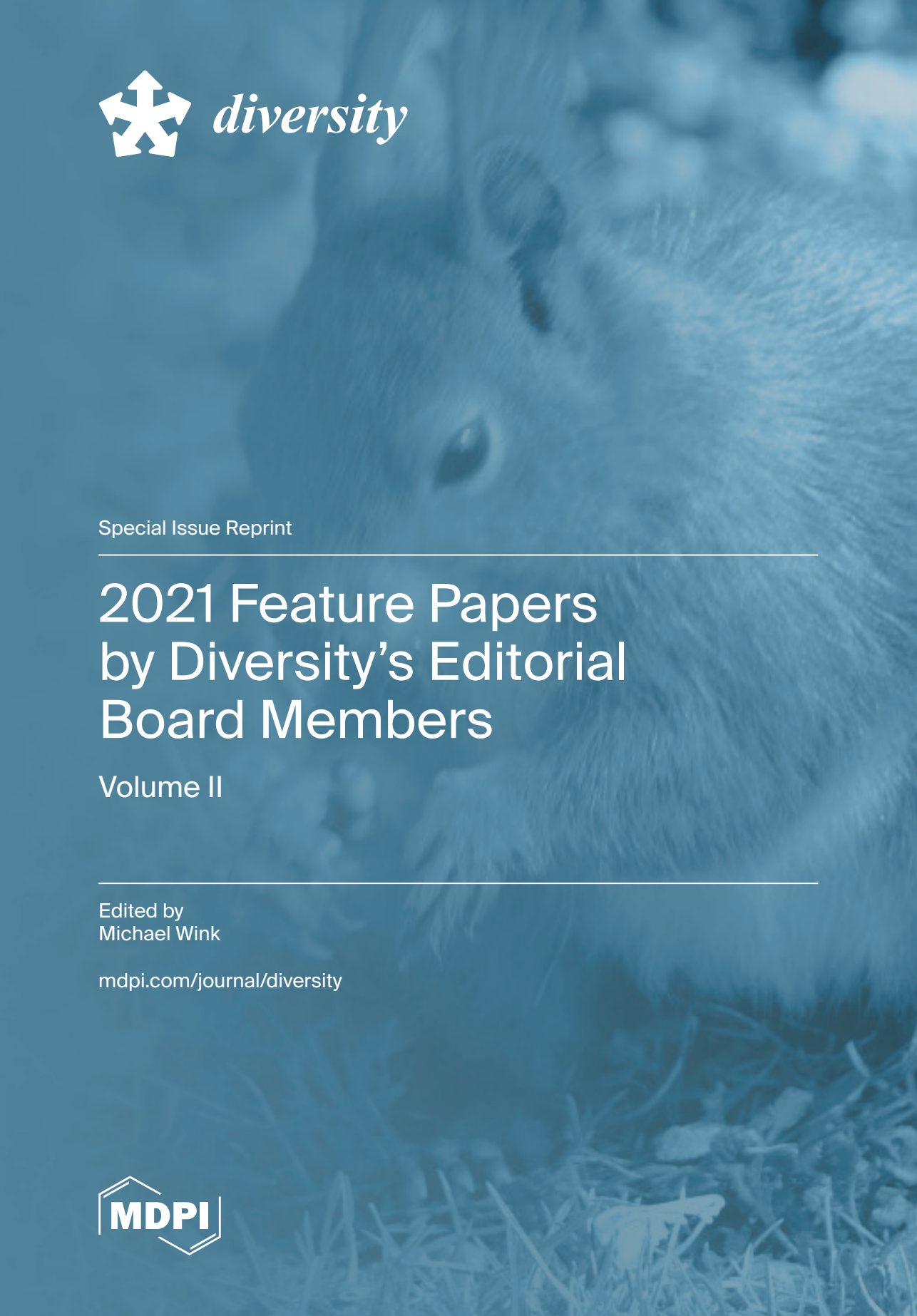

diversity

Special Issue Reprint

2021 Feature Papers by Diversity's Editorial Board Members

Volume II

Edited by
Michael Wink

mdpi.com/journal/diversity

MDPI

2021 Feature Papers by Diversity's Editorial Board Members—Volume II

2021 Feature Papers by Diversity's Editorial Board Members—Volume II

Editor

Michael Wink

MDPI

Basel • Beijing • Wuhan • Barcelona • Belgrade • Novi Sad • Cluj • Manchester

Editor
Michael Wink
Heidelberg University
Heidelberg, Germany

Editorial Office
MDPI
St. Alban-Anlage 66
4052 Basel, Switzerland

This is a reprint of articles from the Special Issue published online in the open access journal *Diversity* (ISSN 1424-2818) (available at: https://www.mdpi.com/journal/diversity/special_issues/emb_diversity).

For citation purposes, cite each article independently as indicated on the article page online and as indicated below:

Lastname, A.A.; Lastname, B.B. Article Title. *Journal Name* **Year**, *Volume Number*, Page Range.

Volume II
ISBN 978-3-0365-9957-1 (Hbk)
ISBN 978-3-0365-9958-8 (PDF)
doi.org/10.3390/books978-3-0365-9958-8

Set
ISBN 978-3-0365-9953-3 (Hbk)
ISBN 978-3-0365-9954-0 (PDF)

Cover image courtesy of Michael Wink

Contents

Preface

This is a Special Issue of high-quality papers in open access form by the Editorial Board Members of Diversity, or those recommended and invited by the Editorial Board Members and the Editor-in-Chief. The Special Issue comprises publications on all aspects of ecology and evolution of plants, animals, marine organisms and microbes, their biodiversity, phylogeny and evolution, and conservation.

Michael Wink
Editor

diversity

MDPI

Article

Transcriptome Analyses Reveal Circadian-Related Expression Features in the Visual Systems of Two Snakes

Chen-Yang Tang [1,2], Meng-Huan Song [2,3], Zhong-Liang Peng [2,3], Wei Wu [2,3], Changjun Peng [2,3], Kong Yang [1,*] and Jia-Tang Li [2,3,*]

[1] Institute of Qinghai-Tibetan Plateau, Southwest Minzu University, Chengdu 610041, China; phtcy97@163.com
[2] CAS Key Laboratory of Mountain Ecological Restoration and Bioresource Utilization & Ecological Restoration and Biodiversity Conservation Key Laboratory of Sichuan Province, Chengdu Institute of Biology, Chinese Academy of Sciences, Chengdu 610041, China; songmh@cib.ac.cn (M.-H.S.); pengzl@cib.ac.cn (Z.-L.P.); wuwei@cib.ac.cn (W.W.); pengcj@cib.ac.cn (C.P.)
[3] University of Chinese Academy of Sciences, Beijing 100049, China
* Correspondence: lx-yk@163.com (K.Y.); lijt@cib.ac.cn (J.-T.L.)

Abstract: The visual characteristics of animals with different circadian habits, especially colubrid snakes, exhibit highly variable photoreceptor morphology. While studies have reported on the diversity in retinal cell morphology among snakes with different circadian patterns, few studies have examined the expression of genes related to vision. To explore gene expression patterns in the eyes between diurnal and nocturnal snakes, we carried out RNA sequencing of six tissues (eye, heart, liver, lung, kidney, and muscle) in two colubrids with disparate circadian activities, i.e., diurnal *Ahaetulla prasina* and nocturnal *Lycodon flavozonatum*, followed by weighted gene co-expression network analysis (WGCNA). The genes in the two most correlated modules were primarily enriched in different functional pathways, thus suggesting different biological functions. Three opsin genes (*RH1*, *LWS*, and *SWS*) were differentially expressed between the two species. Moreover, in the phototransduction pathway, different genes were highly expressed in the eyes of both species, reflecting specific expression patterns in the eyes of snakes with different circadian activity. We also confirmed the dominance of cone- and rod-related genes in diurnal and nocturnal adaptation, respectively. This work provides an important foundation for genetic research on visual adaptation in snakes and provides further insight into the adaptive evolution of such species.

Keywords: transcriptome; gene expression pattern; Colubridae; visual adaption; phototransduction; circadian

Citation: Tang, C.-Y.; Song, M.-H.; Peng, Z.-L.; Wu, W.; Peng, C.; Yang, K.; Li, J.-T. Transcriptome Analyses Reveal Circadian-Related Expression Features in the Visual Systems of Two Snakes. *Diversity* **2021**, *13*, 621. https://doi.org/10.3390/d13120621

Academic Editor: Michael Wink

Received: 2 November 2021
Accepted: 23 November 2021
Published: 26 November 2021

1. Introduction

The evolution of perception has long fascinated evolutionary biologists, especially the complex visual systems that have evolved over millions of years to adapt to diverse habitats with various spectral ranges and illumination intensities [1]. The initial process of vertebrate vision is the absorption of light by retinal photoreceptor cells (rods and cones), and subsequent activation of the biochemical phototransduction cascade, which converts light signals into electrical signals transmitted through nerves [2]. Visual pigments (or opsins) play a core role in visual photosensitivity. Photons are absorbed by visual pigments, i.e., G protein-coupled receptors [3]. Rhodopsin visual pigments are found in rod cells, whereas color visual pigments are found in cone cells [4]. Animal lifestyle often reflects the content of cones and rods [5]. Nocturnal terrestrial animals have an abundance of rods, which mediate dim-light vision, whereas diurnal vertebrates contain more cones with good color vision [6]. For instance, daytime visual capabilities, including cone densities, cone: rod ratios, and photopic a-wave amplitudes, can discriminate wading bird species [7]; among reptiles, the nocturnal gecko (*Gekko gekko*) has pure rod retinas [8] while the diurnal chameleon (*Anolis carolinensis*) has pure cone retinas [9].

Snakes are globally distributed taxa, and their distribution patterns are affected by diffusion corridors [10] or isolation barriers [11] produced by geological changes. More than 3500 extant snake species are currently recognized, which exhibit considerable diversity in habitat requirements and circadian patterns [12]. Snakes usually perceive their prey by chemosensory or visual stimuli, and exhibit diverse diurnal and nocturnal lifestyles [13]. Diversified constitute of photoreceptors in retinas of snakes was described, especially in colubrids [14] (e.g., pure cone retina in some diurnal colubrids, and pure rod retina in some nocturnal colubrids). Thus, snakes are good model animals for exploring adaptive molecular evolution of vertebrate vision. However, most related research has focused on mammals, birds, and fish, revealing the adaptations of retinal morphology [15]. Several studies have explored the evolutionary changes in snake opsin genes, indicating exceptional diversity in snake visual systems [16,17]. Different from other vertebrate taxa, most snakes only express three visual opsin genes [18], i.e., the rhodopsin (*RH1*) gene, which is mainly expressed in rods, the short-wavelength-sensitive (*SWS1*) gene, which is primarily located in small singles cones, and the long-wavelength-sensitive (*LWS*) gene, which is mainly found in large single cones [19]. Divergence in snake circadian activity has led to the adaptation of retinal morphology to either photopic or scotopic vision, which may result in differences in gene expression patterns [20,21].

To explore the similarities and differences in eye gene expression patterns in snakes with different habits, we performed transcriptome sequencing and weighted gene co-expression network analysis (WGCNA) of two Colubridae snakes: i.e., *Ahaetulla prasina*, a common arboreal snake with acute diurnal vision in Southeast Asia and Indochina [22], and *Lycodon flavozonatum*, a nocturnal snake with yellow stripes mainly distributed in southern China, northern Vietnam, and Myanmar [23]. The WGCNA results revealed that eye-related genes were assigned to two modules involved in different function. Moreover, the three opsin genes and several genes vital in phototransduction cascade showed disparate expression patterns between the two species. These expression changes were in accordance with their circadian activity patterns, indicating that differences in expression may be a key molecular basis for adaptation to different circadian rhythms. Our results showed that the expression patterns of vision-related genes differed between diurnal and nocturnal snakes, providing an important basis for further molecular evolution research of snake vision.

2. Materials and Methods

2.1. Sequencing Samples Collection

To understand the genetic mechanisms underlying the visual adaption between two snakes with different habits, we collected a total of six individuals for transcriptome sequencing. Three individuals of *A. prasina* were collected from Xishuangbanna, Yunnan Province and three *L. flavozonatum* were from Mangshan, Hunan Province. Six tissues (heart, liver, lung, kidney, muscle, eyes) of each snake were sampled, immediately frozen in liquid nitrogen for 10 min, and stored at −80 °C prior to RNA isolation.

2.2. cDNA Library Construction and mRNA Sequencing

QIAGEN® RNA Mini Kit was used to extract total RNA. After degradation and contamination monitored on 1% agarose gels, RNA purity was checked using the NanoPhotometer® spectrophotometer (IMPLEN, Calabasas, CA, USA). RNA concentration was measured using the Qubit® RNA Assay Kit in Qubit® 2.0 Flurometer (Life Technologies, Carlsbad, CA, USA). RNA integrity was assessed using the RNA Nano 6000 Assay Kit of the Agilent Bioanalyzer 2100 system (Agilent Technologies, Santa Clara, CA, USA). A total amount of 1.5 μg RNA per sample was used as input material for the RNA sample preparations. Sequencing libraries were generated using NEBNext® UltraTM RNA Library Prep Kit for Illumina® (NEB, Ipswich, MA, USA), following the manufacturer's recommendations, and index codes were added to attribute sequences to each sample. The clustering of the index-coded samples was performed on a cBot Cluster Generation System using TruSeq PE Cluster Kit v3-cBot-HS (Illumina), according to the manufacturer's instructions.

After cluster generation, the library preparations were sequenced on an Illumina Novaseq 6000 platform, and 150 bp paired-end reads were generated.

2.3. De Novo Transcriptome Assembly and Transcription Abundance Statistic

Original reads data was processed using seqtk v1.3-r106 to remove low-quality reads for obtaining clean data. The high-quality filtered reads data of six tissues of one species (three biological replicates each) were pooled together for *de novo* assembly. Trinity v2.4.0 was used for *de novo* transcriptome assembly and to remove redundant sequences, yielding unigenes of each species. We compared the assembly results (Table S1) obtained by setting different parameters, and finally applied parameters "-group_pairs_distance 230 -min_contig_length 600 -min_glue 4". Clean reads was aligned to unigenes using bowtie2 with parameters "-no-discordant -gbar 1000 -end-to-end -k 200 -q -X 800". The longest transcripts were retrieved as the gene body to avoid redundant gene counts. Abundance of each unigene was calculated by RSEM tool, and the TPM (Transcripts Per Million) method was chosen to represent expression level of each unigene.

2.4. Transcriptome Assembly Statistics and Functional Annotation

We used TransDecoder v3.0.1 to predict open reading frames (ORFs) and predict amino acid sequence of each unigene. BUSCO (Benchmarking Universal Single-Copy Orthologs) was used to evaluate the completeness of the unigenes against the vertebrate lineages (vertebrata_odb9, based on 2586 vertebrate core BUSCOs). Local ncbi-blast-2.7.1+ was used for the homology search of unigenes against the non-redundant SWISS-Prot database (https://ftp.uniprot.org/pub/databases/uniprot/, accessed on 22 September 2021), using a BLASTP algorithm with parameters "-line 2 -word_size 4 -evalue 1e-5 -top 3" to retrieve the best hit results of unigenes; the same protocol was processed against NCBI non-redundant protein database (NR) and Kyoto Encyclopedia of Genes and Genomes (KEGG) database. Gene ontology (GO) functional categorization analysis of unigenes was performed using in-house perl scripts, based on the SWISS-Prot annotated results retrieved associated GO terms from idmapping.tb.gz (ftp://ftp.pir.georgetown.edu/databases/idmapping/, accessed on 22 September 2021). Gene ontology (GO) annotation classified unigenes into various pathways and functions through three sub catalogs: biological process, molecular function, and cellular component. Statistics of functional prediction and GO annotation results were performed through jvenn (http://jvenn.toulouse.inra.fr/app/example.html, accessed on 2 September 2021) [24] and WEGO 2.0 (https://wego.genomics.cn/, accessed on 22 September 2021) [25], respectively.

2.5. Orthologous Genes Identification and Principal Component Analysis (PCA)

Based on amino acid sequence of two species, we identified orthologous genes using BLASTP algorithm. Sequence alignments were conducted for transcripts between two species with parameter E-value of 1e-5; reciprocal best hits in each pair were obtained, and orthologous genes shared by both species were retained. Principal component analysis (PCA) was proceeded to check the cluster of tissues based on expression data of orthologous genes by using R package FactoMineR and factoextra.

2.6. Weighted Gene Co-Expression Network Analysis (WGCNA) and Screening of Differential Expression Genes

The co-expression network of the orthologous genes was constructed using R package WGCNA v1.69 based on expression level (TPM). A network based on the approximate scale-free topology was constructed by selecting the most suitable soft threshold power of 10, which resulted in a scale-free R2 fit. A topological overlap dendrogram was used to define modules with a minimum module size of 100 genes, and the threshold cut height for merging modules was set to 0.2. Genes were clustered with similar expression patterns into a co-expression module with specific molecular mechanisms. The module eigengenes (ME) were subsequently calculated for each module. We treated the eyes of two snakes as different phenotypes, and identified the most relevant gene modules respectively. Pearson's

correlation coefficient was used to analyze the correlation between the module eigengene and eyes, and the modules with the highest correlations were selected as eye-correlated module. Gene significance (GS) and module membership (MM), which represented the correlation of gene expression profile with the ME, were identified. We compared the TPM results of key genes in correlation modules between two species to identify different expression genes (DEGs) by using R package limma v3.48.2. To reduce the false positive rate, only genes with adjusted *p*-value < 0.05 and $|\log2FC| \geq 1$ were recognized as DEGs.

2.7. Gene Functional Enrichment and Pathways Analysis

Gene ontology enrichment analysis of genes in eye-correlated modules was performed using R package clusterProfiler v3.14.3 [26]. We identified significantly enriched GO terms of genes in eye-correlated modules by using the GO annotations of all annotated unigenes as the background. The *p*-value was adjusted by Benjamini–Hochberg FDR, and terms with adjusted *p*-value of <0.05 were recognized as significant. REViGO [27] was then used to cluster the overrepresented GO terms, and construct the interactions of terms. KEGG pathway mapping analysis was utilized by using KEGG mapping tools (https://www.kegg.jp/kegg/mapper/, accessed on 12 October 2021). We searched genes annotated from KEGG by KOs against KEGG pathway maps and other network entities. Of all the results, we concentrated on KEGG pathways of interest and crucial genes in the pathway.

3. Results

3.1. Transcriptome De Novo Assembly

We collected three individuals of *A. prasina* (Figure 1A) and *L. flavozonatum* (Figure 1B), respectively. cDNA libraries were constructed for both species, with three replicates per group. In total, 307.77 Gb of raw data were obtained from 36 samples (six tissues per individual) using the Illumina sequencing platform (Table S2). After quality control, a total of 298.35 Gb of clean reads were generated for downstream analysis. Using Trinity tools, 218,220 transcripts and 90,635 unigenes with a contig N50 of 3345 were assembled for *A. prasina*, and 226,292 transcripts and 98,838 unigenes with a contig N50 of 2996 were assembled for *L. flavozonatum* (Table S3). Of all transcripts, 73,147 and 78,359 contained open reading frames (ORFs) that predicted peptides >100 amino acids (aa) in length, respectively, of which, 36,902 and 40,445 were full-length for predicting coding protein sequence. After removing redundancy and clustering, 26,540 and 29,877 longest sequences were obtained for orthologous gene analysis, respectively. Transcriptome assembly quality was evaluated using benchmarking universal single-copy orthologs (BUSCO) with protein mode and lineage data from vertebrates, which showed comparable completeness (65.6% and 68.3%) (Table S4).

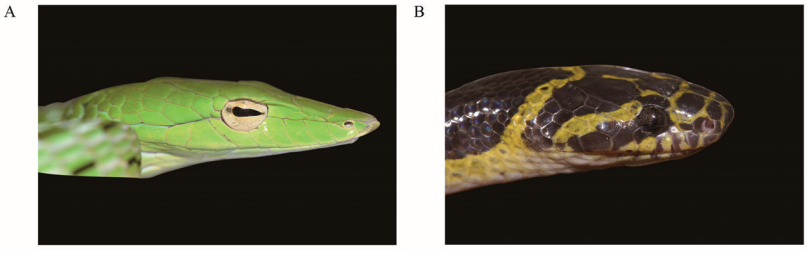

Figure 1. Schematic diagram of the eyes of (**A**) *Ahaetulla prasina* (diurnal) and (**B**) *Lycodon flavozonatum* (nocturnal). Photos by Chen-Yang Tang and Jin-Long Ren.

3.2. Unigene Functional Annotation

Unigenes from *A. prasina* and *L. flavozonatum* were searched against the NR, SwissProt, Gene Ontology (GO), and Kyoto Encyclopedia of Genes and Genomes (KEGG) databases.

In total, 17,978 unigenes (67.74% of 26,540) and 20,868 unigenes (69.85% of 29,877) were annotated to one or more functions for *A. prasina* (Figure 2A) and *L. flavozonatum* (Figure 2B), respectively. Subsequently, 15,616 and 17,932 unigenes were co-annotated in all databases for *A. prasina* and *L. flavozonatum*, respectively. Based on GO functional annotation, 15,734 and 18,082 unigenes were assigned to three categories: biological processes, molecular function, and cellular component. Results revealed that unigenes related to cellular process (GO: 0009987), biological regulation (GO: 0065007), metabolic process (GO: 0008152), and regulation of biological process (GO: 0050789) were highly represented in the biological processes category; unigenes related to binding (GO: 0005488) and catalytic activity (GO: 0003824) were highly represented in the molecular function category; and unigenes related to cell (GO: 0005623), cell part (GO: 0044464), and organelle (GO: 0043226) were highly represented in the cellular component category in both species (Figure 2C).

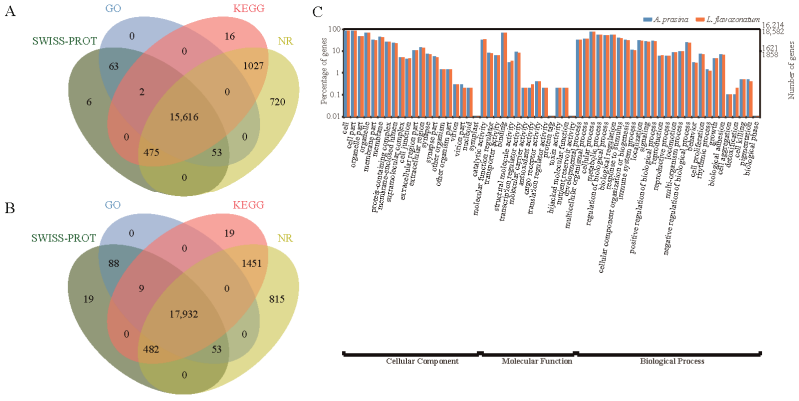

Figure 2. Annotative summary of *de novo* transcriptome assembly. (**A**) Annotated unigenes of *A. prasina* and (**B**) *L. flavozonatum* from 4 different databases. (**C**) Comparison of Gene Ontology (GO) classifications based on *de novo* transcriptome assembly of two snakes.

3.3. Gene Expression and Cluster Analysis

A total of 13,605 orthologous genes were identified by BLASTP. WGCNA and gene expression analysis were based on these orthologous genes. We first performed principal component analysis (PCA) to assess differences in expression between the eyes and other tissues. Results revealed that the 36 samples could be assigned to six groups, according to tissue types, and the first two PCs explained 41.6% of the variance (Figure 3). The same tissues from all six individuals clustered together, indicating that the transcriptome data could be used for further analysis. Furthermore, the eyes were well distinguished, suggesting differences in the expression patterns between eyes and other tissues.

3.4. Co-Expression Network Construction

Co-expression analysis is commonly used to clarify gene association patterns in samples or species [28]. Through WGCNA, connectivity among genes in the network showed scale-free network distribution when the correlation coefficient threshold was set to 0.9, the best soft-thresholding power was set to 10 (Figure 4A), and modules with high ME correlations ($R > 0.8$) were merged (Figure 4B). A total of 13,605 orthologous genes were divided into 21 co-expression modules, which were independent of each other (Figure 4C). The dark-green module contained the most genes, followed by the midnight blue module. Genes that could not be assigned to any module were placed in the gray module, which contained genes identified as not co-expressed.

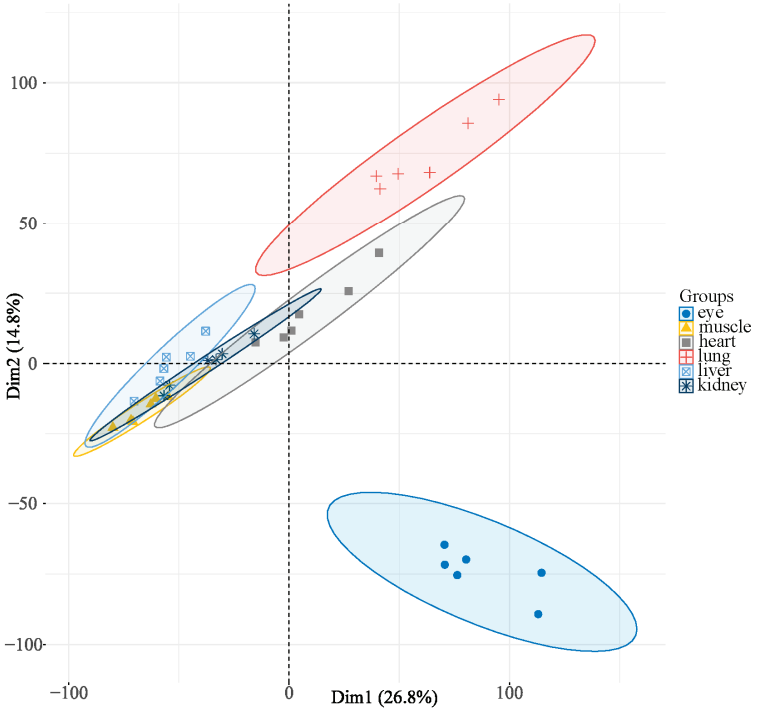

Figure 3. PCA plot of 36 samples from two snakes.

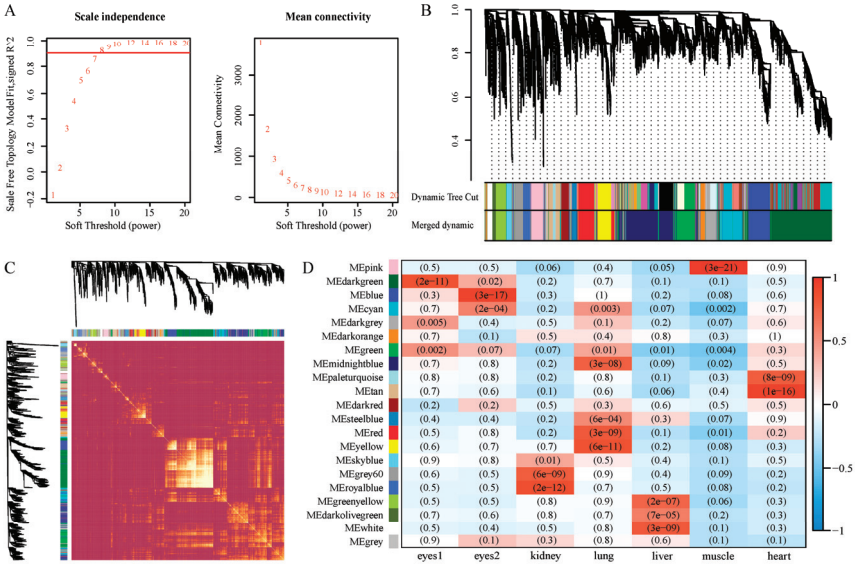

Figure 4. Co-expression analysis for orthologous genes from two snakes. (**A**) Analysis of soft-thresholding powers based on scale independence (left) and mean connectivity (right). (**B**) The cluster dendrogram of genes. Modules considered with high similarity were merged. (**C**) Network heatmap plots of all genes in WGCNA. (**D**) Heatmap of correlation between modules and traits. Shades of color represent correlation and the numbers in parentheses represent *p*-value.

3.5. Identification and GO Enrichment of Significant Eye Correlation Modules

To identify the modules most relevant to phenotype, we performed correlation analysis between module and trait. Results showed that the dark-green (R = 0.86, p = 2e-11) and blue (R = 0.94, p = 3e-17) modules were the best correlated modules for the eyes of the two species, and included 2641 and 878 genes, respectively (Figure 4D). GO functional enrichment analysis of the key modules showed that genes in dark-green module were mainly enriched in biological processes related to response to stimulus (GO: 0050896), signal transduction (GO: 0007165), ion transmembrane transport (GO: 0034220), G protein-coupled receptor signaling pathway (GO: 0007186), and nervous system development (GO: 0007399), which were mainly related to signal transmission (Figure 5A,B, Table S5). The top GO terms enriched by genes in the blue module included visual perception (GO: 0007601), photoreceptor cell maintenance (GO: 0045494), and response to stimulus (GO: 0050896), suggesting that these genes were highly related to vision formation and light perception (Figure 5C, Table S6).

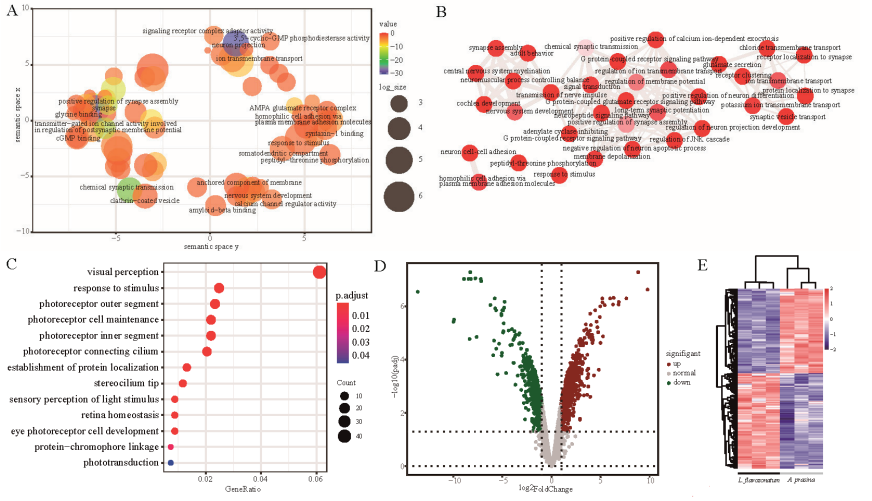

Figure 5. GO terms enriched by module genes and differential expression pattern. (**A**) REVIGO clusters of significantly overrepresented GO terms for genes in dark-green module. (**B**) Interactive graph of significantly overrepresented GO terms in dark-green module. (**C**) Dot plot of significant GO terms enriched by genes in blue module. (**D**) Volcano plot of differential expression genes (DEGs) in two modules between two snakes. The green dots indicate the genes upregulated in eyes of *A. prasina* and red dots represent genes upregulated in *L. flavozonatum* (**E**) Heatmap shows expression pattern of DEGs in two modules.

3.6. Expression Pattern and Screening of Genes in Phototransduction Pathway

Of the eye-related genes, 596 were up-regulated in the eyes of *A. prasina* and 673 were up-regulated in the eyes of *L. flavozonatum* (Figure 5D, Table S7), and gene expression showed opposite trends (Figure 5E). To explore the differences in gene expression patterns between the two species, we concentrated on genes in the key modules enriched in visual-related pathways. For KEGG pathway mapping analysis, 1799 and 528 genes in the key modules were assigned to the KEGG database, respectively. In addition, 354 and 330 pathways were mapped by all these genes, with phototransduction (map04744) found to be the most concerned, due to its key role in light perception (Figure 6). In the dark-green module, *LWS* was significant, with high GS and MM scores. Rhodopsin kinase GRK7 (*GRK7*), regulator of G-protein signaling 9 (*RGS9*), calmodulin-2 B (*CALM2B*), cyclic nucleotide-gated cation channel beta-3 (*CNGB3*), cyclic nucleotide-gated channel cone photoreceptor subunit alpha 3 (*CNGA3*), and cone cGMP-specific 3′, 5′-cyclic phosphodiesterase subunit alpha

(*PDE6C*) were noticed particularly in the phototransduction pathway. Most of these genes are involved in signal transmission, especially in cone cells. In the blue module, *SWS1*, *RH1*, cyclic nucleotide gated channel alpha 1 (*CNGA1*), cyclic nucleotide gated channel beta 1 (*CNGB1*), guanylate cyclase activator 1 (*GUCA1*), and retinal guanylyl cyclase 2D/E (*GUCY2E*) were key genes involved in the phototransduction pathway. They mostly play a part in rod cells.

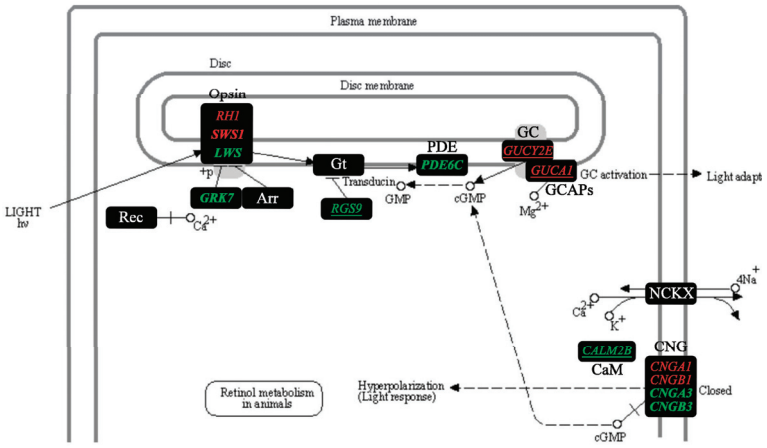

Figure 6. Genes of interest involved in phototransduction pathway (modified from KEGG pathway: map04744). Genes not involved in this study are shown in white. Genes assigned to modules correlated with eyes of *A. prasina* and *L. flavozonatum* are shown in green and red, respectively. The genes specifically involved in phototransduction in cones are shown in bold, and in rods shown in regular font, while underlined texts indicate genes in both cones and rods.

4. Discussion

Different diurnal and nocturnal habits can lead to differences in the adaptive evolution of visual systems. For instance, activity patterns can be well discriminated based on morphometric analysis and signatures of selection [15,16,29]. However, studies on differences in gene expression remain limited. In the current study, we explored the expression patterns of vision-related genes based on transcriptome data of multiple tissues from two snakes with diverse circadian activity. *De novo* assembly of the transcriptome uncovered 13,605 orthologous genes between the two snake species, providing important support for snake vision research.

Based on PCA, we showed that gene expression patterns in the eyes differed from those in other tissues in both species, which proves the high specificity of gene expression and functional specialization of eyes. Furthermore, WGCNA showed that 2641 genes in the diurnal vision-related module were involved in nervous system development, ion transmembrane transport, and the G protein-coupled receptor signaling pathway, indicating dominance of light signal transmission. Diurnal snakes generally contain a higher density of ganglion cells, which contact directly onto cones with synaptic for responding rapidly [6,30]. In retinal photoreceptor cells, when the status of ion channels varies due to photon absorption, the concentration of ions in the outer segment changes quickly, and transforms the polarization state of the photoreceptors, resulting in visual regulation [31]. Ion transport can affect the synthesis and degradation of cGMP [32] and modulate the sensitivity of visual pigment itself [33]. Based on our analysis of *L. flavozonatum* eyes, we identified 878 correlated genes in the blue module, most of which were related to visual perception, photoreceptors, and phototransduction. In nocturnal vertebrates, rod cells serve as dim-light photoreceptors, and are normally related to night vision [6,34]. Due to night-based activities and predation, nocturnal snakes always have a higher density

of rod photoreceptors to increase sensitivity for light perception [35]. The significant expression of genes enriched in visual signal transmission in *A. prasina* eyes increases its adaptability to daylight conditions and rapid reactions, whereas the significant expression of photosensory-related genes in *L. flavozonatum* eyes increases its sensitivity to light in dark environments. Thus, the main functions of the genes expressed in the eye were specific to the circadian activities of the two snakes.

During phototransduction cascade, opsins in retinal photoreceptor cells perform crucial functions in light perception [36,37]. Previous research has demonstrated that the density of cones in the retina of diurnal animals is significantly higher, while the number of rods in the retina of nocturnal animals is markedly higher [38]. Moreover, gene loss and signatures of selection of opsins were discovered in owls, which possess large and rod-dominant retinas as a kind of special night-time raptor [39]; in snakes, visual opsin genes were detected containing signals of positive selection in sites of functional importance that are associated with shifts in ecology and retinal anatomy [29]. Thus, changes in opsin genes may affect circadian activities. Here, we concentrated on the expression of three opsin genes (i.e., *RH1*, *SWS1*, and *LWS*) in two snake species. Although all three photopigment genes (*RH1*, *LWS*, and *SWS1*) were expressed in the eyes of both snakes, only *LWS* was highly expressed in *A. prasina*, and only *SWS1* and *RH1* were highly expressed in *L. flavozonatum*. Research shows that some diurnal snakes cut out shorter wavelength (including UVA), whereas UV vision is predicted to be widely present in most nocturnal snakes [16]. Of note, removal of UV light has been linked to increased visual acuity [40], and it is supported by morphological research on *Ahaetulla* species, which are highly visual hunters with the least transparent lenses, horizontal pupils, binocular vision, and a fovea in eyes that are indicative of high visual acuity [41]. Photoreceptors can display evolutionarily transitions between cell types in squamates [42], as supported by the expression of cone-like rod photoreceptors in the all-cone retina of garter snake, which restore spectral sensitivity and chromatic discrimination [43]. As such, transmuted rod photoreceptors may exist in the retinas of *A. prasina*. The expression difference in our analysis acts as a reminder that, as nocturnal snake, rod photoreceptor genes highly express in eyes of *L. flavozonatum* for adapting dim-light condition, and shows sensitivity to short-wavelength light, versus eyes of *A. prasina* is more sensitive to long-wavelength light with a preponderance of cones photoreceptor, probably due to filtering shorter wavelength, which shows consistency with previous circadian activity studies.

Visual phototransduction represents one of the best-characterized signaling pathways in vertebrate vision [44]. In Shaw's sea snake (*Hydrophis curtus*), phototransduction-related genes are reported to be under positive selection to improve visual sensitivity [45]. The expression level of phototransduction proteins in visual cells also accounts for visual adaption to light [6]. Our WGCNA results demonstrated specific expression of phototransduction-related genes in the eyes of both snakes. We identified six genes (*GRK7*, *CNGB3*, *CNGA3*, *PDE6C*, *RGS9*, and *CALM2B*) involved in the phototransduction pathway in *A. prasina*, four of which were cone-specific, thus showing the dominant role of cones in the eyes of *A. prasina*. *GRK7* encodes a member of the G protein-coupled receptor kinase subfamily, which is involved in shutting down the light response and adapting to changing light conditions through opsin phosphorylation [46]. *CNGB3* encodes the beta subunit of a cyclic nucleotide-gated ion channel, which plays a role in modulation of channel function in cone photoreceptors and is essential for the generation of light-evoked electrical responses in the red-, green-, and blue-sensitive cones [47]. *CNGA3* plays a role in cation channel opening and causes depolarization of cone photoreceptors after activation by cGMP [48]. As a cone-specific cGMP phosphodiesterase, *PDE6C* participates in light detection and cone phototransduction by rapidly reducing the intracellular levels of cGMP [49]. *RGS9* and *CALM2B* play crucial roles in signal transduction [50] and regulation of calcium ion concentrations [51] in photoreceptor light adaptation, respectively.

Of note, differences in the expression of cone-specific genes may indicate changes in cone cells, and high cone cell density may indicate increased color discrimination [52],

similar to the double cones found in *A. prasina* with skin color polymorphism [16,53]. Since skin color can be used in mate-choice and other intraspecific signals, or may be involved in predator avoidance (e.g., aposematism and mimicry), color vision is very important [54]. However, further research is required to elucidate this ability in *A. prasina*.

In the correlation module of the *L. flavozonatum* eyes, several important genes related to rods were mapped to the same pathway, including *CNGA1*, *CNGB1*, *GUCA1*, and *GUCY2E*. *CNGA1* encodes a subunit of the rod cyclic GMP-gated cation channel to depolarize rod photoreceptors in the last step of the phototransduction pathway [55]. Analogously, *CNGB1* is involved in the regulation of ion flow in rod photoreceptor outer segments in response to light-induced changes in the levels of intracellular cGMP associated with *CNGA1* [56]. *GUCA1* and *GUCY2E* play essential roles in regulating retinal guanylyl cyclase-1 (GC1) [57] and mediating cGMP replenishment during phototransduction [58], respectively. Thus, these genes suggest the vital role of rods in *L. flavozonatum* of light perception.

In summary, we used WGCNA to identify key co-expression modules and functional pathways related to the vision of two snakes with different circadian activities. We also revealed the different expression patterns in phototransduction in the two species. Although our research is preliminary and needs further verification, these findings provide new insights into the genetic adaptations of vision related to circadian activity.

Supplementary Materials: The following are available online at https://www.mdpi.com/article/10.3390/d13120621/s1, Table S1: Summary of transcriptome *de novo* assembly tests of two snakes, Table S2: Summary of samples and RNA sequencing, Table S3: Summary of transcriptome assembly of two snakes, Table S4: BUSCO scores of transcriptome assembly of two snakes, Table S5: Significant GO terms enriched by genes in dark-green module, Table S6: Significant GO terms enriched by genes in blue module, Table S7: Differential expression of genes in two modules correlated to eyes.

Author Contributions: J.-T.L. and K.Y. conceived the study; C.-Y.T. and Z.-L.P. collected experimental samples; C.-Y.T. and C.P. performed data analyses; J.-T.L. and C.-Y.T. prepared the initial manuscript draft; M.-H.S. and W.W. worked on the approval of the manuscript. All authors have read and agreed to the published version of the manuscript.

Funding: This work was supported by the National Natural Science Foundation of China (32000296); the International Partnership Program of Chinese Academy of Sciences (151751KYSB20190024); Key Research Program of Frontier Sciences, CAS (QYZDB-SSW-SMC058); the Sichuan Science and Technology Program (2021JDJQ0002); and the CAS "Light of West China" Program (2018XBZG_JCTD_001).

Institutional Review Board Statement: Not applicable.

Informed Consent Statement: Not applicable.

Data Availability Statement: The RNA-seq data generated in this study are available in the China National GeneBank DataBase (CNGBdb), under accession number CNP0002398.

Acknowledgments: We would like to thank Di-Hao Wu and Dan Wang for snake samples; and Jin-Long Ren for photos and insightful suggestions.

Conflicts of Interest: The authors declare no conflict of interest.

References

1. Katti, C.; Stacey-Solis, M.; Coronel-Rojas, N.A.; Davies, W.I.L. Opsin-based photopigments expressed in the retina of a South American pit viper, *Bothrops atrox* (Viperidae). *Vis. Neurosci.* **2018**, *35*, E027. [CrossRef]
2. Strader, C.D.; Fong, T.M.; Tota, M.R.; Underwood, D. Structure and Function of G Protein-Coupled Receptors. *Annu. Rev. Biochem.* **1994**, *63*, 101–132. [CrossRef]
3. Kefalov, V.J. Rod and cone visual pigments and phototransduction through pharmacological, genetic, and physiological approaches. *J. Biol. Chem.* **2012**, *287*, 1635–1641. [CrossRef]
4. Sakmar, T.P.; Fahmy, K. Properties and Photoactivity of Rhodopsin Mutants. *Isr. J. Chem.* **1995**, *35*, 325–337. [CrossRef]
5. Yokoyama, S. Molecular evolution of vertebrate visual pigments. *Prog. Retin. Eye Res.* **2000**, *19*, 385–419. [CrossRef]
6. Lamb, T.D. Evolution of phototransduction, vertebrate photoreceptors and retina. *Prog. Retin. Eye Res.* **2013**, *36*, 52–119. [CrossRef]
7. Rojasa, L.M.; McNeila, R.; Cabanaa, T.; Lachapelleb, P. Behavioral, Morphological and Physiological Correlates of Diurnal and Nocturnal Vision in Selected Wading Bird Species. *Brain Behav. Evol.* **1999**, *53*, 227–242. [CrossRef] [PubMed]

8. Yokoyama, S.; Blow, N.S. Molecular evolution of the cone visual pigments in the pure rod-retina of the nocturnal gecko, *Gekko gekko*. *Gene* **2001**, *276*, 117–125. [CrossRef]
9. Crescitelli, F. *The Visual Cells and Visual Pigments of the Vertebrate Eye*; Springer: Berlin, Germany, 1972; Volume VII/1, pp. 245–363.
10. Jiang, D.; Klaus, S.; Zhang, Y.P.; Hillis, D.M.; Li, J.T. Asymmetric biotic interchange across the Bering land bridge between Eurasia and North America. *Natl. Sci. Rev.* **2019**, *6*, 739–745. [CrossRef] [PubMed]
11. Hu, Y.; Fan, H.; Chen, Y.; Chang, J.; Zhan, X.; Wu, H.; Zhang, B.; Wang, M.; Zhang, W.; Yang, L.; et al. Spatial patterns and conservation of genetic and phylogenetic diversity of wildlife in China. *Sci. Adv.* **2021**, *7*, eabd5725. [CrossRef]
12. Torello-Viera, N.F.; Marques, O.A.V. Daily Activity of Neotropical Dipsadid Snakes. *South Am. J. Herpetol.* **2017**, *12*, 128–135. [CrossRef]
13. Mullin, S.J.; Cooper, R.J. The Foraging Ecology of the Gray Rat Snake (*Elaphe obsoleta spiloides*)—Visual Stimuli Facilitate Location of Arboreal Prey. *Am. Midl. Nat.* **1998**, *140*, 397–401. [CrossRef]
14. Hauzman, E. Adaptations and evolutionary trajectories of the snake rod and cone photoreceptors. *Semin. Cell Dev. Biol.* **2020**, *106*, 86–93. [CrossRef]
15. Schmitz, L.; Motani, R. Morphological differences between the eyeballs of nocturnal and diurnal amniotes revisited from optical perspectives of visual environments. *Vis. Res.* **2010**, *50*, 936–946. [CrossRef]
16. Simoes, B.F.; Sampaio, F.L.; Douglas, R.H.; Kodandaramaiah, U.; Casewell, N.R.; Harrison, R.A.; Hart, N.S.; Partridge, J.C.; Hunt, D.M.; Gower, D.J. Visual Pigments, Ocular Filters and the Evolution of Snake Vision. *Mol. Biol. Evol.* **2016**, *33*, 2483–2495. [CrossRef]
17. Cronin, T.W. Sensory Ecology: In Sea Snake Vision, One Plus One Makes Three. *Curr. Biol.* **2020**, *30*, R763–R766. [CrossRef]
18. Simoes, B.F.; Sampaio, F.L.; Jared, C.; Antoniazzi, M.M.; Loew, E.R.; Bowmaker, J.K.; Rodriguez, A.; Hart, N.S.; Hunt, D.M.; Partridge, J.C.; et al. Visual system evolution and the nature of the ancestral snake. *J. Evol. Biol.* **2015**, *28*, 1309–1320. [CrossRef]
19. Davies, W.L.; Cowing, J.A.; Bowmaker, J.K.; Carvalho, L.S.; Gower, D.J.; Hunt, D.M. Shedding light on serpent sight: The visual pigments of henophidian snakes. *J. Neurosci.* **2009**, *29*, 7519–7525. [CrossRef]
20. Bhattacharyya, N.; Darren, B.; Schott, R.K.; Tropepe, V.; Chang, B.S.W. Cone-like rhodopsin expressed in the all-cone retina of the colubrid pine snake as a potential adaptation to diurnality. *J. Exp. Biol.* **2017**, *220*, 2418–2425. [CrossRef] [PubMed]
21. Simoes, B.F.; Sampaio, F.L.; Loew, E.R.; Sanders, K.L.; Fisher, R.N.; Hart, N.S.; Hunt, D.M.; Partridge, J.C.; Gower, D.J. Multiple rod-cone and cone-rod photoreceptor transmutations in snakes: Evidence from visual opsin gene expression. *Proc. Biol. Sci.* **2016**, *283*, 20152624. [CrossRef]
22. Amber, E.D.; Strine, C.T.; Suwanwaree, P.; Waengsothorn, S. Intra-Population Color Dimorphism of *Ahaetulla prasina* (Serpentes: Colubridae) in Northeastern Thailand. *Curr. Herpetol.* **2017**, *36*, 98–104. [CrossRef]
23. Zhao, E. *Snakes of China*; Anhui Science Technology Publishing House: Hefei, China, 2006; p. 372.
24. Bardou, P.; Mariette, J.; Escudié, F.; Djemiel, C.; Klopp, C. jvenn: An interactive Venn diagram viewer. *BMC Bioinform.* **2014**, *15*, 293. [CrossRef]
25. Ye, J.; Zhang, Y.; Cui, H.; Liu, J.; Wu, Y.; Cheng, Y.; Xu, H.; Huang, X.; Li, S.; Zhou, A.; et al. WEGO 2.0: A web tool for analyzing and plotting GO annotations, 2018 update. *Nucleic Acids Res.* **2018**, *46*, W71–W75. [CrossRef] [PubMed]
26. Yu, G.; Wang, L.G.; Han, Y.; He, Q.Y. clusterProfiler: An R package for comparing biological themes among gene clusters. *OMICS* **2012**, *16*, 284–287. [CrossRef]
27. Supek, F.; Bosnjak, M.; Skunca, N.; Smuc, T. REVIGO summarizes and visualizes long lists of gene ontology terms. *PLoS ONE* **2011**, *6*, e21800. [CrossRef]
28. Langfelder, P.; Horvath, S. WGCNA: An R package for weighted correlation network analysis. *BMC Bioinform.* **2008**, *9*, 559. [CrossRef] [PubMed]
29. Hauzman, E.; Bonci, D.M.O.; Suarez-Villota, E.Y.; Neitz, M.; Ventura, D.F. Daily activity patterns influence retinal morphology, signatures of selection, and spectral tuning of opsin genes in colubrid snakes. *BMC Evol. Biol.* **2017**, *17*, 249. [CrossRef]
30. Hauzman, E.; Bonci, D.M.O.; Ventura, D.F. Visual ecology of snakes: Comparative study of the density and distribution of retinal neurons in diurnal and nocturnal species. *Investig. Ophthalmol. Vis. Sci.* **2016**, *57*, 4667.
31. Krizaj, D.; Copenhagen, D.R. Calcium regulation in photoreceptors. *Front. Biosci.* **2002**, *7*, d2023–d2044. [CrossRef] [PubMed]
32. Koch, K.-W.; Stryer, L. Highly cooperative feedback control of retinal rod guanylate cyclase by calcium ions. *Nature* **1988**, *334*, 64–66. [CrossRef] [PubMed]
33. Dizhoor, A.M.; Ray, S.; Kumar, S.; Niemi, G.; Spencer, M.; Brolley, D.; Walsh, K.A.; Philipov, P.P.; Hurley, J.B.; Stryer, L. Recoverin: A Calcium Sensitive Activator of Retinal Rod Guanylate Cyclase. *Science* **1991**, *251*, 915–918. [CrossRef] [PubMed]
34. Ridge, K.D.; Palczewski, K. Visual rhodopsin sees the light: Structure and mechanism of G protein signaling. *J. Biol. Chem.* **2007**, *282*, 9297–9301. [CrossRef]
35. Baylor, D.A.; Lamb, T.D.; Yau, K.W. Responses of retinal rods to single photons. *J. Physiol.* **1979**, *288*, 613–634. [CrossRef] [PubMed]
36. Fain, G.L.; Hardie, R.; Laughlin, S.B. Phototransduction and the evolution of photoreceptors. *Curr. Biol.* **2010**, *20*, R114–R124. [CrossRef]
37. Bowmaker, J.K. Evolution of vertebrate visual pigments. *Vision Res.* **2008**, *48*, 2022–2041. [CrossRef] [PubMed]
38. Wikler, K.C.; Rakic, P. Distribution of photoreceptor subtypes in the retina of diurnal and nocturnal primates. *J. Neurosci.* **1990**, *10*, 3390–3401. [CrossRef] [PubMed]

39. Wu, Y.; Hadly, E.A.; Teng, W.; Hao, Y.; Liang, W.; Liu, Y.; Wang, H. Retinal transcriptome sequencing sheds light on the adaptation to nocturnal and diurnal lifestyles in raptors. *Sci. Rep.* **2016**, *6*, 33578. [CrossRef]
40. Douglas, R.H.; Jeffery, G. The spectral transmission of ocular media suggests ultraviolet sensitivity is widespread among mammals. *Proc. R. Soc. B Biol. Sci.* **2014**, *281*, 20132995. [CrossRef]
41. Rasmussen, J.B. The retina of *Psammodynastes pulverulentus* (Boie, 1827) and *Telescopus fallax* (Fleischmann, 1831) with a discussion of their phylogenetic significance (Colubroidea, Serpentes). *J. Zool. Syst. Evol.* **1990**, *28*, 269–276. [CrossRef]
42. Walls, G. *The Vertebrate Eye and Its Adaptive Radiation*; Fafner Publishing Company: New York, NY, USA, 1942.
43. Schott, R.K.; Muller, J.; Yang, C.G.; Bhattacharyya, N.; Chan, N.; Xu, M.; Morrow, J.M.; Ghenu, A.H.; Loew, E.R.; Tropepe, V.; et al. Evolutionary transformation of rod photoreceptors in the all-cone retina of a diurnal garter snake. *Proc. Natl. Acad. Sci. USA* **2016**, *113*, 356–361. [CrossRef]
44. Ridge, K.D.; Abdulaev, N.G.; Sousa, M.; Palczewski, K. Phototransduction: Crystal clear. *Trends Biochem. Sci.* **2003**, *28*, 479–487. [CrossRef]
45. Peng, C.; Ren, J.L.; Deng, C.; Jiang, D.; Wang, J.; Qu, J.; Chang, J.; Yan, C.; Jiang, K.; Murphy, R.W.; et al. The Genome of Shaw's Sea Snake (*Hydrophis curtus*) Reveals Secondary Adaptation to Its Marine Environment. *Mol. Biol. Evol.* **2020**, *37*, 1744–1760. [CrossRef]
46. Osawa, S.; Weiss, E.R. A tale of two kinases in rods and cones. *Adv. Exp. Med. Biol.* **2012**, *723*, 821–827. [CrossRef] [PubMed]
47. Kohl, S.; Baumann, B.; Broghammer, M.; Jägle, H.; Sieving, P.; Kellner, U.; Spegal, R.; Anastasi, M.; Zrenner, E.; Sharpe, L.T.; et al. Mutations in the *CNGB3* gene encoding the β-subunit of the cone photoreceptor cGMP-gated channel are responsible for achromatopsia (*ACHM3*) linked to chromosome 8q21. *Hum. Mol. Genet.* **2000**, *9*, 2107–2116. [CrossRef]
48. Gerstner, A.; Zong, X.; Hofmann, F.; Biel, M. Molecular Cloning and Functional Characterization of a New Modulatory Cyclic Nucleotide-Gated Channel Subunit from Mouse Retina. *J. Neurosci.* **2000**, *20*, 1324–1332. [CrossRef]
49. Grau, T.; Artemyev, N.O.; Rosenberg, T.; Dollfus, H.; Haugen, O.H.; Cumhur Sener, E.; Jurklies, B.; Andreasson, S.; Kernstock, C.; Larsen, M.; et al. Decreased catalytic activity and altered activation properties of *PDE6C* mutants associated with autosomal recessive achromatopsia. *Hum. Mol. Genet.* **2011**, *20*, 719–730. [CrossRef] [PubMed]
50. Nishiguchi, K.M.; Sandberg, M.A.; Kooijman, A.C.; Martemyanov, K.A.; Pott, J.W.R.; Hagstrom, S.A.; Arshavsky, V.Y.; Berson, E.L.; Dryja, T.P. Defects in RGS9 or its anchor protein R9AP in patients with slow photoreceptor deactivation. *Nature* **2004**, *427*, 75–78. [CrossRef] [PubMed]
51. Hsu, Y.-T.; Molday, R.S. Modulation of the cGMP-gated channel of rod photoreceptor cells by calmodulin. *Nature* **1993**, *361*, 76–79. [CrossRef]
52. Burns, M.E.; Lamb, T.D. *Visual Transduction by Rod and Cone Photoreceptors*; MIT Press: Cambridge, MA, USA, 2004; Volume 1, pp. 215–233.
53. Pignatelli, V.; Champ, C.; Marshall, J.; Vorobyev, M. Double cones are used for colour discrimination in the reef fish, Rhinecanthus aculeatus. *Biol. Lett.* **2010**, *6*, 537–539. [CrossRef] [PubMed]
54. Cyriac, V.P.; Kodandaramaiah, U. Conspicuous colours reduce predation rates in fossorial uropeltid snakes. *PeerJ* **2019**, *7*, e7508. [CrossRef] [PubMed]
55. Kaupp, U.B.; Niidome, T.; Tanabe, T.; Terada, S.; Bonigk, W.; Stiihmert, W.; Cooka, N.J.; Kangawa, K.; Matsuo, H.; Hirosell, T.; et al. Primary structure and functional expression from complementary DNA of the rod photoreceptor cyclic GMP.gated channel. *Nature* **1989**, *342*, 762–766. [CrossRef] [PubMed]
56. Chen, T.Y.; Illing, M.; Molday, L.L.; Hsu, Y.T.; Yau, K.W.; Molday, R.S. Subunit 2 (or β) of retinal rod cGMP-gated cation channel is a component of the 240-kDa channel-associated protein and mediates Ca2+-calmodulin modulation. *Proc. Natl. Acad. Sci. USA* **1994**, *91*, 11757–11761. [CrossRef] [PubMed]
57. Kitiratschky, V.B.D.; Behnen, P.; Kellner, U.; Heckenlively, J.R.; Zrenner, E.; Jägle, H.; Kohl, S.; Wissinger, B.; Koch, K.-W. Mutations in the *GUCA1A* Gene Involved in Hereditary Cone Dystrophies Impair Calciummediated Regulation of Guanylate Cyclase. *Hum. Mutat.* **2009**, *30*, E782–E796. [CrossRef] [PubMed]
58. Baehr, W.; Karan, S.; Maeda, T.; Luo, D.-G.; Li, S.; Bronson, J.D.; Watt, C.B.; Yau, K.-W.; Frederick, J.M.; Palczewski, K. The Function of Guanylate Cyclase 1 and Guanylate Cyclase 2 in Rod and Cone Photoreceptors. *J. Biol. Chem.* **2007**, *282*, 8837–8847. [CrossRef]

diversity

MDPI

Article

Mitogenomics and the Phylogeny of Mantis Shrimps (Crustacea: Stomatopoda)

Cassandra Koga * and Greg W. Rouse *

Scripps Institution of Oceanography, University of California San Diego, La Jolla, CA 92093-0202, USA
* Correspondence: ckoga@ucsd.edu (C.K.); grouse@ucsd.edu (G.W.R.)

Abstract: Stomatopoda, commonly known as mantis shrimps, are notable for their enlarged second maxillipeds encompassing the raptorial claw. The form of the claw can be used to divide them into two basic groups: smashers and spearers. Previous phylogenetic studies of Stomatopoda have focused on morphology or a few genes, though there have been whole mitochondrial genomes published for 15 members of Stomatopoda. However, the sampling has been somewhat limited with key taxa not included. Here, nine additional stomatopod mitochondrial genomes were generated and combined with the other available mitogenomes for a phylogenetic analysis. We used the 13 protein coding genes, as well as 12S rRNA, 16S rRNA genes, and included nuclear 18S rRNA gene sequences. Different rooting options were used for the analyses: (1) single and multiple outgroups from various eumalocostracan relatives and (2) a stomatopod-only dataset, with *Hemisquilla californiensis* used to root the topologies, based on the current hypothesis that *Hemisquilla* is the sister group to the rest of Stomatopoda. The eumalocostracan-rooted analyses all showed *H. californiensis* nested within Stomatopoda, raising doubts as to previous hypotheses as to its placement. Allowing for the rooting difference, the *H. californiensis* outgroup datasets had the same tree topology as the eumalocostracan outgroup datasets with slight variation at poorly supported nodes. Of the major taxonomic groupings sampled to date, Squilloidea was generally found to be monophyletic while Gonodactyloidea was not. The position of *H. californiensis* was found inside its superfamily, Gonodactyloidea, and grouped in a weakly supported clade containing *Odontodactylus havanensis* and *Lysiosquillina maculata* for the eumalocostracan-rooted datasets. An ancestral state reconstruction was performed on the raptorial claw form and provides support that spearing is the ancestral state for extant Stomatopoda, with smashing evolving subsequently one or more times.

Keywords: mitochondrial genome; molecular phylogeny; gene order

Citation: Koga, C.; Rouse, G.W. Mitogenomics and the Phylogeny of Mantis Shrimps (Crustacea: Stomatopoda). *Diversity* **2021**, *13*, 647. https://doi.org/10.3390/d13120647

Academic Editor: Bert W. Hoeksema

Received: 2 September 2021
Accepted: 1 December 2021
Published: 5 December 2021

1. Introduction

Mantis shrimps (Stomatopoda Latreille, 1817) [1] are marine crustaceans well known for their feeding mechanism and complex eyes. Stomatopods construct or occupy burrows and mainly occur in tropical and subtropical regions [2]. These marine carnivores capture prey by spearing or smashing depending on their distinctive second maxilliped appendages, the raptorial claws [3] (Figure 1). Smashers strike with the heel of the dactyl (calcified tip of the claw shaped like a club) after energy is loaded in a saddle spring mechanism [4]. This allows the claw to strike hard-shelled prey. Spearers are ambush predators with elongated serrated raptorial claws enhanced for soft-bodied prey [5]. In addition to their claws, mantis shrimps are of research interest for their complex visual system due to their compound eyes with around 12–16 photoreceptors, capable of seeing ultraviolet, linear, and circular polarized light [6,7]. Stomatopods have many important roles including used as food, as bioindicators of pollution, and their role as predators in marine ecosystems [8–13].

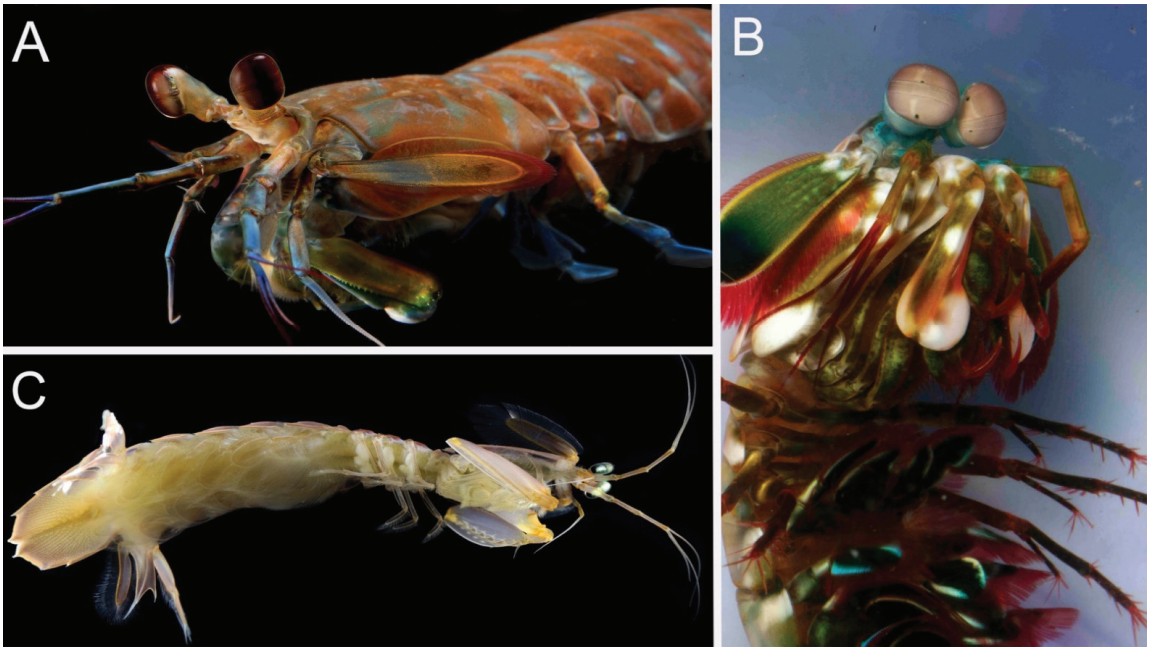

Figure 1. Photographs of Stomatopoda showing the range of raptorial claws. (**A**) 'Intermediate' claw form: *Hemisquilla californiensis* from California. (**B**) Smasher: *Odontodactylus scyllarus* from New Guinea (not used in this study). (**C**) Spearer: *Squilla biformis* from off Pacific Costa Rica.

Within Stomatopoda, the suborder Unipeltata Latreille, 1825 [14] contains all extant stomatopods, while the other two suborders are for extinct taxa, Palaeostomatopodea and Archaeostomatopodea [15,16]. Unipeltata contains 7 superfamilies, 17 families, and over 100 genera, and nearly 500 accepted species [17,18]: Squilloidea Latreille, 1802 [19]; Gonodactyloidea Giesbrecht, 1910 [20]; Lysiosquilloidea Giesbrecht, 1910 [20]; Bathysquilloidea Manning, 1967 [21]; Eurysquilloidea Manning, 1977 [22]; Erythrosquilloidea Manning & Bruce, 1984 [23]; and Parasquilloidea Manning, 1995 [24]. Most mantis shrimp species are contained within Squilloidea, Gonodactyloidea, and Lysioquilloidea [25].

One of the more speciose superfamilies, Gonodactyloidea, contains the only four families of smashers out of all the superfamilies, as well as some taxa with spearers. The rest of the stomatopod superfamilies consist only of spearers. Gonodactyloidea has been found to be non-monophyletic in previous molecular studies, owing mainly to the position of the 'intermediate' raptorial claw family, Hemisquillidae Manning, 1980 [26]. Morphological data supports Hemisquillidae as a member of Gonodactyloidea [3,17]; however, previous molecular phylogenetic studies that combined mitochondrial and nuclear genes have recovered it as a sister group to all other superfamilies [18,25,27]. Pseudosquillidae Manning, 1977 [22], one of the families of spearers in Gonodactyloidea, also has an unclear position. Some molecular phylogenetic results show Pseudosquillidae to be outside of the rest of the superfamilies, including Gonodactyloidea [25,27], while Van Der Wal et al. [18] showed Pseudosquillidae within Gonodactyloidea. To date, no studies have resolved the potential non-monophyly of Gonodactyloidea regarding the positions of Hemisquillidae and Pseudosquillidae.

Inferring the evolutionary history of smashers and spearers and whether smashers and spearers diverged early [17,25], or whether smashers evolved from a lineage of spearers [3,28] continues to be a topic of study. The results of morphology-based phylogeny by Ahyong and Harling [17] led them to suggest an early divergence of spearing and smashing clades, yet the position of Hemisquillidae and Pseudosquillidae complicates this

hypothesis. The molecular phylogenies of Ahyong and Jarman [25] and Porter et al. [27] show a single origin of smashing forms, though the positions of Hemisquillidae and Pseudosquillidae suggest spearing may be plesiomorphic for Stomatopoda. The results of the most recent broadscale phylogenetic analysis by Van Der Wal et al. [18] show smashers nested deeply among spearers with a reversal to spearing in Pseudosquillidae. However, they lacked support for key nodes concerning the origin for smashing and spearing nodes in their phylogeny, meaning the evolution of the raptorial claws is still in question [18].

As next-generation sequencing (NGS) technology, such as genome skimming (shallow, low pass sequencing), becomes more accessible, studies using whole mitochondrial genomes in their phylogenies have had better resolution and support compared to those of analyses with partial mitogenomic data [29–32]. To date, 15 complete mitogenomes of Stomatopoda have been published, though phylogenetic studies [33–36] have used only a proportion of these. The study by Yang et al. [36] used the most, with 13 stomatopod mitogenomes and rooted their analysis with Penaeidae Rafinesque, 1815 [37] (Decapoda). They showed a grade of spearing forms relative to a clade of smashers within Gonodactyloidea and overall support values were better than those shown in Van Der Wal et al. [18]. However, more taxon sampling is needed and particularly important is the absence to date of mitogenomic data for Hemisquillidae. Here, we present nine newly sequenced mantis shrimp mitochondrial genomes, including a member of Hemisquillidae. We combine this data with the 15 other available stomatopod mitogenomes and available nuclear 18S rRNA gene data to assess the phylogeny of Stomatopoda and the placement of Hemisquillidae.

2. Materials and Methods

2.1. Sampling

Samples were collected from the field or from commercial aquarium suppliers (Table 1). Voucher specimens were fixed and preserved in 50% ethanol and deposited at the Scripps Institution of Oceanography, Benthic Invertebrate Collection, La Jolla, California, USA. Identification was determined by morphology based on the keys of Manning [38] for SIO-BIC C14383 *Mesacturoides brevisquamatus* Paulson, 1875 [39], and Ahyong [40] for SIO-BIC C12730 *Gonodactylus* sp. and SIO-BIC C12514 *Gonodactylellus* sp. Mitochondrial COI sequences were also used in assessing the identification of some specimens.

2.2. DNA Extraction and Sequencing

DNA was extracted from claws, pleopods, and/or pereiopods using the Zymo Quick-DNA Miniprep plus kit, following the manufacturer's protocol. A fragment of the mitochondrial COI gene was amplified using LCO1490(f) and HCO2198(r) primers [41]. Samples were prepared with 8.5 µL of water, 12.5 µL of Apex 2X Taq RED Master Mix DNA polymerase (Genesee Scientific), 1 µL each of forward and reverse primers, and 2.0 µL of extracted DNA from specimens. The Eppendorf thermocycler was used to carry out the rest of the PCR with the temperature settings at: 94 °C/3 min.; (94 °C/30 s, 47 °C/45 s, 72 °C/1 min, 94 °C/30 s, 52 °C/45 s, 72 °C/1 min) x35 cycles, 72 °C/5 min. Products were purified with 2 µL of ExoSAP-IT and run in a thermocycler with the settings: 37 °C/20 min and 80 °C/15 min. Sanger sequencing was completed by Eurofins Genomics (Louisville, KY, USA). COI sequences obtained from Sanger sequencing for six of the nine taxa studied here are provided in Table 1 with separate accession numbers.

2.3. Mitochondrial Genome Assembly and Annotation

Extracted DNA was prepared and sequenced by Novogene (Sacramento, CA, USA) using genome skimming, generating 2 Gb worth of reads. Data statistics were checked with SeqKit v.0.13.2 [42] and the raw reads were trimmed with Trimmomatic v. 0.39 [43]. The mitochondrial genomes were assembled with Mitofinder v. 1.4 [44] using the Trimmomatic output files. Parameters chosen were Megahit metagenomic assembler v. 1.2.9 [45] and tRNAs were annotated with Arwen v.1.2.3 [46]. The Mitofinder contigs were checked with

MITOS [47] web server under the mitochondrial code for invertebrates and the annotations were manually edited in Geneious v 11.1.5 [48] if necessary to reflect accurate positions.

Table 1. Collection information, vouchers, GenBank accession numbers (COI, mitogenome, 18S rRNA), and mitogenome length. New COI sequences and mitogenomes are in bold.

Taxon	SIO-BIC Catalog Number	Locality	COI Accession Number	Mitogenome Accession Number	18S rRNA Accession Number	Mitogenome Length
Gonodactyloidea Hemisquillidae ***Hemisquilla californiensis*** Stephenson, 1967 [49]	C14449	California	**MZ742104**	**MW867302**	HM138876	**16,030**
Odontodactylidae ***Odontodactylus havanensis*** Bigelow, 1893 [50]	C14408	Florida		**MW867300**	HM138884	**16,035**
Gonodactylidae ***Neogonodactylus oerstedii*** Hansen, 1895 [51]	C14405	Florida		**MW867303**	HM138882	**16,327**
Neogonodactylus bredini Manning, 1969 [52]	C14428	Florida	**MZ742108**	**MW867301**	HM138881	**16,342**
Gonodactylus smithii Pocock, 1893 [53]		-		MW574903	HM138873	16,260
Gonodactylus chiragra Fabricius, 1781 [54]		-		DQ191682	HM138870	16,279
Gonodactylaceus randalli Manning, 1978 [55]		-		MW019425	-	15,907
Gonodactylus sp.	C12730	Red Sea	**MZ742105**	**MW867306**	-	**16,032**
Gonodactylellus sp.	C12514	Red Sea	**MZ742107**	**MW867308**	-	**16,011**
Takuidae ***Mesacturoides brevisquamatus***	C14383	Red Sea	**MZ742109**	**MW867304**	-	**16,151**
Taku spinosocarinatus Fukuda, 1909 [56]		-		MT672285	HM138899	15,960
Pseudosquillidae *Pseudosquilla ciliata* Fabricius, 1787 [57]		-		AY947836	HM138888	14,621 (incomp.)
Protosquillidae *Chorisquilla orientalis* Hwang et al., 2018 [58]		-		MT672286	-	15,880
Squilloidea Squillidae *Oratosquilla oratoria* De Haan, 1844 [59]		-		GQ292769	-	15,783
Squilla mantis Linnaeus, 1758 [60]		-		AY639936	GQ328958	15,994
Squilla empusa Say, 1818 [61]		-		DQ191684	HM138897	15,828
Squilla biformis Bigelow, 1891 [62]	C13808	Costa Rica		**MW867305**	-	**15,688**
Squilloides leptosquilla Brooks, 1886 [63]		-		KR095170	-	16,376
Harpiosquilla harpax De Haan, 1844 [59]		-		AY699271	-	15,714
Lophosquilla costata De Haan, 1844 [59]		-		MT276143	-	15,771
Alima pacifica Ahyong, 2001 [40]	C12719	Red Sea	**MZ742106**	**MW867307**	HM138858	**15,678**
Dictyosquilla foveolata Wood-Mason, 1895 [64]		-		MW864094	-	15,733
Lysiosquilloidea Lysiosquillidae *Lysiosquillina maculata* Fabricius, 1793 [65]		-		DQ191683	HM138878	16,325
Parasquilloidea Parasquillidae *Faughnia haani* Holthuis, 1959 [66]		-		MW632159	-	16,089
Outgroups Euphausiacea *Euphausia pacifica* Hansen, 1911 [67]		-		EU587005	AY141010	16,898
Mysida *Neomysis japonica* Nakazawa, 1910 [68]		-		KR006340	-	17,652
Isopoda *Cymothoa indica* Schioedte & Meinert, 1884 [69]		-		MH396438	-	14,475

2.4. Phylogenetic Analyses

Recent phylogenomic studies of Malacostraca have confirmed Stomatopoda as part of Eumalocostraca. It may either be the sister group to all other Eumalocostraca, or nested within [70,71]. Based on these studies, we chose as outgroups three other members of Eumalocostraca with relatively close phylogenetic proximity to Stomatopoda: *Euphausia pacifica* (Euphausiacea), *Cymothoa indica* (Isopoda), and *Neomysis japonica* (Mysida). These were aligned and analyzed with the stomatopod data. Further supplemental analyses were conducted using *Euphausia pacifica*, *Cymothoa indica,* and *Neomysis japonica* as individual outgroups. Stomatopod-only analyses were also performed with *Hemisquilla californiensis* chosen to root the trees, since previous works [18,25,27] placed *Hemisquilla* Hansen, 1895 [51] as a sister group to the rest of Stomatopoda. Datasets included the 13 mitochondrial protein coding genes plus the 12S rRNA and 16S rRNA genes, and nuclear 18S rRNA gene. The analyses were conducted with nucleotide-only sequences or as amino acid sequences of the 13 protein coding genes and nucleotide sequences of the 3 rRNA genes: (1) Eumalocostraca outgroups, nucleotide only (EumalNuc); (2) Eumalocostraca outgroups, amino acids and rRNAs (EumalAA); (3) *Hemisquilla californiensis* outgroup, nucleotide only (HemiNuc); and (4) *Hemisquilla californiensis* outgroup, amino acids and rRNAs (HemiAA); (5) *Euphausia pacifica*, *Cymothoa indica,* and *Neomysis japonica* as individual outgroups, amino acids, and rRNA genes (Supplementary Materials Figure S1). The 13 protein coding genes were translated to amino acids to mitigate saturation effects from the third codon position. The fraction of parsimony informative characters out of total characters for each dataset is shown in Supplementary Materials Table S1. The NADH6 nucleotide and amino acid data for *Chorisquilla orientalis* were excluded owing to poor alignment caused by possible contamination. To remove a four base pair insertion, 194 nucleotides were also removed starting at position 941 and on from the cytochrome b gene alignment of *Chorisquilla orientalis.* Gblocks v. 0.91b [72] was used to remove poorly aligned regions of the 3 rRNA genes with the least stringent settings. Sequences were aligned with MAFFT v. 7.475 [73] under the G-INSI-i method with 1000 iterations, with all three outgroups, each of the three outgroups separately or with members of Stomatopoda only.

Three phylogenetic analyses were performed on each dataset: maximum likelihood (ML), maximum parsimony (MP), and Bayesian inference (BI). The ML analyses were performed in the RaXML v. 2.0.5 [74] interface using RAxML-NG v. 1.0.1 [75]. Gene sequences were concatenated in RAxML-NG and partitioned with variations of the substitution models determined by ModelTest-NG v. 0.1.6 [76] (Supplementary Materials Table S2). The program parameters were set to ML + thorough bootstrap + consensus with 10 ML searches and 1,000 bootstrap pseudoreplicates for each dataset. Mesquite v. 3.61 [77] was used to concatenate the mixed amino acid and nucleotide datasets for the MP and BI analyses. For the MP analysis, heuristic searches of concatenated datasets were run in PAUP* v. 4.0a168 [78] with TBR branch swapping and 100 random addition replicates. Bootstrap values were gathered via 1000 pseudoreplicates. The BI analysis was conducted in MrBayes v. 3.2.7a [79]. The GTR + I + G model was applied for the nucleotide partitions except for GTR + G for the ND4L and 12S nucleotide partitions in the eumalocostracan outgroup analyses based on the models chosen with ModelTest-NG from the ML analyses. The WAG model was chosen for amino acid partitions in MrBayes. Parameters set for posterior distributions were under the Markov chain Monte Carlo (MCMC) sampling for multiple runs of 20,000,000 generations and 4 chains, with trees sampled every 1000 generations. The first 10% of the sampled trees were cut away as burn-in after examination of the likelihood scores using Tracer [80].

Approximately Unbiased (AU) tests [81] were performed to assess if one placement of *Hemisquilla californiensis* was significantly better than another in the phylogenetic results. A constraint tree was made with *H. californiensis* positioned as the sister to a clade of the rest of the stomatopods (as a polytomy), with the eumalocostracan outgroups. The best ML constrained tree topology was generated in RAxML-NG under the same settings as the best unconstrained tree. Whether the best unconstrained tree was significantly better than

the best constrained tree for the EumalAA and EumalNuc datasets was assessed via the AU test using the default settings in IQ tree v. 1.6.12 [82,83], partitioned as for the original ML analyses. Likelihood-based and most parsimonious ancestral reconstructions of the raptorial claw were mapped onto the Eumalocostrata outgroup EumalAA and EumalNuc ML tree topologies in Mesquite. For the likelihood ancestral state reconstruction, the Mk1 probability model was used. To assess variation in the ancestral state reconstruction owing to alternative tree topologies, 18,000 post-burnin trees from the EumalAA BI analysis were traced under the Mk1 probability model on the EumalAA ML tree topology using the 'Trace Character Over Trees' option in Mesquite. Raptorial claws are classified as spearers or smashers based on the shape of the dactyl. The states are as follows: 0: spearers, 1: smashers, and 2: no claw for the outgroup. *Hemisquilla californiensis* was scored as 0/1 (assigned either of these states, depending on the transformation used) since it is regarded as an intermediate form [3,84].

3. Results

The newly sequenced mitogenomes ranged in total length from 15,678 base pairs (*Alima pacifica*) to 16,342 base pairs (*Neogonodactylus bredini*). The usual 13 protein-coding, 2 rRNA and 22 tRNA genes were all present (Figure 2), and the length variation range fell within the range previously found in the complete mitogenomes of other Stomatopoda (Table 1). Most differences can be attributed to variation in the control region. For instance, in *Alima pacifica*, the control region was found to be 755 base pairs in length while in Neogonodactylus bredini, it was 1,407 base pairs long and this accounted for nearly all the length difference between the mitogenomes. There was otherwise minor variation in the rRNA and tRNA gene lengths. Gene order and direction were conserved among newly sequenced stomatopod genomes and all the available GenBank sequences for stomatopods (Figure 2).

Figure 2. Gene order arrangement of the mitochondrial genome for all stomatopod species used in this study. Blue boxes represent protein coding genes, orange boxes are rRNA genes, and green boxes are tRNA genes. The NAD1, NAD4, NAD4L, NAD5, rrnL, and rrnS genes were in the reverse direction and the rest were in the forward direction.

Figures 3 and 4 show the phylogenetic results produced from the analyses based on the four datasets, two with three outgroup taxa (Figure 3) and two with Stomatopoda only and rooted with *Hemisquilla* (Figure 4). The nucleotide datasets had similar tree topologies to their respective mixed amino acid and nucleotide datasets, albeit the mixed datasets had lower support than the nucleotide only datasets (Figures 3 and 4). Variations between datasets were due to a few nodes that had low support. The ML and BI trees were congruent in tree topology for the nucleotide only datasets but showed a few differing nodes in the mixed datasets. Incongruence with the ML, BI, and MP analyses occurred at the low supported nodes (Figures 3 and 4). Most differences between trees were from the MP analyses compared to the others. The root position was stable with the three outgroup analyses compared to rooting with individual outgroups (Figures 3 and S1).

There were recurring patterns in all the dataset analyses: Squilloidea was monophyletic and well supported as a spearing clade for three analyses (Figures 3A and 4), with the exception being the ML and BI analyses with the EumalAA dataset (Figures 3B and S1), where it formed a grade. There was high support for a clade of smashers within Gonodactyloidea containing members of Gonodactylidae Giesbrecht, 1910 [20], Protosquillidae Manning, 1980 [26], and Takuidae Manning, 1980 [26]. Gonodactyloidea, however, was non-monophyletic for all analyses (Figures 3, 4 and S1). In the Eumalocostraca-rooted analyses, Lysiosquilloidea and Parasquilloidea terminals nested inside Gonodactyloidea (Figures 3 and S1) and in the *Hemisquilla*-rooted analyses, Gonodactyloidea was also

paraphyletic (Figure 4). A clade containing *Hemisquilla californiensis*, *Odontodactylus havanensis*, and *Lysiosquillina maculata* was recovered for all Eumalocostraca outgroup analyses (Figures 3 and S1) and it was grouped with the remaining Gonodactyloidea. In the *H. californiensis* outgroup analyses, the tree topology was essentially the same as those rooted with Eumalocostraca. However, the alternative rooting resulted in *H. californiensis*, *O. havanensis*, and *L. maculata* forming a grade with respect to the rest of Stomatopoda (Figure 4). The nested position of *H. californiensis* within Stomatopoda, as shown in Figure 3, was tested against the constrained tree with *H. californiensis* as the sister group to Stomatopoda, as in Figure 4, using AU tests. The unconstrained ML tree was significantly better in the EumalNuc dataset ($p = 0.0001$), though for the EumalAA dataset, the two topologies were not significantly different ($p = 0.128$).

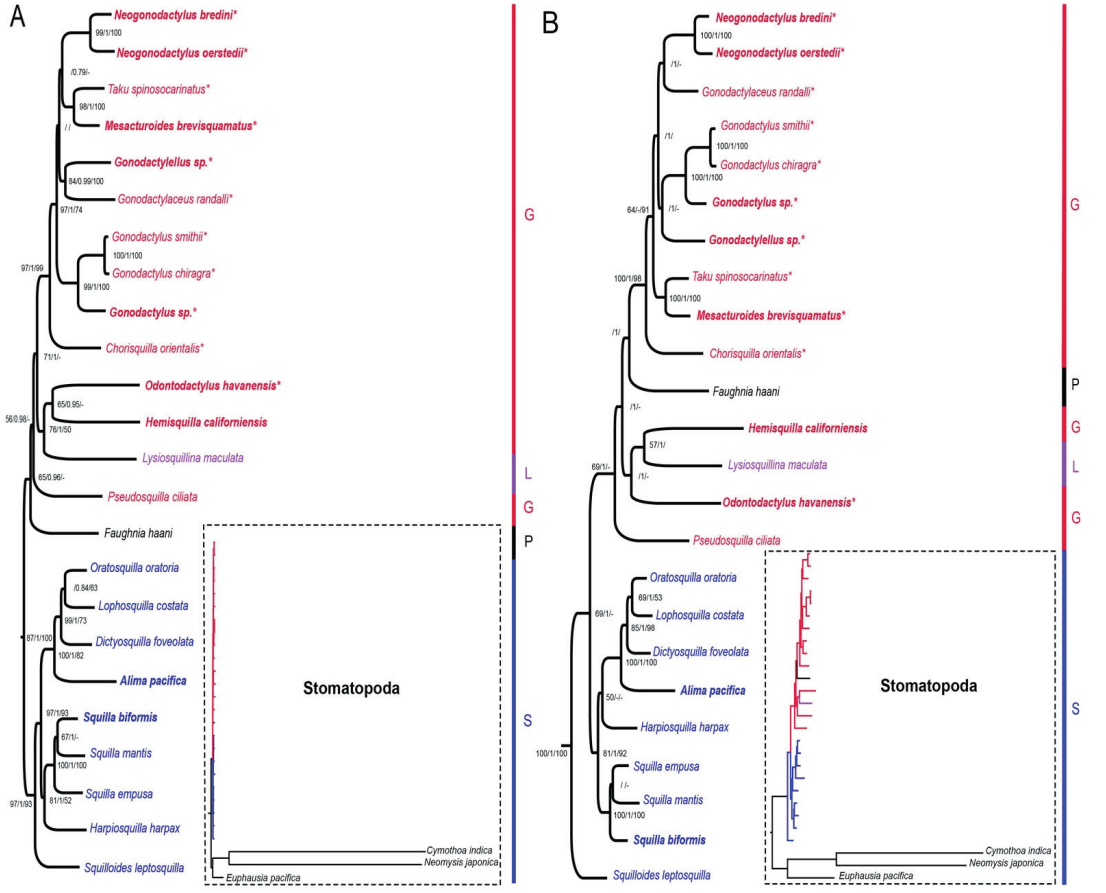

Figure 3. Stomatopoda phylogeny based on the concatenated mitochondrial genes and 18S rRNA sequences; rooted with *Euphausia pacifica*, *Cymothoa indica*, and *Neomysis japonica* (not shown in main figures, they are indicated in the dotted boxes). Newly sequenced taxa are in bold. Each superfamily is coded by the color of the taxon name. Superfamily abbreviations are G: Gonodactyloidea, L: Lysiosquilloidea, S: Squilloidea, P: Parasquilloidea. Asterisks (*) after the taxon name denote smashers. Values at the nodes represent the bootstrap values of ML and MP and the posterior probability of BI in the format (ML/BI/MP). Values not listed were below 50 for bootstrap or below 0.70 for posterior probabilities. Hyphens (-) represent nodes not recovered by the MP or BI analyses. Branch lengths relative to the outgroups are shown in the dotted boxes to the right of each main figure. (**A**) Maximum likelihood tree from the nucleotide dataset (EumalNuc). (**B**) Maximum likelihood tree from the mixed amino acid and nucleotide dataset (EumalAA).

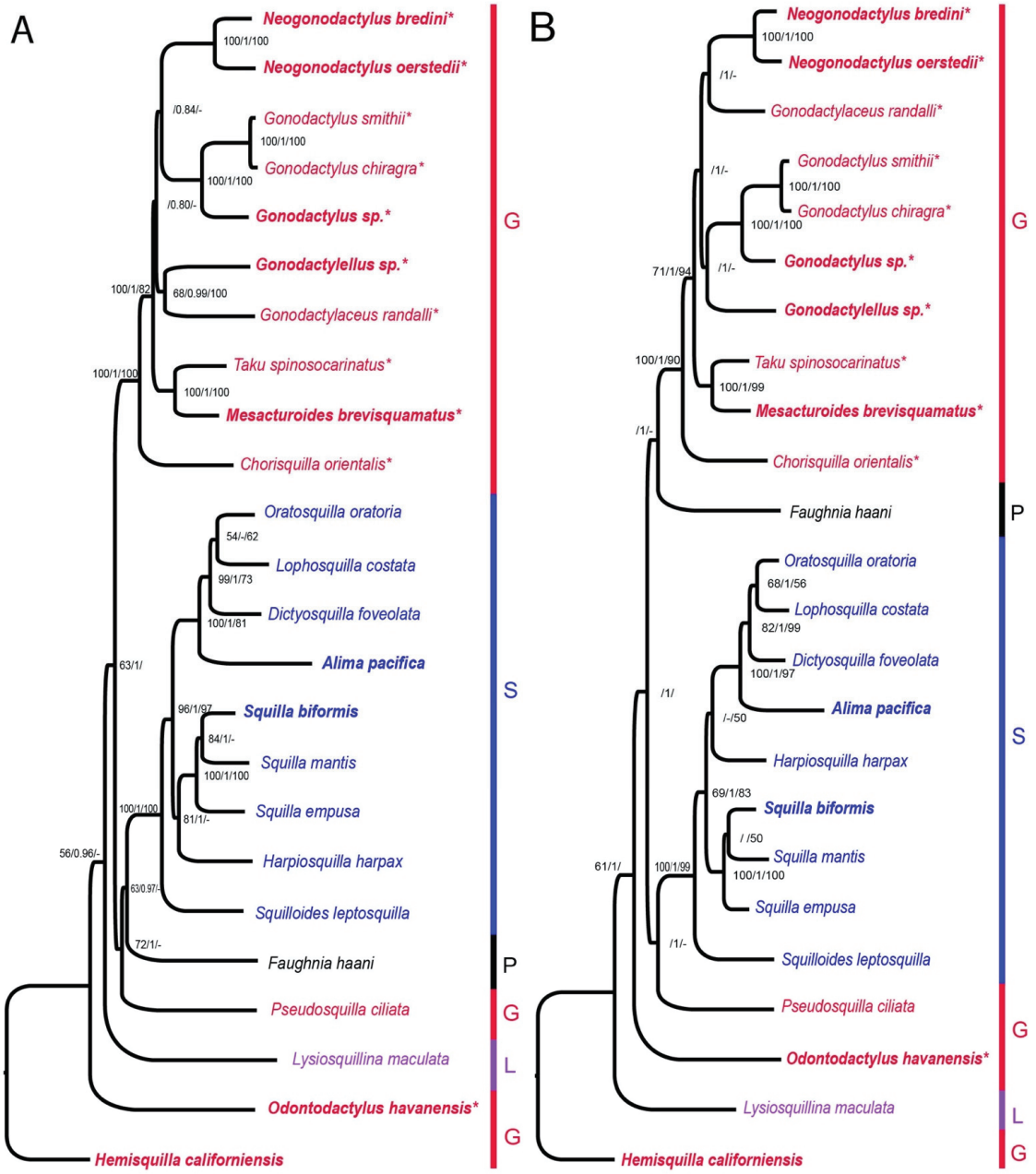

Figure 4. Stomatopoda phylogeny based on the concatenated mitochondrial genes and 18S rRNA sequences; rooted with *Hemisquilla californiensis*. (**A**) Maximum likelihood tree from the nucleotide dataset (HemiNuc). (**B**) Maximum likelihood tree from the mixed amino acid and nucleotide dataset (HemiAA). Newly sequenced species are in bold. Each superfamily is coded by color of the taxon name. Superfamily abbreviations are G: Gonodactyloidea, L: Lysiosquilloidea, S: Squilloidea, P: Parasquilloidea. Asterisks (*) after the taxon name denote smashers. Values at the nodes represent the bootstrap values of ML and MP and the posterior probability of BI in the format (ML/BI/MP). Values not listed were below 50 for bootstrap or below 0.70 for posterior probabilities. Hyphens (-) represent nodes not recovered by the MP or BI analyses.

The EumalNuc and EumalAA ML tree topologies (Figure 3) were each used for illustrating the ancestral state reconstruction of raptorial claws in Stomatopoda since the tree topologies varied slightly. The Mk1 likelihood ancestral state reconstruction found a proportional likelihood greater that 0.95 for spearers at the ancestral node for Stomatopoda (Figures 5A and 6A). Smashing would appear to have evolved twice at least within Gonodactyloidea. There were three most parsimonious reconstructions (MPRs) for this character in the EumalNuc ML tree, resulting in several scenarios for the raptorial claw evolution, though in all cases spearing was plesiomorphic for Stomatopoda: (1) two origins of smashing, one for *O. havanensis* and the other for the clade of smashers in Gonodactyloidea, with *H. californiensis* optimized as a spearer (Figure 5B); (2) one origin of smashing with a reversal to spearing for *Lysiosquillina maculata* (Figure 5C); and (3) two origins of smashing, one in the clade of *Hemisquilla californiensis* + *Odontodactylus havanensis*), and for the clade of smashers in Gonodactyloidea, with *H. californiensis* optimized as a smasher (Figure 5D). The EumalAA ML tree topology showed a single MPR that essentially matched the scenario in Figure 5B, with two origins of smashing from spearing. One origin was for *O. havanensis* and the other for the clade of smashers in Gonodactyloidea, with *H. californiensis* optimized as a spearer. Exploration of the effect of suboptimal tree topologies on the ancestral state reconstruction for raptorial claws is summarized in Figure 6C. Here 18,000 post-burnin trees from the EumalAA BI analysis were traced under the Mk1 probability model on the EumalAA ML tree topology (Figure 4A) using the Trace Character Over Trees option in Mesquite. There was some incongruity between the BI analysis and the ML tree, largely in the nodes of Squilloidea (Figure 4A). This is reflected in the summary tree, where two nodes were often absent in the 18,000 post-burnin trees. However, the overall implications for the ancestral state reconstruction of raptorial claws in Stomatopoda were consistent across the 18,000 post-burnin trees (Figure 6C). This supports the transformations shown in Figures 5A and 6A and suggests an ancestral state of spearing for Stomatopoda with one to three transformations to smashing.

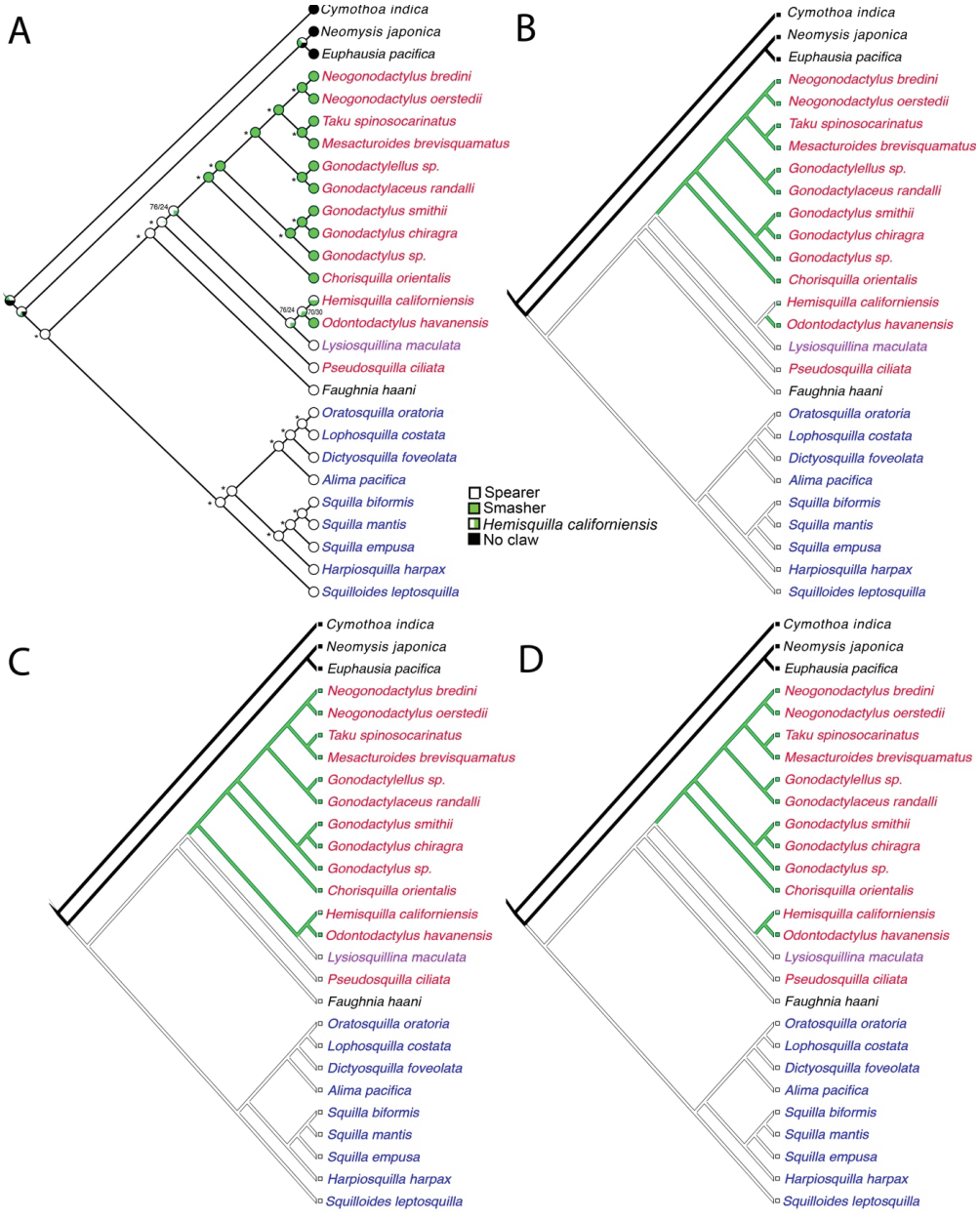

Figure 5. Ancestral state reconstruction, using Mesquite, of the raptorial claws mapped onto the Eumalocostraca outgroup maximum likelihood tree for the EumalNuc dataset. (**A**) Maximum likelihood reconstruction. Asterisks represent nodes with proportional likelihood estimations of >95%. Other scores for the ingroup are provided in order of most likely states and separated with a forward slash. (**B**–**D**) The three most parsimonious reconstructions. Coloring of terminal names as in Figures 2 and 3. *Hemisquilla californiensis* was coded as either spearer or smasher.

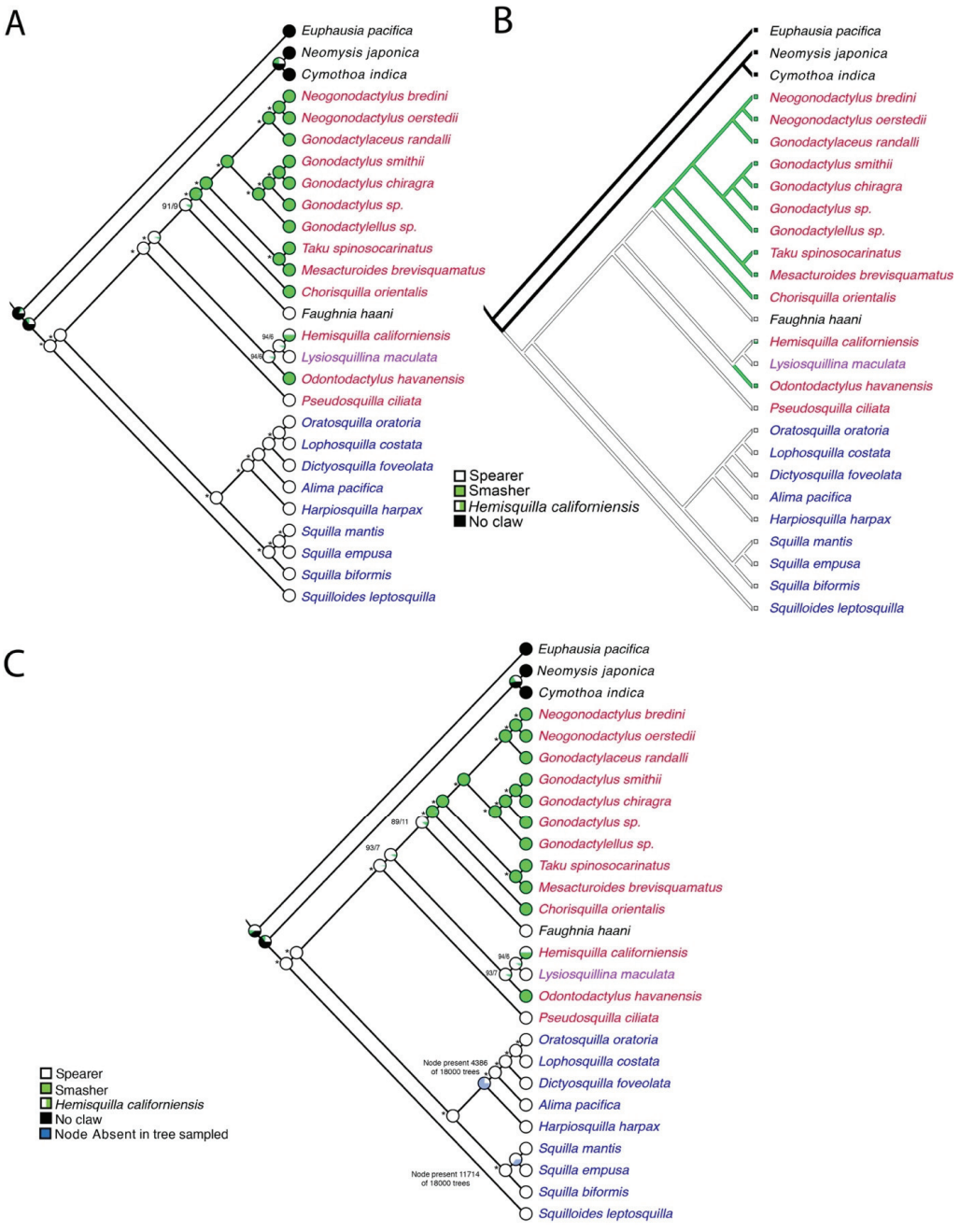

Figure 6. Ancestral state reconstruction, using Mesquite, of the raptorial claws mapped onto the Eumalocostraca outgroup maximum likelihood tree for the EumalAA dataset. (**A**) Maximum likelihood reconstruction. Asterisks represent nodes with proportional likelihood estimations of >95%. Other scores for the ingroup are provided in order of most likely states and separated with a forward slash. (**B**) The single most parsimonious reconstruction for this topology. Coloring of terminal names as in Figures 2 and 3. *Hemisquilla californiensis* was coded as either spearer or smasher. (**C**) 'Trace Character Over Trees' summary of ancestral state reconstructions over 18,000 post-burnin trees from the EumalAA BI analysis, traced under the Mk1 probability model on the EumalAA ML tree topology.

4. Discussion

This study provided the first mitogenome phylogenetic analyses of Stomatopoda containing *Hemisquilla californiensis*, a member of Hemisquillidae, which has been proposed to have an 'intermediate' claw form [3,84]. Furthermore, eight other new stomatopod mitochondrial genomes were also sequenced. Hemisquillidae has been inferred to be the sister group to all other extant stomatopods in recent molecular phylogenetic analyses, and this has led to proposals that its claw form represents the ancestral state [18,27], yet support for this hypothesis appears to be weak (see below). However, all the analyses shown here that were rooted with other Eumalocostraca recovered *H. californiensis* nested within a paraphyletic Gonodactyloidea (Figures 3 and S1). The results shown in Figure 3 are somewhat like the findings of Barber and Erdmann [85], where Hemisquillidae grouped with Odontodactylidae Manning, 1980 [26], although they only used one mitochondrial gene in that study. The results of our study were significantly better (AU test results) with the EumalNuc dataset (Figure 3A) than the phylogenetic hypotheses of the two most recent comprehensive previous studies [18,27]. However, the EumalAA ML result (Figure 3B) was not significantly better. Additionally, several key nodes in both analyses summarized in Figure 3 showed low support, suggesting that mitochondrial genomes do not have the phylogenetic signal to resolve the overall phylogeny of Stomatopoda.

Other results found here also conflicted with recent molecular phylogenetics analyses of Stomatopoda in other ways. For instance, the Eumalocostraca-rooted ML analyses (Figures 3 and S1) resulted in a near monophyletic Gonodactyloidea, except for *Lysiosquillina* Manning, 1995 [24] or *Lysiosquillina* and *Faughnia haani***.** In the EumalNuc analyses, *Pseudosquilla* Dana, 1852 [86], the only member of Pseudosquillidae in this study, was the sister group to *Lysiosquillina* plus all the other terminals of Gonodactyloidea (Figure 3A). In the amino acid analyses, it had a similar position, though *Faughnia haani* (Parasquillidae) also made Gonodactyloidea paraphyletic. These results contrasted with some previous studies [25,27], where Pseudosquillidae was quite distant from the smashing members of Gonodactyloidea. It also differed from the results of Van Der Wal et al. [18], where Pseudosquillidae, a group of spearing stomatopods, was nested within the smashing forms of Gonodactyloidea, implying a reversal from smashing to spearing. In contrast, our results showed a highly supported clade of smashing taxa comprising members of the families Gonodactylidae, Takuidae, and Protosquillidae (Figures 3, 4 and S1). A clade of spearing taxa, Squilloidea, was recovered consistently as well supported in the nucleotide analyses (Figures 3A and 4), congruent with other studies [18,33–36]. However, the various Eumalocostraca-rooted mixed amino acid nucleotide analyses recovered Squilloidea as a grade (Figures 3B and S1) and the position of *Squilloides leptosquilla* deserves further investigation.

The previous studies that conflict with the results shown here [18,25,27] were the most comprehensive molecular phylogenetic analyses of Stomatopoda until now, but each relied on only a few mitochondrial genes and the nuclear genes 18S rRNA and 28S rRNA, far less data than was used here. The study by Porter et al. [27] showed support values based on approximate likelihood ration tests instead of the bootstrap and posterior probability support values used in other studies on Stomatopoda and in this study. This makes direct comparisons of support difficult. However, the datasets used in Porter et al. [27] and Van der Wal et al. [18] were similar in terms of the genes used and taxon sampling. The values shown by Porter et al. [27] were inferred by those authors to reflect high support, but they contrast markedly with Van der Wal et al. [18], where most major nodes showed very low bootstrap and posterior probability values.

One of the charismatic features of mantis shrimps is the raptorial claws that are used to informally group species into smashers and spearers based on morphology and the way they strike. The evolution and diversification of this raptorial claw form has been a subject of much discussion. Our ancestral state reconstruction of the raptorial claw evolution in Stomatopoda using the Eumalocostraca-rooted datasets (Figures 5 and 6) showed unequivocally that spearing is the ancestral state for extant Stomatopoda. This

corroborates the views of Caldwell [28] and Ahyong [3] but contrasts markedly with to the findings of Ahyong and Harling [17] and Van Der Wal et al. [18]. The position of *Hemisquilla californiensis* within Gonodactyloidea (Figures 3 and 5) contradicts theories of a *Hemisquilla*-like ancestor having an 'intermediate' claw form [18]. Hemisquillidae can strike with either a closed and open dactyl [25,87] and so either spear or smash their prey. The most parsimonious reconstructions of this character transformation allow for some lability in the evolution of smashing and spearing (Figures 5B–D and 6B) and it is not clear what the original state for the ancestor for Hemisquillidae was. Spearing and smashing are more of a continuum and not binary states and deVries et al. [88] and deVries [89] confirm spearers and smashers can eat hard- and soft-bodied prey and have a more generalist diet than thought before.

5. Conclusions

This study added nine complete mitochondrial genomes to the 15 available stomatopod mitogenomes, bringing the total to 24. The new mitogenomes came from the large superfamilies Gonodactyloidea and Squilloidea, and *Hemisquilla californiensis*, which is in the key taxon Hemisquillidae. The gene order and direction were found to be highly conserved across Stomatopoda and followed the Crustacea ancestral state gene order [90,91]. The new sequences were combined with available mantis shrimp mitogenomes and 18S nuclear gene data to allow for further assessment of the phylogeny of Stomatopoda. When non-stomatopod outgroups were used, in combination and singly, Hemisquillidae was found in a relatively derived position instead of being the sister group to all Stomatopoda, as proposed in previous molecular studies. The tree topologies were identical with Stomatopoda-only analyses, which were done here to allow for rooting with Hemisquillidae. The results suggest that the placement of Hemisquillidae as the sister group to Stomatopoda can be seriously questioned. From the outgroup-rooted phylogenies, the ancestral state was inferred to be spearing with several scenarios for the origin or even loss of smashing. Despite showing better support than in previous molecular systematics analysis of Stomatopoda, the results showed several poorly supported nodes. Mitochondrial genomes therefore, do not appear to provide the signal required for the overall phylogeny of Stomatopoda, but will likely be useful for more restricted analyses within the clade.

Supplementary Materials: The following are available online at https://www.mdpi.com/article/10.3390/d13120647/s1, Table S1: Fraction of parsimony informative characters out of the total characters for each gene, Table S2: Models used for each gene in the datasets for maximum likelihood analyses. Figure S1: Maximum likelihood tree topologies from the mixed amino acid and nucleotide dataset analyzed with three different outgroups from Eumalocostraca.

Author Contributions: Conceptualization and resources G.W.R.; formal analysis and data curation, C.K. and G.W.R.; writing—original draft preparation, C.K.; writing—review and editing, C.K. and G.W.R.; supervision, G.W.R. All authors have read and agreed to the published version of the manuscript.

Funding: The collection of *Squilla biformis* was funded by USA National Science Foundation (NSF) grant number OCE-1634172.

Institutional Review Board Statement: Ethical review and approval were waived for this study, due to Stomatopoda not requiring approval for study.

Informed Consent Statement: Not applicable.

Data Availability Statement: All mitogenomes and Sanger-sequencing data is publicly available on GenBank (www.ncbi.nlm.nih.gov, accessed on 30 November 2021).

Acknowledgments: We thank Mary 'Dewy' White for being the inspiration behind the project. We are also grateful to Phil Zerofski for the collection of *Hemisquilla californiensis* from California. The specimen of *Squilla biformis* was collected under a permit issued by the Ministerio de Ambiente y Energía of Costa Rica (Sistema Nacional de Áreas de Conservación/Comisión Nacional para la

Gestión de la Biodiversidad) for granting a collection permit (SINAC-SE-064-2018). Thanks also to the captain, crew, science party, *Alvin* team on RV *Atlantis* AT42-03 for collecting this specimen. The stomatopods from Saudi Arabia were collected thanks to an invitation to GWR by Tim Ravasi and King Abdullah University of Science and Technology. Thank you to Avery Hiley and Marina McCowin for their support in mentoring and preparing DNA extractions. Thank you to Charlotte Seid for cataloging the specimens into SIO-BIC. We also thank the four anonymous reviewers for their helpful and constructive comments.

Conflicts of Interest: The authors declare no conflict of interest.

References

1. Latreille, P.A. Les Crustacés, Les Arachnides et Les Insectes. In *La Regne Animal Distribue d'Apres son Organisation, pour Servir de Base a l'Histoire Naturelle des Animaux et d'Introduction a l'Anatomie Compare*; Chez Déterville: Paris, France, 1817; Volume 3, pp. 1–653.
2. Caldwell, R.L.; Dingle, H. Ecology and evolution of agonistic behavior in stomatopods. *Naturwissenschaften* **1975**, *62*, 214–222. [CrossRef]
3. Ahyong, S.T. Phylogenetic Analysis of the Stomatopoda (Malacostraca). *J. Crustacean Biol.* **1997**, *17*, 695–715. [CrossRef]
4. Patek, S.N.; Korff, W.L.; Caldwell, R.L. Deadly strike mechanism of a mantis shrimp. *Nature* **2004**, *428*, 819–820. [CrossRef]
5. DeVries, M.S.; Murphy, E.A.K.; Patek, S.N. Strike mechanics of an ambush predator: The spearing mantis shrimp. *J. Exp. Biol.* **2012**, *215*, 4374–4384. [CrossRef]
6. Marshall, N.J. A unique colour and polarization vision system in mantis shrimps. *Nature* **1988**, *333*, 557–560. [CrossRef]
7. Thoen, H.H.; How, M.J.; Chiou, T.H.; Marshall, J. A Different Form of Color Vision in Mantis Shrimp. *Science* **2014**, *343*, 411–413. [CrossRef]
8. Sukumaran, K.K. Study on the fishery and biology of the mantis shrimp *Oratosquilla nepa* (Latreille) of south Kanara coast during 1979–1983. *Indian J. Fish.* **1987**, *34*, 292–305.
9. Abelló, P.; Martín, P. Fishery dynamics of the mantis shrimp Squilla mantis (Crustacea: Stomatopoda) population off the Ebro delta (northwestern Mediterranean). *Fish. Res.* **1993**, *16*, 131–145. [CrossRef]
10. Erdmann, M.V.; Caldwell, R.L. Stomatopod crustaceans as bioindicators of marine pollution stress on coral reefs. In Proceedings of the Eighth International Coral Reef Symposium, Panama City, Panama, 24–29 June 1996; Smithsonian Tropical Research Institute: Panama City, Panama, 1997; Volume 2, pp. 1521–1526.
11. Kodama, K.; Shimizu, T.; Yamakawa, T.; Aoki, I. Changes in reproductive patterns in relation to decline in stock abundance of the Japanese mantis shrimp *Oratosquilla oratoria* in Tokyo Bay. *Fish. Sci.* **2006**, *72*, 568–577. [CrossRef]
12. Ng, J.S.S.; Lui, K.K.Y.; Lai, C.-H.; Leung, K.M.Y. *Harpiosquilla harpax* (Crustacea, Stomatopoda) as a biomonitor of trace metal contamination in benthic sediments in Hong Kong waters. *Mar. Pollut. Bull.* **2007**, *54*, 1523–1529. [CrossRef]
13. Antony, P.J.; Dhanya, S.; Lyla, P.S.; Kurup, B.M.; Ajmal Khan, S. Ecological role of stomatopods (mantis shrimps) and potential impacts of trawling in a marine ecosystem of the southeast coast of India. *Ecol. Modell.* **2010**, *221*, 2604–2614. [CrossRef]
14. Latreille, P.A. *Familles Naturelles Du Règne Animal: Exposées Succinctement et Dans Un Ordre Analytique, Avec Lindication de Leurs Genres*; J.-B. Baillière: Paris, France, 1825; p. 283.
15. Schram, F.R. Paleozoic proto-mantis shrimp revisited. *J. Paleontol.* **2007**, *81*, 895–916. [CrossRef]
16. Haug, J.T.; Haug, C.; Maas, A.; Kutschera, V.; Waloszek, D. Evolution of mantis shrimps (Stomatopoda, Malacostraca) in the light of new Mesozoic fossils. *BMC Evol. Biol.* **2010**, *10*, 290. [CrossRef]
17. Ahyong, S.T.; Harling, C. The phylogeny of the stomatopod Crustacea. *Aust. J. Zool.* **2000**, *48*, 607–642. [CrossRef]
18. Van Der Wal, C.; Ahyong, S.T.; Ho, S.Y.W.; Lo, N. The evolutionary history of Stomatopoda (Crustacea: Malacostraca) inferred from molecular data. *PeerJ* **2017**, *5*, e3844. [CrossRef]
19. Latreille, P.A. *Histoire Naturelle, Générale et Particulière des Crustacés et des Insectes: Ouvrage Faisant Suite aux Owuvres de Leclerc de Buffon, et Partie du Cours Complet d'Histoire Naturelle Rédigé par C. S. Sonnini, Membre de Plusieurs Sociétés Savantes*; Dufart: Paris, France, 1802; p. 56.
20. Giesbrecht, W. Stomatopoden. *Erster Theil. Fauna Flora Golf. Neapel* **1910**, *33*, 1–239.
21. Manning, R.B. Preliminary account of a new genus and a new family of Stomatopoda. *Crustaceana* **1967**, *13*, 238–239. [CrossRef]
22. Manning, R.B. *A Monograph of the West African Stomatopod Crustacea*; Atlantide Rep. 12; Scandinavian Science Press: Copenhagen, Denmark, 1977; pp. 1–181.
23. Manning, R.B.; Bruce, A.J. Erythrosquilla megalops, a remarkable new stomatopod from the western Indian Ocean. *J. Crustacean Biol.* **1984**, *4*, 329–332. [CrossRef]
24. Manning, R.B. Stomatopod Crustacea of Vietnam: The legacy of Raoul Serène. *Crustac. Res.* **1995**, *4*, 1–339. [CrossRef]
25. Ahyong, S.T.; Jarman, S.N. Stomatopod interrelationships: Preliminary results based on analysis of three molecular loci. *Arthropod Syst. Phylogeny* **2009**, *67*, 1864–8312.
26. Manning, R.B. The superfamilies, families and genera of recent stomatopod Crustacea, with diagnoses of six new families. *Proc. Biol. Soc. Wash.* **1980**, *93*, 362–372.

27. Porter, M.L.; Zhang, Y.; Desai, S.; Caldwell, R.L.; Cronin, T.W. Evolution of anatomical and physiological specialization in the compound eyes of stomatopod crustaceans. *J. Exp. Biol.* **2010**, *213*, 3473–3486. [CrossRef]
28. Caldwell, R.L. Stomatopods: The better to see you with my dear. *Aust. Nat. Hist.* **1991**, *23*, 696–705.
29. Trevisan, B.; Alcantara, D.M.C.; Machado, D.J.; Marques, F.P.L.; Lahr, D.J.G. Genome skimming is a low-cost and robust strategy to assemble complete mitochondrial genomes from ethanol preserved specimens in biodiversity studies. *PeerJ* **2019**, *7*, e7543. [CrossRef]
30. Lin, F.J.; Liu, Y.; Sha, Z.; Tsang, L.M.; Chu, K.H.; Chan, T.Y.; Liu, R.; Cui, Z. Evolution and phylogeny of the mud shrimps (Crustacea: Decapoda) revealed from complete mitochondrial genomes. *BMC Genom.* **2012**, *13*, 631. [CrossRef]
31. Cheng, J.; Chan, T.-Y.; Zhang, N.; Sun, S.; Sha, Z.-L. Mitochondrial phylogenomics reveals insights into taxonomy and evolution of Penaeoidea (Crustacea: Decapoda). *Zool. Scr.* **2018**, *47*, 582–594. [CrossRef]
32. González-Castellano, I.; Pons, J.; González-Ortegón, E.; Martínez-Lage, A. Mitogenome phylogenetics in the genus *Palaemon* (Crustacea: Decapoda) sheds light on species crypticism in the rockpool shrimp *P. elegans*. *LoS ONE* **2020**, *15*, e0237037. [CrossRef]
33. Kang, H.-E.; Kim, J.N.; Yoon, T.-H.; Park, K.D.; Park, W.G.; Park, H.; Kim, H.W. Total mitochondrial genome of mantis shrimp, *Squilloides leptosquilla* (Brooks, 1886) (Crustacea: Stomatopoda: Squillidae) in Korean waters. *Mitochondrial DNA A DNA Mapp. Seq. Anal.* **2016**, *27*, 2842–2843. [CrossRef]
34. Zhang, Y.; Bi, Y.; Feng, M. The complete mitochondrial genome of *Lophosquillia costata* (Malacostraca: Stomatopoda) from China and phylogeny of stomatopods. *Mitochondrial DNA Part B* **2020**, *5*, 2495–2497. [CrossRef]
35. Hwang, H.-S.; Shin, J.; Jung, J. Complete mitochondrial genome of the mantis shrimp *Taku spinosocarinatus* (Fukuda, 1909) (Stomatopoda: Gonodactyloidea: Takuidae) in South Korea. *Mitochondrial DNA Part B* **2020**, *5*, 3609–3610. [CrossRef]
36. Yang, M.; Liu, H.; Wang, R.; Tan, W. The complete mitochondrial genome of purple spot mantis shrimp *Gonodactylus smithii* (Pocock, 1893). *Mitochondrial DNA Part B* **2021**, *6*, 2028–2030. [CrossRef]
37. Rafinesque, C.S. *Analyse de la Nature, ou Tableau de l'Univers et des Corps Organisés*; Self-Published: Palermo, Italy, 1815.
38. Manning, R.B. *Stomatopod Crustacea Collected by the Yale Seychelles Expedition, 1957–1958*; Yale Peabody Museum of Natural History: Edinburgh, UK, 1962; Volume 68.
39. Paul'son, O. *Studies on Crustacea of the Red Sea with Notes Regarding Other Seas. Part I. Podophthalmata and Edriophthalmata (Cumacea)*; S.V. Kul'zhenko: Kiev, Ukraine, 1875; pp. 1–144. (In Russian)
40. Ahyong, S.T. Revision of the Australian stomatopod Crustacea. *Rec. Aust. Mus.* **2001**, *26*, 1–326. [CrossRef]
41. Folmer, O.; Black, M.; Hoeh, W.; Lutz, R.; Vrijenhoek, R. DNA primers for amplification of mitochondrial cytochrome c oxidase subunit I from diverse metazoan invertebrates. *Mol. Mar. Biol. Biotechnol.* **1994**, *3*, 294–299.
42. Shen, W.; Le, S.; Li, Y.; Hu, F. SeqKit: A Cross-Platform and Ultrafast Toolkit for FASTA/Q File Manipulation. *PLoS ONE* **2016**, *11*, e0163962. [CrossRef] [PubMed]
43. Bolger, A.M.; Lohse, M.; Usadel, B. Trimmomatic: A flexible trimmer for Illumina sequence data. *Bioinformatics* **2014**, *30*, 2114–2120. [CrossRef] [PubMed]
44. Allio, R.; Schomaker-Bastos, A.; Romiguier, J.; Prosdocimi, F.; Nabholz, B.; Delsuc, F. MitoFinder: Efficient automated large-scale extraction of mitogenomic data in target enrichment phylogenomics. *Mol. Ecol. Resour.* **2020**, *20*, 892–905. [CrossRef] [PubMed]
45. Li, D.; Luo, R.; Liu, C.-M.; Leung, C.-M.; Ting, H.-F.; Sadakane, K.; Yamashita, H.; Lam, T.-W. MEGAHIT v1.0: A fast and scalable metagenome assembler driven by advanced methodologies and community practices. *Methods* **2016**, *102*, 3–11. [CrossRef]
46. Laslett, D.; Canbäck, B. ARWEN: A program to detect tRNA genes in metazoan mitochondrial nucleotide sequences. *Bioinformatics* **2008**, *24*, 172–175. [CrossRef]
47. Bernt, M.; Donath, A.; Jühling, F.; Externbrink, F.; Florentz, C.; Fritzsch, G.; Pütz, J.; Middendorf, M.; Stadler, P.F. MITOS: Improved de novo metazoan mitochondrial genome annotation. *Mol. Phylogenet. Evol.* **2013**, *69*, 313–319. [CrossRef]
48. Kearse, M.; Moir, R.; Wilson, A.; Stones-Havas, S.; Cheung, M.; Sturrock, S.; Buxton, S.; Cooper, A.; Markowitz, S.; Duran, C.; et al. Geneious Basic: An integrated and extendable desktop software platform for the organization and analysis of sequence data. *Bioinformatics* **2012**, *28*, 1647–1649. [CrossRef]
49. Stephenson, W. A comparison of Australasian and American Specimens of Hemisquilla ensigera (Owen, 1832) (Crustacea: Stomatopoda). *Proc. U. S. Natl. Mus.* **1967**, *120*, 1–18. [CrossRef]
50. Bigelow, R.P. Preliminary notes on the Stomatopoda of the Albatross collections and on other specimens in the National Museum. *Johns Hopkins Univ. Circ.* **1893**, *12*, 100–102.
51. Hansen, J.H. Isopoden, Cumaceen Und Stomatopoden Der Plankton-Expedition. *Ergeb. Plankton-Exped. Der Humboldt-Stift.* **1895**, *2*, 1–105.
52. Manning, R.B. Stomatopod Crustacea of the western Atlantic. *Stud. Trop. Oceanogr.* **1969**, *8*, 1–380.
53. Pocock, R.I. Report upon the stomatopod crustaceans obtained by P. W. Bassett-Smith, Esq., Surgeon, R. N., during the cruise, in the Australian and China seas, of H.M.S. "Penguin," Commander W. U. Moore. *Ann. Mag. Nat. Hist.* **1893**, *11*, 473–479. [CrossRef]
54. Fabricius, J.C. *Species Insectorum Exhibentes Eorum Differentias Specificas, Synonyma Auctorum, Loca Natalia, Metamorphosin Adiectis, Observationibus, Descriptionibus*; C.E. Bohnii: Hamburg, Germany; Kiel, Germany, 1781; Volume 1, pp. 1–552.
55. Manning, R.B. Notes on some species of the *Falcatus* group of *Gonodactylus* (Crustacea: Stomatopoda: Gonodactylidae). *Smithson. Contrib. Zool.* **1978**, *258*, 1–15. [CrossRef]
56. Fukuda, T. The Stomatopoda of Japan. *Dobutsugaku Zasshi* **1909**, *21*, 54–62.

57. Fabricius, J.C. *Mantissa Insectorum, Sistens Eorum Species Nuper Detectas, Adjectis Characteribus Genericis, Differentiis Specificis, Emendationibus Observationibus*; C. G. Proft: Copenhagen, Germany, 1787; Volume 1, p. 348.
58. Hwang, H.-S.; Ahyong, S.T.; Kim, W. A new species of *Chorisquilla* Manning, 1969 (Stomatopoda: Protosquillidae) from Korea and Japan with redescription of C. mehtae Erdmann Manning, 1998. *Zootaxa* **2018**, *4483*, 365–374. [CrossRef]
59. De Haan, W. Crustacea. In *Von Siebold, P.F., Fauna Japonica sive Descriptio Animalium, quae in Itinere per Japoniam, Jussu et Auspiciis Superiorum, qui Summum in India Batava Imperium Tenent, Suspecto, Annis 1823–1830 Collegit, Notis*; Observationibus et Adumbrationibus Illustravit: Leiden, The Netherlands, 1844; pp. 1–243.
60. Linnaeus, C. *Systema Naturae per Regna Tria Naturae, Secundum Classes, Ordines, Genera, Species, cum Characteribus, Differentiis, Synonymis, Locis*; Laurentius Salvius Holmiae: Stockholm, Sweden, 1758; Volume 1, p. 824.
61. Say, T. An account of the Crustacea of the United States. *J. Acad. Nat. Sci. Phila.* **1818**, *1*, 445–458.
62. Bigelow, R.P. Preliminary notes on some new species of Squilla. *Johns Hopkins Univ. Circle* **1891**, *10*, 93–94.
63. Brooks, W.K. Report on the Stomatopoda collected by HMS Challenger during the years 1873–76. *Rep. Sci. Results Voyag. HMS Chall. Zool.* **1886**, *16*, 1–115.
64. Wood-Mason, J. *Figures and Descriptions of Nine Species of Squillidae from the Collection in the Indian Museum*; Indian Museum: Calcutta, India, 1895; pp. 1–11.
65. Fabricius, J.C. *Entomologia Systematica Emendata et Aucta. Secundum Classes, Ordines, Genera, Species Adjectis Synonimis, Locis, Observationibus, Descriptionibus*; Christ. Gottl. Proft: Copenhagen, Denmark, 1793; Volume 2, pp. 1–519.
66. Holthuis, L.B. Stomatopod Crustacea of Suriname. *Stud. Fauna Suriname Other Guyanas* **1959**, *3*, 173–191.
67. Hansen, H.J. The genera and species of the order Euphausiacea, with account of remarkable variation. *Bull. L'institut Océanographique Monaco* **1911**, *210*, 1–54.
68. Nakazawa, K. Notes on Japanese Schizopoda. *Annot. Zool. Jpn.* **1910**, *7*, 247–261.
69. Schioedte, J.C.; Meinert, F.W. Symbolae ad Monographiam Cymothoarum Isopodum Familiae 4. *Cymothoidae. Trib. II. Cymothoinae. Trib. III. Livonecinae. Nat. Tidsskr.* **1884**, *3*, 221–454.
70. Schwentner, M.; Richter, S.; Rogers, D.C.; Giribet, G. Tetraconatan phylogeny with special focus on Malacostraca and Branchiopoda: Highlighting the strength of taxon-specific matrices in phylogenomics. *Proc. Biol. Sci.* **2018**, *285*, 20181524. [CrossRef]
71. Lozano-Fernandez, J.; Giacomelli, M.; Fleming, J.F.; Chen, A.; Vinther, J.; Thomsen, P.F.; Glenner, H.; Palero, F.; Legg, D.A.; Iliffe, T.M.; et al. Pancrustacean Evolution Illuminated by Taxon-Rich Genomic-Scale Data Sets with an Expanded Remipede Sampling. *Genome Biol. Evol.* **2019**, *11*, 2055–2070. [CrossRef]
72. Castresana, J. Selection of conserved blocks from multiple alignments for their use in phylogenetic analysis. *Mol. Biol. Evol.* **2000**, *17*, 540–552. [CrossRef]
73. Katoh, K.; Standley, D.M. MAFFT Multiple Sequence Alignment Software Version 7: Improvements in Performance and Usability. *Mol. Biol. Evol.* **2013**, *30*, 772–780. [CrossRef]
74. Edler, D.; Klein, J.; Antonelli, A.; Silvestro, D. raxmlGUI 2.0: A graphical interface and toolkit for phylogenetic analyses using RAxML. *Methods Ecol. Evol.* **2021**, *12*, 373–377. [CrossRef]
75. Kozlov, A.M.; Darriba, D.; Flouri, T.; Morel, B.; Stamatakis, A. RAxML-NG: A fast, scalable and user-friendly tool for maximum likelihood phylogenetic inference. *Bioinformatics* **2019**, *35*, 4453–4455. [CrossRef]
76. Darriba, D.; Posada, D.; Kozlov, A.M.; Stamatakis, A.; Morel, B.; Flouri, T. ModelTest-NG: A New and Scalable Tool for the Selection of DNA and Protein Evolutionary Models. *Mol. Biol. Evol.* **2020**, *37*, 291–294. [CrossRef]
77. Maddison, W.P.; Maddison, D.R. Mesquite: A Modular System for Evolutionary Analysis. Version 3.61. 2019. Available online: http://www.mesquiteproject.org (accessed on 30 November 2021).
78. Swofford, D.L. *PAUP *. Phylogenetic Analysis Using Parsimony (* and Other Methods)*; Version 4; Sinauer Associates: Sunderland, MA, USA, 2003.
79. Ronquist, F.; Teslenko, M.; van der Mark, P.; Ayres, D.L.; Darling, A.; Höhna, S.; Larget, B.; Liu, L.; Suchard, M.A.; Huelsenbeck, J.P. MrBayes 3.2: Efficient Bayesian Phylogenetic Inference and Model Choice across a Large Model Space. *Syst. Biol.* **2012**, *61*, 539–542. [CrossRef]
80. Rambaut, A.; Drummond, A.J.; Xie, D.; Baele, G.; Suchard, M.A. Posterior summarisation in Bayesian phylogenetics using Tracer 1.7. *Syst. Biol.* **2018**, *67*, 901–904. [CrossRef] [PubMed]
81. Shimodaira, H. An Approximately Unbiased test of phylogenetic tree selection. *Syst. Biol.* **2002**, *51*, 492–508. [CrossRef] [PubMed]
82. Nguyen, L.-T.; Schmidt, H.A.; von Haeseler, A.; Minh, B.Q. IQ-TREE: A fast and effective stochastic algorithm for estimating maximum-likelihood phylogenies. *Mol. Biol. Evol.* **2015**, *32*, 268–274. [CrossRef] [PubMed]
83. Chernomor, O.; von Haeseler, A.; Minh, B.Q. Terrace aware data structure for phylogenomic inference from supermatrices. *Syst. Biol.* **2016**, *65*, 997–1008. [CrossRef]
84. Schram, F.R.; Ahyong, S.T.; Patek, S.N.; Green, P.A.; Rosario, M.V.; Bok, M.J.; Cronin, T.W.; Vetter, K.S.M.; Caldwell, R.L.; Scholtz, G.; et al. Subclass Hoplocarida Calman, 1904: Order Stomatopoda Latreille, 18171. In *Treatise on Zoology-Anatomy, Taxonomy, Biology. The Crustacea, Volume 4 Part A*; Brill: Leiden, The Netherlands, 2013; pp. 179–355.
85. Barber, P.H.; Erdmann, M.V. Molecular systematics of the Gonodactylidae (Stomatopoda) using mitochondrial cytochrome oxidase C (Subunit 1) DNA sequence data. *J. Crustacean Biol.* **2000**, *20*, 20–36. [CrossRef]
86. Dana, J. *United States Exploring Expedition. During the Year 1838, 1839, 1840, 1841, 1842*; C. Sherman: Philadelphia, PA, USA, 1852; Volume 13, pp. 615–623.

87. Caldwell, R.L.; Dingle, H. Stomatopods. *Sci. Am.* **1976**, *234*, 80–89. [CrossRef]
88. DeVries, M.S.; Stock, B.C.; Christy, J.H.; Goldsmith, G.R.; Dawson, T.E. Specialized morphology corresponds to a generalist diet: Linking form and function in smashing mantis shrimp crustaceans. *Oecologia* **2016**, *182*, 429–442. [CrossRef] [PubMed]
89. DeVries, M.S. The role of feeding morphology and competition in governing the diet breadth of sympatric stomatopod crustaceans. *Biol. Lett.* **2017**, *13*, 20170055. [CrossRef]
90. Boore, J.L.; Lavrov, D.V.; Brown, W.M. Gene translocation links insects and crustaceans. *Nature* **1998**, *392*, 667–668. [CrossRef]
91. Kilpert, F.; Podsiadlowski, L. The complete mitochondrial genome of the common sea slater, *Ligia oceanica* (Crustacea, Isopoda) bears a novel gene order and unusual control region features. *BMC Genom.* **2006**, *7*, 241. [CrossRef] [PubMed]

diversity

MDPI

Article

Risk of Infection, Local Prevalence and Seasonal Changes in an Avian Malaria Community Associated with Game Bird Releases

Jesús T. García [1,*], Javier Viñuela [1], María Calero-Riestra [1,2], Inés S. Sánchez-Barbudo [1], Diego Villanúa [1,3] and Fabián Casas [1,4]

[1] Instituto de Investigación en Recursos Cinegéticos, IREC (CSIC, UCLM, JCCM), Ronda de Toledo 12, E-13071 Ciudad Real, Spain; Javier.Vinuela@uclm.es (J.V.); maria.caleroriestra@gmail.com (M.C.-R.); Ines.Sanchez@uclm.es (I.S.S.-B.); dvillani@ganasa.es (D.V.); fabiancasas1979@gmail.com (F.C.)
[2] Instituto Pirenaico de Ecología (IPE-CSIC), Avda. Nuestra Señora de la Victoria, 16, E-22700 Jaca, Spain
[3] Navarra Environmental Management (GAN-NIK), c/Padre Adoain, 219, Navarra, E-31015 Pamplona, Spain
[4] Dehesa de El Lobillo S.A., E-13248 Ciudad Real, Spain
* Correspondence: jesusgarcia.irec@gmail.com

Abstract: Anthropogenic activities, such as the translocation or introduction of animals, may cause a parallel movement of exotic parasites harboured by displaced animals. Although introduction and/or relocation of animals for hunting purposes is an increasingly common management technique, the effects of gamebird release as a major vehicle for the introduction of parasites into new geographic regions have rarely been reported. We examined the prevalence and distribution of avian malaria parasites infecting resident avian hosts (red-legged partridge *Alectoris rufa*) at a local scale, with a particular emphasis on the effects of releasing farm-reared birds for hunting on the spatial and temporal structure of the parasite community. We collected blood samples from adult partridges from two game estates with partridge releases and two sites without releases over two periods (spring and autumn). We tested the probability of infection and differences in the parasite community in relation to the management model (releases vs. non releases) and sampling period, comparing autumn (when farm-reared birds are released) and spring (after hunting season, when mostly wild birds can be found in the population). We found a high prevalence (54%) of *Plasmodium* spp., and substantial differences in the spatial and temporal distribution of parasite lineages among the populations studied. Some parasite lineages occurred at high frequencies in game estates without introduction of farm-reared partridges, while other lineages were more abundant in game estates with releases than in those without releases. Overall, the prevalence of avian malaria was similar between spring and autumn at non-release sites, whereas in sites with releases, it was higher in autumn than in spring—probably due to artificial restocking with infected farm-reared birds at the onset of the hunting season. In short, humans may be an important agent driving the alteration of the spatial structure of local parasite fauna via the introduction of exotic parasites by gamebird release, which could cause avian malaria outbreaks with severe repercussions for native avifauna.

Keywords: avian malaria; *Alectoris rufa*; host-parasite co-evolution; hunting; farm-reared birds; *Plasmodium*; introduced parasites

Citation: García, J.T.; Viñuela, J.; Calero-Riestra, M.; Sánchez-Barbudo, I.S.; Villanúa, D.; Casas, F. Risk of Infection, Local Prevalence and Seasonal Changes in an Avian Malaria Community Associated with Game Bird Releases. *Diversity* **2021**, *13*, 657. https://doi.org/10.3390/d13120657

Academic Editor: Michael Wink

Received: 15 November 2021
Accepted: 3 December 2021
Published: 10 December 2021

1. Introduction

The anthropogenic actions affecting the distribution and dispersal of animals have a global and continuing influence on the evolutionary course of wild populations. There is now a large body of literature showing remarkable large-scale responses in some animal populations affected by human disturbance [1–3]. Among these perturbations, common practices used today such as the relocation and introduction of animals have played a significant role on the emergence and spread of several diseases [4–10], with significant consequences for wildlife, domestic animals, and humans [11,12]. The human-based spread of infectious agents over new areas jeopardizes wild animal populations by exposure

to exotic pathogens [13–16], some of which may be parasites harboured by introduced animals [17–21]. Avian malaria is a paradigmatic case of a widespread vector-transmitted disease with negative effects on the survival and fitness of many bird species [22–25]. The introduction of parasites into new environments can largely influence parasite evolution, host population dynamics, and host—parasite interactions [26–28], and growing empirical evidence indicates that these kinds of human-induced changes in ecosystems are more common than previously thought [27].

The management of wild species for hunting is probably one of the human activities responsible for much of the alteration occurring at a large scale on wild populations of many species. Introduction and/or relocation of animals is an increasingly common management technique that represents a good example in which humans modify on a large scale the genetic structures, community compositions, and life histories of both parasites and hosts [28–35]. Gamebird releases, particularly those of red-legged partridges (*Alectoris rufa*), provide a suitable model for evaluating the consequences of this kind of wildlife management. The red-legged partridge is a medium-sized *Phasianidae* native to the Iberian Peninsula, France, and Italy, that has suffered a sharp decline in wild numbers during the last decades [36,37]. The reinforcement of wild populations with farm-reared birds is today the most widely used tool in the management of this gamebird, involving millions of released birds over huge areas [32,34,38]. The percentage of released birds that survive after their first "hunting season" (from October to January) is potentially low [39–42], but settlement and successful breeding into the wild of some released individuals has been proven [39]. On the other hand, the habitual conditions of partridge farms (very high densities of animals and increased stress factors) may be particularly favourable for the acquisition of malaria parasites from local avifauna, which has been established afterwards in distant areas where partridges are released in large numbers. Furthermore, releases suddenly increase host density at local scales and, consequently, the number of both intra- and inter-specific contacts between infected and uninfected individuals. Such a phenomenon may indeed be of great conservation concern since it operates on a country-wide scale in the case of Iberian partridges, but also globally in a wide range of species, including fish, mammals, and birds [11]. The importance of hunting management as a pathway for the introduction of new parasites and its potential consequences for wildlife has received increased attention recently [9,12,43], but little has been done to address the importance of farm-reared bird releases as a putative reservoir of infections and avian malaria outbreaks.

The aim of this study was therefore to determine the importance of hunting releases as a way of propagating exotic (i.e., parasites previously non-existent in the receiving host population) avian malaria parasites. Furthermore, we explore potential changes in the prevalence of native parasites as a consequence of releases. We address this question by comparing the parasite community among sites with releases and sites without releases, and between autumn (when farm-reared birds are released) and spring (when mostly wild birds can be found in the population) in both types of sites. Basically, if malaria prevalence (i.e., the percentage of infected birds) and the community composition (the occurrence of each parasite strain) differs between both periods in populations reinforced by releases but not in sites without releases, then the difference may be associated with releases. To further assess the existence of artificial restocking in our populations, we explored the occurrence of partridges with allochthonous mtDNA haplotypes (mainly from *Alectoris chukar*), which is expected to increase after releases due to the liberation of hybrids (*A. chukar* × *A. rufa*) among the captive stock [32,34,42,44,45].

We discuss our findings in relation to how releases may alter the spatial structure of local pathogenic fauna via the introduction of exotic avian malaria parasites, and the potential consequences for the host—parasite system, for wild populations of game species, and for sympatric populations of non-game species.

2. Materials and Methods

2.1. Study Populations and Field Procedure

The study area comprised 7.779 ha located in the Campo de Calatrava region (Central Spain, 38°80′ N, 3°80′ W, 610 m a.s.l.). The habitat was characterized by undulated farmlands aimed at cereal cultivation (mostly barley *Hordeum* spp.), with interspersed patches of olive groves (*Olea* sp.), vineyards, dry annual legume crops (mainly vetch *Vicia sativa*) and sugar beet (*Beta rubra*).

We collected 189 blood samples from adult red-legged partridges between 2003 and 2005 from four game estates (hereafter "sites" A, B, C, and D) 1.8–11.1 km apart from each other (Figure 1 and Table 1). We considered the four sites as independent in our analyses in relation to hosts, because radio-tracked partridges usually have low dispersion rates after releases (average lower than 600 m, see [41]). However, the capacity of some vectors to travel was within this range of distances [46], and parasite transmission could also be vectored by other avian species. Hence, the distance between pairs of sites does not guarantee independence regarding vectors and/or other avian host species movements. The four sampling sites had similar landscape features, climate and the same type of "dry cultivation" without irrigated lands, but differed markedly in game management systems [47]. One of the game estates sampled (site B, 1484 ha.) followed an intensive management model with about 2000 farm-reared partridges released per year, representing 75–90% of the total partridge captures each year. This site maintains the same hunting pressure every year, having an overall hunting bag of 1.35 birds/ha. Site C (548 ha.) showed occasional releasing activity, with hunting pressure adjusted to autumn numbers and an average hunting bag of 0.15 birds/ha. Finally, sites A (3145 ha.) and D (1009 ha.) have followed a traditional management model without captive-bred gamebird restocking for over 10 years. In both sites, hunting pressure was adjusted to autumn numbers, with an average hunting bag of 0.26 and 0.55 birds/ha, respectively [47].

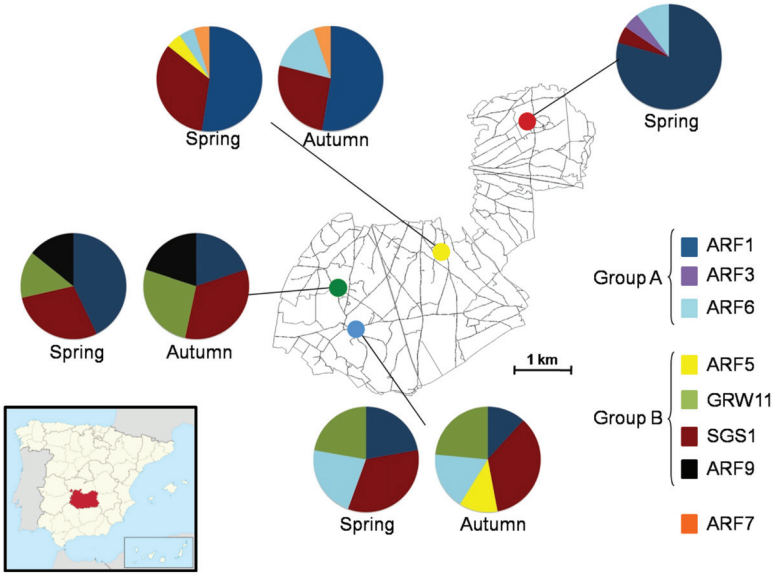

Figure 1. Spatial and temporal distribution of malaria-parasite lineages recorded in four populations of red-legged partridges in Ciudad Real, central Spain (inset shows the location of the Ciudad Real province within the Iberian peninsula). The two main groups of lineages according to Figure 2 are indicated. Pie charts indicate the relative importance of all sequenced *Plasmodium* infections in a given population. The four host sites are labelled by different colours: yellow—game estate A, blue—game estate B, green—game estate C, and red—game estate D. Percentage values are given in Table 1.

Table 1. Number of red-legged partridges infected by each malaria lineage (*Plasmodium* spp.) in four study sites in central Spain.

			Game Estate									
			Site A		Site B		Site C		Site D		Total	
Parasite Taxon	**Lineage**	**GenBank**	**AT**	**SP**	**AT**	**SP**	**AT**	**SP**	**AT**	**SP**	**AT**	**SP**
Plasmodium sp.	ARF1	EU395835	10	11	2	2	3	3	-	11	29.4	51.9
P. relictum	SGS1	AF495571	5	7	6	3	5	2	-	1	31.4	25.0
Plasmodium sp.	ARF3	EU395836	0	0	0	0	0	0	-	1	0.0	1.9
Plasmodium sp.	ARF5	EU395838	0	1	2	0	0	0	-	0	3.9	1.9
Plasmodium sp.	ARF6	EU395839	3	1	3	2	0	0	-	2	11.8	9.6
Plasmodium sp.	ARF7	EU395840	1	1	0	0	0	0	-	0	2.0	1.9
P. relictum	GRW11	AY831748	0	0	4	2	4	1	-	0	15.7	5.8
Plasmodium sp.	ARF9	EU395841	0	0	0	0	3	1	-	0	5.9	1.9
N° of samples			31	39	25	35	21	9	-	29	77	112
N° of infections			19	21	17	9	15	7	-	15	51	52
Prevalence			61.2	53.8	68	25.7	71.4	77.7	-	51.7	66.2	46.4

Note: Autumn and spring sampling periods are designated by AT and SP, respectively. The last two columns show the percentage of infected hosts by each parasite lineage in each of the two periods.

Our analyses were based on two different sampling periods: spring samples (n = 112) were collected in the four populations from wild partridges caught using cage traps with live adult partridges as a decoy [47]; autumn samples (when hunters restocked partridge populations) were taken from 77 hunter-harvested partridges sampled in sites A, B, and C (samples from site D were not available, see Table 1). We were limited in our autumn data collection to hunter-harvested birds rather than birds previous to releases because of the noticeable reticence of hunting managers to allow sampling from farmed stocks. All partridges captured were ringed in order to avoid resampling.

2.2. Avian Malaria Diagnosis

Blood samples were obtained by ulnar venipuncture in live partridges (spring samples) or taken from the heart in hunter-harvested partridges (autumn samples) and stored in 99% ethanol until molecular analysis. DNA was extracted using a standard ammonium acetate precipitation method, and diluted to a working concentration of 25 ng/µL. Samples were screened for the presence of *Plasmodium* and *Haemoproteus* using a widespread nested polymerase chain reaction (PCR) protocol [48] designed to amplify a 479 bp fragment of the mitochondrial cytochrome b gene of both parasite geni. The PCR tests were performed in two separate runs with positive (i.e., DNA from individuals with known malarial infections) and negative (ddH_2O) controls. Pre- and post-PCR work was performed with different materials and in different laboratory sections to avoid contamination. We repeated the protocol three times to confirm negative infections. All samples with positive PCR reactions were successfully sequenced from both ends. We used MicroSpin s-400 HR columns (Amersham Biosciences) to purify PCR products, which were sequenced using the same PCR primers and the Big Dye Terminator Kit (Applied Biosystems, Thermo Fisher Brand, Foster City, CA, USA). The sequencing reactions were purified on standard Sephadex columns and DNA sequences were obtained using an ABI 3130 automated sequencer (Applied Biosystems). Reading data were processed with the ABI PRISM1 Sequencing Analysis Software v3.7 (Applied Biosystems).

2.3. Defining Parasite Lineages

We aligned and edited parasite DNA sequences using Clustal W [49] and Bioedit [50] with the published sequences of other avian malaria parasites registered in GenBank. Lineages differing by one nucleotide were re-sequenced for verification purposes. Many of the sequences obtained differed by as few as one or two nucleotides over the 479 bp examined. Thus, because some avian malaria *Cyt b* lineages with less than 0.5% sequence

divergence may represent different species [51], the same person (JTG) carefully examined each sequence at least twice, discarding those with ambiguous sites (then amplified and sequenced again) to assess the quality of the data. We did not find any individual showing double peaks in the sequences which could indicate the presence of multiple infections [52,53]. Here, we used a threshold of one nucleotide divergence to define separated lineages [54]. All new sequences have been deposited in GenBank (accession numbers EU395835–EU395841).

Although we did not have information on the morphological identity of our lineages, we inferred taxonomic identity by assessing the phylogenetic relatedness of partridge-isolated *Plasmodium* spp. lineages with published sequences from GenBank of morphologically identified parasites (see [55] for a similar procedure) and compiled in the MalAvi database [56]. We estimated the phylogenetic relationships among avian malaria haplotypes using BEAST v.2.5 [57]. The analysis was conducted for 36 lineages of *Plasmodium* and 3 lineages of *Haemoproteus*, together with the 8 *Plasmodium* lineages detected in *A. rufa* (see results). We conducted BEAST analyses using the GTR + I + G model (α = 0.3810; p.inv = 0.312), as selected using jModelTest 2.1.4 [58] under the Akaike Information Criterion (AIC), with estimated base frequencies, relaxed lognormal clock, and two independent MCMC runs of 10 million generations each, sampling every 1000 generations. We checked for convergence using Tracer v. 1.7.1 [59], confirming that ESS values for likelihoods and all parameters were >200. We then combined runs with LogCombiner [60] using 20% burn-in, and generated a maximum clade credibility (MCC) tree in TreeAnnotator [61] from 8002 posterior trees.

Sequence divergence values between *Plasmodium* spp. lineages were analysed using uncorrected P distance.

2.4. Host Mitochondrial Lineages

To differentiate host mtDNA haplotypes within our samples we used sequence variation in the mitochondrial NADH dehydrogenase subunit 2 gene (ND2). We amplified the first part of the ND2 gene using the primers L5216 and H5766 [62]. All samples were sequenced from both ends using the BigDye Terminator Kit, and DNA sequences were determined using an ABI 3100 automated sequencer (Applied Biosystems). Sequence alignment was performed with BioEdit 7.0 [50], together with the sequences of *A. chukar* published in GenBank and *A. magna*, which was used as outgroup. We constructed a neighbour-joining (NJ) tree via PAUP* 4.0 [63], using previously characterized *A. rufa* specimens [32] and published sequences from *A. chukar*. We then assigned each of our *Alectoris* samples to one (*A. rufa*) or the other (*A. chukar*) of the haplogroups.

2.5. Statistical Analysis

Statistical analyses were conducted in Statistica 8.0 [64]. We tested the probability of infection (0 for absence and 1 for presence) in a generalized linear model with logit link function and binomial distribution of errors. First, we investigated the relationship between the infection status (binary variable) and two explanatory variables: the management (game estates with releases vs. game estates without releases) and the sampling period (autumn vs. spring). Second, we performed additional analyses for the two groups of parasites inferred from the phylogenetic analyses (see the Results section). For this, we pooled these parasite lineages with high bootstrap support (>80% posterior probability, Group A and B; Figure 2), categorizing each host sample as either being infected or not infected by each parasite group.

For the subset of infected hosts, we used a log-linear analysis to determine whether the proportion of hosts infected by parasites belonging to Groups A and B was independent of management type and period ($2 \times 2 \times 2$ contingency table; [64]). The Log-Linear analysis is considered an ANOVA-like design for frequency data. Specifically, it is used to test the different factors that are used in a crosstabulation with categorical factors and their interactions for statistical significance [64].

To assess the incidence of partridge restocking in our sample set we compared the occurrence of allochthonous host mtDNA haplotypes (mtDNA corresponding with A. chukar lineages) between autumn and spring in sites with releasing activity by means of a generalized non-linear model (GLZ procedure in Statistica software), and in the single site without releasing activity using a Fisher exact test.

3. Results

Malaria infections were detected in 103 individuals out of 189 red-legged partridges screened, which represented an overall prevalence of 54% (Table 1). All parasite *Cyt b* lineages recorded corresponded to *Plasmodium* spp. (Figure 2), whereas sequences belonging to *Haemoproteus* spp. were absent in our sample set. Eight unique *Plasmodium* lineages were defined according to 43 variable nucleotide sites. There were no insertions or deletions, and thus the nucleotide alignment was unambiguous.

Two of the parasite lineages found in red-legged partridges (SGS1 and GRW11; Figure 2) are considered cosmopolitan in distribution, highly invasive, and have been recorded in more than 140 bird species—principally passerines—in over 43 countries [4,56]. The remaining six lineages corresponded to new parasite lineages, showing divergences between 0.2% and 7.8% with respect to any other *Plasmodium* morphospecies recorded to date in avian hosts. The most common parasite lineage was ARF1 (41% of detected lineages), followed by SGS1 (28%), ARF6 (10.7%), and GRW11 (10.7%). The remaining four lineages (ARF3, ARF5, ARF7 and ARF9) were detected at low rates (less than 5% of infections).

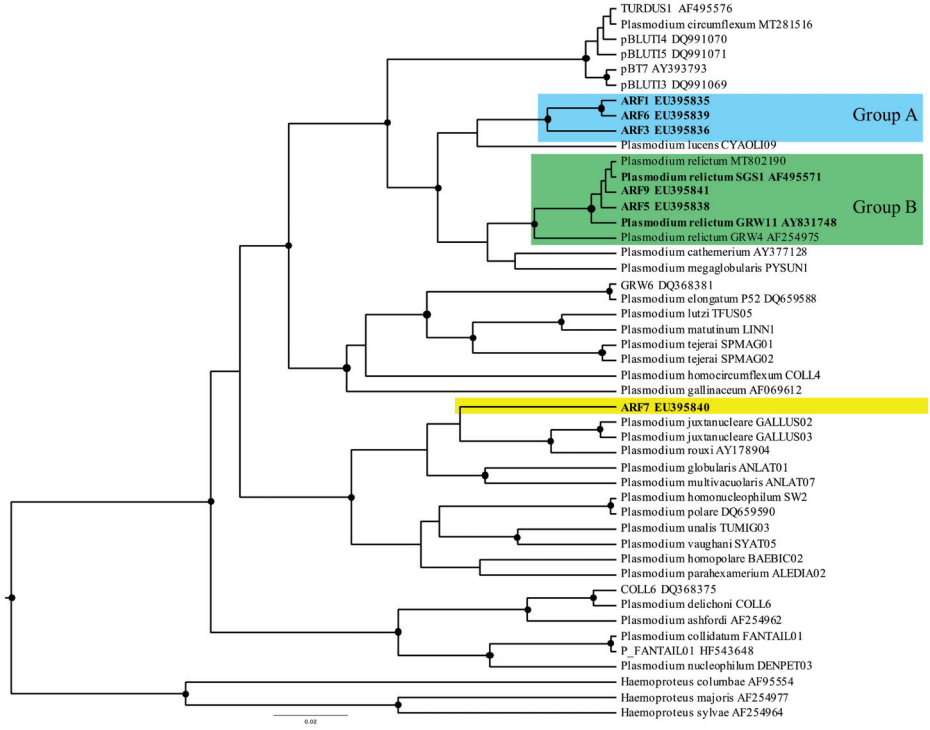

Figure 2. Phylogram of Plasmodium spp. cytochrome b lineages found in *Alectoris rufa* sampled in central Spain. Lineages detected in this study are shown in bold. Principal groups are indicated by colours and correspond to closely related lineages that belong, or likely belong, to the same parasite morphospecies. *Haemoproteus majoris*, *H. columbae* and *H. sylvae* were used as outgroups. Bayesian posterior probabilities above 0.5 are depicted (black dots) at each node. GenBank accession numbers or MalAvi database morphospecies are indicated after lineage names.

3.1. Releasing Activity and Distribution of Host Genotypes

We detected two *A. chukar* and eight *A. rufa* haplotypes in the sample. The alignment of the partridge ND2 sequences yielded a NJ tree in which *A. rufa*, and *A. chukar* haplotypes clustered into two different groups (Figure 3). As predicted, the temporal distribution of partridge haplotypes in sites with releasing activity, but not in sites without releases, showed widespread occurrence of allochthonous mtDNA lineages principally during the hunting season (autumn). In sites with releases, haplotypes belonging to the *A. chukar* clade were significantly higher in autumn (59% of *A. chukar* haplotypes vs. 41% of *A. rufa* clade) than in spring (18% of haplotypes vs. 82% belonging to *A. rufa* clade) ($\chi^2_1 = 4.5$, $p = 0.033$). The occurrence of *A. chukar* haplotypes was similar between both sites with partridge releases ($\chi^2_1 = 0.53$, $p = 0.47$), and the interaction site x period was also non-significant in the model $\chi^2_1 = 0.12$, $p = 0.73$). In contrast, in the game estate without releases (site A), the occurrence of allochthonous mtDNA haplotypes remained seasonally stable (12% *A. chukar* vs. 87% *A. rufa* in autumn, and 8% *A. chukar* vs. 92% *A. rufa* in spring; Fisher exact test, $p = 0.63$). Thus, allochthonous mtDNA haplotypes (i.e., the *A. chukar* clade) appeared more frequently in areas where farm-bred partridges were released for hunting, and principally during the hunting season.

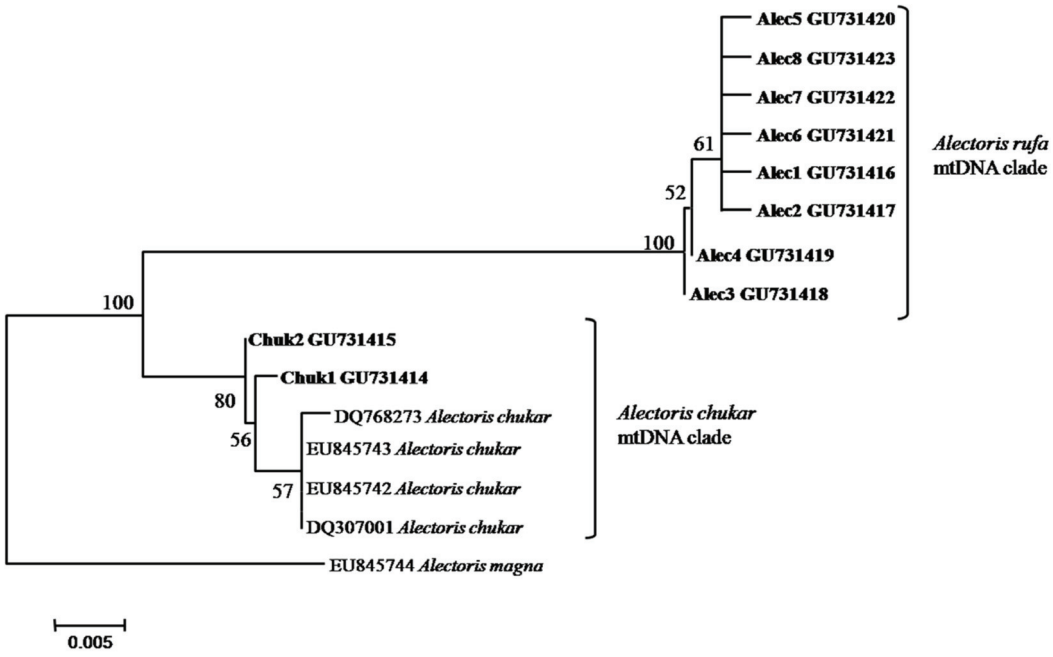

Figure 3. Neighbour-joining tree of mtDNA haplotypes from samples classified morphologically as Alectoris rufa (in bold). The tree was rooted using the Alectoris magna sequence (Genbank accession numbers of sequences are indicated on the tree). Bootstrap support to internal branches (>50; 10, 000 replicates) is indicated by numbers.

3.2. Avian Malaria Lineages of Red-Legged Partridges

The phylogenetic tree (Figure 2) supported the existence of at least three different parasite species among our samples. Three of the lineages (ARF1, ARF3, and ARF6) clustered together into a well-supported clade (>80% posterior probability, Group A; Figure 2), which did not contain sequences of any of the morphospecies included in the analysis. Our isolates SGS1, ARF5, GRW11 and ARF9 did fall together into the *P. relictum* clade (Group B; Figure 2) and we tentatively considered these lineages as belonging to the same morphospecies (*P. relictum*) for further analyses. The genetic distances between

the lineages of Group A ranged from 0.2% to 1.7%, and in Group B from 0.2% to 2.3% (Figure 2). Finally, ARF7 did not match any described morphological species and was placed in the resulting phylogeny in a different clade, thus corresponding to a separate species. Between-group mean genetic distances varied from 2.9% (Group A/Group B) to 16.9% (Group A—*P. tejerai*). Lineage ARF7 exhibited much larger differences with respect to all other lineages, ranging from 5.3% (ARF 7—*P. paraxehamerium*) to 27.8 % (ARF 7—*P. juxtanucleare*). This lineage was excluded from further analyses due to its low occurrence in our populations (Table 1).

3.3. Seasonal Distribution of Parasites and Releasing Activity

We detected red-legged partridges infected by *Plasmodium* spp. in all four sampled sites, and during both sampling periods. The frequency of the eight lineages isolated in red-legged partridges was not randomly distributed among sites (Table 1; Figure 1). Among infected birds, we found large between-population variations in the occurrence of each lineage (Figure 1). Even when considering only lineages present in all the four sampling sites (ARF1 and SGS1), large differences in the relative frequency among different host populations were observed (Figure 1). Tentatively, and considering isolates of the same parasite cluster as belonging to the same species (Figure 2), we observed differences in the probability of being infected in relation to releasing activity and period. Overall, *Plasmodium* spp. prevalence was significantly higher in autumn than in spring (Table 2), with no significant differences between types of management. The interaction of period x management was also non-significant.

Table 2. Generalized linear model (GLZ) for effects of period and management on infection by avian malaria parasites in red-legged partridges.

	Wald $\chi 2$	d.f.	p
All Parasites Pooled			
Period	7.77	1	0.005
Management	0.24	1	0.6
Period x Management	2.76	2	0.1
Parasites of Group A			
Period	0.13	1	0.71
Management	12.12	1	0.0004
Period x Management	0.04	2	0.95
Parasites of Group B			
Period	4.51		0.033
Management	9.04	1	0.0026
Period x Management	2.57		0.11

At the parasite-group level, the prevalence showed a significant but opposite effect, with a higher prevalence in sites with releases than sites without releases for Group B, whereas Group A exhibited the inverse, with a higher prevalence in non-releasing than in releasing sites (Table 2). Indeed, we found a season effect on Group B prevalence, with a higher prevalence during autumn than during spring. No effect of period was found on the prevalence of Group A, and neither was the interaction period x management significant. The distribution of parasite lineages among infected hosts gave similar results. The Log-Linear analysis indicated that the best model for parasite distribution included all the second-order interactions, with no single or three-way interaction (all $p > 0.05$). The management-by-period interaction ($\chi^2_4 = 19.38$, $p = 0.006$; Figure 4) indicates that parasites were more frequent in autumn than in spring in sites with releasing activity, whereas no between-period differences were found at game estates without releases. Parasites belonging to Group A were more frequent in sites without releases than in sites with releases (Figure 4) whereas the opposite was found for Group B (management-by-group

interaction: $\chi^2_4 = 11.97$, $p = 0.017$). Furthermore, the frequency of parasites in Group A did not vary significantly between spring and autumn. In contrast, Group B lineages were much more frequent in autumn than in spring in sites with releases, but not in sites without releases (group-by-period interaction: $\chi^2_4 = 23.78$, $p = 0.00009$; Figure 4).

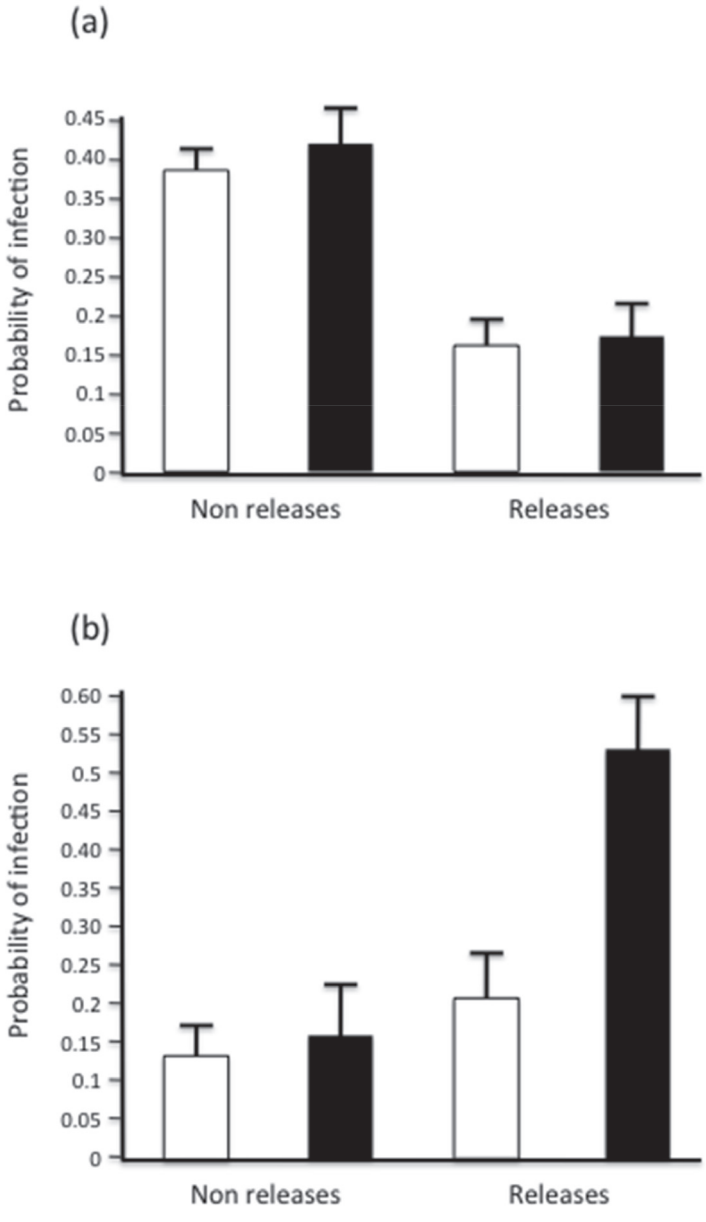

Figure 4. Probability of infection in red-legged partridges in game estates with releases and without releases with avian malaria parasites belonging to (**a**) Group A or (**b**) Group B of parasites, according to Figure 2. We show the weighted marginal means (±S.E.) during both spring (white bars) and autumn (black bars) sampling periods.

The parasites detected here can be further split into relation-to-host haplotypes: lineages infecting the *A. chukar* clade and lineages infecting the *A. rufa* clade. Six out of the eight parasite lineages were present in both host haplotypes, while two parasite lineages (ARF3 and ARF7) were absent from *A. chukar* hosts. Overall, parasites belonging to Group A were more frequent in *A. rufa* hosts (57.5% of all infections in these hosts) than in *A. chukar* hosts (34.8%), while parasites of Group B were more frequent in *A. Chukar* (65%) than in *A. rufa* hosts (40%).

4. Discussion

As humans continuously alter landscapes and ecological communities, the knowledge of how parasites and their hosts respond to these changes and the implications and consequences for the transmission and distribution of infectious agents are of paramount importance [10–12]. We found a quite high prevalence of avian malaria parasites in red-legged partridges in central Spain. The results presented here revealed malaria prevalences that are among the highest found in bird populations, particularly for *Plasmodium* [4,65–68], including studies on species from comparable habitats in Spain [69]. We also found notable differences in the spatial and temporal distribution of parasites at a local scale. Our results show that parasite species can differ in their distribution and temporal abundance with regard to game management type (sites with red-legged partridge releases and sites without releases). This distribution of parasites may potentially be caused by the effect of large-scale and widespread human activity (releases into the wild of farm-reared birds), as recently reported for the highly invasive lineage SGS1 in passerine birds of the USA [4].

Despite the socioeconomic and conservation relevance of red-legged partridges, there is still very limited knowledge on some pathogens that can threaten their long-term conservation [30,70]. In particular, very few studies are available on avian malaria in this species (a recent review of partridge diseases can be found in [70]) and we were unable to find similar studies based on DNA analyses for this group of parasites. Therefore, we can only compare our results with studies based on the analyses of blood smears. [71] reported an overall prevalence of *Plasmodium relictum* in wild partridge populations from western Spain of between 3.2% and 16.6%, while [72] examined farm-reared partridges from central Spain and found that *Haemoproteus* spp. occurred in 10% of birds. Apart from the few studies carried out in Spain, the occurrence of *Haemoproteus* sp. in *A. rufa* was reported for the first time recently in NW Italy [73].

The high prevalence of *Plasmodium* spp. in our study as compared with previous works may be related to spatial heterogeneity and/or temporal shifts in infestation rates [74], or to differences in the detection power of research protocols (blood smears vs. molecular identification, [48]). In general, the absence or low prevalence of hematozoan recorded in many host species inhabiting open and arid environments has been commonly attributed to a reduced transmission rate of parasites due to the scarcity of suitable vectors in those habitats (review in [75]). However, our findings suggest that the abundance of suitable vectors (Culicidae mosquitoes; [69] should not be a limiting factor for the existence and dispersion of malaria parasites in agricultural habitats, at least in our study area (see also [67] for the Mediterranean island of Sardinia). Higher prevalences of these parasites in birds have been found in areas with elevated summer NDVI (a widely used index of vegetal productivity) at the continental level [65], but our study area has a semi-arid climate with very dry summers and consequently is expected to have a low summer NDVI. Future research should measure the density and the parasites that the (infected) vectors carry to confirm this hypothesis.

The absence of *Haemoproteus* infections in our sample set may be due to the primer sequences being more similar to *Plasmodium* than to *Haemoproteus*, or because *Plasmodium* reaches higher parasitemias than *Haemoproteus* [53]. This is expected if the PCR assays are developed using conserved *Plasmodium* spp. sequences, and hence often preferentially amplify the DNA of parasites of this genus (see [76] for the shortcomings of different PCR assays)

At the local scale of our study, there was compelling evidence of a relationship between releasing activity and parasite infection. The seasonal distribution of parasites in game estates where partridge restocking had occurred differed from that of game estates without releases. In the two sites with releasing activity, parasite prevalence was higher in autumn (when hunters restocked partridge populations) than in spring (when most of the released partridges had been hunted; [77]), while the high frequency of allochthonous host mtDNA haplotypes among the autumn samples confirmed the captive breeding origin of hunted birds [32]. This is consistent with the findings of [30,78], who suggested that partridge releases promote parasite opportunities for infecting wild populations and generating subsequent host-to-host transmission (see also [79]). Most of the released partridges do not survive the first hunting season [39–41], as suggested by the sharp reduction observed in the abundance of hybrids (*A. chukar* haplotypes) after the hunting season in sites with releases, but the overall host-to-host transmission rate would depend on both the survival rate of the released birds and the number of partridges released yearly. In the study area over the years, the mean number of red-legs released in traditional shooting partridge estates was about 8465 birds per season, although in intensive estates, the mean was 21,408 birds, with some estates releasing up to 90,000 birds [80]. Consequently, although the number of survivors was usually very low, the total transmission rate to wild birds could be not negligible. We cannot definitively discard the potential effect of sampling bias between periods, due to the noticeable reticence of hunting managers in allowing sampling from farmed stocks previous to releases. Since we only have data on hunter-harvested birds, one could argue that this handicap may affect the results obtained, as infected birds might be more susceptible to being hunted than uninfected birds. However, the hunting modality used in our study area where long beater rows, often with dogs running ahead, drive the partridges towards another row of shooters, do not necessarily imply selection against weak, infected or low-condition individuals. Rather, the probability of killing a partridge is more related to the ability of the shooter than to the condition of birds.

On the other hand, the parasite assemblage included the presence of two previously described lineages of *Plasmodium* (SGS1 and GRW11), which emphasizes the general idiosyncrasy of these parasite lineages, both geographically and taxonomically (i.e., regarding the broad range of hosts infected [4,54,56,81–83]). Of the eight parasite lineages isolated in partridges, six *Plasmodium* spp. have not been previously detected in avian hosts. This may reflect the limited sampling of avian hosts at our study sites or the specificity for hosts of these lineages.

The prevalence of 'generalist' parasites (Group B) was higher in the two sites with releases than in sites without them, and principally during autumn. In contrast, the prevalence of 'partridge-specific' parasites belonging to Group A (Figure 2) was higher in sites without releases than in sites with releases, and was found in similar proportions in spring and autumn samples. It is plausible that the potential for transmission at different points of the year may differ between different parasite species, although the knowledge on the seasonal variation of prevalences of these parasites is quite limited [84]. For example, the seasonal pattern of prevalence in partridges is clearly different from the two *Plasmodium* species infecting blue tits (*Cyanistes caeruleus*) in UK [85]. The general seasonal pattern seems to be that the prevalence of avian malaria parasites increases during the breeding season in temperate wild bird populations, reaching maximal values during summer and then declining through autumn [84,86], a pattern corroborated by the *P. relictum* data [85]. However, recent work with house sparrows (*Passer domesticus*) in Spain reported a double peak pattern of *Plasmodium* prevalence in spring and autumn [87]. Overall, the most likely explanation for the seasonal pattern we found in partridges is that parasites belonging to Group B (that included generalist lineages) correspond with the parasites harbored by farm-reared partridges that were released into the wild in autumn. Indeed, the distribution of parasites within the two host groups (allochthonous vs. autochthonous mtDNA haplotypes) further supports this hypothesis.

The acquisition of generalist lineages from infected (local) hosts is likely to occur at game bird facilities from local avifauna. Partridges born and bred on farms were often infected by avian malaria before the time of release, especially via host-to-host transmission from passerines that come to farms in high densities to exploit partridge feeders and drinkers (authors, unpublished data). Thus, relocation of farming stocks in distant locations may lead to local differences in parasite composition and specific abundance. An alternative explanation for the higher prevalence of this group of parasites in autumn than in spring in sites with releases is the greater susceptibility of released birds to local parasite lineages once they are in the field. However, when releases occur in the study area (late summer/early autumn) the abundance of suitable vectors in the field should be low (mean temperatures in October averaged 16 °C and minimum temperatures averaged 11 °C). Consequently, at that time, it is more likely that the parasites sampled already existed in the hosts rather than resulting from new infections after releases. The strong decline of Group B prevalence from autumn to spring in game estates with releases may be explained by the disappearance of released birds due to hunting, or to the high natural mortality typical of traditional restocking [40,77].

5. Conclusions

Further work is needed to determine if captive game breeding facilities could be considered as reservoir hosts and foci of malaria parasites, which can potentially spill out to attack new hosts of distant areas via introductions or translocations of infected animals, as the available information is very scarce. Gamebird releasing is a broadly accepted and very common activity in most countries, and the potential effects of parasite introduction into new environments should not be discarded—on the contrary, it should be increasingly considered in evolutionary ecology and conservation biology. A human-induced increase in prevalence or diversification of the parasite community would induce new immune challenges in wild bird populations [88], maybe reducing survival or jeopardizing other host life history traits in new hosts [25,89]. Evidence concerning the effects of blood parasites in wild non-passerine birds is however limited, and in red-legged partridges, completely absent. In light of our results, the potential pathogenic effects of avian malaria parasites in wild partridge populations may be added to the other negative effects of releases for wild host populations [42], such as the spreading of intestinal parasites [28,29], genetic introgression [32,34,90], or over-hunting [77,91]. Given the potential of partridge releases to introduce new avian malaria parasites into wild populations, studies on the pathologic effects of these parasites are urgently needed. Tens of millions of game birds are released yearly in Europe [92], but the use of captive stocks for shooting may be harmful for wild populations of target species and may also cause serious side effects on many non-target sympatric avian species [93].

Author Contributions: Conceptualization, J.T.G., F.C. and J.V.; Fieldwork, F.C., D.V.; Laboratory work, J.T.G., I.S.S.-B., M.C.-R., statistics and analysis, J.T.G.; writing—original draft preparation, J.T.G.; writing—review and editing, all authors; funding acquisition, J.V. All authors have read and agreed to the published version of the manuscript.

Funding: This research was funded by the Spanish Ministry for Science and Innovation (CYCIT project CGL2004-06147-CO2/BOS), and by Junta de Comunidades de Castilla-La Mancha (JCCM) projects PAC06-0137-2179, and PII1C09-0128-4724.

Institutional Review Board Statement: This study was made following the Spanish Ministry for Science and Innovation and the University of Castilla–La Mancha Ethics Committee regulations.

Informed Consent Statement: Not applicable.

Data Availability Statement: Not applicable.

Acknowledgments: We are very grateful to the game managers for permission to work in their hunting lands. Salvador Luna provided technical support during fieldwork. F.C. was supported by a Torres Quevedo contract (PTQ-17-09549) co-funded by the Ministerio de Economía, Industria y Competitividad while writing this paper.

Conflicts of Interest: The authors declare no conflict of interest.

References

1. Palumbi, S.R. Humans as the World's Greatest Evolutionary Force. *Science* **2001**, *293*, 1786–1790. [CrossRef]
2. Bell, G.; Collins, S. Adaptation, Extinction and Global Change. *Evol. Appl.* **2008**, *1*, 3–16. [CrossRef] [PubMed]
3. Cable, J.; Barber, I.; Boag, B.; Ellison, A.R.; Morgan, E.R.; Murray, K.; Pascoe, E.L.; Sait, S.M.; Wilson, A.J.; Booth, M. Global Change, Parasite Transmission and Disease Control: Lessons from Ecology. *Philos. Trans. R. Soc. B Biol. Sci.* **2017**, *372*, 20160088. [CrossRef] [PubMed]
4. Theodosopoulos, A.N.; Grabenstein, K.C.; Bensch, S.; Taylor, S.A. A Highly Invasive Malaria Parasite Has Expanded Its Range to Non-Migratory Birds in North America. *Biol. Lett.* **2021**, *17*, 20210271. [CrossRef]
5. Cunningham, A. Disease Risks of Wildlife Translocations. *Conserv. Biol.* **1996**, *10*, 349–353. [CrossRef]
6. Fessl, B.; Kleindorfer, S.; Tebbich, S. An Experimental Study on the Effects of an Introduced Parasite in Darwin's Finches. *Biol. Conserv.* **2006**, *127*, 55–61. [CrossRef]
7. Miura, O.; Torchin, M.; Kuris, A.; Hechinger, R.; Chiba, S. Introduced Cryptic Species of Parasites Exhibit Different Invasion Pathways. *Proc. Natl. Acad. Sci. USA* **2006**, *103*, 19818. [CrossRef]
8. Shakman, E.; Kinzelbach, R.; Trilles, J.; Bariche, M. First Occurrence of Native Cymothoids Parasites on Introduced Rabbitfishes in the Mediterranean Sea. *Acta Parasitol.* **2009**, *54*, 380–384. [CrossRef]
9. Díaz-Sánchez, S.; Moriones, A.M.; Casas, F.; Höfle, U. Prevalence of *Escherichia Coli*, *Salmonella* sp. and *Campylobacter* sp. in the Intestinal Flora of Farm-Reared, Restocked and Wild Red-Legged Partridges (*Alectoris rufa*): Is Restocking Using Farm-Reared Birds a Risk? *Eur. J. Wildl. Res.* **2012**, *58*, 99–105. [CrossRef]
10. Welchman, D. Diseases in Gamebirds: An Update. *Practice* **2016**, *38*, 189–192. [CrossRef]
11. Daszak, P.; Cunningham, A.; Hyatt, A. Emerging Infectious Diseases of Wildlife—Threats to Biodiversity and Human Health. *Science* **2000**, *287*, 443. [CrossRef]
12. Cunningham, A.A.; Daszak, P.; Wood, J.L. One Health, Emerging Infectious Diseases and Wildlife: Two Decades of Progress? *Philos. Trans. R. Soc. B Biol. Sci.* **2017**, *372*, 20160167. [CrossRef] [PubMed]
13. Cooper, J. Historical Survey of Disease in Birds. *J. Zoo Wildl. Med.* **1993**, *24*, 256–264.
14. Burdon, J.; Thrall, P. Pathogen Evolution across the Agro-Ecological Interface: Implications for Disease Management. *Evol. Appl.* **2008**, *1*, 57–65. [CrossRef]
15. Keim, P.; Wagner, D. Humans and Evolutionary and Ecological Forces Shaped the Phylogeography of Recently Emerged Diseases. *Nat. Rev. Microbiol.* **2009**, *7*, 813–821. [CrossRef]
16. Keatts, L.O.; Robards, M.; Olson, S.H.; Hueffer, K.; Insley, S.J.; Joly, D.O.; Kutz, S.; Lee, D.S.; Chetkiewicz, C.-L.B.; Lair, S.; et al. Implications of Zoonoses from Hunting and Use of Wildlife in North American Arctic and Boreal Biomes: Pandemic Potential, Monitoring, and Mitigation. *Front. Public Health* **2021**, *9*, 451. [CrossRef] [PubMed]
17. Dobson, A. Restoring Island Ecosystems: The Potential of Parasites to Control Introduced Mammals. *Conserv. Biol.* **1988**, *2*, 31–39. [CrossRef]
18. Torchin, M.; Lafferty, K.; Kuris, A. Release from Parasites as Natural Enemies: Increased Performance of a Globally Introduced Marine Crab. *Biol. Invasions* **2001**, *3*, 333–345. [CrossRef]
19. Torchin, M.E.; Lafferty, K.D.; Dobson, A.P.; McKenzie, V.J.; Kuris, A.M. Introduced Species and Their Missing Parasites. *Nature* **2003**, *421*, 628–630. [CrossRef]
20. Smith, K.; Carpenter, S. Potential Spread of Introduced Black Rat (*Rattus rattus*) Parasites to Endemic Deer Mice (*Peromyscus maniculatus*) on the California Channel Islands. *Divers. Distrib.* **2006**, *12*, 742–748. [CrossRef]
21. Lindahl, J.F.; Grace, D. The Consequences of Human Actions on Risks for Infectious Diseases: A Review. *Infect. Ecol. Epidemiol.* **2015**, *5*, 30048. [CrossRef] [PubMed]
22. Atkinson, C.; van Riper, C., III. Pathogenicity and Epizootiology of Avian Haematozoa: *Plasmodium*, *Leucocytozoon*, and *Haemoproteus*. In *Bird-Parasite Interactions. Ecology, Evolution, and Behavior*; Oxford University Press: London, UK, 1991; pp. 19–48.
23. Valkiunas, G. Pathogenic Influence of Haemosporidians and Trypanosomes on Wild Birds in the Field Conditions: Facts and Hypotheses. *Ekologija* **1993**, *1*, 47–60.
24. Merino, S.; Moreno, J.; Sanz, J.; Arriero, E. Are Avian Blood Parasites Pathogenic in the Wild? A Medication Experiment in Blue Tits (*Parus caeruleus*). *Proc. R. Soc. B Biol. Sci.* **2000**, *267*, 2507. [CrossRef] [PubMed]
25. Dadam, D.; Robinson, R.A.; Clements, A.; Peach, W.J.; Bennett, M.; Rowcliffe, J.M.; Cunningham, A.A. Avian Malaria-Mediated Population Decline of a Widespread Iconic Bird Species. *R. Soc. Open Sci.* **2019**, *6*, 182197. [CrossRef]
26. Benkman, C.; Siepielski, A.; Parchman, T. The Local Introduction of Strongly Interacting Species and the Loss of Geographic Variation in Species and Species Interactions. *Mol. Ecol.* **2008**, *17*, 395–404. [CrossRef] [PubMed]
27. Smith, T.; Bernatchez, L. Evolutionary Change in Human-Altered Environments. *Mol. Ecol.* **2008**, *17*, 1–8. [CrossRef]

28. Villanua, D.; Perez-Rodriguez, L.; Casas, F.; Alzaga, V.; Acevedo, P.; Vinuela, J.; Gortazar, C. Sanitary Risks of Red-Legged Partridge Releases: Introduction of Parasites. *Eur. J. Wildl. Res.* **2008**, *54*, 199–204. [CrossRef]
29. Millan, J.; Gortazar, C.; Villafuerte, R. A Comparison of the Helminth Faunas of Wild and Farm-Reared Red-Legged Partridge. *J. Wildl. Manag.* **2004**, *68*, 701–707. [CrossRef]
30. Millán, J. Diseases of the Red-Legged Partridge (*Alectoris rufa* L.): A Review. *Wildl. Biol. Pract.* **2009**, *5*, 70–88. [CrossRef]
31. Gortázar, C.; Acevedo, P.; Ruiz-Fons, F.; Vicente, J. Disease Risks and Overabundance of Game Species. *Eur. J. Wildl. Res.* **2006**, *52*, 81–87. [CrossRef]
32. Blanco Aguiar, J.; Gonzalez-Jara, P.; Ferrero, M.; Sanchez Barbudo, I.; Virgós, E.; Villafuerte, R.; Dávila, J. Assessment of Game Restocking Contributions to Anthropogenic Hybridization: The Case of the Iberian Red Legged Partridge. *Anim. Conserv.* **2008**, *11*, 535–545. [CrossRef]
33. Randi, E. Detecting Hybridization between Wild Species and Their Domesticated Relatives. *Mol. Ecol.* **2008**, *17*, 285–293. [CrossRef] [PubMed]
34. Barbanera, F.; Pergams, O.R.W.; Guerrini, M.; Forcina, G.; Panayides, P.; Dini, F. Genetic Consequences of Intensive Management in Game Birds. *Biol. Conserv.* **2010**, *143*, 1259–1268. [CrossRef]
35. Farfán, M.A.; Duarte, J.; Meriggi, L.R.; Viñuela, J.V.; Vargas, J.M. The red-legged Partridge: A historical overview on distribution, status, research and hunting. In *The Future of the Red-Legged Partridge: Science, Hunting and Conservation*; Wildlife Research Monographs; Springer International: Cham, Switzerland, 2022.
36. Aebischer, N.; Potts, G. Red-Legged Partridge (*Alectoris rufa*). In *Birds in Europe: Their Conservation Status*; BirdLife International: Cambridge, UK, 1994.
37. BirdLife International. Birdlife Species Factsheet: Alectoris rufa. Available online: http://www.birdlife.org (accessed on 2 November 2021).
38. Garrido, J.L. Capturas de Perdiz Roja (Economía Inducida Por La Caza de Perdiz). In *Aportaciones a la Gestión Sostenible de la Caza*; Fedenca: Madrid, Spain, 2002; Volume I, pp. 141–147.
39. Duarte, J.; Vargas, J. Field Interbreeding of Released Farm-Reared Red-Legged Partridges (*Alectoris rufa*) with Wild Ones. *Game Wildl. Sci.* **2004**, *21*, 55–61.
40. Gortázar, C.; Villafuerte, R.; Martín, M. Success of Traditional Restocking of Red-Legged Partridge for Hunting Purposes in Areas of Low Density of Northeast Spain Aragón. *Z. Jagdwiss.* **2000**, *46*, 23–30. [CrossRef]
41. Alonso, M.; Pèrez, J.; Gaudioso, V.; Diez, C.; Prieto, R. Study of Survival, Dispersal and Home Range of Autumn-Released Red-Legged Partridges (*Alectoris rufa*). *Br. Poult. Sci.* **2005**, *46*, 401–406. [CrossRef]
42. Sánchez-García, C.; Sokos, C.; Santilli, F.; Ponce, F.; Sagel, R.B.; Bro, E.; Buner, F.D. Enough Reared Red-Legs for Today, but Fewer Wild Ones for Tomorrow? The Dilemma of Gamebird Rearing and Releasing. In *The Future of the Red-Legged Partridge: Science, Hunting and Conservation*; Wildlife Research Monographs; Springer International: Cham, Switzerland, 2022.
43. Kruse, H.; Kirkemo, A.-M.; Handeland, K. Wildlife as Source of Zoonotic Infections. *Emerg. Infect. Dis.* **2004**, *10*, 2067. [CrossRef]
44. Negro, J.; Torres, M.; Godoy, J. RAPD Analysis for Detection and Eradication of Hybrid Partridges (*Alectoris rufa* A. Graeca) in Spain. *Biol. Conserv.* **2001**, *98*, 19–24. [CrossRef]
45. Casas, F.; Mougeot, F.; Ferrero, M.E.; Sánchez-Barbudo, I.; Dávila, J.A.; Viñuela, J. Phenotypic Differences in Body Size, Body Condition and Circulating Carotenoids between Hybrid and "Pure" Red-Legged Partridges (*Alectoris rufa*) in the Wild. *J. Ornithol.* **2013**, *154*, 803–811. [CrossRef]
46. Bogojević, M.S.; Merdić, E.; Bogdanović, T. The Flight Distances of Floodwater Mosquitoes (*Aedes vexans*, *Ochlerotatus sticticus* and *Ochlerotatus caspius*) in Osijek, Eastern Croatia. *Biologia* **2011**, *66*, 678–683. [CrossRef]
47. Casas, F.; Viñuela, J. Agricultural Practices or Game Management: Which Is the Key to Improve Red-Legged Partridge Nesting Success in Agricultural Landscapes? *Environ. Conserv.* **2010**, *37*, 177–186. [CrossRef]
48. Waldenström, J.; Bensch, S.; Hasselquist, D.; Östman, Ö. A New Nested Polymerase Chain Reaction Method Very Efficient in Detecting Plasmodium and Haemoproteus Infections from Avian Blood. *J. Parasitol.* **2004**, *90*, 191–194. [CrossRef] [PubMed]
49. Thompson, J.D.; Higgins, D.G.; Gibson, T.J. CLUSTAL W: Improving the Sensitivity of Progressive Multiple Sequence Alignment through Sequence Weighting, Position-Specific Gap Penalties and Weight Matrix Choice. *Nucleic Acids Res.* **1994**, *22*, 4673. [CrossRef]
50. Hall, T.A. BioEdit: A User-Friendly Biological Sequence Alignment Editor and Analysis Program for Windows 95/98/NT. *Nucleic Acids Symp. Ser.* **1999**, *41*, 95–98.
51. Bensch, S.; Pèarez-Tris, J.; Waldenströum, J.; Hellgren, O. Linkage between Nuclear and Mitochondrial DNA Sequences in Avian Malaria Parasites: Multiple Cases of Cryptic Speciation? *Evolution* **2004**, *58*, 1617–1621. [CrossRef]
52. Perez-Tris, J.; Bensch, S. Diagnosing Genetically Diverse Avian Malarial Infections Using Mixed-Sequence Analysis and TA-Cloning. *Parasitology* **2005**, *131*, 15–23. [CrossRef]
53. Ciloglu, A.; Ellis, V.A.; Bernotienė, R.; Valkiūnas, G.; Bensch, S. A New One-Step Multiplex PCR Assay for Simultaneous Detection and Identification of Avian Haemosporidian Parasites. *Parasitol. Res.* **2019**, *118*, 191–201. [CrossRef]
54. Waldenström, J.; Bensch, S.; Kiboi, S.; Hasselquist, D.; Ottosson, U. Cross-Species Infection of Blood Parasites between Resident and Migratory Songbirds in Africa. *Mol. Ecol.* **2002**, *11*, 1545–1554. [CrossRef]

55. Njabo, K.Y.; Cornel, A.J.; Bonneaud, C.; Toffelmier, E.; Sehgal, R.N.M.; Valkiūnas, G.; Russell, A.F.; Smith, T.B. Nonspecific Patterns of Vector, Host and Avian Malaria Parasite Associations in a Central African Rainforest. *Mol. Ecol.* **2011**, *20*, 1049–1061. [CrossRef]
56. Bensch, S.; Hellgren, O.; Pérez-Tris, J. MalAvi: A Public Database of Malaria Parasites and Related Haemosporidians in Avian Hosts Based on Mitochondrial Cytochrome b Lineages. *Mol. Ecol. Resour.* **2009**, *9*, 1353–1358. [CrossRef]
57. Bouckaert, R.; Vaughan, T.G.; Barido-Sottani, J.; Duchêne, S.; Fourment, M.; Gavryushkina, A.; Heled, J.; Jones, G.; Kühnert, D.; De Maio, N.; et al. BEAST 2.5: An Advanced Software Platform for Bayesian Evolutionary Analysis. *PLoS Comput. Biol.* **2019**, *15*, e1006650. [CrossRef]
58. Darriba, D.; Taboada, G.L.; Doallo, R.; Posada, D. JModelTest 2: More Models, New Heuristics and Parallel Computing. *Nat. Methods* **2012**, *9*, 772. [CrossRef] [PubMed]
59. Rambaut, A.; Drummond, A.J.; Xie, D.; Baele, G.; Suchard, M.A. Posterior Summarization in Bayesian Phylogenetics Using Tracer 1.7. *Syst. Biol.* **2018**, *67*, 901. [CrossRef] [PubMed]
60. Rambaut, A.; Drummond, A.J. *LogCombiner, Version 2.3.0*; Part of the BEAST Package; University of Auckland: Auckland, New Zealand, 2014.
61. Rambaut, A.; Drummond, A. *TreeAnnotator*, version 2.4.3; BEAST Package. 2016.
62. Sorenson, M.; Ast, J.; Dimcheff, D.; Yuri, T.; Mindell, D. Primers for a PCR-Based Approach to Mitochondrial Genome Sequencing in Birds and Other Vertebrates. *Mol. Phylogenetics Evol.* **1999**, *12*, 105–114. [CrossRef]
63. Swofford, D. *PAUP*. Phylogenetic Analysis Using Parsimony (* and Other Methods), version 4*; Sinauer Associates: Sunderland, MA, USA, 2002.
64. StatSoft Inc. *STATISTICA (Data Analysis Software System), version 8.0*; StatSoft: Tulsa, OK, USA, 2008.
65. Clark, N.J.; Drovetski, S.V.; Voelker, G. Robust Geographical Determinants of Infection Prevalence and a Contrasting Latitudinal Diversity Gradient for Haemosporidian Parasites in Western Palearctic Birds. *Mol. Ecol.* **2020**, *29*, 3131–3143. [CrossRef] [PubMed]
66. Muriel, J.; Marzal, A.; Magallanes, S.; García-Longoria, L.; Suarez-Rubio, M.; Bates, P.J.; Lin, H.H.; Soe, A.N.; Oo, K.S.; Aye, A.A.; et al. Prevalence and Diversity of Avian Haemosporidians May Vary with Anthropogenic Disturbance in Tropical Habitats in Myanmar. *Diversity* **2021**, *13*, 111. [CrossRef]
67. Pellegrino, I.; Ilahiane, L.; Boano, G.; Cucco, M.; Pavia, M.; Prestridge, H.L.; Voelker, G. Avian Haemosporidian Diversity on Sardinia: A First General Assessment for the Insular Mediterranean. *Diversity* **2021**, *13*, 75. [CrossRef]
68. Schumm, Y.R.; Bakaloudis, D.; Barboutis, C.; Cecere, J.G.; Eraud, C.; Fischer, D.; Hering, J.; Hillerich, K.; Lormée, H.; Mader, V.; et al. Prevalence and Genetic Diversity of Avian Haemosporidian Parasites in Wild Bird Species of the Order Columbiformes. *Parasitol. Res.* **2021**, *120*, 1405–1420. [CrossRef]
69. Jiménez-Peñuela, J.; Ferraguti, M.; Martínez-de la Puente, J.; Soriguer, R.C.; Figuerola, J. Urbanization Effects on Temporal Variations of Avian Haemosporidian Infections. *Environ. Res.* **2021**, *199*, 111234. [CrossRef]
70. Díaz-Sánchez, S.; Höfle, U.; Villanúa, D.; Gortázar, C. Health Monitoring and Disease Control in Red-Legged Partridges. In *The Future of the Red-Legged Partridge: Science, Hunting and Conservation*; Wildlife Research Monographs; Springer International: Cham, Switzerland, 2022.
71. Encinas, A. *Plasmodium relictum* y *P. cathemerium* en aves del area salmantina. *Rev. Ibérica Parasitol.* **1982**, *42*, 289–306.
72. Millán, J.; Gortazar, C.; Villafuerte, R. First Record of Haemoproteus sp. Parasiting Red-Legged Partridges (Alectoris rufa). In Proceedings of the European Association of Zoo and Wildlife Veterinarians (EAZWV) 4th Scientific Meeting, Joint with the Annual Meeting of the European Wildlife Disease Association (EWDA), Heidelberg, Germany, 8–12 May 2002.
73. Tizzani, P.; Fanelli, A.; Negri, E.; Silvano, F.; Menzano, A.; Molinar, A.; Meneguz, P.G. Haemoparasites in Red-Legged Partridge (*Alectoris rufa*): First Record of *Haemoproteus* sp. in Italy? *J. Parasit. Dis.* **2020**, *44*, 462–466. [CrossRef]
74. Fecchio, A.; Clark, N.J.; Bell, J.A.; Skeen, H.R.; Lutz, H.L.; De La Torre, G.M.; Vaughan, J.A.; Tkach, V.V.; Schunck, F.; Ferreira, F.C.; et al. Global Drivers of Avian Haemosporidian Infections Vary across Zoogeographical Regions. *Glob. Ecol. Biogeogr.* **2021**, *30*, 2393–2406. [CrossRef]
75. Martínez-Abraín, A.; Esparza, B.; Oro, D. Lack of Blood Parasites in Bird Species: Does Absence of Blood Parasite Vectors Explain It All? *Ardeola* **2004**, *51*, 225–232.
76. Bernotienė, R.; Palinauskas, V.; Iezhova, T.; Murauskaitė, D.; Valkiūnas, G. Avian Haemosporidian Parasites (Haemosporida): A Comparative Analysis of Different Polymerase Chain Reaction Assays in Detection of Mixed Infections. *Exp. Parasitol.* **2016**, *163*, 31–37. [CrossRef]
77. Casas, F.; Arroyo, B.; Viñuela, J.; Guzmán, J.L.; Mougeot, F. Are Farm-Reared Red-Legged Partridge Releases Increasing Hunting Pressure on Wild Breeding Partridges in Central Spain? *Eur. J. Wildl. Res.* **2016**, *62*, 79–84. [CrossRef]
78. Villanúa, D.; Casas, F.; Viñuela, J.; Gortázar, C.; de la Morena, E.L.G.; Morales, M. First Occurrence of *Eucoleus contortus* in a Little Bustard *Tetrax tetrax*: Negative Effect of Red-Legged Partridge *Alectoris rufa* Releases on Steppe Bird Conservation? *Ibis* **2007**, *149*, 405–406. [CrossRef]
79. Gortázar, C.; Ferroglio, E.; Höfle, U.; Frölich, K.; Vicente, J. Diseases Shared between Wildlife and Livestock: A European Perspective. *Eur. J. Wildl. Res.* **2007**, *53*, 241–256. [CrossRef]
80. Caro, J.; Delibes-Mateos, M.; Vicente, J.; Arroyo, B. A Quantitative Assessment of the Release of Farm-Reared Red-Legged Partridges (*Alectoris rufa*) for Shooting in Central Spain. *Eur. J. Wildl. Res.* **2014**, *60*, 919–926. [CrossRef]

81. Hellgren, O.; Kriûanauskiene, A.; Valkiūnas, G.; Bensch, S. Diversity and Phylogeny of Mitochondrial Cytochrome B Lineages from Six Morphospecies of Avian Haemoproteus (Haemosporida: Haemoproteidae). *J. Parasitol.* **2007**, *93*, 889–896. [CrossRef]
82. Beadell, J.; Ishtiaq, F.; Covas, R.; Melo, M.; Warren, B.; Atkinson, C.; Bensch, S.; Graves, G.; Jhala, Y.; Peirce, M.; et al. Global Phylogeographic Limits of Hawaii's Avian Malaria. *Proc. R. Soc. B Biol. Sci.* **2006**, *273*, 2935. [CrossRef]
83. Dimitrov, D.; Zehtindjiev, P.; Bensch, S. Genetic Diversity of Avian Blood Parasites in SE Europe: Cytochrome B Lineages of the Genera Plasmodium and Haemoproteus (Haemosporida) from Bulgaria. *Acta Parasitol.* **2010**, *55*, 201–209. [CrossRef]
84. Huang, X.; Jönsson, J.; Bensch, S. Persistence of Avian Haemosporidians in the Wild: A Case Study to Illustrate Seasonal Infection Patterns in Relation to Host Life Stages. *Int. J. Parasitol.* **2020**, *50*, 611–619. [CrossRef] [PubMed]
85. Cosgrove, C.; Wood, M.; Day, K.; Sheldon, B. Seasonal Variation in Plasmodium Prevalence in a Population of Blue Tits *Cyanistes caeruleus*. *J. Anim. Ecol.* **2008**, *77*, 540–548. [CrossRef] [PubMed]
86. Valkiunas, G. *Avian Malaria Parasites and Other Haemosporidia*; CRC Press: Boca Raton, FL, USA, 2005; ISBN 0-415-30097-5.
87. Neto, J.M.; Mellinger, S.; Halupka, L.; Marzal, A.; Zehtindjiev, P.; Westerdahl, H. Seasonal Dynamics of Haemosporidian (Apicomplexa, Haemosporida) Parasites in House Sparrows *Passer domesticus* at Four European Sites: Comparison between Lineages and the Importance of Screening Methods. *Int. J. Parasitol.* **2020**, *50*, 523–532. [CrossRef]
88. De Roode, J.; Read, A. Evolution and Ecology, after the Malaria Genomes. *Trends Ecol. Evol.* **2003**, *18*, 60–61. [CrossRef]
89. McClure, K.M.; Fleischer, R.C.; Kilpatrick, A.M. The Role of Native and Introduced Birds in Transmission of Avian Malaria in Hawaii. *Ecology* **2020**, *101*, e03038. [CrossRef]
90. Casas, F.; Mougeot, F.; Sánchez-Barbudo, I.; Dávila, J.A.; Viñuela, J. Fitness consequences of anthropogenic hybridization in wild red-legged partridge (*Alectoris rufa*, *Phasianidae*) populations. *Biol. Invasions* **2012**, *14*, 295–305. [CrossRef]
91. Keane, A.; Brooke, M.; McGowan, P. Correlates of Extinction Risk and Hunting Pressure in Gamebirds (Galliformes). *Biol. Conserv.* **2005**, *126*, 216–233. [CrossRef]
92. Viñuela, J.; Arroyo, B. *Gamebird Hunting and Biodiversity Conservation: Synthesis, Recommendations and Future Research Priorities*; CSIC-UCLM-Instituto de Investigación en Recursos Cinegéticos (IREC): Brussels, Belgium, 2002.
93. Mustin, K.; Arroyo, B.; Beja, P.; Newey, S.; Irivine, R.J.; Kestler, J.; Redpath, S.M. Consequences of Game Bird Management for Non-game Species in Europe. *J. Appl. Ecol.* **2018**, *55*, 2285–2295. [CrossRef]

diversity

MDPI

Article

Bigger Is Better, Sometimes: The Interaction between Body Size and Carcass Size Determines Fitness, Reproductive Strategies, and Senescence in Two Species of Burying Beetles

Mark C. Belk [1,*], Peter J. Meyers [1,2] and J. Curtis Creighton [3]

[1] Department of Biology, Brigham Young University, Provo, UT 84602, USA; pmeyers85@gmail.com
[2] Department of Biology, Grinnell College, Grinnell, IA 50112, USA
[3] Department of Biological Sciences, Purdue University Northwest, Hammond, IN 46323, USA; Creighto@pnw.edu
* Correspondence: mark_belk@byu.edu

Abstract: The cost of reproduction hypothesis suggests that allocation to current reproduction constrains future reproduction. How organisms accrue reproductive costs and allocate energy across their lifetime may differ among species adapted to different resource types. We test this by comparing lifetime reproductive output, patterns of reproductive allocation, and senescence between two species of burying beetles, *Nicrophorus marginatus* and *N. guttula,* that differ in body size, across a range of carcass sizes. These two species of burying beetles maximized lifetime reproductive output on somewhat different–sized resources. The larger *N. marginatus* did better on large and medium carcasses while the smaller *N. guttula* did best on small and medium carcasses. For both species, reproduction is costly and reproduction on larger carcasses reduced lifespan more than reproduction on smaller carcasses. Carcass size also affected lifetime reproductive strategies. Each species' parental investment patterns were consistent with terminal investment on carcasses on which they performed best (optimal carcass sizes). However, they exhibited reproductive restraint on carcass sizes on which they did not perform as well. Reproductive senescence occurred largely in response to carcass size. For both species, reproduction on larger carcasses resulted in more rapid senescence. These data suggest that whether organisms exhibit terminal investment or reproductive restraint may depend on type and amount of resources for reproduction.

Keywords: senescence; reproductive allocation; terminal investment; reproductive restraint; resource availability

Citation: Belk, M.C.; Meyers, P.J.; Creighton, J.C. Bigger Is Better, Sometimes: The Interaction between Body Size and Carcass Size Determines Fitness, Reproductive Strategies, and Senescence in Two Species of Burying Beetles. *Diversity* **2021**, *13*, 662. https://doi.org/10.3390/d13120662

Academic Editor: Michael Wink

Received: 24 November 2021
Accepted: 10 December 2021
Published: 11 December 2021

1. Introduction

For iteroparous organisms, fitness is maximized through balancing current reproductive effort with future reproductive opportunities [1]. When an organism allocates resources to current reproduction, that energy is unavailable for somatic maintenance, growth, or future reproduction. Because of this tradeoff, organisms are expected to balance current and future reproduction to maximize total lifetime reproductive output [2–5]. As individuals age, this balance between current and future reproduction shifts, which potentially causes a change in how they allocate resources for reproduction. Two general patterns of reproductive resource allocation have been predicted. First, older individuals invest terminally in reproduction because future opportunities are unlikely (the terminal investment hypothesis [6]). Second, individuals decrease investment in reproduction as they age to increase the likelihood of additional breeding opportunities (reproductive restraint hypothesis [7]). However, it is not clear under what circumstances selection will favor one or the other of these allocation strategies.

Inherent in the tradeoff between current and future reproduction is the cost of reproduction and the onset of senescence [1]. As a consequence of patterns of reproductive

allocation and aging, organisms experience variation in the rate of senescence [6,7]. Reproduction at an early age and high levels of allocation typically lead to earlier onset of senescence; whereas, later reproduction and decreased allocation to reproduction results in delayed senescence [8]. In addition to the timing and level of allocation to reproduction, availability and type of resources for consumption can influence onset and rates of senescence [9]. How resource type and availability interacts with patterns of reproductive allocation to modify onset and rates of senescence is less well studied.

Organisms are adapted to use specific types of resources for reproduction, and the type and quantity of resources available may determine how an organism allocates to reproduction over a lifetime and the resulting rate of senescence. Optimal resource type and availability should result in maximization of fitness measured as number of offspring over a lifetime. Availability of optimal resources may ameliorate the tradeoff inherent in the cost of reproduction hypothesis and allow allocation of energy to both current and future reproduction [9] while delaying senescence. Conversely, optimal resources for reproduction may require additional effort to acquire and process, as well as defend from competitors [10]. As such, optimal resources for reproduction may come with additional costs of acquisition that are not embodied in the traditional current versus future reproduction tradeoff. Thus, it is unclear how resource type and availability affect reproductive allocation and senescence, and strategies of allocation may depend on matching between species–specific adaptations and type and availability of resources.

Can adaptation to specific resource types and the availability of those types influence the way individuals allocate to reproduction and experience senescence across their lifetime? Patterns indicative of terminal investment [11–22] and reproductive restraint [11,12,14,20–28] have been documented in several taxa. Some taxa may exhibit both patterns as either a direct or indirect response to environmental conditions [8]. For instance, in the burying beetle, *N. orbicollis*, females exhibited terminal investment patterns on larger carcasses, but not on smaller carcasses [15], and the degree to which terminal investment occurs in this species was dependent on previous reproductive experience [12]. Male mealworm beetles (*Tenebrio molitor*) changed reproductive strategies depending on the availability of food; they exhibited terminal investment in the absence of food, and were more restrained in reproduction when food resources were readily available [19]. Different populations of alpine chamois (*Rupicapra rupicapra*) showed patterns consistent with both terminal investment and reproductive restraint; males in two populations had smaller reproductive effort late in life (suggesting restraint), while males in a third population had greater reproductive effort late in life (suggesting terminal investment [20]). Taken together, these studies suggest that the pattern of reproductive allocation over a lifetime may depend on the availability of optimal resources for reproduction. In conditions where optimal resources are rare or not available, organisms may exhibit reproductive restraint to maximize reproductive lifetime; whereas, under conditions where optimal resources are available, organisms will exhibit terminal investment [29,30]. Thus, type and availability of resources may account for some of the wide variation in observed patterns of reproductive allocation within and among species.

Burying beetles (genus *Nicrophorus*) are model organisms for studies of reproductive allocation over a lifetime and senescence because of their use of discrete, quantifiable resources in reproduction, and their ease of manipulation in the laboratory. Burying beetles reproduce exclusively on small vertebrate carcasses where they provision offspring through post–hatching parental care [31]. Reproductive allocation is unambiguous because both adults and offspring feed on the same carcass, and thus the number of offspring represents allocation to current reproduction and the change in mass of the resident parents represents allocation to future reproduction [15]. Burying beetles can use a range of carcass sizes from only a few grams to several hundred grams and brood size and offspring body size typically increase with carcass size. Thus, for burying beetles, carcass size represents a quantifiable measure of resource quality [10,32,33]. Typically, larger species are reproductively more successful on larger carcasses, while smaller species are reproductively more successful

on smaller carcasses [10]. Because of their ability to breed on a range of carcass sizes, and the range of body sizes found among species of burying beetles, we can use them to experimentally determine optimal carcass sizes for each species and then evaluate effects of carcass size on lifetime patterns of reproductive allocation and senescence.

In this paper, we compare two species of burying beetles to address two fundamental questions about reproductive allocation and reproductive senescence and the relationship to carcass size. First, are species adapted to specific carcass sizes as measured by the lifetime number of offspring produced, or are bigger carcasses always better for maximizing the number of offspring over a lifetime? For burying beetles, we predict that optimal carcass size (i.e., the size that results in the greatest number of offspring over a lifetime) should scale with body size of the beetle; thus, optimal carcass size should be larger for larger–bodied species. Second, do burying beetles that are reproducing on optimal carcass sizes exhibit a different pattern of reproductive allocation over a lifetime compared with those reproducing on non–optimal carcass sizes? Specifically, we predict that beetles reproducing on optimal carcass sizes will engage in terminal investment strategies and experience earlier reproductive senescence, and beetles reproducing on non–preferred carcass sizes will engage in reproductive restraint and experience delayed reproductive senescence. We test these predictions by comparing reproductive allocation and patterns of reproductive output between two species of burying beetles, *N. marginatus* and *N. guttula*, across a range of carcass sizes. We chose these two species because they are phylogenetically similar (*N. marginatus* is the outgroup to the sister species *N. guttula* and *N. obscurus* [34]): they overlap in their distribution and co–occur in the same habitats [35,36]; however, they differ somewhat in body size in the wild (*N. marginatus* mean pronotum width: 6.75, SE = 0.06, n = 232; *N. guttula* mean pronotum width: 6.07, SE = 0.07, n = 116; A. N. Smith, unpublished data from populations in this study).

2. Materials and Methods

2.1. Burying Beetle Natural History

Burying beetles locate small vertebrate carcasses and use them as food resources for themselves and their offspring. Males and females compete with individuals of the same sex until a single pair, typically those with the largest body sizes, dominate the carcass [37,38]. Similar to within species competitive dynamics, larger species will displace smaller species when they co–occur on a carcass [10,31]. The winning pair of beetles buries the carcass under the soil, removes the feathers or hair, shapes the carcass into a ball, and coats it with oral and anal secretions that help prevent microbial growth. During carcass preparation, the female lays eggs in the soil, and larvae usually hatch on or after the fourth day. Parents adjust brood size through filial cannibalism, regurgitate food to newly hatched larvae, and provide defense of the carcass and larvae from conspecifics. Parental care continues until larvae disperse into the soil to pupate [31].

2.2. Experimental Design

We collected both *N. marginatus* and *N. guttula* at Goshen Ponds (39°57.476′ N, 111°51.426′ W) and Utah Lake Wetland Preserve (40°6.933′ N, 111°47.589′ W) in central Utah during June 2011 and July 2012 using pitfall traps baited with aged chicken. We transported beetles back to Brigham Young University and established laboratory populations for each species by breeding wild–caught pairs on a 30 g carcass. We kept newly eclosed offspring in small plastic containers (11.3 cm L × 7.6 cm W × 5.7 cm H), provided them ad libidum raw chicken liver, and maintained them on a 14L:10D cycle (a natural photoperiod for the summer breeding season at the source location). Beetles used in this experiment were F1, F2, and F3 individuals, and all crosses used different family lines to ensure no inbreeding occurred.

At 28 days (±1 day) from eclosion, we randomly assigned females from both species to one of six carcass size treatments and one nonreproductive treatment (12 replicates for each treatment for a total of 84 females of each species). In six of the treatments, we allowed

females to reproduce throughout their lifetime on one of six carcass sizes (5 g, 10 g, 20 g, 30 g, 40 g, or 50 g, ±1.0 g lab mouse carcasses; this range in size covers the range of carcass sizes available in the natural environment). For each reproductive bout, we placed each female with a virgin male (at least 21 days old, to ensure sexual maturity) on a carcass of their assigned size in a plastic container (20.3 cm L × 15.2 cm W × 9.8 cm H) filled with approximately 4.5 cm (depth) of commercially purchased topsoil and allowed them to reproduce. After 48 h, we removed males from the carcass to isolate the reproductive investment patterns of females (males were present only during the beginning of the carcass preparation phase). At the end of each reproductive attempt (defined as the point when all larvae dispersed from the carcass into the soil), we removed the females, placed them each in a small, individual container, and provided them with a moistened paper towel for water and chicken liver ad libidum. After 48 h, we placed females on a new carcass (of the same size as their previous reproductive attempt) with a virgin male and allowed them to produce offspring. This cycle was repeated until the female died. To assess effects of reproduction on lifespan, our seventh treatment was a "non–reproducing" treatment where females were fed on chicken liver (0.5 g to 1 g twice per week), but were not allowed to breed throughout their life.

For each treatment, we weighed females and measured their pronotum width at 28 days of age (±1 day), and when the female died we recorded her lifespan. For the six reproducing treatments, we weighed females before and after each reproductive attempt. We monitored each female and her brood daily to determine brood size and timing of larval dispersal. If, after 7 days, no offspring had appeared on the carcass, we designated the brood as a failure, and removed the female, gave her food, and isolated her for 48 h, then allowed her to breed again on a fresh carcass with a new virgin male. We recorded the initial and final number of offspring and mass of offspring as they dispersed into the soil for each reproductive attempt.

2.3. Statistical Analyses

2.3.1. Analysis of Optimal Carcass Size

Our first goal in the experiment was to determine optimal carcass sizes for each species. We defined "optimal" as the carcass size that resulted in the greatest number of offspring produced over a lifetime. To determine optimal carcass size, we used a general linear model to examine the effects of carcass size and species on lifetime number of offspring (GLM procedure; SAS 9.3 SAS Institute, Cary, NC, USA). In the model, carcass size and species were main effects, and we included an interaction between carcass size and species, and standardized female body size (pronotum width) as a covariate. As noted above, body size varies between the two species. We were interested in effects of body size within each species, and we did not want to confound differences in body size between species with within species variation, so we standardized body size across species by creating a z–score centered on the mean of each species. The response variable, lifetime total number of offspring, was log transformed to meet assumptions for the parametric model. One *N. guttula* female from the 20 g carcass size never reproduced and was removed from all analyses.

Total mass of offspring over the lifetime (i.e., total number of offspring multiplied by mean offspring mass per brood) is sometimes used to represent evolutionary fitness. We analyzed patterns of total mass of offspring over a lifetime using the same model as that used for total number of offspring. Results were consistent with results obtained from total number of offspring, so we present only total number of offspring in this paper.

2.3.2. Analysis of Patterns of Reproductive Allocation

Our second goal was to determine if reproductive allocation and resulting senescence followed a pattern of terminal investment or reproductive restraint. We used four response variables to characterize contrasting patterns of reproductive allocation as follows: lifespan, lifetime number of reproductive bouts, mass change of females through time, and

proportion of offspring culled through time. Terminal investment would be characterized by shorter lifespans, fewer reproductive bouts, negative or neutral mass gain, and fewer offspring culled at older ages. In contrast, reproductive restraint would be characterized by longer lifespans, more reproductive bouts, positive mass gain, and more offspring culled at older ages.

To test for differences in lifespan, we used a general linear model (GLM procedure; SAS 9.3 SAS Institute, Cary, NC, USA) and for differences in number of reproductive bouts we used a generalized linear model (GenMod procedure; SAS 9.3 SAS Institute, Cary, NC, USA). For each model, carcass size and species were main effects, and we included an interaction between carcass size and species, and standardized female body size (pronotum width) as a covariate. As noted above, body size varies between the two species. We were interested in effects of body size within each species and we did not want to confound differences in body size between species with within species variation, so we standardized body size across species by creating a z–score centered on the mean of each species. The non–reproducing treatment was only included in the model for lifespan. Data for lifespan met the assumptions of the parametric model and was not transformed. For the number of successful reproductive bouts, we assumed a Poisson distribution and used a log–link function.

To test for differences in mass change and proportion brood culled within lifetimes, we used a generalized linear mixed model (GLMM; GLIMMIX procedure; SAS 9.3 SAS Institute, Cary, NC, USA). Mass change was measured as mass of female at the end of the reproductive bout minus mass of the female at the beginning of the reproductive bout. Mass loss would be observed as a negative number and mass gain would be positive. Mass change is a continuous variable, and raw data met assumptions for a parametric model, so no transformations were used. Proportion brood culled was measured as number of offspring culled relative to initial brood size, so we assumed a binomial distribution with a logit–link function. We used a repeated measures design to analyze patterns of allocation through time. Species, carcass size, and age (indexed by reproductive bout) were predictor variables (i.e., main effects). We used standardized female body size as a covariate and included all two–way and three–way interactions among main effects. A single *N. guttula* female never reproduced and thus we removed her from all analyses. Because we had multiple measures of the same individual through time, individual ID was used as a random effect in the model.

2.3.3. Analysis of Patterns of Reproductive Senescence

To assess patterns of reproductive senescence, we used three response variables as follows: initial brood size, final brood size, and offspring body mass at dispersal. An increased rate of senescence would be characterized by a negative slope of initial offspring number and final offspring number with increasing age; whereas, a decreased rate of senescence or delayed senescence would be characterized by a zero slope of initial offspring number and final offspring number with increasing age. Because both the female and the offspring feed exclusively on the carcass during brood development, fewer offspring should result in larger offspring body size. Thus, senescence would result in fewer but larger offspring in older individuals; whereas, delayed senescence would result in about the same number and size of offspring with increasing age.

To test for differences in initial brood size, final brood size, and individual offspring mass within lifetimes we used generalized linear mixed models (GLMM; GLIMMIX procedure; SAS 9.3 SAS Institute, Cary, NC, USA). We ran separate models for each of the three response variables. Initial brood size was the number of larvae that first appeared on the carcass before culling had occurred. Final brood size was the number of larvae that dispersed into the soil and represents the brood size after culling has occurred. For each trait we used a repeated measures design to analyze patterns of senescence through time. Species, carcass size, and reproductive bout (age) were predictor variables (i.e., main effects). We used standardized female body size as a covariate and included all two–way

and three–way interactions. For both initial and final brood sizes, we assumed a Poisson distribution and used a log–link function. Offspring mass was a continuous variable, so we used a log–link function. Because we had multiple measures of the same individual through time, individual ID was used as a random effect in the model. A single *N. guttula* female never reproduced and thus we removed her from all analyses. In addition, we removed two bouts from a single female from the analysis for mean offspring mass because in each bout, only two offspring were produced and they were abnormally small (1/5 the size of any other offspring).

3. Results

3.1. Optimal Carcass Size

Lifetime number of offspring differed by species, carcass size, and their interaction, but not by body size (Table 1). The number of offspring for *N. marginatus* increased with carcass size up to 20 g and then plateaued on larger carcass sizes. Lifetime number of offspring on carcasses 20 g or greater was about three times that on 5 g carcasses and nearly double that on 10 g carcasses (Figure 1). Number of offspring for *N. guttula* peaked on 10 g and 20 g carcasses and declined on carcasses larger than 20 g. Lifetime number of offspring on 10 g and 20 g carcasses was about double that on larger or smaller carcasses (Figure 1).

Table 1. Results of ANCOVA for lifetime number of offspring. Significant effects are bolded.

Effect.	DF (num/den)	F	*p*
species	1/132	54.07	**<0.0001**
carcass	5/132	4.78	**0.0005**
carcass × species	5/132	5.36	**0.0002**
standardized size	1/132	0.16	0.6891

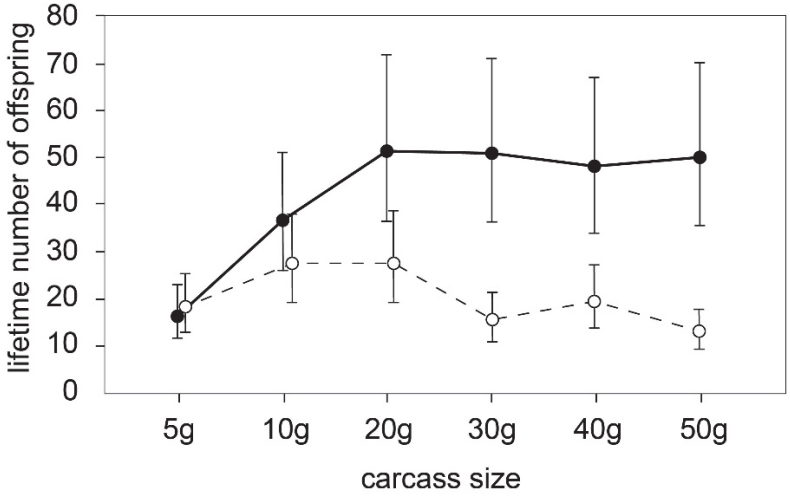

Figure 1. Mean lifetime number of offspring (error bars are 95% confidence interval) produced by *N. marginatus* (solid circle and line) and *N. guttula* (open circles and dashed line) across six carcass sizes.

3.2. Patterns of Reproductive Allocation

Lifespan differed significantly between species, among carcass size treatments, and by body size, but the interaction between species and carcass size was not significant (Table 2). On average, *N. marginatus* lived slightly longer than *N. guttula*, and the difference was most pronounced on carcass sizes $\geq$ 20 g. Across both species, beetles that reproduced

on smaller carcasses lived longer than those on larger carcasses and non–reproducing individuals lived the longest at about 120 days. Lifespan declined with carcass size until carcass size equaled 30 g at which lifespan was about 70 days. However, there was no decline in lifespan on carcasses $\geq$ 30 g (Figure 2a). On average, the largest individuals lived about 30 days longer than the smallest individuals within both species and across all carcass size treatments.

Table 2. Results of ANCOVA for lifespan. Significant effects are bolded.

Effect	DF (num/den)	F	*p*
species	1/153	5.60	**0.0192**
carcass	6/153	35.78	**<0.0001**
carcass × species	6/153	0.32	0.9244
standardized size	1/153	16.75	**<0.0001**

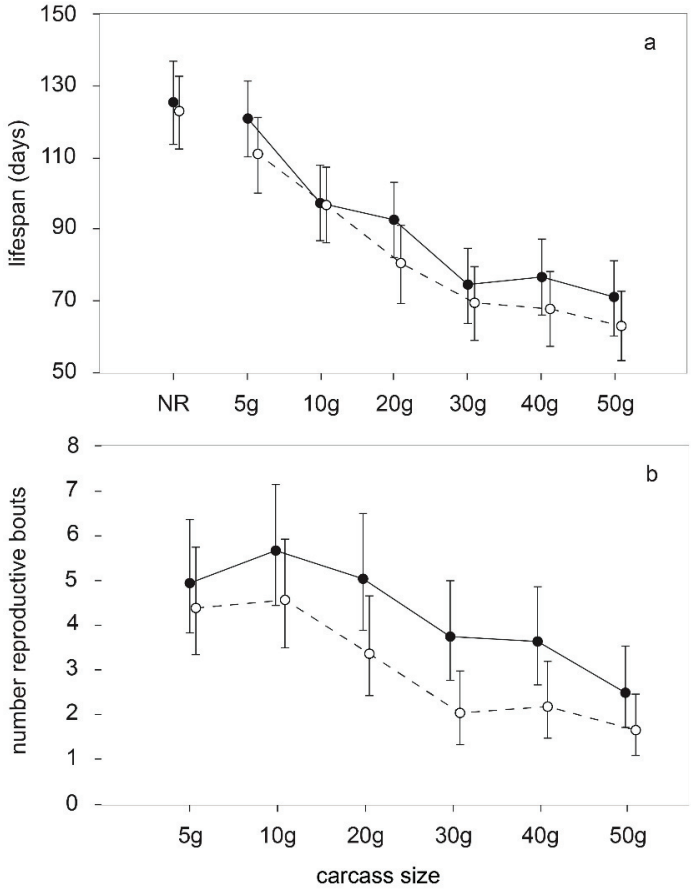

Figure 2. (**a**) Mean lifespan (in days; error bars are 95% confidence interval) of *N. marginatus* (solid circle and line) and *N. guttula* (open circles and dashed line) across six carcass sizes. NR indicates nonreproductive treatment. (**b**) Mean number of reproductive bouts (error bars are 95% confidence interval) for *N. marginatus* (solid circle and line) and *N. guttula* (open circles and dashed line) across six carcass sizes.

The number of successful reproductive bouts differed by species and among carcass size treatments, but not by body size. The interaction between species and carcass size

treatment was not significant (Table 3). For *N. marginatus*, the number of successful reproductive bouts was highest and about equal for 5 g to 20 g carcasses, dropped by about 1 for 30 g and 40 g carcasses, and dropped again for 50 g carcasses. For *N. guttula*, the number of successful reproductive bouts was highest and about equal for 5 g and 10 g carcasses, dropped by about 1 for 20 g carcasses, and dropped again and was about equal for 30 g to 50 g carcasses. On average, *N. marginatus* had about 1.5 more successful reproductive bouts than *N. guttula* across all carcass sizes (Figure 2b).

Table 3. Results of ANCOVA for number of reproductive bouts. Significant effects are bolded.

Effect	DF	χ^2	*p*
species	1	16.79	**<0.0001**
carcass	5	51.88	**<0.0001**
carcass × species	5	3.80	0.5784
standardized size	1	1.50	0.2202

The change in mass of females was not significantly affected by main effects or interactions among main effects or the covariate, female body size (Table 4). Change in mass varied widely among individuals and no patterns were evident between species, among carcass sizes, or with age (Figure 3a,b).

Table 4. Results of repeated measures ANCOVA for mass change, and proportion brood culled. Significant effects are bolded.

Effect	DF (num/den)	F	*p*
Mass Change			
species	1/462	0.04	0.8387
carcass	5/462	0.79	0.5565
age	1/462	0.05	0.824
standardized size	1/462	0.73	0.3923
species × carcass	5/462	0.73	0.602
age × species	1/462	1.12	0.2915
age × carcass	5/462	0.86	0.5065
age × species × carcass	5/462	0.58	0.719
Proportion Brood Culled			
species	1/212.8	5.65	**0.0184**
carcass	5/167.2	2.88	**0.0072**
age	1/202	8.71	**0.0035**
standardized size	1/135.8	8.45	**0.0043**
species × carcass	5/186.4	2.58	**0.0275**
age × species	1/265.6	0.29	0.5892
age × carcass	5/117.1	0.75	0.6305
age × species × carcass	5/129.2	2.03	0.0788

The proportion of brood culled differed significantly by species, carcass size, and by age. Moreover, the interaction between species and carcass size was significant, and the three–way interaction was marginally significant (Table 4). For *N. marginatus* on small carcasses (5 g and 10 g) the proportion of the brood culled was higher and remained high with increasing age; however, on larger carcasses (20 g to 50 g) the proportion of the brood culled decreased with increasing age (Figure 3c). In *N. guttula* on 5 g and 10 g carcasses the proportion of brood culled was high to begin with but declined with age and on 20 g and 30 g carcasses the proportion of brood culled was intermediate to begin with but declined with age; however, on 40 g and 50 g carcasses the proportion of the brood culled was lower to begin with and remained constant or increased with age (Figure 3d).

3.3. Patterns of Reproductive Senescence

Initial brood size differed significantly by species, among carcass sizes, and with age. Moreover, the interaction between species and carcass size, the interaction between species and age, and the interaction between age and carcass size were all significant (Table 5). Females on larger carcasses tended to produce larger initial broods than females on smaller carcasses at early ages (Figure 4a,b). Initial brood size for *N. marginatus* stayed relatively constant with age at the lowest carcass sizes (5 g and 10 g) but dropped with increasing age for larger carcass size treatments (Figure 4a). For *N. guttula*, initial brood size decreased with age for every carcass size treatment and the rate of decrease was greater as carcass size increased (Figure 4b). Initial brood size was about equal between *N. marginatus* and *N. guttula* on the smallest two carcass sizes. However, initial brood size on larger carcasses at early ages was substantially larger in *N. marginatus* compared with *N. guttula*.

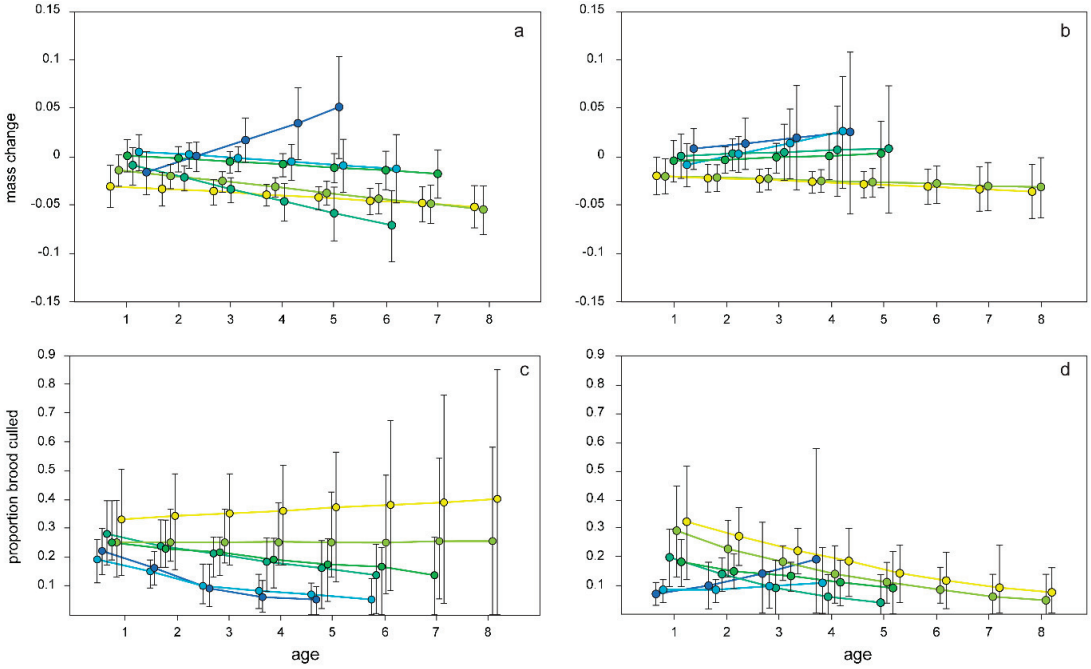

Figure 3. (**a**) Mean mass change (in grams, error bars are 95% confidence intervals, same on all panels) of female *N. marginatus* during reproduction on six carcass sizes (5 g = yellow, 10 g = yellow/green, 20 g = green, 30 g = blue/green, 40 g = light blue, 50 g = dark blue; same on all panels) by reproductive bout as age. (**b**) Mean mass change of female *N. guttula* during reproduction on six carcass sizes by reproductive bout as age. (**c**) Mean proportion of the brood culled by female *N. marginatus* on six carcass sizes by reproductive bout as age. (**d**) Mean proportion of the brood culled by female *N. guttula* on six carcass sizes by reproductive bout as age.

Mean offspring mass differed significantly between species, among carcass sizes, and by age. The interaction between age and carcass size was also significant (Table 5). For both species, mean offspring mass increased with age (except for 5 g and 10 g carcasses for *N. marginatus* and 5 g carcasses for *N. guttula*), and mean offspring mass increased with age at a greater rate for females breeding on larger carcasses (Figure 4e,f). Offspring mass was similar between *N. marginatus* and *N. guttula* on the smallest carcass size, but larger in *N. marginatus* at all larger carcass sizes.

Table 5. Results of repeated measures ANCOVA for initial brood size, final brood size, and mean offspring mass. Significant effects are bolded.

Effect	DF (num/den)	F	*p*
Initial Brood Size			
species	1/118.7	9.87	**0.0021**
carcass	5/117.4	12.54	**<0.0001**
age	1/337	135.6	**<0.0001**
standardized size	1/100.6	0.03	0.8525
species × carcass	5/117.5	1.97	0.0885
age × species	1/341.6	4.35	**0.0378**
age × carcass	5/236.5	10.07	**<0.0001**
age × species × carcass	5/236.9	1.25	0.2845
Final Brood Size			
species	1/139	6.86	**0.0098**
carcass	5/131.8	22.28	**<0.0001**
age	1/489	116.9	**<0.0001**
standardized size	1/94.6	0.15	0.6982
species × carcass	5/132	1.64	0.153
age × species	1/489	6.81	**0.0093**
age × carcass	5/395.3	9.35	**<0.0001**
age × species × carcass	5/396.1	2.01	0.0764
Mean Offspring Mass			
species	1/212	12.43	**0.0005**
carcass	5/191.6	7.53	**<0.0001**
age	1/447.2	18.84	**<0.0001**
standardized size	1/100.5	0.61	0.4382
species × carcass	5/191.9	0.75	0.5834
age × species	1/449.6	0.27	0.6038
age × carcass	5/414.9	2.8	**0.0169**
age × species × carcass	5/415.1	1.02	0.4041

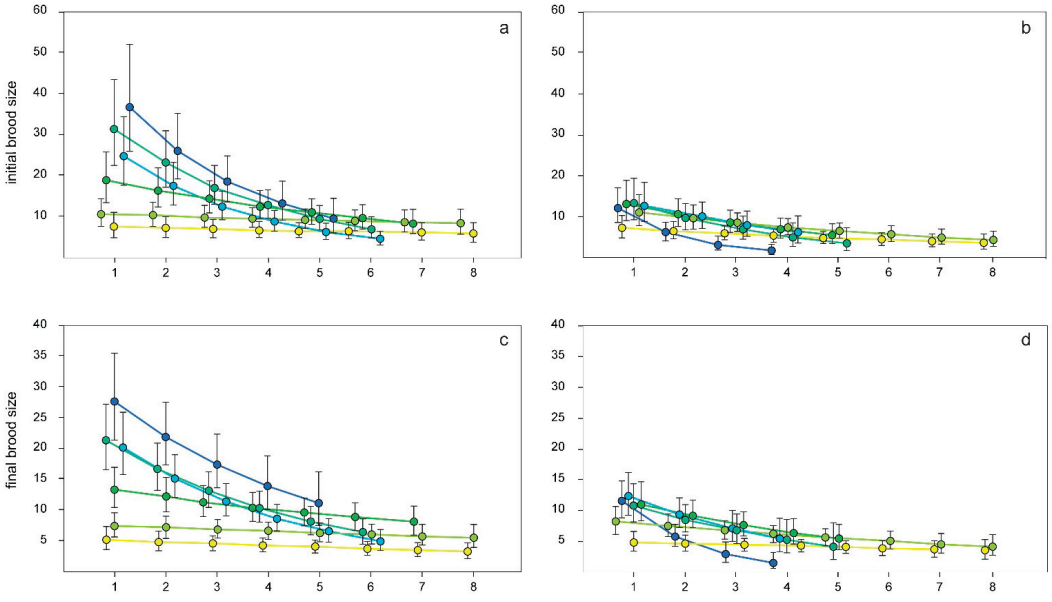

Figure 4. *Cont.*

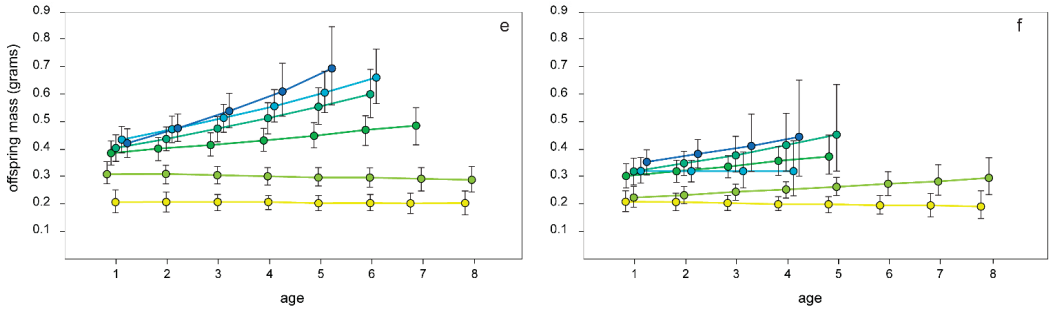

Figure 4. (**a**) Mean initial brood size (error bars are 95% confidence intervals on all panels) of *N. marginatus* across six carcass sizes (yellow circles represent the smallest carcass sizes grading to blue for the largest carcass sizes; same across all panels) by reproductive bout as age. (**b**) Mean initial brood size of *N. guttula* across six carcass sizes by reproductive bout as age. (**c**) Mean final brood size of *N. marginatus* across six carcass sizes by reproductive bout as age. (**d**) Mean final brood size of *N. guttula* across six carcass sizes by reproductive bout as age. (**e**) Mean offspring mass of *N. marginatus* across six carcass sizes by reproductive bout as age. (**f**) Mean offspring mass of *N. guttula* across six carcass sizes by reproductive bout as age.

4. Discussion

N. marginatus and *N. guttula* achieve the highest fitness on different–sized carcasses. The larger *N. marginatus* had higher lifetime reproductive success on medium and large carcasses (carcasses $\geq$ 20 g), and *N. guttula* had highest lifetime reproductive success on small and medium carcasses (10 g and 20 g carcasses). On larger carcasses, female *N. marginatus* survived longer and for more reproductive bouts than did *N. guttula*, although both species had similar lifespans and number of reproductive bouts on small carcasses. Similarly, *N. marginatus* was able to take advantage of carcasses $\geq$ 30 g by producing broods equal in size to those produced on 20 g carcasses; whereas, brood sizes produced by *N. guttula* declined on carcasses $\geq$ 30 g and varied less across the range of carcass sizes. Brood sizes on the smallest carcasses were similar between the species. Thus, optimal carcass size for the larger *N. marginatus* was large and medium carcasses ($\geq$20 g), and optimal carcass size for the smaller *N. guttula* was small and medium carcasses (10 g and 20 g, but not the smallest, 5 g size). Interestingly, the 20 g carcass size was included in the optimal carcass sizes for both species, indicating partial overlap in optimal carcass sizes between species. Differences in optimal carcass sizes between the two species suggest they have markedly different reproductive and competitive strategies.

Female *N. marginatus* and *N. guttula* differed considerably in their reproductive allocation strategies (i.e., terminal investment versus reproductive restraint). On small and medium carcasses (5 g, 10 g, 20 g, and 30 g), *N. guttula* females culled a smaller proportion of their brood as they aged, suggesting that they were investing more into each reproductive bout (i.e., terminal investment) whereas *N. marginatus* females tended to cull a constant proportion of their broods as they aged on the two smallest carcasses (5 g and 10 g) indicating reproductive restraint. Conversely, on the largest two carcass sizes (40 g and 50 g), *N. guttula* culled a constant or increasing proportion of their broods with age (i.e., reproductive restraint), while *N. marginatus* decreased the proportion of the brood culled with age on 20 g, to 50 g carcasses (terminal investment). Thus, both species behaved much less conservatively (i.e., more likely to incur reproductive costs) on the carcass sizes with which they performed best and more conservatively on carcass sizes with which they normally performed worst. Consistent with our hypothesis that each species is adapted for different carcass sizes, their differing investment patterns are likely due to their species–specific adaptation to different carcass sizes. Work with *N. orbicollis* has demonstrated a similar pattern of resource–quality based reproductive investment. On smaller carcasses, *N. orbicollis* initially invests more in body maintenance and less in offspring, and on larger carcasses, it invests less in body maintenance and more in offspring [12,15]. The pattern

shifts to increased investment in offspring as the female ages across carcass sizes [15], although the degree to which this shift occurs is dependent on previous experience [12]; *N. orbicollis* females invested more into reproduction when presented with a large carcass if they had first reproduced on a smaller carcass, but were more conservative in reproduction if they only reproduced on small carcasses or were given a small carcass after having reproduced on a large carcass [12]. Work with mealworm beetles similarly confirms the importance of resources in determining reproductive strategies. When immune challenged, starved male mealworm beetles suppressed their immune response and invested more heavily into pheromones to increase attractiveness to females, while males fed food ad libitum acted much more conservatively when immune challenged [19]. Our study and the others we have highlighted here suggest general consistency with the dynamic terminal investment threshold model [8]; however, in our study the external factor that determines whether individuals exhibit terminal investment or reproductive restraint is carcass size relative to optimal carcass sizes.

Mass change of the female during a reproductive bout has been shown in *N. orbicollis* to vary based on carcass size and the resulting reproductive strategy [15]. Female *N. orbicollis* on 30 g carcasses exhibited negative mass change with increasing age; whereas, females on 20 g carcasses exhibited positive or neutral mass change with increasing age 15]. We expected to see similar patterns in our study. We predicted that females exhibiting terminal investment on preferred carcass sizes would be characterized by negative or neutral mass change, and females exhibiting reproductive restraint on non–optimal carcass sizes would be characterized by positive mass change. However, mass change in the two species in our study varied widely among individuals in all treatments but did not vary significantly with any of the experimental predictors. Rather, the proportion of the brood culled appears to be the main mechanism whereby terminal investment or reproductive restraint is realized. In burying beetles, proportion of the brood culled has been suggested to vary based on the size of the carcass as a mechanism for matching brood size to carcass size to avoid errors of over or under allocation [10,15,31]. However, our study suggests that the rate of culling the brood is also an indication of reproductive strategy across a female's lifetime.

Our results suggest that differences in allocation patterns observed across populations and species in a number of other taxa may be a result of differential adaptation to and use of varying resource qualities. For example, older female alpine chamois were less likely to reproduce in "poor" years ("poor" being indicated by adult mortality) even when weighing more than younger females, suggesting that such strategies may be tied to resource abundance or resource quality [27]. Male alpine chamois exhibited different patterns of late–life allocation based on population [20]. Competition between male chamois is intense, with males losing up to 28% of their body mass during the breeding season [20]. In two populations, males peak in reproductive effort (as measured by mass loss during the breeding season) and then decrease reproductive effort as they age, suggesting that older males are restraining reproduction [20]. Males in a third population exhibited the opposite pattern, with older males terminally investing by increasing reproductive effort [20]. While resource qualities were not explicitly tied to these patterns, Mason et al. [20] did observe that the third population's environment is more calcareous, suggesting that the plant community may be a more nitrogen–rich resource than in the other two environments. Thus, males in the third population may be simply taking advantage of increased resource quality, or they may be better adapted to their environment. Neither of these experiments explicitly tested for the effect of resource quality on reproductive allocation. Thus, how resource quality leads to one or the other strategy is not necessarily clear. Our study is the first to demonstrate the effect that resource quality and species–specific adaptation to different resources has on lifetime patterns of reproductive allocation.

Reproduction is costly for both *N. marginatus* and *N. guttula*. Females that did not reproduce lived longer than those that reproduced, and lifespan and number of reproductive bouts decreased with increasing carcass size, suggesting that reproduction on larger carcasses may incur greater reproductive costs than on smaller carcasses. Resource quality

also affected the rate of senescence. Both species had declining brood sizes on larger carcasses as they aged, although the rate at which brood sizes declined varied between species. Brood sizes of *N. marginatus* on larger carcasses declined more rapidly across bouts than *N. guttula*. However, *N. marginatus* initially produced significantly larger broods on larger carcasses. The pattern of declining brood size in later reproductive bouts observed in this study is consistent with previous work on *N. orbicollis* [12,15]. Interestingly, both species in our study reach a similar limit on the decline in lifespan on carcasses $\geq$ 30 g. Lifespans of these two species are remarkably similar to those observed in *N. orbicollis* [15]. Even though the two species in this study showed substantially different patterns of allocation and reproductive output on larger carcasses, the lower limit on lifespan of reproducing females is quite similar. Reproductive females may reach a limit where they are providing all they can to reproduction and further increases in time or energy are simply not possible. Handicap experiments that focus on changes in reproductive effort with reduced effort of the partner come to a similar conclusion [39]; females cannot increase reproductive effort to fully compensate for lack of male effort because they are already expending energy and time at a maximal level [39]. Interestingly, senescence does not follow the same pattern as fitness (lifetime number of offspring), especially in *N. guttula*. For both species, larger carcasses incur a progressively larger cost, but do not yield increased reproductive output.

With lower fecundity, how does *N. guttula* persist in this area with *N. marginatus*? *Nicrophorus marginatus* is larger than *N. guttula* and likely outcompetes *N. guttula* in competitive interactions on carcasses. Additionally, *N. marginatus* had more and larger offspring than *N. guttula* on all but the smallest carcass sizes (5 g and 10 g). Burying beetles segregate niches to avoid competitive interactions on a number of different axes (seasonal activity, habitat preference, resources; [40–46]). One such case is *N. defodiens*, a smaller burying beetle species, which is often displaced from larger carcasses by the larger *N. orbicollis*, but is successful on small carcasses, likely due to a higher finding and processing efficiency on smaller carcasses [41]. Because reproductive potential is much greater on larger carcasses, *N. marginatus* may simply ignore small carcass sizes in nature, and *N. guttula* may have uncontested access to these small carcasses. This is consistent with recent results seen intraspecifically in *N. vespilloides*, where large individuals tended to use large carcasses for reproduction but disproportionately rejected smaller carcasses [46]. Small mammal abundances may also favor sizes preferred by *N. guttula*. For example, deer mice (*Peromyscus maniculatus*) are within the size range used efficiently by *N. guttula* and were the most abundant small mammal in nearby Juab County, UT, in similar habitat to our study [47]. Increased numbers of these smaller carcasses may decrease competitive interactions between the two species and allow for *N. guttula* to persist despite lower reproductive output on these carcass sizes.

It is interesting to note that *N. guttula* appears to be incapable of producing large numbers of offspring, even on large carcasses. This may suggest that in the natural, selective environment, there is little opportunity for *N. guttula* to successfully find, compete for, and use large carcasses for reproduction. It also suggests that *N. guttula* may be a brood parasite on *N. marginatus* on larger carcasses. A previous study tested the potential for brood parasitism in *N. guttula* [48] and indicated that there is some probability, albeit low, that *N. guttula* could be successful as a brood parasite. In addition, the well–developed ability of *N. marginatus* to detect and differentially cull brood parasites suggests an evolutionary history of brood parasitism from *N. guttula* or other species of burying beetles [48].

The reduced fecundity of *N. guttula* relative to *N. marginatus* seems to be a species–specific effect unrelated to body size because even small–bodied *N. marginatus* that would be similar in size to medium–sized *N. guttula* produce far more offspring on larger carcasses. This comparison suggests that although body size may be an important differentiating trait between these two species, it does not account for most of the differences we observed. As further confirmation of this idea, we reran the three lifetime analyses (Figures 1 and 2) using raw size values, rather than standardized values within species, as the covariate. Results for lifetime number of offspring and lifetime number of reproductive bouts were

unchanged when using raw values of body size as the covariate; species was a significant predictor, but body size was not. In the case of lifespan as the response variable, the initial analysis, with standardized size as a covariate, showed both species and standardized size as significant predictors, and we reported that the largest individuals lived about 30 days longer than the smallest (standardized) individuals. When we used raw size scores for the covariate, species was no longer a significant effect, but body size was still a significant effect on lifespan. Similar to the effect of standardized body size, the largest individuals lived about 30 days longer than the smallest (raw size values) individuals. This suggests that all of the variation in lifespan between species can be accounted for by body size, but that most of that variation is observed within species rather than between species.

It is important to remember that these experiments were conducted in isolated lab conditions such that many of the pressures found in natural environments (i.e., competitors, parasites, predators, carcass availability; [31,32]) were missing. Competition, predation, parasitism, and carcass availability may influence realized fitness [32,41,46], and these potential selective effects have been part of the selective history of the source populations for this study. Presumably, the selective environment that created the patterns we observed in the lab included all influences embodied in the natural environment. Thus, although the specific value of our measure of fitness (i.e., lifetime number of offspring) is unlikely to be realized in the natural environment, the general pattern of differences between species and among carcasses should be robust. Our results should be viewed as evolved differences evaluated in an isolated environment.

5. Conclusions

In this study, we showed that two phylogenetically similar species of burying beetles that differ in body size are adapted to maximize reproductive output on different–sized resources. The larger species, *N. marginatus*, did better on larger carcasses while the smaller species, *N. guttula*, did best on smaller carcasses, although *N. marginatus* did as well, or better, overall. Carcass size affected lifetime reproductive strategies for both species. Each species' parental investment patterns were consistent with terminal investment on carcasses on which they normally performed best, but they responded conservatively (reproductive restraint) on carcass sizes on which they performed poorly. These data provide strong support for a dynamic threshold for terminal investment [8] based on size of carcass used for reproduction. The differences in how the two species use carcasses and incur reproductive costs may facilitate their co–occurrence in nature.

Author Contributions: Conceptualization, M.C.B., P.J.M. and J.C.C.; methodology, P.J.M. and J.C.C.; formal analysis, M.C.B. and P.J.M.; investigation, P.J.M.; resources, M.C.B.; data curation, M.C.B.; writing—original draft preparation, P.J.M. and M.C.B.; writing—review and editing, M.C.B., P.J.M. and J.C.C.; visualization, M.C.B. and P.J.M.; supervision, M.C.B. and J.C.C.; funding acquisition, M.C.B. All authors have read and agreed to the published version of the manuscript.

Funding: This research received no external funding.

Institutional Review Board Statement: Ethical review and approval were waived for this study because all live animals used in the study were invertebrates.

Informed Consent Statement: Not applicable.

Data Availability Statement: Data are deposited in Dryad data repository with the following identifier, https://doi.org/10.5061/dryad.rv15dv48t.

Acknowledgments: We thank Bruce Schaalje for help with statistical analyses and Eric Billman and Clint Laidlaw for helping to design and execute this experiment. Jerry Johnson provided important comments that helped shape the manuscript. We also thank a myriad of undergraduate researchers for their help in collecting data, especially Mason Segura. We thank the Department of Biology, Brigham Young University for support.

Conflicts of Interest: The authors declare no conflict of interest.

References

1. Williams, G.C. Natural selection, the costs of reproduction, and a refinement of Lack's principle. *Am. Nat.* **1966**, *100*, 687–690. [CrossRef]
2. Carlisle, T.R. Brood success in variable environments: Implications for parental care allocation. *Anim. Behav.* **1982**, *30*, 824–836. [CrossRef]
3. Heimpel, G.E.; Rosenheim, J.A. Dynamic host feeding by the parasitoid *Aphytis melinus*: The balance between current and future reproduction. *J. Anim. Ecol.* **1995**, *64*, 153–167. [CrossRef]
4. Rosenheim, J.A. Characterizing the cost of oviposition in insects: A dynamic model. *Evol. Ecol.* **1999**, *13*, 141. [CrossRef]
5. Pianka, E.R.; Parker, W.S. Age–Specific Reproductive Tactics. *Am. Nat.* **1975**, *109*, 453–464. [CrossRef]
6. Clutton–Brock, T.H. Reproductive effort and terminal investment in iteroparous animals. *Am. Nat.* **1984**, *123*, 212–229. [CrossRef]
7. McNamara, J.M.; Houston, A.I.; Barta, Z.; Scheuerlein, A.; Fromhage, L. Deterioration, death and the evolution of reproductive restraint in late life. *Proc. Royal Soc. B Biol. Sci.* **2009**, *276*, 4061–4066. [CrossRef]
8. Duffield, K.R.; Bowers, E.K.; Sakaluk, S.K.; Sadd, B.M. A dynamic threshold model for terminal investment. *Behav. Ecol. Sociobiol.* **2017**, *71*, 185. [CrossRef] [PubMed]
9. van Noordwijk, A.J.; de Jong, G. Acquisition and allocation of resources: Their influence on variation in life history tactics. *Am. Nat.* **1986**, *128*, 137–142. [CrossRef]
10. Trumbo, S.T. Monogamy to communal breeding: Exploitation of a broad resource base by burying beetles (*Nicrophorus*). *Ecol. Entomol.* **1992**, *17*, 289–298. [CrossRef]
11. Billman, E.J.; Belk, M.C. Effect of age–based and environment–based cues on reproductive investment in *Gambusia affinis*. *Behav. Ecol.* **2014**, *4*, 1611–1622. [CrossRef] [PubMed]
12. Billman, E.J.; Creighton, J.C.; Belk, M.C. Prior experience affects allocation to current reproduction in a burying beetle. *Behav. Ecol.* **2014**, *25*, 813–818. [CrossRef]
13. Brannelly, L.A.; Webb, R.; Skerratt, L.F.; Berger, L. Amphibians with infectious disease increase their reproductive effort: Evidence for the terminal investment hypothesis. *Open Biol.* **2016**, *6*, 150251. [CrossRef] [PubMed]
14. Cotter, S.C.; Littlefair, J.E.; Grantham, P.J.; Kilner, R.M. A direct physiological trade–off between personal and social immunity. *J. Anim. Ecol.* **2013**, *82 4*, 846–853. [CrossRef]
15. Creighton, J.C.; Heflin, N.D.; Belk, M.C. Cost of reproduction, resource quality, and terminal investment in a burying beetle. *Am. Nat.* **2009**, *174*, 673–684. [CrossRef] [PubMed]
16. Duffield, K.R.; Hunt, J.; Rapkin, J.; Sadd, B.M.; Sakaluk, S.K. Terminal investment in the gustatory appeal of nuptial food gifts in crickets. *J. Evol. Biol.* **2015**, *28*, 1872–1881. [CrossRef] [PubMed]
17. Farchmin, P.; Eggert, A.; Duffield, K.; Sakaluk, S. Dynamic terminal investment in male burying beetles. *Anim. Behav.* **2020**, *163*, 1–7. [CrossRef]
18. Heinze, J.; Schrempf, A. Terminal investment: Individual reproduction of ant queens increases with age. *PLoS ONE* **2012**, *7*, e35201. [CrossRef]
19. Krams, I.A.; Krama, T.; Moore, F.R.; Rantala, M.J.; Mänd, R.; Mierauskas, P.; Mänd, M. Resource availability as a proxy for terminal investment in a beetle. *Oecologia* **2015**, *178*, 339–345. [CrossRef] [PubMed]
20. Mason, T.H.E.; Chirichella, R.; Richards, S.A.; Stephens, P.A.; Willis, S.G.; Apollonio, M. Contrasting life histories in neighbouring populations of a large mammal. *PLoS ONE* **2011**, *6*, e28002. [CrossRef] [PubMed]
21. Reavey, C.E.; Silva, F.W.S.; Cotter, S.C. Bacterial infection increases reproductive investment in burying beetles. *Insects* **2015**, *6*, 926–942. [CrossRef] [PubMed]
22. Velando, A.; Drummond, H.; Torres, R. Senescent birds redouble reproductive effort when ill: Confirmation of the terminal investment hypothesis. *Proc. Biol. Sci.* **2006**, *273*, 1443–1448. [CrossRef] [PubMed]
23. Balbontín, J.; Møller, A.P.; Hermosell, I.G.; Marzal, A.; Reviriego, M.; de Lope, F. Geographical variation in reproductive ageing patterns and life–history strategy of a short–lived passerine bird. *J. Evol. Biol.* **2012**, *25*, 2298–2309. [CrossRef] [PubMed]
24. Elliott, K.H.; O'Reilly, K.M.; Hatch, S.A.; Gaston, A.J.; Hare, J.F.; Anderson, W.G. The prudent parent meets old age: A high stress response in very old seabirds supports the terminal restraint hypothesis. *Horm. Behav.* **2014**, *66*, 828–837. [CrossRef] [PubMed]
25. Lecomte, V.J.; Sorci, G.; Cornet, S.; Jaeger, A.; Faivre, B.; Arnoux, E.; Gaillard, M.; Trouvé, C.; Besson, D.; Chastel, O.; et al. Patterns of aging in the long–lived wandering albatross. *Proc. Natl. Acad. Sci. USA* **2010**, *107*, 6370–6375. [CrossRef] [PubMed]
26. McCallum, M.L.; Trauth, S.E. Physiological trade–offs between immunity and reproduction in the northern cricket frog (*Acris crepitans*). *Herpetologica* **2007**, *63*, 269–274. [CrossRef]
27. Morin, A.; Rughetti, M.; Rioux–Paquette, S.; Festa–Bianchet, M. Older conservatives: Reproduction in female Alpine chamois (*Rupicapra rupicapra*) is increasingly risk–averse with age. *Canad. J. Zool.* **2016**, *94*, 311–321. [CrossRef]
28. Smith, A.N.; Belk, M.C.; Creighton, J.C. Residency time as an indicator of reproductive restraint in male burying beetles. *PLoS ONE* **2014**, *9*, e109165. [CrossRef]
29. Davison, R.; Boggs, C.L.; Baudisch, A. Resource allocation as a driver of senescence: Life history tradeoffs produce age patterns of mortality. *J. Theor. Biol.* **2014**, *360*, 251–262. [CrossRef] [PubMed]
30. Le Lann, C.; Visser, B.; Van Baaren, J.; Van Alphen, J.J.; Ellers, J. Comparing resource exploitation and allocation of two closely related aphid parasitoids sharing the same host. *Evol. Ecol.* **2012**, *26*, 79–94. [CrossRef]
31. Scott, M.P. The ecology and behavior of burying beetles. *Annu. Rev. Entomol.* **1998**, *43*, 595–618. [CrossRef]

32. Trumbo, S.T.; Fiore, A.J. Interspecific competition and the evolution of communal breeding in burying beetles. *Am. Mid. Nat.* **1994**, *131*, 169–174. [CrossRef]
33. Smith, R.J.; Heese, B. Carcass selection in a high altitude population of the burying beetle, *Nicrophorus investigator* (Silphidae). *Southwest. Nat.* **1995**, *40*, 50–55.
34. Sikes, D.S.; Venables, C. Molecular phylogeny of the burying beetles (Coleoptera: Silphidae: Nicrophorinae). *Mol. Phylogenet. Evol.* **2013**, *69*, 552–565. [CrossRef] [PubMed]
35. Peck, S.B.; Kaulbars, M.M. A synopsis of the distribution and bionomics of the carrion beetles (Coleoptera, Silphidae) of the conterminous United States. *Proc. Entomol. Soc. Ont.* **1987**, *118*, 47–81.
36. Ratcliffe, B.C. The Carrion Beetles (Coleoptera: Silphidae) of Nebraska. *Bull. Univ. Neb. State Mus.* **2011**, *13*, 100.
37. Bartlett, J.; Ashworth, C.M. Brood size and fitness in *Nicrophorus vespilloides* (Coleoptera: Silphidae). *Behav. Ecol. Sociobiol.* **1988**, *22*, 429–434. [CrossRef]
38. Müller, J.K.; Eggert, A.-K.; Dressel, J. Intraspecific brood parasitism in the burying beetle, *Necrophorus vespilloides* (Coleoptera: Silphidae). *Anim. Behav.* **1990**, *40*, 491–499. [CrossRef]
39. Creighton, J.C.; Smith, A.N.; Komendat, A.; Belk, M.C. Dynamics of biparental care in a burying beetle: Experimental handicapping results in partner compensation. *Behav. Ecol. Sociobiol.* **2015**, *69*, 265–271. [CrossRef]
40. Anderson, R.S. Resource partitioning in the carrion beetle (Coleoptera:Silphidae) fauna of southern Ontario: Ecological and evolutionary considerations. *Canad. J. Zool.* **1982**, *60*, 1314–1325. [CrossRef]
41. Trumbo, S.T. Interference competition among burying beetles (Silphidae, Nicrophorus). *Ecol. Entomol.* **1990**, *15*, 347–355. [CrossRef]
42. Lomolino, M.; Creighton, C.; Schnell, G.; Certain, D. Ecology and conservation of the endangered American burying beetle (*Nicrophorus americanus*). *Conserv. Biol.* **1995**, *9*, 605–614. [CrossRef]
43. Hocking, M.; Darimont, C.; Christie, K.; Reimchen, T. Niche variation in burying beetles (*Nicrophorus* spp.) associated with marine and terrestrial carrion. *Canad. J. Zool.* **2007**, *85*, 437–442. [CrossRef]
44. Smith, G.; Trumbo, S.T.; Sikes, D.S.; Scott, M.P.; Smith, R.L. Host shift by the burying beetle, *Nicrophorus pustulatus*, a parasitoid of snake eggs. *J. Evol. Biol.* **2007**, *20*, 2389–2399. [CrossRef] [PubMed]
45. Keller, M.L.; Howard, D.R.; Hall, C.L. Spatiotemporal niche partitioning in a specious silphid community (Coleoptera: Silphidae *Nicrophorus*). *Sci. Nat.* **2019**, *106*, 57. [CrossRef]
46. Hopwood, P.; Moore, A.; Tregenza, T.; Royle, N. Niche variation and the maintenance of variation in body size in a burying beetle. *Ecol. Entomol.* **2015**, *41*. [CrossRef]
47. Smith, C.B.; Urness, P.J. Small mammal abundance on native and improved foothill ranges, Utah. *J. Range Manag.* **1984**, *37*, 353–357. [CrossRef]
48. Smith, A.N.; Belk, M.C. Evidence for interspecific brood parasite detection and removal in burying beetles. *Psyche* **2018**. [CrossRef] [PubMed]

diversity

MDPI

Article

Determining Plant Diversity within Interconnected Natural Habitat Remnants (Ecological Network) in an Agricultural Landscape: A Matter of Sampling Design?

Francesco Liccari [1,2], Maurizia Sigura [2], Enrico Tordoni [3], Francesco Boscutti [2] and Giovanni Bacaro [1,*]

[1] Department of Life Sciences, University of Trieste, Via L. Giorgieri 10, 34127 Trieste, Italy; francesco.liccari@phd.units.it
[2] Department of Agricultural, Food, Environmental and Animal Sciences, University of Udine, Via delle Scienze 206, 33100 Udine, Italy; maurizia.sigura@uniud.it (M.S.); francesco.boscutti@uniud.it (F.B.)
[3] Department of Botany, Institute of Ecology and Earth Science, University of Tartu, Lai 40, 51005 Tartu, Estonia; enrico.tordoni@ut.ee
* Correspondence: gbacaro@units.it

Abstract: In intensively used and human-modified landscapes, biodiversity is often confined to remnants of natural habitats. Thus, identifying ecological networks (ENs) necessary to connect these patches and maintain high levels of biodiversity, not only for conservation but also for the effective management of the landscape, is required. However, ENs are often defined without a clear a-priori evaluation of their biodiversity and are seldom even monitored after their establishment. The objective of this study was to determine the adequate number of replicates to effectively characterize biodiversity content of natural habitats within the nodes of an EN in north-eastern Italy, based on vascular plant diversity. Plant communities within habitat types of the EN's nodes were sampled through a hierarchical sampling design, evaluating both species richness and compositional dissimilarity. We developed an integrated method, consisting of multivariate measures of precision (*MultSE*), rarefaction curves and diversity partitioning approaches, which was applied to estimate the minimum number of replicates needed to characterize plant communities within the EN, evaluating also how the proposed optimization in sampling size affected the estimations of the characteristics of habitat types and nodes of the EN. We observed that reducing the total sampled replicates by 85.5% resulted to sufficiently characterize plant diversity of the whole EN, and by 72.5% to exhaustively distinguish plant communities among habitat types. This integrated method helped to fill the gap regarding the data collection to monitor biodiversity content within existing ENs, considering temporal and economic resources. We therefore suggest the use of this quantitative approach, based on probabilistic sampling, to conduct pilot studies in the context of ENs design and monitoring, and in general for habitat monitoring.

Keywords: α diversity; β diversity; multivariate pseudo-standard error; plant biodiversity; protected areas; sampling optimization

Citation: Liccari, F.; Sigura, M.; Tordoni, E.; Boscutti, F.; Bacaro, G. Determining Plant Diversity within Interconnected Natural Habitat Remnants (Ecological Network) in an Agricultural Landscape: A Matter of Sampling Design?. *Diversity* **2022**, *14*, 12. https://doi.org/10.3390/d14010012

Academic Editor: Maurizio Rossetto

Received: 17 November 2021
Accepted: 23 December 2021
Published: 27 December 2021

1. Introduction

Biodiversity loss is one of the main concerns in the Anthropocene, happening at a faster rate than ever, driven by many factors such as land use change, habitat fragmentation, pollution, natural resources exploitation, climate change, biological invasion, and many others [1–3]. Although protected areas (PAs) were designed to face these problems through conservation actions focused on endangered target habitats and species, it is now clear that biodiversity protection should rely on a more efficient management of the anthropogenic surrounding landscapes and no longer be confined only to PAs [4–6]. Urgent actions to mitigate habitat loss and fragmentation are needed. These actions must be achieved through a management approach that coherently considers all the landscape components,

integrating also information about functional traits of species and landscape structures through connectivity models [7]. In this context, the Ecological Network (EN) was established as a useful tool to provide an integrated protection of biodiversity also considering biotic interactions among species in an ecosystem [8]. ENs were described and used as tools for conservation planning that rely on the concept of ecological connectivity between the more natural portions of a landscape (so called "nodes" of the EN), with the final aim to limit the effects of fragmentation of habitat patches [9–12]. ENs were thought as a patch matrix model [13], a vision of landscape in which discrete homogeneous habitat patches, surrounded by a more or less inhospitable matrix, are connected in a network structure to support ecological connectivity at landscape scale [14]. Research concerning ENs have developed different approaches directed to assess both the structural connectivity, that is a property of the landscape and concerns the spatial pattern of habitat patches and is independent of the ecological characteristics of the species [15,16], and the functional connectivity, defined as the behavioral movement response of organisms towards habitat patches [17,18]. In this respect, many analytical tools were developed in recent decades such as least-cost modeling, circuit theory, and graph-theoretic methods, aiming at design connectivity models [14].

The concept of EN is increasingly accepted as an operational tool for protecting biodiversity, improving ecological connectivity, and sustainable development of landscapes [19–22]. Several studies have focused on the application of ENs, both from the theoretical and practical point of view, highlighting the complex interaction between structural and functional features of ENs, and the need for further research on the effects of their planning and implementation [14,23–25]. In particular, the definition of the EN follows often an approach oriented only to the structure of the network, while there is a lack of standards in EN projects (e.g., no clear objectives, no monitoring activities) to make them a suitable tool for biodiversity conservation [25–27]. Thus, it is essential to assess the spatial distribution of the habitats within the EN and to quantify their biodiversity content as they may be potentially altered due to anthropic activities of the surrounding matrix, or even by application of improper management of the nodes [28–30]. Moreover, the identification of the habitats suitable for a species should consider the plant communities that are fundamental to habitat type definition, adopted also in modern European classifications [31–34]. The term "habitat" has been used in various contexts with different meanings. In the context of EN, we refer to habitat as an assemblage of animals and plants, together with their abiotic environment, that contribute as patches of the network. Plant communities also have a key role in primary productivity, capturing that portion of solar energy that can support the life of all components of the biosphere, as well as in regulation of the nutrients' cycle and in soil protection [35] and stand for a large part of biodiversity of landscapes.

In this light, a robust and replicable method to detect the biological and structural characteristics of plant communities within the ENs is needed. It should also aim at monitoring the distribution and biodiversity content of the habitat types. A robust methodological approach which is based on probabilistic sampling of plant communities is fundamental to estimate how suitable a sample is for seizing the species diversity and relative abundance, avoiding bias [36]. The adequacy of sampling methods able to reliably characterize ecological communities within a habitat have long been debated in literature (e.g., Yoccoz et al. [37], Balmford et al. [38], Del Vecchio et al. [39], Maccherini et al. [40]). One recently introduced approach which proved to be useful consists of evaluating multivariate differences in the composition of plant communities [41], using a measure of precision based on dissimilarity matrices called pseudo multivariate dissimilarity-based standard errors (*MultSE*), which allow for determination of sample-size adequacy within communities. The *MultSE* is the multivariate analog of the standard error and measures the variability in the position of the centroid in the space of a chosen dissimilarity measure under repeated sampling for a given sample size [41]. This measure of multivariate precision was recently used in the context of European habitats monitoring for costal sand dunes by Maccherini et al. [40],

and it can represent a valid approach to estimating the optimal sample-size required to adequately characterize plant communities within habitats.

In this study, we provide an integrated method to determine the adequate number of replicates to effectively characterize biodiversity within habitat types (considered as EUNIS habitat types [33]) and nodes in an EN whose main novelty relies on the combination of (i) *MultSE*, (ii) rarefaction curves, and (iii) diversity partitioning approaches. Our main contribution is to provide a methodological framework for practitioners to support biodiversity data collection planning, in the EN design process or in the monitoring of existing ENs and PAs, as requested by the European Biodiversity Strategy for 2030 [42].

In an EN, modeled in the context of the regional landscape planning process at the regional level, we sampled 193 vegetation plots in 14 habitat types contained within 74 nodes, aiming at estimating how many replicates are sufficient (a) to distinguish and maintain the typification among different habitat types and (b) to gather data on species diversity and heterogeneity within the whole EN. We tested our framework on an EN in Friuli Venezia Giulia region (north-eastern Italy), which was developed in the context of the regional landscape planning project [43]. The sampled EN is composed of numerous PAs and biotopes, as well as several patches of semi-natural and natural habitats in an agricultural landscape matrix. These habitat types, forming the nodes of the EN, consist mainly of wetlands, linked to the presence of rivers and fens, which are well-known for their ecological role and for the high levels of biodiversity [44]. These environments are usually underrepresented in EN studies and the few studies concerning wetlands tend to give more weight to animal diversity instead of plant diversity [45].

2. Materials and Methods

2.1. Study Area and EN Model

This study was carried out in a local EN in the Friulian lowland (Friuli Venezia Giulia region, NE Italy; centroid coordinates: 45°48′13.4″ N–13°08′11.0″ E; Figure 1).

The study area has an extent of 298 km^2 and is included in an agricultural context bounded by two river systems (Stella and Corno rivers, respectively). The landscape is characterized by a mixed mosaic of intensively and extensively cultivated areas, settlements, semi-natural (hedgerows and watercourses) and natural habitats (woodlands, shrubs, meadows and fens), including eight Natura 2000 Special Area of Conservation (Habitats Directive 92/43/EEC) and nine regional protected sites (biotopes), connecting mainly wetland habitat types.

The geology of the area is mainly composed of Quaternary sand sediments, silt sediments and silt-clay sediments generated by glacial fluvial transport during Pleistocene and by alluvial deposit during Holocene. The area is characterized by an average annual temperature of ca. 13 °C and an average annual rainfall between 1100 and 1400 mm.

In this intensively cultivated landscape, connectivity was mapped on a habitat-species based model (flora and fauna), developed at the local scale in the context of the regional landscape planning process [43]. The model is based on least-cost path analysis and graph theory used to obtain species-specific ENs which were later merged into the final composite multi-species network (Figure S1), where the nodes (natural habitats), corridors and stepping stones (links between natural habitats) were obtained for a set of 19 target species (10 animal species and 9 plant communities, assumed to be crucial for several plant species of conservation concern) to capture favorable conditions for biodiversity. Specifically, the EN was originally modeled from the habitat map of the region [46], using the habitat classification proposed by Poldini et al. [47] (see Table 1), and crossing costs for species were attributed by expert assessment and literature review data. However, for a more comparable interpretation and replicability of this study, the adopted habitat classification was converted according to the European Nature Information System (EUNIS, [33]) classification which has a one-to-one correspondence with the previous classification (Table 1). The term habitat is here understood as an assemblage of plants together with their abiotic

environment. The EN is composed of 108 nodes and 17 different habitat types, for a total extent of 5900 ha of which 1700 ha represent nodes and 4200 ha ecological corridors.

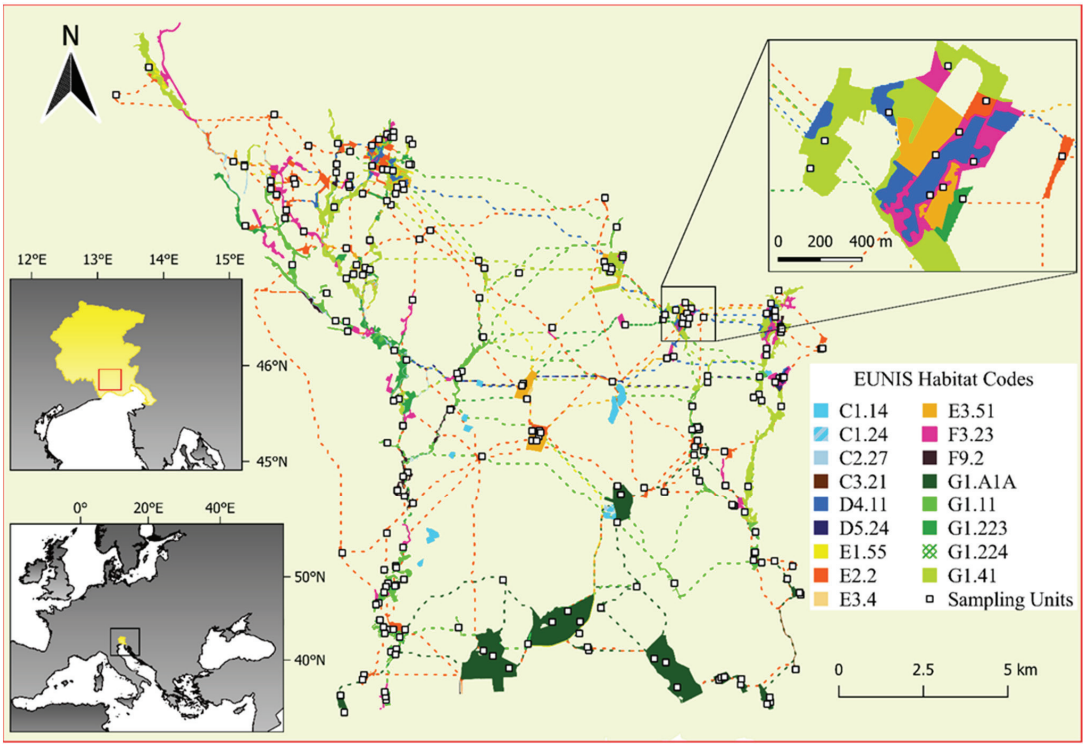

Figure 1. Study area location (Friuli Venezia Giulia region is represented in yellow) and ecological network representation (all the nodes of the EN are shown, including aquatic and smaller than 1 ha nodes). EUNIS Habitat Codes are as follows: C1.14 Charophyte submerged carpets in oligotrophic water bodies; C1.24 Rooted floating vegetation of mesotrophic water bodies; C2.27 Mesotrophic vegetation of fast flowing streams; C3.21 *Phragmites australis* beds; D4.11 *Schoenus nigricans* fens; D5.24 Fen *Cladium mariscus* beds; E1.55 Eastern sub-Mediterranean dry grassland; E2.2 Low and medium altitude hay meadows; E3.4 Moist or wet eutrophic and mesotrophic grassland; E3.51 *Molinia caerulea* meadows and related communities; F3.23 Tyrrhenian sub-Mediterranean deciduous thickets; F9.2 *Salix* carr and fen scrub; G1.A1A Illyrian *Quercus-Carpinus betulus* forests; G1.11 Riverine *Salix* woodland; G1.223 Southeast European *Fraxinus-Quercus-Alnus* forests; G1.224 Po *Quercus-Fraxinus-Alnus* forests; G1.41 *Alnus* swamp woods not on acid peat. Colored lines and patches are corridors and nodes of the network, representing different habitat types and species-specific networks. An example of the hierarchical sampling design in which each node was sampled stratified by habitat type proportionally to habitat extent within the node is showed.

Table 1. Habitat codes of the area according to Poldini et al. [47] and correspondence with EU and EUNIS habitat classification along with descriptive statistics of the study area (i.e., area, number of patches, number of plots and average richness). Asterisk (*) in EU habitat codes denotes priority habitats according to Habitats Directive. Plus (+) before EUNIS habitat codes denotes habitat types that were updated after the sampling (see main text).

Habitat [46]	EU Habitat (Directive 92/43/EEC)	EUNIS Habitat	Area (ha)	*N* Patches	*N* Plots	Average Richness (±SD)
AC6	3260—Water courses of plain to montane levels with the *Ranunculion fluitantis* and *Callitricho-Batrachion* vegetation	C2.27—Mesotrophic vegetation of fast flowing streams	48.6	7	Not sampled	Not sampled
AF5	3140—Hard oligo-mesotrophic waters with benthic vegetation of *Chara* spp.	C1.14—Charophyte sub-merged carpets in olig-otrophic water bodies	59.3	10	Not sampled	Not sampled
AF6	/	C1.24—Rooted floating vegetation of mesotrophic water bodies	5.0	1	Not sampled	Not sampled
BL13	91L0—Illyrian oak-hornbeam forests (*Erythronio-Carpinion*)	G1.A1A—Illyrian *Quercus*—*Carpinus betulus* forests	599.4	17	34	23.3 ± 5.7
BU10	91E0*—Alluvial forests with *Alnus glutinosa* and *Fraxinus excelsior* (*Alno-Padion*, *Alnion incanae*, *Salicion albae*)	G1.41—*Alnus* swamp woods not on acid peat	410.5	43	28	23.3 ± 5.0
BU11	/	F9.2—*Salix* carr and fen scrub	45.8	8	12	25.0 ± 5.2
BU5	92A0—*Salix alba* and *Populus alba* galleries	G1.11—Riverine *Salix* woodland	186.4	31	39	23.6 ± 6.9

Table 1. *Cont.*

Habitat [46]	EU Habitat (Directive 92/43/EEC)	EUNIS Habitat	Area (ha)	*N* Patches	*N* Plots	Average Richness (±SD)
BU7	91F0—Riparian mixed forests of *Quercus robur*, *Ulmus laevis* and *Ulmus minor*, *Fraxinus excelsior* or *Fraxinus angustifolia*, along the great rivers (*Ulmenion minoris*)	G1.223—Southeast European *Fraxinus*—*Quercus*—*Alnus* forests	112.4	20	8	25.9 ± 4.8
BU8	91F0—Riparian mixed forests of *Quercus robur*, *Ulmus laevis* and *Ulmus minor*, *Fraxinus excelsior* or *Fraxinus angustifolia*, along the great rivers (*Ulmenion minoris*)	G1.224—Po *Quercus*-*Fraxinus*—*Alnus* forests	1.9	1	1	18
GM11	/	F3.23—Tyrrhenian sub-Mediterranean deciduous thickets	153.1	41	27	22.5 ± 4.7
PC8	62A0—Eastern sub-Mediterranean dry grasslands (*Scorzoneretalia villosae*)	+E1.55—Eastern sub-Mediterranean dry grassland	2.9	1	1	35

Table 1. *Cont.*

Habitat [46]	EU Habitat (Directive 92/43/EEC)	EUNIS Habitat	Area (ha)	*N* Patches	*N* Plots	Average Richness (±SD)
PM1PM2	6510—Lowland hay meadows (*Alopecurus pratensis*, *Sanguisorba officinalis*)	E2.2—Low and medium altitude hay meadows	127.2	37	19	29.7 ± 5.8
PU1	6430—Hydrophilous tall herb fringe communities of plains and of the montane to alpine levels	+E3.4—Moist or wet eutrophic and mesotrophic grassland	4.1	1	2	12 ± 14.1
PU3	6410—*Molinia* meadows on calcareous, peaty or clayey-siltladen soils (*Molinion caeruleae*)	E3.51—*Molinia caerulea* meadows and related communities	71.7	20	7	33.9 ± 8.5
UC1	/	+C3.21—*Phragmites australis* beds	3.7	1	1	21
UC11	7210 *—Calcareous fens with *Cladium mariscus* and species of the *Caricion davallianae*	D5.24—Fen *Cladium mariscus* beds	9.9	2	3	14.3 ± 4.2
UP4UP5	7230—Alkaline fens	D4.11—*Schoenus nigricans* fens	75.5	28	10	14.9 ± 6.2

2.2. Sampling Design and Data Collection within the EN

Among the nodes, we selected and sampled all the nodes larger than 1 ha. Purely aquatic habitat types (i.e., C1.14, C1.24, C2.27, EUNIS codes; see Table 1) within the nodes were not sampled, since they require completely different assumptions for connectivity than terrestrial ones. Ecological corridors were not sampled. Thus, the final dataset relies on 74 nodes and 14 habitat types. The adopted sampling design was hierarchical (Figure 1), where each habitat type was sampled within each node (that could contain more than one habitat type), proportionally to habitat extent within the node. The sampling density with respect to the habitat extent was chosen as follows: a squared plot of 100 m^2 was randomly placed for a habitat area <5 ha, 2 plots for an area $\geq$5 and $\leq$10 ha and, finally, 3 plots for an area >10 ha. In total, 193 plots were randomly selected within the EN corresponding to an overall sampling density of 0.11 plot/ha. Occurrence and abundance (% visual cover estimation) of vascular plant species were recorded within each plot. Nomenclature and

taxonomy of species followed Bartolucci et al. [48] for native species and Galasso et al. [49] for alien species. Data were collected during spring and summer 2019.

2.3. Data Analysis

Habitat types and nodes within the EN were analyzed in terms of species richness (alpha diversity) and compositional dissimilarity as a measure of species complementarity among sampling units (*sensu* Whittaker [50] defined as beta diversity). The latter was analyzed using the Bray–Curtis (BC) dissimilarity index [51]. This index is defined as the sum over the whole species of the ratio between the difference of abundance values and the sum of abundance values for each species, and it represents the vegetation plots pairwise differences using quantitative species abundance data. The BC dissimilarity index ranges between 0, when two plots share the same elements, to 1, when the two sampling units are totally different). First, we performed a preliminary analysis to evaluate statistical differences in species richness among habitat types and nodes using ANOVA test followed by Tukey post-hoc test (using the "multcomp" R package *version 1.4-17*, [52]) when significant. These differences represented our baseline diversity values characterizing the EN in terms of biodiversity and its variability among habitat types/nodes, given the maximum sampling effort available. Then, we characterized diversity patterns through sample-based rarefaction curves (RCs) using exact method and spatially explicit rarefaction curves (SERs, [53–55]), using the function available in "Rarefy" package *(version 1.1)* [56] and in "vegan" R package *(version 2.5-7)* [57]. We compared first the habitat-based curve and node-based curve to the rarefaction curve for the whole dataset (both RC and SER) and then the curves for each habitat (RCs and SERs) to the whole dataset curve (both RC and SER). Finally, we compared RC for each node with respect to the whole dataset RC. The difference between RC and SER somehow expresses the amount of spatial autocorrelation among sampling units, based on the spatial structure of the collected data and already proved to be effective in different habitat types [55,58].

Species richness patterns across different spatial scales (plot, habitat/node, whole EN) were also evaluated by means of additive partitioning techniques [59,60] using the "adipart" function in the "vegan" R package [57] and their significance was tested using a null model that permutes the original data matrix 999 times to assess deviation from random expectations.

Pseudo multivariate dissimilarity-based standard error (*MultSE*) was computed following the method described by Anderson and Santana-Garcon [41], and using the code and functions provided therein. *MultSE* (Equations (1) and (2)) is based on the chosen dissimilarity measure, thus providing a powerful tool to examine the relative precision of a sampling procedure. It is calculated as follows:

$$MultSE = \sqrt{V/n} \tag{1}$$

where V is a multivariate measure of pseudo variance in the space of the chosen dissimilarity measure:

$$V = \frac{1}{(n-1)} \sum_{i=1}^{(n-1)} \sum_{j=(i+1)}^{n} \frac{d_{ij}^2}{n} \tag{2}$$

where n is the number of sampling units and d represents the squared distance between individual sampling points to their centroid, given a chosen dissimilarity measure.

To calculate *MultSE*, we first downweighted the abundance of the plant community matrix using a log (x + 1) transformation and then we computed the BC dissimilarity index. This was computed both for habitat types and habitat types aggregated within nodes, and then for the whole dataset. A double resampling scheme was used to generate means for each sample size and 95% confidence intervals; in particular the first was obtained from 10,000 permutations and the latter from 10,000 bias-adjusted bootstrap resamples. When the profile of *MultSE* in relation to the increasing sampling size reaches an asymptote, we can consider that sample size as an adequate number of replicates beyond which only small

fluctuations of sampling precision can be observed. The point where the slope of *MultSE* profile changes, was estimated using R package "segmented" *version 1.3-4* [61,62]. These were calculated only for the habitat types and for the whole dataset. The number of plots for each node profile was often not large enough to estimate breaking points.

To verify if and how the proposed reduction in sampling size affects diversity, we reduced the whole dataset adopting resampling strategies as suggested by the results of *MultSE*. In particular, the complete dataset was resampled both randomly and stratified by habitat types. The plots were resampled from the whole dataset, using the number of plots derived from *MultSE* estimation for the habitat types (999 random resamples) and for the whole EN (999 random resamples). These subsets of plots were then tested to investigate if there were significant differences in species richness between habitat types (only for habitat types resampling). Species diversity patterns across different scales (plot/habitat/whole EN and plot/node/whole EN) were evaluated both for the habitats resampled subset (HRS) and for the whole EN resampled subset (ENRS). Finally, the resulting statistics were compared with those of the original dataset to determine the effect in sampling reduction in the ability to discriminate among habitat types and EN nodes.

3. Results

Overall, 74 nodes of the EN were sampled, of which 56 were formed by a singular habitat and 18 by multiple habitat types. The most common habitat types within the nodes were G1.11 Riverine *Salix* woodland (present within 26 nodes, see Table 1 for more details on habitat types), F3.23 Tyrrhenian sub-Mediterranean deciduous thickets (19), G1.A1A Illyrian *Quercus-Carpinus betulus* forests (17), G1.41 *Alnus* swamp woods not on acid peat (14), E2.2 Low and medium altitude hay meadows (13), while the less common were F9.2 *Salix* carr and fen scrub (7), D4.11 *Schoenus nigricans* fens, E3.51 *Molinia caerulea* meadows and related communities, G1.223 Southeast European *Fraxinus-Quercus-Alnus* forests (5), D5.24 Fen *Cladium mariscus* beds (2), other habitat types were present only within a singular node. Most of these habitat types (11) were attributable to wetland habitat types and were present in 78% of the nodes, occupying 84% of the total extent of the EN's nodes.

A total of 399 plant species were sampled in the EN, of which 42 were aliens and 20 were protected, rare or endemic species according to European, Italian, or Regional red lists. The most frequent native species were *Rubus caesius* (occurring in 126 plots), *Rubus ulmifolius* (118), *Quercus robur* (107), *Hedera helix* (106), *Cornus sanguinea* (104) and *Salix alba* (94). Concerning alien species, the most frequent were *Platanus hispanica* (61), *Robinia pseudoacacia* (33) and *Potentilla indica* (28). Finally, the most frequent protected species were *Ruscus aculeatus* (Habitat Directive 92/43/CEE Annex V, 18 occurrences) and *Neottia ovata* (CITES and (CE) N. 407/2009 Annex B, 8 occurrences).

The sampling activity, that aimed at verifying the biodiversity content of the EN, helped also to verify the correspondence between cartography and ground-data. Moreover, it permitted us to update the habitat attribution to a precise habitat type thanks to a greater level of detail and considering natural dynamism among plant communities (e.g., see Table 1 habitat types distinguished by the symbol +).

Concerning species richness calculated at the habitat level (Figure 2), the higher values were in meadows (31.3 ± 8.8 species), the lowest ones in fens (14.9 ± 5.3 species), while intermediate values were observed in shrublands and forests (23.3 ± 5.8 species). Species richness was significantly different among these 3 groups, but not within the groups. Conversely, no significant differences emerged for species richness between EN nodes.

Rarefaction curves (RCs, Figure S2) calculated from the whole dataset confirmed that spatially explicit rarefaction curve (SER) accumulated a lower number of species than RC and revealed that the habitat-based RC accumulated species less rapidly than the node-based RC and SER. RCs for habitat types (Figure S3) showed that none of the curves reached a plateau. A similar trend was observed also in the RCs for nodes (Figure S4).

Additive partitioning (Figure 3) for habitat types showed how within habitat type diversity (i.e., the average inventory diversity) accounted for 15.61% of the total EN diversity

and it was lower than between habitat type diversity (78.43% of total diversity). For nodes, this pattern was even more evident, with a diversity within nodes (3.84% of total diversity) lower than between them (90.2% of total EN diversity).

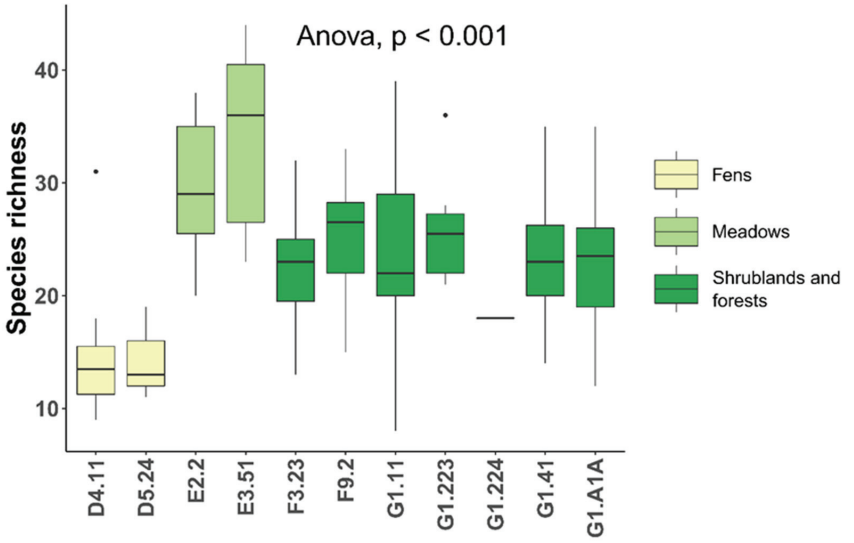

Figure 2. Species richness in habitat types and ANOVA resulting *p*-value. The color scale identifies the 3 groups with significant differences resulting from ANOVA post-hoc analysis ($\alpha < 0.05$): fens (light yellow), meadows (light green) and shrublands and forests (green).

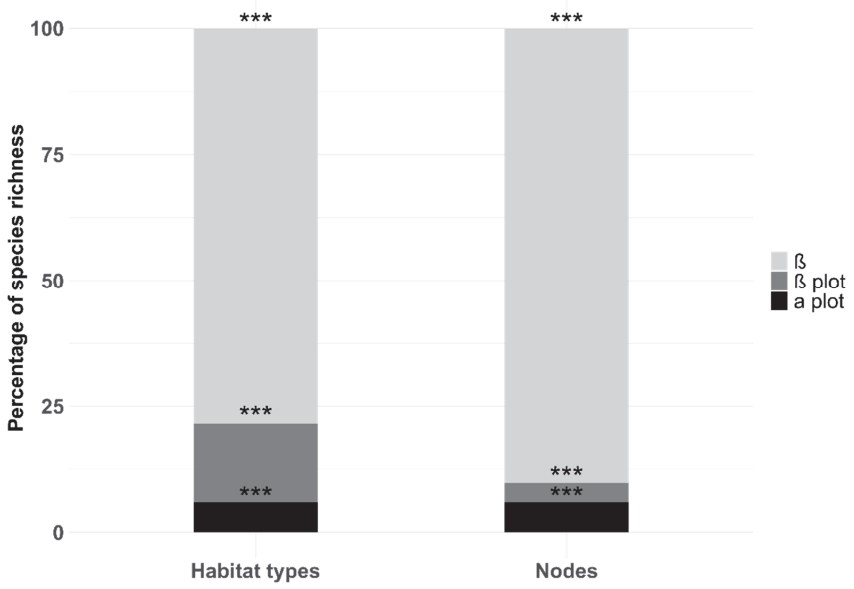

Figure 3. Additive partitioning of diversity across different scales: within each plot (α plot), within each habitat type or node (β plot) and between habitat types or nodes (β). Asterisks indicate a significant difference from random expectations resulting from a null model (*** $p < 0.001$).

MultSE profiles in relation to sample size for each habitat type within the EN (Figure 4) flattened out between seven and ten plots depending on habitat type, a similar trend was observed also in the *MultSE* profiles of the nodes (Figure S5). The *MultSE* profile for the whole dataset (Figure S6) flattened out at around 25 plots.

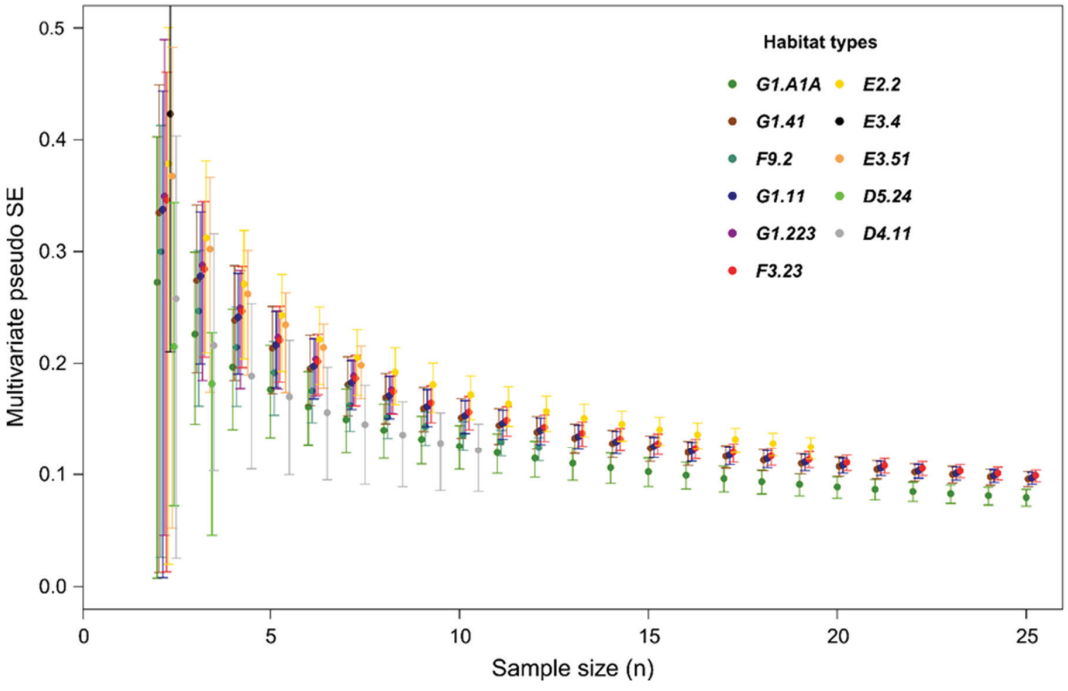

Figure 4. *MultSE* profile based on Bray–Curtis dissimilarity for each habitat within the ecological network. The white space on the left is due to a *MultSE* higher than 0.5 in the first plots.

Based on habitats' *MultSE* profiles, the minimum number of replicates needed to characterize the main features of each habitat was reported in Table S1, while the minimum number of replicates needed for the whole EN was 27.77 ± 1.77 (mean ± SD) according to the point where the slope of *MultSE* profile changed.

In addition, our results proved to be robust when reducing the size of the dataset to the ones suggested by the previous analysis (i.e., 53 plots for HRS, 28 for ENRS) detecting similar patterns in terms of species richness and additive partitioning of diversity (Tables 2 and 3).

Table 2. Summary statistics of additive partitioning results showing the differences in species richness (α) at plot and habitat/node level vs. dissimilarity (β) at plot and network level derived from 999 stratified resampling of the original dataset based on the plot numbers given by the decay of habitats *MultSE* and from 999 random resampling of the original dataset based on the plot numbers given by the decay of whole EN *MultSE*.

Term	Distribution of Values	α Plot	Rate of Significance (% of Permutations with $p < 0.05$)	β Plot	Rate of Significance (% of Permutations with $p < 0.05$)	α (Habitat/node)	Rate of Significance (% of Permutations with $p < 0.05$)	β Network	Rate of Significance (% of Permutations with $p < 0.05$)
Habitat	Min.	0.08	100%	0.16	100%	0.25	100%	0.70	100%
	1st quart.	0.09		0.18		0.27		0.72	
	Median	0.09		0.18		0.28		0.72	
	3rd quart.	0.10		0.19		0.28		0.73	
	Max.	0.10		0.20		0.30		0.75	
Node	Min.	0.10	100%	0.0000	60.2%	0.11	96.1%	0.80	96%
	1st quart.	0.11		0.02		0.14		0.85	
	Median	0.12		0.03		0.14		0.86	
	3rd quart.	0.12		0.03		0.15		0.86	
	Max.	0.14		0.06		0.20		0.89	

Table 3. Summary statistics of ANOVA results derived from 999 stratified resampling of the original dataset based on the plot numbers given by the decay of habitats *MultSE*. Fisher values (F) and measures of effect size (η^2) are shown along with the overall rate of significance of the tests.

Term	Distribution of Values	F	η^2	Rate of Significance (% of Permutations with $p < 0.05$)
Habitat	Min.	1.17	0.17	93.9%
	1st quart.	3.23	0.37	
	Median	4.14	0.43	
	3rd quart.	5.21	0.49	
	Max.	13.16	0.70	

4. Discussion

Sampling diversity of plant communities, in terms of species richness and composition, allowed us to verify and update the distribution of the habitat types within the nodes of the EN. In fact, the field survey can reach a higher level of detail than cartographic data, thus being able to capture and interpret the different aspects of plant mosaics and their dynamism over time, potentially caused by global change and/or anthropic pressure [63]. Moreover, this verification between ground and map data in EN planning should be required [25] and it should be undertaken independently of the cartographic reference checks, which are completed during map drafting. In fact, these incongruences between maps and the observed environment can be a limit in the planning and design phase of the EN and in the application of indexes for connectivity analysis, where weight evaluation of the nodes is requested (e.g., probability of connectivity index). Moreover, it highlights once again the need for verification and monitoring of the modeled EN once implemented. This issue is well known in literature, and Foltete et al. [45] recently highlighted the weakness of approaches based on landscape structure data, suggesting to not use landscape graphs in operational contexts without validating them beforehand with empirical data on species or communities.

As expected, the species richness and rarefaction curves for habitat types and nodes (Figures 2 and S2–S4) described the high heterogeneity existing between nodes, in fact, the method used to identify the EN has been developed to cover the functional areas needed to host the highest number of different species [43], assuming that the species and habitat types used for modeling the EN stand as a proxy for many other species. Moreover, the SERs for habitat types (Figure S3) showed an increasing species richness going from moist or wet grasslands and fens (D4.11, D5.24, E3.4), to shrublands and forests (F3.23, F9.2, G1.A1A, G1.11, G1.223, G1.41) and meadows (E2.2, E3.51). A similar trend was found by De Simone et al. [64] studying patterns of biodiversity in cultivated landscapes, where meadows and woodlands proved to be hotspots of biodiversity. Furthermore, the habitat-based RC accumulated species less rapidly than the node-based RC (Figure S2) while the SER first displayed a trend similar to the node-based RC, and then to the habitat-based one. This feature indicated a higher similarity among habitat types in terms of species composition, than nodes. Nodes were also generally more extended than habitats and therefore they accumulated species more rapidly [65]. Additionally, some of the nodes were often composed by more habitat types, allowing for a faster accumulation of species.

These results pointed out that node-based RC accumulated more species than habitat-based RC, suggesting that a sampling design based on nodes is more efficient in capturing the EN heterogeneity: similar habitat types, sharing similar species composition and structure (e.g., shrublands and forests shared numerous species: *Salix* spp., *Alnus glutinosa*, *Populus* spp., *Quercus robur*, *Fraxinus* spp., etc.), include indeed a high redundant composition of species that can be characterized with fewer sampling units. This is further corroborated by additive partition of diversity (Figure 3), which showed as nodes were more diverse between them than habitat types themselves.

Regarding *MultSE* profiles, the number of plots required for characterizing habitat types ranged from 4 to 8 (Figure 4 and Table S1). Grassland habitat types needed fewer plots than woodland habitat types, due to the lower degree of habitat complexity. Probably the applied plot size was too small for forest habitat types due to the scale of the vegetation patchiness but, even though the plot size might not completely proper in every habitat type, a uniform plot size was needed for the aims of this work and for further research concerning the EN under study. The number of plots required for nodes ranged from two to ten (Figure S5), depending on the number of habitat types present within the node. It is interesting to note that if we consider the whole dataset (Figure S6), 28 replicates (14.51% of the original dataset) are sufficient to maintain the same level of heterogeneity of the network as observed with all the sampling units. Indeed, the additive partitioning of diversity for the reduced dataset, showed a minimum variation of α plot, β plot and β (Table 2) thus the overall signal for the whole EN remained comparable to the original. This suggests that sampling all the nodes of the EN leads to a redundancy in the data, if the aim is to point out an overall plant diversity contained within the EN.

Conversely, the approach that allows for distinguishing best among plant communities is the habitat-based sampling design. Indeed, when considering the HRS' analysis (53 plots, 27.46% of the original dataset), we noticed that the significant difference between habitat composition remained constant (Table 3) and the partitioning of diversity underwent a slight variation (Table 2). In this case, the observed variation in the diversity partitioning was due to a lower redundancy of sampled species; in fact, oversampling habitat types that had many species in common (e.g., shrublands and forests) led to a lower diversity between habitat types (72.38% in the reduced dataset vs. 66.64% of the original dataset).

Considering the results in their totality, the best approach between habitat-based and node-based depends on the aims of the research: in our study case the habitat-based approach gave us important information both on the heterogeneity of the network and on habitat types' structure and composition, but a node-based approach can be a valid alternative when time and resources are scarce and the aim is to point out an overall richness for the studied EN.

It is worth noting that our results give a general indication on the adequate sampling effort that can be applied in similar contexts. It should be highlighted that our EN is predominantly wetlands based, so more studies would be needed if applied to other habitat types (e.g., an EN based primarily on grasslands would probably need more plots). Moreover, the proposed methodology can be useful for monitoring the ENs over time, considering that ENs are never monitored after being implemented [25]. That is, starting with a sampling design proportional to the extent of the EN under study, it is possible to establish the minimum and sufficient number of sampling units to subsequently monitor diversity variation over time. Finally, our results on *MultSE* profiles, albeit applied in a completely different context, are consistent with previous studies [40,41], thus confirming it to be a useful statistic for assessing sample-size adequacy in studies of ecological communities.

Since ENs are often modeled on the basis of species-habitat interactions and designed based on graph theory [66,67], it is extremely important to join biological data in the graph's early construction stage [44] to confirm the distribution of the habitat types in the area and their composition in terms of plant communities, as they are the primary component for habitat types determination [31–34] and the basis on which the interaction species-habitat are set up.

As already acknowledged in literature, it is not recommended to analyze plant communities by preferential sampling [68,69] which may lead to biased results, and for this reason the sampling design must be probabilistic and replicates independent, and it is essential to establish a measure of sampling adequacy to exhaustively distinguish different plant communities.

A final consideration regarding wetlands should be made. These environments are reported to be less studied in ENs' literature [45] and they are known to be vulnerable ecosystems extremely important for the maintenance of biodiversity, as they are peculiar environments extremely rich in both plant and animal diversity. More than 78% of the habitat types within our EN were attributable to wetland habitat types and 4 of those resulted to be rich of rare, protected, or endemic species. In particular, *Schoenus nigricans* dominated fens (D4.11) presented seven species as well as *Molinia caerulea* meadows (E3.51), while Illyrian *Quercus robur-Carpinus betulus* forests (G1.A1A) and *Alnus glutinosa* swamp woods (G1.41), respectively, five and four species. This result confirms that these habitat types are particularly important for the conservation of biodiversity in this region [70–74] and should be paid particular attention.

5. Conclusions

In this study, we used an innovative integrated approach in order to estimate the adequate sample size to maintain the observed features of plant communities within the habitat types and nodes of the EN. This integrated method helped to fill the gaps regarding the collection of biodiversity data before the definition of an EN as well as the monitoring of biodiversity content within existing ENs.

The importance of validating ENs obtained through graph analysis, based on land cover maps and/or habitat maps, is widely known (e.g., Foltete et al. [45]). It is fundamental to optimize sampling design to enhance temporal and economic resources and define the minimum effort to adequately represent the biodiversity content of the networks.

Overall, our results gave us important information on the biodiversity conserved within the EN, the composition of plant communities and the sufficient sampling effort. One of the future developments of this study could be to distinguish between different ecological roles (e.g., Deák et al. [75]) of plant species within the habitat types for fine-tuning the methodology for applied practical conservation. In fact, the use of total biodiversity in our models is perfect for testing the integrated method but, in practical conservation planning, distinguishing between different ecological roles would be better. However, this study represents a novel approach to be applied in the context of designing and monitoring ENs, and thus more tests are needed to validate its suitability in different habitat types and organisms. In addition, we would recommend the use of this approach for conducting

pilot studies on ENs, both for designing and monitoring, aiming at optimizing resources and in general for habitat monitoring.

Supplementary Materials: The following are available online at https://www.mdpi.com/article/10.3390/d14010012/s1, Figure S1: Flow chart of the main steps applied to model the multi-species Ecological Network: starting from a map of the habitat types of the study area and combining it with a table of costs (time and effort to travel through an environment) it was obtained a map of costs for all 10 animal species and 9 plant communities (habitats) present in the landscape. From the overlay of all species-specific networks the multi-species ecological network was obtained as the sum of all identified elements. Figure S2: Spatially explicit rarefaction curve (SER, blue dashed line), traditional rarefaction curve (RC, black dotted line), habitat-based rarefaction curve (red solid line) and node-based rarefaction curve (green solid line) calculated from the whole dataset. Figure S3: Spatially explicit rarefaction curves (SERs, dashed lines) and traditional rarefaction curves (RCs, solid lines) calculated for each habitat of the ecological network. The black solid line represents the RC calculated from the whole dataset, Figure S4: Classic rarefaction curves (RCs) calculated for each node of ecological network. The black dashed line represents the RC calculated from the whole dataset, Figure S5: *MultSE* profile based on Bray–Curtis dissimilarity for each node within the ecological network, Figure S6: *MultSE* profile based on Bray–Curtis dissimilarity for the whole dataset within the ecological network, Table S1: Estimated sample size for each habitat based on the slope change in the linear relation between *MultSE* and sample size. The value could not be estimated in habitat types with 3 or less replicates (NA = Not assessed, see main text).

Author Contributions: Conceptualization, G.B. and M.S.; methodology, E.T., G.B. and M.S.; formal analysis, F.L. and E.T.; data curation, F.L. and F.B.; writing—original draft preparation, F.L.; writing—review and editing, G.B., M.S., E.T. and F.B.; supervision, G.B. and M.S. All authors have read and agreed to the published version of the manuscript.

Funding: This research received no external funding.

Institutional Review Board Statement: Not applicable.

Informed Consent Statement: Not applicable.

Data Availability Statement: All data are available on request.

Acknowledgments: We would like to thank two anonymous reviewers for providing valuable advice to improve the final version of the article. In addition, we would also like to thank the handling editor.

Conflicts of Interest: The authors declare no conflict of interest.

References

1. Landi, P.; Minoarivelo, H.O.; Brännström, Å.; Hui, C.; Dieckmann, U. Complexity and stability of ecological networks: A review of the theory. *Popul. Ecol.* **2018**, *60*, 319–345. [CrossRef]
2. IPBES. *Summary For Policymakers of the Global Assessment Report on Biodiversity and Ecosystem Services of the Intergovernmental Science-Policy Platform on Biodiversity and Ecosystem Services*; Díaz, S., Settele, J., Brondízio, E.S., Ngo, H.T., Guèze, M., Agard, J., Arneth, A., Balvanera, P., Brauman, K.A., Butchart, S.H.M., et al., Eds.; IPBES: Bonn, Germany, 2019; p. 56. [CrossRef]
3. EEA. *State of Nature in the EU Report European Environment Agency 2020. State of Nature in the EU. Results from Reporting under the Nature Directives 2013–2018*; Publication office of European Unions: Luxembourg, 2020; p. 142. ISBN 978-92-9480-259-0. [CrossRef]
4. UN (United Nation). *Transforming our World: The 2030 Agenda for Sustainable Development, A/RES/70/L.1. Resolution Adopted by the General Assembly*; United Nations: New York, NY, USA, 2015. Available online: https://sustainabledevelopment.un.org/post2015/transformingourworld/publication (accessed on 12 November 2021).
5. UN (United Nations). *Sustainable Development Goals*; United Nations: New York, NY, USA, 2015. Available online: http://www.un.org/sustainabledevelopment/sustainable-development-goals/ (accessed on 12 November 2021).
6. European Commission. Communication from the Commission to the European Parliament, the Council, the European Economic and Social Committee and the Committee of the Regions EU Biodiversity Strategy for 2030 Bringing Nature Back into Our Lives COM/2020/380 Final 20.5.2020 Brussels 2020. Available online: https://eur-lex.europa.eu/legal-content/EN/TXT/?uri=CELEX:52020DC0380 (accessed on 16 November 2021).
7. Cushman, S.A.; McRae, B.; Adriaensen, F.; Beier, P.; Shirley, M.; Zeller, K. Biological corridors and connectivity. In *Key Topics in Conservation Biology 2*; Macdonald, D.W., Willis, K.J., Eds.; Wiley-Blackwell: Hoboken, NJ, USA, 2013; pp. 384–404.

8. Pascual, M.; Dunne, J. *Ecological Networks: Linking Structure to Dynamics in Food Webs*; Oxford University Press: New York, NY, USA, 2006.
9. Fahrig, L. Effects of habitat fragmentation on biodiversity. *Annu. Rev. Ecol. Evol. Syst.* **2003**, *34*, 487–515. [CrossRef]
10. Battisti, C. *Frammentazione Ambientale Connettività Reti Ecologiche: Un Contributo Teorico E Metodologico Con Particolare Riferimento Alla Fauna Selvatica*; Provincia di Roma Assessorato alle Politiche Agricole, Ambientali e Protezione Civile: Rome, Italy, 2004. (In French)
11. Biondi, E.; Nanni, L. Geosigmeti, Unità Di Paesaggio E Reti Ecologiche. In *Identificazione E Cambiamenti Nel Paesaggio Contemporaneo*; Blasi, C., Paolella, A., Eds.; Atti del Terzo Congresso IAED: Roma, Italy, 2005; pp. 134–140.
12. Rosati, L.; Fipaldini, M.; Marignani, M.; Blasi, C. Effects of fragmentation on vascular plant diversity in a Mediterranean forest archipelago. *Plant. Biosyst.* **2010**, *144*, 38–46. [CrossRef]
13. Forman, R.T.T. *Land Mosaics*; Cambridge University Press: Cambridge, UK, 1995.
14. Foltête, J.C. How ecological networks could benefit from landscape graphs: A response to the paper by Spartaco Gippoliti and Corrado Battisti. *Land Use Policy* **2019**, *80*, 391–394. [CrossRef]
15. Tischendorf, L.; Fahrig, L. On the usage and measurement of landscape connectivity. *Oikos* **2000**, *90*, 7–19. [CrossRef]
16. Taylor, P.D.; Fahrig, L.; With, K.A. Landscape connectivity: A return to the basics. In *Connectivity Conservation*; Cambridge University Press: Cambridge, UK, 2006.
17. Taylor, P.D.; Fahrig, L.; Henein, K.; Merriam, G. Connectivity is a vital element of landscape structure. *Oikos* **1993**, *68*, 571–573. [CrossRef]
18. LaPoint, S.; Balkenhol, N.; Hale, J.; Sadler, J.; van Der Ree, R. Ecological connectivity research in urban areas. *Funct. Ecol.* **2015**, *29*, 868–878. [CrossRef]
19. Damschen, E.I. Landscape Corridors. In *Encyclopedia of Biodiversity*, 2nd ed.; Levin, S.A., Ed.; Academic Press: Cambridge, MA, USA, 2013; pp. 467–475. [CrossRef]
20. De Montis, A.; Caschili, S.; Mulas, M.; Modica, G.; Ganciu, A.; Bardi, A.; Ledda, A.; Dessena, L.; Laudari, L.; Fichera, C.R. Urban–rural ecological networks for landscape planning. *Land Use Policy* **2016**, *50*, 312–327. [CrossRef]
21. Keeley, A.T.H.; Ackerly, D.D.; Cameron, D.R.; Heller, N.E.; Huber, P.R.; Schloss, C.A.; Thorne, J.H.; Merenlender, A.M. New concepts, Models, and assessments of climate-wise connectivity. *Environ. Res. Lett.* **2018**, *13*, 073002. [CrossRef]
22. Xu, H.; Plieninger, T.; Primdahl, J. A systematic comparison of cultural and ecological landscape corridors in Europe. *Land* **2019**, *8*, 41. [CrossRef]
23. Battisti, C. Ecological network planning—From paradigms to design and back: A cautionary note. *J. Land Use Sci.* **2013**, *8*, 215–223. [CrossRef]
24. Boitani, L.; Strand, O.; Herfindal, I.; Panzacchi, M.; St Clair, C.C.; van Moorter, B.; Saerens, M.; Kivimaki, I. Predicting the continuum between corridors and barriers to animal movements using step selection functions and randomized shortest paths. *J. Anim. Ecol.* **2015**, *85*, 32–42. [CrossRef]
25. Gippoliti, S.; Battisti, C. More cool than tool: Equivoques, Conceptual traps and weaknesses of ecological networks in environmental planning and conservation. *Land Use Policy* **2017**, *68*, 686–691. [CrossRef]
26. Kareksela, S.; Moilanen, A.; Tuominen, S.; Kotiaho, J.S. Use of inverse spatial conservation prioritization to avoid biological diversity loss outside protected areas: Inverse spatial conservation prioritization. *Conserv. Biol.* **2013**, *27*, 1294–1303. [CrossRef] [PubMed]
27. Jalkanen, J.; Toivonen, T.; Moilanen, A. Identification of ecological networks for land-use planning with spatial conservation prioritization. *Landscape Ecol.* **2020**, *35*, 353–371. [CrossRef]
28. Brooks, T.M.; Mittermeier, R.A.; Mittermeier, C.G.; da Fonseca, G.A.B.; Rylands, A.B.; Konstant, W.R.; Flick, P.; Pilgrim, J.; Oldfield, S.; Magin, G.; et al. Habitat loss and extinction in the hotspots of biodiversity. *Conserv. Biol.* **2002**, *16*, 909–923. [CrossRef]
29. Wiegand, T.; Revilla, E.; Moloney, K.A. Effects of habitat loss and fragmentation on population dynamics. *Conserv. Biol.* **2005**, *19*, 108–121. [CrossRef]
30. Thiele, J.; Kellner, S.; Buchholz, S.; Schirmel, J. Connectivity or area: What drives plant species richness in habitat corridors? *Landscape Ecol.* **2018**, *33*, 173–181. [CrossRef]
31. Devillers, P.; Devillers-Terschuren, J.; Ledant, J.P. *CORINE Biotopes Manual. Habitats of the European Community*; Data Specifications—Part 2; EUR 12587/3 EN; European Commission: Luxembourg, 1991.
32. Devillers, P.; Devillers-Terschuren, J. *A Classification of Palaearctic Habitats*; Nature and Environment, No 78; Council of Europe: Strasbourg, France, 1996.
33. Davies, C.E.; Moss, D.; Hill, M.O. *EUNIS Habitat Classification Revised 2004*; Report to the European Topic Centre on Nature Protection and Biodiversity; European Environment Agency: Copenhagen, Denmark, 2004.
34. European Commission. *Interpretation Manual of European Union Habitats*; EUR 28, April 2013, DG Environment, Nature ENV B.; European Commission: Luxembourg, 2013; p. 144.
35. Lieth, H. Primary production: Terrestrial ecosystems. *Hum. Ecol.* **1973**, *1*, 303–332. [CrossRef]
36. Cao, Y.; Larsen, D.P.; Hughes, R.M.; Angermeier, P.L.; Patton, T.M. Sampling effort affects multivariate comparisons of stream assemblages. *J. N. Am. Benthol. Soc.* **2002**, *21*, 701–714. [CrossRef]
37. Yoccoz, N.G.; Nichols, J.D.; Boulinier, T. Monitoring of biological diversity in space and time. *Trends Ecol. Evol.* **2001**, *16*, 446–453. [CrossRef]

38. Balmford, A.; Green, R.E.; Jenkins, M. Measuring the changing state of nature. *Trends Ecol. Evol.* **2003**, *18*, 326–330. [CrossRef]
39. Del Vecchio, S.; Fantinato, E.; Silan, G.; Buffa, G. Trade-offs between sampling effort and data quality in habitat monitoring. *Biodivers. Conserv.* **2019**, *28*, 55–73. [CrossRef]
40. Maccherini, S.; Bacaro, G.; Tordoni, E.; Bertacchi, A.; Castagnini, P.; Foggi, B.; Gennai, M.; Mugnai, M.; Sarmati, S.; Angiolini, C. Enough is enough? Searching for the optimal sample size to monitor european habitats: A case study from coastal sand dunes. *Diversity* **2020**, *12*, 138. [CrossRef]
41. Anderson, M.J.; Santana-Garcon, J. Measures of precision for dissimilarity-based multivariate analysis of ecological communities. *Ecol. Lett.* **2015**, *18*, 66–73. [CrossRef] [PubMed]
42. Directorate-General for Environment. *EU Biodiversity Strategy for 2030: Bringing Nature Back into Our Lives*; European Commission: Luxembourg, 2020.
43. Sigura, M.; Boscutti, F.; Buccheri, M.; Dorigo, L.; Glerean, P.; Lapini, L. La rel dei paesaggi di pianura, Di area montana e urbanizzati. Piano Paesaggistico regionale del Friuli-Venezia Giulia (Parte Strategica) E1-allegato alla scheda di RER. Regione Friuli-Venezia Giulia. 2017. Available online: http://www.regione.fvg.it/rafvg/cms/RAFVG/ambiente-territorio/pianificazione-gestione-territorio/FOGLIA21/#id9 (accessed on 12 November 2021).
44. Liccari, F.; Castello, M.; Poldini, L.; Altobelli, A.; Tordoni, E.; Sigura, M.; Bacaro, G. Do habitats show a different invasibility pattern by alien plant species? A test on a wetland protected area. *Diversity* **2020**, *12*, 267. [CrossRef]
45. Foltête, J.C.; Savary, P.; Clauzel, C.; Bourgeois, M.; Girardet, X.; Sahraoui, Y.; Vuidel, G.; Garnier, S. Coupling landscape graph modeling and biological data: A review. *Landscape Ecol.* **2020**, *35*, 1035–1052. [CrossRef]
46. ISPRA. La Carta della Natura della Regione Friuli-Venezia Giulia (Aggiornamento 2017). Available online: https://www.isprambiente.gov.it/it/servizi/sistema-carta-della-natura/carta-della-natura-alla-scala-1-50.000/la-carta-della-natura-della-regione-friuli-venezia-giulia-aggiornamento-2017 (accessed on 12 November 2021).
47. Poldini, L.; Oriolo, G.; Vidali, M.; Tomasella, M.; Stoch, F.; Orel, G. Manuale degli habitat del Friuli-Venezia Giulia. Strumento a Supporto della Valutazione D'impatto Ambientale (VIA), Ambientale Strategica (VAS) e D'incidenza Ecologica (VIEc). Regione Autonoma Friuli-Venezia Giulia—Direz. Centrale Ambiente e Lavori Pubblici—Servizio Valutazione Impatto Ambientale, Univ. Studi Trieste Dipart. Biologia. 2006. Available online: http://www.regione.fvg.it/ambiente/manuale/home.htm (accessed on 12 November 2021).
48. Bartolucci, F.; Peruzzi, L.; Galasso, G.; Albano, A.; Alessandrini, A.; Ardenghi, N.M.G.; Astuti, G.; Bacchetta, G.; Ballelli, S.; Banfi, E.; et al. An updated checklist of the vascular flora native to Italy. *Plant. Biosyst.* **2018**, *152*, 179–303. [CrossRef]
49. Galasso, G.; Conti, F.; Peruzzi, L.; Ardenghi, N.M.G.; Banfi, E.; Celesti-Grapow, L.; Albano, A.; Alessandrini, A.; Bacchetta, G.; Ballelli, S.; et al. An updated checklist of the vascular flora alien to Italy. *Plant. Biosyst.* **2018**, *152*, 556–592. [CrossRef]
50. Whittaker, R. Evolution and measurement of species diversity. *Taxon* **1972**, *21*, 213–215. [CrossRef]
51. Bray, J.R.; Curtis, J.T. An ordination of the upland forest communities of Southern Wisconsin. *Ecol. Monogr.* **1957**, *27*, 325–349. [CrossRef]
52. Hothorn, T.; Bretz, F.; Westfall, P.; Heiberger, R.M. Multcomp: Simultaneous Inference in General Parametric Models. R Package. 2008. Available online: http://CRAN.R-project.org (accessed on 12 November 2021).
53. Chiarucci, A.; Bacaro, G.; Rocchini, D.; Ricotta, C.; Palmer, M.; Scheiner, S. Spatially constrained rarefaction: Incorporating the autocorrelated structure of biological communities into sample-based rarefaction. *Commun. Ecol.* **2009**, *10*, 209–214. [CrossRef]
54. Bacaro, G.; Rocchini, D.; Ghisla, A.; Marcantonio, M.; Neteler, M.; Chiarucci, A. The spatial domain matters: Spatially constrained species rarefaction in a Free and Open Source environment. *Ecol. Complex.* **2012**, *12*, 63–69. [CrossRef]
55. Bacaro, G.; Altobelli, A.; Cameletti, M.; Ciccarelli, D.; Martellos, S.; Palmer, M.W.; Ricotta, C.; Rocchini, D.; Scheiner, S.M.; Tordoni, E.; et al. Incorporating spatial autocorrelation in rarefaction methods: Implications for ecologists and conservation biologists. *Ecol. Indic.* **2016**, *69*, 233–238. [CrossRef]
56. Thouverai, E.; Pavoine, S.; Tordoni, E.; Rocchini, D.; Ricotta, C.; Chiarucci, A.; Bacaro, G. Rarefy. R Package Version 1.0.0. 2020. Available online: http://CRAN.R-project.org (accessed on 12 November 2021).
57. Oksanen, J.; Blanchet, G.F.; Friendly, M.; Kindt, R.; Legendre, P.; McGlinn, D.; Minchin, P.R.; O'Hara, R.B.; Simpson, G.L.; Solymos, P.; et al. Vegan: Community Ecology Package. R package version 2.5-6. 2019. Available online: https://CRAN.R-project.org/package=vegan (accessed on 12 November 2021).
58. Tordoni, E.; Napolitano, R.; Maccherini, S.; Da Re, D.; Bacaro, G. Ecological drivers of plant diversity patterns in remnants coastal sand dune ecosystems along the northern Adriatic coastline. *Ecol. Res.* **2018**, *33*, 1157–1168. [CrossRef]
59. Lande, R. Statistics and partitioning of species diversity, and similarity among multiple communities. *Oikos* **1996**, *76*, 5–13. [CrossRef]
60. Crist, T.O.; Veech, J.A.; Gering, J.C.; Summerville, K.S. Partitioning species diversity across landscapes and regions: A hierarchical analysis of α, β, and γ-diversity. *Am. Nat.* **2003**, *162*, 734–743. [CrossRef] [PubMed]
61. Muggeo, V.M.R. Estimating regression models with unknown break-points. *Stat. Med.* **2003**, *22*, 3055–3071. [CrossRef] [PubMed]
62. Muggeo, V.M.R. Segmented: An R package to fit regression models with broken-line relationships. *R News* **2008**, *8*, 20–25.
63. Franklin, J.; Serra-Diaz, J.M.; Syphard, A.D.; Regan, H.M. Global change and terrestrial plant community dynamics. *Proc. Natl. Acad. Sci. USA* **2016**, *113*, 3725–3734. [CrossRef] [PubMed]
64. De Simone, S.; Sigura, M.; Boscutti, F. Patterns of biodiversity and habitat sensitivity in agricultural landscapes. *J. Environ. Plan. Manag.* **2016**, *60*, 1173–1192. [CrossRef]

65. Arrhenius, O. Species and area. *J. Ecol.* **1921**, *9*, 95–99. [CrossRef]
66. Urban, D.L.; Minor, E.S.; Treml, E.A.; Schick, R.S. Graph models of land mosaics. *Ecol. Lett.* **2009**, *12*, 260–273. [CrossRef] [PubMed]
67. Galpern, P.; Manseau, M.; Fall, A. Patch-based graphs of landscape connectivity: A guide to construction, analysis and application for conservation. *Biol. Conserv.* **2011**, *144*, 44–55. [CrossRef]
68. Diekmann, M.; Kühne, A.; Isermann, M. Random vs non-random sampling: Effects on patterns of species abundance, species richness and vegetation-environment relationships. *Folia Geobot.* **2007**, *42*, 179. [CrossRef]
69. Lájer, K. Statistical tests as inappropriate tools for data analysis performed on non-random samples of plant communities. *Folia Geobot.* **2007**, *42*, 115–122. [CrossRef]
70. Poldini, L.; Oriolo, G. Alcune entità nuove e neglette per la flora italiana. *Inf. Bot. Ital.* **2002**, *34*, 105–114.
71. Wassen, M.J.; Venterink, H.O.; Lapshina, E.D.; Tanneberger, F. Endangered plants persist under phosphorus limitation. *Nature* **2005**, *437*, 547–550. [CrossRef]
72. Dybkjær, J.B.; Baattrup-Pedersen, A.; Kronvang, B.; Thodsen, H. Diversity and distribution of riparian plant communities in relation to stream size and eutrophication. *J. Environ. Qual.* **2012**, *41*, 348–354. [CrossRef]
73. Natlandsmyr, B.; Hjelle, K.L. Long-term vegetation dynamics and land-use history: Providing a baseline for conservation strategies in protected *Alnus glutinosa* swamp woodlands. *For. Ecol. Manag.* **2016**, *372*, 78–92. [CrossRef]
74. Della Longa, G.; Boscutti, F.; Marini, L.; Alberti, G. Coppicing and plant diversity in a lowland wood remnant in North–East Italy. *Plant. Biosyst.* **2020**, *154*, 173–180. [CrossRef]
75. Deák, B.; Rádai, Z.; Lukács, K.; Kelemen, A.; Kiss, R.; Bátori, Z.; Kiss, P.J.; Valkó, O. Fragmented dry grasslands preserve unique components of plant species and phylogenetic diversity in agricultural landscapes. *Biodivers. Conserv.* **2020**, *29*, 4091–4110. [CrossRef]

diversity

MDPI

Article

Structure and Functionality of the Mesozooplankton Community in a Coastal Marine Environment: Portofino Marine Protected Area (Liguria)

Paolo Vassallo [1,*], Daniele Bellardini [1,2], Michela Castellano [1], Giulia Dapueto [1] and Paolo Povero [1]

[1] Department for the Earth, Environment and Life Sciences, University of Genoa, 16132 Genoa, Italy; daniele.bellardini@szn.it (D.B.); michela.castellano@unige.it (M.C.); giulia.dapueto@edu.unige.it (G.D.); povero@unige.it (P.P.)

[2] Department of Research Infrastructures for Marine Biological Resources, Stazione Zoologica Anton Dohrn, Villa Comunale, 80121 Naples, Italy

* Correspondence: paolo.vassallo@unige.it; Tel.: +39-01-0353-8069

Abstract: This research is part of the LTER (Long-Term Ecological Research) project, a network of terrestrial, freshwater, transitional water and marine sites, on which ecological research is conducted on a multi-decade scale. LTER studies ecosystems, their dynamics and evolution, the relationships between biodiversity and ecological functionality, water quality, productivity, the role of resource availability, the effects of pollution and climate change. The research focuses on the study of the variability of zooplankton groups in the Portofino marine protected area, in Punta Faro. The samplings were carried out in the years 2018–2019, and the results were compared with the values of the years 2003–2005, interesting from a meteorological climatic and biological point of view. The plankton community of the Punta Faro system was analyzed by means of a modeling approach to obtain information on the functionality and health status of the system and to verify whether this has undergone any alterations in the last decade. The analyses carried out show a clear difference between the three-year period 2003–2005 and the two-year period 2018–2019, highlighting how environmental changes, such as the increase in temperature, have led to higher costs of system functioning in the last two years. The mesozooplankton community has changed both in terms of abundance of organisms and in terms of organization and functionality.

Keywords: ecological network analysis; emergy analysis; ascendency; Ligurian Sea; Mediterranean Sea

Citation: Vassallo, P.; Bellardini, D.; Castellano, M.; Dapueto, G.; Povero, P. Structure and Functionality of the Mesozooplankton Community in a Coastal Marine Environment: Portofino Marine Protected Area (Liguria). *Diversity* **2022**, *14*, 19. https://doi.org/10.3390/d14010019

Academic Editor: Michael Wink

Received: 3 December 2021
Accepted: 25 December 2021
Published: 29 December 2021

1. Introduction

The LTER-Italy Network is based on the general principles of the International LTER network and has the primary objective of promoting and supporting the acquisition of data and information relating to the basic variability and evolutionary trends of ecological processes and to support the development of sustainable management strategies of ecosystems, which can favor the integration of terrestrial and aquatic ecological research. The Protected Marine Area of Portofino has been part of the LTER network (site IT15 Ligurian Sea) since 2007 with two coastal stations, one in front of Punta Faro (zone B) and one in correspondence with Cala dell'Oro (zone A). The research is aimed at continuing the study of the structure and dynamics of zooplankton groups in the Portofino MPA, in Punta Faro.

Zooplankton plays a vital role in marine ecosystems. In particular, the organisms that make up mesozooplankton feed directly on phytoplankton, microzooplankton, other mesozooplankton and detritus and they are among the largest organisms that still have a significant feedback interaction with primary production [1].

Globally they are one of the main players in the flow of vertical particles in the oceans, so they are important both in the pelagic food web and in export processes, influencing the biogeochemical cycle of carbon and other nutrients in marine environment. Therefore,

understanding the structure and functioning of the planktonic community is crucial for tracking biogeochemical cycles and predicting the future responses of aquatic ecosystems to environmental changes [2,3].

Several studies have investigated whether these organisms could be used in the assessment of environmental quality status [4,5] and therefore be considered as indicators of ecosystem changes [6–8], organisms or group of organisms (populations, communities) which through a biochemical, physiological or ecological response allow to evaluate an alteration in the quality of the environment [9].

The zooplankton composition and abundance are influenced by various chemical, physical and biological variables, among these it is known how the zooplankton density is influenced by the properties of the water masses in which they live [10].

Several studies on zooplankton organisms as biological indicators focus on two main aspects: on the one hand, the analysis of the medium and long-term variations of the community in relation to the alterations induced by hydro-climatic variables on a local scale [11], regional [12] and global [13]; on the other hand, zooplankton changes due to the heavy anthropic impact on the coastal marine system [14].

Climate change is one of the aspects that have received the most attention in recent years; in fact, there are many studies that focus on how the increase in temperature can affect the marine ecosystem [15]. In several works, it is evident how these changes are reflected above all at the base of the trophic network (planktonic communities) which undergoes both quantitative and qualitative changes, such as the alteration of seasonal cycles, vertical migrations, and algal blooms.

All of this leads to important consequences at the ecosystem level, both from a socio-economic point of view, by decreasing the availability of fish resources [13,16], and from an ecological point of view, as variations of zooplankton communities affect the regeneration of nutrients [17] and the transport of organic matter.

In the works of Ribera d'Alcalà et al. [18] and Molinero et al. [19], it is highlighted that in different areas of the Mediterranean Sea, since the second half of the Eighties, the increase in temperatures influenced the zooplankton component, causing an increase in the population of gelatinous organisms and the consequent decline in copepod abundance.

A first attempt to analyze the changes in the planktonic community in LTER Italia sites was made by Morabito et al. [20]. In the Portofino site in the Ligurian Sea, an increase in the total abundance of mesozooplankton is evident, characterized by a reduction in the percentage contribution of copepods and an increase in Cladocera. Key species such as *Centropages typicus* decreased while small copepods (0.5–1 mm) increased, along with Appendicularia.

While the identification of changes in the community composition is important to detecting variations in the species composition and abundance, it gives poor information on the functioning of the system and on the adaptation strategies that complex natural systems may put in place to cope with changes in the surrounding environment. In this context, a series of whole system analyses based on the assessment and the investigation of the system functioning are here proposed. With the aim to cover different aspects of the complex functioning of the plankton community Energy Systems Theory and Emergy Analysis (Emergy is defined as the sum of the available energy of one kind, e.g., solar joules, which is used-up, directly and indirectly, within an ecosystem for the production of goods and services) were applied to quantify the health of these benthic ecosystems and evaluate differences in their structure, organization and functional capacities.

The application of a whole system perspective for the evaluation of the structure and functionality of the zooplankton community is not widely reported in the scientific literature. The role of these indices allows a more in-depth study of the observed system and thanks to these it has been possible to search for signals that can highlight changes at the environmental level. This study compared two periods 13 years apart (2003–2005; 2018–2019), highlighting an ongoing climate change which is leading to functional changes in the system.

2. Materials and Methods

2.1. Study Site

The Portofino Promontory (Figure 1) has a very complex circulation because it is linked both to the meteo-climatic (wind direction and intensity) and hydrodynamic (dominant circulation) forcing, and to the interference of the promontory itself together with the narrow continental shelf [21–24]. Current historical series show that the current off Sestri Levante in winter has a North-West direction (Ligurian Provençal current), consistent at all depths, while on the other side of the promontory it has the opposite direction (South-East) with some variation in the vertical component and, finally, off the coast of Bogliasco or 15 km downstream of the promontory it again has a north-west direction and consistency at all depths, also confirmed by numerical models [22].

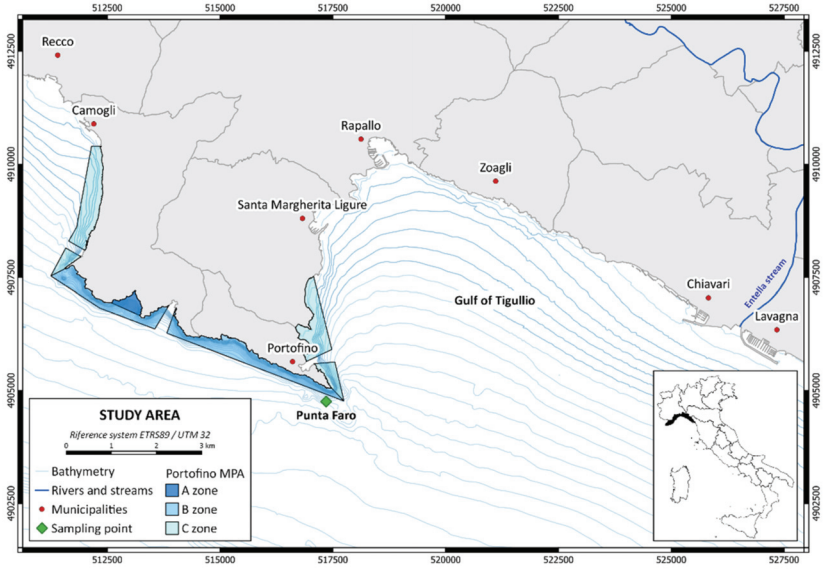

Figure 1. Study area.

The predominance of the current towards the Southeast during the surveys near Camogli suggests the existence of a recirculation or anticyclonic vortex with an intensity of the order of 10% of the inlet current and with an extension of less than 15 km. This vortex was highlighted in the spring by a superficial drifter, caught by the coastal current [23], but the presence of a fish trap, "tonnarella", in the area overlooking Camogli since 1600, testifies how the vortex is a regularly occurring structure in the area. Occasional current reversals off Camogli can be induced by local winds. Facing the western cape of the Promontory (Punta del Faro), the main stream from east to west can intensify and be moved away from the promontory towards the open sea (in case of winds from NE and SE), while occasionally, in case of winds from SSW, the coastal circulation inside the Gulf of Tigullio intensifies, as a consequence of water accumulation along the coast, generating an upstream vortex and one against the coastal current from West to East [21].

Several torrential water courses flow into the Gulf of Tigullio, but generally do not lead to high inputs of fresh water. For this reason, the coastal waters around the Promontory maintain a marked oligotrophy [20], like the waters further offshore, which tends to be more pronounced in recent years than in the past [25]. The main supply of fresh water comes from the Entella stream that flows between Chiavari and Lavagna. The Entella stream, in fact, together with the other minor watercourses that flow into the Gulf of Tigullio, is important as it modifies the physical chemical and biological conditions of the

marine environment, both as an input of inorganic nutrients and as it favors stability of the water column, decreasing the salinity; this influences the dynamics of phytoplankton biomasses which are affected in a short time by the input of nutrients [26,27].

2.2. Field Activity

Both the zooplankton samplings and the seawater features were investigated as part of LTER program monitoring in Punta Faro station (Figure 1), around 80 m depth, every 15 days, according to the meteo-marine situation, on board the "M/B Veliger", since 2000 for environmental features and since 2003 for zooplankton.

2.2.1. Environmental Features

Sea temperature and fluorescence were acquired by an Idronaut 301 (2003–2005) and 316 plus (2018–2019) probe equipped with a Turner Cyclops 7™ fluorometer along the entire water column. To calibrate the fluorometer, in situ seawater samples were collected and chlorophyll-a was determined in the laboratory [28]. CTD data were averaged for each meter and the monthly means were calculated in the 0–50 m layer.

2.2.2. Zooplankton Sampling and Laboratory Procedures

The collection of mesozooplankton was carried out using a WP2 type plankton net with 200 μm meshes, a mouth with a diameter of 57 cm for the years 2003–2005 and a General Oceanics net with a 200 μm mesh, a mouth with a diameter of 50 cm for the years 2018–2019. A vertical descent from −50 m depth to the surface was carried out. The collected samples were transferred into containers and suitably fixed for storage (final 4% formaldehyde solution) to perform taxonomic studies and to identify the feeding strategy. All samples were split with a Folsom plankton splitter into subsamples according to their abundance and were sorted into different taxa and identified under a stereomicroscope (Zeiss) to group level, while for copepods an aliquot of the whole samples was considered where at least 100 copepods could be identified [29] to species or genus level. A total of 100 samples were analyzed in this study (2003:24; 2004:20; 2005:19; 2018:18; 2019:19). In 2018–2019 two replicates were collected in order to determine also the total biomass (dry weight) filtering the samples through pre-weighted 200-μm nets. The zooplanktonic biomass was calculated by weighing the collected nets after drying overnight (60 °C).

2.3. Abundance to Biomass Conversion

The application of a mass balance trophic network model needs the estimation of biomass values for the functional groups in the system.

Chlorophyll-a concentrations were converted into carbon equivalents by applying the coefficient 40 μg C μg chl-a [30]. The abundance of zooplankton was converted into biomass through the application of conversion factors available in the literature (e.g., [31]). Whenever this conversion was not available, biomass was estimated by means of procedures based on the length/biomass ratio (e.g., [32]). This latter procedure was applied in this study to the pteropods. In particular, the length (L, mm) of the organisms was first converted to wet weight (WW, mg) and then transformed into DW using conversion factors available in the literature [32,33]. Finally, the biomass was transformed into carbon using a conversion factor of 0.25 [34]. Conversion factors applied in this study are reported in Appendix A (Table A1).

Aiming at a validation of the abundance of biomass conversion, the sum of all the estimated biomasses was compared to the total measured biomass values in each sample. Differences were always moderate and statistically not relevant (one-way ANOVA, $p > 0.1$)

2.4. Data Processing

Monthly standardized anomalies (zero mean and unit variance) were calculated for temperature (0–50 m average and 0–5 m average) and fluorescence (0–50 m average)

removing to each monthly mean the five years monthly mean and dividing for the five years standard deviation.

Differences in the anomalies and zooplankton biomass values were tested with ANOVA.

Moreover, the Redundancy Analysis multivariate technique (RDA) [35] was used to verify the influence of seawater temperature and fluorescence on the average annual zooplankton biomass of the functional groups. The response variables (zooplankton variables) were log-transformed prior to the analysis and then standardized to minimize the effects of outliers and extreme values, while standardized monthly anomalies of temperature in the 0–50 m layer (T_An), temperature in the 0–5 m layer (T5_An) and fluorescence in the 0–50 m layer (Chl_An) were used as explanatory variables.

To test the order of importance of the explanatory variables, an automated forward selection model was applied. First the "marginal effects", namely the variance expressed by only one explanatory variable, were calculated; then the "conditional effects" that show the increase in total sum of eigenvalues after including a new variable during the forward selection. RDA analysis was performed using Brodgar 2.5.6 (2011, Highland Statistics Ltd., Newburgh, United Kingdom).

2.5. Modelling Approach

The plankton community has been analyzed through an ecosystem approach in terms of structure and functioning based on the quantification and characterization of flows acting within the system [36]. System flow analysis was performed through the development and calibration of simulations of the trophic web by means of Ecopath software. Ecopath uses a set of linear equations in order to balance the flows (in and out) of each element or functional group (species or groups of species) [37]. The simulation's routine is based on a system of linear equations, which can be expressed for an arbitrary time period by:

$$B_i \times \left(\frac{P}{B}\right)_i \times EE_i = \sum_{j=1}^{n}\left[B_j \times \left(\frac{Q}{B}\right)_j \times DC_{ij}\right] \quad (1)$$

Five parameters are needed for each group: biomass (B), production/biomass ratio (P/B), consumption/biomass ratio (Q/B), ecotrophic efficiency (EE) and diet matrix (DC). If one of these parameters is not available, it could be calculated knowing 4 further parameters: unassimilated/consumption (Un/Q), net migration rate (E), biomass accumulation (BA), catch mortality (Y). Since ecotrophic efficiency was always lacking it has been estimated considering E, BA and Y null for each simulation. Employed data of P/B, Q/B and Un/Q are reported in Appendix A (Table A2) together with their reference sources. Whenever two or more species were characterized by the same parameters, they were collapsed into one single functional group in the simulations).

The software routine gives an error message if the simulation output is not realistic. If inconsistencies were detected (i.e., EE > 1) the diet matrix was slightly adjusted to get to a successful simulation [38]. Whenever the diet matrix was modified, the number (and obviously the position) of fluxes remained unchanged.

2.5.1. Model Outputs

Ecological indices were used to analyze the structure and functioning of the plankton community based on trophic flows analysis, thermodynamic concepts, information theory and trophodynamic indicators [38].

Mixed Trophic Impact

Direct and indirect trophic interactions among functional groups were analyzed by means of the Mixed Trophic Impact (MTI) approach [39,40].

Mixed trophic impact is able to account for the relative direct and indirect effects of any group within the mesozooplankton community on another group by applying hypothetical biomass changes.

MTI was calculated in accord with Ulanowicz and Puccia [40]:

$$\lfloor M \rfloor = ([I] - [Q])^{-1} - [I] \quad (2)$$

where M (MTI) is all the mixed trophic impacts that occur in the food web, Q is the net impact matrix involving all impacts, and I is the identity matrix. Each q_i element of the Q matrix results from the differences between the positive effects d_{ji} (the fraction of the prey i in the diet of the predator j) and negative effects f_{ij} (the fraction of total consumption of i used by predator j) [40,41].

The MTI range from −1 to +1, and values close to these limits indicate strong effects. For the sake of clarity in this research only the five groups having the highest positive impacts and the highest negative impacts were taken into consideration.

Ecological Network Analysis

Functionality, efficiency, and ability to exploit, move and convey energy and matter are emergent properties of a complex living system. A whole system approach is necessary to identify, measure and combine the web of fluxes acting within the ecosystem. A set of metrics (here referred to as network analysis) based on a statistical approach to the study of ecosystem fluxes was proposed by Ulanowicz [42]. Network analysis is able to measure key signals of ecosystem functioning and to provide information regarding the ecosystem status. Total trophic flows within the community in terms of consumption, production, respiration, exports and imports and flow to detritus were quantified for the analyzed plankton community. The sum of all these flows represents the Total System Throughput (TST) that is here intended as the measure of the activity or size of the system functioning [43]. Complementary to the quantitative information provided by TST, the level of organization of the exchanges among components of the system can be assessed. Average mutual information (AMI) is based on the statistical evaluation of how much each flux acting in the considered web is forced to enter a specific compartment (j) when released by another one (i) [42,44] suggested the formulation for its calculation as:

$$AMI = \sum_{i=1}^{n} \sum_{j=1}^{n} \frac{T_{ij}}{T} \log\left(\frac{T_{ij} B^2}{B_i B_j T}\right) \quad (3)$$

where T_{ij} is the flux of biomass out of i-group and going in j-group, T is the sum of all the fluxes of biomass in the system and B_i and B_j are the biomasses of i-group a j-group, respectively. Ascendency (A) incorporates aspects of both a system's size (TST) and the degree of organization (AMI) with which the material is being processed [44]. Computation of Ascendency used the following equation:

$$A = TST * AMI = \sum_{i=1}^{n} \sum_{j=1}^{n} T_{ij} \log\left(\frac{T_{ij} B^2}{B_i B_j T}\right) \quad (4)$$

Emergy Analysis

Emergy accounting is an environmental accounting method proposed by [45] as a metric able to account for the differences in the energies flowing in a system that are not equivalent in terms of their ability to perform work. In this method, all inputs supporting a system are accounted for in terms of their solar emergy, defined as the total amount of solar available energy (exergy) directly or indirectly required to make a given product or support a given flow, and measured as solar equivalent Joule (sej) [45]. An accounting method for the assessment of the emergy content of marine system has been recently proposed [46] (refer to this study for the methodology description) and applied to different systems from benthic [47,48] to oceans [49]. The emergy content of each element of the system is accounted for in function of different properties depending on the size of each element (i.e., biomass) and on the organization or complexity (i.e., rate of consumption and trophic level)

that are information retrieved by the modelling approach applied in this study. In this study, the accounting system for the emergy evaluation has been applied for the assessment of both the natural capital (i.e., the stock of biomass) and the functioning of the system (i.e., the resources exploited on a yearly basis).

In thermodynamic terms, the increase in size and complexity (and in turn in emergy) means that ecosystems gain order and move away from the state of thermodynamic equilibrium, and this thermodynamic property of natural systems can be used to assess the ecological condition (e.g., the health) of ecosystems [50].

3. Results

3.1. Environmental Features

Figure 2A shows the temperature trend along the water column in relation to the depth in the years 2003–2005.

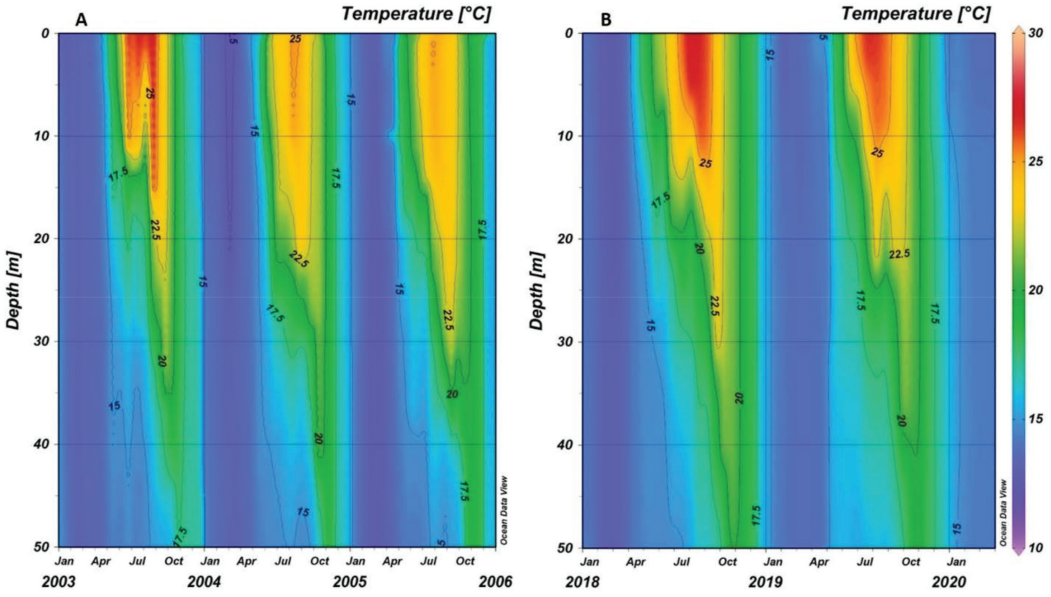

Figure 2. Temperature trend (°C) in the water column during the three years (**A**) and the two years (**B**).

The graph shows a regular trend of this variable, with high summer-spring surface values (21.7 ± 3.4 °C) and low autumn-winter surface values (16.6 ± 3.3 °C), but high interannual variations are evident. The maximum temperatures were recorded on the surface in August 2003 (26.5 °C); the minimums on the surface were recorded in March 2004 (12.5 °C).

Figure 2B shows the temperature trend along the water column in the years 2018–2019, a regular trend of the variable is observed, with high surface values in the warm seasons (23.3 ± 2.5 °C) and low surface values in the winter autumn seasons (15.4 ± 2.5 °C). The maximum temperatures were recorded on the surface in August 2018 (27.2 °C); the surface minima were measured in March 2018 (12.6 °C). Differences were analyzed using a one-way ANOVA followed by a Fischer post hoc test ($p < 0.01$)

In both graphs we can see the progressive establishment of the thermocline, which is evident in the months of July–August, with very warm surface waters and colder deep waters. In the following months, the surface heat is transferred to the deeper layers. Summer 2003 experienced a positive temperature anomaly, similar to those of summer 2018 and 2019.

Autotrophic biomass (Figure 3), expressed as chlorophyll-a (μg/L), in the 50 m-surface layer shows a clear seasonal cycle (one-way ANOVA, $p < 0.01$) with higher values in winter and decreasing trend up to summer, and an increase in autumn. The major interannual variation occurred in winter due to the high variability of the late winter/early spring blooms. The highest autotrophic biomass occurred in winter 2018 and in winters 2003 and 2004 the seasonal average values exceeded 0.50 μg/L. Conversely, in autumn 2018 and 2004 the increase in concentration was almost missing, as the seasonal average values were very similar to the ones of the summer in those years (<0.2 μg/L). Analyzing the annual average values, the difference in the 2003–2005 period is low (0.30 ± 0.19 μg/L in 2003; 0.31 ± 0.19 μg/L in 2004 and 0.29 ± 0.08 μg/L in 2005), while 2018 shows the highest average and 2019 the lowest (0.36 ± 0.25 μg/L and 0.25 ± 0.11 μg/L, respectively).

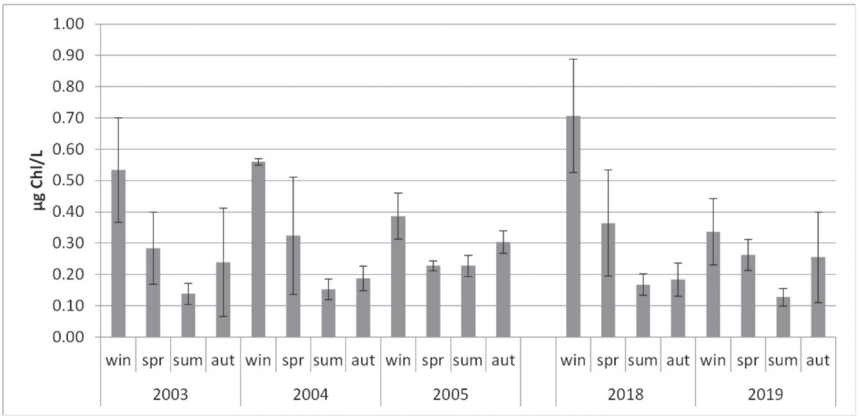

Figure 3. Seasonal autotrophic biomass as average chlorophyll-a (μg/L) in the 50 m-surface layer. Win: January–March; spr: April–June; sum: July–September; aut: October–December. Bars denote standard deviation.

3.2. Zooplankton Community

The complete list of the mesozooplankton species collected is reported in Appendix A (Tables A3–A7) together with abundances and sampling frequencies. Considering the annual mean abundance of the mesozooplankton organisms (both adults and juveniles) (Figure 4), it appears clear that copepods were the main abundant taxa in the five years, and the most abundant trophic group (ind/m^3) was represented by herbivorous copepods (HC). It accounted for more than 50% each year, with peaks of abundance in 2003, 2005 and 2019, close to 1000 ind/m^3 (46%), but only in 2005 they accounted for more than 60% of the total organisms. Among copepods, the least represented group were detritivorous copepods (DC), which accounted for less than 2% in the 2003–2005 period but increased their contribution in 2018 and 2019 (3.2 and 2.5%, respectively) with a percentage of about 3%. The omnivorous copepods (OC) contribution varied from 16.5 to 26.4% not showing differences between the periods. Carnivorous copepods (CC), as detritivorous, were less abundant in 2003–2005 period (1.2–2.2%) and increased in 2018–2019 reaching a percentage contribution like that of DC (3.3% and 2.6%, respectively, in 2018 and 2019).

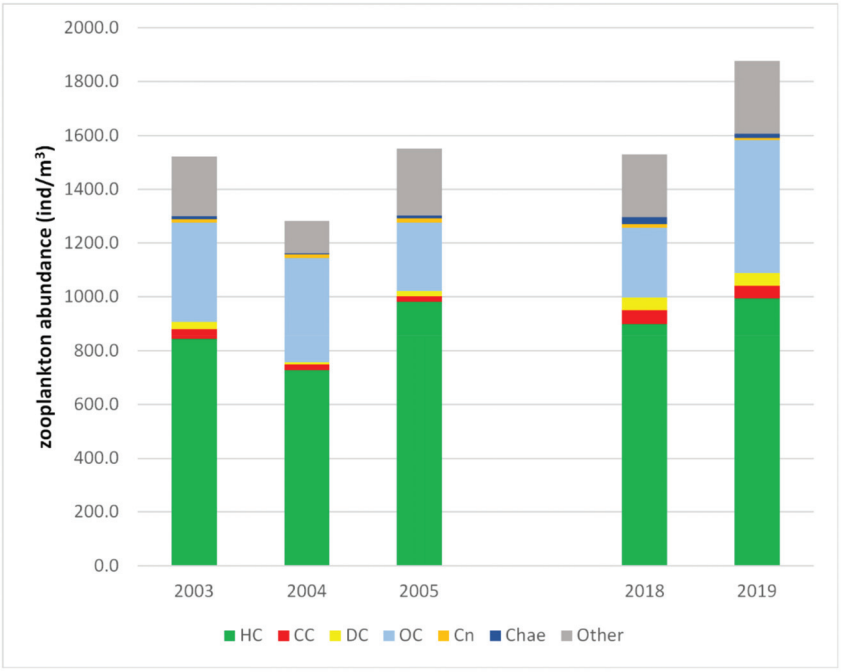

Figure 4. Zooplankton average abundance (ind/m^3) in the five years according to main taxa (Copepods are divided by trophic strategy: HC-herbivorous copepods, CC-carnivorous copepods, DC-detritivorous copepods, OC omnivorous copepods; Cn-Cnidarians; Chae-Chaetognata; Other- other organisms mainly Cladocera, Appendicularia, Thaliacea and Thecosomata-Pteropoda).

Other carnivorous organisms, Cnidaria (Cn) and Chaetognata (Chae), showed low abundance: 22.30 ± 4.23 ind/m^3 in 2003–2005 and a slightly higher 31.36 ± 12.81 ind/m^3 in 2018–2019, while the contribution of other organisms (Other), mainly Cladocera, Appendicularia, Thaliacea and Pteropoda, varied from 7.9% to 16.1% according to the years.

Total abundance was higher in 2019 (>1800 ind/m^3) and lower in 2004 (<1300 ind/m^3).

The contribution of each taxa/trophic group in terms of biomass (mgC/m^3) has been drawn up and Figure 5 shows the changes in the relationships between the years and between the trophic groups. Since most of the copepods have a small size, their overall contribution shifts below 50%. The HC are always the dominant group, but the percentage contribution of this trophic group is reduced to 43.5% in 2003–2005 period and to 39.7% in 2018–2019, with minimum percentages in 2018 (30.1%). The OC contributes for around 2% each period, while CC and DC contribute for even less, but their biomass is higher in 2018–2019 period (one-way ANOVA, $p < 0.05$ and $p < 0.001$, respectively, for CC and DC). Carnivorous larger organisms such as Cnidaria (Cn) and Chaetognata (Chae) acquire relevance every year: Cn contribution varies from 12.2% in 2019 to 31.9% in 2005 and Chae from 8.3% in 2004 to 41.2% in 2018, together accounting for nearly 50% of the total biomass. In particular, Chae have higher biomass in 2018–2019 period (one-way ANOVA, $p < 0.05$). The contribution of Other, conversely, decreases to less than 6%.

Total biomass was highest in 2018 (13.1 ± 9.2 mgC/m^3) and lowest in 2004 (7.7 ± 3.0 mgC/m^3) despite differences were not statistically relevant (one-way ANOVA, $p > 0.1$).

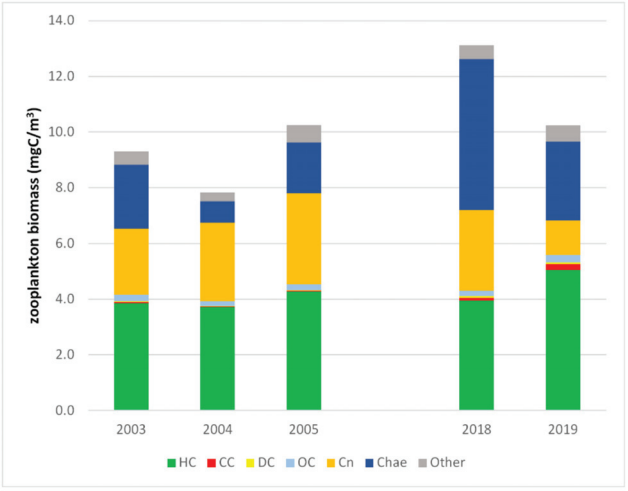

Figure 5. Zooplankton average biomass (mgC/m^3) for five years according to main taxa (Copepods are divided by trophic strategy: HC-herbivorous copepods, CC-carnivorous copepods, DC-detritivorous copepods, OC omnivorous copepods; Cn-Cnidarians; Chae-Chaetognata; Other- other organisms mainly Cladocera, Appendicularia, Thaliacea and Thecosomata-Pteropoda).

3.3. Influence of Environmental Features on Zooplankton

Redundancy analysis developed considering the three explanatory variables (T_An, Chl_An and T5_An) explains 84% of the variation in the annual zooplankton biomass data. The two-dimensional approximation in Figure 6 explains 80.0% of this (59.5% on axis 1 and 20.5% on axis 2). Therefore, the first two axes explain 67.2% of the total variation in the annual zooplankton biomass data.

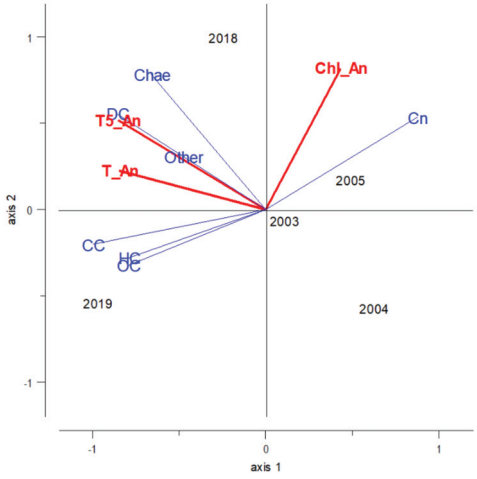

Figure 6. RDA correlation triplot for annual average zooplankton biomass and environmental variables anomalies. In blue: the response variables (zooplankton biomass functional groups); in red: the explanatory variables (monthly anomalies of temperature in the 0–50 m layer T_An, temperature in the 0–5 m layer T5_An, and fluorescence in the 0–50 m layer Chl_An); in black: the five years. (Copepods are divided by trophic strategy: HC-herbivorous copepods, CC-carnivorous copepods, DC-detritivorous copepods, OC omnivorous copepods; Cn-Cnidarians; Chae-Chaetognata; Other-other organisms mainly Cladocera, Appendicularia, Thaliacea and Thecosomata-Pteropoda).

The results of the forward selection and the permutation tests continue to explain a high percentage of variance (84.5%) and indicate that temperature anomalies have the main "marginal" effect (58.03% and 52.97%, respectively, T5_An and T_An, while Chl_An alone only explains 30.39%) and considering the "conditional effects" T5_An has the highest explained variation (0.49). The increase in explained variation due to adding an extra explanatory variable show Chl_An followed by T_An (0.27 and 0.08, respectively). The triplot in Figure 6 indicates that T5_An and T_An were positively related and T5_An was highly positively related to DC, Other and chaetognats, while T_An was partially positively correlated to CC, HC and OC. Chl_An instead was positively related to cnidarians. The five years grouped in different ways: the years of the period 2003–2005 grouped closer in the first and second quadrant while 2018 and 2019 were more apart in the third and fourth.

3.4. Modelling Approach

The main statistics describing the output of the ecological models estimated in each simulation together with the network flows and information indices were reported in Table 1.

Table 1. Output parameters from the Punta Faro mesozooplankton community model (TL: trophic level, TST: total system throughput).

	Groups Number	TL Mean	TL Max	Production (Sum)	Respiration (Tot)	Flows to Detritus	TST
					mgC/m^3/year		
				2003			
Minimum	16.00	1.26	1.61	7.40	2.00	5.23	12.91
Maximum	22.00	1.98	2.41	31.06	8.44	29.15	45.12
Mean	19.83	1.67	2.10	17.57	4.50	12.76	28.90
St.dev.	1.59	0.26	0.22	9.94	2.24	8.46	12.43
				2004			
Minimum	13.00	1.31	1.49	7.61	1.86	4.94	12.17
Maximum	23.00	1.79	2.35	28.26	6.52	26.53	42.17
Mean	18.45	1.53	1.95	16.13	3.66	13.94	26.87
St.dev.	2.46	0.17	0.28	10.08	1.36	9.40	10.22
				2005			
Minimum	15.00	1.23	1.41	12.71	1.42	6.83	20.22
Maximum	20.00	1.94	2.48	25.96	10.48	20.14	53.01
Mean	17.82	1.62	2.00	17.21	4.90	12.13	30.10
St.dev.	1.60	0.20	0.27	4.15	2.30	4.13	9.00
				2018			
Minimum	16.00	1.31	1.77	8.13	2.59	4.17	15.44
Maximum	22.00	2.22	2.45	47.97	7.40	41.42	56.06
Mean	19.09	1.75	2.18	22.13	4.54	16.37	33.36
St.dev.	1.76	0.27	0.19	14.05	1.61	12.69	15.38
				2019			
Minimum	17.00	1.38	2.00	8.01	1.31	4.33	11.23
Maximum	22.00	2.26	2.66	36.93	13.67	17.64	50.45
Mean	19.58	1.77	2.26	21.12	5.28	10.75	28.93
St.dev.	1.44	0.24	0.19	5.85	3.29	3.96	10.92

A number of functional groups showed low variability among simulations and ranged from a minimum of 13 groups to a maximum of 23. The sum of all production displayed higher values in 2018–2019 while respiration, flow to detritus and the sum of all the flows in the network (total system throughput) did not show clear differences among years.

Both the average and the maximum values of the trophic levels show consistent trends in the two considered periods with higher values in the period 2018–2019. The highest trophic levels corresponded to the presence of Cnidaria (average TL = 3.06) and Chaetognata (average TL = 2.72). Differences in the average trophic levels of the networks are also mirrored by variations in the organization of the food chain and in the groups targeted for consumption (Figure 7). Despite the consumption of autotrophs playing a major role in all the considered years, the average food chain organization in 2018–2019 has shifted towards higher consumption of detritus and heterotrophs reducing the share of autotrophs consumption.

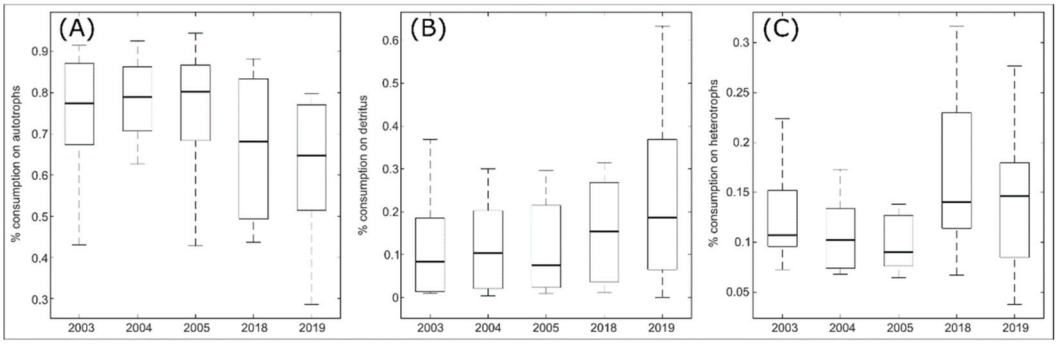

Figure 7. Percentage of total consumption on autotrophs (**A**), detritus (**B**) and heterotrophs (**C**).

3.4.1. Mixed Trophic Impact

The total MTI analysis was carried out for each simulation in order to identify the functional group with the highest influence on the biomass of the others in the analyzed trophic web. In all the simulated networks, primary producers played the top positive role in the system. For the sake of clarity, results are shown excluding the primary producers' role and taking into consideration the frequency each functional group was identified among ones having of the top five positive or negative effects (Figure 8). Juvenile copepods played a major positive role in the plankton community during the entire period, together with herbivorous copepods, despite these latter losing importance in recent years. During the 2003–2005 period Thecosomata often had a negative impact while *Oncaea* spp. as well as omnivorous cyclopoids (mainly *Oithona* spp.) played a major positive role only in the 2018–2019 samples. Regarding the negative overall effects, the highest impact on the web was always due to Appendicularia, Chaetognata, Cnidaria, Thecosomata and other omnivorous juveniles (as crustaceans' larvae).

3.4.2. Ecological Network Analysis

Average mutual information variations are very narrow ranging from 1.02 to 1.22 with an overall average value of 1.14 ± 0.05 (Figure 9). AMI values are consistent between the considered periods with the highest values during the warm season (spring and summer) and the lowest values in winter.

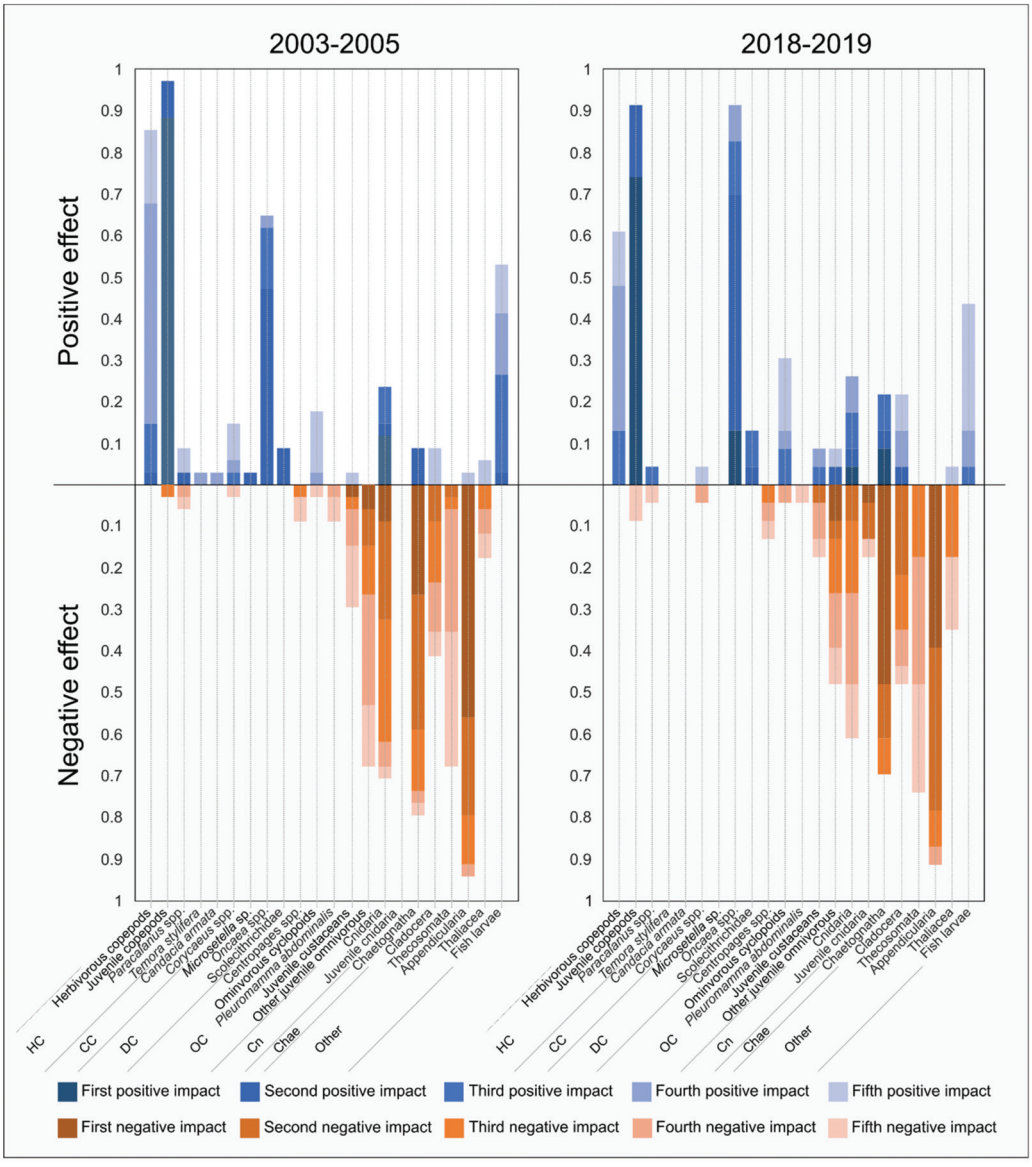

Figure 8. Positive and negative effects of considered functional group (values reported as frequency of appearance).

Ascendency ranges from 8.16 to 55.47 mgC/m^3/year averaging 26.23 $\pm$ 10.81 mgC/m^3/year. Maximum values and highest variability are displayed in spring (Figure 9). Ascendency in the two years period 2018–2019 always displayed larger maximum, minimum and average values than 2003–2005.

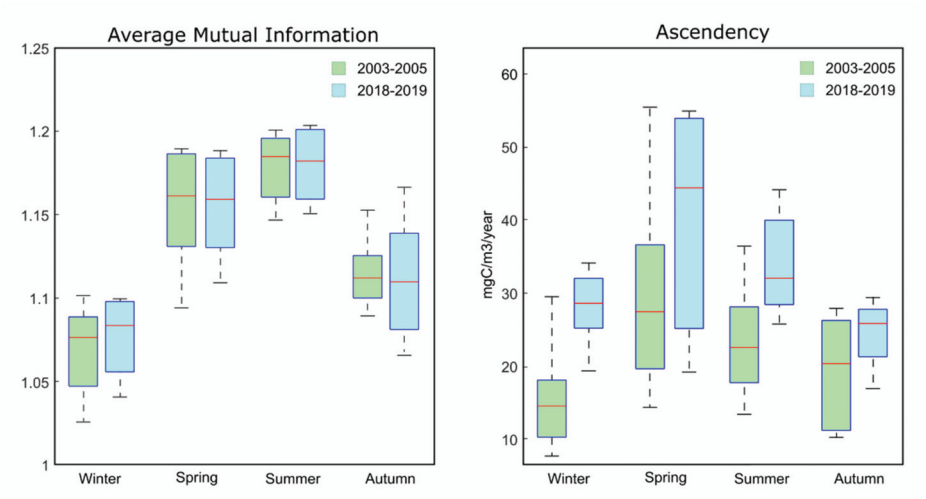

Figure 9. Seasonal Average Mutual Information and Ascendency (mgC/m^3/year) in the two periods (2003–2005 and 2018–2019).

3.4.3. Emergy Analysis

Emergy, intended here as a metric of the natural capital stored in the living biomass, ranged from 3.89×10^{10} sej to 4.46×10^{11} sej with an average value of $1.76 \times 10^{11} \pm 1.18 \times 10^{11}$ sej (Figure 10). Emergy showed similar values in both the considered periods with minimum average values in summer and highest average values in spring. Emergy exploited per unit of time (empower) ranged from 3.80×10^{9} sej/year to 2.31×10^{10} sej/year averaging $1.19 \times 10^{10} \pm 8.55 \times 10^{9}$ sej/year (Figure 10). Despite natural capital stored did not differ in the considered periods, the functioning of the plankton community measured through the emergy exploited to maintain the system (empower) always showed higher average values in 2018–2019. The two periods also showed different trends with maximum values in spring during 2003–2005 while empower kept growing until summer in 2018–2019.

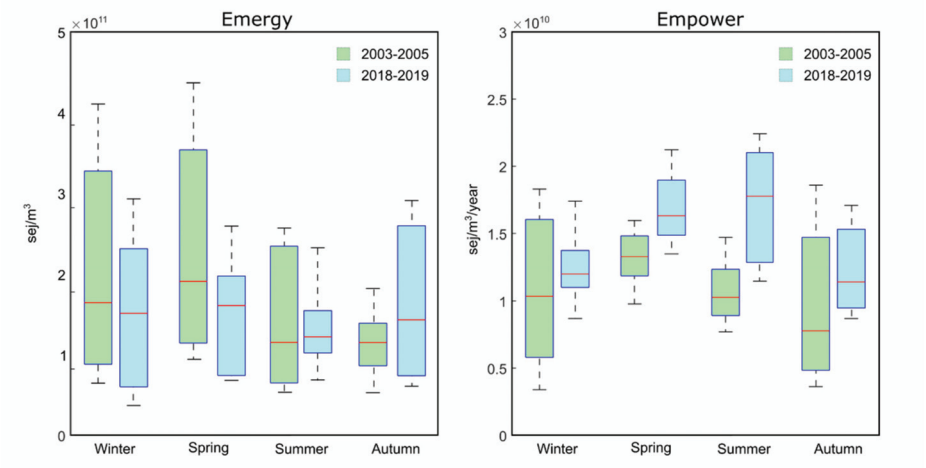

Figure 10. Seasonal average Emergy (sej/m^3) and Empower (sej/m^3/year) in the two periods (2003–2005 and 2018–2019).

4. Discussion

Numerous long-term studies regarding the variations of plankton community due to climate and hydrological changing conditions are available mainly regarding the oceans [51–56]. Despite being recognized as an important hot spot of biodiversity, Mediterranean Sea is less studied and research regarding the plankton community is somewhat rare because of the lack of long-term datasets [52,57–62] although efforts have been made in recent years carrying on long-term programs (e.g., [63–67]). Even when the plankton community is investigated, the studies focused on the analysis of the variations in the composition of the community, comparing abundances of different species or assemblages of species. Very few studies are referred to the analysis of the plankton community functioning [68,69] while it is complementary information crucial for the interpretation of the ecosystem state, maturity and health status. Therefore, in this study, we analyzed the functioning of the plankton community sampled on a monthly base in front of the coast of Portofino (NW Mediterranean) comparing two periods 13 years apart (2003–2005 and 2018–2019). The functional analyses, based on whole system approaches such as network analysis and emergy analysis, allowed to analyze the functioning of the system in terms of its ability to store, move and exploit available energy. Both network and emergy analysis outputs have been considered as goal functions of the system since all the considered indicators are expected to increase when a system is free to develop and move towards a more mature and stable state [42,45].

The temperature of the water column showed that the environmental conditions have changed, leading to less diversified seasons with warmer seasons lasting longer and colder seasons showing higher temperature values all over the water column. This is expected to have relevant consequences in terms of system functionality and is in accord with a general increase in the surface temperatures of the Ligurian Sea but, in general, also of the Mediterranean Sea, although presenting interannual variations [23]. From the analyses carried out, in fact, it can be observed that 2005 is characterized by a low stratification, as the warm waters are not limited to the surface area but reach up to about 35–40 m deep, while 2003 shows a superficial thermal anomaly with very high temperature values compared to the average. In recent years, there has been a marked increase in temperatures which translates into a decidedly positive normalized anomaly for both 2018 and 2019, especially in late summer and autumn [70].

Autotrophic biomass in the two considered periods is generally low, reflecting the oligotrophy of the Ligurian Sea [71] and the characteristics of the Portofino Promontory marine area [20,72,73]. The seasonal cycle (principal blooms in late winter/early spring and an occasional secondary bloom in autumn) are typical of the Mediterranean Sea and at Punta Faro LTER site are also influenced by torrents discharge [27,74]. Since the 2000s a process of oligotrophication was highlighted in the area [25], and this process was also observed in other Italian LTER sites up to the middle 1990s/early 2000s, followed by a stabilization or a new increase, together with a reduction of the mean phytoplankton size [20].

Considering this scenario, possible structural (biomass composition) and functional differences of the system were investigated. For the zooplankton component, what is known for this study area is confirmed, namely that the zooplankton abundance is mainly dominated by copepods [62,73] which cover about 62% of the sampled community, among them the component mainly represented is that of herbivorous copepods. The main peak of abundance occurs in spring, after the late winter-early spring phytoplankton bloom. These five years are part of a context of increased abundance of zooplankton organisms, mainly due to the increase in small to medium-sized copepods (1 mm–0.5 mm) that were reported in other Tyrrhenian sites, although with interannual and decadal fluctuations [20,67]. Despite the increase in total mesozooplankton abundance in the 2000s compared to the past, specific organisms or groups showed different behaviors, such as the most abundant spring copepods *Centropages* spp. that is also decreasing because of an anticipation of the end of the season in relation to summer temperature anomalies in the Tyrrhenian Sea,

but other groups such as the Appendicularia and Chaetognata groups are increasing in abundance. Moreover, in Portofino LTER site an increase is reported in the abundance of small organisms, such as *Oithona* spp. and *Oncaea* spp. and the same process also occurs in the Northern Adriatic Sea [20]. This trend seems to be amplified in 2018–2019 biennium where average detritivores copepods contribution increased, together with CC and Chae contributions.

Looking at the biomass values, they are coherent with other findings in the oligotrophic Mediterranean Sea [75] (<10 mgC/m^3). A high percentage contribution is due to herbivorous copepods (adults and juveniles) but also to Cnidaria and Chaetognata, which were particularly elevated in 2018 (41.2%), contributing to the highest value of mean annual biomass for that year. The year 2004, on the other hand, is the one with the lowest values in terms of biomass, as it was for the abundance values, but the difference in biomass is even more marked.

The web organization in the two considered periods showed an increase in the share of consumption directed towards detritus and heterotrophs coupled with a decrease in the share of primary producers' consumption. Primary producers in the water column and the primary productivity available for consumption do not display significant variations during the considered periods. We may hypothesize two different reasons for the decrease in the primary producers' consumption. In 2018, primary productivity and food availability were high due to the maximum values of primary producers biomass in the system (Figure 3) but this corresponds to the moment when the maximum values of non-herbivorous consumers biomass was detected (mainly Chaetognata and Cnidaria) (Figure 5) forcing the web organization to a functional change driven by the presence of a different set of organisms composing the zooplankton community rather than by a lack of resources availability (top-down effect). On the contrary, in 2019 the highest herbivorous biomass was sampled, and it was expected to address the consumption towards the autotrophs. This was not the case, due to a lack of primary productivity in the system which was not able to support the expected consumption that was diverted towards detritus exploitation (bottom-up effect). Primary productivity was in fact simulated to be completely consumed by autotrophs 5 out of 12 months in 2019.

Despite different forcing factors, the changes in the food web organization might identify a shift of the plankton community from a grazing food web towards a detritus or microbial loop food web, typical of the tropical area [76], but already discussed for the Mediterranean Sea [19,68].

This is also supported by the analysis of the mixed trophic impact: the network functioning is characterized by the positive effect of herbivorous copepods and the negative overall effect due to Cnidaria, Chaetognata and other consumers. Still, in the 2018–2019 biennium the herbivorous copepods are less important being mainly compensated by the increased positive effect of *Oncaea* spp. and a few other minor changes (in example omnivorous copepods such as *Oithona* spp.) that may indicate an increased complexity in the web organization and a lower relevance of the first trophic levels in the web. Regarding the species with negative effects, changes are less evident highlighting that the community is changing mainly from the perspective of resource provisioning rather than from the resource exploitation one.

The modeling approach made it possible to investigate the functionality of the plankton community and its seasonal and interannual variations. The average mutual information here intended as a proxy of the organization and efficiency of the system displayed a decreasing seasonal trend with minimum values in autumn and consistent values throughout the years. Despite the species composition having changed, the system is able to maintain the flow organization, efficiently adapting to the changing conditions. On the contrary, ascendency displayed consistently higher values in recent years, meaning that the overall level of activity of the system has increased and more energy is flowing in the system. Ecological network analysis theory states that this is expected to be correlated to an increase in maturity and complexity [42] but in this case this is not mirrored by a similar

trend of average mutual information indicating that the system is accelerating the rate of energy exchange without increasing its organization.

Ecological network analysis has been complemented by the analysis of the system complexity measured assessing the natural capital stored in the biomass (emergy) and the natural cost of maintaining the system complexity (empower). The comparison between the two analyzed periods displayed little variation in the system's capability to store natural capital in the plankton community that, despite being composed of a different set of organisms and being organized in a different way, kept the quantity of emergy stored in the living structures unchanged. On the contrary, the same complexity has been kept at a higher annual cost in recent years, pointing out that the plankton community has become less efficient at keeping the complexity level stable, having to spend more energy to maintain the natural capital.

As a matter of fact, the whole system analyses proposed here are able to analyze the system's functioning and complexity revealing that the plankton community has changed the species' composition, moving towards a more regeneration-dominated ecosystem [19] where small detritivorous copepods such as *Oncaea* spp. and omnivorous copepods such as *Oithona* spp., advantaged in an oligotrophic area [77], acquired importance. This is also mirrored by the different roles played by functional groups in the system with primary consumers (herbivores) that are losing relevance and an increasing importance of more complex species feeding on different resources and with higher trophic levels (increased contribution of detritivorous and carnivorous copepods, and carnivorous organisms). Considering the functional analyses, the system is able to organize the web of connections keeping the same level of exchange efficiency despite being characterized by an increase in the flow intensity and in the overall energy flowing in the system. This behavior was previously detected in benthic system under anthropic pressure [78,79] and was referred to as an increase effort put in place by the natural system to face or cope with the external disturbance. In this case, the plankton community affected by an increase in water temperature seems to react in the same way, accelerating processes without improving the general condition. This was also confirmed by the natural capital evaluation that showed the system was able to keep the stored capital at a constant level but at the cost of higher flows feeding the system. Again, the system is able to organize itself in a new, modified structure, probably adapted to the changed surrounding conditions but this is possible at the cost of higher energy flows and higher costs in terms of resources exploited by the system.

Author Contributions: Conceptualization, P.V. and P.P.; methodology, P.V., D.B. and P.P.; investigation, M.C. and D.B.; writing, P.V., D.B., M.C., G.D. and P.P.; supervision, P.V. and P.P. All authors have read and agreed to the published version of the manuscript.

Funding: This research received no external funding.

Institutional Review Board Statement: Not applicable.

Informed Consent Statement: Not applicable.

Data Availability Statement: The data presented in this study are available in the text and in the Appendix A.

Conflicts of Interest: The authors declare no conflict of interest.

Appendix A

Table A1. Individual Carbon weight for mesozooplankton species.

Functional Group	Species/Taxa	IC (mgC)
HC	*Acartia clausi*	0.0029
	Acartia italica	0.0029
	Acartia margalefi	0.0029
	Acartia teclae	0.0029
	Calocalanus contractus	0.0029
	Calocalanus styliremis	0.0029
	Calocalanus tenuis	0.0029
	Clausocalanus arcuicornis	0.0029
	Clausocalanus furcatus	0.0029
	Clausocalanus lividus	0.0029
	Clausocalanus parapergens	0.0029
	Clausocalanus paululus	0.0029
	Clausocalanus pergens	0.0029
	Clausocalanus spp.	0.0029
	Ctenocalanus vanus	0.0029
	Euterpina acutifrons	0.0029
	Nannocalanus minor	0.0049
	Paracalanus denudatus	0.0019
	Paracalanus nanus	0.0019
	Paracalanus parvus	0.0019
	Paracalanus spp.	0.0019
	Temora stylifera	0.0102
	Juvenile copepods	0.0038
CC	*Candacia armata*	0.0020
	Corycaeus spp.	0.0022
DC	*Microsetella* sp.	0.0012
	Oncaea spp.	0.0022
	Scolecithricidae	0.0063
OC	*Centropages kroyeri*	0.0065
	Centropages typicus	0.0065
	Isias clavipes	0.0068
	Oithona nana	0.0004
	Oithona plumifera	0.0004
	Oithona similis	0.0004
	Pleuromamma abdominalis	0.1000
	Pleuromamma gracilis	0.0020

Table A1. *Cont.*

Functional Group	Species/Taxa	IC (mgC)
Cn	Cnidaria	0.1885
	Juvenile Cnidarians	0.1885
Che	Chaetognatha	0.1885
Other	*Evadne spinifera*	0.0017
	Evadne spp.	0.0017
	Penilia avirostris	0.0017
	Podon spp.	0.0017
	Thecosomata	2.41×10^{-5}
	Appendicularia	0.0030
	Thaliacea	0.0028
	Fisch larvae	0.0016
Other Juvenile	Malacostraca	0.0016
	Polychaeta	0.0016
	Bivalvia larvae	0.0016
	Bryozoa larvae	0.0016
	Echinodermata	0.0016
	Cirripedia	0.0016
	Crustacea	0.0016

Table A2. List of model parameters.

			Model Parameters			
	Functional Group	**Species**	**P/B**	**Q/B**	**U/Q**	**References**
Chl*a*			1.278			
HC	Herbivorous copepods		0.04	0.631	0.53	[31,80,81]
	Paracalanus spp.		0.116	0.667	0.53	
	Temora spp.	*Temora stylifera*	0.04	0.223	0.53	
CC	*Candacia* spp.	*Candacia armata*	0.04	0.631	0.53	
	Corycaeus spp.		0.108	0.289	0.323	
	Euchaeta spp.		0.04	0.631	0.53	
DC	*Microsetella* sp.		0.04	0.631	0.53	
	Oncaea spp.		0.04	0.631	0.53	
	Scolecithricella spp.		0.04	0.631	0.53	
OC	*Centropages* spp.		0.108	0.289	0.323	
	Omivores Cyclopoida		0.055	0.297	0.53	
	Isias spp.	*Isias clavipes*	0.04	0.631	0.53	
	Pleuromamma spp.	*Pleuromamma abdominalis*	0.04	0.631	0.53	
		Pleuromamma gracilis	0.04	0.631	0.53	
Cn	Cnidaria		0.25	0.192	0.195	
Che	Chaetognata		0.25	0.192	0.195	
Other	Cladocera		0.793	1.452	0.496	
	Thecosomata		0.25	0.192	0.195	
	Appendicularia		0.494	14.012	0.604	
	Thaliacea		1.35	1.392	0.22	

Table A3. Abundance and frequency of species in 2003 samplings.

			2003							
Functional Group	**Trophic Refs.**	**Species/Taxa**	**Winter**		**Spring**		**Summer**		**Autumn**	
			Ab.	**Freq. (%)**	**Ab.**	**Freq. (%)**	**Ab.**	**Freq. (%)**	**Ab.**	**Freq. (%)**
HC	[82–86]	*Acartia clausi*	14.59	20	184.46	50	45.19	50	3.93	33
		Acartia italica	-	-	-	-	-	-	-	-
		Acartia margalefi	-	-	-	-	-	-	-	-
		Acartia teclae	-	-	-	-	-	-	-	-
		Calocalanus contractus	-	-	-	-	-	-	-	-
		Calocalanus styliremis	35.08	40	24.88	50	24.59	50	29.01	50
		Calocalanus tenuis	-	-	-	-	-	-	-	-
		Clausocalanus arcuicornis	19.94	20	3.13	33	7.36	33	6.17	33
		Clausocalanus furcatus	19.97	40	4.55	33	39.26	50	31.95	50
		Clausocalanus lividus	3.71	40	2.11	17	-	-	1.68	17
		Clausocalanus parapergens	-	-	-	-	-	-	-	-
		Clausocalanus paululus	56.35	60	7.91	33	145	50	20.90	50
		Clausocalanus pergens	38.40	40	41.22	50	5.67	50	15.96	50
		Clausocalanus spp.	47.97	20	12.22	33	28.54	26	19.94	50
		Ctenocalanus vanus	8.60	-	10.32	17	0.92	17	0.67	17
		Euterpina acutifrons	22.57	60	17.20	33	5.67	33	17.09	50
		Nannocalanus minor	-	-	-	-	-	-	2.18	17
		Paracalanus denudatus	2.32	40	22.05	33	-	-	-	-
		Paracalanus nanus	12.41	40	2.29	17	15.14	50	12.06	50
		Paracalanus parvus	54.57	40	128.65	50	23.46	50	43.87	50
		Paracalanus spp.	7.80	20	11.95	50	3.40	17	2.09	33
		Temora stylifera	3.11	-	-	-	5.47	50	10.29	50
		Juvenile copepods	784.09	40	1251.86	50	414.17	50	643.67	50
CC	[87–90]	*Candacia armata*	-	-	-	-	2.22	17	-	-
		Corycaeus spp.	15.15	40	9.95	50	24.17	50	46.03	50
DC	[87,91–93]	*Microsetella* sp.	-	-	-	-	1.65	17	-	-
		Oncaea spp.	11.71	20	11.95	50	3.93	33	7.34	50
		Scolecithricidae	-	-	-	-	2.45	17	1.09	17
OC	[82,83,94–96]	*Centropages kroyeri*	-	-	6.88	45	8.36	55	-	-
		Centropages typicus	13.61	20	27.69	54	5.39	10	4.89	09
		Isias clavipes	-	20	14.87	59	7.41	30	2.73	11
		Oithona nana	3.27	-	-	-	-	-	-	-
		Oithona plumifera	-	-	6.88	19	19.92	55	9.39	26
		Oithona similis	80.18	40	102.19	46	17.16	08	23.02	10
		Pleuromamma abdominalis	-	-	-	-	-	-	-	-
		Pleuromamma gracilis	-	-	-	-	-	-	0.67	17
Cn	[19,97,98]	Cnidaria	5.31	60	15.06	50	19.55	50	10.40	50
		Juvenile Cnidarians	-	-	-	-	-	-	-	-
Che	[99–102]	Chaetognatha	3.61	60	8.59	50	12.81	50	23.47	50

Table A3. *Cont.*

			2003							
Functional Group	**Trophic Refs.**	**Species/Taxa**	**Winter**		**Spring**		**Summer**		**Autumn**	
			Ab.	**Freq. (%)**	**Ab.**	**Freq. (%)**	**Ab.**	**Freq. (%)**	**Ab.**	**Freq. (%)**
Other	[103–105]	*Evadne spinifera*	1.10	-	117.42	50	11.66	50	0.21	33
		Evadne spp.	0.21	-	3.35	50	7.79	50	-	-
		Penilia avirostris	-	-	2.82	50	73.14	50	0.26	33
		Podon spp.	11.66	40	11.03	50	2.88	50	-	-
		Thecosomata	14.90	60	75.60	50	19.08	50	21.64	50
		Appendicularia	69.22	60	156.26	50	184.08	50	61.64	50
		Thaliacea	0.94	40	24.78	50	2.40	50	4.08	33
		Fisch larvae	0.52	20	4.71	50	2.14	50	0.31	33
Other Juvenile		Malacostraca	20.86	40	8.42	50	6.85	50	9.51	50
		Polychaeta	5.96	40	0.68	50	1.15	50	5.76	50
		Bivalvia larvae	23.84	40	58.61	50	2.67	50	2.35	50
		Bryozoa larvae	5.44	40	11.66	50		-	0.26	33
		Echinodermata	6.12	40	27.86	50	1.15	50	1.52	50
		Cirripedia	0.05	-	0.05	17	0.05	17	-	-
		Crustacea	10.87	40	2.67	50	4.55	50	1.46	50

Table A4. Abundance and frequency of species in 2004 samplings.

			2004							
Functional Group	**Trophic Refs.**	**Species/Taxa**	**Winter**		**Spring**		**Summer**		**Autumn**	
			Ab.	**Freq. (%)**	**Ab.**	**Freq. (%)**	**Ab.**	**Freq. (%)**	**Ab.**	**Freq. (%)**
HC	[82–86]	*Acartia clausi*	3.35	25	55.99	50	8.36	50	18.90	33
		Acartia italica	-	-	-	-	-	-	-	-
		Acartia margalefi	-	-	-	-	-	-	-	-
		Acartia teclae	-	-	-	-	-	-	-	-
		Calocalanus contractus	-	-	-	-	-	-	-	-
		Calocalanus styliremis	60.48	50	9.95	50	24.96	50	8.53	67
		Calocalanus tenuis	-	-	-	-	-	-	-	-
		Clausocalanus arcuicornis	4.56	25	3.14	33	4.42	50	-	-
		Clausocalanus furcatus	4.87	50	-	-	2.03	33	12.43	33
		Clausocalanus lividus	7.59	50	1.33	17	-	-	-	-
		Clausocalanus parapergens	-	-	-	-	-	-	-	-
		Clausocalanus paululus	27.27	75	17.17	50	20.51	33	33.77	67
		Clausocalanus pergens	38.40	50	46.15	50	12.23	33	3.36	67
		Clausocalanus spp.	12.87	25	6.02	17	7.87	33	55.77	67
		Ctenocalanus vanus	-	-	-	-	-	-	-	-
		Euterpina acutifrons	18.46	75	5.86	33	2.73	33	1.00	33
		Nannocalanus minor	-	-	0.51	17	-	-	-	-

Table A4. *Cont.*

			2004							
Functional Group	**Trophic Refs.**	**Species/Taxa**	**Winter**		**Spring**		**Summer**		**Autumn**	
			Ab.	**Freq. (%)**	**Ab.**	**Freq. (%)**	**Ab.**	**Freq. (%)**	**Ab.**	**Freq. (%)**
HC	[82–86]	*Paracalanus denudatus*	8.68	50	-	-	-	-	-	-
		Paracalanus nanus	11.93	50	3.27	33	3.04	17	2.00	33
		Paracalanus parvus	56.13	50	40.74	50	60.45	50	17.79	67
		Paracalanus spp.	6.70	25	18.02	50	9.09	33	-	-
		Temora stylifera	-	-	-	-	2.74	33	2.09	33
		Juvenile copepods	1057.50	50	1211.49	50	413.90	50	555.83	1.00
CC	[87–90]	*Candacia armata*	-	-	0.51	17	1.12	17	-	-
		Corycaeus spp.	6.33	50	7.23	50	7.28	50	29.88	67
DC	[87,91–93]	*Microsetella* sp.	-	-	-	-	-	-	-	-
		Oncaea spp.	10.05	25	3.27	33	2.73	33	-	-
		Scolecithricidae	-	-	-	-	1.21	17	-	-
OC	[82,83,94–96]	*Centropages kroyeri*	-	-	-	-	1.36	17	-	-
		Centropages typicus	8.93	25	32.10	50	12.85	50	2.36	33
		Isias clavipes	1.77	25	1.59	17	11.91	33	2.36	33
		Oithona nana	-	-	52.13	50	4.80	33	4.17	33
		Oithona plumifera	-	-	-	-	5.00	50	7.72	67
		Oithona similis	80.89	50	73.20	50	12.06	50	8.53	67
		Pleuromamma abdominalis	-	-	-	-	-	-	-	-
		Pleuromamma gracilis	-	-	-	-	-	-	-	-
Cn	[19,97,98]	Cnidaria	16.42	75	14.06	50	15.84	50	12.63	67
		Juvenile Cnidarians	-	-	-	-	-	-	-	-
Che	[99–102]	Chaetognatha	4.13	75	3.61	50	1.88	50	8.00	67
Other	[103–105]	*Evadne spinifera*	-	-	5.38	33	8.36	50	2.67	33
		Evadne spp.	-	-	0.21	17	3.55	50	0.47	33
		Penilia avirostris	-	-	0.31	17	35.97	50	1.57	67
		Podon spp.	19.81	50	12.49	50	3.82	50	1.49	67
		Thecosomata	12.97	75	35.71	50	9.67	50	8.16	67
		Appendicularia	27.76	75	86.94	50	136.82	50	86.42	67
		Thaliacea	2.25	50	9.31	33	0.73	50	3.29	67
		Fisch larvae	0.05	25	3.08	33	1.15	50	0.16	67
Other Juvenile		Malacostraca	18.14	50	11.61	50	5.23	50	2.12	1.00
		Polychaeta	3.14	50	1.46	50	1.88	50	1.57	1.00
		Bivalvia larvae	5.33	50	12.01	50	1.57	50	0.71	67
		Bryozoa larvae	4.65	50	1.93	50	0.05	33	-	-
		Echinodermata	5.86	50	1.93	50	0.94	33	0.78	1.00
		Cirripedia	-	-	-	-	0.10	17	-	-
		Crustacea	10.19	50	1.10	50	1.46	50	1.49	1.00

Table A5. Abundance and frequency of species in 2005 samplings.

			2005							
Functional Group	**Trophic Refs.**	**Species/Taxa**	**Winter**		**Spring**		**Summer**		**Autumn**	
			Ab.	**Freq. (%)**	**Ab.**	**Freq. (%)**	**Ab.**	**Freq. (%)**	**Ab.**	**Freq. (%)**
HC	[82–86]	*Acartia clausi*	131.20	75	183.61	50	42.75	40	4.30	25
		Acartia italica	-	-	-	-	3.27	20	-	-
		Acartia margalefi	-	-	-	-	-	-	-	-
		Acartia teclae	-	-	-	-	-	-	-	-
		Calocalanus contractus	-	-	-	-	-	-	-	-
		Calocalanus styliremis	46.90	75	24.54	50	8.48	40	12.33	25
		Calocalanus tenuis	-	-	-	-	-	-	-	-
		Clausocalanus arcuicornis	6.84	50	7.69	17	4.14	40	3.28	50
		Clausocalanus furcatus	11.35	50	-	-	1.42	20	33.23	50
		Clausocalanus lividus	10.40	50	4.06	33	3.63	20	8.61	25
		Clausocalanus parapergens	-	-	4.03	17	-	-	-	-
		Clausocalanus paululus	29.44	75	6.31	33	9.08	40	7.67	25
		Clausocalanus pergens	28.66	75	23.15	50	17.06	40	3.72	25
		Clausocalanus spp.	32.73	75	45.86	50	61.35	60	31.71	50
		Ctenocalanus vanus	3.75	25	-	-	3.27	20	-	-
		Euterpina acutifrons	14.59	50	2.40	33	-	-	7.03	50
		Nannocalanus minor	-	-	-	-	-	-	-	-
		Paracalanus denudatus	-	-	-	-	10.89	20	-	-
		Paracalanus nanus	4.54	25	15.38	17	1.42	20	6.33	23
		Paracalanus parvus	47.09	50	174.69	50	129.95	60	46.68	12
		Paracalanus spp.	-	-	5.16	17	18.05	60	-	-
		Temora stylifera	-	-	0.87	17	1.42	20	1.24	35
		Juvenile copepods	906.54	75	1266.04	50	686.01	60	515.98	50
CC	[87–90]	*Candacia armata*	13.56	27	7.75	16	10.56	21	17.68	36
		Corycaeus spp.	4.18	50	31.73	33	15.30	60	18.51	50
DC	[87,91–93]	*Microsetella* sp.	-	-	-	-	-	-	-	-
		Oncaea spp.	22.31	75	16.30	33	1.36	20	1.24	25
		Scolecithricidae	-	-	-	-	-	-	-	-
OC	[82,83,94–96]	*Centropages kroyeri*	-	-	3.19	17	3.27	20	-	-
		Centropages typicus	5.56	25	43.32	50	18.83	60	1.13	25
		Isias clavipes	0.91	25	-	-	7.26	20	-	-
		Oithona nana	2.11	25	9.41	33	3.27	20	1.13	25
		Oithona plumifera	2.11	25	10.35	33	13.89	40	29.64	50
		Oithona similis	78.39	75	74.55	50	33.57	40	39.12	50
		Pleuromamma abdominalis	-	-	-	-	-	-	-	-
		Pleuromamma gracilis	-	-	-	-	-	-	4.96	25
Cn	[19,97,98]	Cnidaria	4.18	75	31.73	50	15.30	60	18.51	50
		Juvenile Cnidarians	-	-	-	-	-	-	-	-
Che	[99–102]	Chaetognatha	5.02	75	1.57	33	6.27	40	34.11	50

Table A5. *Cont.*

			2005							
Functional Group	**Trophic Refs.**	**Species/Taxa**	**Winter**		**Spring**		**Summer**		**Autumn**	
			Ab.	**Freq. (%)**	**Ab.**	**Freq. (%)**	**Ab.**	**Freq. (%)**	**Ab.**	**Freq. (%)**
Other	[103–105]	*Evadne spinifera*	-	-	26.82	33	16.68	34	5.80	12
		Evadne spp.	-	-	2.77	17	8.21	60	1.25	50
		Penilia avirostris	0.10	25	1.88	17	217.53	60	46.97	50
		Podon spp.	9.10	75	10.19	50	10.40	60	0.71	50
		Thecosomata	13.17	75	38.01	50	19.81	60	26.35	50
		Appendicularia	73.98	75	198.03	50	157.10	60	99.91	50
		Thaliacea	-	-	16.76	50	22.06	60	50.19	50
		Fisch larvae	0.21	25	2.67	50	0.31	40	0.24	50
Other Juvenile		Malacostraca	9.41	75	8.84	50	8.52	60	2.27	50
		Polychaeta	4.91	75	1.20	50	1.20	60	4.78	50
		Bivalvia larvae	9.41	75	9.51	50	3.29	60	3.92	50
		Bryozoa larvae	3.35	50	4.08	33	0.05	20	0.63	50
		Echinodermata	5.23	75	3.71	50	0.73	40	11.61	50
		Cirripedia	-	-	0.31	17	0.10	20	-	-
		Crustacea	26.56	75	0.84	50	0.63	40	1.88	50

Table A6. Abundance and frequency of species in 2018 samplings.

			2018							
Functional Group	**Trophic Refs.**	**Species/Taxa**	**Winter**		**Spring**		**Summer**		**Autumn**	
			Ab.	**Freq. (%)**	**Ab.**	**Freq. (%)**	**Ab.**	**Freq. (%)**	**Ab.**	**Freq. (%)**
HC	[82–86]	*Acartia clausi*	25.46	50	6.17	33	10.14	60	9.79	67
		Acartia italica	-	-	-	-	-	-	-	-
		Acartia margalefi	-	-	-	-	-	-	0.25	67
		Acartia teclae	5.66	25	-	-	1.77	20	-	-
		Calocalanus contractus	-	-	1.83	17	3.54	20	-	-
		Calocalanus styliremis	12.73	75	20.49	50	15.13	60	22.03	67
		Calocalanus tenuis	-	-	0.91	17	1.77	0.20	0.10	33
		Clausocalanus arcuicornis	21.29	75	9.97	33	5.29	40	4.43	33
		Clausocalanus furcatus	16.16	50	7.21	33	18.24	40	24.14	67
		Clausocalanus lividus	-	-	1.42	17	3.54	20	4.30	67
		Clausocalanus parapergens	-	-	-	-	-	-	-	-
		Clausocalanus paululus	70.14	75	20.38	50	12.38	20	8.03	33
		Clausocalanus pergens	36.82	50	11.53	33	9.26	60	7.24	67
		Clausocalanus spp.	14.01	50	18.00	33	39.53	60	7.24	67
		Ctenocalanus vanus	11.97	75	0.98	17	3.54	20	3.06	67
		Euterpina acutifrons	26.32	75	12.31	17	1.09	20	5.28	67
		Nannocalanus minor	-	-	-	-	1.09	20	-	-

Table A6. *Cont.*

			2018							
Functional Group	**Trophic Refs.**	**Species/Taxa**	**Winter**		**Spring**		**Summer**		**Autumn**	
			Ab.	**Freq. (%)**	**Ab.**	**Freq. (%)**	**Ab.**	**Freq. (%)**	**Ab.**	**Freq. (%)**
HC	[82–86]	*Paracalanus denudatus*	-	-	-	-	-	-	-	-
		Paracalanus nanus	11.08	50	-	-	1.09	20	0.85	33
		Paracalanus parvus	90.57	75	104.94	50	88.21	60	10.44	33
		Paracalanus spp.	-	-	2.93	17	2.65	20	-	-
		Temora stylifera	2.93	25	5.73	33	11.01	40	3.40	33
		Juvenile copepods	1332.10	75	947.31	50	633.76	60	366.42	67
CC	[87–90]	*Candacia armata*	-	-	-	-	-	-	-	-
		Corycaeus spp.	27.84	75	46.84	50	52.12	60	43.17	67
DC	[87,91–93]	*Microsetella* sp.	-	-	-	-	-	-	-	-
		Oncaea spp.	35.94	75	23.57	50	21.15	60	18.78	67
		Scolecithricidae	-	-	-	-	-	-	6.27	33
OC	[82,83,94–96]	*Centropages kroyeri*	-	-	-	-	-	-	-	-
		Centropages typicus	36.88	75	15.77	50	3.98	20	2.09	33
		Isias clavipes	10.15	25	-	-	1.39	20	-	-
		Oithona nana	38.50	50	5.62	17	-	-	-	-
		Oithona plumifera	8.06	50	11.52	50	10.23	40	19.44	67
		Oithona similis	23.32	50	52.28	50	5.72	40	15.32	67
		Pleuromamma abdominalis	-	-	-	-	-	-	-	-
		Pleuromamma gracilis	-	-	-	-	-	-	0.85	33
Cn	[19,97,98]	Cnidaria	6.79	75	35.97	50	9.51	60	6.32	67
		Juvenile Cnidarians	-	-	-	-	-	-	-	-
Che	[99–102]	Chaetognatha	26.73	75	54.15	50	8.70	60	23.44	67
Other	[103–105]	*Evadne spinifera*	-	-	79.76	33	34.90	60	11.72	33
		Evadne spp.	-	-	12.54	50	18.48	60	2.75	33
		Penilia avirostris	-	-	14.47	33	169.58	60	53.61	67
		Podon spp.	1.70	50	21.84	50	6.52	60	0.92	67
		Thecosomata	32.61	75	77.86	50	17.26	60	12.13	67
		Appendicularia	32.61	75	109.32	50	136.49	60	67.87	67
		Thaliacea	10.97	75	10.70	50	9.92	60	46.68	67
		Fisch larvae	0.20	25	1.90	50	2.85	40	0.31	67
Other Juvenile		Malacostraca	9.24	75	8.90	50	5.77	60	1.83	67
		Polychaeta	5.37	75	1.83	50	0.41	40	2.96	67
		Bivalvia larvae	11.62	75	9.61	50	1.36	40	1.12	33
		Bryozoa larvae	10.87	75	24.63	50	-	-	-	-
		Echinodermata	9.99	75	14.85	50	3.94	60	11.21	67
		Cirripedia	-	-	-	-	0.14	20	-	-
		Crustacea	14.88	75	2.65	50	1.49	60	0.51	67

Table A7. Abundance and frequency of species in 2019 samplings.

			2019							
Functional Group	**Trophic Refs.**	**Species/Taxa**	**Winter**		**Spring**		**Summer**		**Autumn**	
			Ab.	**Freq. (%)**	**Ab.**	**Freq. (%)**	**Ab.**	**Freq. (%)**	**Ab.**	**Freq. (%)**
HC	[82–86]	*Acartia clausi*	8.52	33	40.54	75	13.48	75	0.64	20
		Acartia italica	-	-	-	-	-	-	-	-
		Acartia margalefi	-	-	-	-	2.18	25	1.22	20
		Acartia teclae	-	-	-	-	-	-	-	-
		Calocalanus contractus	3.41	17	-	-	-	-	-	-
		Calocalanus styliremis	31.31	50	7.83	50	16.14	75	39.04	60
		Calocalanus tenuis	1.42	17	-	-	-	-	1.29	20
		Clausocalanus arcuicornis	1.21	17	19.07	50	14.48	50	-	-
		Clausocalanus furcatus	9.32	50	9.64	50	36.69	50	55.71	60
		Clausocalanus lividus	2.57	17	5.23	25	-	-	-	-
		Clausocalanus parapergens	-	-	-	-	-	-	-	-
		Clausocalanus paululus	47.13	50	42.03	75	10.29	50	17.21	20
		Clausocalanus pergens	49.41	50	131.02	75	3.25	50	-	-
		Clausocalanus spp.	8.29	17	38.15	75	43.20	75	27.32	60
		Ctenocalanus vanus	3.71	33	9.44	25	4.30	50	2.43	20
		Euterpina acutifrons	60.11	50	1.81	25	1.62	25	5.67	40
		Nannocalanus minor	2.92	33	-	-	-	-	3.69	20
		Paracalanus denudatus	1.25	17	-	-	-	-	-	-
		Paracalanus nanus	1.42	17	-	-	3.76	50	1.21	20
		Paracalanus parvus	50.41	50	26.61	50	80.71	75	42.24	60
		Paracalanus spp.	2.63	17	9.44	25	-	-	-	-
		Temora stylifera	4.28	17	-	-	17.24	75	18.61	40
		Juvenile copepods	1170.71	50	2064.95	75	534.42	75	614.77	60
CC	[87–90]	*Candacia armata*	-	-	-	-	-	-	1.85	20
		Corycaeus spp.	14.62	33	5.73	25	64.11	75	65.79	60
DC	[87,91–93]	*Microsetella* sp.	-	-	-	-	-	-	-	-
		Oncaea spp.	13.06	50	8.33	50	35.70	75	21.07	60
		Scolecithricidae	-	-	6.79	25	-	-	0.64	20
OC	[82,83,94–96]	*Centropages kroyeri*	-	-	-	-	-	-	-	-
		Centropages typicus	8.09	33	58.89	75	37.28	75	1.33	20
		Isias clavipes	2.50	33	4.92	25	-	-	-	-
		Oithona nana	8.00	50	20.68	50	5.86	50	9.45	60
		Oithona plumifera	1.70	17	-	-	3.74	50	46.67	60
		Oithona similis	27.46	50	83.79	50	15.54	75	55.76	60
		Pleuromamma abdominalis	-	-	-	-	-	-	1.21	20
		Pleuromamma gracilis	-	-	1.31	25	-	-	1.33	20
Cn	[19,97,98]	Cnidaria	5.16	50	5.98	75	13.79	75	4.42	60
		Juvenile Cnidarians	-	-	2.65	50	0.14	25	0.14	20
Che	[99–102]	Chaetognatha	10.94	50	7.34	75	11.96	75	29.62	60

Table A7. *Cont.*

			2019							
Functional Group	**Trophic Refs.**	**Species/Taxa**	**Winter**		**Spring**		**Summer**		**Autumn**	
			Ab.	**Freq. (%)**	**Ab.**	**Freq. (%)**	**Ab.**	**Freq. (%)**	**Ab.**	**Freq. (%)**
Other	[103–105]	*Evadne spinifera*	1.29	33	10.60	50	14.62	75	0.34	20
		Evadne spp.	-	-	2.17	50	18.28	75	0.61	20
		Penilia avirostris	-	-	8.42	50	425.24	75	52.38	60
		Podon spp.	6.59	50	4.01	75	8.97	75	0.20	20
		Thecosomata	12.30	50	9.72	75	25.27	75	19.57	60
		Appendicularia	62.64	50	119.44	75	172.37	75	53.13	60
		Thaliacea	4.62	50	6.45	75	31.12	75	10.87	60
		Fisch larvae	0.204	33	2.310	50	1.223	50	0.272	40
Other Juvenile		Malacostraca	5.16	50	12.70	75	5.16	75	14.61	60
		Polychaeta	4.01	50	0.48	50	0.82	75	12.03	60
		Bivalvia larvae	4.21	50	4.01	75	1.97	75	1.56	60
		Bryozoa larvae	0.54	50	4.14	75	0.14	25	1.29	20
		Echinodermata	11.28	50	2.38	75	1.49	75	7.95	60
		Cirripedia	0.14	17	-	-	0.20	50	-	-
		Crustacea	15.35	50	4.01	50	0.54	50	3.87	40

References

1. Buitenhuis, E.; Le Quéré, C.; Aumont, O.; Beaugrand, G.; Bunker, A.; Hirst, A.; Ikeda, T.; O'Brien, T.; Piontkovski, S.; Straile, D. Biogeochemical Fluxes through Mesozooplankton. *Glob. Biogeochem. Cycles* **2006**, *20*. [CrossRef]
2. De Senerpont Domis, L.N.; Elser, J.J.; Gsell, A.S.; Huszar, V.L.M.; Ibelings, B.A.S.W.; Jeppesen, E.; Kosten, S.; Mooij, W.M.; Roland, F.; Sommer, U.; et al. Plankton Dynamics under Different Climatic Conditions in Space and Time. *Freshw. Biol.* **2013**, *58*, 463–482. [CrossRef]
3. Behrenfeld, M.J.; Boss, E.S. Resurrecting the Ecological Underpinnings of Ocean Plankton Blooms. *Ann. Rev. Mar. Sci.* **2014**, *6*, 167–194. [CrossRef]
4. Webber, M.; Edwards-Myers, E.; Campbell, C.; Webber, D. Phytoplankton and Zooplankton as Indicators of Water Quality in Discovery Bay, Jamaica. *Hydrobiologia* **2005**, *545*, 177–193. [CrossRef]
5. White, S.; Rakhesh, M.; Sarma, V.S.; Rajanna, B.; Raman, A.V. Discriminating Zooplankton Assemblages through Multivariate Methods: A Case for a Tropical Polluted Harbour and Bar-Built Estuary. *Chem. Ecol.* **2006**, *22*, 225–237. [CrossRef]
6. Valdés, L.; Moral, M. Time-Series Analysis of Copepod Diversity and Species Richness in the Southern Bay of Biscay off Santander, Spain, in Relation to Environmental Conditions. *ICES J. Mar. Sci.* **1998**, *55*, 783–792. [CrossRef]
7. Valdés, L.; Harris, R.; Ikeda, T.; McKinnell, S.; Peterson, W.T. The Role of Zooplankton in Global Ecosystem Dynamics: Comparative Studies from the World Oceans. *ICES J. Mar. Sci.* **2004**, *61*, 441–444. [CrossRef]
8. Hooff, R.C.; Peterson, W.T. Copepod Biodiversity as an Indicator of Changes in Ocean and Climate Conditions of the Northern California Current Ecosystem. *Limnol. Oceanogr.* **2006**, *51*, 2607–2620. [CrossRef]
9. Blandin, P. Bioindicateurs et Diagnostic Des Systèmes Écologiques. *Bull. Ecol.* **1986**, *17*, 215–307.
10. Boucher, J.; Ibanez, F.; Prieur, L. Daily and Seasonal Variations in the Spatial Distribution of Zooplankton Populations in Relation to the Physical Structure in the Ligurian Sea Front. *J. Mar. Res.* **1987**, *45*, 133–173. [CrossRef]
11. Bonnet, D.; Frid, C. Seven Copepod Species Considered as Indicators of Water-Mass Influence and Changes: Results from a Northumberland Coastal Station. *ICES J. Mar. Sci.* **2004**, *61*, 485–491. [CrossRef]
12. Beaugrand, G.; IbaHez, F. Monitoring Marine Plankton Ecosystems. II: Long-Term Changes in North Sea Calanoid Copepods in Relation to Hydro-Climatic Variability. *Mar. Ecol. Prog. Ser.* **2004**, *284*, 35–47. [CrossRef]
13. Perry, R.I.; Batchelder, H.P.; Mackas, D.L.; Chiba, S.; Durbin, E.; Greve, W.; Verheye, H.M. Identifying Global Synchronies in Marine Zooplankton Populations: Issues and Opportunities. *ICES J. Mar. Sci.* **2004**, *61*, 445–456. [CrossRef]
14. Jamet, J.-L.; Jean, N.; Bogé, G.; Richard, S.; Jamet, D. Plankton Succession and Assemblage Structure in Two Neighbouring Littoral Ecosystems in the North-West Mediterranean Sea. *Mar. Freshw. Res.* **2005**, *56*, 69–83. [CrossRef]
15. Philippart, C.; Anadón, R.; Danovaro, R.; Dippner, J.; Drinkwater, K.; Hawkins, S.; Oguz, T.; O'Sullivan, G.; Reid, P.C. Impacts of Climate Change on European Marine Ecosystems: Observations, Expectations and Indicators. *J. Exp. Mar. Biol. Ecol.* **2011**, *400*, 52–69. [CrossRef]

16. Beaugrand, G.; Brander, K.M.; Alistair Lindley, J.; Souissi, S.; Reid, P.C. Plankton Effect on Cod Recruitment in the North Sea. *Nature* **2003**, *426*, 661–664. [CrossRef]
17. Alcaraz, M.; Saiz, E.; Estrada, M. Excretion of Ammonia by Zooplankton and Its Potential Contribution to Nitrogen Requirements for Primary Production in the Catalan Sea (NW Mediterranean). *Mar. Biol.* **1994**, *119*, 69–76. [CrossRef]
18. Ribera d'Alcala, M.; Conversano, F.; Corato, F.; Licandro, P.; Mangoni, O.; Marino, D.; Mazzocchi, M.G.; Modigh, M.; Montresor, M.; Nardella, M.; et al. Seasonal Patterns in Plankton Communities in Pluriannual Time Series at a Coastal Mediterranean Site (Gulf of Naples): An Attempt to Discern Recurrences and Trends. *Sci. Mar.* **2004**, *68*, 65–83. [CrossRef]
19. Molinero, J.C.; Ibanez, F.; Souissi, S.; Buecher, E.; Dallot, S.; Nival, P. Climate Control on the Long-Term Anomalous Changes of Zooplankton Communities in the Northwestern Mediterranean. *Glob. Chang. Biol.* **2008**, *14*, 11–26. [CrossRef]
20. Morabito, G.; Mazzocchi, M.G.; Salmaso, N.; Zingone, A.; Bergami, C.; Flaim, G.; Accoroni, S.; Basset, A.; Bastianini, M.; Belmonte, G.; et al. Plankton Dynamics across the Freshwater, Transitional and Marine Research Sites of the LTER-Italy Network. Patterns, Fluctuations, Drivers. *Sci. Total Environ.* **2018**, *627*, 373–387. [CrossRef] [PubMed]
21. Doglioli, A.M.; Griffa, A.; Magaldi, M.G. Numerical Study of a Coastal Current on a Steep Slope in Presence of a Cape: The Case of the Promontorio Di Portofino. *J. Geophys. Res. Ocean.* **2004**, *109*. [CrossRef]
22. Doglioli, A.M.; Magaldi, M.G.; Vezzulli, L.; Tucci, S. Development of a Numerical Model to Study the Dispersion of Wastes Coming from a Marine Fish Farm in the Ligurian Sea (Western Mediterranean). *Aquaculture* **2004**, *231*, 215–235. [CrossRef]
23. Cattaneo-Vietti, R.; Cappanera, V.; Castellano, M.; Povero, P. Yield and Catch Changes in a Mediterranean Small Tuna Trap: A Warming Change Effect? *Mar. Ecol.* **2015**, *36*, 155–166. [CrossRef]
24. Vietti, R.C.; Albertelli, G.; Aliani, S.; Bava, S.; Bavestrello, G.; Cecchi, L.B.; Bianchi, C.N.; Bozzo, E.; Capello, M.; Castellano, M.; et al. The Ligurian Sea: Present Status, Problems and Perspectives. *Chem. Ecol.* **2010**, *26*, 319–340. [CrossRef]
25. Parravicini, V.; Micheli, F.; Montefalcone, M.; Morri, C.; Villa, E.; Castellano, M.; Povero, P.; Bianchi, C.N. Conserving Biodiversity in a Human-Dominated World: Degradation of Marine Sessile Communities within a Protected Area with Conflicting Human Uses. *PLoS ONE* **2013**, *8*, e75767. [CrossRef]
26. Povero, P.; Misic, C.; Castellano, M.; Ruggieri, N.; Fabiano, M. Response of a Coastal Marine Ecosystem to Atmospheric Forcing (Portofino, Ligurian Sea). In Proceedings of the First Italian IGBP Conference, Paestum (Salerno), Italy, 14–16 November 2002.
27. Ruggieri, N.; Castellano, M.; Misic, C.; Gasparini, G.; Cattaneo-Vietti, R. Seasonal and Interannual Dynamics of a Coastal Ecosystem (Portofino, Ligurian Sea) in Relation to Meteorological Constraints. *Geophys. Res. Abstr.* **2006**, *8*, 07774.
28. Holm-Hansen, O.; Lorenzen, C.J.; Holmes, R.W.; Strickland, J.D.H. Fluorometric Determination of Chlorophyll. *ICES J. Mar. Sci.* **1965**, *30*, 3–15. [CrossRef]
29. Frontier, S. Calcul de l'erreur Sur Un Comptage de Zooplancton. *J. Exp. Mar. Biol. Ecol.* **1972**, *8*, 121–132. [CrossRef]
30. Fabiano, M.; Danovaro, R.; Fraschetti, S. A Three-Year Time Series of Elemental and Biochemical Composition of Organic Matter in Subtidal Sandy Sediments of the Ligurian Sea (Northwestern Mediterranean). *Cont. Shelf Res.* **1995**, *15*, 1453–1469. [CrossRef]
31. D'Alelio, D.; Libralato, S.; Wyatt, T.; Ribera d'Alcalà, M. Ecological-Network Models Link Diversity, Structure and Function in the Plankton Food-Web. *Sci. Rep.* **2016**, *6*, 21806. [CrossRef] [PubMed]
32. Little, W.; Copley, N. *WHOI Silhouette DIGITIZER Version 1.0 User's Guide*; Woods Hole Oceanographic Institution: Woods Hole, MA, USA, 2003. [CrossRef]
33. Bednaršek, N.; Možina, J.; Vogt, M.; O'Brien, C.; Tarling, G. The Global Distribution of Pteropods and Their Contribution to Carbonate and Carbon Biomass in the Modern Ocean. *Earth Syst. Sci. Data* **2012**, *4*, 167–186. [CrossRef]
34. Larson, R.J. Water Content, Organic Content, and Carbon and Nitrogen Composition of Medusae from the Northeast Pacifi. *J. Exp. Mar. Biol. Ecol.* **1986**, *99*, 107–120. [CrossRef]
35. Zuur, A.; Ieno, E.; Smith, G. *Analysing Ecological Data*; Springer Science and Business Media LLC: New York, NY, USA, 2007; Volume 75, ISBN 978-0-387-45967-7.
36. Paoli, C.; Morten, A.; Bianchi, C.N.; Morri, C.; Fabiano, M.; Vassallo, P. Capturing Ecological Complexity: OCI, a Novel Combination of Ecological Indices as Applied to Benthic Marine Habitats. *Ecol. Indic.* **2016**, *66*, 86–102. [CrossRef]
37. Christensen, V. A Model of Trophic Interactions in the North Sea in 1981, the Year of the Stomach. *Dana* **2003**, *11*, 1–28.
38. Christensen, V.; Walters, C. Ecopath With Ecosim: Methods, Capabilities and Limitations. *Ecol. Model.* **2004**, *172*, 109–139. [CrossRef]
39. Leontief, W.W. *The Structure of {American} Economy, {1919–1939}; An Empirical Application of Equilibrium Analysis*; Oxford University Press: New York, NY, USA, 1951.
40. Ulanowicz, R.E.; Puccia, C.J. Mixed trophic impacts in ecosystems. *Coenoses* **1990**, *5*, 7–16.
41. Libralato, S.; Christensen, V.; Pauly, D. A Method for Identifying Keystone Species in Food Web Models. *Ecol. Model.* **2006**, *195*, 153–171. [CrossRef]
42. Ulanowicz, R.E. *Growth and Development: Ecosystem Phenomenology*; Springer: New York, NY, USA, 1986.
43. Finn, T.J. Measures of Ecosystem Structure and Function Derived from Analysis of Flows. *J. Theor. Biol.* **1976**, *56*, 363–380. [CrossRef]
44. Ulanowicz, R.E.; Abarca-Arenas, L.G. An Informational Synthesis of Ecosystem Structure and Function. *Ecol. Model.* **1997**, *95*, 1–10. [CrossRef]
45. Odum, H.T. *Environmental Accounting. Emergy and Environmental Decision Making*; John Wiley and Sons: New York, NY, USA, 1996.

46. Vassallo, P.; Paoli, C.; Buonocore, E.; Franzese, P.P.; Russo, G.F.; Povero, P. Assessing the Value of Natural Capital in Marine Protected Areas: A Biophysical and Trophodynamic Environmental Accounting Model. *Ecol. Model.* **2017**, *355*, 12–17. [CrossRef]
47. Paoli, C.; Povero, P.; Burgos, E.; Dapueto, G.; Fanciulli, G.; Massa, F.; Scarpellini, P.; Vassallo, P. Natural Capital and Environmental Flows Assessment in Marine Protected Areas: The Case Study of Liguria Region (NW Mediterranean Sea). *Ecol. Model.* **2018**, *368*, 121–135. [CrossRef]
48. De La Fuente, G.; Asnaghi, V.; Chiantore, M.; Thrush, S.; Povero, P.; Vassallo, P.; Petrillo, M.; Paoli, C. The Effect of Cystoseira Canopy on the Value of Midlittoral Habitats in NW Mediterranean, an Emergy Assessment. *Ecol. Model.* **2019**, *404*, 1–11. [CrossRef]
49. Mattei, F.; Buonocore, E.; Franzese, P.P.; Scardi, M. Global Assessment of Marine Phytoplankton Primary Production: Integrating Machine Learning and Environmental Accounting Models. *Ecol. Model.* **2021**, *451*, 109578. [CrossRef]
50. Jorgensen, S.E.; Nielsen, S.N.; Meyer, H.F. Emergy, Environ, Exergy and Ecological Modelling. *Ecol. Model.* **1995**, *77*, 99–109. [CrossRef]
51. McGowan, J.A. Climate and Change in Oceanic Ecosystems: The Value of Time-Series Data. *Trends Ecol. Evol.* **1990**, *5*, 293–299. [CrossRef]
52. Ménard, F.J.; Fromentin, M.; Goy, J.; Dallot, S. Temporal Fluctuations of Doliolid Abundance in the Bay of Ville-Franche-Sur-Mer (Northwestern Mediterranean Sea) from 1967 to 1990. *Oceanol. Acta* **1997**, *20*, 733–742.
53. Fevre-Lehoerff, G.; Ibanez, F.; Poniz, P.; Fromentin, J.-M. Hydroclimatic Relationships with Planktonic Time Series from 1975 to 1992 in the North Sea off Gravelines, France. *Mar. Ecol. Ser.* **1995**, *129*, 269–281. [CrossRef]
54. Fromentin, J.; Planque, B. Calanus and Environment in the Eastern North Atlantic. II. Influence of the North Atlantic Oscillation on C. Finmarchicus and C. Helgolandicus. *Mar. Ecol. Prog. Ser.* **1996**, *134*, 111–118. [CrossRef]
55. Alvarez-Fernandez, S.; Licandro, P.; van Damme, C.J.G.; Hufnagl, M. Effect of Zooplankton on Fish Larval Abundance and Distribution: A Long-Term Study on North Sea Herring (Clupea Harengus). *ICES J. Mar. Sci.* **2015**, *72*, 2569–2577. [CrossRef]
56. Monteiro, M.; Azeiteiro, U.M.; Martinho, F.; Pardal, M.A.; Primo, A.L. Long-Term Changes of Ichthyoplankton Communities in an Iberian Estuary Are Driven by Varying Hydrodynamic Conditions. *J. Plankton Res.* **2021**, *43*, 33–45. [CrossRef]
57. Pucher-Petković, T. Recherches Sur La Production Primaire et La Densite Des Populations Du Phyfcoplancton En Adriatique Moyenne (1962–1967) (Research on Primary Production and Population Density of Phycoplankton in the Middle Adriatic). *Rapp. Comm. Int. Mer. Medit.* **1971**, *20*, 339–343.
58. Goy, J.; Pie, O. Long-Term Fluctuations of Pelagia Noctiluca (Cnidaria, Scyphomedusa) in the Western Mediterranean Sea: Prediction by Climatic Variables. *Deep Sea Res. Part I Oceanogr. Res. Pap.* **2002**, *36*, 269–279. [CrossRef]
59. Ménard, F.S.; Dallot, G.T.; Braconnot, J.C. Temporal Fluctuations of Two Mediterranean Salp Populations From1967 to 1990. Analysis of the Influence of Environmental Variables Using a Markov Chain Model. *Mar. Ecol. Prog. Ser.* **1994**, *104*, 139–152. [CrossRef]
60. Cataletto, B.; Feoli, E.; Umani, S.F.; Cheng-Yong, S. Eleven Years of Time-Series Analysis on the Net-Zooplankton Community in the Gulf of Trieste. *ICES J. Mar. Sci.* **1995**, *52*, 669–678. [CrossRef]
61. Solic, M.; Krstulovic, N.; Marasović, I.; Baranovic, A.; Puciier-Petkovic, T.; Vucetic, T. Analysis of Time Sertes of Planktonic Communities in the Adriatic Sea: Distinguishing between Natural and Man-Induced Changes. *Oceanol. Acta* **1997**, *20*, 131–143.
62. Licandro, P.; Ibanez, F. Changes of Zooplankton Communities in the Gulf of Tigullio (Ligurian Sea, Western Mediterranean) from 1985 to 1995. Influence of Hydroclimatic Factors. *J. Plankton Res.* **2000**, *22*, 2225–2253. [CrossRef]
63. García-Comas, C.; Stemmann, L.; Ibanez, F.; Berline, L.; Mazzocchi, M.G.; Gasparini, S.; Picheral, M.; Gorsky, G. Zooplankton Long-Term Changes in the NW Mediterranean Sea: Decadal Periodicity Forced by Winter Hydrographic Conditions Related to Large-Scale Atmospheric Changes? *J. Mar. Syst.* **2011**, *87*, 216–226. [CrossRef]
64. Mazzocchi, M.G.; Licandro, P.; Dubroca, L.; Di Capua, I.; Saggiomo, V. Zooplankton Associations in a Mediterranean Long-Term Time-Series. *J. Plankton Res.* **2011**, *33*, 1163–1181. [CrossRef]
65. Vandromme, P.; Stemmann, L.; Berline, L.; Gasparini, S.; Mousseau, L.; Prejger, F.; Passafiume, O.; Guarini, J.-M.; Gorsky, G. Inter-Annual Fluctuations of Zooplankton Communities in the Bay of Villefranche-Sur-Mer from 1995 to 2005 (Northern Ligurian Sea, France). *Biogeosciences* **2011**, *8*, 3143–3158. [CrossRef]
66. Berline, L.; Siokou-Frangou, I.; Marasović, I.; Vidjak, O.; de Puelles, M.L.F.; Mazzocchi, M.G.; Assimakopoulou, G.; Zervoudaki, S.; Fonda-Umani, S.; Conversi, A.; et al. Intercomparison of Six Mediterranean Zooplankton Time Series. *Prog. Oceanogr.* **2012**, *97*, 76–91. [CrossRef]
67. Fullgrabe, L.; Grosjean, P.; Gobert, S.; Lejeune, P.; Leduc, M.; Engels, G.; Dauby, P.; Boissery, P.; Richir, J. Zooplankton Dynamics in a Changing Environment: A 13-Year Survey in the Northwestern Mediterranean Sea. *Mar. Environ. Res.* **2020**, *159*, 104962. [CrossRef]
68. D'Alelio, D.; Mazzocchi, M.G.; Montresor, M.; Sarno, D.; Zingone, A.; Di Capua, I.; Franzè, G.; Margiotta, F.; Saggiomo, V.; Ribera d'Alcalà, M. The Green–Blue Swing: Plasticity of Plankton Food-Webs in Response to Coastal Oceanographic Dynamics. *Mar. Ecol.* **2015**, *36*, 1155–1170. [CrossRef]
69. Marouan, M.; Niquil, N.; Grami, B.; Mejri, K.; Haraldsson, M.; Chaalali, A.; Pringault, O.; Hlaili, A. A New Type of Plankton Food Web Functioning in Coastal Waters Revealed by Coupling Monte Carlo Markov Chain Linear Inverse Method and Ecological Network Analysis. *Ecol. Indic.* **2019**, *104*, 67–85. [CrossRef]

70. Betti, F.; Venturini, S.; Merotto, L.; Cappanera, V.; Ferrando, S.; Aicardi, S.; Mandich, A.; Castellano, M.; Povero, P. Population Trends of the Fan Mussel Pinna Nobilis from Portofino MPA (Ligurian Sea, Western Mediterranean Sea) before and after a Mass Mortality Event and a Catastrophic Storm. *Eur. Zool. J.* **2021**, *88*, 18–25. [CrossRef]
71. Misic, C.; Fabiano, M. Ectoenzymatic Activity and Its Relationship to Chlorophyll- a and Bacteria in the Gulf of Genoa (Ligurian Sea, NW Mediterranean). *J. Mar. Syst.* **2006**, *60*, 193–206. [CrossRef]
72. Misic, C.; Castellano, M.; Covazzi Harriague, A. Organic Matter Features, Degradation and Remineralisation at Two Coastal Sites in the Ligurian Sea (NW Mediterranean) Differently Influenced by Anthropogenic Forcing. *Mar. Environ. Res.* **2011**, *72*, 67–74. [CrossRef]
73. Coppari, M.; Ferrier-Pagès, C.; Castellano, M.; Massa, F.; Olivari, E.; Bavestrello, G.; Povero, P.; Bo, M. Seasonal Variation of the Stable C and N Isotopic Composition of the Mesophotic Black Coral Antipathella Subpinnata (Ellis \& Solander, 1786). *Estuar. Coast. Shelf Sci.* **2020**, *233*, 106520.
74. D'Ortenzio, F.; Ribera d'Alcalà, M. On the Trophic Regimes of the Mediterranean Sea: A Satellite Analysis. *Biogeosciences* **2009**, *6*, 139–148. [CrossRef]
75. Frangoulis, C.; Grigoratou, M.; Zoulias, T.; Hannides, C.C.S.; Pantazi, M.; Psarra, S.; Siokou, I. Expanding Zooplankton Standing Stock Estimation from Meso- to Metazooplankton: A Case Study in the N. Aegean Sea (Mediterranean Sea). *Cont. Shelf Res.* **2017**, *149*, 151–161. [CrossRef]
76. Anjusha, A.; Jyothibabu, R.; Jagadeesan, L.; Mohan, A.P.; Sudheesh, K.; Krishna, K.; Ullas, N.; Deepak, M. Trophic Efficiency of Plankton Food Webs: Observations from the Gulf of Mannar and the Palk Bay, Southeast Coast of India. *J. Mar. Syst.* **2013**, *115*, 40–61. [CrossRef]
77. Hannides, C.C.S.; Popp, B.N.; Close, H.G.; Benitez-Nelson, C.R.; Ka'apu-Lyons, C.A.; Gloeckler, K.; Wallsgrove, N.; Umhau, B.; Palmer, E.; Drazen, J.C. Seasonal Dynamics of Midwater Zooplankton and Relation to Particle Cycling in the North Pacific Subtropical Gyre. *Prog. Oceanogr.* **2020**, *182*, 102266. [CrossRef]
78. Vassallo, P.; Fabiano, M. Trophodynamic Variations on Microtidal North Mediterranean Sandy Beaches. *Oceanologia* **2005**, *47*, 351–364.
79. Vassallo, P.; Paoli, C.; Schiavon, G.; Albertelli, G.; Fabiano, M. How Ecosystems Adapt to Face Disruptive Impact? The Case of a Commercial Harbor Benthic Community. *Ecol. Indic.* **2013**, *24*, 431–438. [CrossRef]
80. D'Alelio, D.; Montresor, M.; Mazzocchi, M.G.; Margiotta, F.; Sarno, D.; D'Alcalà, M.R. Plankton Food-Webs: To What Extent Can They Be Simplified? *Adv. Oceanogr. Limnol.* **2016**, *7*, 67–92. [CrossRef]
81. Cianelli, D.; D'Alelio, D.; Uttieri, M.; Sarno, D.; Zingone, A.; Zambianchi, E.; d'Alcalà, M.R. Disentangling Physical and Biological Drivers of Phytoplankton Dynamics in a Coastal System. *Sci. Rep.* **2017**, *7*, 15868. [CrossRef] [PubMed]
82. Martynova, D.; Kazus, N.; Bathmann, U.; Graeve, M.; Sukhotin, A. Seasonal Abundance and Feeding Patterns of Copepods Temora Longicornis, Centropages Hamatus and Acartia Spp. in the White Sea (66° N). *Polar Biol.* **2011**, *34*, 1175–1195. [CrossRef]
83. Wiadnyana, N.N.; Wiadnyana, N.W.; Rassoulzadegan, F. Selective Feeding of Acartia Clausi and Centropages Typicus on Microzooplankton. *Mar. Ecol. Prog. Ser.* **1989**, *53*, 37–45. [CrossRef]
84. Razouls, C.; Kouwenberg, J.; Desreumaux, N. Diversity and Geographic Distribution of Marine Planktonic Copepods (Sensu lato) A Pan-European Species-Directories Infrastructure (PESI) View Project. 2005. Available online: https://doi.org/10.13140/RG.2.1.2077.4241 (accessed on 15 December 2021).
85. Swadling, K.M.; Slotwinski, A.; Davies, C.; Beard, J.; McKinnon, A.D.; Coman, F.; Murphy, N.; Tonks, M.; Rochester, W.; Conway, D.V.P.; et al. Australian Marine Zooplankton: A Taxonomic Guide and Atlas. Available online: http://www.imas.utas.edu.au/zooplankton (accessed on 15 December 2021).
86. Dam, H.G.; Lopes, R.M. Omnivory in the Calanoid Copepod Temora Longicornis: Feeding, Egg Production and Egg Hatching Rates. *J. Exp. Mar. Biol. Ecol.* **2003**, *292*, 119–137. [CrossRef]
87. Yamaguchi, A.; Watanabe, Y.; Ishida, H.; Harimoto, T.; Furusawa, K.; Suzuki, S.; Ishizaka, J.; Ikeda, T.; Takahashi, M. Mac Community and Trophic Structures of Pelagic Copepods down to Greater Depths in the Western Subarctic Pacific (WEST-COSMIC). *Deep Sea Res. Part I Oceanogr. Res. Pap.* **2002**, *49*, 1007–1025. [CrossRef]
88. Kouwenberg, J. Copepod Distribution in Relation to Seasonal Hydrographics and Spatial Structure in the North-Western Mediterranean (Golfe Du Lion). *Estuar. Coast. Shelf Sci.* **1994**, *38*, 69–90. [CrossRef]
89. Ohtsuka, S.; Onbé, T. Evidence of Selective Feeding on Larvaceans by the Pelagic Copepod Candacia Bipinnata (Calanoida: Candaciidae). *J. Plankton Res.* **1989**, *11*, 869–872. [CrossRef]
90. López-Urrutia, Á.; Harris, R.P.; Smith, T. Predation by Calanoid Copepods on the Appendicularian Oikopleura Dioica. *Limnol. Oceanogr.* **2004**, *49*, 303–307. [CrossRef]
91. Ohtsuka, S.; Kubo, N.; Okada, M.; Gushima, K. Attachment and Feeding of Pelagic Copepods on Larvacean Houses. *J. Oceanogr.* **1993**, *49*, 115–120. [CrossRef]
92. Nishida, S.; Ohtsuka, S. Ultrastructure of the Mouthpart Sensory Setae in Mesopelagic Copepods of the Family Scolecitrichidae. *Plankt. Biol. Ecol.* **1997**, *44*, 81–90.
93. Maar, M.; Visser, A.; Nielsen, T.G.; Stips, A.; Saito, H. Turbulence and Feeding Behaviour Affect the Vertical Distributions of Oithona Similis and Microsetella Norwegica. *Mar. Ecol. Ser.* **2006**, *313*, 157–172. [CrossRef]
94. Calbet, A.; Carlotti, F.; Gaudy, R. The Feeding Ecology of the Copepod Centropages Typicus (Kröyer). *Prog. Oceanogr.* **2007**, *72*, 137–150. [CrossRef]

95. Turner, J.T. The Importance of Small Planktonic Copepods and Their Roles in Pelagic Marine Food Webs. *Zool. Stud.* **2004**, *43*, 255–266.
96. Lampitt, R.S.; Gamble, J.C. Diet and Respiration of the Small Planktonic Marine Copepod Oithona Nana. *Mar. Biol.* **1982**, *66*, 185–190. [CrossRef]
97. Boero, F.; Bucci, C.; Colucci, A.M.R.; Gravili, C.; Stabili, L. Obelia (Cnidaria, Hydrozoa, Campanulariidae): A Microphagous, Filter-Feeding Medusa. *Mar. Ecol.* **2007**, *28*, 178–183. [CrossRef]
98. Purcell, J.E. A Review of Cnidarians and Ctenophores Feeding on Competitors in the Plankton. *Hydrobiologia* **1991**, *216*, 335–342. [CrossRef]
99. Pearre, S., Jr. Vertical Migration and Feeding in Sagitta Elegans Verrill. *Ecology* **1973**, *54*, 300–314. [CrossRef]
100. Giesecke, R.; González, H.E. Feeding of Sagitta Enflata and Vertical Distribution of Chaetognaths in Relation to Low Oxygen Concentrations. *J. Plankton Res.* **2004**, *26*, 475–486. [CrossRef]
101. Kehayias, G.; Kourouvakalis, D. Diel Vertical Migration and Feeding of Chaetognaths in Coastal Waters of the Eastern Mediterranean. *Biologia* **2010**, *65*, 301–308. [CrossRef]
102. Bonnet, D.; Lindeque, P.K.; Harris, R.P. Sagitta Setosa Predation on Calanus Helgolandicus in the English Channel. *J. Plankton Res.* **2010**, *32*, 725–737. [CrossRef]
103. Katechakis, A.; Stibor, H. Feeding Selectivities of the Marine Cladocerans Penilia Avirostris, Podon Intermedius and Evadne Nordmanni. *Mar. Biol.* **2004**, *145*, 529–539. [CrossRef]
104. Lipej, L.; Mozetič, P.; Turk, V.; Malej, A. The Trophic Role of the Marine Cladoceran Penilia Avirostris in the Gulf of Trieste. *Hydrobiologia* **1997**, *360*, 197–203. [CrossRef]
105. Atienza, D.; Saiz, E.; Calbet, A. Feeding Ecology of the Marine Cladoceran Penilia Avirostris: Natural Diet, Prey Selectivity and Daily Ration. *Mar. Ecol. Ser.* **2006**, *315*, 211–220. [CrossRef]

diversity

MDPI

Article

Diversity of Land Snail Tribe Helicini (Gastropoda: Stylommatophora: Helicidae): Where Do We Stand after 20 Years of Sequencing Mitochondrial Markers?

Ondřej Korábek [1,*], Lucie Juřičková [2] and Adam Petrusek [1]

[1] Department of Ecology, Faculty of Science, Charles University, Viničná 7, 12844 Prague, Czech Republic; petrusek@natur.cuni.cz
[2] Department of Zoology, Faculty of Science, Charles University, Viničná 7, 12844 Prague, Czech Republic; lucie.jurickova@seznam.cz
* Correspondence: ondrej.korabek@gmail.com

Abstract: Sequences of mitochondrial genes revolutionized the understanding of animal diversity and continue to be an important tool in biodiversity research. In the tribe Helicini, a prominent group of the western Palaearctic land snail fauna, mitochondrial data accumulating since the 2000s helped to newly delimit genera, inform species-level taxonomy and reconstruct past range dynamics. We combined the published data with own unpublished sequences and provide a detailed overview of what they revealed about the diversity of the group. The delimitation of *Helix* is revised by placing *Helix godetiana* back in the genus and new synonymies are suggested within the genera *Codringtonia* and *Helix*. The spatial distribution of intraspecific mitochondrial lineages of several species is shown for the first time. Comparisons between species reveal considerable variation in distribution patterns of intraspecific lineages, from broad postglacial distributions to regions with a fine-scale pattern of allopatric lineage replacement. To provide a baseline for further research and information for anyone re-using the data, we thoroughly discuss the gaps in the current dataset, focusing on both taxonomic and geographic coverage. Thanks to the wealth of data already amassed and the relative ease with which they can be obtained, mitochondrial sequences remain an important source of information on intraspecific diversity over large areas and taxa.

Keywords: *Helix*; *Codringtonia*; *Caucasotachea*; *Levantina*; taxonomy; phylogeography; Western Palaearctic; Europe; Middle East; gastropod

Citation: Korábek, O.; Juřičková, L.; Petrusek, A. Diversity of Land Snail Tribe Helicini (Gastropoda: Stylommatophora: Helicidae): Where Do We Stand after 20 Years of Sequencing Mitochondrial Markers?. *Diversity* **2022**, *14*, 24. https://doi.org/10.3390/d14010024

Academic Editor: Michael Wink

Received: 30 November 2021
Accepted: 23 December 2021
Published: 31 December 2021

1. Introduction

Intraspecific diversity is an important source of information about the mechanisms responsible for the current species distributions. The phylogeographic perspective reveals geographic structuring, informs about past distribution range extensions and population size changes and is able to distinguish between different scenarios responsible for accumulation of diversity in a given area and lack thereof in another (e.g., [1]). For example, genetic diversity allows differentiating between species evolved in situ and recent immigrants. Uncovering how biodiversity emerges and is maintained thus requires combining both inter- and intraspecific perspectives.

Unfortunately, datasets covering simultaneously intra- and interspecific diversity patterns within a taxon above the genus level remain rare and highly incomplete (e.g., [2–5]). It is difficult to obtain a broader picture of the diversity and phylogeny of, say, a family-level taxon across its whole distribution range, sampling all genera, species and the intraspecific diversity. To this day, collections of sequences of mitochondrial genes remain, along with microsatellites, the main source of information on the intraspecific variation on large taxonomic and spatial scales (e.g., [5–7]). Describing internal diversity of its constituent species in terms of both intrapopulation genetic variation and geographic structure is a mammoth

task. Comprehensive and reliable information about diversity and its distribution is only obtained by a dense and geographically balanced sampling of populations. Data can be often repurposed from earlier studies, but utilization of published data is often difficult: they may be published in a summarized form [8] and they are often not appropriately georeferenced (e.g., [2,9]. Moreover, the sampling may be spatially and taxonomically biased depending on the goals of the original studies and filling the gaps in coverage then promises a diminished chance of discovery, which may lower the motivation to do such work.

We present here a dataset that covers both the species-level and intraspecific diversity of a Western Palaearctic tribe of land snails, Helicini. The tribe comprises the largest land snails in the region, several of which are very common and represent a prominent part of the local faunas. Thanks to several recent studies compiled here, this group is currently among the most thoroughly studied land snail taxa considering the distribution of intraspecific lineages. Its parent family, Helicidae, currently represents probably the best sampled land snail family, with more publicly available sequences than much more diverse Clausiliidae or Camaenidae, whose members have also been the target of numerous studies. Intraspecific diversity, however, is covered in a substantial part of the species only within the tribe Helicini, the intraspecific data for other helicid clades are less comprehensive or outright missing.

We collated georeferenced mitochondrial sequence data from published sources combined with rich own unpublished data, together spanning nearly 20 years of research on this group across over 80 species (according to https://www.molluscabase.org (accessed on 25 December 2021), but note that the taxonomy of this group is still not fully settled) and totalling to 2566 analysed individuals. We review what these data revealed about the taxonomy of Helicini and phylogenetic relationships between taxa, but the main focus is a qualitative comparison of the intraspecific diversity between species and, in particular, between different regions. For the first time we are able to compare the geographic patterns of distribution of intraspecific lineages across the whole group, including species broadly distributed as well as those with restricted ranges, by putting side-by-side species from different clades and regions. As we aim to provide a comprehensive primer on this model group for anyone interested in its diversity or in reusing the data further, we thoroughly discuss the strengths and weaknesses of the dataset, focusing on the gaps in taxonomic and geographic coverage.

2. Materials and Methods

2.1. The Model Group

The members of Helicini are medium- to large-sized land snails (greatest shell dimension ca 2–6 cm, e.g., [10,11]). The tribe is naturally distributed in the Western Palaearctic (ca. 20–54° N, 0–53° E, possibly extending further up to 68° E) and contains around 85 currently accepted species (see below). Neiber and Hausdorf [11] estimated the minimum crown age of the tribe to ca 31 Mya. This dating may be disputed because the placement of the fossil used for calibration is ambiguous (see [12]), but the estimates it yields are compatible with other lines of evidence [13,14] and the Oligocene age of the group is likely given the helicid fossil record [15].

The first sequence of a partial mitochondrial gene of a Helicini specimen (AF126144) was published in GenBank on 21 April 1999. It was a 372 bp fragment of 16S rRNA gene from *Helix pomatia*, with no locality given and misidentified as *Helix lucorum*, which was used as an outgroup in a phylogeographic analysis of another helicid species [16]. Other early uses of *Helix* mitochondrial sequences focused on identification of processed snail meat [17]. Manganelli et al. [18] were the first to provide phylogenetic insight into the systematics of Helicini using mitochondrial data, when they found indications that its type genus *Helix*, as usually delimited at that time, was polyphyletic. *Helix pomatia* was the subject of the first study focused on a Helicini taxon, presented at the World Congress of Malacology in 2007 [19], but the results were published only years later [20]. In 2012, Kotsakiozi et al. [21] published an analysis of the genus *Codringtonia*, which became the

first published comprehensive molecular phylogenetic treatment of any Helicini genus. The foundations for the phylogenetics of the whole tribe were laid between 2015 and 2016, when its internal relationships as well as its position within the family Helicidae were explored [11,22–24]. Since then, further studies involving representatives of the tribe appeared. In 2019, *Helix pomatia* became the first Helicini species with a complete mitogenome sequence [25,26]. By now, the mitochondrial sequences still represent the bulk of existing genetic data for the Helicidae family (including Helicini). Nuclear sequence markers used to date consist mostly of the internal transcribed spacers 1 and 2 of the ribosomal rRNA cluster [20,27] and a gene for histone H3 (e.g., [24,28,29]). Genomic data are currently starting to be used [30] and the first draft genome of a helicid species has been published recently [31].

2.2. Data Acquisition

The dataset analysed here includes sequences publicly available from GenBank and our own as yet unpublished sequences accumulated since 2011. We also re-sequenced some DNA isolates analysed earlier (mainly in [23]) to obtain longer fragments. Only data available to us as of 31 December 2020 were included. The published data were collated from 33 peer-reviewed publications published between 2004 and 2021 [11,18,20–27,32–54]. The Barcode of Life Data System (BOLD, https://www.boldsystems.org/ (accessed on 25 December 2021)) did not yield additional data, as only three *Caucasotachea vindobonensis* sequences available in BOLD were not represented in GenBank.

Four mitochondrial markers have been used so far for phylogenetic analyses involving representatives of Helicini. Most commonly these were the genes for 16S rRNA (16S hereafter; in two different lengths of the amplified region: ca. 400 or ca. 810 bp) and cytochrome c oxidase subunit I (*cox1*; 655 bp). Kotsakiozi et al. [21] also included a part of the cytochrome c oxidase subunit II (*cox2*; 505 bp) and partial sequences of the 12S rRNA (12S) were used in some studies attempting to reconstruct relationships between species or genera [24,35,37]. Here, we also successfully tested the amplification and sequencing of the 361 bp part of cytochrome b (*cytb*), used by [28] in a study of the helicid subfamily Ariantinae, on several samples across the diversity of Helicini. We also sequenced the 3′ half of the *cox1* gene and the span between the *cox1* and *16S* genes, including the *tRNA-Val* gene, in representatives of major lineages within Helicini (as in [41]). Additional data extending beyond the five loci above come from transcriptome sequencing [25]. Five individuals (1 *Caucasotachea*, 4 *Helix* species) were analysed and the data also contained partial sequences of mitochondrial protein coding genes. We visualized the availability for different loci by plotting the distribution of the sequence data along the mitogenome of *H. pomatia*.

The new data were largely produced using the primers listed in Table 1 as the first for each locus. Other primer combinations were employed for amplification and sequencing when the standard combinations failed. For example, an incomplete sequence was originally obtained for the *cox1* fragment in *Helix godetiana*, so the rest of the fragment has been amplified and sequenced with a forward primer specific to that sequence and H2198-Alb as the reverse primer.

Table 1. List of primer pairs used for PCR amplification.

Forward Primer	Reverse Primer	Notes on Use	References
	cox1		
LCO1490: 5′-GGTCAACAAATCATAAAGATATTGG-3′	HC02198: 5′-TAAACTTCAGGGTGACCAAAAAATCA-3′	most samples	[55] *
p-cox1-f: 5′-TCGGGACGGGTCTCTCTTTG-3′	HC02198: 5′-TAAACTTCAGGGTGACCAAAAAATCA-3′	a few *Helix pomatia* samples	forward: this study
COI-vind-f: 5′-TACTGTTTGGTGTTTGATGTGG-3′	COI-vind-r: 5′-ACAACATAG TAATTGCCCCAGC-3′	*Caucasotachea vindobonensis*	[40]
LCO1490: 5′-GGTCAACAAATCATAAAGATATTGG-3′	H2198-Alb: 5′-TATACTTCAGGATGACCAAAAAATCA-3′	a few samples	reverse [32]
g-COX1-f: 5′-TGGGACAGGTTTATCGTTACTG-3′	H2198-Alb: 5′-TATACTTCAGGATGACCAAAAAATCA-3′	3′ part of *Helix godetiana* sequence	forward: this study
COI_OK1F: 5′-TTGTWACTGCYCAYGCRTTTG-3′	HC02198: 5′-TAAACTTCAGGGTGACCAAAAAATCA-3′	used for some samples that failed to amplify with the standard primer pair, mostly from museum ethanol material	forward [42]
LCO1490: 5′-GGTCAACAAATCATAAAGATATTGG-3′	COI_OK3R: 5′-AAAGGTGGRTAAACAGTYCANCC-3′		reverse [42]
	16S rRNA		
16Scs1: 5′-AAACATACCTTTTGCATAATGG-3′	16Scs2: 5′-AGAAACTGACCTGGCTTACG-3′	most samples	both [56] **
Scs1-p: 5′-GAATTACCTTTTGCATAATGGA-3′	Scs2-p: 5′-GAAACTGACCTGGCTTACG-3′	a couple of *Helix pomatia* samples	this study
16Scs1: 5′-AAACATACCTTTTGCATAATGG-3′	16S_MN3R: 5′-GCTACCTTTGCACAGTCAGWG-3′	the 16S sequence in two parts, mainly used for older or improperly preserved samples	reverse [57]
16S-F: 5′-CGGCCGCCTGTTTATCAAAAACAT-3′	16S-R: 5′-GGAGCTCCGGTTTGAACTCAGATC-3′		[58] ***
16S-F: 5′-CGGCCGCCTGTTTATCAAAAACAT-3′	16S-Helcentr-R: 5′-AAGYTTCTAGGGTCTTCTCGTCT-3′	the 3′ half of the 16S sequence in three parts, used for particularly fragmented templates	reverse [23]
16S-Helcentr-F: 5′-AGACGAGAAGACCCTAGAARCTT-3′	16S-R: 5′-GGAGCTCCGGTTTGAACTCAGATC-3′		forward [23]
16S-Helinter-F: 5′-GTACYYTGACTGTGCAAAGGT-3′	16S-Helinter-R: 5′-CTAGTCCAACATCGAGGTCAC-3′		[23]
16S-F: 5′-CGGCCGCCTGTTTATCAAAAACAT-3′	g-centr-R: 5′-AGACAGTTACCGCCCATGCT-3′	the 3′ half of the 16S sequence in three parts, for an old sample of *Helix godetiana*	reverse: this study
g-centr-F: 5′-AGCATGGGCGGTAACTGTCT-3′	16S-R: 5′-GGAGCTCCGGTTTGAACTCAGATC-3′		forward: this study
g-inter-F: 5′-TGGCCCATGATTGGGGTCTA-3′	16S-Helinter-R: 5′-CTAGTCCAACATCGAGGTCAC-3′		this study
	cox2		

Table 1. *Cont.*

Forward Primer	Reverse Primer	Notes on Use	References
COII-F: 5′-AAATAATGCTATTTCATGAYCAYGC-3′	COII-R: 5′-GCTCCGCAAATCTCTGARCAYTG-3′		[59]
	12S rRNA		
12SGast_fwd2: 5′-AGTGACGGGCGATTTGT-3′	12SGast_rev3: 5′-TAAGCTGTTGGGCTCATAAC-3′	most samples	[35]
12Sam: 5′-AACTAGGATTAGATACCCCAYTAT-3′	12bm: 5′-CGAGAGTGACGGGCGATTTGT-3′	a few samples, shorter amplicon than with the other pair	[60]
	cytb		
UCYTB151F: 5′-TGTGGRGCNACYGTWATYACTAA-3′	UCYTB270R: 5′-AANAGGAARTAYCAYTCNGGYTG-3′		[61]

* A shorter version of the reverse primer [60] may also be used. ** Combinations 16S-F+16Scs2 and 16Scs1+16S-R were also used in some cases. *** Alternatively, primers 16Sar+16Sbr [62] may also be used.

PCR conditions varied depending on primer pair, the polymerase used and quality of the DNA isolate. Lately we used the following protocol as it appeared most efficient with the best PCR and sequencing results. We run PCRs in 20 μL volume containing 1 μL of the DNA isolate, 1.5 mM $MgCl_2$, 1X Platinum II PCR buffer (Invitrogen), 0.2 mM each dNTP, 0.2 μM each primer and 0.16 μL Platinum™ II Taq Hot-Start DNA polymerase (Invitrogen). The PCR cycle was set to 2 min at 94 °C and 35 cycles of 15 s at 94 °C, 15 s at 50 °C, 15 s at 68 °C.

Amplification and sequencing of the 16S locus was without problems with the 16Scs1 and Scs2 primer pair using the protocol presented here. The primers LCO1490 and HC02198 worked well for *cox1* in most cases, except for *Helix lutescens* and some *Helix schlaeflii* lineages, where PCRs were mostly unsuccessful. For 12S the 12SGast_fwd2 and 12SGast_rev3 primer pair worked well, but for *cox2* most samples produced reads where the same sequence was visible in the background shifted by one nucleotide, meaning that either the primers or the PCR protocol were not optimal. With *cytb* (and occasionally 12S), we encountered sequencing difficulties with some samples due to stretches of 8–11 thymine bases in a row.

The chromatograms of all new sequences were visually checked for reading errors. Sequences downloaded from GenBank had in some cases to be edited. Remnants of primer sequences or poorly read sequence ends were trimmed and in rare cases (when multiple lines of evidence suggested that data from the given study were carelessly curated) highly suspect substitutions (in conserved positions of *16S* or non-synonymous in *cox1*) were given ambiguity codes. Although it is possible that they are actually accurate, some sequences were omitted altogether (e.g., KR705008, KF114835, JQ240036) due to suspected sequencing errors and/or long branches when compared to closely related samples.

An infrequent, but existing issue encountered with mitochondrial markers is the amplification of nuclear pseudogene sequences (NUMTs; e.g., [63]). We identified several instances of probable NUMT amplification in the Helicidae family as well as in Helicini. In *Helix ceratina* and one *Cepaea nemoralis* (Linnaeus, 1758) from Italy, we initially obtained two different sequences for *cox1* by varying reagent concentrations and cycling conditions for the PCR with the same DNA isolate. We identified the genuine *cox1* by amplifying and sequencing the region spanning from the standard *cox1* fragment into *16S* (*H. ceratina* [41]) or by comparison with *16S* phylogeny (*C. nemoralis*). In another *C. nemoralis* individual from Italy, belonging to the clade E of Grindon & Davison [64], the sequencing resulted in a chromatogram with numerous double-peaks, suggesting that we co-amplified two distinct fragments simultaneously. Other possible NUMT examples are MF564162 from *Helix melanostoma* and MF564169 from *Eobania* P. Hesse, 1913 [29], which do not contain unexpected stop codons but, unlike the *16S* from the same specimens, fall outside the correct clades when included in phylogenetic analysis.

All sequences, both newly obtained and retrieved from published studies, are listed with their metadata in Table S1. The geographic coordinates of sampling sites are given with varying precision, depending on how precisely the original location was known. In some cases, museum samples or published sequences have been used where the locality has been only verbally described, sometimes vaguely (for example, providing only the name of the closest settlement) or referring to places that we could not trace. In a few cases the published coordinates were corrected to correspond with the locality description. The museum lots indicated as vouchers include any shell material of the given species collected at the same site on the same occasion. Occasionally, these do not include shells of the sequenced individuals, typically when only small juveniles were found alive, which were preserved whole and directly used for DNA extraction.

2.3. Phylogenetic Analyses

2.3.1. Outgroup Selection

Currently, the best supported hypothesis on the relationships within the subfamily Helicinae assumes that the subfamily consists of two major clades, with centres of diversity

in the western and eastern Mediterranean, respectively [11,25,27]. The tribe Helicini equals the eastern clade; the western clade consists of Allognathini Westerlund, 1903, Maculariini Neiber, Korábek, Glaubrecht and Hausdorf, 2021 and Thebini Wenz, 1923 [27] (but see [65] for an alternative system). Being sister to Helicini, the western clade is a natural outgroup choice.

For the outgroup, we collated only the *16S* and *cox1* data, because the other loci are available for only a few species. To avoid long branches as much as possible we employed a broad sampling of the outgroup by including most of the species recognized by the most recent revisions; more than one sample per species were included for *Cepaea nemoralis* (due to its very high intraspecific diversity) and for *Cornu* Born, 1778 (as the taxonomic splitting to species level is uneven across the genus). We mostly relied on published sequences [11–13,16,20,22,23,27,29,49,64–82]. The respective GenBank accession numbers are listed in Table S2. Some species could not be included due to lack of available samples or sequences at the time of dataset collation (see [14] for additional data published meanwhile).

2.3.2. Alignment

The alignment of *cox1*, *cox2* and *cytb* was straightforward since there were no indels when aligned with MAFFT 7.471, G-INS-i algorithm [83]. In contrast, alignment of the two rRNA genes is problematic due to the stem-and-loop structure of the rRNA, where the positions within loops may be non-homologous between distantly related sequences. Homology may be expected more safely among related species and these regions may also hold valuable phylogenetic information at the finest phylogenetic levels. In order to give priority to correct alignment of the loops among more closely related taxa, we performed the alignment in several steps. First, we aligned the sequences in each genus separately with MAFFT's E-INS-i algorithm (default settings). The only exception was *Cepaea*, where we enforced the assumption of global homology by using G-INS-i. The sequences of the two *Cepaea* species are highly divergent and *Cepaea hortensis* (O. F. Müller, 1774) was underrepresented, which resulted in long unaligned blocks.

The resulting alignment blocks were checked and occasionally corrected when misplaced parts of incomplete sequences or apparently misaligned positions were observed at the end of aligned sequences. Then, we aligned these blocks within well-supported clades found in a recent analysis employing also the nuclear ITS2 (including partial 5.8S and 28S rRNA) data [27]: *Otala+Loxana+Massylaea+Eobania+Gyrostomella*, *Cornu+Cantareus+Rossmaessleria*, *Allognathus+Hemicycla* and *Helix+Maltzanella*. Within Thebini and Helicini, the resulting alignments were then aligned with each other and the remaining genera. In Allognathini there was an additional step of aligning all genera with the exclusion of *Cepaea* (see Figure 4 in [27]). We then aligned Thebini with Maculariini, these two with Allognathini and, finally, this complete outgroup with Helicini. Aligning the sub-alignments was done using the *–merge* option of MAFFT and the E-INS-i algorithm.

The data from the transcriptome sequencing were aligned by codons with MUSCLE [84] in MEGA 7 [85]. For phylogenetic analyses, only the *cox1*, *cox2*, *cytb* genes recovered from the transcriptome were used.

2.3.3. Maximum Likelihood Analysis of Backbone Phylogeny

We first examined the species-level backbone phylogeny of Helicini using two datasets: one consisting of the partial *cox1* and 16S sequences and including the outgroup ("outgroup" dataset), the other without outgroup and aiming to maximize the length of the alignment ("maxloci" dataset) by including full *cox1* and partial *cytb*, *cox2*, 16S and 12S where available. The nuclear ITS2 alignment used in analyses of multiple concatenated genes by Neiber et al. [27] was also analysed to show potential differences to the mitochondrial phylogeny.

For each dataset, the partition scheme and substitution models were selected with ModelFinder in IQ-TREE 1.6.12 [86,87] after initially partitioning the data into three codon positions for each protein-coding gene and separate partitions for each rRNA gene. Maxi-

mum likelihood analyses were then run with IQ-TREE and branch support was assessed with standard bootstrap (1000 pseudoreplicates) and SH-aLRT [88] (1000 replicates).

The inferred position of the genera *Theba* Risso, 1826 and *Eremina* L. Pfeiffer, 1855 within the outgroup, although without support, conflicted with expectations based on previous phylogenetic analyses (e.g., [27]) and morphology (*Eremina* appeared sister to Allognathini, *Theba* to *Rossmaessleria* P. Hesse, 1907). This appears to be driven at least in part by uneven nucleotide composition in different genera of the outgroup (see Results in Section 3). We also repeated the analysis with constraints on the outgroup topology to ensure that it had no effect on the inferred root position of Helicini. In this constrained analysis, we enforced the monophyly of Thebini with the exclusion of *Macularia* Albers, 1850 (according to [27]) and assigned *Theba* as sister to *Eremina* (due to shared preference for arid habitats, thick digitiform glands with reduced terminal branches and a small protoconch that is darkly coloured in some individuals).

2.3.4. Complete Phylogeny of Helicini

The strength of the presented dataset is in the coverage of intraspecific diversity of a number of the Helicini species. In order to describe and visualise the intraspecific lineage diversity in a manner allowing for comparison between species and regions, a unified objective approach to the delimitation of intraspecific groupings is needed. To this end, we constructed a complete time-tree of the samples and defined species-level clades and intraspecific clades by applying common clade age thresholds across the whole tree. The focus here were the phylogenetic relationships within species and the relative timing of diversification in different clades, not the relationships between more distantly related species and absolute dating of the tree.

Phylogenetic analysis of the complete dataset is challenging for several reasons. The number of samples is high, the alignment short and there is a great variation in the sequence length due to missing data [89]. Many of the samples yielded identical or nearly identical sequences and the loci available are insufficient to resolve deeper nodes within Helicini, especially relationships between related species and between genera [11,23,27,37,41], so it would be difficult if not impossible to obtain the complete phylogeny in one analysis. We therefore followed an approach inspired by that of Upham et al. [90]. We first constructed a backbone phylogeny using a dataset containing representatives from all major clades within Helicini and all samples of species unassigned to any of these, then we analysed each clade separately and, finally, we combined the resulting trees to create a complete phylogeny of all samples. The following datasets were analysed: Helicini backbone (*cox1*, 16S, 12S), *Caucasotachea* (*cox1*, 16S), *Codringtonia* (*cox1*, 16S, 12S, *cox2*), *Levantina* (*cox1*, 16S, 12S), *Helix* (*Pelasga*) (*cox1*, 16S, 12S), *Helix* Anatolian clade (*cox1*, 16S, 12S), *Helix* Mediterranean clade (*cox1*, 16S, 12S) and *Helix* European clade (*cox1*, 16S, 12S). We have run the single clade analyses without outgroups, because while each of the datasets (except for the backbone) comprises a well-supported clade, their closest relatives are in all cases uncertain [23,27] (see Results in Section 3 and Figure S1) and rooting of the clades could be biased if the outgroup is chosen arbitrarily.

For each dataset, partition scheme and substitution models were selected by IQ-TREE; we initially partitioned the data into three codon positions for each protein-coding gene and separate partition for each rRNA gene, but in all cases the model selection suggested four partitions: three codon positions and the rRNAs. We used BEAST 2.6.3 [91] for the phylogenetic analysis. We linked the tree and clock model between partitions. Bayesian Skyline was used as a flexible tree prior suitable for combination of inter- and intraspecific data [92] and a relaxed lognormal clock with mean rate of 0.02 substitutions per site per million years [13] was assumed for all analyses. In some cases, the selected substitution model has been downgraded from GTR to TN93 due to convergence problems of some of the model's substitution rates in preliminary runs.

We run analyses of all sub-alignments in two replicates for 70 million generations sampling each 10,000th. 28% generations were discarded as burn-in after checking that

parameter estimates converged within these and effective sample sizes over 200 were reached in the post-burn-in. This resulted in 10,000 trees for each sub-alignment. An exception was the European clade of *Helix*, the largest dataset (1292 tips) containing large amounts of very closely related samples mostly from *H. pomatia*. Analysis of this dataset was run in four replicates for 21 million generations.

The results for each single-clade dataset were summarized on a maximum clade credibility (MCC) tree with mean node heights (trees available from the Dryad repository). There were large differences in support for the position of the root between the single clade analyses and the backbone BEAST tree, with resolved root position only in the latter analysis (except for *Levantina* and *Codringtonia* supported in both). In the case of the European clade of *Helix*, there was a strong support for a root between *Helix lutescens* and the remainder in the backbone analysis (Figure S3). *Helix lutescens* is the only species in the clade which does not live in the Balkans [10] and lives syntopically with other members of the clade without any sign of past or present hybridization (own observations). Therefore, we consider this rooting very likely; it also appeared in earlier analysis with an outgroup [37]. In addition, the root for *Caucasotachea* was fully supported in the backbone tree. Its position corresponded to that uncovered in an earlier analysis [24] and is likely based on conchological and geographic grounds. Finally, we considered more likely that the root of the Mediterranean clade is between *H. ceratina* (or *H. ceratina+H. ligata* complex) and the remainder of the clade than among the conchologically similar species with brown shell apertures [41], as the single-clade analysis suggested (although without statistical support). We therefore accepted the root positions as inferred in the backbone analysis, despite uncertainty in case of *Pelasga* and the fact that the high supports for the root positions from the BEAST backbone analysis (Figure S3) were not mirrored in the ML analyses. We excluded from the posterior of the backbone and single-clade analyses trees not conforming the respective root positions. MCC trees were calculated for these filtered posterior samples and used for constructing the complete phylogeny. We found no appreciable effect on the support values for species-level and intraspecific clades (which were the focus of our analysis, see below); the differences only concerned the basal relationships between species which were not statistically supported in either analysis. The filtering led to varying reductions in the number of the posterior trees: for example, while no trees were excluded for *Codringtonia* and *Levantina*, almost a half did not correspond to the assumed root position in *Caucasotachea* and only ca. 10% of the posterior trees conformed to the selected rooting with *H. ceratina* in case of the Mediterranean clade.

The MCC trees from single-clade analyses were then grafted onto the MCC tree from the filtered posterior of the backbone analysis in place of the respective clades. The tree heights were adjusted to the height of the most common recent ancestor (MRCA) of the respective clades in the backbone tree. Note that there were substantial differences in the heights between single clade analyses and the backbone analysis despite using the same average clock rate, which corresponds to variability in the inferred clock rates for major branches in the backbone tree.

2.4. Distribution Maps of Intraspecific Lineages

We recognized two levels of clades for the visualization of the distributions of mitochondrial diversity ("species-level" and "intraspecific") to obtain comparable units for plotting the distribution. We set these common age thresholds in the complete phylogeny and recognized the (sub)clades, whose crown ages were younger and stem ages older than these thresholds. Note that due to variation in molecular clock rate within the tree and the assembly of the complete tree from several subtrees, these thresholds may in fact, correspond to somewhat different absolute ages in different clades and subclades.

The "species-level" threshold has been set only for plotting and does not reflect any taxonomic opinion. No such threshold, however, would fit all situations. For our purpose, the "species-level" threshold was set so that well-established species were not split into multiple "species-level" clades, but in some cases the resulting clades contain more than

one currently recognized species (e.g., *Helix lucorum* and *Helix nicaeensis*; *Levantina*). The MRCA of *Codringtonia parnassia* was used to set the "species-level" threshold. The threshold defining the intraspecific clades delimits subclades corresponding to or finer than divisions used in earlier phylogeographic studies [38,40]. The threshold was set at the base of *Helix pomatia* clade F *sensu* Korábek et al. [38] and adjusted so that several lineages represented by 1–2 individuals became included in larger intraspecific groups.

The geographic distributions of intraspecific lineages of all "species-level" clades were mapped using the same map scale and projection for direct comparability.

2.5. Non-Native Populations

Several large helicids (*C. nemoralis*, *C. aspersum* (O. F. Müller, 1774), *T. pisana* (O. F. Müller, 1774), *E. vermiculata* (O. F. Müller, 1774); for Helicini, see [23,38,39,41,42]) have been subject to countless intentional or unintentional introductions beyond their natural range limits. For meaningful biogeographic considerations, samples originating from such non-native populations must be identified and filtered out. We considered a sample to be from a native population when it was taken in a part of the species' range where there is no a priori reason to doubt its natural occurrence. Populations from parts of the range which are known or suspected by us to be a result of introductions were labelled as non-native. The status of samples from near the tentative limits of natural distribution of *H. pomatia* and *H. lucorum* was given as unknown.

3. Results and Discussion

3.1. Mitogenome Representation

The mitogenomes of Helicidae sequenced so far are from 14,050 (*Cornu aspersum*) to 14,795 (*Theba pisana*) bp long [73,93,94]; the three sequenced mitogenomes of *H. pomatia* were very similar and 14,070–14,072 bp long [25,26]. For most samples, only about 10% of the mitogenome length or less was sequenced (Figure 1). In the presented dataset, only 33 out of the total of 2566 analysed individuals were sequenced for all four focal genes (*cox1*, *cox2*, 16S and 12S). 1421 were analysed for *cox1* (max. fragment length 1506 bp, min. 133 bp, median 655 bp), 122 for *cox2* (max. 658 bp, min. 360 bp, median 505 bp), 2313 for *16S* (max. 851 bp, min. 122 bp, median 776 bp) and 121 for *12S* (max. 675 bp, min. 240 bp, median 640 bp). The *cox1* fragment is generally under-represented in comparison to 16S, but in *Caucasotachaea* many individuals were sequenced for *cox1* only.

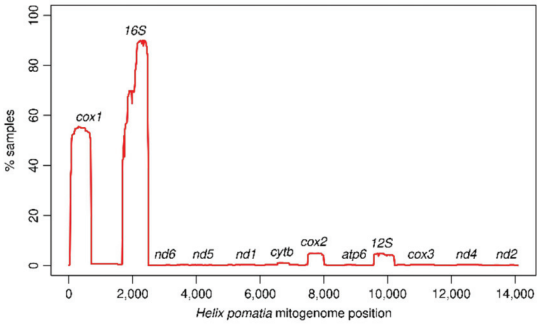

Figure 1. Representation of the mitogenome among the available sequences of mitochondrial markers of Helicini, plotted along the mitogenome of *Helix pomatia*. All sequences were aligned with the mitogenome and positions with gaps in the mitogenome were removed. For each position of the alignment, we calculated the percentage of all analysed individuals (out of 2566 included in this study) in which that position was covered. The percentages were averaged and plotted in 10 bp bins.

3.2. Dataset Coverage

The coverage of the distribution range of Helicini by currently available mitochondrial sequence data is highly uneven (Figure 2). The most densely sampled region are Central Europe and the Balkans. Towards the east, the sampling gradually becomes sparser. Those less covered areas include vast expanses of Eastern Europe with only few broadly distributed lineages of Helicini, as well as Anatolia and the Middle East where many endemic lineages occur.

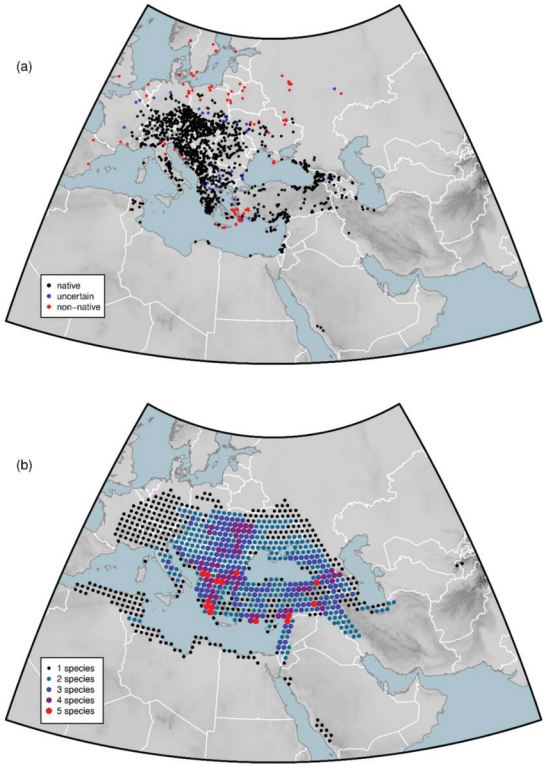

Figure 2. (**a**) sites of origin of the mitochondrial sequences in the tribe Helicini collated here and (**b**) a schematic representation of the spatial distribution of species diversity in the tribe. Sampling sites where only (presumably) non-native species have been sampled are shown in red, those where the native status is uncertain are in blue. Without prior knowledge, the unbiased way to uncover the distribution of intraspecific lineages would be a regular and indiscriminate sampling across the whole species ranges. In (**b**), we illustrate this by regularly spaced points covering the natural range of Helicini. Point size and colour corresponds to the number of species occurring in its vicinity, reflecting thus not only sympatric diversity, but also boundaries between species ranges (no more than four species were found syntopic, usually no more than two). The high diversity in southern Greece is due to proximity among ranges of several closely related and narrowly distributed species of *Codringtonia*. In addition, note that the plotted diversity is, in part, an approximation, because there are poorly explored areas in the east and clades with problematic taxonomy (in particular *Levantina*); in Iran we assume that the actual species distributions may be broader than currently known. Non-native distributions were excluded, but populations with uncertain origin were in part considered (e.g., *Helix nucula*, *Helix lucorum*) as these need to be properly analysed in order to resolve their status. As shown by the presented data, some areas would in fact require considerably denser sampling than the figure suggests.

The phylogenetic coverage is biased as well. Some species (especially *H. pomatia*, *C. vindobonensis*) are very well sampled across most of their range, but there are also species represented by samples from a single locality and genera like *Levantina* and *Isaurica* are only incompletely sampled at the species level. In fact, *H. pomatia* alone makes for 40% of the sequenced individuals and *C. vindobonensis* for additional 14%. This is partly due to studies dedicated to the phylogeography of these two species [38,40,51], but also due to their exceptionally large distribution range and high abundances in well accessible parts of Europe. In contrast, *Helix salomonica* from eastern Turkey, northern Iraq and Iran is an example of a broadly distributed species with very sparse coverage (three localities only).

In total, only 6% of the analysed individuals came from non-native populations and in further 4% the origin was classified unknown. However, in the extreme case of *Helix cincta* s. str., only one out of 30 analysed samples originated from its presumed native range.

3.3. Phylogeny

The phylogenetic analyses yielded, as expected, results similar to earlier studies. The available data do not provide a resolved mitochondrial phylogeny of Helicini (even with the "maxloci" dataset, Figure 3). The tribe Helicini is consistently recovered as monophyletic with both mitochondrial (Figure S1) and ITS2 data (Figure S2; see [27] for results of a concatenated analysis), but the only grouping between genera, supported unambiguously by the mitochondrial data, is the sister relationship between *Helix* and *Maltzanella*. The root position suggested by the analysis with outgroup (Figure S1; regardless of the outgroup topology) as well as the molecular clock analysis (Figure S3) is between *Helix+Maltzanella* and the rest of the tribe, but without unambiguous support. The supported groupings of species correspond to genera and the clades within *Helix* recognized by Korábek et al. [23]. Relationships among species are generally unresolved, but well-supported clades are found at the level of species and within species.

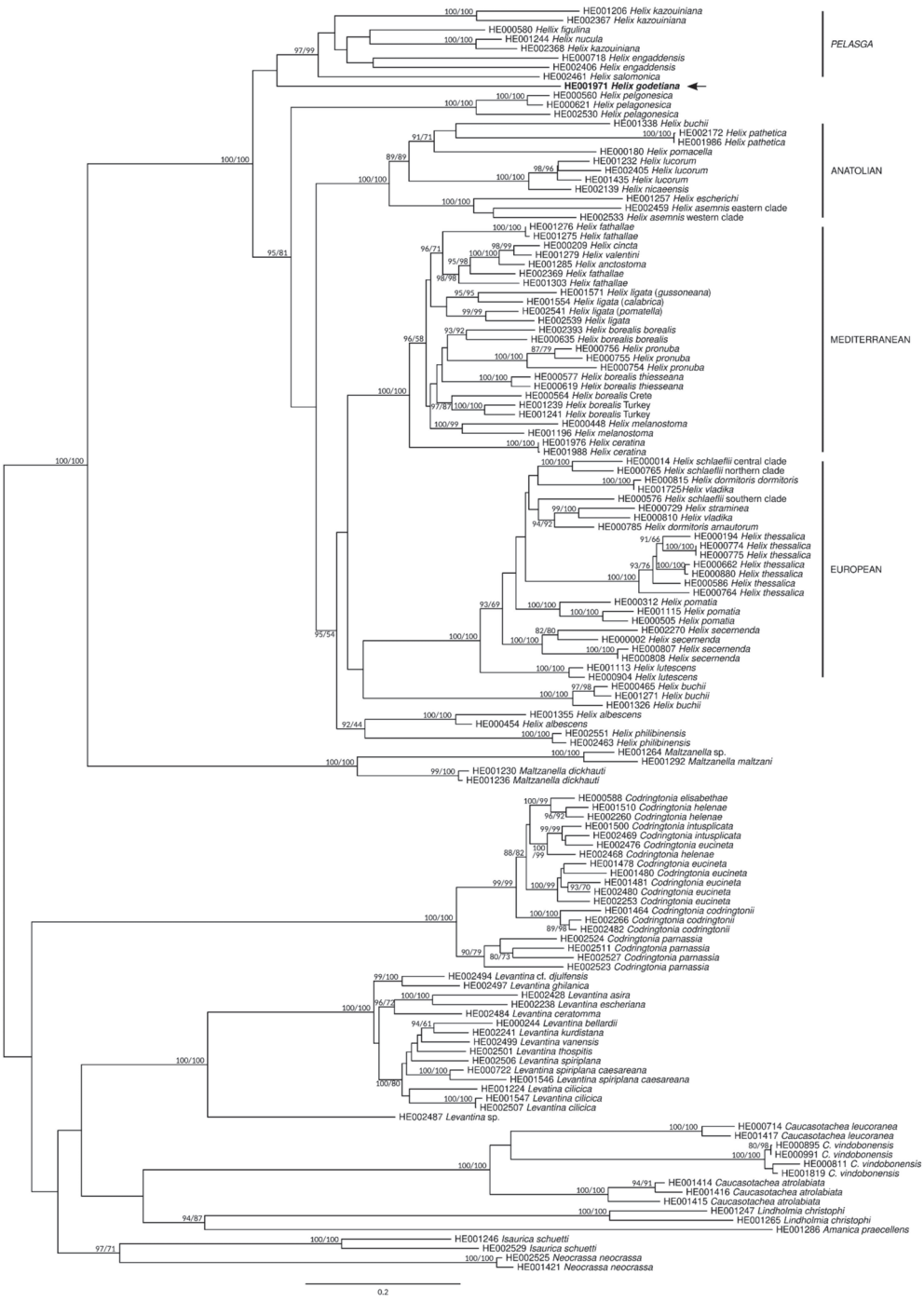

Figure 3. Unrooted maximum likelihood phylogeny of Helicini, based on concatenated *cox1*, *cytb*, *cox2*, 16S and 12S sequences. Support values are given as SH-aLRT/bootstrap percentages, support is shown only for branches with SH-aLRT value >90 or bootstrap >70% is shown. The position of *Helix godetiana* is marked with an arrow and major clades within *Helix*, discussed in the text, are labelled.

3.4. Diversity of Helicini

The tribe Helicini is unambiguously supported by molecular phylogeny, geographically well-defined and its delimitation is now agreed upon. The phylogenetic relationships among the genera within the tribe, however, are not resolved with the available mitochondrial data or by ITS2 data (Figure S2). In addition, the limited information content of the sequenced genes and missing data in the matrix, the evolutionary history of the group also contributes to the issue. Two genera are monotypic, in 3–5 others the crown group is young relative to the age of their branch. The situation is similar within *Helix*, as relationships among the main clades remain obscure. Furthermore, at least two of these clades (Mediterranean, European) seem to have undergone a rapid initial diversification, another factor contributing to poor resolution of the phylogeny.

3.4.1. *Caucasotachea* C. Boettger, 1909

In their morphology-based revision, Neubert and Bank [95] restricted the genus *Caucasotachea* to four species distributed in the Caucasus region, Alborz mountain range in Iran and along the southeast of the Black Sea by excluding species of the former subgenus *Lindholmia* P. Hesse, 1919. Molecular phylogenetic studies supported this split, but nevertheless led to changes in both the genus delimitation and species-level taxonomy. The very broadly distributed east-European *Caucasotachea vindobonensis* (C. Pfeiffer, 1828) has been transferred to this genus from *Cepaea* Held, 1838 [11,23,24,35] and the original four species were reduced to only two by Neiber et al. [47] following a detailed molecular genetic study.

The phylogeography of two species, *C. vindobonensis* (Figure S4) and *Caucasotachea atrolabiata* (Krynicki, 1833) (Figure S5), has been studied comprehensively [40,47,51]. The distribution of the former is well covered by sampling except for its eastern part from eastern Ukraine and south-western Russia to the river Volga and the Caucasus. In addition, its eastern range limits are not yet clarified. Due to the long distance between glacial refugia in the Balkans [40] and the eastern range extremes and the ubiquity of the species, *C. vindobonensis* may be a good model for studying how the genetic diversity becomes depleted with increasing distance from the postglacial expansion source in the absence of major dispersal barriers. For such a purpose, additional data from its eastern populations would be beneficial.

In *C. atrolabiata*, our new data from Abkhazia reveal that all major mtDNA clades are present, possibly in a parapatric pattern, in the western end of the Greater Caucasus, suggesting that its diversification centre lies here. To confirm the pattern, more samples from Abkhazia would be desirable to fill a gap in sampling.

Only a few sequences were available for *Caucasotachea leucoranea* (Mousson, 1863), which is distributed around the south of the Caspian Sea from Azerbaijan to Golestan in Iran (Figure S6).

3.4.2. *Neocrassa* Subai, 2005

Neocrassa has been distinguished first as a subgenus of *Codringtonia* [96], but the mitochondrial phylogeny indicates that it has to be separated at the genus level [23,27]. Its only species, *Neocrassa neocrassa* (Zilch, 1952), has a very limited range at the Greek–Albanian frontier (Figure S7). The available data revealed only shallow intraspecific divergences; no samples were available from Albania.

3.4.3. *Isaurica* Kobelt, 1901

The genus *Isaurica* is distributed in a small area in south-western Anatolia. The last revision [97] distinguished six species. However, Nordsieck [98] suggested that *Isaurica callirhoe* (Rolle, 1894) belongs, based on shell microsculpture, to *Levantina* and *Amanica praecellens* (Nägele, 1901) has been excluded from the genus by molecular phylogeny even earlier [23]. Of the remaining four species, *Isaurica riedeli* Subai, 1994 from north of Manavgat and near Akseki in the Antalya Province and *Isaurica pamphylica* Subai, 1994 from around Sütçüler and the Köprülü Canyon in the Isparta and Antalya Provinces of

Turkey remain unsampled for molecular analyses. The phylogeny revealed samples of *Isaurica schuetti* Subai, 1994 as paraphyletic relative to *Isaurica lycia* (Martens, 1889), but the significance of this is unclear as only two individuals were analysed for each of these taxa (Figure S8). Introgression from *I. lycia* seems a plausible explanation.

3.4.4. *Amanica* Nordsieck, 2017

Amanica is a narrowly distributed monotypic genus separated from *Isaurica* after sequence data became available [23,98]. It only comprises *Amanica praecellens* (Nägele, 1901) from the Hatay province of Turkey (Figure S9).

3.4.5. *Levantina* Kobelt, 1871

Levantina comprises more than 20 currently accepted rock-dwelling species broadly distributed in the Middle East from Cyprus, Central Taurus mountains and the Levant to western Iran, Iraqi Kurdistan and south-western Arabia. The centre and origin of the present diversity of *Levantina* lies in eastern Turkey in the area south and south-west of Lake Van towards the Syrian Desert [42]. The species-level taxonomy is not resolved due to scarcity of samples from some regions and taxa on the one hand and variability of shell characters on the other hand. A thorough revision would require extensive new sampling. Intraspecific variability and its distribution are virtually unknown within *Levantina*. The genus has been recently newly delimited by excluding one former subgenus as a completely unrelated lineage and merging *Assyriella* P. Hesse, 1909 and *Levantina* (*Laevihelix*) Neubert, 1998 with the nominotypic subgenus [27]. In a follow-up study, the first mitochondrial phylogeny of the genus was presented [42], which forms the basis of the data shown here.

The western limits of the natural distribution of *Levantina* are uncertain. The populations of *Levantina spiriplana spiriplana* (Olivier, 1801) and *L. spiriplana caesareana* (Mousson, 1854) in the south-eastern Aegean and on Cyprus are most likely introduced [42], but there are two additional taxa from the western end of *Levantina*'s range, which have not been studied yet by molecular methods. One is *Levantina rechingeri* Fuchs & Käufel, 1936, known only from a few empty shells found on the slopes of the Kali Limni mountain on Karpathos island in the south-eastern Aegean [99–101]. The other is the above-mentioned *Isaurica callirhoe* (Rolle, 1894), which Nordsieck [98] reassigned to *Levantina*. It is known only from shells of the type series collected at an unknown location on the northern slopes of Akdağlar between Fethiye and Elmalı [102] in the very south-east of Anatolia.

Similarly, the range extent of *Levantina* in the east is not well documented. The known distribution extends roughly to Tehran [102], but *Levantina longinqua* (Schütt & Subai, 1996) has been described based on shells allegedly from "Hasrat Sultan Gebirge" south-east of Samarqand, Uzbekistan [103]. It remains known only from its type series and the type locality is not given precisely: Khazret-Sultan (Hazrati Sulton) at the Tajikistan border is the highest peak in Uzbekistan, but a broad area around it has to be considered. Finally, the true extent of distribution of *Levantina* in the west of the Arabian Peninsula is unclear and *Levantina semitecta* Neubert, 1998 from an unknown locality (probably in an area roughly between Jabal al-Lawz and al-Wajh in the north-west of Saudi Arabia) is known only from its two types collected in the 19th century [104].

In addition, the four problematic taxa above, no data are currently available also for *Levantina mahanica* Kobelt, 1910, described from near Lake Urmia and distributed south of it into Iraqi Kurdistan, and *Levantina ninivita* (Galland, 1885), described from near Mosul and recorded also near Cizre in Turkey [102]. In addition, samples from type localities would be desirable for *Levantina guttata* (Olivier, 1804) (Turkey, Şanlıurfa Castle hill) and *Levantina thospitis* (Schütt and Subai, 1996) (Turkey, between Bitlis and Baykan, Kermate/Alaniçi SW of Şetek/Ortakapı). They are likely conspecific with *Levantina vanensis* (Schütt and Subai, 1996) and *Levantina mardinensis* Kobelt, 1900, respectively, but because the intraspecific variation and significance of conchological characters in *Levantina* are poorly understood, the two pairs were not formally synonymized based on the available samples [42].

The majority of *Levantina* taxa, including the type species *L. spiriplana*, group in a large, broadly distributed clade with very short and unresolved branches at its base (Figures S10 and S11). This group is similarly aged as the Peloponnese radiation of *Codringtonia* (Figure S3; see also Figure 4 in [27]), but its range extends from southern Israel, Cyprus and the Cilician Taurus to the very south-east of Turkey. We presume that *L. mahanica* also belongs here as a potential close relative of *Levantina kurdistana* (L. Pfeiffer, 1862), which would extend the distribution of this clade up to Iraqi Kurdistan and western Iran.

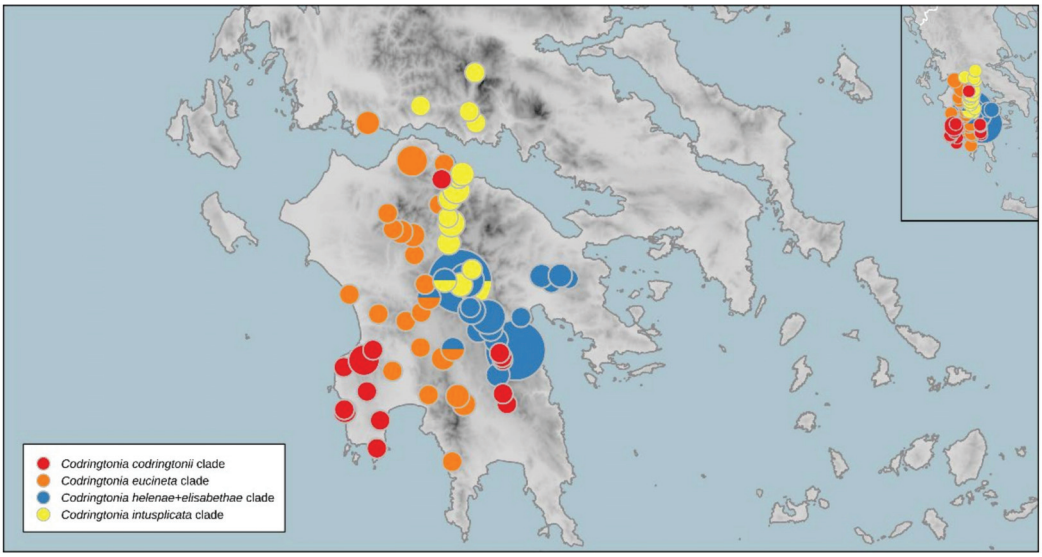

Figure 4. Distribution of mitochondrial clades corresponding to presently recognized *Codringtonia* species from the Peloponnese. The inset shows the distribution on the same map scale as the European clade of *Helix* in Figure 5. These four clades fall below the "species" threshold and thus represent finer divisions than in Figure 5. The sampling is mostly sufficient, samples are only missing for *Codringtonia intusplicata* populations from the north-eastern Peloponnese. See Figures S17–S20 for the internal diversity of the clades shown here.

A clade comprising *Levantina djulfensis* (Dubois de Montpéreux, 1840) and its relatives *Levantina ghilanica* (Mousson, 1876) and *Levantina mazenderanensis* (Kobelt, 1883) is distributed in the north-eastern part of the range of the genus (Figure S12). *Levantina djulfensis* has been reported also from an isolated area south of Siirt (Schütt and Subai 1996), a record whose identification may be worth a revision using molecular data due to its position in a region of high diversity of *Levantina*. *Levantina ceratomma* (L. Pfeiffer, 1856) (Figure S13) appears to be an isolated and well recognizable species, its samples from Iran west of Lake Urmia are nevertheless missing. *Levantina escheriana* (Bourguignat, 1864) is relatively broadly distributed (Figure S14). It is likely closely related to or conspecific with *L. ninivita*, judging from conchological similarity. It was found to be a sister clade of the three Arabian taxa *Levantina asira* Neubert, 1998, *Levantina symensi* Neubert, 1998 and *Levantina asagittata* Neubert, 1998, which are very closely related and for which samples were available only from their type localities (Figure S15).

The basal-most mitochondrial lineage in *Levantina* was recovered from a population sampled near the south-western end of Lake Van (Figure S16). We could not assign this sample reliably to any of the species accepted by Schütt and Subai [102]. The lineage is deeply divergent from the rest of the genus; however, the nuclear ITS2 data do not confirm the deep divergence between this sample and the remaining *Levantina* sequences (Figure S2).

3.4.6. *Codringtonia* Kobelt, 1898

Codringtonia comprises large rock-dwelling snails from Central Greece and the Peloponnese. The last taxonomic revision [96] distinguished, based on morphology, seven parapatric species. They are, except for *Codringtonia parnassia* Roth, 1855, mutually similar and very closely related. There is substantial geographic variation in details of shell shape and colour also within some of the species, suggesting geography as the main driver of diversification of *Codringtonia*. In the first molecular phylogeny, Kotsakiozi et al. [21] found support for the proposed classification with the exception of *Codringtonia gittenbergeri* Subai, 2005.

Our new data, which also include original material from the Subai's revision [96], suggest a more complicated situation. Two samples from within the range of *C. gittenbergeri* as indicated by Subai [96] were identified as *Codringtonia codringtonii* (Gray, 1834) by Kotsakiozi et al. [21]. After excluding these, they concluded that *C. gittenbergeri* shares the same mtDNA clade with *Codringtonia elisabethae* Subai, 2005. However, the typical *C. gittenbergeri* shells including the holotype have an appearance similar to *C. codringtonii*, they are just darker, and the two paratypes we analysed also had mtDNA corresponding to *C. codringtonii*. Therefore, we consider *C. gittenbergeri* a junior synonym of *C. codringtonii*. Samples identified as *C. gittenbergeri* in Kotsakiozi et al. [21] were collected where Subai [96] reported *C. elisabethae* and likely indeed belonged to that species as the mtDNA suggests. The ranges of *C. elisabethae* and *C. gittenbergeri*, as indicated by Subai [96], adjoin and there is some overlap in the distribution of the corresponding mtDNA lineages.

After revising the status of *C. gittenbergeri*, *C. codringtonii* has apparently a disjunct range in the Peloponnese (Figure S17), formed by two areas separated by the range of *Codringtonia eucineta* (Bourguignat, 1857) (Figure S18). The sample from the northern Peloponnese carrying a haplotype of *C. codringtonii* was originally identified as *C. eucineta* by Subai [96] but that author already noted that there is a similarity to *C. codringtonii* with regard to shell characters.

The most diverse species within *Codringtonia* is clearly *C. eucineta* (Figure S18), which is also the most broadly distributed and most conchologically variable one. Samples of *Codringtonia intusplicata* (L. Pfeiffer, 1851) belong to a clade distributed eastward of *C. eucineta* (Figure S19) and two shallowly differentiated sister clades corresponding to *Codringtonia helenae* Subai, 2005 and *C. elisabethae* (Figure S20) occur even more to the east.

The clade uniting *C. codringtonii*, *C. eucineta*, *C. intusplicata*, *C. helenae* and *C. elisabethae* falls below the "species" threshold, so the divergences between these taxa are comparable to those often seen within other species of Helicinae. In the central Peloponnese, we have found multiple cases of discrepancy between the identification based on shell characters and the mtDNA lineage of the respective individual. Most involve *C. helenae*, where haplotypes of the clades characteristic for *C. intusplicata* and *C. eucineta* were found. In three cases these occurred in the same population together with haplotypes of the *C. helenae* clade. In addition, one individual identified as *C. eucineta* was found to have mtDNA belonging to a clade characteristic for *C. helenae*. A lineage from the *C. intusplicata* clade was found also in *C. eucineta* at one site in southern Aetolia. These discrepancies are mostly attributable to introgression as they occur at the contact between specie ranges, but incomplete lineage sorting seems possible for two lineages at the base of the *C. intusplicata* clade. Despite overlap in the ranges of the mitochondrial clades (Figure 4), we are not aware of syntopic occurrence of two currently recognized *Codringtonia* species except for a shared locality of *C. helenae* and *C. intusplicata* reported by Kotsakiozi et al. [21]. In light of our results, we doubt that this was indeed a case of coexistence of two separate populations.

There is a considerable phylogenetic diversity within *C. parnassia* (Figure S21), comparable to that within the clade uniting all other species of the genus. We have uncovered additional divergent mitochondrial lineages within this taxon on top of those reported by Kotsakiozi et al. [21] and slightly extended the known distribution to the north-east compared to Subai [96]. Various populations of *C. parnassia* also differ substantially in shell

size and shape. Apparently, the taxonomic treatment is not comparable between *C. parnassia* and the rest of the genus and further revisions within the genus would be warranted.

3.4.7. *Lindholmia* P. Hesse, 1919

This genus comprises two recognised species [94], both of which were sampled and analysed. *Lindholmia christophi* (O. Boettger, 1881) is known from a small area in north-western Turkey near Artvin in the vicinity of Borçka and Ardanuç (Figure S22; the samples come from the latter locality). *Lindholmia nordmanni* (Mousson, 1854) has a distribution extending considerably more to the west than is the extent of the sampled sites (Figure S23), up to the west of the Yozgat Province of Turkey.

3.4.8. *Maltzanella* P. Hesse, 1917

In his revision, Schütt [105] recognized two species within this genus: *Maltzanella dickhauti* (Kobelt, 1903) and *Maltzanella maltzani* (Kobelt, 1883). We have found two lineages above the "species" threshold in *M. dickhauti* (Figure S24) from south-western Anatolia, suggesting that there may be additional diversity of mtDNA lineages yet to be uncovered. *Maltzanella maltzani* is known only from a small area near İzmir in western Turkey, but Korábek et al. [23] reported a single *Maltzanella* individual collected in the European part of Turkey in Kuru Dağı which yielded a mtDNA haplotype close to the *M. maltzani* sample (Figure S25). The specimen (SMF 342502) was conchologically more similar to *M. dickhauti*; apparently, the conchological diversity of the genus and its relationship to phylogeny and taxonomy is not yet sufficiently known.

3.4.9. *Helix* Linnaeus, 1758

Helix was the first helicid genus, in which molecular phylogenetics demonstrated the necessity of changes in its taxonomic delimitation [18,106]. Some of those changes were proposed even earlier on the grounds of genital system anatomy [107,108], namely the exclusion of *Cornu aspersum* and *Cantareus apertus* (Born 1778) from *Helix*. Later works included within *Helix* the following two genera: *Tacheopsis* C. R. Boettger, 1909 from north-western Anatolia [11,23] and *Tyrrhenaria* P. Hesse, 1918, endemic to Corsica [20]. The first nearly complete molecular phylogeny of the genus distinguished four major clades and four unassigned species within the genus [23]. Neubert [10] recognized only two subgenera based on morphology of the genital system, *Helix* and *Pelasga* P. Hesse, 1908, but whether *Helix* is monophyletic in respect to *Pelasga* remains still unclear due to unresolved relationships between major groups within the genus.

We resolve here the last remaining issue regarding what taxa should be included in *Helix*. Neubert [10] proposed to transfer *Helix godetiana* Kobelt, 1878 from islands in the southern Aegean (Figure S26) to *Maltzanella*. There are substantial conchological similarities between those taxa and only a very short fragment of 16S was available at the time, which did not refute that hypothesis [23]. We were now able to obtain the complete 16S and *cox1* fragments from a dry museum specimen collected in the late 19th century (a syntype of *Helix dacoronae* Letourneux, 1884). The results (Figure 3 and Figures S1 and S3) show *H. godetiana* with full support as a member of *Helix*. Its precise position is unresolved, but the results suggest it could be either the basal-most *Helix* species or a sister clade to the subgenus *Pelasga*. Further analysis of this rare species is warranted.

Subgenus *Pelasga* P. Hesse, 1908

Species of the subgenus *Pelasga* are distributed from Greece and North Macedonia along the Mediterranean coast to Israel and Jordan, with one species extending eastwards to Iran. The diagnostic character of the group is the epiphallus, at least twice as long as the penis. The shells are, except for some large forms from the Levant, also very similar between species and their shape and sculpture is characteristic for the subgenus. Neubert [10] recognized six species, but this will probably need a future revision.

Of all major *Helix* clades, *Pelasga* remains the least sampled because the snails are buried in the soil when inactive, so live individuals can usually be found only for a limited part of the year [109] and/or shortly after rain. Therefore, even the type species of the subgenus, *Helix figulina* Rossmässler, 1839, is not well represented in our dataset (Figure S27), although it is very abundant in a large part of Greece. Similarly, *Helix salomonica* Naegele, 1899, a species with the eastern-most distribution, has a vast range in south-eastern Turkey (westwards at least to Adıyaman Province), western Iran and the Iraqi Kurdistan, but samples were available from only three localities (Figure S28).

Helix kazouiniana (Pallary, 1939) was recovered monophyletic, but with two divergent lineages (Figure S29). Even more divergent lineages were found within *Helix engaddensis* Bourguignat, 1852 (Figure S30), although samples from only two localities just 36 km apart were analysed. *Helix engaddensis* is a common species in much of Israel and Palestine and western Jordan. Heller [110] distinguished an undescribed form from high elevations at Mount Hermon as a probable separate species (but see [10]) and the darkly coloured forms from east and south of Lake Kinneret as a subspecies *Helix engaddensis prasinata* Roth, 1855. A similar dark form has been found at the ruins of the crusaders' castle Krak des Chevaliers in the Homs Governorate in Syria. All these potentially distinct forms are yet to be sampled and assessed phylogenetically.

The remaining two *Pelasga* species recognized by Neubert [10] are characterized by marked spiral sculpture on the shell: *Helix nucula* Mousson, 1854 distributed along the south-western coast of Anatolia, some Aegean islands and Cyprus and *Helix pachya* Bourguignat, 1860 from the Levant. While the former is often small, the latter reaches 5 cm in shell diameter. Surprisingly, the mitochondrial phylogeny showed that these two cannot be separated [23]. There is a clade specific to Cyprus, but samples from the west of Anatolia and Aegean islands on the one hand and from the Levant on the other are intermingled in the tree (Figure S31). The very large form found from Syria to Mt. Hermon in northern Israel (represented in our dataset, however, by just one sampling site in Lebanon) does not seem to be phylogenetically distinct from smaller forms, which are found in the northern Levant, south-western Anatolia and south-eastern Aegean. We therefore conclude that *H. pachya* is a junior synonym of *H. nucula* and we suspect that *H. nucula* is naturally distributed in the Levant, while the distribution in south-western Anatolia and the Aegean may be a result of anthropogenic translocations. Such distribution parallels the cases of *Levantina* [42] and *Helix cincta* with its relatives [41]. However, this remains a speculative hypothesis until further detailed phylogeographic analysis is performed in the Levant.

European Clade

The so-called European clade [23] is a well-supported group of *Helix* species with diversity centre in the western Balkans, comprising eight currently recognized species including the type species of the genus. Relationships between species within the clade remain largely unresolved, but their intraspecific diversity is usually very well sampled. Further detailed sampling may reveal details of contact zones or origin of specific populations. Of the currently recognized species, *Helix lutescens* Rossmässler, 1837, *Helix pomatia* Linnaeus, 1758, *Helix secernenda* Rossmässler, 1847 and *Helix thessalica* O. Boettger, 1886 are well supported by the data as monophyletic groups and are well defined conchologically. The remaining species, all found in the western Balkans, are more complicated and their relationships cannot be fully resolved with mtDNA data only.

Only shallow divergences were detected within *Helix lutescens*, which is the only species of the clade distributed exclusively outside the area of the Balkan glacial refugia (Figure S32). It is the only Carpathian biogeographic element within Helicini and, like in *H. pomatia* or *H. thessalica*, it apparently performed better in the warmer periods of the last glacial cycles [111,112]. Glacial refugia of *H. lutescens* may be expected somewhere in Romania, but the existing data do not provide strong hints of their location.

Helix pomatia has been detailed elsewhere [38] and we only provide denser sampling in some areas, especially northern Italy and Croatia (Figure S33). In *H. secernenda*, our data reveal a

centre of diversity in northern Albania and southern Montenegro, in particular around Prokletije Mts. and Lake Skadar, and a late colonization of Dalmatia (Figure S34). For *H. thessalica*, we provide additional data (mainly from Ukraine) compared to Korábek et al. [40] (Figure S35). Three minor issues remain for this species: the eastward extent of its range is not yet clear, there may be further populations between the southernmost occurrences in Pelion, Greece, and those sampled in Macedonia (see [113]) and the diversity of lineages in a presumed source area for postglacial expansion in the south-western Carpathians [40] needs to be better explored.

A complicated issue is the classification of populations and taxa currently included in *Helix dormitoris* Kobelt, 1898. So far, this name has been used for several similar forms living predominantly in higher altitudes of the western Balkans [10,114–116] and our observations suggest that these may comprise up to four different evolutionary lineages. The typical *H. dormitoris* is a species from eastern Bosnia and Herzegovina, Montenegro and south-western Serbia (type locality in Durmitor, Montenegro), characterized by a mitochondrial lineage without any close relatives and with a shallowly differentiated crown (Figure S36). *Helix dormitoris arnautorum* Knipper, 1939 from high altitudes of Šar Planina and Korab yielded a mitochondrial lineage basal to *Helix straminea* and *Helix vladika* (Figure S37). Samples from Hajla (*Helix dormitoris hajlensis* Knipper, 1939) yielded a lineage sister to a small form of *H. secernenda* from high altitudes of Prokletije (south of Hajla) and is by us provisionally included in *H. secernenda* (yellow in Figure S34). The last form included in the past within *H. dormitoris* comes from an isolated limestone massif Mali i Tomorrit in central Albania. The shells there closely resemble typical *H. dormitoris* or sometimes *H. secernenda*, but the single tissue sample from the massif yielded a *H. schlaeflii* haplotype typical for central Albania. The summit area of the massif, where the shells resemble most the other high-altitude "*dormitoris*" forms, needs to be sampled to resolve the identity of those populations.

Helix straminea Briganti, 1825 and *Helix vladika* Kobelt, 1898 are very closely related (Figure S37) and there are conchologically intermediate populations. *Helix straminea* probably colonized the Apennine Peninsula from the territory of current Albania [36]; the present data reveal Albanian populations with an even closer relationship to the Apennine populations than known before. The area along the borders between Albania, Northern Macedonia and Kosovo should be explored in detail to shed light on the degree of isolation between *H. straminea*, *H. vladika* and *H. dormitoris arnautorum*.

Three mtDNA lineages above the "species" threshold exist in *Helix schlaeflii* Mousson, 1859. Their relationships and the potential monophyly of *H. schlaeflii* in the mtDNA are unresolved. There do not seem to be readily identifiable conchological differences between individuals of these three clades and their distributions overlap (Figure 5). The northern clade is found in central Albania (Figure S38), roughly north and east of Pogradec, Elbasan and Tiranë. A geographically central clade is broadly distributed in southern Albania, but it has been recorded also from Greece (Figure S39). The third, southern clade was found only in north-western Greece (Epirus, Western Macedonia; Figure S40).

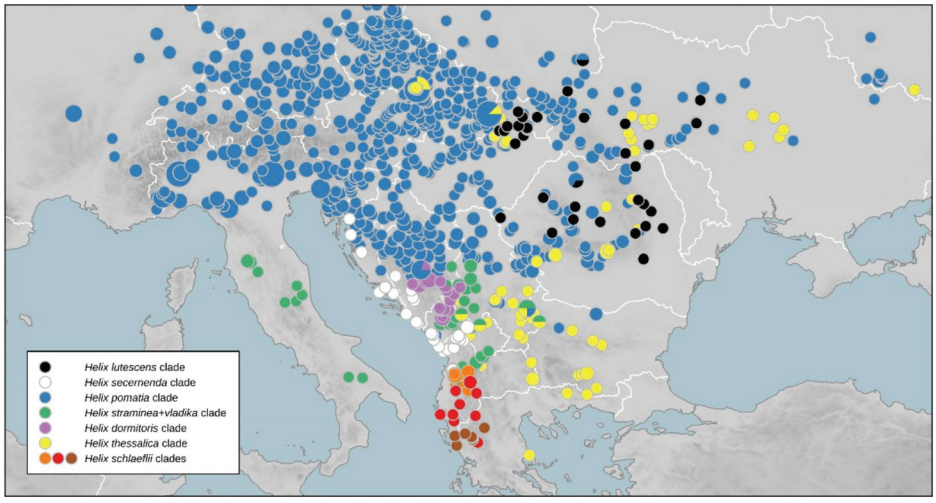

Figure 5. Distribution of "species-level" mitochondrial clades in the European clade of *Helix*. The distribution of the clades largely corresponds to that of accepted morphospecies except for some samples at range contacts where we assume effects of interspecific hybridization and introgression. The relationships between the three clades found in *Helix schlaeflii* are unresolved.

Our new data on the European clade (Table S1) revealed additional cases of discordance between identifications based on shells and the retrieved mitochondrial lineages to those reported earlier [23,37,38]. Haplotypes belonging to a mtDNA lineage typical for *H. pomatia* have been found in individuals identified as *H. thessalica* and *H. vladika* (Figure S33), lineage of *H. vladika* in *H. dormitoris* (Figure S37) and vice versa (Figure S36), lineage of *H. thessalica* in *H. pomatia* (Figure S35), lineage of *H. dormitoris* in *H. pomatia* (Figure S36), lineage of *H. schlaeflii* in *H. straminea* (Figure S38) and lineage of *H. secernenda* in *H. schlaeflii* (Figure S34). Sometimes, morphologically intermediate individuals or populations can be found: we have observed these between *H. pomatia* and *H. thessalica*, *H. pomatia* and *H. dormitoris*, *H. vladika* and *H. dormitoris*, *H. pomatia* and *H. vladika*. Overall, it seems that interspecific hybridization occurs in very localized contact zones (as we observed in the case of *H. pomatia* and *H. thessalica*) because contact of populations of parental species is limited. However, there are areas with populations that are probably of admixed origin as well as possible cases of mitochondrial capture. The discrepancies between shell-based identification and mitochondrial lineages may be a result of contacts between species during range contractions and expansions over the Quaternary glacial cycles [117,118]. This is especially likely in the case of *H. dormitoris dormitoris* (Figure S36), whose lineage is more broadly distributed than the taxon itself. They were found in *H. pomatia* and *H. vladika* at the north-western and southern limits of the range of the *H. dormitoris* mtDNA lineage, respectively. *Helix dormitoris* is probably adapted to higher altitudes than these two species and might have been replaced by them after the LGM, leaving behind the introgressed mitogenomes (and probably additional genomic heritage as well, as some of the *H. pomatia* and *H. vladika* populations in question have atypical conchological characters). Such events likely occurred also earlier in the evolution of this group, so even if fully resolved, the mitochondrial phylogeny may not fully capture the true relationships between the species.

The European clade of *Helix* is, besides *Codringtonia*, the only group where the currently accepted species are distributed in a pattern with a substantial element of parapatric replacement; in other groups the ranges do not adjoin, they overlap more, or the parapatry is limited to two or a few lineages. This is also reflected in the distribution of the "species-level" mitochondrial clades (Figure 5), although their distribution does not fully correspond to that of morphospecies, in particular in the case of the *H. dormitoris dormitoris* clade. The main

exception to the pattern is *H. lutescens*, which is sympatric with *H. pomatia* and *H. thessalica* and is often found in syntopy with these. The frequency of syntopy is not fully apparent from the data because of the difficulty to collect live *H. lutescens* at some of the visited sites. The ranges of *Helix thessalica* and *H. pomatia* overlap mainly in the postglacially colonized areas [38,40] and the two apparently hybridize upon contact [37]. *Helix thessalica* also lives in sympatry and syntopy with *H. vladika*, but we saw no phenotypically intermediate individuals. The ranges of *Helix straminea* and *H. schlaeflii* overlap in Albania, but no syntopic occurrence is known to us.

The limited overlap of most species' distributions can be probably partly explained by differing habitat and climate preferences. In particular, *Helix pomatia* and *H. secernenda* probably do not come into contact in Croatia as they markedly differ in their climatic niche, the latter being adapted to exposed summer-dry rocky Mediterranean habitats (own observations). *Helix schlaeflii* has similar preferences. *Helix thessalica* seems to favour warmer areas than *H. pomatia*, but both prefer relatively humid sites. There are also forms that seem to be adapted to high altitudes, like *H. dormitoris*.

Mediterranean Clade

The Mediterranean clade of *Helix* can be divided into two groups, whose close relationship has only been revealed by molecular phylogenetic analyses: *Helix ceratina* Shuttleworth, 1843 from Corse and the Apennine complex of lineages related to *Helix ligata* O. F. Müller, 1774 on the one hand and species related to *Helix cincta* O. F. Müller, 1774 and *Helix melanostoma* Draparnaud, 1801 on the other hand [41]. The former group is in a need of a formal taxonomic revision, as Fiorentino et al. [20] only suggested available names for the mitochondrial clades they recovered within the *H. ligata* complex and not all clades were assigned a name. The authors could not find phenotypic traits that would distinguish members of the different clades. Phylogeny and biogeography of the latter group has been revised recently [41]. The relationships between species are even less resolved than in the European clade, but in this case also the distribution of mitochondrial lineages is poorly known in some species.

Helix ceratina is an extremely threatened species known only from a single small site near Ajaccio, Corse (Figure S41), which is a remnant of a once broader distribution documented by findings of subfossil shells elsewhere on the island [119].

The earliest split within the Apennine *Helix ligata* complex divides its diversity into a southern and a northern clade (Figure 3). Both are highly diverse. The results suggest marked geographic structuring within the southern clade, but sympatric occurrence of haplotypes from different lineages suggests that this is at least in part due to differences in frequency of individual lineages within populations rather than strict allopatry (Figure S42). Furthermore, the number of sampled populations is too low to reveal the real geographic structure. The distribution of the southern clade overlaps with that of the northern one. Within the latter, lineages overlap in distribution (Figure S43) and we found no apparent geographic structure among them.

Regardless of the systematic status of all mitochondrial lineages, the *Helix ligata* complex likely contains more than one species. Within the northern clade, there is a peculiar morphotype with white rounded shells with narrow bands, which is, at least in part, associated with high altitudes near or above the treeline (Gran Sasso, Monti Reatini, Majella). It used to be identified as *Helix delpretiana* Paulucci, 1878 [120,121] and our samples of this form fall within a clade labelled as *Helix pomatella* Kobelt, 1876 by Fiorentino et al. [20]. In Abruzzo, from where we analysed samples, its range overlaps with the clade considered *H. ligata* s. str. by Fiorentino et al. [20], but they apparently live in different habitats. However, there appear to be populations of intermediate appearance and the corresponding mitochondrial lineage is more broadly distributed, including lower altitudes. We do not know how closely the distribution of this clade is mirrored by the distribution of the conchological varieties. In addition, another isolated mitochondrial lineage has been recorded from high altitude in Monti Marsicani [20]. We hypothesize that these populations from high altitudes represent relics of lineages more

broadly distributed during the Quaternary glacial periods. The spread of *H. ligata* s. str. then might have led to admixed populations in lower altitudes. Of course, genomic-scale data would be needed to test this hypothesis. Type localities of all nominal taxa in the Apennine *Helix* need to be sampled to associate phylogenetic clades with available names.

The distribution of several species of the Mediterranean clade has been affected by introductions to new areas within the Mediterranean basin [41]. All but one sequence of *H. cincta* currently available come from populations outside its native range (Figure S44), which lies probably largely in Syria. In the mitochondrial phylogeny, this species is one of the terminal branches of a "species" level clade from the northern Levant that includes three more recognized species [10]. The two most closely related to *H. cincta* are not sufficiently known: the typical form of *Helix anctostoma* von Martens, 1874 from Belen pass in the Hatay province [10] has not been sampled and the known range of *Helix valentini* Kobelt, 1891 extends to Syria [10], but samples were available only from Turkey. The distribution, monophyly and morphological distinctiveness of these three taxa across their distribution range still need to be established. The combined range of these three overlaps with that of *Helix fathallae* Nägele, 1901, which is paraphyletic to them in the mitochondrial tree. Its most basal lineage comes from an atypical population and fell above our "species" threshold (Figure S45).

Helix borealis Mousson, 1859 is well sampled. The monophyly of the species is uncertain: it consists of three divergent allopatric clades. The nominotypical form lives in western Greece in three parapatric lineages (Figure S46). The other two clades seem to be relictual and their distribution is limited. One is found on northern Evvia and in Northern Sporades (Figure S47), the other in two isolated areas on Crete and in south-western Anatolia (Figure S48).

The two African species, *Helix melanostoma* and *Helix pronuba* Westerlund & Blanc, 1979, are also poorly sampled. For *H. melanostoma* (Figure S49), there is no sequence available from Algeria, which comprises approximately two thirds of its range in the west. The data for *H. pronuba* (Figure S50) are fragmentary, as no fresh or properly preserved samples were analysed. The core of its Holocene broad range may be Cyrenaica, with subfossil shells dated to 17,000–14,000 cal. BP [122].

Anatolian Clade

The Anatolian clade comprises six currently accepted species [23]. All live in Anatolia, although the ranges of two extend also into south-eastern Europe and one lives also in the Caucasus.

Helix asemnis Bourguignat, 1860 is, compared to other *Helix* species, currently broadly delimited in respect to conchological variation and the divergences between its mtDNA lineages [10,23]. It consists of two clades, eastern (Figure S51) and western (Figure S52), whose ranges adjoin along the Ecemiş fault zone in southern Turkey (roughly along the line Pozantı–Mersin; a corresponding divide probably exists also in *Levantina cilicica* (Kobelt, 1895), Figure S11). Both clades are diverse and the individual lineages within both seem distributed in an allopatric manner. There is also a substantial corresponding geographic conchological variation, suggesting that *H. asemnis* may comprise several narrowly distributed species. As in the *H. ligata* complex and *Codringtonia*, finer sampling would be needed to reveal the degree of isolation or distribution overlap between the uncovered lineages. We suggest that the north-eastern and altitudinal range limits of *H. asemnis* should also be better explored.

A species closely related to *H. asemnis* is *Helix escherichi* O. Boettger, 1898 from north-western Anatolia (Figure S53). Its current range is only poorly known and there are no recent samples available from anywhere near its type locality Akşehir in the Konya Province [10]. As regards *Helix pathetica* Mousson, 1854, the species has a very broad distribution range in inner Anatolia, which is probably young, perhaps of only Holocene age, because of the very small differences between haplotypes from across central Anatolia (Figure S54). We hypothesize that more mitochondrial diversity within the species might

be found in the as yet unsampled north-west of its range, because north-western Anatolia appears to be a diversification centre of the Anatolian clade. Anatolian samples are missing altogether for *Helix pomacella* Mousson, 1854 (Figure S55), which lives around the Sea of Marmara and up to Burgas [10] and is so far represented by only one analysed individual from Bulgaria.

The divergence between the mitochondrial clades of *Helix nicaeensis* Férussac, 1821 and *Helix lucorum* Linnaeus, 1758 is in a range observed within some species (Figure S56). However, the two species are morphologically so different that *H. nicaeensis* has even been placed into its own genus *Tacheopsis* prior to molecular phylogenetic analyses [123]. *Helix lucorum* has been recently extending its range through introductions to anthropogenic habitats ([39] and references therein) and data posted online at the iNaturalist website (https://www.inaturalist.org (accessed on 25 December 2021)) suggest a far greater extent of the introductions than covered by peer-reviewed literature, for example in Central Asia. The present data on the distribution of its intraspecific lineages are nevertheless insufficient for identifying the geographic origins of the lineages involved in the expansion. Published figures and photos posted on iNaturalist show that most of the newly emerging non-native populations are of a morphotype distributed from Europe along the southern Black Sea coast up to the western Caucasus and associated with a specific mitochondrial lineage [39]. The natural distribution limits of this lineage Europe and western Caucasus are disputed [39,124], leaving northern Anatolia as its possible cradle.

Species Unassigned to Clades

Four *Helix* species cannot be assigned to any of the above four major mitochondrial clades. *Helix buchii* Dubois de Montpéreux, 1840 lives in north-eastern Turkey, in Georgia and in part of Armenia [10]. Like in *H. nucula*, there are remarkable differences in shell shape and size between populations (3–6 cm in diameter [10]): individuals from some of those located westerly are very small (e.g., from Espiye) while other populations more to the east make the species the largest helicid. Two divergent, unrelated lineages have been recovered from *H. buchii*. One lineage, belonging to the Anatolian clade but distinct from other species, was recovered from a single individual collected near the Sümela monastery in the Trabzon Province of Turkey (Figure S57). All other *H. buchii* individuals analysed so far yielded an unrelated lineage outside the Anatolian clade, but given that the deviating individual shared the shell characteristics typical for *H. buchii* in the same region, we consider unlikely that the sample represents a distinct species. This case may represent a "ghost" mitochondrial lineage from a past introgression, the source of which is either extinct or yet to be uncovered. The data from the remaining samples point to a decrease in diversity from west to east (Figure S58) with an overlapping distribution of mitochondrial lineages, but remain too scarce for a reliable description of the phylogeographic pattern.

Helix pelagonesica (Rolle, 1898) has a small range extending from Thessaly and Macedonia, Greece, to south-east North Macedonia. The available data indicate substantial mtDNA diversity but are insufficient for description of potential geographic structure within its small range (Figure S59). However, an isolated locality lying outside the known range is reported here from Morfovouni near Karditsa in Central Greece, which yielded a lineage basal to the other *H. pelagonesica* samples.

The current range of *Helix philibinensis* Rossmässler, 1939, stretching from Lake Prespa in the west to Asenovgrad near Plovdiv in Bulgaria is apparently young, as samples from all the range extremes yielded identical or very similar haplotypes (Figure S60). Interestingly, its distribution appears to be in large part patchy, which cannot be explained by patchiness of suitable habitats. We have found *H. philibinensis* on different bedrock from limestone to granite and although it prefers warm open habitats, we found it also in shaded places under tree cover.

Helix albescens Rossmässler, 1839 has a large range stretching from Azerbaijan to Ukraine (Mykolaiv, Odessa), but sequence data from autochthonous populations are available only from the Caucasus and Crimea (Figure S61). The single presented sample from

Bulgaria (an individual from a site without GPS coordinates near Ivaylovgrad [10,23]) is problematic. *Helix albescens* is not known anywhere else in Bulgaria (I. Dedov, pers. comm.) or from Romania [125]. Neubert [10] lists additional Bulgarian localities, but we did not find *H. albescens* at any of these and, upon inspection of the original material, we conclude that these records are based on misidentified material. We did not find the species in the immediate vicinity of Ivaylovgrad (instead, *H. figulina* was present), but the sampling site probably lies farther from the town by the Ivyalovgrad Reservoir (Table S1).

3.5. Distribution of Intraspecific Diversity

Even though insufficient data are available for many species at the moment, several observations can already be made regarding the intraspecific diversity and its distribution that emerge from the comparison across the tribe (Figure 6).

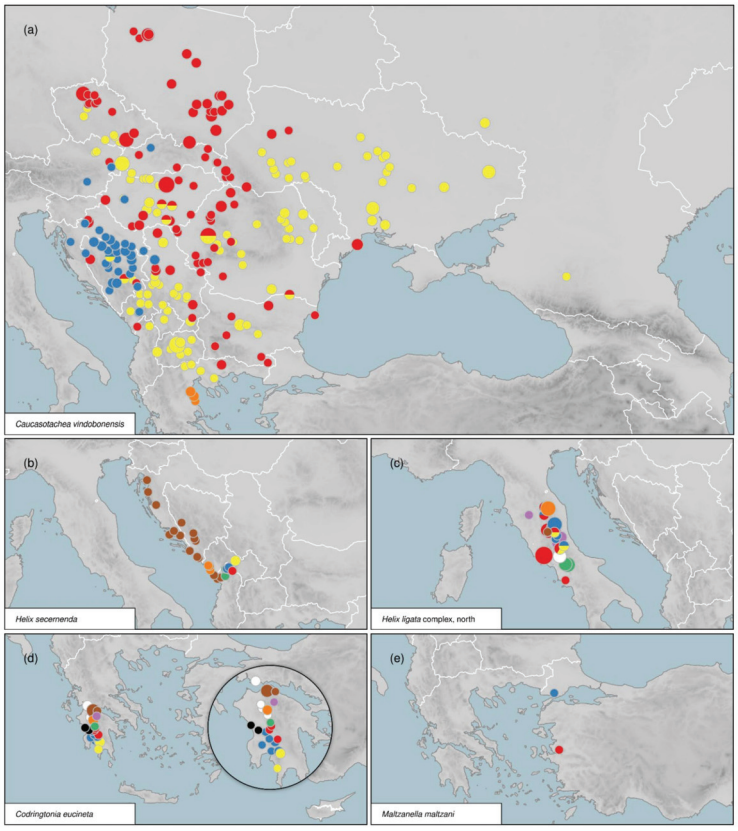

Figure 6. Examples of different patterns in distribution of intraspecific mitochondrial lineages: (**a**) large distribution ranges, a spatially restricted lineage in a southern refugium and marked differences in lineage frequencies between a glacial refugium in Bosnia and Montenegro and other parts of the range in *Caucasotachea vindobonensis*; (**b**) number of spatially restricted lineages, some of them limited to high latitudes, along with a recent expansion of one clade in *Helix secernenda*; (**c**) high number of lineages overlapping in distribution in the northern clade of the *Helix ligata* complex in the Apennine Peninsula; (**d**) similarly high but geographically arranged diversity in *Codringtonia eucineta*; (**e**) two spatially isolated lineages in the clade of *Maltzanella maltzani*, which is known from these two restricted disjunct areas only. For other maps and the underlying phylogenies, see Figures S1–S61.

Clades of similar age vary profoundly in their range size; largest range dimension between small and large ranges may differ by two orders of magnitude. The largest ranges of intraspecific lineages are mostly located in central and eastern Europe and result from postglacial range expansions [38,40]. A specific case is the only broadly distributed intraspecific lineage within *H. lucorum*, the spread of which was apparently greatly facilitated by anthropogenic dispersal even before the documented establishment of many newly founded populations since the late 19th century [39]. This species has been collected and transported for food, but its spread is clearly facilitated also by its broad ecological valence and tolerance for anthropogenic habitats. Similar ecological characteristics helped the expansion of *H. pomatia*. Tolerance to soils with relatively low calcium content might be an advantageous trait for both species. A factor contributing to expansion of *H. thessalica* and *C. vindobonensis* could be also the relative topographic homogeneity and zonal distribution of biomes in eastern Europe in comparison with the geographically complex Balkans.

In contrast to the large ranges of the postglacial colonizers, there are whole species with extremely restricted distributions (*A. praecellens*, *N. neocrassa*, *L. christophi*). *Amanica praecellens* and *N. neocrassa* are particularly isolated old lineages (Figure 3), whose ranges may be relictual. There are also somewhat more broadly distributed taxa with strong intraspecific geographic structure of narrowly distributed mitochondrial lineages (*H. asemnis*, *Codringtonia*). Both situations require long-term environmental stability allowing for differentiation and persistence of the lineages in question and are thus informative about the history of the respective regions. There are several areas with a pattern of allopatric, narrowly distributed lineages (or where this pattern may be suspected based on the current data). One such region is in the Taurus Mts. in Cilicia, southern Turkey, where similar structure is observed in sympatric *H. asemnis* and *L. cilicica*. Additional such areas are found in Europe. These include the Peloponnese (with *Codringtonia*), Albania (*H. schlaeflii*, *H. straminea*, *H. secernenda*), southern Apennine Peninsula (*H. ligata* complex) and likely the western edge of the Greater Caucasus (*C. atrolabiata*).

It is not uncommon that two or more divergent intraspecific lineages are distributed sympatrically and even co-occur within local populations. This may happen in postglacially colonized areas thanks to colonization from multiple sources (*H. pomatia*; [38]), but the same pattern may be found also in diversifications centres where the species survived through the glacials. The pattern in *H. pomatia* combines a geographic structure observed in Bosnia and co-occurrence of several lineages in potential refugia in western Romania [38]. Additional possible examples of high diversity in a stable range core are not yet sufficiently sampled (*H. pronuba*, *C. leucoranea*). Geographic structuring means lower local lineage diversity than when the lineages are sympatric, but both patterns may indicate regional environmental stability; the situations differ in the population connectivity across the region. The cases of the finest geographic structure like in *H. asemnis* or *Codringtonia* would require extremely dense sampling to evaluate whether boundaries between the ranges of the intraspecific clades are sharp or rather overlapping. In addition, the sample sizes per sampling site would have to be larger to capture the rare lineages within each sampled population, because what appears to be a strict allopatry may in fact be just differences in lineage frequencies. These characteristics are relevant for answering questions regarding the role of dispersal barriers in the origin and persistence of phylogeographic structures.

An important point to consider is the range of spatial dynamics suggested by the available data. On the one hand, there are species comprising deeply divergent lineages which might have persisted in the same region for millions of years (possible examples: *M. dickhauti*, *H. kazouiniana*, *H. engaddensis*); on the other hand, there are some remarkable postglacial expansions (*H. pomatia*, *H. thessalica*, *C. vindobonensis*) and some relatively old species that have recent crown ages (*C. vindobonensis*, *H. philibinensis*, *H. lutescens*, possibly *H. pathetica*). While the stem ages of these species are around 10 My or more, their crown groups may be more than ten times younger than their stems (depending on the magnitude of time-dependency of the clock rate [126,127]). If not caused by selection, this could be a result of past range contractions, as documented for the glacial cycles in central and Eastern

Europe. For example, fossils attributable to the stem lineage of *C. vindobonensis* occur in deposits of the late Miocene age (most likely Tortonian [128]) near Kavarna in eastern Bulgaria (own observations) and its closest relatives live in the Caucasus and Alborz [24], yet the crown group likely originated in the western Balkans during the second half of the Pleistocene and large parts of the current distribution range of *C. vindobonensis* date to less than 12,000 years [40]. That indicates that most of the biogeographic history of these species captured in mitochondrial genomes has been lost due to extinctions and this hidden past might have involved substantial and repeated changes in range extent and position.

3.6. Outlook

The phylogenetic and phylogeographic studies based on sequences of mitochondrial markers revolutionized the understanding of (not only) land snail diversity and its roots and had a tremendous impact on taxonomy. That holds also for the group detailed here and it is very likely that for some time the mitochondrial data will remain indispensable.

3.6.1. Mitochondrial Data in Helicini Taxonomy

Despite some persisting problems, the potential of the mitochondrial-only data for taxonomy and phylogenetics is now nearly exhausted in Helicini. They enabled great progress in the systematics of Helicini, allowing to sort the many described forms (e.g., [10]) into natural groups. Genera are now reliably delimited, groupings of closely related species revealed, several species redefined and taxa warranting further systematic attention identified. However, the limitations of the mitochondrial data are obvious (see [129] for an illustrative example) and we expect that with detailed studies using genomic-scale data and considering ecology of the snails, the species-level taxonomy would see additional changes.

There are subtle indications that the biological species are in some cases smaller units than recognized by the current taxonomy. While the intraspecific mitochondrial diversity may be substantial and old (e.g., in *Helix pomatia*, *H. thessalica*), there may also be species characterized by young mitochondrial lineages and some of them may have indeed formed recently. In central Italy, there appear to be specialized high-latitude forms which may deserve recognition as distinct species. In the Balkans, the high-latitude populations from Prokletije and Hajla, placed here in *H. secernenda*, probably also have a different set of adaptations than the typical *H. secernenda* from the warm Dalmatian coastland. A particular case presents *H. asemnis*, where the locally distributed intraspecific mitochondrial lineages seem to be associated with specific morphotypes, indicating differentiation far beyond the mitochondrial genomes. Another similar case may be *H. cincta* with its relatives, but the distribution of the conchological forms known as *H. cincta*, *H. valentini* and *H. anctostoma* and their association with a particular lineage needs to be clarified with good sampling from the Hatay region and Syria. Finally, crossing experiments showed reduced fitness of hybrids between populations classified as subspecies of *L. spiriplana* [130], also suggesting an advanced stage of speciation.

3.6.2. Mitochondrial Data in Phylogeography

Further sequencing of selected mitochondrial genes remains the most feasible approach to learn more about the variation in phylogeographic histories and about the distribution of diversification centres and refugia of land snails in the Western Palaearctic. Taxonomic and geographic coverage offered by the mitochondrial data in land snails is not in sight with multilocus data, for reasons that include not only the costs of alternative methods (decreasing but still substantial) and their complexity, but especially the availability of suitable samples. The mitochondrial data accumulated over many years of research thus represent a unique resource, which would be reasonable to improve further by expanding the geographic and taxonomic coverage in understudied regions to fully exploit its potential. Furthermore, taxonomy, to serve its purpose, must maintain its continuity dating back to the second half of the 18th century and new taxonomic research should relate to earlier hypotheses. The data compiled here include material used for ear-

lier morphology-based taxonomic revisions of the genera *Codringtonia*, *Levantina*, *Isaurica* and *Helix* [10,95,96,101], allowing for connecting taxonomic hypotheses with phylogenetic lineages, though only mitochondrial ones. This makes it meaningful to include an analysis of mitochondrial sequences also in parallel to future genomic-scale studies in order to provide the link from the new types of data to the earlier work. We recommend that both most commonly used fragments of mitochondrial genes for 16S and *cox1*, defined by the primer pairs 16Scs1+16Scs2 and LCO1490+HC02198 (Table 1), respectively, are targeted in such cases, with priority given to 16S when only one is used. However, adding additional loci or sequencing of whole mitogenomes would be helpful for some research questions. Despite the wealth of data, well resolved mitochondrial phylogeny is lacking, preventing for example comparison of mitochondrial and nuclear phylogenies and divergence dates. For phylogeography, including faster evolving mitochondrial genes could be helpful as the variability in the relatively slowly evolving 16S and *cox1* limits their use for locating glacial refugia.

The sampling density needed to uncover the regional diversity and its structure widely differs between regions, but for an unbiased view of the distribution of intraspecific diversity, it is vital that species and areas are sampled indiscriminately at least in the beginning, without preference for species with problematic taxonomies or where readily interpretable phylogeographic structure is expected. The data collated here show a broad range of different phylogeographic structures and histories. They suggest several relatively recent range expansions of different extent and uncover several regional diversification centres or refugia. If the sampling focused only on well-established refugia and diversity centres, the full extent of variability in population histories and the dynamic nature of the distribution of many of the species and intraspecific lineages would be obscured. However, very fine sampling is still necessary to characterize the distribution of lineages in the diversity centres, as in the case of *H. asemnis* or the *H. ligata* complex.

Further progress in documenting the diversity of Helicini heavily depends on collecting new samples from the eastern half of the tribe's distribution. That holds in particular for *Isaurica* and *Levantina*, where even some of the currently accepted species are not sampled at all and for all Helicini members in the Levant, eastern Turkey and adjacent regions of Iraq and Iran. It is difficult, or almost impossible, to move forward without a broad participation of local zoologists. Geographically complete sampling is easiest for locals, who may also leverage on their knowledge of the regional biogeography to identify populations worth sampling (e.g., by considering known regional dispersal barriers and diversity hotspots) as well as phenology, distribution of suitable habitats (Figure S62) and other factors when planning the sampling. We are open for cooperation and willing to help anyone interested in the diversity of the Helicini.

Supplementary Materials: The following supporting information can be downloaded at: https://www.mdpi.com/article/10.3390/d14010024/s1, Figures S1–S62: phylogeny, distribution of intraspecific lineages and examples of habitats of Helicini, Tables S1 and S2: list of Helicini and outgroup sequences with metadata, including sampling locality and voucher information and GenBank accession numbers.

Author Contributions: Conceptualization, O.K.; methodology O.K. and A.P.; formal analysis, O.K.; investigation, O.K., L.J. and A.P.; resources, O.K., L.J. and A.P.; data curation, O.K.; writing—original draft preparation, O.K.; writing—review and editing, O.K., L.J. and A.P.; visualization, O.K.; supervision, L.J. and A.P.; funding acquisition, L.J. and A.P. All authors have read and agreed to the published version of the manuscript.

Funding: This research was funded by Charles University, Prague (project SVV 260436 and its predecessors) and Charles University Grant Agency (project no. 615).

Institutional Review Board Statement: Not applicable.

Data Availability Statement: All sequence metadata are provided in Tables S1 and S2. Newly generated sequences were deposited in GenBank (accession numbers listed in Tables S1 and S2). Aligned sequences (with details about the sites of origin) and the complete Helicini phylogeny along with the subtrees used to assemble it are available from the Dryad repository. Available online: doi:10.5061/dryad.pnvx0k6p5.

Acknowledgments: We would like to thank all colleagues who over the years helped to collect or contributed samples for this study. We are thankful for every single sample, but the help of Eike Neubert, Zoltán Fehér, Emanuel Tardy, Ira Richling, František Šťáhlavský, David Král, Tereza Kosová, Petr Dolejš, Petr Šípek and Jasna Vukić was particularly important for this work.

Conflicts of Interest: The authors declare no conflict of interest. The funders had no role in the design of the study; in the collection, analyses, or interpretation of data; in the writing of the manuscript, or in the decision to publish the results.

References

1. Schluter, D.; Pennell, M.W. Speciation gradients and the distribution of biodiversity. *Nature* **2017**, *546*, 48–55. [CrossRef] [PubMed]
2. Miraldo, A.; Li, S.; Borregaard, M.K.; Flórez-Rodríguez, A.; Gopalakrishnan, S.; Rizvanovic, M.; Wang, Z.; Rahbek, C.; Marske, K.A.; Nogués-Bravo, D. An Anthropocene map of genetic diversity. *Science* **2016**, *353*, 1532–1535. [CrossRef] [PubMed]
3. Carstens, B.C.; Morales, A.E.; Field, K.; Pelletier, T.A. A global analysis of bats using automated comparative phylogeography uncovers a surprising impact of Pleistocene glaciation. *J. Biogeogr.* **2018**, *45*, 1795–1805. [CrossRef]
4. Reid, B.N.; Naro-Maciel, E.; Torres Hahn, A.; FitzSimmons, N.N.; Gehara, M. Geography best explains global patterns of genetic diversity and postglacial co-expansion in marine turtles. *Mol. Ecol.* **2019**, *28*, 3358–3370. [CrossRef]
5. Theodoridis, S.; Fordham, D.A.; Brown, S.C.; Li, S.; Rahbek, C.; Nogues-Bravo, D. Evolutionary history and past climate change shape the distribution of genetic diversity in terrestrial mammals. *Nat. Commun.* **2020**, *11*, 2557. [CrossRef]
6. Lawrence, E.R.; Benavente, J.N.; Matte, J.-M.; Marin, K.; Wells, Z.R.R.; Bernos, T.A.; Krasteva, N.; Habrich, A.; Nessel, G.A.; Koumrouyan, R.A.; et al. Geo-referenced population-specific microsatellite data across American continents. The MacroPopGen Database. *Sci. Data* **2019**, *6*, 14. [CrossRef]
7. Manel, S.; Guerin, P.-E.; Mouillot, D.; Blanchet, S.; Velez, L.; Albouy, C.; Pellissier, L. Global determinants of freshwater and marine fish genetic diversity. *Nat. Commun.* **2020**, *11*, 692. [CrossRef]
8. Paz-Vinas, I.; Jensen, E.L.; Bertola, L.D.; Breed, M.F.; Hand, B.K.; Hunter, M.E.; Kershaw, F.; Leigh, D.M.; Luikart, G.; Mergeay, J.; et al. Macrogenetic studies must not ignore limitations of genetic markers and scale. *Ecol. Lett.* **2021**, *24*, 1282–1284. [CrossRef]
9. Gratton, P.; Marta, S.; Bocksberger, G.; Winter, M.; Trucchi, E.; Kühl, H. A world of sequences: Can we use georeferenced nucleotide databases for a robust automated phylogeography? *J. Biogeogr.* **2017**, *44*, 475–486. [CrossRef]
10. Neubert, E. Revision of *Helix* Linnaeus, 1758 in its eastern Mediterranean distribution area, and reassignment of *Helix godetiana* Kobelt, 1878 to *Maltzanella* Hesse, 1917 (Gastropoda, Pulmonata, Helicidae). *Contrib. Nat. Hist.* **2014**, *26*, 1–200.
11. Neiber, M.T.; Hausdorf, B. Molecular phylogeny reveals the polyphyly of the snail genus *Cepaea* (Gastropoda: Helicidae). *Mol. Phylogenet. Evol.* **2015**, *93*, 143–149. [CrossRef]
12. Hausdorf, B.; Bamberger, S.; Walther, F. A Sicilian-Cretan biogeographical disjunction in the land snail group *Cornu* (Gastropoda: Helicidae). *Zool. J. Linn. Soc.* **2021**, *192*, 59–74. [CrossRef]
13. Chueca, L.J.; Madeira, M.J.; Gómez-Moliner, B.J. Biogeography of the land snail genus *Allognathus* (Helicidae): Middle Miocene colonization of the Balearic Islands. *J. Biogeogr.* **2015**, *42*, 1845–1857. [CrossRef]
14. Neiber, M.T.; Chueca, L.J.; Caro, A.; Teixeira, D.; Schlegel, K.A.; Gómez-Moliner, B.J.; Walther, F.; Glaubrecht, M.; Hausdorf, B. Incorporating palaeogeography into ancestral area estimation can explain the disjunct distribution of land snails in Macaronesia and the Balearic Islands (Helicidae: Allognathini). *Mol. Phylogenet. Evol.* **2021**, *162*, 107196. [CrossRef]
15. Harzhauser, M.; Neubauer, T.A. A review of the land snail faunas of the European Cenozoic—Composition, diversity and turnovers. *Earth-Sci. Rev.* **2021**, *217*, 103610. [CrossRef]
16. Guiller, A.; Coutellec-Vreto, M.A.; Madec, L.; Deunff, J. Evolutionary history of the land snail *Helix aspersa* in the Western Mediterranean: Preliminary results inferred from mitochondrial DNA sequences. *Mol. Ecol.* **2001**, *10*, 81–87. [CrossRef]
17. Abdulmawjood, A.; Bülte, M. Snail species identification by RFLP-PCR and designing of species-specific oligonucleotide primers. *J. Food Sci.* **2001**, *66*, 1287–1293. [CrossRef]
18. Manganelli, G.; Salomone, N.; Giusti, F. A molecular approach to the phylogenetic relationships of the western palaearctic Helicoidea (Gastropoda: Stylommatophora). *Biol. J. Linn. Soc.* **2005**, *85*, 501–512. [CrossRef]
19. Ketmaier, K.; Fiorentino, V.; Tiedemann, R.; Manganelli, G.; Giusti, F. Morphological and molecular characterization of the Roman snail *Helix pomatia* with data on the phylogeny of the genus *Helix* (Pulmonata, Helicidae). In Proceedings of the World Congress of Malacology, Antwerp, Belgium, 15–20 July 2007.
20. Fiorentino, V.; Manganelli, G.; Giusti, F.; Ketmaier, V. Recent expansion and relic survival: Phylogeography of the land snail genus *Helix* (Mollusca, Gastropoda) from south to north Europe. *Mol. Phylogenet. Evol.* **2016**, *98*, 358–372. [CrossRef]

21. Kotsakiozi, P.; Parmakelis, A.; Giokas, S.; Papanikolaou, I.; Valakos, E.D. Mitochondrial phylogeny and biogeographic history of the Greek endemic land-snail genus *Codringtonia* Kobelt 1898 (Gastropoda, Pulmonata, Helicidae). *Mol. Phylogenet. Evol.* **2012**, *62*, 681–692. [CrossRef]
22. Razkin, O.; Gómez-Moliner, B.J.; Prieto, C.E.; Martínez-Ortí, A.; Arrébola, J.R.; Muñoz, B.; Chueca, L.J.; Madeira, M.J. Molecular phylogeny of the western Palaearctic Helicoidea (Gastropoda, Stylommatophora). *Mol. Phylogenet. Evol.* **2015**, *83*, 99–117. [CrossRef]
23. Korábek, O.; Petrusek, A.; Neubert, E.; Juřičková, L. Molecular phylogeny of the genus *Helix* (Pulmonata: Helicidae). *Zool. Scr.* **2015**, *44*, 263–280. [CrossRef]
24. Neiber, M.T.; Sagorny, C.; Hausdorf, B. Increasing the number of molecular markers resolves the phylogenetic relationship of '*Cepaea*' *vindobonensis* (Pfeiffer 1828) with *Caucasotachea* Boettger 1909 (Gastropoda: Pulmonata: Helicidae). *J. Zool. Syst. Evol. Res.* **2016**, *54*, 40–45. [CrossRef]
25. Korábek, O.; Petrusek, A.; Rovatsos, M. Mitogenome of *Helix pomatia* and the basal phylogeny of Helicinae (Gastropoda, Stylommatophora, Helicidae). *ZooKeys* **2019**, *827*, 19–30. [CrossRef]
26. Groenenberg, D.S.J.; Duijm, E. The complete mitogenome of the Roman snail *Helix pomatia* Linnaeus 1758 (Stylommatophora: Helicidae). *Mitochondrial DNA Part B* **2019**, *4*, 1494–1495. [CrossRef]
27. Neiber, M.T.; Korábek, O.; Glaubrecht, M.; Hausdorf, B. A misinterpreted disjunction: The phylogenetic relationships of the Libyan land snail *Gyrostomella* (Gastropoda: Stylommatophora: Helicidae). *Zool. J. Linn. Soc.* **2021**, in press. [CrossRef]
28. Groenenberg, D.S.J.; Subai, P.; Gittenberger, E. Systematics of Ariantinae (Gastropoda, Pulmonata, Helicidae), a new approach to an old problem. *Contrib. Zool.* **2016**, *85*, 37–65. [CrossRef]
29. Bouaziz-Yahiatene, H.; Inäbnit, T.; Medjdoub-Bensaad, F.; Colomba, M.S.; Sparacio, I.; Gregorini, A.; Liberto, F.; Neubert, E. Revisited—the species of Tweeting vineyard snails, genus *Cantareus* Risso, 1826 (Stylommatophora, Helicidae, Helicinae, Otalini). *ZooKeys* **2019**, *876*, 1–26. [CrossRef]
30. Bober, S.; Glaubrecht, M.; Hausdorf, B.; Neiber, M.T. One, two or three? Integrative species delimitation of short-range endemic *Hemicycla* species (Gastropoda: Helicidae) from the Canary Islands based on morphology, barcoding, AFLP and ddRADseq data. *Mol. Phylogenet. Evol.* **2021**, *161*, 107153. [CrossRef]
31. Saenko, S.V.; Groenenberg, D.S.J.; Davison, A.; Schilthuizen, M. The draft genome sequence of the grove snail *Cepaea nemoralis*. *G3 Genes Genomes Genet.* **2021**, *11*, jkaa071. [CrossRef]
32. Gittenberger, E.; Piel, W.H.; Groenenberg, D.S.J. The Pleistocene glaciations and the evolutionary history of the polytypic snail species *Arianta arbustorum* (Gastropoda, Pulmonata, Helicidae). *Mol. Phylogenet. Evol.* **2004**, *30*, 64–73. [CrossRef]
33. Mumladze, L.; Tarkhnishvili, D.; Murtskhvaladze, M. Systematics and evolutionary history of large endemic snails from the Caucasus (*Helix buchii* and *H. goderdziana*) (Helicidae). *Am. Malacol. Bull.* **2013**, *31*, 225–234. [CrossRef]
34. Parmakelis, A.; Kotsakiozi, P.; Rand, D. Animal mitochondria, positive selection and cyto-nuclear coevolution: Insights from Pulmonates. *PLoS ONE* **2013**, *8*, e61970. [CrossRef]
35. Cadahía, L.; Harl, J.; Duda, M.; Sattmann, H.; Kruckenhauser, L.; Fehér, Z.; Zopp, L.; Haring, E. New data on the phylogeny of Ariantinae (Pulmonata, Helicidae) and the systematic position of *Cylindrus obtusus* based on nuclear and mitochondrial DNA marker sequences. *J. Zool. Syst. Evol. Res.* **2014**, *52*, 163–169. [CrossRef]
36. Korábek, O.; Juřičková, L.; Petrusek, A. Resurrecting *Helix straminea*, a forgotten escargot with trans-Adriatic distribution: First insights into the genetic variation within the genus *Helix* (Gastropoda: Pulmonata). *Zool. J. Linn. Soc.* **2014**, *171*, 72–91. [CrossRef]
37. Korábek, O.; Juřičková, L.; Petrusek, A. Splitting the Roman snail *Helix pomatia* Linnaeus, 1758 (Stylommatophora: Helicidae) into two: Redescription of the forgotten *Helix thessalica* Boettger, 1886. *J. Molluscan Stud.* **2016**, *82*, 11–22. [CrossRef]
38. Korábek, O.; Petrusek, A.; Juřičková, L. Glacial refugia and postglacial spread of an iconic large European land snail, *Helix pomatia* (Pulmonata: Helicidae). *Biol. J. Linn. Soc.* **2018**, *123*, 218–234. [CrossRef]
39. Korábek, O.; Juřičková, L.; Balashov, I.; Petrusek, A. The contribution of ancient and modern anthropogenic introductions to the colonization of Europe by the land snail *Helix lucorum* Linnaeus, 1758 (Helicidae). *Contrib. Zool.* **2018**, *87*, 61–74. [CrossRef]
40. Korábek, O.; Juřičková, L.; Petrusek, A. Inferring the sources of postglacial range expansion in two large European land snails. *J. Zool. Syst. Evol. Res.* **2020**, *58*, 944–956. [CrossRef]
41. Korábek, O.; Kosová, T.; Dolejš, P.; Petrusek, A.; Neubert, E.; Juřičková, L. Geographic isolation and human-assisted dispersal in land snails: A Mediterranean story of *Helix borealis* and its relatives (Gastropoda: Stylommatophora: Helicidae). *Zool. J. Linn. Soc.* **2021**, *193*, 1310–1335. [CrossRef]
42. Korábek, O.; Glaubrecht, M.; Hausdorf, B.; Neiber, M.T. Phylogeny of the land snail *Levantina* reveals long-distance dispersal in the Middle East. *Zool. Scr.*. in review.
43. Dahirel, M.; Olivier, E.; Guiller, A.; Martin, M.-C.; Madec, L.; Ansart, A. Movement propensity and ability correlate with ecological specialization in European land snails: Comparative analysis of a dispersal syndrome. *J. Anim. Ecol.* **2015**, *84*, 228–238. [CrossRef]
44. Giusti, F.; Fiorentino, V.; Manganelli, G. A neotype for *Helix cincta* Müller, 1774 (Gastropoda, Pulmonata, Helicidae). *J. Conchol.* **2015**, *42*, 209–212.
45. Psonis, N.; Vardinoyannis, K.; Mylonas, M.; Poulakakis, N. Evaluation of the taxonomy of *Helix cincta* (Muller, 1774) and *Helix nucula* (Mousson, 1854); insights using mitochondrial DNA sequence data. *J. Nat. Hist.* **2015**, *49*, 383–392. [CrossRef]
46. Jaksch, K.; Eschner, A.; von Rintelen, T.; Haring, E. DNA analysis of molluscs from a museum wet collection: A comparison of different extraction methods. *BMC Res. Notes* **2016**, *9*, 348. [CrossRef]

47. Neiber, M.T.; Sagorny, C.; Sauer, J.; Walther, F.; Hausdorf, B. Phylogeographic analyses reveal Transpontic long distance dispersal in land snails belonging to the *Caucasotachea atrolabiata* complex (Gastropoda: Helicidae). *Mol. Phylogenet. Evol.* **2016**, *103*, 172–183. [CrossRef]
48. Schmera, D.; Pizá, J.; Reinartz, E.; Ursenbacher, S.; Baur, B. Breeding system, shell size and age at sexual maturity affect sperm length in stylommatophoran gastropods. *BMC Evol. Biol.* **2016**, *16*, 89. [CrossRef]
49. Bouaziz-Yahiatene, H.; Pfarrer, B.; Medjdoub-Bensaad, F.; Neubert, E. Revision of *Massylaea* Möllendorff, 1898 (Stylommatophora, Helicidae). *ZooKeys* **2017**, *694*, 109–133. [CrossRef]
50. Cesaroni, D.; De Felici, S.; Riccarducci, G.; Ciambotta, M.; Ventura, A.; Bianchi, E.; Sbordoni, V. DNA Barcodes of the animal species occurring in Italy under the European "Habitats Directive" (92/43/EEC): A reference library for the Italian National Biodiversity Network. *Biogeogr. J. Integr. Biogeogr.* **2017**, *32*, 5–23. [CrossRef]
51. Kajtoch, Ł.; Davison, A.; Grindon, A.; Deli, T.; Sramkó, G.; Gwardjan, M.; Kramarenko, S.; Mierzwa-Szymkowiak, D.; Ruta, R.; Tóth, J.P.; et al. Reconstructed historical distribution and phylogeography unravels non-steppic origin of *Caucasotachea vindobonensis* (Gastropoda: Helicidae). *Org. Divers. Evol.* **2017**, *17*, 679–692. [CrossRef]
52. Sei, M.; Robinson, D.G.; Geneva, A.J.; Rosenberg, G. Doubled helix: Sagdoidea is the overlooked sister group of Helicoidea (Mollusca: Gastropoda: Pulmonata). *Biol. J. Linn. Soc.* **2017**, *122*, 697–728. [CrossRef]
53. Dimzas, D.; Morelli, S.; Traversa, D.; Di Cesare, A.; Van Bourgonie, Y.R.; Breugelmans, K.; Backeljau, T.; Frangipane di Regalbono, A.; Diakou, A. Intermediate gastropod hosts of major feline cardiopulmonary nematodes in an area of wildcat and domestic cat sympatry in Greece. *Parasites Vectors* **2020**, *13*, 345. [CrossRef]
54. Petraccioli, A.; Niero, A.; Carandente, F.; Crovato, P.; de Vico, G.; Odierna, G.; Picariello, O.L.A.; Tardy, E.; Viglietti, S.; Guarino, F.M.; et al. *Helix straminea* Briganti, 1825 in Italy (Gastropoda: Pulmonata): Taxonomic history, morphology, biology, distribution and phylogeny. *Eur. Zool. J.* **2021**, *88*, 390–416. [CrossRef]
55. Folmer, O.; Black, M.; Hoeh, W.; Lutz, R.; Vrijenhoek, R. DNA primers for amplification of mitochondrial cytochrome c oxidase subunit I from diverse metazoan invertebrates. *Mol. Mar. Biol. Biotechnol.* **1994**, *3*, 294–299.
56. Chiba, S. Accelerated evolution of land snails *Mandarina* in the oceanic Bonin Islands: Evidence from mitochondrial DNA sequences. *Evolution* **1999**, *53*, 460–471. [CrossRef]
57. Neiber, M.T.; Razkin, O.; Hausdorf, B. Molecular phylogeny and biogeography of the land snail family Hygromiidae (Gastropoda: Helicoidea). *Mol. Phylogenet. Evol.* **2017**, *111*, 169–184. [CrossRef]
58. Misof, B.; Erpenbeck, D.; Sauer, K.P. Mitochondrial gene fragments suggest paraphyly of the genus *Panorpa* (Mecoptera, Panorpidae). *Mol. Phylogenet. Evol.* **2000**, *17*, 76–84. [CrossRef]
59. Hugall, A.; Moritz, C.; Moussalli, A.; Stanisic, J. Reconciling paleodistribution models and comparative phylogeography in the Wet Tropics rainforest land snail *Gnarosophia bellendenkerensis* (Brazier 1875). *Proc. Natl. Acad. Sci. USA* **2002**, *99*, 6112–6117. [CrossRef]
60. Hausdorf, B.; Röpstorf, P.; Riedel, F. Relationships and origin of endemic Lake Baikal gastropods (Caenogastropoda: Rissooidea) based on mitochondrial DNA sequences. *Mol. Phylogenet. Evol.* **2003**, *26*, 435–443. [CrossRef]
61. Merritt, T.J.S.; Shi, L.; Chase, M.C.; Rex, M.A.; Etter, R.J.; Quattro, J.M. Universal cytochrome b primers facilitate intraspecific studies in molluscan taxa. *Mol. Mar. Biol. Biotechnol.* **1998**, *7*, 7–11.
62. Palumbi, S.; Martin, A.; Romano, S.; McMillan, W.O.; Stice, L.; Grabowski, G. *The Simple Fool's Guide to PCR, Version 2*; Department of Zoology, University of Hawaii: Honolulu, HI, USA, 1991.
63. Song, H.; Buhay, J.E.; Whiting, M.F.; Crandall, K.A. Many species in one: DNA barcoding overestimates the number of species when nuclear mitochondrial pseudogenes are coamplified. *Proc. Natl. Acad. Sci. USA* **2008**, *105*, 13486–13491. [CrossRef] [PubMed]
64. Grindon, A.J.; Davison, A. Irish *Cepaea nemoralis* land snails have a cryptic Franco-Iberian origin that is most easily explained by the movements of mesolithic humans. *PLoS ONE* **2013**, *8*, e65792. [CrossRef] [PubMed]
65. Holyoak, D.T.; Holyoak, G.A.; Gómez-Moliner, B.J.; Chueca, L.J. Phylogeny, species-limits and taxonomic revision of Otalini (Helicidae) from north-west Africa. *J. Conchol.* **2020**, *43*, 551–611.
66. Elejalde, M.A.; Muñoz, B.; Arrébola, J.R.; Gómez-Moliner, B.J. Phylogenetic relationships of *Iberus gualtieranus* and *I. alonensis* (Gastropoda: Helicidae) based on partial mitochondrial 16S rRNA and COI gene sequences. *J. Molluscan Stud.* **2005**, *71*, 349–355. [CrossRef]
67. Elejalde, M.A.; Madeira, M.J.; Arrébola, J.R.; Muñoz, B.; Gómez-Moliner, B.J. Molecular phylogeny, taxonomy and evolution of the land snail genus *Iberus* (Pulmonata: Helicidae). *J. Zool. Syst. Evol. Res.* **2008**, *46*, 193–202. [CrossRef]
68. Greve, C.; Hutterer, R.; Groh, K.; Haase, M.; Misof, B. Evolutionary diversification of the genus *Theba* (Gastropoda: Helicidae) in space and time: A land snail conquering islands and continents. *Mol. Phylogenet. Evol.* **2010**, *57*, 572–584. [CrossRef] [PubMed]
69. Greve, C.; Gimnich, F.; Hutterer, R.; Misof, B.; Haase, M. Radiating on oceanic islands: Patterns and processes of speciation in the land snail genus *Theba* (Risso 1826). *PLoS ONE* **2012**, *7*, e34339. [CrossRef]
70. Greve, C.; Haase, M.; Hutterer, R.; Rödder, D.; Ihlow, F.; Misof, B. Snails in the desert: Species diversification of *Theba* (Gastropoda: Helicidae) along the Atlantic coast of NW Africa. *Ecol. Evol.* **2017**, *7*, 5524–5538. [CrossRef]
71. Neiber, M.T.; Vega-Luz, R.; Vega-Luz, R.; Koenemann, S. *Hemicycla* (*Adiverticula*) *diegoi* (Gastropoda: Pulmonata: Helicidae), a new species from Tenerife, Canary Islands, with a phylogenetic analysis of conchologically similar species in the genus *Hemicycla* Swainson, 1840. *Zootaxa* **2011**, *2757*, 29–46. [CrossRef]

72. Guiller, A.; Martin, M.-C.; Hiraux, C.; Madec, L. Tracing the invasion of the mediterranean land snail *Cornu aspersum aspersum* becoming an agricultural and garden pest in areas recently introduced. *PLoS ONE* **2012**, *7*, e49674. [CrossRef]
73. Gaitán-Espitia, J.D.; Nespolo, R.F.; Opazo, J. C The complete mitochondrial genome of the land snail *Cornu aspersum* (Helicidae: Mollusca): Intra-specific divergence of protein-coding genes and phylogenetic considerations within Euthyneura. *PLoS ONE* **2013**, *8*, e67299. [CrossRef]
74. Martínez-Ortí, A.; Robles, F. El viaje del Prof. Emil, A. Rossmässler en 1853 por España y la localidad tipo de *Iberus angustatus* (Rossmässler, 1854) (Gastropoda, Helicidae). *Anim. Biodivers. Conserv.* **2013**, *36*, 187–194. [CrossRef]
75. Haase, M.; Greve, C.; Hutterer, R.; Misof, M. Amplified fragment length polymorphisms, the evolution of the land snail genus *Theba* (Stylommatophora: Helicidae), and an objective approach for relating fossils to internal nodes of a phylogenetic tree using geometric morphometrics. *Zool. J. Linn. Soc.* **2014**, *171*, 92–107. [CrossRef]
76. Colomba, M.S.; Gregorini, A.; Liberto, F.; Reitano, A.; Giglio, S.; Sparacio, I. The genus *Erctella* Monterosato, 1894: New molecular evidence (Pulmonata Stylommatophora Helicidae). *Biodivers. J.* **2015**, *6*, 401–411.
77. Ali, R.F.; Neiber, M.T.; Walther, F.; Hausdorf, B. Morphological and genetic differentiation of *Eremina desertorum* (Gastropoda, Pulmonata, Helicidae) in Egypt. *Zool. Scr.* **2016**, *45*, 48–61. [CrossRef]
78. Böckers, A.; Greve, C.; Hutterer, R.; Misof, B.; Haase, M. Testing heterogeneous base composition as potential cause for conflicting phylogenetic signal between mitochondrial and nuclear DNA in the land snail genus *Theba* Risso 1826 (Gastropoda: Stylommatophora: Helicoidea). *Org. Divers. Evol.* **2016**, *16*, 825–846. [CrossRef]
79. Walther, F.; Neiber, M.T.; Hausdorf, B. Species complex or complex species? Integrative taxonomy of the land snail genus *Rossmaessleria* (Gastropoda, Helicidae) from Morocco and Gibraltar. *Syst. Biodivers.* **2016**, *14*, 394–416. [CrossRef]
80. Neiber, M.T. On the status of *Rossmaessleria scherzeri scherzeri* (Zelebor in Pfeiffer & Zelebor, 1867) (Gastropoda: Pulmonata: Helicidae). *Zootaxa* **2017**, *4286*, 116–120. [CrossRef]
81. Holyoak, D.T.; Holyoak, G.A.; Chueca, L.J.; Gómez-Moliner, B.J. Evolution and taxonomy of the populations of *Eremina* (Gastropoda, Pulmonata, Helicidae) in Morocco. *J. Conchol.* **2018**, *43*, 17–57.
82. Kneubühler, J.; Hutterer, R.; Pfarrer, B.; Neubert, E. Anatomical and phylogenetic investigation of the genera *Alabastrina* Kobelt, 1904, *Siretia* Pallary, 1926, and *Otala* Schumacher, 1817 (Stylommatophora, Helicidae). *ZooKeys* **2019**, *843*, 1–37. [CrossRef]
83. Katoh, K.; Standley, D.M. MAFFT Multiple Sequence Alignment Software Version 7: Improvements in Performance and Usability. *Mol. Biol. Evol.* **2013**, *30*, 772–780. [CrossRef]
84. Edgar, R.C. MUSCLE: Multiple sequence alignment with high accuracy and high throughput. *Nucleic Acids Res.* **2004**, *32*, 1792–1797. [CrossRef]
85. Kumar, S.; Stecher, G.; Tamura, K. Molecular Evolutionary Genetics Analysis Version 7.0 for bigger datasets. *Mol. Biol. Evol.* **2016**, *33*, 1870–1874. [CrossRef]
86. Nguyen, L.-T.; Schmidt, H.A.; von Haeseler, A.; Minh, B.Q. IQ-TREE: A fast and effective stochastic algorithm for estimating maximum likelihood phylogenies. *Mol. Biol. Evol.* **2015**, *32*, 268–274. [CrossRef]
87. Kalyaanamoorthy, S.; Minh, B.Q.; Wong, T.K.F.; von Haeseler, A.; Jermiin, L.S. ModelFinder: Fast model selection for accurate phylogenetic estimates. *Nat. Methods* **2017**, *14*, 587–589. [CrossRef]
88. Guindon, S.; Dufayard, J.-F.; Lefort, V.; Anisimova, M.; Hordjik, W.; Gascuel, O. New algorithms and methods to estimate maximum-likelihood phylogenies: Assessing the performance of PhyML 3.0. *Syst. Biol.* **2010**, *59*, 307–321. [CrossRef]
89. Smirnov, V.; Warnow, T. Phylogeny estimation given sequence length heterogeneity. *Syst. Biol.* **2021**, *70*, 268–282. [CrossRef]
90. Upham, N.S.; Esselstyn, J.A.; Jetz, W. Inferring the mammal tree: Species-level sets of phylogenies for questions in ecology, evolution, and conservation. *PLoS Biol.* **2019**, *17*, e3000494. [CrossRef]
91. Bouckaert, R.; Vaughan, T.G.; Barido-Sottani, J.; Duchêne, S.; Fourment, M.; Gavryushkina, A.; Heled, J.; Jones, G.; Kühnert, D.; De Maio, N.; et al. BEAST 2.5: An advanced software platform for Bayesian evolutionary analysis. *PLoS Comput. Biol.* **2019**, *15*, e1006650. [CrossRef]
92. Ritchie, A.M.; Lo, N.; Ho, S.Y.W. The impact of the tree prior on molecular dating of data sets containing a mixture of inter- and intraspecies sampling. *Syst. Biol.* **2017**, *66*, 413–425. [CrossRef]
93. Groenenberg, D.S.J.; Pirovano, W.; Gittenberger, E.; Schilthuizen, M. The complete mitogenome of *Cylindrus obtusus* (Helicidae, Ariantinae) using Illumina next generation sequencing. *BMC Genom.* **2012**, *13*, 114. [CrossRef] [PubMed]
94. Wang, P.; Yang, S.-P.; Lin, J.-H.; Zhang, M.-Z.; Zhou, W.-C. The mitochondrial genome of the land snail *Theba pisana* (Müller, 1774) (Stylommatophora: Helicidae): The first complete sequence in the genus *Theba*. *Mitochondrial DNA Part B Resour.* **2018**, *3*, 798–800. [CrossRef] [PubMed]
95. Neubert, E.; Bank, R. Notes on the species of *Caucasotachea*, C. Boettger 1909 and *Lindholmia*, P. Hesse 1919, with annotations to the Helicidae. *Arch. Molluskenkd.* **2006**, *135*, 101–132. [CrossRef]
96. Subai, P. Revision der Gattung *Codringtonia* Kobelt 1898 [Revision of the genus *Codringtonia* Kobelt 1898] (Gastropoda: Pulmonata: Helicidae: Helicinae). *Arch. Molluskenkd.* **2005**, *134*, 56–119.
97. Subai, P. Vergleich der mit *Levantina* verwandten großen Heliciden, sowie Revision der Gattung *Isaurica* (Kobelt). *Arch. Molluskenkd.* **1994**, *123*, 49–87. [CrossRef]
98. Nordsieck, H. Amanica n. gen., a new genus of Helicidae (Helicini) from Turkey. In *Pulmonata, Stylommatophora, Helicoidea: Systematics with Comments*; Nordsieck, H., Ed.; ConchBooks: Harxheim, Germany, 2017; pp. 82–89.
99. Pfeiffer, K.L.; Wächtler, W. Über *Codringtonia* and *Isaurica*. *Arch. Molluskenkd.* **1939**, *71*, 57–74.

100. Glaubrecht, M. Systematics and biogeography of *Assyriella rechingeri* (Gastropoda, Pulmonata, Helicidae) on Kárpathos, Greece. *Verh. Nat. Ver. Hambg.* **1994**, *34*, 373–384.
101. Grano, M.; Cattaneo, C. Rediscovery of *Assyriella rechingeri* (Fuchs et Käufel, 1936) (Gastropoda Helicidae) in Karpathos Island (Dodecanese, Greece). *Biodivers. J.* **2021**, *12*, 467–474. [CrossRef]
102. Schütt, H.; Subai, P. Revision der Gattung *Assyriella*, P. Hesse 1908 (Gastropoda: Pulmonata: Helicidae: Helicinae). *Arch. Molluskenkd.* **1996**, *125*, 117–161. [CrossRef]
103. Dohrn, H. Ueber einige centralasiatische Landschnecken. *Jahrbücher Dtsch. Malakozool. Ges.* **1882**, *9*, 115–120.
104. Neubert, E. Annotated checklist of the terrestrial and freshwater molluscs of the Arabian Peninsula with descriptions of new species. *Fauna Arab.* **1998**, *17*, 333–461.
105. Schütt, H. Über die *Helix*-Untergattung *Maltzanella* Hesse 1917. *Arch. Molluskenkd.* **1976**, *107*, 63–71.
106. Wade, C.M.; Hudelot, C.; Davison, A.; Naggs, F.; Mordan, P.B. Molecular phylogeny of the helicoid land snails (Pulmonata: Stylommatophora: Helicoidea), with special emphasis on the Camaenidae. *J. Molluscan Stud.* **2007**, *73*, 411–415. [CrossRef]
107. Schileyko, A. Nazemnye mollyuski nadsemeystva Helicoidea. In *Fauna SSSR, Mollyuski*; Skarlato, O.A., Ed.; Nauka: Leningrad, Russia, 1978; Volume III, pp. 1–384.
108. Giusti, F.; Manganelli, G.; Schembri, P.J. The non-marine molluscs of the Maltese Islands. *Monogr. Mus. Reg. Sci. Nat.* **1995**, *15*, 1–607.
109. Heller, J.; Ittiel, H. Natural history and population dynamics of the land snail *Helix texta* in Israel (Pulmonata: Helicidae). *J. Molluscan Stud.* **1990**, *56*, 189–204. [CrossRef]
110. Heller, J. *Land Snails of the Land of Israel. Natural History and Field Guide*; Pensoft: Sofia, Bulgaria; Moscow, Russia, 2009.
111. Ložek, V. Quartärmollusken der Tschechoslowakei. *Rozpr. Ústředního Ústavu Geol.* **1964**, *31*, 1–374.
112. Popiuk, Y.; Ridush, B.; Solovey, T. Middle and Late Pleistocene terrestrial snails from the Middle Dniester area, Ukraine (based on Mykola Kunytsia's collections). *Geol. Q.* **2021**, *65*, 6. [CrossRef]
113. Blume, W. Einige mazedonische Schnecken. *Arch. Molluskenkd.* **1920**, *52*, 89–92.
114. Knipper, H. Systematische, anatomische, ökologische und tiergeographische Studien an südosteuropäischen Heliciden (Moll. Pulm.). *Z. Wiss. Zool. Abt. B Archiv. Nat. Neue Folge.* **1939**, *8*, 327–517.
115. Urbański, J. Beiträge zur Kenntnis balkanischer Vertreter des Genus *Helix*, L. I (Systematische, zoogeographische und ökologische Studien über die Mollusken der Balkan-Halbinsel X). *Bull. Société Amis Sci. Lett. Poznań Série D* **1970**, *11*, 63–79.
116. Urbański, J. Beiträge zur Kenntnis balkanischer Vertreter des Genus *Helix*, L. II. (Systematische, zoogeographische und ökologische Studien über die Mollusken der Balkan-Halbinsel XIV). *Bull. Société Amis Sci. Lett. Poznań Série D* **1975**, *15*, 99–107.
117. Phuong, M.A.; Bi, K.; Moritz, C. Range instability leads to cytonuclear discordance in a morphologically cryptic ground squirrel species complex. *Mol. Ecol.* **2017**, *26*, 4743–4755. [CrossRef]
118. Dufresnes, C.; Nicieza, A.G.; Litvinchuk, S.N.; Rodrigues, N.; Jeffries, D.L.; Vences, M.; Perrin, N.; Martínez-Solano, Í. Are glacial refugia hotspots of speciation and cytonuclear discordances? Answers from the genomic phylogeography of Spanish common frogs. *Mol. Ecol.* **2020**, *29*, 986–1000. [CrossRef]
119. Bouchet, P.; Ripken, T.; Recorbet, B. Redécouverte de l'escargot de Corse *Helix ceratina* au bord de l'extinction. *Rev. Écologie* **1997**, *52*, 97–111.
120. Giusti, F. Notulae malacologicae XVI. I molluschi terrestri e di acqua dolce viventi sul massiccio dei Monti Reatini (Appennino Centrale). *Lav. Soc. Ital. Biogeogr. Nuova Ser.* **1971**, *11*, 423–574, pl. 1–7. [CrossRef]
121. Welter-Schultes, F.W. *European Non-Marine Molluscs, a Guide for Species Identification*; Planet Poster Editions: Göttingen, Germany, 2012.
122. Douka, K.; Jacobs, Z.; Lane, C.; Grün, R.; Farr, L.; Hunt, C.; Inglis, R.H.; Reynolds, T.; Albert, P.; Aubert, M.; et al. The chronostratigraphy of the Haua Fteah cave (Cyrenaica, northeast Libya). *J. Hum. Evol.* **2014**, *66*, 39–63. [CrossRef]
123. Schütt, H.; Subai, P. Beitrag zur Kenntnis von *Tacheopsis nicaeensis* (FÉRUSSAC) (Gastropoda Pulmonata: Helicidae: Helicinae). *Mitt. Dtsch. Malakozool. Ges.* **1989**, *44/45*, 31–34.
124. Mumladze, L. Sympatry without co-occurrence: Exploring the pattern of distribution of two *Helix* species in Georgia using an ecological niche modelling approach. *J. Molluscan Stud.* **2014**, *80*, 249–255. [CrossRef]
125. Grossu, A.V. *Gastropoda Romaniae 4, Ordo Stylommatophora, Suprafam.: Arionacea, Zonitacea, Ariophantacea și Helicacea*; Editura Litera: Bucuresti, Romania, 1983.
126. Molak, M.; Ho, S.Y.W. Prolonged decay of molecular rate estimates for metazoan mitochondrial DNA. *PeerJ* **2015**, *3*, e821. [CrossRef]
127. Ho, S.Y.W.; Duchêne, S.; Molak, M.; Shapiro, B. Time-dependent estimates of molecular evolutionary rates: Evidence and causes. *Mol. Ecol.* **2015**, *24*, 6007–6012. [CrossRef]
128. Kojumdgieva, E. *Fosilite na Balgaria, VII, Sarmat*; Bulgarian Academy of Science: Sofia, Bulgaria, 1969.
129. Dufresnes, C.; Mazepa, G.; Jablonski, D.; Caliari Oliveira, R.; Wenseleers, T.; Shabanov, D.A.; Auer, M.; Ernst, R.; Koch, C.; Ramírez-Chaves, H.E.; et al. Fifteen shades of green: The evolution of *Bufotes* toads revisited. *Mol. Phylogenet. Evol.* **2019**, *141*, 106615. [CrossRef] [PubMed]
130. Heller, J. Distribution, hybridization and variation in the Israeli landsnail *Levantina* (Pulmonata: Helicidae). *Zool. J. Linn. Soc.* **1979**, *67*, 115–148. [CrossRef]

diversity

MDPI

Article

Unrecognized Ant Megadiversity in Monsoonal Australia: Diversity and Its Distribution in the Hyperdiverse *Monomorium nigrius* Forel Group

Alan N. Andersen [1,*], François Brassard [1] and Benjamin D. Hoffmann [1,2]

[1] Research Institute for the Environment and Livelihoods, Charles Darwin University, Darwin, NT 0909, Australia; francois.brassard@cdu.edu.au (F.B.); ben.hoffmann@csiro.au (B.D.H.)
[2] CSIRO Tropical Ecosystems Research Centre, PMB 44, Winnellie, NT 0822, Australia
* Correspondence: alan.andersen@cdu.edu.au; Tel.: +61-457-539-513

Abstract: We document diversity and its distribution within the hyperdiverse *Monomorium nigrius* Forel group of the Australian monsoonal tropics, an unrecognized global centre of ant diversity. The group includes a single described species, but several distinct morphotypes each with multiple clearly recognizable taxa are known. Our analysis is based on 401 CO1-sequenced specimens collected from throughout the Australian mainland but primarily in the monsoonal north and particularly from four bioregions: the Top End (northern third) of the Northern Territory (NT), the Sturt Plateau region of central NT, the Kimberley region of far northern Western Australia, and far North Queensland. Clade structure in the CO1 tree is highly congruent with the general morphotypes, although most morphotypes occur in multiple clades and are therefore shown as polyphyletic. We recognize 97 species among our sequenced specimens, and this is generally consistent (if not somewhat conservative) with PTP analyses of CO1 clustering. Species turnover is extremely high both within and among bioregions in monsoonal Australia, and the monsoonal fauna is highly distinct from that in southern Australia. We estimate that the *M. nigrius* group contains well over 200 species in monsoonal Australia, and 300 species overall. Our study provides further evidence that monsoonal Australia should be recognized as a global centre of ant diversity.

Keywords: ant diversity; PTP; species complex; species delimitation; tropical savanna

Citation: Andersen, A.N.; Brassard, F.; Hoffmann, B.D. Unrecognized Ant Megadiversity in Monsoonal Australia: Diversity and Its Distribution in the Hyperdiverse *Monomorium nigrius* Forel Group. *Diversity* **2022**, *14*, 46. https://doi.org/10.3390/d14010046

Academic Editors: Simone Fattorini and Michael Wink

Received: 6 November 2021
Accepted: 5 January 2022
Published: 11 January 2022

1. Introduction

The Australian monsoonal tropics, encompassing the vast tropical savanna landscapes of the northern third of the continent (Figure 1), is a centre of exceptional but largely unrecognized ant diversity. Many taxa that are formally recognized as single, widespread species are in fact hyperdiverse species complexes [1,2]. For example, *Melophorus rufoniger* Heterick, Castalanelli and Shattuck was recently described as a single species occurring throughout mainland Australia but most commonly in the monsoonal tropics [3]. However, a subsequent analysis that integrated genetic, morphological and distributional information revealed that at least 30 species within the taxon occur in the Top End (high rainfall northern third) of the Northern Territory (NT) alone. It was concluded that the total *M. rufoniger* fauna included up to 100 species from monsoonal Australia, none of which are described [4].

The *Monomorium nigrius* Forel group is another case in point. It is an intractably diverse assemblage of very small, brownish-black species with 11-segmented antenna occurring throughout mainland Australia but with its centre of diversity in the monsoonal north [5,6]. In a recent revision of the Australian *Monomorium* fauna the group was described as representing a single species, *M. fieldi* Forel [7], despite morphological variation that is obviously interspecific.

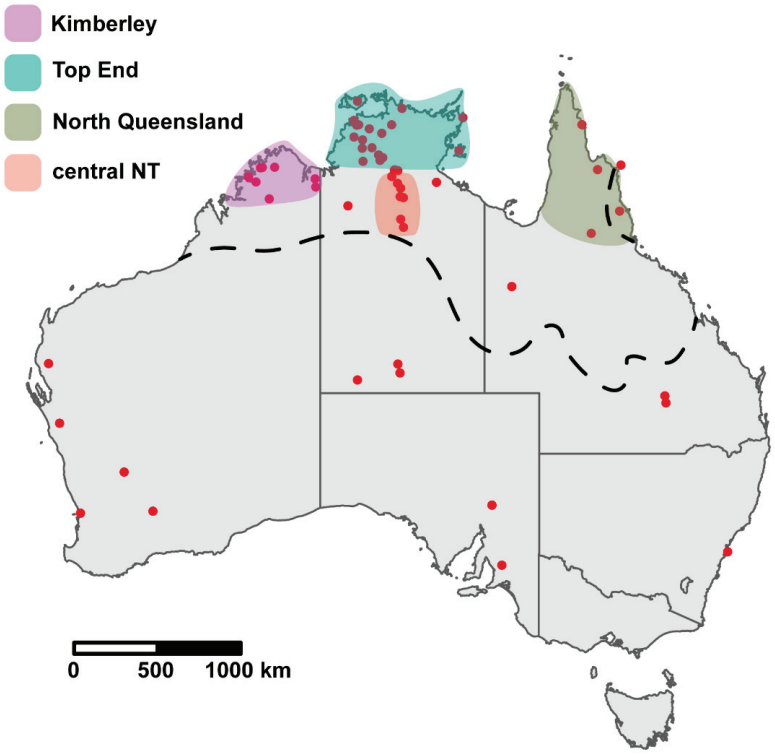

Figure 1. Map of Australia showing the approximate boundary of the monsoonal tropics (dashed line), where rainfall is very heavily concentrated in a summer wet season. Collection localities (red dots) for sequenced specimens of the *Monomorium nigrius* group are indicated, as are the four regions in the monsoonal zone where collections are concentrated.

Six general morphotypes, each with multiple species, can be recognized based on variation in body size, length of antennal scapes, shape of the propodeum and petiolar node, and pilosity (the '*fieldi*', '*donisthorpei*', 'sp. 50', 'sp. 14', 'sp. 13' and 'sp. 9' morphotypes, using the species nomenclature of [8]: Figure 2). A key to the morphotypes is as follows:

1. Antennal scapes relatively long, reaching occipital margin or nearly so 1
   Antennal scapes relatively short, failing to reach occipital margin by a distance greater than their maximum width 4
2. Mesosoma with particularly long hairs; metanotal notch deep and propodeum rather prominently rounded; petiole often unusually broad in profile (Figure 2a,b) . . . . . '*...fieldi*'
   Not as above 2
3. Relatively large and robust, often with a squarish head; metanotal notch feeble and propodeum not at all prominently rounded (Figure 2c,d) . . . . . '*donisthorpei*'
   Smaller, with a rectangular head; metanotal notch more pronounced and propodeum more rounded (Figure 2e,f) . . . . . 'sp. 50'
4. Petiolar node very small, lower than long in profile 5
   Petiolar node as high as long in profile (Figure 2g,h) . . . . . 'sp. 14'
5. Tiny species, propodeum short and obliquely angled in profile (Figure 2i,j) .... 'sp. 13'
   Larger species; propodeum more broadly rounded in profile (Figure 2k,l) . . . ... 'sp. 9'

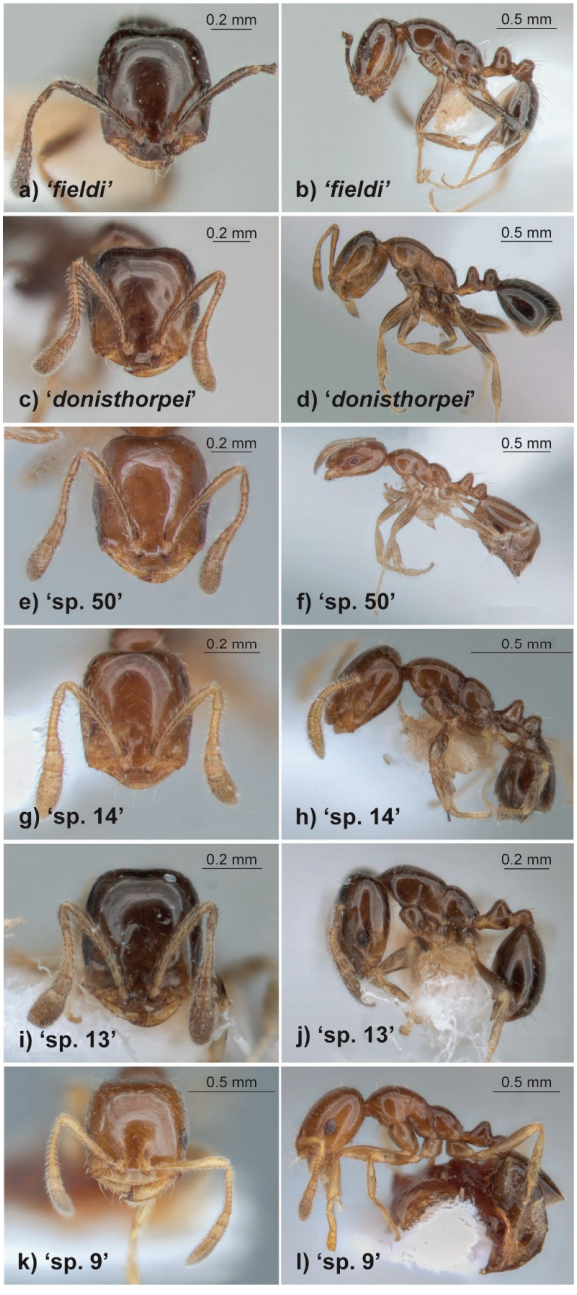

Figure 2. Images of the six general morphotypes of species within the *Monomorium nigrius* group. (**a**,**b**) 'fieldi' (sequenced specimen ID OZBOL4003-21; species A15); (**c**,**d**) 'donisthorpei' (OZBOL4454-21; species C3); (**e**,**f**) 'sp. 50' (MONO197-16; species B19); (**g**,**h**) 'sp. 14' (OZBOL4460-21; species G6); (**i**,**j**) 'sp. 13' (OZBOL4013-21; species H9); (**k**,**l**) 'sp. 9' (not sequenced, collected from the Territory Wildlife Park, near Darwin, NT; species L).

The different morphotypes commonly occur in close sympatry; indeed, nine species shown to be differentiated genetically and morphologically, and representing all six morphotypes, have been recorded from a savanna woodland site (Territory Wildlife Park) near Darwin [8]. Remarkably, seven of these species were recorded from a single 10 × 10 m plot and six in another. If so many species of the *M. nigrius* group can occur at such a small spatial scale, and the species group occurs throughout most of mainland Australia, then how many species are there in total? A recent compilation of the known ant fauna of the Top End of the NT lists 17 species from the group [9], but otherwise there has been no attempt at a broader quantification of total diversity within the taxon.

In this paper, we present an integrated genetic (CO1), morphological and distributional analysis of the *M. nigrius* group in order to provide an estimate of the total number of species within it and to document spatial patterns of species richness and turnover. We specifically address the following questions:

What are indicative levels of total diversity based on available morphological, CO1 and distributional information?

What is the extent of congruence between the six general morphotypes and CO1 phylogeny?

How diverse is the *M. nigrius*-group fauna within Australia, and what are the spatial patterns of species richness and turnover?

2. Materials and Methods

This study was based on pinned specimens of the *M. nigrius* group held in the ant collection at the CSIRO laboratory in Darwin, which holds by far the most extensive collection of the taxon. For CO1 analysis we used the 40 *M. nigrius*-group sequences from [8] and obtained sequences from an additional 361 specimens collected from throughout mainland Australia (Supplementary Table S1). One of these (from urban Sydney) is a perfect morphological match with the New Zealand species *M. antipodum* Forel [10], and we refer to it as *M.?antipodum*. We also sequenced a specimen of the closely related *M. carinatum* Heterick group to be used as the outgroup for building a CO1 tree. Geographic coverage of samples within mainland Australia was extremely patchy (Figure 1). The most intensively sampled region was the Top End of the NT (1000–2000 mm mean annual rainfall), but even here large areas are unrepresented. Other regions of relatively high sampling intensity within monsoonal Australia are the Sturt Plateau region of central Northern Territory (550–800 mm), the Kimberley region of far northern Western Australia (500–1700 mm) and far North Queensland (north of the Townsville region) (Figure 1). Vast areas of central and southern Australia are not represented.

Many localities represent multiple sites. The four major biogeographic regions of relatively high collection effort in northern Australia are indicated. Total annual rainfall in the monsoonal zone ranges from approximately 2000 mm on the Tiwi Islands in the Top End to 500 mm on the southern boundary with the central arid zone.

DNA extraction (from foreleg or whole-body tissue) and CO1 sequencing were conducted through the Barcode of Life Data (BOLD) System (for extraction details, see http://ccdb.ca/resources, accessed on 4 January 2022). Each sequenced specimen was assigned a unique identification code that combines the batch within which it was processed, its number within the batch and the year of sequencing (e.g., MONO244-16). All specimens are labeled with their respective BOLD identification numbers in the Darwin collection.

DNA sequences were checked and edited in MEGA [11]. Sequences were aligned using the UPGMB clustering method in MUSCLE [12], and then translated into (invertebrate) proteins to check for stop codons and nuclear paralogues. The aligned sequences were trimmed accordingly, resulting in 822 base pairs.

To explore overall CO1 diversity in the samples, the mean genetic pairwise distances between sequences were calculated in MEGA. This was done using the Kimura-2 parameter (K2P) model [13] to ensure that results were comparable with those of most other studies of insect DNA barcoding, with 500 bootstrap replicates and the 'pairwise deletion' option

of missing data (to remove all ambiguous positions for each sequences pair). Analysis involved all nucleotide sequences, excluding those of the outgroup. Codon positions included were 1st + 2nd + 3rd.

The level of CO1 variation within ant species is typically 1–3% [14] but there is no specific level of CO1 divergence that can be used to define a species. For species delimitation we adopted the species concept based on reproductive isolation and evolutionary independence as evidenced by morphological differentiation between sister (i.e., most closely related) clades (considering all available samples from the same collections as those of sequenced specimens) and sympatric distribution. We thus delimited species based on the integration of morphological variation, CO1 clustering and distance, and geographic distribution [15]. We compared our species delimitations using such an integrated approach with two statistical methods using CO1 data alone. We used the MEGA genetic distances to produce a tree file with IQ-TREE [16] and then ran this into two models. The first was the Poisson Tree Processes (PTP) model, which infers species boundaries using the number of substitutions within and between species in a maximum likelihood tree [17]. The second was the Bayesian implementation of the PTP model (bPTP), which adds Bayesian values to delimited species on the input tree [17]. We subjected trees including all specimens, as well as a tree of each major clade within the full tree separately, to PTP and bPTP algorithms on the web server (http://species.h-its.org/ptp/, accessed on 8 October 2021), using the settings of 500,000 MCMC generations, 100 thinning and 0.1 burn in. We elected to increase the number of MCMC generations from 100,000 to 500,000 to increase the rate of convergence for the MCMC chain. Nevertheless, we did not reach convergence for several clades, and thus discarded these results.

We imaged representative specimens using a Leica DMC4500 camera mounted on a Leica M205C dissecting microscope. We took image montages using the Leica Application suite v. 4.13 and stacked them in Zerene stacker.

3. Results

3.1. Diversity

By integrating morphological variation with CO1 data and distributional information we recognize 97 species among our sequenced samples. Nearly one-third (32) of these species are known from single records in the Darwin collection. The CO1 tree contains ten major clades (A–J) that collectively contain 388 of the 401 sequenced specimens and 91 of our recognized species (Figure 3, Table 1; see Supplementary Figure S1 for the full CO1 tree). The mean CO1 distance between species from different clades ranges from 13.1% (between species from clades A and F) to 19.5% (clades E and I). The number of species within a clade ranges from 3 (clade C) to 20 (clade A), with mean CO1 distances among species within a clade ranging from 4.9% (range 1.5–11.3%) in clade A to 15.8% (13.8–17.2%) in clade I (Table 1). The six 'outlier' species occur in five independent clades, one of which is represented by *M.* ?*antipodum*.

Table 1. Number of indicated species within each of the ten major clades (A–J; see Figure 3). Data are for PTP (maximum likelihood), bPTP (Bayesian inference), and integrated assessment (considering morphological, distributional and CO1 information). For PTP and bPTP analyses, data are provided for assessments of the full tree (A) and each clade individually (B). The totals include specimens outside the ten major clades. For the integrated assessment, the CO1 distances among species (calculated in MEGA) within each clade are shown.

Clade	No. Indicated Species					CO1 Distance (%)	
	PTP		bPTP		Integrated	Mean	Range
	A	B	A	B			
A	2	31	15	nc	20	4.9	1.5–11.3
B	16	14	16	16	19	10.9	2.3–15.9

Table 1. *Cont.*

Clade	No. Indicated Species					CO1 Distance (%)	
	PTP		bPTP		Integrated	Mean	Range
	A	B	A	B			
C	5	5	9	34	3	11.7	11.5–12.1
D	3	9	7	15	5	5.6	3.7–7.2
E	9	14	12	15	9	8.3	5.7–10.9
F	5	6	5	6	5	5.8	4.2–7.7
G	8	6	16	10	6	6.8	2.9–8.9
H	2	15	2	nc	10	6.6	1.8–19.3
I	4	4	4	4	4	15.8	13.8–17.2
J	9	7	9	8	10	11.3	2.6–15.5
TOTAL	**72**	**120**	**102**	nc	**97**		

nc = not converged and so results have been discarded.

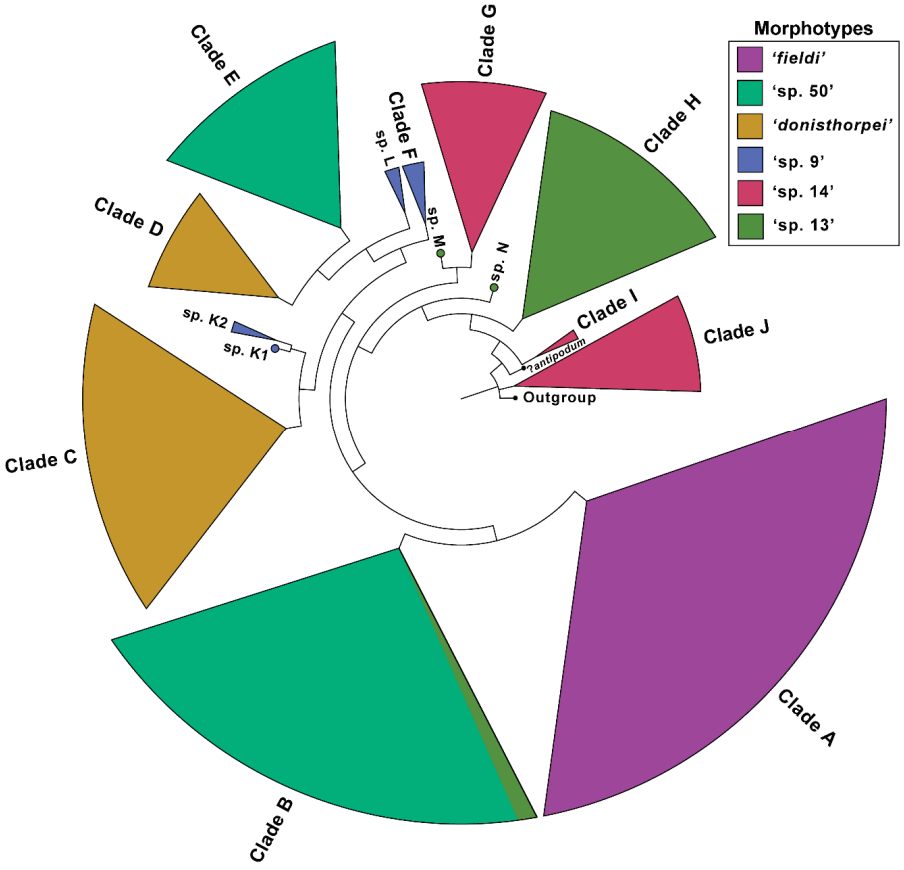

Figure 3. Summary CO1 tree showing the ten major clades (A–J) and distribution of the six morphotypes (see Figure 2).

There is strong concordance between clade structure and the six recognized morphotypes: all major clades except B contained a single morphotype; and in clade B, 18 of the 19 recognized species are of the same ('sp. 50') morphotype (Figure 3). However, all morphotypes other than '*fieldi*' (Figure 2a,b and Figure 4) occur in multiple clades. The '*donisthorpei*'

morphotype (Figure 2c,d and Figure 5) occurs in two clades, one containing '*donisthorpei*' in the strict sense (clade C, with three species recognized) and the other including 'sp. 37' from the Territory Wildlife Park study [8] (clade D, five species). The 'sp. 50' morphotype (Figure 6) likewise occurs in two clades, represented by 18 of the 19 species in clade B and all nine species in clade E, whereas the 'sp. 14' morphotype (Figure 7) occurs in three clades (G, I and J). The 'sp. 13' (Figure 8) and 'sp. 9' (Figure 9) morphotypes each occur in a single major clade (H and F, respectively) but are both also represented by 'outlier' species (Figure 3).

Figure 4. Images of species from the '*fieldi*' morphotype. (**a**) Specimen MONO237-16; Kakadu NP, NT; (**b**) specimen OZBOL1366-21; Douglas Daly, NT; (**c**) specimen DARW347-15; Eurardy Stn, WA; (**d**) specimen MONS028-18; Nitmiluk NP, NT; (**e**) specimen OZBOL1364-21; Lakefield NP, Qld; (**f**) specimen OZBOL4008-21; Forrest Hill Stn., NT; (**g**) specimen MONO254-16; Lizard Island, Qld; (**h**) specimen OZBOL4004-21; Hayfield Shenandoah Stn, NT.

PTP analyses provided variable results according to whether they were based on maximum likelihood or Bayesian probability, and whether the full tree was analyzed simultaneously or by individual clades (Table 1). The total number of indicated species by Bayesian analysis of the full tree (102) was very similar to our 97 recognized species (Figure S1). However, maximum likelihood analysis of the full tree indicated only 72 species (Figure S1). This difference is due primarily to clades A ('*fieldi*' morphotype) and H ('sp. 13' morphotype), where only two species were indicated in each compared with 20 and 10, respectively, recognized by integrated analysis (Figure S1). Mean CO1 distances among our recognized species in clade A (4.9%) are well above the typical 1–3% for conspecific variation but are the lowest for any clade, which appears to explain the low number of PTP-indicated species when the full tree is analyzed. Geographic distribution was a key factor in our recognition of 20 species within the clade (Figure S1). For example, specimens from south-western WA fall into two subclades that we recognize as separate species, A1 and A6. A1 belongs to a broader subclade that includes several species from the NT, whereas A6 represents a subclade separate to this. Such a distribution indicates that specimens from the two southwestern WA subclades are reproductively isolated and therefore represent different species. Similarly, specimens from the Top End are represented in subclades that are scattered throughout clade A, separated by subclades consisting of specimens from distant locations. Moreover, there is substantial morphological variation among the species relating to pilosity and shape of the promesonotum, propodeum and petiolar node (Figures 1a and 4). Notably, when clade A is analyzed separately the number of PTP (maximum likelihood)-indicated species increases dramatically, from two to 31 (Table 1). The low number of PTP-indicated species in clade H appears to be driven by the outlier species H10 (Figure 8c and Figure S1), which has 14–19% CO1 distance from other species in the clade, compared with 2–7% among the other species. If clade H is analyzed separately without H10 then 14 species are indicated by PTP (maximum likelihood) analysis. PTP (maximum likelihood) analysis of each clade separately indicates a total of 120 species among our sequenced specimens (Table 1).

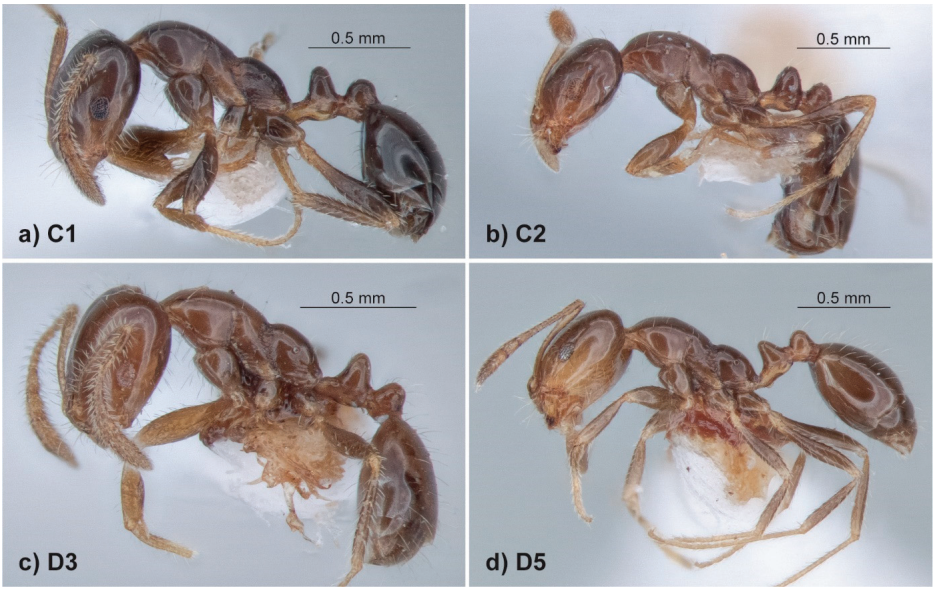

Figure 5. Images of species from the '*donisthorpei*' morphotype. (**a**) Specimen OZBOL4021-16; Hayfield Shenandoah Stn; NT; (**b**) specimen OZBOL4451-21; Gove Peninsula, NT; (**c**) specimen MONO257-16; Mitchell Falls, WA; (**d**) specimen 318 from Andersen et al. 2013.

Figure 6. Images of species from the 'sp. 50' morphotype. (**a**) Specimen OZBOL3995-16; Forrest Hill Stn, NT; (**b**) specimen OZBOL3996-21; Forrest Hill Stn, NT; (**c**) specimen MONO225-16; Pine Creek, NT; (**d**) specimen MONO266-16; Eurardy Stn, WA; (**e**) specimen OZBOL4005; Hayfield Shenandoah Stn, NT; (**f**) specimen OZBOL1353-21; Ranger Uranium Mine, NT; (**g**) specimen OZBOL1348-21; Gove Peninsula, NT; (**h**) specimen OZBOL4030-21; Hayfield Shenandoah Stn, NT.

Figure 7. Images of species from the 'sp. 14' morphotype. (**a**) specimen MONM613-18; Mt Elizabeth, WA; (**b**) specimen DARW225-15; Currawarra Stm, Qld; (**c**) specimen MONO110-16; Claravale Stn, Qld; (**d**) specimen MONO111-16; Glendonnel Stn, Qld; (**e**) specimen MONO170-16; Jilbadji Nat Res, WA: (**f**) specimen DARW237-15; Eurardy Stn, WA.

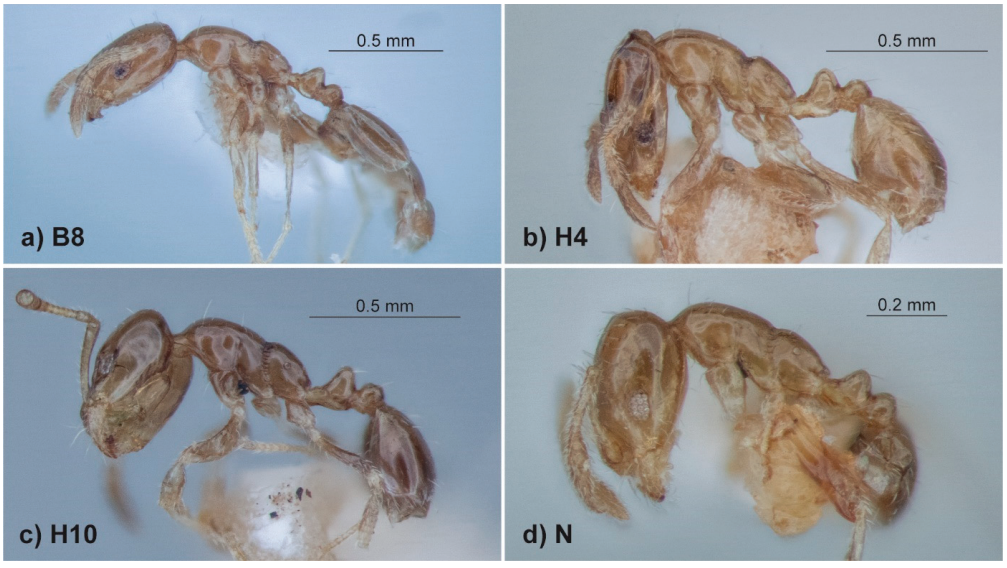

Figure 8. Images of species from the 'sp. 13' morphotype. (**a**) Specimen OZBOL1330-21; Maryfield Stn, NT; (**b**) specimen MONM594-18; Mt Elizabeth, WA; (**c**) MONOM595-18; Cascade Ck, WA; (**d**) specimen DARW206-15; Theda Stn, WA.

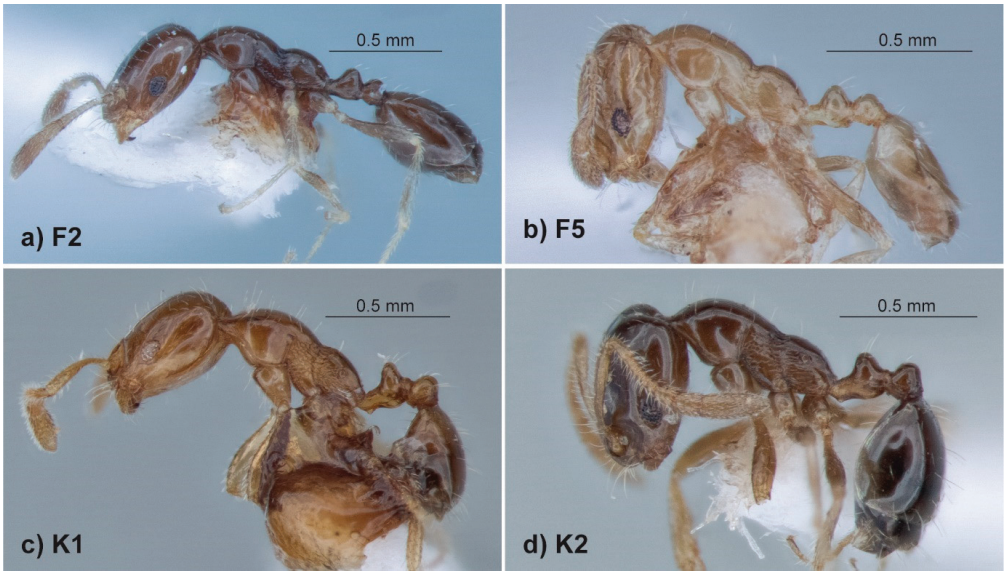

Figure 9. Images of species from the 'sp. 9' morphotype. (**a**) Specimen DARW250-15; Maryfield Stn, NT; (**b**) specimen MONM591-18; Mt Elizabeth, Kimberley, WA; (**c**) specimen MONS008-18; Nitmiluk NP, NT; (**d**) specimen OZBOL4039-21; Hayfield Shenandoah Stn, NT.

3.2. Geographic Distribution

The most widely distributed morphotype geographically is '*fieldi*', which occurs throughout semi-arid southern Australia as well as throughout the monsoonal zone (Table S1). Of the 20 species we recognize within '*fieldi*', five (A3, A4, A5, A9, A15; 3–

5% CO1 distances among them) occur in the Top End of the NT, including three in each of Kakadu (A3, A4, A15) and Nitmiluk (A4, A9 and A15) National Parks (Table S1). The 'sp. 14' morphotype includes a species-rich clade (clade J, with 10 species) of exclusively southern Australian species (Table S1). Six of these occur in south-eastern Queensland (two of them also in South Australia, and so are likely distributed throughout semi-arid south-eastern Australia) and the other four are from southwestern Western Australia (one of these also occurs in South Australia). The clade includes four glabrous species (J1–4; Figure 7c,d), a condition unique to them. None of our sequenced specimens from the '*donisthorpei*', 'sp. 9', 'sp. 13' or 'sp. 50' morphotypes are from southern Australia, but all these morphotypes occur throughout the monsoonal north (Table S1).

A total of 34 of our 97 recognized species occur in the Top End of the NT, where there is very high species turnover among subregions (Figure 10a). Of the combined 25 species recorded from the Kakadu/Nitmiluk and Darwin-Litchfield subregions, only two (8.0%) are in common, and only 6% of the 32 total species were recorded from all three subregions. Subregional richness is especially high in the central Kakadu/Nitmiluk subregion, where 20 of our recognized species have been recorded. Despite Kakadu and Nitmiluk National Parks being contiguous, only five (25%) of the 20 species are known from both.

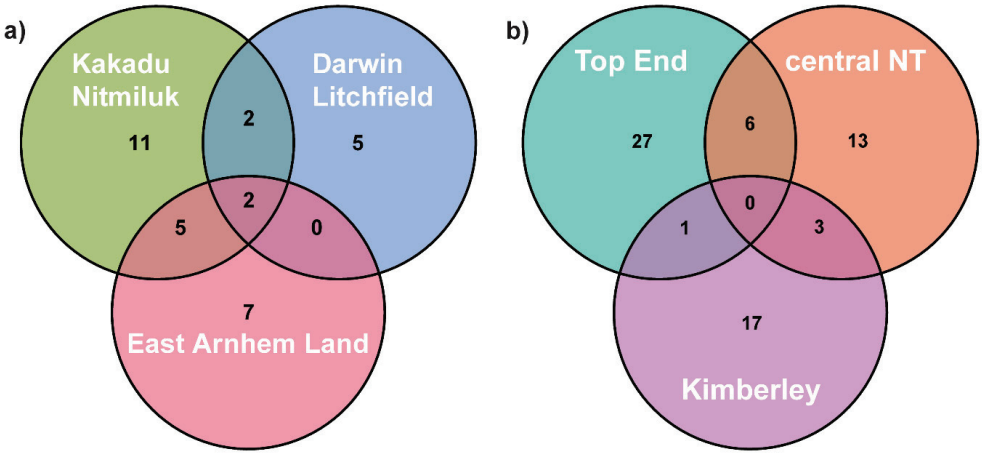

Figure 10. Species overlap among subregions within (**a**) the Top End of the NT, and (**b**) major regions in north-western Australia. Data are numbers of unique and shared species represented by the sequenced specimens.

Unsurprisingly, species turnover is even higher among broader regions across northern Australia. None of the 34 Top End species are among the seven species from far North Qld, and only one (C3) is among the 21 species from the Kimberley region of far northern WA. The Top End fauna is also very distinct from that of the Sturt Plateau bioregion of central NT, with only six of the combined 50 species recorded from both regions (Figure 10b).

4. Discussion

We have revealed remarkable hyperdiversity within the *Monomorium nigrius* group, recognizing 97 species from limited geographic coverage of sequenced specimens. PTP analysis of CO1 clustering suggests that this figure is conservative. Given (1) the high levels of spatial turnover, (2) the fact that much of the taxon's range remains unsampled, (3) that nearly one-third of the species are known from single records, and (4) many additional species (that are too old to yield sequences) are held in the Darwin collection, the sequenced specimens are likely to represent just a fraction of total diversity within the group.

We acknowledge that our sampling is limited when viewed at a continental scale, but we do not believe that this significantly affects our species delimitations. More than

one-third (34) of our 97 recognized species occurs in a single region (Top End of the NT), and this region has been the most intensively sampled. The Top End fauna has very limited overlap with those of the region immediately south (central NT) that connects the Top End with the rest of Australia, which has also been intensively sampled. This indicates that further sampling would not show that species from other regions that we have recognized as different from those from the Top End are in fact conspecific. A detailed examination of sister relationships among our recognized species (Figure S1) further supports our view that our species delimitations are not an artefact of limited sampling. For example, we recognize 20 species (all of the '*fieldi*' morphotype) in clade A. A1 is represented by ten specimens, all of which occur in southwestern western Australia. Its two sister species (A2 and A3) are from the Top End of the NT (furthest north) rather than from central or southern NT (which connect the Top End to southern Australia). These three species belong to a clade that includes two other, clearly distinct species, one (A4; Figure 4a) known only from the Top End and the other (A5; Figure 4b) occurring both in the Top End and central NT. The sister to this clade is another species from southwestern Australia (A6; Figure 4c), which obviously cannot be the same as A1. Similar reasoning can be applied to other species.

The 34 species that we recognize from the Top End of the NT is twice as many as listed by [9], and it does not include several species on that list (Figure 11). Many of the species appear to have narrow ranges. For example, species E1, H1 and L are all known only from the same one site near Darwin [8], and species G1 is known only within a 20 km range from that site. Given the limited spatial coverage of samples (Figure 1), it is likely that the total Top End fauna comprises at least 50 species.

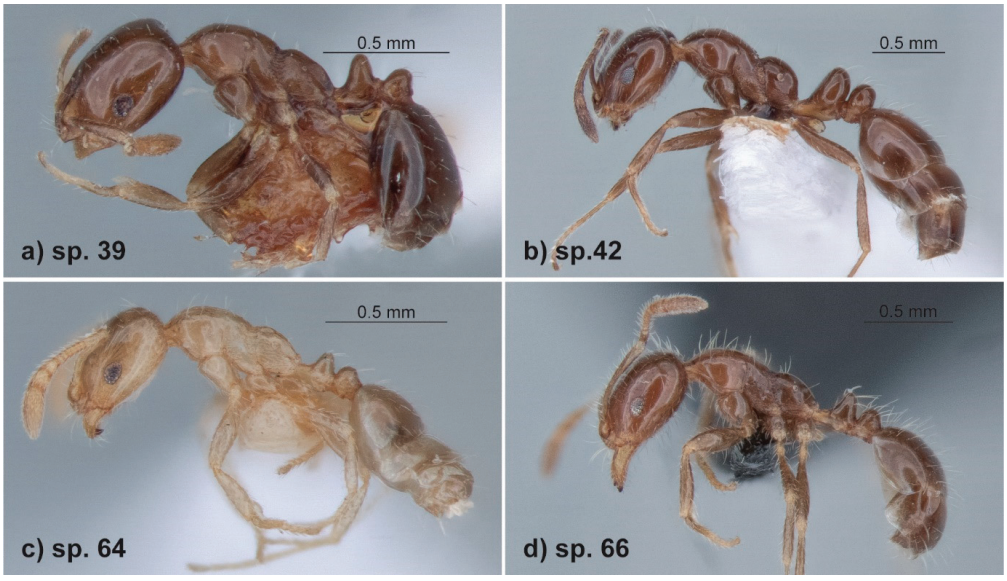

Figure 11. Additional species known from the Top End of the NT (not sequenced in this study). The species belong to the 'sp. 14' (**a**), '*fieldi*' (**b**), 'sp. 9' (**c**) and '*donisthorpei*' (**d**) morphotypes. Species codes follow [8].

We recorded far fewer species in the two other high-rainfall regions of northern Australia: the Kimberley with 21 species, and far North Queensland with only seven. However, these figures are proportionate to sampling effort (Figure 1, Table S1) and there is no reason to believe that the faunas of these regions are substantially less diverse than in the Top End. Given the very little species overlap among them, the three regions collectively

can be expected to have around 150 species. The high diversity (22 species) of the Sturt Plateau subregion of central NT is presumably repeated throughout the semi-arid north of the continent, suggesting that over 200 species occur just in monsoonal Australia. Diversity is also high in semi-arid central and southern Australia, with virtually no overlap with the monsoonal fauna, and so a reasonable estimate of the total *M. nigrius*-group fauna is a phenomenally high 300 species.

An analysis of other (especially nuclear) genes is required for testing the robustness of the deeper clade structure within our CO1 tree. However, the high concordance between CO1 clade structure and our six previously recognized morphotypes suggests that they have a strong phylogenetic basis. Clade A contained all specimens of the '*fieldi*' morphotype, and so this is likely to represent a phylogenetically robust species complex. However, all other morphotypes are shown in the CO1 tree as polyphyletic. The '*donisthorpei*' morphotype occurs in two (disjunct) clades, one including '*donisthorpei*' in the strict sense (clade C, with three recognized species), and the other including sp. 37 from [8] (clade D, with five recognized species). Despite their close morphological affinity (Figure 5) they likely represent separate species complexes. Notably, not only did two of the three '*donisthorpei*' species from clade C occur at the same site but they did so in the same 10 × 10 m plot (plot 3 in [8]). One of these (C2; Figure 5b) is known only from the Top End, whereas the other (C1; Figure 2c,d) occurs also in the Kimberley region.

The 'sp. 14', 'sp. 13' and 'sp. 9' morphotypes appear to be particularly diverse phylogenetically. The 'sp. 14' morphotype occurs as three (G, I and J) of the ten major clades and is distributed throughout mainland Australia. Clade J consists exclusively of species from outside the monsoonal zone, ranging throughout southern semi-arid Australia from central Queensland to southwestern Western Australia. The only other sequenced specimens from southern Australia are from the '*fieldi*' morphotype, one species (A6) of which is from southwestern Western Australia, and a distantly related species (A20) occurring throughout semi-arid southeastern Australia. Both are shown in the CO1 tree as being most closely related to (different) species from central NT.

The 'sp. 13' morphotype is heavily concentrated in just one (H) of the ten major clades, but it is also represented in clade B (B8) and in two other locations on the CO1 tree (sp. M and sp. N; Figure 3). This strongly indicates that despite being highly distinctive and relatively uniform (Figure 2i,j and Figure 8), the morphotype has evolved multiple times. The 'sp. 9' morphotype occurs in three locations (clades F and K and sp. L) on the CO1 tree and these are associated with conspicuous morphological differences, suggesting that they represent three separate species complexes. Species L (sp. 9 from [8]) is unique among known species within the *M. nigrius* group in being somewhat polymorphic (with head size and shape showing considerable allometric variation) and having an anterior clypeal margin that is only weakly convex (Figure 2k). The two species from clade K (Figure 9c,d) are unusual in having a mesosoma that is conspicuously sculptured postero-laterally; the unsequenced sp. 64 (Figure 11c) shares this trait and presumably belongs to this complex.

Our *M.* ?*antipodum* sample is an outlier on the CO1 tree. It was collected from suburban Sydney and the only other specimens in the Darwin collection that match it morphologically are from suburban Brisbane. Together, this strongly suggests that it is introduced and is indeed *M. antipodum* from New Zealand, where it is commonly associated with human settlements (Don 2007).

5. Conclusions

What are the implications of our findings for total richness within the ant fauna of monsoonal Australia? Two decades ago, the fauna was estimated to contain approximately 1500 species, which at the time seemed remarkably high [6]. In that analysis, the *Melophorus rufoniger* group (then referred to as the *M. aeneovirens* group, before *M. rufoniger* was described) was estimated to contain ten species and the *Monomorium nigrius* group twenty, estimates that have now been shown to be an order of magnitude too low. The more recent analysis of the ant fauna of the Top End of the NT recognized 901 native species,

with a remarkable 60% of these apparently endemic to the region [9]. Subsequent surveys in the Top End (e.g., [18]) have recorded over 100 additional species. Detailed analyses of the *Melophorus rufoniger* and *Monomorium nigrius* groups have revealed that richness in these taxa is at least twice as high as was then recognized, and that levels of regional endemism are far higher than 60%. Our unpublished CO1 data show that this is true for many other species groups within *Melophorus* and *Monomorium*, as well as in other genera such as *Tetramorium*, *Rhytidoponera*, *Meranoplus*, *Camponotus* and *Iridomyrmex*. Given the highly patchy sampling within the Top End (Figure 1), we estimate that its total ant fauna comprises at least 1300 species.

Ant diversity and endemism are also exceptionally high in the Kimberley region of far northern Western Australia [19–21]. Other biogeographical regions in monsoonal Australia have been even less intensively sampled, but their levels of species richness and endemism are also likely to be extremely high (see [21] for a broader discussion of this). This means that the total monsoonal fauna likely numbers in the several thousand.

Such diversity is truly remarkable for a tropical savanna landscape. For example, although the ant fauna of the similarly sized Brazilian savanna ('cerrrado') is considered particularly diverse [22], it is estimated to comprise only approximately 700 species (R. Feitosa, personal communication). Peak ant diversity globally is generally considered to occur in lowland tropical rainforest and especially in Amazonia [23]. However, our analysis suggests that monsoonal Australia may in fact be the true global centre of ant diversity. How can such remarkable richness—and that of arid Australia more generally, be explained? It is presumably a product of historical processes given that the contemporary Australian environment is not so dramatically different from elsewhere in the world. The remarkable diversity occurs within species complexes rather than at the genus level, indicating that it was generated over recent evolutionary time. One explanation [24] is that it is a product of the Pleistocene glaciations that caused massive movement of sand across Australia during these times of peak aridity, when up to 85% of the continent was covered by desert dunes. Such dunes are hostile for most ant species, whose distributions would have retracted to isolated refugia scattered within the vast sand-dominated landscape, allowing for speciation on a mass scale.

Supplementary Materials: The following supporting information can be downloaded at: https://www.mdpi.com/article/10.3390/d14010046/s1, Table S1: List of sequenced specimens of the *Monommorium nigrius* group, along with their collection localities. Figure S1: Full CO1 tree of sequenced specimens of the *Monomorium nigrius* group, showing recognized species delimited by an integration of morphological, genetic and distributional information, along with those indicated by PTP (maximum likelihood) and ePTP analyses of the full tree.

Author Contributions: A.N.A. conceived this study, led the development of the Darwin ant collection, and wrote the first draft of the manuscript. F.B. undertook the analysis of the CO1 data, prepared the figures and contributed to the writing of this paper. B.D.H. helped develop the Darwin ant collection and contributed to the writing of this paper. All authors have read and agreed to the published version of the manuscript.

Funding: This research received no external funding.

Institutional Review Board Statement: Not applicable.

Data Availability Statement: CO1 sequence data are available from the authors upon request.

Acknowledgments: We thank our many collaborators who collected the specimens analyzed in this study, and especially Magen Pettit, Tony Hertog and Jodie Hayward from CSIRO, as well as staff from the Flora and Fauna Division of the NT Department of Environment and Natural Resources who conducted biodiversity monitoring in Kakadu, Nitmiluk and Litchfield National Parks in the Northern Territory. We also thank Stefanie Oberprieler for providing access to imaging facilities.

Conflicts of Interest: The authors declare no conflict of interest.

References

1. Oberprieler, S.K.; Andersen, A.N.; Moritz, C.C. Ants in Australia's monsoonal tropics: CO1 barcoding reveals extensive unrecognised diversity. *Diversity* **2018**, *10*, 36. [CrossRef]
2. Andersen, A.N.; Hoffmann, B.D.; Oberprieler, S.K. Integrated morphological, CO1 and distributional analysis confirms many species in the *Iridomyrmex anceps* (Roger) complex of ants. *Zool. Syst.* **2020**, *45*, 219–230.
3. Heterick, B.E.; Castalanelli, M.; Shattuck, S.O. Revision of the ant genus *Melophorus* (Hymenoptera, Formicidae). *Zookeys* **2017**, 1–420. [CrossRef] [PubMed]
4. Andersen, A.N.; Hoffmann, B.D.; Oberprieler, S.K. Megadiversity in the ant genus *Melophorus*: The *M. rufoniger* Heterick, Castalanelli and Shattuck species group in the top end of Australia's northern territory. *Diversity* **2020**, *12*, 386. [CrossRef]
5. Andersen, A.N. Ant diversity in arid Australia: A systematic overview. In *Advances in Ant Systematics (Hymenoptera: Formicidae): Homage to E. O. Wilson—50 Years of Contributions*; Snellling, R.R., Fisher, B.L., Ward, P.S., Eds.; Memoirs American Entomological Institute Series; American Entomological Institute: Logan, UT, USA, 2007; pp. 19–51.
6. Andersen, A. *The Ants of Northern Australia: A Guide to the Monsoonal Fauna*; CSIRO Publishing: Melbourne, Australia, 2000; ISBN 0643066039.
7. Heterick, B.E. Revision of the Australian ants of the genus *Monomorium* (Hymenoptera: Formicidae). *Invertebr. Syst.* **2001**, *15*, 353–459. [CrossRef]
8. Andersen, A.N.; Arnan, X.; Sparks, K. Limited niche differentiation within remarkable co-occurrences of congeneric species: *Monomorium* ants in the Australian seasonal tropics. *Austral Ecol.* **2013**, *38*, 557–567. [CrossRef]
9. Andersen, A.N.; Hoffmann, B.D.; Oberprieler, S. Diversity and biogeography of a species-rich ant fauna of the Australian seasonal tropics. *Insect Sci.* **2018**, *25*, 519–526. [CrossRef] [PubMed]
10. Don, W. *Ants of New Zealand*; Otago University Press: Dunedin, New Zealand, 2007; ISBN 1877372471.
11. Kumar, S.; Stecher, G.; Li, M.; Knyaz, C.; Tamura, K. MEGA X: Molecular evolutionary genetics analysis across computing platforms. *Mol. Biol. Evol.* **2018**, *35*, 1547–1549. [CrossRef]
12. Edgar, R.C. MUSCLE: Multiple sequence alignment with high accuracy and high throughput. *Nucleic Acids Res.* **2004**, *32*, 1792–1797. [CrossRef]
13. Kimura, M. A simple method for estimating evolutionary rates of base substitutions through comparative studies of nucleotide sequences. *J. Mol. Evol.* **1980**, *16*, 111–120. [CrossRef] [PubMed]
14. Smith, M.A.; Fisher, B.L.; Hebert, P. DNA barcoding for effective biodiversity assessment of a hyperdiverse arthropod group: The ants of Madagascar. *Philos. Trans. R. Soc. B Biol. Sci.* **2005**, *360*, 1825–1834. [CrossRef] [PubMed]
15. Schlick-Steiner, B.C.; Steiner, F.M.; Moder, K.; Seifert, B.; Sanetra, M.; Dyreson, E.; Stauffer, C.; Christian, E. A multidisciplinary approach reveals cryptic diversity in Western Palearctic *Tetramorium* ants (Hymenoptera: Formicidae). *Mol. Phylogenet. Evol.* **2006**, *40*, 259–273. [CrossRef] [PubMed]
16. Nguyen, L.T.; Schmidt, H.A.; Von Haeseler, A.; Minh, B.Q. IQ-TREE: A fast and effective stochastic algorithm for estimating maximum-likelihood phylogenies. *Mol. Biol. Evol.* **2015**, *32*, 268–274. [CrossRef] [PubMed]
17. Zhang, J.; Kapli, P.; Pavlidis, P.; Stamatakis, A. A general species delimitation method with applications to phylogenetic placements. *Bioinformatics* **2013**, *29*, 2869–2876. [CrossRef] [PubMed]
18. Oberprieler, S.K.; Andersen, A.N.; Yeates, D.K. Selecting complementary target taxa for representing terrestrial invertebrate diversity in the Australian seasonal tropics. *Ecol. Indic.* **2020**, *109*, 105836. [CrossRef]
19. Andersen, A.N.; Lanoue, J.; Radford, I. The ant fauna of the remote Mitchell Falls area of tropical north-western Australia: Biogeography, environmental relationships and conservation significance. *J. Ins. Cons.* **2010**, *14*, 647–661. [CrossRef]
20. Cross, A.T.; Myers, C.; Mitchell, C.N.A.; Cross, S.L.; Jackson, C.; Waina, R.; Mucina, L.; Dixon, K.W.; Andersen, A.N. Ant biodiversity and its environmental predictors in the North Kimberley region of Australia's seasonal tropics. *Biodivers. Conserv.* **2016**, *25*, 1727–1759. [CrossRef]
21. Bowman, D.M.J.S.; Brown, G.K.; Braby, M.F.; Brown, J.R.; Cook, L.G.; Crisp, M.D.; Ford, F.; Haberle, S.; Hughes, J.; Isagi, Y.; et al. Biogeography of the Australian monsoon tropics. *J. Biogeogr.* **2010**, *37*, 201–216. [CrossRef]
22. Hölldobler, B.; Wilson, E.O. *The Ants*; Belknap Press of Harvard University Press: Cambridge, MA, USA, 1990; ISBN 0674040759.
23. Campos, R.I.; Vasconcelos, H.L.; Andersen, A.N.; Frizzo, T.L.M.; Spena, K.C. Multi-scale ant diversity in savanna woodlands: An inter-continental comparison. *Austral Ecol.* **2011**, *36*, 983–992. [CrossRef]
24. Andersen, A.N. Ant megadiversity and its origins in arid Australia. *Austral Entomol.* **2016**, *55*, 132–147. [CrossRef]

diversity

MDPI

Article

Bill Variation of Captive and Wild Chukar Partridge Populations: Shape or Size

Tamer Albayrak [1,*] and Ahmet İhsan Aytek [2]

[1] Department of Biology, Science and Art Faculty, Burdur Mehmet Akif Ersoy University, 15100 Burdur, Turkey
[2] Department of Anthropology, Science and Art Faculty, Burdur Mehmet Akif Ersoy University, 15100 Burdur, Turkey; aytek@mehmetakif.edu.tr
* Correspondence: talbayrak@mehmetakif.edu.tr

Abstract: Traditionally, morphological characters are widely used to distinguish between interspecies and intraspecies. In addition to the size of morphological characters, shape has also been used as an indicator in the last decades. We evaluated the geometric morphometry and morphometric of the bill of Chukar Partridge, *Alectoris chukar* from captive and wild populations to determine the bill variation and population relationships. Although there was a size difference between the sexes, no shape difference was found. However, captive populations differed from wild populations in both size and shape. Although there was no difference in shape among wild populations, some differences were found in size. Moreover, bill sizes of captive populations were statistically longer than western, centre, and eastern wild populations. It was also shown that the western populations had the most significant variation among the wild populations. The results revealed that using the size and shape together was more effective in comparing populations.

Keywords: *Alectoris chukar*; gamebirds; geometric morphometrics; morphometry; morphological diversity

1. Introduction

Morphological differences in species with the effect of evolutionary forces are significant in species identification, and these differences may be in the shape and the size of the morphological character. Moreover, Darwin described the finch species and explained their evolutionary relationship using bill characters. Supporting this argument, the size of the morphological characters was found to be important in distinguishing similar species from each other, such as Insecta [1], Amphibia [2], Reptilia [3], Mammalia [4], and Aves [5]. Although the size of morphometric characters is the same, species can be distinguished each other based on their shape [6–8]. In the morphological comparisons of different populations of the same species, geometric morphometry studies based on the shape of the morphological character, as well as the classical size comparison, have become increasingly common in the last decades [6,9–13].

Geometric morphometric is a method of shape analysis defined as the analysis of all geometric information taken from Cartesian coordinates of anatomical points [14]. Many scholars have argued that shape is more relevant than size because the shape is more variable than size between groups within a species [15,16]. Many shape differences can be seen between individuals due to different biological processes. Some shape differences can be attributed to disease or injury, ontogenetic development, adaptation to local geographic factors, and long-term evolutionary diversification [17]. Using geometric morphometry, species can be grouped into different animal classes, such as Mammalia [18,19], Reptilia and Amphibia [6,20,21], and Insecta [13,22,23].

The interest in using geometric morphometry on avian species has increased in the last decade [8–10,24–27]. In addition to actual specimens, geometric morphometry reveals significant results in avian fossil specimens [28]. Though most of the studies have focused

Citation: Albayrak, T.; Aytek, A.İ. Bill Variation of Captive and Wild Chukar Partridge Populations: Shape or Size. *Diversity* **2022**, *14*, 48. https://doi.org/10.3390/d14010048

Academic Editor: Luc Legal

Received: 16 December 2021
Accepted: 8 January 2022
Published: 12 January 2022

on the skull shape of avian species, some studies have provided valuable results with respect to bill shape changes. For example, Foster et al. [11] assessed Darwin finches' bill size and shape, and they reported that geometric morphometric analysis had better results than traditional measurements to discriminate specimens. In another study by Myczko et al. [8], three woodpecker species (*Dendrocopos major*, *Dendrocopos syriacus*, and *Dendrocopos leucotos*) were evaluated by traditional and geometric morphometric methods. The results showed that the species significantly differed in bill shapes, although the standard measurements were similar. Contrary to these studies, Kass et al. [29] reported that traditional morphometrics could separate two different skua species (*Catharacta antartica lonnbergi* and *Catharacta maccormcki*), but geometric morphometry could not separate them.

Morphological studies in birds are usually used to determine the size of the morphological characters [30] and to determine their differentiation between populations [2]. For example, Albayrak et al. [31] determined the description of the morphological characters of Kurper's Nuthatch, *Sitta krueperi* and revealed that some morphological characters were significantly different between the northern and southern populations in Anatolia.

Whereas morphometrical studies are concerned with the character's size, geometric morphometry is concerned with shape rather than size. In this respect, evaluating the size and shape of a morphological character together can be more efficient for comparing intraspecific and interspecific differentiation. We evaluated Chukar Partridge, *Alectoris chukar* samples from different wild and captive populations to compare their morphometric and geomorphometric differences and to determine their population relationship. The Chukar Partridge is farmed in many countries and released into nature since it is an important game bird. Its range is from the Balkans to the Middle East and Central Asia up to the Yellow Sea [32]. This study is based on the hypothesis that the size and shape of bills of Chukar Partridges may be different in wild and captive populations since the species is a non-migratory native species and the same lineage is used at the breeding stations. The bill of Chukar Partridge was studied to determine both the morphometry (size) and geometric morphometry (shape). In the light of the facts mentioned above, in this study, we aimed (i) to find out whether there is sexual dimorphism, (ii) to test the differences among different wild and captive populations, and (iii) to compare the shapes and sizes of the bills of Chukar Partridges.

2. Materials and Methods

2.1. Study Area

Wild Chukar Partridges were randomly sampled during the 2018–2019 hunting seasons in four western (Burdur: BUR, Çanakkale: CAN, Eskişehir: ESK, Muğla: MUG), three centre (Çankırı: CNK, Niğde: NIG, Sivas: SIV), and three eastern (Bitlis: BIT, Erzurum: ERZ, Van: VAN) localities throughout Turkey. We used three breeding stations (in Afyon: BSA, in Kahramanmaraş: BSK, in Malatya: BSM) belonging to the ministry. Approximately 10,000 Chukar Partridges are produced with the same bloodline in each breeding station annually. Captive ones were randomly selected and euthanized by the principal veterinary of each station. In total, 128 wild and 44 captive Chukar Partridges were sampled. All captive samples were used together in the analyses because they came from the same bloodline. All legal permissions required for study were obtained from the ministry. The MAKU-HADYEK-169 protocol controlled all the experiments on Chukar Partridges by MAKU, Local Ethical Committee on Animal Experiments regulations.

2.2. Molecular Sexing

The secondary sex characters of male and female Chukar Partridge are not wholly reliable in sex determination, for example, spur occurs in males and old females. For this reason, molecular sexing methods should be used to determine their sexes precisely. Muscle or blood tissues were preserved at room temperature in absolute ethanol. According to the manufacturer's instructions, total DNA was extracted using the Thermo, GeneJET Genomic DNA Purification Kit, or Qiagen Dneasy Blood & Tissue Kit. Molecular sex

determination was performed using 2550 F (5′-GTTACTGATTCGTCTACGAGA-3′) and 2718 R (5′-ATTGAAATGATCCAGTGCTTG-3′) primers. These primers were designed to amplify the homologous parts of CHD-W and the related gene CHD- Z. The PCR conditions were as follows: 100 to 200 ng/µL total DNA, 1 µL for each primer (2550F, 2718R), 0.2 µL Taq DNA Polymerase (Thermo Scientific), 5 µL dNTP mix, 2.5 µL MgCl2, 5 µL 10X PCR Buffer (Invitrogen), and sterile dH_2O up to a total volume of 50 µL. The PCR profile was performed with an initial denaturation step at 94 °C for 7 min, followed by 30 cycles of 94 °C denaturations for 60 s, annealing at 55.5 °C for 120 s, and extension at 72 °C for 60 s. A final 10 min extension at 72 °C completed the PCR profile. PCR products were separated by electrophoresis for 60 min at 80 V in a 3% agarose gel stained with cyber green and visualized under UV light. Due to size differences between the W and Z fragments, females displayed two bands, W and Z copies while males display one band, two copies of the Z fragment (Figure 1).

Figure 1. Molecular sexing results. One band is male, and two bands are female.

2.3. Morphometry

As suggested by Svensson [33], four morphometrical bill characters of the Chukar Partridge were measured using a digital calliper (0.01 mm) by the same researcher in the laboratory: bill length (**BL**), bill width (**BW**), bill height (**BH**), and length of the nostril to bill apex (**LNBa**) (File S1). Descriptive statistics, such as mean and standard deviation (SD) of the four bill sizes by locations and gender, were investigated before the further analyses. A quantile-quantile (Q-Q) plot showing these data distributions against the expected normal distribution and the Shapiro-Wilk normality test were used to investigate the morphometric characters for normal distributions. To determine whether there was sexual dimorphism (aim i) and differences among different wild and captive populations (aim ii), we used a *t*-test and Principal Component Analysis (PCA). Each bill character was used for the *t*-test to understand the potential differences between two groups, such as gender and location. Using all four bill characters together, Principal Component Analysis (PCA) was performed to determine whether there was a difference between genders and locations. PCA is a statistical analysis that allows us to summarize the information contained in large data tables by means of smaller set of summary indices that can be more easily visualized and analysed.

To understand the overall differentiation between the size or shape of the bill of Chukar Partridges (aim iii), we used all the samples without using sex information. All characters were used together in the Hopkins statistic and cluster analysis. The Hopkins statistic was conducted to understand whether our data could be clustered or not. The Hopkins

statistic is a way of measuring the cluster tendency of a dataset, and Hopkins statistic values greater than 0.5 indicate a tendency of data to cluster. This statistic measures the nearest-neighbour distance for each point in the dataset and compares this with the nearest distances from simulated datapoints to a real datapoint. Cluster analysis was performed to understand how many clusters the entire dataset would be grouped in without any location information. All statistical analyses were conducted using R Studio software [34].

2.4. Geometric Morphometry

We captured 2-dimensional photographs of the skull (18 × 205 Canon EOS 1000D with Sigma lens) from the right lateral side. The pictures were taken from 50 cm by a camera placed on a tripod with a water gauge. The landmarks were detected in two phases using Tps programs over 2-dimensional photographs. In the first phase, the pictures were introduced into the tpsUtil Version 1.60 [35] and saved as tps files. The landmarks were marked on the photographs in the second phase through the tpsDig2 Version 2.18 program [36], and the Cartesian coordinates were determined. Totally 7 landmarks were taken on the bill (Figure 2). To remove the effect of direction, position, and size on variation over the Cartesian coordinates obtained by marking the landmarks, these data were overlapped by Generalized Procrustes Analysis using the MorphoJ 1.06 [37]. We performed Prinicpal Component Analysis over the new coordinates obtained by overlapping, and the shape variation was revealed. In addition, it was shown that the principal components caused shape changes the landmarks' program using the MorphoJ 1.06. Data on the landmarks were saved as a text file for statistical analyses (File S1). The PAST 3.21 software was used for statistical analyses [38].

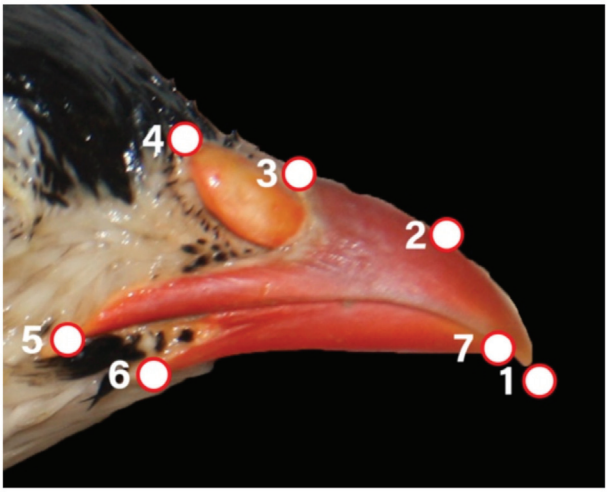

Figure 2. Landmarks used to describe the shape of Chukar Partridge's bill (the side of upper mandible, 1: tips, 2: middle, 3: the first place the feathers come out, 4: apex of nostril, 5: angle of the mouth; the side of under mandible, 6: rictus, 7: tips).

3. Results

3.1. Population Differences

The data of the morphometric characters and sizes of the bill were found to be normally distributed by a Shapiro-Wilk's test ($p < 0.05$) and a visual inspection of Q-Q plots (Figure 3). We found that 48 females and 50 males, accounted for 56.9% of the 172 samples using the molecular sexing method (File S1). Three sets of morphometric (**M**; size), geometric morphometric (**GM**; shape), and **M + GM** analyses were conducted to determine the sex differences of the Chukar Partridge's bill.

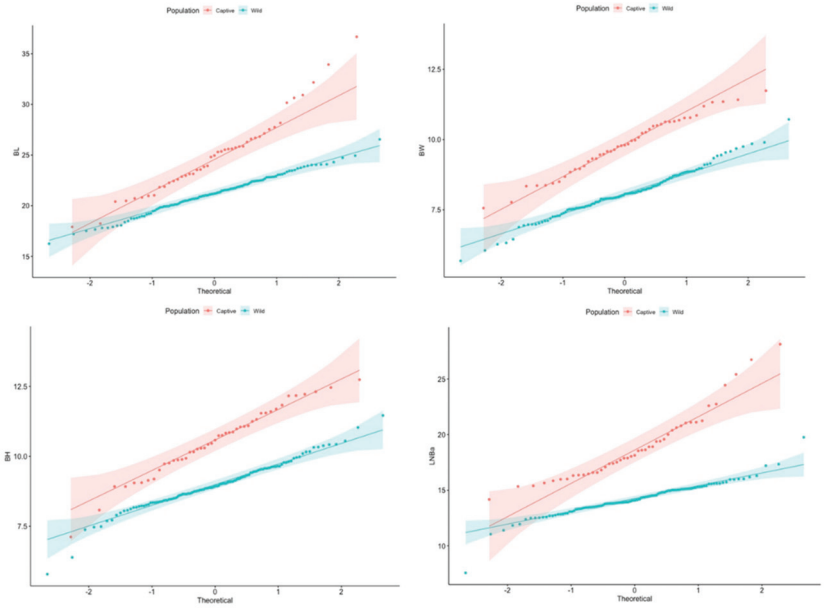

Figure 3. Visual inspection of the Q-Q plots of morphometric data of the wild and captive populations for each bill character.

We found some differentiation between male and female bill sizes, **M**, but not **BW** (Table 1). Chukar Partridge males were found to have bigger bill sizes than females. However, the PCA did not support the differentiation when using the four **M** characters together (Figure 4). In addition, no significant difference in bill shape, **GM**, was found between male and female specimens in wild, captive, and together (Figure 4). Furthermore, we did not find differences between sexes using **M + GM** together (Figure 4).

All specimens were evaluated together for comparison of the localities. The smallest bill length in the western populations was CAN and ESK for **BL**, ESK for **BH**, CAN for **BW**, and ESK for **LNBa**. The largest bill length was VAN for **BL**, SIV for **BH**, MUG for **BW**, and VAN for **LNBa** (Table 2). The bill sizes of captive populations were statistically bigger than the western, centre, and eastern wild populations ($p < 0.05$; Figure 5).

Table 1. Descriptive statistics of the morphometric data of bill characters and overall corporations of sexes using the *t*-test. ns: nonsignificant; *: $p < 0.05$; **: $p < 0.01$.

	Captive		Wild		Overall		
	Female (*n* = 12)	**Male (*n* = 10)**	**Female (*n* = 36)**	**Male (*n* = 40)**	**Female (*n* = 48)**	**Male (*n* = 50)**	***p***
BL							**
Mean (SD)	23.8 (3.18)	26.9 (4.48)	20.3 (1.85)	21.8 (1.42)	21.2 (2.71)	22.9 (3.07)	
Median [Min, Max]	23.5 [17.9, 30.6]	26.1 [20.8, 36.7]	20.1 [16.3, 23.4]	21.6 [18.9, 24.9]	21.1 [16.3, 30.6]	21.9 [18.9, 36.7]	
BW							ns
Mean (SD)	9.50 (0.907)	10.3 (0.861)	7.81 (0.814)	8.25 (0.766)	8.23 (1.11)	8.66 (1.14)	
Median [Min, Max]	9.56 [7.77, 11.2]	10.6 [8.34, 11.4]	7.89 [5.68, 9.85]	8.09 [6.05, 9.90]	8.02 [5.68, 11.2]	8.21 [6.05, 11.4]	
BH							
Mean (SD)	9.96 (1.01)	11.3 (1.04)	8.52 (0.704)	9.39 (0.715)	8.88 (1.00)	9.77 (1.09)	**
Median [Min, Max]	10.0 [8.08, 11.3]	11.6 [9.19, 12.5]	8.67 [5.79, 9.93]	9.44 [7.69, 11.5]	8.76 [5.79, 11.3]	9.57 [7.69, 12.5]	
LNBa							*
Mean (SD)	17.6 (1.60)	20.8 (2.99)	14.0 (1.07)	14.7 (1.02)	14.9 (2.01)	15.9 (2.92)	
Median [Min, Max]	16.9 [16.0, 21.0]	20.0 [17.5, 28.1]	13.9 [11.4, 16.0]	14.6 [12.7, 17.3]	14.4 [11.4, 21.0]	15.1 [12.7, 28.1]	

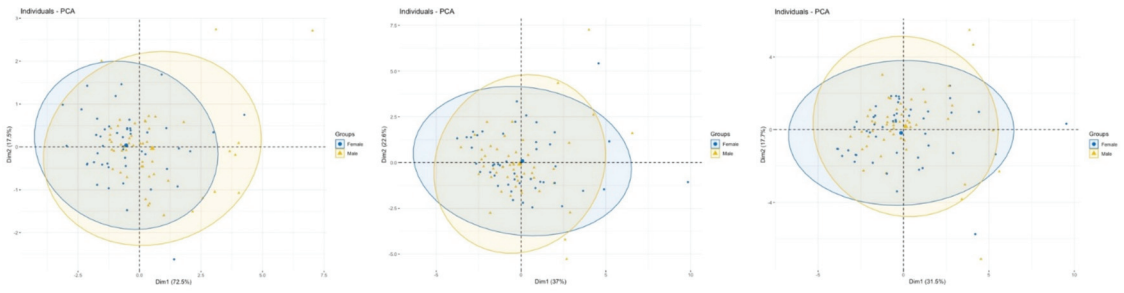

(**a**) (**b**) (**c**)

Figure 4. PCA of male (yellow) and female (blue) Chukar Partridges bills. (**a**) Morphometric (**M**; size), (**b**) geometric morphometric (**GM**; shape), and (**c**) **M + GM** together.

Table 2. Basic descriptive statistics of the bill for wild and captive populations. SD is given in parent brackets.

		Bill			
Location	***n***	**BL**	**BH**	**BW**	**LNBa**
Western					
BUR	13	21.8 (1.6)	9.2 (0.7)	8.5 (0.8)	14.4 (0.8)
CAN	9	20.4 (1.9)	8.8 (1.4)	7.5 (0.8)	13.9 (1.6)
ESK	21	20.4 (1.6)	8.6 (0.8)	7.9 (0.4)	13.6 (0.9)
MUG	8	20.3 (2.6)	9.3 (0.6)	8.9 (0.7)	13.7 (2.9)
Centre					
CNK	14	21.1 (1.3)	8.7 (0.6)	7.7 (0.9)	14.6 (1.1)
NIG	3	20.5 (0.7)	8.7 (0.4)	8.2 (0.9)	13.8 (1.2)
SIV	11	21.2 (1.6)	9.5 (0.9)	8.4 (0.7)	14.2 (0.9)
Eastern					
BIT	12	21.8 (1.7)	8.9 (0.5)	7.9 (0.5)	14.7 (0.9)
ERZ	12	20.9 (1.6)	8.8 (0.8)	7.9 (0.6)	14.1 (1.1)
VAN	11	22.8 (1.5)	9.3 (0.6)	7.9 (0.9)	14.9 (0.9)
Unknown	14	22.1 (3.1)	9.2 (0.8)	8.4 (1.0)	14.7 (2.9)
Captive					
BSA	6	25.4 (3.5)	9.0 (1.0)	8.2 (0.5)	19.0 (2.9)
BSK	21	26.4 (4.1)	11.0 (1.1)	10.1 (0.8)	20.2 (3.4)
BSM	17	22.8 (2.6)	10.4 (0.9)	10.0 (0.9)	17.0 (1.4)
Total					
Wild	128	21.3 (1.9)	8.9 (0.8)	8.1 (0.8)	14.3 (1.5)
Captive	44	24.9 (3.8)	10.5 (1.2)	9.8 (1.0)	18.8 (3.1)
Total	172	22.2 (3.0)	9.4 (1.1)	8.5 (1.1)	15.4 (2.8)

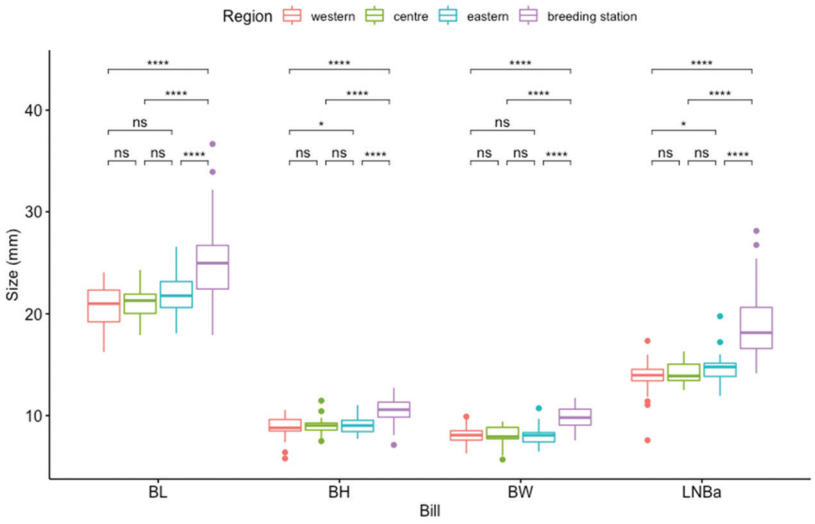

Figure 5. Comparison of bill length by regions. ns: nonsignificant, *: $p < 0.05$, ****: $p < 0.0001$.

3.2. Comparison of Size and Shape

The principle component analysis showed that the variation in captive specimens was more remarkable than wild specimens for **M**, **GM**, and **M + GM** (Figure 6). All wild populations—western, centre, and eastern—were mixed in the PCA of **M**, **GM**, and **M + GM**. Although the **M** and **M + GM** of captive Chukar Partridges were different than the wild populations separated from Dim 1, the difference of **GM** was not fully observed (Figure 6).

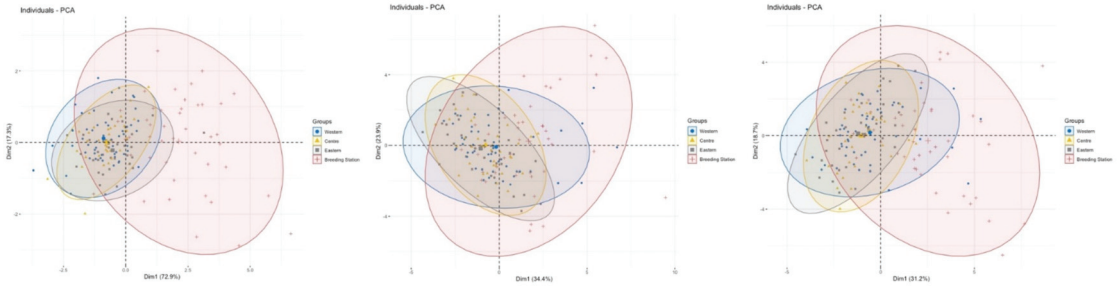

(**a**) (**b**) (**c**)

Figure 6. PCA of the bills from the locations of Chukar Partridges. The colours represent localities, blue: western, yellow: centre, grey: eastern, red: breeding station. (**a**) Morphometric (**M**; size), (**b**) geometric morphometric (**GM**; shape), and (**c**) **M + GM** together.

The Hopkins statistic shows that these data are highly clustered. The lowest similarity was the size, followed by the shape and size + shape, respectively (**M** = 0.83, **GM** = 0.77, **M + GM** = 0.75; Figure 7), when using all samples together without any location information. The optimal number of clusters was one for the **M**, **GM**, and **M + GM** data using all samples together in cluster analysis. The second optimal number of clusters was three for **M** and **GM** but four for **M + GM** (Figure 7).

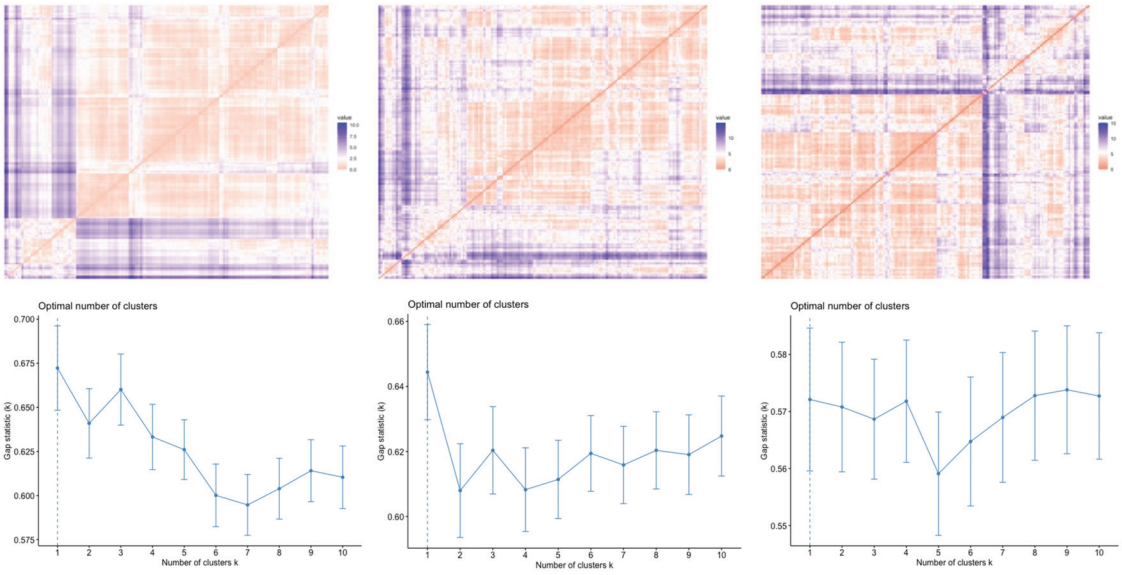

(**a**) (**b**) (**c**)

Figure 7. The top is the Hopkins statistic (Red: high similarity (i.e., low dissimilarity) | Blue: low similarity). Hopkins statistic: **M** = 0.83, **GM** = 0.77, **M + GM** = 0.75). The bottom is a cluster analysis of all bills of Chukar Partridges using all samples together without any locations information. (**a**) Morphometric (**M**; size), (**b**) geometric morphometric (**GM**; shape), and (**c**) **M + GM** together.

4. Discussion

Our results indicate the population diversity of the bill in wild and captive Chukar Partridges populations located in Turkey. The bill size and shape of Chukar Partridges were compared between sexes and locations.

4.1. Population Differences

Chukar Partridge is one of the most famous game birds throughout America, Europe, and Asia [39]. Although both sexes are very similar morphologically, the traditional method of identifying males with a spur at the tarsus is unreliable because old females have also spurred. Sex ratios need to be known to analyse the population's effective population size and trend. In general, the proportion of sexes in the population is theoretically expected to be 1:1 if the production costs of males and females are equal, and this ratio is essential in protecting endangered species [40,41]. The molecular sexing method, which helps determine the sexes of species such as the Black Francolin (*Francolinus francolinus*) [42] and Woodcock (*Scolopax rusticola*) [43] without secondary sex characteristics and chicks [44], was also used for Chukar Partridges. As a result of using the molecular sexing method on 98 randomly selected Chukar Partridges, the sex ratio was found in the population with the theoretically expected 1:1 ratio (F:M, 0.98:1.02), showing that there is no selection on one sex in the population. Males of Chukar Partridges are larger than females [39]. This was also found in bill size, with males having a more extended bill size. We found that captive Chukar Partridges have a longer bill than wild individuals. Although there were some differences in morphometric size (**M**) between the sexes, no difference was found in shape based on the geometric morphometric (**GM**) analysis. We understood that the sizes of the morphometric characters of the bill are different except for **BW**, but the shape is same in male and female Chukar Partridges. The reason why the bill shape is the same while the size is different between genders may be related to the fact the only difference

between partridges of different sexes is body size [39]. However, the PCA showed that when size (**M**), shape (**GM**), and size + shape (**M + GM**) were evaluated, there was no size or shape difference between the sexes. As a result, all samples were assessed together without gender information. We used the PCA because the values could be log-transformed and standardized. Kark et al. [45] suggested that there were two possibilities for applying a PCA: one could run (i) a separate PCA of the individuals in each population or (ii) an overall PCA of individuals in all populations combined, and then project each population onto the new global principle component variables and calculate variances.

When we evaluated all samples together, similar results were only found with sex-specific evaluation, revealing that the lengths of all **M** characters of Chukar Partridges in breeding stations were statistically larger than the wild ones ($p < 0.05$). A larger bill in captive individuals may be due to the feeding strategy in breeding stations and the fact that partridges are produced in small cage environments. Moreover, while Chukar Partridges feed in the natural environment, they prevent their bills from elongating by rubbing them on the ground and stones. Captive Chukar Partridges' bills may have been longer because they could not perform these behaviours in a cage environment. Areas of environmental transition, ecotone, and heavy metal affected the bill size of Chukar Partridges [45,46]. When only wild populations were evaluated, it was determined that the eastern Chukar Partridges had statistically longer **BL** and **LNBa** than western populations. This longer bill of eastern Chukar Partridges may be related to the Bergmann hypothesis that individuals living in cold regions are larger than individuals living in hot regions. The eastern region has a colder climate than the western region in Turkey. Similarly, it was found that the populations living in cold areas are larger [47]. When localities were compared with respect to bill shape (**GM**), individuals in breeding stations were more diverse but were not statistically different from wild ones. Although **GM** studies on *Geospiza fortis* [11] and *Tyrannus savana* species [25] found a shape difference between populations, no such difference was determined between the populations of Chukar Partridge.

4.2. Comparison of Size and Shape

Traditionally, **M** characters, i.e., size, are important markers used to distinguish species [1] and to determine differences between populations of the same species [5]. **GM** studies developed in the last decade have been used to distinguish morphometric characters, such as the bill, based on shape differences rather than size [10,24,28,29]. Thus, it was found that there is a significant difference in bill shape, whereas the traditional body measurements between the Great Spotted Woodpecker and Syrian Woodpecker are similar [8]. Furthermore, geometric morphometry is also valuable for showing shape differences in different populations of the same species [9,10,26]. In differentiating species of the Scolopacidae family from each other, in addition to bill size, the shape is also important in the distinction of the species identification, i.e., whether the bill is flat, down, or upwardly curved [48]. Bill lengths of Chukar Partridges in the breeding station were statistically separated from the wild ones, but an absolute difference was not found in shape. This is because the bill shapes of Chukar Partridges are the same, but their sizes are different. When only wild populations were evaluated, although the shape variation was high, no statistical difference was found in terms of shape or size. Moreover, when **M + GM** were assessed together, no significant difference was found.

The Hopkins statistics revealed different levels of general clustering tendency for bird songs [49]. The Hopkins statistic values were found as **M** = 0.83, **GM** = 0.77, **M + GM** = 0.75 when all samples were evaluated without locality information. The Hopkins statistic values of our data were found to be greater than 0.5. This value indicated that our data were suitable to cluster. In addition, the Hopkins' statistic values greater than 0.5 with larger k values indicate a tendency of data to cluster in larger cluster sizes. The highest Hopkins statistic value was found in **M**, followed by **GM** and **M + GM**. When we performed cluster analyses, we found that in all three cluster analyses for **M**, **GM**, and **M + GM**, the optimal number of the cluster was determined as 1. However, the second optimal cluster number

was **M**, whereas **GM** was 3 and **M + GM** was 4. This is compatible with the four regions, the western, centre, eastern, and breeding stations used in the study. Klingenberg [7] suggested that not only size but also shape should be used in allometric studies. Allometry refers to the size-related changes of morphological traits and remains an essential concept for studying evolution and development. This has led to the conclusion that, in addition to comparing populations in terms of size and shape of the morphological character, both **M** and **GM** may be more effective in grouping the populations.

5. Conclusions

We compared the size and shape of the bill of Chukar Partridge from captive and wild populations. Although there was a difference between the sexes of Chukar Partridges in bill length, no difference was found in shape. In addition, we found a significant difference in size between captive and wild populations, but difference was found in shape. Moreover, there was no significant difference in size or shape between the wild populations evaluated. The hypothesis of the study that "the size and shape of bills of Chukar Partridges may be different in wild and captive populations" was partially confirmed for size, but it was not confirmed for shape. The morphological characters used to compare populations should not be evaluated only as size or shape. Instead, both size and shape should be considered together to make a more efficient grouping.

Supplementary Materials: The following supporting information can be downloaded at: https://www.mdpi.com/article/10.3390/d14010048/s1, File S1: Data of M and GM.

Author Contributions: A.İ.A. and T.A. designed and directed the study. T.A. provided material, conducted genetic tests for sex determination, and conducted metric analysis. A.İ.A. conducted the geometric morphometric analysis. All authors have read and agreed to the published version of the manuscript.

Funding: This research was funded by TUBITAK, 117O580.

Institutional Review Board Statement: The animal study protocol was approved by The MAKU-HADYEK-169 protocol controlled all the experiments on Chukar Partridges by MAKU, Local Ethical Committee on Animal Experiments regulations.

Informed Consent Statement: Not applicable.

Data Availability Statement: The data presented in this study are available in Supplementary Material File S1.

Acknowledgments: The authors would like to thank the farmers, hunters, lab volunteers, and the DKMPGM for their help and cooperation. Furthermore, the authors would like to thank Özlem Özmen for preparing the samples.

Conflicts of Interest: The authors declare no conflict of interest.

References

1. Rivas, N.; Sánchez Espíndola, M.E.; Camacho, A.D.; Moreno, E.R.; Rocha-Gómez, M.A.; Aguilar, R.A. Morphology and morphometry of the scutellum of six species in the genus *Meccus* (Hemiptera: Triatominae). *J. Vector Ecol.* **2014**, *39*, 14–20. [CrossRef] [PubMed]
2. Papežík, P.; Kubala, M.; Jablonski, D.; Doležálková-Kaštánková, M.; Choleva, L.; Benovics, M.; Mikulíček, P. Morphological differentiation of endemic water frogs (Ranidae: *Pelophylax*) from the southwestern balkans. *Salamandra* **2021**, *57*, 105–123.
3. Kadry, M.A.M.; Al-Qahtani, A.R.; Amer, S.A.M. Morphometric and molecular differentiation between Egyptian *Stellagama stellio vulgaris* and *S. stellio salehi* (Reptilia: Agamidae). *Zool. Middle East* **2020**, *66*, 295–301. [CrossRef]
4. Islam, M.M.; Farag, E.; Mahmoudi, A.; Hassan, M.M.; Atta, M.; Mostafavi, E.; Alnager, I.A.; Farrag, H.A.; Eljack, G.E.A.; Bansal, D.; et al. Morphometric study of *Mus musculus*, *Rattus norvegicus*, and *Rattus rattus* in Qatar. *Animals* **2021**, *11*, 2162. [CrossRef]
5. Kayvanfar, N.; Aliabadian, M.; Ghasempouri, S.M. Morphometric and morphological differentiation of the subspecies of *Phasianus colchicus* (Linnaeus, 1758) on the Iranian Plateau (Aves: Galliformes). *Zool. Middle East* **2015**, *61*, 9–17. [CrossRef]
6. Liu, Q.; Xiong, J.; Gou, J.; Gao, X. Geographic variation in the skull morphometry of four populations of *Batrachuperus karlschmidti* (Urodela: Hynobiidae). *Asian Herpetol. Res.* **2020**, *11*, 194–204. [CrossRef]

7. Klingenberg, C.P. Size, shape, and form: Concepts of allometry in geometric morphometrics. *Dev. Genes Evol.* **2016**, *226*, 113–137. [CrossRef]
8. Myczko, Ł.; Mizerová, Z.; Kubicka, A.M.; Sparks, T.H.; Hromada, M. Bill morphology and biometrics of three sibling woodpecker species from sympatric populations. *Bird Study* **2020**, *67*, 8–18. [CrossRef]
9. Angst, D.; Barnoud, J.; Cornette, R.; Chinsamy, A. Sex and Ontogenetic Variation in the Crest of *Numida meleagris*: Implications for Crested Vertebrates. *Anat. Rec.* **2020**, *303*, 1018–1034. [CrossRef]
10. Dalton, H.A.; Wood, B.J.; Widowski, T.M.; Guerin, M.T.; Torrey, S. An analysis of beak shape variation in two ages of domestic turkeys (*Meleagris gallopavo*) using landmark-based geometric morphometrics. *PLoS ONE* **2017**, *12*, e0185159. [CrossRef]
11. Foster, D.J.; Podos, J.; Hendry, A.P. A geometric morphometric appraisal of beak shape in Darwin's finches. *J. Evol. Biol.* **2008**, *21*, 263–275. [CrossRef]
12. Souza, A.T.; Soukalová, K.; Děd, V.; Šmejkal, M.; Blabolil, P.; Říha, M.; Jůza, T.; Vašek, M.; Čech, M.; Peterka, J.; et al. Ontogenetic and interpopulation differences in otolith shape of the European perch (*Perca fluviatilis*). *Fish. Res.* **2020**, *230*, 105673. [CrossRef]
13. Wells, C.; Munn, A.; Woodworth, C. Geomorphic Morphometric Differences between Populations of *Speyeria diana* (Lepidoptera: Nymphalidae). *Florida Entomol.* **2018**, *101*, 195–202. [CrossRef]
14. Slice, D.E. Geometric morphometrics. *Annu. Rev. Anthropol.* **2007**, *36*, 261–281. [CrossRef]
15. Ariza-Marín, E.R.; De Luna, E. Linear and geometric morphometric analyses of variation of the plectrum in four species of bess beetles, tribe Proculini (Coleoptera: Passalidae). *Arthropod Struct. Dev.* **2020**, *59*, 100994. [CrossRef]
16. Corruccini, R.S. Shape in morphometrics: Comparative analyses. *Am. J. Phys. Anthropol.* **1987**, *73*, 289–303. [CrossRef]
17. Zelditch, M.; Swiderski, D.; Sheets, H.; Fink, W. *Geometric Morphometrics for Biologists*; Elsevier: New York, NY, USA, 2004; ISBN 9780127784601.
18. Cardini, A. Modern morphometrics and the study of population differences: Good data behind clever analyses and cool pictures? *Anat. Rec.* **2020**, *303*, 2747–2765. [CrossRef]
19. Cardini, A.; Elton, S.; Kovarovic, K.; Strand Viðarsdóttir, U.; Polly, P.D. On the Misidentification of Species: Sampling Error in Primates and Other Mammals Using Geometric Morphometrics in More than 4000 Individuals. *Evol. Biol.* **2021**, *48*, 190–220. [CrossRef]
20. Gray, J.A.; McDowell, M.C.; Hutchinson, M.N.; Jones, M.E.H. Geometric morphometrics provides an alternative approach for interpreting the affinity of fossil lizard jaws. *J. Herpetol.* **2017**, *51*, 375–382. [CrossRef]
21. Kaliontzopoulou, A. Geometric morphometrics in herpetology: Modern tools for enhancing the study of morphological variation in amphibians and reptiles. *Basic Appl. Herpetol.* **2011**, *25*, 5–32. [CrossRef]
22. Tatsuta, H.; Takahashi, K.H.; Sakamaki, Y. Geometric morphometrics in entomology: Basics and applications. *Entomol. Sci.* **2018**, *21*, 164–184. [CrossRef]
23. Sumruayphol, S.; Chaiphongpachara, T. Geometric morphometrics as a tool for three species identification of the firefly (Coleoptera: Lampyridae) in Thailand. *Biodiversitas* **2019**, *20*, 2388–2395. [CrossRef]
24. Bright, J.A.; Marugán-Lobón, J.; Cobb, S.N.; Rayfield, E.J. The shapes of bird beaks are highly controlled by nondietary factors. *Proc. Natl. Acad. Sci. USA* **2016**, *113*, 5352–5357. [CrossRef]
25. Carvalho Provinciato, I.C.; Araújo, M.S.; Jahn, A.E. Drivers of wing shape in a widespread Neotropical bird: A dual role of sex-specific and migration-related functions. *Evol. Ecol.* **2018**, *32*, 379–393. [CrossRef]
26. Gündemir, O.; Özkan, E.; Dayan, M.O.; Aydoğdu, S. Sexual analysis in Turkey (*Meleagris gallopavo*) neurocranium using geometric morphometric methods. *Turkish J. Vet. Anim. Sci.* **2020**, *44*, 681–687. [CrossRef]
27. Tokita, M.; Yano, W.; James, H.F.; Abzhanov, A. Cranial shape evolution in adaptive radiations of birds: Comparative morphometrics of Darwin's finches and Hawaiian honeycreepers. *Philos. Trans. R. Soc. B Biol. Sci.* **2017**, *372*, 20150481. [CrossRef]
28. Haidr, N.S.; Acosta Hospitaleche, C. Fossil penguin beaks from the Eocene of Antarctica: New materials from La Meseta Formation. *Contrib. MACN* **2017**, *1*, 57–68.
29. Kass, N.; Montalti, D.; Acosta Hospitaleche, C. Comparison of the skull of Brown Skua (*Catharacta antarctica lonnbergi*) and South Polar Skua (*Catharacta maccormicki*): Differentiation source identification and discriminant analysis. *Polar Biol.* **2018**, *41*, 1049–1053. [CrossRef]
30. Ottvall, R.; Gunnarsson, G. Morphological and molecular sex identification of Redshanks *Tringa totanus*. *Bird Study* **2007**, *54*, 127–129. [CrossRef]
31. Albayrak, T.; Besnard, A.; Erdogan, A. Morphometric Variation and Population Relationships of Kruper's Nuthatch (*Sitta krueperi*) in Turkey. *Wilson J. Ornithol.* **2011**, *123*, 734–740. [CrossRef]
32. Madge, S.; McGowan, P. *Pheasants, Partridges, and Grouse: A Guide to the Pheasants, Partridges, Quails, Grouse, Guineafowl, Buttonquails, and Sandgrouse of the World*; Christopher Helm, A & C Black: London, UK, 2002.
33. Svensson, L. *Identification Guide to European Passerines*; British Trust for Ornithology: Norfolk, UK, 1992.
34. R Core Team. *R: A Language and Environment for Statistical Computing*; R Foundation for Statistical Computing: Vienna, Austria, 2021. Available online: http://www.R-project.org (accessed on 3 March 2021).
35. Rohlf, F.J. *TpsUtil*, Version 1.60; Department of Ecology and Evolution, State University of New York: Stone Brook, NY, USA, 2013.
36. Rohlf, F.J. *TpsDig2*, Version 2.18; Department of Ecology and Evolution, State University of New York: Stone Brook, NY, USA, 2015.
37. Klingenberg, C.P. MorphoJ: An integrated software package for geometric morphometrics. *Mol. Ecol. Resour.* **2011**, *11*, 353–357. [CrossRef] [PubMed]

38. Hammer, Ø.; Harper, D.A.T.; Ryan, P.D. Past: Paleontological statistics software package for education and data analysis. *Palaeontol. Electron.* **2001**, *4*, 1–9.
39. Christensen, G.C. Chukar (*Alectoris chukar*), version 1.0. In *Birds of the World*; Poole, A.F., Gill, F.B., Eds.; Cornell Lab of Ornithology: Ithaca, Greece, 2020.
40. Ewen, J.G.; Clarke, R.H.; Moysey, E.; Boulton, R.L.; Crozier, R.H.; Clarke, M.F. Primary sex ratio bias in an endangered cooperatively breeding bird, the black-eared miner, and its implications for conservation. *Biol. Conserv.* **2001**, *101*, 137–145. [CrossRef]
41. Robertson, B.C.; Elliott, G.P.; Eason, D.K.; Clout, M.N.; Gemmell, N.J. Sex allocation theory aids species conservation. *Biol. Lett.* **2006**, *2*, 229–231. [CrossRef] [PubMed]
42. Forcina, G.; Guerrini, M.; Khaliq, I.; Khan, A.A.; Barbanera, F. Human-modified biogeographic patterns and conservation in game birds: The dilemma of the black francolin (*Francolinus francolinus*, Phasianidae) in Pakistan. *PLoS ONE* **2018**, *13*, e0205059. [CrossRef]
43. Aradis, A.; Landucci, G.; Tagliavia, M.; Bultrini, M. Sex determination of Eurasian Woodcock *Scolopax rusticola*: A molecular and morphological approach. *Avocetta* **2015**, *39*, 83–89.
44. Kabasakal, B.; Albayrak, T. Offspring sex ratios and breeding success of a population of the Great Tit, *Parus major* (Aves: Passeriformes). *Zool. Middle East* **2012**, *57*, 27–34. [CrossRef]
45. Kark, S.; Mukerji, T.; Safriel, U.N.; Noy-Meir, I.; Nissani, R.; Darvasi, A. Peak morphological diversity in an ecotone unveiled in the chukar partridge by a novel Estimator in a Dependent Sample (EDS). *J. Anim. Ecol.* **2002**, *71*, 1015–1029. [CrossRef]
46. Albayrak, T.; Pekgöz, A.K. Heavy metal effects on bird morphometry: A case study on the house sparrow *Passer domesticus*. *Chemosphere* **2021**, *276*, 130056. [CrossRef]
47. Asthon, K.G. Patterns of Within-Species Body Size Variation of Birds: Strong Evidence for Bergmann's. *Glob. Ecol. Biogeogr.* **2002**, *11*, 505–523.
48. Barbosa, A.; Moreno, E. Evolution of foraging strategies in shorebirds: An ecomorphological approach. *Auk* **1999**, *116*, 712–725.
49. Lachlan, R.F.; Verhagen, L.; Peters, S.; Ten Cate, C. Are There Species-Universal Categories in Bird Song Phonology and Syntax? A Comparative Study of Chaffinches (*Fringilla coelebs*), Zebra Finches (*Taenopygia guttata*), and Swamp Sparrows (*Melospiza georgiana*). *J. Comp. Psychol.* **2010**, *124*, 92–108. [CrossRef]

diversity

MDPI

Communication

Multi-Locus Phylogenetic Analyses of the Almadablennius Clade Reveals Inconsistencies with the Present Taxonomy of Blenniid Fishes

Luca Vecchioni [1], Andrew C. Ching [2,3], Federico Marrone [1], Marco Arculeo [1], Peter J. Hundt [2,3,*] and Andrew M. Simons [2,3]

[1] Department of Biological, Chemical and Pharmaceutical Sciences and Technologies (STEBICEF), University of Palermo, Via Archirafi 18, 90123 Palermo, Italy; luca.vecchioni@unipa.it (L.V.); federico.marrone@unipa.it (F.M.); marco.arculeo@unipa.it (M.A.)
[2] Department of Fisheries, Wildlife and Conservation Biology, University of Minnesota, Saint Paul, MN 55108, USA; ching051@umn.edu (A.C.C.); asimons@umn.edu (A.M.S.)
[3] Bell Museum, University of Minnesota, Saint Paul, MN 55113, USA
* Correspondence: hundt002@umn.edu

Abstract: We used a multi-locus phylogenetic approach (i.e., combining both mitochondrial and nuclear DNA fragments) to address some long-standing taxonomic inconsistencies within the diverse fish clade of Combtooth Blennies (Blenniidae—unranked clade Almadablennius). The obtained phylogenetic trees revealed some major inconsistencies in the current taxonomy of Parablennini, such as the paraphyletic status of the *Salaria* and *Parablennius* genera, casting some doubt regarding their actual phylogenetic relationship. Furthermore, a scarce-to-absent genetic differentiation was observed among the three species belonging to the genus *Chasmodes*. This study provides an updated taxonomy and phylogeny of the former genus *Salaria*, ascribing some species to the new genus *Salariopsis* gen. nov., and emphasizes the need for a revision of the genus *Parablennius*.

Keywords: Blenniidae; phylogeny; *Parablennius*; *Salaria*

Citation: Vecchioni, L.; Ching, A.C.; Marrone, F.; Arculeo, M.; Hundt, P.J.; Simons, A.M. Multi-Locus Phylogenetic Analyses of the Almadablennius Clade Reveals Inconsistencies with the Present Taxonomy of Blenniid Fishes. *Diversity* **2022**, *14*, 53. https://doi.org/10.3390/d14010053

Academic Editor: Michael Wink

Received: 14 December 2021
Accepted: 11 January 2022
Published: 14 January 2022

1. Introduction

Combtooth blennies (Blenniidae Rafinesque 1810; herein, blennies) are a diverse clade (>400 species) of nearshore, cryptobenthic fishes that inhabit temperate and tropical marine environments and inland water bodies worldwide [1]. The first major revisions of blenny taxonomy since Norman [2], subdivided the family into six tribes [3,4], each of which was characterized by generic revisions based on morphological characters (Salariini, [5], Omobranchini [6], Phenablenniini [4]; Nemophini [7], and Parablenniini and Blenniini [8–10]). The specific membership of these tribes, and generic boundaries within, have remained relatively stable, with the exception of Parablenniini and Blenniini, which have been the subject of great disagreement since Zander [9] rejected the new genera set by Bath [8] (See Table 1 in [11] for history of generic revisions).

Our understanding of the taxonomy of this group has changed significantly with the advent of molecular systematics. In particular, the Almadablennius clade (Parablenniini + Blenniini [12]) has received much attention since Almada et al. [11] published a phylogeny where Blenniini *sensu* Williams [13] was nested within Parablennini *sensu* Williams [13] and the genus *Lipophrys* was paraphyletic, demonstrating that the available taxonomy was inconsistent with phylogeny. Subsequent efforts to investigate the relationships and clarify taxonomy within the Almadablennius clade (e.g., [12,14–17]), have led to useful taxonomic changes, such as *Microlipophyrs* being split from *Lipophrys* (e.g., [15]) and the resolution of species membership within Blenniini and Parablenniini. Despite these updates and multiple lines of evidence suggesting problems, the taxonomy of the Almadablennius clade remains unresolved (e.g., paraphyly of *Parablennius*, *Hypleurochilus* and

Salaria, and deep split between Mediterranean and Atlantic specimens of *Scartella cristata*; see Hundt and Simons [16]). In the light of these problems, we re-examined the phylogenetic relationships of the Almadablennius clade using partial sequences of two nuclear and two mitochondrial loci with the explicit aim of testing the monophyly and revising the taxonomy of the genus *Salaria*.

2. Methods

A total of 49 specimens of blennies belonging to 32 morphospecies were collected in the field or obtained as gifts from the colleagues listed in the acknowledgment section (Table 1). Specimens were fixed in 96% ethanol in situ and identified in the laboratory, using the most updated morphological identification keys [18–20].

Table 1. List of species sampled, catalog number, locality, and GenBank accession number for molecular loci sampled. Novel GenBank accession numbers are reported in bold. * *Salariopsis* gen. nov. Roman numbers in brackets refer to analysed specimens shown in Figure 1.

Species	Taxonomical Remarks	Catalog Number	Locality	*ENC1*	*MYH6*	*16S*	*Dloop*
Aidablennius sphynx (Valenciennes, 1836)	-	MNHN 2012-0219	Balearic Islands, Spain	KF678553	KF678648	**MW980003**	**MZ026013**
Blennius ocellaris Linnaeus, 1758	-	MNHN 2012-0221	Balearic Islands, Spain	KF678554	KF678649	**MW980004**	**MZ026014**
Chasmodes bosquianus (Lacepède, 1800)	-	JFBM 46472-2	Virgnia, USA	KF678501	KF678601	**MW980005**	**MZ026015**
Chasmodes longimaxilla Williams, 1983	-	JFBM 46845-1433	Texas, USA	KF678530	KF678627	**MW980006**	**MZ026016**
Chasmodes saburrae Jordan and Gilbert, 1882	-	JFBM 46414-2	Florida, USA	KF678500	KF678600	**MW980007**	**MZ026017**
Hypleurochilus bananensis (Poll, 1959)	-	EFMM-20-201013	Bacoli, Italy	**MZ025976**	**MZ025994**	**MW980008**	**MZ026018**
Hypleurochilus fissicornis (Quoy and Gaimard, 1824)	-	-	Chile	MG779097	MG779132	**MW980009**	**MZ026019**
Hypleurochilus geminatus (Wood, 1825)	-	JFBM 46839-TX-002	Texas, USA	KF678526	KF678623	**MW980010**	**MZ026020**
Parablennius incognitus (I) Miranda Ribeiro, 1915	-	MNHN 2012-0237	Balearic Islands, Spain	KF678558	KF678653	**MW980011**	-
Parablennius incognitus (II)	-	EFMM-8-090815	Milazzo, Italy	**MZ025977**	**MZ025995**	**MW980012**	**MZ026021**
Parablennius incognitus (III)	-	EFMM-12–140815	Avola, Italy	**MZ025978**	**MZ025996**	**MW980013**	**MZ026022**
Parablennius intermedius Miranda Ribeiro, 1915	-	AMS I.45631-021	New South Wales, Australia	KF678474	KF678576	**MW980014**	**MZ026023**
Parablennius pilicornis Miranda Ribeiro, 1915	-	MNHN 2012-0240	Banyuls sur Mer, France	KF678560	KF678655	**MW980015**	**MZ026024**
Parablennius rouxi Miranda Ribeiro, 1915	-	MNHN 2012-0242	Banyuls sur Mer, France	KF678561	MG779139	**MW980016**	**MZ026025**
Parablennius salensis Miranda Ribeiro, 1915	-	JFBM 47280-1	Cape Verde	MG779103	-	**MW980017**	**MZ026026**
Parablennius tasmanianus Miranda Ribeiro, 1915	-	SAMAF 12607	Sturt Bay, Australia	MG779104	MG779141	**MW980018**	**MZ026027**

Table 1. *Cont.*

Species	Taxonomical Remarks	Catalog Number	Locality	*ENC1*	*MYH6*	*16S*	*Dloop*
Parablennius tentacularis Miranda Ribeiro, 1915	-	MNHN 2012-0406-BPS2265	Port-Vendres, France	MG779105	-	**MW980019**	**MZ026028**
Parablennius yatabei Miranda Ribeiro, 1915	-	JFBM 47154-1568	Kochi, Japan	KF678540	KF678636	**MW980020**	**MZ026029**
Parablennius zvonimiri (I) Miranda Ribeiro, 1915	-	EFMM-25-100716	Avola, Italy	**MZ025979**	**MZ025997**	**MW980021**	**MZ026030**
Parablennius zvonimiri (II)	-	MNHN 2012-0247	Banyuls sur Mer, France	KF678564	KF678657	**MW980022**	**MZ026031**
Hypsoblennius hentz (Lesueur, 1825)	-	JFBM 46471-VIMS10-78	Virgnia, USA	KF678572	KF678666	**MW980023**	**MZ026032**
Hypsoblennius sordidus (Bennett, 1828)	-	-	Chile	MG779098	MG779133	**MW980024**	**MZ026033**
Parablennius gattorugine (I) Miranda Ribeiro, 1915	-	MNHN 2012-0229	Banyuls sur Mer, France	KF678557	KF678652	**MW980025**	**MZ026034**
Parablennius gattorugine (II)	-	EFMM-16-060915	Avola, Italy	**MZ025980**	**MZ025998**	**MW980026**	**MZ026035**
Parablennius parvicornis Miranda Ribeiro, 1915	-	MNHN 2012-0238	Terceira, Azores	KF678559	KF678654	**MW980027**	**MZ026036**
Parablennius ruber Miranda Ribeiro, 1915	-	MNHN 2012-0243	Terceira, Azores	KF678562	MG779140	**MW980028**	**MZ026037**
Parablennius sanguinolentus (I) Miranda Ribeiro, 1915	-	EFMM-23-181115	Ognina, Italy	**MZ025981**	**MZ025999**	**MW980029**	**MZ026038**
Parablennius sanguinolentus (II)	-	EFMM-27-100716	Avola, Italy	**MZ025982**	**MZ026000**	**MW980030**	**MZ026039**
Parablennius sanguinolentus (III)	-	MNHN 2012-0246	Banyuls sur Mer, France	KF678563	KF678656	**MW980031**	**MZ026040**
Salaria basilisca (I) (Valenciennes, 1836)	-	MZFU-17633	Ghar El Melh, Tunisia	-	-	MH724822	MH715446
Salaria basilisca (II)	-	MZFU-17634	Sayeda, Tunisia	-	-	MH724823	MH715447
Salaria pavo (I) (Risso, 1810)	-	-	Palermo, Italy	**MZ025983**	**MZ026001**	MH724841	MH715465
Salaria pavo (II)	-	-	Palermo, Italy	**MZ025984**	**MZ026002**	MH724842	MH715466
Salaria pavo (III)	-	MNHN 2003-1994	Ile-Tudy, France	KF678551	KF678646	**MW980032**	**MZ026041**
*Salariopsis * atlantica* (I) Doadrio, Perea & Yahyaoui, 2011	Previously the genus referred to *Salaria* Forsskål, 1775	MNCN 279641-279660	Ouerrha R. Morocco	-	-	FJ465736	FJ465527
*Salariopsis * atlantica* (II)	Previously the genus referred to *Salaria* Forsskål, 1775	MNCN 279641-279660	Ouerrha R. Morocco	-	-	FJ465737	FJ465526
*Salariopsis * economidisi* (I) (Kottelat, 2004)	Previously the genus referred to *Salaria* Forsskål, 1775	-	Lake Trichonis, Greece	**MZ025985**	**MZ026003**	**MW980033**	**MZ026042**
*Salariopsis * economidisi* (II)	Previously the genus referred to *Salaria* Forsskål, 1775	-	Lake Trichonis, Greece	**MZ025986**	**MZ026004**	**MW980034**	**MZ026043**
*Salariopsis * economidisi* (III)	Previously the genus referred to *Salaria* Forsskål, 1775	-	Lake Trichonis, Greece	**MZ025987**	**MZ026005**	**MW980035**	**MZ026044**

Table 1. *Cont.*

Species	Taxonomical Remarks	Catalog Number	Locality	*ENC1*	*MYH6*	*16S*	*Dloop*
*Salariopsis * fluviatilis* (I) (Asso, 1801)	Previously the genus referred to *Salaria* Forsskål, 1775	MZFU-17635	Stream Frattina, Italy	**MZ025988**	**MZ026006**	MH724847	MH715471
*Salariopsis * fluviatilis* (II)	Previously the genus referred to *Salaria* Forsskål, 1775	MZFU-17636	Lake Garda, Italy	**MZ025989**	**MZ026007**	MH724848	MH715472
*Salariopsis * fluviatilis* (III)	Previously the genus referred to *Salaria* Forsskål, 1775	-	-	HM050017	HM050075	-	-
Scartella caboverdiana (Bath, 1990)	-	JFBM 47282	Cape Verde	MG779110	MG779147	**MW980036**	**MZ026045**
Scartella cristata (I) (Linnaeus, 1758)	-	TIUFRN3520	-	**MZ025990**	**MZ026008**	**MW980037**	**MZ026046**
Scartella cristata (II)	-	BPS3411	Eastern Atlantic	**MZ025991**	**MZ026009**	**MW980038**	**MZ026047**
Scartella cristata (III)	-	EFMM-4-060815	Avola, Italy	**MZ025992**	**MZ026010**	**MW980039**	**MZ026048**
Scartella cristata (IV)	-	EFMM-24-090716	Avola, Italy	**MZ025993**	**MZ026011**	**MW980040**	**MZ026049**
Scartella emarginata (Günther, 1861)	-	JFBM 47159-1576	Kochi, Japan	KF678541	KF678637	**MW980041**	**MZ026050**
Scartella itajobi (Rangel and Mendes, 2009)	-	TIUFRN3508	-	-	**MZ026012**	**MW980042**	**MZ026051**
Diademichthys lineatus (Sauvage, 1883)	-	-	-	JX188985	JX189754	-	-
Enneapterygius minutus (Günther, 1877)	-	JFBM 46377-1224	-	KF678492	KF678594	-	-

Total genomic DNA was extracted from muscle or fin clips using a Qiagen DNeasy Blood and Tissue Kit (Qiagen, Valencia, CA, USA), according to manufacturer suggested protocol. Polymerase chain reaction (PCR) was used to amplify fragments of two nuDNA exons (ectodermal-neural cortex 1-like protein, Enc1, and the cardiac muscle myosin heavy chain 6 alpha, myh6) and two mtDNA fragments (16S ribosomal RNA, 16S, and the control region, D-loop). PCR reactions contained 1.5 μL template DNA, 2.75 μL water, 6.25 μL GoTaqR Green Master Mix (Promega, Madison, WI), with 1.0 μL of each primer (10μM) (see [12,21,22] for the primer pairs used for the different loci). Exonuclease 1 and shrimp alkaline phosphatase were added to PCR products for enzymatic purification at manufacturer-suggested thermal profiles. Automated Sanger sequencing of purified PCR products was performed using ABI Prism R BigDye Terminator v. 3.1 chemistry (Applied Biosystems, Foster City, CA, USA) at the Biomedical Genomics Center DNA Sequencing and Analysis Facility at the University of Minnesota, USA. Complementary heavy and light strands were aligned into contiguous sequences (contigs) and edited in Geneious v. 6.1.8 (Biomatters Ltd., Auckland, New Zealand). Alignments were visually inspected for potential misalignments and, when appropriate, verified by checking amino acid translations.

All sequences were aligned with the software MEGAX [23], using the ClustalW method [24]. All novel sequences were deposited in GenBank (see Table 1 for their Accession Numbers). The alignment of the novel fragments and those downloaded from GenBank were trimmed to fragments of 801 bp (Enc1) 754 bp (myh6) 517 bp (16S) 308 bp (D-loop), respectively. In addition, publicly available sequences belonging to the study taxa and the outgroups *Diademichthys lineatus* (Sauvage, 1883) (Gobiesocidae) and *Enneapterygius minutus* (Günther, 1877) (Tripterygiidae) were downloaded from GenBank and included in the analyses (see Table 1 for their GenBank Accession Number, AN).

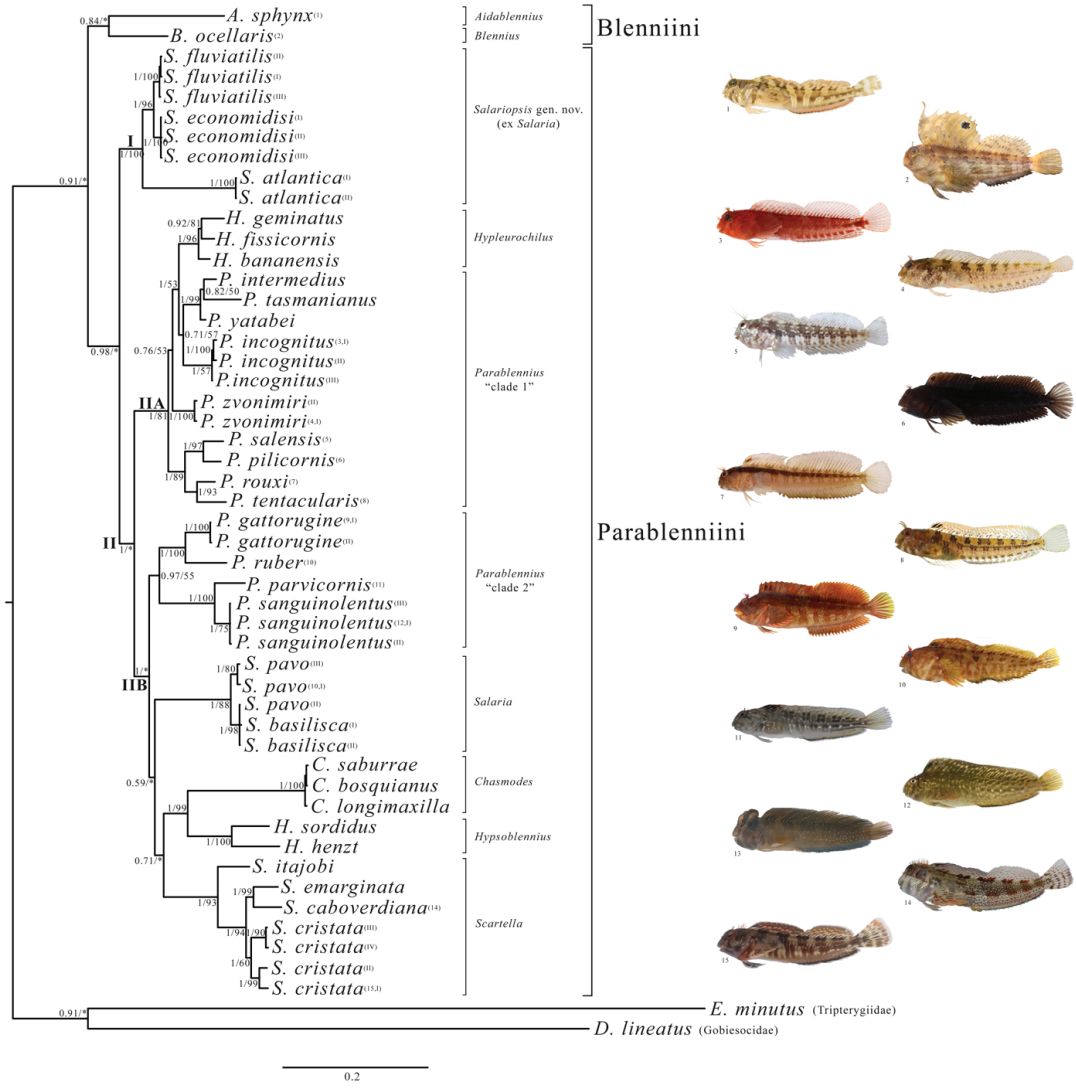

Figure 1. Bayesian phylogram of the studied Blenniidae samples based on the concatenated mtDNA and nuDNA dataset. Node statistical support is reported as nodal posterior probabilities (Bayesian Inference of phylogeny, BI)/bootstrap values (maximum likelihood, ML). Asterisks indicate a bootstrap support value lower than 50. Square brackets group the samples according to the current taxonomy. Arabic numbers in brackets refer to the blennies' images attached next to the phylogram. Roman numbers in brackets refer to specimens listed in Table 1. (I), freshwater *Salariopsis* gen. nov. (ex *Salaria*) clade; (II), marine Parablenniini clade; (IIA), *Hypleurochilus* and *Parablennius* "clade 1" subclades; (IIB), *Parablennius* "clade 2", *Salaria*, *Chasmodes*, *Hypsoblennius* and *Scartella* subclades.

In order to test whether the mitochondrial and nuclear fragments could be combined for joint analyses, the incongruence length difference test (ILD, [25]) as implemented in PAUP* v. 4.0b10 [26] was used. According to Cunningham [27], if $p > 0.01$, pooling the data improves the phylogenetic accuracy, and thus it is admissible to merge the tested datasets into a single matrix. This condition was fulfilled both for the concatenation of all the genetic markers analysed in the frame of this study ($p = 1$). Therefore, the fragments of both the

mtDNA and nuDNA loci were concatenated in a single, partitioned dataset. The best evolutionary model for each locus was selected among models analysed by MrBayes v. 3.2.6 [28] using Bayesian model choice criteria (nst = mixed, rates = gamma). The phylogenetic analyses of the partitioned concatenated dataset, including the fragments of the amplified DNA loci, were conducted using Bayesian Inference (BI) and Maximum Likelihood (ML) framework in the software package MrBayes and PhyMl v. 3 [29], respectively. Bootstrap values [30] were calculated with 1000 replicates in the ML trees, whereas the node posterior probability values were reported in the BI tree. In the BI analyses, two independent Markov Chain Monte Carlo analyses were performed with 1 million generations (temp.: 0.2; default priors). Trees and parameter values were sampled every 100 generations, with the result of 10,000 trees for each analysis. Convergence of chains was assessed to ensure proper mixing (Effective Sample Size, ESS, greater than 200 in all the analyses performed). The initial 25% of trees were discarded as "burn-in".

3. Results

All phylogenetic analyses based on the concatenated DNA dataset were congruent and nodes were well-supported. Most of the genera included in the analyses proved to be monophyletic, with the noteworthy exception of *Salaria* Forsskål, 1775 and *Parablennius* Miranda Ribeiro, 1915, which were paraphyletic.

The Parablenniini are separated from Blenniini by a cladogenetic event, with an uncorrected *p*-distance between the two tribes of 15.5% (Figure 1). There are two well-supported major subclades within Parablenniini: a clade that includes the investigated freshwater *Salaria* species (see Figure 1, clade "I"), and a clade that includes the remaining analysed ingroup taxa (see Figure 1, clade "II"). Within clade "II", the genus *Parablennius* is split into two different subclades; one subclade includes *Parablennius intermedius*, *P. tasmanianus*, *P. yatabei*, *P. incognitus*, *P. zvonimiri*, *P. salensis*, *P. pilicornis*, *P. rouxi*, *P. tentacularis* and the genus *Hypleurochilus* Gill, 1861 (subclade "IIA", see Figure 1); the second subclade includes the rest of the analysed *Parablennius* species (i.e., *P. gattorugine*, *P. ruber*, *P. parvicornis*, and *P. sanguinolentus*) along with representatives of the genera *Chasmodes* Valenciennes, 1836, *Hypsoblennius* Gill, 1861, *Scartella* Jordan, 1886 and *Salaria* (subclade "IIB", see Figure 1). The uncorrected *p*-distance between the two subclades (i.e., "IIA" and "IIB") is 13.4%.

4. Discussion

The phylogenetic trees obtained in the present study highlight some important inconsistencies in the current taxonomy of Parablenniini: (i) the genera *Parablennius* and *Salaria* are paraphyletic; (ii) some alleged *Parablennius* species cluster with the genus *Hypleurochilus*; (iii) a scarce-to-absent genetic differentiation was observed between the three species belonging to the genus *Chasmodes.* Our study strongly supports prior findings which suggested a sharp differentiation between the marine and freshwater species currently ascribed to the genus *Salaria* (e.g., [12,17]). To date, three species are formally described within the freshwater clade of *Salaria*: the widespread *S. fluviatilis*; *S. economidisi*, endemic to Lake Trichonis (Greece), and *S. atlantica*, endemic to Morocco. Moreover, a further undescribed taxon of putative species rank occurs in the Middle East (see [31,32]).

This group of freshwater blennies is deeply divergent from its alleged marine congeneric taxa, by an extent much greater than that reported by Doadrio et al. [33], Hundt et al. [12] and Vecchioni et al. [17], thus stressing the inappropriateness of their current generic assignment. Even though some studies (e.g., [34]) found some clear osteological differences between *S. pavo* and *S. fluviatilis*, to date, the absence of morphological synapomorphies is a recurrent issue [35]). Based on these results, the taxonomical status of the freshwater species currently ascribed to the genus *Salaria* must be revised. Considering that the type taxon of the genus *Salaria* is *S. basilisca* (Valenciennes, 1836) (see also [36]), the species of the marine clade belong to *Salaria* s.s.. Conversely, no genus-level epithet is available for the divergent freshwater clade currently ascribed to "*Salaria*". We propose the

new genus *Salariopsis*, which includes the species *Salariopsis fluviatilis*, *S. economidisi* and *S. atlantica*.

5. Systematics

Family: Blenniidae Rafinesque, 1910

Genus: *Salariopsis* new genus (Zoobank link LSID: http://zoobank.org/urn:lsod:zoobank.org:pub:1884E670-F6E7-48F8-AF7F-19380579DB8)

Type species of the genus: *Salariopsis fluviatilis* (Asso, 1801)

Synonyms: none

Etymology: By adding the suffix—opsis, from the ancient Greek ὄψῐς (view, appearance), to the epithet "*Salaria*", we want to highlight its apparent, but misleading, morphological similarity to the blenniid genus *Salaria* Forsskål, 1775

Morphological diagnosis: Fishes of the genus *Salariopsis* and *Salaria* have many overlapping meristic counts. However, *Salariopsis* possess fewer soft dorsal and anal fin elements than *Salaria*. In fact, *Salariopsis* has 16–17 dorsal and 16–19 anal fin rays, whereas *Salaria* has 22–25 and 23–28 fin rays, respectively (see Table 2).

Table 2. Meristic data compiled from literature for comparison of fin element counts. Superscripts indicate source: [a] Bath [8], [b] Kottelat [37], [c] Doadrio et al. [33], and [d] Tiralongo [20]. Presence of two spines in the pelvic fins of *Salaria atlantica* could not be confirmed. Tiralongo [20] added two new observations from *S. basilisca*: a specimen with 28 anal fin rays and another with 2 pelvic fin rays.

Species	Dorsal Fin	Anal Fin	Pectoral Fin	Pelvic Fin
Salariopsis fluviatilis	XII-XIII, 16–17 [d]	II, 16–19 [c]	12–14 [d]	I, 3 [a]
Salariopsis economidisi	XII-XIII, 16–17 [b]	II, 16–19 [c]	13–14 [b]	I, 3 [d]
Salariopsis atlantica	XII-XIII, 16–17 [c]	II, 16–17 [c]	10–11 [c]	II, 2–4 [c]
Salaria pavo	XI-XIII, 22–25 [b]	II, 23–26 [c]	14 [a]	I, 3 [a]
Salaria basilisca	XI-XIII, 23–27 [a]	II, 25–28 [c,d]	14 [a]	I, 2–3 [a,d]

The novel data used in this study provided results in accordance with previous molecular studies of the Almadablennius clade (e.g., [11,12,16,17,35]): the genus *Parablennius* s.l. proved to be paraphyletic, supporting the likely presence of at least two distinct and distantly related genera currently joined together within this name. Furthermore, the genus *Hypleurochilus* s.l. was nested within *Parablennius* (Figure 1, subclade "IIA"). Considering that these two genera share similar morphological features [35] and that the phylogenetic relationships are not in accordance with the current systematics, the taxonomic status of these two genera should be reassessed.

The remaining results largely agree with previous phylogenetic studies and taxonomy, while also providing direction for future studies of speciation and phylogeography. For example, a clade containing *Chasmodes*, *Scartella*, and *Hypsoblennius* was recovered, similar to previous studies (e.g., [16]).

The genus *Chasmodes* includes three species, *Chasmodes saburrae*, *C. bosquianus* and *C. longimaxilla*. Recently, Javonillo and Harold [38] highlighted the existence of a scarce interspecific divergence among the species of this genus, and their sister group relationship with a clade including the genera *Scartella*, *Hypsoblennius* and *Hypleurochilus* based on 12S mitochondrial DNA sequences. Our results are partially in contrast to those reported by Javonillo and Harold [38]. In fact, even if we detected a very low interspecific divergence (mean uncorrected *p*-distance about 0.22%) among the *Chasmodes* species and a sister group relationship between *Chasmodes* and the genera *Scartella* and *Hypsoblennius*, we did not observe the same phylogenetic relationship with the *Hypleurochilus* taxa (see Figure 1). This is probably due to our richer sampling effort, which includes more species than those investigated by Javonillo and Harold [38]. The scarce differentiation detected between the *Chasmodes* species is possibly related to their recent origin linked to sea-level fluctuations,

as proposed by Javonillo and Harold [38]. However, bearing in mind that these species have a different ecology, phenotypic plasticity, i.e., an adaptive response to different local habitats and ecology, might be playing a major role in driving the diversification of the three *Chasmodes* lineages and might be accountable for their morphological variations.

Finally, our phylogenetic analyses confirm the monophyly of the genus *Scartella*, as already proposed by other authors [12,35,39], finding a sister clade relationship of this genus with the clade that includes *Chasmodes* spp. and *Hypsoblennius* spp. Within the *Scartella* clade, an uncorrected *p*-distance of 5.23% separating the Mediterranean versus the Atlantic specimens of *S. cristata* (see Table 1) suggests the possible presence of well-characterised parapatric lineages within this species, whose taxonomical rank should be the object of dedicated research.

Author Contributions: Conceptualization, P.J.H., M.A. and A.M.S.; methodology, P.J.H., A.C.C., F.M. and L.V.; writing—original draft preparation, L.V. and P.J.H. All authors have read and agreed to the published version of the manuscript.

Funding: This research received no external funding.

Institutional Review Board Statement: Not applicable.

Informed Consent Statement: Not applicable.

Data Availability Statement: The data presented in this study are available in GenBank (see Table 1 for their Accession Numbers).

Acknowledgments: We wish to thank Stamatis Zogaris (Hellenic Centre for Marine Research, Greece) for the help he provided us with the collection of Greek samples of *Salariopsis economidisi* (Hellenic Ministry of Environment and Energy licence no. 173241/1497/27-8-2018). Samuel P. Iglésias (Muséum National d'Histoire Naturelle, France) and Francesco Tiralongo (Ente Fauna Marina Mediterranea, Italy) kindly provided blenniid photos included in Figure 1.

Conflicts of Interest: The authors declare no conflict of interest.

References

1. Fricke, R.; Eschmeyer, W.N.; Fong, J.D. Species by Family/Subfamily. 2018. Available online: http://researcharchive.calacademy.org/research/ichthyology/catalog/SpeciesByFamily.asp (accessed on 10 December 2021).
2. Norman, J.R. Notes on the blennioid fishes. I. A provisional synopsis of the genera of the family Blenniidae. *Ann. Mag. Nat. Hist.* **1943**, *11*, 793–812. [CrossRef]
3. Springer, V.G. Osteology and classification of the fishes of the family Blenniidae. *Bull. Am. Mus. Nat.* **1968**, *284*, 1–85.
4. Springer, V.G.; Smith-Vaniz, W.F. A new tribe (*Phenablenniini*) and genus (*Phenablennius*) of blenniid fishes based on *Petroscirtes heyligeri* Bleeker. *Copeia* **1972**, *1*, 64–71. [CrossRef]
5. Smith-Vaniz, W.F.; Springer, V.G. Synopsis of the tribe Salariini, with description of five new genera and three new species (Pisces: Blenniidae). *Smithson. Cont. Zool.* **1971**, *73*, 1–72. [CrossRef]
6. Springer, V.G. Synopsis of the tribe Omobranchini with descriptions of three new genera and two new species (Pisces: Blenniidae). *Smithson. Cont. Zool.* **1972**, *130*, 1–31. [CrossRef]
7. Smith-Vaniz, W.F. The saber-toothed blennies, tribe Nemophini (Pisces, Blenniidae). *Monogr. Acad. Nat. Sci. Phila.* **1976**, *19*, 1–196.
8. Bath, H. Revision der Blenniini (Pisces: Blenniidae). *Senckenb. Biol.* **1977**, *57*, 167–234.
9. Zander, C.D. Kritische Anmerkungen zur "Revision der Blenniini (Pisces: Blenniidae)" von H. Bath (1977). *J. Zool. Syst. Evol. Res.* **1978**, *16*, 290–296. [CrossRef]
10. Bock, M.; Zander, C.D. Osteological characters as tool for blenniid taxonomy—A generic revision of European Blenniidae (Percomorphi; Pisces). *J. Zool. Syst. Evol. Res.* **1986**, *24*, 138–143. [CrossRef]
11. Almada, F.; Almada, V.C.; Guillemaud, T.; Wirtz, P. Phylogenetic relationships of the north-eastern Atlantic and Mediterranean blenniids. *Zool. J. Linn. Soc.* **2005**, *86*, 283–295. [CrossRef]
12. Hundt, P.J.; Iglésias, S.P.; Hoey, A.S.; Simons, A.M. A multilocus molecular phylogeny of combtooth blennies (Percomorpha: Blennioidei: Blenniidae): Multiple invasions of intertidal habitats. *Mol. Phylogenetics Evol.* **2014**, *70*, 47–56. [CrossRef]
13. Williams, J.T. Phylogenetic relationships and revision of the blenniid fish genus *Scartichthys*. *Smithson. Contrib. Zool.* **1990**, *492*, 1–30. [CrossRef]
14. Almada, V.C.; Robalo, J.I.; Levy, A.; Freyhof, J.; Bernardi, G.; Doadrio, I. Phylogenetic analysis of Peri-Mediterranean blennies of the genus *Salaria*: Molecular insights on the colonization of freshwaters. *Mol. Phylogenetics Evol.* **2009**, *52*, 424–431. [CrossRef] [PubMed]

15. Levy, A.; Wirtz, P.; Floeter, S.R.; Almada, V.C. The Lusitania Province as a center of diversification: The phylogeny of the genus *Microlipophrys* (Pisces: Blenniidae). *Mol. Phylogenetics Evol.* **2011**, *58*, 409–413. [CrossRef] [PubMed]
16. Hundt, P.J.; Simons, A.M. Extreme dentition does not prevent diet and tooth diversification within combtooth blennies (Ovalentaria: Blenniidae). *Evolution* **2018**, *72*, 930–943. [CrossRef]
17. Vecchioni, L.; Marrone, F.; Belaiba, E.; Tiralongo, F.; Bahri-Sfar, L.; Arculeo, M. The DNA barcoding of Mediterranean combtooth blennies suggests the paraphyly of some taxa (Perciformes. Blenniidae). *J. Fish Biol.* **2019**, *94*, 339–344. [CrossRef]
18. Nakabo, T. (Ed.) *Fishes of Japan with Pictorial Keys to the Species*, 3rd ed.; Tokai University Press: Tokyo, Japan, 2013.
19. Iglésias, S.P. *Actinopterygians from the North-Eastern Atlantic and the Mediterranean (A Natural Classification Based on Collection Specimens, with DNA Barcodes and Standardized Photographs*; Provisional Version 08, 1 April 2012; MNHN: Paris, France, 2013; Volume I (plates), 245p. Available online: http://www.mnhn.fr/iccanam (accessed on 16 March 2021).
20. Tiralongo, F. *Blennies of the Mediterranean Sea*; Amazon Fulfillment: Poland, 2020.
21. Ostellari, L.; Bargelloni, L.; Penzo, E.; Patarnello, P.; Patarnello, T. Optimization of single-strand conformation polymorphism and sequence analysis of the mitochondrial control region in *Pagellus bogaraveo* (Sparidae. Teleostei): Rationalized tools in fish population biology. *Anim. Genet.* **1996**, *27*, 423–427. [CrossRef]
22. Li, C.; Orti, G.; Zhang, G.; Lu, G. A practical approach to phylogenomics: The phylogeny of ray-finned fish (Actinopterygii) as a case study. *BMC Ecol. Evol.* **2007**, *7*, 1–11. [CrossRef]
23. Kumar, S.; Stecher, G.; Li, M.; Knyaz, C.; Tamura, K. MEGA X: Molecular Evolutionary Genetics Analysis across Computing Platforms. *Mol. Biol. Evol.* **2018**, *35*, 1547–1549. [CrossRef]
24. Thompson, J.D.; Higgins, D.G.; Gibson, T.J. CLUSTAL W: Improving the sensitivity of progressive multiple sequence alignment through sequence weighting. position-specific gap penalties and weight matrix choice. *Nucleic Acids Res.* **1994**, *22*, 4673–4680. [CrossRef]
25. Farris, J.S.; Kallersjo, M.; Kluge, A.G.; Bult, C. Testing significance of incongruence. *Cladistics* **1995**, *10*, 315–319. [CrossRef]
26. Swofford, D.L. *Phylogenetic Analysis Using Parsimony (*and Other Methods)*; Version 4; Sinauer Associate: Sunderland, MA, USA, 2004.
27. Cunningham, C.W. Can three incongruence tests predict when data should be combined? *Mol. Biol. Evol.* **1997**, *14*, 733–740. [CrossRef] [PubMed]
28. Ronquist, F.; Teslenko, M.; Van der Mark, P.; Ayres, D.L.; Darling, A.; Höhna, S.; Larget, B.; Liu, L.; Suchard, M.A.; Huelsenbeck, J.P. MrBayes v. 3.2: Efficient bayesian phylogenetic inference and model choice across a large model space. *Syst. Biol.* **2012**, *61*, 539–542. [CrossRef] [PubMed]
29. Guindon, S.; Gascuel, O. A simple. fast. and accurate algorithm to estimate large phylogenies by maximum likelihood. *Syst. Biol.* **2003**, *52*, 696–704. [CrossRef] [PubMed]
30. Felsenstein, J. Confidence-limits on phylogenies: An approach using the bootstrap. *Evolution* **1985**, *39*, 783–791. [CrossRef]
31. Belaiba, E.; Marrone, F.; Vecchioni, L.; Bahri-Sfar, L.; Arculeo, M. An exhaustive phylogeny of the combtooth blenny genus *Salaria* (Pisces. Blenniidae) shows introgressive hybridization and lack of reciprocal mtDNA monophyly between the marine species *Salaria basilisca* and *Salaria pavo*. *Mol. Phylogenetics Evol.* **2019**, *135*, 210–221. [CrossRef]
32. Wagner, M.; Zogaris, S.; Berrebi, P.; Freyhof, J.; Koblmüller, S.; Magnan, P.; Laporte, M. Diversity and biogeography of Mediterranean freshwater blennies (Blenniidae, *Salaria*). *Divers. Distrib.* **2021**, *27*, 1832–1847. [CrossRef]
33. Doadrio, I.; Perea, S.; Yahyaoui, A. A new species of the genus *Salaria* Forsskål, 1775 (Actinopterygii, Blennidae) in Morocco. *Graellsia* **2011**, *67*, 151–173. [CrossRef]
34. Ferrito, V.; Mauceri, A.; Minniti, F.; Isaja, M.; Maisano, M.; Tigano, C. Comparative morphological studies of the neurocranium and the gills of two species of blennies living in different habitats. *Acta Histochem.* **2007**, *109*, 428–436. [CrossRef] [PubMed]
35. Levy, A.; von der Heyden, S.; Floeter, S.R.; Bernardi, G.; Almada, V.C. Phylogeny of *Parablennius* Miranda Ribeiro, 1915 reveals a paraphyletic genus and recent Indo-Pacific diversification from an Atlantic ancestor. *Mol. Phylogenetics Evol.* **2013**, *67*, 1–8. [CrossRef]
36. Krupp, F.; Schneider, W. *The Fishes of the Jordan River Drainage Basin and Azraq Oasis*; Pro Entomologia c/o Natural History Museum: Basel, Switzerland, 1989.
37. Kottelat, M. *Salaria economidisi*, a new species of freshwater fish from Lake Trichonis, Greece, with comments on variation in *S. fluviatilis* (Teleostei: Blenniidae). *Rev. Suisse Zool.* **2004**, *111*, 121–137. [CrossRef]
38. Javonillo, R.; Harold, A.S. A systematic review of the genus *Chasmodes* (Teleostei: Perciformes: Blenniidae). *Zootaxa* **2010**, *2558*, 1–16. [CrossRef]
39. Araujo, G.S.; Vilasboa, A.; Britto, M.R.; Bernardi, G.; von der Heyden, S.; Levy, A.; Floeter, S.R. Phylogeny of the comb-tooth blenny genus *Scartella* (Blenniiformes: Blenniidae) reveals several cryptic lineages and a trans-Atlantic relationship. *Zool. J. Linn. Soc.* **2020**, *190*, 54–64. [CrossRef]

diversity

MDPI

Article

Alien Invasive Plant Effect on Soil Fauna Is Habitat Dependent

Tania De Almeida [1], Estelle Forey [2] and Matthieu Chauvat [2,*]

[1] AgroParisTech, INRAE, Université Paris-Saclay, UMR ECOSYS, 78850 Thiverval-Grignon, France; tania.almeida@outlook.fr
[2] ECODIV, INRAE, Normandie Université, UNIROUEN, 76000 Rouen, France; Estelle.forey@univ-rouen.fr
* Correspondence: matthieu.chauvat@univ-rouen.fr

Abstract: Invasive alien plants often modify the structure of native plant communities, but their potential impact on soil communities is far less studied. In this study, we looked at the impact of invasive Asian knotweed (*Reynoutria* spp.) on two major soil mesofauna (Collembola) and microfauna (Nematodes) communities. We expected ingress of knotweed to differentially affect faunal groups depending on their trophic position, with the lower trophic levels being more impacted than the higher trophic groups according to the closer relationship to plants for basal trophic groups. Furthermore, we expected the knotweed impact to depend on habitat type (forest vs. meadow) with more pronounced changes in abundances of soil invertebrate in invaded meadows. Plant and soil invertebrates were sampled in six sites (three forest and three meadows) in northern France in both control and invaded plots. Our results showed that the presence of knotweed strongly reduced native plant species' diversity and abundance. Soil fauna also responded to the invasion by Asian knotweed with different responses, as hypothesized, according to trophic position or life-forms. Furthermore, abundances of several collembolan life-forms were influenced by the interaction between the factors "Habitat" and "Knotweed". This may explain the difficulty to easily generalize and predict the consequences of plant invasion on belowground diversity, although this is of crucial importance for alleviating negative consequences and costs of biological invasion.

Keywords: *Reynoutria* ssp.; Collembola; Nematodes; habitat type; novel ecosystems

Citation: De Almeida, T.; Forey, E.; Chauvat, M. Alien Invasive Plant Effect on Soil Fauna Is Habitat Dependent. *Diversity* **2022**, *14*, 61. https://doi.org/10.3390/d14020061

Academic Editor: Michael Wink

Received: 14 December 2021
Accepted: 16 January 2022
Published: 18 January 2022

1. Introduction

Biological invasions are a main concern globally as they have drastic economic and ecological impacts through replacement of native species, change in habitat structure or alteration of ecosystem functioning [1,2]. Recently, Diagne et al. [3] estimated the costs of biological invasions to consistently increase over time with an average threefold increase per decade, reaching a reported worldwide annual cost of around USD 162.7 billion in 2017. Furthermore, biological invasions are expected to increase in the future, being exacerbated by globalization and interactions with a number of other components including urbanization, over-exploitation, climate change and agricultural intensification.

Despite progress in generalizing the impacts of invasive alien species, species that have successfully been introduced, established and spread beyond their native range, there remain considerable uncertainties regarding the underlying mechanisms of such impacts [4]. Native plant communities suffer from establishment and development of invasive alien plant species. Success of invasive species may result from both direct effects (e.g., allelopathy or competition with natives; [5]) or indirectly through changes in the environment [2].

Development and dynamics of terrestrial ecosystems are partly regulated by interactions taking place between above and belowground compartments. Briefly, while plants provide organic matter to the belowground system, soil organisms, e.g., soil fauna and soil microorganisms, through decomposition and mineralization processes, regulate the delivery rate of nutrients back to the plants. Recently, Forey et al. [6] showed that an invasive

palm tree, *Pinanga coronata*, on a South Pacific Island, led to weakening of the plant–soil fauna relationships (i.e., trait-matching) compared to the more stable relationships in non-invaded plots. In different recent meta-analyses, it was shown that habitat-context, mainly open (e.g., meadows) versus closed habitats (e.g., forests), strongly interact with the trophic position of an organism to determine the response of soil fauna to the presence of invasive species, and that stronger responses were observed in open habitats [7,8]. This supports the hypothesis that invasive alien plant (IAP) species can alter the quantity, quality and timing of litter production. This would alter nutrient inputs into the soil, altering linkages with biota belowground and their associated functions such as mineralization, and inducing feedbacks to the plant assemblages' structure and dynamic [9]. These plant–soil feedbacks may in turn contribute to promote seedling establishment of invasive species (results from a meta-analysis performed on 68 species, [10]).

Several IAP species are described to release allelopathic compounds into their environment. This refers to the novel weapon hypothesis (NWH) suggesting that alien plant species may become invasive according to their possession of deleterious secondary compounds unknown to the native species in the invasion range. This is the case of a well-known invasive plant complex in Europe, the Asian knotweed species complex. Composed of two distinct species *Reynoutria japonica* (Houttuyn), *R. sachalinensis* (F. Schmidt) and a hybrid *R.* × *bohemica* (Chrtek & Chrtková), these species originating from eastern Asia have now colonized numerous countries on both hemispheres [11]. Their impacts have been recently reviewed [12] and, although studies agree on their negative effects on the diversity of native flora and aboveground fauna, mostly due to a considerable amount of litter-leaf and stems produced, their impacts on soil biota are, so far, little investigated and difficult to generalize, especially regarding soil meso- or microfauna. Additionally, this large amount of knotweed litter input may be more contrasting in meadows than in forests where trees already provide a high amount of leaf litter [13]. In a microcosm experiment, Abgrall et al. [13] showed that adding knotweed rhizome extract alters the soil food webs (with a positive or negative effect depending on the concentration and trophic levels), and Skubala and Mierny [14] reported a significant negative effect of knotweed on oribatid mites but no effect on Collembola. To our knowledge, only one publication [14] assessed the impact of spontaneous invaded sites upon soil mesofauna, and none have reported field data on Nematodes' responses to knotweed.

We wanted to partly fill this gap in the current knowledge by investigating the response of soil Collembola and Nematodes as members of the meso- and the microfauna, respectively, to the spontaneous and long-term invasion by Asian knotweed (>10 years). Nematode species belong to different trophic groups, e.g., bacterivores, fungivores, herbivores, omnivores or predators. As reported by Abgrall et al. [13] in a laboratory study, we expect that knotweed will exert a strong influence on basal trophic groups such as herbivores or microbial-feeders, and that higher trophic levels, such as predatory Nematodes, will be less affected. By comparison, Collembola species can be separated into three eco-morphological life-forms: epedaphic, hemiedaphic, and euedaphic. These life-forms differ in fundamental ecological properties such as reproduction, vertical distribution, metabolic activity and dispersal [15,16], in addition to trophic position and niche, with different food resources ranging from plant materials to microorganisms [17,18]. These life-forms differ thus in their sensitivity to environmental conditions and are commonly used to depict consequences of environmental changes [19–23]. We thus expect epedaphic species living in the litter to be impacted by the amount of litter produced by the knotweeds, especially in the invaded meadows.

Thus, we hypothesize that the litter produced by knotweed will generate new habitats for epedaphic Collembola species in invaded meadows sites, whereas in forest it will be less critical according to the pre-existing litter before invasion. However, we also cannot exclude that the decrease in resource diversity resulting from the invasion may negatively impact epedaphic species. In contrast, we expect euedaphic Collembola (i.e., deep-living species)

to be less responsive to changes in organic matter delivery under knotweed invasion, either in forest or in meadow habitat types.

2. Materials and Methods

2.1. Study Area

We identified 1123 sites where knotweed was present in Normandy (France) through a literature and field survey. In Normandy all three knotweed species—*R. japonica*, *R.* × *bohemica* and *R. sachalinensis*—are present. These species can be morphologically very similar and only genetic analyses would allow a rigorous identification. Therefore, in the following text, the term knotweed refers to *Reynoutria* spp.

We selected six riparian sites (see Table S1) where introduced knotweed has been present for more than 10 years but has not been managed for at least seven years. At each site, both the monospecific stands of knotweed (invaded plots) and the uninvaded areas with only native vegetation (control plots) were larger than 60 m^2. To compare two contrasting habitat types, we chose three sites in forest and three in meadows. For forest sites, we only sampled patches located in the core of riparian forests and we excluded sites with knotweed located at the border of stands. All sites were situated at an altitude of between 10 and 100 m asl.

On each site, sampling was carried out in spring 2017, in three 2 m^2 quadrats in both knotweed cover classes: control (uninvaded area) and invaded (monospecific stands of knotweed). Thus, a total of 36 plots for soil fauna were sampled overall. Additionally, we also characterized habitat properties that could drive soil communities (soil variables and vegetation) on these 36 plots.

2.2. Soil Variables

In each quadrat, 500 g of soil was collected to the depth of 10 cm in spring 2017 to measure edaphic properties. To perform the following standard methods of analyses, the fresh soil was sieved (2 mm). Microbial carbon biomass (microbial C) was determined by means of the fumigation-extraction method [24]. Microbial C was extracted from fumigated and unfumigated soil samples with K_2SO_4 (at 0.2 g L^{-1}) using a Shimadzu TOC-L analyzer (Shimadzu Corporation SL, Kyoto, Japan). Soil ergosterol content, a proxy of soil fungal biomass, was measured using the method proposed by Gong et al. [25]. Ammonium and nitrate content in the soil were quantified by calorimetry with a Gallery analyzer (Thermo Fisher Scientific, Waltham, MA, USA). Twenty grams of sieved fresh soil was dried at 105 °C for 48 h to determine the soil humidity. The remaining soil samples were air-dried for 2 weeks for the other soil analyses. Soil pH was measured in a suspension with 1 mol·L^{-1} of potassium chloride (1:5, w/v) using a FiveEasy pH meter (Mettler Toledo, Columbus, OH, USA). The dried soil samples were ground with a ball mill (MM 200, Retsch), and used to determine the total carbon and nitrogen contents with an elemental analyzer (CHN Flash 2000 Thermo Scientific, Waltham, MA, USA). In each quadrat, we also measured the average litter thickness in triplicate (in cm).

2.3. Vegetation Survey

Plant communities were sampled in the 2 m^2 quadrats in June 2017. The abundance of each plant species was defined using a Braun-Blanquet scale [26]. They were then converted into plants' cover percentage using the median value of each Braun-Blanquet cover class. For forest sites, quadrats were placed avoiding trunks; therefore, only the understory communities were sampled.

2.4. Soil Fauna Survey

Soil fauna was sampled on the same day as the soil collection in spring 2017. Springtime corresponds to a common period of high soil biological activity in Normandy.

2.4.1. Soil Collembola

Soil Collembola were collected in the middle of each quadrat using a 5-cm-diameter steel cylinder from the upper 10 cm of soil. A single core was performed per quadrat. Collembola were extracted for twelve days according to the Berlese–Tullgren method [27] and stored in 70% ethyl alcohol. Collembola individuals were assigned to each of the 3 life-forms, i.e., epedaphic, hemiedaphic, and euedaphic, according to their morphological attributes [28]. Epedaphic species were rather large species characterized by the presence of pigmentation and more than 4 ocelli on each side and a well-developed furca (i.e., *Lepidocyrtus* sp., *Pogonognathellus* sp., *Neanura muscorum*, *Dicyrtoma fusca*, *Dicyrtomina minuta*, *Isotoma* sp., *Isotomurus* sp., *Deuterosminthurus* sp., *Orchesella* sp., *Tomocerus* sp.); in contrast, euedaphic species were blind with no pigmentation and without a functional furca (i.e., *Protaphorura* sp., *Mesaphorura* sp., *Paratullbergia callipygos*, *Isotomiella minor*, *Megalothorax minimus*, *Willemia* sp., *Stenaphorurella* sp., *Arrhopalites* sp.). Finally, species that did not fall into the previous two categories were considered as hemiedaphic (i.e., *Folsomia quadrioculata*, *F. manolachei*, *Parisotoma notabilis*, *Friesea* sp., *Ceratophysella* sp., *Pseudosinella* sp., *Sminthurinus aureus*, *Sphareridia pumilis*).

2.4.2. Soil Nematoda

Soil Nematoda were sampled using the same protocol as for Collembola with a steel corer. Then, for each sample, to facilitate extraction, two subsamples of 100 g fresh soil were extracted for two days using the Baermann funnel method [29]. After extraction, both subsamples of a single sample were combined for further analyses. First, live specimens were counted under a stereomicroscope. Then, they were fixed in 4% formalin solution and mounted on glass slides. Under a microscope the first two hundred individuals encountered were divided into the following trophic groups [30]: bacterial feeder, fungal feeder, plant feeder and omnivorous-predatory, based on their morphological attributes.

2.5. Data Analyses

Prior to statistical analyses, all data distributions were examined using the Shapiro–Wilk test of normality. To test the effect of two factors—"Knotweed" with 2 levels: absence or presence, and "Habitat" with two levels: forest or meadow—and their interaction, on soil variables, plant community and soil fauna abundance, generalized linear mixed models (GLMMs) with nested design were computed (R package "glmmTMB" [31]). In all models, a random factor was used with the samples nested in sites that were nested in "Habitats". Total carbon, total nitrogen, C:N ratio, nitrate, microbial biomass, ergosterol and humidity were fitted with a Gaussian distribution. Other abiotic variables and plant community parameters were fitted with a gamma distribution, whereas soil fauna abundances were fitted with a zero-inflated negative binomial model (with family "nbinom2" [32]). Models were followed by Tukey HSD post-hoc tests using the package "emmeans". Significance thresholds for post hoc analyses were set at p-value < 0.05.

Changes in plant community composition were visualized via non-metric multidimensional scaling (NMDS) based on the Bray–Curtis dissimilarity index to ordinate the characteristics of plant communities (composition and abundance). Differences in plant community composition were tested by permutation multivariate analysis using the Adonis function (R package "vegan" [33]). To complement previous analyses, we conducted a principal component analysis (PCA) ordination of 10 variables (C:N ratio, nitrate, microbial biomass, ergosterol, relative soil humidity, litter thickness, plant species richness, total plant cover, total Collembola and total Nematoda abundances) based on the 36 quadrats monitored (R package "FactoMineR" [34]).

All statistical analyses were performed using R software v. 4.1.0 (R Foundation for Statistical Computing). Soil (abiotic and biotic) and vegetation data are compiled within Table S2.

3. Results

3.1. Soil Variables

Three variables were impacted by the factor "Knotweed", litter thickness and C:N ratio, with significantly higher values in invaded plots than in control plots (Table 1; Figure 1a) and microbial C biomass, with an opposite pattern being significantly lower in invaded plots than in control plots (Table 1). C:N ratio was also significantly influenced by the interaction between "Knotweed" and "Habitat", as were soil nitrate and relative soil humidity. Although the C:N ratio did not differ between invaded plots and control plots in meadows, it did in forests with higher values (+33%) in invaded forests compared to control forests. Although soil nitrate content was not different between the two knotweed levels (absence or presence) in forest habitats, soil nitrate content in invaded plots was more than twice as high as that in control plots in meadow habitats (Table 1). Soil humidity in both control and invaded plots in forest habitats was significantly higher than in control plots in meadow habitats.

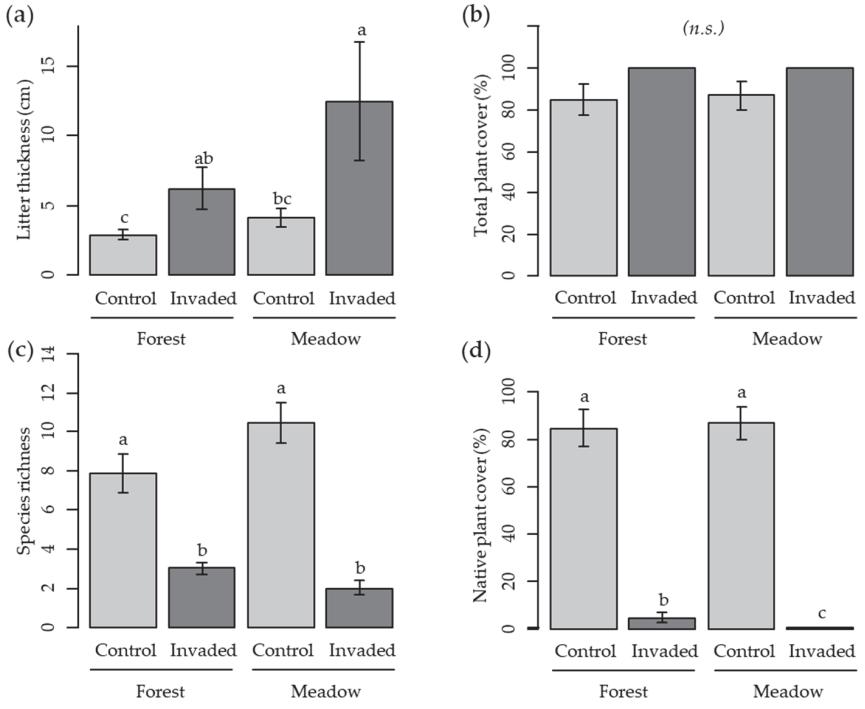

Figure 1. Effects of habitat (forest and meadow) and knotweed on (**a**) litter thickness and plant community parameters: (**b**) total plant cover; (**c**) plant species richness; (**d**) native plant cover. Values are means ± standard errors. Significant differences according to Tukey post hoc tests are indicated by different letters. n.s.: not significant.

Finally, several variables were impacted by the factor "Habitat" with more nitrate (+38.7%) and a higher soil humidity (+21.2%) in forest soils compared to meadow soils, and an opposite pattern was found for ergosterol content, which was 1.8 times higher in meadows than in forests.

Table 1. Effects of the factors "Knotweed" with two levels: presence or absence, "Habitat" with two levels: forest or meadow, and their interaction on soil variables. Values are means ± standard errors. z-values and associated *p*-values were obtained from GLMM with gamma or Gaussian distributions. Two values in the same row with a different letter are significantly different according to Tukey post hoc tests. *, **, and *** denote statistical significance at $p = 0.05$, 0.01, and 0.001, respectively. When the *p*-values obtained from GLMM were not significant, the post hoc test results are not reported.

			Forest		Meadow	
	z-Value	***p*-Value**	**Control**	**Invaded**	**Control**	**Invaded**
Total carbon ($mg \cdot g^{-1}$)						
Knotweed	1.14	0.25	5.84 ± 0.77	6.9 ± 1.47	4.77 ± 0.45	5.67 ± 0.38
Habitat	−0.68	0.49				
Knotweed × Habitat	−0.12	0.9				
Total nitrogen ($mg \cdot g^{-1}$)						
Knotweed	−1.48	0.14	0.39 ± 0.05	0.31 ± 0.05	0.28 ± 0.04	0.33 ± 0.03
Habitat	−1.56	0.11				
Knotweed × Habitat	1.69	0.09				
C:N ratio						
Knotweed	3.23	0.001 **	$15.15^{B} \pm 0.91$	$20.33^{A} \pm 2.31$	$17.55^{AB} \pm 1.27$	$17.73^{AB} \pm 0.83$
Habitat	0.97	0.33				
Knotweed × Habitat	−2.2	0.03 *				
Nitrate ($mg \cdot g^{-1}$)						
Knotweed	−0.56	0.58	$1.61^{AB} \pm 0.31$	$1.47^{AB} \pm 0.23$	$0.67^{B} \pm 0.2$	$1.56^{A} \pm 0.12$
Habitat	−2.44	0.01 *				
Knotweed × Habitat	2.86	0.004 **				
Ammonium ($mg \cdot g^{-1}$)						
Knotweed	−1.39	0.16	0.91 ± 0.23	0.65 ± 0.14	0.73 ± 0.08	0.59 ± 0.1
Habitat	−0.12	0.91				
Knotweed × Habitat	0.15	0.88				
pH						
Knotweed	0.55	0.59	6.97 ± 0.23	7.04 ± 0.26	7.56 ± 0.09	7.56 ± 0.04
Habitat	1.58	0.12				
Knotweed × Habitat	−0.4	0.69				
Microbial biomass ($mgC \cdot g^{-1}$)						
Knotweed	−2.82	0.0049 **	$0.23^{A} \pm 0.04$	$0.14^{B} \pm 0.03$	$0.2^{AB} \pm 0.02$	$0.16^{AB} \pm 0.02$
Habitat	−0.8	0.43				
Knotweed × Habitat	1.09	0.28				
Ergosterol ($\mu g \cdot g^{-1}$)						
Knotweed	−1.28	0.2	$1.7^{AB} \pm 0.5$	$1.1^{B} \pm 0.3$	$3.1^{A} \pm 0.4$	$2.0^{AB} \pm 0.4$
Habitat	1.98	0.048 *				
Knotweed × Habitat	−0.7	0.48				
Humidity (%)						
Knotweed	−1.1	0.27	$33.4^{A} \pm 1.6$	$31.5^{A} \pm 1.4$	$24.5^{B} \pm 1.8$	$29.0^{AB} \pm 1.2$
Habitat	−3.71	<0.001 ***				
Knotweed × Habitat	2.54	0.011 *				
Litter thickness (cm)						
Knotweed	2.71	0.0068 **	$2.9^{B} \pm 0.4$	$6.2^{AB} \pm 1.5$	$4.1^{B} \pm 0.7$	$12.4^{A} \pm 4.3$
Habitat	0.61	0.54				
Knotweed × Habitat	0.29	0.78				

3.2. Plant Communities

All three measured variables, plant species richness, total plant cover and native plant cover, were significantly affected by the factor "Knotweed", with species richness and native plant cover being considerably reduced in invaded plots compared to control plots, by 2.5 times and 32 times, respectively (Table 2, Figure 1). Conversely, the total plant cover increased from around 86% in control plots to 100% in invaded plots. Of the three variables, only total plant cover was not impacted by the interaction between "Knotweed" and "Habitat". Both species richness and native plant cover showed the same pattern, being significantly higher in control plots than in invaded plots, by 2.6 and 17.2 times in forests, respectively, and by 5.2, and 217 times in meadows, respectively (Table 2; Figure 1d). By contrast no significant differences were found in total plant cover between the four modalities (Table 2; Figure 1b). Finally, none of the variables responded to the factor "Habitat".

The NMDS ordination (stress = 0.11) discriminated on axis 1 the control plots from the invaded ones (Figure 2). In both habitats, plant community composition and abundance differed between control and invaded quadrats (both p-value < 0.001). The NMDS ordination discriminated on axis 2 the control plots (Figure 2). Plant community composition and abundance differed between the two habitats' control plots (p-value < 0.001). The forest control plots were characterized by *Urtica dioica* L., *Galium aparine* L. and *Rubus fruticosus* L. within the understory layer. In contrast, the meadow control plots were characterized by *Achillea millefolium* L., *Potentilla reptans* L. and *Agrostis capillaris* L. No significant difference was found between the two habitats' invaded plots (p-value = 0.99). Both invaded plots were mainly characterized by *Reynoutria* spp.

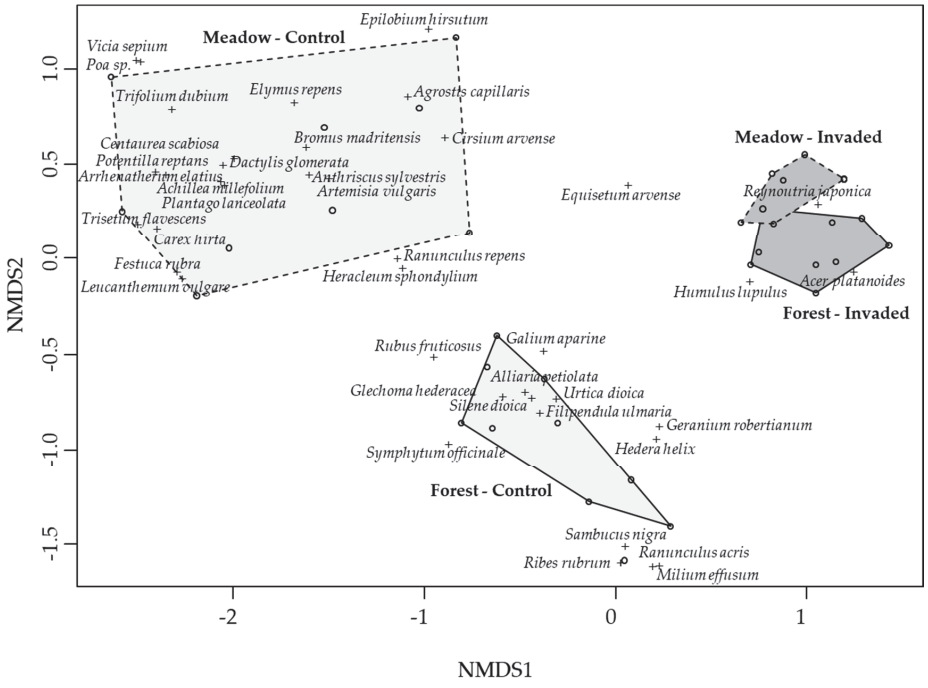

Figure 2. Non-metric multidimensional scaling (NMDS) (stress = 0.11) performed on the plant community composition. The 9 samples of each treatment are grouped in polygons, with dashed lines for the meadow sites and full lines for the forest sites (control plots in light grey and invaded plots in dark grey). Dots represent the 36 quadrats and crosses represent the spatial location of each species. For clarity, only the plant species most correlated to the two first axes are shown.

3.3. Soil Fauna

Regarding Collembola, both total and hemiedaphic abundances were impacted by the factor "Knotweed", with a decrease of 6.7% in the total collembolan abundance in invaded plots compared to control plots, but with an increase of 14.5% in hemiedaphic Collembola in invaded plots. However, with the exception of euedaphic abundance, all variables, i.e., total Collembola abundance, epedaphic abundance, and hemiedaphic abundance, were affected by the interaction term between "Knotweed" and "Habitat" (Table 2), with a different response pattern between control and invaded plots according to the habitat type. However, only the abundance of epedaphic Collembola differed significantly between the four modalities, with three times more individuals in control meadow plots than in invaded meadow plots, whereas no difference was found between control forest plots and invaded forest plots (Table 2). Finally, only the epedaphic abundance was significantly influenced by the factor "Habitat", with more individuals in meadows than in forests.

With the exception of the abundance of plant feeder Nematodes, which had about 6 times more individuals in control plots vs. invaded plots, the other trophic groups and the total Nematodes did not respond to the factors "Knotweed", "Habitat" or their interaction (Table 3). In forest habitats, abundance of plant feeders was seven times higher in control plots than in invaded plots, whereas no difference was observed between control and invaded plots in meadows (Table 3).

3.4. Global Effect of Knotweed on Habitats

The PCA did not show any clear separation between the four modalities (Figure 3). The control plots are more heterogeneous than the invaded ones in both habitat types. Invaded forest plots tend to be characterized by low Collembola and nematode abundances and plant species richness, and high litter thickness, humidity, nitrate content and total plant cover. In contrast, invaded meadows plots tend to be characterized by high Collembola and Nematoda abundances, total plant cover and litter thickness.

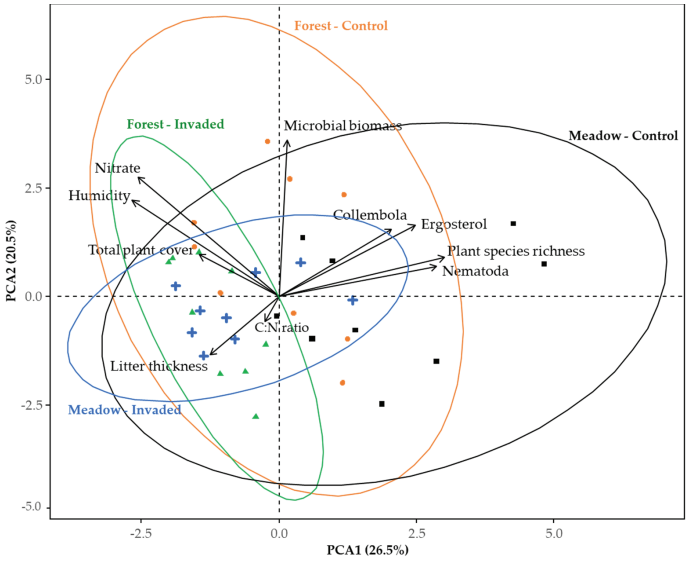

Figure 3. Principal component analysis (PCA) ordination of 10 variables (C:N ratio, nitrate, microbial biomass, ergosterol, relative soil humidity, litter thickness, plant species richness, total plant cover, total Collembola and total Nematoda abundances) based on the 36 quadrats of control forest (orange circle), invaded forest (green triangle), control meadow (black square) and invaded meadow (blue cross). Samples from each treatment (n = 9) are grouped within ellipses. Variables are represented by arrows.

Table 2. Effects of the factors "Knotweed" with two levels: presence or absence, "Habitat" with two levels: forest or meadow and their interaction on plant community variables and Collembola variables (ind.m^{-2}). Values are means ± standard errors. z-values and associated *p*-values were obtained from GLMM with a binomial negative distribution (zero-inflated models) for Collembola variables and with a gamma distribution for plant community parameters. Two values in the same row with a different letter are significantly different according to Tukey post hoc tests. *, **, and *** denote statistical significance at p = 0.05, 0.01, and 0.001, respectively. When the *p*-values obtained from GLMM were not significant, the post hoc test results are not reported.

			Forest		Meadow	
	z-Value	***p*-Value**	**Control**	**Invaded**	**Control**	**Invaded**
Plant community variables						
Species richness						
Knotweed	−4.28	<0.001 ***	7.9 ^{A} ± 1	3.0 ^{B} ± 0.3	10.4 ^{A} ± 1.1	2.0 ^{B} ± 0.4
Habitat	1.49	0.14				
Knotweed × Habitat	−2	0.045 *				
Total plant cover (%)						
Knotweed	2.26	0.024 *	84.7 ^{A} ± 7.8	100 ^{A} ± 0	86.9 ^{A} ± 6.8	100 ^{A} ± 0
Habitat	0.25	0.8				
Knotweed × Habitat	−0.20	0.84				
Native plant cover (%)						
Knotweed	−4.32	<0.001 ***	84.7 ^{A} ± 7.8	4.9 ^{B} ± 1.9	86.9 ^{A} ± 6.8	0.4 ^{C} ± 0.3
Habitat	−0.5	0.61				
Knotweed × Habitat	−3.54	<0.001 ***				
Collembola abundance						
Knotweed	−2.5	0.013 *	26,056 ^{A} ± 5594	13,333 ^{A} ± 3593	22,611 ^{A} ± 8924	32,055 ^{A} ± 9320
Habitat	−0.74	0.46				
Knotweed × Habitat	3.21	0.0013 **				
Epedaphic abundance						
Knotweed	1.48	0.14	556 ^{B} ± 155	556 ^{AB} ± 242	1722 ^{A} ± 657	556 ^{B} ± 194
Habitat	3.4	<0.001 ***				
Knotweed x Habitat	−2.8	0.0052 **				
Hemiedaphic abundance						
Knotweed	−2.09	0.037 *	15,278 ^{A} ± 3436	9611 ^{A} ± 2652	10,000 ^{A} ± 3123	19,333 ^{A} ± 5428
Habitat	−0.49	0.62				
Knotweed × Habitat	2.59	0.0097 **				
Euedaphic abundance						
Knotweed	−1.52	0.13	10,167 ± 2981	4055 ± 823	10,889 ± 6628	12,167 ± 4349
Habitat	−0.06	0.95				
Knotweed × Habitat	1.65	0.098				

Table 3. Effects of the factors "Knotweed" with two levels: presence or absence, "Habitat" with two levels: forest or meadow and their interaction on Nematoda abundances (ind.100 g of dry soil). Values are means ± standard errors. z-values and associated *p*-values were obtained from GLMM with a binomial negative distribution (zero-inflated models). Two values in the same row with a different letter are significantly different according to Tukey post hoc tests. ** denotes statistical significance at $p = 0.01$. When the *p*-values obtained from GLMM were not significant, the post hoc test results are not reported.

			Forest		Meadow	
	z-Value	***p*-Value**	**Control**	**Invaded**	**Control**	**Invaded**
Nematoda abundance						
Knotweed	−1.43	0.15	351 ± 98	233 ± 69	941 ± 490	238 ± 58
Habitat	0.89	0.37				
Knotweed × Habitat	−0.94	0.35				
bacterial feeder						
Knotweed	−1.4	0.16	224 ± 65	149 ± 52	655 ± 326	180 ± 55
Habitat	1.05	0.29				
Knotweed × Habitat	−0.93	0.35				
fungal feeder						
Knotweed	−1.11	0.27	122 ± 35	81 ± 29	260 ± 155	52 ± 6
Habitat	0.44	0.66				
Knotweed × Habitat	−0.38	0.71				
plant feeder						
Knotweed	−2.86	0.004 **	$14^{A} \pm 5$	$2^{B} \pm 0.8$	$24^{A} \pm 13$	$4^{AB} \pm 2$
Habitat	0.28	0.78				
Knotweed × Habitat	1.04	0.3				
omnivorous-predatory						
Knotweed	−0.51	0.61	0.3 ± 0.3	0.2 ± 0.2	0.9 ± 0.7	0.3 ± 0.2
Habitat	0.45	0.66				
Knotweed × Habitat	−0.62	0.54				

4. Discussion

4.1. Knotweed Effects on Native Plants and Soil Variables

Knotweed invasion strongly reduced the heterogeneity of both forest and meadow habitats. Indeed, invasion by knotweeds led to a strongly significant decrease in native understory plant diversity in both meadows (−62%) and forests (−81%). Such negative effects of knotweed on plant diversity are well known and have been recently compiled in the review of Lavoie [12]: from 28 studies, 23 studies showed a negative effect of knotweed on plant diversity, and two studies found a null effect. Functional diversity was also reported to be lower in knotweed plots compared to control ones with a marked effect in meadows comparted to in forested areas [35]. In all these studies, this loss of diversity was coupled with a strong decrease in native plant cover and biomass [12]. In our study, native cover dropped by 80% on average, but this negative impact was higher in open habitat. Such Habitat × Knotweed interaction can be explained by the lowest ability of meadows species to compete for light compared to forest understory species. Indeed, the productivity, high stem density, and biomass (up to 13 times higher than the native one) of knotweeds contribute to the suppression of native understory species by competition for light and space [12]. In forest habitats, understory species are more adapted to low light availability, and have developed strategies to avoid light competition (e.g., liana: *Hedera helix*, *Galium aparine*), allowing them to climb over knotweeds. Thus, although invasion by knotweed did not lead to a change in the total plant cover (when including the contribution of knotweed), we can argue that knotweed invasion induced a strong

alteration of habitat for soil fauna, with vegetation resource being less diverse and plant ground cover architecture being extremely reduced, and made only of knotweed stems. Indeed, knotweeds have shoots that can reach over 2 m in height, and these aerial parts (stems and leaves) die back to the ground in autumn, producing a threefold increase in litter amount compared to our control plots. This knotweed litter production (i.e., thickness) was similar between our two habitats. As hypothesized, this increase in litter following knotweed invasion was more significant in meadow habitats compared to forest habitats. The litter of knotweeds generally decomposes 3–4 times slower than litter of native species ([36], measurements in meadows) and is commonly of lower quality than the litter of the displaced plant species, thus potentially altering the nutrient cycling of the invaded ecosystems [37–39]. Most of the soil variables we measured responded to the knotweed invasion; for example, nitrate available for plants strongly increased in the invaded sites in meadow habitats and C:N ratio was highest in invaded forest habitats. Similarly to Stefanowicz et al. [40], our soils from forest-invaded plots had a much lower microbial biomass than soils from uninvaded plots. It is, therefore, possible that knotweed affects microbial biomass through competition for N due to the increase in soil C:N ratio, and/or through allelopathy on microbial communities, which may ultimately cascade through Collembola and Nematoda groups feeding on these microorganisms. Knotweed invasion altered soil properties and simplified the habitat structure for soil fauna, but this effect is highly habitat dependent.

4.2. Knotweed Effects on Collembola

Overall, the presence of invasive knotweed led to reduce the total number of Collembola. Furthermore, as hypothesized, this negative effect was habitat dependent (significant interactive terms of Knotweed × Habitat) with an opposite response pattern of invasion in forests, where half of the Collembola disappeared compared to the invasion in meadows, with an increase in collembolan abundance of about 41.8%. The importance of habitat characteristics or ecosystem type in invasion ecology was previously highlighted by other authors such as McCary et al. [7] and Liebhold et al. [41], suggesting that IAP rather indirectly influence soil fauna through modifications/alterations of environmental variables that may or not differ according to habitat type. Interestingly, this habitat-dependent differential response to the invasion of total Collembola was expressed by two of the three collembolan life-forms, the most and the less abundant, i.e., the hemiedaphic and the epedaphic, respectively. By contrast, the euedaphic species living deep in the soil were not significantly influenced by the presence of knotweed. This validates our hypothesis that collembolan species have contrasting responses to knotweed invasion according to their life-forms and that these responses were driven by contrasting ecological factors among different functional groups. Interestingly, euedaphic species not influenced by the presence of knotweed are assumed to be K-strategists and, therefore, more sensitive to changes in environmental conditions than r-strategists, such as epedaphic species [16] which can rapidly adapt to a fluctuating environment. Knotweed invasion strongly affects the vegetation community by changing the habitat for topsoil-living Collembola species, i.e., epedaphic and several hemiedaphic Collembola. Several studies previously highlighted the importance of vegetation community structure and composition as drivers of Collembola life-forms abundance [22,42]. Changes deeper in the soil, such as organic matter content or pH, may be less important or may take more time to occur, and therefore be less important for euedaphic species that are used to coping with organic matter that is already processed. For example, euedaphic Collembola were shown to be much less reactive than epedaphic or hemiedaphic species to understory vegetation changes during forest clear-cutting [43]. From our results, it is clear that knotweed invasion in meadows led, first, to unfavorable habitat conditions or a trophic niche for epedaphic Collembola, and, second, to the promotion of hemiedaphic species. In contrast, in forests, the opposite pattern was found for the hemiedaphic species, and no response was found in the epedaphic Collembola. Although we do not have a clear explanation for the mechanisms behind these contrasting patterns, we can hypothesize that

epedaphic species living in meadows, in contrast to species living in forests, are not used to dealing with a large amount of litter in autumn. Additionally, this monospecific litter also presents contrasted functional leaf attributes compared to monocotyledons leaves that are dominant in meadows. The presence of knotweed in meadows is radically changing the topsoil habitat with a high amount of litter. This may also have a strong effect on the available trophic resources for Collembola. The different collembolan life-forms are known to have distinct trophic regimes and this may also partly explain their differential responses to knotweed invasion in different habitat types [17]. Changes in abiotic variables, such as nitrate or soil humidity, are also more important in post-invasion meadows than in post-invasion forests, possibly affecting epedaphic and hemiedaphic species. Furthermore, we cannot exclude that secondary compounds released by knotweed roots or litter may differently interact with soil components in a forest or in a meadow soil, according to their chemical nature and/or physical matrices. Plant exudation is known to be controlled by soil abiotic variables such as pH, temperature and humidity [44]. Regardless of the underlying mechanisms, however, changes in abundance of ep- and hemiedaphic species a few years after invasion may have considerable functional implications for soil processes. Surface-dwelling species have been shown, for example, to significantly enhance decomposition rates by facilitating the microbial use of organic matter [45–47].

4.3. Knotweed Effects on Nematoda

Overall, the total abundance of Nematodes we found in our study is comparable to abundances found in other studies reporting on riparian habitats in both forests or meadows [48–51]. The total abundance of Nematoda did not respond to the ingress of knotweed, regardless of the initial habitat structure. The abundance of total Nematodes seems to be positively correlated with plant species' richness and soil fungal biomass (i.e., ergosterol). We could not find any study in the literature reporting results on nematode abundances in the context of knotweed invasion. However, Abgrall et al. [13], in a microcosm experiment, found the total nematode abundance to significantly respond to knotweed rhizome extract; however, the direction of the effect (positive, neutral or negative) was dependent on the concentration of the rhizome extract, making a generalization difficult. Furthermore, Mc Cary et al. [7] and Abgrall et al. [8], in two meta-analyses, found the effect of invasive alien plant species on belowground fauna to depend on the feeding regime of the soil faunal group considered. Therefore, the lack of general effect on Nematodes in our case is not surprising, as Nematodes encompass a wide array of different trophic groups spanning from root herbivores to predators. Separating Nematodes into trophic groups helped us to reveal that plant feeders were the only trophic groups influenced by the invasion of knotweed, with their populations being strongly impoverished after knotweed invasion, either in forest or in meadow habitats. Plant feeders are primary consumers and have direct relationships with alien plant roots in the context of invasion. There is evidence for a high level of specificity aboveground, with over 90% of insect herbivores, for example, that feed only on plants belonging to a single genus or family [52]. Accordingly, McCary et al. [7] found that the abundance of aboveground herbivores declined in invaded areas dominated by one plant species, limiting the choice of resources for herbivores. Our results support this point of view. Furthermore, Asian knotweeds are known to deliver complex secondary metabolic compounds such as catechin or trans-resveratrol, which are known as being allelopathic [53–55]. Knotweed root systems consist of strong rhizomes with only a few fine roots. Both aspects (root architecture and release of allelopathic compounds) are likely to limit the accessibility of roots by plant feeders, explaining their strong decrease observed in our study. The decrease in microbial biomass observed in invaded plots compared to control plots did not lead to a significant decrease in microbivorous Nematodes, either bacterial or fungal feeders, even if a clear negative trend was observed, with a five-fold decrease and a three-fold decrease in bacterivores and fungivores in invaded plots compared to controls (forests and meadows merged together), respectively. Unfortunately, the statistical power was probably too weak to enable us to reveal statistical differences

between treatments in this case. Finally, abundances of predators were relatively constant between all situations, supporting the idea that higher soil faunal trophic groups are less impacted than basal ones by the invasion of a plant species [8]. Brousseau et al. [35], at the same sites, also found that the lower species and functional diversity of plants in knotweed plots did not markedly cascade to the macrodetritivores and predators at either the taxonomic or the functional level. They also demonstrated that knotweed strongly reduced the trait matching (i.e., correlation between traits) between the functional diversity of detritivores and predators. Furthermore, a meta-analysis by Zhang et al. [56] showed that the effects of invasive plants can be separated into litter-based effects and rhizosphere effects, even though both compartments can facilitate plant invasion through positive feedback of nutrient cycling in soil systems. According to their research, invasive plant litter increases the abundance of aboveground decomposers, whereas the roots of invasive plants have a negative impact on belowground herbivores and predators. The latter also undergo changes in habitat structure due to the knotweed's rhizomes [57].

5. Conclusions

Further investigations are needed to clearly identify the abiotic or biotic factors responsible for changes in Collembola and Nematoda communities after knotweed invasion. However, our findings support the conclusions of previous studies by demonstrating that soil fauna abundance is impacted by plant invasions [58–60], with the initial habitat structure as a strong moderator of knotweed presence outcome [8]. Responses within the soil fauna also differ between trophic levels and life-forms, potentially leading to different food-web structures and performances. Our results reveal the need to further investigate belowground response to IAP because, in the context of biological invasions, the importance of plant species' identity and composition as drivers of soil biodiversity is predominant [6,61]. This is most likely explained by trait differences between plant species, which can determine litter quality and physical structure, with subsequent consequences for trophic resources and microhabitat conditions [6,62].

Supplementary Materials: The following are available online at https://www.mdpi.com/article/10.3390/d14020061/s1, Table S1: Study sites description with the dominant plant species found in control sites, Table S2: Full dataset of soil variables (abiotic and biotic) and vegetation in 6 studied sites invaded or not by Asian knotweed.

Author Contributions: Conceptualization, T.D.A., M.C. and E.F.; methodology, T.D.A., M.C. and E.F.; validation, T.D.A., M.C. and E.F.; formal analysis, T.D.A., M.C. and E.F.; investigation, T.D.A., M.C. and E.F.; resources, T.D.A., M.C. and E.F.; data curation, T.D.A.; writing—original draft preparation, T.D.A., M.C. and E.F.; writing—review and editing, T.D.A., M.C. and E.F.; funding acquisition, E.F. and M.C. All authors have read and agreed to the published version of the manuscript.

Funding: This research was partly funded by "the Agence de l'Eau Seine-Normandie—AESN".

Institutional Review Board Statement: Not applicable.

Informed Consent Statement: Not applicable.

Data Availability Statement: Data are available as part of the Supplementary Material.

Acknowledgments: We thank the Ecodiv lab members for field and laboratory assistance as well as the AESN for site accessibility.

Conflicts of Interest: The authors declare no conflict of interest. The funders had no role in the design of the study; in the collection, analyses, or interpretation of data; in the writing of the manuscript, or in the decision to publish the results.

References

1. Vilà, M.; Espinar, J.L.; Hejda, M.; Hulme, P.E.; Jarošík, V.; Maron, J.L.; Pergl, J.; Schaffner, U.; Sun, Y.; Pyšek, P. Ecological impacts of invasive alien plants: A meta-analysis of their effects on species, communities and ecosystems. *Ecol. Lett.* **2011**, *14*, 702–708. [CrossRef]
2. Pyšek, P.; Jarošík, V.; Hulme, P.E.; Pergl, J.; Hejda, M.; Schaffner, U.; Vilà, M. A global assessment of invasive plant impacts on resident species, communities and ecosystems: The interaction of impact measures, invading species' traits and environment. *Glob. Change Biol.* **2012**, *18*, 1725–1737. [CrossRef]
3. Diagne, C.; Leroy, B.; Vaissière, A.-C.; Gozlan, R.E.; Roiz, D.; Jarić, I.; Salles, J.-M.; Bradshaw, C.J.A.; Courchamp, F. High and rising economic costs of biological invasions worldwide. *Nature* **2021**, *592*, 571–576. [CrossRef]
4. Schirmel, J.; Bundschuh, M.; Entling, M.H.; Kowarik, I.; Buchholz, S. Impacts of invasive plants on resident animals across ecosystems, taxa, and feeding types: A global assessment. *Glob. Change Biol.* **2016**, *22*, 594–603. [CrossRef]
5. Callaway, R.M.; Ridenour, W.M. Novel weapons: Invasive success and the evolution of increased competitive ability. *Front. Ecol. Environ.* **2004**, *2*, 436–443. [CrossRef]
6. Forey, E.; Lodhar, S.; Gopaul, S.; Boehmer, H.J.; Chauvat, M. A functional trait-based approach to assess the impact of an alien palm invasion on plant and soil communities on a South Pacific island. *Austral Ecol.* **2021**, *46*, 398–410. [CrossRef]
7. McCary, M.A.; Mores, R.; Farfan, M.A.; Wise, D.H. Invasive plants have different effects on trophic structure of green and brown food webs in terrestrial ecosystems: A meta-analysis. *Ecol. Lett.* **2016**, *19*, 328–335. [CrossRef] [PubMed]
8. Abgrall, C.; Forey, E.; Chauvat, M. Soil fauna responses to invasive alien plants are determined by trophic groups and habitat structure: A global meta-analysis. *Oikos* **2019**, *128*, 1390–1401. [CrossRef]
9. Wardle, D.A.; Peltzer, D.A. Impacts of invasive biota in forest ecosystems in an aboveground–belowground context. *Biol. Invasions* **2017**, *19*, 3301–3316. [CrossRef]
10. Aldorfová, A.; Knobová, P.; Münzbergová, Z. Plant–soil feedback contributes to predicting plant invasiveness of 68 alien plant species differing in invasive status. *Oikos* **2020**, *129*, 1257–1270. [CrossRef]
11. Martin, F.-M. The Study of the Spatial Dynamics of Asian Knotweeds (*Reynoutria* spp.) across Scales and its Contribution for Management Improvement. Ph.D. Thesis, Université Grenoble Alpes, Grenoble, France, 2019.
12. Lavoie, C. The impact of invasive knotweed species (*Reynoutria* spp.) on the environment: Review and research perspectives. *Biol. Invasions* **2017**, *19*, 2319–2337. [CrossRef]
13. Abgrall, C.; Forey, E.; Mignot, L.; Chauvat, M. Invasion by *Fallopia japonica* alters soil food webs through secondary metabolites. *Soil Biol. Biochem.* **2018**, *127*, 100–109. [CrossRef]
14. Skubala, P.; Mierny, A. Invasive *Reynoutria* taxa as a contaminant of soil. Does it reduce abundance and diversity of microarthropods and damage soil habitat? *Pestycydy* **2009**, *1–4*, 57–62.
15. Chauvat, M.; Perez, G.; Ponge, J.-F. Foraging patterns of soil springtails are impacted by food resources. *Appl. Soil Ecol.* **2014**, *82*, 72–77. [CrossRef]
16. Petersen, H. General aspects of collembolan ecology at the turn of the millennium: Proceedings of the Xth international colloquium on Apterygota, České Budějovice 2000: Apterygota at the beginning of the third millennium. *Pedobiologia* **2002**, *46*, 246–260. [CrossRef]
17. Potapov, A.A.; Semenina, E.E.; Korotkevich, A.Y.; Kuznetsova, N.A.; Tiunov, A. V Connecting taxonomy and ecology: Trophic niches of collembolans as related to taxonomic identity and life forms. *Soil Biol. Biochem.* **2016**, *101*, 20–31. [CrossRef]
18. Potapov, A.M.; Pollierer, M.M.; Salmon, S.; Šustr, V.; Chen, T. Multidimensional trophic niche revealed by complementary approaches: Gut content, digestive enzymes, fatty acids and stable isotopes in Collembola. *J. Anim. Ecol.* **2021**, *92*, 161–188. [CrossRef]
19. Rusek, J. Biodiversity of Collembola and their functional role in the ecosystem. *Biodivers. Conserv.* **1998**, *7*, 1207–1219. [CrossRef]
20. Chauvat, M.; Wolters, V.; Dauber, J. Response of collembolan communities to land-use change and grassland succession. *Ecography* **2007**, *30*, 183–192. [CrossRef]
21. da Silva, P.M.; Carvalho, F.; Dirilgen, T.; Stone, D.; Creamer, R.; Bolger, T.; Sousa, J.P. Traits of collembolan life-form indicate land use types and soil properties across an European transect. *Appl. Soil Ecol.* **2016**, *97*, 69–77. [CrossRef]
22. Henneron, L.; Aubert, M.; Archaux, F.; Bureau, F.; Dumas, Y.; Ningre, F.; Richter, C.; Balandier, P.; Chauvat, M. Forest plant community as a driver of soil biodiversity: Experimental evidence from collembolan assemblages through large-scale and long-term removal of oak canopy trees *Quercus petraea*. *Oikos* **2017**, *126*, 420–434. [CrossRef]
23. Yin, R.; Gruss, I.; Eisenhauer, N.; Kardol, P.; Thakur, M.P.; Schmidt, A.; Xu, Z.; Siebert, J.; Zhang, C.; Wu, G.-L. Land use modulates the effects of climate change on density but not community composition of Collembola. *Soil Biol. Biochem.* **2019**, *138*, 107598. [CrossRef]
24. Jenkinson, D.S.; Powlson, D.S. The effects of biocidal treatments on metabolism in soil–I. Fumigation with chloroform . . . V. A method for measuring soil biomass. *Soil Biol. Biochem.* **1976**, *8*, 179. [CrossRef]
25. Gong, P.; Guan, X.; Witter, E. A rapid method to extract ergosterol from soil by physical disruption. *Appl. Soil Ecol.* **2001**, *17*, 285–289. [CrossRef]
26. Braun-Blanquet, J.; Roussine, N.; Nègre, R.; Emberger, L. *Les Groupements Végétaux de la France Méditerranéenne*; CNRS Edition: Paris, France, 1952.
27. Macfadyen, A. Improved funnel-type extractors for soil arthropods. *J. Anim. Ecol.* **1961**, *30*, 171–184. [CrossRef]

28. Gisin, H. *Ökologie und Lebensgemeinschaften der Collembolen im Schweizerischen Exkursionsgebiet Basel, Inauguraldissertation*; Universität Basel: Basel, Switzerland, 1943.
29. Barker, K.R. *Nematode Extraction and Bioassays*; Barker, K., Barker, K.R., Carter, C.C., Sasser, J.N., Eds.; North Carolina State University Graphics: Raleigh, NC, USA, 1985.
30. Yeates, G.W.; Bongers, T.; De Goede, R.G.M.; Freckman, D.W.; Georgieva, S.S. Feeding habits in soil nematode families and genera—an outline for soil ecologists. *J. Nematol.* **1993**, *25*, 315–331.
31. Magnusson, A.; Skaug, H.; Nielsen, A.; Berg, C.; Kristensen, K.; Maechler, M.; van Bentham, K.; Bolker, B.; Brooks, M.; Brooks, M.M. Package 'glmmTMB.' R Packag. Version 0.2. 0. 2017. Available online: http://cran.uni-muenster.de/web/packages/glmmTMB/glmmTMB.pdf (accessed on 15 January 2021).
32. Brooks, M.E.; Kristensen, K.; van Benthem, K.J.; Magnusson, A.; Berg, C.W.; Nielsen, A.; Skaug, H.J.; Mächler, M.; Bolker, B.M. glmmTMB balances speed and flexibility among packages for zero-inflated generalized linear mixed modeling. *R J.* **2017**, *9*, 378–400. [CrossRef]
33. Oksanen, J.; Blanchet, F.; Kindt, R.; Legendre, P.; O'Hara, R. Vegan: Community ecology package. *R Packag.* **2016**, *2*, 2–3.
34. Lê, S.; Josse, J.; Husson, F. FactoMineR: An R package for multivariate analysis. *J. Stat. Softw.* **2008**, *25*, 1–18. [CrossRef]
35. Brousseau, P.-M.; Chauvat, M.; De Almeida, T.; Forey, E. Invasive knotweed modifies predator–prey interactions in the soil food web. *Biol. Invasions* **2021**, *23*, 1987–2002. [CrossRef]
36. Mincheva, T.; Barni, E.; Varese, G.C.; Brusa, G.; Cerabolini, B.; Siniscalco, C. Litter quality, decomposition rates and saprotrophic mycoflora in Fallopia japonica (Houtt.) Ronse Decraene and in adjacent native grassland vegetation. *Acta Oecol.* **2014**, *54*, 29–35. [CrossRef]
37. Urgenson, L.S.; Reichard, S.H.; Halpern, C.B. Community and ecosystem consequences of giant knotweed (*Polygonum sachalinense*) invasion into riparian forests of western Washington, USA. *Biol. Conserv.* **2009**, *142*, 1536–1541. [CrossRef]
38. Mincheva, T.; Barni, E.; Siniscalco, C. From plant traits to invasion success: Impacts of the alien *Fallopia japonica* (Houtt.) Ronse Decraene on two native grassland species. *Plant Biosyst. Int. J. Deal. Asp. Plant Biol.* **2016**, *150*, 1348–1357. [CrossRef]
39. Bardon, C.; Poly, F.; el Zahar Haichar, F.; Le Roux, X.; Simon, L.; Meiffren, G.; Comte, G.; Rouifed, S.; Piola, F. Biological denitrification inhibition (BDI) with procyanidins induces modification of root traits, growth and N status in *Fallopia x bohemica*. *Soil Biol. Biochem.* **2017**, *107*, 41–49. [CrossRef]
40. Stefanowicz, A.M.; Kapusta, P.; Stanek, M.; Frąc, M.; Oszust, K.; Woch, M.W.; Zubek, S. Invasive plant *Reynoutria japonica* produces large amounts of phenolic compounds and reduces the biomass but not activity of soil microbial communities. *Sci. Total Environ.* **2021**, *767*, 145439. [CrossRef]
41. Liebhold, A.M.; Brockerhoff, E.G.; Kalisz, S.; Nuñez, M.A.; Wardle, D.A.; Wingfield, M.J. Biological invasions in forest ecosystems. *Biol. Invasions* **2017**, *19*, 3437–3458. [CrossRef]
42. Perez, G.; Decaëns, T.; Dujardin, G.; Akpa-Vinceslas, M.; Langlois, E.; Chauvat, M. Response of collembolan assemblages to plant species successional gradient. *Pedobiologia* **2013**, *56*, 169–177. [CrossRef]
43. Chauvat, M.; Zaitsev, A.S.; Wolters, V. Successional changes of Collembola and soil microbiota during forest rotation. *Oecologia* **2003**, *137*, 269–276. [CrossRef]
44. Badri, D.V.; Vivanco, J.M. Regulation and function of root exudates. *Plant. Cell Environ.* **2009**, *32*, 666–681. [CrossRef]
45. Takeda, H. A 5 year study of pine needle litter decomposition in relation to mass loss and faunal abundances. *Pedobiologia* **1988**, *32*, 221–226.
46. Faber, J.H.; Teuben, A.; Berg, M.P.; Doelman, P. Microbial biomass and activity in pine litter in the presence of *Tomocerus minor* (Insecta, Collembola). *Biol. Fertil. Soils* **1992**, *12*, 233–240. [CrossRef]
47. Hasegawa, M.; Takeda, H. Changes in feeding attributes of four collembolan populations during the decomposition process of pine needles. *Pedobiologia* **1995**, *39*, 155–169.
48. Young-Mathews, A.; Culman, S.W.; Sánchez-Moreno, S.; O'Geen, A.T.; Ferris, H.; Hollander, A.D.; Jackson, L.E. Plant-soil biodiversity relationships and nutrient retention in agricultural riparian zones of the Sacramento Valley, California. *Agrofor. Syst.* **2010**, *80*, 41–60. [CrossRef]
49. Briar, S.S.; Culman, S.W.; Young-Mathews, A.; Jackson, L.E.; Ferris, H. Nematode community responses to a moisture gradient and grazing along a restored riparian corridor. *Eur. J. Soil Biol.* **2012**, *50*, 32–38. [CrossRef]
50. Čerevková, A.; Bobuľská, L.; Miklisová, D.; Renčo, M. A case study of soil food web components affected by *Fallopia japonica* (Polygonaceae) in three natural habitats in Central Europe. *J. Nematol.* **2019**, *51*, e2019-42. [CrossRef]
51. Renčo, M.; Čerevková, A.; Homolová, Z. Nematode communities indicate the negative impact of *Reynoutria japonica* invasion on soil fauna in ruderal habitats of tatra national park in Slovakia. *Glob. Ecol. Conserv.* **2021**, *26*, e01470. [CrossRef]
52. Ali, J.G.; Agrawal, A.A. Specialist versus generalist insect herbivores and plant defense. *Trends Plant Sci.* **2012**, *17*, 293–302. [CrossRef]
53. Vrchotová, N.; Šerá, B. Allelopathic properties of knotweed rhizome extracts. *Plant Soil Environ.* **2008**, *54*, 301–303. [CrossRef]
54. Vrchotová, N.; Sera, B.; Triska, J. The stilbene and catechin content of the spring sprouts of Reynoutria species. *Acta Chromatogr.* **2007**, *19*, 21–28.
55. Vastano, B.C.; Chen, Y.; Zhu, N.; Ho, C.-T.; Zhou, Z.; Rosen, R.T. Isolation and identification of stilbenes in two varieties of polygonum c uspidatum. *J. Agric. Food Chem.* **2000**, *48*, 253–256. [CrossRef]

56. Zhang, P.; Li, B.; Wu, J.; Hu, S. Invasive plants differentially affect soil biota through litter and rhizosphere pathways: A meta-analysis. *Ecol. Lett.* **2019**, *22*, 200–210. [CrossRef] [PubMed]
57. Bailey, J.P.; Bímová, K.; Mandák, B. Asexual spread versus sexual reproduction and evolution in Japanese Knotweed s.l. sets the stage for the "battle of the Clones". *Biol. Invasions* **2009**, *11*, 1189–1203. [CrossRef]
58. Morriën, E.; Duyts, H.; Van der Putten, W.H. Effects of native and exotic range-expanding plant species on taxonomic and functional composition of Nematodes in the soil food web. *Oikos* **2012**, *121*, 181–190. [CrossRef]
59. Tanner, R.A.; Varia, S.; Eschen, R.; Wood, S.; Murphy, S.T.; Gange, A.C. Impacts of an invasive non-native annual weed, *Impatiens glandulifera*, on above-and below-ground invertebrate communities in the United Kingdom. *PLoS ONE* **2013**, *8*, e67271. [CrossRef]
60. Maceda-Veiga, A.; Basas, H.; Lanzaco, G.; Sala, M.; De Sostoa, A.; Serra, A. Impacts of the invader giant reed (*Arundo donax*) on riparian habitats and ground arthropod communities. *Biol. Invasions* **2016**, *18*, 731–749. [CrossRef]
61. Wardle, D.A. How plant communities influence decomposer communities. *Biol. Divers. Funct. Soils* **2005**, 119–138. [CrossRef]
62. Wardle, D.A. The influence of biotic interactions on soil biodiversity. *Ecol. Lett.* **2006**, *9*, 870–886. [CrossRef]

diversity

MDPI

Review

Diversity and Distribution of *Theileria* Species and Their Vectors in Ruminants from India, Pakistan and Bangladesh

Jehan Zeb [1,2], Baolin Song [1], Muhammad Umair Aziz [1], Sabir Hussain [1], Riaz Zarin [3] and Olivier Sparagano [1,*]

[1] Department of Infectious Diseases and Public Health, Jockey Club College of Veterinary Medicine and Life Sciences, City University of Hong Kong, Kowloon, Hong Kong SAR, China; jehanzeb2@cityu.edu.hk (J.Z.); Baolin.Song@my.cityu.edu.hk (B.S.); muhamaziz3-c@my.cityu.edu.hk (M.U.A.); sahussain8-c@my.cityu.edu.hk (S.H.)
[2] Department of Zoology, Abdul Wali Khan University Mardan, Mardan 23200, Pakistan
[3] Elementary & Secondary Education Department Government of Khyber Pakhtunkhwa, Chitral 17200, Pakistan; geospatial571@gmail.com
* Correspondence: olivier.sparagano@cityu.edu.hk

Abstract: Tropical theileriosis, caused by the apicomplexan hemoparasite of the genus *Theileria*, is a major constraint to livestock production in various parts of world, including South Asia. Several studies have been carried out over the last five decades; however, comprehensive information in this region regarding the diversity and distribution of *Theileria* is lacking. Therefore, keeping in mind the economic importance of theileriosis, we have systematically reviewed the current knowledge about *Theileria* spp. diversity and distribution affecting cattle, water buffaloes, goats and sheep in three countries included India, Pakistan and Bangladesh of the Indian sub-continent. The data collected indicated that the microscopic method is the widely used method for evaluating *Theileria* species in the three countries from 1970 to 2021. This is the first study in this region to compile a comprehensive knowledge about the diversity and distribution of *Theileria*. Our study revealed the existence of 11 different species of *Theileria*, including *Theileria* spp. *Theleria annulata*, *T. orientalis*, *T. mutans*, *T. velifera* circulating in cattle and buffalo while *T. annulata*, *T. lestoquardi*, *T. luwenshuni T. ovis*, *Theileria* spp. and *T. lestoquardi-like* spp., were infecting goats and sheep from various regions of India, Pakistan and Bangladesh. We find that *T. annulata* can be found in both small and large ruminants and is widely distributed in the different regions of India, Pakistan and Bangladesh. In addition, our analysis revealed that the existence of possible tick vectors of the genera *Hyalomma*, *Haemophysalis*, *Rhipicephalus* and *Amblyomma* may be responsible for the diverse and wide distribution of different *Theileria* species. However, the competence of these tick vectors for different *Theileria* species still need to be explored. Therefore, further studies are needed to bridge this gap and to improve the health and production of livestock and reduce economic losses due to theileriosis in India, Pakistan and Bangladesh. Furthermore, we selected representative 18S rRNA sequences for *T. annulata* from the different regions to infer phylogenetic relationship. Phylogenetic analysis of the selected isolates clustered in different clades which might be due to the variation in a hypervariable region of *18S rRNA*. The outcome of this analysis is expected to provide a coherent and integrated framework about the different *Theileria* species prevailing in these countries and contribute to improving the surveillance and control plans of various *Theileria* species in the region.

Keywords: diversity; distribution; *Theileria*; tick vectors; South Asia

Citation: Zeb, J.; Song, B.; Aziz, M.U.; Hussain, S.; Zarin, R.; Sparagano, O. Diversity and Distribution of *Theileria* Species and Their Vectors in Ruminants from India, Pakistan and Bangladesh. *Diversity* **2022**, *14*, 82. https://doi.org/10.3390/d14020082

Academic Editor: Michael Wink

Received: 28 December 2021
Accepted: 19 January 2022
Published: 25 January 2022

1. Introduction

Tick-borne diseases (TBDs) are considered to be one of the main threats to the ruminants' health in both tropical and sub-tropical regions of the world, representing a serious obstacle to livestock farming. Several TBDs cause significant economic losses associated

with high mortality rate and decreased production output in domestic livestock worldwide [1,2]. Among these, theileriosis is considered one of the significant tick-borne diseases and a major constraint in the growth of the livestock business in many areas of the world [3,4] (Ica et al., 2007; Jenkins 2018). It causes severe morbidity and mortality in livestock, reducing meat and milk production, leading to significant economic losses each year worldwide. The estimated range of economic losses due to theileriosis is 5–25% of the total farm losses worldwide [5]. Resource-poor farming communities are at a greater risk due to the lack of systematic acaricide use and limited access to veterinary health care centers leading to a high mortality rate in untreated animals [6,7].

The lifecycle of *Theileria* parasites in the ruminant host and tick vector has been reviewed [8,9]. Shortly, the lifecycle of *Theileria* is completed in two stages i.e., the vertebrate host stage (asexual reproduction) and tick vector stage (sexual reproduction). The lifecycle begins when an infected tick bites and transmits sporozoites into vertebrate hosts during blood-feeding, where it may transform into schizonts [10]. Subsequently, upon releasing from the infected leukocytes, the merozoites may infect host erythrocytes (RBCs) and then develop into piroplasms. Further multiplication of the piroplasms (merogony) takes place in the RBCs [11]. In non-transforming *Theileria*, merogony has been observed in RBCs [12]. Finally, the tick acquires blood-stage *Theileria* parasites including the gametes, when they feed on an infected host. Sexual reproduction of the gametes occurs in the midgut of the competent vector tick species, where, during meiosis, genetic recombination occurs [13,14]. In this way, *Theileria* parasites' transmission occurs trans-stadially by the tick vectors, and therefore, the known transmission vectors may be 2- or 3-host tick species [9]. The modified form of life cycle of *Theileria* species is shown in Figure 1.

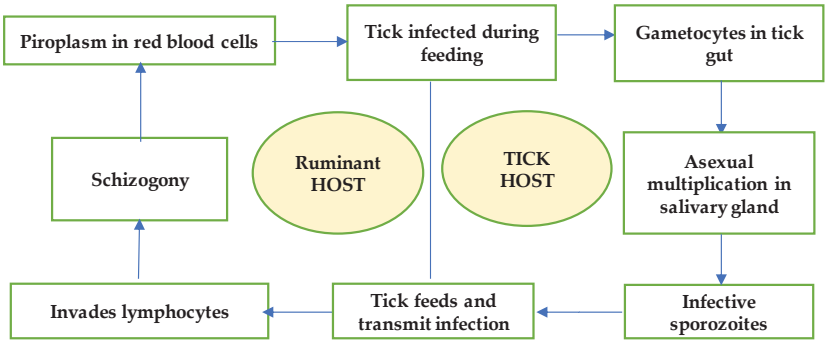

Figure 1. Life cycle of *Theileria* showing different stages in ruminants and tick hosts.

Theileria is distributed worldwide and is a significant cause of disease in livestock in tropical and subtropical regions of the world, including Asia. The most pathogenic and economically important *Theileria* species infecting large ruminants (Cattle; *Bos Taurus* and *Bos indicus*, and water buffalo; *Bubalus bubalis*) are *T. annulata*, which causes Tropical theileriosis (TT) or Mediterranean theileriosis, *T. parva*, which causes East Coast fever (ECF), and *T. mutans*, which causes benign theileriosis and *T. orientalis*, (*T. orientalis/buffeli* group), which causes Oriental theileriosis (OT) or *Theileria*-associated bovine anemia (TABA). However, on the other hand, *T. lestoquardi*, which causes malignant ovine theileriosis (MOT) *T. uilenbergi* and *T. luwenshuni* are the most pathogenic species of economic significance infecting small ruminants (goats; *Capra aegagrus hircus* and sheep; *Ovis aries*), *T. taurotragi*, and *T. ovis*, mostly cause asymptomatic infections in livestock [2,15]. Depending upon the *Theileria* species, different tick vector species of the genera *Hyalomma*, *Rhipicephalus*, *Haemaphysalis*, and *Amblyomma* are involved in disease transmission [16].

Different diagnostic techniques are used for the detection of *Theileria*. Most widely used and standard techniques are Giemsa-stained blood smears and lymph node needle biopsy smears. These methods are more useful in acutely infected animals than the chroni-

cally infected carriers due to the low level of parasitaemia. Furthermore, species-specific identification based on Giemsa staining is difficult as most *Theileria* piroplasms share morphological identity except for *T. parva*, *T. annulata* and *T. velifera*. Similarly, schizonts cannot always be detected in the superficial lymph nodes during the disease time. In addition, these methods need more field investigation [15,17]. As an alternative, a serological method for detecting parasites antibodies has been developed. However, these methods may only detect previous exposure to the infection as compared to the current one due to its poor sensitivity and specificity [15,18]. New advanced techniques such as next-generation genomic resources have been adapted to overcome these limitations of traditional gross parasitological diagnostic techniques. Different piroplasm species can be differentiated based on variations in the hyper-variable region of 18S rDNA sequence [19–25]. For the amplification of the 18S region, various PCR methods like reverse line blot (RLB)-PCR, quantitative PCR (qPCR) and multiplex PCR have been described to [19,26–28].

The seasonal fluctuations have been found as one of the important risk factors that affect the distribution of this parasite. There are several species of this parasite, and they have substantial differences in their ecoepidemiology in significant parts of the Asian countries including India, Pakistan and Bangladesh. In addition, lack of proper management practices in these areas may lead to heavy economic losses [29–31]. Keeping in view the importance of the above discussion, the present review data related to the *Theileria* species diversity infecting ruminant species and distribution concerning its tick vectors in specific region of the Asia including India, Pakistan and Bangladesh. The outcome of this analysis is expected to provide an integrated scientific baseline for future vaccination programs and other control measures either at the pathogen or vector level.

2. Materials and Methods

2.1. Study Protocol

In this review study, we systemically reviewed the relevant articles published on *Theileria* in small and large ruminants in the three important countries from the livestock perspectives of South Asia, including India, Pakistan and Bangladesh as shown in Figure 2. The different studies were divided into various zones based on administrative and geomorphic features such as India divided into five zones viz Central, North, East, North-east, West, South, while Pakistan divided into four provinces such as Punjab, Khyber Pakhtunkhwa, Sindh and Balochistan and FATA and Bangladesh was divided into six zones like Central, South Eastern, North Central, Northern, and Western.

2.2. Literature Search Strategy

Our procedure was based on searching different databases such as PubMed, Science Direct, Springer, Scopus, Google Scholar and Web of Science for retrieving relevant articles published in these three countries, which mainly focused on the time period from 1970 to 2021. Furthermore, to back trace the past years published articles on *Theileria*, all collected peer- reviewed articles, and references cited from the retrieved studies were searched again. Different terms such as *Theileria*, tick borne pathogens, *Theileria* vectors, tick vectors, large ruminants, small ruminants, and region of the concerned country were used for retrieving data.

2.3. Data Extraction and Qualitative Assessment

The diversity and distribution studies were analyzed carefully and reviewed systematically before initiating the data entry process onto predesigned Microsoft Excel 2010 sheets. To further maximize the accuracy, the extracted information compiled in Microsoft Excel 2010 by the author (JZ) was screened to remove repeated studies. After the data were entered, another author (OS) checked the dataset thoroughly to avoid errors, duplications and to further enhance the quality of extracted data.

Theileria Species Name

Country: Pakistan

Host: Cattle and Baffaloes

T. annulata
T. orientalis
Theileria spp

Host: Goats and sheep

T. annulata
T. lestoquardi
T. luwenshuni T. ovis
Theileria spp.
lestoquardi-like spp.

Country: India

Host: Cattle and Baffaloes

T. orientalis, T. mutans
T. velifera
Theileria spp. T. annulata

Host: Goats and sheep

T. luwenshuni & T. ovis
Theileria spp. T. lestoquardi
Country: Bangladesh

Country: Bangladesh

Host: Cattle and Baffaloes

T. Mutans
T. orientalis
Theileria Spp. T. annulata

Host: Goats and sheep

T. annulata

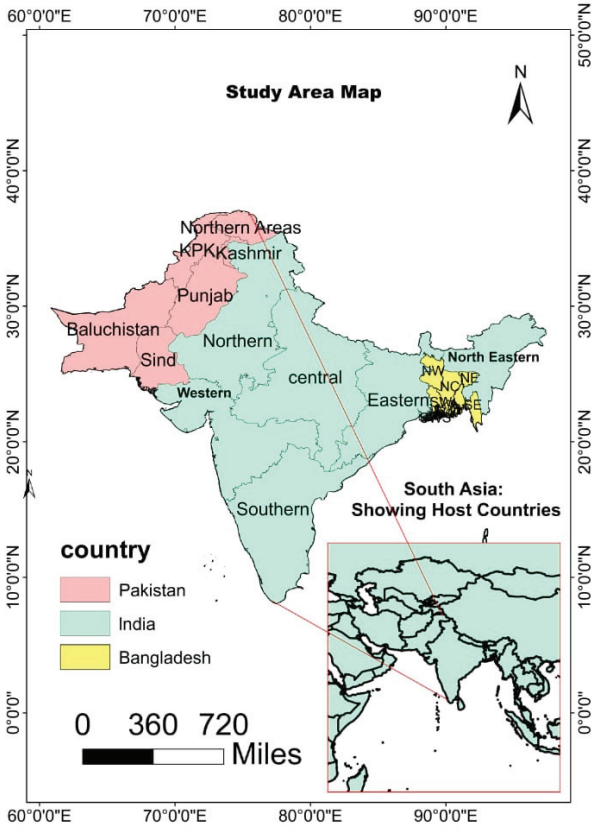

Figure 2. Map showing the location of the study area (India, Pakistan, and Bangladesh) and a list of *Theileria* Species present in each country.

Furthermore, all studies regarding *Theileria*/theileriosis conducted on large (cattle and buffaloes) and small ruminants (goats and sheep) in the region were selected for analysis. Five key pieces of information was extracted from the literature: (1) *Theileria* species and possible tick vectors detection (2) region, state or location of the study, (3) time of the study conducted, (4) study type and (5) studies that have used the standard methodology of confirmatory tests including blood smear examination with different staining methods, molecular methods by different PCRs, and serological diagnosis.

During the first step of screening, 410 articles, including $n = 250$ from India, $n = 130$ from Pakistan and $n = 30$ from Bangladesh were retrieved. Following the data retrieval step, the data were compiled in Microsoft Excel 2010 and all the duplicated studies $n = 60$ were removed from further screening while $n = 130$ theses and full length papers which were not available online were also excluded. In addition, all the irrelevant data and papers ($n = 75$) published in a language other than English were also removed. To further enhance the quality assessment, we removed the conference proceedings, which were not available with full text. Finally, a total of 136 were identified to be eligible for data analysis which included $n = 67$, $n = 56$ and $n = 13$ from India, Pakistan and Bangladesh, respectively (Figure 3). The studies were carried out between 1975 and 2021, and were grouped in three different periods: (1) 1975–2010, (2) 2011–2015, (3) 2016–2021, and were differentiated between molecular and direct diagnostic tests, as shown in Figures 4 and 5.

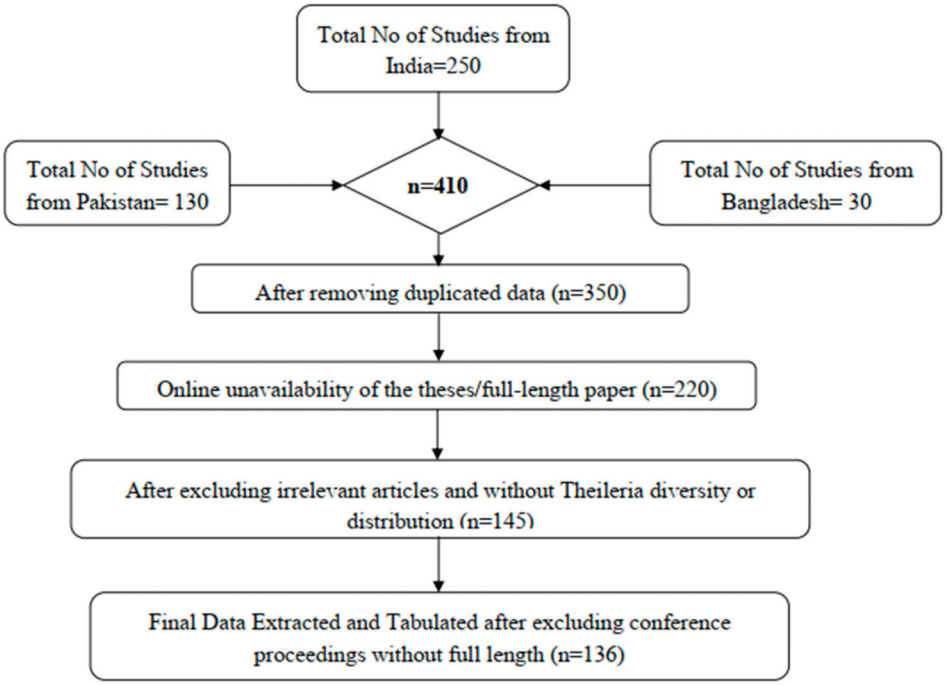

Figure 3. Flow chart diagram showing the data retrieving and extraction procedure.

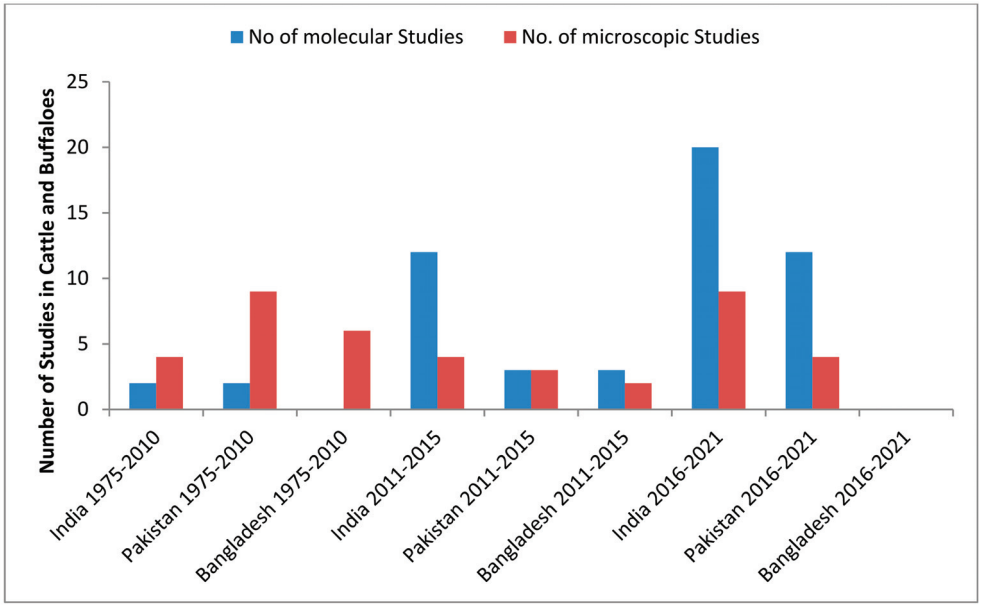

Figure 4. Comparison of the number of epidemiological studies detecting *Theileria* spp. in water buffalo and cattle using molecular and microscopic diagnostic methods in India, Pakistan and Bangladesh, according to three different periods between 1975 and 2021.

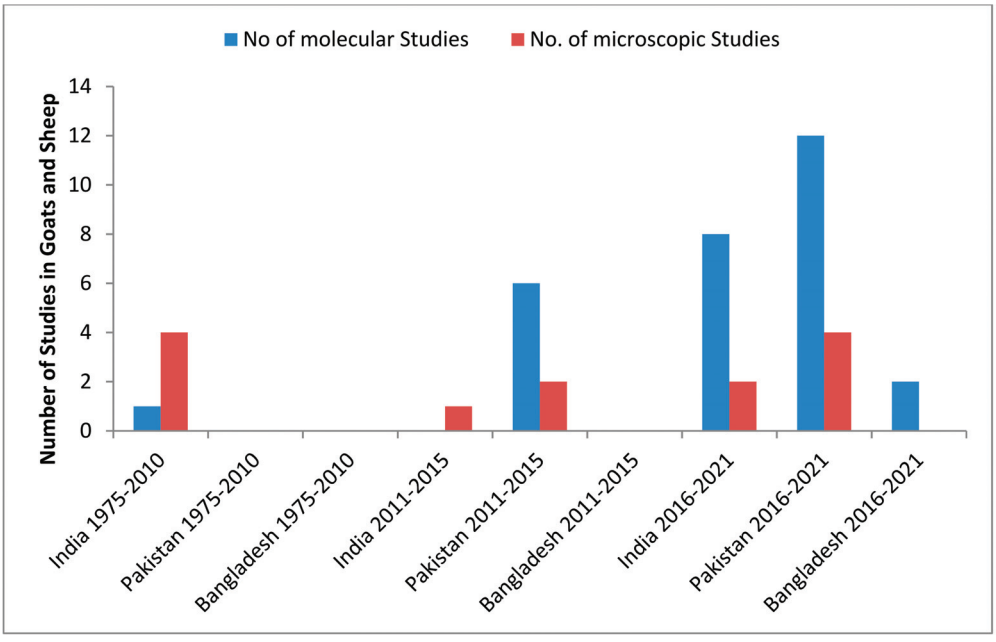

Figure 5. Comparison of the number of epidemiological studies detecting *Theileria* spp. in goats and sheep using molecular and microscopic diagnostic methods in India, Pakistan and Bangladesh, according to three different periods between 1975 and 2021.

2.4. Phylogenetic Analysis and Evolutionary Divergence

Representative sequences with accession numbers were selected from the previously published studies and were used for phylogenetic and evolutionary (genetic) divergence analysis. The sequences selected from the different regions of India were included, MF287947.1 (Central India), MF287920.1, (West India), MF287949.1 (Eastern India), MF287937.1 *T_annulata* South India and MF287934.1 (North India) while sequences with accession numbers from Pakistan are included JQ743631.1 (Pakistan), JQ743636.1, (Pakistan), MW046053.1 (Pakistan) and MW046054.1 (Pakistan). The phylogenetic tree of the selected *T. annulata* isolates was inferred using the *18S rRNA* genetic marker. Phylogenetic analyses were conducted with a Tamura 3-parameter (T92 + G) Model using MEGA version 7.0 [32]. CLUSTAL W alignment was performed to align the selected sequences retrieved from the GenBank. The neighbor-joining algorithm was used to establish the phylogenetic analysis. Bootstrap values were obtained with 1000 replicates.

3. Results and Discussion

3.1. Diversity and Distribution of Theileria Species Infecting Livestock

A general overview of the *Theileria* species identified in the three countries is depicted in the Table 1. We have collected the data regarding different species of *Theileria* infecting livestock i.e., large (cattle & buffalo) and small ruminants (goats & sheep) conducted in the different geographical regions of the three selected countries of South Asia. Our analysis revealed that different species of *Theileria* in these countries circulating in large ruminants include *T. annulata*, *T. orientalis T. mutans*, *T. Ovis* and *T. velifera* and *Theileria* spp., while in small ruminants, the different species of *Theileria* reported were *T. annulata*, *T. lestoquardi*, *T. luwenshuni T. ovis*, *Theileria* spp. and *T. lestoquardi*-like spp. from various geographical locations of India, Pakistan and Bangladesh. Among these, the most common and widespread species circulating in all ruminants is *T. annulata*.

Table 1. Common *Theileria* species found in India, Pakistan and Bangladesh.

Country	Host	*Theileria* Species Name
India	Cattle & Buffaloes	*Theileria* spp. *T. annulata*, *T. orientalis*, *T. mutans* & *T. velifera*
	Goats & Sheep	*Theileria* spp. *T. lestoquardi T. luwenshuni* & *T. ovis*
Pakistan	Cattle & Buffaloes	*T. annulata*, *T. orientalis* & *Theileria* spp.
	Goats & Sheep	*T. annulata*, *T. lestoquardi*, *T. luwenshuni T. ovis* & *Theileria* spp. *T. lestoquardi*-like spp.
Bangladesh	Cattle & Buffaloes	*Theileria* spp. *T. annulata*, *T. orientalis*, *T. Mutans*,
	Goats & Sheep	*T. annulata*

3.2. Diversity and Distribution of Theileria Species Infecting Livestock in the Different Regions of India

Theileria species reported from different regions of India are listed in Table 2. According to the data collected, only one species of *Theileria* reported in cattle and buffalo from the central region of India is *T. annulata*, [33,34] while, on the other hand, in Eastern India, two species of *Theileria*. (*T. mutans* & *T. velifera*) were identified; however, no *Theileria* species were reported in small ruminants from these two regions [35,36]. Furthermore, *Theileria* species identified in the large ruminants from South India included *Theileria* spp., *T. annulata* [37–39] and new *T. orientalis* genotype [40–43], whereas, in East and North East India, trans placental transmission of *T. annulata* in young borne calves and its detection in tick *Hy. anatolicum* has been identified [44,45]. In the case of small ruminants, *T. lestoquardi* was identified molecularly. *T. luwenshuni* & *T. ovis* [46–48] were detected in South India while only *T. luwenshuni* has been recorded in the East and Northeast region of India [49,50]. Furthermore, *Theileria* spp., [51] *T. annulata*, [52–57] and *T. orientalis* [58] were detected to be circulating in cattle and buffalo while *T. annulata*, [59], *Theileria* spp. [60] and *T. luwenshuni* [61–63] were found infecting goats and sheep (small ruminants) from West Bangal and North India. The difference in the distribution of diversity of various *Theileria* species in different regions may be attributed to various factors such as competent vector tick species, geo-climatic conditions favoring different vector tick species growth, lack of education of farmers, and improper use of acaricidal use.

Table 2. Regional wise distribution of *Theileria* Species in different regions of India.

India					
Province/State	***Theileria* spp.**	**Identification Method**	**Host**	**Year of Study**	**References**
		Central India			
		Cattle & Buffaloes			
Central India	*T. annulata*	Microscopy	Ticks & Cattle	1975	[64]
Uttar Pradesh	*T. annulata*	Molecular	Cattle	1977	[65]
Uttar Pradesh	*T. annulata*	Microscopy	Cattle	2012	[66]
Uttar Pradesh	*T. annulata*	Molecular	Cattle	2015	[67]
Chhattisgarh	*T. annulata*	Microscopy	Cattle	2016	[34]
Central India	*T. annulata*	Molecular	Cattle	2017	[68]
Uttar Pradesh	*T. annulata*	Molecular	Cattle	2018	[69]
Hisar	*T. annulata*	Microscopy	Cattle	1989	[33]
		Eastern India			
West Bangal	*T. annulata*	Molecular	Cattle	2003	[35]
Guinea	*T. mutans* & *T. velifera*	Molecular	Cattle	2021	[36]
		South India			
North Banglore	*T. annulata*	Microscopy	Cattle	2009	[37]
Kerala	*Theileria* spp. & *T. annulata*	Microscopy & Molecular	Cattle	2011	[38]
South India	*T. orientalis*	Molecular	Cattle	2011	[70]
South India	*T. annulata* & *Theileria* spp.	Molecular	Cattle	2013	[40]
Tamil Nadu	*Theileria* spp.	Microscopy	Cattle	2014	[71]
Telangana and Andhra Pradesh	*T. orientalis*	Molecular	Cattle	2015	[41]
Karnataka	*T. annulata*	Microscopy	Cattle	2016	[42]

Table 2. *Cont.*

India					
Province/State	***Theileria* spp.**	**Identification Method**	**Host**	**Year of Study**	**References**
Southwest India	*T. annulata*	Microscopy	Buffalo & Cattle	2016	[39]
Karnataka	*T. annulata*	Microscopy	Cattle	2017	[72]
Kerala	*T. orientalis*	Molecular	*R. annulatus* Ticks	2019	[43]
South India	*Theileria* spp.	Molecular	Ticks & Cattle	2021	[73]
		Goats & Sheep			
West Bengal	*T. hirci* (*T. lestoquardi*)	Microscopy	Goat	1990	[46]
Karnataka	*Theileria* spp.	Microscopy	Sheep	1985	[74]
South India	*Theileria* spp.	Microscopy	Goat & Ticks	2017	[47]
Kerala	*Theileria* spp.	Microscopy & Molecular	Goats	2017	[75]
Karnataka	*T. luwenshuni*	Molecular	Goats & Sheep	2017	[48]
Karnataka	*T. luwenshuni* & *T. ovis*	Molecular	Sheep	2019	[76]
Karnataka	*Theileria* spp.	Microscopy	Sheep	2020	[77]
Assam	*T. annulata* & *T. orientalis*	Molecular	Cattle	2015	[78]
Odisha	*T. annulata* & *T. orientalis*	Microscopy & Molecular	Cattle	2017	[79]
Odisha	*T. annulata*	Microscopy and Molecular	Cattle	2017	[80]
Odisha	*T. orientalis*	Molecular	Cattle	2020	[81]
Odisha	*T. annulata*	Molecular	Cattle	2021	[44]
Odisha	*T. annulata*	Molecular	Cattle	2021	[45]
		Goats & Sheep			
Assam	*T. luwenshuni*	Microscopy & Molecular	Goat	2018	[50]
Guwahati of Assam	*T. luwenshuni*	Microscopy & Molecular	Goat	2019	[49]
		West India			
Anand	*T. annulata*	Molecular	Buffalo & Cattle	2014	[52]
Gujrat	*T. annulata*	Microscopy and Molecular	Cattle	2015	[54]
Gujrat	*T. annulata*	Microscopy & Molecular	Cattle & Buffalo	2015	[53]
Maharashtra	*T. annulata* & *T. orientalis*	Molecular	Cattle	2017	[58]
Bihar	*T. annulata*	Microscopy	Buffalo	2018	[82]
Anand	*T. annulata* & *T. orientalis*	Molecular	Cattle	2019	[55]
Maharashtra & tamil Nadu	*T. annulata*	Molecular	Buffalo & Cattle	2019	[58]
Telangana, Gujarat, Haryana, and Bihar	*T. annulata*	Molecular	Vaccine Isolate	2019	[83]
Maharashtra	*Theileria* spp.	Microscopy	Buffalo	2020	[51]
Bihar	*Theileria* spp.	Microscopy	Cattle	2021	[84]
Tamil Nadu	*T. annulata*	Molecular	Cattle	2021	[57]
Bihar	*T. annulata*	Microscopy & Molecular	Cattle	2021	[85]
Haryana	*T. annulata*	Microscopy	Goat, cattle, sheep Sera	1998	[86]
Tamil Nadu	*Theileria* Spp.	Microscopy	Sheep	2005	[87]
Haryana	*T. annulata*	Molecular	Tick	2006	[59]
Tamil Nadu	*Theileria* spp.	Microscopy	Goats & Sheep	2015	[60]
Tamil Nadu	*T. luwenshuni*	Molecular	Gaots & Sheep	2019	[61]
Maharashtra	*T. luwenshuni*	Microscopy & Molecular	Sheep	2021	[62]
Punjab	*T. annulata*	Microscopy	Tick Hy. anatolicum	2010	[88]
Gujrat	*Theileria* spp.	Microscopy	Buffalo & Cattle	2021	[89]
Ludhiana Punjab	*T. annulata*	Microscopy	Cattle	2012	[90]
Punjab	*T. annulata*	Molecular	Cattle	2015	[91]
Ludhiana Punjab	*T. annulata*	Molecular	Tick & Cattle	2015	[92]
Rajasthan	*Theileria*	Microscopy	Cattle	2015	[93]
Uttara hand	*Theileria* genus	Microscopy & Molecular	Cattle	2014	[94]
Haryana	*T. annulata*	Microscopy	Cattle	2017	[95]
Haryana	*T. annulata*	Molecular	Cattle	2020	[96]
Telangana, Gujarat, Haryana, and Bihar	*T. annulata*	Molecular	Vaccine	2021	[83]
Gujrat	*T. annulata*	Molecular	Cattle	2021	[97]
Himachal Pradesh	*T. orientalis*	Molecular	Cattle	2021	[98]
		Goats & Sheep			
Himachal Pradesh	*T. luwenshuni*	Molecular	Goats & Sheep	2021	[63]

3.3. Possible Tick Vectors for Theileria Species in India

The diverse array of *Theileria* species in the region may be due to different tick vectors infesting livestock, which is shown in Table 3. Several studies have reported different vector tick species from different regions of India included *R. microplus Hae. Bispinosa*

Hy. truncatum Hy. dromedarii Hy. anatolicum R. Sanguineous [70,78,99]. It may be assumed that the presence of different species of *Theileria* circulating in large and small ruminants may be linked to the presence of a wide variety of these tick vectors in the particular area as these ticks have the potential to transmit various *Theileria* species reported from other parts of the world [100,101]. For example, it has been found in Uttar Pradesh that *H. anatolicum* and *R. appenticulatus* could play a vector role in the *T. annulata* and *T. lestoquardi* transmission in large and small ruminants, respectively [64]. Similarly, *Hy. anatolicum* and *R. microplus Hy. m. isaaci* have been identified to transmit *T. annulata* in cattle, while, in buffalo, *Hy. anatolicum* may be the only vector transmitting *T. buffeli* (*T. orientalis*). On the other hand, *Hy. anatolicum* and *Haemaphysalis* are widely distributed in different regions of India [64,102], which may transmit various species of *Theileria* such as *T. lestocardi* (*hirci*) and other *Theileria* species in goats and sheep. Recently, in India, some studies have also confirmed the role of various tick species such as *R. microplus*, *Hy. anatolicum* and *Hae. bispinosa* in the transmission of *T. orientalis* [70,78]. Similar reports have been observed in Africa [103]. Besides the above-mentioned tick species, *Hy. detritum*, *Hy. dromedarii*, and *Hy. lusitanicum* can also be the potential vectors for the transmission of this pathogen in different hosts [9].

Table 3. Distribution of the possible vector tick species of *Theileria* in different regions of India.

Tick Species	Host	States/Region	References
R. microplus. R. haemaphysaloides	Cattle & Buffalo	It is found in all places except Manipur, Kerala, Nagaland, Tripura & Maharashtra	[78,102]
Hy. anatolicum	Ruminants	It may be present in all parts except Andhra Pradesh, Jharkhand, Manipur, Mega laya, Stkin, Tripuri	[33,46,103]
Hae. Bispinosa	Goats & Sheep	Widely distributed except Delhi, Haryana, Kerala, Nagaland, Uttar Pradesh and Chhattisgarh	[47,64,70,99]
Hy. truncatum	Goats & Sheep	It is restricted to only Gujrat, Maharashtra & Uttar Pradesh	[102]
Hy. dromedarii	Goats & Sheep	It can be found only in Andhra Pradesh, Delhi, Gujrat, Haryana, Himachal Pradesh, Jammu & Kashmir, Odisha, Punjab, Rajasthan, Uttar Pradesh	[102]
R. Sanguineus	Goats & Sheep	It is reported from all places except Gora, Delhi, Manipur, Megha laya, Nagaland, Tripuri and Uttar Pradesh	[47,64,102]

3.4. Diversity and Distribution of Theileria Species in Different Regions of Pakistan

Theileria species that have been reported in different provinces of Pakistan are listed in Table 4. Approximately three different species of *Theileria*, including *Theileria* spp., *T. annulata* and *T. orientalis* have been reported in cattle and buffalo from different places of the Punjab province. Among these, the predominant and widely distributed pathogen is *T. annulata*, which many authors have reported across the province either microscopically or molecularly [104–107]. In addition to *T. annulata*, other *Theileria* species such as *T. orientalis* [108–110] and *Theileria* spp. have also been identified recently [111–113]. On the other hand, different species of *Theileria* identified in small ruminants (goats and sheep) from various geographic areas of Punjab included *Theileria* spp. and *T. annulata*, [114–116] *T. ovis* and *T. ovis*, *T. lestoquardi*, [115,117–119]. In Khyber Pakhtunkhwa province, several studies from different areas investigated that *T. annulata* is the only species circulating in cattle and buffalo [101,120–122]; however, diverse species of *Theileria* such as *T. annulata*, *T. lestoquardi*, *T. luwenshuni T. ovis* and *Theileria* spp. have been identified in goats and sheep [123–126]. *Theileria* spp. and *T. annulata* were identified in cattle and buffalo from Sindh and Balochistan Province [116,127]. No single study has reported *Theileria* species infecting ruminants from Sindh province; however, in Balochistan and FATA, different species *Theileria* identified from small ruminants include *T. annulata*, *T. ovis* and *T. lestoquardi* [7,107,116]. Some studies were carried out in the adjoining areas of two provinces and reported different species of *Theileria*; for example, in a study Ghafar et al. [128] interestingly identified *T. lestoquardi-like* spp., *T. orientalis* and *T. annulata*

from the ticks collected from the cattle and buffalo in different agro-ecological zones of Punjab and Sindh Province, while, on the other hand, Durrani et al. [129] and Karim et al. [130] identified *T. ovis* and *T. annulata* in small and large ruminants from the different regions of Punjab and Khyber Pakhtunkhwa, respectively.

Table 4. Provincial wise distribution of the different *Theileria* species in Pakistan.

Pakistan					
Province/State	***Theileria* Species**	**Identification Method**	**Host**	**Year**	**Reference**
Punjab					
Cattle & Buffaloes					
Punjab	*Theileria* spp.	Microscopy	Cattle	1983	[131]
Faisalabad	*Theileria* spp.	Microscopy	Cattle	1999	[132]
Faisalabad	*T. annulata*	Microscopy	Buffaloes & Cattle	2004	[133]
Kasur	*Theileria* spp.	Microscopy	Cattle	2005	[134]
Punjab	*T. annulata*	Microscopy	Buffaloes	2006	[135]
Kasur	*T. annulata*	Molecular	Cattle	2008	[136]
Punjab	*T. annulata*	Microscopy & Molecular	Cattle	2008	[137]
Sahiwal	*Theileria* spp.	Microscopy	Cattle	2010	[111]
Southern Punjab	*T. annulata*	Microscopy	Cattle	2011	[104]
Sargodha	*T. annulata*	Microscopy	Cattle	2012	[138]
Faisalabad, Jhang, Khanewal	*T. annulata*	Molecular	Ticks of Cattle & Buffaloes	2013	[105]
Faisalabad	*T. annulata*	Molecular	Cattle & Buffaloes	2013	[106]
Punjab	*T. orientalis*	Molecular	Cattle	2021	[108]
Punjab	*T. annulata*	Molecular	Cattle	2018	[109]
Punjab	*T. annulata* & *T. orientalis*	Molecular	Cattle	2018	[139]
Lahore	*T. annulata*	Microscopy	Cattle	2018	[5]
Agro-ecological Zones Punjab	*T. orientalis* & *T. annulata*	Molecular	Ruminants	2019	[110]
Agro-ecological Zones Punjab	*T. annulata*	Molecular	Cattle	2020	[107]
Layyah	*T. annulata* & *T. orientalis*	Molecular	Cattle	2021	[113]
Dera Ghazi Khan & Lodhran	*T. annulata*	Molecular	Cattle	2021	[112]
Attock	*Theileria* spp.	Microscopy	Goats & Sheep	2010	[140]
Okara	*Theileria* spp.	Microscopy	Sheep	2010	[141]
Lahore	*T. lestoquardi* & *T. ovis*	Microscopy & Molecular	Sheep	2011	[142]
Lahore	*Theileria* spp.	Microscopy	Goats & Sheep	2011	[143]
Okara	*T. ovis*	Molecular	Sheep	2013	[114]
Southern Punjab	*T.lestoquardi*	Molecular	Goats & Sheep	2015	[144]
Multan	*T. ovis* & *T. lestoquardi*	Microscopy & Molecular	Goats & Sheep	2017	[115]
Multan	*T. lestoquardi* & *T. ovis*	Microscopy & Molecular	Goats & Sheep	2017	[145]
Punjab	*T. annulata T.ovis* & *T. lestoquardi*	Molecular	Ruminants	2019	[117]
Multan	*T. lestoquardi &*& *T. ovis*	Molecular & Microscopy	Goats	2019	[118]
Layyah	*T. annulata*	Molecular	Sheep	2021	[119]
Lahore	*Theileria* Spp.	Microscopy	Goats & Sheep	2021	[116]
Peshawar	*T. annulata*	Microscopy	Buffalo & Cattle	2005	[146]
KPK (Southern KP)	*T. annulata*	Molecular	Cattle	2012	[147]
KPK	*T. annulata*	Molecular	Cattle	2017	[120]
Northern Pakistan	*T. annulata*	Molecular	Cattle (Ticks)	2019	[101]
North-Western Pakistan	*T. annulata*	Molecular	Cattle	2021	[148]
DI Khan	*Theileria* spp.	Microscopy	Cattle	2021	[149]
Central KPK	*T. annulata*	Microscopy & Molecular	Cattle	2021	[122]
KPK	*T. lestoquardi* & *T. ovis*	Molecular	Goats & Sheep	2013	[147]
KPK	*T.lestoquardi*	Molecular	Goats & Sheep	2015	[150]
Peshawar & Periphery	*Theileria* spp.	Microscopy	Ruminants	2017	[151]
Peshawar & Khyber Agency	*Theileria*	Microscopy	Goats & Sheep	2017	[152]
Southern KPK	*T. ovis T. lestoquardi*	Molecular	Goats & Sheep	2018	[123]

Table 4. *Cont.*

Pakistan					
Province/State	***Theileria* Species**	**Identification Method**	**Host**	**Year**	**Reference**
Southern KPK	*Theileria* spp.	Microscopy	Sheep	2018	[153]
KPK	*T. annulata*, *T. lestoquardi*, *T. luwenshuni T. ovis* & *Theileria* spp.	Molecular	Goats & Sheep	2020	[124]
Malakand Division	*Theileria* spp.	Microscopy	Buffalo, Cattle, Goat & Sheep	2021	[125]
KPK	*Theileria* Spp. *T. annulata*, *T. lestoquardi*, *T. ovis*	Molecular	Goats & Sheep	2021	[126]
		Sindh			
Hyderabad	*Theileria* spp.	Microscopy	Cattle	1994	[154]
Karachi	*Theileria*	Microscopy	Buffalo	2012	[127]
Quetta	*T. annulata*	Microscopy	Cattle	2021	[116]
Baluchistan	*Theileria ovis* & *T. lestoquardi*	Molecular	Goats & Sheep	2017	[7]
FATA	*T. ovis*	Molecular	Goats & Sheep	2020	[107]
Punjab & KPK	*T. ovis*	Microscopy & Molecular	Goats & Sheep	2012	[129]
Pakistan/Punjab-KPK	*T. annulata*	Molecular	Ruminants	2017	[130]
Sindh & Punjab	*T. lestoquardi*-like spp., *T. orientalis* & *T. annulata*	Molecular	Cattle	2021	[128]

3.5. Tick Vectors for Transmission of Theileria in Pakistan

In Pakistan, different studies have reported a wide variety of tick species from various geographical areas as shown in Table 5. In these studies, different tick species have been identified, which may be due to different prevailing conditions in the country such as seasonal fluctuation, relative humidity, temperature, association and lifestyle of different species of animals, lack of education in farmers, and farm management practices which may favor tick growth and survival. In the current study, existence of a wide variety of *Theileria* species may be due to the presence of different tick vectors, which may possibly play a role in the transmission of these pathogens. Common genera which may be possibly involved in the transmission of these pathogens include *Hyalomma*, *Rhipicephalus* and *Haemaphysalis*. Several studies have reported different tick species across the country such as *Hy. hussaini*, *Hy. scupense*, *Hy. anatolicum*, *Hy. scupense*, *Hy. excavatum*, *R. microplus*, *R. sanguineus* [105,123,138,155–158]. These ticks may have the capacity to transmit different *Theileria* species in different hosts [103,107]. However, further molecular studies are needed to find out their vector competencies.

Table 5. Distribution of various tick vectors for the transmission of *Theileria* species in Pakistan.

Ticks	Host	References
Punjab		
R. microplus, *Hy. anatolicum*, *Hy. aegyptium*, *Hy. dromedarii*, *R. appendiculatus*, *R. sanguineus*	Cattle and buffaloes	[102,105,138,147,153,157–162]
Khyber Pakhtunkhwa		
R. microplus, *R. appendiculatus*, *Hy. anatolicum*	Cattle & buffaloes	[101,163]
Sindh		
Hy. hussaini, *Hy. scupense*, *R. annulatus*, *R. microplus*, *Hy. anatolicum*, *Hy. scupense*, *Hy. excavatum*	Buffaloes	[155,156,164]
Balochistan		
R. microplus, *Hy. anatolicum*, *Hy. scupense*, *Hy. aegyptium*, *Haemaphysalis*	Cattle & buffaloes	[107,165–169]
Punjab		
Hy. anatolicum, *Hy. excavatum R. appendiculatus*, *Hy. dromedarii*, *R. microplus*, *R. sanguineus*, *R. Turanicus*	Goats & Sheep	[158,160,170–174]
Khyber Pakhtunkhwa		
Hy. anatolicum, *Hy. detritum*, *Hy. excavatum*, *Hy. scupense*, *Haemaphysalis longicornis*, *Hyalomma impeltatum*, *R. appendiculatus*, *R. microplus*	Goats & Sheep	[107,175–180]
Sindh		
Hae. bispinosa, *Hy. anatolicum*, *Hy. detritum*, *Hy. dromedarii*, *Hy. hussaini*, *Hy. impeltatum*, *Hy. marginatum isaaci*, *R. microplus*, *R. Sanguineus*	Goats & Sheep	[181,182]
Balochistan		
Hy. anatolicum, *Hy. dromedarii*, *Hy. excavatum*, *Hy. scupense*, *R. microplus*	Goats & Sheep	[168,183–185]

3.6. Regional Wise Distribution of Theileria Species and Its Possible Tick Vectors in Bangladesh

Different species of *Theileria* from large and small ruminants from various geographical regions are listed in Table 6. Among these, most of the species such as *Theileria* spp., *T. annulata*, *T. mutans* and *T. orientalis* have been identified from the large ruminants of Central and North Central regions of Bangladesh [186–189] while, from the Southwestern, Northern and Western region, only *Theileria* spp. and *T. annulata* have been reported [190–193]. Furthermore, only one species, i.e., *T. annulata*, was reported in goats and sheep from the central part of Bangladesh [189,194].

Table 6. Regional wise distribution and diversity of *Theileria* species in various regions of Bangladesh.

Bangladesh					
City	***Theileria* spp.**	**Identification Method**	**Host**	**Year of Study**	**References**
		Central Region			
Dhaka Targil	*T. annulata*	Microscopy	Cattle	1983	[195]
Dhaka	*T. annulata* and *T. mutans*	Microscopy	Cattle	1989	[196]
Dhaka, Sirajganj and Nikhangsori	*T. annulata*	Microscopy & Molecular	Cattle goats & Sheep	2019	[194]
		Goats & Sheep			
Dhaka	*Theileria* spp.	Microscopy & Molecular	Goats	2021	[189]
		South Eastern Region			
Chittagong	*Theileria* spp.	Microscopy	Cattle	2010	[190]
		North Central Region			
Sirajganj	*Theileria* spp.	Microscopy	Cattle	2015	[187]
Sirajganj	*T. annulata* & *T. mutans*	Microscopy	Cattle	1976	[186]
Sirajganj	*T. annulata*	Molecular	Cattle	1977	[197]
Mymensingh	*T. orientalis*	Molecular	Cattle	2018	[188]
		Northern Region			
Dinajpur	*Theileria* spp.	Microscopy	Cattle	2016	[191]
		Western region			
Rajshahi	*T. annulata*	Molecular	Cattle	2016	[192]
Natores	*T. annulata*	Molecular	Cattle	2019	[193]

The possible vector tick species from the different geographical places of Bangladesh that could be involved in the transmission of various *Theileria* species in small and large ruminants are shown in Tables 7 and 8. The common tick species responsible for the transmission of *Theileria* in cattle and buffalo are *R. microplus*, *Hae. bispinosa*, *R. sanguineus*, and *Hy. anatolicum anatolicum* [102], while, in the case of small ruminants (goats and sheep), these may be *R. sanguineus* and *Hy. anatolicum anatolicum* [102].

Table 7. Distribution of possible tick vectors for *Theileria* species in various regions of Bangladesh.

Divisions	**Possible Tick Vector**	**Reference**
Braisel, Dhaka, Savar, Narayanganj, Tangali	*R. microplus*	[102]
Dhaka, Rajshahi, Savar	*Hae. bispinosa*	[102]
North western dry Region (Rajshahi, Rangpur, and Dinajpur districts)	*Hy. anatolicum anatolicum*	[102]
Savar	*Hy. Truncatum*	[102]
Braisal, Chitagang, Dhaka, Narayanganj, Tangail, Rangpur, Sylhet	*R. sanguineus*	[102]

Table 8. Common tick species in different hosts in Bangladesh.

Possible Tick Vectors for TT	**Host**	**References**
R. microplus, *Hae. bispinosa*, *R. sanguineus*, *Hy. anatolicum anatolicum*	Cattle & Buffaloes	[102]
R. sanguineus, *Hy. anatolicum anatolicum*	Goats & Sheep	[102]

3.7. Phylogenetic Analysis, Genetic Divergence and Multiple Sequence Alignment

We have selected *T. annulata* for phylogenetic and genetic divergence analysis as this species may infect all ruminants and could be of great economic concern. The evolutionary history was inferred using an *18S rRNA* taxonomic marker. Homology searches of the selected *18S rRNA* isolates shared 99–100% similarities with local and global isolates deposited in the NCBI GenBank. The neighbor-joining algorithm was used to establish a phylogenetic relationship among different selected isolates. The selected *18S rRNA* isolates were clustered into different clades (Figure 6). However, no single isolate was selected from Bangladesh as *18S RNA* sequence was not available for *T. annulata* from Bangladesh. We select the *18S rRNA* genetic marker as several previously published studies used this genetic marker in Pakistan, India and other parts of the world to identify and establish the phylogenetic profile of *T. annulata* circulating in ruminants [41,101,106,109,198]. The *18S rRNA* gene play an important role in genetic variability of *Theileria* spp. due to the presence of conserved sequences and some hypervariable regions which are crucial in determining the evolutionary patterns and discriminating the various *Theileria* species [16,199]. Furthermore, targeting the amplification of the hypervariable V4 region of the *18S rRNA* gene is preferably used for the accurate identification, classification and exploring the population structures of the piroplasm parasites [117,200]. Nucleotide sequence heterogeneity analysis (evolutionary/genetic divergence) showed that *T. annulata* isolates were different from each other by 0–4.7 bp as shown in Table 9. Maximum divergence (4.7 bp) was observed with isolates from Pakistan. Additionally, the multiple alignment analysis also showed changes in the nucleotide sequences of different isolates as can be seen in Figure 7. These genetic variations may be due to genetic variability contributed by the deletions, insertions and substitutions in the nucleotide sequences of different isolates [41,55], which may result in the various degrees of pathogenecity and treatment measures in the field. Thus, on the basis of this analysis and previous findings, we concluded that, due to the presence of a hypervariable region and genetic variability, vaccine development against *Theileria* species is still challenging, and we may suggest that using a single diagnostic or immunogenic molecule may not be sufficient in achieving the required goals.

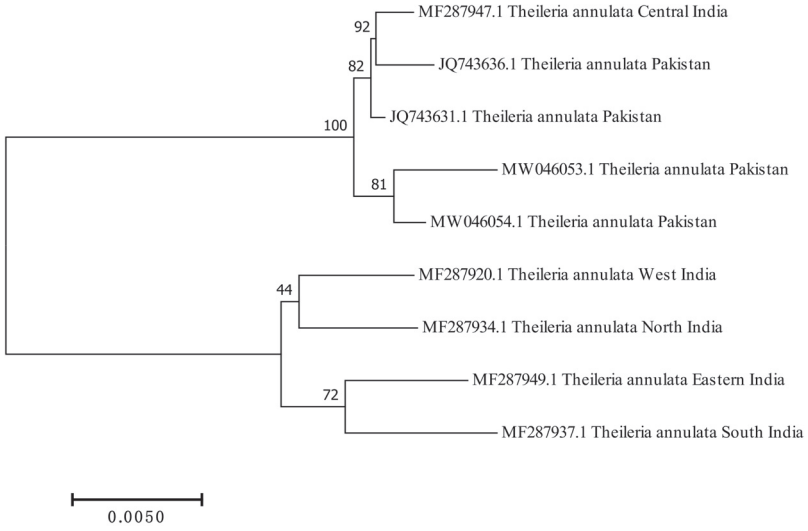

Figure 6. Phylogenetic analysis of selected *T. annulata* isolates (*18 S rRNA* gene).

Table 9. Evolutionary divergence analysis of *T. annulata 18S rRNA* gene isolates.

	1	2	3	4	5	6	7	8	9
MF287947.1 *T annulata* Central India									
MF287920.1 *T annulata* West India	0.58								
MF287949.1 *T annulata* Eastern India	0.62	0.22							
MF287937.1 *T annulata* South India	0.63	0.25	0.19						
MF287934.1 *T annulata* North India	0.58	0.16	0.19	0.28					
JQ743631.1 *T annulata* Pakistan	0.4	0.55	0.59	0.6	0.56				
JQ743636.1 *T annulata* Pakistan	0.7	0.6	0.63	0.065	0.6	0.5			
MW046053.1 *T annulata* Pakistan	2.14	1.65	4.7	4.7	0.65	0.12	0.15		
MW046054.1 *T annulata* Pakistan	0.9	0.57	2.63	3.62	0.57	3.8	0.11	0.0	
	1	2	3	4	5	6	7	8	9

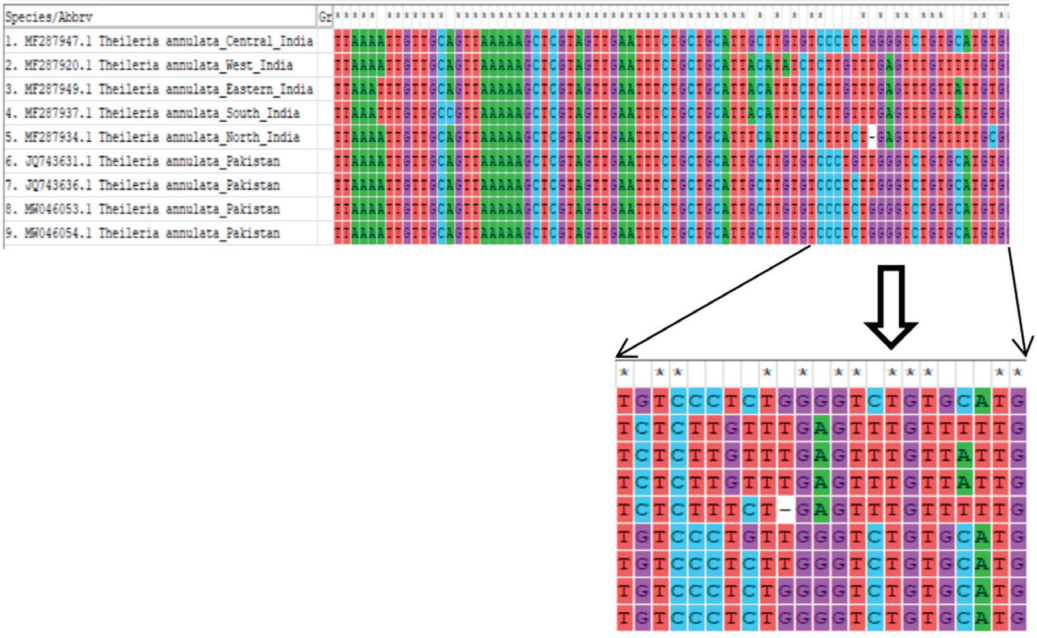

Figure 7. CLUSTAL W multiple sequence alignment analysis for the different *T. annulata* isolates from India and Pakistan. The box below showing the changes in nucleotide sequences between *T. annulata* isolates from Pakistan and India. * means nucleotide similarities.

3.8. Overall Comparison (Why Vector-Borne Diseases like Theileria Are Increasing Day by Day)

The global climate has been changing over the last century due to greenhouse gas emissions. It will continue to change over this century, accelerating without effective global efforts to reduce emissions. Ticks and tick-borne diseases (TTBDs) are inherently climate-sensitive due to the sensitivity of tick lifecycles to climate. Key direct climate and weather sensitivities include survival of individual ticks and the duration of development and questing (host-seeking) activity of ticks [201].

We have concluded that our data contribute to the knowledge of *Theileria* species diversity and distribution circulating in ruminants in different regions of India, Pakistan and Bangladesh. The diverse species and wide distribution of *Theileria* in the region may be linked with the presence of their possible vector tick species belonging to the main four genera including *Hyalomma*, *Haemaphysalis*, *Rhipicephalus* and *Amblyomma* as they have been identified as *Theileria* vectors from several parts of the world [101–103,107,117]. Paucity still exists; however, molecular studies have been updated and increased during the last decade regarding *Theileria* species identification and their possible vectors. Different

ticks have been adapted to diverse climatic conditions such as aridity in the desert, and seasonal and daily fluctuations may result in widespread distribution of these ticks and subsequently lead to the diversity in *Theileria* species. This adaptation offers the tick a significant comparative advantage over other tick species under the predicted scenarios for climate change [103], particularly in the context of South Asian countries where these tick species might gain importance in the future. Our analysis suggests the needs of further molecular studies to discover different species and strains, and their potential vectors as microscopic studies have not been so effective in identifying different species and strains. Additionally, genetic variation among different *T. annulata* isolates may be due to the mutations in the hypervariable region and genetic variability, which makes the therapeutic and single molecule based vaccine development against *Theilera* challenging and necessitates the needs for alternative control measures. This study also helps in providing a baseline for devising integrated control measures to reduce the losses due to these pathogens being either at the pathogen or vector level.

Thus, on the basis of this analysis and previous findings, we may suggest that using a single diagnostic or immunogenic molecule may not be sufficient in achieving the required goals regarding *Theileria* control strategies.

Author Contributions: J.Z. designed the study, searched the literature, identified and screened articles, and extracted data which was reviewed by O.S., J.Z., B.S., S.H. and M.U.A. wrote the first draft of the manuscript. J.Z. performed molecular and genetic analysis. R.Z. conducted geographic and regional analysis of data. O.S. revised the manuscript critically. All the authors approved the final version of the manuscript. All authors have read and agreed to the published version of the manuscript.

Funding: O.S. is a Principal Investigator of an internal research fund of the Department of Infectious Diseases and Public Health of the City University of Hong Kong (Project number 9380108).

Institutional Review Board Statement: Not applicable.

Informed Consent Statement: Not applicable.

Acknowledgments: We are thankful to all authors whose articles are included in this study.

Conflicts of Interest: The authors declare that there is no conflict of interest.

References

1. Lew-Tabor, A.E.; Valle, M.R. A review of reverse vaccinology approaches for the development of vaccines against ticks and tick borne diseases. *Ticks Tick-Borne Dis.* **2016**, *7*, 573–585. [CrossRef]
2. Nene, V.; Kiara, H.; Lacasta, A.; Pelle, R.; Svitek, N.; Steinaa, L. The biology of Theileria parva and control of East Coast fever–current status and future trends. *Ticks Tick-Borne Dis.* **2016**, *7*, 549–564. [CrossRef]
3. Ica, A.; Vatansever, Z.; Yildirim, A.; Duzlu, O.; Inci, A. Detection of Theileria and Babesia species in ticks collected from cattle. *Vet. Parasitol.* **2007**, *148*, 156–160. [CrossRef]
4. Jenkins, C. Bovine theileriosis in Australia: A decade of disease. *Microbiol. Aust.* **2018**, *39*, 215–219. [CrossRef]
5. Rashid, M.; Akbar, H.; Rashid, I.; Saeed, K.; Ahmad, L.; Ahmad, A.S.; Shehzad, W.; Islam, S.; Farooqi, S. Economic significance of tropical theileriosis on a Holstein Friesian dairy farm in Pakistan. *J. Parasitol.* **2018**, *104*, 310–312. [CrossRef]
6. Gul, N.; Ayaz, S.; Gul, I.; Adnan, M.; Shams, S.; Akbar, N. Tropical theileriosis and east coast fever in cattle: Present, past and future perspective. *Int. J. Curr. Microbiol. Appl. Sci.* **2015**, *4*, 1000–1018.
7. Khan, M.A.; Khan, M.; Ahmad, I.; Khan, M.; Anjum, A.; Durrani, A.; Hameed, K.; Kakar, I.; Wajid, A.; Ramazan, M. Risk factors assessment and molecular characterization of Theileria in small ruminants of Balochistan. *J. Anim. Plant Sci.* **2017**, *27*, 1190–1196.
8. Shaw, M.K.; Tilney, L.G. How individual cells develop from a syncytium: Merogony in Theileria parva (Apicomplexa). *J. Cell Sci.* **1992**, *101*, 109–123. [CrossRef]
9. Bishop, R.; Musoke, A.; Morzaria, S.; Gardner, M.; Nene, V. Theileria: Intracellular protozoan parasites of wild and domestic ruminants transmitted by ixodid ticks. *Parasitology* **2004**, *129*, S271–S283. [CrossRef]
10. Dobbelaere, D.; Heussler, V. Transformation of Leukocytes by *Theileria parva* and *T. annulata*. *Annu. Rev. Microbiol.* **1999**, *53*, 1–42. [CrossRef]
11. Conrad, P.A.; Denham, D.; Brown, C.G.D. Intraerythrocytic multiplication of Theileria parva in vitro: An ultrastructural study. *Int. J. Parasitol.* **1986**, *16*, 223–229. [CrossRef]
12. Kawamoto, S.; Takahashi, K.; Kurosawa, T.; Sonoda, M.; Onuma, M. Intraerythrocytic schizogony of *Theileria* sergenti in cattle. *Jpn. J. Vet. Sci.* **1990**, *52*, 1251–1259. [CrossRef] [PubMed]

13. Katzer, F.; Ngugi, D.; Oura, C.; Bishop, R.P.; Taracha, E.L.N.; Walker, A.R.; McKeever, D.J. Extensive genotypic diversity in a recombining population of the apicomplexan parasite Theileria parva. *Infect. Immun.* **2006**, *74*, 5456–5464. [CrossRef] [PubMed]
14. Weir, W.; Ben-Miled, L.; Karagenç, T.; Katzer, F.; Darghouth, M.; Shiels, B.; Tait, A. Genetic exchange and sub-structuring in Theileria annulata populations. *Mol. Biochem. Parasitol.* **2007**, *154*, 170–180. [CrossRef] [PubMed]
15. OIE. *THEILERIOSIS Aetiology Epidemiology Diagnosis Prevention and Control References*; OIE: Paris, France, 2021. Available online: https://www.oie.int/app/uploads/2021/03/theileriosis.pdf (accessed on 26 December 2021).
16. Sivakumar, T.; Hayashida, K.; Sugimoto, C.; Yokoyama, N. Evolution and genetic diversity of Theileria. *Infect. Genet. Evol.* **2014**, *27*, 250–263. [CrossRef]
17. Böse, R.; Jorgensen, W.K.; Dalgliesh, R.J.; Friedhoff, K.T.; De Vos, A.J. Current state and future trends in the diagnosis of babesiosis. *Vet. Parasitol.* **1995**, *57*, 61–74. [CrossRef]
18. Passos, L.M.F.; Bell-Sakyi, L.; Brown, C.G.D. Immunochemical characterization of in vitro culture-derived antigens of Babesia bovis and Babesia bigemina. *Vet. Parasitol.* **1998**, *76*, 239–249. [CrossRef]
19. Gubbels, J.M.; De Vos, A.P.; Van der Weide, M.; Viseras, J.; Schouls, L.M.; De Vries, E.; Jongejan, F. Simultaneous detection of bovine Theileria and Babesia species by reverse line blot hybridization. *J. Clin. Microbiol.* **1999**, *37*, 1782–1789. [CrossRef]
20. Rougemont, M.; Van Saanen, M.; Sahli, R.; Hinrikson, H.P.; Bille, J.; Jaton, K. Detection of four Plasmodium species in blood from humans by 18S rRNA gene subunit-based and species-specific real-time PCR assays. *J. Clin. Microbiol.* **2004**, *42*, 5636–5643. [CrossRef]
21. Mens, P.F.; Schoone, G.J.; Kager, P.A.; Schallig, H.D.F.H. Detection and identification of human Plasmodium species with real-time quantitative nucleic acid sequence-based amplification. *Malar. J.* **2006**, *5*, 80. [CrossRef]
22. Steenkeste, N.; Incardona, S.; Chy, S.; Duval, L.; Ekala, M.-T.; Lim, P.; Hewitt, S.; Sochantha, T.; Socheat, D.; Rogier, C. Towards high-throughput molecular detection of Plasmodium: New approaches and molecular markers. *Malar. J.* **2009**, *8*, 86. [CrossRef] [PubMed]
23. Agudelo, O.; Arango, E.; Maestre, A.; Carmona-Fonseca, J. Prevalence of gestational, placental and congenital malaria in north-west Colombia. *Malar. J.* **2013**, *12*, 341. [CrossRef] [PubMed]
24. Haanshuus, C.G.; Mohn, S.C.; Mørch, K.; Langeland, N.; Blomberg, B.; Hanevik, K. A novel, single-amplification PCR targeting mitochondrial genome highly sensitive and specific in diagnosing malaria among returned travellers in Bergen, Norway. *Malar. J.* **2013**, *12*, 26. [CrossRef] [PubMed]
25. Lee, Y.-H.; Lai, Y.-H. Fabrication and Characterization of HER2 Cell Receptor-Targeted Indocyanine Green-Encapsulated Poly (Lactic-co-Glycolic Acid) Nanoparticles. *Peertechz J. Biomed. Eng.* **2015**, *1*, 15–20.
26. Bilgiç, H.B.; Karagenç, T.; Simuunza, M.; Shiels, B.; Tait, A.; Eren, H.; Weir, W. Development of a multiplex PCR assay for simultaneous detection of Theileria annulata, Babesia bovis and Anaplasma marginale in cattle. *Exp. Parasitol.* **2013**, *133*, 222–229. [CrossRef]
27. Chaisi, M.E.; Janssens, M.E.; Vermeiren, L.; Oosthuizen, M.C.; Collins, N.E.; Geysen, D. Evaluation of a Real-Time PCR Test for the Detection and Discrimination of Theileria Species in the African Buffalo (Syncerus caffer). *PLoS ONE* **2013**, *8*, e75827. [CrossRef]
28. Kundave, V.R.; Ram, H.; Banerjee, P.S.; Garg, R.; Mahendran, K.; Ravikumar, G.; Tiwari, A.K. Development of multiplex PCR assay for concurrent detection of tick borne haemoparasitic infections in bovines. *Acta Parasitol.* **2018**, *63*, 759–765. [CrossRef]
29. Ayadi, O.; Gharbi, M.; Elfegoun, M.C.B. Milk losses due to bovine tropical theileriosis (Theileria annulata infection) in Algeria. *Asian Pac. J. Trop. Biomed.* **2016**, *6*, 801–802. [CrossRef]
30. Kerario, I.I.; Simuunza, M.; Laisser, E.L.K.; Chenyambuga, S. Exploring knowledge and management practices on ticks and tick-borne diseases among agro-pastoral communities in Southern Highlands, Tanzania. *Vet. World* **2018**, *11*, 48. [CrossRef]
31. Elsheikha, H. Management of ticks and tick-borne diseases: Challenges and opportunities. *Vet. Nurse* **2019**, *10*, 60–63. [CrossRef]
32. Kumar, S.; Stecher, G.; Tamura, K. MEGA7: Molecular evolutionary genetics analysis version 7.0 for bigger datasets. *Mol. Biol. Evol.* **2016**, *33*, 1870–1874. [CrossRef]
33. Sangwan, A.K.; Chhabra, M.B.; Samantaray, S. Relative role of male and female Hyalomma anatolicum anatolicum ticks in Theileria transmission. *Vet. Parasitol.* **1989**, *31*, 83–87. [CrossRef]
34. Naik, B.S.; Maiti, S.K.; Raghuvanshi, P.D.S. Prevalence of tropical theileriosis in cattle in Chhattisgarh State. *J. Anim. Res.* **2016**, *6*, 1043–1045. [CrossRef]
35. Das, G.; Ray, D. PCR-based detection of Theileria annulata infection in ticks collected from cattle of West Bangal, India. *J. Vet. Parasitol.* **2003**, *17*, 11–14.
36. Kartashov, M.Y.; Naidenova, E.V.; Zakharov, K.S.; Yakovlev, S.A.; Skarnovich, M.O.; Boumbaly, S.; Nikiforov, K.A.; Plekhanov, N.A.; Kritzkiy, A.A.; Ternovoi, V.A. Detection of Babesia caballi, Theileria mutans and Th. velifera in ixodid ticks collected from cattle in Guinea in 2017–2018. *Vet. Parasitol. Reg. Stud. Rep.* **2021**, *24*, 100564. [CrossRef]
37. Ananda, K.J.; D'Souza, P.E.; Puttalakshmamma, G.C. Prevalence of Haemoprotozoan diseases in crossbred cattle in Banglore north. *Vet. World* **2009**, *2*, 15. [CrossRef]
38. Nair, A.S.; Ravindran, R.; Lakshmanan, B.; Kumar, S.S.; Tresamol, P.V.; Saseendranath, M.R.; Senthilvel, K.; Rao, J.R.; Tewari, A.K.; Ghosh, S. Haemoprotozoa of cattle in northern Kerala, India. *Trop. Biomed.* **2011**, *28*, 68–75.
39. Maharana, B.R.; Kumar, B.; Prasad, A.; Patbandha, T.K.; Sudhakar, N.R.; Joseph, J.P.; Patel, B.R. Prevalence and assessment of risk factors for haemoprotozoan infections in cattle and buffaloes of South-West Gujarat, India. *Indian J. Anim. Res.* **2016**, *50*, 733–739.

40. Aparna, M.; Vimalkumar, M.B.; Varghese, S.; Senthilvel, K.; Ajithkumar, K.G.; Raji, K.; Syamala, K.; Priya, M.N.; Deepa, C.K.; Jyothimol, G. Phylogenetic analysis of bovine Theileria spp. isolated in south India. *Trop. Biomed.* **2013**, *30*, 281–290.
41. George, N.; Bhandari, V.; Reddy, D.P.; Sharma, P. Emergence of new genotype and diversity of Theileria orientalis parasites from bovines in India. *Infect. Genet. Evol.* **2015**, *36*, 27–34. [CrossRef]
42. Ananda, K.J.; Adeppa, J. Prevalence of Haemoprotozoan infections in bovines of Shimoga region of Karnataka state. *J. Parasit. Dis.* **2016**, *40*, 890–892.
43. Nimisha, M.; Devassy, J.K.; Pradeep, R.K.; Pakideery, V.; Sruthi, M.K.; Pious, A.; Kurbet, P.S.; Amrutha, B.M.; Chandrasekhar, L.; Deepa, C.K. Ticks and accompanying pathogens of domestic and wild animals of Kerala, South India. *Exp. Appl. Acarol.* **2019**, *79*, 137–155. [CrossRef] [PubMed]
44. Selim, A.M.; Das, M.; Senapati, S.K.; Jena, G.R.; Mishra, C.; Mohanty, B.; Panda, S.K. Transplacental transmission of Theileria annulata in cattle confirmed by molecular techniques. *J. Parasit. Dis.* **2021**, *45*, 336–340. [CrossRef] [PubMed]
45. Dehuri, M.; Panda, M.; Sahoo, N.; Mohanty, B.; Behera, B. Nested PCR assay for detection of *Theileria annulata* in *Hyalomma anatolicum* infesting cattle from coastal Odisha, India. *Anim. Biotechnol.* **2021**, 1–6. [CrossRef] [PubMed]
46. Banerji, P.K.; Samaddar, J.; Gupta, R.; Paul, J.; Guha, C. Natural infection with Theileria hirci in Jumnapari goat—A case report. *Indian Vet. J.* **1990**, *67*, 677–678.
47. Shruthi, R.; Thimmareddy, P.M.; Mamatha, G.S.; Chandranaik, B.M.; Puttalakshmamma, G.C. Studies on theileriosis in goats from Karnataka, South India. *J. Parasit. Dis.* **2017**, *41*, 1082–1085. [CrossRef]
48. Mamatha, G.S.; Shruthi, R.; Chandranaik, B.M.; D'Souza, P.E.; Thimmareddy, P.M.; Shivashankar, B.P.; Puttalakshmamma, G.C. Molecular epidemiology and phylogenetic characterisation of Theileria luwenshuni in India: A first report. *Small Rumin. Res.* **2017**, *154*, 52–57. [CrossRef]
49. Begam, R.; Talukdar, S.K.; Sarmah, P.C.; Bulbul, K.H.; Kakati, P.; Tamuly, S.; Islam, S. Molecular and microscopic detection of Theileria luwenshuni infection in goats in and around Guwahati of Assam, India. *Biol. Rhythm Res.* **2019**, 1–8. [CrossRef]
50. Begam, R.; Talukdar, S.; Sarmah, P.C.; Bulbul, K.H.; Kakati, P.; Neog, R.; Saleque, A.; Tamuly, S.; Tamuli, S.M. Emergence of Theileria luwenshuni infection in goats of Assam, India. *J. Entomol. Zool. Stud.* **2018**, *6*, 100.
51. Bhosale, A.A.; Bhikane, A.U.; Chavhan, S.G.; Jadhav, R.K.; Mohan, A.; Kushwaha, N. Prevalence and Clinico-Therapeutic Management of Bubaline Theileriosis in Marathwada Region of Maharashtra. *Int. J. Livest. Res.* **2020**, *10*, 155–165. [CrossRef]
52. Kundave, V.R.; Patel, A.K.; Patel, P.V.; Hasnani, J.J.; Joshi, C.G. Qualitative and quantitative assessment of Theileria annulata in cattle and buffaloes Polymerase Chain Reaction. *Trop. Biomed.* **2014**, *31*, 728–735. [PubMed]
53. Kundave, V.R.; Patel, A.K.; Patel, P.V.; Hasnani, J.J.; Joshi, C.G. Detection of theileriosis in cattle and buffaloes by polymerase chain reaction. *J. Parasit. Dis.* **2015**, *39*, 508–513. [CrossRef] [PubMed]
54. Chauhan, H.C.; Patel, B.K.; Bhagat, A.G.; Patel, M.V.; Patel, S.I.; Raval, S.H.; Panchasara, H.H.; Shrimali, M.D.; Patel, A.C.; Chandel, B.S. Comparison of molecular and microscopic technique for detection of Theileria annulata from the field cases of cattle. *Vet. World* **2015**, *8*, 1370–1374. [CrossRef] [PubMed]
55. Kundave, V.R.; Ram, H.; Shahzad, M.; Garg, R.; Banerjee, P.S.; Nehra, A.K.; Rafiqi, S.I.; Ravikumar, G.; Tiwari, A.K. Genetic characterization of Theileria species infecting bovines in India. *Infect. Genet. Evol.* **2019**, *75*, 103962. [CrossRef] [PubMed]
56. Larcombe, S.D.; Kolte, S.W.; Ponnudurai, G.; Kurkure, N.; Magar, S.; Velusamy, R.; Rani, N.; Rubinibala, B.; Rekha, B.; Alagesan, A. The impact of tick-borne pathogen infection in Indian bovines is determined by host type but not the genotype of Theileria annulata. *Infect. Genet. Evol.* **2019**, *75*, 103972. [CrossRef]
57. Azhahianambi, P.; Madhanmohan, M.; Madan, N.; Kumaran, D.; Priyadharshini, M.L.M.; Bharathi, R.; Senthilkumar, T.M.A.; Manoharan, S. Successful treatment of severe form of bovine tropical theileriosis in dairy cattle and genotyping of Theileria annulata isolates of Tamil Nadu, India. *Vet. Parasitol. Reg. Stud. Rep.* **2021**, *26*, 100628. [CrossRef]
58. Kolte, S.W.; Larcombe, S.D.; Jadhao, S.G.; Magar, S.P.; Warthi, G.; Kurkure, N.V.; Glass, E.J.; Shiels, B.R. PCR diagnosis of tick-borne pathogens in Maharashtra state, India indicates fitness cost associated with carrier infections is greater for crossbreed than native cattle breeds. *PLoS ONE* **2017**, *12*, e0174595. [CrossRef]
59. Manuja, A.; Malhotra, D.V.; Sikka, V.K.; Sangwan, A.K.; Sharma, R.; Kumar, B.; Mehta, B.D.; Gulati, B.R.; Nichani, A.K. Isolates of Theileria annulata collected from different parts of India show phenotypic and genetic diversity. *Vet. Parasitol.* **2006**, *137*, 242–252. [CrossRef]
60. Velusamy, R.; Rani, N.; Ponnudurai, G.; Anbarasi, P. Prevalence of intestinal and haemoprotozoan parasites of small ruminants in Tamil Nadu, India. *Vet. World* **2015**, *8*, 1205. [CrossRef]
61. Jayaram, A.S.; Soundararajan, C.; Latha, B.R.; Senthilkumar, T.M.A. Molecular detection of Theileria Luwenshuni in sheep and goats of Chennai, Tamil Nadu. *Indian J. Small Rumin.* **2019**, *25*, 242–246. [CrossRef]
62. Dhaygude, V.S.; Kundu, K.; Kamdi, B.P.; Bagal, U.R.; Bhosale, S.B.; Sabharwal, D. Investigations on first confirmed outbreak of ovine theileriosis (Theileria luwenshuni) from Maharashtra state, India. *Indian J. Anim. Res.* **2021**, *55*, 951–955. [CrossRef]
63. Devi, G.; Ajith, Y.; Mal, G.; Dimri, U.; Preena, P.; Jairath, G.; Kattoor, J.J.; Jacob, S.S.; Singh, B.; Dhar, J.B. Migratory Gaddi sheep and goats as potential carriers of Theileria infection: A molecular survey. *Trop. Anim. Health Prod.* **2021**, *53*, 302. [CrossRef] [PubMed]
64. Bhattacharyulu, Y.; Chaudhri, R.P.; Gill, B.S. Transstadial transmission of Theileria annulata through common ixodid ticks infesting Indian cattle. *Parasitology* **1975**, *71*, 1–7. [CrossRef] [PubMed]

65. Srivastava, P.S.; Sharma, N.N. Potential of immunoprophylaxis using cobalt-60 irradiated Theileria annulata in salivary gland suspensions of the tick Hyalomma anatolicum. *Vet. Parasitol.* **1977**, *3*, 183–188. [CrossRef]
66. Sudan, V.; Sharma, R.L.; Yadav, R.; Borah, M.K. Turning sickness in a cross bred cow naturally infected with Theileria annulata. *J. Parasit. Dis.* **2012**, *36*, 226–229. [CrossRef]
67. Sudan, V.; Singh, S.K.; Jaiswal, A.K.; Parashar, R.; Shanker, D. First molecular evidence of the transplacental transmission of Theileria annulata. *Trop. Anim. Health Prod.* **2015**, *47*, 1213–1215. [CrossRef]
68. Kumar, A.; Gaur, G.K.; Gandham, R.K.; Panigrahi, M.; Ghosh, S.; Saravanan, B.C.; Bhushan, B.; Tiwari, A.K.; Sulabh, S.; Priya, B. Global gene expression profile of peripheral blood mononuclear cells challenged with Theileria annulata in crossbred and indigenous cattle. *Infect. Genet. Evol.* **2017**, *47*, 9–18. [CrossRef]
69. Mohmad, A.; Chandra, D.; Saravanan, B.C.; Manjunathchar, H.V.; OR, V.K.; Fular, A.; Chigure, G.; Kaur, N.; Ghosh, S. Development of a recombinant TaSP-based Dot-ELISA for detection of Theileria annulata infection in cattle. *Ticks Tick. Borne. Dis.* **2018**, *9*, 1416–1420. [CrossRef]
70. Aparna, M.; Ravindran, R.; Vimalkumar, M.B.; Lakshmanan, B.; Rameshkumar, P.; Kumar, K.G.A.; Promod, K.; Ajithkumar, S.; Ravishankar, C.; Devada, K. Molecular characterization of Theileria orientalis causing fatal infection in crossbred adult bovines of South India. *Parasitol. Int.* **2011**, *60*, 524–529. [CrossRef]
71. Velusamy, R.; Rani, N.; Ponnudurai, G.; Harikrishnan, T.J.; Anna, T.; Arunachalam, K.; Senthilvel, K.; Anbarasi, P. Influence of season, age and breed on prevalence of haemoprotozoan diseases in cattle of Tamil Nadu, India. *Vet. World* **2014**, *7*, 574–578. [CrossRef]
72. Dharanesha, N.K.; Giridhar, P.; Byregowda, S.M.; Venkatesh, M.D.; Ananda, K.J. Seasonal prevalence of blood parasitic diseases in crossbred cattle of Mysore and its surrounding districts of Karnataka. *J. Parasit. Dis.* **2017**, *41*, 773–777. [CrossRef] [PubMed]
73. Krishnamoorthy, P.; Sudhagar, S.; Goudar, A.L.; Jacob, S.S.; Suresh, K.P. Molecular survey and phylogenetic analysis of tick-borne pathogens in ticks infesting cattle from two South Indian states. *Vet. Parasitol. Reg. Stud. Rep.* **2021**, *25*, 100595. [CrossRef] [PubMed]
74. Srinivas, R.P.; Renukaprasad, C.; Keshvamurthy, B.S. A note on occurrence of outbreak of theileriosis in sheep in Karnataka. *Indian J. Comp. Microbiol. Immunol. Infect. Dis.* **1985**, *6*, 165–166.
75. Hitaishi, V.N.; Lakshmanan, B.; Shameem, H.; Jose, P.E.; Jain Jose, K.; Sabu, L. Molecular identification of theileriosis in goats of Kerala. *Int. J. Sci. Environ. Technol.* **2017**, *6*, 1979–1984.
76. Biradar, S.S.; D'Souza, P.E.; Mamatha, G.S.; Yathish, H.M.; Siju, S.J. Molecular epidemiology and phylogenetic analysis of Theileria species in sheep. *Indian J. Small Rumin.* **2019**, *25*, 192–198. [CrossRef]
77. Satbige, A.S.; Patil, N.A. Therapeutic Management of Theileriosis in Sheep. *Int. J. Livest. Res.* **2020**, *10*, 168–170. [CrossRef]
78. Kakati, P.; Sarmah, P.C.; Ray, D.; Bhattacharjee, K.; Sharma, R.K.; Barkalita, L.M.; Sarma, D.K.; Baishya, B.C.; Borah, P.; Stanley, B. Emergence of oriental theileriosis in cattle and its transmission through Rhipicephalus (Boophilus) microplus in Assam, India. *Vet. World* **2015**, *8*, 1099. [CrossRef] [PubMed]
79. Sahoo, N.; Behera, B.K.; Khuntia, H.K.; Dash, M. Prevalence of carrier state theileriosis in lactating cows. *Vet. World* **2017**, *10*, 1471. [CrossRef]
80. Acharya, A.P.; Panda, S.K.; Prusty, B.K. Diagnosis and confirmation of Theileria annulata infection in cattle in Odisha, India. *J. Entomol. Zool. Stud.* **2017**, *5*, 1543–1546.
81. Selim, A.M.; Senapati, S.K.; Das, M.; Mishra, C.; Patra, R.C.; Panda, S.K. Molecular, epidemiological and haematological evaluation in Theileria orientalis infected cattle from an endemic region in India. *Anim. Biotechnol.* **2020**, *32*, 663–670. [CrossRef]
82. Kala, S.; Gopal Deo, B.; Kumari, N. Prevalence of Theileriosis in Buffaloes during Rainy Season in and Around Patna, Bihar. *Int. J. Curr. Microbiol. Appl. Sci.* **2018**, *7*, 2762–2766. [CrossRef]
83. Roy, S.; Bhandari, V.; Dandasena, D.; Murthy, S.; Sharma, P. Genetic profiling reveals high allelic diversity, heterozygosity and antigenic diversity in the clinical isolates of the Theileria annulata from India. *Front. Physiol.* **2019**, *10*, 673. [CrossRef] [PubMed]
84. Sinha, B.S.; Sarkar, S.; Lodh, C.; Gupta, A.R.; Batabyal, S.; Jas, R. Prevalence of Bovine Theileriosis in South Bihar. *Pharma Innov. J.* **2021**, *SP-10*, 776–780.
85. Prabhakaran, H.S.; Ghosh, K.K.; Kumari, R.R.; Kumar, P.; Kumar, M. Evaluation of sporozoite and macroschizont antigen (Spm2) of Theileria annulata for its diagnostic potential. *Ticks Tick-Borne Dis.* **2021**, *12*, 101691. [CrossRef] [PubMed]
86. Sharma, G.; Sharma, R.D.; Nichani, A.K. Successful long-term in vitro cultivation of Theileria annulata schizonts in media supplemented with homologous and heterologous sera. *Vet. Parasitol.* **1998**, *79*, 135–141. [CrossRef]
87. Govindarajan, R.; Pazhanivel, N.; Sunder, N.; Sekar, M.; Jawahar, T.P.; Purusothaman, V. An outbreak of concurrent infection of theileriosis and sheep pox in Tamil Nadu, India. *Indian J. Anim. Sci.* **2005**, *75*, 787–788.
88. Haque, M.; Singh, N.K.; Rath, S.S. Prevalence of Theileria annulata infection in Hyalomma anatolicum anatolicum in Punjab state, India. *J. Parasit. Dis.* **2010**, *34*, 48–51. [CrossRef]
89. Vahora, S.P.; Patel, J.V.; Patel, B.B.; Patel, S.B.; Umale, R.H. Seasonal incidence of Haemoprotozoal diseases in crossbred cattle and buffalo in Kaira and Anand districts of Gujarat, India. *Vet. World* **2012**, *5*, 223. [CrossRef]
90. Singh, N.K.; Singh, H.; Haque, M.; Rath, S.S. Prevalence of parasitic infections in cattle of Ludhiana district, Punjab. *J. Parasit. Dis.* **2012**, *36*, 256–259. [CrossRef]
91. Tuli, A.; Das Singla, L.; Sharma, A.; Bal, M.S.; Filia, G.; Kaur, P. Molecular epidemiology, risk factors and hematochemical alterations induced by Theileria annulata in bovines of Punjab (India). *Acta Parasitol.* **2015**, *60*, 378–390. [CrossRef]

92. Tiwari, A.; Singh, N.K.; Singh, H.; Bhat, S.A.; Rath, S.S. Prevalence of Theileria annulata infection in Hyalomma anatolicum anatolicum collected from crossbred cattle of Ludhiana, Punjab. *J. Parasit. Dis.* **2015**, *39*, 57–61. [CrossRef]
93. Bhatnagar, C.S.; Bhardawaj, B.; Sharma, D.K.; Meena, S.K. Incidence of Haemoprotozoan diseases in cattle in Southern Rajasthan, India. *Int. J. Curr. Microbiol. Appl. Sci.* **2015**, *4*, 509–514.
94. Afifi, N.A.; Shihata, I.M.; El-Zorba, H.Y.; Ismail, I.M. Prevalence of theileriosis in cross-bred cattle: Its detection through blood smear examination and polymerase chain reaction in Dehradun district, Uttarakhand, India. *Vet. World* **2014**, *7*, 168.
95. Ganguly, A.; Bisla, R.S.; Singh, H.; Bhanot, V.; Kumar, A.; Kumari, S.; Maharana, B.R.; Ganguly, I. Prevalence and haemato-biochemical changes of tick borne haemoparasitic diseases in crossbred cattle of Haryana, India. *Indian J. Anim. Sci.* **2017**, *87*, 552–557.
96. Ganguly, A.; Maharana, B.R.; Ganguly, I. Pentaplex PCR assay for rapid differential detection of Babesia bigemina, Theileria annulata, Anaplasma marginale and Trypanosoma evansi in cattle. *Biologicals* **2020**, *63*, 81–88. [CrossRef] [PubMed]
97. Kundave, V.R.; Nehra, A.K.; Ram, H.; Kumari, A.; Shahzad, M.; Vinay, T.S.; Garg, R.; Banerjee, P.S.; Singh, G.; Tiwari, A.K. Genetic diversity in the Tams1 gene of Theileria annulata (Duschunkowsky and Luhs, 1904) infecting cattle. *Acta Trop.* **2021**, *224*, 106121.
98. Patial, V.; Gupta, T.; Angaria, S.; Bali, D.; Katoch, A.; Gautam, M.; Singh, N.K.; Sharma, M.; Chahota, R. Theileria orientalis outbreak in an organized cattle breeding farm. *Vet. Parasitol. Reg. Stud. Rep.* **2021**, *24*, 100572. [CrossRef]
99. Kamau, J.; de Vos, A.J.; Playford, M.; Salim, B.; Kinyanjui, P.; Sugimoto, C. Emergence of new types of Theileria orientalis in Australian cattle and possible cause of theileriosis outbreaks. *Parasit. Vectors* **2011**, *4*, 22.
100. Jongejan, F.; Uilenberg, G. The global importance of ticks. *Parasitology* **2004**, *129*, S3–S14. [CrossRef] [PubMed]
101. Zeb, J.; Szekeres, S.; Takács, N.; Kontschán, J.; Shams, S.; Ayaz, S.; Hornok, S. Genetic diversity, piroplasms and trypanosomes in Rhipicephalus microplus and Hyalomma anatolicum collected from cattle in northern Pakistan. *Exp. Appl. Acarol.* **2019**, *79*, 233–243. [CrossRef]
102. Ghosh, S.; Bansal, G.C.; Gupta, S.C.; Ray, D.; Khan, M.Q.; Irshad, H.; Shahiduzzaman, M.D.; Seitzer, U.; Ahmed, J.S. Status of tick distribution in Bangladesh, India and Pakistan. *Parasitol. Res.* **2007**, *101*, 207–216. [CrossRef] [PubMed]
103. Gharbi, M.; Darghouth, M.A.; Elati, K.; AL-Hosary, A.A.T.; Ayadi, O.; Salih, D.A.; El Hussein, A.M.; Mhadhbi, M.; Khamassi Khbou, M.; Hassan, S.M.; et al. Current status of tropical theileriosis in Northern Africa: A review of recent epidemiological investigations and implications for control. *Transbound. Emerg. Dis.* **2020**, *67*, 8–25. [CrossRef] [PubMed]
104. Shahnawaz, S.; Ali, M.; Aslam, M.A.; Fatima, R.; Chaudhry, Z.I.; Hassan, M.U.; Iqbal, F. A study on the prevalence of a tick-transmitted pathogen, Theileria annulata, and hematological profile of cattle from Southern Punjab (Pakistan). *Parasitol. Res.* **2011**, *109*, 1155–1160. [CrossRef] [PubMed]
105. Ali, Z.; Maqbool, A.; Muhammad, K.; Khan, M.; Younis, M. Prevalence of Theileria annulata infected hard ticks of cattle and buffalo in Punjab, Pakistan. *DNA* **2013**, *862*, 846.
106. Khan, M.K.; He, L.; Hussain, A.; Azam, S.; Zhang, W.-J.; Wang, L.-X.; Zhang, Q.-L.; Hu, M.; Zhou, Y.-Q.; Zhao, J. Molecular epidemiology of Theileria annulata and identification of 18S rRNA gene and ITS regions sequences variants in apparently healthy buffaloes and cattle in Pakistan. *Infect. Genet. Evol.* **2013**, *13*, 124–132. [CrossRef]
107. Ghafar, A.; Cabezas-Cruz, A.; Galon, C.; Obregon, D.; Gasser, R.B.; Moutailler, S.; Jabbar, A. Bovine ticks harbour a diverse array of microorganisms in Pakistan. *Parasit. Vectors* **2020**, *13*, 1. [CrossRef]
108. Gebrekidan, H.; Abbas, T.; Wajid, M.; Ali, A.; Gasser, R.B.; Jabbar, A. Molecular characterisation of Theileria orientalis in imported and native bovines from Pakistan. *Infect. Genet. Evol.* **2017**, *47*, 19–25. [CrossRef]
109. Hassan, M.A.; Liu, J.; Sajid, M.S.; Mahmood, A.; Zhao, S.; Abbas, Q.; Guan, G.; Yin, H.; Luo, J. Molecular detection of Theileria annulata in cattle from different regions of Punjab, Pakistan, by using recombinase polymerase amplification and polymerase chain reaction. *J. Parasitol.* **2018**, *104*, 196–201. [CrossRef]
110. Rehman, A.; Conraths, F.J.; Sauter-Louis, C.; Krücken, J.; Nijhof, A.M. Epidemiology of tick-borne pathogens in the semi-arid and the arid agro-ecological zones of Punjab province, Pakistan. *Transbound. Emerg. Dis.* **2019**, *66*, 526–536.
111. Qayyum, M.; Farooq, U.; Samad, H.A.; Chauhdry, H.R. Prevalence, clinicotherapeutic and prophylactic studies on theileriosis in district Sahiwal (Pakistan). *J. Anim. Plant Sci.* **2010**, *20*, 266–270.
112. Parveen, A.; Alkhaibari, A.M.; Asif, M.; Almohammed, H.I.; Naqvi, Z.; Khan, A.; Aktas, M.; Ozubek, S.; Farooq, M.; Iqbal, F. Molecular Epidemiology of Theileria annulata in Cattle from Two Districts in Punjab (Pakistan). *Animals* **2021**, *11*, 3443. [CrossRef] [PubMed]
113. Parveen, A.; Ashraf, S.; Khan, A.; Asif, M.; Iqbal, F. Tick and tick-borne diseases in Pakistan. In *The Entomological Guide to Rhipicephalus*, 1st ed.; Kumar, S., Bayugar, R.C., Sharma, A.K., Miranda, E.M., Chaubey, A.K., Eds.; Nova Science Publishers: New York, NY, USA, 2021.
114. Shahzad, W.; Haider, N.; Mansur-ud-Din, A.; Munir, R.; Saghar, M.S.; Mushtaq, M.H.; Ahmad, N.; Akbar, G.; Mehmood, F. Prevalence and molecular diagnosis of Babesia ovis and Theileria ovis in Lohi sheep at livestock experiment station (LES), Bahadurnagar, Okara, Pakistan. *Iran. J. Parasitol.* **2013**, *8*, 570. [PubMed]
115. Riaz, M.; Tasawar, Z. Identification of Theileria species (Theileria ovis and Theileria lestoquardi) by PCR in apparently healthy small ruminants in and around Multan, Southern Punjab, Pakistan. *Pakistan. J. Anim. Plant Sci.* **2017**, *27*, 809–818.
116. Habib, F.; Tabbasum, R.; Awais, T.; Sakhawat, A.; Khalil, R.; Sharif, A.; Yousaf, A.; Arshad, M.; Shahnawaz, R.; Shaheen, S.; et al. Prevalence of Bovine Tropical Theileriosis in Cattle in Quetta Balochistan-Pakistan. *Arch. Anim. Husb. Dairy Sci.* **2021**, *2*, 1–3.

117. Chaudhry, U.; Ali, Q.; Rashid, I.; Shabbir, M.Z.; Ijaz, M.; Abbas, M.; Evans, M.; Ashraf, K.; Morrison, I.; Morrison, L.; et al. Development of a deep amplicon sequencing method to determine the species composition of piroplasm haemoprotozoa. *Ticks Tick-Borne Dis.* **2019**, *10*, 101276. [CrossRef]
118. Riaz, M.; Nazir, M.M.; Tasawar, Z.; Ahmed, A.N.; Ayaz, M.M.; Akram, Q.; Lindsay, D.S. Molecular epidemiology and prevalence of Theileria lestoquardi and Theileria ovis infection in goats infested with tick vectors from Multan, Pakistan. *J. Med. Entomol.* **2019**, *56*, 844–848. [CrossRef]
119. Abid, K.; Bukhari, S.; Asif, M.; Sattar, A.; Arshad, M.; Aktas, M.; Ozubek, S.; Shaikh, R.S.; Iqbal, F. Molecular detection and prevalence of Theileria ovis and Anaplasma marginale in sheep blood samples collected from Layyah district in Punjab, Pakistan. *Trop. Anim. Health Prod.* **2021**, *53*, 439. [CrossRef]
120. Farooqi, S.; Ijaz, M.; Saleem, M.; Rashid, M.; Ahmad, S.; Islam, S. Prevalence and molecular diagnosis of Theileria annulata in bovine from three distinct zones of Khyber Pakhtunkhwa province, Pakistan. *J. Anim. Plant Sci.* **2017**, *27*, 1836–1841.
121. Zeb, J.; Shams, S.; Din, I.U.; Ayaz, S.; Khan, A.; Nasreen, N.; Khan, H.; Khan, M.A.; Senbill, H. Molecular epidemiology and associated risk factors of Anaplasma marginale and Theileria annulata in cattle from North-western Pakistan. *Vet. Parasitol.* **2020**, *279*, 109044. [CrossRef]
122. Ullah, R.; Shams, S.; Khan, M.A.; Ayaz, S.; ul Akbar, N.; ud Din, Q.; Khan, A.; Leon, R.; Zeb, J. Epidemiology and molecular characterization of Theileria annulata in cattle from central Khyber Pakhtunkhwa, Pakistan. *PLoS ONE* **2021**, *16*, e0249417. [CrossRef]
123. Ullah, N.; Durrani, A.Z.; Avais, M.; Nisar, A.; Ullah, S.; Khan, M.S.; Mehmood, K.; Khan, M.A.; Haq, I. Prevalence, risk factors and host biomarkers of ovine theileriosis. *Pak. J. Zool.* **2018**, *50*, 1211–1216. [CrossRef]
124. Khan, A.; Niaz, S.; Khan, A.; Ahmed, H.; Khattak, I.; Zeb, J.; Naeem, H.; Hassan, M.A.; Ulucesme, M.C.; Ozubek, S. Molecular detection of small ruminant piroplasmosis and first report of Theileria luwenshuni (Apicomplexa: Theileridae) in small ruminants of Pakistan. *Exp. Parasitol.* **2020**, *212*, 107872.
125. Mohsin, M.; Hameed, K.; Kamal, M.; Ali, A.; Rafiq, N.; Usman, T.; Khan, W.; Abbasi, A.A.; Khan, R.U.; Yousafzai, G.J. Prevalence and risk factors assessment of theileriosis in livestock of Malakand Division, Pakistan. *J. Saudi Soc. Agric. Sci.* **2021**. [CrossRef]
126. Niaz, S.; Zia Ur Rahman, I.A.; Cossío-Bayúgar, R.; Amaro-Estrada, I.; Alanazi, A.D.; Khattak, I.; Zeb, J.; Nasreen, N.; Khan, A. Molecular prevalence, characterization and associated risk factors of Anaplasma spp. and *Theileria* spp. in small ruminants in Northern Pakistan. *Parasite* **2021**, *28*, 3. [CrossRef]
127. Bhutto, B.; Gadahi, J.A.; Khuhro, A.; Rajput, H.M.; Bhutto, F.; Rajput, M.A.; Talpur, A.R. A survey on haemo-protozoan parasites in buffaloes of Landhi Dairy Colony, Karachi-Pakistan. *Int. J. Agro Vet. Med. Sci.* **2012**, *6*, 73–76. [CrossRef]
128. Ghafar, A.; Koehler, A.V.; Hall, R.S.; Gauci, C.G.; Gasser, R.B.; Jabbar, A. Targeted next-generation sequencing and informatics as an effective tool to establish the composition of bovine piroplasm populations in endemic regions. *Microorganisms* **2021**, *9*, 21. [CrossRef]
129. Durrani, S.; Khan, Z.; Khattak, R.M.; Andleeb, M.; Ali, M.; Hameed, H.; Taqddas, A.; Faryal, M.; Kiran, S.; Anwar, H.; et al. A comparison of the presence of Theileria ovis by PCR amplification of their SSU rRNA gene in small ruminants from two provinces of Pakistan. *Asian Pac. J. Trop. Dis.* **2012**, *2*, 43–47. [CrossRef]
130. Karim, S.; Budachetri, K.; Mukherjee, N.; Williams, J.; Kausar, A.; Hassan, M.J.; Adamson, S.; Dowd, S.E.; Apanskevich, D.; Arijo, A. A study of ticks and tick-borne livestock pathogens in Pakistan. *PLoS Negl. Trop. Dis.* **2017**, *11*, e0005681. [CrossRef]
131. Ashfaque, M.; Ajmal, M.; Ahmad, S. An outbreak of theileriosis in crossbred neonate calves. *Pak. Vet. J.* **1983**, *3*, 44–46.
132. Muhammad, G. Clinico-epidemiological and therapeutic aspects of bovine theileriosis. *Bull Calf Appear Female* **1999**, *36*, 32.
133. Khan, M.Q.; Zahoor, A.; Jahangir, M.; Mirza, M.A. Prevalence of blood parasites in cattle and buffaloes. *Pak. Vet. J.* **2004**, *24*, 193–194.
134. Zahid, I.A.; Latif, M.; Baloch, K.B. Incidence and treatment of theileriasis and babesiasis. *Pak. Vet. J.* **2005**, *25*, 137.
135. Durrani, A.; Kamal, N.; Khan, M.S. Incidence of theileriosis and estimation of packed cell volume, total erythrocyte count and hemoglobin in buffaloes. *J. Anim. Plant Sci.* **2006**, *16*, 85–88.
136. Durrani, A.Z.; Kamal, N. Identification of ticks and detection of blood protozoa in friesian cattle by polmerase chain reacton test and estimation of blood parameters in district Kasur, Pakistan. *Trop. Anim. Health Prod.* **2008**, *40*, 441–447. [CrossRef] [PubMed]
137. Azizi, H.; Shiran, B.; Dehkordi, A.F.; Salehi, F.; Taghadosi, C. Detection of Theileria annulata by PCR and its comparison with smear method in native carrier cows. *Biotechnology* **2008**, *7*, 574–577. [CrossRef]
138. Atif, F.A.; Khan, M.S.; Iqbal, H.J.; Arshad, G.M.; Ashraf, E.; Ullah, S. Prevalence of Anaplasma marginale, Babesia bigemina and Theileria annulata infections among cattle in Sargodha District, Pakistan. *Afr. J. Agric. Res.* **2012**, *7*, 302–3307.
139. Hassan, M.A.; Liu, J.; Sajid, M.S.; Rashid, M.; Mahmood, A.; Abbas, Q.; Guan, G.; Yin, H.; Luo, J. Simultaneous detection of Theileria annulata and Theileria orientalis infections using recombinase polymerase amplification. *Ticks Tick-Borne Dis.* **2018**, *9*, 1002–1005. [CrossRef]
140. Irshad, N.; Qayyum, M.; Hussain, M.; Khan, M.Q. Prevalence of tick infestation and theileriosis in sheep and goats. *Pak. Vet. J.* **2010**, *30*, 178–180.
141. Shabbir, M.Z.; Khan, J.A. Prevalence of theileriosis in sheep in Okara District, Pakistan. *Pak. J. Zool.* **2010**, *42*, 639–643.
142. Durrani, A.Z.; Younus, M.; Kamal, N.; Mehmood, N.; Shakoori, A.R. Prevalence of ovine Theileria species in district Lahore, Pakistan. *Pak. J. Zool.* **2011**, *43*, 57–60.

143. Naz, S.; Maqbool, A.; Ahmed, S.; Ashraf, K.; Ahmed, N.; Saeed, K.; Latif, M.; Iqbal, J.; Ali, Z.; Shafi, K. Prevalence of theileriosis in small ruminants in Lahore-Pakistan. *J. Vet. Anim. Sci.* **2012**, *2*, 16–20.
144. Fatima, M.; Saeed, S.; Shaikh, R.S.; Ali, M.; Iqbal, F. A study on molecular detection of Theileria lestoquardi by PCR amplification in apparently healthy small ruminants from five districts of Southern Punjab. *Pak. J. Zool.* **2015**, *47*, 441–446.
145. Riaz, M.; Tasawar, Z. A study on molecular surveillance of Theileria spp. infection and its impact on hematological and biochemical changes in naturally infected small ruminants at Multan, Pakistan. *Pure Appl. Biol.* **2017**, *6*, 1427–1435. [CrossRef]
146. Afridi, Z.K.; Ahmad, I. Incidence of anaplasmosis, babesiosis and theileriosis in dairy cattlein Peshawar [Pakistan]. *Sarhad J. Agric.* **2005**, *21*, 311–316.
147. Iqbal, F.; Khattak, R.M.; Ozubek, S.; Khattak, M.N.K.; Rasul, A.; Aktas, M. Application of the reverse line blot assay for the molecular detection of Theileria and Babesia sp. in sheep and goat blood samples from Pakistan. *Iran. J. Parasitol.* **2013**, *8*, 289.
148. Zeb, J.; Shams, S.; Ayaz, S.; Din, I.U.; Khan, A.; Adil, N.; Ullah, H.; Raza, A. Epidemiology of ticks and molecular characterization of Rhipicephalus microplus in cattle population in North-Western Pakistan. *Int. J. Acarol.* **2020**, *46*, 335–343. [CrossRef]
149. Khan, A.; Jamil, M.; Ali, A.; Ali, A.; Imdad, S.; Zeeshan, M. Prevalence of Theileriosis in Buffaloes at Government and Private Farms in Tehsil Paharpur, Dera Ismail Khan. *Int. J. Mod. Agric.* **2021**, *10*, 4360–4363.
150. Saeed, S.; Jahangir, M.; Fatima, M.; Shaikh, R.S.; Khattak, R.M.; Ali, M.; Iqbal, F. PCR based detection of Theileria lestoquardi in apparently healthy sheep and goats from two districts in Khyber Pukhtoon Khwa (Pakistan). *Trop. Biomed.* **2015**, *32*, 225–232.
151. Anwar, K.; Din, A. Epidemiology of Tick Borne Heamoprotozoan Infection in Ruminants in District Peshawar, and Periphery, Khyber Pakhtunkhwa,(Pakistan). *Am. Sci. Res. J. Eng. Technol. Sci.* **2017**, *35*, 191–200.
152. Shah, S.S.A.; Khan, M.I.; Rahman, H.U. Epidemiological and hematological investigations of tick-borne diseases in small ruminants in Peshawar and Khyber agency. *Pak. J. Adv. Parasitol.* **2017**, *4*, 15–22.
153. Ullah, N.; Durrani, A.Z.; Ullah, S.; Ullah, S.; Shah, M.K.; Khan, A.Z.; Khan, M.S.; Khan, N.U.; Khan, M.A. A study on potential factors and physiological biomarkers associated with the occurrence of ovine theileriosis. *Small Rumin. Res.* **2018**, *168*, 32–38. [CrossRef]
154. Buriro, S.N.; Phulan, M.S.; Arijo, A.H.; Memon, A.B. Incidence of some haemo-protozoans in Bos indicus and Bubalis bubalis in Hyderabad. *Pak. Vet. J.* **1994**, *14*, 28–29.
155. Abbasi, F.; Abbasi, I.H.R.; Nissa, T.F.; Bhutto, Z.A.; Arain, M.A.; Soomro, R.N.; Siyal, F.A.; Fazlani, S.A. Epidemiological study of tick infestation in buffalo of various regions of district Khairpur, Pakistan. *Vet. World* **2017**, *10*, 688–694. [CrossRef] [PubMed]
156. Soomro, M.H.; Soomro, S.P.; Bhutto, M.B.; Akbar, Z.; Yaqoob, M.; Arijo, A.G. Prevalence of ticks in buffaloes in the upper Sindh Pakistan. *Buffalo Bull.* **2014**, *33*, 323–327.
157. Durrani, A.Z.; Shakoori, A.R. Study on ecological growth conditions of cattle Hyalomma ticks in Punjab, Pakistan. *Iran. J. Parasitol.* **2009**, *14*, 19–25.
158. Rehman, A.; Nijhof, A.M.; Sauter-Louis, C.; Schauer, B.; Staubach, C.; Conraths, F.J. Distribution of ticks infesting ruminants and risk factors associated with high tick prevalence in livestock farms in the semi-arid and arid agro-ecological zones of Pakistan. *Parasit. Vectors* **2017**, *10*, 190. [CrossRef]
159. Zahida, T.; Sumaira, N.; Lashari, M.H. The prevalence of ixodid ticks on buffaloes at private animal farm Bibipur, Multan. *Glob. Vet.* **2014**, *12*, 154–157.
160. Khan, M.N.; Hayar, C.S.; Iqbal, Z.; Hayat, B. Prevalence of ticks on livestock in Faisalabad (Pakistan). *Pak. Vet. J.* **1993**, *13*, 182.
161. Ramzan, M.; Khan, M.S.; Avais, M.; Khan, J.A.; Pervez, K.; Shahzad, W. Prevalence of ecto parasites and comparative efficacy of different drugs against tick infestation in cattle. *J. Anim. Plant Sci.* **2008**, *18*, 17–19.
162. Ahmed, S.; Numan, M.; Manzoor, A.W.; Ali, F.A. Investigations into Ixodidae ticks in cattle in Lahore, Pakistan. *Vet. Ital.* **2012**, *48*, 185–191.
163. Nasreen, N.; Niaz, S.; Khan, A.; Ayaz, S.; Rashid, M.; Khattak, I.; Yu, Z.; Wang, T.; Al Sarraf, M.; Ali, A. Molecular characterization of ticks infesting livestock in Khyber Pakhtunkhwa Province, Pakistan. *Int. J. Acarol.* **2020**, *46*, 165–170. [CrossRef]
164. Hussain, S.I.; Kumar, G.A. Prevalence of ticks (Ixodoidea, Ixodidae) of buffaloes at Thatta and its adjoining areas in the Province of Sindh, Pakistan. *Pak. Congr. Zool.* **1990**, *10*, 11–16.
165. Rafique, N.; Kakar, A.; Iqbal, A.; Masood, Z.; Razzaq, W.; Iqbal, F. Impact assessment of tick species, Rhipicephalus (Boophilus) microplus on the milk productions of cattle's in the Quetta City of Province Balochistan, Pakistan. *Glob. Vet.* **2015**, *15*, 19–23.
166. Sajid, M.S.; Iqbal, Z.; Khan, M.N.; Muhammad, G. Point prevalence of hard ticks (Ixodids) infesting domestic ruminants of lower Punjab, Pakistan. *Int. J. Agric. Biol.* **2008**, *10*, 349–351.
167. Rafiq, N.; Kakar, A.; Ghani, A.; Iqbal, A.; Achakzai, W.M.; Sadozai, S.; Shafiq, M.; Mengal, M.A. Ixodid ticks (Arachnida: Acari) prevalence associated with risk factors in the bovine host in District Quetta, Balochistan. *Pak. J. Zool.* **2017**, *46*, 2113–2121. [CrossRef]
168. Bibi, S.; Rafique, N.; Kareem, A.; Taj, M.K.; Iqbl, K.; Bibi, A.; Shafiq, M.; Ghafoor, G.; Ghafoor, A.; Ijaz, A. 15. Prevalence and taxonomic identification of hard ticks (Ixodidea) found in livestock of Harnai District, Balochistan, Pakistan. *Pure Appl. Biol.* **2020**, *9*, 2330–2338. [CrossRef]
169. Cruz, D.D.; Arellano, E.; Denis Ávila, D.; Ibarra-Cerdeña, C.N. Identifying Chagas disease vectors using elliptic Fourier descriptors of body contour: A case for the cryptic dimidiata complex. *Parasit. Vectors* **2020**, *13*, 332. [CrossRef]
170. Batool, M.; Nasir, S.; Rafique, A.; Yousaf, I.; Yousaf, M. Prevalence of tick infestation in farm animals from Punjab, Pakistan. *Pak. Vet. J.* **2019**, *39*, 406–410. [CrossRef]

171. Sajid, M.S.; Iqbal, Z.; Khan, M.N.; Muhammad, G.; Needham, G.; Khan, M.K. Prevalence, associated determinants, and in vivo chemotherapeutic control of hard ticks (Acari: Ixodidae) infesting domestic goats (Capra hircus) of lower Punjab, Pakistan. *Parasitol. Res.* **2011**, *108*, 601–609. [CrossRef]
172. Iqbal, A.; Siddique, F.; Mahmood, M.S.; Shamim, A.; Zafar, T.; Rasheed, I.; Saleem, I.; Ahmad, W. Prevalence and impacts of ectoparasitic fauna infesting goats (*Capra hircus*) of district Toba Tek Singh, Punjab Pakistan. *Glob. Vet.* **2014**, *12*, 158–164.
173. Ramzan, M.; Naeem-Ullah, U.; Abbas, H.; Adnan, M.; Rasheed, Z.; Khan, S. Diversity of hard ticks in goats and sheep in Multan, Punjab, Pakistan. *Int. J. Agric. Biol. Res.* **2019**, *35*, 7–9.
174. Ramzan, M.; Naeem-Ullah, U.; Saba, S.; Iqbal, N.; Saeed, S. Prevalence and identification of tick species (Ixodidae) on domestic animals in district Multan, Punjab Pakistan. *Int. J. Acarol.* **2020**, *46*, 83–87. [CrossRef]
175. Siddiqi, M.N.; Jan, A.H. Ixodid ticks (ixodidae) of NWFP (Pakistan). *Pak. Vet. J.* **1986**, *6*, 124–126.
176. Shah, A.; Shah, S.R.; Rafi, M.A.; Noorrahim, M.S.; Mitra, A. Identification of the prevalent ticks (Ixodid) in goats and sheep in Peshawar, Pakistan. *J. Entomol. Zool. Stud.* **2015**, *3*, 11–14.
177. Ali, A.; Khan, M.A.; Zahid, H.; Yaseen, P.M.; Qayash Khan, M.; Nawab, J.; Ur Rehman, Z.; Ateeq, M.; Khan, S.; Ibrahim, M. Seasonal Dynamics, Record of Ticks Infesting Humans, Wild and Domestic Animals and Molecular Phylogeny of Rhipicephalus microplus in Khyber Pakhtunkhwa Pakistan. *Front. Physiol.* **2019**, *10*, 793. [CrossRef] [PubMed]
178. Aziz, S.; Shah, S.F.; Amin, F.; Khan, M.A.; Ahmad, M. Taxonomic Study of Arthropod Pests of Livestock in District Peshawar, Khyber Pakhtunkhwa. *Pak. J. Life Soc. Sci.* **2018**, *16*, 85–96.
179. Khatoon, N.; Noureen, S.; Khan, Z.; Gul, S.U.; Ur, H. Domestic animals ectoparasite fauna of district Karak, KP, Pakistan. *Int. J. Biosci.* **2018**, *13*, 384–388.
180. Khan, A.; Nasreen, N.; Niaz, S.; Sajjad Ali Shah, S.; Mitchell III, R.D.; Ayaz, S.; Naeem, H.; Khan, L.; De León, A.P. Tick burden and tick species prevalence in small ruminants of different agencies of the Federally Administered Tribal Areas (FATA), Pakistan. *Int. J. Acarol.* **2019**, *45*, 374–380. [CrossRef]
181. Hussain, S.I.; Kumar, G.A. Prevalence of ixodid ticks (Ixodoidea, Ixodidae) of goats at Khairpur Mir's and its adjoining areas [Pakistan]. *Pak. J. Zool.* **1983**, *15*, 51–55.
182. Hussain, S.I.; Kumar, G.A. The incidence of ticks (Ixodoidea: Ixodidae) infesting sheep and goats in Sind province, Pakistan. *Pak. J. Zool.* **1985**, *17*, 89–97.
183. Iqbal, A.; Nawaz, M. Taxonomic studies of Haemaphysalis flava (Neumann), its seasonal prevalence and role in parasitic diseases of sheep/goat in Balochistan. *Pak. Entomol.* **2007**, *29*, 1–4.
184. Haneef, M.; Kakar, A.; Naseem, M.; Kurd, A.; Rafiq, N.; Kakar, B.; Uddin, S. 40. Incidence of ectoparasite in chiltan wild goat (Artiodactyla: Caprinae) native of Hazarganji chiltan national park (HCNP), Balochistan, Pakistan. *Pure Appl. Biol.* **2019**, *8*, 389–396.
185. Kasi, K.K.; von Arnim, F.; Schulz, A.; Rehman, A.; Chudhary, A.; Oneeb, M.; Sas, M.A.; Jamil, T.; Maksimov, P.; Sauter-Louis, C. Crimean-Congo haemorrhagic fever virus in ticks collected from livestock in Balochistan, Pakistan. *Transbound. Emerg. Dis.* **2020**, *67*, 1543–1552. [CrossRef] [PubMed]
186. Ahmed AKNU Blood parasites of domestic animals in Bangladesh. *Bangladesh Vet. J.* **1976**, *10*, 69–71.
187. Al Mahmud, M.A.; Belal, S.M.S.H.; Hossain, M.A. Prevalence of theileriosis and babesiosis in cattle in Sirajganj district of Bangladesh. *Res. Agric. Livest. Fish.* **2015**, *2*, 79–86. [CrossRef]
188. Roy, B.C.; Estrada-Peña, A.; Krücken, J.; Rehman, A.; Nijhof, A.M. Morphological and phylogenetic analyses of Rhipicephalus microplus ticks from Bangladesh, Pakistan and Myanmar. *Ticks Tick-Borne Dis.* **2018**, *9*, 1069–1079. [CrossRef]
189. Islam, M.F.; Rudra, P.G.; Singha, S.; Das, T.; Gebrekidan, H.; Uddin, M.B.; Chowdhury, M.Y.E. Molecular Epidemiology and Characterization of Theileria in Goats. *Protist* **2021**, *172*, 125804. [CrossRef]
190. Siddiki, A.Z.; Uddin, M.B.; Hasan, M.B.; Hossain, M.F.; Rahman, M.M.; Das, B.C.; Sarker, M.S.; Hossain, M.A. Coproscopic and Haematological Approaches to Determine the Prevalence of Helminthiasis and Protozoan Diseases of Red Chittagong Cattle (RCC) Breed in Bangladesh. *Pak. Vet. J.* **2010**, *30*, 1–6.
191. Kispotta, S.; Islam, M.F.; Hoque, M.F.; Rahman, M.S.; Borman, A.; Haque, M.A.; Rahman, M.R. Study of prevalence and associated risk factors of anaplasmosis and theileriasis in cattle. *Asian J. Med. Biol. Res.* **2016**, *2*, 567–576. [CrossRef]
192. Ali, M.W.; Alauddin, M.; Azad, M.T.A.; Hasan, M.A.; Appiah-Kwarteng, C.; Takasu, M.; Baba, M.; Kitoh, K.; Rahman, M.; Takashima, Y. Theileria annulata seroprevalence among different cattle breeds in Rajshahi Division, Bangladesh. *J. Vet. Med. Sci.* **2016**, *78*, 1577–1582. [CrossRef]
193. Moni, M.I.Z.; Hayashi, K.; Sivakumar, T.; Rahman, M.; Nahar, L.; Islam, M.Z.; Yokoyama, N.; Kitoh, K.; Appiah-Kwarteng, C.; Takashima, Y. First Molecular detection of Theileria annulata in Bangladesh. *J. Vet. Med. Sci.* **2019**, *81*, 1197–1200. [CrossRef] [PubMed]
194. Hassan, M.Z.; Giasuddin, M.; Rahman, M.M.; Ershaduzzaman, M.; Hasan, M. Identification of vector-borne blood protozoa in cattle and sheep in Bangladesh. *J. Virol. Antivir.* **2019**, *2*, 4.
195. Samad, A.; Dhar, S.; Gautam, O.P. Prevalence of Theileria annulata infection among cattle of Bangladesh. *Indian J. Parasitol.* **1983**, *7*, 61–63.
196. Samad, M.A.; Bashar, S.A.; Shahidullah, M.; Ahmed, M.U. Prevalence of haemoprotozoan parasites in cattle of Bangladesh. *Indian Vet. Med. J.* **1989**, *13*, 50–51.

197. Dhar, S.; Gautam, O.P. Theileria annulata infection of cattle I complement fixation and coagulating absorption tests for serodiagnosis. *Indian J. Anim. Sci.* **1977**, *47*, 389–394.
198. Ros-García, A.; Nicolás, A.; García-Pérez, A.L.; Juste, R.A.; Hurtado, A. Development and evaluation of a real-time PCR assay for the quantitative detection of Theileria annulata in cattle. *Parasit. Vectors* **2012**, *5*, 171. [CrossRef]
199. Chae, J.; Allsopp, B.A.; Waghela, S.D.; Park, J.; Kakuda, T.; Sugimoto, C.; Allsopp, M.T.E.P.; Wagner, G.G.; Holman, P.J. A study of the systematics of Theileria spp. based upon small-subunit ribosomal RNA gene sequences. *Parasitol. Res.* **1999**, *85*, 877–883. [CrossRef]
200. Glidden, C.K.; Koehler, A.V.; Hall, R.S.; Saeed, M.A.; Coppo, M.; Beechler, B.R.; Charleston, B.; Gasser, R.B.; Jolles, A.E.; Jabbar, A. Elucidating cryptic dynamics of Theileria communities in African buffalo using a high-throughput sequencing informatics approach. *Ecol. Evol.* **2020**, *10*, 70–80. [CrossRef]
201. Ogden, N.H.; Ben Beard, C.; Ginsberg, H.S.; Tsao, J.I. Possible Effects of Climate Change on Ixodid Ticks and the Pathogens They Transmit: Predictions and Observations. *J. Med. Entomol.* **2021**, *58*, 1536–1545. [CrossRef]

diversity

MDPI

Article

Is Diversity the Missing Link in Coastal Fisheries Management?

Stuart Kininmonth [1,2,3,*], Thorsten Blenckner [1], Susa Niiranen [1], James Watson [1,4], Alessandro Orio [5], Michele Casini [5,6], Stefan Neuenfeldt [7], Valerio Bartolino [5] and Martin Hansson [8]

1 Stockholm Resilience Centre, Stockholm University, SE-106 91 Stockholm, Sweden; thorsten.blenckner@su.se (T.B.); susa.niiranen@su.se (S.N.); jrwatson@coas.oregonstate.edu (J.W.)
2 Heron Island Research Station, University of Queensland, Gladstone, QLD 4680, Australia
3 School of Agriculture Geography Environment Oceans and Natural Sciences, University of the South Pacific, Suva, Fiji
4 College of Earth, Ocean and Atmospheric Sciences, Oregon State University, Corvallis, OR 97330, USA
5 Department of Aquatic Resources, Institute of Marine Research, Swedish University of Agricultural Sciences, Turistgatan 5, SE-453 30 Lysekil, Sweden; alessandro.orio@slu.se (A.O.); michele.casini@slu.se (M.C.); valerio.bartolino@slu.se (V.B.)
6 Department of Biological, Geological and Environmental Sciences, University of Bologna, Via Selmi 3, 40126 Bologna, Italy
7 National Institute of Aquatic Resources, Section for Oceans and Arctic, Technical University of Denmark, Kemitorvet 202, 2800 Kongens Lyngby, Denmark; stn@aqua.dtu.dk
8 Oceanographic Unit, Swedish Meteorological and Hydrological Institute—SMHI, Sven Källfelts Gata 15, SE-426 71 Västra Frölunda, Sweden; martin.hansson@smhi.se
* Correspondence: stuart@kininmonth.com.au; Tel.: +61-487-281-689

Abstract: Fisheries management has historically focused on the population elasticity of target fish based primarily on demographic modeling, with the key assumptions of stability in environmental conditions and static trophic relationships. The predictive capacity of this fisheries framework is poor, especially in closed systems where the benthic diversity and boundary effects are important and the stock levels are low. Here, we present a probabilistic model that couples key fish populations with a complex suite of trophic, environmental, and geomorphological factors. Using 41 years of observations we model the changes in eastern Baltic cod (*Gadus morhua)*, herring *(Clupea harengus)*, and Baltic sprat (*Sprattus sprattus balticus*) for the Baltic Sea within a Bayesian network. The model predictions are spatially explicit and show the changes of the central Baltic Sea from cod- to sprat-dominated ecology over the 41 years. This also highlights how the years 2004 to 2014 deviate in terms of the typical cod–environment relationship, with environmental factors such as salinity being less influential on cod population abundance than in previous periods. The role of macrozoobenthos abundance, biotopic rugosity, and flatfish biomass showed an increased influence in predicting cod biomass in the last decade of the study. Fisheries management that is able to accommodate shifting ecological and environmental conditions relevant to biotopic information will be more effective and realistic. Non-stationary modelling for all of the homogeneous biotope regions, while acknowledging that each has a specific ecology relevant to understanding the fish population dynamics, is essential for fisheries science and sustainable management of fish stocks.

Keywords: benthic coupling; fisheries modelling; Bayesian networks; spatially explicit; Baltic Sea; non-stationary; regime shift; resilience; sustainability

Citation: Kininmonth, S.; Blenckner, T.; Niiranen, S.; Watson, J.; Orio, A.; Casini, M.; Neuenfeldt, S.; Bartolino, V.; Hansson, M. Is Diversity the Missing Link in Coastal Fisheries Management?. *Diversity* **2022**, *14*, 90. https://doi.org/10.3390/d14020090

Academic Editor: Michael Wink

Received: 19 November 2021
Accepted: 18 January 2022
Published: 28 January 2022

1. Introduction

Ecosystem-based modeling approaches to fisheries management require models that can include the fundamental interaction present in the fisheries systems [1]. Even for relatively simple fisheries regions, such as the Baltic Sea, models can be improved if they account for localized diversity, species interactions at chosen trophic levels, environmental drivers, and human pressures [2]. Indeed, many models have extended their complexity

to achieve this level of comprehension [3,4]. Despite these advances, there still exists a mismatch between modeling output and fisheries management—particularly in the spatial realm of marine reserve design, local seasonal closures, and real-time probabilistic assessment of fish biomass given field observations. Many fisheries models, despite containing many complex interaction components, still consider the fisheries ecosystem as a single homogeneous resource pool [5,6]. Spatial interactions of biota with the habitat and benthic structure are simplified or ignored in order to maintain traction with complicated mechanistic models [7].

Evidence of critical transitions occurring in marine ecosystems is dominated by coastal and inland sea systems [8]. The role of benthic dynamics in determining the character of the ecosystem dynamics, due to environmental fluctuations and the interaction with biotic elements, is well known [9,10], but remains challenging from a modelling perspective [7,11]. At one level, the mechanistic models lack the suitable experimental and observational data to determine the parameters for such a responsive system. On another level, the modeling frameworks that are often used struggle to include spatial processes—especially in continuous-time logistic models [12]. This is primarily due to the difficulty in defining the interaction suite for each habitat type and the mechanics of interaction processes between habitat zones.

In general, the term habitat has been widely used in relation to areas that are homogeneous in terms of their geophysical environment [13]. Therefore, in these cases, no information on the biota in that area is required. However, in this paper, we refer to the concept of biotopes, which are homogeneous units that are characterized by a typical species assemblage that exists in the geophysical environment [13]. For spatial mapping and conservation purposes, it is of fundamental importance to include biotope classes (distinct units with a homogeneous species composition) that are representative of their distributions, and to adapt the scale of observation and modelling to the scale of the patches that they form.

New modelling approaches are being explored that limit model complexity while maintaining predictive skill, negotiating uncertainty limits, and offering spatially valid explicit estimates of fisheries dynamics [7]. One such approach is to base the predictions on correlations between observations over space and time, rather than formulate a set of precise interaction equations. Correlations in a trophodynamic systems do not necessarily directly equate to metabolic, behavioral, or ecological processes, but the trade-off is the ability to predict with increased precision in a diverse and uncertain environment [10]. The trade-off between limiting models to well-defined causation links versus expanded models based on including correlations can be critical to management imperatives.

Bayesian Networks

Bayesian networks (BNs) offer the capacity to encompass complex interactions of disparate data types within a probabilistic framework with only a few limitations [14–18]. Bayes' rule combined with the chain rule enables the propagation of conditional probability throughout a network structure. The network design is typically the result of expert opinion, although algorithms exist to formulate a possible structure through analysis of correlations. The parameterization of a model is achieved through the inclusion of observational cases that fully or partially describe a system's state. The more cases used to inform the model's conditional probabilities, the more accurate the predictions, but algorithms such as expectation maximization can assist in adjusting for missing data. Expert opinion, equations, and numerical (i.e., continuous, discrete, and censored) and categorical data can be included in the model, which is particularly useful for models of socioecological systems such as fisheries [19,20].

The development of a BN for a system that has been comprehensively observed for many decades while undergoing rapid change was an outstanding opportunity not only to increase knowledge of ecosystem dynamics, but also to advance fisheries ecosystem modeling. The Baltic Sea was such a system, with records of fishing catches combined

with changing environmental conditions and fluctuating biota [19–21]. Such changes induced a fishery- and climate-induced regime shift that changed the food web from being dominated by the predator eastern Baltic cod (*Gadus morhua*, hereafter referred to as cod) to an alternative configuration dominated by planktivorous fish, e.g., Baltic sprat (*Sprattus sprattus balticus*) [22,23]. Even after the reduction in the cod catch, several biological changes occurred to the cod stock [24], which did not recover. Critically, the benthic pelagic coupling was particularly important in the Baltic Sea (largely due to the shallow nature of the sea), and also the young cod were dependent on benthic prey (the availability of which was closely linked to hypoxia) [21,25]. In order to better understand the dynamics of the cod that could help foresee their evolution and, therefore, aid in their management, thus-far overlooked pieces of information are needed. One of these could be represented by spatially explicit habitat information in relation to the cod stock dynamics [26]. Spatial dynamics across habitats or better biotopes are very important [27], and can have major effects on marine food webs [28].

Here, we present a spatially explicit trophodynamic model for the Baltic Sea based on 41 years of observations, including structural, environmental, and trophic data. With this model we answer two questions: (1) Are changes in diversity through alteration of biotopic conditions the key to shaping cod dynamics? (2) Are trophic, environmental, and biotopic feedbacks—and, consequently, cod biomasses—non-stationary?

2. Materials and Methods

2.1. Baltic Sea Study Area

The Baltic Sea (Figure 1) is an inland sea measuring 393,000 km^2 and with a mean depth of only 54 m. The most significant environmental gradient is the surface salinity, which declines to almost fresh water in the innermost and northernmost areas. A highly saline region in the deeper locations causes stagnation of the bottom waters; the 85 million residents living in the adjacent catchments exacerbate this stagnation [29]. The latitudinal span from 53 N to 66 N creates a temperature gradient resulting in large variations from summer to winter. In general, the depth, substrate, wave exposure, and salinity gradient determine the benthic composition [30]. Habitat zones based on these factors with six levels of resolution were modeled by Wikstrom et al. [30]. Associated fisheries have concentrated on a diverse range of species, but primarily dominated by cod, herring, and sprat [31]. The collapse of the Baltic cod fisheries in the 1980s highlighted the transition of the Baltic Sea to an alternative state dominated by the commercially less valuable herring and sprat [21,32].

2.2. Modeling Framework

To address the question regarding the factors influencing cod biomass, we needed a model framework that integrates environmental and structural components into a trophic network with the inclusion of fisheries' catch influences. Motivating this model design were two practical limitations: Firstly, the variables included in the model needed to be based on raw observational data rather than model outputs, in order to minimize bias towards contemporary modeling approaches. Secondly, the spatial scale of the model needed to reflect the Baltic Sea management requirements yet concede to the spatial and temporal resolution of the observational data. The BN model is scale-invariant, but the prediction outputs are required to fit a spatial scale that can be mapped. The units of analysis selected were the EUSeaMap biotope polygons that vary in size and shape throughout the Baltic Sea [30]. This has the advantage that adjacent homogeneous areas (based on the classification level) could be merged into a larger area with a higher likelihood of being coincident with observational data (Figure 2). However, despite this spatial simplification, the analysis was based on predicting the cod biomass for 28,712 biotope polygons.

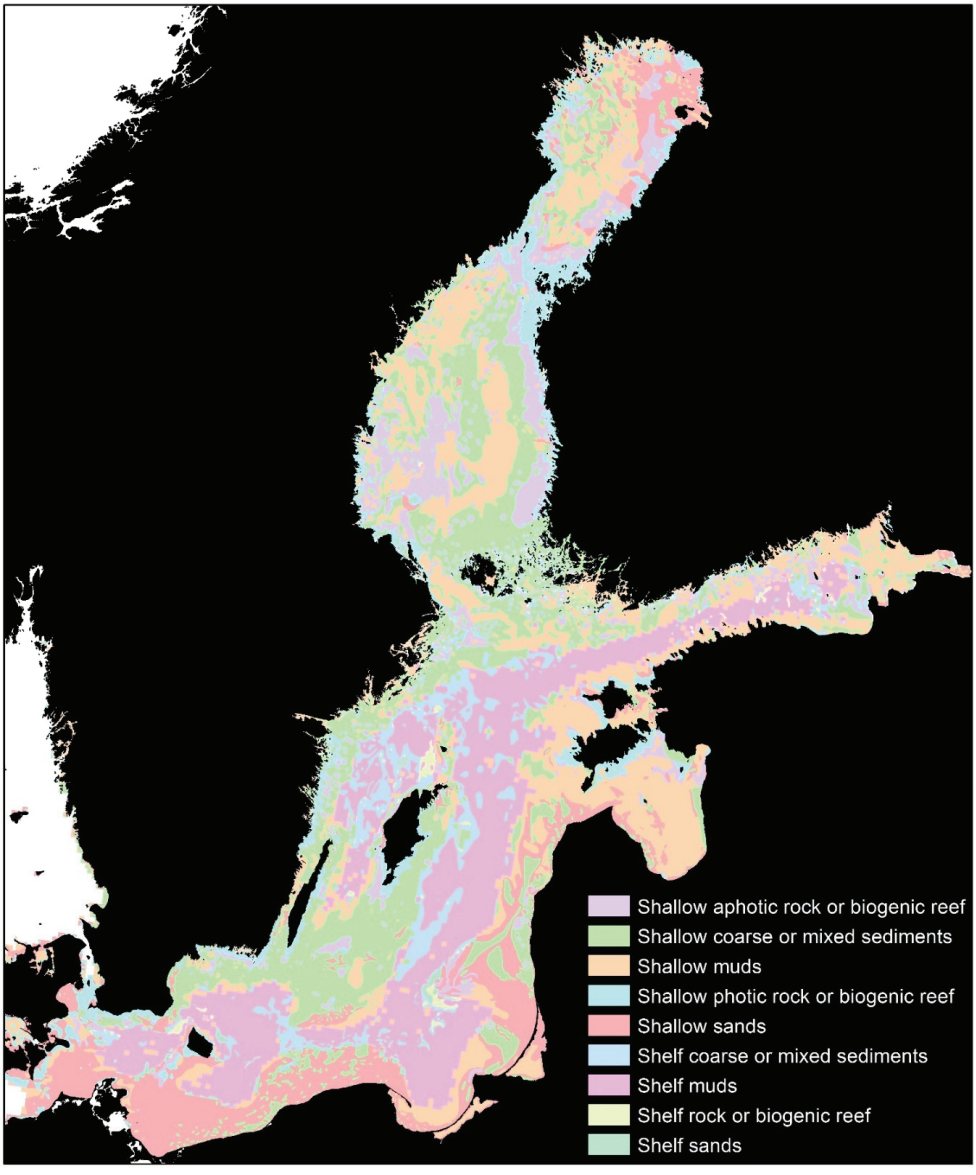

Figure 1. Biotopes of the Baltic Sea, showing the polygons grouped into 9 categories [30].

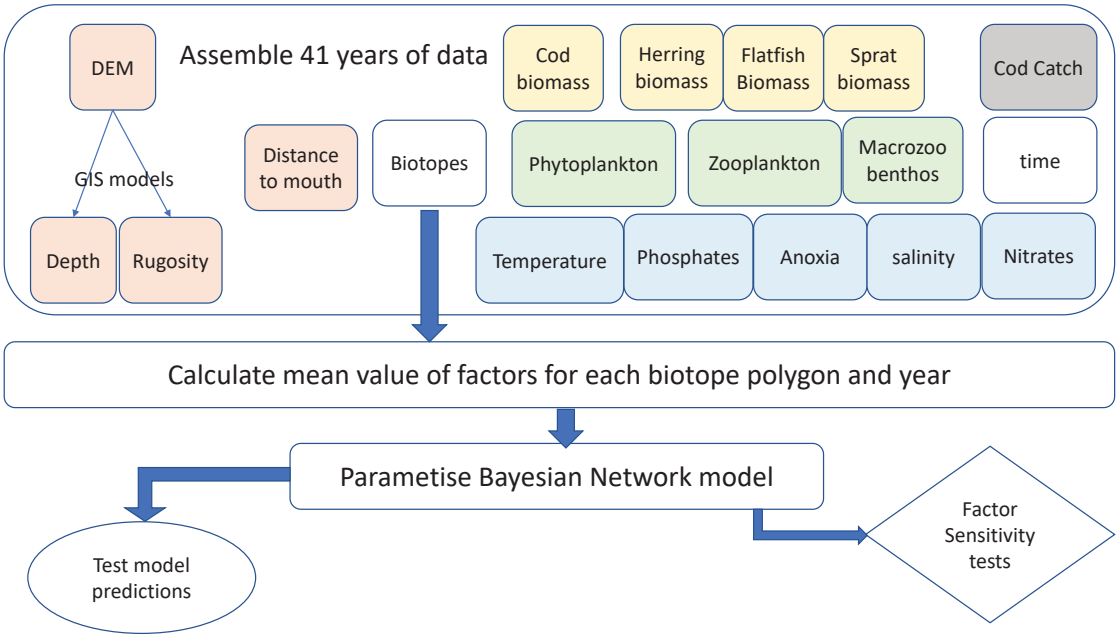

Figure 2. Flow model of Bayesian network development. The spatial data (rounded boxes) were first checked for quality across 41 years. The data were then aggregated based on the biotope polygons for every year. The BN was then parameterized from this large dataset. The model was subsequently used to make predictions with comparison to the actual observations (oval shape). The factors that make up the model were assessed in terms of sensitivity in order to understand the model influences (diamond shape).

2.3. Development and Application of the BN Model

The development and application of the BN model consists of six phases:

- Causal diagram design resulting in the network structure;
- Variables present in the model;
- Parametrization of the BN from observational data;
- Model testing;
- Scale and non-stationary nature of the BN cod biomass;
- Prediction of cod biomass for biotope for each time period.

2.4. Causal Diagram Design and Bayesian Network Construction

The first step was to construct a diagram of the key environmental correlates and other variables that influenced the species of interest. In this regard, we used expert opinion from the authors and INSPIRE (https://www.bonus-inspire.org/ accessed on 10 January 2022) project partners combined with influences from the literature. The guiding principles regarding which variables to include were the relevance to the ecological dynamics, the state of the data quality, the spatial coverage, and the temporal integrity over the period 1974 to 2014. The causal diagram was assembled with 24 variables and 55 linkages, with an essentially bottom-up perspective on cod biomass (Figure 3). The casual diagram has five major components reflecting the key influences on cod biomass. The structural nodes (grey nodes in Figure 3) do not alter over time, but provide a foundation for the benthic and environmental interactions. The environmental nodes (blue nodes in Figure 3) critically influence the lower trophic components. The plankton nodes capture a selected set of phytoplankton and zooplankton that are influenced by the environmental conditions [33].

The macrozoobenthos node was a combined selection of smaller benthic organisms that are likely to be eaten by cod; this selection was based on the analysis of cod stomach data [34]. The final group was the fish biomass in both the benthic and pelagic zones for cod, sprat, herring, and flatfish (primarily flounder and plaice). Included in the fish group were the cod catch estimates. Attempts were made to include additional variables at the "top end" of the trophic scale [35], including sea bird abundances, seal abundances, and fishing fleet sizes, but these variables had too many gaps across the time period. Linkages between the variables (nodes) are based on expected causal influences extracted from the literature. This diagram then becomes a causal network and the foundation for the expert opinion for the project. Finally, the causal network was developed into a BN by converting each node to a set of discrete states.

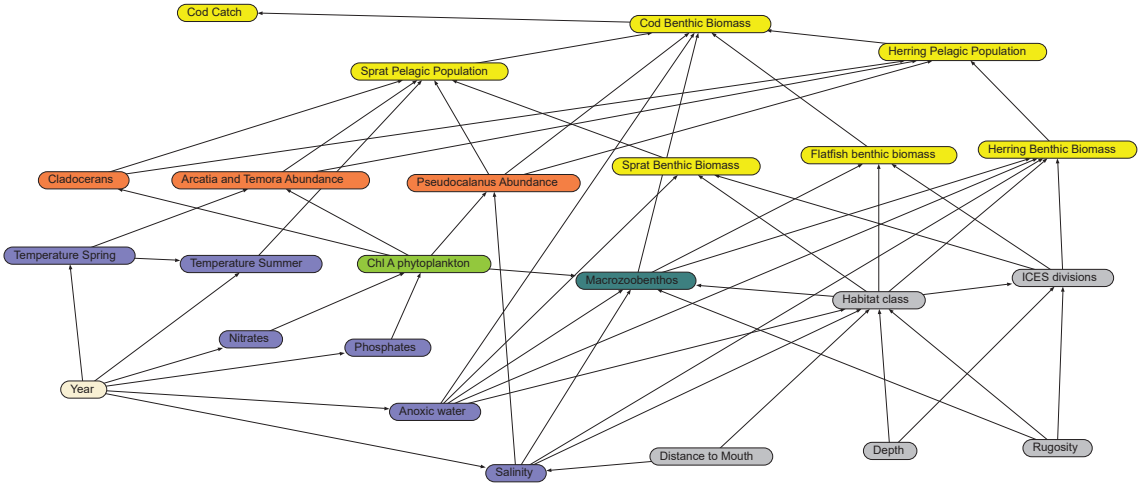

Figure 3. The completed BN with boxes and arrows showing the parameters and dependencies included. The box colors highlight the structural (grey), environmental (purple), phytoplankton (light green), zooplankton (orange), macrozoobenthos (brown), fish (yellow), and time (beige) components. Each arrow represents a modelled conditional probability element. The data that underpin each node in the BN are described above.

2.5. Variables Present in the Model

The following is a description of the variables or nodes (bold text with shorthand denotations used in figures) present in the model. Cod catch (CC) shows the commercial catch by ICES subdivision 1974 to 2013 [36,37], with equal-frequency bins based on abundance in millions. Cod benthic biomass (CB) was based on scientific bottom trawl data from 1974 to 2014 [38], with equal-frequency bins, and based on biomass calculated from length and abundance data N*W = a*L^b, where a = 0.0079 and b = 3.05. Herring pelagic biomass (HA) was based on acoustic surveys verified by catch data and extrapolated to the ICES rectangles between 1984 and 2014 [36,37], as well as older data [39]; the bins were equal frequency, and the biomass was calculated from length and abundance data N*W = a*L^b, where a = 0.0069 and b = 3.04. Sprat pelagic biomass (SpA) was based on acoustic surveys verified by catch data and extrapolated to the ICES rectangles from 1984 to 2014 [36,37], as well as older data [39]; the bins were equal frequency, and the biomass was calculated from length and abundance data N*W = a*L^b, where a = 0.0055 and b = 3.06. Herring benthic biomass (HB) was based on bottom trawl data from 1974 to 2014 [38]; the bins were equal frequency, and the biomass was calculated from length and abundance data N*W = a*L^b, where a = 0.0069 and b = 3.04. Flatfish benthic biomass (FF) was based on bottom trawl data combined for flounder and plaice from 1974 to 2014 [38]; the bins were equal frequency, and the biomass was calculated from length and abundance data N*W = a*L^b, where a = 0.0093

and b = 3.05 (flounder) and a = 0.0093 and b = 3.03 (plaice). Sprat benthic biomass (SpB) was based on bottom trawl data from 1974 to 2014 [38], with equal-frequency bins, and biomass calculated from length and abundance data N*W = a*L^b, where a = 0.0055 and b = 3.06. Cladocerans abundance (CL), Acartia and Temora abundance (AT), and Pseudocalanus abundance (psu) were based on multi-depth tow samples of plankton collected by the Finnish Institute of Marine Research (1979–2008) and the Finnish Environment Institute Marine Research Centre (2009+) from 1979 to 2013; these data were retrieved from the Global Plankton Database, NOAA [40], with the assistance of Maiju Lehtiniemi, the manager of the collection; the bins were equal frequency, and showed the abundance per volume. Macrozoobenthos (BG) was based on benthic grab data and filtered for species relevant to cod consumption from 1974 to 2007 by MarBEF [41]; the bins were equal frequency for the abundance data. Chl A phytoplankton (CHL) was based on in situ samples from 1974 to 2009 and stored in the Baltic Nest data [42,43]; the bins were split into the following groups: 0 to 1, 1 to 2, and 2 to 9.5, in units of chlorophyll (μg/L). Spring temperature (TSp) was based on in situ samples averaged for the depths 0 to 40 m for the months March, April, and May from 1974 to 2009 and stored in the Baltic Nest data [42,43]; the bins were equal frequency, in units of degrees Celsius. Similarly, the summer temperature (TSu) was based on in situ samples averaged for the depths 0 to 20 m for the months June, July, and August from 1974 to 2009, and also stored in the Baltic Nest data [42,43], with equal-frequency bins and in units of degrees Celsius. Nitrates (no3) were based on in situ samples collected in January and February from 1974 to 2009 and stored in the Baltic Nest data [42,43]; the bins were split as follows: 0 to 2, 2 to 5, and 5 to 22, in units of μmol/L. Phosphates (po4) were based on in situ samples collected in January and February from 1974 to 2009 and stored in the Baltic Nest data [42,43]; the bins were split as follows: 0 to 1, 1 to 1.5, and 1.5 to 4, in units of μmol/L. Salinity (sal) was based on in situ samples restricted to 10–50 m from 1974 to 2009 and stored in the Baltic Nest data [42,43]; the bins were split as follows: 0 to 7.5 and 7.5 to 34, in units of psu, as described in [44]. Anoxic water (anox) was based on in situ samples restricted to 20 m from the sea floor from 1974 to 2009 and stored in the Baltic Nest data [42,43]; the bins were split as follows: −2 to 6 and 6 to 11, in units of total oxygen mL/L. Habitat class (Hab) was derived from modelled habit based on bathymetry, halocline, substrate, and energy from the EUSeaMap project [32]; the bins were based on grouped classes: shallow muds, shallow sands, shallow coarse or mixed sediments, shallow photic rock or biogenic reef, shallow aphotic rock or biogenic reef, shelf muds, shelf coarse or mixed sediments, shelf rock or biogenic reef, and shelf sands. Distance to mouth (dis) was based on the modelled travel cost from the surface to a point located at 58.0666 N and 9.2666 E (the mouth of the Baltic Sea); the bins were equal frequency, in units of meters from the mouth along a direct path. Depth (Depth) was based on a bathymetry model stored in the Baltic Nest data [42,43], with bins of equal frequency and in units of meters. Rugosity (rug) was based on a neighborhood measure calculated from minimum depth per depth range for 3 × 3 neighborhood pixels; the bins were equal frequency, with units of rugosity measured from 0.24 (low) to 0.74 (high). ICES (International Council for the Exploration of the Sea) divisions (div) are the polygon rectangles based on the published ICES divisions and stored in the ICES data portal [42,43]; the bins were grouped by 2 ICES IDs to reduce bin numbers, and included divisions 22 to 32. Year (Yr) was a time counter of the data collection grouped into 4 periods from 1974 to 2014; the periods include the calendar years 1974–1986, 1986–1993, 1993–2004, and 2004–2014. Each biotope has a unique identification number (ID), but this was not used with the model directly.

As recommended by Marcot et al. [14], the number of bins was minimized for enhanced performance and tractability of the underlying conditional probability tables (CPTs). For nodes where a known threshold exists, such as for salinity (7 psu threshold [33]), the bin classes are adjusted accordingly. The years were grouped to capture the major changes in cod biomass in 4 periods (1974–1986, 1986–1993, 1993–2004, and 2004–2014). Habitat class was maintained as a discrete variable describing 9 grouped habitat types. The 11 ICES subdivisions were numbered sequentially from south to north, and were grouped into

7 continuous classes. Bottom oxygen concentration, salinity, and chlorophyll a were allocated bins based on published thresholds [36]. All other variables were binned to represent equal frequency from the observation files (In the Supplementary Figure S1).

2.6. BN Parametrization from Observational Data

The observational data for the Baltic Sea were assembled from a variety of sources. The primary directive was to obtain a spatial location (point or polygon) of a field-based observation. This included benthic grabs and plankton sampling as well as fish population estimates from acoustic surveys and bottom trawl surveys. Additionally, structural aspects (depth and rugosity) were modelled from a digital elevation model. Extrapolation of the data to extend the coverage was specifically avoided in order to reduce the compound effect of multiple model assemblage. A notable exception was the cod catch estimates that were only available at an ICES subdivision polygon scale. The data were then aggregated at a biotope polygon scale and for each year using the mean of the values within the biotope boundaries.

The BN was developed in the modeling shell Netica (version 6.05, Norsys Systems Corp., Vancouver, BC, Canada). The BN before parametrization was considered naïve, since the conditional probability tables (CPTs) will reflect equal distributions for each bin in every node. In order to update the probabilities in the CPTs, we used the expectation maximization learning algorithm [37] within Netica; this approach updates the CPTs automatically as the observational data are considered case by case. Each case here was essentially a row in a table that identifies the habitat polygon, the year, and any relevant information known about the 23 environmental variables in the model. The complete case file (with missing data included) was 1,177,192 rows with 26 columns depicting every habitat polygon and year combination possible. However given that observational data were commonly represented as spatial points, and we were reluctant to extrapolate this spatially limited set across the Baltic Sea environment using some statistical interpolation technique, there were consequently many cases of missing data (~60%)—especially for small habitat polygons. Figure 4 highlights the pattern of the missing data, reflecting the difficulty in obtaining samples for many of these variables. The 397 observations of the cladocerans were an example of scarce data, as shown by Figure 5, whilst noting that only 42 out of 28,712 biotope polygons were sampled across those years. Within the BN, each observation or case was as directly linked to the biotope polygon as possible without the confounding effects of geospatial extrapolations. Biotopes with insufficient data, as defined by 60% missing, were considered to be outside the scope of this model.

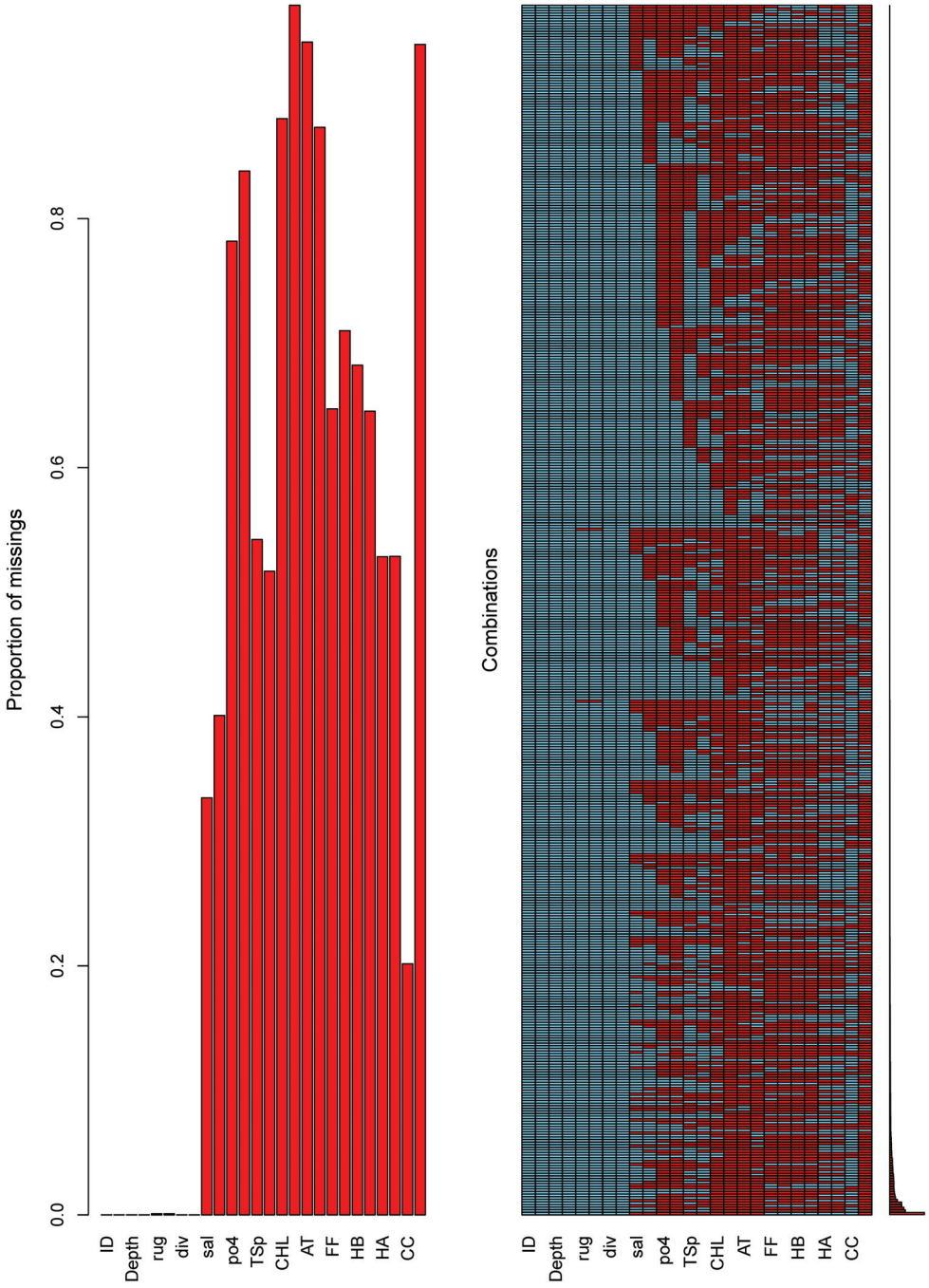

Figure 4. The graph of the missing data using the *aggr* function in the VIM R package [38]. The data were a reduced set based on including only cases with at least 14 observations out of a possible 26. The shortened variable names are linked in the data description above.

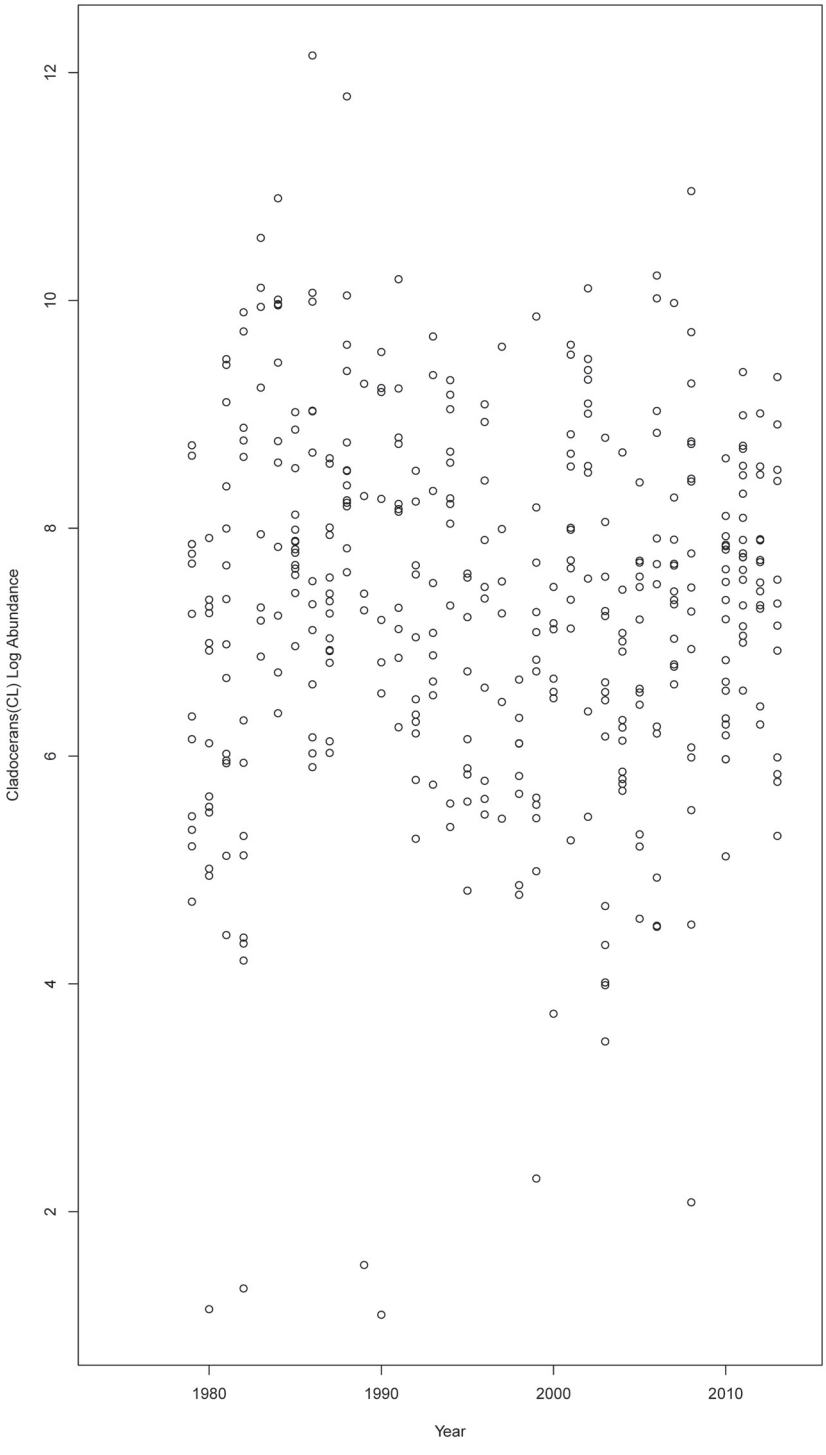

Figure 5. Graph of the cladoceran observations across the years.

In order to evaluate the model performance using validation, the BN was updated from a naïve state with a random subset of the case file (across all years) containing 70% (81,657) of the cases. The prediction accuracy of the model for the cod biomass node was then tested with the remainder 30% (34,995) of the cases. For every one of the 34,995 cases, the model predicted the likelihood of the cod biomass in each bin, and then compared the prediction directly to the observed value, where it existed for that case within a confusion matrix. An error rate was calculated, meaning that for a percentage of the cases for which the case file supplied a cod biomass value, the network predicted the wrong value. Various other statistical approaches—such as logarithmic loss, quadratic loss, spherical payoff, and area under the receiver operating characteristic (ROC) curve—were calculated [14,39]. Logarithmic loss values (Equation (1) [40]) were calculated using the natural log, and were constrained to 0 and infinity, with 0 indicating the best performance. Quadratic loss (Equation (2) [40]) was restricted between 0 and 2, with 0 being the best, while spherical payoff (Equation (3) [40]) was limited between 0 and 1, with 1 being the best. These measures are defined as follows:

$$\text{Logarithmic loss} = \text{MOAC}\left(-\log\left(\mathrm{P_c}\right)\right) \tag{1}$$

$$\text{Quadratic loss} = \text{MOAC}\left(1 - 2\mathrm{P_c} + \sum_{i=1}^{n} p_i^2\right), \tag{2}$$

$$\text{Spherical payoff} = \text{MOAC}\left(\frac{\mathrm{P_c}}{\sqrt{\sum_{i=1}^{n} p_i^2}}\right) \tag{3}$$

where $\mathrm{P_c}$ is the probability predicted for the correct state, p_i is the probability predicted for state i, n is the number of states, and MOAC stands for the mean over all cases [40]. Finally receiver operating characteristic (ROC) curves for ICES only, ICES with habitat classes, and ICES with biotopes were generated based on the classification success of the model where the percentage of true positive classification (sensitivity) was greater than the false positives (1 sensitivity) [14,39]. Each point on an ROC curve represents a sensitivity/specificity pair. A model with perfect discrimination between predicted classes has an ROC curve that passes through the upper left corner (100% sensitivity, 100% specificity). Hence, the greater the area under the curve (towards the upper left) relative to the diagonal, the higher the accuracy of the model. Similarly, if the curve goes below the diagonal, the predictions of the model are considered poor discrimination of the classes. The final model was updated with 100% of the cases in order to utilize the full information suite contained in the observational data.

To examine the predictive capacity of the model, we compared three data profiles:

1. Data averaged for each biotope polygon for each year (30% random subset);
2. Data averaged for each ICES polygon for each year;
3. Data averaged for each habitat class in each ICES polygon for each year.

This provides a way to compare the scale of the data and test the model accuracy. To complete this task the BN model was used to predict the cod biomass based on values where they existed. The cod biomass predictions were compared to the observed values, and the ROC curves were compared.

2.7. Scale and Non-Stationary Nature of the BN Cod Biomass

To address the questions about an effective scale for estimating cod biomass and the value of a non-stationary approach, we focused on the relative influence of each factor in the BN on the cod biomass. The magnitude of changes in cod biomass based on changes in the influencing factors as compared when the spatial unit selected was at the course ICES subdivision scale versus the biotope classification within ICES subdivisions. The changes were measured using a variance reduction technique from the Netica toolbox that produces a table with the magnitude of contribution for each node in the BN [39]. To examine the scale effect, we specified the probability distribution of observing a particular

ICES subdivision (i.e., number 28) to be 100% likely, and this then recalculated the marginal probabilities for the remaining BN. The variance reduction calculation was based on this limited probability set and, thus, we were able to estimate the factors that influence the probability distribution given changes in spatial scale (noting that the influences of shape are ignored). Modelling time series based on a stationary stochastic process relies on two assumptions: the independence and identical distribution of the mean and variance of key parameters [41]. If the ecosystem characteristics have changed over time, these assumptions will be violated. In the non-stationary framework, the statistical properties of distributions are specified as a function of different predictors. To examine the effectiveness of adopting a non-stationary approach, we selected two ICES subdivisions and examined the impact of habitat information on the relative influence of significant parameters across the time series. The temporal changes for ICES subdivisions 25 and 28. with and without biotope information, were examined. The nodes with more than 1% influence were recorded. Ideally, the model network topology would also change reflecting the alterations in parameter dependencies, but this would require a machine learning approach to the model's development.

2.8. Prediction of Cod Biomass per Biotope for Each Time Period

Using the BN model, we predicted the cod and sprat biomass for each period (1974–1986, 1986–1993, 1993–2004, and 2004–2014) and for each biotope polygon based on observed environmental and trophic data, where they existed. The BN model then output an estimate of the probability that a particular cod biomass would be observed for each biotope and for each time period, and this was mapped. This spatially explicit prediction of the cod biomass based on abiotic and biotic factors was a key output of the BN, but other products—such as scenario exploration—are possible.

3. Results

3.1. Model Testing

The isolated 30% case set used to test the model's capacity to predict Baltic cod biomass showed an overall score of 32.5% error rate for the entire temporal period based on the confusion matrix; it also showed a logarithmic loss value of 0.66, a quadratic loss value of 0.44, and a spherical payoff of 0.75, demonstrating a robust model—especially given the data scarcity. The ROC (Figure 6) shows a high classification success (area under the ROC = 0.7572) of the model. Overall, the model appears robust, with a high degree of prediction capacity—especially when biotope data were included.

3.2. Predictive Changes with Scale

The predictive power of the model altered significantly when habitat information was included, and even more when the unit of analysis was the biotope. The ROC provides a comparison of the prediction of true positives verses false positives for cod biomass (Figure 6). The first dataset, consisting of aggregated ICES subdivisions as the only information (861 cases, 41 years by 21 ICES subdivisions), had a poor predictive capacity (error rate of 64.2%), with an ROC of 0.5015 and the ROC curve dropping below the line of equal distribution separation. This dataset did not contain any benthic biotope information, but did include all the rest where it existed. The next dataset was the 41 years of Baltic data aggregated for the ICES subdivisions partitioned with the biotope classes (5617 cases). This data structure showed an overall error rate of 55.5% and an ROC of 0.6449. As shown in Figure 6, the predictions of the true positives were better than those of the false positives. The final dataset was the aggregated observed data (30% isolated random subset) for each biotope for each year. For this data structure, the error rate was 32.5%, while the ROC was 0.7575. The substantial increase in predictive power was evident across all years when the biotopic data were used to structure the data. In many cases the biotopes crossed the ICES boundaries and had a unique shape.

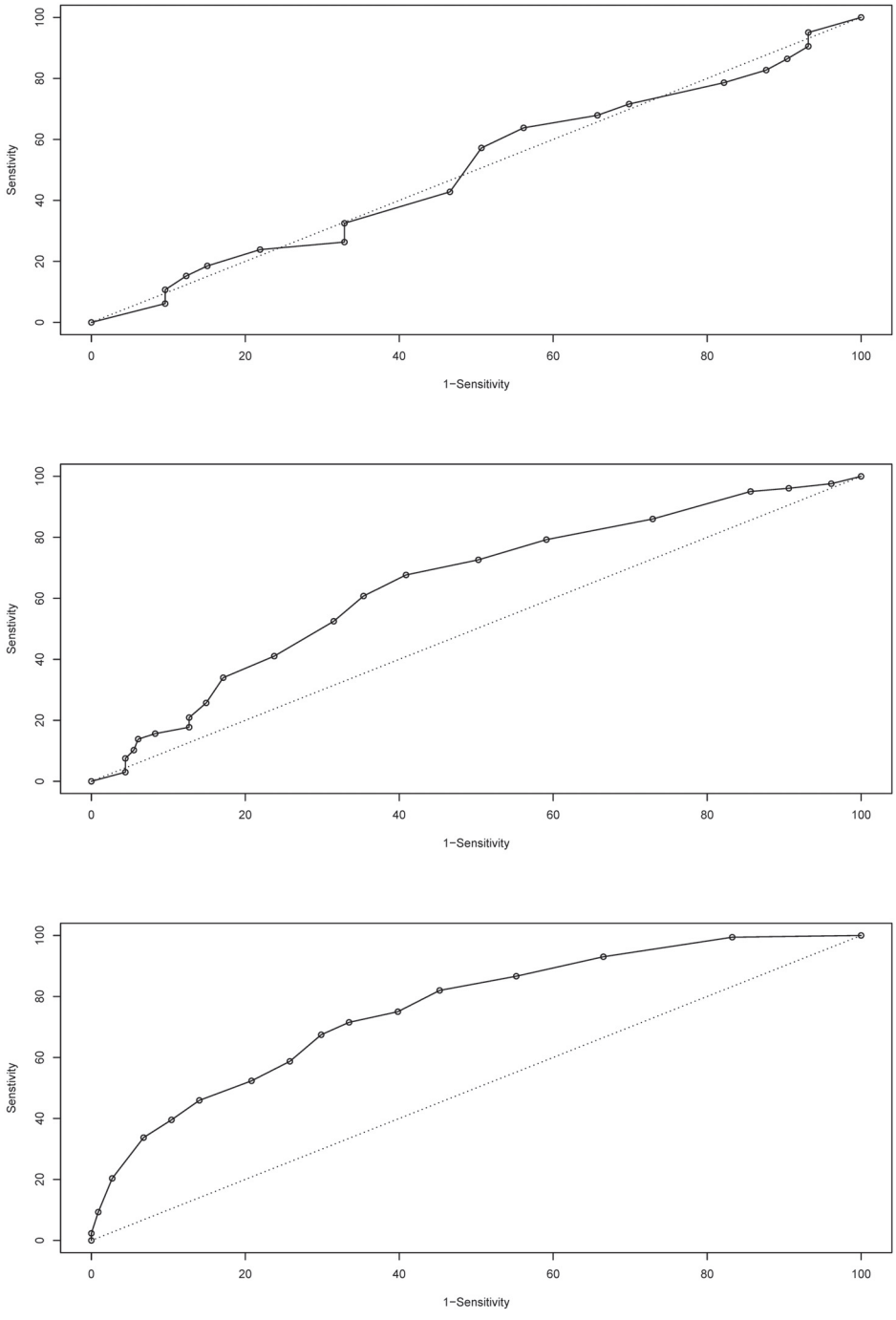

Figure 6. Receiver operating characteristic (ROC) curves for ICES only (**top**), ICES with habitat classes (**middle**) and ICES with biotopes (**bottom**) [14,39].

3.3. Non-Stationary Modelling Based on Selected ICES and Biotope Polygons

To highlight the non-stationary nature of the relationships in the BN model, we closely examined two ICES subdivision polygons (25 and 28, Figure 7) across the time series. The sensitivity of the factors to cod biomass was partitioned into four time periods (Figure 8), and the ICES subdivision 25 with biotope information included (Figure 8, top left) shows an increase in the influence of the factors, particularly with cod biomass. In the last time period—i.e., 2004 to 2014—the sensitivity of the factors decreased. When habitat information was not used to inform the network (Figure 8, top right), there was a steady reduction in sensitivity, with the salinity factor reducing the most. The ICES subdivision 28 showed a constant reduction when no biotope information was included (Figure 8, bottom left); however, the sensitivity of cod catch remained constant across these time periods. When habitat information was included (Figure 8, bottom right), the factor sensitivity magnitude remained constant until the last time period, when macrozoobenthos, flatfish [42], and rugosity emerged as informative (which was likely to be directly related to oxygen stratification [26,43]). Note that the biotope information did not alter during the time series, but the character of the biotope changed as the various environmental factors altered the biotic interactions. This highlights the importance of the model in adjusting the impact of the dependent factors as the other factors change over time.

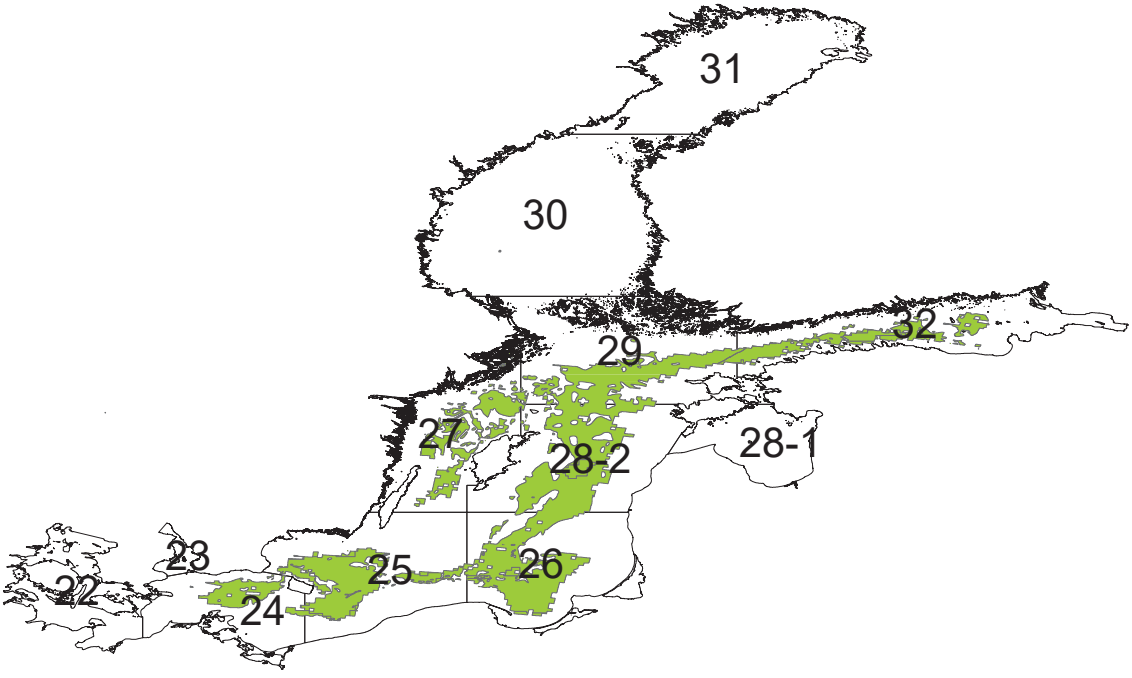

Figure 7. Spatial map of ICES subdivisions with biotopes that have the shelf mud grouped class type.

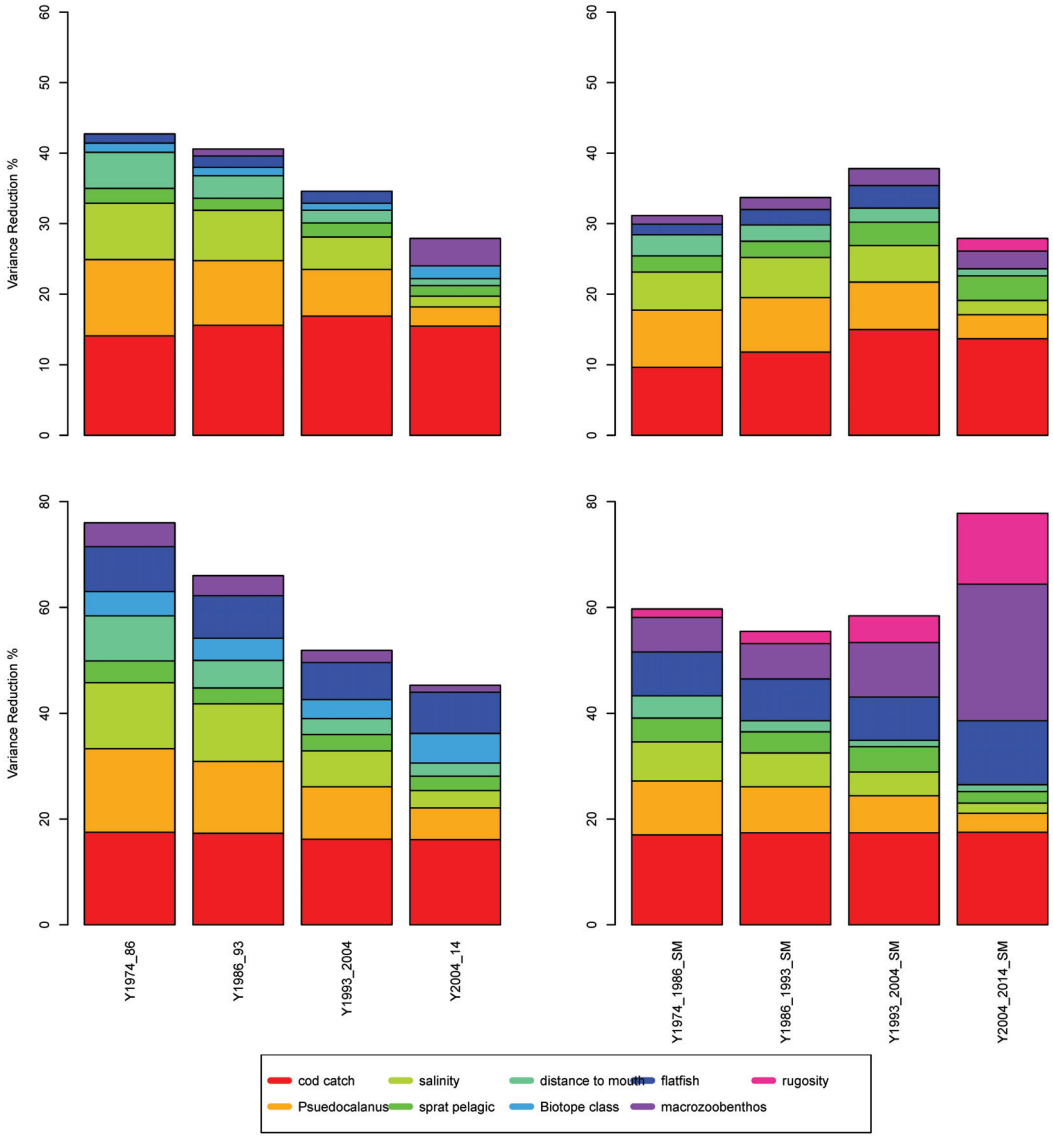

Figure 8. The magnitude of the dominant influential factors for time periods 1974, 1986, 1993, 2004, and 2014 for ICES 25 (**top**) and 28 (**bottom**) without biotope information (**left**) and with biotope information (**right**).

Predictions of the cod spatial distributions can be contrasted with the sprat biomass predictions, as shown in Figure 9. Biotopes with more than 61.5% null data values were excluded from predictions in order to reduce uncertainty. The map composite highlights the changes in the spatial usage of the central and coastal Baltic Sea regions by cod and sprat. In particular, the dominance of the central Baltic region by cod was replaced by sprat dominance in the 1993 to 2004 period. However, in the decade 2004 to 2014, the central region exhibited high uncertainty in the fish population dynamics—especially compared to the western areas.

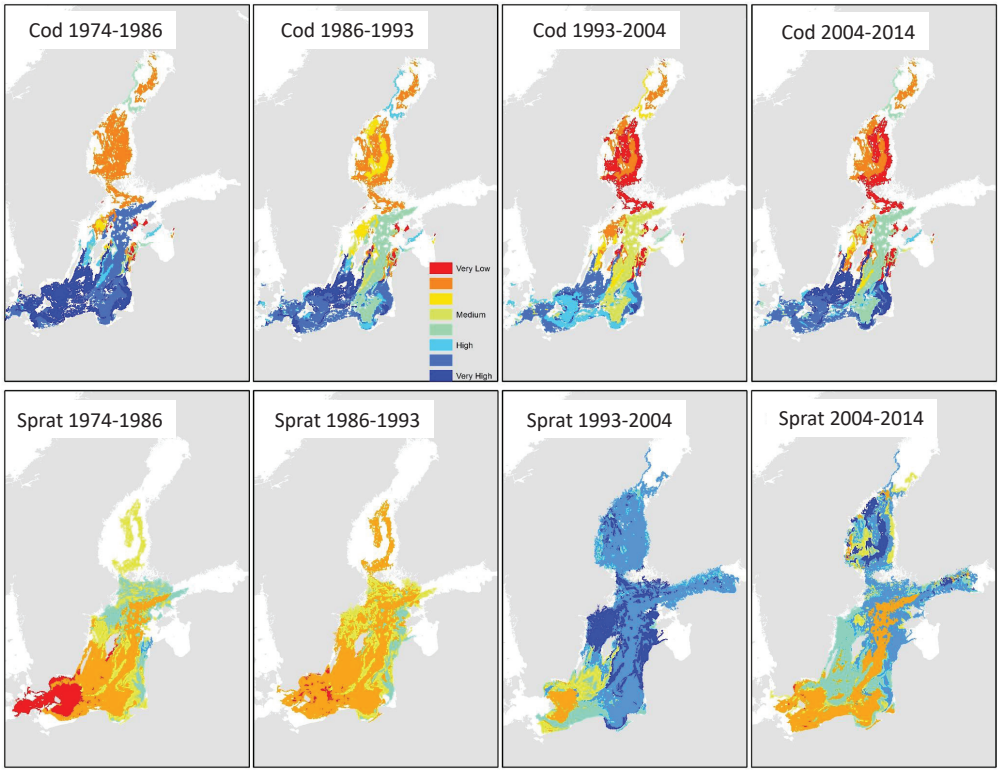

Figure 9. Predictions of high cod and sprat biomass in 4 periods. White areas represent biotopes where the level of information for that year group was below the threshold of missing data; consequently, these were excluded from the predictions.

4. Discussion

This use of 41 years of environmental and biotic data within a Bayesian network demonstrates that biotopic information increases predictive capacity for this enclosed region. Understanding the benthic character and incorporating this information into a BN model shows that biotopic conditions are important to developing a spatially explicit and temporally bound model of cod dynamics in the Baltic Sea. Removing this biotopic information or aggregating the model spatial resolution in order to ignore the biotopic boundaries degraded the predictive capacity of the model. In particular, the model was able to accurately predict (within the periods observed) cod biomass across the region, although the predictions for the biotope polygons with insufficient data were discarded. The BN model was not suitable to predict into the future, given the uncertainty of the underlying abiotic and biotic factors, but various future scenarios can be rapidly explored.

Using a variance reduction method to evaluate the contribution of the model factors to the prediction of cod biomass highlighted that trophic, environmental, and biotopic feedbacks—and thus, cod biomasses—were non-stationary. Factors such as macrozoobenthos, flatfish, and rugosity only became influential in the later years of the data, and when environmental factors were different. In contrast, the cod catch factor remained stable in terms of influence, highlighting the fact that while fish catch data were a contributing factor in cod biomass predictions, the model was stationary for this factor. This was despite the substantial decrease in cod catches across this period. A non-stationary approach to a time series is not about the overall changes in a given factor but, rather, the capacity of the time-series model to include the changes in dependencies. Our BN model structure

(i.e., the linkages between nodes), however, remained stationary, and there is potential to facilitate the change in network structure as a function of non-stationary changes in correlations observed.

While our model addresses 41 years of observations, it is possible to predict outside this time period (with the addition of extra observational data), and this places extra emphasis on the importance of the non-stationary capacity of the model. Particularly as climate change alters the relationships commonly observed, the inclusion of dynamics in parameter coefficients is required in order to better capture possible future trajectories. However, in agreement with this BN model's predictions, the recent 2021 ICES advice on fishing opportunities for cod states that catch should be zero in 2022 in order to protect the stock [44,45]. The ICES reports [44,45] continue to note that "The poor status of the eastern Baltic cod is largely driven by biological changes in the stock during the last decades. Growth, condition (weight-at-length), and size-at-maturation have substantially declined. These developments indicate that the stock is distressed and is expected to have reduced reproductive potential"; also important for fisheries management is the statement [44,45] that "Natural mortality has increased and is estimated to be considerably higher than the fishing mortality in recent years".

The model's scale was based on the published biotope polygons, and these appear to be a sensible compromise between model size and accuracy. Smaller homogeneous regions could be defined, but the boundary accuracy would demand increased spatial mapping. Models based on a regular raster grid containing fixed cell sizes are restricted in the independence of their observations; either the number of observations is increased (by increasing cell size), or the observations are extrapolated across cells using a selected technique. In either case, the justification for extending the likelihood of occurrence data is problematic, and is isolated from the environmental and ecological associations. Biotopes offer a solution that links ecological processes to benthic structure and, hence, provides a justifiable case for assuming that the observations could have occurred equally within the biotope polygon.

The BN model presented here (Figures 3 and S1) represents one class of model that was employed to understand and predict changes in the biomass of fished species; it is a statistical model, trained on data, and there are numerous examples of different types of statistical models used for similar purposes. For example, to answer similar questions, we could have employed a random forests approach [46]. The strength of the BN approach is that it includes explicit description of the interaction of dependent factors [47]; this was relevant in our study to evaluate the importance of biotopic information that directly affected cod biomass in the Baltic BN. In contrast, the other classes of fisheries/ecosystem models are those that are based on dynamical system representations of food-web interactions and abiotic factors. These models are also well known for their applications in the Baltic Sea, and include large-scale end-to-end models intended to capture the whole-ecosystem dynamics [48,49], models of intermediate complexity that capture the dynamics and strong trophic interactions of only a small subset of species with high detail [50–52], and more simple models based on ecological theory such as the size spectra of ecosystems [53–56]. The important difference between these models and the BN is that the dynamical models often have nonlinear interaction terms. Furthermore, unlike BNs, dynamical models typically do not implicitly account for parameter uncertainty (although parameter sensitivity simulation tests are standard). BNs with discrete bins have linear interaction terms, and it would be interesting to conduct future work to explore whether the nonlinear aspects of dynamical systems models and the parameter uncertainty aspect of BNs could be employed simultaneously.

The selection of the ICES subdivisions for comparison aligned the model evaluation with current fisheries management [44,57]. For instance, in the case of eastern Baltic cod, the management area spans from SD25 to SD29, while for sprat it is even larger, spanning from SD22 to SD32 (Figure 7). These regions are managed based on the advice of scientists, but here we demonstrate that increasing the resolution from subdivisions to biotope polygons

significantly increases the predictive capacity. This was especially important when the uncertainty of the observations was high, or when the number of missing data was great. The conclusion in this regard is that the evaluation of stock dynamics and status should reconcile with the spatial scale of the dominant ecological processes, as suggested by the arrangement based on benthic classification.

Fisheries decisions that are based on environmental flows, fish catch statistics, or simple trophic indicators are limited in their management confidence [47]. Including a range of parameters that can characterize the linkage of fish dynamics as a function of overall system characteristics is more likely to generate meaningful advice on fish catch quotas and restrictions. The BN model shown here was able to integrate a wide array of observations while also using the marginal probabilities to assist with predictions, despite missing data.

The BN model does contain a number of assumptions and limitations. The primary limitation is that the BN configuration is assumed to represent the system without being overly complicated. While BNs are generally robust to variations in network structure, the influence on the conditional probabilities is significant, and cannot be ignored. The BN is also based on the observations that occur within the boundaries of the biotopic polygons, and this implies a direct linkage to ecological processes at this scale, as well as a homogeneous character. In some cases, the processes linking one factor to other factors (i.e., pelagic cod partially feeding on macrozoobenthos, which was not included in our model) may not be tightly constrained to benthic structures. An additional limitation is that the model does not include parameters that have inadequate data but may be influential. For example, the role of expanding seal populations or the influence of seabird colonies was recognized [45], but was not incorporated, due to limited data. One limitation of BNs is their incapacity to incorporate feedback loops, such as the population information from previous years [58]. Dynamic BNs can link factors across time periods, but this is only feasible for simple BNs with large numbers of observations. The model presented here was able to make predictions (within the periods specified) without the knowledge of past observations and, despite this limitation, the implicit incorporation of past trends was expected to increase the accuracy of the model.

The BN model's complexity and resolution were a compromise between data availability and expert opinion on the ecological processes in the Baltic Sea. Some of the nodes—such as flatfish and phytoplankton—were aggregates of the biota in the respective classes, while other classes—such as sprat and herring—were split into benthic and pelagic components. Similarly, the inclusion of some factors while excluding others—particularly environmental categories—remains in the realm of expert opinion. Additionally, the BN's behavior was improved by adhering to rules of simplicity for bin number and linkage density [14,15]. Future improvements in exploring the model complexity are likely to be fruitful for fisheries management [47].

The approach taken here to evaluate a BN model of the Baltic Sea fisheries demonstrates a clear need to include the benthic influences, and to do so within a modelling framework that is non-stationary and spatially relevant to the ecological process(es) determining the key variables. The understandable nature of the model flow combined with a robust capacity to deal with missing or inaccurate data is attractive for the managers of fisheries in coastal or enclosed waters.

5. Conclusions

Fisheries science has struggled to accurately inform the management of coastal fisheries. We suggest that this is due to the absence of two key factors: benthic coupling, and non-stationary modelling. The role of the benthic environment as expressed by biotope models provides a linkage to the structural components of the marine interaction. The model presented here using a Bayesian network approach was able to integrate the structural, environmental, and biotic components of the system. Critically, the use of biotope information in the form of polygons of variable shape and size, rather than repeated rectan-

gles, increased the ecological linkages within the model, resulting in enhanced predictive capacity. Coastal systems have commonly undergone change during the short and long term; consequently, the nature of variable interactions needed to be dynamic. The BN model can adjust the relationships across the modelled periods and, hence, enable the inclusion of variables that are important only in certain situations. In this regard, we observed the increased influence of the macrozoobenthos, flatfish biomass, and rugosity towards the later period of the 41-year data observation period. Our results strongly suggest that fisheries management that is able to encompass a spatially relevant suite of abiotic and biotic factors is likely to improve sustainable fisheries programs.

Supplementary Materials: The following supporting information can be downloaded at https://www.mdpi.com/article/10.3390/d14020090/s1, Figure S1. The completed BN with colors highlighting the structural (grey), environmental (purple), phytoplankton (light green), zooplankton (orange), macrozoobenthos (brown), fish (yellow), and time (beige) components. Each node (box) shows the discrete bins and marginal probabilities (as numbers and a bar graphic). Each arrow represents a modelled conditional probability element.

Author Contributions: Conceptualization, S.K. and T.B.; methodology, S.K. and T.B.; software, S.K.; validation, S.K., S.N. (Susa Niiranen), J.W. and T.B.; formal analysis, S.K.; investigation, S.K., S.N. (Susa Niiranen) and T.B.; resources, A.O., M.C., S.N. (Stefan Neuenfeldt), V.B. and M.H.; data curation, S.K.; writing—original draft preparation, S.K.; writing—review and editing, S.K., T.B. and S.N. (Susa Niiranen); visualization, S.K.; supervision, T.B.; project administration, T.B.; funding acquisition, T.B. All authors have read and agreed to the published version of the manuscript.

Funding: This work resulted from the Joint Baltic Sea Research and Development Programme (BONUS) project "Integrating spatial processes into ecosystem models for sustainable utilisation of fish resources" (INSPIRE), which were supported by BONUS (Art 185), funded jointly by the European Union, Innovation Fund Denmark, Swedish Research Council Formas, and the Latvian Academy of Science (grant/award number: 2012-60).

Institutional Review Board Statement: Not applicable.

Informed Consent Statement: Not applicable.

Data Availability Statement: The Baltic Environment Database contains the data from this research: http://nest.su.se/bed/. Accessed on 1 July 2015.

Acknowledgments: This work was initiated within the Study Group on Spatial Analysis for the Baltic Sea (SGSPATIAL), 4–6 November 2014, Gothenburg, Sweden.

Conflicts of Interest: The authors declare no conflict of interest.

References

1. Van Hoof, L. Fisheries management, the ecosystem approach, regionalisation and the elephants in the room. *Mar. Policy* **2015**, *60*, 20–26. [CrossRef]
2. Levontin, P.; Kulmala, S.; Haapasaari, P.; Kuikka, S. Integration of biological, economic, and sociological knowledge by Bayesian belief networks: The interdisciplinary evaluation of potential management plans for Baltic salmon. *ICES J. Mar. Sci.* **2011**, *68*, 632–638. [CrossRef]
3. Harvey, C.; Cox, S. An ecosystem model of food web and fisheries interactions in the Baltic Sea. *J. Mar. Sci.* **2003**, *3139*, 939–950. [CrossRef]
4. Bauer, B.; Gustafsson, B.G.; Hyytiäinen, K.; Meier, H.E.M.; Müller-Karulis, B.; Saraiva, S.; Tomczak, M.T. Food web and fisheries in the future Baltic Sea. *Ambio* **2019**, *48*, 1337–1349. [CrossRef]
5. Mahévas, S.; Pelletier, D. ISIS-Fish, a generic and spatially explicit simulation tool for evaluating the impact of management measures on fisheries dynamics. *Ecol. Modell.* **2004**, *171*, 65–84. [CrossRef]
6. Pelletier, D.; Mahevas, S. Spatially explicit fisheries simulation models for policy evaluation. *Fish Fish.* **2005**, *6*, 307–349. [CrossRef]
7. Collie, J.S.; Botsford, L.W.; Hastings, A.; Kaplan, I.C.; Largier, J.L.; Livingston, P.A.; Plagányi, É.; Rose, K.A.; Wells, B.K.; Werner, F.E. Ecosystem models for fisheries management: Finding the sweet spot. *Fish Fish.* **2016**, *17*, 101–125. [CrossRef]
8. Lees, K.; Pitois, S.; Scott, C.; Frid, C.; Mackinson, S. Characterizing regime shifts in the marine environment. *Fish Fish.* **2006**, *7*, 104–127. [CrossRef]
9. Hagerman, L.; Josefson, A.B.; Jensen, J.N. Benthic Macrofauna and Demersal Fish. *Eutrophication Coast. Mar. Ecosyst.* **2013**, *52*, 155–178. [CrossRef]

10. Snickars, M.; Gullström, M.; Sundblad, G.; Bergström, U.; Downie, A.-L.; Lindegarth, M.; Mattila, J. Species–environment relationships and potential for distribution modelling in coastal waters. *J. Sea Res.* **2014**, *85*, 116–125. [CrossRef]
11. Griffiths, J.R.; Kadin, M.; Nascimento, F.J.A. The importance of benthic—Pelagic coupling for marine ecosystem functioning in a changing world. *Glob. Chang. Biol.* **2017**, *23*, 2179–2196. [CrossRef] [PubMed]
12. Geritz, S.A.H.; Kisdi, E. On the mechanistic underpinning of discrete-time population models with complex dynamics. *J. Theor. Biol.* **2004**, *228*, 261–269. [CrossRef] [PubMed]
13. Gonzalez-Mirelis, G.; Buhl-Mortensen, P. Modelling benthic habitats and biotopes off the coast of Norway to support spatial management. *Ecol. Inform.* **2015**, *30*, 284–292. [CrossRef]
14. Marcot, B.G.; Steventon, J.D.; Sutherland, G.D.; McCann, R.K. Guidelines for developing and updating Bayesian belief networks applied to ecological modeling and conservation. *Can. J. For. Res.* **2006**, *36*, 3063–3074. [CrossRef]
15. McCann, R.K.; Marcot, B.G.; Ellis, R. Bayesian belief networks: Applications in ecology and natural resource management. *Can. J. For. Res.* **2006**, *36*, 3053–3062. [CrossRef]
16. Borsuk, M.E.; Reichert, P.; Peter, A.; Schager, E.; Burkhardt-Holm, P. Assessing the decline of brown trout (Salmo trutta) in Swiss rivers using a Bayesian probability network. *Ecol. Modell.* **2006**, *192*, 224–244. [CrossRef]
17. Johnson, S.; Mengersen, K. Integrated Bayesian Network Framework For Modeling Complex Ecological Issues. *Integr. Environ. Assess. Manag.* **2011**, *8*, 480–490. [CrossRef]
18. Eklöf, A.; Tang, S.; Allesina, S. Secondary extinctions in food webs: A Bayesian network approach. *Methods Ecol. Evol.* **2013**, *4*, 760–770. [CrossRef]
19. Bartolino, V.; Tian, H.; Bergström, U.; Jounela, P.; Aro, E.; Dieterich, C.; Markus Meier, H.E.; Cardinale, M.; Bland, B.; Casini, M. Spatio-temporal dynamics of a fish predator: Density-dependent and hydrographic effects on baltic sea cod population. *PLoS ONE* **2017**, *12*, 1–17. [CrossRef]
20. Otto, S.A.; Kornilovs, G.; Llope, M.; Möllmann, C. Interactions among density, climate, and food web effects determine long-term life cycle dynamics of a key copepod. *Mar. Ecol. Prog. Ser.* **2014**, *498*, 73–84. [CrossRef]
21. Orio, A.; Bergström, U.; Florin, A.B.; Lehmann, A.; Šics, I.; Casini, M. Spatial contraction of demersal fish populations in a large marine ecosystem. *J. Biogeogr.* **2019**, *46*, 633–645. [CrossRef]
22. Casini, M.; Hjelm, J.; Molinero, J.-C.; Lövgren, J.; Cardinale, M.; Bartolino, V.; Belgrano, A.; Kornilovs, G. Trophic cascades promote threshold-like shifts in pelagic marine ecosystems. *Proc. Natl. Acad. Sci. USA* **2009**, *106*, 197–202. [CrossRef]
23. Möllmann, C.; Diekmann, R.; Müller-Karulis, B.; Kornilovs, G.; Plikshs, M.; Axe, P. Reorganization of a large marine ecosystem due to atmospheric and anthropogenic pressure: A discontinuous regime shift in the Central Baltic Sea. *Glob. Chang. Biol.* **2009**, *15*, 1377–1393. [CrossRef]
24. Eero, M.; Hjelm, J.; Behrens, J.; Buchmann, K.; Cardinale, M.; Casini, M.; Gasyukov, P.; Holmgren, N.; Horbowy, J.; Hussy, K.; et al. Food for Thought Eastern Baltic cod in distress: Biological changes and challenges for stock assessment. *ICES J. Mar. Sci.* **2015**, *72*, 2180–2186. [CrossRef]
25. Kristensen, E.; Delefosse, M.; Quintana, C.O.; Flindt, M.R.; Valdemarsen, T. Influence of benthic macrofauna community shifts on ecosystem functioning in shallow estuaries. *Front. Mar. Sci.* **2014**, *1*, 1–14. [CrossRef]
26. Casini, M.; Hansson, M.; Orio, A.; Limburg, K. Changes in population depth distribution and oxygen stratification are involved in the current low condition of the eastern Baltic Sea cod (*Gadus morhua*). *Biogeosciences* **2021**, *18*, 1321–1331. [CrossRef]
27. Aarestrup, K.; Økland, F.; Hansen, M.M.; Righton, D.; Gargan, P.; Castonguay, M.; Bernatchez, L.; Howey, P.; Sparholt, H.; Pedersen, M.I.; et al. Oceanic spawning migration of the european eel (anguilla anguilla). *Science* **2009**, *325*, 1660. [CrossRef]
28. Casini, M.; Blenckner, T.; Möllmann, C.; Gårdmark, A.; Lindegren, M.; Llope, M.; Kornilovs, G.; Plikshs, M.; Stenseth, N.C. Predator transitory spillover induces trophic cascades in ecological sinks. *Proc. Natl. Acad. Sci. USA* **2012**, *109*, 8185–8189. [CrossRef]
29. Andersson, A.; Meier, H.E.M.; Ripszam, M.; Rowe, O.; Wikner, J.; Haglund, P.; Eilola, K.; Legrand, C.; Figueroa, D.; Paczkowska, J.; et al. Projected future climate change and Baltic Sea ecosystem management. *Ambio* **2015**, *44*, 345–356. [CrossRef]
30. Wikstrom, S.A.; Daunys, D.; Leinikki, J. *A Proposed Biotope Classification System for the Baltic Sea*; AquaBiota Water Research: Stockholm, Sweden, 2011.
31. Österblom, H.; Hansson, S.; Larsson, U.; Hjerne, O. Human-induced trophic cascades and ecological regime shifts in the Baltic Sea. *Ecosystems* **2007**, 877–889. [CrossRef]
32. Tomczak, M.T.; Heymans, J.J.; Yletyinen, J.; Niiranen, S.; Otto, S.A.; Blenckner, T. Ecological Network Indicators of Ecosystem Status and Change in the Baltic Sea. *PLoS ONE* **2013**, *8*, 1–11. [CrossRef] [PubMed]
33. Neuenfeldt, S.; Bartolino, V.; Orio, A.; Andersen, K.H.; Andersen, N.G.; Niiranen, S.; Bergström, U.; Ustups, D.; Kulatska, N.; Casini, M. Feeding and growth of Atlantic cod (*Gadus morhua* L.) in the eastern Baltic Sea under environmental change. *ICES J. Mar. Sci.* **2020**, *77*, 624–632. [CrossRef]
34. Tomczak, M.T.; Niiranen, S.; Hjerne, O.; Blenckner, T. Ecosystem flow dynamics in the Baltic Proper-Using a multi-trophic dataset as a basis for food-web modelling. *Ecol. Modell.* **2012**, *230*, 123–147. [CrossRef]
35. Telesh, I.V.; Schubert, H.; Skarlato, S.O. Revisiting Remane's concept: Evidence for high plankton diversity and a protistan species maximum in the horohalinicum of the Baltic Sea. *Mar. Ecol. Prog. Ser.* **2011**, *421*, 1–11. [CrossRef]
36. Elmgren, R.; Blenckner, T.; Andersson, A. Baltic Sea management: Successes and failures. *Ambio* **2015**, *44*, 335–344. [CrossRef]

37. Spiegelhalter, D.J.; Dawid, A.P.; Lauritzen, S.L.; Cowell, R.G. Bayesian analysis in expert systems. *Stat. Sci.* **1993**, *8*, 219–283. [CrossRef]
38. Templ, M.; Alfons, A.; Filzmoser, P. Exploring incomplete data using visualization techniques. *Adv. Data Anal. Classif.* **2012**, *6*, 29–47. [CrossRef]
39. Marcot, B.G. Metrics for evaluating performance and uncertainty of Bayesian network models. *Ecol. Modell.* **2012**, *230*, 50–62. [CrossRef]
40. Pearl, J. An economic basis for certain methods of evaluating probabilistic forecasts. *Int. J. Man. Mach. Stud.* **1978**, *10*, 175–183. [CrossRef]
41. Hesarkazzazi, S.; Arabzadeh, R.; Hajibabaei, M.; Rauch, W.; Kjeldsen, T.R.; Prosdocimi, I.; Castellarin, A.; Sitzenfrei, R. Stationary vs non-stationary modelling of flood frequency distribution across northwest England. *Hydrol. Sci. J.* **2021**, *66*, 729–744. [CrossRef]
42. Orio, A.; Bergström, U.; Florin, A.B.; Šics, I.; Casini, M. Long-term changes in spatial overlap between interacting cod and flounder in the Baltic Sea. *Hydrobiologia* **2020**, *847*, 2541–2553. [CrossRef]
43. Orio, A.; Heimbrand, Y.; Limburg, K. Deoxygenation impacts on Baltic Sea cod: Dramatic declines in ecosystem services of an iconic keystone predator. *Ambio* **2021**, 1–12. [CrossRef]
44. ICES. Benchmark Workshop on Baltic Cod Stocks (WKBALTCOD2). *ICES Sci. Rep.* **2019**, *1*, 310.
45. ICES. Cod (Gadus morhua) in subdivisions 24–32, eastern Baltic stock (eastern Baltic Sea). *Rep. ICES Advis. Committee* **2020**, *27*, 1–8.
46. De'ath, G. Boosted trees for ecological modeling and prediction. *Ecology* **2007**, *88*, 243–251. [CrossRef]
47. Uusitalo, L.; Blenckner, T.; Puntila-Dodd, R.; Skyttä, A.; Jernberg, S.; Voss, R.; Müller-Karulis, B.; Tomczak, M.T.; Möllmann, C.; Peltonen, H. Integrating diverse model results into decision support for good environmental status and blue growth. *Sci. Total Environ.* **2022**, *806*, 150450. [CrossRef]
48. Fulton, E.A. Approaches to end-to-end ecosystem models. *J. Mar. Syst.* **2010**, *81*, 171–183. [CrossRef]
49. Bossier, S.; Palacz, A.P.; Nielsen, J.R.; Christensen, A.; Hoff, A.; Maar, M.; Gislason, H.; Bastardie, F.; Gorton, R.; Fulton, E.A. The Baltic sea Atlantis: An integrated end-to-end modelling framework evaluating ecosystem-wide effects of human-induced pressures. *PLoS ONE* **2018**, *13*, e0199168. [CrossRef]
50. Plagányi, É.E.; Punt, A.E.; Hillary, R.; Morello, E.B.; Thébaud, O.; Hutton, T.; Pillans, R.D.; Thorson, J.T.; Fulton, E.A.; Smith, A.D.M.; et al. Multispecies fisheries management and conservation: Tactical applications using models of intermediate complexity. *Fish Fish.* **2014**, *15*, 1–22. [CrossRef]
51. Kulatska, N.; Neuenfeldt, S.; Beier, U.; Elvarsson, B.Þ.; Wennhage, H.; Stefansson, G.; Bartolino, V. Understanding ontogenetic and temporal variability of Eastern Baltic cod diet using a multispecies model and stomach data. *Fish. Res.* **2019**, *211*, 338–349. [CrossRef]
52. Kulatska, N.; Woods, P.J.; Elvarsson, B.Þ.; Bartolino, V. Size-selective competition between cod and pelagic fisheries for prey. *ICES J. Mar. Sci.* **2021**, *78*, 1900–1908. [CrossRef]
53. Carozza, D.A.; Bianchi, D.; Galbraith, E.D. The ecological module of BOATS-1.0: A bioenergetically constrained model of marine upper trophic levels suitable for studies of fisheries and ocean biogeochemistry. *Geosci. Model Dev.* **2016**, *9*, 1545–1565. [CrossRef]
54. Jennings, S.; Mélin, F.; Blanchard, J.L.; Forster, R.M.; Dulvy, N.K.; Wilson, R.W. Global-scale predictions of community and ecosystem properties from simple ecological theory. *Proc. Biol. Sci.* **2008**, *275*, 1375–1383. [CrossRef] [PubMed]
55. Blanchard, J.L.; Dulvy, N.K.; Jennings, S.; Ellis, J.J.R.; Pinnegar, J.K.; Tidd, A.; Kell, L.T. Do climate and fishing influence size-based indicators of Celtic Sea fish community structure? ICES J Mar Sci. *ICES J. Mar. Sci.* **2005**, *62*, 405–411. [CrossRef]
56. Watson, J.R.; Stock, C.A.; Sarmiento, J.L. Exploring the role of movement in determining the global distribution of marine biomass using a coupled hydrodynamic@_ Size-based ecosystem model. *Prog. Oceanogr.* **2015**, *138*, 521–532. [CrossRef]
57. Lee, J.; South, A.B.; Jennings, S. Developing reliable, repeatable, and accessible methods to provide high-resolution estimates of fishing-effort distributions from vessel monitoring system (VMS) data. *ICES J. Mar. Sci.* **2010**, *67*, 1260–1271. [CrossRef]
58. Uusitalo, L. Advantages and challenges of Bayesian networks in environmental modelling. *Ecol. Modell.* **2007**, *203*, 312–318. [CrossRef]

diversity

MDPI

Review

Vegetation Ecology of Debris-Covered Glaciers (DCGs)—Site Conditions, Vegetation Patterns and Implications for DCGs Serving as Quaternary Cold- and Warm-Stage Plant Refugia

Thomas Fickert [1,*], Donald Friend [2], Bruce Molnia [3], Friederike Grüninger [4] and Michael Richter [5]

[1] German Alpine Club, Baden-Wuerttemberg Branch, Nature Conservancy Unit, Rotebühlstr. 59 A, 70178 Stuttgart, Germany
[2] Department of Geography, Minnesota State University, 206 Morris Hall, Mankato, MN 56001, USA; donald.friend@mnsu.edu
[3] US Geological Survey, Reston, VA 20192, USA; glacier1@verizon.net
[4] TNL Environmental Planning, Hochstraße 21, 92637 Weiden in der Oberpfalz, Germany; friederike.grueninger@posteo.de
[5] Institute for Geography, Friedrich-Alexander-University, Wetterkreuz 15, 91058 Erlangen, Germany; sairecabur@posteo.de
* Correspondence: thomas.fickert@posteo.de

Abstract: Scientific interest in debris-covered glaciers (DCGs) significantly increased during the last two decades, primarily from an abiotic perspective, but also regarding their distinctive ecology. An increasing body of evidence shows that, given a minimum of debris thickness and sufficient substrate stability, DCGs host surprisingly diverse plant assemblages, both floristically and structurally, despite being obviously cold and in parts also highly mobile habitats. As a function of site conditions, floristic composition and vegetation structure, DCGs represent a mosaic of environments, including subnival pioneer communities, glacier foreland early- to late-successional stages, morainal locations, and locally, even forest sites. On shallow supraglacial debris layers, cryophilous alpine/subnival taxa can grow considerably below their common elevational niche due to the cooler temperatures within the root horizon caused by the underlying ice. In contrast, a greater debris thickness allows even thermophilous plant species of lower elevations to grow on glacier surfaces. Employing the principle of uniformitarianism, DCGs are assumed to have been important and previously undocumented refugia for plants during repeated Quaternary cold and warm cycles. This review and recent study summarize the current knowledge on the vegetation ecology of DCGs and evaluates their potential function as plant habitat under ongoing climate warming.

Keywords: high mountain biogeography; climate change ecology; refugia; niche heterogeneity

Citation: Fickert, T.; Friend, D.; Molnia, B.; Grüninger, F.; Richter, M. Vegetation Ecology of Debris-Covered Glaciers (DCGs)—Site Conditions, Vegetation Patterns and Implications for DCGs Serving as Quaternary Cold- and Warm-Stage Plant Refugia. *Diversity* **2022**, *14*, 114. https://doi.org/10.3390/d14020114

Academic Editor: Michael Wink

Received: 16 January 2022
Accepted: 2 February 2022
Published: 5 February 2022

1. Introduction

DCGs are globally distributed landforms, occurring in mountain ranges of all major climatic zones, from subpolar into the tropics, with a spatial concentration at mid-latitudes [1,2]. DCGs are more common in mountainous terrain compared to polar ice sheets, because unglaciated rock faces and scree slopes serving as sources for both, debris and vegetation, are limited in polar environments. Estimates of mountain glacier area covered by supraglacial debris range from 4.4% [1] to 7.3% [2], and the relative share of DCGs is increasing as clean-ice glaciers shrink globally under current climate warming [3,4]—apart from regional exceptions such as the "Karakoram anomaly" [5]. At the same time rockfall events in high cirques are increasing due to destabilized slopes from intensified freeze–thaw cycles, downwasting glaciers and permafrost degradation [6–8].

DCGs might resemble rock glaciers by shape and appearance (Figure 1a), but actually are different landforms regarding their formation, a fact that is not consistently respected in the scientific literature [9–13]. Here we treat DCGs sensu Kirkbride [14] as "true"

glaciers partly to almost fully overlain by a mantle of rock material, in the ablation zone in particular (Figure 1a–d). Rock glaciers, in contrast, consist of a perennially frozen mixture of ice (40–70%) and coarse rock material, slowly moving down-valley. Ground ice within rock glaciers commonly originates by congelation [11] but can also have a glacial origin, i.e., an evolution from debris-covered glaciers cannot be excluded [12,15,16] (Figure 1e). Recently, Anderson et al. [17] highlighted that there is a continuum between clean-ice glaciers, debris-covered glaciers and rock glaciers.

Figure 1. Aspects of DCGs: (**a**) fully covered Miage Glacier (European Alps, Italy); (**b**) debris cover restricted to the lateral margins on Batura Glacier (Karakorum, Pakistan); (**c**) debris cover originating from medial moraines on Jamtalferner (European Alps, Austria); (**d**) supraglacial lake on debris-covered Kinzl Glacier (Peruvian Andes); (**e**) rock glacier of most likely glacial origin in front of a clean-ice glacier (Sailiskji Alatau, Kazakhstan) (photos: (**a**,**d**) M. Richter; (**b**,**c**,**e**) T. Fickert).

At the beginning of the 21st century it was noted: " . . . debris covered glaciers comprise a significant fraction of the global population of glaciers and despite their relatively common occurrence, they have not been well studied" ([18], p. 261). Scientific interest in DCGs has significantly increased since then. There have been at least 500 publications on the subject with the majority focusing on the abiotic (i.e., glaciological, hydrological and geomorphological, along with natural hazard and mapping related issues, Figure 2). As supraglacial debris modifies the energy balance of glacier surfaces, DCGs show a different behavior with regard to glacier mass balance than clean-ice glaciers in times of climate warming [19–25]. In general, a thin layer of debris enhances melting rates due to a lowered albedo, while a thicker debris cover insulates glacier ice, reduce ablation and slows mass loss considerably [26,27]. However, contradicting observations of very similar surface elevation change rates for debris-covered and clean-ice glaciers are reported from High Mountain Asia, which are referred to as "debris-covered (glacier) anomaly" [27–29], but the underlying reasons are not yet fully understood [30]. In addition, efforts to enhance mapping accuracy were intensified, for glacier monitoring archives such as the Randolph Glacier Inventory [31,32], the World Glacier Monitoring Service [33], the Global Land Ice Measurements from Space initiative [34,35] and the Glacier Thickness Database [36,37]. Identifying an exact differentiation between DCGs and other landforms with similar spectral signature outside the glacier boundary is crucial to reduce bias in glacier area change estimations [38–43].

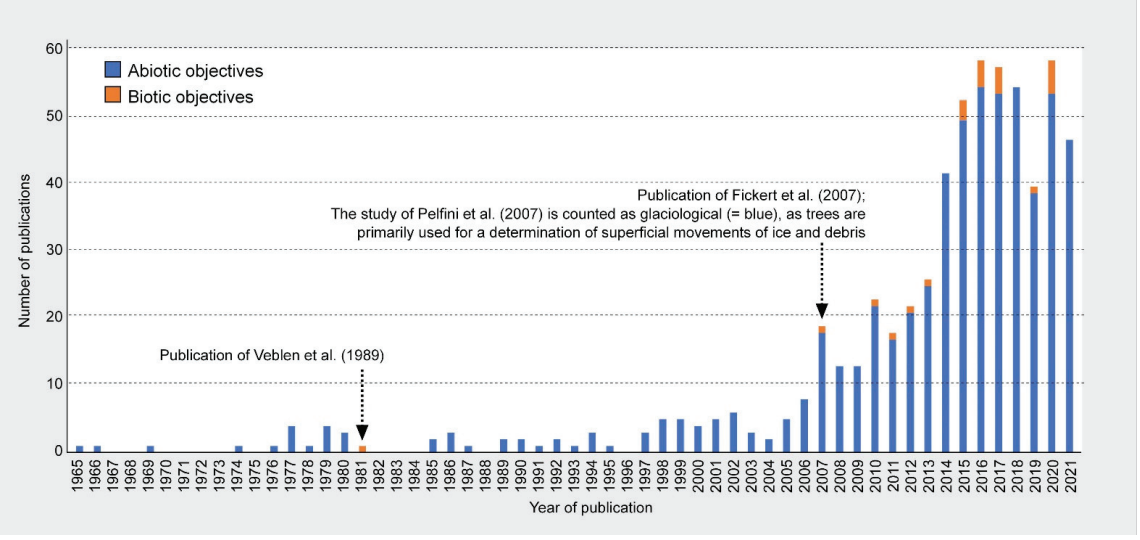

Figure 2. Bibliometric search (as of 10/2021) in the "Dimensions" Database for English language publications including the keyword "debris-covered glacier" in title or abstract. Matches were screened for objective and classified into publications with a primarily abiotic (i.e., glaciological, hydrological, geomorphological, climatological and mapping issues) and with a primarily biotic focus (i.e., flora, fauna, microbes and interactions). Papers dealing exclusively with rock glaciers, with a paleo perspective (i.e., Pleistocene, early Holocene) or with related features on Mars are excluded.

Increasing attention is also paid to DCGs from an ecological perspective, including a focus on flora [44–50], fauna [48,51–55], microbes [56] and interactions between different organism groups [57] (Figure 2). The increasing ecological interest on DCGs is also related to the fact that these landforms were recognized as potential refugia for plants (and other organisms) during warm and cold stages in the past [44,45,47,53,54,58]. This has implications in space and time for post-glacial recolonization patterns [45], for primary succession in glacier forelands [59,60] and for the survival of cryophilous taxa under cur-

rent climate warming due to the thermal inertia of DCGs [47,53,54]. Early notes on plant growth on DCGs date back well into the late 19th and 20th century. They come from all around the globe (for the Alps [61–65]; for Scandinavia and Iceland [59,66]; for Alaska and Canada [67–75]; for Southern Chile [76]; for the Himalaya [77,78]), including reports about mature forests with stem-diameters of more than 50 cm (DBH) on more than a dozen debris-covered glaciers in southcentral Alaska, including Bering, Malaspina, Fairweather and Yakataga Glaciers. (Figure 3, [41]). With the exception of [76], all of these reports are observational rather than quantitative studies.

Figure 3. North-looking oblique aerial photograph of part of the vegetation-covered, stagnant ice terminus of Malaspina Glacier at Sitkagi Bluffs. The cliff of stagnant ice is approximately 15–20 m high, topped by a thin debris layer. A dense forest, composed of alders, willows, and conifers is rooted in this glacial sediment layer. As the ice melts, the trees topple into the lagoon. Maximum tree height is >15 m. The banding on the ice surface is composed of a thin drape of sediment deposited by meltwater (photo: B. F. Molnia in the 1980s).

One of the earlier accounts on plant growth on DCGs employing systematic vegetation sampling was our paper titled "Did debris-covered glaciers serve as Pleistocene refugia for plants? A new hypothesis derived from observations of recent plant growth on glacier surfaces", published in Arctic, Antarctic and Alpine Research in 2007 [45]. This publication was pioneering at the time it was published, as it included both phytosociological sampling on the debris mantled glacier surface of Carbon Glacier on Mount Rainier (Washington, DC, USA), together with short-term microclimatic measurements and determination of debris thickness and particle size spectra to allow for a rough ecological interpretation of the vegetation patterns found. In addition, the paper presented unconventional ideas about the survival of plants under a different climate in the past. This publication catalyzed a more intense engagement with the ecology of DCGs, carried out primarily by a group of Italian scientists from different disciplines in the European Alps [46,47,49,50,53,54,57], but also additional sources provide new insights into the ecology of DCGs and other cold rocky landforms [48,58]. Thus, we believe it is the right time for summarizing the current ecological knowledge about these distinctive habitats.

This paper is based on an extensive screening of published literature. It discusses general aspects of DCGs as plant habitat, the ecological heterogeneity within and between DCGs, and their function as potential cold and warm stage plant refugia. To further illustrate and support our original hypotheses [44,45], we also report results from additional

research on three mid-latitude DCGs, namely Carbon Glacier on Mount Rainier (Cascade Range, Washington, DC, USA), Miage Glacier (European Alps, Italy, one of the best studied DCGs in the world) and Lang Glacier (European Alps, Switzerland), along with new observations made on additional DCGs across the globe. These three model DCGs terminate in the montane (low- to mid-elevation forests), subalpine (i.e., below treeline) and alpine (i.e., above treeline) environments, respectively. To not distract from this review, Appendix A describes our materials and methods.

2. Origin of Debris Cover and Its Effect on Glacier Movement and Glacier Mass Balance

DCGs come in different types with regard to distribution, thickness and arrangement of supraglacial debris (Figure 1, [79]). Their surface is commonly characterized by mounds and hollows, locally disrupted by ice cliffs, thermokarst ponds and supraglacial lakes, acting as points of origin for enhanced ice melt. Particularly intriguing features of DCGs are so-called ice sails, pyramid-shaped clean-ice sections protruding the debris layer, which are especially common in the Karakoram [80,81]. Debris cover on glacier surfaces derives from rock falls and landslides originating from destabilized rock faces and debris slopes most commonly in cirques of deeply incised glacial valleys after glacier melt, after permafrost degradation, by earthquakes in seismically active mountain regions, and/or from existing medial and eroded lateral moraines [6,8,82–85] (Figure 4a). Additional debris sources include periglacial (solifluction), fluvial or aeolian sediment-transport processes, basal thrusting, as well as the melt-out of englacial debris [17,21,30,85–87] (Figure 4a).

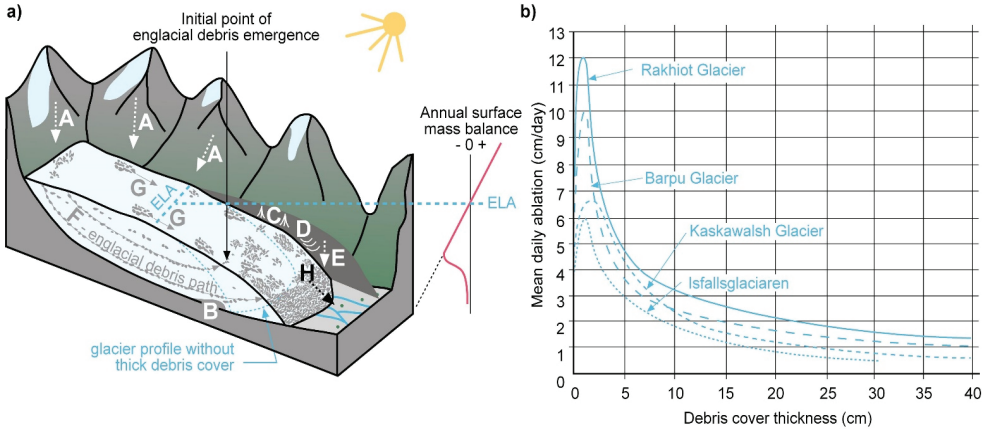

Figure 4. (**a**) Schematic diagram displaying debris supply processes, debris fluxes and debris features on DCGs: rock falls and landslides from surrounding walls and slopes (A); basal thrusting (B); debris flows (C), solifluction (D) and rock falls (E) from lateral moraines; debris transport (within (F) and upon the glacier (G)), debris concentration near the glacier terminus and eventual debris transfer to the glacier foreland (H); a debris cover surpassing a critical thickness has a significant effect on the annual surface mass balance of a glacier by reducing the ablation and consequently the ice discharge and length reduction (redrawn from [21,85,86]; (**b**) relationship between debris cover thickness and measured mean daily ablation on different DCGs (adapted from [88]).

Supraglacial debris might cover the entire glacier surface (Figure 1a), or is concentrated in particular regions depending on the debris origin: on the lateral glacier margins, if rockfalls from the valley slopes and/or the lateral moraines are the prime debris sources (Figure 1b); or in the center, if one or more medial moraines are the prime debris sources (Figure 1c). In the case of piedmont glaciers protruding from larger glacier networks, the commonly unglaciated outer margins of mountain ranges deliver debris by rockfalls (e.g., Malaspina Glacier in Figure S1).

Debris thickness may be as little as a couple of millimeters but may reach more than two meters [27]. The supraglacial debris has significant effects on the mass balance of glaciers and on flow dynamics. While a thin debris cover enhances melt rate due to reduced surface albedo compared to clean-ice glaciers and consequently a higher absorption of solar radiation, a supraglacial debris mantle of a couple of centimeters or more significantly reduces melt rate and glacier mass loss as heat transfer to the upper edge of the ice body is reduced [27,89,90]. The critical debris thickness separating the two opposing glaciological controls is around 2 cm ([89], Figure 4b), although substrate color may cause deviations from this value in either direction.

Generally, debris thickness on DCGs increases down-glacier towards the termini due to a "conveyor-belt-like nature of the glacier surface in the ablation zone (debris can typically only be added but not removed)", as Anderson and Anderson point out ([91], p. 1). The debris thickening on the lower parts of DCGs make debris-covered glacier tongues slow moving or even stagnant [26]. Thus, DCG termini are commonly located at lower elevations than termini of clean-ice glaciers, under otherwise equal settings, and termini reaching below alpine (i.e., thermal) tree line are common. At the upper margin of the debris cover, in contrast, thickness is often less than the critical threshold, thus increasing melt occurs there. As a result, DCGs often have convex to concave debris thickness profile towards the glacier terminus, which is ablation controlled up-glacier and velocity controlled down-glacier [91]. Over time, DCG profiles as a whole become concave by slow downwasting of the glacial surface [85], favoring the formation of supraglacial meltwater ponds as drainage is topographically impeded (Figure 1d).

3. DCGs as Habitats for Plants

As observations, reports and phytosociological samples from DCGs demonstrate, a shallow debris mantle of a few centimeters can host surprisingly diverse vegetation, both floristically and structurally (Figure 5, [44,45,47,49,74,76]). This is not intuitive at first glance, as slowly moving DCGs are cold and, at least in up-glacier locations, mobile habitats, offering plants (and other organisms) an environment far from welcoming. The underlying ice bestows temperatures rather low for plant roots to thrive, and can initiate both passive (i.e., caused by motion of the underlying ice) and active debris movement (i.e., caused by the hummocky supraglacial debris topography) [92] that creates considerable mechanical stress for plants by constant disturbance from shifting debris.

3.1. Physical Setting of DCGs

The fact that a broad array of different plant species is able to grow on DCG surfaces indicates that the seemingly challenging issues for plant establishment and growth such as substrate mobility, low soil temperature or limited root horizon are offset by other factors facilitating plant growth. Supraglacial debris cover is commonly a mixture of fine- and coarse-grained (up to boulder size) material, similar to that found in recently deglaciated glacier forelands. A sufficient amount of fine-grained substrate is crucial for retaining water essential for plant growth and to allow plants to set roots, while larger rocks often serve as "safe sites" for colonizing species [93] and act as stable spots in a loose unconsolidated surrounding. In addition, such safe sites provide a more favorable microclimate from earlier snow melt, a longer growing season and/or warmer temperatures while at the same time larger rocks also create shadow preventing plants from overheating during heat waves [94]. Thus, both fine and coarse substrates support plant growth, each one in a different way. This was documented in our original study where particle size analyses of soil samples collected from the debris layer on Carbon Glacier showed no significant correlation between the states of vegetation (i.e., species numbers or ground cover) and the amount of coarse debris particles [45]. More important than the grain size distribution is the thickness of the debris layer, i.e., the spacing between the root horizon and the underlying ice, as direct contact between roots and ice adversely affects plants physiological processes and commonly leads to stunted growth forms and/or death of plants [44].

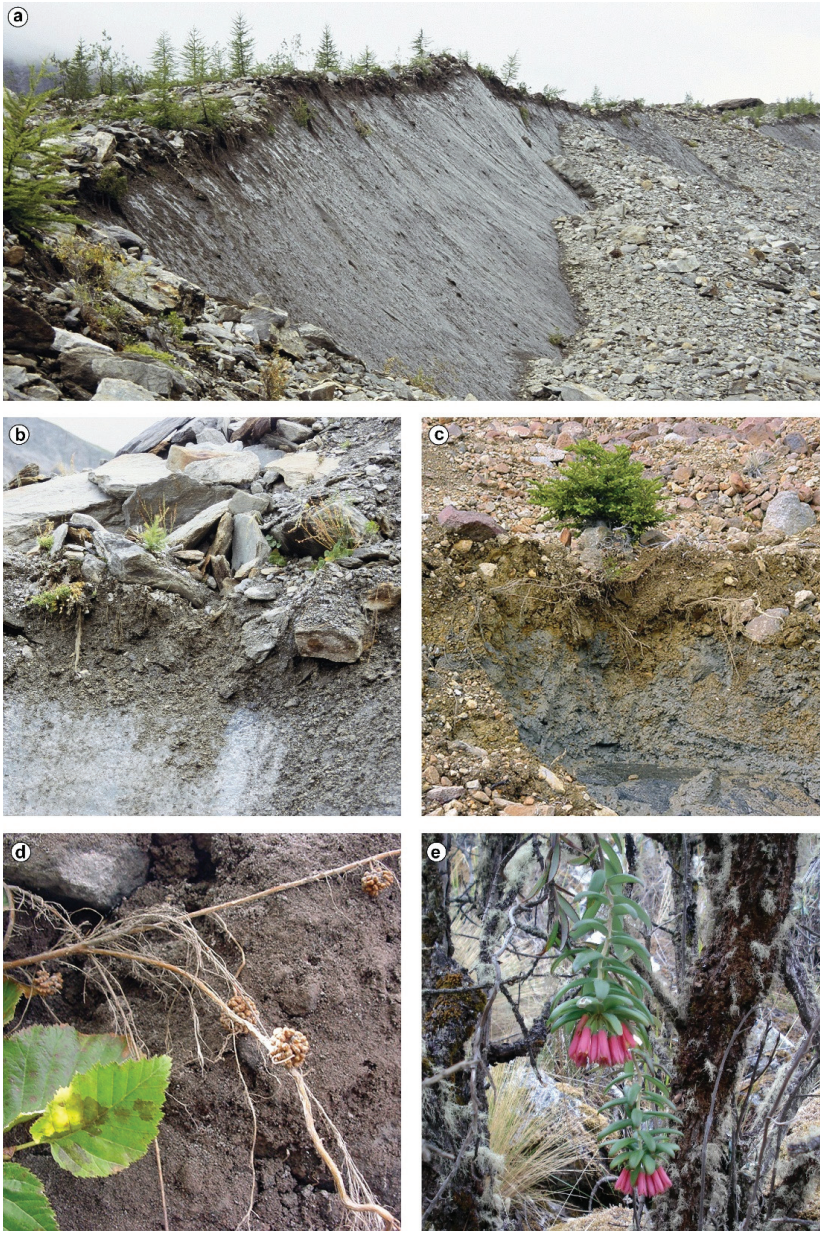

Figure 5. Aspects of plant growth on debris-covered glacier surfaces: (**a**) *Larix decidua* dominated plant community on Miage Glacier (European Alps, Italy); (**b**) detail view of the contact zone of ice and plants (amongst others: *Oxyria digyna*, *Cerastium uniflorum* and a *Larix decidua* seedling) on debris-covered Miage Glacier (European Alps, Italy); (**c**) *Nothofagus dombeyi* on debris-covered Ventisquero Blanco (Andes, Southern Chile)—note the gleyic soil due to water saturation caused by the underlying ice; (**d**) *Alnus viridis* ssp. *sinuata* on debris-covered Carbon Glacier with the symbiotic actinomycete filamentous nitrogen-fixing bacterium *Frankia alni* on its roots (Mount Rainier, Washington, DC, USA); (**e**) the epiphytic lily-of-the-Incas *Bomarea albimontana* on a *Polylepis*-tree growing on the supraglacial debris of Kinzl Glacier (Peruvian Andes) (photos: (**a**,**b**) Th. Fickert; (**c**,**d**) F. Grüninger; (**e**) M. Richter).

There are some analogies between supraglacial debris layers and recently deglaciated glacier forelands with regard to environmental setting, species composition and vegetation structure [47]. A major difference, however, is that on moving glaciers the debris layer is quite mobile, while the coarse morainal debris left by receding glaciers is commonly settled and stabilized by early colonizers within a short period of time [95,96]. In fact, where DCGs move over subglacial rock outcrops or bend while following the topography of glacial valleys, crevasses and serac zones with highly mobile debris layers occur, impairing the chances for plant establishment. The lower parts of DCGs, however, are often stagnant and characterized by a slow downwasting of the glacier body causing a lowering of the overlaying debris layer without major effects on the substrate stability and the debris layer is thus readily available for plant colonization.

Besides substrate characteristics, microclimate is a major control of plant growth [97]. As plant growth on DCGs occurs in a broad range of environments from high to low latitudes (e.g., the Coast Ranges of Alaska to the Cordillera Blanca in Peru) and under very variable moisture conditions (perhumid–maritime in the Andes of Southern Chile or the US Cascade Range, to arid continental in the Northwestern Karakoram or the Eastern Pamir), macroclimate seems not to be a major control for presence or absence of supraglacial vegetation. However, microclimate is a major control of plant growth and plays an important role for colonization and survival, as well as for species composition and groundcover development on DCGs. Depending on the thickness of the debris layer and the color of the material present, the heat flow from above into the root horizon and the cooling effects from the underground ice variably overlap (Figure 6).

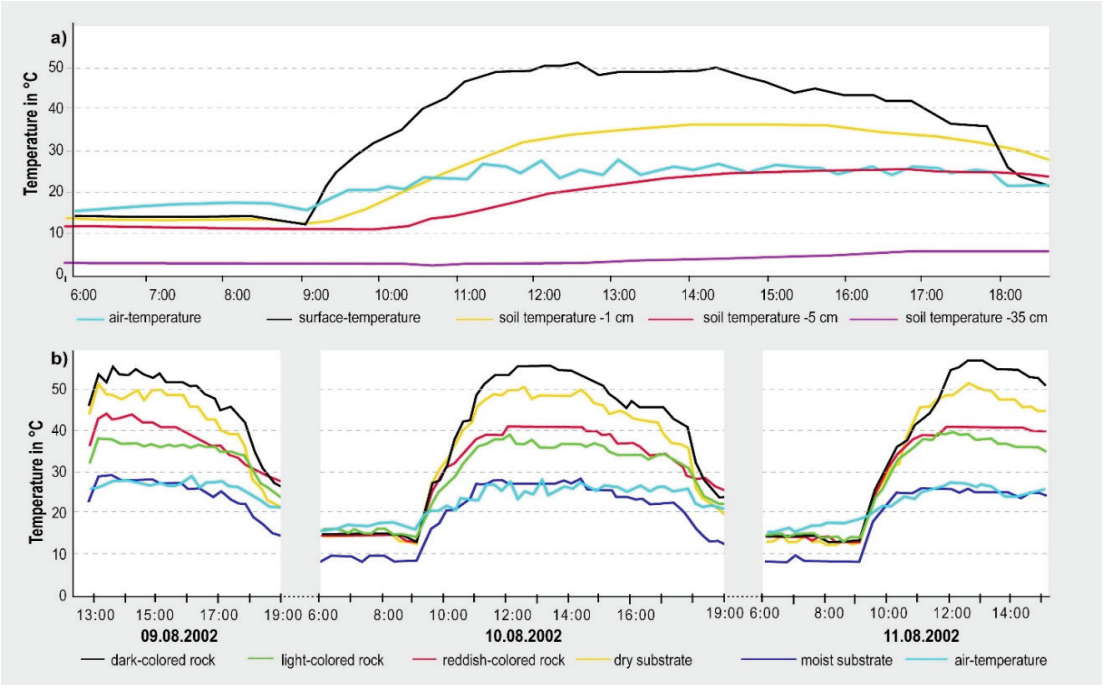

Figure 6. (**a**) Air temperatures (2 m), debris surface temperature and soil temperature at various depths, recorded on 10 August 2002 with cloudless skies on Carbon Glacier; (**b**) surface temperatures of differently colored debris together with air temperature recorded with cloudless skies on Carbon Glacier between 9 August and 11 August 2002 (redrawn and modified from [45]).

Short term measurements of soil temperatures at different depths on Carbon Glacier at Mount Rainier (Washington, DC, USA) at a study site with a debris cover of 40 cm

showed that no substantial cooling effects exist in the upper layers down to about −35 cm (i.e., 5 cm above the ice) (Figure 6a). At depths of −1 and −5 cm, heat flow is slightly delayed but follows the daily course of air and surface temperatures and offers a rather warm root horizon. At a depth of −35 cm, daily temperatures fluctuate between 3 and 7 °C, indicating that heat flow from the surface is recognizable with slightly increasing temperatures in late afternoon; thus, even at greater depths, heat transfer from the debris surface is evident (Figure 6a). Measurements of surface temperatures on differently colored substrates on the debris layer of Carbon Glacier (Figure 6b) revealed high microclimatic niche variability in close proximity. On dry and/or dark substrates, daytime ground surface temperatures of more than 50 °C were measured, a temperature potentially lethal for cryophilous plants [94], yet they survive in areas of wet substrates and/or a thin debris cover which allow for cooler root zone temperatures. Those same high surface temperatures offer growth conditions for thermophilous taxa from lower elevations on areas where surface debris is thicker. In general, wide daily temperature fluctuations are a common surface characteristic of DCGs [45,47,49].

3.2. Source Areas and Dispersal Pathways of Plants Colonizing DCGs

Potential source areas for plants colonizing DCGs are plant communities in the wider surrounding area. These vary depending on the location of the glacier tongue, which is a function of climate, aspect, elevation and topography, along with size of the glacier accumulation zone and the debris thickness governing ice melt in the ablation zone. The vast majority of plant species colonizing the supraglacial debris is anemochochorous, i.e., wind dispersed (Figure 7), reaching the glacier surface by mesoscale diurnal mountain-valley wind systems [98]. Anemochorous species commonly show a leptokurtic diaspore dispersal behavior [99], i.e., most diaspores are deposited in close proximity to the mother plant, and only few are transported over longer distances during strong wind events; thus, the chances to reach a particular location decrease with distance to the source area.

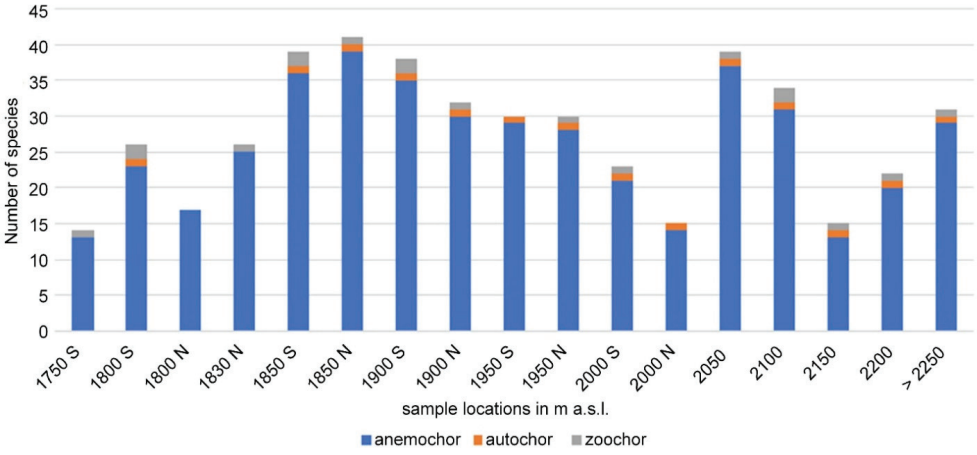

Figure 7. Predominant seed dispersal pathways (according to [100]) of species growing on Miage Glacier: anemochor = wind dispersed, autochor = without external forces by the plant itself, zoochor = dispersed by animals.

Figure 8 shows the provenances of species growing on "montane" Carbon Glacier (i.e., located within montane conifer forests), on "subalpine" Miage Glacier (i.e., located within the subalpine treeline ecotone), and on "alpine" Lang Glacier (i.e., located in the alpine belt above treeline). While on all three glaciers a broad range of species from montane (=low elevation) to subnival (=high elevation) origin grow side by side, it becomes very clear that plant communities of the immediate surroundings contribute the most to the

DCGs species composition; at Carbon Glacier, half of the species encountered are low- to mid-elevation taxa (montane and montane–subalpine), while high-elevation taxa (alpine and alpine–subnival) are underrepresented. In contrast, on Lang Glacier, which terminates above alpine treeline, three-quarters of the taxa growing on its surface originate from plant communities of the treeline ecotone upwards. Miage Glacier shows a more balanced contribution of species originating from different elevational belts. Either way, even on Lang Glacier some taxa from lower elevations occur (e.g., *Larix decidua* well above tree line) if debris cover is sufficiently thick, while on Carbon and Miage glaciers several high-elevation taxa benefit from lowered soil temperatures at locations with shallow debris cover and consequently occur well below their usual lower distribution limit. For example, on Carbon Glacier the alpine species *Luetkea pectinata* and the alpine–subnival pioneer *Oxyria digyna* grow virtually side by side with montane conifers such as *Pseudotsuga menziesii* var. *menziesii* or *Tsuga heterophylla*. On Miage Glacier the subnival species *Ranunculus glacialis*, one of the highest ascending vascular plants in the European Alps and commonly found between 2300 and 4200 m a.s.l, occurs as low as 1850 m a.s.l., together with montane *Salix mysinifolia* or the subalpine conifer *Larix decidua*.

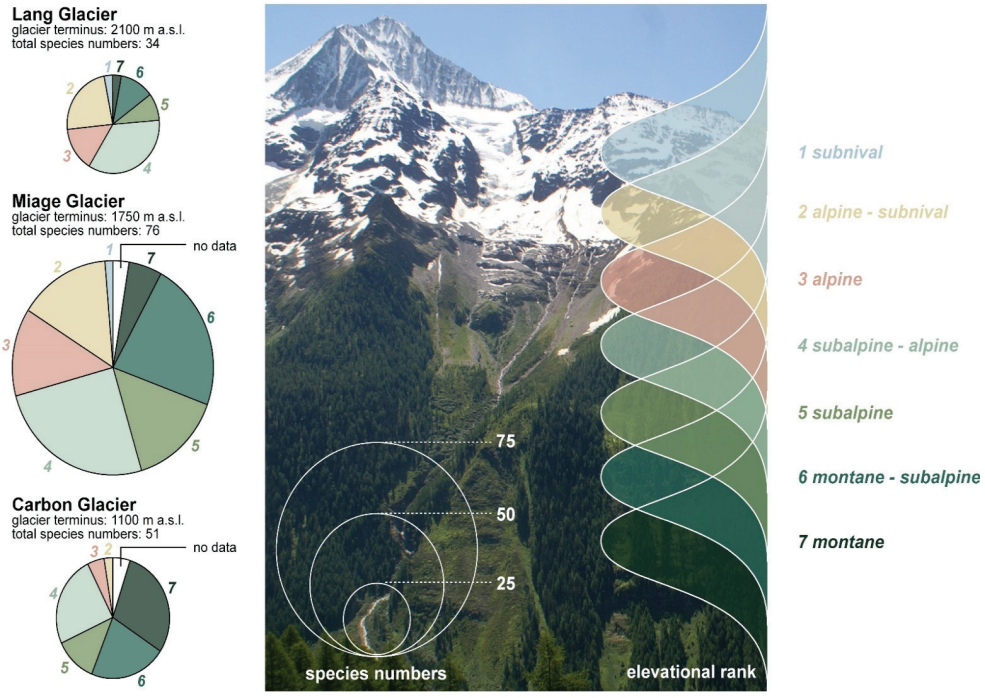

Figure 8. According to their primarily temperature-determined distribution along the elevational gradient, plant species refer to different elevational belts, here montane to subnival. The species distribution can be used as an ecological indicator for the respective temperature preferences, so for each plant species a particular elevational rank value can be assigned, here 1 (=subnival) to 7 (=montane) (according to information given in [101,102]). The pie charts on the left show the relative contribution of species from different provenances for the "montane" Carbon Glacier, the "subalpine" Miage Glacier and the "alpine" Lang Glacier.

To answer the question of whether plants from a particular plant community in the immediate surroundings of a DCG are superior in colonizing the supraglacial debris, vegetation sampling on Carbon Glacier was supplemented by samples from forest locations and scree slopes in close proximity to the glacier. A canonical correspondence analysis (CCA, Figure 9) including samples from the supraglacial debris as well as from forest and

scree slope sites, shows, not surprisingly, that scree slope samples are well separated from the forest sites due to a low floristic similarity. The DCG samples are located between these two diverging environments, with some samples floristically more similar to forests sites, some to scree slope sites and some with a co-occurrence of species present in both habitats (including *Alnus viridis* ssp. *sinuata*, *Poa secunda*, *Polystichum muntium* or *Saxifraga ferruginea* var. *ferruginea*). Thus, depending on debris properties, a wide range of site characteristics, some more closely related to scree slopes and others more to forest sites, allow for plants from very different provenances to find suitable habitats on supraglacial debris. Consequently, a clear attribution of supraglacial vegetation to phytosociological units (plant communities, associations) is difficult [49].

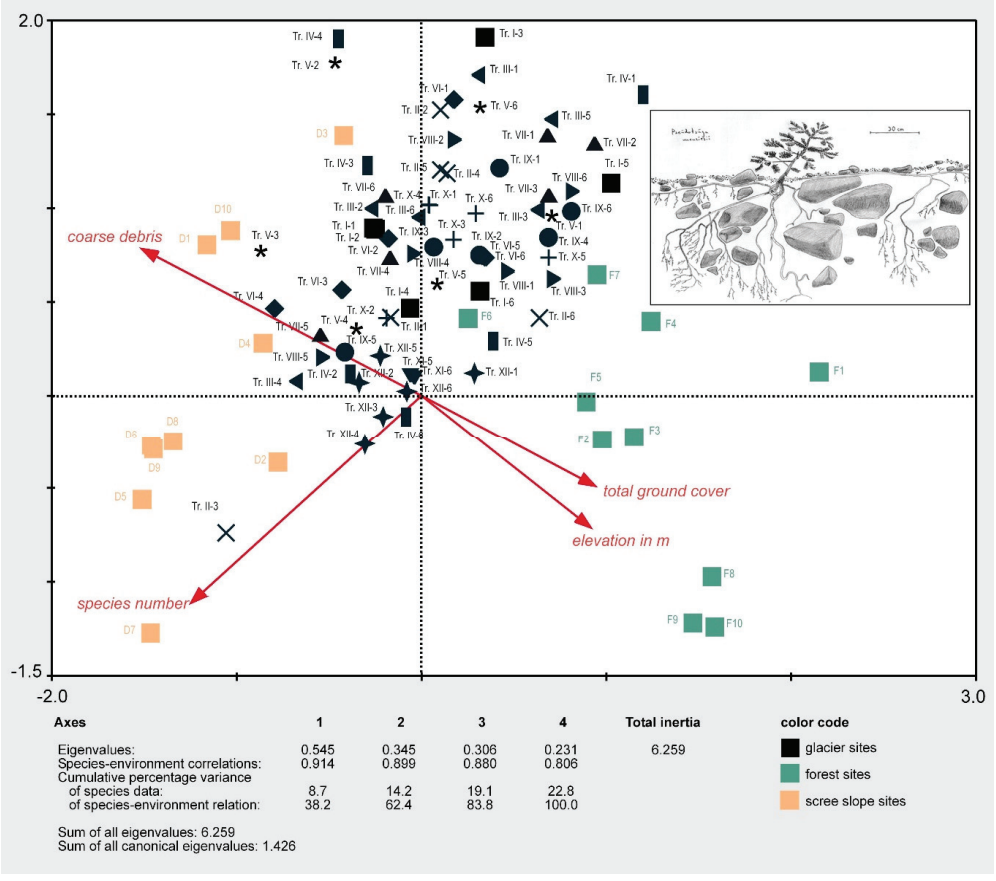

Figure 9. A canonical correspondence analysis (CCA) ordination biplot showing the floristic similarity of samples on the debris-covered surface of Carbon Glacier on Mount Rainier (Washington, DC, USA) in relation to samples from forest and scree slope sites in the immediate surroundings. The inset shows the disproportionally long roots of a small *Pseudotsuga menziesii* var. *menziesii* treelet growing on the supraglacial debris of Carbon Glacier (drawing by M. Richter).

Plant growth on debris-covered glacier surfaces is not restricted to a highly specialized set of plants. Rather, most available species tolerating underground ice and substrate mobility to some degree potentially can colonize supraglacial debris [47,49]. A shallow and wide-spreading root-system (Figure 9, inset), which is a common feature in high mountain plant species [103] seems to be beneficial in terms of keeping distance to the ice, thereby preventing negative effects on the plants' physiological processes and to withstand the

permanent rearrangement of the substrate. Only very few taxa have special adaptations such as *Alnus* species which lives in symbiosis with the actinomycete filamentous nitrogen-fixing bacterium *Frankia alni* (Figure 5d), and hence has a better nutrient supply.

The colonization of supraglacial debris has certain analogies to the colonization of glacier forelands [47]. In both settings, successful vegetation development requires three important steps (according to [104]): (1) plants, or rather their diaspores, have to get there, i.e., the colonization process itself; (2) plant seeds reaching the debris-covered glacier surface have to establish, i.e., successful germination; and (3) once established, the plants have to persist, grow and spread, i.e., survival. The prevailing anemochorous plant species set up an "autochthonous" vegetation type with in situ germination of seeds carried primarily by wind from the surroundings to the debris layer. This colonization pathway, however, is not the only one. Often plants reach the glacier surface by landslides from vegetated lateral moraines and/or adjacent bordering mountain slopes [76], setting up a patchier, "allochthonous" vegetation type [44]. Plant colonization via this pathway is particularly common on the tropical Kinzl Glacier in the Cordillera Blanca of the Peruvian Andes, where most of the plants growing on the debris-covered glacier surface, including small tree individuals of *Polylepis sericea* (Figure 1d), are derived from landslides originating from Little Ice Age (LIA) moraines after substantial post-LIA downwasting of the debris-covered glacier surface [105]. Once established, even those plant species that reached the supraglacial debris via long distance dispersal now propagate on the glacier surface and persist through a cycle of a slow downward migration via glacier flow and upward dispersal of diaspores by valley winds without the necessity of further stochastic long distance dispersal events.

3.3. Spatiotemporal Plant Diversity Patterns on DCGs

DCGs can host a large number of different plant species. Among the three case studies presented here (i.e., Carbon Glacier, Miage Glacier and Lang Glacier), the highest total species number (76 taxa) and highest species number per 100 m^2 sample location (up to 25 species) are encountered at Miage Glacier. This is most likely due to its intermediate subalpine location, which allows for an overlap of species from low and high elevations (Figure 8). On montane Carbon Glacier and alpine Lang Glacier, chances for high- and low-elevation species, respectively, to reach and successfully establish on the debris layer are less than at Miage Glacier's intermediate elevation, consequently species numbers are lower (Carbon Glacier: 41 taxa, Lang Glacier: 34 taxa, [44]). Similar counts are reported at Belvedere Glacier in the European Alps (31 taxa, [49]), at Ventisquero Blanco in Southern Chile (37 taxa, [44]), and at Hailuogou and Gonga Gomba Glaciers in the Chinese Gonga Shan (32 taxa and 38 taxa, respectively, [44]). This astonishing species richness on DCGs is linked to the highly variable microclimate and surface characteristics with sunny, dry, and/or coarse-grained habitats occurring side-by-side with shady, humid, and/or fine-grained habitats, offering growth conditions for both, xerophytic, or at least desiccation tolerant species, together with more hygrophilous and/or cryophilous species in close proximity.

Structural diversity of the supraglacial vegetation is affected by the location of a DCG relative to the respective elevational zonation, too. On DCGs terminating within the forested belt such as Carbon and Miage Glaciers, different life-forms including trees and higher shrubs (i.e., micro- to macrophanerophytes) co-occur and ground cover values are as high as 20% (though highly variable), while on higher elevation Lang glacier ground cover is much less (rarely exceeding 0.3%), with herbs and subshrubs (i.e., hemicryptophytes and chamaephytes) being the predominant life-forms (Figure 10a). The overall highest structural complexity on a DCG was observed on the tropical Kinzl Glacier. Because the debris-covered portion of the glacier is located some 500 m below the local treeline at 4800 m a.s.l., small tree individuals of *Polylepis sericea*, taller shrub species (*Berberis lutea*, *Gynoxys oleifolia*), several dwarf to medium-sized shrubs (*Baccharis genistelloides*, *Phyllactis rigida*, *Loricaria ferruginea*, *Diplostephium foliosissimum*, *Vaccinium floribundum*), perennial

herbs (e.g., the ferns *Cheilanthes pruinata* and *Elaphoglossum engelii*, the club moss *Lycopodium crissum*, the herbs *Gentiana prostrata*, *Castilleja nubigena*, *Neobartsia diffusa*, *Senecio nivalis* and *Werneria nubigena*) as well as grasses (*Stipa ichu* and *Deyeuxia ovata*) are present. Further supraglacial oddities on Kinzl Glacier include the cushion cactus *Austrocylindropuntia floccosa*, the terricolous orchid *Aa mathewsii* and even epiphytes such as *Bomarea albimontana* (Figure 5e) are found growing on older *Polylepis*-trees.

Apart from locations close to the glacier front or ice cliffs where debris shifting activity is more pronounced, species richness, ground cover, and structural complexity expressed by the co-occurrence of different life-forms, is generally higher in the less mobile lower elevation sections of DCGs. Up-glacier floristic and structural diversity successively decreases due to combined effects of a change in elevation, a reduction of debris cover and a faster glacier velocity, and thus increased debris cover mobility (Figure 10). On Carbon Glacier, for example, a steep serac zone around 1450 m is responsible for a decrease in ground cover and species richness. On Miage Glacier a similar pattern appears, where the glacier turns from a southern into an eastward flow direction (Figure 1a). In both cases, ground cover and species richness decrease toward the high mobility zone, and increase again once the high mobility zone is passed (Figure 10a,b). Caccianiga et al. [47] also found that glacier velocity (0.3–16 m/yr.), which affects debris stability, and elevation were the best predictors for species richness on Miage Glacier. Lang Glacier, in contrast, shows a continuously decreasing ground cover and species richness with increasing elevation; this is likely related to a decreasing debris thickness and to increasingly adverse growth conditions on the glacier surface, better suited for high elevation species as expressed by the decreasing elevational rank score S (Figure 10c).

Besides spatial gradients in plant diversity patterns, temporal changes during vegetation development, i.e., succession, can be assumed to occur on debris-covered glacier surfaces. However, as scientific engagement in supraglacial vegetation is a rather recent phenomenon, no data on long-term vegetation dynamics or successional trajectories are available. Tree ages determined by dendrochronological methods allow for a rough estimate of the date of their first arrival, which occurred on some Alaskan glaciers in the second half of the 19th century, which is post Little Ice Age [67–69,71]. The same is documented on Casa Pangue Glacier in Southern Chile from the early 20th century [76] and on Miage Glacier in the European Alps the oldest trees established around the middle of the 20th century [46]. On Casa Pangue and Miage Glacier no indications for different successional stages exist yet, but Stephens [71] describes an earlier Sitka alder (*Alnus crispa* ssp. *sinuata*) stage which is eliminated later by a Sitka spruce (*Picea sitchensis*) stage for Kushtaka Glacier in Alaska where plant colonization started earlier. This pattern resembles successional stages described by Lawrence [107] from Alaskan glacier forelands, where an earlier *Alnus sinuata* dominated successional stage is also replaced by a late successional *Picea sitchensis* stage.

This, again, underpins ecological similarities between recently deglaciated glacier forelands and DCGs. A repeated vegetation sampling in the Alpine glacier foreland of Jamtalferner (Silvretta, Austria) in 2016 and 2021, provides some insights on the pace of the early colonization dynamics on stagnant DCG termini (Figure 11). These sample sites were placed a couple of meters in front of the ice margin in 2016 and deemed as recently deglaciated as they became ice-free only one to two years prior to sampling. In fact, these samples are still underlain by ice, as later indicated by high resolution elevation models, which show an ongoing lowering of the surface elevation due to melt-out of the underlying ice [108]. The ice does not seem to be dead ice, rather it is still connected to the clean-ice glacier several tens of meters up-valley. Thus, these sites represent an early-stage colonization of stagnant DCG terminus. The resurvey in 2021 indicates a highly dynamic colonization with exponentially increasing ground cover values and species numbers (Figure 11), comparable to recently deglaciated glacier foreland samples [60,95,109,110]. While this location may not be representative of the dynamics on a moving DCG with high substrate mobility and ongoing stress for plants by the constant rearrangement of debris, it does demonstrate that the stagnant termini of DCGs are characterized by progressive vegetation development, i.e., succession, and that those sites can be important refugia for plants.

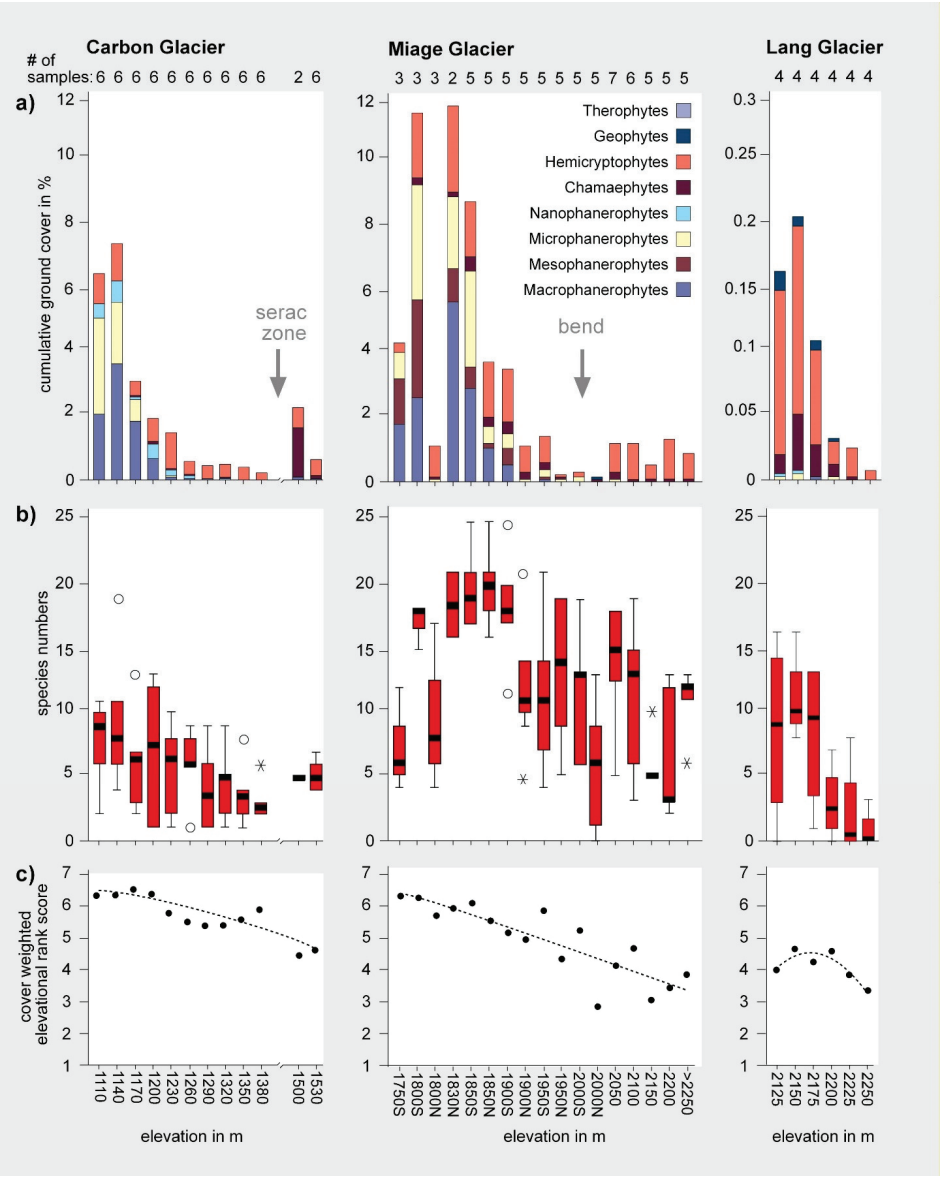

Figure 10. Gradual changes in vegetation structure and diversity measures from the glacier terminus upwards for the three mid-latitude DCGs—Carbon Glacier (terminating in the montane belt), Miage Glacier (terminating in the subalpine belt) and Lang Glacier (terminating in the alpine belt): (**a**) Life-form spectra, showing the contribution of individual life-forms to the mean total ground cover of vascular plants per sample location. (**b**) Boxplots for vascular plant species number per sample location showing the minimum and maximum values, the range of the middle half of the scores (25th to 75th percentile) and the median and outliers, if present. (**c**) Cover-weighted elevational rank score S for each sample location, based on the elevational rank values of vascular plants as displayed in Figure 8 and calculated using the formula in [106] (see also Appendix A).

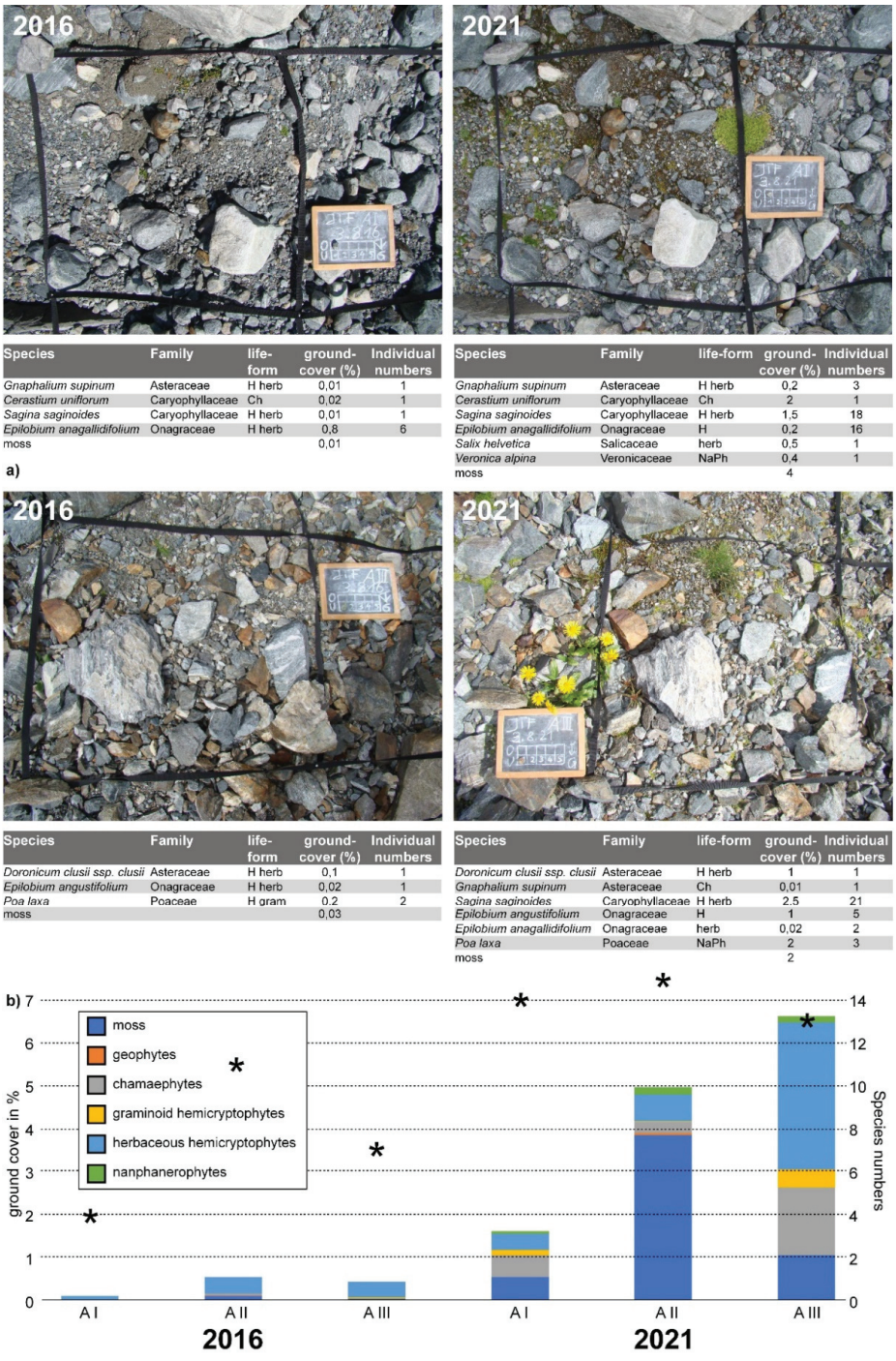

Figure 11. Rapid colonization of newly emerged supraglacial debris on Jamtalferner (European Alps, Austria): (**a**) illustrative photo-pairs of two 1 m^2 sample plots in 2016 and 2021; (**b**) changes in ground cover and life-form composition (bars) along with species numbers (asterisks) of three samples AI, AII and AIII (10 m^2 each) between 2016 and 2021.

4. DCGs as Potential Cold Stage Refugia in the Past

An increasing number of studies focus on vegetation on DCGs [44–47,49,50]. They indicate that even a shallow debris cover allows for establishment and survival of plants. Employing the principle of uniformitarianism (sensu [111]), DCGs could have provided habitats for plants during repeated cold and warm cycles (Figure 12a) caused by climatic oscillations in the past as well.

In 2007 we hypothesized that DCGs functioned as habitats for plants during Pleistocene cold phases [45]. Before our publication there were two competing hypotheses on the fate of plants during Pleistocene ice ages [112–114]. The first, tabula rasa, theorized a complete replacement of plants to milder refugia in the foreland or farther away and a subsequent recolonization after glacier retreat, i.e., the slate (tabula) was wiped clean (rasa) by glacial ice, and plants then grew back on the clean slate. The second hypothesis is survival of plants during ice ages on nunataks, isolated unglaciated mountain peaks within extensive ice sheets that then allowed for a fast recolonization from these mountain refugia. While there are studies, primarily employing DNA analyses, in support for either one of these hypotheses, current perspectives abandon such a sort of exclusiveness. Instead, individualistic responses of species to climatic changes are assumed [115], and the existence of many different "cryptic" (micro)refugia are proposed as the key explanation for present day species distribution and genetic patterns [115–117]. Our assumption of Pleistocene plant survival on debris-covered glacier surfaces introduced a new, hitherto unrecognized cryptic microrefugia for plants, from which a post-glacial recolonization of mountain areas was possible without relying exclusively on either long-distance remigration from peripheral refugia (i.e., the tabula rasa hypothesis) or a plant survival on extremely cold and isolated ice-free areas within extended ice sheets (i.e., the nunatak hypothesis). Pleistocene DCGs were located in a much milder low-elevation climatic setting compared to high-elevation nunataks, thus offering better chances for survival for many different plant species. Glaciers in mid-latitude mountains such as the European Alps descended to the base of the mountains as piedmont glaciers [118], similar to present day Alaskan glaciers such as Malaspina or Bering. These two examples also provide insight as to the Pleistocene debris sources which were primarily the less glaciated valley entrances and outer margins of the mountain ranges (see Figure S1). In addition, basal thrusting (Figure 4) might have brought basal sediments to the surface in the lower parts of the glaciers enhancing the supraglacial debris mantle. Thus, even if the source area for supraglacial debris was limited in the center of the ice sheets during full glacial conditions, where clean-ice glaciers prevailed, and just as exist in contemporary analogues, piedmont glaciers flowing to low-elevation mountain forelands were able to accumulate a significant amount of debris on their termini. As debris sources were reduced, debris cover extent may have been proportionally less than today. Nevertheless, unglaciated rock faces and slopes above piedmont glaciers provided sufficient suitable substrate and refugia for plant growth, especially when considering the warmer temperatures at lower elevations. Pleistocene mid-latitude mountain glaciers such as those in the Alps terminated some 2000 m below their current position. Assuming a vertical temperature lapse rate of 0.6 °C/100 m, this corresponds to a difference in temperature of 12 °C, what is roughly the value of cooling during the last cold phase of the Pleistocene in Central Europe (Figure 12b). Thus, cold-adapted high-elevation plants of the Alps may have found comparable site conditions, in terms of both substrate (coarse debris) and climate, to their present-day natural habitats on Pleistocene DCGs (Figure 12c). With an increasing debris thickness on Pleistocene piedmont glaciers, even lower elevation taxa were able to survive on supraglacial debris, especially when considering small-scale microclimatic differentiation described by Scherrer and Körner [119].

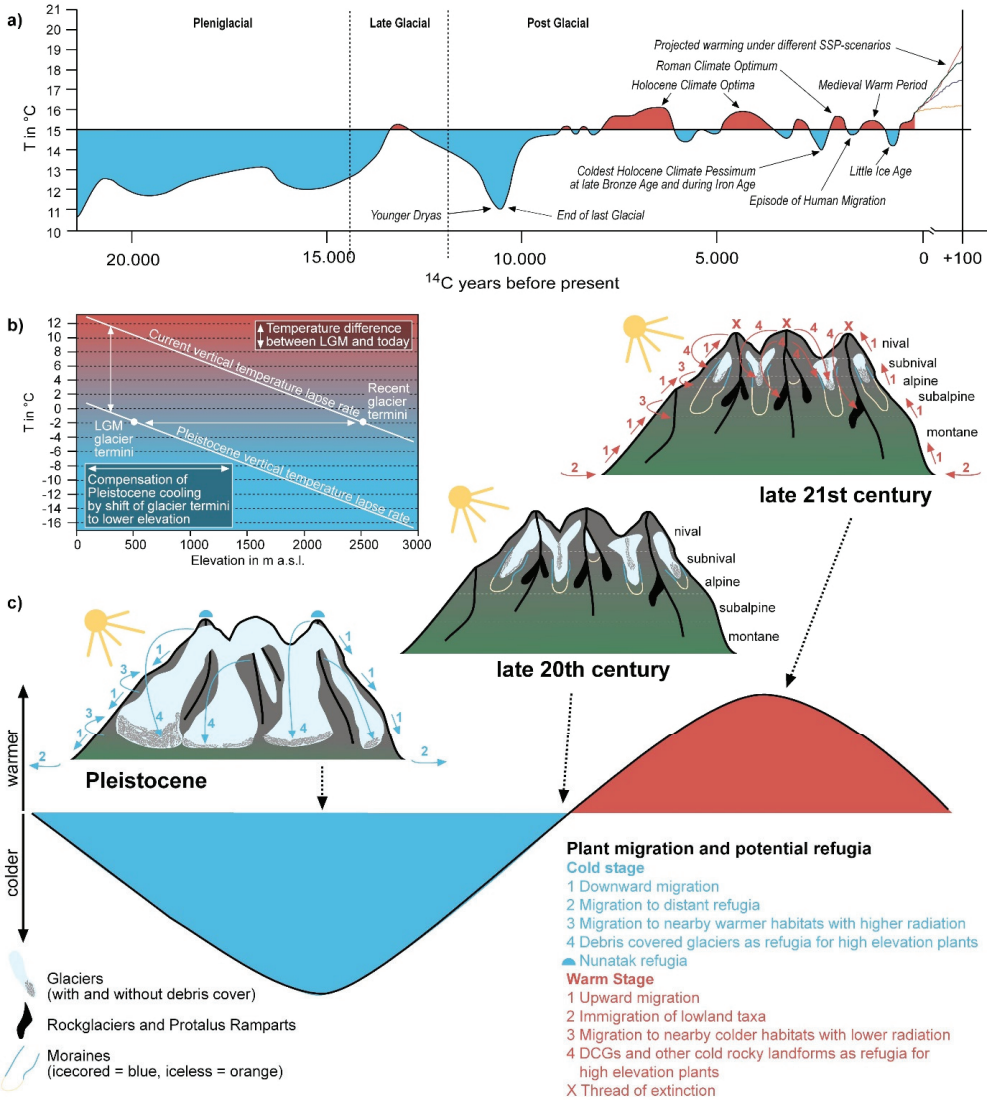

Figure 12. Plant migration and potential plant refugia under colder and warmer temperatures than today: (**a**) North hemispheric mean air temperature change and variability during the last 20k years (adapted and modified from [120]), together with projections under different IPCC–SSP (shared socioeconomic pathways) scenarios (according to [121]). (**b**) Schematic vertical temperature lapse rates today and during the last glacial maximum (LGM), illustrating the comparable thermal conditions at LGM (at lower elevations but under colder climate) and current glacier termini, making debris-covered LGM piedmont glaciers potential plant refugia temperature-wise. (**c**) Potential plant migration directions and refugia under colder (e.g., Pleistocene) and warmer (e.g., projected for late 21st century) conditions compared to late 20th century.

Our assumption of Pleistocene DCGs as plant refugia was recently supported by Zale et al. [122], who found macrofossil evidence of vascular plant growth on debris-covered Late Weichselian ice sheet during Greenland interstadial 1 (GI-1 or Bølling–Allerød interstadial) in Fennoscandia, three millennia before final deglaciation. For the final deglaciation phase

the presence of shrubs (*Salix* div. spec., *Betula* div. spec. and *Ericaceae* div. spec.) and tree species (*Larix*) is reported. Comparable "plant trash" originating from supraglacial forests on Late Pleistocene ice sheets were found in lake sediments from North America [123], likewise indicating the presence of a supraglacial forest containing *Picea* spec., *Larix laricina*, *Juniperus communis*, *Cornus stolonifera*, *C. canadensis*, *Rubus pubescens*, *Fragaria virginiana* and *Viola* sp. on debris-covered dead ice remnants of the Late Pleistocene Laurentide ice sheet. Even earlier, Stephens [71] assumed that vegetation on supraglacial debris on Late Wisconsin ice in Alaska could have hastened the post-glacial extension of plant ranges.

5. The Role of DCGs and Other Cold Rocky Landforms as Refugia under Current Climate Warming

Based on the fact that cold-adapted high-elevation taxa are commonly found well below their natural distribution on DCGs, a complementary hypothesis was proposed: DCGs as refugia for cold-adapted taxa during Holocene warm stages [47,54,58,124]. Crucial for that kind of habitat function is a shallow debris layer, favoring cryophilic plants with a sufficiently cool root horizon. This has important implications for the survival of cold-adapted high-elevation plants under current climate warming.

Climate-warming-induced upward range shift of plant species, plant communities and/or elevational belts are well-documented phenomena in high mountains globally [106,125–131]. Within an increasingly warmer world, many high-elevation plant species, whose distribution is primarily determined by cold temperatures, migrate upwards to higher colder elevations (Figure 12c) to find suitable habitats [106,127,131,132]. For species already restricted to the upper margin of the elevational relief, summit locations could easily become a trap. Ongoing climate warming is expected to cause their extinction, as they fall victim to competition from upward migrating plants from lower elevation (Figure 12c, see also [106,127,133,134]). For these species, alternative cold habitats in their surrounding region will enhance their chance for survival. The increasing area of glacier forelands left by the receding glaciers are assumed to provide to a certain degree suitable habitats for cryophilous species [60]. However, glacier forelands alone, for which an area gain of 0.126 Mio km^2 is calculated under a 2.2 °C warming scenario, are not able to compensate the area loss (1.5 Mio km^2) of high-elevation ecosystems by advancing tree lines [135]. Thus, the existence of other refugia is crucial for their survival. Brighenti et al. [58] and Gentili et al. [124] introduce several additional glacial and periglacial landforms, aptly termed "cold rocky landforms" [58] with similar and/or additional functions to DCGs, contributing to a mosaic of strongly diverging microhabitats for plant (and other) life in high mountain environments [135].

Besides the already mentioned recently deglaciated glacier forelands, ice-cored and iceless moraines, nivation niches, rock glaciers (supposedly more common in dry continental climates [10]) and protalus ramparts, talus slopes along with composite debris cones and channels created by the coexistence of different erosive and depositional processes, must be taken into account as potential cold and rocky plant habitats in warming mountain environments [48]. Underground ice and/or natural convection within the debris inducing a seasonally reversible circulation pattern [58] keep these landforms cold year-round, creating habitat conditions similar to DCGs even with geomorphological processes causing a certain degree of substrate mobility. Consequently, many of the plant species mentioned for such cold rocky landforms [47,58,124] are present on northern hemisphere DCGs, too. They include: *Oxyria digyna* on Carbon Glacier, Miage Glacier, Belvedere Glacier, Lang Glacier and Hailuogou Glacier (Gonga Shan, China); *Poa alpina* on Miage Glacier, Belvedere Glacier, Lang Glacier and Oytagh Glacier (Eastern Pamir, China); and *Ranunculus glacialis*, *Leucanthemopsis alpina*, *Saxifraga bryoides* and *Linaria alpina* on Miage Glacier, Belvedere Glacier and Lang Glacier of the European Alps.

6. Conclusions

Cold rocky landforms including DCGs with surface and/or subsurface ice in close proximity might provide appropriate habitats for cryophilous plant species, and, if so, significantly enlarge the areal extent of potential refugia for those species. In contrast to clean-ice glaciers and snowfields, these landforms are less responsive to climate warming due to insulating effects and the thermal inertia of the debris layer [17,58]. Thus, these coarse-grained, more-or-less mobile and cold environments will persist despite climate warming, at least for the near future. They will provide suitable habitats for cryophilous species possessing physiological and/or physiognomic adaptations to cope with the special habitat conditions and allows them—at least in the near- to medium-term—to escape the threat of extinction by climate warming induced upward migrating taxa from lower elevation and/or the decreasing amount of available space [58,124,128]. In summary, such landforms may help to prevent both local disappearances of species and general species extinction.

Mountains in general are known to provide important refugia for organisms under a changing climate (Figure 12c), allowing for easier vertical range shifts (upward during warmer phases, downward during cooler phases) compared to the lowlands, where significantly greater distances have to be conquered to find suitable habitats. In addition, topographically (and thus microclimatically) diverse mountain terrain provides opportunity for many species to survive climatic changes due to the mosaic of strongly diverging microhabitats [135]. DCGs and other cold rocky landforms decrease the chances for mountains to become traps for the survival of plants under changing climates, in the past, present and future, as they provide refugia during both warming and cooling climates. Under warming conditions cold-adapted plant species can survive in the cold microclimate offered by DCGs and other such landforms. Under cooling and cold conditions, DCGs descend to lower elevation with milder climate and offer chances for plant survival.

Supplementary Materials: The following supporting information can be downloaded at: https://www.mdpi.com/article/10.3390/d14020114/s1, Figure S1: Satellite imagery of Malaspina Glacier (source: NASA, https://earthobservatory.nasa.gov/images/86767/malaspina-glacier-alaska), Table S1: Species list of Carbon Glacier (Mt. Rainier, Washington, DC, USA), Table S2: Species list of Miage Glacier (Alps, Italy), Table S3: Species List of Lang Glacier (Alps, Switzerland).

Author Contributions: Conceptualization, M.R. and T.F.; methodology, M.R., T.F. and F.G.; formal analysis, T.F. and F.G.; writing—original draft preparation, T.F.; writing—review and editing, all authors; funding acquisition, M.R. All authors have read and agreed to the published version of the manuscript.

Funding: Field sampling of data presented here was funded by the Deutsche Forschungsgemeinschaft (DFG, German Research Foundation) under grant number RI370/13–1. Vegetation sampling and data analyses for Jamtalferner (Silvretta, Tyrol, Austria) were supported by Verein Gletscher–Klima (Glacier–Climate Society) and Österreichische Akademie der Wissenschaften (ÖAW, Austrian Academy of Science).

Institutional Review Board Statement: Not applicable.

Data Availability Statement: The data used are available upon request to the corresponding author.

Acknowledgments: The authors are grateful to Constance I. Millar (Scientist Emerita, USDA Forest Service, Pacific Southwest Research Station, Lee Vining, CA 93541, USA) for valuable comments on an earlier version of the manuscript and to two anonymous reviewers for their suggestions which greatly improved the outcome. Biol. Eric F. Rodríguez-Rodríguez at the Herbarium Truxillense of the National University of Trujillo (HUT), Perú, helped with identification of plant species from Kinzl Glacier in the Cordillera Blanca.

Conflicts of Interest: The authors declare no conflict of interest.

Appendix A. Materials and Methods

Vegetation data for the three mid-latitude model DCGs presented here, namely Carbon Glacier on Mount Rainier (Cascade Range, Washington, DC, USA), Miage Glacier (European Alps, Italy) and Lang Glacier (European Alps, Switzerland) were collected on quadratic 100 m^2 sample sites arranged along transversal transects across the DCGs. The number of sampling sites and distance between them varied, depending on area, elevational range and terrain characteristics of the debris-covered glacier surface. Vegetation data recorded include percent ground cover of all occurring vascular plant species and the respective life-form affiliation (therophytes = annual herbaceous plants; geophytes = plants with tuberous subterranean organs; hemicryptophytes = graminoid and herbaceous perennial plants; chamaephytes = woody dwarf shrubs growing less than 0.5 m tall; nanophanerophytes = shrubs growing 0.5–2 m tall; microphanerophytes = shrubs growing 2–5 m tall; mesophanerophytes = trees growing 5–20 m tall; macrophanerophytes = trees growing 20–50 m tall). Sampling occurred from the glacier terminus up-glacier to the uppermost occurrence of plants. In addition, site characteristics (aspect, slope angle, proportion of coarse rock and, when possible, depth of debris cover) were recorded. At Carbon Glacier, 12 transects with a total of 68 plots were sampled between 1110 and 1530 m a.s.l., in vertical steps of 30 m; a sampling gap exists between 1400 and 1500 m a.s.l. due to an inaccessible serac zone. In addition to the DCG samples, further vegetation sampling was carried out at ten forest and ten scree slope locations next to Carbon Glacier on equally sized sample sites. At Miage Glacier a total of 17 transects with 79 plots were sampled between 1700 and 2315 m a.s.l, in vertical steps of mostly 50 m. At Lang Glacier six transects with 24 plots were sampled between 2125 and 2250 m a.s.l. in vertical steps of 25 m. Plant taxonomy for Carbon Glacier follows Biek [101] and for Miage and Lang Glacier, Fischer et al. [102]. Additional vegetation data come from Jamtalferner in the European Alps (Silvretta, Tyrol, Austria) where a repeated plant survey (2016, 2021) on species composition and ground cover on three 10m^2 samples (5 × 2 m) was conducted. On Carbon Glacier also short-term surface- and soil-temperature measurements were carried out.

Vegetation data analyses include standard uni- and multivariate statistical procedures. Life-form composition is displayed separately for each transversal transect by bar graphs (Figure 10) showing the relative contribution (i.e., mean ground cover) of a particular life-form to total ground cover. Species numbers per transect are displayed by boxplots. In addition, for each transect a ground-cover-weighted elevational rank score S is calculated. The elevational rank of a particular species is specified by its primarily temperature determined distribution along the elevational gradient, ranging here from montane (7) to subnival (1) (information on elevational species distribution from [101,102]). Considering all species with their respective elevational ranks and the mean ground cover per transect, a composite elevational rank score is calculated to depict changes within and differences between DCGs. Calculation is by the following equation (according to [106]):

$$S = \frac{\sum \text{ elevational rank}(\text{species}_i) \cdot \text{ground cover}(\text{species}_i)}{\sum \text{ groundcover}(\text{species}_i)}$$

A canonical correspondence analysis (CCA) was employed to identify similarities regarding species composition between DCG samples on Carbon Glacier and samples on forest and scree slope locations in the immediate surroundings. The CCA results are displayed by an ordination scatterplot (Figure 9), arranging samples along underlying gradients. Samples are shown as symbols and explaining variables as arrows, pointing from the origin of the coordinates into the direction where samples with above-average values of the respective variable are located (Figure 9). The arrangement of samples within the ordination space indicates the floristic (dis)similarity. The CCA analysis was performed with the software Canoco 4.5 (Biometrics, Wageningen and České Budějovice). Species data were log-transformed ($x' = \log(x + 1)$) prior to CCA calculation to place the data within acceptable limits of normality [136,137].

References

1. Scherler, D.; Wulf, H.; Gorelick, N. Global assessment of supraglacial debris-cover extents. *Geophys. Res. Lett.* **2018**, *45*, 11798–11805. [CrossRef]
2. Herreid, S.; Pellicciotti, F. The state of rock debris covering Earth's glaciers. *Nat. Geosci.* **2020**, *13*, 621–627. [CrossRef]
3. Zemp, M.; Frey, H.; Gärtner-Roer, I.; Nussbaumer, S.; Hoelzle, M.; Paul, F.; Haeberli, W.; Denzinger, F.; Ahlstrom, A.P.; Anderson, B.; et al. Historically unprecedented global glacier decline in the early 21st century. *J. Glaciol.* **2015**, *61*, 745–762. [CrossRef]
4. Hugonnet, R.; McNabb, R.; Berthier, E.; Menounos, B.; Nuth, C.; Girod, L.; Farinotti, D.; Huss, M.; Dussaillant, I.; Brun, F.; et al. Accelerated global glacier mass loss in the early twenty-first century. *Nature* **2021**, *592*, 726–731. [CrossRef]
5. Farinotti, D.; Immerzeel, W.W.; de Kok, R.J.; Quincey, D.J.; Dehecq, A. Manifestations and mechanisms of the Karakoram glacier. *Anomaly. Nat. Geosci.* **2020**, *13*, 8–16. [CrossRef]
6. Haeberli, W.; Noetzli, J.; Arenson, L.; Delaloye, R.; Gärtner-Roer, I.; Gruber, S.; Isaksen, K.; Kneisel, C.; Krautblatter, M.; Phillips, M. Mountain permafrost: Development and challenges of a young research field. *J. Glaciol.* **2011**, *56*, 1043–1058. [CrossRef]
7. McColl, S.T. Paraglacial rock-slope stability. *Geomorphology* **2012**, *153–154*, 1–16. [CrossRef]
8. Stoffel, M.; Huggel, C. Effects of climate change on mass movements in mountain environments. *Prog. Phys. Geog.* **2012**, *36*, 421–439. [CrossRef]
9. Wahrhaftig, C.; Cox, A. Rock glaciers in the Alaska Range. *Geol. Soc. Am. Bull.* **1959**, *70*, 383–436. [CrossRef]
10. Barsch, D. *Rockglaciers. Indicators for the Present and Former Geoecology in High Mountain Environments*; (Springer Series in Physical Environment Book Series); Springer: Berlin, Germany, 1996; Volume 16.
11. Haeberli, W. Modern Research Perspectives Relating to Permafrost Creep and Rock Glaciers: A Discussion. *Permafr. Periglac.* **2000**, *11*, 290–293. [CrossRef]
12. Berthling, I. Beyond confusion: Rock glaciers as cryo-conditioned landforms. *Geomorphology* **2011**, *131*, 98–106. [CrossRef]
13. Whalley, B.; Matsuoka, N.; Sik, A.; Kereszturi, A.; Hargitai, H. Rock Glacier and Debris-Covered Glacier. In *Encyclopedia of Planetary Landforms*; Hargitai, H., Kereszturi, A., Eds.; Springer: New York, NY, USA, 2015; pp. 1811–1828. [CrossRef]
14. Kirkbride, M.P. Debris-Covered Glaciers. In *Encyclopedia of Snow, Ice and Glaciers*; Singh, V.P., Singh, P., Haritashya, U.K., Eds.; Springer: Dordrecht, The Netherlands, 2011; pp. 190–192. [CrossRef]
15. Johnson, P.G. Glacier—Rock glacier transition in the Southwest Yukon Territory, Canada. *Arct. Alp. Res.* **1980**, *12*, 195–204. [CrossRef]
16. Whalley, B.; Martin, H. Rock glaciers: II models and mechanisms. *Prog. Phys. Geog.* **1992**, *16*, 127–186. [CrossRef]
17. Anderson, R.; Anderson, L.; Armstrong, W.; Rossi, M.; Crump, S. Glaciation of alpine valleys: The glacier—Debris-covered glacier—Rock glacier continuum. *Geomorphology* **2018**, *311*, 127–142. [CrossRef]
18. Fountain, A.G.; Raymond, C.F.; Nakawo, M. International Workshop examines debris-covered glaciers. *Eos* **2001**, *82*, 261–262.
19. Nicholson, L.; Benn, D.I. Calculating ice melt beneath a debris layer using meteorological data. *J. Glaciol.* **2006**, *52*, 463–470. [CrossRef]
20. Reid, T.; Brock, B. An energy-balance model for debris-covered glaciers including heat conduction through the debris layer. *J. Glaciol.* **2010**, *56*, 903–916. [CrossRef]
21. Evatt, G.; Abrahams, I.; Heil, M.; Mayer, C.; Kingslake, J.; Michell, S.; Fowler, A.; Clark, C. Glacial melt under a porous debris layer. *J. Glaciol.* **2015**, *61*, 825–836. [CrossRef]
22. Naegeli, K.; Huss, M. Sensitivity of mountain glacier mass balance to changes in bare-ice albedo. *Ann. Glaciol.* **2017**, *58*, 119–129. [CrossRef]
23. Fyffe, C.L.; Brock, B.W.; Kirkbride, M.P.; Mair, D.W.F.; Arnold, N.S.; Smiraglia, C.; Diolaiuti, G.; Diotri, F. Do debris-covered glaciers demonstrate distinctive hydrological behaviour compared to clean glaciers? *J. Hydrol.* **2019**, *570*, 584–597. [CrossRef]
24. Ferguson, J.C.; Vieli, A. Modelling steady states and the transient response of debris-covered glaciers. *Cryosphere* **2021**, *15*, 3377–3399. [CrossRef]
25. Huo, D.; Chi, Z.; Ma, A. Modeling Surface Processes on Debris-Covered Glaciers: A Review with Reference to the High Mountain Asia. *Water* **2021**, *13*, 101. [CrossRef]
26. Mayr, E.; Hagg, W. Debris-Covered Glaciers. In *Geomorphology of Proglacial Systems. Geography of the Physical Environment*; Heckmann, T., Morche, D., Eds.; Springer: Cham, Switzerland, 2019. [CrossRef]
27. Rounce, D.; Hock, R.; McNabb, R.; Millan, R.; Sommer, C.; Braun, M.; Malz, P.; Maussion, F.; Mouginot, J.; Seehaus, T.; et al. Distributed Global Debris Thickness Estimates Reveal Debris Significantly Impacts Glacier Mass Balance. *Geophys. Res. Lett.* **2021**, *48*, e2020GL091311. [CrossRef] [PubMed]
28. Banerjee, A. Brief Communication: Thinning of debris-covered and debris-free glaciers in a warming climate. *Cryosphere 11* **2017**, 133–138. [CrossRef]
29. Salerno, F.; Thakuri, S.; Tartari, G.; Nuimura, T.; Sunako, S.; Sakai, A.; Fujita, K. Debris-covered glacier anomaly? Morphological factors controlling changes in the mass balance, surface area, terminus position, and snow line altitude of Himalayan glaciers. *Earth Planet Sci. Lett.* **2017**, *471*, 19–31. [CrossRef]
30. Huo, D.; Bishop, M.P.; Bush, A.B.G. Understanding Complex Debris-Covered Glaciers: Concepts, Issues, and Research Directions. *Front. Earth Sci.* **2021**, *9*, 358. [CrossRef]

31. Pfeffer, W.T.; Arendt, A.A.; Bliss, A.; Bolch, T.; Cogley, J.G.; Gardner, A.S.; Hagen, J.-O.; Hock, R.; Kaser, G.; Kienholz, C.; et al. The Randolph Glacier Inventory: A globally complete inventory of glaciers. *J. Glaciol.* **2014**, *60*, 537–552. [CrossRef]
32. RGI Consortium. *Randolph Glacier Inventory—A Dataset of Global Glacier Outlines: Version 6.0: Technical Report, Global Land Ice Measurements from Space*; Digital Media; RGI Consortium: Boulder, CO, USA, 2017. [CrossRef]
33. WGMS; NSIDC. *World Glacier Inventory. Compiled and Made Available by the World Glacier Monitoring Service*; Updated 2012; Zurich, Switzerland, and The National Snow and Ice Data Center: Boulder, CO, USA, 1989. [CrossRef]
34. Raup, B.; Racoviteanu, A.; Khalsa, S.J.S.; Helm, C.; Armstrong, R.; Arnaud, Y. The GLIMS geospatial glacier database: A new tool for studying glacier change. *Glob. Planet Change* **2007**, *56*, 101–110. [CrossRef]
35. GLIMS; NSIDC. *Global Land Ice Measurements from Space Glacier Database*; Compiled and made available by the international GLIMS community and the National Snow and Ice Data Center, updated 2018; National Snow and Ice Data Center: Boulder, CO, USA, 2005. [CrossRef]
36. GlaThiDa Consortium. *Glacier Thickness Database 3.1.0*; World Glacier Monitoring Service: Zurich, Switzerland, 2020. [CrossRef]
37. Welty, E.; Zemp, M.; Navarro, F.; Huss, M.; Fürst, J.J.; Gärtner-Roer, I.; Landmann, J.; Machguth, H.; Naegeli, K.; Andreassen, L.M.; et al. Worldwide version-controlled database of glacier thickness observations. *Earth Syst. Sci. Data* **2020**, *12*, 3039–3055. [CrossRef]
38. Paul, F.; Huggel, C.; Kääb, A. Combining satellite multispectral image data and a digital elevation model for mapping debris-covered glaciers. *Remote Sens. Environ.* **2004**, *89*, 510–518. [CrossRef]
39. Brenning, A.; Trombotto, D. Logistic regression modeling of rock glacier and glacier distribution: Topographic and climatic controls in the semi-arid Andes. *Geomorphology* **2006**, *81*, 141–154. [CrossRef]
40. Brenning, A.; Grasser, M.; Friend, D.A. Statistical estimation and generalized additive modeling of rock glacier distribution in the San Juan Mountains, Colorado, USA. *J. Geophys. Res. Earth* **2007**, *112*, F02S15. [CrossRef]
41. Molnia, B.F. *Satellite Image Atlas of the Glaciers of the World: Alaska*; US Geological Survey Professional Paper 1386-K; U.S. Geological Survey: Reston, VA, USA, 2008; 750p.
42. Shukla, A.; Gupta, R.P.; Arora, M.K. Delineation of debris-covered glacier boundaries using optical and thermal remote sensing data. *Remote Sens. Lett.* **2010**, *1*, 11–17. [CrossRef]
43. Xie, Z.; Haritashya, U.; Asari, V.; Young, B.; Bishop, M.; Kargel, J. GlacierNet: A Deep-Learning Approach for Debris-Covered Glacier Mapping. *IEEE Access* **2020**, *8*, 83495–83510. [CrossRef]
44. Richter, M.; Fickert, T.; Grüninger, F. Pflanzen auf schuttbedeckten Gletschern—Wandernde Kuriositäten. *Geoöko* **2004**, *25*, 225–256.
45. Fickert, T.; Friend, D.; Grüninger, F.; Molnia, B.; Richter, M. Did Debris-Covered Glaciers Serve as Pleistocene Refugia for Plants? A New Hypothesis Derived from Observations of Recent Plant Growth on Glacier Surfaces. *Arct. Antarct. Alp. Res.* **2007**, *39*, 245–257. [CrossRef]
46. Pelfini, M.; Santilli, M.; Leonelli, G.; Bozzoni, M. Investigating surface movements of debris-covered Miage Glacier (Western Italian Alps) using dendroglaciological analysis. *J. Glaciol.* **2007**, *53*, 141–152. [CrossRef]
47. Caccianiga, M.; Andreis, C.; Diolaiuti, G.; D'Agata, C.; Mihalcea, C.; Smiraglia, C. Alpine debris-covered glaciers as a habitat for plant life. *Holocene* **2011**, *21*, 1011–1020. [CrossRef]
48. Millar, C.I.; Westfall, R.D.; Evenden, A.; Holmquist, J.G.; Schmidt-Gengenbach, J.; Franklin, R.S.; Nachlinger, J.; Delany, D.L. Potential climatic refugia in semi-arid, temperate mountains: Plant and arthropod assemblages associated with rock glaciers, talus slopes, and their forefield wetlands, Sierra Nevada, California, USA. *Quatern. Int.* **2015**, *387*, 106–121. [CrossRef]
49. Tampucci, D.; Citterio, C.; Gobbi, M.; Caccianiga, M. Vegetation outlines of a debris-covered glacier descending below the treeline. *Plant Sociol.* **2016**, *53*, 45–54. [CrossRef]
50. Vezzola, L.; Diolaiuti, G.; D'Agata, C.; Smiraglia, C.; Pelfini, M. Assessing glacier features supporting supraglacial trees: A case study of the Miage debris-covered Glacier (Italian Alps). *Holocene* **2016**, *26*, 1138–1148. [CrossRef]
51. Gobbi, M.; Isaia, M.; De Bernardi, F. Arthropod colonisation of a debris-covered glacier. *Holocene* **2011**, *21*, 343–349. [CrossRef]
52. Gobbi, M.; Ballarin, F.; Brambilla, M.; Compostella, C.; Isaia, M.; Losapio, G.; Maffioletti, C.; Seppi, R.; Tampucci, D.; Caccianiga, M. Life in harsh environments: Carabid and spider trait types and functional diversity on a debris-covered glacier and along its foreland. *Ecol. Entomol.* **2017**, *42*, 838–848. [CrossRef]
53. Gobbi, M. Global warning: Challenges, threats and opportunities for ground beetles (Coleoptera: Carabidae) in high altitude habitats. *Acta Zool. Hung.* **2020**, *66*, 5–20. [CrossRef]
54. Tampucci, D.; Azzoni, R.S.; Boracchi, P.; Citterio, C.; Compostella, C.; Diolaiuti, G.; Isaia, M.; Marano, G.; Smiraglia, C.; Gobbi, M.; et al. Debris-covered glaciers as habitat for plant and arthropod species: Environmental framework and colonization pattern. *Ecol. Complex* **2017**, *32*, 42–52. [CrossRef]
55. Valle, B.; Ambrosini, R.; Caccianiga, M.; Gobbi, M. Ecology of the cold-adapted species *Nebria germari* (Coleoptera: Carabidae): The role of supraglacial stony debris as refugium during the current interglacial period. *Acta Zool. Hung.* **2020**, *66*, 199–220. [CrossRef]
56. Franzetti, A.; Tatangelo, V.; Gandolfi, I.; Bertolini, V.; Bestetti, G.; Diolaiuti, G.; D'Agata, C.; Mihalcea, C.; Smiraglia, C.; Ambrosini, R. Bacterial community structure on two alpine debris-covered glaciers and biogeography of Polaromonas phylotypes. *ISME J.* **2013**, *7*, 1483–1492. [CrossRef]

57. Losapio, G.; Jordán, F.; Caccianiga, M.; Gobbi, M. Structure-dynamic relationship of plant–insect networks along a primary succession gradient on a glacier foreland. *Ecol. Model.* **2015**, *314*, 73–79. [CrossRef]
58. Brighenti, S.; Hotaling, S.; Finn, D.A.; Fountain, A.G.; Hayashi, M.; Herbst, D.; Saros, J.E.; Tronstad, L.M.; Millar, C.I. Rock glaciers and related cold rocky landforms: Overlooked climate refugia for mountain biodiversity. *Glob. Change Biol. Vol.* **2021**, *27*, 1504–1517. [CrossRef]
59. Matthews, J.A. *The Ecology of Recently-Deglaciated Terrain. A Geoecological Approach to Glacier Forelands and Primary Succession*; Cambridge University Press: Cambridge, UK, 1992.
60. Erschbamer, B.; Caccianiga, M.S. Glacier forelands: Lessons of plant population and community development. *Prog. Bot.* **2017**, *78*, 259–284.
61. Lüdi, W. *Die Pflanzengesellschaften des Lauterbrunnentales und ihre Sukzession*; Beiträge zur Geobotanischen Landesaufnahme der Schweiz; Verlag: Zürich, Switzerland, 1921; Volume 9, pp. 1–364.
62. Negri, G. La vegetazione delle morene del Ghiacciaio del Lys (Monte Rosa). *Boll. Del Com. Glaciol. Ital.* **1934**, *15*, 105–172.
63. Negri, G. Osservazioni di U. Monterin su alcuni casi di invasioni delle morene galleggianti dei ghiacciai del Monte Rosa da parte della vegetazione. *Nuovo G. Bot. Ital.* **1935**, *42*, 699–712.
64. Negri, G. Nuovi dati sull'invasione delle morene galleggianti dei ghiacciai alpini da parte della vegetazione. *Nuovo G. Bot. Ital.* **1942**, *49*, 448–459.
65. Valbusa, U. Florula di due isole glaciali del Rutor con appendice morenica epiglaciale. *Nuovo G. Bot. Ital.* **1937**, *44*, 705–714.
66. Porter, P.R.; Evans, A.J.; Hodson, A.; Lowe, A.T.; Crabtree, M.D. Sediment-moss interactions on a temperate glacier: Falljökull, Iceland. *Ann. Glaciol.* **2008**, *48*, 25–31. [CrossRef]
67. Russell, I.C. An expedition to Mount St. Elias. *Natl. Geogr.* **1891**, *3*, 53–191.
68. Russell, I.C. *Second Expedition to Mount St. Elias*; U.S. Geological Survey 13th Annual Report Part 2; US Government Printing Office: Washington, DC, USA, 1893; pp. 1–91.
69. Tarr, R.S.; Martin, L. *Alaskan Glacier Studies*; National Geographic Society: Washington, DC, USA, 1914.
70. Sharp, R.P. The latest major advance of Malaspina Glacier, Alaska. *Geogr. Rev.* **1958**, *48*, 16–26. [CrossRef]
71. Stephens, F.R. A forest ecosystem on a glacier in Alaska. *Arctic* **1969**, *22*, 441–444. [CrossRef]
72. Rampton, V. Neoglacial fluctuations of the Natazhat and Klutlan glaciers, Yukon Territory, Canada. *Can. J. Earth Sci.* **1970**, *7*, 1236–1263. [CrossRef]
73. Post, A.; Streveler, G. The tilted forest: Glaciological-geological implications of vegetated neoglacial ice at Lituya Bay, Alaska. *Quat. Res.* **1976**, *6*, 111–117. [CrossRef]
74. Birks, H.J.B. The present flora and vegetation of the moraines of the Klutlan Glacier, Yukon Territory, Canada: A study in plant succession. *Quat. Res* **1980**, *1*, 60–86. [CrossRef]
75. Benn, D.I.; Evans, D.J.A. *Glaciers and Glaciation*; Routledge: New York, NY, USA, 2010; 802p.
76. Veblen, T.T.; Ashton, D.H.; Rubulis, S.; Lorenz, D.; Cortes, M. *Nothofagus* Stand Development on In-Transit Moraines, Casa Pangue Glacier, Chile. *Arct. Alp. Res.* **1989**, *21*, 144–155. [CrossRef]
77. Miehe, G. *Langtang Himal—Flora und Vegetation als Klimazeiger und -zeugen im Himalaya*; Dissertationes Botanicae 158; Borntaeger: Berlin, Germany; Stuttgart, Germany, 1990; 529p.
78. Hambrey, M.; Quincey, D.; Glasser, N.; Reynolds, J.; Richardson, S.; Clemmens, S. Sedimentological, geomorphological and dynamic context of debris-mantled glaciers, Mount Everest (Sagarmatha) region, Nepal. *Quat. Sci Rev.* **2009**, *28*, 2361–2389. [CrossRef]
79. Janke, J.; Bellisario, A.; Ferrando, F. Classification of debris-covered glaciers and rock glaciers in the Andes of central Chile. *Geomorphology* **2015**, *241*, 98–121. [CrossRef]
80. Evatt, G.; Mayer, C.; Mallinson, A.; Abrahams, I.; Heil, M.; Nicholson, L. The secret life of ice sails. *J. Glaciol.* **2017**, *63*, 1–14. [CrossRef]
81. Fowler, A.C.; Mayer, C. The formation of ice sails. *Geophys Astro Fluid* **2017**, *111*, 411–428. [CrossRef]
82. Ravanel, L.; Magnin, F.; Deline, P. Impacts of the 2003 and 2015 summer heat waves on permafrost-affected rock-walls in the Mont Blanc massif. *Sci. Total. Environ.* **2017**, *609*, 132–143. [CrossRef]
83. Mollaret, C.; Hilbich, C.; Pellet, C.; Flores-Orozco, A.; Delaloye, R.; Hauck, C. Mountain permafrost degradation documented through a network of permanent electrical resistivity tomography sites. *Cryosphere* **2019**, *13*, 2557–2578. [CrossRef]
84. Hartmeyer, I.; Delleske, R.; Keuschnig, M.; Krautblatter, M.; Lang, A.; Schrott, L.; Otto, J.-C. Current glacier recession causes significant rockfall increase: The immediate paraglacial response of deglaciating cirque walls. *Earth Surf. Dynam.* **2020**, *8*, 729–751. [CrossRef]
85. Van Woerkom, T.; Steiner, J.F.; Kraaijenbrink, P.D.A.; Miles, E.S.; Immerzeel, W.W. Sediment supply from lateral moraines to a debris-covered glacier in the Himalaya. *Earth Surf. Dynam.* **2019**, *7*, 411–427. [CrossRef]
86. Anderson, L.S.; Anderson, R.S. Modeling debris-covered glaciers: Response to steady debris deposition. *Cryosphere* **2016**, *10*, 1105. [CrossRef]
87. Fleischer, F.; Otto, J.-C.; Junker, R.; Hölbling, D. Evolution of debris cover on glaciers of the Eastern Alps, Austria, between 1996 and 2015. *Earth Surf. Proc. Land.* **2021**, *46*, 1673–1691. [CrossRef]

88. Mattson, L.E.; Gardner, J.S.; Young, G.Y. Ablation on Debris Covered Glaciers: An Example from the Rakhiot Glacier, Punjab, Himalaya. In *Snow and Glacier Hydrology, Proceedings of the Kathmandu Symposium, Kathmandu, Nepal, 16–21 November 1992*; IAHS Publ. no. 218; IAHS: Wallingford, UK, 1993; pp. 289–296.
89. Boxall, K.; Willis, I.; Giese, A.; Liu, Q. Quantifying Patterns of Supraglacial Debris Thickness and Their Glaciological Controls in High Mountain Asia. *Front. Earth Sci.* **2021**, *9*, 504. [CrossRef]
90. Mayer, C.; Licciulli, C. The concept of steady state, cyclicity and debris unloading of debris-covered glaciers. *Front. Earth Sci.* **2021**, *9*, 710276. [CrossRef]
91. Anderson, L.; Anderson, R. Debris thickness patterns on debris-covered glaciers. *Geomorphology* **2018**, *311*, 1–12. [CrossRef]
92. Moore, P.L. Numerical Simulation of Supraglacial Debris Mobility: Implications for Ablation and Landform Genesis. *Front. Earth Sci.* **2021**, *9*, 595. [CrossRef]
93. Jumpponen, A.; Väre, H.; Mattson, K.; Ohtonen, R.; Trappe, J. Characterization of 'safe sites' for pioneers in primary succession on recently deglaciated terrain. *J. Ecol.* **2003**, *87*, 98–105. [CrossRef]
94. Marcante, S.; Erschbamer, B.; Buchner, O.; Neuner, G. Heat tolerance of early developmental stages of glacier foreland species in the growth chamber and in the field. *Plant Ecol.* **2014**, *215*, 747–758. [CrossRef]
95. Fickert, T.; Grüninger, F. High-speed colonization of bare ground—Permanent plot studies on primary succession of plants in recently deglaciated glacier forelands. *Land Degrad. Dev.* **2018**, *29*, 2668–2680. [CrossRef]
96. Eichel, J. Vegetation succession and biogeomorphic interactions in glacier forelands: Landform and Sediment Dynamics in Recently Deglaciated Alpine Landscapes. In *Geomorphology of Proglacial Systems*; Heckmann, T., Morche, D., Eds.; Springer: Cham, Switzerland, 2019; pp. 327–349. [CrossRef]
97. Woodward, F.I.; McKee, I.F. Vegetation and climate. *Environ. Int.* **1991**, *17*, 535–546. [CrossRef]
98. Barry, R.G. *Mountain Weather and Climate*, 3rd ed.; Cambridge University Press: Cambridge, UK, 2008; 532p.
99. Tackenberg, O.; Stöcklin, J. Wind dispersal of alpine plant species: A comparison with lowland species. *J. Veg. Sci.* **2008**, *19*, 109–118. [CrossRef]
100. Landolt, E.; Bäumler, B.; Erhardt, A.; Hegg, O.; Klötzli, F.A.; Lämmler, W.; Nobis, M.; Rudmann-Maurer, K.; Schweingruber, F.H.; Theurillat, J.-P.; et al. *Flora Indicativa: Ökologische Zeigerwerte und Biologische Kennzeichen zur Flora der Schweiz und der Alpen*; Haupt: Bern, Germany, 2010; 376p.
101. Biek, D. *Flora of Mount Rainier National Park*; Oregon State University Press: Corvallis, OR, USA, 2000; 506p.
102. Fischer, M.A.; Adler, W.; Oswald, K. *Exkursionsflora für Österreich, Liechtenstein und Südtirol*; Land Oberösterreich, Biologiezentrum der OÖ Landesmuseen: Linz, Germany, 2005; 1392p.
103. Körner, C. *Alpine Plant Life*, 2nd ed.; Springer: Berlin/Heidelberg, Germany; New York, NY, USA, 2003; 344p.
104. Bradshaw, A.D. Understanding the fundamentals of succession. In *Primary Succession on Land*; Miles, J., Walton, D.W.H., Eds.; Blackwell Scientific Publications: Oxford, UK, 1993; pp. 1–3.
105. Emmer, A.; Klimeš, J.; Hölbling, D.; Abad, L.; Draebing, D.; Skalák, P.; Štěpánek, P.; Zahradníček, P. Distinct types of landslides in moraines associated with the post-LIA glacier thinning: Observations from the Kinzl Glacier, Huascarán, Peru. *Sci. Total Environ.* **2020**, *739*, 139997. [CrossRef] [PubMed]
106. Gottfried, M.; Pauli, H.; Futschik, A.; Akhalkatsi, M.; Barančok, P.; Alonso, J.L.B.; Coldea, G.; Dick, J.; Erschbamer, B.; Calzado, M.R.F.; et al. Continent-wide response of mountain vegetation to climate change. *Nat. Clim. Change* **2012**, *2*, 111–115. [CrossRef]
107. Lawrence, D.B. Primary versus secondary succession at Glacier Bay National Monument, southeastern Alaska. In *Proceedings of the First Conference on Scientific Research in the National Parks, Orleans, LA, USA, 9–12 November 1976*; Transactions and Proceedings Series No. 5.; United States Department of the Interior, National Park Service: Washington, DC, USA, 1979; pp. 213–224.
108. Fischer, A. *Personal communication on subsurface ice on Jamtalferner*; Silvretta: Tyrol, Austria, 2021.
109. Cannone, N.; Diolaiuti, G.; Guglielmin, M.; Smiraglia, C. Accelerating climate change impacts on alpine glacier forefield ecosystems in the European Alps. *Ecol. Appl.* **2008**, *18*, 637–648. [CrossRef]
110. Fischer, A.; Fickert, T.; Schwaizer, G.; Patzelt, G.; Groß, G. Vegetation dynamics in Alpine glacier forelands tackled from space. *Sci. Rep.* **2019**, *9*, 13918. [CrossRef]
111. Gould, S.J. Is uniformitarianism necessary? *Am. J. Sci.* **1965**, *263*, 223–228. [CrossRef]
112. Ives, J.D. Biological refugia and the nunatak hypothesis. In *Arctic and Alpine Environments*; Ives, J.D., Barry, R.G., Eds.; Methuen: London, UK, 1974; pp. 605–636.
113. Stehlik, I. Nunataks and peripheral refugia for alpine plants during Quaternary glaciation in the middle parts of the Alps. *Bot. Helv.* **2000**, *110*, 25–30.
114. Brochmann, C.; Gabrielsen, T.; Nordal, I.; Landvik, J.; Elven, R. Glacial Survival or tabula rasa? The History of North Atlantic Biota Revisited. *Taxon* **2003**, *52*, 417–450. [CrossRef]
115. Stewart, J.R.; Lister, A.M.; Barnes, I.; Dalen, M. Refugia revisited: Individualistic response of species in space and time. *Proc. R. Soc. B: Biol. Sci.* **2009**, *277*, 661–671. [CrossRef]
116. Birks, H.J.B.; Willis, K.J. Alpines, trees, and refugia in Europe. *Plant Ecol. Divers.* **2008**, *1*, 147–160. [CrossRef]
117. Gavin, D.; Fitzpatrick, M.; Gugger, P.; Heath, K.; Rodríguez-Sánchez, F.; Dobrowski, S.; Hampe, A.; Hu, F.; Ashcroft, M.; Bartlein, P.; et al. Climate refugia: Joint inference from fossil records, species distribution models and phylogeography. *N. Phytol.* **2014**, *204*, 37–54. [CrossRef] [PubMed]

118. Seguinot, J.; Ivy-Ochs, S.; Jouvet, G.; Huss, M.; Funk, M.; Preusser, F. Modelling last glacial cycle ice dynamics in the Alps. *Cryosphere* **2018**, *12*, 3265–3285. [CrossRef]
119. Scherrer, D.; Körner, C. Topographically controlled thermal habitat differentiation buffers alpine plant diversity against climate warming. *J. Biogeogr.* **2011**, *38*, 406–416. [CrossRef]
120. Schönwiese, C. *Klimaänderungen: Daten, Analysen, Prognosen*; Springer: Berlin/Heidelberg, Germany, 1995; 224p.
121. O'Neill, B.; Kriegler, E.; Ebi, K.; Kemp-Benedict, E.; Riahi, K.; Rothman, D.; van Ruijven, B.; Vuuren, D.; Birkmann, J.; Kok, K.; et al. The roads ahead: Narratives for shared socioeconomic pathways describing world futures in the 21st century. *Glob. Env. Chang.* **2015**, *42*, 169–180. [CrossRef]
122. Zale, R.; Huang, Y.-T.; Bigler, C.; Wood, J.R.; Dalén, L.; Wang, X.-R.; Segerström, U.; Klaminder, J. Growth of plants on the Late Weichselian ice-sheet during Greenland interstadial-1? *Quat. Sci Rev* **2018**, *185*, 222–229. [CrossRef]
123. Wright, H.E.; Stefanova, I. Plant trash in the basal sediments of glacial lakes. *Acta Palaeobot.* **2004**, *44*, 141–146.
124. Gentili, R.; Baroni, C.; Caccianiga, M.; Armiraglio, S.; Ghiani, A.; Citterio, S. Potential warm-stage microrefugia for alpine plants: Feedback between geomorphological and biological processes. *Ecol. Complex* **2015**, *21*, 87–99. [CrossRef]
125. Parolo, G.; Rossi, G. Upward migration of vascular plants following a climate warming trend in the Alps. *Basic Appl. Ecol.* **2008**, *9*, 100–107. [CrossRef]
126. Chen, I.-C.; Hill, J.; Ohlemüller, R.; Roy, D.B.; Thomas, C. Rapid Range Shifts of Species Associated with High Levels of Climate Warming. *Science* **2011**, *333*, 1024–1026. [CrossRef]
127. Pauli, H.; Gottfried, M.; Dullinger, S.; Abdaladze, O.; Akhalkatsi, M.; Benito Alonso, J.-L.; Coldea, G.; Dick, J.; Erschbamer, B.; Calzado, R.F.; et al. Recent plant diversity changes on Europe's mountain summits. *Science* **2012**, *336*, 353–355. [CrossRef]
128. Carlson, B.; Georges, D.; Rabatel, A.; Randin, C.; Renaud, J.; Delestrade, A.; Zimmermann, N.; Choler, P.; Thuiller, W. Accounting for tree line shift, glacier retreat and primary succession in mountain plant distribution models. *Divers. Distrib.* **2014**, *20*, 1379–1391. [CrossRef]
129. Cannone, N.; Pignatti, S. Ecological responses of plant species and communities to climate warming: Upward shift or range filling processes? *Clim. Change* **2014**, *123*, 201–214. [CrossRef]
130. Lenoir, J.; Svenning, J.C. Climate-related range shifts—A global multidimensional synthesis and new research directions. *Ecography* **2015**, *38*, 15–28. [CrossRef]
131. Steinbauer, M.; Grytnes, J.A.; Jurasinski, G.; Kulonen, A.; Lenoir, J.; Pauli, H.; Rixen, C.; Winkler, M.; Bardy-Durchhalter, M.; Barni, E.; et al. Accelerated increase in plant species richness on mountain summits is linked to warming. *Nature* **2018**, *556*, 231–234. [CrossRef] [PubMed]
132. Lenoir, J.; Gégout, J.C.; Marquet, P.A.; de Ruffray, P.; Brisse, H. A significant upward shift in plant species optimum elevation during the 20th century. *Science* **2008**, *320*, 1768–1771. [CrossRef]
133. Engler, R.; Randin, C.F.; Thuiller, W.; Dullinger, S.; Zimmermann, N.E.; Araújo, M.B.; Pearman, P.B.; Lay, G.L.; Piedallu, C.; Albert, C.H.; et al. 21st century climate change threatens mountain flora unequally across Europe. *Glob. Change Biol.* **2011**, *17*, 2330–2341. [CrossRef]
134. Dullinger, S.; Gattringer, A.; Thuiller, W.; Moser, D.; Zimmermann, N.E.; Guisan, A.; Willner, W.; Plutzar, C.; Leitner, M.; Mang, T.; et al. Extinction debt of high-mountain plants under twenty-first-century climate change. *Nat. Clim. Change* **2012**, *2*, 619–622. [CrossRef]
135. Körner, C.; Hiltbrunner, E. Why is the Alpine Flora Comparatively Robust against Climatic Warming? *Diversity* **2021**, *13*, 383. [CrossRef]
136. Ter Braak, C.J.F.; Šmilaur, P. *CANOCO for Windows Version 4.5*; Biometris, Plant Research International: Wageningen, The Netherlands, 2002.
137. Lepš, J.; Šmilauer, P. *Multivariate Analysis of Ecological Data Using CANOCO*; Cambridge University Press: New York, NY, USA, 2003.

diversity

MDPI

Review

Purely Australian Essential Oils Past and Present: Chemical Diversity, Authenticity, Bioactivity, and Commercial Value

Nicholas John Sadgrove

Royal Botanic Gardens, Kew, Richmond, Surrey TW9 3DS, UK; n.sadgrove@kew.org

Abstract: In this comprehensive commentary, Australian essential oils and their components are listed and discussed in the context of their value to industry and aesthetics. The historic and cultural significance of endemic essential oils is explained. Several promising candidates are identified that have commercial potential and will enter the marketplace in the not-too-distant future. This text elaborates on the current progress in research, and explains the up-to-date view of 'bioactive,' with reference to insect repellence, antimicrobial activity, anti-inflammatory activity, and potential toxicity. The concept of chemotypes and chemophenetics is explained in detail to justify why chemically variable species in Australia require standardisation practices to ensure reproducibility of their derived natural products: standardisation practice includes cultivar development and authentication protocols. Thereafter, some of the more significant essential oils are defined and some background information provided. This review concludes with a comprehensive table of aromatic species that were studied by Joseph Brophy over the last 30 years, thereby providing the most comprehensive overview available, on the chemistry of Australian essential oil yielding species.

Keywords: industry; commerce; business; farming; chemistry; health; medicine

Citation: Sadgrove, N.J. Purely Australian Essential Oils Past and Present: Chemical Diversity, Authenticity, Bioactivity, and Commercial Value. *Diversity* **2022**, *14*, 124. https://doi.org/10.3390/d14020124

Academic Editor: Michael Wink

Received: 24 January 2022
Accepted: 8 February 2022
Published: 9 February 2022

1. Introduction

The two most famous Australian essential oils are tea tree oil (TTO) from *Melaleuca alternaifolia* (Maiden et Betche) Cheel., and eucalyptus oil from various species of *Eucalyptus*, particularly *E. radiata* Sieber ex DC (syn. *E. australiana*), and formerly *E. globulis* Labill. Both TTO and eucalyptus oil are sold in nearly every country of the world, making them two of the most successful natural products to enter the market since the start of the industrial revolution.

TTO and eucalyptus oil are defined in the British Pharmacopoeia and the International Standards Organisation (ISO) according to a specific chemical profile. Eucalyptus oil must contain >70% of a monoterpene oxide called 1,8-cineole [1], and TTO must include 14 ingredients, such as terpinen-4-ol, within a specific concentration range according to gas chromatography [2].

Standardisation across industry is a necessary measure to ensure that consumers pay for the same item as advertised [3]. While, today, most of the commercial crops give a product that adheres to the standards, they were established 50–100 years ago, so the farmers, wholesalers, and retailers are no longer interacting with wild plants. The wild Australian flora is highly chemically diverse, and chemical diversity occurs even within species. When aromatic species produce different types of essential oils, they are divided into varieties called chemotypes [2]. Thus, if farmers started new crops of TTO or Eucalyptus that were propagated from wild species, there is a strong chance that their product will differ dramatically from the defined standard.

All commercial crops were originally established from wild plants, and extensive bioprospecting, following by propagation from a single genotype, was a necessary undertaking to create today's industrial scale plantations that conform to the pharmacopoeia

standards. Commercial crops must, therefore, start from a single genotype, called a cultivar, so that there is chemical uniformity across the natural products in industry.

When studying essential oils, natural product chemists first look at the chemical phenotype (chemophenetics) of a species, then divide the species according to chemotypes [2]. Occasionally, the opposite happens; rather than finding chemotypes within species, the chemistry of one species is identical to another closely related species, meaning that one chemotype is assigned for several species. For this reason, even if it is from the wrong species, the chemistry of an essential oil can meet the requirements of the standard defined by the ISO.

For example, both the Australian standard (AS 2782-2009) and the ISO (ISO 4730:2004) define TTO as an oil produced from any one of multiple species, such as *M. alternifolia*, *M. linariifolia* Smith, and *M. dissitiflora* F.Muell. They also specify that any other species in *Melaleuca* that can produce an essential oil that matches the standard chemical profile is classified as TTO [2].

Paradoxically, the eucalyptus oil that is defined according to 1,8-cineole content (ISO 770:2002), usually has little to no globulol, which is an antimicrobial sesquiterpene [4] that is etymologically related to the name of the species *E. globulus*. So much value has been attributed to 1,8-cineole in meeting the pharmacopoeia standard that perceptions have conflated the value of 1,8-cineole and globulol is largely forgotten about. However, a well-rounded oil that is rich in 1,8-cineole with moderate amounts of globulol and aromadendrene is theoretically better for antimicrobial applications [5], particularly because of the synergistic antimicrobial combination between aromadendrene and 1,8-cineole [6]. Such a well-rounded essential oil can be produced by ensuring that the fruits (gum nuts or capsules) of *Eucalyptus* are included in the distillation with the leaves. However, today, this cannot be done, as the essential oil will not meet the pharmacopoeia standard.

There are several other Australian essential oils that are achieving national and international commercial success. For example, Australian sandalwood oil, from *Santalum spicatum* A.DC has been feeding the international market for over 185 years [7] as a variant of the East Indian and Indonesian sandalwood oil, from the species *S. album* L [8].

Another Australian oil that was called 'bastard sandalwood,' from *Eremophila mitchellii* Benth. [9,10], was also marketed as an alternative to Indian sandalwood, but it was a failure. It should have been branded separately because it was considered inferior to sandalwood. However, it would have been successful under another name, such as 'buddha wood oil,' which is adapted from its vernacular name 'buddha wood.' Fortunately, today, there is a market for buddha wood oil, and the branding has incorporated yogic stereotypes as a hook for practitioners of new age crafts.

There are several other Australian essential oils that have had a long history of moderate success in international trade. There are also many more that were never developed or have only recently been discovered. The current review article summarises the potential value of Australia as a source of unique essential oils, their roles in aesthetics or therapy, and how they are facing up to the marketplace.

2. Progress in Research

Research in the last 30 years on Australian essential oils has created a comprehensive overview of nearly all the aromatic species (Table 1 and Section 3) [11]. However, with repeated sampling of species that were previously studied, new information has emerged about the chemical diversity within each taxon. Some of this chemical information has supported taxonomic revision of species, but in most cases, taxa are split into chemotypes [12].

In going beyond chemical reports, studies of Australian essential oils and natural volatiles also focus on antimicrobial activity and their possible involvement in Aboriginal traditional medicine (ethnopharmacology) [12,13]. Antimicrobial effects from essential oils generally place them as antiseptic ingredients, such as topical anti-infectives and surface

sprays. Essential oil components are also known to exert immunological effects, but these are not explained by the outcomes of antimicrobial assays [14].

Antimicrobial outcomes are also influenced by synergistic effects between volatile organic compounds and fixed components in extracts [15,16], the concentrations are still many orders of magnitude above antibiotics [17]. Furthermore, antimicrobial outcomes are augmented when essential oils are delivered as vapours in warm air [18,19], but again, the inhibitory concentrations are only significant in the context of household usage, topical antiseptic use or in ethnopharmacology. Thus, the industrial development of essential oils should continue to focus on development of fragrances, aesthetics, and products for dermatological end uses.

During the last 50 years or so, studies of the Australian flora have described countless new molecules to science [2]. For this reason, there is minimal information related to the biological effects, or toxicity of exclusively Australian volatile organic compounds. Information is usually restricted to toxicity data from effects observed over the span of hundreds of years against grazing stock. Information of antimicrobial data is also readily available because it is generated quite easily in standard university labs [14,17].

2.1. Bioactivity of Australian Essential Oils

There is a significant number of volatile molecules that are only found in Australian aromatic plants. Many Australian essential oils contain these exclusive components, but they also include components that are familiar to other parts of the world. For this reason, an educated guess of the biological effects of Australian essential oils can be made by extrapolating from pharmacological information produced in other parts of the world.

2.1.1. Insect Repellent or Insecticidal Essential Oils

Cedrol and 8,14-cedranoxide are sesquiterpenes familiar to Mediterranean and Asian species in the family Cupressaceae [20–24]. Because both of these components were identified in *Eremophila sturtii* R.Br. [9], it is expected that biological effects converge between products from *E. sturtii* and Mediterranean Cupressaceae. To evidence this, 8,14-cedranoxide is the major insecticidal component of *Juniperus recurva* Buch.-Ham. ex D.Don [25]. As it is also present in leaves of *E. sturtii*, this explains the fly repellent effects achieved in traditional use of this species [9,26].

Australia is home to many insecticidal plants, but those that entered industry are limited to the termite resistance timbers. The observation of termite resistance in native timbers occurred in several waves. It is possible that Aboriginal people and early colonialists observed this phenomenon in wild trees, but no detailed records were found to confirm this. However, when the timbers were arbitrarily used in construction, their resistant properties were realized, and commercial initiatives quickly followed. The first to promote the use of these timbers was Joseph Henry Maiden [27,28], who made the knowledge public in the late 1800s to early 1900s.

Use of the timbers from *Eremophila mitchellii* was based on the observation that fence posts coincidentally made from the timber were still standing a century later [29], whereas other posts littered along the same fence line had disintegrated. A research group in Lismore (NSW) later demonstrated that the essential oils from the timber of *E. mitchellii* are a repellent against termites [30]. The active components are in the eudesmane and eremophilone class, including eremophilone, santalcamphor, and 9-hydroxy-7(11), 9-eremophiladien-8-one [10].

Maiden's observations were based on the timbers used to make houses. Timbers made from Australian species of cypress, from the genus *Callitris* (Cupressaceae), were resistant to termite infestation. He encouraged the establishment of a plantation of *Callitris endlicheri* (Parl.) F.M.Bailey as an export timber [28], but the costs of transporting the timber from NSW to the shipping ports in the Northern Territory proved economically unfeasible. However, several years after Maiden died (1859–1925), a plantation of *Callitris intratropica* R.T.Baker & H.G.Sm (accepted name is *C. columellaris* F.Muell. [31]) was initiated in the region near Darwin (Northern Territory).

During the years 1950–1974, the timber from *C. intratropica* entered the market and was being used in the construction of houses. However, in the year of 1974, a category 4 cyclone arrived on Darwin's shores, Cyclone Tracey. Most of the houses constructed from timber of *Callitris* were destroyed [2]. Thereafter, the plantation of *C. intratropica* was abandoned as a source of timber. In later years the plantation was accessed for the blue essential oil, which is used today in aesthetics. A possible dermatological application may involve inhibition of *Demodex* [32], which is a human ectoparasite that causes skin complaints in some individuals [33].

Lastly, there is an Australian essential oil that is rich in pregeijerene, which is a known insecticidal molecule, with activity against the tobacco cutworm, *Spodoptera litura* (F.) [34]. It is also an attractant to subterranean nematodes that feed on herbivorous insect larvae. A study of entomopathogenic nematodes demonstrated that the roots of species of the genus *Citrus* express pregeijerene. This sesquiterpene increases when herbivorous larvae, such as *Diaprepes abbreviatus*, graze on the roots, indicating that it is possibly a phytoalexin. The presence of pregeijerene then attracts nematodes that eat the herbivorous larvae and reduce their population density. These effects were also replicated in blueberry fields by attracting nematodes that eat the respective blueberry larvae, *Galleria mellonella* and *Anomala orientalis* [35].

2.1.2. Antimicrobial Effects of Essential Oils

There is a wide selection of possible applications for essential oils in aesthetics where antimicrobial activity is needed. Although essential oils are not considered a primary treatment for dermatological infections, they are preventative and can be used like a disinfectant [17]. Essential oils are better for antibacterial and antifungal applications than pure alcohol, because alcohol is quickly evaporated, whereas the essential oil components absorb into the dermis and confer protection for longer.

For example, medical practitioners will discourage self-treatment for potentially dangerous infections, such as staph or septic wounds, but they will accept use of essential oils to prevent spreading the infection, or to support antibiotic treatment. Some dermatological problems that will benefit from the antimicrobial effects of essential oils include acne [36], hair loss pathologies where overgrowth of *Propionibacterium* and *Malassezia* promote microinflammation [37,38], foot odours [39], athletes foot [40], and protection of skin grazes, cuts, or non-infected wounds.

Australian essential oils that have strong antimicrobial effects include TTO [41,42], some chemotypes of *Eremophila longifolia* [18,19,40], essential oil from some species of *Eucalyptus* [43], or from some species of *Prostanthera* [44–46]. Although there are many antimicrobial essential oils, the antimicrobial effects can be traced to active ingredients that are either common or are common in Australian species. For example, the antifungal oil from the Australian species *Zieria smithii* Jacks. is rich in elemicin [47], a known antifungal component [48].

In another example, several chemotypes of *Geijera parviflora* L. were identified and some demonstrated antimicrobial and antifungal activity. The most active essential oils were the green oils rich in geijerene and pregeijerene (35–50%), which are the components that taint the oil to the colour green. The antimicrobial effects of these components, in combination with linalool, were demonstrated against Gram-positive bacteria, and some fungal species in the genus *Trichophyton* [49]. This green essential oil is currently being developed for the market under the brand name 'green lavender.'

Geijerene and pregeijerene were also identified in the chemical profile of another Australian species, *Flindersia maculosa* (Lindl.) Benth [50]. Although these components, geijerene and pregeijerene, were first described in Australia, they have also been detected in essential oils distilled from African species [51]. They were also characterised at high abundance in a south Indian species, *Chloroxylon swietenia* DC. [34], which was used traditionally in anti-fungal applications by the south Indian people, giving a parallel to

in vitro data obtained on the Australian essential oil [49]. Lastly, pregeijerene is expressed in the roots of citrus, as previously mentioned [35].

Another exclusively Australian antimicrobial sesquiterpene comes from the genus *Prostanthera*. Essential oils from some species demonstrated relatively interesting inhibitory activity against Gram-positive organisms. The active component of the oils is named 'prostantherol,' which is evidently etymologically related to the genus from where it was first isolated [52]. The antimicrobial values were in the range of 125–250 ug.mL^{-1} [45], which is regarded as good in the context of an essential oil. As a comparison, a similar inhibitory concentration is achieved from TTO [53]. Furthermore, when the essential oils from *Prostanthera* were encapsulated using α-cyclodextrin, the antimicrobial effects were augmented by 2–5 folds, and Gram-negative organisms were also inhibited [46]. It is possible that the hydrophilic cyclodextrin exterior of the complex acts as a vehicle for the transport of lipophilic compounds across the periplasmic space, enabling essential oils to have inhibitory activity against Gram-negative microbes.

These types of synergistic antimicrobial effects also occur in nature, between two or more essential oil components [6], or in mixtures of essential oils and non-volatile components in the source plant material [15,16]. Synergistic antimicrobial effects are evident in TTO [54], and in the fruit essential oil from *Eucalyptus globulus* [6].

A very common essential oil component is globulol, which is one of the main ingredients from fruits of *Eucalytpus* and is responsible for the antimicrobial effects of many essential oils against Gram-positive organisms [4]. Another common component is aromadendrene, which was demonstrated to have an optimal synergistic combination with 1,8-cineole in antimicrobial outcomes [6].

Although the synergistic antimicrobial effects between 1,8-cineole and non-volatile components has not been investigated, it is encouraged to examine combinations between 1,8-cineole and the known antimicrobial meroterpenes. These unique meroterpenes represent condensation products between phloroglucinols and terpenes [55]. In a similar way to the effects of prenylation of flavonoids in augmenting antimicrobial outcomes [56], it is possible that the lipophilic terpene moiety of the antimicrobial meroterpene euglobal series [57] enhances the penetration ability into Gram-positive bacterial cells, conferring significant antimicrobial outcomes. The effects of terpenes to bacterial cell walls should, therefore, be explored in research of synergy between essential oil components and phloroglucinols.

2.1.3. Toxic Australian Essential Oils

Although essential oils cannot be compared to poisonous substances, such as the taxines from the genus *Taxus*, or the toxic pesticide strychnine from *Strychnos nux-blanda* A.W.Hill, some can be toxic at high doses. An example of such a compound known to be lethal with a high dose is ngaione [58], which is responsible for the deaths of grazing stock animals.

Sheep and cattle graze harmlessly on the species *Eremophila deserti* (A.Cunn. ex Benth.) Chinnock, which normally expresses a high yield of the iridoid methoxymyodesert-3-ene. However, the species is made up of several chemotypes, and one is the ngaione type [59], or types that include related furanosesquiterpenes. Because stock animals graze heavily on the species, *E. deserti* has been associated with animal fatalities, but the inconsistency in poisonings was a mystery until it was realized that toxicity was caused by a ngaione chemotype. The Australian desert genus *Eremophila* has several species that express furanosesquiterpenes like ngaione [59], and they should all be regarded as inedible.

Controversy over claims of toxicity also prevails in the context of essential oils. For example, a chemotype of *Eremophila longifolia* F. Muell. produced high yields of an essential oil with only two components, safrole and methyl eugenol [60]. Safrole was previously used as a flavour ingredient in soft drinks, but it was banned after a study in the 1960s demonstrated hepatotoxicity in mice, leading to the formation of liver cancers [61]. The mice were administered extremely high doses of safrole, and hepatotoxicity was related to some phase 1 metabolites [62], which have not been detected in humans. Safrole is

present in several herbs and spices that form part of a standard oriental diet. However, it is not natural for humans to be exposed to the levels like those mice in the assays that demonstrated hepatotoxicity.

Essential oils may also be considered toxic if they cross the blood-brain barrier and enact psychotropic effects that are either recreational, or at higher concentrations, dangerous. An example of a psychotropic essential oil component is elemicin. Elemicin is the major component of essential oil from *Myristica fragrans* Houtt., a herb that has been used and abused for its psychotropic effects [63,64]. While nutmeg is not an Australian species, several species in Australia express elemicin in their essential oil profiles. The best example is one of the chemotypes of *Zieria smithii* Jacks., which expressed 50% of elemicin, and an essential oil yield of 2% [47].

As a final example, animal studies were conducted to determine the toxic dose of 1,8-cineole. The 50% oral lethal dose of 1,8-cineole in mice is approximately 3.8 $g.kg^{-1}$ [65]. This is the equivalent of a human drinking approximately 200–500 mL of 1,8-cinoele liquid. It was later determined that reversable signs of toxicity occur over the course of 2–3 months with an oral dose of 0.19 $g.kg^{-1}$ (10–20 mL equivalent in humans). In the same study, no adverse effect was noticed at one third of that dose [65]. This illustrates that toxicity is relative to dose, and that even a household product, eucalyptus oil, that is widely considered safe, can be branded as a toxic item if it were not for the long history of safe use.

Although the above study reiterates that toxicity is dose and context specific, some consumers of essential oil products experience sensitisation due to allergy [66], which is not easy to predict using data from animal studies. However, it is more common that natural products are therapeutic within a reasonable concentration range, then become toxic above that concentration [3], as in the above example. Toxic effects can also either be persistent (chronic) or they reverse when the toxin has been metabolised and removed from the system.

In 1994, a case of poisoning from TTO was reported to the Journal of Toxicology: Clinical Toxicology [67]. It described the experience of a 23-month-old boy who ingested an entire 10 mL bottle of the liquid. According to the child's parents, he became confused and incapacitated (unable to walk) 30 min after ingestion, before being taken to a nearby hospital. Allegedly his condition steadily improved, he became completely asymptomatic after five hours and endured no long-term effects.

Unfortunately, knowledge of long-term effects of natural products from the Australian flora is unavailable, because Australia's recorded history is still young. Detailed records of long-term safe use are not available for most natural products and medicines. Although there is a rich ethnobotanical history with the Aboriginal people, so much of the information has been lost because of the cultural fragmentation that occurred with colonization. However, as previously mentioned, tentative knowledge of Australian botanicals will largely come from examples of chemically similar species in other nations that have more comprehensive written records and pharmacopoeias.

2.2. Chemophenetics of Natural Volatiles and Essential Oils

The chemical signature of natural volatiles and essential oils has found place in taxonomy, but not as a tool to delimitate taxa, but rather, as a tool for exploration. Chemophenetics may be defined as an exploration of chemical relationships, which can be either intraspecific (within species) or interspecific (across species). Chemophenetics focuses on small molecules, often natural volatiles, and essential oils, but it is not restricted to volatiles, because fixed components, such as flavonoids, saponins, coumarins and others, are also of interest in exploration of taxa.

The term chemophenetics was introduced as a replacement for the previous outdated terms, chemosystematics, or chemotaxonomy [68]. The new term was necessary because the older terms have become obsolete. When chemotaxonomy was initially finding place as a tool in taxonomic delimitation, the sudden development of complex phylogenetic and macro-molecular systematic techniques overshadowed chemotaxonomy. It is explained that

most importantly, chemophenetics contributes to the phenetic description of taxa, i.e., just like shape, colour and other physical characters, the chemical profile is a description of the specimen's phenotype, however, chemical profiles are not as easily determined as observable morphology.

In chemophenetic studies of taxa, if multiple specimens within or across taxa are chemically characterised, the data can be analysed by multivariate analysis, such as principal component analysis, or cluster hierarchical analysis. Thereafter, chemical patterns are determined within and between taxa. The type of data used for such studies can come from any chemical group, such as flavonoids, coumarins, saponins and volatile organic compounds. When volatiles are studied, they can either be in the form of an essential oil or as a solvent extract. Furthermore, chemophenetic studies can be enriched by acknowledging biosynthetic relatedness between components, or by using oxidation indices to add another layer of complexity to the analysis and tease out more relationships, particularly in the context of circadian rhythms [69].

2.2.1. Examples of Essential Oils in Australian Chemophenetic Studies

From hundreds of hydrodistillations of *Eremophila longifolia*, 12 or 13 potential chemotypes were discovered [59,60]. Samples were taken from across the continent, from a transect that spans 3300 km from east to west, and 1500 km north to south. It was revealed that chemical diversity within a radius of several hundred kilometres is similar to right across the country, from Sydney to Perth. For example, the borneol/fenchol type of *E. longifolia* in NSW is like the fenchol/borneol type in the Murchison district of WA. The only difference between the two is the relative expression of the two compounds, fenchol and borneol. Furthermore, the random populations or individuals that express karahanaenone are found purely by chance, right across the country [60].

In NSW, there is also a diploid population of *E. longifolia* that expresses high yields of a terpenoid essential oil with menthone and isomenthone as major components [40]. Another diploid population is in WA, also giving high yields of essential oil, but the major components are the phenylpropanoids, safrole and methyl eugenol [70]. A latter study demonstrated that diploid specimens of *E. longifolia* express high yields of essential oils from their leaves, in contrast to the tetraploids that express low yields [60]. Furthermore, within the distribution of the eastern Australian diploids that span from NSW into central Qld, there are several chemotypes, such as the karahanaenone type (White Cliff, Wilcannia, Cobar), the isomenthone/menthone type (White Cliff), and the piperitol type (Grey Ranges, Qld) [59].

According to biogeographic theory, the flora of the Murchison district of Australia is remnants of an 'eremaeon' stock of diploid species. It is postulated that in ancient history a post glaciation drought caused a continent-wide die-back of indigenous flora and the surviving species in the far west of WA recolonised the continent by developing polyploidy, increasing drought tolerance. Hence, the observation that tetraploid species of *E. longifolia* express lower yields of specialised metabolites is a validation of that hypothesis because the tetraploids are more resource efficient.

The chemophenetic study of *E. longifolia* cast doubt over the taxonomic rank of the diploid chemotype in WA. This is because it is the only chemotype among the 13 that has phenylpropanoid essential oils, whereas all others follow terpenoid biosynthesis. In this regard, the location in NSW known as Mutawintji NP should be explored as another potential 'eremaeon' stock, and it should be considered whether the Australia-wide tetraploids are descendants of the eastern diploids from that region, because they follow terpenoid biosynthesis, rather than the western diploids [60].

Furthermore, the leaves of the western diploid are a greyish green colour, and the growth habit is distinctly different. However, Robert Chinnock mentions that no floral or leaf characters are available to justify the splitting of the diploids [71]. Hence, it is necessary to investigate this further, perhaps by following a macro-molecular approach.

A chemophenetic approach was followed in exploration of the *Phebalium squamulosum* Vent heterogeneous species aggregate [72], using hydrodistilled essential oils. Patterns were identified that agreed with the newest taxonomic placements. The first finding came from a study of *P. squamulosum* subsp. *verrucosum* Paul G.Wilson, which has a stronger morphological relationship to the *Phebalium glandulosum* Hook., heterogeneous species aggregate. Hydrodistillation produced an essential oil at a yield of 2%, and the major component identified as dihydrotagetone [73]. This chemical observation validated the morphological relationship to *P. glandulosum* [74]. However, rather than correct subspecies placement, *P. squamulosum* subsp. *verrucosum* was elevated to species rank as *P. verrucosum* (Paul G.Wilson) I.Telford & J.J.Bruhl [75].

Hydrodistilled essential oils were also used in a chemophenetic study of the *Prostanthera lasianthos* Labill., heterogeneous species aggregate, which identified chemotypes within single taxa that resulted from phenotypic plasticity of volatiles, in response to soils, moisture and shading [76]. In this latter case, the chemophenetic data was not taxonomically informative [77]. Conn et al., [77] stated that:

> "no dataset has primacy in defining segregate taxa, and ... a combination of morphological and molecular data was required to determine the taxa within."

This reiterates the objective of chemophenetics, which is not to use a chemical profile as a taxonomic tool, but rather, to describe the phenotype and look for patterns, which could be related to taxa or to other variables, such as abiotic factors. Whether or not it supports taxonomic delimitation is a matter of context and if it represents the converging effect of multiple lines of evidence, as was explained by De Queiroz [78].

2.2.2. Examples of Solvent Extracted Volatiles in Australian Chemophenetic Studies

Chemophenetic studies have recently started to use single leaf extracts as an alternative to essential oils that require laborious, time consuming and energy-taxing hydrodistillation. In this approach, a small leaf, or fragment of big leaf, is extracted into approximately 2 mL of solvent, which is usually dichloromethane, hexane, or ethyl acetate, and less commonly ethanol or methanol.

Organic solvents extract the volatile components and non-volatile or semi-volatile components that have vapour pressures too high to be afforded by hydrodistillation. Some of these compounds still have a vapour pressure, but it is not high enough for the component to be driven into the essential oil during hydrodistillation. However, their vapour pressures are still high enough for them to be detected by GC-MS. This means that the chemical profiles of solvent extracts often include more than just the essential oil components. If the GC-MS operating conditions are manipulated so that the column is heated to its highest temperature and held for 20–30 min, components with lower vapour pressures will also be detected, even if they are absent from the essential oils.

An example of where a solvent extract was used as part of a chemophenetic study, includes the work of Collins et al. [79,80], who created a taxonomic revision of *Eucalyptus magnificata* L.A.S.Johnson & K.D.Hill. This species normally produces a high yield of an essential oil in hydrodistillation, made up of the three eudesmol isomers, i.e., α-, β-, and γ-eudesmol. However, when using solvent extracts in the place of essential oils the dominant component was cryptomeridiol [79,80], which is a biosynthetic precursor to the eudesmol isomers. In hydrodistillation, cryptomeridiol undergoes a heat-driven elimination of the hydroxyl moiety (loss of water) at position four, which instils a double bond that randomly occurs in one of three directions, i.e., α- = 3(4), β- = 4(14), and γ- = 4(5), creating the three isomers. Hence, a solvent extract is significantly different by comparison with the essential oil.

In another example, the heat labile precursor to spathulenol, bicyclogermacrene [81], was of high relative abundance in solvent extracts of taxa in the *Phebalium nottii* (F.Muell.) Maiden & Betche heterogeneous species aggregate [82], whereas hydrodistillation afforded spathulenol-rich essential oils. Furthermore, the use of solvent extracts revealed several semi-volatile coumarins that are too 'heavy' to be driven into the essential oils. From

this study the semi-volatile coumarin myrsellin stood out as a taxonomic marker for the putative new taxa, *P.* sp. Goobang and *P.* sp. Texas, which have subsequently been joined as a single taxon awaiting a taxonomic rank. In this context, the use of solvent extracts in the place of essential oils was more informative in the chemophenetic study, because more chemical information was obtained.

2.2.3. Chemophenetics as an Authentication Tool

In the current paradigm of natural products in health, the opportunism in industry has become polarised between honest and dishonest marketing. The consumer is understandably concerned that their turn to health is contradicted by products that are not authentic, that harm health rather than confer the effects described in scientific studies. The rise in counterfeited items in the marketplace has been met with authentication initiatives that aim to help the consumer to have faith in the product, and to help the company be rewarded for their honesty [3].

Chemophenetic studies may be regarded as a powerful tool to be used in the authentication of essential oils and aromatic extracts. This is because chemophenetics is the best procedure for the determination of natural variation in essential oil profiles, before standards are stipulated. The authenticator might observe chemical variation of an essential oil and determine that it is natural and not a sign of tampering or adulteration, because a chemophenetic study demonstrated the same variation.

Furthermore, chemophenetic studies identify chemotypes. Knowledge of chemotypes informs authenticators about expected differences within a single species. Armed with this knowledge the authenticator will recognise that an apparent substitution is the unintended outcome of harvesting plant material from a different chemotype, but not the wrong species, causing a non-match to the known standard defined in the pharmacopoeia or by ISO. Chemotypes can be recognised according to a unique chemical profile but claims in the marketplace need to be consistent with the standard described for that chemotype.

3. Natural Volatiles in Ethnopharmacology

In Australia there is a high proportion of endemic aromatic species, by comparison with the other continents. There are also a significant number of aromatic species utilised by the Aboriginal people, past and present. Thus, volatile organic compounds feature prominently in the *materia medica* of Australia's first people.

3.1. The Eucalyptus Paradox

Paradoxically, there is limited information on how species of *Eucalyptus* were used in traditional medicine. Although there are numerous articles on the web, and in the published literature [83], that present *Eucalyptus* as an ethnobotanically significant genus, the truth is that records of traditional use are scarce. Lassak and McCarthy [84] also observed this paradox and stated that the northern species of *Eucalyptus* contain irritants and were unlikely to have been used in fumigation type medicine, however, the southern and eastern species were an obvious good choice for therapeutic use. They went on to present the theory that because the south-eastern part of the country was the first place to be colonized, the culture of the Aboriginal people was fragmented before ethnobotanical records were made of their use of *Eucalyptus*.

While it seems odd that there are no records, it is also possible that species in *Eucalyptus* were used as warm vapours. Although this was not observed, it has been extrapolated from archaeological findings of 'hot oven rock' that are associated with procedures designed to drive vapours out of the leaves of aromatic species [85]. The procedure involved the lining of a hole in the earth with hot rocks that were heated over a fire. The hot rocks were then overlaid with aromatic foliage, followed by the patient, then sealed. The ground oven was closed with enough soil to cover the body, but not the face or head of the living patient. The reason archaeologists believed that species from *Eucalyptus* were chosen for this procedure is that the vegetation in the respective region was limited to that genus.

3.2. How Volatile Organic Compounds Were Used in Ancient Australian History

In the Australian flora there are several antimicrobial and anti-inflammatory compounds that are present in the essential oils [2]. The traditional Australian people did not use essential oils per se, because distillation apparatus was not available. Instead, they utilised volatile organic compounds in the form of poultices, fat extracts and vapours [86].

Volatile organic compounds are often directly responsible for the therapeutic outcome of a medicinal application, but they are also involved in synergy with fixed medicinal compounds. While there is limited empirical work to support this latter observation in the Australian context, studies on African aromatic species have confirmed that synergistic effects occur between fixed and volatile components [15,16,87].

One way that the volatiles of aromatic plants were used by traditional Australian people was by direct inhalation of the vapours emitted by crushed aromatic plant material. The aromatic poultice was held to the nose, or near the nose, and the vapours inhaled. Species with written records confirming this include *Eremophila bignoniiflora* (Benth.) F.Muell. [88], and *Pittosporum angustifolium* G.Lodd. [89]. However, it is likely that vastly more species were used in this way, but records were not made by the colonialists or early ethnobotanists who observed this.

Aromatic species were also pulverised and applied to the surface of the skin. Because volatile organic compounds are lipophilic, they partition into and across the dermis. Thus, aromatic species that were applied to the skin as a poultice targeted both superficial and deeper ailments, possibly related to infection or inflammation [86].

Volatile organic compounds were also extracted into animal fat (and maybe fixed plant oils). The aromatic species were pulverised and mixed with fat, and the fat used for topical applications [84,90]. This method was possibly chosen to improve the longevity of aromatic species (for travel) and to encapsulate volatiles to improve flux into the dermis.

Evidently in all the above scenarios, the volatile organic compounds are delivered to the dermis in combination with fixed compounds. In such cases, synergistic effects are possible between volatiles and fixed components. However, in the final example, vapours were also utilised by placing aromatic foliage over the smouldering embers of an extinguished fire. Although records of how many species were utilised this way are limited, there is strong evidence that species in *Eremophila* were used, such as *E. sturtii*, *E. longifolia*, *E. bignoniiflora*, and *E. freelingii* F.Muell. [85]. Furthermore, a desert species named *Prostanthera striatiflora* F.Muell., and two temperate species, *P. angustifolium* and *G. parviflora* were also observed in such modalities and recorded before the information was lost [85].

One variation of body fumigation with aromatic vapours involved the use of a bark hut to contain vapours (and artefact aerosols). This was evidently practiced with species from *Eremophila* and may have been practiced using other species. Communications from surviving traditional elders of the Gamilaraay nation describe using *E. bignoniiflora* and *E. longifolia* this way [86].

When the fumigation ritual of *E. longifolia* was replicated in a university laboratory, a heart-derived artefact was produced that had antimicrobial activity that was stronger than the volatile organic compounds naturally present in the leaves. The product was a furan aldehyde; thus it was named 'genifuranal' because it is believed to be a derivative from geniposidic acid [18]. Genifuranal may be a contributor to other biological effects that have been described for this species.

The use of *E. longifolia* in fumigation rituals, either over open embers or in a closed hut, was practiced widely across the Australian continent, but there are some places where this practice was not active. In the same study that identified genifuranal, it was observed that some specimens of *E. longifolia* did not yield genifuranal, despite having the same essential oil profile as the ones that did. Furthermore, the diploid specimens did not yield genifuranal on any occasion [18]. This explains why there was variation in traditional use of this species in fumigation rituals.

4. Significant Genera and Industrial Progress

Several species and genera have potential but have not yet found a niche in the essential oils industry. In this section, some of the most promising candidates are discussed, with consideration to feasible yield and novelty.

4.1. Prostanthera (Lamiaceae)

This genus is currently undergoing extensive taxonomic revision, particularly the *Prostanthera ovalifolia* R.Br. [44,45,52,91–93], and *P. lasianthos* Labill. [76,77], heterogeneous species aggregates. In the *P. ovalifolia* group, several sesquiterpenes are expressed singularly or in combinations, commonly diluted by 1,8-cineole [44]. The sesquiterpenes, such as maaliol, prostantherol, cis-dihydroagarofuran and kessane, have minimal dedicated pharmacological research (Figure 1). However, in the *P. lasianthos* group, the essential oils are predominantly monoterpenoid in character, including 1,8-cineole, linalool, linalyl acetate, butanoic esters, and occasionally, pinene isomers [76].

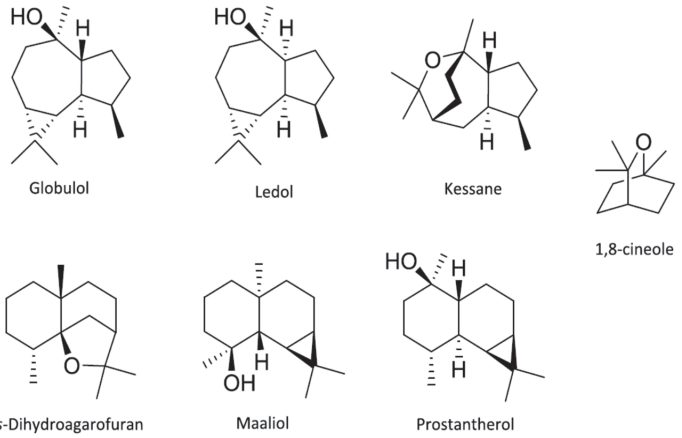

Figure 1. Major sesquiterpenes and 1,8-cineole in the *Prostanthera ovalifolia* heterogeneous species aggregate.

4.2. Eremophila and Myoporum (Scrophylariaceae)

These two genera are regarded as clade sisters. Chemophenetic discoveries of *E. longifolia* were elaborated upon in Section 2.2.1. *Eremophila* is a genus of over 200 species [71], but the number is rising as new species are discovered or segregated. Similarly, *Myoporum* is also comprised of a phenotypic and chemical diversity that is nearly comparable to that of *Eucalyptus*.

Species in Myoporum are occasionally revised and placed into *Eremophila*. This is what happened to *Eremophila deserti* (A.Cunn. ex Benth.) Chinnock, which was chemically characterised under its previous name, *Myoporum deserti*, during the late 20th century. This species is morphologically consistent across its distribution, yet its chemophenetic pattern is varied significantly. The combination of past and present data confirms that *E. deserti* includes over five chemotypes [59]. It is noteworthy that there is no geographical pattern to these chemotypes. Furthermore, multiple chemotypes of *E. deserti* are often found growing together in the same population.

Due to the high yield of the essential oil from leaves of *E. deserti*, that is sometimes dominated by a single component, there is an opportunity to use the components as precursors for industrial scale synthesis to produce known or therapeutic compounds. A similar observation is made for *Eremophila dalyana* F.Muell., which produces a high yield of an essential oil dominated by myodesert-1-ene [94].

4.3. Correa (Rutaceae)

It is strange that the chemical character of the essential oils has not been published for members of this genus. However, this may be due to the chemical diversity within the essential oil profile, which is an apparent insurmountable obstacle to quality data reporting. This was experienced by the author who produced essential oils from the three known variants within *Correa glabra* Lindl., which are *C. glabra* var *glabra*, *C. glabra* var *leucoclada* (Lindl.) Paul G.Wilson and *C. glabra* var *turnbullii* (Ashby) Paul G.Wilson. The essential oils from all three variants were populated by hundreds of components in some cases. However, by focusing on only the major components, comments on the chemical character can be made.

The essential oil from the taxon known only as *C. glabra* is rich in the phenylpropanoid elemicin and two other phenylpropanoids that were not successfully identified. This taxon also had several sesquiterpenes in its profile, including cubebene and bisabolene. The taxon *C. glabra* var *glabra* has two morphological variants, one with long leaves and the other with shorter leaves. The two had strikingly different chemical profiles, with the long leaf variant dominated by sesquiterpenes, mostly azulene derivatives, and the short leaved variant had a monoterpenoid composition, thujene and terpinolene. The taxon named *C. glabra* var *turnbullii* produced an essential oil that was part terpenoid and part pheylpropanoid, comprising elemicin, β-phellandrene and thujene. A similar essential oil profile was determined for *C. glabra* var *leucoclada*, but the phenylpropanoids were more diverse, also including anethole and estragole, in addition to elemicin, phellandrene and thujene. The essential oils that were mixtures between phenylpropanoids and monoterpenes demonstrated the strongest antimicrobial effects, which were evident against both Gram-positive and Gram-negative bacteria.

4.4. Geiera (Rutaceae)

Nearly 90 years ago today, Arthur Penfold encouraged the commercialization of essential oils from *Geijera parviflora* [95]. The species includes several chemotypes, and strong overlap with *G. salicifolia* Schott [49]. Among the several chemotypes is the xanthoxylin type (phloroacetophenone dimethyl ether). During hydrodistillation the compound crystallises onto the condenser, creating the appearance of a paraffin-type wax, but it is evidently a volatile compound. Xanthoxylin is also known under the vernacular name brevifolin, which is the name used with reference to pomegranate (*Punica granatum* L). This chemotype is currently being explored as a supply for Australian natural product industries and a topical cream is under development that includes xanthoxylin at a concentration of 0.1%.

Another chemotype from *G. parviflora* is the geijerene/pregeijerene chemotype described earlier. The green essential oil will be marketed under the vernacular name 'green lavender' and it will also be used in dermatological applications. The reason for using the name 'lavender' in the branding is due to an old vernacular, lavender bush, used to describe this chemotype. The note that influences likeness to lavender is the co-major component linalool [49].

4.5. Melaleuca (Myrtaceae)

The TTO industry was starting to gain momentum in the 1920s [95]. In 1929, Penfold wrote under the image of *M. linariifolia*:

> "The essential oil derived from this tree, which is one of a number of trees and shrubs known collectively as Tea Trees, is about to be placed upon the markets of the world." [96]

Only three years after Penfold's prescient observation, he reported back on the progress that had been made in the commercial development of TTO. He reported that the oil had achieved an exalted status in medicine and dentistry, and that those who had entered the market with the oil disguised the ingredient to protect their commercial interest. Thus, TTO was marketed as 'ti-trol' as a pure oil, and in a 40% soap solution, it was branded

as 'melasol' or 'intol' [95]. These brands were still in the market by 1954 (22 years later) according to a much older Penfold [97].

Penfold was also insistent that the 1,8-cineole content must be kept below 10% to avoid dilution of the medicinal benefit, particularly when used in surgery for sterilisation. His earlier comments influenced the formation of the modern ISO standard for the terpinen-4-ol type. He also described the use of TTO in munitions factories during WW2, by incorporation of 1% into machine cutting oil to reduce infection of skin injuries. TTO was also used by the soldiers in the WW2, as it was a compulsory item in the first aid kit, also for sterilization and prevention of infections.

After WW2 demand for TTO declined and the success of antibiotics overshadowed TTO for another 20 years, until a renaissance of nature occurred in the 1970s [41]. At this time plantations were established and TTO entered the market as a lifestyle product, rather than a medical liquid. One of the major suppliers of TTO today is the Thursday Plantation.

4.6. Backhousia (Myrtaceae)

A species that captured the attention of Penfold was *Backhousia angustifolia* F.Muell., which contained a very unusual triketone called angustione [95]. Although the species has since been demonstrated to contain five chemotypes, three of which include unusual monoterpenes [98], they never had the same success as *B. citriodora* F.Muell. Today the species is used to flavour soaps that have a market across the globe. The essential oil of the popular chemotype is dominated by citral [98], which is a mixture of two aldehydes, namely geranial and neral [99].

In the 1950s, Penfold described the *l*-citronellal chemotype of *B. citriodora,* which was a serendipitous discovery made by a farmer who noticed the difference of aroma between leaves he was foraging for distillation [97]. Brophy et al. [100] commented that this chemotype was 'lost' for nearly 40 years before it was rediscovered in 1996. The concern was that it became of interest, because of yields of approx. 3%, making it feasible as a feedstock for the perfume industry. The citral chemotype of *B. citriodora* is already a well establish commercial essential oil, however, it is likely that Brophy's work has led to the establishment of plantations that use the citronellal chemotype.

4.7. Leptospermum and Kunzea (Myrtaceae)

Leptospermum and *Kunzea* are regarded as clade sisters. The two produce chemically diverse essential oils across the genus. One that is worth mentioning is *Leptospermum micromyrtus* Miq., which grows as thick impenetrable scrub at the top of mountains in Australia's capital territory, south of Canberra. The leaves yield an essential oil on hydrodistillation at 1–2%, dominated by the eudesmol isomers (α-, β-, and γ-) [101]. This sesquiterpenoid oil solidifies shortly after its production, taking on the appearance of a camphor block.

It was demonstrated that the chemistry of essential oil from species of *Leptospermum* can be influenced by availability of soil nitrogen [102]. This was evident in two out of the three species examined, *L. petersonii* F.M.Bailey., and *L. flavescens* Sm. Higher nitrogen content resulted in reduced expression of α- and β-pinene.

Penfold was fond of *L. liversidgei* R.T.Baker & H.G.Sm., as a source of essential oil [96], which is rich in citral, and another chemotype is rich in citronellal. However, both chemical profiles can be produced by two chemotypes of *Backhousia* that have higher yields, thus interest in these species waned.

Despite the efforts of Penfold, only two species of *Leptospermum* are commercialised today, which are unfortunately not those that captured his interest. One is produced from *L. petersonii* by the company "Essentially Australia." They branded it as 'Australian rose' or 'rose myrtle' and the chemistry demonstrates why this name was chosen. The chosen chemotype, chemotype b, is rich in geranyl acetate, γ-terpinene, geraniol, terpinolene, α-pinene, p-cymene, and linalool [103]. This is like the chemistry in the headspace of some roses [104].

The other species that is marketed by "Essentially Australia" is *L. scoparium* J.R.Forst. & G.Forst., which is being called manuka essential oil. It is the same species that produces the flowers that bees use to make manuka honey. The essential oil is dominated by a β-triketone named grandiflorone [105]. Although this species is from New Zealand, a similar essential oil is produced from *L. morrisonii* Joy Thomps [106]. Furthermore, the triketone grandiflorone was first described by Penfold's successor, Hellyer, who isolated it from the Australian species *Leptospermum grandiflorum* G.Lodd., and *Leptospermum lanigerum* (Aiton) Sm [107].

The sister genus of *Leptospermum*, namely *Kunzea*, includes several putative new species. Several of the new or known species have been chemical studied. *Kunzea ambigua* (Sm.) Druce is a Tasmanian species that has the vernacular name 'tick bush,' due to the tick repellent effect. This property was realized when farmers observed that wild animals preferred to shelter under this bush. It was eventually discovered that the foliage protected them from tick infestation. The essential oil from this species is available from 'Essentially Australia.' The chemistry includes α-pinene, 1,8 cineole, globulol, viridifloral, and bicyclogermacrene [108].

4.8. Philotheca and Eriostemon (Rutaceae)

Many species that were once in the genus *Eriostemon* have been placed into *Philotheca*. One of the species know previously as *Eriostemon myoporoides* is now known under the accepted name of *Philotheca myoporoides* (DC.) Bayly. The species is also divided into five subspecies.

In 1925, Penfold published a chemical characterization of the essential oil of *E. myoporoides*, that is known today as *P. myoporoides* subsp. *myoporoides*, which grows in the mountains of the Hunter Valley in NSW. Penfold reported that the essential oil is dominated by α-pinene, camphor and ocimene [109].

The author has been to the place where Penfold made his collection (Mt Dangar, Sandy Hollow), and it was found growing alongside *Prostanthera prunelloides* R.Br. It is likely that Penfold also collected *P. prunelloides* because nearly 40 years later his successor, Hellyer, found an essential oil in Penfold's retired laboratory that was dominated by maaliol [110]. In a recent study, the essential oil from the leaves of *P. prunelloides* was characterized and demonstrated to be dominated by maaliol [44]. However, the sample was mislabelled as *E. myoporoides*, thus Hellyer incorrectly described the essential oil from *E. myoporoides* as maaliol. This was in error, because Penfold had previously published the composition, as mentioned above.

Thus, it is likely that Penfold had incorrectly labelled the sample of *P. prunelloides* that he collected the same day of collection of *E. myoporoides*. He probably declined to publish the composition when he saw an inconsistency. This error is likely to have occurred because the leaves of *P. prunelloides* radically change shape in mountainous cliffs, becoming morphologically like *Eriostemon*. Thus, on the day of collection the samples were incorrectly labelled.

4.9. Syzygium (Myrtaceae)

The essential oil from *Syzygium oleosum* (F.Muell.) B.Hyland. is being called 'mango myrtle' in the Australian essential oils market (Essentially Australia). This species is commonly known as 'lily pily' and produces a little pink-red fruit that is edible. The essential oil was previously available commercially, but the plantation has been very recently established and it may take time to reach sustainable levels. Greg Trevena is currently growing a plantation outside of Byron Bay, NSW.

Another species is *Syzygium anisatum* (Vickery) Craven & Biffin, previously known as *Backhousia anisata*, and *Anetholea anisata*. The essential oil is very similar to that of anise, with phenylpropanoids that confer the liquorice aroma. This essential oil has had more success in the industry than other species in the same genus.

4.10. Calytrix (Myrtaceae)

Another essential oil from 'Essentially Australia' is made from a species endemic to Western Australia, named *Calytrix exstipulata* DC., or by the vernacular 'Kimberley Heather.' The essential oil is dominated by the pinene isomers, pulegol, isopulegol, aromadendrene, and ledene [111].

4.11. Cassinia (Asteraceae)

The genus *Cassinia* is known widely as 'native rosemary,' but the resemblance is poor. The species has foliage that can be mistaken for that of *Rosmarinus*, or *Melaleuca*, but *Cassinia* belongs to Asteraceae, and this is evident when in flower. The best essential oil from *Cassinia quinquefaria* R.Br. was produced by the author from the flower calyx, which gave a high yield of a predominantly monoterpenoid oil. This is consistent with a chemical report of an oil dominated by the pinene isomers from the same species [112].

The other common species is *C. laevis* R.Br., which has a subspecies by the name of *Cassinia laevis* subsp. *rosmarinifolia* (A.Cunn. ex DC.) Orchard. This is probably due to the apparent resemblance to rosemary. The essential oil is also dominated by α-pinene, but also includes some spathulenol and viridiflorol [113].

4.12. Eucalyptus and Corymbia (Myrtaceae)

The vernacular name used for the smooth barked Australian eucalyptus tree is the 'gum tree.' Most people are unaware that the name derives from the ironbark species and not the smooth bark. The name was also given in error, because the intention was to define a tree that exudes a water-soluble sap called a 'gum.' But the actual product is correctly known as a 'kino,' which is an astringent tannin that was used as a 'bitter' for general health in the 1800s. The kino was produced from the bark of the ironbark [84,96].

In 1929, Penfold explained that the first medicinal oil used from a species of *Eucalyptus* was far removed from the current standard prescribed by the ISO (ISO 3065:2021). It was distilled from *E. piperita* J.White., in 1788, by a surgeon on the first fleet, Dr John White, who was initially attracted by its resemblance to the mint familiar to Europe. The major component is piperitone, which is used today to manufacture menthol by reduction, or thymol by oxidation. Today the main species used to feed the piperitone industry is *E. dives* S.Schauer. Nevertheless, Penfold commented that the standard for eucalyptus oil, with a requirement of >70% 1,8-cineole, is at odds with the oils that are used in therapy, or for that matter, the oil that was first used in commerce [96].

Although the first cineole oil was produced from *E. globulus*, this species is no longer the major biota that feeds the eucalyptus oil industry. This is because the yield of 0.75% is lower than that from a chemically similar alternative, *E. radiata*, which gives a yield of 2–3%.

More recent work by Boland et al. [114] demonstrates that the essential oils across the 300 or so species in the genus *Eucalyptus* are extraordinarily chemically diverse. Some of the more common species in industry include *E. phellandra* R.T.Baker & H.G.Sm., which is etymologically related to its major component phellandrene, *E. macarthurii* H.Deane & Maiden, which is a source of geranyl acetate, and *E. citriodora*, which has recently been taxonomically revised to *Corymbia citriodora* (Hook.) K.D.Hill & L.A.S.Johnson. This latter species has the vernacular name 'lemon scented gum' and is a popular fragrance in remote communities. The dominant component in the essential oil is citronellal [96], which can be used as an insect repellent [115].

4.13. Phebalium and Leionema (Rutaceae)

Phebalium and *Leionema* are regarded as clade sisters. Aside from taxa in the *P. glandulosum* complex [73], the two genera do not produce high yields of essential oils. Thus, research on volatiles has centered on chemophenetics in heterogeneous species aggregates. As mentioned in Section 2, much work needs to be done on *P. squamulosum* to get it taxonomically correct. An initial study was completed by Brophy et al. [116], which

gave single specimens from each species. Then when more samples were analysed, it was realized that intraspecific variability is common. Furthermore, during that chemophenetic study it was realized that the etymologically related sesquiterpene 'squamulosone' is detected in only a limited number of taxa. The remaining taxa yields predominantly hedycaryol, which is converted to elemol in hydrodistillation [72].

One of the best known species from the genus *Leionema* is the 'fruit salad plant' known botanically as *Leionema ambiens* (F.Muell.) Paul G.Wilson. The species grows in the granite mountainous terrain of regional NSW and when in flower it puts a fruity scent into the air that can be perceived from hundreds of metres away. The aroma was studied by Brophy et al. [117] and revealed to be dominated by the *cis*/*trans* isomers of β-ocimene.

4.14. Boronia (Rutaceae)

For well over 100 years, an essential oil has been marketed from Tasmania that is extracted, not distilled, from the flowers of *Boronia megastigma* Nees ex Bartlett. In earlier practice, the flower was hydrodistilled, but Penfold explained that the aroma changes considerably in hydrodistillation and a significant loss of volatile organic compounds occurs. To retain the compounds and to maintain a pleasing aroma, the plant is extracted into petroleum ether (pentane/hexane) and a 'concrete' is produced, which is an aromatic resin that contains the volatile component β-ionone and the flower's waxes [95].

This is consistent with the author's observations in distillation of other species in *Boronia*. Although the leaves and flowers are strongly aromatic and the odour is pleasant, on distillation the odour becomes unpleasant and scarcely any of the volatiles are captured. This is because of the high solubility of components in the hydrosol, which prevents phase separation of the volatile organic compounds.

In 1929, Penfold listed four species of *Boronia* that he considered of potential commercial value. These are *B. pinnata* Sm, *B. muelleri* (Benth.) Cheel., *B. thujona* Penfold & M.B.Welch., and *B. safrolifera* Cheel. It is noteworthy that the latter two species are named according to the dominant component in their essential oil, i.e., *B. thujona* expresses thujone in its essential oil and *B. safrolifera* expresses safrole. Unsurprisingly, Penfold is an authority on the species named *B. thujona* [96].

4.15. Callitris (Cupressaceae)

Although there are 20 or so accepted species of *Callitris*, there are four that are known widely in Australia [32,118]. Two of these major species are *C. endlicheri* (Parl.) F.M.Bailey., and *C. columellaris* F.Muell. As of today, the World Checklist of Vascular Plants does not recognise the two other major species. Both *C. glaucophylla* J.Thomps. & L.A.S.Johnson and *C. intratropica* R.T.Baker & H.G.Sm. are currently regarded as synonyms of *C. columnellaris*, yet they stand out as distinct chemical entities in chemophenetic analysis [32]. Today they are tentatively regarded as chemotypes before an international audience but are regarded as distinct species within Australia.

Whether *C. columellaris* occupies a large or small geographic area is a matter of debate. If *C. glaucophylla* is recognised internationally, as it is in Australia, then it occupies the greatest land area of all *Callitris* and the range of *C. columellaris* is reduced to coastal areas in the Brisbane area.

The chemical differences between species are evident in the essential oil from timber and leaves, and in the non-volatile components too. The leaves of *C. glaucophylla* express the abietanes pisiferic acid, pisiferal and pisiferol. These were not detected in the leaves of *C. columellaris* or *C. intratropica*. The timber of *C. intratropica* is rich in guaiazulene, which is responsible for the blue colour of the oil. This component is not present in the timber essential oil of the other two species. However, despite their chemical differences, all four of the species yield a wood oil that is dominated by guaiol, which has an earthy aroma that can also be detected when burning the timber [32]. Today, there are still some Australians from remote regions who understand the following quote from Sir Joseph Henry Maiden more than 100 years ago in reference to *C. glaucophylla* (White Cypress Pine):

> "there is nothing more delightful in the approach, on a winter evening, to a township where Cypress pine is used as a fuel. Its delicious perfume is borne on the air for miles, and is often the first intimation that the weary traveller experiences that he is approaching a human habitation, and that his long journey is drawing to a close." [119]

4.16. Santalum (Santalaceae)

For over 185 years, the essential oil from *Santalum spicatum* was used to produce one of the most popular forms of sandalwood essential oil [95]. However, the species is facing sustainability issues, which is a consequence of over harvesting from wild populations. Because the tree is a hemiparasite, it is difficult for the seedlings to become established, making it difficult for the population to recover naturally. Today it is illegal to harvest the species from the wild in South Australia, but it is not recognised as a threatened species in Western Australia, even though the same population decline is evident in that state [7].

Due to population decline of wild specimens, most of the timber to make sandalwood essential oil is harvested from commercial plantations. This is good from a sustainability perspective, but it may also be the reason that sandalwood essential oil no longer adheres to the standard chemical profile defined by the ISO (2002). According to a study from RBG Kew, most commercial sandalwood essential oils that are derived from *S. spicatum* contain a significantly lower santalol content than specified, at approximately 25%, compared to ISO's recommended 90% [8]. These results contrast with those put forth by Penfold in 1932, who described Australian sandalwood as being comprised of 60% santalols [95].

Most of the commercial essential oils from the original sandalwood, Indian sandalwood (*S. album*), also fail to meet the standard specified by ISO, with a santalol content of 60% [8]. However, Penfold again reported in 1932 that the santalol content of the Indian sandalwood is 90% [95].

There are three possible reasons for the change to modern day essential oils, which are: (1) Hydrodistillation technology has improved so that condensation and technique is optimised. This improves the capture of compounds with higher vapour pressures, which dilutes the lower vapour pressure ingredients, such as the santalols; (2) By using cultivated trees in the place of wild specimens, younger trees are harvested. In the wild, *S. spicatum* takes 90–115 years to reach ecological maturity, but in traditional wild harvesting older trees were chosen for essential oil production, because they contained a greater mass of timber (thicker trunk). These older trees take 250–300 years to build that quantity of biomass, which is a much longer timespan than the life of the sandalwood essential oil industry [7]. It is possible that older trees retain santalols while the higher vapour pressure terpenes, such as the monoterpenes, diffuse through the timber layers and evaporate over time; (3) Distillation time will influence the successful exhaustion of lower vapour pressure ingredients from the source plant material. In the modern age, distillation times have been minimised because of the higher costs of fossil fuel energy. Shorter distillation times produce essential oils with higher monoterpene content [2].

Two other species from the genus *Santalum* are also common in Australia, which are *S. acuminatum* (R.Br.) A.DC., and *S. lanceolatum* R.Br. In the former, *S. acuminatum* is known by its vernacular name 'quandong.' It produces a sweet red edible fruit that is used in home cooking in Australia's remote areas. The kernel from quandong is also edible and when roasted has a pleasant taste [120,121].

In the mid to late 1800s, RBG Kew supplied the University of Strasburg with wood samples labelled as sandalwood that allegedly came from *S. acuminatum*, under the previous older synonyms *Fusanus acuminatus* and *Eucarya acuminata*. These specimens were later revealed to be misidentified and the actual identity remains a mystery [122]; however, an 'oil' sample that was made from this old specimen, and retained in an old collection at RBG Kew, was used in the more recent study of sandalwood essential oils [8]. No santalols were detected. Since the identification was wrong, it is not known if the timber of the quandong produces an essential oil. There is currently no confirmation that the timber is

even aromatic. However, a fixed oil is produced from the quandong kernel, and this may cause confusion among scientists or the lay community.

In the same study, an essential oil that was allegedly from Australia under the name of *S. latifolium* Meurisse, was also rich in the santalol isomers [8]. However, this is not an Australian species, it is Hawaiian and is currently known under the accepted name *S. paniculatum* var. *paniculatum* [123]. The chemical profile of this specimen is consistent with the Hawaiian species [124], but it is also consistent with the Australian species *S. lanceolatum* [125]. It is therefore unclear whether the mistake was in the provenance or the species identification.

Nevertheless, *S. lanceolatum*, is known commonly as east Australian sandalwood. The essential oil from the timber was previously used as an adulterant to *S. spicatum* to make it more like the Indian sandalwood oil, by changing the optical rotation of the oil (in the days before GC-MS) [95,122]. However, the use of east Australian sandalwood was very short lived because the yield was below an economically feasible threshold [95].

4.17. Lagarostrobos franklinii (Hook.F.) Quinn (Podocarpaceae)

Lagarostrobos franklinii is a conifer that is endemic to Tasmania, known by the vernacular Huon Pine. Penfold referred to it by its older synonym *Dacrydium franklinii* and lamented that it was one of Australia's few wood-based essential oils to be used in industry, before the wild population was decimated [97]. The timber essential oil was chemically characterised by Penfold and Morrison [126], and it was revealed to be rich in the phenylpropanoids elemicin and methyl eugenol.

In 1995, just over 40 years since Penfold published his comment on the species, a hectare-wide stand of trees containing specimens that had remained genetically unchanged for over 10,500 years was found in western Tasmania on Mount Read [127]. Within this stand are wild specimens just over 2000 years old [128]. Because these trees are slow growers and are among the oldest living beings, their conservation status is critical. Hence, they are no longer used to produce essential oils.

4.18. Pittosporum (Pittosporaceae)

Essential oils from species in *Pittosporum* are sometimes difficult to produce in hydrodistillation, due to the saponins in the leaves. This was a challenge faced when studying *P. angustifolium* G.Lodd., to produce essential oils from both leaves and fruits. The problem was overcome by adding a thick layer of pearlite obsidian to the still, which floats over the aqueous phase and crushes the bubbles as they are formed [129].

The essential oil of fruits and leaves of *P. angustifolium* were dominated by saturated alkanes, cycloalkanes, alkanols, and alkane esters. Furthermore, some chemotypes expressed caryophyllene in their profiles. This contrasts with *Pittosporum undulatum* Vent. which produced essential oil from leaves and fruits dominated by limonene and bicyclogermacrene, with no issues related to saponins [129]. However, the latter species, *P. undulatum*, is introduced. It is expected that all native Australian *Pittosporum* will express saponins in their organs.

4.19. Zieria (Rutaceae)

Species in the tri-folate genus *Zieria* yield high quantities of essential oil, generally 1.5–2.5% wet leaf weight. The chemistry between species is considerably varied, with components that are either terpenoid, phenolic, or phenylpropanoid. The major terpenoids are car-3-en-2-one and chrysanthenone, the major phenol is benzaldehyde (same as almond flavour) and the major phenylpropanoids are safrole, methoxystyrene, methyl eugenol, and elemicin [47].

During the years of chemotaxonomy, the efforts to recognise chemical fingerprints across species within the genus *Zieria* were thwarted by intraspecific chemotypes. For example, *Zieria smithii* Jacks., is made up of at least five chemotypes that are predominantly phenylpropanoid, except for the chrysanthenyl acetate type [130–132]. However,

there are examples of chemical convergence for morphologically similar species, such as *Z. floydii* J.A.Armstr., which is morphologically like *Z. furfuracea* R.Br. ex Benth., and *Z. granulata* C.Moore ex Benth., all of which express car-3-en-2-one as dominant in their gas chromatography spectrums [47].

4.20. Citrus (Rutaceae)

The Australian finger lime, *Citrus australasica* F.Muell., yields an essential oil from its leaves that is dominated by limonene, γ-terpinene, β-citronellol, and citronellal [133]. This edible lime is distributed in the rainforest regions of coastal eastern and east-northern Australia. The arid version is the desert lime, *Citrus glauca* (Lindl.) Burkill, which is distinguished by two furanoid forms of linalool oxide in the essential oil profile [134]. The limes are a favourite bush fruit among the Australian Aboriginal people, particularly those in arid communities.

4.21. Tasmannia (Winteraceae)

There are several species of *Tasmannia* that grow in Australia and Tasmania. Each of the species is described as having a peppery flavour, thus their fruits have become an alternative pepper. However, the work by Southwell and Brophy demonstrated that the chemical profile of volatiles from the seven Australian species did not include components known to confer a peppery flavour. Rather, they were dominated by monoterpenes (pinene isomers, limonene, sabinene phellandrene, 1,8-cineole and linalool), sesquiterpene components (caryophyllene, copaene, elemol, eudesmol isomers and viridiflorol) and phenylpropanoids [135].

This contrasts with the chemistry of the commercial pepper, the Tasmanian species *Tasmannia lanceolata* (Poir.) A.C.Sm., which is dominated by the drimane sesquiterpene polygodial [136]. The drimane sesquiterpenes are also known for the peppery aroma they confer to the African pepper bark tree, *Warburgia salutaris* (G.Bertol.) Chiov [137]. The drimane sesquiterpenes were originally identified as the peppery aroma constituents of the water pepper plant *Persicaria hydropiper* (L.) Delarbre, published under the old name *Polygonum hydropiper* L [138].

4.22. Agonis fragrans (syn. Taxandria) (Myrtaceae)

Australian fragonia is a commercial essential oil from *Taxandria fragrans* (J.R.Wheeler & N.G.Marchant) J.R.Wheeler & N.G.Marchant, which was previously known under the name *Agonis fragrans*. This species is from coastal Western Australia, south of Perth, and the essential oil that is now commercialised represents one of several chemotypes that was selected by husband-and-wife John and Peta Day, respectively. The chemistry of the essential oil they had chosen includes 1,8-cineole, linalool, geraniol, and terpinen-4-ol. Another chemotype that was later identified by John Day had no 1,8-cineole, but included α-pinene, linalool, and myrtenol as dominant components [139].

A selection of mostly unrecognised species from the genus *Agonis* (*A. pariceps*, *A. juniperina*, *A. flexuosa* (Willd.) Sweet, A. sp. nov. 'Swamp' and S. sp. nov. 'Rose') were studied and the chemistry of their essential oils was reportedly dominated by the monoterpenes sabinene, β-pinene, limonene, linalool, terpinene-4-ol and α-terpineol [140].

5. Miscellaneous GC-MS Characterisations by Joseph Brophy (UNSW)

Table 1 summarises the Australian essential oils that were characterised over the last 30 years by Joseph Brophy (from his google scholar page). The species are provided in order of most recently published. The species are listed according to their arrangement in the publications. The essential oil components are listed in order of relative abundance.

Table 1 only includes Australian native species but does not include species mentioned in the earlier text. Because *Melaleuca* and *Eucalyptus* were comprehensively covered in Brophy's published books, that information is not included here. For more information, see Brophy's book on *Melaleuca* [141] and his book on *Eucalyptus* [114].

Table 1. Australian essential oils that were chemically studied by Joseph Brophy from the School of Chemistry, The University of New South Wales, Sydney, NSW 2052, Australia; (J.Brophy@unsw.edu.au).

Species	Chemistry Info from Abstract	Family	Year and Ref.
Acmenosperma claviflorum (Roxb.) E. Kausel	Bicyclogermacrene (36%), α-copaene (7%), δ-cadinene (4.9%), globulol (5.2%)	Myrtaceae	1999, [142]
Acradenia euodiiformis (F.Muell.), *A. frankliniae* Kippist	*A. euodiiformis*: type 1, α-pinene (16%), limonene (8%), p-cymene (13%), type 2, aromadendrene (11–22%), caryophyllene oxide (4–13%), globulol (11–13%), spathulenol (12–18%). *A. frankliniae*: 1.2–3.0% yield, type 1, xanthoxylin (90%), type 2, α-pinene (19–21%), camphene (13–14%), β-pinene (24–25%), (E)-β-ocimene (8–10%)	Rutaceae	2001, [143]
Acronychia aberrans, *A. acuminata*, *A. acidula*, *A. acronychioides*, *A. baeuerlenii*, *A. chooreechillum*, *A. crassipetala*, *A. eungellensis*, *A. imperforata*, *A. laevis*, *A. wilcoxiana*, *A. littoralis*, *A. octandra*, *A. oblongifolia*, *A. parviflora*, *A. pubescens*, *A.* sp. (Batavia Downs, J.R.Clarkson + 8511), *A. suberosa*, *A. vestita*	*A. aberrans*: (Z)-ocimenone (40–55%), (E)-ocimenone (23–28%). *A. acuminata*: α-pinene (33–64%). *A. acidula*: δ-3-carene (32–40%), terpinolene (13–46%) α-santalene (2–15%), aromadendrene (2–8%), germacrene B (0.6–18%). *A. acronychioides*: spathulenol (37–52%). *A. baeuerlenii*: α-pinene (65%). *A. chooreechillum*: α-pinene (45–66%). *A. crassipetala*: 40% monoterpenes. *A. eungellensis*: α-pinene (21–26%). *A. imperforata*: β-caryophyllene (13–20%), bicyclogermacrene (21–26%). *A. laevis*: elemol, α-pinene, bicyclogermacrene. *A. wilcoxiana* and *A. littoralis:* β-caryophyllene, pregeijerene, geijerene. *A. octandra*: (Z)-β-ocimene (15–23%), (E)-β-ocimene (15–23%), limonene (4–21%). *A. oblongifolia*: α-pinene (34–87%), limonene (0.1–26%), terpinolene (0.1–29%). *A. parviflora*: β-caryophyllene (2–34%), allo-aromadendrene (0.3–20%). *A. pauciflora*: α-pinene (14–45%), β-caryophyllene (10–24%). *A. pubescens*: β-caryophyllene (15–39%). *A.* sp. (Batavia Downs): (3–21%). *A. suberosa*: (Z)-ocimenone (20–23%), (E)-ocimenone (9–13%), β-caryophyllene (4–10%). *A. vestita*: α-pinene (40%), β-caryophyllene (23.5%), limonene (67–80%)	Rutaceae	2004, [144]
Actinodium cunninghamii	90% α-Pinene	Myrtaceae	1994, [145]
Actinostrobus pyramidalis, *A. arenarius*, *A. acuminatus*	*A. pyramidalis*: α-pinene (60–78%), limonene (1–17%), citronellal, citronellyl acetate, citronellol. *A. arenarius*: α-pinene (40–76%), limonene (1–28%), citronellal, citronellyl acetate, citronellol. *A. acuminatus*: α-pinene (17–79%), limonene (1–39%), spathulenol (6–17%)	Cupressaceae	2004, [146]
Agathis atropurpurea, *A. microstachya*, *A. robusta*, *A. australis*, *A. macrophylla*, *A. moorei*, *A. ovata*	*A. atropurpurea*: phyllocladene (13%), 16-kaurene (19%), α-pinene (8%), δ-cadinene (9%). *A. microstachya*: α-pinene (18%) myrcene (7%), bicyclogermacrene (6%), δ-cadinene (6%). *A. robusta*: spathulenol (37%), rimuene (6%). *A. australis*: 16-kaurene (37%), sclarene (5%) germacrene-D (9%). *A. macrophylla*: 5,15-rosadiene (60%), 16-kaurene (7%). *A. moorei*: allo-aromadendrene (6%), germacrene-D, δ-cadinene (10%), 16-kaurene (6%). *A. ovata*: caryophyllene oxide (15%), phyllocladene (39%)	Araucariaceae	2000, [147]

Table 1. *Cont.*

Species	Chemistry Info from Abstract	Family	Year and Ref.
Agonis obtusissima F.Muell., (syn. Agonis baxteri (Benth.) J.R.Wheeler & N.G.Marchant)	α-Pinene (12%), trans-β-ocimene (16%), globulol (39%)	Myrtaceae	2004, [148]
Allosyncarpia ternata S.T.Blake	β- and α-Pinene, limonene, β-caryophyllene, globulol, spathulenol	Myrtaceae	1992, [149]
Angasomyrtus salina	α-Pinene (77–83%), campholenic aldehyde (1%), 1,8-cineole (0.1–1.0%), β-pinene (1–2%), bicyclogermacrene (1–3%)	Myrtaceae	1994, [150]
Angophora spp.	Essential oils overlap with *Eucalyptus*	Myrtaceae	1999, [151]
Araucaria angustifolia, A. bidwillii, A. columnaris, A. cunninghamii, A. heterophylla, A. hunsteinii, A. luxurians, A. montana, A. muelleri, A. scopulorum,	*A. angustifolia*: germacrene-D (9%), hibaene (30%), phyllocladene (20). *A. bidwillii*: hibaene (76%). *A. columnaris*: hibaene (9%), sclarene (6%), luxuriadiene (13-epi-dolabradiene) (23%). *A. cunninghamii*: 16-kaurene (53%), hibaene (29%). *A. heterophylla*: α-pinene (52%), phyllocladene (32%). *A. hunsteinii*: α-Pinene (18%), sclarene (11%), germacrene-D (5%).*A. luxurians*: 5,15-rosadiene (20%), luxuriadiene (13-epi-dolabradiene) (66%). *A. montana*: phyllocladene (61%), 16-kaurene (23%). *A. muelleri*: sclarene (20%), luxuriadiene (19%). *A. scopulorum*: 16-α-phyllocladanol (41%), luxuridiene (10%), δ-cadinene, α-copaene	Araucariaceae	2000, [147]
Archirhodomyrtus beckleri (F. Muell.) A.J. Scott	Type 1, (E)-β-ocimene (69–87%), type 2, α-pinene, β-caryophyllene, α-terpineol, (E)-nerolidol and α-, β, and γ-eudesmol	Myrtaceae	1996, [152]
Arillastrum gummiferum (Brongriart & Gris) Pancher ex Baillon	80% (−)-limonene, α- and β-pinene, caryophyllene (3–7%)	Myrtaceae	1994, [153]
Artabotrys sp. (Claudie River B.Gray 3240)	Oxygenated sesquiterpenes	Annonaceae	2004, [154]
Asteromyrtus angustifolia, A. arnhemica, A. brassii, A. lysicephala, A. symphyocarpa	*A. angustifolia*: α-pinene (10%), 1,8-cineole (31%), β-caryophyllene (23%). *A. arnhemica*: α-pinene (92%). *A. brassii*: α-pinene (6%), 1,8-cineole (24%), γ-terpinene (21%). *A. lysicephala*: α-pinene (11.2%), 1,8-cineole (49%), α-terpinyl acetate (4%). A. magnifica: α-pinene (14%), β-pinene (20%), 1,8-cineole (36%). *A. symphyocarpa*: α-pinene (16%), 1,8-cineole (40%)	Myrtaceae	1994, [155]
Austrobaileya scandens	β-Pinene (1.3–44.2%), α-pinene (3.1–30.3%), β-caryophyllene (2.3–13.0%), δ-cadinene (2.8–9.0%), spathulenol (0.9–11.9%)	Austrobaileyaceae	1994, [156]
Austromatthea elegans L. S. Smith	Type 1, benzyl benzoate (96.25%), type 2, benzyl salicylate, benzyl benzoate	Austrobaileyaceae	1995, [157]
Austromyrtus sp. nov.	(E)-β-Ocimene (83%), myrcene	Austrobaileyaceae	1995, [158]
Austromyrtus dulcis (C. T. White) L. S. Smith, *A. tenuifolia* (Sm.) Burret.,	*A. dulcis*: type 1, isobaeckeol (80%), type 2, β-pinene (34–45%), 1,8-cineole (24–35%). *A. tenuifolia*: 1.8–3.0% yield of isobaeckeol (97–98%)	Austrobaileyaceae	1995, [159]

Table 1. *Cont.*

Species	Chemistry Info from Abstract	Family	Year and Ref.
Austromyrtus gonoclada, *A. floribunda*, *A. hillii*, *A. inophloia*, *A. minutiflora*, *A. pubiflora*, *A. shepherdii*, *A.* sp. (Bamaga, B. P. Hyland 10235), *A.* sp. (Brookfield, L. W. Jessup 155), *A.* sp. (McIlwraith Range, B. P. Hyland 11148), *A.* sp. (Pinnacle Track, P.I. Forster PIF15535), *A. acmenoides*, *A. bidwillii*, *A. dallachiana*, *A. fragrantissima*, *A. hillii* type 2, *A. racemulosa*, *A.* sp. (Byerstown Range, G. P. Guymer 2037), *A.* sp. (Forty Mile Scrub, G. C. Stocker 1758), *A.* sp. (Mt. Beatrice, P. I. Forster PIF14662), *A.* sp. (Mt. Lewis, P.I. Forster PIF15613), *A.* sp. (Mt. White, P.I. Forster PIF13461), *A.* sp. (Danbulla, L. S. Smith 10123), *A.* sp. (Spencer Creek, P. I. Forster PIF13701)	*A. gonoclada*: 2-hydroxy-4,6-dimethoxy-3,5-dimethylacetophenone. Sesquiterpenoid oils: *A. floribunda*, *A. hillii*, *A. inophloia*, *A. minutiflora*, *A. pubiflora*, *A. shepherdii*, *A.* sp. (Bamaga), *A.* sp. (Brookfield), *A.* sp. (McIlwraith Range), *A.* sp. (Pinnacle Track). Monoterpenoid oils: *A. acmenoides*, *A. bidwillii*, *A. dallachiana*, *A. fragrantissima*, *A. hillii* type 2, *A. racemulosa*, *A.* sp. (Byerstown Range), *A.* sp. (Forty Mile Scrub), *A.* sp. (Mt. Beatrice), *A.* sp. (Mt. Lewis), *A.* sp. (Mt. White), *A.* sp (Danbulla), *A.* sp. (Spencer Creek)	Austrobaileyaceae	1996, [160]
Austromyrtus lasioclada (F. Muell.) L.S. Sm., *A.* sp. (Blackall Range P.R. Sharpe 5387), *A* sp. (Upper Mudgeeraba Creek N.B. Byrnes +4069), *A.* sp. (Main Range P.R. Sharpe 4877)	*A. lasioclada*: δ-cadinene (8–14%), germacrene-D (4–12%). *A.* sp. (Blackall Range P.R. Sharpe 5387): α-copaene (12–16%), β-caryophyllene (4–20%), allo-aromadendrene (3–13%). *A* sp. (Upper Mudgeeraba Creek N.B. Byrnes +4069): α-copaene (8–15%), β-caryophyllene (3–8%) and allo-aromadendrene (8–14%). *A.* sp. (Main Range P.R. Sharpe 4877): spathulenol (8–12%), allo-aromadendrene (7–9%)	Austrobaileyaceae	1995, [161]
Athrotaxis cupressoides, *A. selaginoides*, *A. laxifolia*	*A. cupressoides*: limonene (46–56%), spathulenol (3–10%), α-acorenol (8–13%) and 8-β-hydroxyisopimarene (2–24%). *A. selaginoides*: limonene (40–48%), spathulenol (4–11%), α-bisabolol (6–14%), rimuene (0.8–7%), 8-β-hydroxyisopimarene (11–29%). *A. laxifolia*: limonene (34–58%), spathulenol (4–10%), α-acorenol (7–18%), γ-acorenol (0.1–0.5%), α-bisabolol (0.6–4%), rimuene (1–4%) and 8-β-hydroxyisopimarene (2–18%)	Cupressaceae	2002, [162]
Backhousia angustifolia F. Muell, *B. anisata* Vickery, *B. bancroftii* F. M. Bailey & F. Muell., *B. citriodora* F. Muell, *B. hughesii* C. T. White, *B. kingii* Guymer, *B. myrtifolia* Hooker & Harvey, *B. sciadophora* F. Muell., *Backhousia* sp. (Didcot P.I. Forster PIF12671)	*B. angustifolia*: 1,8-cineole, (E)-β-ocimene, angustifolenone, angustifolionol, dehydroangustione and angustione. *B. anisata*: type 1, (E)-anethole, type 2, methyl chavicol. *B. bancroftii*: octyl acetate (0.3–61.7%), dodecyl acetate (0.2–21.0%), dodecanol (trace—22.9%), decyl acetate (0.5–39.0%), decanol (0.1–17.4%), 2,4,6-trimethoxy-3-methylacetophenone (trace—23.0%), bancroftinone (trace—90.0%). *B. citriodora*: type 1, citral, type 2, citronellal. *B. hughesii*: β-bisabolene (1.0–44.0%) unidentified (8.0–54.0%). *B. kingii*: α-pinene (24.0–49.0%), limonene (7.0–24.0%), 1,8-cineole (10.0–17.0%). *B. myrtifolia*: type 1, methyl eugenol, type 2, (E)-methyl isoeugenol, type 3, elemicin, type 4, (E)-isoelemicin. B. sciadophora: α-pinene (44.0–55.0%), β-pinene (2.4–8.0%), limonene (6.5?12.7%), linalool (2.8–6.7%). *Backhousia* sp. (Didcot): α-pinene (11.0%), β-pinene (5.3%), β-caryophyllene (12.0%), dodecyl acetate (8.1%), dodecanol (8.2%)	Myrtaceae	1995, [98]

Table 1. *Cont.*

Species	Chemistry Info from Abstract	Family	Year and Ref.
Backhousia anisata Vickery	Type 1: *E*-anethole (90+ %), methyl chavicol (<5%), Z-anethole (<0.1%). Type 2: methyl chavicol (60–75%), E-anethole (<25%), Z-anethole (<0.1%)	Myrtaceae	1991, [163]
Backhousia citriodora F. Muell.	The *l*-citronellal type of *B. citriodora* described by Penfold was lost until 1996: 85–89% citronellal, 6–9% isopulegol isomers, citronellol (approx. 3%)	Myrtaceae	2001, [100]
Barongia lophandra	α-Pinene (58%), β-pinene (19%)	Myrtaceae	2003, [164]
Bosistoa brassii, *B. floydii*, *B. medicinalis*, *B. pentacocca*, *B. pentacocca var. connaricarpa*, *B. pentacocca var. dryanderensis*, *B. pentacocca var. pentacocca*, *B. selwynii*, and *B. transversa*	*B. brassii*: β–caryophyllene (2–12%), α-humulene (1–18%,), bicyclogermacrene (trace—24%). *B. floydii*: α-pinene (46–67%). *B. medicinalis*: α–pinene (13–57%), β–caryophyllene (1–9%). *B. pentacocca*: δ–cadinene (6–11%), α–copaene (2–7%), germacrene D (4–14%), α–cadinol (2–8%). *B. transversa*: α–pinene (24–83%)	Rutaceae	2007, [165]
Bouchardatia neurococca (F. Muell.) Baillon	β-Caryophyllene (38.5%), α-humulene (16.1%), bicyclogermacrene (10.8%), caryophyllene oxide (13.0%)	Rutaceae	1994, [166]
Brombya platynema, B. sp. (Gap Creek L.S. Smith 11116)	*B. platynema*: germacrene D (11–78%), β-bisabolene (0.8–22%), bicyclogermacrene (14–22%), kessane (1–17%), type 2: β-bisabolene (19–53%), curcumene (26.7%), bicyclogermacrene (7.7%), ar-curcumene (10.6%). *B.* sp. (Gap Creek): β-bisabolene (22.9%), ar-curcumene (14.6%), α-santalene (9.2%)	Rutaceae	2004, [167]
Callistemon viminalis (Sol. ex Gaertner) G.Don ex Loudon	α-Pinene, β-pinene, myrcene, 1,8-cineole, leptospermone, flavesone.	Myrtaceae	1997, [168]
Callistemon spp (high yields), low yield species, *C. brachyandrus*, *C. montanus*, *C. polandii*, *C. teretifolius*, *C.* sp. (Walsh's Pyramid P.I. Forster 13767), *C.* sp. nov. Oakey, *C. pachyphyllus*,	High yielding species: 1,8-cineole (45–80%), α-pinene (2–40%), limonene (2–9%), α-terpineol (1–13%). Low yielding species: 1,8-cineole (<20%), sesquiterpenoid	Myrtaceae	1998, [169]
Cananga odorata	β-Caryophyllene (34–52%), sabinene (1–20%), α-humulene (6–11%), α-pinene (1–17%)	Annonaceae	2004, [154]
Choricarpia subargentea (C.T. White) L.A.S. Johnson, *C. leptopetala* (F. Muell.) Domin	*C. subargentea*: α-pinene (30–76%), limonene (2–55%), 1,8-cineole (2–20%), jensenone. *C. leptopetala*: α-pinene, limonene, p-cymene, 1,8-cineole	Myrtaceae	1994, [170]
Cinnamomum baileyi, *C. oliveri*, *C. baileyi*, *C. oliveri*, *C. propinquum*, *C. virens*	*C. baileyi*: methyl eugenol, bicyclogermacrene. *C. oliveri*: camphor, safrole, methyl eugenol. *C. laubatii*: type 1, safrole, methyl eugenol, elemicin and bicyclogermacrene, type 2, bicyclogermacrene, β-selinene, spathulenol and γ-eudesmol. *C. propinquum*: p-cymene, β-eudesmol. *C. virens*: α-pinene, (E)-nerolidol	Lauraceae	2001, [171]
Clausena brevistyla Oliv. and *C. smyrelliana* P.I.Forst.	*C. brevistyla*: type 1, myrcene (72.4%), type 2, limonene (83.3%), type 3, β-caryophyllene (19.4%), α-humulene (4.3%), bicyclogermacrene (9.5%), caryophyllene oxide (7.6%), spathulenol (10.6%). *C. smyrelliana*: α-pinene (73.3%), β-caryophyllene (8.5%)	Rutaceae	2016, [172]
Coatesia paniculata F.Muell., syn. *Geijera paniculata*.	Leaf oil: α-pinene (27–57%), β-caryophyllene (4–12%)	Rutaceae	2005, [173]

Table 1. *Cont.*

Species	Chemistry Info from Abstract	Family	Year and Ref.
Coleonema pulchellum Williams	α- and β-Pinene, myrcene, β-phellandrene, linalool, terpinen-4-ol, caryophyllene, germacrene-D, bicyclogermacrene	Rutaceae	1986, [174]
Corymbia dallachiana (Benth.) K.D.Hill & L.A.S.Johnson	Papuanone	Myrtaceae	1999, [175]
Crowea exalata, *C. saligna*, *C. angustifolia* var. *angustifolia*	*C. exalata*: Type 1, safrole (81–88%), type 2, (E)-methyl isoeugenol (18–25%), (E)-carpacin (47–51%), type 3, safrole (27–35%), (E)-methyl isoeugenol (29–46%), α-pinene (12–25%), type 4, safrole (6–29%), asaricin (57–74%), type 5, exalatacin, croweacin (10–20%). C. saligna: croweacin (84–94%), safrole. *C. angustifolia* var. *angustifolia*: β-asarone (68%), exalatacin (13%), croweacin (7%)	Rutaceae	1997, [176]
Crowea exalata F.Muell	exalaticin	Rutaceae	2000, [11]
Cryptocarya bellendenkerana, *C. cocosoides*, *C. cunninghamii*, and *C. lividula* (Lauraceae)	*C. cocosoides*: bicyclogermacrene (3–26%), spathulenol (16–47%), massoia lactone (11–15%), (6-heptyl-5,6-dihydro-2H-pyran-2-one (0.3–3%) and benzyl benzoate (0.2–5%). *C. cunninghamii*: benzyl benzoate (80.2%). *C. bellendenkerana*: limonene (8.3%), β-phellandrene (11.8%), viridiflorene (9.1%). *C. lividula*: bicyclogermacrene (26.1%), spathulenol (21.1%), β-eudesmol (6.1%)	Lauraceae	2016, [177]
Cryptocarya cunninghamii Meissner	Type 1, bicyclogermacrene (52.4%), type 2, 6-nonyl-5,6-dihydro-2H-pyran-2-one (78–88%)	Lauraceae	1998, [178]
Cyathostemma micranthum	Caryophyllene oxide (26%), spathulenol (11%), benzyl benzoate (4%)	Annonaceae	2004, [154]
Darwinia citriodora (Endl.) Benth	Yield: 0.5% to 1.1%: methyl myrtenate (56–76%) methyl geranate (49–75%), α-pinene (7.8%), (Z)-β-ocimene (2.0%), linalool (1.7%), bicyclogermacrene (1.3%), viridiflorol (2.3%)	Myrtaceae	2001, [179]
Darwinia procera, *D. fascicularis* subsp. *fascicularis* and *D. peduncularis*	*D. procera*: myrtenyl acetate (6.1–29.6%), α-pinene (6.9–25.1%), γ-terpinene (6.2–13.6%), bicyclogermacrene (5.5–10.8%), (E)-nerolidol (3.4–9.7%). *D. fascicularis* ssp. *fascicularis:* (E)-nerolidol (33.0%), α-pinene (15.1%), γ-terpinene (10.2%). *D. peduncularis*: α-pinene (33.5%), γ-terpinene (23.1%), bicyclogermacrene (6.7%)	Myrtaceae	2010, [180]
Decaspermum humile (Sweet ex G.Don) A.J.Scott, *D. struckoilicum* N.Snow & Guymer	*D. struckoilicum*: α-pinene (37.5%), β-caryophyllene (2.4%), α-humulene (2.2%) and α- and β-eudesmol (8.2% and 8.1%, respectively). *D. humile*: a-thujene (0.1–13%), α-pinene (0.2–21%), limonene (0.2–8%), myrcene (0.3–10%), β-phellandrene (0.1–5%), linalool (0.3–9%) and terpinen-4-ol (0.3–6%), β-caryophyllene (0.7–5%), aromadendrene (1–6%), viridiflorene (1–7%), δ-cadinene (0.4–14%), bicyclogermacrene (0.2–10%), globulol (1–9%)	Myrtaceae	2005, [181]
Desmos goezeanus, *D.* spp. (Mossman River L.W. Jessup 550), *D. wardianus*,	*D. goezeanus*: benzyl benzoate, benzyl salicylate. *D.* spp. (Mossman River): benzyl benzoate (52%). *D. wardianus*: α-pinene (37%)	Annonaceae	2002, [182]

Table 1. *Cont.*

Species	Chemistry Info from Abstract	Family	Year and Ref.
Dinosperma erythrococca, *D. stipitata*, *D. melanophloia*,	*D. erythrococca*: type 1, geranyl acetate (80%), type 2, (E)-β-ocimene (3–28%), geranyl acetate (2–32%), linalool (2–10%), β-caryophyllene (7–11%), bicyclogermacrene (2–10%), spathulenol (1–10%), type 3, spathulenol (30%), type 4, furanoid linalool oxides (5–8%), (E)-β-ocimene (13%), γ-elemene (36.4%), type 5, myrcene (13.3%), limonene (26.3%), (E)-β-ocimene (18.5%). *D. stipitata*: type 1, bicyclogermacrene (22–32%), germacrene B (11–12%) evodionol methyl ether (11.5%), (E)-methyl isoeugenol (6–11%), type 2, hydrocarbon C15H,4 (9–26%), bicyclogermacrene (7–16%), γ-elemene (7–9%). *D. melanophloia*: methyl chavicol (59%), (E)-methyl isoeugenol (15%)	Rutaceae	2002, [183]
Dinosperma longifolium T.G. Hartley (Rutaceae)	Niranin, S-methylthiocarboxylic acid-N-methyl-N-phenylethylamide, (39–62%), β-caryophyllene (5–12%), (E)-β-farnesene (5–12%), bicyclogermacrene (10–14%)	Rutaceae	2004, [184]
Diselma archeri Hook.f.	Yield 0.6–0.8%: Leaves, α-pinene (45–73%), δ-3-carene (1–15%), limonene	Cupressaceae	2003, [185]
Doryphora sassafras Endl., *D. aromatica* (F. M. Bail.) L. S. Smith	*D. sassafras*: methyl eugenol (27–47%), safrole (15–30%), camphor (15–19%). *D. aromatica*: α-, β- and γ-eudesmol, spathulenol, elemol, guaiol	Atherospermataceae	1993, [186]
Drummondita calida (F.Muell.) Paul G.Wilson	α-pinene (79–86%)	Rutaceae: Boronieae	2006, [187]
Dryadodaphne sp. (Mt. Lewis B.P. Hyland RFK1496)	Leaves: δ-cadinene (10.7%), globulol (4.6%), T-cadinol (3.7%). Bark and wood: guaiol, bulnesol	Atherospermataceae	1998, [188]
Endressia wardellii (F.Muell.) Whiffin	*E. wardellii*: α-humulene (14–17%), bicyclogermacrene (17–24%)	Apiaceae	2009, [189]
Eremaea pauciflora (Endl.) Druce	1,8-Cineole (22%), eudesmols (α-, β-, γ-; 26%)	Myrtaceae	2004, [148]
Eriostemon banksii A. Cunn. ex Endl, *E. australasius*	*E. australasius* and *E. banksia*: cis and trans-methyl-4-isoprenoxycinnamate, β-elemene (7.2–8.1%), β-caryophyllene (7.7–8.4%) sesquiterpene n.d. (12.3–15.1%), α-pinene (2.8–8.3%), β-pinene (0.2–0.8%), limonene (0.4–0.5%)	Rutaceae	1998, [190]
Eryngium expansum F. Muell, *E. pandanifolium* Cham. et Schlecht, *E. rostratum* Cav., *E. vesiculosum* Labill.	*E. expansum*: 7-epi-α-selinene (38.3%), cis-β-guaiene (10.8%), 2,3,6-trimethylbenzaldehyde (8.0%), (E,E)-α-farnesene (7.3%). *E. pandanifolium*: bornyl acetate (20.8%), β-selinene (13.8%), α-selinene (11.3%), α-muurolene (8.0%). *E. rostratum*: spathulenol (20.0%), β-bisabolol (8.6%), fruit oil: β-bisabolol (65.3%). *E. vesiculosum*: β-caryophyllene (20.3%), germacrene D (19.2%), α-humulene (8.8%)	Apiaceae	2003, [191]
Eryngium paludosum (C.Moore) P.W.Michael	γ-terpinene (12.9%), β-bisabolene (12.2%), germacrene D (7.6%), myrcene (7.3%), β-caryophyllene (7.0%), limonene (6.0%), α-humulene (5.1%)	Apiaceae	2008, [192]

Table 1. *Cont.*

Species	Chemistry Info from Abstract	Family	Year and Ref.
Eryngium rosulatum P.W. Michael Ined	β-elemene (16.0%), bicyclogermacrene (12.5%), δ-elemene (7.0%), (E)-caryophyllene (5.9%)	Apiaceae	2006, [193]
Eryngium vesiculosum Labill.	Caryophyllene (20.3%), germacrene D (19.2%), α-humulene (8.8%), bicyclogermacrene	Apiaceae	2003, [194]
Euodia hylandii, *E. pubifolia*	*E. hylandii*: spathulenol (12–20%). *E. pubifolia*: spathulenol (18.3%)	Rutaceae	2004, [195]
Fitzalania heteropetala F. Muell.	β-Caryophyllene (33–8%), aromadendrene (14.0%)	Annonaceae	1997, [196]
Flindersia acuminata, *F. australis*, *F. bennettiana*, *F. bourjotiana*, *F. brassii*, *F. brayleyana*, *F. collina*, *F. dissosperma*, *F. ifflaiana*, *F. laevicarpa*, *F. maculosa*, *F. oppositifolia*, *F. pimenteliana*, *F. schottiana*, and *F. xanthoxyla*	*F. maculosa*/*F. dissosperma*: geijerene, pregeijerene, methyl geranate, α-pinene, β-caryophyllene and bicyclogermacrene. *F. acuminata*/*F. australis*: bicyclogermacrene, guaiol, bulnesol. *F. australis* type 2: β-caryophyllene, spathulenol. *F. bennettiana*: bicyclogermacrene. *F. bourjotiana*: β-caryophyllene. *F. brassiii*: α-cadinol, δ-cadinene. *F. brayleyana*: spathulenol, caryophyllene oxide. *F. collina*: (E,E)-farnesol. *F. ifflaiana*: β-caryophyllene, α-humulene, bicyclogermacrene. *F. Laevicarpa*: β-caryophyllene, germacrene D, bicyclogermacrene, elemol. *F. oppositifolia*: diverse. *F. pimenteliana*: β-caryophyllene, bicyclogermacrene, chemotype 2: α-pinene. *F. schottiana*: α-pinene, sabinene. *F. xanthoxyla*: bicyclogermacrene, δ-cadinene, β-caryophyllene	Rutaceae	2005, [50]
Galbulimima baccata F.M.Bailey (Himantandraceae)	Elemol/hedycaryol (12–30%), α-, β- and γ-eudesmol (0.6–3%, 0.4–3% and 0.2–3%, respectively), spathulenol (1–3%)	Himantandraceae	2005, [197]
Geijera linearifolia (DC.) J.M.Black	Leaf oil: spathulenol (10–17%), geranyl acetate (4–9%), bicyclogermacrene (3–6%), (E,E)-farnesol (23–30%)	Rutaceae	2005, [173]
Geleznowia verrucosa Turcz	Leaves: α-pinene (80%), flower, α-pinene + eugenyl acetate	Rutaceae	1995, [198]
Goniothalamus australis Jessup	Type 1, pinocarvone (10%), trans-pinocarveol (17%), type 2, α-pinene (10–11%)	Annonaceae	2004, [154]
Gyrocarpus americanus Jacq., subsp. *americanus*	α-pinene, β-pinene, germacrene D (31%)	Hernandiaceae	2000, [199]
Halfordia kendack (Montrouz.) Guillaumin S.L.	methyl eugenol and elemicin	Rutaceae	2004, [200]
Haplostichanthus johnsonii F.Muell., *H.* sp. (Coopers Creek B.Gray 2433), *H.* sp. (Johnstone River L.W Jessup+ 471), *H.* sp. (Mt. Finnigan L.W Jessup 632), *H.* sp. (Rocky River Scrub P.I. Forster+ PIF10617), *H.* sp. (Topaz L.W. Jessup 520)	*H.* sp. (Rocky River Scrub): caryophyllene oxide (26.2%), humulene oxide (10.1%), spathulenol (31.6%). *H.* sp. (Mt. Finnigan): spathulenol (15.4%). *H.* sp. (Coopers Creek): β-caryophyllene (10%), γ-muurolene (12.4%), bicyclogermacrene (9.6%). *H.* sp. (Johnstone River): β-caryophyllene (trace—27%), α-humulene (trace—10%), caryophyllene oxide (3–19%), spathulenol (6–31%). *H.* sp. (Topaz): spathulenol (24–38%). *H. johnsonii*: spathulenol (21–36%)	Annonaceae	2006, [201]
Haplostichanthus johnsonii	Yield 1.5–2%. 2,3,4,5-tetramethoxyallylbenzene (79%), elemicin (5.9%), α-copaene (5%), elemene (2%)	Annonaceae	1992, [202]

Table 1. *Cont.*

Species	Chemistry Info from Abstract	Family	Year and Ref.
Hedycarya angustifolia A.Cunn. and *H. loxocarya* (Benth.) W.D.Francis	Elemol and α-, β- and γ-eudesmol	Monimiaceae	2005, [203]
Hernandia albiflora, *H. bivalvis*, *H. nymphaeifolia*	*H. albiflora*: bicydogermacrene (trace -19%), β-caryophyllene (5–9%), caryophyllene oxide (7–18%), globulol (4–6%). *H. bivalvis*: bicyclogermacrene (20–30%), β-caryophyllene (4–13%), α-copaene (11–13%), germacrene D (7–12%). *H. nymphaeifolia*: β-caryophyllene (11–44%), α-humulene (14–17%), caryophyllene oxide (5–20%)	Hernandiaceae	2000, [199]
Homoranthus biflorus, *H. binghiensis*, *H. cernuus*, *H. flavescens*, *H. montanus*, *H.* sp. nov. Nandewar Range, *H. bornhardtiensis*, *H. decumbens*, *H. homoranthoides*, *H. prolixus*, *H. decumbens*, *H. thomasii*, *H. tropicus*	*H. biflorus*, *H. binghiensis*, *H. cernuus* type 1, *H. flavescens*, *H. montanus* and *H.* sp. nov. Nandewar Range type 1: β-pinene, (Z)-β-Ocimene (>40%), bicyclogermacrene, globulol. *H. bornhardtiensis*, *H. decumbens* type 1, *H. homoranthoides*, *H. prolixus*, *H.* sp. nov. Nandewar Range type 2: β-pinene, limonene, bicyclogermacrene, globulol. *H. decumbens*, *H. thomasii*, *H. tropicus*, H. sp. nov. Nandewar Range type 3: β-pinene, γ-terpinene, bicyclogermacrene, globulol. *H. tropicus*: methyl geranate, bicyclogermacrene, globulol	Myrtaceae	2004, [204]
Homoranthus montanus Craven and S. R. Jones, *H. flavescens* Cunn. ex. Schauer.	*H. montanus*: (Z)-β-ocimene (85%). *H. flavescens*: (Z)-β-ocimene (69–71%)	Myrtaceae	1998, [205]
Idiospermum australiense (Diels) S. T. Blake	Bicyclogermacrene (48%), caryophyllene (8%), globulol, viridiflorol, spathulenol	Calycanthaceae	1992, [206]
Kibara rigidifolia A.C.Sm.	(Z)-β-Ocimene (3–12%), (E)-β-ocimene (1.5%), bicyclogermacrene, germacrene-B, guaiol, spathulenol	Monimiaceae	1998, [188]
Kunzea pulchella (Lindl.) A.S.George	Globulol (83–88%)	Myrtaceae	2004, [148]
Lagarostrobos franklinii (Hook.f.) Quinn	Yield 0.8–0.9%: Leaves, α-pinene (13–36%), δ-3-carene (1–17%), limonene (16–42%), 16-kaurene (3–7%), phyllocladene (4–10%), sclarene (2–23%). Wood, methyl eugenol (74%), (E)-methyl isoeugenol (2%) elemicin (24%)	Podocarpaceae	2003, [185]
Leionema ambiens (F.Muell.) Paul G.Wilson	(E)-β-ocimene (>10%), (Z)-β-ocimene (0.1–4%), viridiflorene (6–7%), bicyclogermacrene (6–13%), globulol (6–7%), viridiflorol (4–6%), (E,E)-farnesol (14–23%)	Rutaceae	2003, [117]
Leptospermum amboinense, *L. emarginatum*, *L. grandiflorum*, *L. liversidgei*, *L. petersonii*, *L. rotundifolium*, *L. wooroonooran*	*L. amboinense*: type 1, geranial (13%), sabinene (13%). *L. emarginatum*: α-eudesmol (7–17%), β-eudesmol (17–26%), γ-eudesmol (9–18%). *L. grandiflorum*: α-, β- and γ-eudesmol. *L. liversidgei*: citronellal (ca. 44%), neral (20%), geranial (35%). *L. petersonii*: type 1, citronellal, low neral/geranial, type 2, low citronellal and high neral/geranial, type 3, Penfold's 'variety A,' monoterpenes, type 4, β-caryophyllene, globulol/viridiflorol/spathulenol, type 4, Penfold's 'variety B,' geranyl acetate (21–38%), geraniol (21–29%). *L. rotundifolium*: α-pinene (16–25%), 1,8-cineole (21–28%). *L. wooroonooran*: α-pinene (4–11%), β-pinene (4–9%), sabinene (9–19%), β-caryophyllene (5–7%), humulene (11–20%)	Myrtaceae	2000, [207]

Table 1. *Cont.*

Species	Chemistry Info from Abstract	Family	Year and Ref.
Leptospermum arachnoides, *L. crassifolium*, *L. deuense*, *L. epacridoideum*, *L. glabrescens*, *L. grandifolium*, *L. lanigerum*, *L. macrocarpum*, *L. nitidum*, *L. petraeum*, *L. riparium*, *L. spectabile*, *L. sphaerocarpum*, *L. thompsonii*, *L. turbinatum*	Oils were dominated by α-, β- and γ-eudesmol. *L. glabrescens*: flavesone, leptospermone, eudesmol isomers	Myrtaceae	1999, [208]
Leptospermum blakelyi, *L. brevipes*, *L. neglectum*, *L. parvifolium*, *L.* sp. (Woodgate, P. I. Forster, PIF 13959), *L. multicaule*, *L. namadgiensis*, *L. microcarpum*	*L. brevipes*, *L. neglectum*, *L. parvifolium*, *L.* sp. (Woodgate): α-pinene. *L. blakelyi*, *L. multicaule*, *L. namadgiensis* and *L. sericatum*: sequiterpenoid. L. divaricatum and *L. microcarpum*: monoterpenoid	Myrtaceae	1998, [209]
Leptospermum brachyandrum (F. Muell.) Druce, *L. luehmannii* F. M. Bailey, *L. madidum* A. R. Bean subsp. *madidum*, *L. purpurascens* Joy Thomps., *L. speciosum* Schauer, *L. whitei* Cheel and *L. pallidum* A. R. Bean	All species produce α-pinene and lesser amounts of β-pinene, β-caryophyllene, aromadendrene, humulene, spathulenol, 1,8-cineole	Myrtaceae	1998, [210]
Leptospermum coriaceum (F. Muell. Ex Miq.) Cheel, *L. fastigiatum* S. Moore, and *L. nitens* Turcz	*L. coriaceum*: α-pinene (25.4%), 1,8-cineole (11.5%), globulol (15.4%). *L. fastigiatum* and *L. nitens*: α-pinene (82.8% and 64.8–70.6% respectively)	Myrtaceae	1999, [211]
Leptospermum spp. *Eudesmol types:* [*L. micromyrtus* Miq., *L. minutifolium* C.T. White, *L. myrtifolium* Sieber ex DC., *L. rupestre* Hook. f., *L. sejunctum* Joy Thomps.] *L. novae-angliae* Joy Thomps., *L. rupicola* Joy Thomps. Sesquiterpenoid types [*L. continentale* Joy Thomps., *L. gregarium* Joy Thomps., *L. juniperinum* Sm, *L. obovatum* Sweet., *L. scoparium* J. R. Forst & G. Forst. and *L. squarrosum* Gaertn.]	Eudesmol types dominated by α-, β- and γ-eudesmol. *L. myrtifolium* type 2: (E,Z)-farnesal (5.8%), (E,E)-farnesal (12.9%), 2,3-dihydro-(E)-farnesol (10.3%), (E,E)-farnesol (26.5%). *L. novae-angliae*: (E)-nerolidol (50%). *L. rupicola*: α- and β-pinene	Myrtaceae	1999, [101]
Leptospermum morrisonlii, *L. oreophilum*, *L. variabile*, *Leptospermum* sp. (Mt Maroon, A.R. Bean 6665), *L. polygalifolium*, ssp. *polygalifolium*, *montanum*, *howense*, *cismontanum*, *transmontanum*, *tropicum* and 'wallum,' *L. madidum* spp. *sativum*	*L. morrisonlii*: grandiflorone. *L. oreophilum*: (E,E)-farnesol. *L. variabile*: type 1, geranyl acetate, β-caryophyllene, humulene, type 2, 1,8-cineole, type 3, α-pinene, β-caryophyllene, α-, β- and γ-eudesmol. *L.* sp. (Mt Maroon): type 1, β-caryophyllene, humulene, type 2, β-caryophyllene, δ-cadinene, calamenene, sesquiterpene n.d. *L. polygalifolium*, ssp. polygalifolium, montanum and howense: α-, β-, and γ-eudesmol. L. ssp. *cismontanum*, *transmontanum*, *tropicum* and '*wallum*': 1,8-cineole. *L. madidum* spp. *sativum*: α-pinene, β-pinene, γ-terpinene α-, β-, and γ-eudesmol	Myrtaceae	2000, [212]
Leptospermum scoparium	Isoleptospermone	Myrtaceae	1999, [175]
Levieria acuminata (F.Muell.) Perkins	n-Dodecanal (28%), δ-cadinene (5.8%), calamenene (5.7%)	Monimiaceae	1998, [188]
Lindera queenslandica B. Hyland	γ-Elemene (21.4%), α-copaene (17.9%), β-caryophyllene (7.4%), α-humulene (9.0%)	Lauraceae	1999, [213]
Lindsayomyrtus racemoides (Greves) Craven	β-Caryophyllene (7.4–13%), humulene (5.2–11.6%), β-trans-ocimene (5.0–7.3%)	Myrtaceae	1996, [214]

Table 1. *Cont.*

Species	Chemistry Info from Abstract	Family	Year and Ref.
Lophostemon Schott spp.	α-Pinene, aromadendrene, allo-aromadendrene, globulol, spathulenol.	Myrtaceae	2000, [215]
Lunasia amara Blanco var. *amara*	γ-Elemene (0.7–19%), germacrene-D (18–51%), bicyclogermacrene (7–26%), bicycloelemene (1–2%), β-bourbonene (0.7–3%), γ-elemene (4–9%), α-farnesene (1–3%), δ-cadinene (3–5%)	Rutaceae	1997, [216]
Lycopus australis R.Br.	β-phellandrene (26–40%), β-caryophyllene (7–16%), α-humulene (18–30%)	Lamiaceae	2005, [217]
Lysicarpus angustifolius (Hook.) Druce	α-Pinene, β-pinene, limonene (8%), α-terpineol (2–5%), viridiflorene (5–8%), aromadendrene (5–8%), globulol (4–5%), spathulenol (2–5%)	Myrtaceae	1994, [218]
Malleostemon tuberculatus (E.Pritz.) J.W.Green	α-Pinene (33%), 1,8-cineole (21%), E,E-farnesol (6%)	Myrtaceae	2004, [148]
Medicosma cunninghamii, *M. elliptica*, *M. fareana*, *M. glandulosa*, *M. obovata*, *M. riparia*, *M. sessiliflora*, *M.* sp. (East Mulgrave River R.L. Jago + 3696), *M.* sp. (Karnak P.I. Forster+ PIF15541), *M.* sp. (Mt Mellum P.I. Forster + PIF25572)	*M. cunninghamii*: evodionol, evodionol methyl ether, α-pinene, myrcene, ocimene. *M. elliptica*: α-pinene (0.6–29%), sabinene (12–55%), myrcene (8–16%), limonene (0.4–13%). *M. fareana*: bicyclogermacrene (15–44%). *M. glandulosa*: α-pinene (t-35%), β-caryophyllene (t-15%), aromadendrene (t-10%), (E,E)-α-farnesene (1–13%), bicyclogermacrene (1–13%), globulol (1–8%), spathulenol (3–10%). *M. obovate*: α-pinene (1–12%), limonene (10–13%), (E)-β-ocimene (14–23%), β-caryophyllene (17–19%), α-humulene (6–14%). *M. riparia*: α-selinene (7–15%), evodionol (1–3%), evodionol methyl ether (30–56%). *M. sessiliflora*: β-caryophyllene (3–11%), aromadendrene (5–14%), humulene (8–19%), spathulenol (3–12%). *M.* sp. (East Mulgrave) bicyclogermacrene (17–21%). *M.* sp. (Karnak): α-pinene (1–40%), bicyclogermacrene (3–8%), spathulenol (10–22%). *M.* sp. (Mt Mellum): α-pinene (38–54%) (Z)-β-ocimene (10–13%)	Rutaceae	2004, [219]
Melicope affinis, *M. bonwickii*, *M. broadbentiana*, *M. elleryana*, *M. fellii*, *M. hayesii*, *M. jonesii*, *M. micrococca*, *M. peninsularis*, *M. rubra*, *M. vitiflora*, *M. xanthoxyloides*	*M. affinis*: bicyclogermacrene (7–18%), bisabolene (t-9%). *M. bonwickii*: zierone (0.3–3%). *M. broadbentiana*: α-pinene (21–76%), limonene (0.6–28%). *M. elleryana*: zierone (26–42%), allo-evodione (4–10%), evodione (10–22%). *M. fellii*: β-caryophyllene (9.9%), α-humulene (8.4%), caryophyllene oxide (7.4%). *M. hayesii*: bicyclogermacrene (22.8%), germacrene D (13.9%), (E,E)-α-farnesene (9.2%), globulol (10.6%). *M. jonesii*: sesquiterpenic. *M. micrococca*: α-pinene (1–46%), (E)-(β-ocimene (t-10%), (β-caryophyllene (0.4–15%), bicyclogermacrene (t-11%), caryophyllene oxide (0.3–23%), spathulenol (1–12%). *M. peninsularis*: β-caryophyllene (30–49%), α-humulene (26?35%). *M. rubra* and *M. vitiflora*: sabinene (31.1%), γ-terpinene, germacrene D (22.6%), sabinene (0.1–54%), limonene (1–47%). *M. xanthoxyloides*: β-caryophyllene (13–47%), spathulenol (1–18%), α-pinene (t-15%)	Rutaceae	2004, [195]

Table 1. *Cont.*

Species	Chemistry Info from Abstract	Family	Year and Ref.
Melicope contermina, M. polybotrya	*M. conterminal*: limonene (33%), elemol (23%). *M. polybotrya*: geijerene (41%), pregeijerene (38%), limonene (9%)	Rutaceae	2004, [220]
Melicope melanophloia C.T. White	Type 1, methyl chavicol (5–13%), methyl eugenol (51–67%), type 2, α-pinene (34–37%), myrcene, α-phellandrene, limonene, 1,8-cineole (4–12%), type 3, limonene (1–8%), (Z)-β-ocimene (12–18%), (E)-β-ocimene (23–56%), 2-hydroxy-4,6-dimethoxyacetophenone (4–6%)	Rutaceae	1997, [221]
Melodorum sp. (Font Hills G. Sankowsky 380), *M*. sp. (Stone Crossing L.W. Jessup 814), *M*. sp. (Topaz G. Sankowsky + 244), *M*. sp. (Claudie River B.P.Hyland 21171V), *M. uhrii, M. leichhardtii,*	*M*. sp. (Font Hills): α-eudesmol (9–5%), β-eudesmol (7–11%), β-caryophyllene (10–16%), bicyclogermacrene (1–9%) and α-pinene (14–15%). *M*. sp. (Stone Crossing): benzyl benzoate (20%), benzyl salicylate (2.7%). *M*. sp. (Topaz): bicyclogermacrene (34–50%), β-caryophyllene (11–16%), spathulenol (2–10%). *M*. sp. (Claudie River): bicyclogermacrene (29.3%), β-caryophyllene (26.7%). *M. uhrii*: bicyclogermacrene (45%), benzyl benzoate (5%). *M. leichhardtii*: germacrene D (6–10%), bicyclogermacrene (15–19%), (Z)-β-ocimene (6?8%), (E)-β-ocimene (2–5%)	Annonaceae	2004, [222]
Mentha diemenica Sprengel	1% Yield, menthone (32%), neomenthyl acetate (0.0–18.3%), pulegone (25–44%), neomenthol (2.5–9.0%), menthyl acetate (2.7–5.7%), menthol (1.8–2.7%), isomenthone (1–3%)	Lamiaceae	1996, [223]
Mentha grandiflora Benth	trans-piperitone oxide (21%), piperitenone oxide (36%), pulegone (19%), menthone (10%)	Lamiaceae	1997, [224]
Microcachrys tetragona (Hook.) Hook.f.	Yield 0.1–0.5%: α-pinene (44–50%), limonene (10–13%)	Podocarpaceae	2003, [185]
Micromelum minutum (G.Forst.) Wight & Arn.	*M. minutum*: δ-elemene (3.3–18.6%), β-caryophyllene (4.8–30.3%), germacrene-D (2–15.8%), germacrene-B (3.9–34.3%)	Rutaceae	2016, [172]
Micromyrtus striata J. W. Green	Isoamylisovalerate (23.0–48.7%), α-pinene (5.9–27.7%)	Myrtaceae	1991, [225]
Microstrobos fitzgeraldii, M. niphophilus	M. fitzgeraldii: α-pinene (22.7%), myrcene (24.1%), hibaene (27.0%). *M. niphophilus*: α-pinene (26.9%), limonene (30.5%) myrcene (20.8%)	Podocarpaceae	2001, [226]
Miliusa traceyi, M. horsfieldii, M. brahei	*Miliusa traceyi*: α-pinene (18.7%), β-pinene (18.6%), β-caryophyllene (13.5%). *M. horsfieldii*: β-caryophyllene (20.2%), caryophyllene oxide (12.5%). *M brahei*: β-caryophyllene (12.8%), α-humulene (11.3%), bicyclogermacrene (12.9%)	Annonaceae	2004, [227]
Mitrantia bilocularis Peter G.Wilson & B.Hyland	β-Caryophyllene (29%) and globulol (13%).	Myrtaceae	2003, [164]
Mitrephora zippeliana Mig.	Type 1, α-pinene (13%), β-pinene (15%), caryophyllene oxide (10%), spathulenol (10%), β-caryophyllene (8%), type 2, β-caryophyllene (18%), α-humulene (7%), γ-curcumene (4%), bicyclogermacrene (4%), ar-curcumene (5%), caryophyllene oxide (3%), spathulenol (5%)	Annonaceae	2004, [154]

Table 1. *Cont.*

Species	Chemistry Info from Abstract	Family	Year and Ref.
Murraya paniculata (L.) Jack.	Small leaves variant: High yield. Big leaves variant: small yield. Both germacrene-D, E-nerolidol	Rutaceae	1994, [228]
Neolitsea australiensis, *N. brassii*	*N. australiensis*: bicyclogermacrene (12–16%), guaiol (13–17%). *N. brassii*: bicyclogermacrene (11–15%), cubenol (6–10%), guaiol (7–10%). Northern chemotypes: germacrone (50%), bicyclogermacrene (12–35%), spathulenol (4–38%), type 2, furanogermenone (43%). Southern chemotypes: γ-eudesmol (3–30%), spathulenol (5–30%)	Lauraceae	2002, [229]
Neofabricia myrtifolia, *N. mjoebergii*, *N. sericisepala*	*N. mjoebergii*: caryophyllene, humulene, β-pinene. *N. sericisepala*: over 50% α-pinene, caryophyllene. *N. myrtifolia*: type 1 α-pinene (>60%) caryophyllene, type 2, α-pinene, caryophyllene (up to 60%)	Myrtaceae	1992, [230]
Osbornia octodonta F. Muell.	α-Pinene (35%), 1, 8-cineole (24%), α-terpineol (11%)	Myrtaceae	1993, [231]
Palmeria F.Muell., spp.	Elemol, spathulenol, bicyclogermacrene, ishwarane	Monimiaceae	2004, [232]
Pentaceras australe (F. Muell.) Benth.	α-Bisabolol (0.3–18%), γ-elemene (11–25%), germacrene D (13–25%), sesquicineole (4–7%)	Rutaceae	2002, [233]
Phebalium distans, *P. glandulosum subsp. glandulosum*, *P. longifolium*, *P. nottii*, *P. squamulosum subsp. squamulosum*, *P. squamulosum subsp. gracile*, *P. whitei*, *and P. woombye*	*P. distans*: α-pinene (0.8–42%), bicyclogermacrene (12–22%). *P. glandulosum* subsp. *glandulosum*: dihydrotagetone, 75–95%. *P. longifolium*: β-caryophyllene (9–20%), bicyclogermacrene (7–23%). *P. nottii*: α-pinene (25–42%), guaiol (t-28%), bulnesol (nil to 34%). *P. squamulosum* subsp. *squamulosum*: α-phellandrene (12–25%), β-phellandrene (14–15%), bicyclogermacrene (2–12%), elemol/hedycaryol (12–36%). *P. squamulosum* subsp. *gracile*: geijerene (4–8%), α-pinene (44–50%), guaiol (9–11%). *P. whitei*: α-pinene (22–42%), limonene (1–12%), bicyclogermacrene (11–20%). *P. woombye*: α-pinene (10–21%), β-phellandrene (12–20%), bicyclogermacrene (11–20%), germacrene D (5–10%)	Rutaceae	2006, [116]
Phyllocladus aspleniifolius (Labill.) Hook.f.	Yield 0.5–1%: α-pinene (44–55%), phyllocladene (15–28%), 8-β-hydroxyisopimarene (5–7%)	Podocarpaceae	2003, [185]
Pilidiostigma glabrum Burret, *P. recurvum* (C.T. White) A.J. Scott, *P. rhytisperma* (F. Muell.) Burret, *P. tetramerum* L.S. Sm., *P. tropicum* L.S. Sm. and *Pilidiostigma* sp. (Mt Lewis G.P. Guymer 2024)	All species: aromadendrene, allo-aromadendrene, β-caryophyllene, α-copaene, viridiflorene, bicyclogermacrene, δ- and γ-cadinene and globulol	Myrtaceae	1999, [234]
Pistacia lentiscus L.	α-Pinene, β-pinene, myrcene, limonene, thymol, carvacrol	Anacardiaceae	1990, [235]
Pitaviaster haplophyllus (F. Muell.) T. G. Hartley	Germacrene D (10–28%), germacrene B (1–30%), bicyclogermacrene (2–10%), elemol (5–21%)	Rutaceae	2002, [236]

Table 1. *Cont.*

Species	Chemistry Info from Abstract	Family	Year and Ref.
Podocarpus dispermus, *P. drouynianus*, *P. elatus*, *P. grayae*, *P. smithii*, *P. spinulosus*	*P. dispermus*: isopimara-9(11),15-diene (10.3%). *P. drouynianus*: bicyclogermacrene (57%). *P. elatus*: α-pinene, β-caryophyllene, bicyclogermacrene. *P. grayae*: Bicyclogermacrene (27–44%), germacrene D (4–11%), spathulenol (3–11%). P. lawrencei: α-pinene (14–18%), β-caryophyllene (3–15%), spathulenol (0.8–19%), rimuene (0.2–30%), sandarocopimara-8(14), 15-diene (0.1–20%), beyerene (7–9%). *P. smithii*: α-copaene (4–8%), β-caryophyllene (5%), cadinene (9–11%). *P. spinulosus*: limonene (13–16%), bicyclogermacrene (15–18%) and viridiflorol (16–18%)	Podocarpaceae	2004, [237]
Polyalthia australis, *P. michaelii*, *P. nitidissima*, *P*. sp. (Wyvuri B.P.Hyland RFK2632)	*P. australis*: β-caryophyllene (4–15%), germacrene D (1–13%), bicyclogermacrene (1–10%), caryophyllene oxide (6–10%), spathulenol (7–24%). *P. michaelii*: spathulenol (42.2%). *P. nitidissima*: type 1, α-pinene (10–12%), limonene (4–6%), (E)-β-ocimene (0.7–2%), δ-cadinene (4–8%), spathulenol (15–17%), type 2, spathulenol (22–28%), bicyclogermacrene (4–24%), β-caryophyllene (2–10%). *P*. sp. (Wyvuri): globulol (1–34%), spathulenol (4–6%), ledol (1–10%), germacrene B (22–39%)	Annonaceae	2001, [238]
Polygonum odoratum Lour	Decanal (27.73%), dodecanal (44.05%), decanol (10.88%)	Polygonaceae	1997, [239]
Pseuduvaria mulgraveana var. mulgraveana, *P. mulgraveana var. glabrescens*, *P. hylandii*, *P. villosa*, and *P. froggattii*	*P. mulgraveana* var. *mulgraveana* and *P. mulgraveana* var. *glabrescens*: elemicin (87%) and methyl eugenol (61%). *P. villosa*: β-caryophyllene (3–13%) and α-copaene (4–11%). *P. froggattii*: caryophyllene oxide (2–22%), froggatt ether (0.1–18%), spathulenol (9–18%). *P. hylandii*: β-caryophyllene (22–28%), α-himachalene (2–10%), α-humulene (8–9%)	Annonaceae	2004, [240]
Ristantia gouldii, *R. pachysperma*, *R. waterhousei*	*R. gouldii*: α-pinene (39–48%), β-pinene (19–34%). *R. pachysperma*: (E)-nerolidol (42%). *R. waterhousei*: α-Pinene (53–66%)	Myrtaceae	2003, [164]
Rhodamnia dumicola, *R. pauciovulata*, *R. rubescens* and *R*. sp. (McIlwraith Range, L.J. Webb + 9527), *R. australis*, *R. blairiana*, *R. costata*, *R. dumicola*, *R. argentea*, *R. whiteana*, *R*. sp. (Cape York, L. S. Smith 12538), *R. glabrescens*, *R. sessiliflora*, and *R. spongiosa*, *R. maideniana*, *R*. sp. (Calliope, N. Gibson 1335)	*R. dumicola*, *R. pauciovulata*, *R. rubescens* and *R*. sp. (McIlwraith Range): α-pinene. *R. australis*, *R. blairiana*, *R. costata*, *R. dumicola*, *R. argentea*, *R. whiteana* and R. sp. (Cape York): α-, β-, and γ-eudesmol, α- and β-pinene. *R. glabrescens*, *R. argentea* type 2, *R. sessiliflora*, *R. spongiosa*: β-caryophyllene, globulol, viridiflorol, spathulenol. *R. maideniana*, *R*. sp. (Calliope): unidentified oxygenated sesquiterpenes	Myrtaceae	1997, [241]

Table 1. *Cont.*

Species	Chemistry Info from Abstract	Family	Year and Ref.
Rhodomyrtus canescens C. T. White & W. D. Francis, *R. effussa* Guymer., *R. macrocarpa* Benth., *R. pervagata* Guymer., *R. psidioides* (G. Don.) Benth., *R. sericea* Burret., *R. trineura* (F. Muell.) F. Muell. ex Benth. subsp. *trineura*, *R. trineura* subsp. *capensis* Guymer	*R. canescens*: α-pinene (20–23%), β-pinene (6–10%), aromadendrene (12?17%). *R. effussa*: globulol (11–22%), viridiflorol (8–10%), spathulenol (5–18%). *R. macrocarpa*: β-caryophyllene (9–44%), aromadendrene (6–11%), globulol (8–10%). R. pervagata: α-pinene (27–35%), β-pinene (18–24%). *R. psidioides*: α-pinene (28–66%), limonene (1–24%). *R. sericea*: α-pinene (28%), β-pinene (21%), β-caryophyllene (13%). *R. trineura* subsp. *trineura*: β-caryophyllene (16–29%), caryophyllene oxide (2–12%), globulol (7–10%). *R. trineura* subsp. *capensis*: α-pinene (tr-26%), globulol (9–19%), viridiflorol (5–12%), spathulenol (4–7%)	Myrtaceae	1997, [242]
Sarcomelicope simplicifolia subsp. *simplicifolia* (Endl.) T.G. Hartley	β-Caryophyllene (14–22%), bicyclogermacrene (10–42%), α-copaene (1–8%), γ-elemene (1–3%), α-humulene (1–4%), δ-cadinene (1–7%), δ-elemene (0.2–2%), spathulenol (1–5%)	Rutaceae	1997, [216]
Sphaerantia chartacea Peter G.Wilson & B.Hyland	β-Bisabolene (t-25%), bicyclogermacrene (15–40%), globulol (6–10%)	Myrtaceae	2003, [164]
Sphaerantia discolor Peter G.Wilson & B.Hyland	Bicyclogermacrene (19%), globulol (15%), viridiflorene (14%), viridiflorol (8%), ar-curcumene (9%)	Myrtaceae	2003, [164]
Steganthera australiana, *S. cooperorum*, *S. hirsute*, *S. laxiflora subsp. laxiflora*, *S. laxiflora subsp. lewisensis*, and *S. macooraia*	*S. australiana*: sesquiterpenoid. *S. cooperorum*: aromadendrene (6–10%), viridiflorene (7–8%), globulol (7–9%), b-eudesmol (8–11%); dodecanal (2–4%), type 2, elemol (30–42%), hedycaryol (approx. 8%), α-, β- and γ-eudesmol (10–14%, 10–14%, 5–9%, respectively). *S. hirsute*: bicyclogermacrene (37–56%), β-caryophyllene (2–17%), germacrene D (2–22%). *S. laxiflora* subsp. *laxiflora*: viridiflorene (13–20%). *S. macooraia*: guaiol (2–23%), bulnesol (0.7–10%), elemol (10–22%). *S. laxiflora* subsp. *lewisensis*: viridiflorene (11.8%), 2-dodecenal (6.3%)	Monimiaceae	2009, [189]
Sundacarpus amarus (Blume) C.N.Page	β-Selinene (67–77%), bicyclogermacrene (9–11%)	Podocarpaceae	2000, [243]
Syncarpia glomulifera (Sm.) Nied. subsp. *glomulifera*, *S. glomulifera* subsp. *glabra* (Benth.) A. R. Bean, *S. verecunda* A. R. Bean, S. hillii F. M. Bailey	*S. glomulifera* (Sm.) Nied. subsp. *glomulifera*, *S. glomulifera* subsp. *glabra* (Benth.) A. R. Bean and S. verecunda A. R. Bean: α-pinene (30–50%), α-thujene (11–27%), aromadendrene (1–13%), globulol (3–8%). S. hillii: hillyl acetate (53–80%), hillone (6–12%), α-pinene (2–22%)	Myrtaceae	1996, [244]
Syncarpia hillii F.M.Bailey	Hillyl acetate, 7-acetoxy-2,2,6,6,8,8-hexamethyl-5-oxo-5,6,7,8-tetrahydro-2H-chromen,	Myrtaceae	1994, [245]
Thaleropia queenslandica (L.S.Sm.) Peter G.Wilson	α-Pinene (61–83%), spathulenol (1–4%), bicyclogermacrene (1–3%)	Myrtaceae	1997, [246]
Thryptomene australis, *T. kochii*	*T. australis*: geranic acid (52%), α-pinene (22%). *T. kochii*: α-pinene (58–60%)	Myrtaceae	2004, [148]
Thryptomene hexandra, *T. parviflora*, *T. oligandra*	*T. hexandra* and *T. parviflora*: 1,8-cineole (up to 70%), α-pinene (up to 16%). *T. oligandra*: γ-terpinene (32–62%), p-cymene (25–50%), α-pinene (1–20%)	Myrtaceae	2000, [247]

Table 1. *Cont.*

Species	Chemistry Info from Abstract	Family	Year and Ref.
Trachymene incisa Rudge	β-selinene, bicyclogermacrene, γ-bisabolene, α-pinene, β-caryophyllene	Araliaceae	2021, [248]
Tristaniopsis collina, T. exiliflora, T. laurina, T. neriifolia	*T. collina*: α-pinene (trace—35–9%), myrcene (5.6–29.3%), cubenol (0–16.6%). *T. exiliflora*: β-caryophyllene (13.4%), δ-cadinene (16.4%). *T. laurina*: type 1, α-pinene (79.4%), type 2, limonene (13.0%), globulol (9.7%). *T. neriifolia*: α-pinene (24.4%), α-eudesmol (17.8%), β-eudesmol (17.2%) and γ-eudesmol (28.0%)	Myrtaceae	1999, [249]
Uromyrtus australis A. J. Scott, *U. metrosideros* (F. M. Bailey), *A.* J. Scott, *U.* sp. (Tinaroo Range G. P. Guymer 2034), *U.* sp. (McPherson Range G. P. Guymer 2000)	*U. australis*: β-caryophyllene (21%), β-, α- and γ-eudesmol (13, 9 and 11% respectively). *U. metrosideros*: α-pinene (13–20%), β-pinene (33–42%), α-terpineol (3–7%), spathulenol (9–15%). *U.* sp. (Tinaroo Range): bicyclogermacrene (14–23%), globulol (9–12%), viridiflorol (5–7%) and spathulenol (3–4%). U. sp. (McPherson Range): terpinen-4-ol (8–13%), α-pinene (3–10%)	Myrtaceae	1996, [250]
Uvaria rufa, U. concave	*U. rufa*: α-humulene (50%), benzyl benzoate *U. concave*: spathulenol (32%)	Annonaceae	2004, [154]
Vitex limonifolia Wall	Caryophyllene (43%), caryophyllene oxide (13%), α-pinene (6%)	Lamiaceae	1990, [251]
Vitex trifolia L., *V. trifolia* L. var. *simplicifolia* Cham	*V. trifolia*: 1,8-cineole, terpinyl acetate, sabinene, α-pinene, caryophyllene. *V. trifolia* var. *simplicifolia*: 1,8-cineole, α-pinene, terpinyl acetate, sabinene	Lamiaceae	1991, [252]
Viticipremna queenslandica Munir (syn. *Vitex queenslandica*)	β-caryophyllene (27–34%), germacrene D (1–16%), bicyclogermacrene (9–15%), spathulenol (2–6%)	Lamiaceae	2008, [253]
Waterhousea floribunda, *W. hedraiophylla*, *W. unipunctata, W. mulgraveana*	*W. floribunda*: α- and β-pinene (17–21%). *W. hedraiophylla*: spathulenol, calamenene, δ-cadinene, bicyclogermacrene. *W. unipunctata*: germacrene D (8.2–25.6%), bicyclogermacrene (3.2–12.3%), globulol (0.4–15.8%), viridiflorol (0.2–9.6%). *W. mulgraveana*: 1,3,5-trimethoxybenzene, 2,4,6-trimethoxyethylbenzene, 2,4,6-trimethoxystyrene, 2,4,6-trimethoxy-3,5-dirnethylstyrene	Myrtaceae	2002, [254]
Wollemia nobilis W.G.Jones, K.D.Hill & J.M.Allen	(+)−16-Kaurene (60%), α-pinene (9%), germacrene-D (8%)	Araucariaceae	2000, [147]
Welchiodendron longivalve (F. Muell.) Peter G. Wilson & J. T. Waterh	β-Trans-ocimene (17–28%), caryophyllene (39–57%), humulene (7–22%)	Myrtaceae	1996, [214]

Table 1. *Cont.*

Species	Chemistry Info from Abstract	Family	Year and Ref.
Wilkiea angustifolia, *W. austroqueenslandica*, *W. cordata*, *W. huegeliana*, *W. longipes*, *W. macrophylla*, *W. pubescens*, *W. rigidifolia*, *W. smithii*, *W.* sp. (McDowall Range J.G.Tracey 14552), *W.* sp. (Palmerston B.P.Hyland 80) and *W.* sp. (Russell Gorge S.J.Dansie 1909)	*W. angustifolia*: β-eudesmol (35%). *W. austroqueenslandica*: (E)- β-ocimene (5–9%), germacrene D (7–18%), bicyclogermacrene (23–26%). *W. cordata*: β-eudesmol (22–25%), spathulenol (11.3%). *W. huegeliana*: α-pinene (10–12%), viridiflorene (4–9%). *W. longipes*: (Z)-β-ocimene (11–15%). *W. macrophylla*: dodecanal (2–35%), (2)-dodecenal (0.1–2%), β-caryophyllene (14–24%). *W. pubescens*: sesquiterpenes. *W. rigidifolia*: (Z)-β-ocimene (3.4–11.5%), bicyclogermacrene (3.2–17.4%), germacrene B (0.3–14.5%). *W. smithii*: β-caryophyllene (10.4%), bicyclogermacrene (9.6%), caryophyllene oxide (8.9%), spathulenol (16.7%). *W.* sp. (McDowall Range): selina-6-en-4-ol (30.7%), germacrene D-4-ol (18.6%). *W.* sp. (Palmerston): spathulenol (22%). *W.* sp. (Russell) elemol (19.2%)	Monimiaceae	2009, [189]
Xylopia maccreae (F.Muell.) L.S. Sm., *Xylopia* sp. (Bertiehaugh Homestead C. Dalliston CC173)	*X. maccreae*: bicyclogermacrene (34%), β-cubebene, β-caryophyllene, germacrene D. *Xylopia* sp. (Bertiehaugh Homestead): spathulenol (31%), globulol, viridiflorol, caryophyllene oxide	Annonaceae	1998, [255]
Zygogynum howeanum, *Z. semecarpoides* var. *semecarpoides*, *Z. queenslandianum* subsp. *queenslandianum*, *Z. queenslandianum* subsp. *australe*	*Z. howeanum*: β-caryophyllene (48.0%), α-humulene (16.5%) and (Z)-β-farnesene (3.2%). *Z. semecarpoides* var. *semecarpoides* spathulenol (24.4%). *Z. queenslandianum* subsp. *queenslandianum*: bicyclogermacrene (10.4%), globulol (7.7%), viridiflorol (4.5%), spathulenol (11.5%). *Z. queenslandianum* subsp. *austral*: elemol (5.1%), bicyclogermacrene, spathulenol	Winteraceae	1994, [256]

6. Conclusions

While many Australian essential oils have risen in the marketplace over the last 200 years, there are many others that experienced a rise and fall, or no rise at all. Some of the species grown on mainland Australia and Tasmania were prized, but their populations became threatened, such as *Lagarostrobos franklinii* and *Santalum spicatum*, and they were not easily cultivated as an alternative. Others were marketed with the wrong branding and were given a bad name, such as *Eremophila mitchellii* which earned the vernacular 'bastard sandalwood.'

Many essential oils are comprised of endemic molecules that were described for the first time after isolation from an Australian species. These molecules were often named after the species or genus, such as geijerene or prostantherol. Occasionally, endemic Australian essential oil components are identified in species from other continents too.

The therapeutic or aesthetic value of Australian oils is demonstrated by the Australian Aboriginal people, and by cultures elsewhere that used *materia medica* that have chemical overlap with Australian aromatic species. Australian essential oils are good candidates for antiseptic effects, as anti-inflammatory ingredients, as anti-depressants, and insect repellents.

Funding: This research received no external funding.

Institutional Review Board Statement: Not applicable.

Data Availability Statement: Not applicable.

Acknowledgments: The author would like to acknowledge Australia's first people who utilized aromatic plants routinely for more than 60,000 years.

Conflicts of Interest: The author declares no conflict of interest.

References

1. Wilson, N.D.; Watt, R.A.; Moffat, A.C. A near-infrared method for the assay of cineole in eucalyptus oil as an alternative to the official BP method. *J. Pharm. Pharm.* **2001**, *53*, 95–102. [CrossRef] [PubMed]
2. Sadgrove, N.J.; Jones, G.L. A contemporary introduction to essential oils: Chemistry, bioactivity and prospects for Australian agriculture. *Agriculture* **2015**, *5*, 48–102. [CrossRef]
3. Sadgrove, N.J. Honest nutraceuticals, cosmetics, therapies, and foods (NCTFs): Standardization and safety of natural products. *Crit. Rev. Food. Sci. Nutr.* **2021**, 1–16. [CrossRef] [PubMed]
4. Tan, M.; Zhou, L.; Huang, Y.; Wang, Y.; Hao, X.; Wang, J. Antimicrobial activity of globulol isolated from the fruits of Eucalyptus globulus Labill. *Nat. Prod. Res.* **2008**, *22*, 569–575. [CrossRef] [PubMed]
5. Mulyaningsih, S.; Sporer, F.; Reichling, J.; Wink, M. Antibacterial activity of essential oils from Eucalyptus and of selected components against multidrug-resistant bacterial pathogens. *Pharm. Biol.* **2011**, *49*, 893–899. [CrossRef] [PubMed]
6. Mulyaningsih, S.; Sporer, F.; Zimmermann, S.; Reichling, J.; Wink, M. Synergistic properties of the terpenoids aromadendrene and 1,8-cineole from the essential oil of Eucalyptus globulus against antibiotic-susceptible and antibiotic-resistant pathogens. *Phytomedicine* **2010**, *17*, 1061–1066. [CrossRef] [PubMed]
7. McLellan, R.C.; Dixon, K.; Watson, D.M. Prolific or precarious: A review of the status of Australian sandalwood (*Santalum spicatum* [R.Br.] A.DC., Santalaceae). *Rangel. J.* **2021**, *43*, 211–222. [CrossRef]
8. Howes, M.J.; Simmonds, M.S.; Kite, G.C. Evaluation of the quality of sandalwood essential oils by gas chromatography-mass spectrometry. *J. Chromatogr. A* **2004**, *1028*, 307–312. [CrossRef]
9. Sadgrove, N.J.; Klepp, J.; Legendre, S.V.A.-M.; Lyddiard, D.; Sumby, C.J.; Greatrex, B.W. Revision of the phytochemistry of *Eremophila sturtii* and *E. mitchellii*. *J. Nat. Prod.* **2018**, *81*, 405–409. [CrossRef]
10. Beattie, K.; Waterman, P.G.; Forster, P.I.; Thompson, D.R.; Leach, D.N. Chemical composition and cytotoxicity of oils and eremophilanes derived from various parts of *Eremophila mitchellii* Benth. (Myoporaceae). *Phytochemistry* **2011**, *71*, 400–408. [CrossRef]
11. Southwell, I.A.; Brophy, J.J. Essential oil isolates from the Australian flora. Part 3. *J. Essent. Oil Res.* **2000**, *12*, 267–278. [CrossRef]
12. Sadgrove, N.J.; Jones, G.L.; Greatrex, B.W.; Watson, K. Ethnopharmacology and Chemotaxonomy of Essential Oil Yielding Australian Plants. Ph.D. Thesis, University of New England, Armidale, Australia, 2014.
13. Jones, G.L.; Sadgrove, N.J. Ethnopharmacology in Australia and Oceania. In *Ethnopharmacology—A Reader*; Heinrich, M., Jäger, A.K., Eds.; John Wiley & Sons: Chichester, UK, 2015.
14. Sadgrove, N.J.; Jones, G.L. From Petri Dish to Patient: Bioavailability Estimation and Mechanism of Action for Antimicrobial and Immunomodulatory Natural Products. *Front. Microbiol.* **2019**, *10*, 2470. [CrossRef] [PubMed]
15. Langat, M.K.; Mayowa, Y.; Sadgrove, N.J.; Danyaal, M.; Prescott, T.A.K.; Kami, T.; Schwikkard, S.; Barker, J.; Cheek, M. Multi-layered antimicrobial synergism of (*E*)-caryophyllene with alkaloids and 13S-hydroxy-9Z,11E,15E-octadecatrienoic acid from the leaves of *Vepris gossweileri* (I. Verd.) Mziray. *Nat. Prod. Res.* 2021. (*in press*) [CrossRef]
16. Sadgrove, N.J. Southern Africa as a 'cradle of incense' in wider African aromatherapy. *Sci. Afr.* **2020**, *9*, e00502. [CrossRef]
17. Sadgrove, N.J.; Padilla-Gonzalez, G.F.; Leuner, O.; Melnikovova, I.; Fernandez-Cusimamani, E. Pharmacology of Natural Volatiles and Essential Oils in Food, Therapy, and Disease Prophylaxis. *Front Pharm.* **2021**, *12*, 740302. [CrossRef]
18. Sadgrove, N.; Jones, G.L.; Greatrex, B.W. Isolation and characterisation of (−)-genifuranal: The principal antimicrobial component in traditional smoking applications of *Eremophila longifolia* (Scrophulariaceae) by Australian Aboriginal peoples. *J. Ethnopharmacol.* **2014**, *154*, 758–766. [CrossRef]
19. Sadgrove, N.; Jones, G.L. A possible role of partially pyrolysed essential oils in Australian Aboriginal traditional ceremonial and medicinal smoking applications of *Eremophila longifolia* (R. Br.) F. Muell (*Scrophulariaceae*). *J. Ethnopharmacol.* **2013**, *147*, 638–644. [CrossRef]
20. Fang, J.-M.; Chen, Y.-C.; Wang, B.-W.; Cheng, Y.-S. Terpenes from the heartwood of *Juniperus chinensis*. *Phytochemistry* **1996**, *41*, 1361–1365. [CrossRef]
21. Lee, C.-H.; Park, J.-M.; Song, H.-Y.; Jeong, E.-Y.; Lee, H.-S. Acaricidal activities of major constituents of essential oil of *Juniperus chinensis* leaves against house dust and stored food mites. *J. Food Prot.* **2009**, *72*, 1686–1691. [CrossRef]
22. Tunalier, Z.; Kirimer, N.; Baser, K.H.C. A potential new source of cedarwood oil: *Juniperus foetidissima* Willd. *J. Essent. Oil Res.* **2004**, *16*, 233–235. [CrossRef]
23. Soković, M.; Ristic, M.; Grubisic, D. Chemical Composition and Antifungal Activity of the Essential Oil from *Juniperus excelsa* Berries. *Pharm. Biol.* **2004**, *42*, 328–331. [CrossRef]
24. Fang, J.-M.; Sou, Y.-C.; Chiu, Y.-H.; Cheng, Y.-S. Diterpenes from the bark of *Juniperus chinensis*. *Phytochemistry* **1993**, *34*, 1581–1584.
25. Oda, J.; Ando, N.; Nakajima, Y.; Inouye, Y. Studies on Insecticidal Constituents of *Juniperus recurva* Buch. *Agric. Biol. Chem.* **1977**, *41*, 201–204. [CrossRef]
26. Richmond, G.S. A review of the use of *Eremophila* (Myoporaceae) by Australian Aborigines. *J. Adel. Bot. Gard.* **1993**, *15*, 101–107.

27. Maiden, J.H. *Forestry Handbook. Part 2. Some of the Principal Commercial Trees of New South Wales*; William Applegate Gullick; Government Printer: Sydney, Australia, 1917.
28. Maiden, J.H. *The Useful Native Plants of Australia*; Published by Compendium in 1975; Alexander Bros Vic: Melbourne, Australia, 1889.
29. Cribb, A.B.; Cribb, J.W. *Useful Wild Plants in Australia*; William Collins Pty. Ltd.: Sydney, Australia, 1981.
30. Beattie, K.D. Phytochemical Studies and Bioactivity of *Centipeda* and *Eremophila* Species. Ph.D. Thesis, Southern Cross University, Lismore, Australia, 2009.
31. Govaerts, R.; Nic Lughadha, E.; Black, N.; Turner, R.; Paton, A. The World Checklist of Vascular Plants, a continuously updated resource for exploring global plant diversity. *Sci. Data* **2021**, *8*, 215. [CrossRef]
32. Sadgrove, N.J.; Senbill, H.; Van Wyk, B.-E.; Greatrex, B.W. New labdanes with antimicrobial and acaricidal activity: Terpenes of *Callitris* and *Widdringtonia* (Cupressaceae). *Antibiotics* **2020**, *9*, 173. [CrossRef]
33. Hay, R. Demodex and skin infection: Fact or fiction. *Curr. Opin. Infect. Dis.* **2010**, *23*, 103–105. [CrossRef]
34. Kiran, S.R.; Reddy, A.S.; Devi, P.S.; Reddy, K.J. Insecticidal, antifeedant and oviposition deterrent effects of the essential oil and individual compounds from leaves of Chloroxylon swietenia DC. *Pest. Manag. Sci.* **2006**, *62*, 1116–1121. [CrossRef]
35. Ali, J.G.; Alborn, H.T.; Campos-Herrera, R.; Kaplan, F.; Duncan, L.W.; Rodriguez-Saona, C.; Koppenhofer, A.M.; Stelinski, L.L. Subterranean, herbivore-induced plant volatile increases biological control activity of multiple beneficial nematode species in distinct habitats. *PLoS ONE* **2012**, *7*, e38146. [CrossRef]
36. Winkelman, W.J. Aromatherapy, botanicals, and essential oils in acne. *Clin. Derm.* **2018**, *36*, 299–305. [CrossRef]
37. Sadgrove, N.J.; Simmonds, M.S.J. Topical and nutricosmetic products for healthy hair and dermal antiaging using "dual-acting " (2 for 1) plant-based peptides, hormones, and cannabinoids. *FASEB Bioadv.* **2021**, *3*, 601–610. [CrossRef]
38. Sadgrove, N.J. The new paradigm for androgenetic alopecia and plant-based folk remedies: 5α-reductase inhibition, reversal of secondary microinflammation and improving insulin resistance. *J. Ethnopharmacol.* **2018**, *227*, 206–236. [CrossRef] [PubMed]
39. Hulley, I.M.; Van Vuuren, S.F.; Sadgrove, N.J.; Van Wyk, B.-E. Antimicrobial activity of *Elytropappus rhinocerotis* (Asteraceae) against micro-organisms associated with foot odour and skin ailments. *J. Ethnopharmacol.* **2019**, *228*, 92–98. [CrossRef] [PubMed]
40. Sadgrove, N.; Mijajlovic, S.; Tucker, D.J.; Watson, K.; Jones, G.L. Characterization and bioactivity of essential oils from novel chemotypes of *Eremophila longifolia* (F. Muell) (Myoporaceae): A highly valued traditional Australian medicine. *Flavour Fragr. J.* **2011**, *26*, 341–350. [CrossRef]
41. Carson, C.F.; Hammer, K.A.; Riley, T.V. *Melaleuca alternifolia* (Tea Tree) oil: A review of antimicrobial and other medicinal properties. *Clin. Microbiol. Rev.* **2006**, *19*, 50–62. [CrossRef]
42. Bejar, E. Tea Tree Oil (*Melaleuca alternifolia* and *M. linariifolia*). Available online: www.botanicaladulterants.org (accessed on 10 May 2021).
43. Wilkinson, J.M.; Cavanagh, H.M.A. Antibacterial activity of essential oils from Australian native plants. *Phytother. Res.* **2005**, *19*, 643–646. [CrossRef]
44. Sadgrove, N.J.; Padilla-González, G.F.; Telford, I.R.H.; Greatrex, B.W.; Jones, G.L.; Andrew, R.; Bruhl, J.J.; Langat, M.K.; Melnikovova, I.; Fernandez-Cusimamani, E. *Prostanthera* (Lamiaceae) as a 'Cradle of Incense': Chemophenetics of Rare Essential Oils from Both New and Forgotten Australian 'Mint Bush' Species. *Plants* **2020**, *9*, 1570. [CrossRef]
45. Collins, T.L.; Jones, G.L.; Sadgrove, N. Volatiles from the rare Australian desert plant *Prostanthera centralis* B.J.Conn (Lamiaceae): Chemical composition and antimicrobial activity. *Agriculture* **2014**, *4*, 308–316. [CrossRef]
46. Sadgrove, N.J.; Greatrex, B.W.; Jones, G.L. α-Cyclodextrin encapsulation enhances antimicrobial activity of cineole-rich essential oils from Australian species of Prostanthera (Lamiaceae). *Nat. Volatiles Essent. Oils* **2015**, *2*, 30–38.
47. Sadgrove, N.; Jones, G.L. Antimicrobial activity of essential oils and solvent extracts from *Zieria* species (Rutaceae). *Nat. Prod. Commun.* **2013**, *8*, 741–745. [CrossRef]
48. Tavares, A.C.; Goncalves, M.J.; Cavaleiro, C.; Cruz, M.T.; Lopes, M.C.; Canhoto, J.; Salgueiro, L.R. Essential oil of Daucus carota subsp. halophilus: Composition, antifungal activity and cytotoxicity. *J. Ethnopharmacol.* **2008**, *119*, 129–134. [CrossRef]
49. Sadgrove, N.J.; Gonçalves-Martins, M.; Jones, G.L. Chemogeography and antimicrobial activity of essential oils from *Geijera parviflora* and *Geijera salicifolia* (Rutaceae): Two traditional Australian medicinal plants. *Phytochemistry* **2014**, *104*, 60–71. [CrossRef] [PubMed]
50. Brophy, J.J.; Goldsack, R.J.; Forster, P.I. The Leaf Oils of the Australian Species of *Flindersia* (Rutaceae). *J. Essent. Oil Res.* **2005**, *17*, 388–395. [CrossRef]
51. Tonzibo, Z.F.; Wognin, E.; Chalchat, J.C.; N'Guessan, Y.T. Chemical Investigation of *Chromolaena odorata* L. King Robinson from Ivory Coast. *J. Essent. Oil Bear. Plants* **2007**, *10*, 94–100. [CrossRef]
52. Dellar, J.E.; Cole, M.D.; Gray, A.I.; Gibbons, S.; Waterman, P.G. Antimicrobial sesquiterpenes from *Prostanthera* aff. melissifolia and P. rotundifolia. *Phytochemistry* **1994**, *36*, 957–960. [CrossRef]
53. Sakkas, H.; Economou, V.; Gousia, P.; Bozidis, P.; Sakkas, V.A.; Petsios, S.; Mpekoulis, G.; Ilia, A.; Papadopoulou, C. Antibacterial Efficacy of Commercially Available Essential Oils Tested Against Drug-Resistant Gram-Positive Pathogens. *Appl. Sci.* **2018**, *8*, 2201. [CrossRef]
54. Tighe, S.; Gao, Y.-Y.; Tseng, S.C.G. Terpinen-4-ol is the Most Active Ingredient of Tea Tree Oil to Kill Demodex Mites. *Transl. Vis. Sci. Technol.* **2013**, *2*, 2. [CrossRef]

55. Qin, X.-J.; Jin, L.-Y.; Yu, Q.; Liu, H.; Khan, A.; Yan, H.; Hao, X.-J.; An, L.-K.; Liu, H.-Y. Eucalypglobulusals A–J, Formyl-Phloroglucinol–Terpene Meroterpenoids from Eucalyptus globulus Fruits. *J. Nat. Prod.* **2018**, *81*, 2638–2646. [CrossRef]
56. Sadgrove, N.J.; Oliveira, T.B.; Khumalo, G.P.; Vuuren, S.F.v.; van Wyk, B.-E. Antimicrobial Isoflavones and Derivatives from Erythrina (Fabaceae): Structure Activity Perspective (Sar & Qsar) on Experimental and Mined Values Against Staphylococcus Aureus. *Antibiotics* **2020**, *9*, 223. [CrossRef]
57. Bharate, S.B.; Bhutani, K.K.; Khan, S.I.; Tekwani, B.L.; Jacob, M.R.; Khan, I.A.; Singh, I.P. Biomimetic synthesis, antimicrobial, antileishmanial and antimalarial activities of euglobals and their analogues. *Bioorg. Med. Chem.* **2006**, *14*, 1750–1760. [CrossRef]
58. Usuki, Y.; Deguchi, T.; Iio, H. A New Concise Synthesis of (+)-Ipomeamarone, (−)-Ngaione, and Their Stereoisomers. *Chem. Lett.* **2014**, *43*, 1882–1884. [CrossRef]
59. Sadgrove, N.J.; Padilla-Gonzalez, G.F.; Green, A.; Langat, M.K.; Mas-Claret, E.; Lyddiard, D.; Klepp, J.; Legendre, S.V.A.; Greatrex, B.W.; Jones, G.L.; et al. The Diversity of Volatile Compounds in Australia's Semi-Desert Genus Eremophila (Scrophulariaceae). *Plants* **2021**, *10*, 785. [CrossRef] [PubMed]
60. Sadgrove, N.J.; Jones, G.L. Cytogeography of essential oil chemotypes of *Eremophila longifolia* F. Muell (Schrophulariaceae). *Phytochemistry* **2014**, *105*, 43–51. [CrossRef] [PubMed]
61. Homburger, F.; Kelley, T.; Friedler, G.; Rusfield, A.B. Toxic and Possible Carcinogenic Effects of 4-Allyl-1,2-methylenedioxybenzene (Safrole) in Rats on Deficient Diets. *Med. Experimentalis. Int. J. Exp. Med.* **1961**, *4*, 1–11.
62. Miller, E.C.; Swanson, A.B.; Phillips, D.H.; Fletcher, T.L.; Liem, A.; Miller, J.A. Structure-Activity Studies of the Carcinogenicities in the Mouse and Rat of Some Naturally Occuring Synthetic Alkenylbenzene Derivatives Related to Safrole and Estragole. *Cancer Res.* **1983**, *43*, 1124–1134.
63. Kalbhen, D.; Abbo, A. Nutmeg as a narcotic. A contribution to the chemistry of pharmacology of nutmeg (*Myristica fragrans*). *Angew. Chem. Int.* **1971**, *10*, 370–374. [CrossRef]
64. Beyer, J.; Ehlers, D.; Maurer, H.H. Abuse of Nutmeg (Myristica fragrans Houtt.): Studies on the metabolism and the toxicologic detection of its ingredients elemicin, myristicin, and safrole in rat and human urine using gas chromagrography/mass spectrometery. *Ther. Drug Monit.* **2006**, *28*, 568–575. [CrossRef]
65. Yonghua, D.; Chuan, W.; Lijun, Z.; Ping, Z.; Qin, W.; Zhongqiong, Y.; Qinjiu, J.; Jihong, J. Effects of sub-chronic intoxication of 1,8-cineole on blood biochemical indexes in mice. *Anim. Husb. Feed Sci.* **2015**, *7*, 167–170.
66. Frosch, P.J.; Johansen, J.D.; Menne, T.; Pirker, C.; Rastogi, S.C.; Andersen, K.E.; Bruze, M.; Goossens, A.; Lepoittevin, J.P.; White, I.R. Further important sensitizers in patients sensitive to fragrances. *Contact Dermat.* **2002**, *47*, 279–287. [CrossRef]
67. Jacobs, M.R.; Hornfeldt, C.S. Melaleuca oil poisoning. *J. Toxicol. Clin. Toxicol.* **1994**, *32*, 461–464. [CrossRef]
68. Zidorn, C. Plant chemophenetics—A new term for plant chemosystematics/plant chemotaxonomy in the macro-molecular era. *Phytochemistry* **2019**, *163*, 147–148. [CrossRef]
69. Ramos, Y.J.; da Costa-Oliveira, C.; Candido-Fonseca, I.; de Queiroz, G.A.; Guimarães, E.F.; Defaveri, A.C.; Sadgrove, N.J.; Moreira, D.d.L. Advanced Chemophenetic Analysis of Essential Oil from Leaves of Piper gaudichaudianum Kunth (Piperaceae) Using a New Reduction-Oxidation Index to Explore Seasonal and Circadian Rhythms. *Plants* **2021**, *10*, 2116. [CrossRef] [PubMed]
70. Della, E.W.; Jefferies, P.R. The Chemistry of *Eremophila Species*. 111. The Essential oil of *Eremophila longifolia* F. Muell. *Aust. J. Chem.* **1961**, *14*, 663–664. [CrossRef]
71. Chinnock, R. *Eremophila and Allied Genera. A Monograph of the Myoporaceae*; Rosenberg Publishing: Kenthurst, Australia, 2007.
72. Sadgrove, N.J.; Telford, I.R.H.; Greatrex, B.W.; Jones, G.L. Composition and antimicrobial activity of essential oils from the *Phebalium squamulosum* species complex (Rutaceae) in New South Wales, Australia. *Phytochemistry* **2014**, *97*, 38–45. [CrossRef] [PubMed]
73. Sadgrove, N.; Telford, I.R.H.; Greatrex, B.W.; Dowell, A.; Jones, G.L. Dihydrotagetone, an unusual fruity ketone, is found in enantiopure and enantioenriched forms in additional Australian native taxa of *Phebalium* (Rutaceae: Boronieae). *Nat. Prod. Commun.* **2013**, *8*, 737–740. [CrossRef]
74. Lassak, E.V.; Southwell, I.A. Occurrence of some unusual compounds in the leaf oils of *Eriostemon obovalis* and *Phebalium glandulosum* subsp. *glandulosum*. *Aust. J. Chem.* **1974**, *27*, 2703–2705. [CrossRef]
75. Telford, I.R.H.; Bruhl, J.J. *Phebalium verrucosum* (Rutaceae: Boronieae), new status for a taxon excluded from *P. squamulosum* on morphological and phytochemical evidence. *Telopea* **2014**, *16*, 127–132. [CrossRef]
76. Sadgrove, N.J. Comparing essential oils from Australia's 'Victorian Christmas Bush' (*Prostanthera lasianthos* Labill., Lamiaceae) to closely allied new species: Phenotypic plasticity and taxonomic variability. *Phytochemistry* **2020**, *176*, 112403. [CrossRef]
77. Conn, B.J.; Henwood, M.J.; Proft, K.M.; Scott, J.A.; Wilson, T.C.; Howes, R.S. An integrative taxonomic approach resolves the *Prostanthera lasianthos* (Lamiaceae) species complex. *Aust. Syst. Bot.* **2021**, *34*, 438–476. [CrossRef]
78. De Queiroz, K. Species concepts and species delimitation. *Syst. Biol.* **2007**, *56*, 879–886. [CrossRef]
79. Collins, T.L.; Andrew, R.L.; Bruhl, J.J. Morphological, phytochemical and molecular analyses define species limits in *Eucalyptus magnificata* (Myrtaceae) and lead to the discovery of a new rare species. *Aust. Syst. Bot.* **2019**, *32*, 12–28. [CrossRef]
80. Collins, T.L.; Andrew, R.L.; Greatrex, B.W.; Bruhl, J.J. Reliable analysis of volatile compounds from small samples of *Eucalyptus magnificata* (Myrtaceae). *Aust. Syst. Bot.* **2018**, *31*, 232–240. [CrossRef]
81. Toyota, M.; Koyama, H.; Mizutani, M.; Asakawa, Y. (−)-ent-spathulenol isolated from liverworts is an artefact. *Phytochemistry* **1996**, *41*, 1347–1350. [CrossRef]

82. Sadgrove, N.J.; Telford, I.R.H.; Padilla-González, G.F.; Greatrex, B.W.; Bruhl, J.J. GC–MS 'chemophenetics' on Australian pink-flowered Phebalium (Rutaceae) using herbarium leaf material demonstrates phenetic agreement with putative new species. *Phytochem. Lett.* **2020**, *38*, 112–120. [CrossRef]
83. Akhtar, M.A.; Raju, R.; Beattie, K.D.; Bodkin, F.; Munch, G. Medicinal Plants of the Australian Aboriginal Dharawal People Exhibiting Anti-Inflammatory Activity. *Evid.-Based Complement. Altern. Med.* **2016**, *2016*, 2935403. [CrossRef] [PubMed]
84. Lassak, E.V.; McCarthy, T. *Australian Medicinal Plants*; Methuen Australia Pty. Ltd.: North Rhyde, Australia, 2011.
85. Sadgrove, N.J.; Lyddiard, D.; Collins, T.L.; Greatrex, B.W.; Jones, G.L. Genifuranal and other derivatives: Smoking desert plants. *Acta Hortic.* **2016**, *1125*, 181–188. [CrossRef]
86. Sadgrove, N.J.; Jones, G.L. Reviewing the importance of aromatic medicinal plants in the traditional pharmacopoeia of Australian Aboriginal people. *Acta Hortic.* **2014**, *1125*, 297–302. [CrossRef]
87. Nsangou, M.F.; Happi, E.N.; Fannang, S.V.; Atangana, A.F.; Waffo, A.F.K.; Wansi, J.D.; Isyaka, S.M.; Sadgrove, N.J.; Sewald, N.; Langat, M.K. Chemical Composition and Synergistic Antimicrobial Effects of a Vegetatively Propagated Cameroonian Lemon, *Citrus x limon* (L.) Osbeck. *ACS Food Sci. Technol.* **2021**, *1*, 354–361. [CrossRef]
88. Sadgrove, N.; Hitchock, M.; Watson, K.; Jones, G.L. Chemical and biological characterization of novel essential oils from *Eremophila bignoniiflora* (F. Muell) (Myoporaceae): A traditional Aboriginal Australian bush medicine. *Phytother. Res.* **2013**, *27*, 1508–1516. [CrossRef]
89. Sadgrove, N.J.; Jones, G.L. Phytochemical variability of *Pittosporum angustifolium* Lodd. (Pittosporaceae): A traditional and contemporary Aboriginal Australian medicine. *Acta Hortic.* **2014**, *1125*, 303–308. [CrossRef]
90. Cribb, A.B.; Cribb, J.W. *Wild Medicine in Australia*; William Collins, Pty. Ltd.: Sydney, Australia, 1981.
91. Baker, R.T.; Smith, H.G. On a new species of *Prostanthera* and its essential oil. *J. Proc. R. Soc. NSW* **1912**, *46*, 103–110.
92. Conn, B.J. A taxonomic revision of *Prostanthera* Labill. section Klanderia (F.v.Muell.) Benth. (Labiatae). *J. Adel. Bot. Gard.* **1984**, *6*, 207–348.
93. Southwell, I.A.; Tucker, D.J. *cis*-Dihydroagarofuran from *Prostanthera* sp. aff. ovalifolia. *Phytochemistry* **1993**, *22*, 857–862. [CrossRef]
94. Sadgrove, N.J.; Collins, T.L.; Legendre, S.V.A.-M.; Klepp, J.; Jones, G.L.; Greatrex, B.W. The Iridoid Myodesert-1-ene and Elemol/Eudesmol are found in Distinct Chemotypes of the Australian Aboriginal Medicinal Plant Eremophila dalyana(Scrophulariaceae). *Nat. Prod. Commun.* **2016**, *11*, 1211–1214. [CrossRef] [PubMed]
95. Penfold, A.R. Natural chemical resources of Australian plant products. Part II. *J. Chem. Educ.* **1932**, *9*, 429. [CrossRef]
96. Penfold, A.R. The natural chemical resources of Australia Plant Products. Part 1. *J. Chem. Educ.* **1929**, *6*, 1195–1205. [CrossRef]
97. Penfold, A.R.; Willis, J.L. The essential oil industry of Australia. *Econ. Bot.* **1954**, *8*, 316–336. [CrossRef]
98. Brophy, J.J.; Goldsack, R.J.; Fookes, C.J.R.; Forster, P.I. Leaf Oils of the Genus Backhousia (Myrtaceae). *J. Essent. Oil Res.* **1995**, *7*, 237–254. [CrossRef]
99. Sadgrove, N.J.; Van Wyk, B.-E. Major volatile compounds in the essential oil of the aromatic culinary herb *Pelargonium crispum* (Geraniaceae). *Nat. Volatiles Essent. OIls* **2018**, *5*, 23–28.
100. Doran, J.C.; Brophy, J.J.; Lassak, E.V. *Backhousia citriodora* F. Muell.—Rediscovery and chemical characterization of the L-citronellal form and aspects of its breeding system. *Flavour Fragr. J.* **2001**, *16*, 325–328. [CrossRef]
101. Brophy, J.J.; Goldsack, R.J.; Bean, A.R.; Forster, P.I.; Lepschi, B.J. Leaf essential oils of the genus *Leptospermum* (Myrtaceae) in eastern Australia. Part 5. Leptospermum continentale and allies. *Flavour Fragr. J.* **1999**, *14*, 98–104. [CrossRef]
102. Diatloff, E. Effects of applied nitrogen fertiliser on the chemical composition of the essential oil of three Leptospermum spp. *Aust. J. Exp. Agric.* **1990**, *30*, 681–685. [CrossRef]
103. Caputo, L.; Smeriglio, A.; Trombetta, D.; Cornara, L.; Trevena, G.; Valussi, M.; Fratianni, F.; De Feo, V.; Nazzaro, F. Chemical Composition and Biological Activities of the Essential Oils of Leptospermum petersonii and Eucalyptus gunnii. *Front. Microbiol.* **2020**, *11*, 409. [CrossRef] [PubMed]
104. Verma, R.S.; Padalia, R.C.; Chauhan, A.; Singh, A.; Yadav, A.K. Volatile constituents of essential oil and rose water of damask rose (Rosa damascena Mill.) cultivars from North Indian hills. *Nat. Prod. Res.* **2011**, *25*, 1577–1584. [CrossRef] [PubMed]
105. Reichling, J.; Koch, C.; Stahl-Biskup, E.; Sojka, C.; Schnitzler, P. Virucidal activity of a beta-triketone-rich essential oil of Leptospermum scoparium (manuka oil) against HSV-1 and HSV-2 in cell culture. *Planta Med.* **2005**, *71*, 1123–1127. [CrossRef]
106. Killeen, D.P.; van Klink, J.W.; Smallfield, B.M.; Gordon, K.C.; Perry, N.B. Herbicidal beta-triketones are compartmentalized in leaves of Leptospermum species: Localization by Raman microscopy and rapid screening. *New Phytol.* **2015**, *205*, 339–349. [CrossRef]
107. Hellyer, R.O.; Pinhey, J.T. The structure of grandiflorone, a new β-triketone. *J. Chem. Soc. C Org.* **1966**, 1496–1498. [CrossRef]
108. Thomas, J.; Narkowicz, C.K.; Jacobson, G.A.; Davies, N.W. An examination of the essential oils of Tasmanian *Kunzea ambigua*, other *Kunzea* spp. and commercial *Kunzea* oil. *J. Essent. Oil Res.* **2010**, *22*, 381–385. [CrossRef]
109. Penfold, A.R. The essential oil of Eriostemon myoporoides (De Candolle). *J. Proc. R. Soc. NSW* **1925**, *59*, 206–211.
110. Hellyer, R.O. Occurence of maaliol, elemol, and globulol in some Australian essential oils. *Aust. J. Chem.* **1962**, *15*, 157. [CrossRef]
111. Curkic, A. *Phytochemistry and Pharmacology of Volatile Components of Calytrix Exstipulata & Cymbopogon Bombycinus*; A 449, Matrikelnummer: 0505534; Universitat Wien: Vienna, Austria, 2012.
112. Doimo, L.; Bartley, J.P.; Michael, G.D. *Cassinia quinquefaria* R. Br. Flower and Leaf Essential Oils. *J. Essent. Oil Res.* **2000**, *12*, 702–704. [CrossRef]

113. Doimo, L.; Bartley, J.P.; Michael, G.D. *Cassinia laevis* R. Br. Flower and Leaf Essential Oils. *J. Essent. Oil Res.* **2001**, *13*, 78–79. [CrossRef]
114. Boland, D.J.; Brophy, J.J.; House, A.P.N. *Eucalyptus leaf Oils: Use, Chemistry, Distillation and Marketing*; Inkata Press—Commonwealth Scientific and Industrial Research Organization: Sydney, Australia, 1991.
115. Kim, J.-K.; Kang, C.-S.; Lee, J.-K.; Kim, Y.-R.; Han, H.-Y.; Yun, H.K. Evaluation of Repellency Effect of Two Natural Aroma Mosquito Repellent Compounds, Citronella and Citronellal. *Entomol. Res.* **2005**, *35*, 117–120. [CrossRef]
116. Brophy, J.J.; Goldsack, R.J.; Forster, P.I. Leaf Essential Oils of the Queensland Species of *Phebalium* (Rutaceae: Boronieae). *J. Essent. Oil Res.* **2006**, *18*, 386–391. [CrossRef]
117. Brophy, J.J.; Goldsack, R.J.; Forster, P.I. What is the Smell of the "Fruit Salad Plant"?: The Leaf Oil of *Leionema ambiens* (Rutaceae). *J. Essent. Oil Res.* **2006**, *18*, 131–133. [CrossRef]
118. Sadgrove, N.J.; Jones, G.L. Medicinal compounds, chemically and biologically characterised from extracts of Australian *Callitris endlicheri* and *C. glaucophylla* (Cupressaceae): Used traditionally in Aboriginal and colonial pharmacopoeia. *J. Ethnopharmacol.* **2014**, *153*, 872–883.
119. Low, T. *Bush Medicine: A pharmacopoeia of Natural Remedies*; Greenhouse Publications Pty Ltd.: Richmond, Australia, 1990.
120. Latz, P. *Bushfires and Bushtucker: Aboriginal plant Use in Central Australia*; IAD Press: Alice Springs, Australia, 2004.
121. Low, T. *Bush Tucker: Australia's Wild Food Harvest*; Angus and Robertson Publishers: Sydney, Australia, 1989.
122. Metcalfe, C.R. The Structure of Some Sandalwoods and Their Substitutes and of Some Other Little Known Scented Woods. *Bull. Misc. Inf. R. Bot. Gard. Kew* **1935**, *1935*, 165–195. Available online: https://www.jstor.org/stable/pdf/4107533.pdf (accessed on 7 December 2021). [CrossRef]
123. RBGK. World Checklist of Vascular Plants. Available online: https://wcvp.science.kew.org/ (accessed on 13 January 2022).
124. Braun, N.A.; Sim, S.; Kohlenberg, B.; Lawrence, B.M. Hawaiian Sandalwood: Oil Composition of Santalum paniculatum and Comparison with Other Sandal Species. *Nat. Prod. Commun.* **2014**, *9*, 1365–1368. [CrossRef]
125. Yan, T.; Chen, Y.; Shang, L.; Li, G. Assessment of essential oils from five Santalum species using ATR-fourier transform mid-infrared spectroscopy and GC-MS combined with chemometric analysis. *J. Essent. Oil Res.* **2020**, *32*, 150–157. [CrossRef]
126. Penfold, A.R.; Morrison, F.R. *Some Australian Essential Oils in Insecticides and Repellents*; Fisher, Knight and Company: St Albans, UK, 1952.
127. Cook, E.; Bird, T.; Peterson, M.; Barbetti, M.; Buckley, B.; D'Arrigo, R.; Francey, R.; Tans, P. Climatic change in tasmania inferred from a 1089-year tree-ring chronology of huon pine. *Science* **1991**, *253*, 1266–1268. [CrossRef]
128. Drew, D.M.; Allen, K.; Downes, G.M.; Evans, R.; Battaglia, M.; Baker, P. Wood properties in a long-lived conifer reveal strong climate signals where ring-width series do not. *Tree Physiol.* **2013**, *33*, 37–47. [CrossRef]
129. Sadgrove, N.; Jones, G.L. Chemical and biological characterisation of solvent extracts and essential oils from leaves and fruit of two Australian species of *Pittosporum* (Pittosporaceae) used in aboriginal medicinal practice. *J. Ethnopharmacol.* **2013**, *145*, 813–821. [CrossRef] [PubMed]
130. Southwell, I.A. Methoxystyrenes from the genus Zieria. *Phytochemistry* **1981**, *20*, 1448–1450. [CrossRef]
131. Flynn, T.M.; Southwell, I.A. Essential oil constituents of the genus Zieria. *Phytochemistry* **1987**, *26*, 1673–1686. [CrossRef]
132. Southwell, I.A.; Armstrong, J.A. Chemical variation within the genus Zieria. *Phytochemistry* **1987**, *26*, 1687–1692. [CrossRef]
133. Johnson, J.B.; Batley, R.; Manson, D.; White, S.; Naiker, M. Volatile compounds, phenolic acid profiles and phytochemical content of five Australian finger lime (*Citrus australasica*) cultivars. *LWT* **2022**, *154*, 112640. [CrossRef]
134. Brophy, J.J.; Goldsack, R.J.; Forster, P.I. The Leaf Oils of the Australian Species of *Citrus* (Rutaceae). *J. Essent. Oil Res.* **2001**, *13*, 264–268. [CrossRef]
135. Southwell, I.A.; Brophy, J.J. Differentiation within the Australian *Tasmannia* by essential oil comparison. *Phytochemistry* **1992**, *31*, 3073–3081. [CrossRef]
136. Cock, I.E. The phytochemistry and chemotherapeutic potential of *Tasmannia lanceolata* (Tasmanian pepper): A review. *Pharmacogn. Commun.* **2013**, *3*, 13–25.
137. Khumalo, G.P.; Sadgrove, N.J.; Van Vuuren, S.F.; Van Wyk, B.-E. Antimicrobial activity of volatile and non-volatile isolated compounds and extracts from the bark and leaves of *Warburgia salutaris* (Canellaceae) against skin and respiratory pathogens. *S. Afr. J. Bot.* **2019**, *122*, 547–550. [CrossRef]
138. Sultana, R.; Hossain, R.; Adhikari, A.; Ali, Z.; Yousuf, S.; Choudhary, M.I.; Ali, M.Y.; Zaman, M.S. Drimane-type sesquiterpenes from Polygonum hydropiper. *Planta Med.* **2011**, *77*, 1848–1851. [CrossRef]
139. Lowe, R.F.; Russell, M.F.; Southwell, I.A.; Robinson, C.J.; Day, J. Composition of an Essential Oil from *Agonis fragrans* J.R. Wheeler et NGMarchant. *J. Essent. Oil Res.* **2007**, *19*, 342–344. [CrossRef]
140. Shellie, R.; Mondello, L.; Dugo, G.; Marriott, P. Enantioselective gas chromatographic analysis of monoterpenes in essential oils of the family Myrtaceae. *Flavour Fragr. J.* **2004**, *19*, 582–585. [CrossRef]
141. Brophy, J.J.; Craven, L.A.; Doran, J.C. *Melaleucas: Their Botany, Essential Oils and Uses*; ACIAR Monograph No. 156; Australian Centre for International Agricultural Research: Canberra, Australia, 2013.
142. Brophy, J.J.; Goldsack, R.J.; Forster, P.I. The Essential Oil of *Acmenosperma claviflorum* (Myrtaceae). *J. Essent. Oil Res.* **1999**, *11*, 162–164. [CrossRef]
143. Brophy, J.J.; Goldsack, R.J.; Forster, P.I.; Southwell, I.A. Leaf Oils of the Genus Acradenia (Rutaceae). *J. Essent. Oil Res.* **2001**, *13*, 136–139. [CrossRef]

144. Brophy, J.J.; Goldsack, R.J.; Forster, P.I. Leaf Essential Oils of the Australian Species of Acronychia (Rutaceae). *J. Essent. Oil Res.* **2004**, *16*, 597–607. [CrossRef]
145. Brophy, J.J.; Goldsack, R.J. Essential Oil of the Leaves and Flowers of Actinodium cunninghamii Schauer (Myrtaceae). *J. Essent. Oil Res.* **1994**, *6*, 639–640. [CrossRef]
146. Brophy, J.J.; Goldsack, R.J.; O'Sullivan, W. Chemistry of the Australian gymnosperms: Part VII. The leaf oils of the genus *Actinostrobus*. *Biochem. Syst. Ecol.* **2004**, *32*, 867–873. [CrossRef]
147. Brophy, J.J.; Goldsack, R.J.; Wu, M.Z.; Fookes, C.J.R.; Forster, P.I. The steam volatile oil of Wollemia nobilis and its comparison with other members of the Araucariaceae (Agathis and Araucaria). *Biochem. Syst. Ecol.* **2000**, *28*, 563–578. [CrossRef]
148. Lassak, E.V.; Brophy, J.J. Steam volatile leaf oils of some Western Australian species of the family Myrtaceae. *Flavour Fragr. J.* **2004**, *19*, 12–16. [CrossRef]
149. Brophy, J.J.; Boland, D.J. The leaf essential oil of *Allosyncarpia ternata* S. T. Blake. *Flavour Fragr. J.* **1992**, *7*, 117–119. [CrossRef]
150. Brophy, J.J.; Goldsack, R.J.; Craven, L.A. The Leaf Essential Oil of Angasomyrtus salina Trudgen & Keighery. *J. Essent. Oil Res.* **1994**, *6*, 69–71. [CrossRef]
151. Dunlop, P.J.; Bignell, C.M.; Brooker, M.I.H.; Brophy, J.J.; Brynn Hibbert, D. Use of gas chromatograms of essential leaf oils to compare eight taxa of genus Angophora (Myrtaceae): Possible relationships to the genus Eucalyptus. *Biochem. Syst. Ecol.* **1999**, *27*, 815–830. [CrossRef]
152. Brophy, J.J.; Goldsack, R.J.; Forster, P.I. Variation in Archirhodomyrtus beckleri (F. Muell.) A.J. Scott (Myrtaceae): Evidence from Volatile Oils. *Flavour Fragr. J.* **1996**, *11*, 11–14. [CrossRef]
153. Boland, D.J.; Brophy, J.J.; Goldsack, R.J. The leaf essential oil of *Arillastrum gummiferum* (Brongriart & Gris) Pancher ex Baillon. *Flavour Fragr. J.* **1994**, *9*, 47–49. [CrossRef]
154. Brophy, J.; Goldsack, R.; Forster, P. Essential Oils from the Leaves of Some Queensland Annonaceae. *J. Essent. Oil Res.* **2004**, *16*, 95–100. [CrossRef]
155. Brophy, J.J.; Clarkson, J.R.; Craven, L.A.; Forresters, R.I. The essential oils of Australian Members of the Genus Asteromyrtus (Myrtaceae). *Biochem. Syst. Ecol.* **1994**, *22*, 409–417. [CrossRef]
156. Brophy, J.J.; Goldsack, R.J.; Forster, P.I. Leaf Essential Oil of Austrobaileya scandens C. White. *J. Essent. Oil Res.* **1994**, *6*, 301–303. [CrossRef]
157. Brophy, J.J.; Goldsack, R.J.; Forster, P.I. Essential Oil of Austromatthaea elegans L.S. Smith (Monimiaceae) Leaves. *J. Essent. Oil Res.* **1995**, *7*, 585–588. [CrossRef]
158. Brophy, J.J.; Goldsack, R.J.; Forster, P.I. (E)-β-Ocimene from Two Species of Austromyrtus (Myrtaceae). *J. Essent. Oil Res.* **1995**, *7*, 1–4. [CrossRef]
159. Brophy, J.J.; Goldsack, R.J.; Fookes, C.J.R.; Forster, P.I. The essential oils of Australian Austromyrtus sens. lat. Part 1. The A. dulcis group. *Flavour Fragr. J.* **1995**, *10*, 69–73. [CrossRef]
160. Brophy, J.J.; Goldsack, R.J.; Fookes, C.J.R.; Forster, P.I. The Essential Oils of Australian Austromyrtus sens. lat. Part 3. The Austromyrtus bidwillii Group. *Flavour Fragr. J.* **1996**, *11*, 275–287. [CrossRef]
161. Brophy, J.J.; Goldsack, R.J.; Forster, P.I. The essential oils of Australian Austromyrtus sens. lat. Part 2. The Austromyrtus lasioclada group. *Flavour Fragr. J.* **1995**, *10*, 293–296. [CrossRef]
162. Brophy, J.J.; Goldsack, R.J.; Fookes, C.J.R.; Rozefelds, A.C. The Chemistry of the Australian Gymnosperms—Part 4: The Leaf Oils of the Genus Athrotaxis D. Don (Cupressaceae). *J. Essent. Oil Res.* **2002**, *14*, 109–113. [CrossRef]
163. Brophy, J.J.; Boland, D.J. The leaf essential oil of two chemotypes of Backhousia anisata vickery. *Flavour Fragr. J.* **1991**, *6*, 187–188. [CrossRef]
164. Brophy, J.J.; Goldsack, R.J.; Forster, P.I. Leaf Oils of the Genera Barongia, Mitrantia, Sphaerantia and Ristantia (Myrtaceae). *J. Essent. Oil Res.* **2003**, *15*, 226–230. [CrossRef]
165. Brophy, J.J.; Goldsack, R.J.; Forster, P.I. Essential Oils from the Leaves of *Bosistoa* F. Muell. ex Benth. (Rutaceae). *J. Essent. Oil Res.* **2007**, *19*, 249–254. [CrossRef]
166. Brophy, J.J.; Goldsack, R.J.; Forster, P.I. Essential Oil of Bouchardatia neurococca (Rutaceae) Leaves. *J. Essent. Oil Res.* **1994**, *6*, 505–506. [CrossRef]
167. Brophy, J.J.; Goldsack, R.J.; Forster, P.i. Leaf Oils of the Genus Brombya (Rutaceae). *J. Essent. Oil Res.* **2004**, *16*, 402–404. [CrossRef]
168. Brophy, J.J.; Forster, P.I.; Goldsack, R.J.; Hibbert, D.B.; Punruckvong, A. Variation in Callistemon viminalis (Myrtaceae): New evidence from leaf essential oils. *Aust. Syst. Bot.* **1997**, *10*, 1–13. [CrossRef]
169. Brophy, J.J.; Goldsack, R.J.; Forster, P.I.; Craven, L.A.; Lepschi, B.J. The Leaf Essential Oils of the Australian Members of the Genus Callistemon (Myrtaceae). *J. Essent. Oil Res.* **1998**, *10*, 595–606. [CrossRef]
170. Brophy, J.J.; Goldsack, R.J.; Forster, P.I. The essential oils of *Choricarpia leptopetala* (F. Muell.) Domin and *C. subargentea* (C.T. White) L.A.S. Johnson (Myrtaceae). *Flavour Fragr. J.* **1994**, *9*, 7–10. [CrossRef]
171. Brophy, J.J.; Goldsack, R.J.; Forster, P.I. The Leaf Oils of the Australian Species of Cinnamomum (Lauraceae). *J. Essent. Oil Res.* **2001**, *13*, 332–335. [CrossRef]
172. Brophy, J.J.; Forster, P.I.; Goldsack, R.J. Leaf oils of the Australian species of *Clausena* and *Micromelum* (Rutaceae). *J. Essent. Oil Res.* **2016**, *28*, 406–412. [CrossRef]
173. Brophy, J.J.; Goldsack, R.J.; Forster, P.I. The leaf oils of *Coatesia* and *Geijera* (Rutaceae) from Australia. *J. Essent. Oil Res.* **2005**, *17*, 169–174. [CrossRef]

174. Brophy, J.J.; Lassak, E.V. Volatile leaf oil of *Coleonema pulchellum* Williams (Rutaceae). *Flavour Fragr. J.* **1986**, *1*, 155–157. [CrossRef]
175. van Klink, J.W.; Brophy, J.J.; Perry, N.B.; Weavers, R.T. β-Triketones from Myrtaceae: Isoleptospermone from Leptospermum scoparium and Papuanone from Corymbia dallachiana. *J. Nat. Prod.* **1999**, *62*, 487–489. [CrossRef]
176. Brophy, J.J.; Goldsack, R.J.; Punruckvong, A.; Forster, P.I.; Fookes, C.J.R. Essential Oils of the Genus Crowea (Rutaceae). *J. Essent. Oil Res.* **1997**, *9*, 401–409. [CrossRef]
177. Brophy, J.J.; Forster, P.I.; Goldsack, R.J. Coconut Laurels: The Leaf Essential Oils from Four Endemic Australian Cryptocarya Species: C. bellendenkerana, C. cocosoides, C. cunninghamii and C. lividula (Lauraceae). *Nat. Prod. Commun.* **2016**, *11*, 255–258. [CrossRef]
178. Brophy, J.J.; Goldsack, R.J.; Forster, P.I. The Leaf Essential Oil of Cryptocarya cunninghamii Meissner (Lauraceae). *J. Essent. Oil Res.* **1998**, *10*, 73–75. [CrossRef]
179. Southwell, I.A.; Brophy, J.J.; Tucker, D.J. Darwinia citriodora (Myrtaceae), a New Source of Methyl Myrtenate and Methyl Geranate. *J. Essent. Oil Res.* **2001**, *13*, 58–60. [CrossRef]
180. Brophy, J.J.; Goldsack, R.J.; Pala-Paul, J.; Copeland, L.M.; Lassak, E.V. Essential oil composition of three Australian endemic species of Darwinia (Myrtaceae). *Nat. Prod. Commun.* **2010**, *5*, 1833–1836. [CrossRef] [PubMed]
181. Brophy, J.J.; Goldsack, R.J.; Forster, P.I. The Leaf Oils of the Australian Species of *Decaspermum* (Myrtaceae). *J. Essent. Oil Res.* **2005**, *17*, 611–613. [CrossRef]
182. Brophy, J.J.; Goldsack, R.J.; Forster, P.I. The Leaf Essential Oils of the Australian Species of Desmos (Annonaceae). *J. Essent. Oil Res.* **2002**, *14*, 298–301. [CrossRef]
183. Brophy, J.J.; Goldsack, R.J.; Forster, P.I. The Leaf Oils of Dinosperma erythrococca and D. stipitata (Rutaceae). *J. Essent. Oil Res.* **2002**, *14*, 443–446. [CrossRef]
184. Brophy, J.J.; Goldsack, R.J.; Forster, P.I. The Rediscovery and Leaf Oil Chemistry of Dinosperma longifolium T.G. Hartley (Rutaceae). *J. Essent. Oil Res.* **2004**, *16*, 350–352. [CrossRef]
185. Brophy, J.J.; Goldsack, R.J.; Rozefelds, A.C. Chemistry of the Australian Gymnosperms—Part 5: Leaf Essential Oils of Some Endemic Tasmanian Gymnosperms: Diselma archeri, Lagarostrobos franklinii, Microcachrys tetragona and Phyllocladus asplenifolius. *J. Essent. Oil Res.* **2003**, *15*, 217–220. [CrossRef]
186. Brophy, J.J.; Goldsack, R.J.; House, A.P.N.; Lassak, E.V. The Essential Oils of the Genus Doryphora. *J. Essent. Oil Res.* **1993**, *5*, 581–586. [CrossRef]
187. Brophy, J.J.; Goldsack, R.J.; Forster, P.I. The Leaf Essential Oils of *Drummondita calida* (Rutaceae: Boronieae). *J. Essent. Oil Res.* **2006**, *18*, 652–653. [CrossRef]
188. Brophy, J.J.; Forster, P.I.; Goldsack, R.J. Essential oils of some Australian monimiaceae. *Flavour Fragr. J.* **1998**, *13*, 273–276. [CrossRef]
189. Brophy, J.J.; Goldsack, R.J.; Forster, P.I. A Preliminary Investigation of the Leaf Essential Oils of the Australian Species of *Endressia*, *Steganthera* and *Wilkiea* (Monimiaceae). *J. Essent. Oil Res.* **2009**, *21*, 115–122. [CrossRef]
190. Bayly, M.J.; Brophy, J.J.; Forster, P.I.; Goldsack, R.J.; Wilson, P.G. Reinstatement of Eriostemon banksii (Rutaceae), with a Report on the Composition of Leaf Essential Oils in E. banksii and E. australasius s. str. *Aust. Syst. Bot.* **1998**, *11*, 13–22. [CrossRef]
191. Brophy, J.J.; Goldsack, R.J.; Copeland, L.M.; Palá-Paúl, J. Essential Oil of Eryngium L. Species from New South Wales (Australia). *J. Essent. Oil Res.* **2003**, *15*, 392–397. [CrossRef]
192. Palá-Paúl, J.; Copeland, L.M.; Brophy, J.J.; Goldsack, R.J. Essential Oil Composition of *Eryngium paludosum* (Moore et Betche) P.W.Michael: An Endemic Species from Eastern Australia. *J. Essent. Oil Res.* **2008**, *20*, 416–419. [CrossRef]
193. Palá-Paúl, J.; Copeland, L.M.; Brophy, J.J.; Goldsack, R.J. Essential oil composition of *Eryngium rosulatum* P.W. Michael ined.: A new undescribed species from eastern Australia. *Biochem. Syst. Ecol.* **2006**, *34*, 796–801. [CrossRef]
194. Palá-Paúl, J.; Brophy, J.J.; Goldsack, R.J.; Copeland, L.M.; Pérez-Alonso, M.J.; Velasco-Negueruela, A. Essential oil composition of the seasonal heterophyllous leaves of *Eryngium vesiculosum* from Australia. *Aust. J. Bot.* **2003**, *51*, 497–501. [CrossRef]
195. Brophy, J.J.; Goldsack, R.J.; Forster, P.I. Composition of the Leaf Oils of the Australian Species of Euodia and Melicope (Rutaceae). *J. Essent. Oil Res.* **2004**, *16*, 286–293. [CrossRef]
196. Brophy, J.J.; Goldsack, R.J.; Forster, P.I. Leaf Essential Oil of Fitzalania heteropetala F. Muell. (Annonaceae). *J. Essent. Oil Res.* **1997**, *9*, 93–94. [CrossRef]
197. Brophy, J.J.; Goldsack, R.J.; Forster, P.I. The Leaf Essential Oil of *Galbulimima baccata* (Himantandraceae) from Queensland, Australia. *J. Essent. Oil Res.* **2005**, *17*, 536–538. [CrossRef]
198. Brophy, J.J.; Goldsack, R.J. Essential Oil of the Leaves and Flowers of Geleznowia verrucosa Turcz. (Rutaceae). *J. Essent. Oil Res.* **1995**, *7*, 663–665. [CrossRef]
199. Brophy, J.J.; Goldsack, R.J.; Forster, P.I. Leaf Essential Oils of the Australian Species of Gyrocarpus and Hernandia (Hernandiaceae). *J. Essent. Oil Res.* **2000**, *12*, 717–722. [CrossRef]
200. Forster, P.I.; Brophy, J.J.; Goldsack, R.J. Variation in Australian populations of *Halfordia kendack* S.L. (Rutaceae): Evidence from leaf essential oils. *Aust. Syst. Bot.* **2004**, *17*, 571–580. [CrossRef]
201. Brophy, J.J.; Goldsack, R.J.; Forster, P.I. Leaf Oils of the Australian Species of the Genus *Haplostichanthus* (Annonaceae). *J. Essent. Oil Res.* **2006**, *18*, 64–67. [CrossRef]
202. Brophy, J.J.; Fookes, C.J.R.; House, A.P.N. The Leaf Essential Oil of Haplostichanthus johnsonii F. Muell. *J. Essent. Oil Res.* **1992**, *4*, 315–316. [CrossRef]

203. Brophy, J.J.; Goldsack, R.J.; Forster, P.I. The Leaf Oils of the Australian Species of *Hedycarya* (Monimiaceae). *J. Essent. Oil Res.* **2005**, *17*, 432–436. [CrossRef]
204. Brophy, J.J.; Goldsack, R.J.; Copeland, L.M. Leaf Oils of the Genus Homoranthus (Myrtaceae). *J. Essent. Oil Res.* **2004**, *16*, 46–60. [CrossRef]
205. Brophy, J.J.; Goldsack, R.J.; Cornwell, C.P.; Leach, D.N.; Wyllie, S.G.; Forster, P.I.; Fookes, C.J.R. (Z)-β-Ocimene from Two Species of Homoranthus (Myrtaceae). *J. Essent. Oil Res.* **1998**, *10*, 229–233. [CrossRef]
206. Brophy, J.J.; Goldsack, R.J. The leaf essential oil of Idiospermum australiense (Diels) S. T. Blake (idiospermaceae). *Flavour Fragr. J.* **1992**, *7*, 79–80. [CrossRef]
207. Brophy, J.J.; Goldsack, R.J.; Punruckvong, A.; Bean, A.R.; Forster, P.I.; Lepschi, B.J.; Doran, J.C.; Rozefelds, A.C. Leaf essential oils of the genus Leptospermum (Myrtaceae) in eastern Australia. Part 7. Leptospermum petersonii, L. liversidgei and allies. *Flavour Fragr. J.* **2000**, *15*, 342–351. [CrossRef]
208. Brophy, J.J.; Goldsack, R.J.; Bean, A.R.; Forster, P.I.; Lepschi, B.J. Leaf essential oils of the genus Leptospermum (Myrtaceae) in eastern Australia. Part 3. Leptospermum arachnoides and allies. *Flavour Fragr. J.* **1999**, *14*, 85–91. [CrossRef]
209. Brophy, J.J.; Goldsack, R.J.; Bean, A.R.; Forster, P.I.; Lepschi, B.J. Leaf essential oils of the genus Leptospermum (Myrtaceae) in eastern Australia. Part 2. Leptospermum blakelyi and allies. *Flavour Fragr. J.* **1998**, *13*, 353–358. [CrossRef]
210. Brophy, J.J.; Goldsack, R.J.; Forster, P.I.; Bean, A.R.; Clarkson, J.R.; Lepschi, B.J. Leaf essential oils of the genus Leptospermum (Myrtaceae) in Eastern Australia. Part 1. Leptospermum brachyandrum and Leptospermum pallidum groups. *Flavour Fragr. J.* **1998**, *13*, 19–25. [CrossRef]
211. Brophy, J.J.; Goldsack, R.J.; Lassak, E.V. Leaf Essential Oils of Some Leptospermum (Myrtaceae) Species from Southern and Western Australia. *J. Essent. Oil Res.* **1999**, *11*, 1–5. [CrossRef]
212. Brophy, J.J.; Goldsack, R.J.; Bean, A.R.; Forster, P.I.; Lepschi, B.J. Leaf essential oils of the genus Leptospermum (Myrtaceae) in eastern Australia, Part 6. Leptospermum polygalifolium and allies. *Flavour Fragr. J.* **2000**, *15*, 271–277. [CrossRef]
213. Brophy, J.J.; Goldsack, R.J.; Forster, P.I. Essential Oil of Lindera queenslandica (Lauraceae). *J. Essent. Oil Res.* **1999**, *11*, 453–455. [CrossRef]
214. Brophy, J.J.; Goldsack, R.J.; Forster, P.I.; Clarkson, J.R. The Essential Oil of Welchiodendron longivalve (F. Muell.) Peter G. Wilson & J. T. Waterh. and Lindsayomyrtus racemoides (Greves) Craven (Myrtaceae) Leaves. *Flavour Fragr. J.* **1996**, *11*, 67–70. [CrossRef]
215. Brophy, J.J.; Goldsack, R.J.; Forster, P.I. Essential oils of the genus *Lophostemon* (Myrtaceae). *Flavour Fragr. J.* **2000**, *15*, 17–20. [CrossRef]
216. Brophy, J.J.; Goldsack, R.J.; Forster, P.I.; Hutton, I. Leaf Essential Oils of Lunasia amara var. amara and Sarcomelicope simplicifolia subsp. simplicifolia (Rutaceae) from Australia. *J. Essent. Oil Res.* **1997**, *9*, 141–144. [CrossRef]
217. Brophy, J.J.; Goldsack, R.J.; Forster, P.I. Leaf Essential Oils of *Lycopus australis* (Lamiaceae), the Australian Gipsywort. *J. Essent. Oil Res.* **2005**, *17*, 133–134. [CrossRef]
218. Brophy, J.J.; Goldsack, R.J.; Forster, P.I. Essential Oil of Lysicarpus angustifolius (Hook.) Druce (Myrtaceae). *J. Essent. Oil Res.* **1994**, *6*, 139–143. [CrossRef]
219. Brophy, J.J.; Goldsack, R.J.; Forster, P.I. The Leaf Oils of the Australian Species of Medicosma (Rutaceae). *J. Essent. Oil Res.* **2004**, *16*, 161–166. [CrossRef]
220. Brophy, J.J.; Goldsack, R.J.; Fookes, C.J.R.; Hutton, I. Leaf Oils of the Endemic Melicope (Rutaceae) of Lord Howe Island. *J. Essent. Oil Res.* **2004**, *16*, 449–452. [CrossRef]
221. Brophy, J.J.; Goldsack, R.J.; Forster, P.I. Chemotype Variation in the Leaf Essential Oils of Melicope melanophloia C.T. White (Rutaceae). *J. Essent. Oil Res.* **1997**, *9*, 279–282. [CrossRef]
222. Brophy, J.J.; Goldsack, R.J.; Forster, P.I. The Leaf Oils of the Queensland Species of Melodorum (Annonaceae). *J. Essent. Oil Res.* **2004**, *16*, 483–486. [CrossRef]
223. Brophy, J.J.; Goldsack, R.J.; Lawrence, B.M.; Forster, P.I. Essential Oil of Mentha diemenica (Lamiaceae). *J. Essent. Oil Res.* **1996**, *8*, 179–181. [CrossRef]
224. Brophy, J.J.; Goldsack, R.J.; Forster, P.I.; Fookes, C.J.R. Leaf Essential Oil of Mentha grandiflora Benth. (Lamiaceae). *J. Essent. Oil Res.* **1997**, *9*, 459–461. [CrossRef]
225. Southwell, I.A.; Brophy, J.J. Isoamyl Isovalerate from Essential Oil of Micromyrtus striata J. W. Green. *J. Essent. Oil Res.* **1991**, *3*, 281–283. [CrossRef]
226. Brophy, J.J.; Goldsack, R.J.; Fookes, C.J.R.; Rozefelds, A.C. Chemistry of Australian Gymnosperms. Part III. Leaf Oils of the Genus Microstrobos (Podocarpaceae). *J. Essent. Oil Res.* **2001**, *13*, 108–109. [CrossRef]
227. Brophy, J.J.; Goldsack, R.J.; Forster, P.I. The Leaf Oils of the Australian Species of Miliusa (Annonaceae). *J. Essent. Oil Res.* **2004**, *16*, 253–255. [CrossRef]
228. Brophy, J.; Forster, P.; Goldsack, R. Diversity in Australian populations of *Murraya paniculate* (Rutaceae): New evidence from volatile leaf oils. *Aust. Syst. Bot.* **1994**, *7*, 409–418. [CrossRef]
229. Brophy, J.J.; Goldsack, R.J.; Fookes, C.J.R.; Forster, P.I. The Leaf Oils of the Australian Species of Neolitsea (Lauraceae). *J. Essent. Oil Res.* **2002**, *14*, 191–195. [CrossRef]
230. Brophy, J.J.; Clarkson, J.R. The essential oils of the genus Neofabricia (Myrtaceae). *Biochem. Syst. Ecol.* **1992**, *20*, 689–696. [CrossRef]
231. Brophy, J.J.; Goldsack, R.J.; Clarkson, J.R. The Essential Oil of Osbornia octodonta F. Muell. *J. Essent. Oil Res.* **1993**, *5*, 1–5. [CrossRef]

232. Brophy, J.J.; Goldsack, R.J.; Forster, P.I. Essential Oils from the Leaves of the Australian Species of Palmeria (Monimiaceae). *J. Essent. Oil Res.* **2004**, *16*, 312–317. [CrossRef]
233. Brophy, J.J.; Goldsack, R.J.; Fookes, C.J.R.; Forster, P.I. The Essential Oils of Pentaceras australe (Rutaceae). *J. Essent. Oil Res.* **2002**, *14*, 348–350. [CrossRef]
234. Brophy, J.J.; Goldsack, R.J.; Punruckvong, A.; Forster, P.I. The leaf essential oils of Pilidiostigma (Myrtaceae). *Flavour Fragr. J.* **1999**, *14*, 143–146. [CrossRef]
235. Wyllie, S.G.; Brophy, J.J.; Sarafis, V.; Hobbs, M. Volatile Components of the Fruit of Pistacia Lentiscus. *J. Food Sci.* **1990**, *55*, 1325–1326. [CrossRef]
236. Brophy, J.J.; Goldsack, R.J.; Forster, P.I. The Leaf Essential Oil of Pitaviaster haplophyllus (F. Muell.) T. G. Hartley. *J. Essent. Oil Res.* **2002**, *14*, 130–131. [CrossRef]
237. Brophy, J.J.; Goldsack, R.J.; Forster, P.I.; Rozefelds, A.C. Chemistry of the Australian Gymnosperms. Part 6. Leaf Oils of the Australian Species of Genus Podocarpus. *J. Essent. Oil Res.* **2004**, *16*, 342–346. [CrossRef]
238. Brophy, J.J.; Goldsack, R.J.; Forster, P.I. Leaf Oils of the Australian Species of Polyalthia (Annonaceae). *J. Essent. Oil Res.* **2001**, *13*, 5–7. [CrossRef]
239. Hunter, M.V.; Brophy, J.J.; Ralph, B.J.; Bienvenu, F.E. Composition of Polygonum odoratum Lour. from Southern Australia. *J. Essent. Oil Res.* **1997**, *9*, 603–604. [CrossRef]
240. Brophy, J.J.; Goldsack, R.J.; Hook, J.M.; Fookes, C.J.R.; Forster, P.I. The Leaf Essential Oils of the Australian Species of *Pseuduvaria* (Annonaceae). *J. Essent. Oil Res.* **2004**, *14*, 362–366. [CrossRef]
241. Brophy, J.J.; Goldsack, R.J.; Forster, P.I. The leaf essential oils of the Australian species of Rhodamnia (Myrtaceae). *Flavour Fragr. J.* **1997**, *12*, 345–354. [CrossRef]
242. Brophy, J.J.; Goldsack, R.J.; Forster, P.I. The Essential Oils of the Australian Species of Rhodomyrtus (Myrtaceae). *Flavour Fragr. J.* **1997**, *12*, 103–108. [CrossRef]
243. Brophy, J.J.; Goldsack, R.J.; Fookes, C.J.R.; Forster, P.I. Essential Oils of Australian Gymnosperms. Part 1. The Leaf Oil of Sundacarpus amarus (Blume) C.N. Page (Podocarpaceae). *J. Essent. Oil Res.* **2000**, *12*, 421–423. [CrossRef]
244. Brophy, J.J.; Goldsack, R.J.; Bean, A.R.; Forster, P.I.; Fookes, C.J.R. The Leaf Essential Oils of the Genus Syncarpia Ten. (Myrtaceae). *Flavour Fragr. J.* **1996**, *11*, 361–366. [CrossRef]
245. Brophy, J.J.; Craig, D.C.; Goldsack, R.J.; Fookes, C.J.R. Hillyl acetate, a keto-acetate from the leaf steam volatiles ofSyncarpia hillii. *Phytochemistry* **1994**, *37*, 1645–1647. [CrossRef]
246. Brophy, J.J.; Goldsack, R.J.; Forster, P.I. The Leaf Essential Oil of Thaleropia queenslandica (Myrtaceae). *J. Essent. Oil Res.* **1997**, *9*, 587–588. [CrossRef]
247. Brophy, J.J.; Goldsack, R.J.; Forster, P.I.; Clarkson, J.R. The Essential Oils of the Queensland Species of Thryptomene (Myrtaceae). *J. Essent. Oil Res.* **2000**, *12*, 11–13. [CrossRef]
248. Pala-Paul, J.; Copeland, L.M.; Brophy, J.J. The Essential Oil Composition of Trachymene incisa Rudge subsp. incisa Rudge from Australia. *Plants* **2021**, *10*, 601. [CrossRef]
249. Brophy, J.J.; Goldsack, R.J.; Forster, P.I. Essential Oils of Australian Species of the Genera Tristaniopsis and Tristania (Myrtaceae). *J. Essent. Oil Res.* **1999**, *11*, 661–665. [CrossRef]
250. Brophy, J.J.; Goldsack, R.J.; Forster, P.I. The Essential Oils of the Australian Species of Uromyrtus (Myrtaceae). *Flavour Fragr. J.* **1996**, *11*, 133–138. [CrossRef]
251. Suksamrarn, A.; Aphaijitt, S.; Brophy, J.J. The volatile leaf oil of *Vitex limonifolia* Wall. *Flavour Fragr. J.* **1990**, *5*, 53–55. [CrossRef]
252. Suksamrarn, A.; Werawattanametin, K.; Brophy, J.J. Variation of essential oil constituents in Vitex trifolia species. *Flavour Fragr. J.* **1991**, *6*, 97–99. [CrossRef]
253. Brophy, J.J.; Goldsack, R.J.; Forster, P.I. The Leaf Essential Oils of Viticipremna queenslandica (Lamiaceae). *J. Essent. Oil Res.* **2008**, *20*, 403–404. [CrossRef]
254. Brophy, J.J.; Goldsack, R.J.; Fookes, C.J.R.; Forster, P.I. Leaf Essential Oils of the Genus Waterhousea (Myrtaceae). *J. Essent. Oil Res.* **2002**, *14*, 31–34. [CrossRef]
255. Brophy, J.J.; Goldsack, R.J.; Forster, P.I. The Essential Oils of the Australian Species of Xylopia (Annonaceae). *J. Essent. Oil Res.* **1998**, *10*, 469–472. [CrossRef]
256. Brophy, J.J.; Goldsack, R.J.; Goldsack, G.; House, A.P.N. Leaf Essential Oils of the Australian Members of the Genus Zygogynum. *J. Essent. Oil Res.* **1994**, *6*, 353–361. [CrossRef]

diversity

MDPI

Article

Pronounced Seasonal Diet Diversity Expansion of Golden Eagles (*Aquila chrysaetos*) in Northern Greece during the Non-Breeding Season: The Role of Tortoises

Lavrentis Sidiropoulos [1], D. Philip Whitfield [2], Christos Astaras [3], Dimitris Vasilakis [4], Haralambos Alivizatos [5] and Vassiliki Kati [1,*]

[1] Biodiversity Conservation Lab., Department of Biological Applications and Technology, University of Ioannina, Ioannina University Campus, 45110 Ioannina, Greece; l.sidiropoulos@uoi.gr
[2] Natural Research Ltd., Brathens Business Park, Hill of Brathens, Banchory, Aberdeenshire AB31 4BY, UK; phil.whitfield@natural-research.org
[3] Hellenic Agricultural Research Organisation "Dimitra", Forest Research Institute, Vasilika, 57006 Thessaloniki, Greece; christos.astaras@fri.gr
[4] Didimoteicho Forestry Service, 58400 Dideimoteicho, Greece; dvasilakis@gmail.com
[5] Independent Researcher, Zaliki 4 st, 11524 Athens, Greece; xaraaliv@gmail.com
* Correspondence: vkati@uoi.gr; Tel.: +30-265-100-7439

Abstract: Golden Eagles are resident in Greece and known to feed mainly on tortoises when breeding. However, information on alternative prey is scarce, especially during the tortoise brumation, that roughly coincides with the eagles' non-breeding season. We analyzed 827 prey items collected from 12 territories over five territory years and 84 records of eagles hunting or feeding behavior. Tortoises dominated the breeding season diet (71% of prey categories on average) and over half of all hunting/feeding observations. While no spatial structure was evident, habitat variables such as forest canopy cover were important associates in golden eagle diet seasonally. A significant seasonal pattern emerged in diet diversity, using a subset of six territories with at least 10 samples per season. Eagles shifted from a narrow, reptile- based breeding season diet dominated by tortoises to a broader non-breeding season diet, that included more carrion, mammals and birds. Breeding season specialization on ectothermic prey is a trait usually associated with migratory raptors in the Western Palearctic. The observed dietary diversity expansion accompanied by residency in the absence of ectothermic prey, highlights the adaptability of the golden eagle, a generalist predator. Tortoise populations in Greece are of conservation concern and land use changes as well as climate change, such as development and land abandonment may increase the prevalence of catastrophic megafires, exacerbating the threats to the golden eagle's main prey when breeding. We discuss this and other diet related conservation implications for the species in northern Greece.

Keywords: *Aquila chrysaetos*; golden eagle; diet diversity; foraging; alternative prey; *Testudo* spp.; Greece; raptors; tortoise predation

Citation: Sidiropoulos, L.; Whitfield, D.P.; Astaras, C.; Vasilakis, D.; Alivizatos, H.; Kati, V. Pronounced Seasonal Diet Diversity Expansion of Golden Eagles (*Aquila chrysaetos*) in Northern Greece during the Non-Breeding Season: The Role of Tortoises. *Diversity* **2022**, *14*, 135. https://doi.org/10.3390/d14020135

Academic Editor: Michael Wink

Received: 15 January 2022
Accepted: 9 February 2022
Published: 14 February 2022

1. Introduction

Food is one of the major limiting factors for raptor populations [1], affecting several population parameters. Food availability and diet metrics have been thus documented to affect densities [2], breeding performance [3,4], convergence of individuals during dispersal in food rich areas [5], nestling condition metrics [6] and long-term population persistence [7]. It is therefore important to have a basic understanding of raptors' diets to inform conservation and further research efforts, such as assessing possible influences of dietary habits and availability of prey species on breeding and occupancy/survival.

Several raptor species tend to consume a few, readily available and profitable taxa given the opportunity, as demonstrated by population level scale studies. However, gener-

alist species can shift their diets towards a broader range during main prey decline periods, according to the Alternative Prey Hypothesis [8].

Golden eagles *Aquila chrysaetos* in general, tend to consume medium sized prey that is abundant and accessible (0.5–4 kg, mainly gamebirds and leporids in Eurasia, and leporids and ground squirrels in N America [9–11]. However, the golden eagle is the most widespread Holarctic eagle, is highly adaptable in its diet as a generalist predator, despite often displaying specialism at low spatial and temporal scales. In northwest Scotland no evidence was found supporting higher productivity in relation to lower diet breadths in some areas; rather, a high diet breadth was attributed to a tendency of utilizing any profitable prey available [12]. In Japan, golden eagles showed considerable temporal plasticity as the breeding season progressed [13]. In Sweden, golden eagles displayed a plasticity on main prey depending on the habitat affecting its availability across its national distribution, and even high specialization locally [14,15]. I In Utah, USA, habitat variables explained best the occurrence of main prey types in golden Eagle diets [16].

In SE Europe, several breeding raptor species specialize on ectothermic prey or consume such prey at higher rates than elsewhere [17–20]. Golden eagles in Greece rely to a great extent on tortoises: Hermann's (*Eurotestudo hermanni*) and Spur-thighed (*Testudo graeca*) in the north, marginated (*T. marginata*) in Peloponnese to the south, especially during the chick rearing period. This raptor is considered the primary predator of adult tortoises in Greece [21]. However, there is scant evidence on alternative prey in periods when tortoises are scarce, as during the reptilian winter phase of brumation, when they should not be readily available to predators.

Our study had the following research objectives: to (a) investigate the diet of the species in northern Greece, (b) assess the variation of diet composition and breadth in the breeding/non-breeding season, (c) assess if the diet is related to spatial and habitat characteristics, (d) describe foraging techniques that may account for prey acquisition, and finally (e) interpret the results in the light of the adaptive significance of tortoise predation for golden eagles and relevant conservation pressures.

2. Materials and Methods

2.1. Study Population and Sampling Sites

The golden eagle is Endangered (EN) in Greece [22] and the national population has been estimated at 105–155 breeding pairs [23]. Productivity has been estimated at 0.5–0.55 fledglings per territorial pair per year, and mean nearest neighbor distance recorded between occupied nest sites in our study area was 8.47 km (±3.18 km) [24]. We sampled dietary material at 15 territories, across over 6600 km^2 in northern Greece (administrative regions of central and east Macedonia and Thrace) (Figure 1). The climate is Mediterranean/continental Mediterranean. The main vegetation types covering a buffer of 6 km around nests were broad leaved woodlands, conifers and sclerophyllous scrub, interspersed with openings and grasslands, and the mean altitude of territories was 440 ± 218 m (range 75–895 m). Main land uses were extensive grazing (goat, sheep, and cattle herds), forestry (usually selective logging) and crop-agriculture on lower altitudinal land.

2.2. Prey Item Sampling

Prey remains and pellets were collected mostly from autumn 2017 to summer 2021 from 15 occupied territories. We defined two sampling seasons: (a) the golden eagle breeding season (mid-March to late November) from egg laying to the late post-fledging dependence period for most pairs), coinciding with the high tortoise activity period; (b) the golden eagle non-breeding period (late November to mid-March) that largely coincides with the low activity period of tortoises that are either brumating or not yet very active [25]. We made 37 and 41 visits during the breeding and non-breeding season respectively (Table S1). We conducted active searching of prey remains and pellets in situ during visits to nests (11 visits to 9 territories), at the tops of nest cliffs, at the base of nest trees, diurnal perches and roosts on trees/cliffs within a buffer of 400 m around nest, where adult

activity is more pronounced [26]. Searched areas at each visit were scoured for any signs of prey consumption.

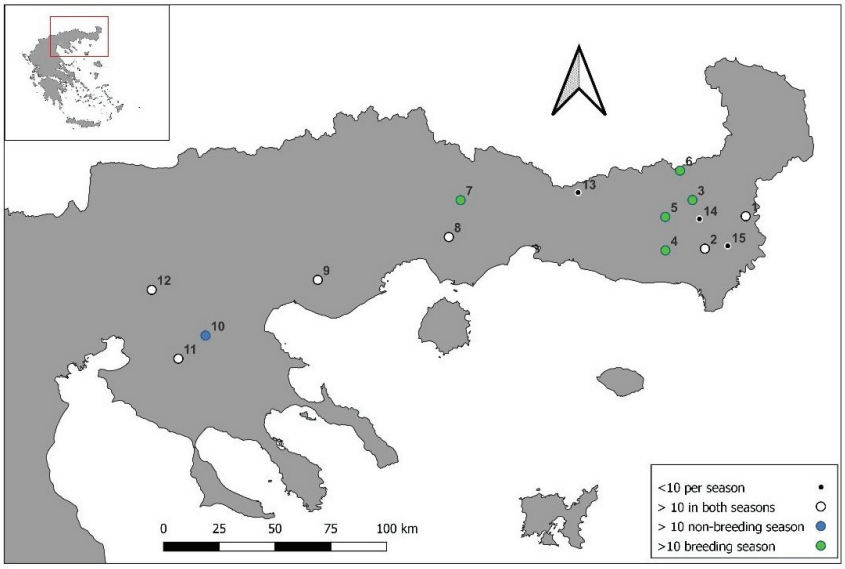

Figure 1. Sampled golden eagle territories in northern Greece. Only data from 11 and 7 territories with ≥10 prey items collected during the breeding and non-breeding seasons respectively were used in the analysis.

Material from localities outside the buffer were included in the analysis (as pertaining to the closest territory), only when members of the pair were known to perch there, or when cast golden eagle feathers were found. Material was not considered when there was evidence (cast feathers, observations) of other predatory species regularly utilizing the localities. Besides direct observations, roost and perch site localization was aided by telemetry data from three territorial adult birds (Movebank study ID 601374863).

2.3. Prey Item Identification and Counting

Prey remains and pellets were collected and removed from the sampling area either for identification in situ (e.g., hedgehog skins, tortoise shells) or in the laboratory. Collected tortoise carapaces were usually identified through the supracaudal scute; the presence of tail nails in pellets was indicative for *T. hermanni*. Whole bird feathers were identified to species when possible, using an online database [27]; feather fragments, mammalian hair and non-testudine reptilian scales were identified microscopically [28–30].

To estimate the number of prey items we combined finds in pellets and prey remains under the following protocol. Each visit to a territory was identified as a single collection event. The minimum number of individuals (MNI) at the lowest possible taxonomic level for each collection was calculated from distinctive anatomical features that were present (e.g., tortoise carapaces, jaws or humeri, flight feathers of birds, skulls or mammal jaws), either by taking the maximum number derived by each source or by combining them [31]. Thus, if for example in a collection we found plucked Eurasian Jay (*Garrulus glandarius*) feathers and a pellet of bones and feather fragments collected contemporaneously identified as belonging to the same species, it would be counted as one item. If on the other hand, we found plucked feathers and an entire head as prey remains and the pellet contained parts of a skull it was counted as two jays since the findings clearly belonged to two individuals. Similarly, one tortoise carapace in remains and two sets of jaws in a pellet were counted as two tortoises, one carapace and no distinct anatomical features in the pellet as one tortoise,

one carapace with the head attached and two sets of jaws in a pellet as three tortoises, and so on.

The sum of all items from each collection per territory, comprised the final territory sample. The above approach is deemed conservative in estimating numbers of prey items per territory.

2.4. Spatial Structure and Environmental Parameters

We applied a Spearman correlation relating the inter-territory distance across all territory pairs and Renkonen's index, which measures dietary overlap [32], as a non sensitive index on the classification of findings to resource categories [33].

We utilised five habitat variables, in terms of percentage cover of four Corine Land Cover Classes: artificial land (codes 100), agricultural land (codes 200 apart from 231), open areas (codes 231, 321, 322, 324, 332 and 333), scrub (code 323) and forests (codes 311–313) [34]. We also calculated the average forest canopy cover using the 25 m resolution Pan–European forest cover dataset [35]. Given that golden eagles are known to range mainly in a radius of up to 6 km from their nests where they utilize mostly ridges [36], habitat variables were calculated in the following steps: we first ran a ridge selection algorithm [37], on a 50×50 m Digital Elevation Model, itself resampled from a global elevation dataset [38]. We subsequently converted the selected ridge pixels to polygons and applied a further 50 m buffer to include more area which eagles may have used, and to take account of possible edge habitats.

2.5. Field Observations

We analyzed a qualitative dataset of 198 observations of golden eagles feeding, hunting or otherwise interacting with prey, including the inspection of a few kill sites derived by telemetry data, collected during fieldwork and supplemented by 11 personal communications (2004–2021). Of these, 96 consisted of observations of golden eagles feeding on carcasses or offal deliberately left in specially designated areas (vulture feeding stations/trapping sites for telemetry purposes) and are just reported indicatively. Each individual recorded attempting to capture, carrying prey, or feeding at prey carcass was counted as one instance. The data were divided in the same categories as with other prey/food items and were examined as percentages. Field observations were not used in the main prey item analysis, but served as a secondary dataset cross-validating the results of prey analysis.

2.6. Data Analysis

Diet diversity: We processed 711 prey remains and 182 pellets. We classified prey items in 13 prey categories: birds, mammals and reptiles comprised five, six and two categories respectively (Table 1). The database used in the analysis comprised 797 items (12 territories) out of 827 items (15 territories) collected overall: we included in the analysis only data from 11 territories (breeding season: 621 items) and from seven territories (non-breeding season: 176 items), where samples included at least 10 items [12]. Data from six territories were used for the seasonal comparison, satisfying the above criterion for both seasons. For each territory we calculated the frequency (%) of the prey category occurrence, as well as the Levin's Diet Breadth index (B) [33] that reflects the diversity of prey in terms of diet breadth, according to the equation $B = 1/\Sigma(p_i^2)$, where p_i is the proportion of each prey category in the territory sample. We also calculated for each prey category its prevalence (P), as the ratio of the number of territories where any item of the prey category was recorded vs. the number of all territories. We ran the same analysis for all territories taken together (population level).

Table 1. Seasonal and annual diet of the golden eagle in northern Greece in terms of number of prey items per category (N), average seasonal (AFs) and average annual (AF) frequency of prey category across territories, as well as prey category prevalence (P) across territories.

Prey Categories	Code	Breeding (n = 11)			Non-Breeding (n = 7)			Annual		
		N	AFs	P	N	AFs	P	N	AF	P
Birds		53	8.9	0.91	54	31.2	1	107	13.4	0.92
Birds all other	B_o	18	2.2	0.64	16	9.1	0.86	34	3.4	0.67
Corvids	B_c	11	3.1	0.73	7	3.7	0.71	18	3.7	0.75
Raptors and Owls	B_ro	2	0.1	0.18	2	0.8	0.29	4	0.3	0.25
Thrushes and Pigeons	B_tp	13	2.1	0.45	19	9.3	0.86	32	3.7	0.58
Waterbirds	B_w	9	1.3	0.36	10	8.2	0.86	19	2.4	0.5
Mammals		89	16.3	1	63	36.1	1	152	19.97	1
Carnivores	M_c	25	4.8	0.73	20	11.1	0.86	45	6.1	0.83
Glirids and Sciurids	M_gs	14	2.4	0.36	6	2.4	0.43	20	2.7	0.5
Hares	M_ha	8	2.7	0.73	6	3.7	0.71	14	2.9	0.83
Hedgehogs	M_he	20	2.6	0.55	13	7.2	0.57	33	3.4	0.58
Mammals all other	M_o	11	2.6	0.64	9	6.4	0.86	20	3.4	0.75
Ungulates	M_u	11	1.2	0.36	9	5.3	0.57	20	1.5	0.42
Reptiles		479	7.8	1	59	32.8	1	538	65.6	1
Snakes and Lizards	R_sl	30	4.6	0.73	12	8.5	0.57	42	6.0	0.75
Tortoises	R_t	449	70.3	1	47	24.2	1	496	60.7	1
Total		**621**			**176**			**797**	**100**	

Spatial and habitat analysis: We performed a Principal Component Analysis (PCA) to visualize in two-dimensional triplots the ecological distance of the territories sampled in terms of their diet composition, in relation to the five environmental variables considered. Due to the small sample size no constrained analysis was possible. Analysis was performed using CANOCO 5.12 [39]. Relationships detected were also checked with univariate Spearman correlations.

Seasonal variation: We ran a binomial chi-square test of proportions [40] for each category at the population level, i.e., prey items pooled per season from all territories of at least 10 items. To pinpoint any significant differences in diet categories between seasons, we first employed an analysis of similarity (ANOSIM) (n = 6 territories). We then ran both a paired Wilcoxon signed ranks test and a Simper test (restricting the permutations within territory blocks to retain the territory as the main sampling unit). For this analysis, since our expectations were for all non-reptilian categories to increase and for reptilian to decrease, we set a one tailed α level of $p \leq 0.1$ and accepted results as important when this was satisfied at both tests. To compare the seasonal diet breadth variation (six territories), we compared the Levin's diet breadth index in the two seasons (Wilcoxon signed rank test), after testing the assumption of symmetry with a Miao, Gel and Gastwirth [41] bootstrap test (Test statistic = 0.77, p= 0.41). We ran the above tests also at the taxonomic class level (birds, mammals, reptiles). Statistical analyses were conducted using vegan package [42] in R 1.12 [43], data were managed with Microsoft Excel^{TM}, and all habitat and spatial data were derived in QGis [44].

3. Results

3.1. Golden Eagle Diet

The overall golden eagle diet database included 827 items from 53 different taxa collected from 15 territories. We identified 21 mammal, 23 bird, and nine reptile species, of which 16 and 10 were unique for breeding and non-breeding seasons respectively (Appendix A). Bird taxa included corvids (mostly *Garrulus glandarius*), pigeons and thrushes (*Columba livia domestica, Columba palumbus* and *Turdus* spp.), raptors and owls, waterbirds (mostly *Larus michahellis* and Anatidae) and all other birds (Phasianidae, smaller passerines, and unidentified). Mammal taxa included carnivores (*Vulpes vulpes, Martes foina* and other mustelids, domestic dogs and cats), hares (*Lepus capensis*), hedgehogs (*Erinaceus*

roumanicus), larger rodents (*Sciurus vulgaris*, *Glis glis*), domestic and wild ungulates (usually taken as carrion although roe deer (*Capreolus capreolus*) might be actively hunted), and others (smaller rodents and unidentified). Reptile taxa included tortoises, snakes and lizards. Reptiles and in particular tortoises comprised the mainstay of the eagle diet in northern Greece during the breeding period, followed by mammals (predominantly carnivores), and birds (Table 1).

3.2. Seasonal Variation of Golden Eagle Diet

During the breeding season golden eagles consumed more reptiles, and particularly tortoises. Birds and mammal prey item categories were not prevalent across all territories and their average frequencies did not exceed 5%. (Table 1, Table S2) In the non-breeding season, the importance of reptiles decreased, as expected, with a consequent increase in birds and mammals. Of all categories, only tortoises were again prevalent across all territories, but most other categories were more prevalent and exceeded 5 % of the total items per territory on average (Table 1, Table S2).

At the population level, the consumption of tortoises decreased by 46 % from the breeding to non-breeding season and inversely the consumption of birds and mammals increased by 20% and 23% respectively (Table 1). Golden eagles took significantly more tortoises in the breeding season than in the non-breeding season, and significantly more thrushes and pigeons, waterbirds, other birds, carnivores, hedgehogs, ungulates, other mammals in the non-breeding season (Table 2).

Table 2. Seasonal variation of golden eagle diet in terms of Wilcoxon matched pairs test and Simper Analysis (n territories = 6, where the number of prey items was $\geq$10). Means and Binomial test of proportions considered 11 breeding territories and 7 non-breeding territories. Mean values refer to item proportions pooled across territories. *p* values: * $\leq$ 0.1, ** < 0.5, *** < 0.01, **** < 0.001.

Prey Category	Means ± SD (%)		Binomial Test of Proportions		Medians	Wilcoxon Matched Pairs Test		Simper Analysis	
	Breeding	Non-Breeding	x^2	*p*	Breeding/Non-Breeding	V	*p*	Contribution	*p*
Birds all other	2.2 ± 2.36	9.1 ± 6.16	11.4	****	0.04/0.09	1	*	0.06	*
Corvids	3.1 ± 3.35	3.7 ± 3.24	2.11	n/s	0.01/0.03	0	n/s	0.02	n/s
Raptors and Owls	0.1 ± 0.35	0.8 ± 1.37	0.55	n/s	0/0	1	n/s	0.01	n/s
Thrushes and Pigeons	2.1 ± 3.65	9.3 ± 9.56	24.7	****	0.027/0.07	3	n/s	0.07	n/s
Waterbirds	1.3 ± 2.77	8.2 ± 10.42	8.82	***	0.01/0.03	0	*	0.07	n/s
BIRDS	8.9 ± 6.61	31.1 ± 13.27	55.98	****	0.08/0.5	0	**	0.31	**
Carnivores	4.8 ± 5.60	11.1 ± 7.55	12.6	****	0.03/0.11	1	*	0.08	**
Glirids and Sciurids	2.4 ± 4.33	2.4 ± 3.29	0.35	n/s	0/0	1	n/s	0.02	n/s
Hares	2.7 ± 3.00	3.7 ± 3.22	2.45	n/s	0.01/0.04	2	*	0.03	*
Hedgehogs	2.6 ± 2.73	7.2 ± 9.78	4.99	**	0.04/0.01	5	n/s	0.07	n/s
Mammals all other	2.6 ± 3.04	6.4 ± 5.57	4.97	**	0.01/0.04	0	*	0.05	n/s
Ungulates	1.2 ± 1.85	5.28 ± 5.01	4.97	**	0.01/0.08	0	*	0.05	*
MAMMALS	16.3 ± 10.16	36.0 ± 13.34	39.55	****	0.14/0.52	0	**	0.38	***
Snakes and Lizards	4.6 ± 4.85	8.51 ± 13.21	0.72	n/s	0.04/0.01	14	n/s	0.07	n/s
Tortoises	70.2 ± 11.05	24.25 ± 11.18	119.4	****	0.72/0.25	21	**	0.4	***
REPTILES	74.8 ± 11.57	32.9 ± 15.11	116.92	****	0.91/0.49	21	**	0.31	***

The territory level analysis (n = 6) also showed significant difference in diet composition between the two seasons (ANOSIM: R = 0.79, p= 0.03 on 63 permutations, p< 0.01 on unrestricted 999 permutations). The prey categories of 'other birds', carnivores, hares were significantly higher in the non-breeding season than in the breeding season, and tortoises significantly lower, across both Wilcoxon and Simper tests. Differences were also significant across all tests at the class level (Table 2).

Diet diversity as expressed by the Levin's diet breadth was higher during the non-breeding season when considering both the 13 prey categories and the three classes (birds, mammals, reptiles) (V = 0, p= 0.03) (Figure 2).

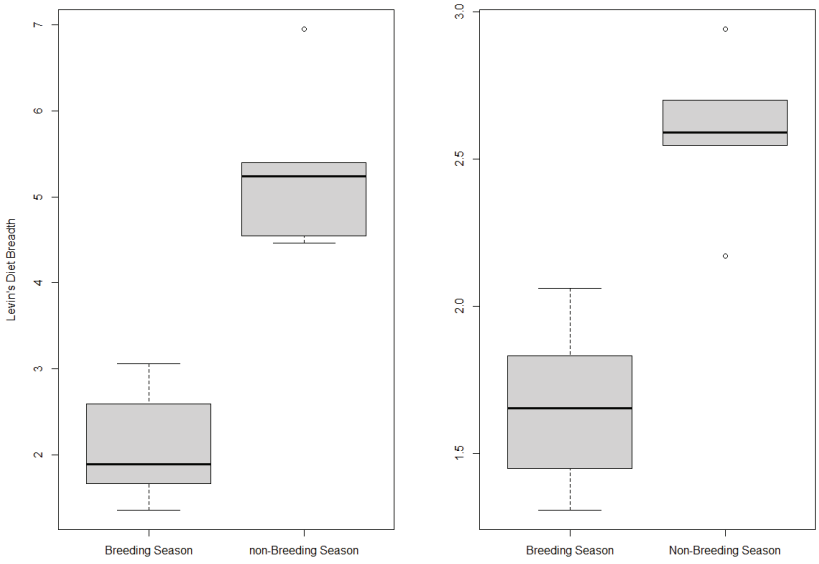

Figure 2. Seasonal Levin's diet breadth indices on the basis of 13 prey categories (see Table 1) (**left**), and the three broad taxonomic classes (birds, mammals, reptiles) (**right**).

3.3. Relationships of Golden Eagle Diet to Spatial and Habitat Characteristics

No spatial structure was evident in the data, as the distance between nests was not significantly correlated with the Renkonen Index of similarity (Spearman rho =0.06, p = 0.55) and this was reflected in the spacing of the territories across the PCA axes. The two first PCA axes explained 92.5% and 67.9% of the diet variability of the breeding and non-breeding datasets respectively (Figure 3). Tortoises (R_t) were more prominent as prey in territories with high canopy cover during the breeding season and in territories with low canopy cover in the non-breeding season (Figure 3, Table S3), the latter also pinpointed by Spearman correlation (rho= −0.86, p = 0.02). Inversely, golden eagles preyed on hares in lower canopy cover habitats during the breeding season (rho = −0.63, p < 0.04) and in more closed habitats during the non-breeding season. Carnivores (M_ca), hedgehogs (M_he) and other birds (B_o) were prominent prey in territories with significant agricultural land cover during the non-breeding season.

3.4. Field Observations

Tortoises comprised 55.1% of the 102 observations of golden eagle hunting/feeding behavior as apparent targets and, combined with snakes and lizards, reached 65.3% (Appendix B). Of the actual instances where the eagles were successful (86), the same percentages reached 67.4 and 76.6% respectively. Only 10% of the reptilian observations happened during the non-breeding season (Appendix B).

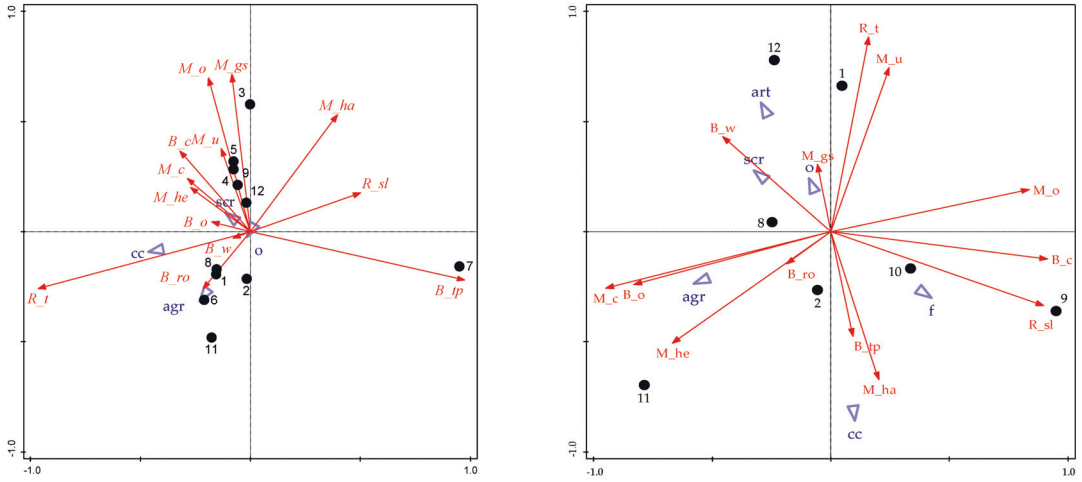

Figure 3. PCA triplot for breeding (**left**) and non-breeding (**right**) seasons, showing the position of territories (dots), environmental parameters (triangles) on ridges at 6.5 km around nests and prey categories (red arrows). agr: agricultural land, cc: canopy cover, scr: scrub and o: open land. Prey categories codified as in Table 1.

The typical reptile hunting method which was observed involved slow descent from a moderate height gained through circling and low gliding flight, prospecting the ground. Eagles were capturing reptilian prey descending slowly, sometimes in seemingly dense canopy, even landing and walking to the base of scrub. Carnivores comprised 6.9% of the 102 records and at least five of the seven instances related to already dead animals visited by pairs. Ungulates comprised also 6.9% and involved mostly carrion and offal but include unsuccessful attempts by a pair on roe deer and attempt at attacking young chamois (*Rupicapra r. balcanica*). All other mammalian categories comprised a further 4.9% of instances. One particular behavior, potentially explaining the presence of glirids in eagle diet was a capture of a small mammal (could not be identified) after an individual perched on a tree canopy, plunged suddenly into the tree. Birds comprised 12.7% of observations with a small percentage of success (3 out of 13 instances). Birds were hunted with aerial maneuvers, including tandem hunting of smaller raptors by pairs (3 instances), corralling of flocking birds by a pair (1), nest raiding (2), aerial chases (3) and near vertical stoops (2) at very high speeds. 10 instances regarded scavenging divided equally between ungulates and carnivores (including a roadkill). An additional 96 observations of eagles feeding on carrion and offal deliberately left for avian scavengers were also registered, 75 of which in the non-breeding season, when the majority of such disposals were made.

4. Discussion

4.1. Golden Eagle Diet

To our knowledge, our analysis has been the first to incorporate findings from the non-breeding season across the Mediterranean. We found 53 taxa in the entire dataset, among which unusual items e.g., a European free-tailed bat (*Tandarida teniotis*) and birds as small as blue tits (*Cyanistes caeruleus*). The number of taxa recorded was unusually large for Balkan golden eagle prey composition [45–47] but higher numbers have been reported, e.g., in Scotland and Bavaria [12,48]. Our findings stressed the importance of tortoises in the golden eagle diet in Greece. Unlike most other studies, we also included data for the non-breeding season and found a shift towards a wider variety of prey categories during that period.

Our tortoise estimate of 62.2% across the entire dataset is within the range of the reported values for the Balkan populations [45–47], with the overall importance of tortoises

not diminishing, despite the inclusion of non-breeding season data (28.3% of the entire dataset). The rest of the prey categories, apart from the hares, are within the limits of published values for the Palearctic [9] and the Balkans [45–47]

Hares accounted for 1.8% in our dataset. This is a relatively low percentage, as is the 3.7 % in the non-breeding season, although during that period consumption increased. Leporids in general and hares where rabbits are absent, will usually form an important part of the eagle's diet, exceeding 10% in several Palearctic populations [9]. Low percentages however for the Mediterranean are not uncommon (e.g., [4] as is the case for the Balkans [45–47]. Hares were generally considered important for golden eagles in Greece [49] and this is even reflected in several common names and traditions in the country [50]. A similar result was recorded with partridges, another species that was considered important [49].

Carrion consumption was relatively low compared to many other populations where it might exceed 10% [9]. However, the consistent response of golden eagles to carrion and offal, supplied or naturally occurring in our behavioral dataset, indicates that especially in winter, carrion would be utilized when encountered, as is the normal for golden eagle populations [2] and carrion did increase substantially during the non-breeding season.

Regarding the role of the golden eagle as a super predator, raptors and owls had a limited incidence, but carnivores were the most important non-reptilian category, especially in the non-breeding season. Carnivores are important at similar magnitudes of 5–20% in several palearctic populations [4,9]. It has been suggested that the presence of golden eagles might alter carnivore and raptor incidence and behavior, thus incurring benefits to small game populations [51,52].

4.2. Seasonal Variation of Eagle Diet

We found a considerable shift from a reptile based diet to a more inclusive of other classes in winter, despite the incidence of tortoises that did not disappear altogether. The only raptor with higher dependence on ectothermic and hibernating prey (reptiles only in this case) in SE Europe, the short–toed eagle (*Circaetus gallicus*), is a Palearctic-Paleotropic migrant [17]. Adult golden eagles in similar latitudes stay year-round in their territories [9] and in our population, they can compensate for the temporary low availability of their main prey by expanding their diet breadth through a shift on other taxa and carrion.

Eagles switch part of their diet on whatever is available during the non-breeding season. At the population level, almost all the non-reptilian prey categories showed considerable increases in the non-breeding season diet. Of avian taxa, increased frequencies of waterbirds and thrushes and pigeons, have been found also in other eagle diet studies during winter, possibly as these taxa more abundant and flocking at this period [53,54]. A tendency to exploit a locally abundant food source was apparent in territory 12 where waterbirds (gulls) were taken at relatively high frequencies as the site is situated close to a large refuse dump (category artificial land). Besides, the fact that some categories were significant at the population level only, indicates that they are highly consumed only in certain territories, instead of uniformly across the population. Across the population, only carnivores, a variety of smaller birds, carrion and hares were retained in both our territory analyses. We believe all the above to indicate that golden eagles respond as generalists in the absence or lower incidence of their main prey, expanding their diet to several taxa and could be thus classified as facultative specialists [55].

4.3. Habitat Variables and Diet

We found that golden eagle hunted tortoises in closed habitats during the breeding season and in more open habitats in the non-breeding season. The higher tortoise abundance in the breeding season, combined with limited escape capabilities, could allow hunting in the more forested areas, whilst in the non-breeding season, any active tortoises during mild, sunny days might be more prevalent in open areas. The inverse pattern was found for hares. Hares might be more abundant in openings [56], and their higher sensory ability and agility facilitates capture in larger openings. In the non-breeding season, the absence

of leaf cover might facilitate detection, allowing hare hunting in more dense areas [13]. Agriculture (in the ridges of our territories mostly low input such as cereal and alfalfa crops) was associated with more carnivores, hedgehogs and other birds. Small scale, low input agriculture increases habitat mosaics and edges and can plausibly attract several taxa on which Mediterranean raptors might feed [57].

4.4. Tortoise Dependence

Golden eagles in the Balkans, including our population, display an unusual diet and to our knowledge, are the highest recorded adult tortoise predators both between conspecific populations and other avian taxa [9,10,17–19,45–47,58–64]. Only [62] noted a 31.9 % of tortoise incidence in golden eagle diet outside the region. From other species in the Balkans, similar magnitude (31.5% albeit on mostly young tortoises) was reported for the Egyptian vulture (*Neophron percnopterus*) [19,64] and for some pairs (up to 30%) of the now locally extinct bearded vulture (*Gypaetus barbatus*) [65].

Eagles capture tortoises in even small openings and to break the carapace open, drop them in a near suitable rocky surface, in a manner similar to the bone dropping behavior of the bearded vulture [66]. Prey and nut dropping to access the interior of hard shells is widely recorded and studied among several bird taxa from different orders, where it has arisen independently and is considered a borderline tool-using behavior, directly linked to foraging innovation rate [67] and such innovations are generally associated with diet-generalist species with larger relative brain metrics [68,69]. This learned behavior might be acquired culturally through vertical transmission. Raptors are known to train through play during the post fledging dependence period, benefitting by adult experience [70,71]. We did observe juveniles following adults with tortoises during this period and even dropping items (pieces of carrion) for which this behavior is unnecessary. Additionally, observations of immature eagles failing to break carapaces in unsuitable substrate (ploughed field), suggest that experience might also be involved.

Golden eagles are reported in N.E. Greece (Dadia National Park) to prefer male individuals over females, *E. hermanni* over *T. graeca* and show a tendency to catch medium sized individuals of both species (1–1.5 kg) [72]. Tortoise predation is costly in terms of prey handling, as golden eagles might need to drop them repeatedly sometimes to break the carapace sufficiently open for consumption. During handling, tortoises might be lost if they roll into very dense vegetation or otherwise inaccessible spots after the drop. However, golden eagles show a clear preference to tortoises for several reasons. First, tortoises are in general easy to capture, and according to our results, they can be captured in fairly dense vegetation where the high speed and maneuverability required to capture other typical eagle prey taxa (e.g., Leporids and birds) is not possible. Indeed, our observed tortoise capture behaviors correspond to the "Low flight and slow descent attack" and "walk and grab attack" described by Watson [9]. Second, tortoises can reach high densities especially during the breeding season, reaching up to 20 tortoises/ha [73], compared to e.g., a reported 0.036 hares/ha [74] reported from Greece. Third, they have a nigh nutritional value, despite the carapace entailing a 31% wastage component [75], further enhanced by scales and bones. Anything apart from the carapace and intestines may be consumed by the eagles although limbs and heads are found nearly intact in pellets and they are not always taken as sometimes they are found attached in carapaces. Data on nutritional value show tortoises to be comparable if not higher to e.g., Leporids (134 Kcal/100 g vs. 112 Kcal/100 g [75,76]. An adult Hermann's tortoise in the preferred size of 1.5 kg, would therefore provide ~950 g of edible mass to a growing chick (7% and 17% dry weight of fat and protein). Finally, specific tortoise behaviors, e.g., sunning in early morning in openings may further augment encounter rates [72]. It is possible therefore, that all the above factors, have contributed to this facultative prey specialization, consistent with the Prey Availability Hypothesis of [12].

We found an unexpectedly high incidence of tortoises in the non-breeding season, in some territories exceeding 25%. Tortoises may become active in mild winter days [25],

and during our sampling winters they could be active during prolonged spells of mild weather. The earliest we have observed eagles with tortoises was the 8th of February, again more than a month before our latest non-breeding period collection. It is possible that only repeated, very intensive sampling before and after very cold spells would provide an accurate picture of the eagle's responses to a complete absence of tortoises.

Our results concerned low to mid-attitude golden eagles' territories. Pairs in the Balkans nesting at higher altitudes may not have access to tortoises, whose distribution is limited at 1500 m asl [46,77] where hares and partridges might be more important as prey. Comparisons of the productivity of pairs with and without access to tortoises (i.e., nesting in the high altitude mt ranges of the Balkans) would provide further answers about the adaptive significance of tortoise hunting.

4.5. Methodological Insights

Non-breeding season samples were smaller than the breeding season in relation to the effort invested (Table S1). Collecting non-breeding season data might yield smaller samples as eagles do not have to feed growing chicks and spread their time in wider areas than the immediate perimeter of the nest [78,79]. Despite the differences in sample sizes, we believe the differences we detected to be genuine due to our minimum requirement for sample inclusion (10 items) and the fact that reptiles would be in any case less abundant.

All raptor diet assessment methods have to some degree inherent biases and different methods might yield different results [31]. In our case, there is the possibility that tortoise carapaces are more prone to detection during prey item collections as they are relatively larger and more persistent in time compared to e.g., fur or feather pellets [19]. However, we believe that the high tortoise predation is not overestimated. Adult golden eagles are known to discard persistent prey remains away from nests, including tortoise carapaces, and even consume pellets [26]. Tortoises also comprised majority of prey remains in nests where the search area is very small and standardized. Furthermore, the overall frequency of tortoises observed as prey during field observations was very high, confirming the dietary dataset. Additionally, our prey item analysis, the MNI method combining pellets and prey remains that has been suggested as the less biased for golden eagles elsewhere, tends to underestimate the most common prey [80]. Ungulates on the other hand might be underrepresented in pellets, especially if the eagles feed on soft parts of a carcass and this might explain a relatively low incidence in diet samples.

Finally, a larger dataset of territories sampled would allow a more robust analysis of the impact of environmental variables on diet selection. However, our results have plausible explanations, and can be considered as a basis for further research in this direction.

4.6. Conservation Implications

Our findings have potentially serious conservation implications for our study population. Golden eagle breeding metrics can be negatively affected where main prey availability (tortoises in our case) declines or altogether collapses [3,81,82]. Both tortoise species have an unfavourable conservation status and a declining population trend, the Hermann's tortoise populations are considered Vulnerable (VU) [77,83], threatened by excess mortality and habitat loss through agricultural intensification, land abandonment, development and wildfires [84]. Such pressures are widespread in Mediterranean woodlands and garrigue [85] that dominate much of our population's distribution range.

Wildfires, endemic in our study area (Table S4), can have abrupt, catastrophic mortality effects on tortoise populations, particularly in the widespread among our territories scrub cover [73]. Especially megafires, are expected to increase in incidence concurrently with extreme heat events [86]. While e.g., hares might recover quickly [74], tortoise population recovery after fires is slow [87], hindered by limited recolonization due to low mobility [88] and the slow growth rates of any new hatchlings that can reach 500 g under optimal conditions only after four years [89]. Wildfire likelihood is enhanced also by the land abandonment that incurs increased fuel loads through the expansion of woody vegetation

where grazing and small-scale farming declines [90]. The land abandonment-induced expansion of canopy cover is documented in parts of our study area [91,92] in the Rhodope mts and Dadia forest. This trend, apart from other negative biodiversity impacts [93,94] reduces the open areas raptors such as the golden eagle rely for hunting [95–97], like the small openings where reptile capture is possible [13] and the open ridges that we found to favor hare predation in the breeding season. Both tortoises and hare abundance has been found to be greater in open habitats such as pasture and scrubland mosaics [56,87,98]. Habitat loss through wildfires and increased canopy cover has been found to affect golden eagle populations and particularly pairs in areas of high density that cannot compensate for this loss through range expansion [99,100]. Habitat management such as grazing and prescribed burning [101,102] promoting habitat mosaics will thus reduce megafire incidence [103], and the associated biodiversity benefits will promote both the main and alternative prey availability [104–106].

Game species encountered in the golden eagle diet collection and behavioral datasets include the wild boar (*Sus scrofa*, whose offal is usually discarded in situ), hares, *Turdus* thrushes, ducks and woodpigeons, that are legally hunted in Greece during the winter months. Especially in winter and by immature individuals, the consumption of such items might be a possible pathway of lead ingestion as has been found elsewhere for this and other eagle species [107–110]. Lead levels have only been investigated incidentally in Greek raptors [111] and relevant studies incorporating tissues of dead birds, feathers and whole blood of handled specimens are required (preliminary findings in four of our territorial eagles have found small but detectable levels, Azmanis and Sidiropoulos, unpublished data).

We found that carrion, although the most likely class taken as such (ungulates) is underrepresented in pellets, can be important for golden eagles. The main carrion source in our area are livestock herds, declining concurrently to extensive grazing with land abandonment [112,113]. It might be particularly important in winter and for inexperienced, dispersing birds [9,114] and can be utilized even during the summer months [115]. Declining carrion availabilities are also exacerbated by the EU legislation on carrion and offal management that forbids the in situ disposal especially as the article 14 of the EC1069/2009 that amends this situation in Special Protection Areas has not been embodied in Greek legislation. Carrion can also be a potential hazard. Wildlife poisoning using offal and carcasses as baits is widespread in the Greek countryside [116] and is the main mortality factor for carrion eating birds. It has devastated vulture populations in mainland Greece [117,118] and accounts for >60% of the recorded golden eagle mortality in our study area in the last 30 years.

5. Conclusions

In conclusion, golden eagles have shown a considerable seasonal dietary plasticity in our study area, shifting from a narrow, reptile based diet to a broader diet more inclusive of various mammalian and avian taxa in the non-breeding season. The declining tortoise populations should be monitored and protected across the golden eagle range in our study area, in terms of management implications, with habitat management promoting landscape heterogeneity. The latter, based on our results where some prey categories where only locally important, should be considered on a territory basis after consideration of local features such as habitat conditions and stocking densities [12].

Supplementary Materials: The following are available online at https://www.mdpi.com/article/10.3390/d14020135/s1, Table S1: Time schedule of the 37 and 41 visits conducted during the breeding (March-November) and non breeding (November-March) season for prey remain collection at the 15 territories. Table S2: Percentage of prey categories and classes, n of items and Levins diversity index per territory and season for sample sizes of at least 10 items. Table S3: Percentage cover of habitat types in the 12 territories and average canopy cover. Table S4: Incidence of wildfires in the regional units of our study territories in the period 1983–2008.

Author Contributions: Conceptualization, L.S., D.P.W. and V.K.; methodology, L.S., D.P.W., H.A. and V.K.; validation, L.S. and V.K.; formal analysis, L.S. and V.K.; investigation, L.S., C.A., H.A. and D.V., resources, C.A. and L.S.; data curation, L.S.; writing—original draft preparation, L.S., V.K., D.P.W.; writing—review and editing, all authors; visualization, V.K., L.S. and D.V.; supervision, V.K.; project administration, L.S.; funding acquisition, D.P.W., L.S. and V.K. All authors have read and agreed to the published version of the manuscript.

Funding: This research was partly supported by a Natural Research Ltd. studentship grant to L.S., who also received support from the A.G. Leventis Scholarships foundation.

Institutional Review Board Statement: All research was conducted under the appropriate annual research permits issued by the Department of Forest Management of the Directorate General of Forests and Forest Environment of the ministry of Environment and Energy of Greece [Protocol codes/dates 4755/134/01.01.2021, 1033/16/04.02.2020, 16563880/80/22.01.2018, 175837/2197/27.11.2018].

Informed Consent Statement: Not applicable.

Data Availability Statement: Not applicable.

Acknowledgments: We are grateful to Konstantinos Poirazidis, WWF–Greece and the Society for Biodiversity Protection of Thrace for invaluable logistical support in the areas of Evros and Rodopi. Archontis Exakoidis, Vladimir Dobrev, Yotam Orchan and Athanasios Chaliveletzios accessed nest sites. Ivaylo Angelov, Panagiotis Azmanis, Vangelis Theodosiadis and Manolia Vougioukalou assisted during some collections. Petros Babakas, Dimitris Kokkinidis, Elzbieta Kret, Despoina Migli, Kostas Papadopoulos, Haritakis Papaioannou, Kyrillos Samaras, Dora Skartsi, Giorgos Spiridakis, Giannis Tsiampazis, Apostolos Tsiompanoudis and Sylvia Zakkak provided eagle observations. Despoina Migli and Maria Petridou provided support in microscopical identification of hair. Elena Papadatou and Christian Dietz identified the bat to species level.

Conflicts of Interest: The authors declare no conflict of interest.

Appendix A

Table A1. The 53 prey taxa of the golden eagle diet in northern Greece, with reference to the 13 class categories used in the analysis. N: the number of prey items, -: unidentified at this taxonomic level. Superscripts indicate prey item found only during the breeding season (^{b}) or only at the non-breeding season (^{nb}).

Class Category	Class	Order	Family	N	%	Lowest Taxonomic Level Identified
Mammals all other	*Mammalia*	-	-	4	0.5	
Mammals all other		Cheiroptera	Molossidae	1	0.1	*Tandarida teniotis* ^{b} (1)
Hedgehogs		Eulipotyphla	Erinaceidae	34	4.1	*Erinaceus concolor* (35)
Mammals all other		Eulipotyphla	Soricidae	3	0.4	-
Hares		Lagomorpha	Leporidae	15	1.8	*Lepus capensis* (15)
Mammals all other		Rodentia	Muridae	15	1.8	*Mus musculus* (1), *Apodemus sp* (3), *Rattus sp* (2), unidentified (9)
Glirids and Sciurids		Rodentia	Gliridae	13	1.6	*Glis glis*
Glirids and Sciurids		Rodentia	Sciuridae	10	1.2	*Sciurus vulgaris*
Carnivores		Carnivora	Canidae	16	1.9	*Canis sp* ^{nb} (2), *V vulpes* (14)
Carnivores		Carnivora	Mustelidae	29	3.5	*M Meles* ^{b} (2), *Martes foina* (19), *Martes sp* (5), *Mustela nivalis* ^{b} (2), *M putorius* ^{b} (1)
Carnivores		Carnivora	Felidae	2	0.2	*Felis catus* ^{nb}
Ungulates		Artiodactyla	Bovidae	15	1.8	*Caprini* (5), *Capra hircus* (7), *Ovis aries*^{nb} (2), *Bos taurus* ^{b} (1)
Ungulates		Artiodactyla	Cervidae	3	0.4	*Capreolus capreolus* ^{nb}
Ungulates		Artiodactyla	Suidae	2	0.2	*Sus domestica* ^{b}
Ungulates		Perissodactyla	Equidae	1	0.1	*Equus sp* ^{b}

Table A1. *Cont.*

Class Category	Class	Order	Family	N	%	Lowest Taxonomic Level Identified
Birds all other	*Aves*	-	-	11	1.3	
Warerbirds		Pelecaniformes	Phalacrocoracidae	1	0.1	*Phalacrocorax carbo* [b]
Waterbirds		Anseriformes	Anatidae	2	0.2	*Anas strepera* [b] (1)
Raptors and Owls		Accipitriformes	Accipitridae	2	0.2	*Buteo buteo* [b] (1)
Raptors and Owls		Falconiformes	Falconidae	1	0.1	
Birds all other		Galliformes	Phasianidae	3	0.4	*Alectoris graeca* [b] (2), *C coturnix* [b] (1)
Waterbirds		Charadriiformes	Laridae	16	1.9	*Larus michahellis* (14), *Larus sp* (2)
Thrushes and pigeons		Columbiformes	Columbidae	12	1.5	*Columba palumbus* (5), *C livia domestica* (5), *Streptopelia turtur* [b] (1), unidentified 1
Birds all other		Apodiformes	Apodidae	1	0.1	*Apus melba* [b]
Birds all other		Caprimulgiformes	Caprimulgidae	2	0.2	*Caprimulgus europaeus* [b]
Raptors and owls		Stringiformes	Stringidae	1	0.1	*Athene noctua* [nb]
Birds all other		Passeriformes	-	9	1.1	
Birds all other		Passeriformes	Alaudidae	1	0.1	*Galerida cristata* [nb]
Thrushes and pigeons		Passeriformes	Turdidae	22	2.7	*Turdus philomelos* 8, *T merula* 5, *Turdus sp*[nb] (5), *T viscivorus* 3, *T pilaris 1*
Birds all other		Passeriformes	Paridae	1	0.1	*Cyanistes caeruleus* [nb]
Birds all other		Passeriformes	Sturnidae	7	0.8	*Sturnus vulgaris*
Corvids		Passeriformes	Corvidae	18	2.2	*Garrulus glandarius* (15), *Corvus cornix* [nb] (2), *Pica pica* (1)
Birds all other		Passeriformes	Fringillidae	2	0.2	
Snakes and lizards	*Reptilia*	Squamata	Anguidae	24	2.9	*Pseudopous apodus*
Snakes and lizards		Squamata	Lacertidae	6	0.7	*Lacerta* spp. 6, Podarcis spp 1
Snakes and lizards		Serpentes	-	3	0.4	
Snakes and lizards		Ophidia	Colubridae	7	0.8	*Elaphe situla* [b] (2), *Dolichophis caspius* (4), *Platyceps najadum* [nb] (1)
Snakes and lizards		Ophidia	Psammophilidae	3	0.4	*Malpolon insignitus*
Tortoises		Chelonia	Testudinidae	511	61.8	*Eurotestudo hermanni* (133), *Testudo graeca* (56), *Testudo* spp. (322)
				827		

Appendix B

Table A2. Summary of the observation dataset. N of instances refers to all behavioral interactions including unsuccessful attacks, N of successes to instances where eagles were seen successfully capturing prey or feeding in prey already captured or scavenged.

Prey Category	N of Instances	N of Successes	Breeding Season	Non–Breeding Season
Corvids	4	0	3	1
Raptors and owls	3	0	2	1
Thrushes and pigeons	1	1	0	1
Waterbirds	1	0	1	0
Other birds	4	2	4	0
Carnivores	7	7	2	5
Glirids and Sciurids	1	1	1	0
Hedgehogs	2	2	1	1
Hares	1	1	1	0
Ungulates	7	5	1	6
Other mammals	1	1	2	2
Snakes and lizards	12	12	9	3
Tortoises	57	57	53	4
Ungulates (carrion and offal) left on designated sites		96	21	75

References

1. Newton, I. *Population Ecology of Raptors*; Poyser: Berkhamstead, UK, 1979.
2. Watson, J.; Rae, S.R.; Stillman, R. Nesting Density and Breeding Success of Golden Eagles in Relation to Food Supply in Scotland. *J. Anim. Ecol.* **1992**, *61*, 543. [CrossRef]
3. Fernandez, C. Effect of the Viral Haemorrhagic Pneumonia of the Wild Rabbit on the Diet and Breeding Success of the Golden Eagle Aquila *Chrysaëtos* (L.). *Revue d'Écol.* **1993**, *48*, 323–329.
4. Clouet, M.; Gerard, J.-F.; Goar, J.-L.; Goulard, M.; González, L.; Rebours, I.; Faure, C. Diet and Breeding Performance of the Golden Eagle *Aquila chrysaetos* at the Eastern and Western Extremities of the Pyrenees: An Example of Intra-Population Variability. *Ardeola* **2017**, *64*, 347–361. [CrossRef]
5. Cadahía, L.; López-López, P.; Urios, V.; Negro, J.J. Satellite telemetry reveals individual variation in juvenile Bonelli's eagle dispersal areas. *Eur. J. Wildl. Res.* **2010**, *56*, 923–930. [CrossRef]
6. Resano-Mayor, J.; Hernández-Matías, A.; Real, J.; Parés, F.; Moleón, M.; Mateo, R.; Ortiz-Santaliestra, M.E. The influence of diet on nestling body condition of an apex predator: A multi-biomarker approach. *J. Comp. Physiol. B* **2016**, *186*, 343–362. [CrossRef]
7. Rutz, C.; Bijlsma, R.G. Food-limitation in a generalist predator. *Proc. R. Soc. B Boil. Sci.* **2006**, *273*, 2069–2076. [CrossRef]
8. Reif, V.; Tornberg, R.; Jungell, S.; Korpimäki, E. Diet variation of common buzzards in Finland supports the alternative prey hypothesis. *Ecography* **2001**, *24*, 267–274. [CrossRef]
9. Watson, J. *The Golden Eagle*, 2nd ed.; Poyser: London, UK, 2010.
10. Bedrosian, G.; Watson, J.W.; Steenhof, K.; Kochert, M.N.; Preston, C.R.; Woodbridge, B.; Williams, G.E.; Keller, K.R.; Crandall, R.H. Spatial and Temporal Patterns in Golden Eagle Diets in the Western United States, with Implications for Conservation Planning. *J. Raptor Res.* **2017**, *51*, 347–367. [CrossRef]
11. Seguin, J.F.; Thibault, J.C.; Torre, J.; Bayle, P.; Vigne, J.D. The Diet of Young Golden Eagles *Aquila chrysaetos* in Corsica: Foraging in a Man-Made Mammal Fauna. *Ardea* **2001**, *89*, 527–535.
12. Whitfield, D.P.; Reid, R.; Haworth, P.F.; Madders, M.; Marquiss, M.; Tingay, R.; Fielding, A.H. Diet specificity is not associated with increased reproductive performance of Golden Eagles *Aquila chrysaetos* in Western Scotland. *Ibis* **2009**, *151*, 255–264. [CrossRef]
13. Takeuchi, T.; Shiraki, S.; Nashimoto, M.; Matsuki, R.; Abe, S.; Yatake, H. Regional and temporal variations in prey selected by Golden Eagles *Aquila chrysaetos* during the nestling period in Japan. *Ibis* **2006**, *148*, 79–87. [CrossRef]
14. Tjernberg, M. Diet of the golden eagle *Aquila chrysaetos* during the breeding season in Sweden. *Ecography* **1981**, *4*, 12–19. [CrossRef]
15. Högström, S.; Wiss, L. Diet of the Golden Eagle *Aquila chrysaetos* (L.) in Gotland, Sweden during the Breeding Season. *Ornis Fennica* **1992**, *69*, 39–44.
16. Brown, J.L.; Bedrosian, G.; Keller, K.R. Habitat Associations of Golden Eagle Prey Inferred from Prey Remains at Nesting Sites in Utah, USA. *J. Raptor Res.* **2021**, *55*, 1–16. [CrossRef]
17. Bakaloudis, D.E.; Vlachos, C.G. Feeding Habits and Provisioning Rate of Breeding Short-Toed Eagles Circaetus Gallicus in Northeastern Greece. *J. Biol. Res.* **2011**, *16*, 166–176.
18. Vlachos, C.G.; Papageorgiou, N.K. Breeding Biology and Feeding of the Lesser Spotted Eagle Aquila Pomarina in Dadia Forest, North-Eastern Greece. In *Eagle Studies*; Meyburg, B.-U., Chancellor, R.D., Eds.; The World Working Group on Birds of Prey (WWGBP): Berlin, Germany, 1996; pp. 337–347.
19. Dobrev, V.; Boev, Z.; Arkumarev, V.; Dobrev, D.; Kret, E.; Saravia, V.; Bounas, A.; Vavylis, D.; Nikolov, S.C.; Oppel, S. Diet is not related to productivity but to territory occupancy in a declining population of Egyptian Vultures *Neophron percnopterus*. *Bird Conserv. Int.* **2015**, *26*, 273–285. [CrossRef]
20. Alivizatos, H.; Goutner, V. Feeding Habits of the Long-Legged Buzzard (*Buteo Rufinus*) during Breeding in Northeastern Greece. *Isr. J. Zool.* **1997**, *43*, 257–266. [CrossRef]
21. Willemsen, R.E.; Hailey, A. Variation in adult survival rate of the tortoise *Testudo hermanni* in Greece: Implications for evolution of body size. *J. Zool.* **2001**, *255*, 43–53. [CrossRef]
22. Handrinos, G.; Kastritis, A. Birds. In *The Red Data Book of Threatened Animals in Greece*; Legakis, A., Maragkou, P., Eds.; Hellenic Zoological Society: Athens, Greece, 2009; pp. 213–354, (In Greek with English Summaries).
23. Ministry of Environment and Energy. Article 12 Reporting for the Implementation of the 2009/147/EC. 2019. Available online: https://cdr.eionet.europa.eu/Converters/run_conversion?file=gr/eu/art12/envxz8njg/GR_birds_reports_20191031-152940.xml&conv=612&source=remote#A091_B (accessed on 15 December 2021).
24. Sidiropoulos, L. The Golden Eagle (*Aquila chrysaetos*, L.) in the Rhodope Mts: Modelling Densities, Distribution and Population Viability to Inform Conservation. Master's Thesis, Division of Biology, Imperial College London, London, UK, 2012.
25. Speybroeck, J.; Beukema, W.; Bok, B.; van der Voort, J.; Velikov, I. *Field Guide to the Amphibians and Reptiles of Britain and Europe*; Bloomsbury: London, UK, 2016.
26. Sulkava, S.; Huhtala, K.; Rajala, P.; Tornberg, R. Changes in the Diet of the Golden Eagle *Aquila chrysaetos* and Small Game Populations in Finland in 1957–96. *Ornis Fennica* **1999**, *76*, 1–16.
27. Featherbase. Featherbase: Online Avian Plumages Collection. Available online: https://www.featherbase.info/en/home (accessed on 6 November 2021).
28. Brom, T.G. Microscopic Identification of Feathers and Feather Fragments of Palearctic Birds. *Bijdragen Dierkunde* **1986**, *56*, 181–204. [CrossRef]
29. Teerink, B.J. *Hair of West-European Mammals*; Cambridge University Press: Cambridge, UK, 1991.

30. Papageorgiou, N.; Sfouggaris, A.; Vlachos, C.; Bakaloudis, D. *Identification of Reptiles through Scale Morphology*; Department of Forestry and the Natural Environment, Aristotle University of Thessaloniki (AUTh): Thessaloniki, Greece, 1993.
31. Marti, C.D.; Bechard, M.; Jaksic, F.M. Food Habits. In *Raptor Research and Management Techniques*; Bildstein, K., Bird, D.M., Eds.; Hanckock House: Blaine, WA, USA, 2007; pp. 129–152.
32. Katzner, T.E.; Bragin, E.A.; Knick, S.T.; Smith, A.T. Spatial structure in the diet of imperial eagles *Aquila heliaca* in Kazakhstan. *J. Avian Biol.* **2006**, *37*, 594–600. [CrossRef]
33. Krebs, C. *Ecological Methodology*; Benjamin/Cummings: Menlo Park, CA, USA, 1999.
34. European Environment Agency/European Union. Copernicus Land Monitoring Service. CORINE Land Cover Dataset 2018. Available online: https://www.eea.europa.eu/data-and-maps/data/copernicus-land-monitoring-service-corine (accessed on 10 December 2021).
35. European Environment Agency/European Union. Copernicus Land Monitoring Service. High Resolution Forest Cover Dataset 2018. pp. 1–4. Available online: https://www.eea.europa.eu/data-and-maps/data/copernicus-land-monitoring-service- (accessed on 10 December 2021).
36. McLeod, D.R.A.; Whitfield, D.P.; McGrady, M.J. Improving Prediction of Golden Eagle (*Aquila chrysaetos)* Ranging in Western Scotland Using GIS and Terrain Modeling. *J. Raptor Res.* **2002**, *36*, 70–77.
37. Fielding, A.H.; Haworth, P.F.; Anderson, D.; Benn, S.; Dennis, R.; Weston, E.; Whitfield, D.P. A simple topographical model to predict Golden Eagle *Aquila chrysaetos* space use during dispersal. *Ibis* **2019**, *162*, 400–415. [CrossRef]
38. NASA. EODIS ASTER Global Digital Elevation Model [Data Set]. NASA EOSDIS Land Processes DAAC. 2009. Available online: https://search.earthdata.nasa.gov/search/granules?p=C1711961296-LPCLOUD&pg[0][v]=f&pg[0][gsk]=-start_date&q=GDEM&tl=1644645645.19!3!! (accessed on 10 December 2021).
39. Leps, J.; Smilauer, P. *Multivariate Analysis of Ecological Data Using CANOCO*; Cambridge University Press: Cambridge, UK, 2003.
40. Crawley, M.J. *The R Book*, 2nd ed.; Wiley: London, UK, 2013.
41. Gastwirth, J.L.; Gel, Y.R.; Hui, W.; Lyubchich, V.; Miao, W.; Noguchi, K. *Package 'Lawstat'*; R Core Team: Vienna, Austria, 2013.
42. Oksanen, A.J.; Blanchet, F.G.; Friendly, M.; Kindt, R.; Legendre, P.; Mcglinn, D.; Minchin, P.R.; Hara, R.B.O.; Simpson, G.L.; Solymos, P.; et al. *Vegan: Community Ecology Package*; Version 2.5-7; R Core Team: Vienna, Austria, 2020.
43. R Core Team. *R: A Language and Environment for Statistical Computing*; R Core Team: Vienna, Austria, 2020.
44. QGIS Development Team. QGIS Geographic Information System. 2021. Available online: http://qgis.osgeo.org. (accessed on 10 December 2021).
45. Grubac, B.R. The Golden Eagle (*Aquila chrysaetos* Chrysaetos) in South-Eastern Yugoslavia. *Larus* **1988**, *38–39*, 95–135.
46. Kuzmanov, G.; Stoyanov, G.; Todorov, R. Sur la Biologie et la Protection de l' Aigle Royal *Aquila chrysaetos* en Bulgarie. In *Eagle Studies*; Meyburg, B.-U., Chanchellor, R.D., Eds.; The World Working Group on Birds of Prey (WWGBP): Berlin, Germany, 1996; pp. 505–516.
47. Georgiev, D.G. Diet of the Golden Eagle (*Aquila chrysaetos)* (Aves: Accipitridae) in Sarnena Sredna Gora Mountains (Bulgaria). *Ecologia Balkanica* **2009**, *2*, 95–98.
48. Schweiger, A.; Fünfstück, H.-J.; Beierkuhnlein, C. Availability of optimal-sized prey affects global distribution patterns of the golden eagle *Aquila chrysaetos*. *J. Avian Biol.* **2014**, *46*, 81–88. [CrossRef]
49. Handrinos, G.I. L'Aigle Royal en Grece. In *Proceedings of the l' Aigle Royal (Aquila chrysaetos) en Europe—Actes de 1er Colloque International sur l Aigle Royal en Europe*; Maison de la Nature: Arvieux, France, 1986; pp. 18–22.
50. Stara, K.; Sidiropoulos, L.; Tsiakiris, R. Bound Eagles, Evil Vultures and Cuckoo Horses. Preserving the Bio-Cultural Diversity of Carrion Eating Birds. *Hum. Ecol.* **2016**, *44*, 751–764. [CrossRef]
51. Lyly, M.S.; Villers, A.; Koivisto, E.; Helle, P.; Ollila, T.; Korpimäki, E. Avian top predator and the landscape of fear: Responses of mammalian mesopredators to risk imposed by the golden eagle. *Ecol. Evol.* **2015**, *5*, 503–514. [CrossRef]
52. Fielding, A.H.; Haworth, P.F.; Morgan, D.H.; Thompson, D.B.A.; Whitfield, D.P. The Impact of Golden Eagles (*Aquila chrysaetos)* on a Diverse Bird of Prey Assemblage. In *Birds of Prey in a Changing Environment*; The Stationary Office: Edinburgh, UK, 2003; pp. 221–244.
53. Moleon, M.; Gil-Sanchez, J.M.; Real, J.; Sanchez-Zapata, J.A.; Bautista, J.; Sanchez-Clemot, J.F. Non-Breeding Feeding Ecology of Territorial Bonelli's Eagles *Hieraaetus fasciatus* in the Iberian Peninsula. *Ardeola* **2007**, *54*, 135–143.
54. Sánchez, R.; Margalida, A.; González, L.M.; Oria, J. Temporal and Spatial Differences in the Feeding Ecology of the Spanish Imperial Eagle *Aquila adatberti* during the Non-Breeding Season: Effects of the Rabbit Population Crash. *Acta Ornithol.* **2009**, *44*, 53–58. [CrossRef]
55. Glasser, J.W. A Theory of Trophic Strategies: The Evolution of Facultative Specialists. *Am. Nat.* **1982**, *119*, 250–262. [CrossRef]
56. Bakaloudis, D.E.; Vlachos, C.G.; Bontzorlos, V.A.; Papakosta, M.; Chatzinikos, E. European Hare (*Lepus europaeus*) Density Response in Mediterranean Ecosystems. In Proceedings of the 29th International Union of Game Biologists, Moscow, Russia, August 2009. Available online: https://www.researchgate.net/publication/260851278_EUROPEAN_HARE_LEPUS_EUROPAEUS_DENSITY_RESPONSE_IN_MEDITERRANEAN_ECOSYSTEMS (accessed on 10 December 2021).
57. Sánchez-Zapata, J.A.; Calvo, J.F. Raptor distribution in relation to landscape composition in semi-arid Mediterranean habitats. *J. Appl. Ecol.* **1999**, *36*, 254–262. [CrossRef]
58. Murgatroyd, M.; Avery, G.; Underhill, L.G.; Amar, A. Adaptability of a specialist predator: The effects of land use on diet diversification and breeding performance of Verreaux's eagles. *J. Avian Biol.* **2016**, *47*, 834–845. [CrossRef]

59. Malan, G.; Branch, W.R. Short Communications: Predation on Tent Tortoise and Leopard Tortoise Hatchlings by the Pale Chanting Goshawk in the Little Karoo. *S. Afr. J. Zool.* **1992**, *27*, 33–35. [CrossRef]
60. Demerdzhiev, D.; Dobrev, D.; Isfendiyaroğlu, S.; Boev, Z.; Stoychev, S.; Terziev, N.; Spasov, S. Distribution, Abundance, Breeding Parameters, Threats and Prey Preferences of the Eastern Imperial Eagle (*Aquila heliaca*) in European Turkey. *Slovak Raptor J.* **2014**, *8*, 17–25. [CrossRef]
61. Shafaeipour, A. Nesting Season Diet of Golden Eagles (*Aquila chrysaetos)* in Western Iran. *J. Raptor Res.* **2015**, *49*, 303. [CrossRef]
62. Varshavski, S.N. Feeding of *Aquila chrysaetos* in Southwestern Ust-Urt [in Russian]. *Ornitologija* **1968**, *9*, 146–149.
63. Longshore, K.; Esque, T.; Nussear, L.; Johnson, D.R.; Simes, M.; Inman, R. *An Assessment of Food Habits, Prey Availability, and Nesting Success of Golden Eagles within the Desert Renewable Energy Conservation Plan Area*; California Energy Commission: Sacramento, CA, USA, 2017.
64. Vlachos, C.G.; Papageorgiou, N.; Bakaloudis, D.E. Effects of the Feeding Station Establishment on the Egyptian Vulture *Neophron percnopterus* in Dadia Forest, North Eastern Greece. In *Holartctic Birds of Prey*; Chancellor, R.D., Meyburg, B.-U., Ferrero, J.J., Eds.; ADENEX & WWGBP: Merida, Germany; Berlin, Germany, 1998; pp. 197–207.
65. Grubac, B.R. Status & Biology of the Bearded Vulture *Gypaetus barbatus* Aureus in Macedonia. *Birds Prey Bull.* **1991**, *4*, 101–117.
66. Margalida, A.; Bertran, J. Function and Temporal Variation in Use of Ossuaries by Bearded Vultures (*Gypaetus barbatus*) during the Nestling Period. *Ornithology* **2001**, *118*, 785–789. [CrossRef]
67. Boire, D.; Nicolakakis, N.; Lefebvre, L. Tools and Brains in Birds. *Behaviour* **2002**, *139*, 939–973. [CrossRef]
68. Ducatez, S.; Clavel, J.; Lefebvre, L. Ecological generalism and behavioural innovation in birds: Technical intelligence or the simple incorporation of new foods? *J. Anim. Ecol.* **2014**, *84*, 79–89. [CrossRef] [PubMed]
69. Lefebvre, L.; Nicolakakis, N. Forebrain Size and Innovation Rate in European Birds: Feeding, Nesting and Confounding Variables. *Behaviour* **2000**, *137*, 1415–1429. [CrossRef]
70. Kitowski, I. Play behaviour and active training of Montagu's harrier (*Circus pygargus*) offspring in the post-fledging period. *J. Ethol.* **2004**, *23*, 3–8. [CrossRef]
71. Kitowski, I. Social learning of hunting skills in juvenile marsh harriers Circus aeruginosus. *J. Ethol.* **2008**, *27*, 327–332. [CrossRef]
72. Capper, S. The Predation of Testudo Spp by Golden Eagles *Aquila chrysaetos* in Dadia Forest Reserve, NE Greece. Master's Thesis, Department of Biology, University of Reading, Reading, UK, 1998.
73. Hailey, A. The effects of fire and mechanical habitat destruction on survival of the tortoise *Testudo hermanni* in northern Greece. *Biol. Conserv.* **2000**, *92*, 321–333. [CrossRef]
74. Kontsiotis, V.; Tsiompanoudis, A.C.; Bakaloudis, D.E. The influence of habitat structure on the European brown hare *Lepus europaeus* food habits in mountainous areas of northern Greece. *Mammalia* **2011**, *75*, 389–394. [CrossRef]
75. Kienzle, E.; Kopsch, G.; Koelle, P.; Clauss, M. Chemical Composition of Turtles and Tortoises. *J. Nutr.* **2006**, *136*, 2053–2054. [CrossRef]
76. Mertin, D.; Slamečka, J.; Ondruška, Ľ.; Zaujec, K.; Jurčík, R.; Gašparík, J. Comparison of Meat Quality between European Brown Hare and Domestic Rabbit. *Slovak J. Anim. Sci.* **2012**, *45*, 89–95.
77. Dimaki, M.; Limperakis, P.; Maragkou, P. Reptiles. In *The Red Data Book of Threatened Animals in Greece*; Legakis, A., Maragkou, P., Eds.; Hellenic Zoological Society: Athens, Greece, 2009; pp. 179–510, (In Greek with English Summaries).
78. Watson, J.; Leitch, A.F.; Rae, S.R. The diet of Golden Eagles *Aquila chrysaetos* in Scotland. *Ibis* **1993**, *135*, 387–393. [CrossRef]
79. Haworth, P.F.; Mcgrady, M.J.; Whitfield, D.P.; Fielding, A.H.; Mcleod, D.R.A.; Haworth, P.F.; Mcgrady, M.J.; Whitfield, D.P.; Fielding, A.H. Ranging distance of resident Golden Eagles *Aquila chrysaetos* in western Scotland according to season and breeding status. *Bird Study* **2006**, *53*, 265–273. [CrossRef]
80. Seguin, J.; Bayle, P.; Thibault, J.; Torre, J.; Vigne, J. A Comparison of Methods to Evaluate the Diet of Golden Eagle in Corsica. *J. Raptor Res.* **1998**, *32*, 314–318.
81. Steenhof, K.; Kochert, M.N. Dietary Responses of Three Raptor Species to Changing Prey Densities in a Natural Environment. *J. Anim. Ecol.* **1988**, *57*, 37. [CrossRef]
82. Preston, C.R.; Jones, R.E.; Horton, N.S.; Reston, C.H.R.P. Golden Eagle Diet Breadth and Reproduction in Relation to Fluctuations in Primary Prey Abundance in Wyoming's Bighorn Basin. *J. Raptor Res.* **2017**, *51*, 334–346. [CrossRef]
83. Ministry of Environment and Energy. Article 17 Reporting for the Implementation of the Habitats Directive. 2019. Available online: https://cdr.eionet.europa.eu/Converters/run_conversion?file=gr/eu/art12/envxz8njg/GR_birds_reports_20191031-152940.xml&conv=612&source=remote#A091_B (accessed on 15 December 2021).
84. Hailey, A.; Willemsen, R. Changes in the status of tortoise populations in Greece 1984–2001. *Biodivers. Conserv.* **2003**, *12*, 991–1011. [CrossRef]
85. Tucker, G.M.; Evans, M.I. *Habitats for Birds in Europe—A Conservation Strategy for the Wider Environment*; BirdLife Conservation Series No. 6; BirdLife International: Cambridge, UK, 1997.
86. Ruffault, J.; Curt, T.; Moron, V.; Trigo, R.M.; Mouillot, F.; Koutsias, N.; Pimont, F.; Martin-StPaul, N.; Barbero, R.; Dupuy, J.-L.; et al. Increased likelihood of heat-induced large wildfires in the Mediterranean Basin. *Sci. Rep.* **2020**, *10*, 13790. [CrossRef] [PubMed]
87. Couturier, T.; Besnard, A.; Bertolero, A.; Bosc, V.; Astruc, G.; Cheylan, M. Factors determining the abundance and occurrence of Hermann's tortoise *Testudo hermanni* in France and Spain: Fire regime and landscape changes as the main drivers. *Biol. Conserv.* **2014**, *170*, 177–187. [CrossRef]

88. Türkozan, O.; Karaman, S.; Yılmaz, C.; Ülger, C. Daily movements and home range of Eastern Hermann's Tortoise, *Testudo hermanni* boettgeri (Reptilia: Testudines). *Zool. Middle East* **2018**, *65*, 28–34. [CrossRef]
89. Robinzon, B.; Nir, I.; Lapid, R. Growth and body composition in captive Testudo graeca terrestris fed with a high-energy diet. *Appl. Herpetol.* **2005**, *2*, 201–209. [CrossRef]
90. Hadjigeorgiou, I. Past, present and future of pastoralism in Greece. *Pastor. Res. Policy Pract.* **2011**, *1*, 24. [CrossRef]
91. Triantakonstantis, D.P.; Kollias, V.J.; Kalivas, D.P. Forest Re-growth Since 1945 in the Dadia Forest Nature Reserve in Northern Greece. *New For.* **2006**, *32*, 51–69. [CrossRef]
92. Poirazidis, K.; Bontzorlos, V.; Xofis, P.; Zakkak, S.; Xirouchakis, S.; Grigoriadou, E.; Kechagioglou, S.; Gasteratos, I.; Alivizatos, H.; Panagiotopoulou, M. Bioclimatic and environmental suitability models for capercaillie (*Tetrao urogallus*) conservation: Identification of optimal and marginal areas in Rodopi Mountain-Range National Park (Northern Greece). *Glob. Ecol. Conserv.* **2019**, *17*, e00526. [CrossRef]
93. Moreira, F.; Russo, D. Modelling the impact of agricultural abandonment and wildfires on vertebrate diversity in Mediterranean Europe. *Landsc. Ecol.* **2007**, *22*, 1461–1476. [CrossRef]
94. Sirami, C.; Brotons, L.; Burfield, I.; Fonderflick, J.; Martin, J.-L. Is land abandonment having an impact on biodiversity? A meta-analytical approach to bird distribution changes in the north-western Mediterranean. *Biol. Conserv.* **2008**, *141*, 450–459. [CrossRef]
95. Pedrini, P.; Sergio, F. Golden Eagle *Aquila chrysaetos* density and productivity in relation to land abandonment and forest expansion in the Alps. *Bird Study* **2001**, *48*, 194–199. [CrossRef]
96. Whitfield, D.P.; McLeod, D.R.A.; Fielding, A.H.; Broad, R.A.; Evans, R.J.; Haworth, P.F. The effects of forestry on golden eagles on the island of Mull, western Scotland. *J. Appl. Ecol.* **2001**, *38*, 1208–1220. [CrossRef]
97. Ontiveros, D.; Pleguezuelos, J.M.; Caro, J. Prey density, prey detectability and food habits: The case of Bonelli's eagle and the conservation measures. *Biol. Conserv.* **2005**, *123*, 19–25. [CrossRef]
98. Nikolić, M.; Cvetković, J.; Stojadinović, D.; Crnobrnja-Isailović, J. Macro- and microhabitat preferences of eastern Hermann's tortoise (*Testudo hermanni* boettgeri). *Amphibia-Reptilia* **2020**, *41*, 313–322. [CrossRef]
99. Steenhof, K.; Kochert, M.N.; McDonald, T.L. Interactive Effects of Prey and Weather on Golden Eagle Reproduction. *J. Anim. Ecol.* **1997**, *66*, 350. [CrossRef]
100. Whitfield, D.P.; Fielding, A.H.; Gregory, M.J.P.; Gordon, A.G.; McLeod, D.R.A.; Haworth, P.F. Complex effects of habitat loss on Golden Eagles *Aquila chrysaetos*. *Ibis* **2006**, *149*, 26–36. [CrossRef]
101. Biswell, H. *Prescribed Burning in California Wildlands Vegetation Management*; University of California Press: Berkeley, CA, USA, 1989.
102. Blondel, J.; Arronson, J. *Biology and Wildlife of the Mediterranean Region*; Oxford University Press: Oxford, UK, 1999.
103. Grove, A.T.; Rackham, O. *The Nature of Mediterranean Europe—An Ecological History*; Yale University Press: New Heaven, CT, USA, 2001.
104. Zakkak, S.; Radovic, A.; Nikolov, S.C.; Shumka, S.; Kakalis, L.; Kati, V. Assessing the effect of agricultural land abandonment on bird communities in southern-eastern Europe. *J. Environ. Manag.* **2015**, *164*, 171–179. [CrossRef]
105. Kati, V.; Foufopoulos, J.; Ioannidis, Y.; Papaioannou, H.; Poirazidis, K.; Lebrun, P. Diversity, ecological structure and conservation of herpetofauna in a Mediterranean area (Dadia National Park, Greece). *Amphibia-Reptilia* **2007**, *28*, 517–529. [CrossRef]
106. Kati, V.; Poirazidis, K.; Dufrêne, M.; Halley, J.M.; Korakis, G.; Schindler, S.; Dimopoulos, P. Towards the use of ecological heterogeneity to design reserve networks: A case study from Dadia National Park, Greece. *Biodivers. Conserv.* **2010**, *19*, 1585–1597. [CrossRef]
107. Herring, G.; Eagles-Smith, C.A.; Buck, J. Characterizing Golden Eagle Risk to Lead and Anticoagulant Rodenticide Exposure: A Review. *J. Raptor Res.* **2017**, *51*, 273–292. [CrossRef]
108. Ganz, K.; Jenni, L.; Madry, M.M.; Kraemer, T.; Jenny, H.; Jenny, D. Acute and Chronic Lead Exposure in Four Avian Scavenger Species in Switzerland. *Arch. Environ. Contam. Toxicol.* **2018**, *75*, 566–575. [CrossRef] [PubMed]
109. Gil-Sánchez, J.M.; Molleda, S.; Sanchez-Zapata, J.A.; Bautista, J.; Navas, I.; Godinho, R.; García-Fernández, A.J.; Moleón, M. From sport hunting to breeding success: Patterns of lead ammunition ingestion and its effects on an endangered raptor. *Sci. Total Environ.* **2017**, *613–614*, 483–491. [CrossRef]
110. Nadjafzadeh, M.; Voigt, C.C.; Krone, O. Spatial, seasonal and individual variation in the diet of White-tailed Eagles *Haliaeetus albicilla* assessed using stable isotope ratios. *Ibis* **2015**, *158*, 1–15. [CrossRef]
111. Bounas, A.; Ganoti, M.; Giannakaki, E.; Akrivos, A.; Vavylis, D.; Zorrilla, I.; Saravia, V. First confirmed case of lead poisoning in the endangered Egyptian Vulture (*Neophron percnopterus*) in the Balkans. *Vulture News* **2018**, *70*, 22. [CrossRef]
112. Caballero, R.; Fernandez-Gonzalez, F.; Perez Badia, R.; Molle, G.; Roggero, P.P.; Bagella, S.; D'Ottavio, P.; Papanastasis, V.P.; Fotiadis, G.; Sidiropoulou, A.; et al. Grazing Systems and Biodiversity in Mediterranean Areas: Spain, Italy and Greece. *Pastos* **2009**, *39*, 9–152.
113. Watson, J. The Golden Eagle and Pastoralism across Europe. In *Birds and Pastoral Agriculture in Europe: Proceedings of the Second European Forum on Birds and Pastoralism, Port Erin, Isle of Man, UK, 26–30 October 1990*; Curtis, D.J., Bignal, E.M., Curtis, M.A., Eds.; Joint Nature Conservation Committee: Inverness, UK; Scottish Chough Study Group: Bridgend, UK, 1991; pp. 56–57.
114. Gjershaug, J.O.; Halley, D.; Stokke, B.G. Predefinitive Plumage in the Golden Eagle (*Aquila chrysaetos*): A Signal of Aggression or Submission? *J. Raptor Res.* **2019**, *53*, 431–435. [CrossRef]

115. Sánchez-Zapata, J.A.; Eguía, S.; Blázquez, M.; Moleón, M.; Botella, F. Unexpected role of ungulate carcasses in the diet of Golden Eagles *Aquila chrysaetos* in Mediterranean mountains. *Bird Study* **2010**, *57*, 352–360. [CrossRef]
116. Ntemiri, K.; Saravia, V.; Angelidis, C.; Baxevani, K.; Probonas, M.; Kret, E.; Mertzanis, Y.; Iliopoulos, Y.; Georgiadis, L.; Skartsi, D.; et al. Animal mortality and illegal poison bait use in Greece. *Environ. Monit. Assess.* **2018**, *190*, 488. [CrossRef] [PubMed]
117. Velevski, M.; Nikolov, S.C.; Hallmann, B.; Dobrev, V.; Sidiropoulos, L.; Saravia, V.; Tsiakiris, R.; Arkumarev, V.; Galanaki, A.; Kominos, T.; et al. Population decline and range contraction of the Egyptian Vulture *Neophron percnopterus* in the Balkan Peninsula. *Bird Conserv. Int.* **2014**, *25*, 440–450. [CrossRef]
118. Sidiropoulos, L.; Tsiakiris, R.; Azmanis, P.; Galanaki, A.; Kastritis, A.; Stara, K.; Konstantinou, P.; Jerrentrup, H.; Xirouchakis, S.; Kominos, T. The Status of Vultures in Greece. In *Vulture Conservation in the Balkan Peninsula and Adjacent Regions—10 Years of Research and Conservation*; Andevski, J., Ed.; Vulture Conservation Foundation: Skopje, North Macedonia, 2013; pp. 20–23.

diversity

MDPI

Article

Biological Interaction as a Possible Ultimate Driver in the Local Extinction of *Cedrus atlantica* in the Iberian Peninsula

Antonio González-Hernández [1,*], Diego Nieto-Lugilde [2], Francisca Alba-Sánchez [1] and Julio Peñas [1]

[1] Department of Botany, University of Granada, C.U. Fuentenueva, 18071 Granada, Spain; falba@ugr.es (F.A.-S.); jgiles@ugr.es (J.P.)
[2] Department of Botany, Ecology and Plant Physiology, University of Cordoba, C.U. Rabanales, 14014 Cordoba, Spain; dnieto@uco.es
* Correspondence: aglezhdez@gmail.com

Abstract: The presence of *Cedrus atlantica* on the European continent, including, especially, the determination of the time of its disappearance from the Iberian Peninsula, is one of the most controversial issues in recent decades regarding the successive extinction of conifers in the Western Mediterranean. This work propounds the possibility that *C. atlantica* and *Pinus nigra* could have co-habited in the past, mutually excluding each other in the areas with suitable conditions for both species, where, ultimately, the one that was the most competitive would have remained. The niche overlap in the two-dimensional ecological space was analyzed. In addition, the potential distribution of both species in the Western Mediterranean today and two past periods (Last Glacial Maximum and Mid-Holocene) was modeled to identify their common geographic area of distribution. The species showed very well differentiated niches and a distribution of their habitats virtually segregated by continents since the Mid-Holocene (*P. nigra* in Europe and *C. atlantica* in Africa), which responds to differences in climatic affinities. However, the contact of the bordering areas of their distributions in the Baetic mountain range suggests that *C. atlantica* could have maintained its presence in the Iberian Peninsula until recent times. *P. nigra* would have displace it in later stages due to its greater prevalence on the continent, so it would have had greater opportunities to occupy the available space.

Keywords: black pine; cedar; competition; ecological niche; paleoecology

Citation: González-Hernández, A.; Nieto-Lugilde, D.; Alba-Sánchez, F.; Peñas, J. Biological Interaction as a Possible Ultimate Driver in the Local Extinction of *Cedrus atlantica* in the Iberian Peninsula. *Diversity* **2022**, *14*, 136. https://doi.org/10.3390/d14020136

Academic Editor: Michael Wink

Received: 16 December 2021
Accepted: 12 February 2022
Published: 15 February 2022

1. Introduction

The presence of *Cedrus atlantica* (Endl.) Carrière on the European continent and the time of its disappearance from the Iberian Peninsula are issues that have raised controversy in recent decades regarding the successive extinction of conifers in the Western Mediterranean [1–3]. The presence of *Cedrus* in the Iberian Peninsula has been referenced from the Eocene to the Holocene [4] and widely in Europe since the Miocene [5]. However, the only fossil macro-remain that confirms its autochthonous origin corresponds to leaves of *C. blombley* found on the island of Rhodes dated to the Middle Pleistocene (500 ka) [6]. The absence of macro-remains (charred wood) of *Cedrus* on the European continent led to the statement that the presence of cedar pollen in the Iberian fossil record responded to its airborne uptake by winds from Africa [2,5,7,8]. However, the constancy of the pollen type in numerous deposits [1,3,7,9–12], its proportion and the low dispersal power of grains [1,13,14]; the *Cedrus–Abies* assemblage in the records [10]; and the low correlation between the presence of pollen and the origin of the winds from Africa [15,16] question this possibility and support the hypothesis that *Cedrus* lived in southern Europe during the Holocene as a component of mixed conifers woods or as small copses [3].

The distribution dynamics of *C. atlantica* in Europe and Africa have been conditioned by climate, especially by the warmer temperatures in winter and the dryness of summer [17,18]. Thus, the warmest periods of the Quaternary, such as the last interglacial

(200–140 ka) or the Holocene (11 ka-present), determined the migration of its populations towards the south and towards higher altitudes, in a progressive reduction in its distribution [17]. In the Iberian Peninsula, its last populations had to take refuge in the southern mountains of the Baetics as small, isolated nuclei [3,15]. In this context, it has been proposed that the definitive extinction of *Cedrus* in Europe during the Holocene could be motivated by human action [16,19,20], or even by competition with other species [3,16]. In this sense, an examination of the pollen diagrams of the available deposits on both sides of the Strait of Gibraltar (Baetic Mountain Range and Rif) revealed inverse patterns in the relative abundance of the *Pinus* and *Cedrus* pollen types; while, in the Baetics, *Pinus* dominates and *Cedrus* is scarce, in the Rif, *Pinus* appears meager where *Cedrus* is the dominant type [1,16,17,21–26]. If the ecological affinities of the species are not mutually exclusive and in the absence of barriers to dispersal, this negative association between species suggests the possibility that species of both genera have interacted in the past, mutually excluding each other in areas where they shared a niche and where the one that was more competitive would have ultimately remained [27,28].

The objective of this study is to identify the interspecific interaction through a niche overlap analysis [29,30]. *Pinus nigra* Arnold was selected among the mountain conifers distributed in the Western Mediterranean due to its ecological affinity with *C. atlantica* [31–34]. Likewise, the distribution of both species in the Iberian Peninsula was explored and the location of the possible common area was identified, both currently and in two moments in the past, Last Glacial Maximum (LGM; 21 ka) and Holocene Climate Optimum (HCO; 6 ka). The variations in the distribution of both species would make it possible to understand their respective historical geographical dynamics.

The use of Species Distribution Models (SDMs) has been a complement to the traditional techniques used in Paleobiogeography that can help identify knowledge gaps derived from inherent geographic, temporal and taxonomic biases [35–39]. In fact, SDMs have been previously applied in the projections of different climatic conditions in the past with *C. atlantica* [14,40,41] and *P. nigra* [31,42,43].

2. Materials and Methods

To identify overlap in the potential geographic distribution of *C. atlantica* and *P. nigra*, Species Distribution Models (SDM) were used. These models were projected into the past (LGM, 21 ka; HCO, 6 ka). On the other hand, the relationship of the niches in the two-dimensional ecological space was revealed by a principal coordinate analysis (PCA), from which the equivalence and similarity of the niches of both species was evaluated.

2.1. Study Area

The study area was framed in the Western Mediterranean, where *C. atlantica* may have reached its maximum extension during the last glaciation (Würm, 21 ka) [5]. It covers the Iberian and Italic peninsulas, the Western Alps and the Dinarides, in Europe; the Atlas Mountains and Rif, in Africa; and Corsica, Sardinia, Sicily and the Balearic Islands.

For the purposes of the different analyses, the study area was defined by the coordinates lat 29° N–46° N; lon 12° W–19° E. For the niche overlap, we defined the surrounding environment of each species as the geographic space delimited by the extreme coordinates of the observations used (Figure 1).

2.2. Species

Cedrus atlantica is currently distributed in mountainous areas of the Rif and Middle Atlas in Morocco and the Tell Atlas and Aures Mountains in Algeria [44], between 1300 and 2600 m of altitude, where annual rainfall ranges between 500 and 2000 mm and the minimum temperatures of the coldest month range from −1 to −8 °C [45]. For the analysis of this work, observations made directly in the field, in Morocco, were used; while in Algeria, the recognition of the species was conducted by photo interpretation (Figure 1).

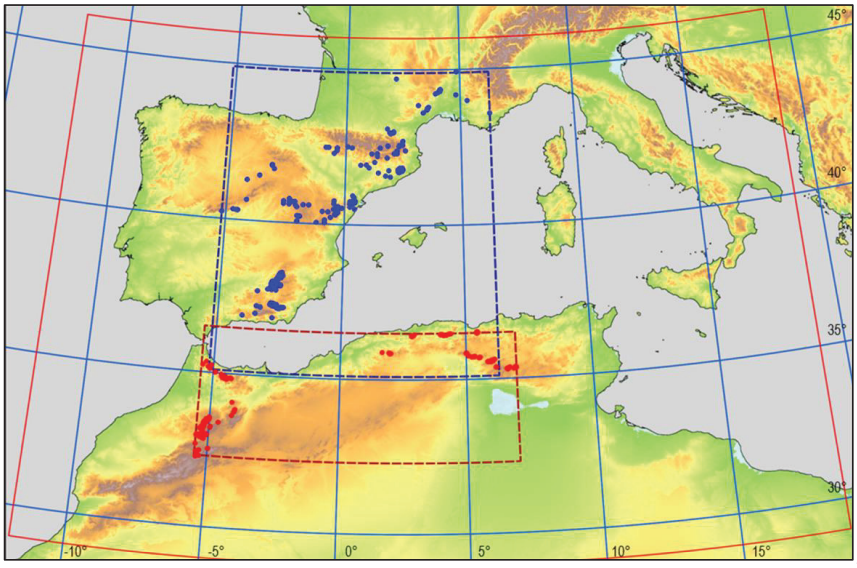

Figure 1. Study area (outlined in red) showing the distribution of the observations for *Pinus nigra* (blue, *n* = 257) and *Cedrus atlantica* (red, *n* = 211). The surrounding environment of each species, marked by dotted lines, were applied in the niche overlap analysis.

Pinus nigra is a species of medium and high mountain (1500–2500 m of altitude) of circum-Mediterranean distribution, which extends through southern Europe, from the Iberian Peninsula to Anatolia, and reaches the Caucasus, with occasional presence in North Africa, in the Rif and Tell Atlas. The subspecies *P. nigra* subsp. *salzmannii* (Dunal) Franco, the one contemplated in this study, is limited to the Western Mediterranean (Cévennes, Pyrenees, Iberian and Central Systems and Baetic mountain range in Europe; Rif and Tell Atlas in Africa). It inhabits rocky terrain where it presents greater resistance to drought than other species of medium- and high-mountain pine [18,32,46]. For the analysis of this work, 257 localities were randomly selected, at the working resolution (30 arc seconds), from the database of the Global Biodiversity Information Facility (GBIF; www.gbif.net). Redundant observations at working resolution were eliminated (Figure 1).

2.3. Variables

The niche predictors were selected from the 19 bioclimatic variables of the 1960–1990 series for the present, from the WorldClim 1.4 portal, (www.worldclim.com, accessed on 1 February 2013). Preliminarily, a survey of the variables that best fit the distribution models of *C. atlantica* was carried out with MAXENT [47], implemented in the 'dismo' R package [48]. Those variables with the highest percentage of contribution and importance of permutation were selected alternatively when the model was adjusted [49], discarding the rest of the highly correlated variables (values higher than 0.7) in each choice (Table A1).

Finally, the following four predictor variables were selected:

- Minimum temperature of the coldest month (bio6);
- Temperature annual range (bio7);
- Mean temperature of the wettest quarter (bio8);
- Precipitation of the driest month (bio14).

To project the niche model in the geographical space, the climatic layers of WorldClim 1.4 were used, at a resolution of 30 arc seconds for current conditions and HCO (6 ka) and at a resolution of 2.5 arc minutes for LGM (21 ka). MIROC-ESM was chosen among the possible general circulation models [50], because it presented the best fit in its evaluation

for the two moments in time in the past for *C. atlantica* (Table A2). In this evaluation, the available evidence of *Cedrus atlantica* in the Western Mediterranean from the fossil record for the two periods referred was used. In this review, the sites of the European Pollen Database [51] were considered, as well as compilations of works in the Iberian Peninsula [22] and in North Africa [14,17,21,23–26].

2.4. Analysis

The niche of each species was modeled and projected in the geographical space using the MAXENT algorithm, included in the 'dismo' R' package [48], a machine learning-type algorithm that only requires presence records and a reference environment (background) to calibrate the models [52–54]. The potential habitat of each species was expressed through the binary transformation of suitability (suitable/unsuitable habitat for the species) applying, as threshold, the maximum of the sum (sensitivity + specificity). The overlap of the potential habitat of both species indicates the favorable areas for both species, thus where interaction between them is possible. There are numerous antecedents in the application of the SDM to the past and, especially, in the Iberian Peninsula [31,35,55].

The validation of the models was carried out by contrasting the value of the observed area under the curve (AUC) with the null model AUC [56]. The null model was built with the distribution of AUC values from 100 SDM iterations built with n randomly selected points (257 for *P. nigra* and 211 for *C. atlantica*) from the background. The null model AUC represents the 0.95 quantile in this distribution and the model is significantly valid ($p < 0.05$) if the observed AUC value is greater than the null model AUC.

On the other hand, the niche overlap in the two-dimensional environmental space was evaluated using the 'ecospat' R' package [57]. This is defined by the two main axes of a PCA built from the values of the four variables selected in the surrounding environment of *C. atlantica* and *P. nigra*. (Figure 2). This two-dimensional environmental space was gridded (100×100 cells) and the density surfaces for the observations were projected on this grid to represent the niches [29]. The relative positions of the niches of both species allowed us to infer possible interspecific relationships.

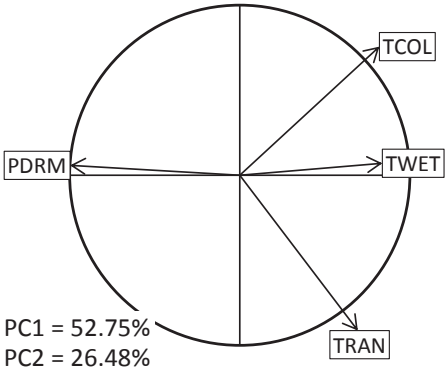

Figure 2. Two-dimensional environmental space, determined by the two main axes of a PCA from four descriptor variables. *TCOL*, minimum temperature of the coldest month; *TRAN*, temperature annual range; *TWET*, mean temperature of the wettest quarter; *PDRM*, precipitation of the driest month.

Niche overlap was measured with Schoener's *D* index (ranging from 0, no overlap, to 1, total overlap). The niche overlap was contrasted using the equivalence and similarity tests [29,30]. In each of them, the observed *D*-value is compared with a null distribution of *D*-values obtained as the result of the iteration of 100 superposition operations between pairs of sets of random observations.

The equivalence test is aimed at identifying identical niches in the whole surrounding area. In this test, each of the two sets of observations of the null distribution is built by

random selection among the whole surrounding area of the two species. The niches of the two species are admitted to be equivalent if the observed overlap value is significantly higher than the 0.95 quantile of the null distribution. That is, the two niches are more similar to each other than any two random sets of the whole surrounding area.

The similarity test assesses the similarity of one niche to another in relation to the surrounding environment in which it is found. The surrounding environment of each species is delimited by the extreme coordinates of the observations (Figure 1). In this test, the total of observations from which the pairs are drawn at random, for the null distribution, was constructed with the observations of one species and an extract from the surrounding environment of the opposite species (in a number equal to that of their observations). Thus, in this test, two asymmetric analyzes are carried out in which the observations of each species are compared with the surrounding environment of the species being confronted. Therefore, two species with environmental affinities would have higher overlap values than expected when comparing the niche of one species with the surrounding environment of the opposite. The niches of the two species are significantly similar if the *D*-value exceeds the 0.95 quantile of the null distribution [29,30].

3. Results

3.1. Geographical Distribution

The four selected environmental variables defined the fundamental niche of both species with a high level of prediction of the optimal habitat for the current conditions. The validation of the models showed that the observed AUC values greatly exceeded those marked for a null distribution [56], with a significance of 95% (Table 1; Figure A1).

Table 1. Evaluation of the distribution models: observed and null model AUC.

SPECIES	*n*	AUC	Null Model AUC
Pinus nigra	257	0.965	0.591
Cedrus atlantica	211	0.995	0.604

The observed AUC (area under the curve) values were significantly higher ($p < 0.05$) than the AUC values of the null model; *n* is the number of presences used in the calibration of the species distribution model and of each iteration in the null model.

According to the projections made in MAXENT, the potential habitats of *C. atlantica* and *P. nigra* are mostly geographically segregated from each other at present (Figure 3c). Currently, the optimal habitat for *C. atlantica* is distributed mainly in North Africa, from the High Atlas in the immediate vicinity of the Atlantic Ocean to the Tell Atlas and Aures Mountains, via the Rif and the Middle Atlas. In Europe, this species finds its optimal habitat in the Iberian Peninsula, Baetic Mountain Range, and in the Central System, extending to the Leon Mountains. The predicted distribution of *P. nigra* is framed in the European Mediterranean basin, from the Iberian and Central Systems and the Cantabrian Mountains, in the Iberian Peninsula; to the Apennines and western Alps, through the Pyrenees and Massif Central. Marginally, it is also represented in the Aures Mountains, Rif and Middle Atlas on the African continent. At present, *C. atlantica* and *P. nigra* would share their distribution in the Baetic Mountain Range and Central System in Europe and in the Middle Atlas and Aures Mountains in Africa (Figure 3c).

Compared with current conditions, the projection to the LGM (21 ka) shows the descent in altitude of the most favorable conditions for *C. atlantica*, where it would share the habitat with *P. nigra* (Figure 3a). This was revealed by a greater extension of the potential habitat of the species throughout the mountain systems of Africa and the prevalence of the plateaus in the Iberian Peninsula, as well as their presence in the mountain systems near the Tyrrhenian. In the Iberian Peninsula, the common areas would extend through the Iberian System and the inland areas close to the Cantabrian Mountains. In Africa, the common habitat would be linked to the High, Middle and Saharan Atlas and the Aures Mountains (Figure 3a).

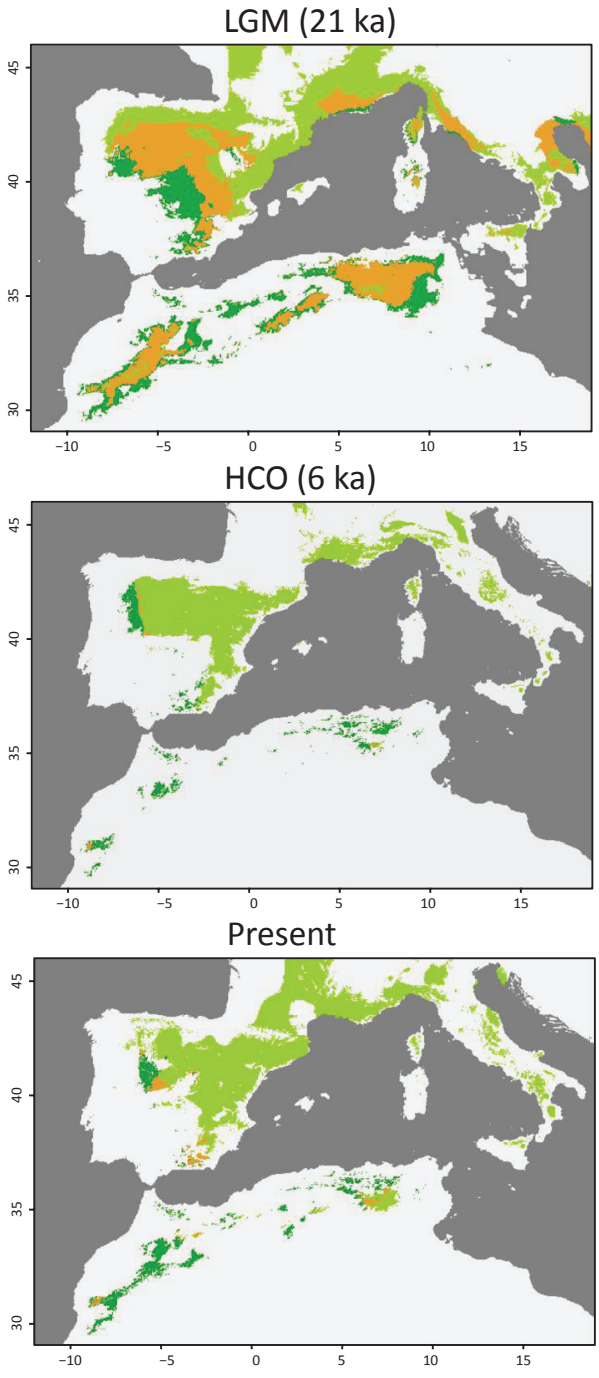

Figure 3. Potential habitat for *Pinus nigra*, *Cedrus atlantica* and their overlap in three time periods: (**a**) Last Glacial Maximum; (**b**) Holocene Climatic Optimum; (**c**) present. These were built from the species distribution model (MAXENT) with environmental variables from the past according to the MIROC-ESM General Circulation Models.

The warmer conditions of the HCO (6 ka) with respect to the LGM would have determined the ascent in altitude of the optimal conditions for both species (Figure 3b). This would have resulted in a drastic reduction in the potential area of *C. atlantica* and its isolation in a number of disjoint areas, largely coinciding with the current distribution of the species. The presence of the habitat of each of the species would have been virtually restricted to one continent, *C. atlantica* to Africa and *P. nigra* to Europe, with negligible presence on the opposite continent, where both species would have shared limits of habitat distribution marginally.

3.2. Niche Overlap

The analysis of niche overlap in the two-dimensional ecological space reflects the overlap with a *D*-value close to 0.37. According to the strict nature of the test, the equivalence test result was that both species niches were non-significantly equivalent (they did not match completely). Contrary to the equivalence test, both similarity tests indicated that both species niches were significantly similar to each other considering their different surrounding environment (Table 2; Figure A2).

Table 2. Niche overlap of *Pinus nigra* and *Cedrus atlantica* and equivalence and similarity tests. Similarity implies two asymmetric analyses (niche→surrounding environment; 1 and 2 represent *P. nigra* and *C. atlantica*, respectively).

SPECIES	Overlap (*D*)	Equivalence	Similarity 1→2	Similarity 2→1
P. nigra–*C. atlantica*	0.365	*ns*	Similar *	Similar **

D, Schoener Overlap Index. * Significant at $p < 0.05$; ** Significant at $p < 0.01$; *ns*, the niches of the species are not significantly equivalent to each other.

The arrangement of the density grids in the two-dimensional ecological space shows a relative displacement between the niches of both species along the second axis of the PCA. (Figure 4). This could be interpreted as a coincidence in the affinity of the species for the variables that determine the first axis of the PCA (precipitation of the driest month and mean temperature of the wettest quarter; Figure 2), while differences appear in the niche determined by the two remaining variables, minimum temperature of the coldest month, whose lowest values are better tolerated by *C. atlantica* (from −6 to −2 °C, compared to −3–2 °C, where *P. nigra* lives); and the temperature annual range, with *C. atlantica* better tolerating higher ranges in temperature (from 29 to 36 °C, compared to 23–26 °C in which *P. nigra* lives; Figures A3 and A4).

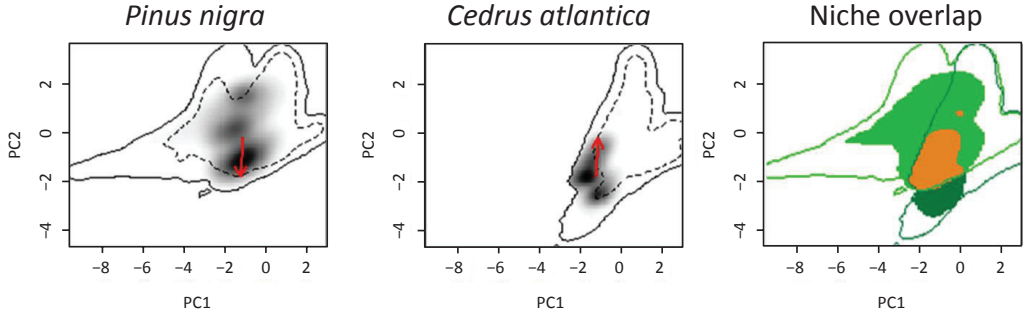

Figure 4. Niche overlap in environmental space. The solid line delimits the surrounding environment and the discontinuous line 50% of its area. The arrows show the relative displacement between the centroids of the niches in the overlap analysis. The overlap diagram shows the niches of *Pinus nigra* and *Cedrus atlantica* (polygons in light and dark green, respectively). The reddish polygon indicates the common niche (overlap).

4. Discussion

According to our results, *C. atlantica* currently extends the distribution of its potential habitat in the Iberian Peninsula even though the species does not currently inhabit Europe. These results are consistent with other models made for *C. atlantica* [17,41]. During the LGM (21 ka), the extension of the habitat would occupy most of the center of the Iberian Peninsula, dominating the plateaus and mountainous areas of the Iberian System, the interior areas near the Cantabrian Mountains and most of the Baetic Mountain Range. The presence of *Cedrus* in the fossil records could support these projections to the past [11,58,59]. The increase in temperature during the HCO (6 ka) determined the increase in altitude of both species. Populations of *C. atlantica* were isolated in the mountain systems, which served as a refuge, from where the species spread to the present day. This is consistent with the dynamics of cedars in North Africa during the Holocene found in fossil records [1,15,17,21,23,24,26]. Therefore, the dynamics of the cedars in Europe have been linked to the climate since the last ice age, so their disappearance on the continent could have been due to a greater extent to a progressive reduction in their potential habitat [17,18].

This would not be incompatible with the existence of biotic relationships as a determining agent of local extinction in the redoubts present in the Baetic Mountain Range (Postigo-Mijarra et al., 2010). Bearing the possibility that *C. atlantica* and *P. nigra* interacted in the Iberian Peninsula in the past, occupying similar environmental spaces, they could mutually have excluded each other in mountainous areas where the more competitive species would have remained. The starting hypothesis arises from the fact that the distribution of each species is restricted to separate continents and that the *Cedrus* and *Pinus* spp. show some negative temporal association in the pollen profiles of the fossil records from both sides of the Mediterranean [1,16,17,21–26]. However, both species show a similar ecological behavior (they form forests in the high Mediterranean mountains), which raises the question of whether and to what extent they share a niche. If so, the negative association of their presence (geographical and temporal) could be associated with biological interaction [27,28].

The results obtained indicate that the distribution of the potential habitat of *C. atlantica* and *P. nigra* overlapped both in Africa and in Europe during the Pleistocene, being able to maintain contact between their populations in their distribution limits. In addition, the niche overlap tests indicate that both species habitats are significantly similar to each other. In the geographical space, the results obtained indicate that the distribution of the potential habitat of *C. atlantica* and *P. nigra* overlapped both in Africa and in Europe during the Pleistocene, being able to maintain contact between their populations in their distribution limits. Warmer temperatures during the Holocene caused both species, *C. atlantica* and *P. nigra*, to migrate upwards [17]. In this situation, both species reduced their shared habitat and, even so, it is possible that their populations maintained contact. Thus, they could have been growing in the same stands as mixed coniferous forests; *Cedrus* could have formed part of pine forests as a companion species, or formed small separate copses in the same territory that *P. nigra* would have inhabited. Going up in altitude, the smaller distribution area of *Cedrus* in the Iberian Peninsula with respect to *Pinus* would make the species more sensitive to certain stochastic processes that would lead to habitat fragmentation and, in the extreme case, to its local disappearance, despite the existence of available habitat.

According to our results, the spatial segregation between species is much greater than that of its niches. Both species share their niches and both species have also shared habitat on the same continent since the Pleistocene. Nevertheless, their current distributions have drifted towards complete spatial segregation. It cannot be ruled out that this fact is due to the interaction between both species. In fact, the geographic segregation may have affected the results of the analysis by introducing a bias in the observations used to calibrate the distribution models. If there had been any observations of *C. atlantica* currently in Europe, the resulting model would likely have been different, with a much larger potential habitat distribution and greater overlap with the *P. nigra* niche.

In conclusion, *C. atlantica* and *P. nigra* show differentiated niches based on greater tolerance to extreme cold and continentality of *Cedrus*. Currently, the distribution of both species, segregated on different continents—*P. nigra* in Europe and *C. atlantica* in Africa—is virtually responding to dissociation from their optimal habitats. However, both species were able to share habitat in their distribution limits on the European continent until the end of the Pleistocene. The increase in temperatures of the Holocene Optimum Climate must have forced the rise of both species in altitude, causing the isolation of their populations in mountain refuges and the consequent loss of connectivity that has lasted until today. Although *C. atlantica* has continuously maintained its ideal habitat in the Baetic Mountains to date, it cannot be ruled out that the higher prevalence of *P. nigra* on mainland Europe has eventually displaced *Cedrus*.

Author Contributions: Conceptualization, A.G.-H., D.N.-L. and J.P.; methodology and formal analysis, A.G.-H. and D.N.-L.; writing—original draft preparation, A.G.-H.; writing—review and editing, D.N.-L., F.A.-S. and J.P.; project administration and funding acquisition, F.A.-S. All authors have read and agreed to the published version of the manuscript.

Funding: This research study was funded by (i) the Spanish government, State R&D Program Oriented to the Challenges of the Society, MED-REFUGIA Research Project (RTI2018-101714-B-I00); (ii) Andalusian Plan for Research, Development and Innovation, OROMEDREFUGIA Research Project (P18-RT-4963); (iii) ERDF Operational Programme in Andalusia (EU regional programme), RELIC-FLORA 2 Research Project (B-RNM-404-UGR18); and (iv) State Program for the Promotion of Scientific Research and Excellence Technique, PALEOPINSAPO Research Project (CSO2017-83576-P). The APC was funded by (i) the Spanish government, State R&D Program Oriented to the Challenges of the Society, MED-REFUGIA Research Project (RTI2018-101714-B-I00); and (ii) Andalusian Plan for Research, Development and Innovation, OROMEDREFUGIA Research Project (P18-RT-4963).

Institutional Review Board Statement: Not applicable.

Informed Consent Statement: Not applicable.

Data Availability Statement: The data used in this study are available upon request from the corresponding author.

Conflicts of Interest: The authors declare no conflict of interest. The funders had no role in the design of the study; in the collection, analyses, or interpretation of data; in the writing of the manuscript; or in the decision to publish the results.

Appendix A

Table A1. Correlation between environmental variables (Pearson). TCOL, min temperature of coldest month; TRAN, temperature annual range; TWET, temperature of wettest quarter; PDRM, precipitation of the driest month.

	TCOL	**TRAN**	**TWET**	**PDRM**
TCOL	1			
TRAN	0.055	1		
TWET	0.464	0.434	1	
PDRM	−0.687	−0.504	−0.436	1

Table A2. Evaluation of the SDM of *Cedrus atlantica* projected into the past: observed and null model AUC.

	HCO		**LGM**	
	CCSM4	**MIROC-ESM**	**CCSM4**	**MIROC-ESM**
Obs. AUC	0.7396	0.7830	0.5011	0.5425
Null AUC	0.7584	0.7398	0.7616	0.7769

The observed AUC (area under the curve) values are only significantly higher ($p < 0.05$) than the null model AUC values in the models projected to the HCO with the MIROC-ESM general circulation model.

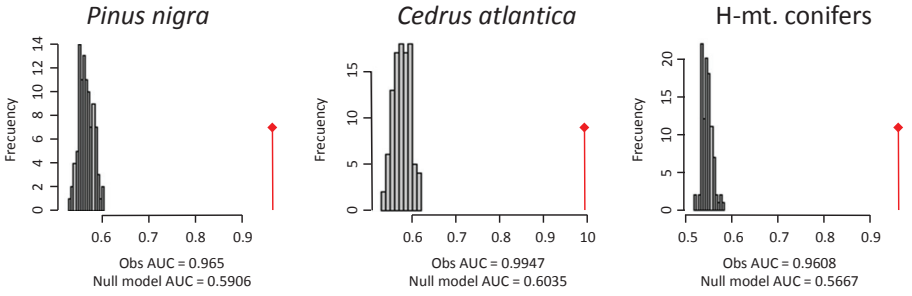

Figure A1. Observed and null model AUC in MAXENT. The null model AUC is the 0.95 quantile in a random distribution. The observed AUC values (red diamond) were significantly ($p < 0.05$) higher than the AUC of the null models.

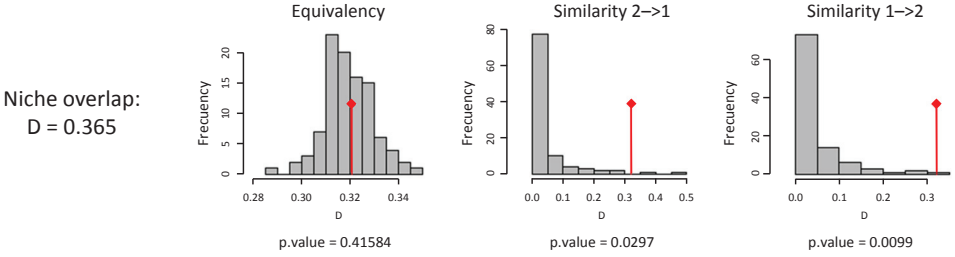

Figure A2. Niche overlap test. Histograms show the observed *D*-value (red diamond) versus the null distribution in the equivalence and similarity tests.

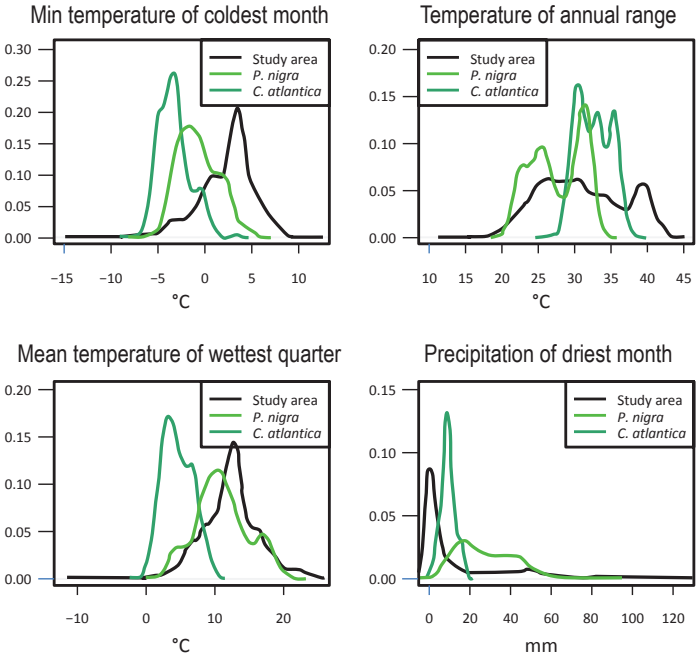

Figure A3. Density curves of the predictor variables for *Pinus nigra*, *Cedrus atlantica* and the background in the study area (see Figure 1).

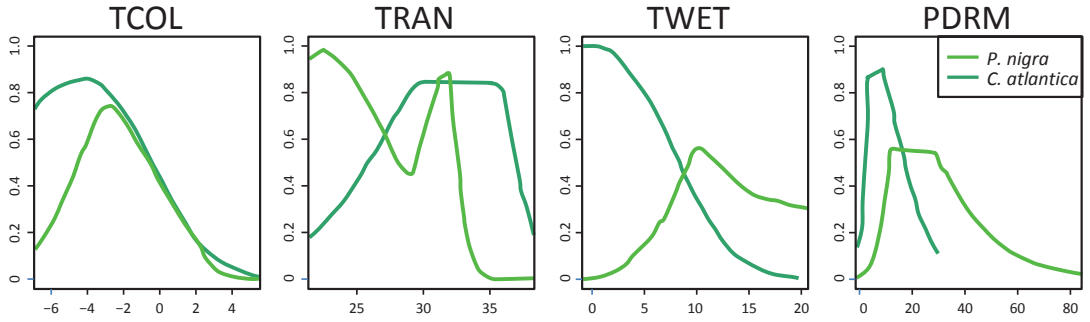

Figure A4. Response curves of the four environmental variables in the models in MAXENT. The differences in the pattern of the curves between the *Pinus nigra* and *Cedrus atlantica* models are consistent with the divergences observed in the distribution of their habitats. TCOL, min temperature of coldest month, TRAN, temperature annual range, TWET, temperature of wettest quarter, PDRM, precipitation of driest month.

References

1. Abel-Schaad, D.; Iriarte, E.; López-Sáez, J.A.; Pérez-Díaz, S.; Sabariego Ruiz, S.; Cheddadi, R.; Alba-Sánchez, F. Are *Cedrus atlantica* forests in the Rif Mountains of Morocco heading towards local extinction? *Holocene* **2018**, *28*, 1023–1037. [CrossRef]
2. Magri, D.; Di Rita, F.; Aranbarri, J.; Fletcher, W.; González-Sampériz, P. Quaternary disappearance of tree taxa from Southern Europe: Timing and trends. *Quat. Sci. Rev.* **2017**, *163*, 23–55. [CrossRef]
3. Postigo-Mijarra, J.M.; Morla, C.; Barrón, E.; Morales-Molino, C.; García, S. Patterns of extinction and persistence of Arctotertiary flora in Iberia during the Quaternary. *Rev. Palaeobot. Palynol.* **2010**, *162*, 416–426. [CrossRef]
4. Postigo-Mijarra, J.M.; Barrón, E.; Gómez Manzaneque, F.; Morla, C. Floristic changes in the Iberian Peninsula and Balearic Islands (South-West Europe) during the Cenozoic. *J. Biogeogr.* **2009**, *36*, 2025–2043. [CrossRef]
5. Magri, D. Quaternary History of *Cedrus* in Southern Europe. *Ann. Bot.* **2012**, *2*, 57–66. [CrossRef]
6. Boyd, A. Relict Conifers from the Mid-Pleistocene of Rhodes, Greece. *Hist. Biol.* **2009**, *21*, 1–15. [CrossRef]
7. Jiménez-Moreno, G.; Anderson, R.S.; Ramos-Román, M.J.; Camuera, J.; Mesa-Fernández, J.M.; García-Alix, A.; Jiménez-Espejo, F.J.; Carrión, J.S.; López-Avilés, A. The Holocene *Cedrus* pollen record from Sierra Nevada (S Spain), a proxy for climate change in N Africa. *Quat. Sci. Rev.* **2020**, *242*, 106468. [CrossRef]
8. Magri, D.; Parra, I. Late Quaternary Western Mediterranean pollen records and African winds. *Earth Planet. Sci. Lett.* **2002**, *200*, 401–408. [CrossRef]
9. Aranbarri, J.; González-Sampériz, P.; Valero-Garcés, B.; Moreno, A.; Gil-Romera, G.; Sevilla-Callejo, M.; García-Prieto, E.; Di Rita, F.; Mata, M.P.; Morellón, M.; et al. Rapid climatic changes and resilient vegetation during the Lateglacial and Holocene in a continental region of South-Western Europe. *Glob. Planet. Chang.* **2014**, *114*, 50–65. [CrossRef]
10. González-Sampériz, P.; Leroy, S.A.G.; Carrión, J.S.; Fernández, S.; García-Antón, M.; Gil-García, M.J.; Uzquiano, P.; Valero-Garcés, B.; Figueiral, I. Steppes, savannahs, forests and phytodiversity reservoirs during the Pleistocene in the Iberian Peninsula. *Rev. Palaeobot. Palynol.* **2010**, *162*, 427–457. [CrossRef]
11. González-Sampériz, P.; Gil-Romera, G.; García-Prieto, E.; Aranbarri, J.; Moreno, A.; Morellón, M.; Sevilla-Callejo, M.; Leunda, M.; Santos, L.; Franco-Múgica, F.; et al. Strong continentality and effective moisture drove unforeseen vegetation dynamics since the Last Interglacial at inland Mediterranean areas: The Villarquemado sequence in NE Iberia. *Quat. Sci. Rev.* **2020**, *242*, 106425. [CrossRef]
12. Manzano, S.; Carrión, J.S.; López-Merino, L.; Ochando, J.; Munuera, M.; Fernández, S.; González-Sampériz, P. Early to Mid-Holocene spatiotemporal vegetation changes and tsunami impact in a paradigmatic coastal transitional system (Doñana National Park, Southwestern Europe). *Glob. Planet. Chang.* **2018**, *161*, 66–81. [CrossRef]
13. Bell, B.A.; Fletcher, W.J. Modern Surface Pollen assemblages from the Middle and High Atlas, Morocco: Insights into pollen representation and transport. *Grana* **2016**, *55*, 286–301. [CrossRef]
14. Cheddadi, R.; Henrot, A.-J.; François, L.; Boyer, F.; Bush, M.; Carré, M.; Coissac, E.; De Oliveira, P.E.; Ficetola, F.; Hambuckers, A.; et al. Microrefugia, climate change, and conservation of *Cedrus atlantica* in the Rif Mountains, Morocco. *Front. Ecol. Evol.* **2017**, *5*, 114. [CrossRef]
15. Alba-Sánchez, F.; Abel-Schaad, D.; López-Sáez, J.A.; Sabariego Ruiz, S.; Pérez-Díaz, S.; González-Hernández, A. Paleobiogeografía de *Abies* spp. y *Cedrus atlantica* en el Mediterráneo Occidental (Península Ibérica y Marruecos). *Rev. Ecosist.* **2018**, *27*, 26–37. [CrossRef]
16. Alba-Sánchez, F.; Abel-Schaad, D.; López-Sáez, J.A.; Sabariego-Ruiz, S.; Pérez-Díaz, S.; Luelmo-Lautenschlaeger, R.; Garrido-García, J.A. Early anthropogenic change in Western Mediterranean mountains (Sierra Nevada, SE Spain). *Anthropocene* **2021**, *33*, 100278. [CrossRef]

17. Cheddadi, R.; Fady, B.; François, L.; Hajar, L.; Suc, J.-P.; Huang, K.; Demarteau, M.; Vendramin, G.G.; Ortu, E. Putative glacial refugia of *Cedrus atlantica* deduced from Quaternary pollen records and modern genetic diversity. *J. Biogeogr.* **2009**, *36*, 1361–1371. [CrossRef]
18. Linares, J.C.; Tíscar, P.A.; Camarero, J.J.; Taïqui, L.; Viñegla, B.; Seco, J.I.; Merino, J.; Carreira, J.A. Tree growth decline on relict Western-Mediterranean mountain forest: Causes and impacts. In *Forest Decline: Causes and Impacts*; Environmental Science, Engineering and Technology; Jenkins, J.A., Ed.; Nova Science Publishers: Hauppauge, NY, USA, 2011; pp. 91–110. ISBN 978-1-61470-002-9.
19. Carrión, J.S.; Sánchez-Gómez, P.; Mota, J.F.; Yll, R.; Chaín, C. Holocene vegetation dynamics, fire and grazing in the Sierra de Gádor, Southern Spain. *Holocene* **2003**, *13*, 839–849. [CrossRef]
20. Carrión, J.S.; Fuentes, N.; González-Sampériz, P.; Sánchez Quirante, L.; Finlayson, J.C.; Fernández, S.; Andrade, A. Holocene environmental change in a montane region of Southern Europe with a long history of human settlement. *Quat. Sci. Rev.* **2007**, *26*, 1455–1475. [CrossRef]
21. Campbell, J.F.E.; Fletcher, W.J.; Joannin, S.; Hughes, P.D.; Rhanem, M.; Zielhofer, C. Environmental drivers of Holocene forest development in the Middle Atlas, Morocco. *Front. Ecol. Evol.* **2017**, *5*, 113. [CrossRef]
22. Carrión, J.S. *Paleoflora y Paleovegetación de la Península Ibérica e Islas Baleares*; Universidad de Murcia, Secretariado PU: Murcia, Spain, 2012; ISBN 978-84-615-9026-1.
23. Muller, S.D.; Rhazi, L.; Andrieux, B.; Bottollier-Curtet, M.; Fauquette, S.; Saber, E.-R.; Rifai, N.; Daoud-Bouattour, A. Vegetation History of the Western Rif Mountains (NW Morocco): Origin, Late-Holocene Dynamics and Human Impact. *Veg. Hist. Archaeobotany* **2015**, *24*, 487–501. [CrossRef]
24. Reille, M. Analyse pollinique de sédiments postglaciaires dans le Moyen Atlas et le Haut Atlas Marocains: Premiers résultats. *Ecol. Mediterr.* **1976**, *2*, 153–170. [CrossRef]
25. Reille, M. Contribution pollenanalytique à l'histoire holocène de la végétation des montagnes du Rif (Maroc septentrional). *Suppl. Bull. AFEQ* **1977**, *50*, 53–76.
26. Stambouli-Essassi, S.; Roche, E.; Bouzid, S. Evolution de la végétation et du climat dans le Nord-ouest de la Tunisie au cours des 40 derniers millénaires. *Geo-EcoTrop* **2007**, *31*, 171–214.
27. Blois, J.L.; Gotelli, N.J.; Behrensmeyer, A.K.; Faith, J.T.; Lyons, S.K.; Williams, J.W.; Amatangelo, K.L.; Bercovici, A.; Du, A.; Eronen, J.T.; et al. A Framework for evaluating the influence of climate, dispersal limitation, and biotic interactions using fossil pollen associations across the Late Quaternary. *Ecography* **2014**, *37*, 1095–1108. [CrossRef]
28. D'Amen, M.; Mod, H.K.; Gotelli, N.J.; Guisan, A. Disentangling Biotic interactions, environmental filters, and dispersal limitation as drivers of species co-occurrence. *Ecography* **2018**, *41*, 1233–1244. [CrossRef]
29. Broennimann, O.; Fitzpatrick, M.C.; Pearman, P.B.; Petitpierre, B.; Pellissier, L.; Yoccoz, N.G.; Thuiller, W.; Fortin, M.-J.; Randin, C.; Zimmermann, N.E.; et al. Measuring ecological niche overlap from occurrence and spatial environmental data. *Glob. Ecol. Biogeogr.* **2012**, *21*, 481–497. [CrossRef]
30. Warren, D.L.; Glor, R.E.; Turelli, M. Environmental niche equivalency versus conservatism: Quantitative approaches to niche evolution. *Evolution* **2008**, *62*, 2868–2883. [CrossRef] [PubMed]
31. Benito Garzón, M.; Sánchez de Dios, R.; Sáinz Ollero, H. Predictive modelling of tree species distributions on the Iberian Peninsula during the Last Glacial Maximum and Mid-Holocene. *Ecography* **2007**, *30*, 120–134. [CrossRef]
32. López-Tirado, J.; Hidalgo, P.J. A high resolution predictive model for relict trees in the Mediterranean-mountain forests (*Pinus sylvestris* L., *P. nigra* Arnold and *Abies pinsapo* Boiss.) from the South of Spain: A Reliable management tool for reforestation. *For. Ecol. Manag.* **2014**, *330*, 105–114. [CrossRef]
33. Navarro-Cerrillo, R.M.; Manzanedo, R.D.; Rodriguez-Vallejo, C.; Gazol, A.; Palacios-Rodríguez, G.; Camarero, J.J. Competition modulates the response of growth to climate in pure and mixed *Abies pinsapo* subsp. *maroccana* forests in Northern Morocco. *For. Ecol. Manag.* **2020**, *459*, 117847. [CrossRef]
34. Valladares, A. Abetales de *Abies pinsapo* Boiss. In *Bases Ecológicas Preliminares para la Conservación de los Tipos de Hábitat de Interés Comunitario en España*; Ministerio Medio Ambiente y Medio Rural y Marino: Madrid, Spain, 2009; Volume 9520, ISBN 978-84-491-0911-9.
35. Alba-Sánchez, F.; López-Sáez, J.A.; Benito de Pando, B.M.; Linares, J.C.; Nieto-Lugilde, D.; López-Merino, L. Past and present potential distribution of the Iberian *Abies* species: A phytogeographic approach using fossil pollen data and species distribution models. *Divers. Distrib.* **2010**, *16*, 214–228. [CrossRef]
36. Blois, J.L. Recent advances in using species distributional models to understand past distributions. *Front. Biogeogr.* **2012**, *3*, 123–124. [CrossRef]
37. Brewer, S.; Jackson, S.T.; Williams, J.W. Paleoecoinformatics: Applying geohistorical data to ecological questions. *Trends Ecol. Evol.* **2012**, *27*, 104–112. [CrossRef]
38. Svenning, J.-C.; Fløjgaard, C.; Marske, K.A.; Nógues-Bravo, D.; Normand, S. Applications of species distribution modeling to paleobiology. *Quat. Sci. Rev.* **2011**, *30*, 2930–2947. [CrossRef]
39. Varela, S.; Lobo, J.M.; Hortal, J. Using species distribution models in paleobiogeography: A matter of data, predictors and concepts. *Palaeogeogr. Palaeoclimatol. Palaeoecol.* **2011**, *310*, 451–463. [CrossRef]

40. Bouahmed, A.; Vessella, F.; Schirone, B.; Krouchi, F.; Derridj, A. Modeling *Cedrus atlantica* potential distribution in North Africa across time: New putative glacial refugia and future range shifts under climate change. *Reg. Environ. Chang.* **2019**, *19*, 1667–1682. [CrossRef]
41. Demarteau, M.; Francois, L.; Cheddadi, R.; Roche, E. Réponses de *Cedrus atlantica* aux changements climatiques passés et futurs. *Geo-Eco-Trop* **2007**, *31*, 105–146.
42. Benito Garzón, M.; Sánchez de Dios, R.; Sáinz Ollero, H. The evolution of the *Pinus sylvestris* L. area in the Iberian Peninsula from the Last Glacial Maximum to 2100 under climate change. *Holocene* **2008**, *18*, 705–714. [CrossRef]
43. Di Pasquale, G.; Saracino, A.; Bosso, L.; Russo, D.; Moroni, A.; Bonanomi, G.; Allevato, E. Coastal pine-oak glacial refugia in the Mediterranean Basin: A biogeographic approach based on charcoal analysis and spatial modelling. *Forests* **2020**, *11*, 673. [CrossRef]
44. Terrab, A.; Hampe, A.; Lepais, O.; Talavera, S.; Vela, E.; Stuessy, T.F. Phylogeography of North African Atlas cedar (*Cedrus atlantica*, Pinaceae): Combined molecular and fossil data reveal a complex Quaternary history. *Am. J. Bot.* **2008**, *95*, 1262–1269. [CrossRef] [PubMed]
45. Thomas, P. *Cedrus atlantica*. The IUCN Red List of Threatened Species. e.T42303A2970716. 2013. Available online: https://www.iucnredlist.org/species/42303/2970716 (accessed on 27 November 2014).
46. Farjon, A. *Pinus nigra*. The IUCN Red List of Threatened Species. e.T42386A2976817. 2013. Available online: https://www.iucnredlist.org/species/42386/2976817 (accessed on 13 January 2020).
47. Phillips, S.J.; Dudık, M.; Shapire, R. Maxent Software for Species Habitat Modeling. 2013. Available online: http://biodiversityinformatics.amnh.org/open_source/maxent/ (accessed on 25 January 2013).
48. Hijmans, R.J.; Phillips, S.J.; Leathwick, J.; Elith, J. Package 'Dismo'. Species Distribution Modeling. R Package Version 0.7-17. 2014. Available online: https://rspatial.org/raster/sdm/ (accessed on 10 September 2014).
49. Phillips, S.J. A Brief Tutorial on Maxent 2017. Available online: https://pdf4pro.com/view/a-brief-tutorial-on-maxent-american-museum-of-natural-5a321d.html (accessed on 2 April 2021).
50. Hijmans, R.J.; Cameron, S.E.; Parra, J.L.; Jones, P.G.; Jarvis, A. Very high resolution interpolated climate surfaces for global land areas. *Int. J. Climatol.* **2005**, *25*, 1965–1978. [CrossRef]
51. EPD European Pollen Database. Available online: http://www.europeanpollendatabase.net/data/ (accessed on 26 April 2012).
52. Booth, T.H.; Nix, H.A.; Busby, J.R.; Hutchinson, M.F. Bioclim: The first species distribution modelling package, its early applications and relevance to most current MaxEnt studies. *Divers. Distrib.* **2014**, *20*, 1–9. [CrossRef]
53. Elith, J.; Phillips, S.J.; Hastie, T.; Dudík, M.; Chee, Y.E.; Yates, C.J. A statistical explanation of MaxEnt for ecologists. *Divers. Distrib.* **2011**, *17*, 43–57. [CrossRef]
54. Merow, C.; Smith, M.J.; Silander, J.A. A practical guide to MaxEnt for modeling species' distributions: What it does, and why inputs and settings matter. *Ecography* **2013**, *36*, 1058–1069. [CrossRef]
55. Rodríguez-Sánchez, F.; Hampe, A.; Jordano, P.; Arroyo, J. Past tree range dynamics in the Iberian Peninsula inferred through phylogeography and palaeodistribution modelling: A review. *Rev. Palaeobot. Palynol.* **2010**, *162*, 507–521. [CrossRef]
56. Raes, N.; ter Steege, H. A null-model for significance testing of presence-only species distribution models. *Ecography* **2007**, *30*, 727–736. [CrossRef]
57. Di Cola, V.; Broennimann, O.; Petitpierre, B.; Breiner, F.T.; D'Amen, M.; Randin, C.; Engler, R.; Pottier, J.; Pio, D.; Dubuis, A.; et al. Ecospat: An R package to support spatial analyses and modeling of species niches and distributions. *Ecography* **2017**, *40*, 774–787. [CrossRef]
58. Camuera, J.; Jiménez-Moreno, G.; Ramos-Román, M.J.; García-Alix, A.; Toney, J.L.; Anderson, R.S.; Jiménez-Espejo, F.; Bright, J.; Webster, C.; Yanes, Y.; et al. Vegetation and climate changes during the last two glacial-interglacial cycles in the Western Mediterranean: A new long pollen record from Padul (Southern Iberian Peninsula). *Quat. Sci. Rev.* **2019**, *205*, 86–105. [CrossRef]
59. Pons, A.; Reille, M. The Holocene- and Upper Pleistocene pollen record from Padul (Granada, Spain): A new study. *Palaeogeogr. Palaeoclimatol. Palaeoecol.* **1988**, *66*, 243–263. [CrossRef]

diversity

MDPI

Article

Small Mammal Diversity in Response to Land Transformation and Seasonal Variation in South Africa

Mmatsawela Ramahlo [1,2,*], Michael John Somers [1,2], Daniel William Hart [1] and Andre Ganswindt [1]

[1] Mammal Research Institute, Department of Zoology and Entomology, University of Pretoria, Private Bag X20, Hatfield 0028, South Africa; michael.somers@up.ac.za (M.J.S.); daniel.hart@up.ac.za (D.W.H.); andre.ganswindt@up.ac.za (A.G.)
[2] Centre for Invasion Biology, Department of Zoology and Entomology, University of Pretoria, Hatfield 0002, South Africa
* Correspondence: jawi.ramahlo@up.ac.za

Abstract: Anthropogenic land transformation is a consequence of human population growth and the associated agricultural, residential, and industrial needs. This study aimed to investigate the effects of anthropogenic activity and human-mediated land transformation on capture/recapture frequencies, species richness, and diversity of native small mammal community assemblages in the Magaliesberg Biosphere, North West province, South Africa. Five anthropogenically transformed land-use types were investigated: an animal rehabilitation and ecotourism center, an agricultural farmstead, a residential farmstead, a mine-adjacent agricultural farmstead, and a protected nature conservancy. We used live traps to sample small mammals during the dry and wet seasons over three consecutive years and compared population numbers and species composition across study sites and seasons. Capture/recapture frequencies differed significantly between sites and seasons, with the highest capture frequencies recorded at the agricultural and residential farmsteads. Species richness and diversity were highest at the residential and mine-adjacent farmsteads, both of which experienced intermediate levels of anthropogenic disturbance throughout the sampling period. The study shows that while natural and protected landscapes with low levels of disturbance are preferred, transformed landscapes can also be managed effectively to benefit native small mammal populations by regulating the frequency and intensity of human-mediated activities.

Keywords: abundance; agriculture; anthropogenic activity; community assemblage; industrial activities; intermediate disturbance; rodents; species richness

Citation: Ramahlo, M.; Somers, M.J.; Hart, D.W.; Ganswindt, A. Small Mammal Diversity in Response to Land Transformation and Seasonal Variation in South Africa. *Diversity* **2022**, *14*, 138. https://doi.org/10.3390/d14020138

Academic Editor: Michael Wink

Received: 29 December 2021
Accepted: 9 February 2022
Published: 16 February 2022

1. Introduction

Due to the rapidly increasing human population and the far-reaching impacts of anthropogenic activities such as agriculture, industrialization and urbanization, fewer ecosystems remain untransformed and undisturbed [1–3]). Monitoring threats to biodiversity that stem from anthropogenic activities is vital in mitigating and managing their effects [4–6]. Ecosystem health is often monitored using several environmental variables, and any one of these variables can be a proxy for health. In the past, similarities in terms of species richness, distribution, and community assemblage in small mammals were investigated across transformed and untransformed landscapes to assess ecosystem health [1,4]. Whereas some studies focus on the impact of one variable at a time, an integrated investigation of several variables can give a more insightful view of the state of both biotic and abiotic components within the system [7,8]. The investigation of the presence of land-use-based species can inform on the impact of various alterations to landscapes and which human activities are most impactful to the ecosystem and resident species [9,10].

Diversity refers to the range and abundance of species in an area and is also a reliable indicator of ecosystem health [7,11,12]. Along with the presence and number of species, it is essential to record the diversity of a region over time, as this further demonstrates how

impactful anthropogenic activities are on natural environments [1,4]. Reduced community evenness can indicate species and diversity declines, resulting in the homogenization of formerly diverse landscapes and the extinction of local species [11,13]. The presence of invasive species in a landscape can also indicate land disturbance, displacement of indigenous species, and most likely declines in biodiversity [8,14].

It is essential to research species prone to population fluctuations in response to landscape changes, as these species are the most vulnerable to environmental and anthropogenic threats [15,16]. To improve the identification of vulnerable species, the IUCN [5] has identified several relevant biological traits that make species more at risk. These include the use of specialized habitats or microhabitats, a narrow environmental tolerance, dependence on environmental cues, a dependence on relationships and interactions with other species, and a poor ability to disperse from low-quality habitats and establish in landscapes with more favorable conditions.

Similarly, it is also important to investigate those taxonomic groups that occur on the other end of the spectrum and do not generally operate within the ecological constraints of at-risk species [17]. However, it can be assumed that environmental changes that affect these tolerant taxonomic groups may have devastating consequences for at-risk species that are dependent on specific ecological and climatic cues [17–19]. Small mammals, such as rodents, are a reliable model for shorter-lived species that can be easily studied, as they have relatively short generation times that can be observed over a human lifetime [20,21]. The use of these adaptive and resilient species in research allows us to investigate the likelihood of wildlife populations and ecosystems recovering from human-induced disturbances. It can also help to improve the management strategies of threatened species in disturbed landscapes.

Most rodents are not on the IUCN Red Data List of Threatened Species and are classified as 'least concern', with only a handful being assessed as threatened or endangered [22]. When assessed using the IUCN-identified biological traits, they are shown to be capable of either adapting to most environmental changes or finding more favorable conditions [23,24]. Although rodents can use microhabitats, they are not restricted by their macrohabitat and can thus persist in a wide range of landscapes [25]. Successful establishment of rodents in a landscape does not require interspecific interactions with other taxonomic groups. They, themselves, are ecosystem drivers who cycle nutrients through the soil, disperse seeds to aid in plant growth, and provide food for predators [23,26]. With increased human expansion and subsequently transformed landscapes, favorable conditions prove more challenging to maintain [27,28]. In addition to an increase in land transformations due to more significant anthropogenic needs, climate change may exaggerate disruptions to ecosystem health, and thus, seasonal variation should be included in diversity-based research [7,29]. Due to the resilient characteristics displayed by rodents, it is essential to monitor them in both natural and transformed landscapes to gauge the critical limit of their tolerance for environmental changes brought about by climate change and anthropogenic activities.

Additionally, due to the heavy reliance of small mammals on resources and shelter in their environments, it is important to monitor any external factors that may influence these environments. Seasonal variation is one such variable, as it can have immediate and delayed effects on natural landscapes. In terms of immediate effects, wet season climatic conditions may lead to physical alterations in the landscapes, such as softer soil substrates, whereas dry season climates can harden said substrates [27]. Many habitats found in southern Africa can be adversely affected by climatic conditions but can also be renewed by wet season rains and produce vegetation that small mammals use for cover and food [28]. Conversely, the dry season may mean that food and cover are limited, often leading to inter- and intraspecific competitive interactions for these resources [18,19]. This study aimed to investigate the effects of land transformation and seasonal variation on small mammal biodiversity in the Magaliesberg Biosphere of South Africa by examining the impacts of season and land transformation on (a) capture frequency; (b) species richness; and (c) community diversity, evenness, and similarity. We predicted that an increase in landscape disturbance would

be inversely proportional to population health and community diversity. Furthermore, we anticipated that seasonal variation would reduce community diversity during the dry season and increase population abundance in the wet season.

2. Materials and Methods

2.1. Study Area

The Magaliesberg mountain range (25°41′00.1″ S 27°57′51.8″ E) expands through the Gauteng and North West provinces, South Africa. The mountain range spans a length of approximately 140 km, with a maximum elevation of 1852 m.a.s.l. The Magaliesberg is primarily characterized by the Savanna Biome, which covers the Gold Reef Mountain Bushveld vegetation type at higher altitudes and Marikana Thornveld and Moot Plains Bushveld in lower-lying areas [30]. The vegetation in these bioregions is woody and consists of a predominantly grassy herbaceous layer. Thorny *Vachellia* species and semi-open thickets dominate the region. The region comprises igneous rocks from the Rustenberg Layered Suite and the Rooiberg Group [30].

Trapping localities were in the De Wildt (25°40′05.5″ S 27°55′23.1″ E) and Zilkaatsnek (25°39′25.8″ S 27°56′34.9″ E) areas, with land-use types such as agriculture, residential, tourism, conservation, and mining (Figure 1). We named the sites as follows: the animal breeding, rehabilitation, and ecotourism center (ABR); the agricultural and residential farmstead (ARF); the residential farmstead (RFS); the industrial and agricultural farmstead (IAR); and the nature conservancy and residential site (NCR). The climate is characterized by hot, wet summers and cold, dry winters, with April until October referred to as the dry season and November to March typically referred to as the wet season [31]. However, the start and patterns of annual rainfall are unpredictable each year. We used five closely located study sites (the maximum distance between sites is 15 km) to discount climatic variability and determine whether the size of study sites and their proximity to each other allows for species turnover (Table 1). All five sites shared similar natural vegetation structures [30], apart from additional cultivation of commercial vegetation in some areas (Table 1). The savanna vegetation composition differs across land-use types, with the level of clearing increasing with an increase in anthropogenic activity. This means that land-use types in the same region with similar vegetation differ in plant species assemblages due to human-mediated land development, clearing, and burning, among other factors. Study sites with infrequent human activity therefore experience less vegetation clearing, resulting in high richness of plant species, with a few examples of cleared areas being roads and footpaths for occasional tourists. Despite the differences in composition, however, the effects of seasonal variation influence the different study sites in similar ways. In the dry season, the area experiences low rainfall conditions, which leaves habitats dry with little green vegetation for animals to use. The soil is dry and compacted, making burrowing more arduous for some species [30]. Due to the dry climate and grass, locals around the area practice controlled burning and slashing techniques to ensure that the areas do not experience uncontrollable and dangerous veld fires. This alters the landscape and may influence natural vegetation and wildlife in various ways. In the wet season, rainfall experienced in the region results in green vegetation and softer soil, which makes burrowing easier for small mammals [31,32]. Additionally, the increase in vegetation can result in increased grazing activity by livestock in the surrounding areas [32].

2.2. Data Collection

For this study, we sampled five study sites during four consecutive seasons (two dry and two wet seasons) for 16,000 trap nights between 2018 and 2021. At each site, we deployed 40 Enviro-Care live traps (imported from Cangzhou Jinglong Technology Co., Ltd., Hebei Province, China), for a total of 3200 trap nights per site. The traps were made of galvanized sheet metal and had the following dimensions (length × height × width): 255 × 78 × 80 mm. We baited each trap with a mixture of oats and peanut butter and placed them 10 m apart in a 5 × 8 trapping grid, following standard procedures [33]. All traps

remained open during the day and night to ensure diurnal and nocturnal species trapping. We checked all traps in the morning from 05:30 until 10:00 and again from 15:00 until 17:00 every day. All captured animals were identified and sexed where possible [23,24,34]. We weighed individuals using a spring scale (PESOLA Präzisionswaagen AG, Schindellegi, Switzerland) and marked them using numbered clipping of toenails to identify recaptured individuals [33]. As many small mammals contain blood vessels in their toenails, which may become damaged if clipped, we treated toenail-clipped individuals with antiseptic Mercurochrome (Barrs Pharmaceutical Industries, Cape Town, South Africa) to prevent infection and ensure that the nails would heal with minimal contamination [35]. Toenail clipping had a dual function of marking individuals and providing keratinized materials to be analyzed in a separate diet-related study. Additionally, we collected <1 mm ear clips by clipping the upper right ear using sterilized dissecting scissors. These ear clips were used as genetic material for resolving individuals from cryptic genera, namely *Aethomys* and *Mastomys*, into their respective species [33]. After processing, we released individuals at their respective capture sites [32,36]. We emptied the traps of all contents, rebaited, and returned them to their original positions in the trapping grid [33]. This study was performed with the approval of the Animal Ethics Committee of the University of Pretoria, Pretoria, South Africa (Ethics clearance number EC044-18).

Figure 1. Orientation map of the North West province showing the locations of the five study sites where rodents were captured between 2018 and 2021 in South Africa.

Table 1. Study-area information on the locations and land-use types from which small mammals were sampled in the Magaliesberg Biosphere, North West province, South Africa. The five land-use types were designated as follows: animal breeding and rehabilitation center (ABR); agricultural and residential farmstead (ARF); residential farmstead (RFS); industrial, agricultural, and residential (IAR); and nature conservancy and residential (NCR).

Study Site	Land Use	Abbreviation	GPS Location	Primary Vegetation	Topography
1	Animal breeding and rehabilitation Ecotourism	ABR	25°40′25.2″ S 27°55′17.4″ E	Thorny, semi-open thickets	Rocky, slight incline near the base of the mountain
2	Agricultural Residential	ARF	25°39′31.3″ S 27°55′08.0″ E	Grassy herbaceous layer	Flat at the base of the mountain
3	Residential	RFS	25°39′20.3″ S 27°55′15.7″ E	Herbaceous and semi-open thickets	Flat at the base of the mountain
4	Industrial Agricultural Residential	IAR	25°38′43.3″ S 27°55′48.8″ E	Herbaceous and semi-open thickets	Flat at the base of the mountain
5	Conservation Residential	NCR	25°40′39.6″ S 27°57′48.9″ E	Herbaceous and semi-open thickets	Rocky, steep incline along the mountain

2.3. Statistical Analysis

All statistical analyses were done with the software program R 4.1.0 (R Core Team 2021) using the RStudio interface (Version 1.4.1103). For the current study, we only included the first capture of an individual. However, a figure with a summary of capture and recapture numbers is provided in the Results section.Sequence analyses, details on DNA extraction and nucleotide sequencing of the genetic material are included in the Supplementary Materials [37]. Sequence chromatographs were visualized and edited in the Chromas program embedded in MEGA 7 and used to generate contiguous sequences (contigs) [38]. The final aligned database for the cryptic species was used to infer a maximum-likelihood (ML) phylogenetic tree in MEGA 7 [38]. Details on the generation of the database are included in the Supplementary Materials document. The best-of-fit model of sequence evolution was determined under the Bayesian information criteria (BIC), and the Akaike information criteria (AIC) in MEGA 7 were used for the ML analysis, with the nodal support being assessed through 5000 bootstrap replications [38].

Cryptic *Aethomys* species were identified as *A. ineptus*, whereas *Mastomys* species were identified as *M. coucha*. These resolved species were specified in the dataset and included in further analysis. Furthermore, all sequences were deposited in GenBank (*A. ineptus*: OM055762, OM055763, OM055764, OM055772, OM055773, OM055774, OM055775, OM055776, OM055777, OM055778; and *M. coucha*: OM055765, OM055766, OM055767, OM055768, OM055769, OM055770, OM055771). The accession numbers represent unique haplotypes identified in the study and include geographical information. The maximum-likelihood tree is included in the Supplementary Materials file. We investigated nestedness and trap dependency in RStudio using the beta.multi function in the *betapart* package, which computes multiple-site dissimilarities and accounts for the nestedness components of beta diversity [39,40]. The function uses beta diversity to measure site dissimilarity resulting from nestedness patterns in the community [40]. In the event of high nestedness between sites, a linear model was employed to account for inter- and intraspecific trap dependency at spatial and temporal scales:

$$\text{Abundance} \sim \text{Season} + \text{Land Use} + \text{Species} + \text{Trapline}$$

where Abundance is the total number of newly captured individuals within a land-use type, Season refers to the dry and wet sampling periods, Land Use denotes the five sites sampled,

and Trapline refers to the numbered trap in the trapping grid where each individual was captured. A *p*-value of $\leq$0.05 was defined as significant.

To compare species richness (alpha diversity), we used descriptive statistics, namely the total number of species captured at each site. To compare diversity across sites, we used the *vegan* package to calculate Shannon and Simpson's diversity indices, as well as Pielou's evenness index [41]. Additionally, we used the *betadisper* analytical function in the package to test for homogeneity of groups (or similarity) by calculating Bray–Curtis distances between land-use types [41,42].

3. Results

Both season (dry season, n = 693; wet season, n = 824; $p < 0.001$; df = 2) and land-use type ($p < 0.0001$; df = 4) resulted in significantly distinct abundance across study sites (Figure 2). Seasonal abundance fluctuated most at the agricultural farmstead (ARF) and the animal breeding and rehabilitation center (ABR) and least at the residential farmstead (RFS) and industrial and agricultural farmstead (IAR). Small mammal captures were low during the dry season at the transformed sites (ABR and ARF), increasing with a decrease in human-intensive land disturbance. Wet season captures showed an inverse trend, except for RFS, which showed consistent capture numbers overall. During the dry season, 66.7% of all encountered individuals were recaptured animals, while the recapture rate during the wet season was 42.6%.

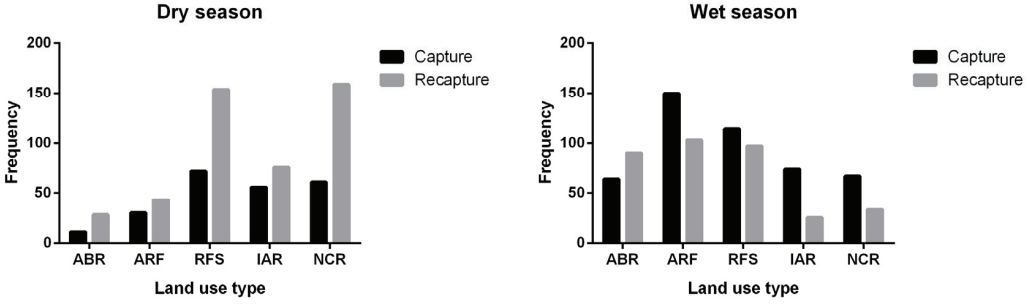

Figure 2. Seasonal capture and recapture numbers for small mammals for a three-year sampling period (2018, 2019, and 2020) across five land-use types: animal breeding and rehabilitation center (ABR); agricultural and residential farmstead (ARF); residential farmstead (RFS); industrial, agricultural, and residential (IAR); and nature conservancy and residential (NCR).

Trap dependency, however, did not have a significant effect on capture and recapture numbers (n = 1516; df = 41; $p = 0.201$) Species nestedness accounted for a large proportion of the beta diversity in the region ($\beta_{NES} = 0.93$).

All captured species were indigenous to southern Africa. Species richness did not differ significantly across seasons ($p = 0.137$; df = 1) or sites ($p = 0.799$; df = 4) (Table 2). Shannon's and Simpson's diversity indices, as well as Pielou's evenness index, were not significantly different between seasons or sites. (Table 2). Beta diversity, represented by Bray–Curtis dissimilarity, varied seasonally and across sites (Table 3). Mean dissimilarity was calculated as 0.37 during the dry season and 0.36 during the wet season.

Table 2. Dry and wet season counts of small mammal species and community structure indices across five land-use types in the Magaliesberg Biosphere, North West province, South Africa. Land-use types were designated as follows: animal breeding and rehabilitation center (ABR); agricultural and residential farmstead (ARF); residential farmstead (RFS); industrial, agricultural, and residential (IAR); and nature conservancy and residential (NCR). * Denotes statistically significant differences between sites.

Species Name	ABR		ARF		RFS		IAR		NCR	
	Dry	Wet	Dry	Wet	Dry	Wet	Dry	Wet	Dry	Wet
Macroscelidea										
Elephantulus brachyrhynchus/myurus [Elephant shrew]	0	0	0	0	0	0	0	0	1	0
Rodentia										
Aethomys ineptus [Tete veld rat]	3	21	0	0	0	0	0	3	10	17
Dendromus mystacalis [Climbing mouse]	0	0	0	0	0	0	0	0	1	0
Gerbilliscus brantsii/leucogaster [Bushveld/Highveld gerbil]	0	0	0	0	0	0	20	2	0	2
Lemniscomys rosalia [Single-striped mouse]	1	8	3	7	15	14	11	10	9	0
Mastomys coucha [Multimammate mouse]	4	19	20	120	45	70	12	29	14	2
Micaelamys namaquensis [Namaqua rock mouse]	2	16	0	18	0	12	0	21	23	46
Mus minutoides [Pygmy mouse]	2	0	6	1	10	0	8	1	2	0
Otomys irroratus [Vlei rat]	0	0	0	0	2	3	0	2	3	0
Rhabdomys pumilio [Three-striped mouse]	0	0	0	0	0	0	2	0	0	0
Saccostomus campestris [Pouched mouse]	0	0	0	3	0	1	2	6	0	0
Steatomys pratensis [Fat mouse]	0	0	0	1	0	15	2	2	0	0
Captures (*N*) *	12	64	29	150	72	115	57	76	63	67
Species richness	5	4	3	6	4	6	7	9	8	4
Shannon diversity index (*H*) *	1.52	1.33	0.82	0.72	0.99	1.20	1.64	1.66	1.66	0.82
Simpson diversity index (*D*)	0.78	0.73	0.47	0.34	0.55	0.59	0.82	0.75	0.76	0.46
Pielou's evenness index (*J*)	0.94	0.96	0.74	0.40	0.71	0.67	0.84	0.76	0.80	0.59

Table 3. Bray–Curtis dissimilarity indices between study sites during the dry and wet seasons across five land-use types in the Magaliesberg Biosphere, North West province, South Africa. Land-use types were designated as follows: animal breeding and rehabilitation center (ABR); agricultural and residential farmstead (ARF); residential farmstead (RFS); industrial, agricultural, and residential (IAR); and nature conservancy and residential (NCR).

	ABR		ARF		RFS		IAR	
	Dry	Wet	Dry	Wet	Dry	Wet	Dry	Wet
ARF	0.25	0.40	-	-	-	-	-	-
RFS	0.33	0.40	0.14	0.17	-	-	-	-
IAR	0.50	0.38	0.40	0.20	0.45	0.20	-	-
NCR	0.23	0.25	0.45	0.60	0.33	0.60	0.60	0.38

4. Discussion

This study demonstrates that seasonal and land-use-specific variation can influence the abundance of small mammal species to different extents in the Magaliesberg Biosphere, South Africa. Monitored minimally transformed landscapes such as the residential farmstead and the nature conservancy had the highest abundance during the dry season. Conversely, study sites that experienced moderate to high levels of anthropogenic activity, i.e., the animal breeding and rehabilitation center and the agricultural and residential farmstead, had fewer captures during the dry season. This could be due to the high fire risks associated with the region, specifically during the dry season, and the resulting management strategies to prevent or reduce fire damage [31]. Fire risk-management efforts appear to increase with an increase in land-use complexity and associated practices. Activities such as controlled burning, livestock grazing, and mechanical slashing directly impact small mammal populations [42,43]. Additionally, in many areas with a high human presence, humans actively try to reduce the number of small mammals and their pest-related activities in and around their households through live and snap trapping, and poison, as well as biological means, such as pets [44,45]. This may further reduce population numbers in transformed areas with a constant human presence. During the wet season, the abovementioned minimally transformed sites had lower capture numbers, as small mammals were no longer reliant on temporary food sources due to improved plant growth after the rains. Conversely, the more transformed sites had more frequent small mammal captures, possibly due to the resurgence and re-establishment of population numbers following the dry season. Additionally, the breeding season of many observed species coincides with the wet season, which could result in an overall increase in capture numbers [24,35,46]. Species ecology and behavior can also impact seasonal population numbers, as many southern African small mammals are seasonal breeders. For example, *M. namaquensis* reproductive behavior is mainly confined to rainy summer months, which correlates with an abundance of nutrient-rich food resources [47]. Similarly, *M. coucha* has been reported to breed primarily during the wet season, and this behavior has been linked to the growth of new grass shoots [48]. Grass shoot growth can also be seen after fire events, and this could explain the upsurge in *M. coucha* during the dry season months after vegetation-control methods are implemented.

In this study, overall species richness was not significantly different across study sites, although a downward trend was associated with increasing and frequent land-use intensification. These findings align with Flynn et al. [49] and Horváth et al. [50], who showed that intensification of agriculture resulted in reduced species richness. Further, species richness did not differ across seasons and sites, but the highest species richness values were recorded at the intermediately disturbed residential farmstead and mine-adjacent farmstead sites. This may be due to the management strategies employed, which involve alternating between rest and intensive tilling and planting activity [51,52]. Intermediately disturbed landscapes have been linked with increased species richness, as some species can persist and even thrive in these environments [53]. At IAR, species from the genus *Gerbilliscus* were captured almost exclusively, suggesting that this particular landscape and level of disturbance are optimal for their survival [54]. Conversely, *L. rosalia* was mainly found across agricultural landscapes, which correlates with several studies that have reported that the species is commonly found along the fringes of agricultural landscapes [55]. Ecological niche preferences often drive habitat selection, and this is seen with *A. ineptus*, a species that prefers rocky outcrops [24]. These outcrops are found primarily at two study sites (ABR and NCR) that are characterized by a rocky incline near the base of the Magaliesberg. Animal behavior can also drive habitat selection and population numbers, as seen in *E. myurus* and *O. irroratus*. The territorial behavior exhibited by these species may explain the low capture numbers observed in our study [24]. Dietary preference may also explain the disappearance of some species from landscapes, as some small mammal species show seasonal shifts in diet [56]. These shifts may result in a change in food selection or a shift in distributional range in search of favorable food resources [48]. Another potential

behavioral driver of species capture numbers can be adjustments in activity patterns, as some small mammals, such as *S. pratensis*, can reportedly go into torpor [57]. These and other drivers are often linked with seasonal variation.

However, the overall lack of significant variation in species richness across seasons and land-use types is consistent with the findings of Sánchez-Cordero [57]. Contrary to our findings, however, Umetsu and Pardini [1] found that species richness across land-use types varied, leading to strong variation in small mammal community assemblages.

As far as beta-diversity-related nestedness, the five land-use types sampled are similar, and a large portion of this similarity is due to nestedness. The disappearance of some species across land-use types and seasons may therefore be a cause for concern, as this may support the theory that specialist species are being excluded from increasingly transformed landscapes and warmer climates [9,17,43]. In our study, the results obtained for community assemblage diversity, evenness, and similarity highlight the importance of holistic approaches to biodiversity research [4]. At first, the results suggest that the animal rehabilitation and ecotourism site has the most diverse and ecologically ordered community assemblage. However, when incorporating the biodiversity variables mentioned above, it appears to be a skewed view. Due to its low sample size, the findings from this heavily transformed site cannot be resolved into an accurate ecological representation. Community diversity and evenness refer to sample size, and a smaller dataset can lead to a distorted output that is heavily biased [13]. By including different ecosystem health and biodiversity measures, such as diversity, richness, evenness, and composition, the actual state of community assemblages could be more accurately interpreted across all sites [4].

The nature conservancy site showed high diversity and evenness during the dry season, which declined during the wet season. This is contrary to the findings of Sánchez-Cordero [49], who demonstrated that small mammal diversity was higher during the wet season. The residential, as well as the industrial and agricultural farmsteads also showed high diversity. These sites were exposed to intermediate levels of activity throughout the year, as the intensity and frequency of farming and grazing at these sites were well managed. Our findings are consistent with those of Horváth et al. [50] and Sánchez-Cordero [58], who reported that small mammal diversity is associated with habitat complexity. They further show that intensively farmed agricultural landscapes reduce habitat heterogeneity and subsequent declines in diversity and balance in community assemblages, whereas heterogeneously managed sites show high diversity.

5. Conclusions

Our study found that seasonal and land-use variation influences small mammal community assemblages, resulting in fluctuations in population numbers, as well as temporal and spatial differences in species richness. As evidenced by our results, particularly those of the natural and intermediately disturbed landscapes, continuously healthy and diverse wildlife populations in a changing world may rely on an environment that experiences some level of periodic disturbance. Although relatively undisturbed landscapes are preferable, it is possible to manage transformed landscapes to safeguard the species richness and community diversity of the region [59]. Therefore, it is important to carefully manage and monitor the frequency and intensity of anthropogenic disturbance to ensure that native populations can re-establish and stabilize after a disturbance event and continue to do so sustainably for extended periods. Considering the ecology, behavior, and physiology of different species, we can implement careful land-use management strategies to reduce the homogenization of natural landscapes and potentially slow the loss of species in southern African environments that are undergoing anthropogenic transformation.

Supplementary Materials: The following supporting information can be downloaded at: https://www.mdpi.com/article/10.3390/d14020138/s1, Details of molecular methodology, Table S1: Summary information of reference sequences used in the construction of the maximum likelihood tree; Figure S1: Maximum likelihood tree.

Author Contributions: Conceptualization, M.R., D.W.H. and A.G.; data curation, M.R.; formal analysis, M.R.; funding acquisition, M.R., M.J.S. and A.G.; methodology, M.R. and D.W.H.; supervision, M.J.S. and A.G.; writing—original draft, M.R.; writing—review and editing, M.R., M.J.S., D.W.H. and A.G. All authors have read and agreed to the published version of the manuscript.

Funding: This research was funded by the DSI-NRF Centre of Excellence for Invasion Biology.

Institutional Review Board Statement: The study was conducted according to the guidelines and approval of the Animal Ethics Committee of the University of Pretoria, Pretoria, South Africa (Ethics clearance number EC044-18; 2018).

Data Availability Statement: The data presented in this study are available on request from the corresponding author or from the DSI-NRF Centre of Excellence for Invasion Biology.

Acknowledgments: We thank the landowners and staff members at our study sites: Ann Van Dyk Cheetah and Wildlife Centre and the Cheetah Lodge, Peglerae Conservancy, the Kemp, Louw, and Van Der Heever farms. Our thanks to E. von Maltitz, J. and J. Wesson, O. and S. Oosthuizen, and P. Viljoen for their logistical fieldwork support. Our thanks to the University of Pretoria (Department of Zoology and Entomology) Molecular Laboratory, A. D. Bastos, O. Seabi, and L. Retief for their invaluable support. We thank our fieldwork volunteers for logistical support during fieldwork.

Conflicts of Interest: The authors declare that they have no other conflict of interest.

References

1. Umetsu, F.; Pardini, R. Small mammals in a mosaic of forest remnants and anthropogenic habitats—evaluating matrix quality in an Atlantic forest landscape. *Landsc. Urban Plan.* **2007**, *22*, 517–530. [CrossRef]
2. Irwin, M.; Junge, R.; Raharison, J.; Samonds, K.E. Variation in physiological health of diademed sifakas across intact and fragmented forest at Tsinjoarivo, eastern Madagascar. *Am. J. Primatol.* **2010**, *72*, 1013–1025. [CrossRef] [PubMed]
3. Waters, C.N.; Zalasiewicz, J.; Summerhayes, C.; Barnosky, A.D.; Poirier, C.; Gauszka, A.; Cearreta, A.; Edgeworth, M.; Ellis, E.C.; Ellis, M.; et al. The Anthropocene is functionally and stratigraphically distinct from the Holocene. *Science* **2016**, *351*, 137–148. [CrossRef] [PubMed]
4. Christie, A.P.; Amano, T.; Martin, P.A.; Shackelford, G.E.; Simmons, B.I.; Sutherland, W.J. Simple study designs in ecology produce inaccurate estimates of biodiversity responses. *J. Appl. Ecol.* **2019**, *56*, 2742–2754. [CrossRef]
5. WWF. *Living Planet Report 2016. Risk and Resilience in a New Era*; WWF International: Gland, Switzerland, 2016.
6. Marris, E. Pre-emptive strike: Outwitting extinction. *Nat. Clim. Change* **2008**, *1*, 140–141. [CrossRef]
7. Cadotte, M.W.; Arnillas, C.A.; Livingstone, S.W.; Yasui, S.L.E. Faunal indicator taxa selection for monitoring ecosystem health. *Funct. Ecol.* **2016**, *92*, 185–197.
8. Wilson, J.R.U.; Faulkner, K.T.; Rahlao, S.J.; Richardson, D.M.; Zengeya, T.A.; van Wilgen, B.W. Indicators for monitoring biological invasions at a national level. *J. Appl. Ecol.* **2018**, *55*, 2612–2620. [CrossRef]
9. Heroldová, M.; Bryja, J.; Zejda, J.; Tkadlec, E. Structure and diversity of small mammal communities in agriculture landscape. *Agric. Ecosyst. Environ.* **2007**, *120*, 206–210. [CrossRef]
10. Foord, S.H.; Swanepoel, L.H.; Evans, S.W.; Schoeman, S.; Erasmus, B.F.N.; Schoeman, M.C.; Keith, M.; Smith, A.; Mauda, E.V.; Maree, N.; et al. Animal taxa contrast in their scale-dependent responses to land use change in rural Africa. *PLoS ONE* **2018**, *13*, e0194336. [CrossRef]
11. Monadjem, A.; Perrin, M. Population fluctuations and community structure of small mammals in a Swaziland grassland over a three-year period. *Afr. Zool.* **2003**, *38*, 127–137. [CrossRef]
12. Simelane, F.N.; Mahlaba, T.A.M.; Shapiro, J.T.; MacFadyen, D.; Monadjem, A. Habitat associations of small mammals in the foothills of the Drakensberg Mountains, South Africa. *Mammalia* **2017**, *82*, 144–152. [CrossRef]
13. Magurran, A.E. *Measuring Biological Diversity*; Blackwell Publishing: Victoria, Australia, 2004.
14. Ramahlo, M.; Chimimba, C.; Pirk, C.; Ganswindt, A. Non-invasive monitoring of adrenocortical activity in free-ranging Namaqua rock mice Micaelamys namaquensis from South Africa in response to anthropogenic land use and season. *Wildl. Biol.* **2019**, *2019*, 1–6. [CrossRef]
15. Cincotta, R.P.; Wisnewski, J.; Engelman, R. Human population in the biodiversity hotspots. *Nature* **2000**, *404*, 990–992. [CrossRef] [PubMed]
16. Scott, D.M.; Brown, D.; Mahood, S.; Denton, B.; Silburn, A.; Rakotondraparany, F. The impacts of forest clearance on lizard, small mammal and bird communities in the arid spiny forest, southern Madagascar. *Biol. Conserv.* **2006**, *127*, 72–87. [CrossRef]
17. Colles, A.; Liow, L.H.; Prinzing, A. Are specialists at risk under environmental change? Neoecological, paleoecological and phylogenetic approaches. *Ecol. Lett.* **2009**, *12*, 849–863. [CrossRef] [PubMed]
18. McKee, J.K.; Sciulli, P.W.; Fooce, C.D.; Waite, T.A. Forecasting global biodiversity threats associated with human population growth. *Biol. Conserv.* **2004**, *115*, 161–164. [CrossRef]

19. Watson, J.E.M.; Whittaker, R.J.; Dawson, T.P. Habitat structure and proximity to forest edge affect the abundance and distribution of forest-dependent birds in tropical coastal forests of southeastern Madagascar. *Biol. Conserv.* **2004**, *120*, 315–331. [CrossRef]
20. Galetti, M.; Giacomini, H.C.; Bueno, R.S.; Bernardo, C.S.S.; Marques, R.M.; Bovendorp, R.S.; Steffler, C.E.; Rubim, P.; Gobbo, S.K.; Donatti, C.I.; et al. Priority areas for the conservation of Atlantic forest large mammals. *Biol. Conserv.* **2009**, *142*, 1229–1241. [CrossRef]
21. Merritt, J.F. *The Biology of Small Mammals*; Johns Hopkins University Press: Baltimore, MD, USA, 2010.
22. IUCN. The IUCN Red List of Threatened Species. Version 2021-1. Available online: https://www.iucnredlist.org (accessed on 8 January 2021).
23. Mills, M.G.L.; Hes, L. *The Complete Book of Southern African Mammals*; Struik Publishers: Cape Town, South Africa, 1997.
24. Skinner, J.; Chimimba, C. *The Mammals of the Southern African Subregion*, 3rd ed.; Cambridge University Press: Cape Town, South Africa, 2005.
25. Skinner, J.; Smithers, R. *The Mammals of the Southern African Subregion*, 2nd ed.; University of Pretoria: Pretoria, South Africa, 1990.
26. Monadjem, A.; Taylor, P.J.; Denys, C.; Cotterill, F.P.D. *Rodents of Sub-Saharan Africa: A Biogeographic and Taxonomic Synthesis*; De Gruyter: Berlin, Germany, 2015.
27. Rymer, T.L.; Pillay, N.; Schradin, C. Extinction or survival? Behavioral flexibility in response to environmental change in the African striped mouse *Rhabdomys*. *Sustainability* **2013**, *5*, 163–186. [CrossRef]
28. Spear, D.; Foxcroft, L.C.; Bezuidenhout, H.; McGeoch, M.A. Human population density explains alien species richness in protected areas. *Biol. Conserv.* **2013**, *159*, 137–147. [CrossRef]
29. Ellis, E.C.; Kaplan, J.O.; Fuller, D.Q.; Vavrus, S.; Klein-Goldewijk, K.; Verburg, P.H. Used planet: A global history. *Proc. Natl. Acad. Sci. USA* **2013**, *110*, 7978–7985. [CrossRef]
30. Rutherford, M.C.; Mucina, L. Biomes and bioregions of southern Africa: The vegetation of South Africa, Lesotho and Swaziland. *Strelitzia* **2006**, *19*, 31–51.
31. Louw, J.; Business Connexions, De Wildt, North West Province, South Africa; Louw, E.; Business Connexions, De Wildt, North West Province, South Africa. Personal communication, 2020. Rainfall statistics for De Wildt, North West province.
32. Newbery, C.H. A key to the Soricidae, Macroscelididae, Gliridae and Muridae of Gauteng, North West province, Mpumalanga and the Northern province, South Africa. *Koedoe* **1999**, *42*, 51–55. [CrossRef]
33. Aplin, K.P.; Brown, P.R.; Jacob, J.; Krebs, C.J.; Singleton, G.R. *Field Methods for Rodent Studies in Asia and the Indo-Pacific. Australian Centre for International Agricultural Research Monograph*; CSIRO Publishing: Canberra, Australia, 2003.
34. Fleckman, P.; Jaeger, K.; Silva, K.A.; Sundberg, J.P. Comparative anatomy of mouse and human nails. *Anat. Rec.* **2013**, *296*, 521–532. [CrossRef]
35. Meheretu, Y.; Welegerima, K.; Sluydts, V.; Bauer, H.; Gebrehiwot, K.; Deckers, J.; Makundi, R.; Leirs, H. Reproduction and survival of rodents in crop fields: The effects of rainfall, crop stage and stone-bund density. *Wildl. Res.* **2015**, *42*, 158. [CrossRef]
36. Anderson, M.J.; Crist, T.O.; Chase, J.M.; Vellend, M.; Inouye, B.D.; Freestone, A.L.; Sanders, N.J.; Cornell, H.V.; Comita, L.S.; Davies, K.F.; et al. Navigating the multiple meanings of β diversity: A roadmap for the practicing ecologist. *Ecol. Lett.* **2011**, *14*, 19–28. [CrossRef]
37. Bastos, A.D.; Nair, D.; Taylor, P.J.; Brettschneider, H.; Kirsten, F.; Mostert, E.; von Maltitz, E.; Lamb, J.M.; van Hooft, P.; Belmain, S.R.; et al. Genetic monitoring detects an overlooked cryptic species and reveals the diversity and distribution of three invasive Rattus congeners in South Africa. *BMC Genet.* **2011**, *12*, 1–18. [CrossRef]
38. Kumar, S.G.; Stecher, G.; Tamura, K. MEGA7: Molecular Evolutionary Genetics Analysis Version 7.0 for bigger datasets. *Mol. Biol. Evol.* **2016**, *33*, 1870–1874. [CrossRef]
39. Baselga, A. The relationship between species replacement, dissimilarity derived from nestedness. *Glob. Ecol. Biogeogr.* **2008**, *21*, 1223–1232. [CrossRef]
40. Baselga, A. Partitioning the turnover and nestedness components of beta diversity. *Glob. Ecol. Biogeogr.* **2009**, *19*, 134–143. [CrossRef]
41. Oksanen, J.; Blanchet, F.G.; Friendly, M.; Kindt, R.; Legendre, P.; McGlinn, D.; Minchin, P.R.; O'Hara, R.B.; Simpson, G.L.; Solymos, P.; et al. *Vegan: Community Ecology Package, R Package*; Version 2.5-7; R Core Team: Vienna, Austria, 2020. Available online: https://CRAN.R-project.org/package=vegan (accessed on 25 October 2021).
42. Saetnan, E.R.; Skarpe, C. The effect of ungulate grazing on a small mammal community in southeastern Botswana. *Afr. Zool.* **2006**, *41*, 9–16. [CrossRef]
43. Blaum, N.; Rossmanith, E.; Jeltsch, F. Land use affects rodent communities in Kalahari savannah rangelands. *Afr. J. Ecol.* **2007**, *45*, 189–195. [CrossRef]
44. Mason, G.; Littin, K. The humaneness of rodent pest control. *Anim. Welf.* **2003**, *12*, 1–38.
45. Welegerima, K.; Meheretu, Y.; Haileselassie, T.H.; Gebre, B.; Kidane, D.; Massawe, A.W.; Mbije, N.E.; Makundi, R.H. Abundance and microhabitat use of rodent species in crop fields and bushland in Ethiopia. *J. Vertebr. Biol.* **2020**, *69*, 1–6. [CrossRef]
46. Van den Heuvel, I.M.; Midgley, J.J. Towards an isotope ecology of Cape Fynbos small mammals. *Afr. Zool.* **2014**, *49*, 195–202. [CrossRef]
47. Muteka, S.P.; Chimimba, C.T.; Bennett, N.C. Reproductive seasonality in *Aethomys namaquensis* (Rodentia: Muridae) from southern Africa. *J. Mammal* **2006**, *87*, 67–74. [CrossRef]

48. Leirs, H.; Verhagen, R.; Verheyen, W. The basis of reproductive seasonality in Mastomys rats (Rodentia: Muridae) in Tanzania. *J. Trop. Ecol.* **1994**, *10*, 55–66. [CrossRef]
49. Flynn, D.F.B.; Gogol-Prokurat, M.; Nogeire, T.; Molinari, N.; Richers, B.T.; Lin, B.B.; Simpson, N.; Mayfield, M.M.; DeClerck, F. Loss of functional diversity under land use intensification across multiple taxa. *Ecol. Lett.* **2009**, *12*, 22–33. [CrossRef]
50. Horváth, A.; March, I.J.; Wolf, J.H.D. Rodent diversity and land use in Montebello, Chiapas, Mexico. *Stud. Neotrop. Fauna Environ.* **2001**, *36*, 169–176. [CrossRef]
51. Schmidt, N.M.; Olsen, H.; Bildsøe, M.; Sluydts, V.; Leirs, H. Effects of grazing intensity on small mammal population ecology in wet meadows. *Basic Appl. Ecol.* **2005**, *6*, 57–66. [CrossRef]
52. Chia, E.K.; Bassett, M.; Leonard, S.W.J.; Holland, G.J.; Ritchie, E.G.; Clarke, M.F.; Bennett, A.F. Effects of the fire regime on mammal occurrence after wildfire: Site effects vs. landscape context in fire-prone forests. *For. Ecol. Manag.* **2016**, *363*, 130–139. [CrossRef]
53. Ferreira, S.; van Aarde, R. Maintaining diversity through intermediate disturbances: Evidence from rodents colonizing rehabilitating coastal dunes. *Afr. J. Ecol.* **2000**, *38*, 286–294. [CrossRef]
54. Wright, N.I. Ecological Impacts of Highveld Gerbils (*Tatera brantsii*) on a Rehabilitated Ash Disposal Site 2006. Doctoral Dissertation, North West University, Potchefstroom, South Africa.
55. Monadjem, A.; Perrin, M. Population dynamics of *Lemniscomys rosalia* (Muridae: Rodentia) in a Swaziland grassland: Effects of food and fire. *Afr. Zool.* **1997**, *32*, 129–135.
56. Field, A.C. Seasonal changes in reproduction, diet and body composition of two equatorial rodents. *Afr. J. Ecol.* **1975**, *13*, 221–235. [CrossRef]
57. Richardson, E.J.; Perrin, M.R. Seasonal changes in body mass, torpidity, and reproductive activity of captive fat mice, *Steatomys pratensis*. *Isr. J. Ecol. Evol.* **1992**, *38*, 315–322.
58. Sánchez-Cordero, V. Elevation gradients of diversity for rodents and bats in Oaxaca, Mexico. *Ecology* **2001**, *10*, 63–76. [CrossRef]
59. Magurran, A.E.; Henderson, P.A. More than the sum of the parts: Annual partitioning within spatial guilds underpins community regulation. *Proc. R. Soc. B* **2008**, *285*, 1–6. [CrossRef]

diversity

MDPI

Review

Riparian Buffers as a Critical Landscape Feature: Insights for Riverscape Conservation and Policy Renovations

Michael P. Graziano [1], Amanda K. Deguire [1,2] and Thilina D. Surasinghe [1,*]

[1] Department of Biological Sciences, Bridgewater State University, Bridgewater, MA 02324, USA; mgraziano@bridgew.edu (M.P.G.); deguire.amanda@gmail.com (A.K.D.)
[2] Department of Ecology and Evolutionary Biology, University of Connecticut, Storrs, CT 06269, USA
* Correspondence: tsurasinghe@bridgew.edu

Abstract: Riparian zones are critical for functional integrity of riverscapes and conservation of riverscape biodiversity. The synergism of intermediate flood-induced disturbances, moist microclimates, constant nutrient influx, high productivity, and resource heterogeneity make riparian zones disproportionately rich in biodiversity. Riparian vegetation intercepts surface-runoff, filters pollutants, and supplies woody debris as well as coarse particulate organic matter (e.g., leaf litter) to the stream channel. Riparian zones provide critical habitat and climatic refugia for wildlife. Numerous conservation applications have been implemented for riparian-buffer conservation. Although fixed-width buffers have been widely applied as a conservation measure, the effectiveness of these fixed buffer widths is debatable. As an alternative to fixed-width buffers, we suggest adoption of variable buffer widths, which include multiple tiers that vary in habitat structure and ecological function, with each tier subjected to variable management interventions and land-use restrictions. The riparian-buffer design we proposed can be delineated throughout the watershed, harmonizes with the riverscape concept, thus, a prudent approach to preserve biodiversity and ecosystem functions at variable spatial extents. We posit remodeling existing conservation policies to include riparian buffers into a broader conservation framework as a keystone structure of the riverscape. Watershed-scale riparian conservation is compatible with landscape-scale conservation of fluvial systems, freshwater protected-area networks, and aligns with enhancing environmental resilience to global change. Sustainable multiple-use strategies can be retrofitted into watershed-scale buffer reservations and may harmonize socio-economic goals with those of biodiversity conservation.

Keywords: riparian zones; riparian buffers; streams; rivers; riverscapes; watersheds; catchments; conservation

Citation: Graziano, M.P.; Deguire, A.K.; Surasinghe, T.D. Riparian Buffers as a Critical Landscape Feature: Insights for Riverscape Conservation and Policy Renovations. *Diversity* **2022**, *14*, 172. https://doi.org/10.3390/d14030172

Academic Editor: Michael Wink

Received: 4 December 2021
Accepted: 20 February 2022
Published: 27 February 2022

1. Introduction

Riparian zones are influenced by hydrodynamic forces in fluvial ecosystems (i.e., lotic systems, such as rivers and streams) and represent transitional aquatic-terrestrial interphase bordering these ecosystems, and as such have numerous functions. They connect terrestrial and aquatic habitats through surface runoff, subsurface flow, and flooding [1–3]. Riparian zones are characterized by saturated soils, elevated water tables, and a three-dimensional configuration, which extends laterally into the river basin, vertically into the riparian canopy and groundwater, and longitudinally along fluvial channels [1–4]. Through surface and subsurface hydrologic processes, riparian buffers colligate waterbodies with adjacent uplands and govern the exchange of energy and matter between aquatic and terrestrial ecosystems [3,5]. The three-dimensional configuration, mediation of energy and matter flow, habitat heterogeneity, and the unique biotic communities make riparian zones an integral constituent of riverscapes [6,7]. The constituents and conceptual framework of riverscapes vary considerably among various disciplines of applied and foundational ecology. Lotic systems and their biota, including the spatiotemporal dynamics (e.g., species-habitat and community-scale interactions) inherent to these systems,

nested within socioecological landscapes are collectively referred to as a riverscape [8,9]. While accommodating this broader viewpoint, riverscapes can be defined as spatially structured, hierarchically organized, heterogeneous habitat mosaics nested within the river continuum [10–14].

Natural disturbances in riparian systems enhance environmental complexity both spatially and temporally [3,15]. Through variable flow regimes, alternative erosion-deposition patterns, and channel migration, fluvial processes have sculpted riparian zones into landform mosaics with modified geomorphology and edaphic conditions [1,3]. Riparian vegetation is substantially structured by the hydrologic gradient (i.e., the variability in the duration, frequency, and timing of inundation). Interspecific differences in flood tolerance and moisture dependence produce spatial and temporal patterns in the riparian community composition and cover types along the hydrologic gradient [16]. Riparian zones have a disproportionate influence on the local ecosystem, yielding a multitude of ecosystem services, thus considered a keystone resource within the landscape [3,4,17].

Studies that have spanned across numerous global ecoregions have emphasized critical and complex functions of riparian zones, including regulation of aquatic thermal properties [3,4]; bank stabilization [1,17]; nutrient assimilation, silt and sediment retention [18,19]; groundwater recharge [3]; and input of woody debris and other allochthonous matter [1,15].

Given these complex ecosystem services and functions and extensive habitat degradation experienced by lotic systems, the scientific community has widely recognized the need for riparian zone conservation. Numerous natural-resource management and conservation authorities have implemented regulatory policies and established guidelines targeting riparian-buffer delineation. The biological effectiveness of existing policies is debatable, while such regulatory enforcement has received substantial criticism [20,21]. Existing policy standards in certain jurisdictions can be outdated, resulting in conflicts with the current scientific comprehension of riparian ecology. Originally intended to mitigate non-point source pollution, riparian buffers can be managed for wildlife conservation as well as to boost ecosystem functions [22,23]. Although the ecological role of riparian zones has been long recognized, scientific literature on riparian buffers mostly focuses on either a single taxon (e.g., fish, amphibians) or a handful of ecosystem functions (e.g., nutrient filtering, pollution remediation). We argue that a review of current literature on riparian systems will lay a foundation for a multi-taxa multi-functional focus on riparian-zone conservation, painting a holistic ecological framework to reinforce policies and regulatory actions. Many studies on riparian-buffer management are shoehorned towards specific localities or geographic regions. Thus, an overview of such region-specific approaches and their applicability across broader geographic contexts are both prudent and timely needs. In this review, specifically targeting temperate North American riparian systems, we intend to (i) explore their overall ecological benefits; (ii) discuss threats and conservation challenges; and (iii) synthesize conservation actions and policy reforms targeting riparian conservation. Our review will help conceptualize conservation potential and ecological values of riparian buffers and thereby provide a foundation to formulate novel conservation approaches to protect and manage riparian zones.

2. Riparian Buffers—A Nexus for Biodiversity

Riparian habitats represent a nexus of biodiversity where both species richness and density of wildlife are disproportionately high compared to nearby terrestrial habitats [1,24]. Many semi-aquatic and aquatic organisms, particularly those with complex life histories (e.g., amphibians), depend on riparian zones for a significant portion of their lifecycles [25–27]. Riparian zones in the United States account for <5% of the land area (15–50 million hectares) yet provide habitat for over 70% of vertebrate species and are thus considered a keystone habitat [28]. In the arid southwestern United States, riparian habitats account for <1% of the landscape yet are enriched with 80–90% of regional wildlife diversity [29]. Riparian zones exhibit high levels of species richness and diversity and

provide habitats for numerous habitat specialists. Riparian systems can act as local refugia for species, thus serving as population sources to support recolonization of disturbed habitats, such as commercial timberlands [30,31]. Bats and birds use forested riparian corridors as flyways, foraging grounds, and roosting sites [32,33]. During the migratory season, the avifaunal richness of riparian zones is at least an order of magnitude higher than the nearby uplands due to increased foraging opportunities and overwintering sites [34]. Amphibian dependency on riparian buffers is pronounced in the Pacific Northwest of the United States, where 47 species are either obligate or facultative stream associates [35]. Many turtles are particularly dependent upon riparian buffers for dispersal, foraging, hibernation, and oviposition. Floral biodiversity, particularly bryophytes, pteridophytes, and herbaceous plants, is remarkably high in riparian buffers [36]. In northern hardwood forests, native vascular plant richness in riparian forests was remarkably higher compared to upland, interior forests, while invasive and ruderal species were less frequent in the former [37]. Marked floristic species turnover rate (beta diversity) between riparian buffers and adjacent uplands heightens species complementarity along the aquatic-upland gradient, which also generates a greater landscape-scale species richness (gamma diversity) [15].

3. Riparian Zones—Ecological Functions

3.1. Reciprocal Energy and Matter Subsidies

Riparian zones, particularly those with mature forests, supply copious amounts of organic matter and allochthonous input to fuel food-web dynamics in lotic systems (Figure 1). Forests provide an abundant supply of woody debris into rivers, which trap sediments, fine and coarse particulate organic matter, and silt, forming habitats and microsites for aquatic macroinvertebrates and fish [38,39]. Coarse particulate organic matter and fine particulate organic matter are the nutrient sources for detritivores and shredders, which in turn become profitable foraging resources for predatory vertebrates [40,41]. Through decomposition, microbial biofilms growth on woody debris yields dissolved and suspended organic matter [42], which is critical for buffering pH and sequestrating heavy metals [17].

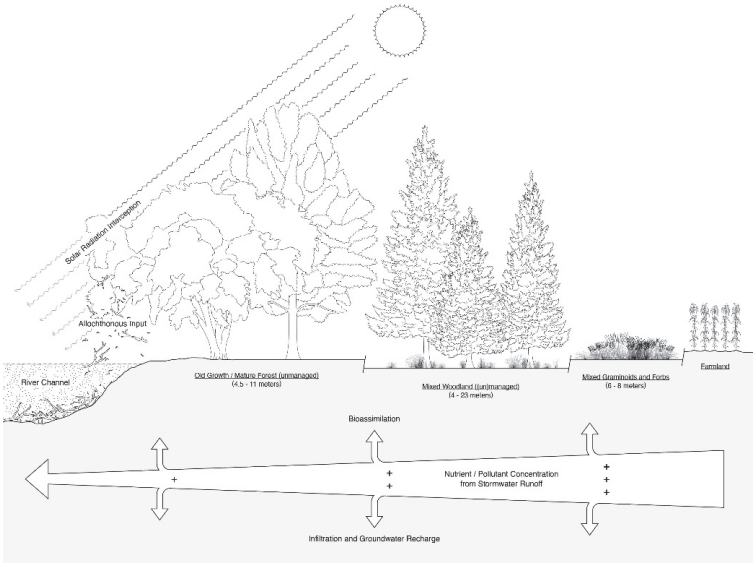

Figure 1. Ecological structure, functions, and multi-tiered delineation of riparian buffers.

Often overlooked or undervalued, the biphasic life histories of many organisms drive aquatic-upland reciprocal energy and nutrient subsidies, highlighting an inextricable connection of the riparian zone to the river itself [43]. Shifting trophic dynamics from

allochthonous to autochthonous production and replacement of specialist feeding guilds (i.e., insectivores, predators) with generalist grazers has been documented after riparian zones have been harvested or otherwise degraded [44–46]. The ultimate consequences of such trophic shifts will likely lead to biotic homogenization where the species turnover and functional diversity of aquatic biodiversity from headwaters to lower reaches attenuate along the river continuum [47].

3.2. Critical Habitat, Channel Stabilization, and Nonpoint-Source Pollution Mitigation

Riparian vegetation supplies particulate organic matter in the form of leaf litter and woody debris of variable sizes and decay classes that structure geomorphology and habitat complexity of the aquatic core-forming microsites and refugia for aquatic fauna [17,40,41]. Woody debris resists erosive water currents and redistributes the flow throughout the riverbed resulting in mosaic patterns of erosion and alluvial depositions along river corridors, which further contribute to habitat heterogeneity [3,23]. Deep-water pools formed by debris dams provide critical habitats for spawning and refugia during low-flow seasons [48]. Further, the abundance of large within-stream woody debris is positively associated with turtle density, as it provides critical thermoregulatory sites [49,50].

By intercepting precipitation and slowing surface runoff, riparian buffers filter silt and sediments, heavy metals, agrochemicals, organic wastes, and pathogens, thereby preventing these contaminants from reaching the aquatic core or groundwater [17,19,39,51]. These buffering functions become crucial in urban and agricultural landscapes where nonpoint-source pollution via surface runoff intensifies during rainstorms [51,52]. The root masses of riparian vegetation assist in maintaining the physical structure of soil and reducing soil erosion [17,39]. Decelerated surface runoff enhances groundwater recharge through the riparian soils, even during storm surges [17,53]. Water quality metrics of buffered aquatic systems are more stable than unbuffered systems. For instance, enhanced siltation elevated peak discharge velocities, and channel incision was reported in unbuffered rivers. In contrast, buffered rivers contained the highest volumes of riverbed woody debris, lower sand/slit content, and reduced river discharge, as well as lowered fecal coliform and nutrient concentrations [54,55].

Riparian buffers intercept sedimentation and prevent the loss of interstitial spaces of stream beds, which represent critical habitat for aquatic organisms [31,53,56]. Buffered streams support a diverse aquatic macroinvertebrate community, including environmentally sensitive taxa [54]. In contrast, freshwater turtles inhabiting streams without adequate riparian buffering, particularly those dissecting urban landscapes, exhibit skewed sex ratios and age structures, reduced juvenile recruitment, heightened incidental mortality, and subsidized predation [56,57].

3.3. Climate Change Resistance and Resilience

Riparian zones are both spatially and temporally dynamic and stochastic; as such, riparian biota has evolved life-history strategies and adaptations under environmental variations, which may make them either more resilient or resistant to climate change [5]. Riparian vegetation exhibits a wide array of adaptive morphological and physiological traits—heterophylly (production of variable leaf forms in response to environmental conditions), heteroblasty (abrupt morphological changes in the ontogenetic development), variable-depth root systems, propagule dormancy, and persistence under variable disturbances (flooding, fluvial, fire) and soil conditions (increased salinity)—that confer resilience to extreme climates [5]. Riparian buffers create spatial connectivity across lateral, longitudinal, and vertical dimensions, which provides multiple pathways for species migrations in response to climate shifts [3,58,59]. Additionally, riparian buffers form climate envelopes with high humidity and thermal stability that function as climate refugia [42]. For instance, large trees typical of intact riparian zones create a continuous canopy, which intercepts solar radiation and regulates stream thermal properties [55]. Indeed, harvesting riverbank vegetation has often resulted in elevated average and maximum water temperatures, in-

creased diel fluctuations and incidences of thermal extremes, and erratic disruptions in seasonal thermal regimens [55,60].

4. Threats and Conservation Challenges

Streams and rivers are among the most imperiled habitats in the United States, as well as across the world [58,59,61]. The current estimates for the riparian-zone surface area of the United States range from 15–50 million hectares, of which >90% are degraded [29,62]. There is growing anthropogenic pressure on riverine ecosystems. In the conterminous United States, a significant proportion of the population dwells within 1-km of a river. Nevertheless, only 2% of stream reaches receive riparian protection [62]. Riparian protection remains uneven across the United States. For instance, compared to eastern North America or the Great Plains, riparian zones of the western United States receive enhanced protection where federal land stewardship ensures appreciable conservation attention. Nationwide, ~480,000 km of rivers exhibit degraded water quality, with impaired riparian buffering being at least partly responsible. Impaired riparian systems experience increased solar incidence, dry microclimatic conditions, and lack of environmental complexity, making them unfit for native wildlife, with the exception of a handful of urban exploiters, urban-adapted human commensals, and invasive species [63].

4.1. Anthropogenic Land-Cover Changes and River Modifications

As ecosystem functions of riparian zones rely heavily on fluvial processes, anthropocentric alterations fundamentally influence riparian dynamics [36]. To facilitate navigation, irrigation, and mitigate threats of catastrophic flooding, rivers have undergone drastic modifications with channelization, diversion, and impoundment, which impacts the riparian zone [36,64,65]. In the United States, there are over 2 million dams that influence nearly 90% of regional drainage basins, disrupting both longitudinal and lateral connectivity [66]. For example, permanent upstream floodplain inundation, downstream sediment and nutrient deprivation, damped hydrologic variability, and downstream peak flow attenuation lead to major modifications in the riparian structure and function [29,63]. Dams also impede downstream hydrochory and plant propagule recruitment, which subsequently suppresses riparian vegetation [67,68].

Channelization and bank-stabilization structures sever the connection between the riparian zone and the in-stream habitats, which prevents recruitment of riparian vegetation, disrupts the riparian microhabitat structure, lowers the riparian water table reduces the frequency of overbank flow, and homogenizes shoreline complexity [29,34]. Channelized river corridors lack soft sandy riverbed substrates, sandbars, and large downed wood, which are critical for basking and nesting turtles [64]. Cumulative effects of flow regulation, drainage, and floodplain reclamations transform anastomosing, meandering, and braiding rivers into oversimplified single-tread channels that are severed from riparian zones [65].

Loss of riparian forest cover is particularly notable in anthropogenic landscapes. Biotic homogenization—reduced species turnover across environmental gradients—as a consequence of urbanization was observed across American riverscapes [69,70]. Declining riparian forest cover changes aquatic productivity, such as the prolific growth of exotic species and filamentous algae at the expense of unicellular phytoplankton and non-vascular plants [47,61]. The proliferation of these primary producers neither contributes to food webs nor is exploited by consumers [42,71]. Sporadic changes in seasonal river temperatures resulting from loss of streamside vegetation can negatively impact juvenile development among fish and trigger adverse behaviors, such as untimely migration and phenological mismatches [23,42].

4.2. Recreation-Based Degradation

Given unique aesthetic and scenic values, recreation-based development and activities (whitewater rafting, canoeing, swimming) are often concentrated within riparian zones [72,73]. Proximity to large rivers is among the most demanding landscape features

sought by recreational developers as well as amenity migrants for secondary and vacation homes [74,75]. Snag removal and vegetation clearance in the riparian zone to boost recreational and scenic values led to declining diversity among turtles in the northern Midwest [38]. Increased cover of invasive and weedy species is frequently observed in riparian zones impacted by human disturbances [34]. For instance, invasive plant species were found to be absent from river reaches where the surrounding land use was largely undisturbed and exhibited greater complexity in vegetation structure, suggesting that these reaches were more resistant to invasion than reaches, which have experienced degradation [76]. Deliberate introduction of exotic species as landscape ornaments is partly responsible for such biological invasions, at least in the early phases of establishment outside the native range. Riparian corridors are conduits for plant propagules, therefore, riparian zones are particularly vulnerable to plant invasions. Recreational activities enhance the human footprints in riparian zones (e.g., vegetation removal, changes in natural land-cover, simplification of the structural complexity) as well as the fluvial channel (e.g., modifications in the riverbed and bank geomorphology), which can further exacerbate biological invasions [76].

4.3. Resource Overuse

Land development in the riparian zones and floodplains increases the acreage of impervious surfaces, which alter local hydrodynamics and fluvial processes. Riparian forests are high in aboveground biomass, making them particularly susceptible for commercial timber harvesting [1]. Logging or clearcutting within the buffer zone can lead to localized extirpation of riparian specialists [36,48]. Additionally, the paper, pulp, and biofuel industries are also attributed to intensified silvicultural practices within the United States. River corridors have been historically used as effective conveyers of harvested timber. However, to facilitate convenient access to river channels to transport timber to sawmills downstream, riparian vegetation and within-stream wood are often removed [77]. River valleys historically were and continue to be targeted by mineral harvesters, particularly for gold mining, resulting in the clearcutting of riparian vegetation as well as the excavation of streambed substrates [59,73]. Indeed, ecosystems within the riparian zone have been and continue to be set on courses exceeding their historical norms due to anthropogenic influences relating to resource overuse [78].

4.4. Agriculture and Farming

Due to high productivity and soil fertility, riparian habitats across the United States have been converted to row-crop farms nationwide [34]. Moreover, nutrient-rich soils of the riparian zones of large, sluggish rivers and dependable access to water have led to the transformation of such riparian zones into extensive croplands [73]. Given high productivity and access to water and shade, riparian zones attract livestock, which results in overgrazing of riparian vegetation and soil compaction. Setting aside forested buffers for conservation is economically costly, thus farming operations usually encroach the riparian zone, resulting in the conversion of diverse native riparian flora into monocrop stands.

4.5. Challenges in Riparian Conservation

Much of America's riparian zones are located within privately owned lands. Unfortunately, many of these landowners prioritize profit over sustainability [39,73]. Streams and rivers crossing private lands, especially low-order reaches, receive little to no legislative protection [79]. Land managers of local jurisdictions are often underinformed about riparian functions and biodiversity, hence policies emerging from local authorities are unlikely to generate tangible conservation benefits [52]. Taking riparian lands out of production and re-vegetating buffers are prohibitively expensive, thus, regulations on riparian zones are often resisted by farmers [52,80]. Consequently, riparian conservation policies in the United States are often distilled into politically palatable decisions driven by what private landowners are willing to concede [17].

5. Conservation Efforts

Maintaining intact riparian zones has long been recognized as a crucial element in biodiversity conservation. During the last few decades, riparian-buffer conservation has undergone paradigm shifts where sustainable resource use, endangered species conservation, landscape-scale connectivity, and climate resilience were incorporated into conservation planning [35,63,81].

5.1. Local Scale and Fixed-Width Buffer Zones

Fixed-width buffer zones are the most popular approach to riparian conservation, where decisions were primarily made at the state level, resulting in significant variations in buffer widths (12–52 m) throughout the United States [77]. The site-specific widths for riparian buffers were often estimated based on the maximum height of dominant plant species along the riverbanks. This baseline may be increased based on the aquatic or terrestrial community targeted for conservation. For instance, fish-bearing perennial rivers may have a buffer zone that is twice the height of the tallest tree height (~90–145 m) [82]. The scientific reasoning behind this baseline remains questionable. Nonetheless, the greater buffer-width variations stipulated by different local land managers for protection of the same target species, communities, or ecosystem functions within similar ecoregions is a significant conservation concern [20].

An array of multi-layered vegetation strips has been recommended to mitigate nonpoint-source pollution in streams associated with commercial farmlands (Figure 1). Multi-layered vegetation strips generate a gradient of structural complexity, thereby maintaining multidimensional niches for numerous taxa, including specialist foraging guilds [83]. For example, a vegetation strip dominated by graminoids and herbaceous vegetation has a rapid biomass turnover rate and thus helps restore biologically optimal soil structures. Multi-layered approaches recommended for the United States include a relatively undisturbed old-growth forest (4.5–11 m wide) closest to the stream channel, followed by managed shrub-mixed woodland layer (4–23 m wide), and a graminoid-dominant herbaceous strip mixed with shrubs and scrubs (6–8 m wide) (Figure 1) [3,18,84]. The innermost strip regulates water temperature, enhances habitat complexity and bank stability, and supplies woody debris to the aquatic core while providing critical wildlife habitats for conservation-dependent biota [40,41]. The middl e strip assimilates nutrients, retains fine sediments, and enhances groundwater recharge. The outermost strip acts as a physical barrier to storm-water runoff, reducing erosion and retaining silt, sediment, and agrochemical contaminants. Conservation Buffer Initiative—which stems from the United States Department of Agriculture Conservation Reserve Program—advocates a three-tiered design comprising perennial grasses, two rows of shrubs, and 4–5 rows of mature woody plants for rivers flowing through farmlands [85].

Numerous taxon-specific fixed-with buffer zones have been proposed for wildlife conservation in the United States. For example, buffer zones ranging from 43–290 m have been recommended for the conservation of 95% of herpetofaunal communities [20]. A forested riparian buffer of 150 m is recommended for the conservation of most North American riverine turtles, especially to support their seasonal navigations [38]. This fixed-width buffer becomes untenable for species with complex and wide-ranging life histories. For example, threatened species of riparian turtles may seek refugia as far as 400 m from the river channel they inhabit [38]. Surprisingly, fixed-width buffer zones intended to support macroinvertebrate, fish, and avian species are often smaller than those recommended for herpetofauna, ranging from a minimum of 30 m (macroinvertebrates and fishes) to 175 m (specialized forest birds) [33,86,87]. Similarly, 100–200 m riparian buffers are effective in protecting passerine assemblages and stabilizing populations of area-sensitive songbirds [88]. However, bank stability, protection of water quality, and channel heterogeneity may be achieved by much smaller buffer widths (10–130 m) and may account for >90% of regional vascular floristic richness [35,37]. Nevertheless, large buffers (>100 m) serve

multiple purposes, such as mitigation of edge effects on nesting birds while providing habitats for riparian-dependent herpetofauna and small mammals [86,89,90].

Fixed-width buffers gained popularity mostly due to their administrative and operational simplicity but are ineffective to sustain ecosystem functions, metacommunity dynamics, and upland habitat associations of semiaquatic fauna [37,77]. Such singular, generic buffers are often homogenous in habitat structure and incongruent with natural processes, thereby over-simplifying riparian zones' bio-physical complexity [53]. For instance, in Canadian boreal forests, fixed-width buffers are at least partly responsible for fire suppression. Small-width homogenous buffers take longer to recover from extreme climatic disturbances and are susceptible to species invasions, insect outbreaks, and forest pathogens. Concerning multi-layered buffers, maintaining the prescribed vegetation structure may warrant intensive management interventions, which can be both financially and logistically challenging.

5.2. Watershed Scale and Variable-Width Buffer Zones

Fixed-width buffer zones are readily employable, sufficiently simple for on-ground delineation, and only warrants management interventions at the local scale. In contrast, variable-width buffer zones are more operationally complex and may necessitate land management beyond the local scale yet are effective at reaching desired conservation goals and may generate lasting benefits across broader spatial extents. For instance, watershed-wide buffer zones are compatible with systematic conservation planning designed for both freshwater and terrestrial ecosystems and align with overreaching environmental themes applicable to riverscapes. Resilience to global environmental change, prevention of nonpoint-source pollution, restoration of trophic dynamics and the riverscape continuum, mitigation of "urban stream syndrome," and augmentation of amphibian and fish biomass in urban and agricultural watersheds can be harmonized with watershed-wide riparian conservation [11,53,64,91]. At the watershed scale, buffered riparian zones support species migrations, assist movements of dispersal-limited species, augment metapopulation dynamics, thereby relieving small, declining, or isolated populations from inbreeding depression, genetic drift, and demographic stochasticity [81,92,93]. For example, streams within extensively forested watersheds yielded enhanced growth and breeding activities, greater body condition, and greater densities of rare salamanders [94]. In anthropocentric landscapes or disturbance-prone watersheds, buffered streams provide refuge for terrestrial source populations [30,31,95]. Watershed-wide riparian buffers established along a north-south orientation or elevation gradients can function as latitudinal migratory corridors aiding poleward or altitudinal range shifts in response to climate change [84].

Buffer zones delineated at the watershed scale restore connectivity integral for rivers and wetlands, including fourfold eco-hydrological dynamics: (1) lateral interactions between aquatic cores and the uplands as well as among different aquatic cores and wetlands; (2) longitudinal dynamics along the river continuum; (3) vertical linkages among the surface water, groundwater and atmosphere; and (4) temporal changes including wetland successions and modifications in channel geomorphology, hydroperiods and flow regimes [11,43,59]. Hence, watershed-wide buffer zones complement biological, hydrological, and geomorphological processes. Effective delineation of watershed-wide buffer zones requires policies that transcend administrative boundaries, focus beyond local scale conservation targets, and warrant participatory management of different jurisdictions and conservation authorities.

5.3. Determinants of Watershed-Scale Buffer Delineation

The magnitude, spatiotemporal extent, and importance of ecological functions of riparian zones depend on both large-scale watershed-wide regional properties and small-scale local habitat characteristics [96]. Thus, the delineation of riparian buffers should be a synergistic product of both local and watershed-scale factors.

Local-scale determinants include channel slope, local topographic relief, riverbank vegetation structure (e.g., stem density, basal area, vegetation successional stages), soil properties, and channel geomorphology [37,53]. Numerous field studies indicated a non-linear relationship between required buffer widths and increasing slope as well as soil erosivity, underpinning the importance of site-specific conditions in delineating buffers [17,23]. Stream order, stream width at bankful discharge, annual discharge regimes, channel dynamics (lateral channel migration and formation of oxbow or scroll lakes) and planform (the quasi-equilibrium channel morphology created by concentration or dissipation of energy and sediment movements), and floodplain complexity should also be considered [58,81,97]. For instance, buffers zones of headwater streams should be sufficiently extensive to protect riverbank seepage formations where the groundwater table approaches the surface. Concerning middle- and higher-order streams, conventional flood-risk assessments [86,87] can be utilized to determine buffer widths, thereby deterring development and industrial farming in flood-prone riparian zones. As private land managers and entrepreneurs are risk aversive, delineating high-risk flood zones as local-scale riparian buffers will carry unintended conservation benefits.

Among watershed-wide determinants—watershed size, basin-wide ecosystem processes, regional geography and climate, current and historical land-use land-cover (the extent of impervious surfaces and modified land-cover types), floodplain characteristics (presence, distribution and types of wetlands), hydrologic connectivity, spatial and temporal distribution of pollutant sources, and types of pollutants—should be accounted when delineating buffer dimensions [11,54,60]. Further, the sociocultural and socioeconomic dimensions cannot be ignored when determining the size and extent of riparian buffers, as local stakeholders must be able to connect the benefits of setting aside tracts of land with their needs and interests [78]. Riparian zones have long been shaped by both human (land-uses and resource extractions) and natural (e.g., climatic, hydrological, geomorphological, fluvial, and biological) processes. Recognizing this multidimensional co-construction will also highlight riparian buffers as an integral component of fluvial ecosystems, which may create a favorable attitude from various sectors (e.g., farmers, agroindustry, policy makers, land-use planners, and land developers) towards riparian-buffer conservation [78]. Thus, watershed-scale buffer delineations must weigh in on anthropocentric uses and values of riparian ecosystems. Both at local and watershed-scale, regional and local wildlife communities that associate riparian buffers as a critical habitat should be factored in as well. Watershed-scale buffer zonation should consider the upland dispersal and migration distance of semiaquatic fauna, which is critical for species with complex life cycles where both breeding migrations and post-natal dispersal occur over long distances [85,95,98,99].

Riparian buffers in managed timberlands should be determined based on harvest regimes, based on the total size of harvested area versus acreage of the unharvested forests in the watershed, harvesting methods, and stand age structure [31,80]. Rivers and wetlands embedded in landscapes with a prolonged land-use past, such as cattle grazing and industrial agriculture, require a lengthy recovering period as well as ample riparian reservations. Thus, land-use legacies, as well as disturbance histories across the watershed, are also critical determinants of buffer zone allocation [54,96]. Legacies resulting from anthropogenic alterations (e.g., riparian timber harvest) induce lasting changes in the entire river corridor (e.g., complete transformation of channel structure and fluvial dynamics), creating alternative states with impoverished ecosystem services [100]. Watershed-scale buffers designed to protect and restore riparian biodiversity and ecosystem functions can be more effective if the lasting effects of historical legacies are recognized.

5.4. Designs for Watershed-Scale Riparian Buffers

Olson et al. [35] proposed watershed-wide buffer conservation, which accounts for lateral and longitudinal linkages of riparian biodiversity as well as riparian-zone ecosystem functions. With the emphasis on cross-ridgeline connectivity to accommodate faunal movements among headwater streams, this conceptual model advocate for wider (200–

400 m) buffers. Olson and Burnett [84] designated ridgeline forests with a high density of headwater streams as "linkage corridors" to facilitate cross ridgeline connectivity of local biota. Dispersal aside, ridgeline forests were habitats for endemic species and harbored stable populations of native vertebrates [35,84]. Attributed to this dual function (dispersal and refugia), we proposed that "linkage corridors" be retrofitted into a riparian-buffer network. If strategically designated with ideal spatial configuration within a watershed, "linkage corridors" enhanced metapopulation interactions and assist safe passage during drought-induced movements and provided access to climate refugia in headwaters.

A two-tiered, riparian buffer design was conceptualized for headwaters of the Pacific Northwest, which can reconcile both commercial land-use operations (logging) and wildlife (amphibian) conservation [89]. Referred to as the "spaghetti-meatball approach," this design comprises non-random alternating configurations of narrow (40–150 m) and wide (400–600 m) buffers [35,92]. The narrow, long buffer strips ("spaghetti") running alongside streams encompass the moist-mesic riparian microclimates via "stream effect" while protecting strictly-aquatic and bank-dwelling species. When protected areas or other critical and rare habitats (e.g., ephemeral wetlands, fluvial lakes, old-growth stands, tributary junctions) neighbor the river channel, particularly at ridgetops, wider buffers ("meatballs") can be applied to enhance the structural heterogeneity and resource availability of the riparian environments. Narrow "spaghetti buffers" are sufficient to confer bank stability and filter runoff, thus making them suitable for streams dissecting timberlands and farmlands. High-value conservation targets, such as stream reaches with a high density of microendemic or threatened species, local hotspots of diversity, and bioclimatic refugia can benefit from "meatball buffers". The "spaghetti-meatball" design also harmonizes economically profitable, yet sustainable land uses with freshwater biodiversity conservation, hence applicable to watershed-scale riverscape conservation.

Riverscapes are spatially complex fluvial systems mosaics of habitat types and environmental gradients, interconnected by dendritic networks with unique spatial configurations and structures that differ markedly from most terrestrial systems and other aquatic systems [11,41]. The spatially heterogeneous structures of the riparian environment (including the floodplains), riparian biotic communities, and matter and energy exchange are particularly important attributes of riverscapes [7,65]. We argue that watershed-wide riparian-buffer conservation will effectively capture all critical attributes of the riverscape.

We recommend the implementation of riparian-habitat conservation criteria by Semlitsch and Bodie [25] and Olson et al. [35] to delineate buffers along river channels at the watershed scale, yet caution against abiding by the suggested buffer widths as canonical rules (Figures 2–4). Instead, we encourage re-tailoring variable buffer widths based on the spatial configuration of critical riverscape elements (i.e., floodplains, isolated channels) and niche dimensions of riparian-dependent biota of the regional species pool. The riverscape is the template for both between-habitat species turnover (beta diversity) and landscape-scale community diversity (gamma diversity); the latter metrics are prudent biodiversity targets representative of the entire riverscape [81]. Incorporating niche dimensions of riparian biotas, such as the lateral navigation distance of both philopatric and vagile species when delineating riparian zones, will make these buffers more biologically productive [90].

Hereto, we first highlight the immediate riparian zones as both core habitats of the riverscape and keystone structures of the watershed (hereafter, critical riparian core), ergo propose the first tier of buffer delineation throughout the drainage system alongside both main stems and tributaries (both perennial and ephemeral), provisionally extending into the floodplain to envelope riparian wetlands and wetland-obligate communities. These buffers can be locally distended at confluences or to connect the river channel with neighboring wetlands. The first tier should be designed to buffer the stream channel from atmospheric and terrestrial stressors, protect water sources, and enhance habitat associations of riparian and semiaquatic biota. Second, we propose delineating a critical terrestrial core beyond the critical riparian core. This second tier will promote metacommunity dynamics [91] and subdue edge effects [101]. To enhance wildlife permeability, we advise restrictions

on both exploitative (subdivision or infrastructure developments, agriculture, grazing, and clearcutting) or non-consumptive (recreational) uses within the critical riparian core while permitting specific land uses (agroforestry, permaculture, forest gardening, selective logging) within the critical terrestrial core.

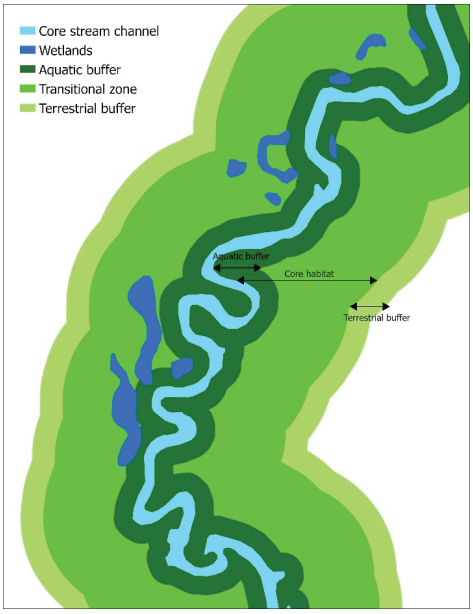

Figure 2. Fixed buffer widths applied to a single mainstem river corridor following multi-tiered buffer widths recommended by Semlitsch and Bodie [25].

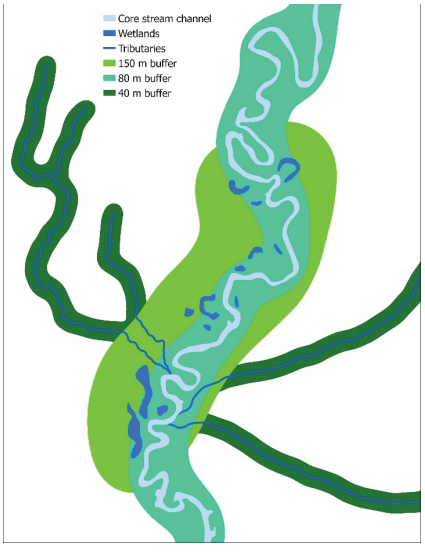

Figure 3. A variation of the Spaghetti-meatball buffer-zone delineation with variable buffer widths as recommended by Olson et al. [35,89] applied to the mainstem river corridor, including the tributaries to the mainstem.

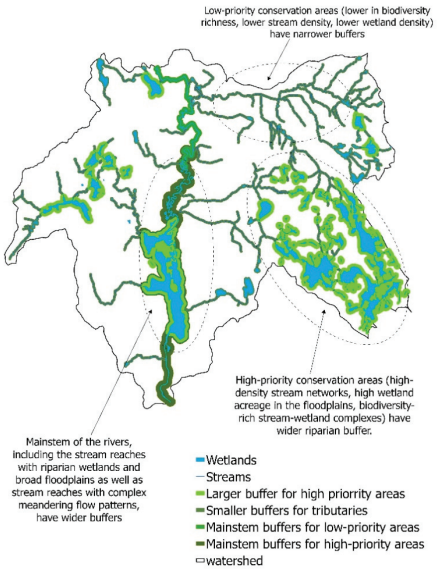

Figure 4. Variable buffer widths applied to stream channels (mainstem and tributaries) and stream-associated wetlands at the watershed scale. Increased riparian buffer widths are applied to regions with high conservation potential and other critical hydrological or ecological features to protect infertility ecosystem structure and functions.

Greater habitat heterogeneity that satisfies natural and life history requirements of riparian obligates is critical in a watershed-wide buffer delineation. Thus, we advocate the inclusion of multiple landscape elements—hibernacula, climatic refugia, high-quality foraging and nesting grounds, heterogeneous wetland complexes with variable hydroperiods, aquatic habitats that offer complementary resources, and a variety of upland habitats—into both riparian and terrestrial core habitats [93]. Moreover, we contend inclusion of forest remnants, commercial timberlands, silvopastoral systems, traditional farmlands, and restored habitats into the critical terrestrial core to reinvigorate beta and gamma diversity and to refuel metacommunity interactions and ecosystem processes [42,102].

5.5. Habitat Management within Buffer Zones

Harvested riparian zones should be characterized by mixed-aged riparian vegetation, vertical stratification, and variable successional stages, thus providing habitats for both seral and climax communities [48,103]. To promote habitat heterogeneity in the riparian buffers where historical disturbances (flooding, fire, debris flow) are suppressed, sustainable forestry operations based on various shelterwood harvesting methods, such as selective thinning in variable-sized patches, and partial cuts may generate spatial patchiness resembling natural disturbances [36,48,83]. Here, it is imperative to mimic historical disturbance regimes in terms of frequency, duration, magnitude, and spatial patterns [103]. Management decisions should weigh in the system resilience, legacy effects (historical fire regimes and grazing), climate conditions (average precipitation), and susceptibility to extreme events (windstorms, floods). A multi-use approach with regulated timber harvesting and extraction of non-woody products in designated riparian buffers will also harmonize conflicts between conservation authorities and resource users [104].

Riparian timber harvest can be connected to the multi-tiered buffer approach we proposed. No logging should be permitted within the immediate riparian zone adjacent to the stream channel (critical riparian core). Variable and transitional timber management operations forming an environmental gradient with respect to stem density, basal area, canopy closure, stand maturity, and species of interest can be permitted in outer tiers (criti-

cal terrestrial core). We urge for minimal use of machinery and motor vehicles, which leads to soil compaction and other disturbances. Availability, diversity, and size of forest-floor cover objects in the riparian buffer are crucial for ameliorating the ill-effects of logging as these cover objects preserve cool, moist microclimatic conditions for forest floor fauna [95]. Thus, we caution against salvage logging or residue removal [35,84]. However, if adequate forest-floor cover exists, some of the logging residuals can be placed alongside banks as microsites to harbor riparian vertebrates and vegetation propagules [96].

To restore longitudinal and lateral connectivity through riparian management, removal of dams, dikes, and levees is imperative to reunite river channels with floodplains and reengineer natural fluvial (meandering, braiding, anastomosing) dynamics [16,96]. Breaching artificial bank stabilization structures such as ripraps also helps restitute surface-to-groundwater movements as well as hydrologic and sediment regimes that are critical for healthy ecosystem functions of riparian zones [16,105]. Dam removal also restores both coarse- and fine-scale geomorphic features, natural flow regimes, and plant successional processes that constitute critical riparian habitats (e.g., floodplain conditions, riparian food webs, plant-community dynamics) and reduce the establishment and persistence of exotic plant species in the riparian zone [16,106,107]. Natural resource managers should estimate site-specific risks of dam removal on riparian zones (e.g., sediment aggradation on riverbanks, habitat homogenization by reducing the variability of bed elevations, biological invasions) for making informed decisions on post-restoration monitoring to detect negative impacts and implement mitigatory measures [97,105]. To improve riparian buffering functions (flood and discharge mitigation, groundwater recharge, and bioremediation), we recommend restoration of floodplain wetlands, which is particularly necessary following dam removal [108]. In impaired (urban and agricultural) watersheds with contaminated runoff, these floodplain wetlands can be an ecologically sound alternative to artificial drainage ponds.

Restoring degraded riparian zones may require the introduction of site-appropriate topsoils and subsoils with adequate soil-particle size distributions and organic matter since plant propagule recruitment, microbial remedial processes, and groundwater movements are functions of soil properties [16]. Introduction of natural cover objects across the riparian buffers in forms of woody debris in variable size and decay classes might be warranted [30,109]. We discourage "landscape manicuring"—removal of downed or standing deadwood for aesthetics and navigation. Spatial arrangement and retention of dead standing trees (snags), rock outcrops, and other vertical geological formations warrant attention as such structures serve as keystone resources for riparian fauna [98]. As degraded riparian zones are species-depauperate and periled with exotic invasions, re-introduction of foundation species (e.g., willows (Salix spp.)) and ecosystem engineers (e.g., American beavers (Castor canadensis)) as well as controlling exotic and invasive species can accelerate recovery with enhanced resilience [82,104,105].

6. Policies and Protection of Riparian Buffers

Numerous United States environmental policies contribute to riparian-buffer conservation [79]. These laws take effect via three mutually nonexclusive avenues: (1) direct acquisition or supporting acquisition of lands and waterways for buffer delineation; (2) restrictions on resource exploitation in riparian environments; and (3) develop environmental standards and guidelines to mitigate water pollution based on buffer-zone management. Herein, we will briefly review a selection of these policies, including their effects and recommendations for enhancing their impact on riparian systems.

Empowered with legislative authority on wetland and riverine buffers, the Clean Water Act (CWA) aims to "restore and maintain the chemical, physical, and biological integrity of the Nation's waters." Administered by the Environmental Protection Agency (EPA) and Army Core of Engineering, the CWA recognizes pollution mitigation and provision of wildlife habitats as critical functions of riparian buffers, thus, mandates avoidance and minimization of damage to riparian zones [99,110]. We advocate that CWA's specifications

on total maximum daily load, the maximum amount of a pollutant permissible in a waterbody to maintain acceptable water-quality standards, be leveraged for buffer delineation as a measure against nonpoint-source pollution [53]. We urge the CWA to recognize the riparian buffer as a "critical habitat complementary to the aquatic core" while underscoring the functional nexus between intact riparian zone and biological integrity of aquatic core habitats, thereby advocating restoration and delineation of riparian buffers as a mitigation strategy [25,26].

Administered by Fish and Wildlife Service and National Oceanic and Atmospheric Administration, the Endangered Species Act (ESA) has the potential to secure riparian environments as "critical habitats" for endangered or threatened species [111]. We encourage the inclusion of the "critical habitat" concept into a panoptic "critical riverscape" perspective to encapsulate watershed-wide environmental complexity and functional diversity inherent to riparian zones. For riparian conservation, we propose that the ESA targets umbrella species such as riparian obligates and riparian-dependent species, particularly those characterized by longevity, delayed reproductive maturity, elevated egg/larval mortality, and high sensitivity to anthropogenic disturbances [112].

Mandated by the United States Department of Agriculture (USDA), the National Forest Management Act (NFMA) requires a minimum of 30 m buffer around perennial rivers and lakes and prohibits land uses that impair water quality or fish habitats [34]. As corroborated by our review, the 30-m minimum threshold might suffice conservation of a subset of stream biota (e.g., headwaters) but is insufficient to maintain upland associations of most riparian communities. In lieu of our variable buffer-width standards, we recommend employing local and watershed-scale biophysical determinants to prescribe variables both buffer widths and length to assure watershed-wide continuity.

The National Wild and Scenic Rivers Act (NWSRA, Departments of Interior and Agriculture) aims to preserve "free-flowing" rivers with remarkable ecological and nonconsumptive (aesthetic and recreational) values [39,88]. The NWSRA recommends a 400 m riparian buffer along designated rivers flowing through federal lands [113]. Given the conservation potential of these rivers, we suggest remodeling NWSRA to recognize the main stem, tributaries, and floodplains (including floodplain wetlands) of designated rivers collectively as "wild and scenic riverscape corridors" while identifying buffers as "critical life zones" of the entire watershed.

Significant extents of riparian zones in the United States are located within private lands. Further, most land development occurs within local jurisdictions where the decision-making officials are likely uninformed about local biodiversity, ecological principles, or sustainable economic benefits associated with riparian buffers [114]. As such, we highlight the urgency to educate local officials as well as private landowners on watershed-scale buffer designs [73]. To cultivate responsible stewardship among public and local officials, we recommend the introduction of citizen-science projects tailored to generate locale-specific long-term data on riparian biodiversity and ecosystem processes, which provide a scientific basis for decision making [30,115]. We also encourage repurposing citizen science as a communication hub among scientific communities, town officials, and private landowners, particularly to disseminate novel approaches on riparian conservation [43]. To enhance public buy-in, we also recommend the adoption of charismatic or flagship species that symbolize riparian habitats (e.g., river otters (*Lontra canadensis*) [102].

For watershed-wide riparian conservation to take effect, rewarding land stewards who adopt riparian best management practices are effective and prudent [78]. Administered by the USDA through the Farm Bill, a number of such programs, Conservation Reserve Program, Conservation Easements, and Environmental Quality Incentive Program, have demonstrated success in optimizing conservation potential and environmental benefits in productive agricultural lands [116]. Program participants offset environmentally sensitive lands from production and establish resource-conserving native plant species in exchange for rental payments, tax breaks, and financial and technical support for improving farming operations [85]. Our recommendations herein include educating farmers on agricultural

benefits through the use of riparian buffers (e.g., flood and erosion prevention) and remodeling incentive programs for recreational entrepreneurs, the timber industry, and non-timber extraction ventures. Given the multitude of ecosystem functions originating from riparian buffers—groundwater recharge, water-quality enhancement, game species conservation, aesthetic and scenic values—we recommend enhancing incentives through Payments for Ecosystem Services for land stewards participating in riparian-buffer conservation [115].

Policy reforms for watershed-scale riparian-buffer conservation will require a paradigm shift from a conventional reach-based perspective to a more inclusive ecosystem-centered approach tailored for the conservation and restoration of hydrogeomorphological processes with the emphasis on ecological integrity and biological dynamics of rivers [117,118]. Herein, the riparian buffers should allocate more physical space to facilitate channel mobility (e.g., lateral migration, meandering) and seasonal flooding [106,118]. Such policy frameworks not only ensure sustainability and resilience of riverine biodiversity but also mitigate flood and erosion risks. Hydrogeomorphology-influenced policies have been successfully implemented in Europe and Canada [107,117]. These legislative frameworks piggyback on the notion of risk aversion (erosion and flooding) as well as ecological integrity, thus are palatable for multiple stakeholders while affording protection to critical riparian features (e.g., floodplain wetlands) and exclude development and detrimental human activities from the riparian buffers. When implemented at watershed scale, these process-driven conservation actions warrant minimal management interventions over time yet are suitable for enhancing the resilience of lotic ecosystems against global environmental change. In addition, such policies simultaneously address multiple regulatory and conservation goals such as the Habitats and Water Framework Directives of the European Union and the Clean Water and Endangered Species Acts in the US [118].

We advocate that policy reforms recognize riparian buffers not only as "critical life zones" or "core habitats" but also a vital riverine and riverscape elements crucial for biodiversity conservation and ecosystem functions [62,104]. Watershed-scale riparian conservation is appropriate for the conservation of aquatic biota, management of all forms of freshwater habitats, and resolution of competing for anthropocentric interests [11,61]. As inter-state and among-municipality collaborations are pivotal to watershed-scale conservation, we suggest that both federal and state funding mechanisms encourage such cross-jurisdictional partnerships. It is of critical importance that policymakers and scientists are cognizant of the sociocultural dimension in management decisions, as overly simplistic approaches to addressing the perceptions, needs, and interests of local communities are likely to result in conservation impasses [78]. Ultimately, if the knowledge gained through research is unable to be contextualized in a manner, which can be readily assimilated and applied, efforts, which would otherwise preserve and enhance ecosystem structure and function while simultaneously meeting the needs of the local populous are likely doomed to failure. Longitudinal and lateral dimensions inherent to watershed-wide riparian reserves will account not only local species richness (alpha diversity) but also between-habitat species turnover (beta diversity) and landscape-scale diversity (gamma diversity) [34]. We encourage state and federal conservation authorities to use these biodiversity metrics to rationalize conservation-focused decision-making.

7. Conclusive Remarks

We advocate for watershed-scale delineation of variable-width riparian buffers with multiple conservation and management objectives in place of conventional reach-scale, uniform-width approaches. Watershed-wide riparian conservation should draw from a robust ecological knowledge base and conform to the dynamics of riparian-zone ecosystem structure and functions, especially with respect to life and natural histories of local and regional species. Herein, we stress the need to protect diverse arrays of habitats—lentic, lotic, and wetland systems as well as floodplains and upland environments—to preserve landscape-scale heterogeneity, thereby configuring and enhancing connectivity. Riparian buffers are cornerstones for landscape-scale conservation planning and pave

a pathway for not only riverscape conservation but also for freshwater protected-area networks. The incongruity between freshwater versus terrestrial protected areas has frequently emerged as a significant conservation challenge, yet little action has been taken to remedy this problem. Riparian buffers define an ecologically meaningful nexus between both stream channels and terrestrial environments, protect and buffer core aquatic habitats, and provide critical resources for biota along the aquatic-terrestrial continuum. Hence, riparian-buffer conservation and management, particularly when implemented at the watershed scale, may have the potential to harmonize disparate conservation goals pertinent to freshwater and terrestrial protected areas.

Author Contributions: T.D.S. developed the concept for this review and provided the overall structure for the manuscript layout and contents, collected relevant literature, subsequently contributed to writing. A.K.D. produced the initial several rounds of drafts. M.P.G. reorganized and rearranged the manuscript layout, tailored it towards a broader audience, and finalized the writing. All authors have read and agreed to the published version of the manuscript.

Funding: This research was funded by the Office of Undergraduate Research at Bridgewater State University.

Acknowledgments: We thank the Office of Undergraduate Research at Bridgewater State University for supporting the student engagement in this research. We also thank Z. Schumacher for his assistance in development of figures used in this manuscript and two anonymous reviewers (R1 and R3) for providing constructive feedback.

Conflicts of Interest: The authors declare no conflict of interest.

References

1. Oakley, A.L.; Collins, J.; Everson, L.; Heller, D.; Howerton, J.; Vincent, R. Riparian zones and freshwater wetlands. In *Management of Wildlife and Fish Habitats in Forest of Western Oregon and Washington*; US Department of Agriculture, Forest Service: Pacific Northwest Region, USA, 1985; pp. 57–80.
2. Blinn, C.R.; Kilgore, M.A. Riparian management practices: A summary of state guidelines. *J. For.* **2001**, *99*, 11–17.
3. Naiman, R.J.; Decamps, H. The ecology of interfaces: Riparian zones. *Annu. Rev. Ecol. Syst.* **1997**, *28*, 621–658. [CrossRef]
4. Gregory, S.V.; Swanson, F.J.; McKee, W.A.; Cummins, K.W. An ecosystem perspective of riparian zones. *Bioscience* **1991**, *41*, 540–551. [CrossRef]
5. Capon, S.J.; Chambers, L.E.; Mac Nally, R.; Naiman, R.J.; Davies, P.; Marshall, N.; Pittock, J.; Reid, M.; Capon, T.; Douglas, M. Riparian ecosystems in the 21st century: Hotspots for climate change adaptation? *Ecosystems* **2013**, *16*, 359–381. [CrossRef]
6. Erős, T.; Lowe, W.H. The landscape ecology of rivers: From patch-based to spatial network analyses. *Curr. Landsc. Ecol. Rep.* **2019**, *4*, 103–112. [CrossRef]
7. Stanford, J.A.; Alexander, L.C.; Whited, D.C. Chapter 1—Riverscapes. In *Methods in Stream Ecology*, 3rd ed.; Hauer, F.R., Lamberti, G.A., Eds.; Academic Press: Boston, MA, USA, 2017; Volume 1, pp. 3–19. [CrossRef]
8. Torgersen, C.E.; Le Pichon, C.; Fullerton, A.H.; Dugdale, S.J.; Duda, J.J.; Giovannini, F.; Tales, É.; Belliard, J.; Branco, P.; Bergeron, N.E. Riverscape approaches in practice: Perspectives and applications. *Biol. Rev.* **2021**. [CrossRef] [PubMed]
9. Peipoch, M.; Brauns, M.; Hauer, F.R.; Weitere, M.; Valett, H.M. Ecological simplification: Human influences on riverscape complexity. *Bioscience* **2015**, *65*, 1057–1065. [CrossRef]
10. Carbonneau, P.; Fonstad, M.A.; Marcus, W.A.; Dugdale, S.J. Making riverscapes real. *Geomorphology* **2012**, *137*, 74–86. [CrossRef]
11. Fausch, K.D.; Torgersen, C.E.; Baxter, C.V.; Li, H.W. Landscapes to Riverscapes: Bridging the Gap between Research and Conservation of Stream Fishes: A Continuous View of the River is Needed to Understand How Processes Interacting among Scales Set the Context for Stream Fishes and Their Habitat. *Bioscience* **2002**, *52*, 483–498. [CrossRef]
12. Benda, L.; Poff, N.L.; Miller, D.; Dunne, T.; Reeves, G.; Pess, G.; Pollock, M. The Network Dynamics Hypothesis: How Channel Networks Structure Riverine Habitats. *Bioscience* **2004**, *54*, 413–427. [CrossRef]
13. Thorp, J.H.; Thoms, M.C.; Delong, M.D. The riverine ecosystem synthesis: Biocomplexity in river networks across space and time. *River Res. Appl.* **2006**, *22*, 123–147. [CrossRef]
14. Davis, C.D.; Epps, C.W.; Flitcroft, R.L.; Banks, M.A. Refining and defining riverscape genetics: How rivers influence population genetic structure. *Wiley Interdiscip. Rev. Water* **2018**, *5*, e1269. [CrossRef]
15. Sabo, J.L.; Sponseller, R.; Dixon, M.; Gade, K.; Harms, T.; Heffernan, J.; Jani, A.; Katz, G.; Soykan, C.; Watts, J. Riparian zones increase regional species richness by harboring different, not more, species. *Ecology* **2005**, *86*, 56–62. [CrossRef]
16. Shafroth, P.B.; Friedman, J.M.; Auble, G.T.; Scott, M.L.; Braatne, J.H. Potential Responses of Riparian Vegetation to Dam Removal: Dam removal generally causes changes to aspects of the physical environment that influence the establishment and growth of riparian vegetation. *Bioscience* **2002**, *52*, 703–712. [CrossRef]
17. Castelle, A.J.; Johnson, A.; Conolly, C. Wetland and stream buffer size requirements—A review. *J. Environ. Qual.* **1994**, *23*, 878–882. [CrossRef]

18. Anbumozhi, V.; Radhakrishnan, J.; Yamaji, E. Impact of riparian buffer zones on water quality and associated management considerations. *Ecol. Eng.* **2005**, *24*, 517–523. [CrossRef]
19. Vidon, P.; Allan, C.; Burns, D.; Duval, T.P.; Gurwick, N.; Inamdar, S.; Lowrance, R.; Okay, J.; Scott, D.; Sebestyen, S. Hot spots and hot moments in riparian zones: Potential for improved water quality management. *J. Am. Water Resour. Assoc.* **2010**, *46*, 278–298. [CrossRef]
20. Marczak, L.B.; Sakamaki, T.; Turvey, S.L.; Deguise, I.; Wood, S.L.; Richardson, J.S. Are forested buffers an effective conservation strategy for riparian fauna? An assessment using meta-analysis. *Ecol. Appl.* **2010**, *20*, 126–134. [CrossRef] [PubMed]
21. Lee, P.; Smyth, C.; Boutin, S. Quantitative review of riparian buffer width guidelines from Canada and the United States. *J. Environ. Manag.* **2004**, *70*, 165–180. [CrossRef] [PubMed]
22. Noon, B.R.; Blakesley, J.A. Conservation of the northern spotted owl under the Northwest Forest Plan. *Conserv. Biol.* **2006**, *20*, 288–296. [CrossRef] [PubMed]
23. Richardson, J.S.; Taylor, E.; Schluter, D.; Pearson, M.; Hatfield, T. Do riparian zones qualify as critical habitat for endangered freshwater fishes? *Can. J. Fish Aquat. Sci.* **2010**, *67*, 1197–1204. [CrossRef]
24. Odum, E.P. *Ecological Importance of the Riparian Zone*; General Technical Report WO-US; Department of Agriculture, Forest Service: Washington, D.C., USA, 1979.
25. Semlitsch, R.D.; Bodie, J.R. Biological criteria for buffer zones around wetlands and riparian habitats for amphibians and reptiles. *Conserv. Biol.* **2003**, *17*, 1219–1228. [CrossRef]
26. Surasinghe, T.D.; Baldwin, R.F. Importance of riparian forest buffers in conservation of stream biodiversity: Responses to land uses by stream-associated salamanders across two southeastern temperate ecoregions. *J. Herpetol.* **2015**, *49*, 83–94. [CrossRef]
27. Baldwin, R.F.; Demaynadier, P.G. Assessing threats to pool-breeding amphibian habitat in an urbanizing landscape. *Biol. Conserv.* **2009**, *142*, 1628–1638. [CrossRef]
28. Raedeke, K. *Streamside Management: Riparian Wildlife and Forest Interactions*; Contribution Number 59; Institute of Forest Resources, University of Washington: Seatle, WA, USA, 1989.
29. National Research Council; Committee on Riparian Zone Functioning and Strategies for Management; Water Science and Technology Board; Board on Environmental Studies and Toxicology; Division on Earth and Life Studies. *Riparian Areas: Functions and Strategies for Management*; National Academies Press: Washington, DC, USA, 2002.
30. Lindenmayer, D.; Hobbs, R.J.; Montague-Drake, R.; Alexandra, J.; Bennett, A.; Burgman, M.; Cale, P.; Calhoun, A.; Cramer, V.; Cullen, P.; et al. A checklist for ecological management of landscapes for conservation. *Ecol. Lett.* **2008**, *11*, 78–91. [CrossRef] [PubMed]
31. de Maynadier, P.G.; Hunter, M.L. The relationship between forest management and amphibian ecology: A review of the North American literature. *Environ. Rev.* **1995**, *3*, 230–261. [CrossRef]
32. O'Keefe, J.M.; Loeb, S.C.; Gerard, P.D.; Lanham, J.D. Effects of riparian buffer width on activity and detection of common bats in the southern Appalachian Mountains. *Wildl. Soc. Bull.* **2013**, *37*, 319–326. [CrossRef]
33. Darveau, M.; Beauchesne, P.; Belanger, L.; Huot, J.; Larue, P. Riparian forest strips as habitat for breeding birds in boreal forest. *J. Wildl. Manag.* **1995**, *59*, 67–78. [CrossRef]
34. Knopf, F.L.; Johnson, R.R.; Rich, T.; Samson, F.B.; Szaro, R.C. Conservation of riparian ecosystems in the United States. *Wilson Bull.* **1988**, *100*, 272–284.
35. Olson, D.H.; Anderson, P.D.; Frissell, C.A.; Welsh, H.H.; Bradford, D.F. Biodiversity management approaches for stream–riparian areas: Perspectives for Pacific Northwest headwater forests, microclimates, and amphibians. *Ecol. Manag.* **2007**, *246*, 81–107. [CrossRef]
36. Kuglerová, L.; Ågren, A.; Jansson, R.; Laudon, H. Towards optimizing riparian buffer zones: Ecological and biogeochemical implications for forest management. *Ecol. Manag.* **2014**, *334*, 74–84. [CrossRef]
37. Spackman, S.C.; Hughes, J.W. Assessment of minimum stream corridor width for biological conservation: Species richness and distribution along mid-order streams in Vermont, USA. *Biol. Conserv.* **1995**, *71*, 325–332. [CrossRef]
38. Bodie, J. Stream and riparian management for freshwater turtles. *J. Environ. Manag.* **2001**, *62*, 443–455. [CrossRef] [PubMed]
39. Lovell, S.T.; Sullivan, W.C. Environmental benefits of conservation buffers in the United States: Evidence, promise, and open questions. *Agric. Ecosyst. Environ.* **2006**, *112*, 249–260. [CrossRef]
40. Allan, J.D.; Castillo, M.M. *Stream Ecology: Structure and Function of Running Waters*; Springer: Dordrecht, The Netherlands, 2007.
41. Allan, J.D. Landscapes and riverscapes: The influence of land use on stream ecosystems. *Annu. Rev. Ecol. Evol. Syst.* **2004**, *35*, 257–284. [CrossRef]
42. Pusey, B.J.; Arthington, A.H. Importance of the riparian zone to the conservation and management of freshwater fish: A review. *Mar. Freshw. Res.* **2003**, *54*, 1–16. [CrossRef]
43. Ekness, P.; Randhir, T. Effects of riparian areas, stream order, and land use disturbance on watershed-scale habitat potential: An ecohydrologic approach to policy. *J. Am. Water Resour. Assoc.* **2007**, *43*, 1468–1482. [CrossRef]
44. Warren, D.R.; Keeton, W.S.; Kiffney, P.M.; Kaylor, M.J.; Bechtold, H.A.; Magee, J. Changing forests—Changing streams: Riparian forest stand development and ecosystem function in temperate headwaters. *Ecosphere* **2016**, *7*, e01435. [CrossRef]
45. Finlay, J.C. Stream size and human influences on ecosystem production in river networks. *Ecosphere* **2011**, *2*, art87. [CrossRef]
46. Lobón-Cerviá, J.; Mazzoni, R.; Rezende, C.F. Effects of riparian forest removal on the trophic dynamics of a Neotropical stream fish assemblage. *J. Fish Biol.* **2016**, *89*, 50–64. [CrossRef] [PubMed]

47. Lorion, C.M.; Kennedy, B.P. Riparian forest buffers mitigate the effects of deforestation on fish assemblages in tropical headwater streams. *Ecol. Appl.* **2009**, *19*, 468–479. [CrossRef] [PubMed]
48. Broadmeadow, S.; Nisbet, T. The effects of riparian forest management on the freshwater environment: A literature review of best management practice. *Hydrol. Earth Syst. Sci. Discuss.* **2004**, *8*, 286–305. [CrossRef]
49. Pitt, A.L.; Nickerson, M.A. Reassessment of the Turtle Community in the North Fork of White River, Ozark County, Missouri. *Copeia* **2012**, *2012*, 367–374. [CrossRef]
50. Brown, G.P.; Weatherhead, P.J. Thermal ecology and sexual size dimorphism in northern water snakes, Nerodia sipedon. *Ecol. Monogr.* **2000**, *70*, 311–330. [CrossRef]
51. Mcelfish, J.; James, M.; Kihslinger, R.; Nichols, S. Setting Buffer sizes for Wetlands. *Nat. Wetl. Newsl.* **2008**, *30*, 6–17.
52. Hickey, M.B.C.; Doran, B. A review of the efficiency of buffer strips for the maintenance and enhancement of riparian ecosystems. *Water Qual. Res. J.* **2004**, *39*, 311–317. [CrossRef]
53. Osborne, L.L.; Kovacic, D.A. Riparian vegetated buffer strips in water-quality restoration and stream management. *Freshw. Biol.* **1993**, *29*, 243–258. [CrossRef]
54. Muenz, T.K.; Golladay, S.W.; Vellidis, G.; Smith, L.L. Stream buffer effectiveness in an agriculturally influenced area, southwestern Georgia: Responses of water quality, macroinvertebrates, and amphibians. *J. Environ. Qual.* **2006**, *35*, 1924–1938. [CrossRef]
55. Wilkerson, E.; Hagan, J.M.; Siegel, D.; Whitman, A.A. The effectiveness of different buffer widths for protecting headwater stream temperature in Maine. *Science* **2006**, *52*, 221–231.
56. Roberts, H.P.; Jones, M.T.; Willey, L.L.; Akre, T.S.B.; Sievert, P.R.; de Maynadier, P.; Gipe, K.D.; Johnson, G.; Kleopfer, J.; Marchand, M.; et al. Large-scale collaboration reveals landscape-level effects of land-use on turtle demography. *Glob. Ecol. Conserv.* **2021**, *30*, e01759. [CrossRef]
57. Marchand, M.N.; Litvaitis, J.A. Effects of habitat features and landscape composition on the population structure of a common aquatic turtle in a region undergoing rapid development. *Conserv. Biol.* **2004**, *18*, 758–767. [CrossRef]
58. Abell, R. Conservation biology for the biodiversity crisis: A freshwater follow-up. *Conserv. Biol.* **2002**, *16*, 1435–1437. [CrossRef]
59. Brinson, M.M.; Malvarez, A.I. Temperate freshwater wetlands: Types, status, and threats. *Environ. Conserv.* **2002**, *29*, 115–133. [CrossRef]
60. Sinokrot, B.A.; Stefan, H.G. Stream temperature dynamics: Measurements and modeling. *Water Resour. Res.* **1993**, *29*, 2299–2312. [CrossRef]
61. Dudgeon, D.; Arthington, A.H.; Gessner, M.O.; Kawabata, Z.I.; Knowler, D.J.; Leveque, C.; Naiman, R.J.; Prieur-Richard, A.H.; Soto, D.; Stiassny, M.L.J.; et al. Freshwater biodiversity: Importance, threats, status and conservation challenges. *Biol. Rev.* **2006**, *81*, 163–182. [CrossRef] [PubMed]
62. Naiman, R.J.; Decamps, H.; Pollock, M. The role of riparian corridors in maintaining regional biodiversity. *Ecol. Appl.* **1993**, *3*, 209–212. [CrossRef]
63. Hunt, S.D.; Guzy, J.C.; Price, S.J.; Halstead, B.J.; Eskew, E.A.; Dorcas, M.E. Responses of riparian reptile communities to damming and urbanization. *Biol. Conserv.* **2013**, *157*, 277–284. [CrossRef]
64. Sterrett, S.; Smith, L.; Golladay, S.; Schweitzer, S.; Maerz, J. The conservation implications of riparian land use on river turtles. *Anim. Conserv.* **2010**, *14*, 38–46. [CrossRef]
65. Ward, J.V. Riverine landscapes: Biodiversity patterns, disturbance regimes, and aquatic conservation. *Biol. Conserv.* **1998**, *83*, 269–278. [CrossRef]
66. US Army Corps of Engineers. National Inventory of Dams; USACE, NID, USA, 2013. Available online: https://nid.usace.army.mil/#/ (accessed on 1 December 2021).
67. Poff, N.L.; Hart, D.D. How Dams Vary and Why It Matters for the Emerging Science of Dam Removal: An ecological classification of dams is needed to characterize how the tremendous variation in the size, operational mode, age, and number of dams in a river basin influences the potential for restoring regulated rivers via dam removal. *AIBS Bull.* **2002**, *52*, 659–668.
68. Bednarek, A.T. Undamming rivers: A review of the ecological impacts of dam removal. *Environ. Manag.* **2001**, *27*, 803–814. [CrossRef] [PubMed]
69. McKinney, M.L.; Lockwood, J.L. Biotic homogenization: A sequential and selective process. In *Biotic Homogenization*; Springer: Boston, MA, USA, 2001; pp. 1–17.
70. Scott, M.C. Winners and losers among stream fishes in relation to land use legacies and urban development in the southeastern US. *Biol. Conserv.* **2006**, *127*, 301–309. [CrossRef]
71. Scott, M.C.; Helfman, G.S. Native invasions, homogenization, and the mismeasure of integrity of fish assemblages. *Fisheries* **2001**, *26*, 6–15. [CrossRef]
72. Woolmer, G.; Trombulak, S.C.; Ray, J.C.; Doran, P.J.; Anderson, M.G.; Baldwin, R.F.; Morgan, A.; Sanderson, E.W. Rescaling the human footprint: A tool for conservation planning at an ecoregional scale. *Landsc. Urban Plan* **2008**, *87*, 42–53. [CrossRef]
73. Keddy, P.A.; Fraser, L.H.; Solomeshch, A.I.; Junk, W.J.; Campbell, D.R.; Arroyo, M.T.; Alho, C.J. Wet and wonderful: The world's largest wetlands are conservation priorities. *Bioscience* **2009**, *59*, 39–51. [CrossRef]
74. Baldwin, R.F.; Trombulak, S.C.; Baldwin, E.D. Assessing risk of large-scale habitat conversion in lightly settled landscapes. *Landsc. Urban Plan* **2009**, *91*, 219–225. [CrossRef]
75. Marcouiller, D.W.; Clendenning, J.G.; Kedzior, R. Natural amenity-led development and rural planning. *J. Plan. Lit.* **2002**, *16*, 515–542. [CrossRef]

76. Zelnik, I.; Mavrič Klenovšek, V.; Gaberščik, A. Complex undisturbed riparian zones are resistant to colonisation by invasive alien plant species. *Water* **2020**, *12*, 345. [CrossRef]
77. Richardson, J.S.; Naiman, R.J.; Bisson, P.A. How did fixed-width buffers become standard practice for protecting freshwaters and their riparian areas from forest harvest practices? *Freshw. Sci.* **2012**, *31*, 232–238. [CrossRef]
78. Dufour, S.; Rodríguez-González, P.M.; Laslier, M. Tracing the scientific trajectory of riparian vegetation studies: Main topics, approaches and needs in a globally changing world. *Sci. Total Environ.* **2019**, *653*, 1168–1185. [CrossRef]
79. Benke, A.C. A perspective on America's vanishing streams. *J. N. Am. Benthol. Soc.* **1990**, *9*, 77–88. [CrossRef]
80. Russell, K.R.; Wigley, T.B.; Baughman, W.M.; Hanlin, H.G.; Ford, W.M. *Responses of Southeastern Amphibians and Reptiles to Forest Management: A Review. General Technical Report SRS–75*; US Department of Agriculture, Forest Service, Southern Research Station: Asheville, NC, USA, 2004; Chapter 27; pp. 319–334.
81. Ficetola, G.F.; Padoa-Schioppa, E.; De Bernardi, F. Influence of landscape elements in riparian buffers on the conservation of semiaquatic amphibians. *Conserv. Biol.* **2009**, *23*, 114–123. [CrossRef]
82. Forest Ecosystem Management Assessment Team. *Forest Ecosystem Management: An Ecological, Economic, and Social Assessment: Report of the Forest Ecosystem Management Assessment Team*; U.S. Government Printing Office: Washington, DC, USA, 1993.
83. Maisonneuve, C.; Rioux, S. Importance of riparian habitats for small mammal and herpetofaunal communities in agricultural landscapes of southern Québec. *Agric. Ecosyst. Environ.* **2001**, *83*, 165–175. [CrossRef]
84. Olson, D.H.; Burnett, K.M. Design and management of linkage areas across headwater drainages to conserve biodiversity in forest ecosystems. *For. Ecol. Manag.* **2009**, *258*, S117–S126. [CrossRef]
85. Schultz, R.; Isenhart, T.; Simpkins, W.; Colletti, J. Riparian forest buffers in agroecosystems–lessons learned from the Bear Creek Watershed, central Iowa, USA. *Agrofor. Syst.* **2004**, *61*, 35–50.
86. Apel, H.; Merz, B.; Thieken, A.H. Quantification of uncertainties in flood risk assessments. *Int. J. River Basin Manag.* **2008**, *6*, 149–162. [CrossRef]
87. Winsemius, H.; Van Beek, L.; Jongman, B.; Ward, P.; Bouwman, A. A framework for global river flood risk assessments. *Hydrol. Earth Syst. Sci.* **2013**, *17*, 1871–1892. [CrossRef]
88. Lambert, J.D.; Hannon, S.J. Short-term effects of timber harvest on abundance, territory characteristics, and pairing success of ovenbirds in riparian buffer strips. *Auk* **2000**, *117*, 687–698. [CrossRef]
89. Olson, D.H.; Leirness, J.B.; Cunningham, P.G.; Steel, E.A. Riparian buffers and forest thinning: Effects on headwater vertebrates 10 years after thinning. *Ecol. Manag.* **2014**, *321*, 81–93. [CrossRef]
90. Roe, J.H.; Georges, A. Heterogeneous wetland complexes, buffer zones, and travel corridors: Landscape management for freshwater reptiles. *Biol. Conserv.* **2007**, *135*, 67–76. [CrossRef]
91. Brown, B.L.; Swan, C.M.; Auerbach, D.A.; Grant, E.H.C.; Hitt, N.P.; Maloney, K.O.; Patrick, C. Metacommunity theory as a multispecies, multiscale framework for studying the influence of river network structure on riverine communities and ecosystems. *J. N. Am. Benthol. Soc.* **2011**, *30*, 310–327. [CrossRef]
92. Rundio, D.E.; Olson, D.H. Influence of headwater site conditions and riparian buffers on terrestrial salamander response to forest thinning. *Science* **2007**, *53*, 320–330.
93. Burbrink, F.T.; Phillips, C.A.; Heske, E.J. A riparian zone in southern Illinois as a potential dispersal corridor for reptiles and amphibians. *Biol. Conserv.* **1998**, *86*, 107–115. [CrossRef]
94. Barrett, K.; Price, S.J. Urbanization and stream salamanders: A review, conservation options, and research needs. *Freshw. Sci.* **2014**, *33*, 927–940. [CrossRef]
95. Kluber, M.R.; Olson, D.H.; Puettmann, K.J. Amphibian distributions in riparian and upslope areas and their habitat associations on managed forest landscapes in the Oregon Coast Range. *Ecol. Manag.* **2008**, *256*, 529–535. [CrossRef]
96. Kauffman, J.B.; Beschta, R.L.; Otting, N.; Lytjen, D. An ecological perspective of riparian and stream restoration in the western United States. *Fisheries* **1997**, *22*, 12–24. [CrossRef]
97. Foley, M.M.; Bellmore, J.; O'Connor, J.E.; Duda, J.J.; East, A.E.; Grant, G.; Anderson, C.W.; Bountry, J.A.; Collins, M.J.; Connolly, P.J. Dam removal: Listening in. *Water Resour. Res.* **2017**, *53*, 5229–5246. [CrossRef]
98. Brooks, R.T.; Nislow, K.H.; Lowe, W.H.; Wilson, M.K.; King, D.I. Forest succession and terrestrial–aquatic biodiversity in small forested watersheds: A review of principles, relationships and implications for management. *Forestry* **2012**, *85*, 315–328. [CrossRef]
99. Hough, P.; Robertson, M. Mitigation under Section 404 of the Clean Water Act: Where it comes from, what it means. *Wetl. Ecol. Manag.* **2009**, *17*, 15–33. [CrossRef]
100. Wohl, E. Forgotten Legacies: Understanding and Mitigating Historical Human Alterations of River Corridors. *Water Resour. Res.* **2019**, *55*, 5181–5201. [CrossRef]
101. Stewart, K.J.; Mallik, A.U. Bryophyte responses to microclimatic edge effects across riparian buffers. *Ecol. Appl.* **2006**, *16*, 1474–1486. [CrossRef]
102. Richardson, J.S.; Naiman, R.J.; Swanson, F.J.; Hibbs, D.E. Riparian communities associated with pacific northwest headwater streams: Assemblages, processes, and uniqueness. *J. Am. Water Resour. Assoc.* **2005**, *41*, 935–947. [CrossRef]
103. Naiman, R.J.; Bilby, R.E.; Bisson, P.A. Riparian ecology and management in the Pacific coastal rain forest. *Bioscience* **2000**, *50*, 996–1011. [CrossRef]
104. Nel, J.L.; Roux, D.J.; Abell, R.; Ashton, P.J.; Cowling, R.M.; Higgins, J.V.; Thieme, M.; Viers, J.H. Progress and challenges in freshwater conservation planning. *Aquat. Conserv. Mar. Freshw. Ecosyst.* **2009**, *19*, 474–485. [CrossRef]

105. Tullos, D.D.; Collins, M.J.; Bellmore, J.R.; Bountry, J.A.; Connolly, P.J.; Shafroth, P.B.; Wilcox, A.C. Synthesis of common management concerns associated with dam removal. *JAWRA J. Am. Water Resour. Assoc.* **2016**, *52*, 1179–1206. [CrossRef]
106. Kondolf, G.M. Setting goals in river restoration: When and where can the river "heal itself". *Stream Restor. Dyn. Fluv. Syst.* **2011**, *194*, 29–43.
107. Ollero, A. Channel changes and floodplain management in the meandering middle Ebro River, Spain. *Geomorphology* **2010**, *117*, 247–260. [CrossRef]
108. Bellmore, J.R.; Pess, G.R.; Duda, J.J.; O'Connor, J.E.; East, A.E.; Foley, M.M.; Wilcox, A.C.; Major, J.J.; Shafroth, P.B.; Morley, S.A.; et al. Conceptualizing Ecological Responses to Dam Removal: If You Remove It, What's to Come? *Bioscience* **2019**, *69*, 26–39. [CrossRef] [PubMed]
109. Semlitsch, R.D.; Todd, B.D.; Blomquist, S.M.; Calhoun, A.J.K.; Gibbons, J.W.; Gibbs, J.P.; Graeter, G.J.; Harper, E.B.; Hocking, D.J.; Hunter, M.L., Jr.; et al. Effects of Timber Harvest on Amphibian Populations: Understanding Mechanisms from Forest Experiments. *Bioscience* **2009**, *59*, 853–862. [CrossRef]
110. National Research Council. *Compensating for Wetland Losses under the Clean Water Act*; National Academies Press: Washington, DC, USA, 2001.
111. Noss, R.F.; O'Connell, M.; Murphy, D.D. *The science of Conservation Planning: Habitat Conservation under the Endangered Species Act*; Island Press: Washington, DC, USA, 1997.
112. Jachowski, C.M.B.; Hopkins, W.A. Loss of catchment-wide riparian forest cover is associated with reduced recruitment in a long-lived amphibian. *Biol. Conserv.* **2018**, *220*, 215–227. [CrossRef]
113. Abell, R.; Allan, J.D.; Lehner, B. Unlocking the potential of protected areas for freshwaters. *Biol. Conserv.* **2007**, *134*, 48–63. [CrossRef]
114. Calhoun, A.J.; Miller, N.A.; Klemens, M.W. Conserving pool-breeding amphibians in human-dominated landscapes through local implementation of Best Development Practices. *Wetl. Ecol. Manag.* **2005**, *13*, 291–304. [CrossRef]
115. González, E.; Felipe-Lucia, M.R.; Bourgeois, B.; Boz, B.; Nilsson, C.; Palmer, G.; Sher, A.A. Integrative conservation of riparian zones. *Biol. Conserv.* **2017**, *211*, 20–29. [CrossRef]
116. Teels, B.M.; Rewa, C.A.; Myers, J. Aquatic condition response to riparian buffer establishment. *Wildl. Soc. Bull.* **2006**, *34*, 927–935. [CrossRef]
117. Biron, P.M.; Buffin-Bélanger, T.; Larocque, M.; Choné, G.; Cloutier, C.-A.; Ouellet, M.-A.; Demers, S.; Olsen, T.; Desjarlais, C.; Eyquem, J. Freedom space for rivers: A sustainable management approach to enhance river resilience. *Environ. Manag.* **2014**, *54*, 1056–1073. [CrossRef] [PubMed]
118. Beechie, T.J.; Sear, D.A.; Olden, J.D.; Pess, G.R.; Buffington, J.M.; Moir, H.; Roni, P.; Pollock, M.M. Process-based Principles for Restoring River Ecosystems. *Bioscience* **2010**, *60*, 209–222. [CrossRef]

diversity

MDPI

Article

Spatial Variability in a Symbiont-Diverse Marine Host and the Use of Observational Data to Assess Ecological Interactions

Edwin Cruz-Rivera [1,*], Mohy-El-Din Sherif [2], Salma El-Sahhar [3] and Thomas Lombardi [4]

[1] Bioenvironmental Science Program, Department of Biology, Morgan State University, 1700 E. Cold Spring Lane, Baltimore, MD 21251, USA
[2] AB Vista NIR Services, AB Agri, Paulerspury N12 7LS, UK; mohyeldin.sherif@abagri.org
[3] School of Life Sciences, University of Essex, Colchester CO4 3SQ, UK; salma.elsahhar@essex.ac.uk
[4] Department of Information Systems and Technology, University of the Virgin Islands, #2 John Brewers Bay, St. Thomas, VI 00802, USA; thomas.lombardi@uvi.edu
* Correspondence: edwin.cruz-rivera@morgan.edu

Abstract: Despite a rich taxonomic literature on the symbionts of ascidians, the nature of these symbioses remains poorly understood. In the Egyptian Red Sea, the solitary ascidian *Phallusia nigra* hosted a symbiotic amphipod and four copepod species, with densities as high as 68 mixed symbionts per host. Correlation analyses suggested no competition or antagonism between symbionts. Ascidian mass, ash-free dry mass per wet mass (AFDM/WM), and both symbiont density and diversity per host, differed significantly among three reefs from El Gouna, Egypt. However, there was no correlation between amphipod, total copepod, or total symbiont densities and host mass or AFDM/WM. A host condition index based on body to tunic mass ratio was significantly related to symbiont density overall, but this positive pattern was only strong at a single site studied. Despite assumptions based on the habit of some of the symbiont groups, our analyses detected little effect of symbionts on host health, suggesting a commensal relationship.

Keywords: ascidian; *Bonnierilla*; *Doropygus*; *Janstockia*; *Leucothoe*; *Styelicola*; Notodelphyidae; *Phallusia nigra*; Red Sea

Citation: Cruz-Rivera, E.; Sherif, M.-E.-D.; El-Sahhar, S.; Lombardi, T. Spatial Variability in a Symbiont-Diverse Marine Host and the Use of Observational Data to Assess Ecological Interactions. *Diversity* **2022**, *14*, 197. https://doi.org/10.3390/d14030197

Academic Editor: Bert W. Hoeksema

Received: 13 January 2022
Accepted: 4 March 2022
Published: 7 March 2022

1. Introduction

Many marine symbioses are poorly understood and have been often classified based on the taxonomy of the animals involved rather than on quantification of costs and benefits [1–3]. While taxon-based inferences have been informative and often correct, they can obscure fundamental differences in the nature of interactions within a clade and the context dependence of symbioses within a parasitism to mutualism continuum [4–8]. For example, apicomplexan protozoa, which have been largely treated as parasites/pathogens, have been increasingly reported as commensals and mutualists of marine invertebrates and vertebrates [9–12]. A recent article on the purported symbiont diversity of the snail *Littorina littorea* (Linnaeus, 1758) also highlights the perils of assuming symbiont roles without considering alternative hypotheses and the complexity of natural interactions [13]. In that study, a more rigorous sampling within a community context elucidated that previously classified snail endosymbionts were, in fact, transient associates trapped in the mucus matrix secreted by the snail.

A cost–benefit analysis of a pairwise interaction within a community context can elucidate the outcome (and ecological classification) of the association between symbiont and host. A manipulative approach in which hosts and symbionts are grown independently from one another, and together, could offer an ideal method to quantify fitness effects for each interacting species. However, this is not feasible in most cases of obligate symbioses and is difficult to achieve when life cycles require multiple hosts or when endosymbiont presence cannot be confirmed without sacrificing the host.

An alternative approach is to take advantage of a natural experiment: sampling of host populations, and comparing fitness of hosts that harbor differing numbers and kinds of symbionts. While such a method only provides information on the host, it can reveal important density-dependent effects as symbiont loads can change in time and space and the nature of the symbiosis can change along a gradient [7,8,14,15]. Sampling natural symbiont populations can also help unravel interactions between multiple symbionts that inhabit the same host [16]. An important consideration in applying this framework is determining what components of host health or fitness can be measured. Techniques such as calculating gonadosomatic or condition indices have been fundamental in assessing how environmental variables affect allometric relations, life history, structural traits, basic health, and fitness components in aquatic and terrestrial animals [17–26]. In shellfish aquaculture, for example, body to shell mass ratios are widely used proxies of animal health [18,19]. Similar approaches have been applied to more ecological studies of echinoderms [21,22], gastropods [27], bivalves [28], and tube-dwelling polychaetes [29], among others.

Here we use two body condition proxies to evaluate the effects of symbiotic crustaceans on the sea squirt *Phallusia nigra* Savingny, 1816 (Tunicata: Ascidiacea). While believed to be a Red Sea endemic by some, this solitary ascidian has a worldwide distribution and serves as host to several invertebrate symbionts [30,31]. It is a shallow-water species found on hard natural and artificial bottoms at depths of up to 14 m [32–34]. Adults are 4–12 cm long and reproduce throughout the year [32,35]. This ascidian is a common member of fouling communities around the world and recruits year-round, although it is more common at early successional community stages [32,36,37]. Population densities can fluctuate seasonally by an order of magnitude [32,38] and surpass $100/m^2$ within native and invaded ranges, with the highest recruitment densities recorded reaching $> 500/m^2$ in the Red Sea [38–40].

The tunic of *P. nigra* accumulates vanadium, acid, and other secondary metabolites, which serve as chemical defenses against predators and fouling organisms and have been proposed as mechanisms promoting the longevity of adults past the initial recruitment stages [41–43]. A diverse symbiont community has evolved to utilize this defended ascidian host around the world (Table 1). In the Red Sea alone, *P. nigra* hosts the amphipod *Leucothoe furina* (Savigny, 1816), a polychaete worm, and at least seven species of copepods that live within different parts of its body [44–48] (Table 1). Outside of this geographic area, five other amphipod symbionts have been reported from *P. nigra* in Belize, Cuba, Florida, Panama, Brazil and Venezuela (Table 1), although records of *L. spinicarpa* and *L. wuriti* from Brazil have been questioned [49,50]. A pinnotherid crab also inhabits *P. nigra* in the Caribbean [51]. Historically, ascidian amphipod symbionts have been considered commensals [45,52,53], whereas copepods have been classified as both commensals and parasites [54–56]. Rarely have these classifications been related to any host traits [14]. Here, we relate amphipod and copepod densities to three ascidian variables that can help elucidate the nature of the symbioses by detecting potential costs for the host. We also assess possible interactions between symbionts. By comparing animals from three reefs in the Red Sea, we evaluate the role of spatial variation in symbiont–host interactions.

Table 1. Listing of all symbionts reported from the ascidian *Phallusia nigra* around the world.

Symbiont	Geographic Location	References
Crustacea		
Amphipoda		
Amphilochus ascidicola Ortiz and Atienza, 2001	Caribbean (Venezuela)	[57]
Leucothoe angraensis Senna, Andrade, Ramos & Skinner, 2021	South Atlantic (Brazil)	[50]
L. flammosa Thomas and Klebba 2007	Caribbean (Cuba)	[57]
L. furina (Savigny, 1816)	Red Sea (Egypt)	[46]
L. spinicarpa (Abildgaard, 1789)	North Atlantic (USA)	[58]

Table 1. *Cont.*

Symbiont	Geographic Location	References
L. wuriti Thomas and Klebba 2007	North Atlantic (USA), Caribbean (Belize, Panama)	[49,52]
Brachiura		
Tunicotheres moseri (Rathbun, 1918)	Caribbean (Jamaica, Venezuela)	[35,51]
Copepoda		
Bonnierilla projecta Stock, 1967	Red Sea (Egypt, Erithrea)	[44,46]
Doropygus humilis [1] Stock, 1967	Red Sea (Egypt, Erithrea)	[44,46]
Janhius brevis [2] (Stock, 1967)	Red Sea (Erithrea)	[44]
Janstockia phallusiella Boxshall & Marchenkov, 2005	Red Sea (Egypt)	[46,59]
Lonchidiopsis tripes Stock, 1967	Red Sea (Erithrea)	[44]
Notodelphys ciliata Schellenberg, 1922	Red Sea (Egypt)	[60]
Notodelphys steinitzi Stock, 1967	Red Sea (Erithrea)	[44]
Paranotodelphys phallusiae (Gurney, 1927)	Red Sea (Egypt)	[61]
Styelicola omphalus Kim I.H., Cruz-Rivera, Sherif & El-Sahhar, 2016	Red Sea (Egypt)	[46]
Annelida		
Polychaeta		
Proceraea exoryxae Martin, Nygren & Cruz-Rivera, 2017	Red Sea (Egypt)	[47]

[1] As *D. apicatus* in [44]; [2] As *Prophioseides brevis* in [44].

2. Materials and Methods

Phallusia nigra were collected from each of three sites (n = 50) around El Gouna, on the Red Sea coast of Egypt (27°23′50.4″ N, 33°40′30.2″ E; Figure 1). Using SCUBA, animals were carefully detached from the substrate and placed individually in resealable plastic bags for transport to the John D. Gerhart Field Station (American University in Cairo, formerly). All organisms were collected with permission from the private administrators of Abu Tig Marina, Mövenpick Hotel, and Zeytouna Beach, as well as the El Gouna local authorities through the American University in Cairo. All specimens came from public areas. Only animals that could be retrieved intact were used in the study. Ascidians were collected randomly at 2–5 m depths along 30 m stretches from reefs around Abu Tig Marina (27°24′34.8″ N 33°40′55.1″ E), Mövenpick Hotel (27°23′41.6″ N 33°41′31.1″ E), and Zeytouna Beach (27°24′06.4″ N 33°41′09.8″ E). The areas of collection were approximately 850 m apart between reefs. All collections were performed over the same ten-day period in October to minimize temporal effects on faunal abundances. El-Gouna is one of the main beach tourism destinations in Egypt and the coastline has been modified by extensive dredging and construction over several decades [62–65]. Nearshore communities have been further affected by sewage and garden runoff and by activities from a local desalination plant [66]. As a result, most local reefs have now low coral, and high algal, cover. Despite being relatively close (ca. 850–900 m from one another), the three reefs sampled had noticeable differences in environmental quality. The reef closest to the Abu Tig Marina lies right off the mouth of the main channel where most charter and commercial boats transit in and out EL Gouna. Suspended sediments were consistently higher, and visibility was considerably lower, in this reef compared to Zeytouna and Mövenpick. Zeytouna had a higher amount of live coral and invertebrate diversity. This is an area frequented by divers and snorkelers and is managed by a private company that enforces fishing and collection restrictions. Mövenpick is southeast of Zeytouna and has a very shallow broad lagoon. Tourists are not discouraged from walking across the patch reefs and reef flat, where signs of trampling are common. However, the slope of the reef breaks several meters deeper than in the other two reefs and is less frequented by divers. While a few studies of environmental impacts for this area are available (e.g., [65,66]), they treat EL Gouna as a single region and, therefore, our description of single reefs is based on qualitative observations over three years of collecting at these sites.

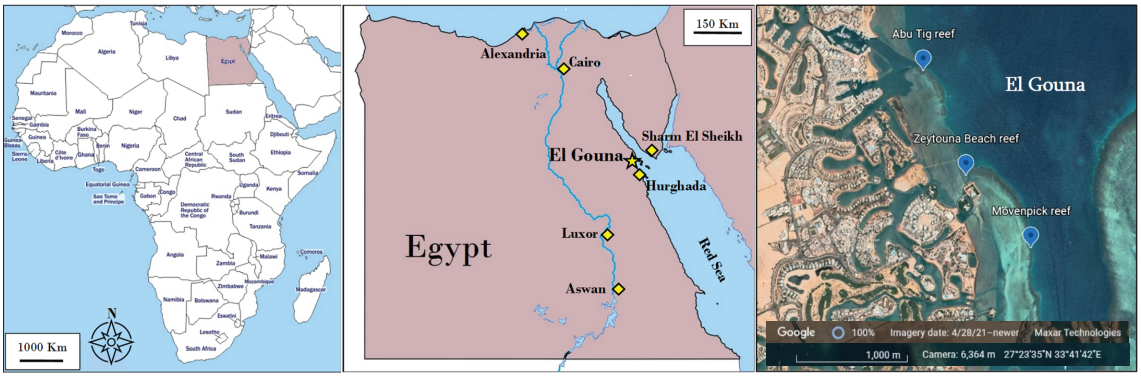

Figure 1. Location of the three reefs in El Gouna, on the Egyptian Red Sea coast, where collections took place. Maps adapted from d-maps.com (https://d-maps.com/carte.php?num_car=4338&lang=en and https://d-maps.com/carte.php?num_car=916&lang=en) and Google Earth (https://earth.google.com/web/).

In the lab, ascidians were dissected by making a peripheral incision and separating each *P. nigra* into two halves [46] (Figure 2). The body of ascidians is encased in a protective outer organic layer called the tunic. This is a carbohydrate-based pliable exoskeleton secreted by the epidermis and may incorporate sand, algae, or spicules produced by the animal, depending on the species [67]. Most of the internal cavity is covered by a large modified ciliated pharynx (the pharyngeal basket) that allows the animal to filter feed by inhaling water through a branchial siphon, trapping edible particles, and expelling the water out an atrial siphon. The rest of the organs occupy a visceral cavity, with the genital ducts and anus opening to the atrium. In *P. nigra*, the tunic is smooth, and it readily separates from the body. The visceral mass (digestive and reproductive systems) and pharyngeal basket were carefully inspected because the location of ascidian faunal associates varied within the host according to symbiont species [46,47] (Figure 2). Using the number of associated animals per ascidian, symbiont diversity was quantified by calculating the Shannon-Wiener and Simpson indices for each collected host containing at least one associated species. The total wet mass of each *P. nigra* was used to approximate host size and was calculated by adding the wet masses of the visceral mass and pharyngeal basket with that of the tunic, after gently padding each with absorbent paper to reduce weighing errors due to water content.

To assess host state in relation to symbiont load, two measurements were used. First, percent of ash-free dry mass per wet mass (AFDM/WM) was calculated by drying each dissected *P. nigra* (tunic + body) at 65 °C for three days and then burning in a furnace at 450 °C for eight hours. This measurement of total organic content has been often used as an indicator of nutritional value of plant and algal food to herbivores [68–70], but can also approximate imbalances between the organic and inorganic components of an animal [71,72]. Second, a condition index was calculated as the percent of body to tunic (=[(WM of viscera + pharyngeal basket)/WM of tunic] × 100). The tunic is a thick external protective and supportive organic layer secreted by the epidermis (mantle) of the ascidian body wall. Despite being seldom calcified with spicules and containing some blood vessels, the tunic has many parallels in function and origin with a molluscan shell (an organic matrix as well, but with higher calcification). Thus, our approach is similar to the broadly used meat-to-shell ratio that is applied to approximate health and quality of shellfish in aquaculture and for human consumption [18,73,74].

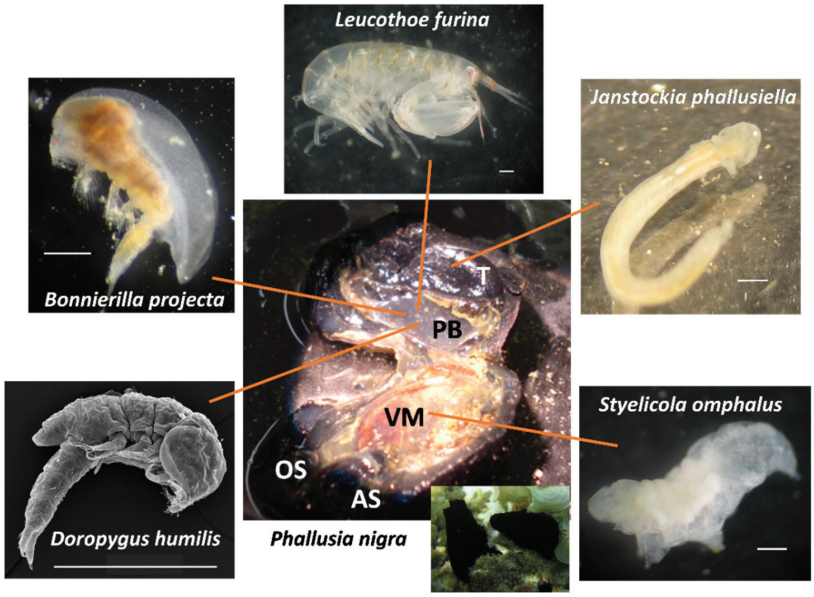

Figure 2. Symbionts found in the ascidian *Phallusia nigra* from the Egyptian Red Sea coast. Lines point the typical location of the symbiont inside the host. At the center, a dissected *P. nigra* (length 4.5 cm) is shown with part of the pharyngeal basket removed to expose the inside of the tunic: OS = oral siphon, AS = atrial siphon, PB = pharyngeal basket, T = tunic, VM = visceral mass. Two living specimens of the ascidian are shown in the insert. The scale bars for all symbionts are 0.5 mm. All photos by E. Cruz-Rivera, except *D. humilis* (by Kolbasov, G.A.).

To analyze differences among reefs in host size, condition, and symbiont loads and diversity, we used one-way ANOVA after testing for normality (Kolmogorov–Smirnov tests) and variance homogeneity (Levene's tests). In some instances, departures from these requirements were corrected by log transformation. When significant differences were found, Tukey's HSD tests were used for post hoc comparisons. The non-parametric Kruskal-Wallis test was applied when data did not conform to ANOVA assumptions despite multiple transformations. When significant differences were found, Kruskal-Wallis were followed by Mann-Whitney U tests, adjusted with Bonferroni corrections, for pairwise comparisons. Data for individual symbionts (1) could not be assumed as independent because multiple species could inhabit the same host replicate, (2) were not normally distributed, and (3) included instances where a particular symbiont was absent from a sampled site. These conditions constrained analyses using multifactorial tests (e.g., two-way ANOVA, Scheirer-Ray-Hare test). Instead, we used the non-parametric Kruskal-Wallis test to assess differences among reefs for each symbiont species quantified.

Pearson correlations were used to evaluate potential interactions between *P. nigra* symbionts by comparing densities between species overall and within each sampled reef separately. While understanding the mechanisms of competition between symbionts requires a manipulative approach, correlations and regression analyses can provide useful insights into interspecific relations between symbionts for a given host (e.g., [16]). Linear regressions were used to determine the effects of host size (mass) on symbiont load and the potential effects of symbiont densities on AFDM/WM and condition index, overall and per reef. Log transformations of data were used in various of the analyses above to conform with the assumptions of these parametric approaches. As different symbionts of *P. nigra* inhabit different parts of the ascidian, regressions with AFDM/WM were conducted on whole animals, ascidian tunic, and ascidian body separately, and against total amphipods

(broadly considered commensals), total copepods (often considered parasites for the two families encountered here), and total symbionts.

3. Results

One sample from Zeytouna Beach was lost during processing and all analyses herein are based on a sample size of 49 for that site. The amphipod *Leucothoe furina* (Savigny, 1816), the ascidicolid copepod *Styelicola omphalus* Kim I.H., Cruz-Rivera, Sherif & El-Sahhar, 2016, and the notodelphyid copepods *Bonnierilla projecta* Stock, 1967, *Doropygus humilis* Stock, 1967, and *Janstockia phallusiella* Boxshall & Marchenkov, 2005, were all found in *P. nigra* from our collections. However, there were spatial differences in distribution. For example, *D. humilis* were never found in Mövenpick reef ascidians.

Data showed no indication of antagonism or tradeoff in the distributions of these symbionts (Table 2). In contrast, a weak, but significant positive correlation between the number of amphipods and the density of the copepod *B. projecta* was observed when all reefs were analyzed together ($p = 0.037$, Pearson correlation coefficient = 0.171). When the three sites were compared, this correlation was only detected for Mövenpick reef ($p = 0.048$, Pearson correlation coefficient = 0.281). The only other significant correlation found was between the presence of *B. projecta* and the copepod *D. humilis* at Zeytouna Beach ($p < 0.001$, Pearson correlation coefficient = 0.836).

Table 2. Correlations between symbiont abundances as proxies for pairwise interactions within ascidian hosts. Analyses were conducted for all studied reefs together and individually. Numbers are *p*-values from two-tailed Pearson correlations. No *Doropygus humilis* were found at Mövenpick reef. Numbers in bold indicate significant correlations. Only positive correlations were detected.

All Field Sites		***Bonnierilla***	***Doropygus***	***Janstockia***	***Styelicola***
	Leucothoe	**0.037**	0.251	0.502	0.773
	Bonnierilla		0.092	0.474	0.817
	Doropygus			0.579	0.078
	Janstockia				0.761
Individual sites					
Abu Tig	*Leucothoe*	0.593	0.526	0.863	0.360
	Bonnierilla		0.861	0.418	0.548
	Doropygus			0.641	0.774
	Janstockia				0.553
Mövenpick	*Leucothoe*	**0.048**	-	0.553	0.832
	Bonnierilla		-	0.985	0.847
	Doropygus			-	-
	Janstockia				0.731
Zeytouna Beach	*Leucothoe*	0.645	0.421	0.81	0.657
	Bonnierilla		**<0.001**	0.950	0.741
	Doropygus			0.656	0.839
	Janstockia				0.755

Phallusia nigra mean wet mass, a proxy for size, was significantly different among reefs ($p = 0.004$, one-way ANOVA [log-transformed data]; Figure 3). Ascidians were significantly larger at Abu Tig than at Zeytouna Beach. Mövenpick ascidians were intermediate in mass and statistically similar to those in the other two reefs. In contrast, total AFDM/WM of the ascidian hosts was significantly lower at Abu Tig than at Zeytouna Beach, although this difference was <7% ($p = 0.003$, Kruskal-Wallis; Figure 3). AFDM/WM of ascidians from Mövenpick reef was statistically equivalent to that of the other sites. Despite differences in other parameters, condition indices were very similar across reefs ($p = 0.767$, one-way ANOVA; Figure 3).

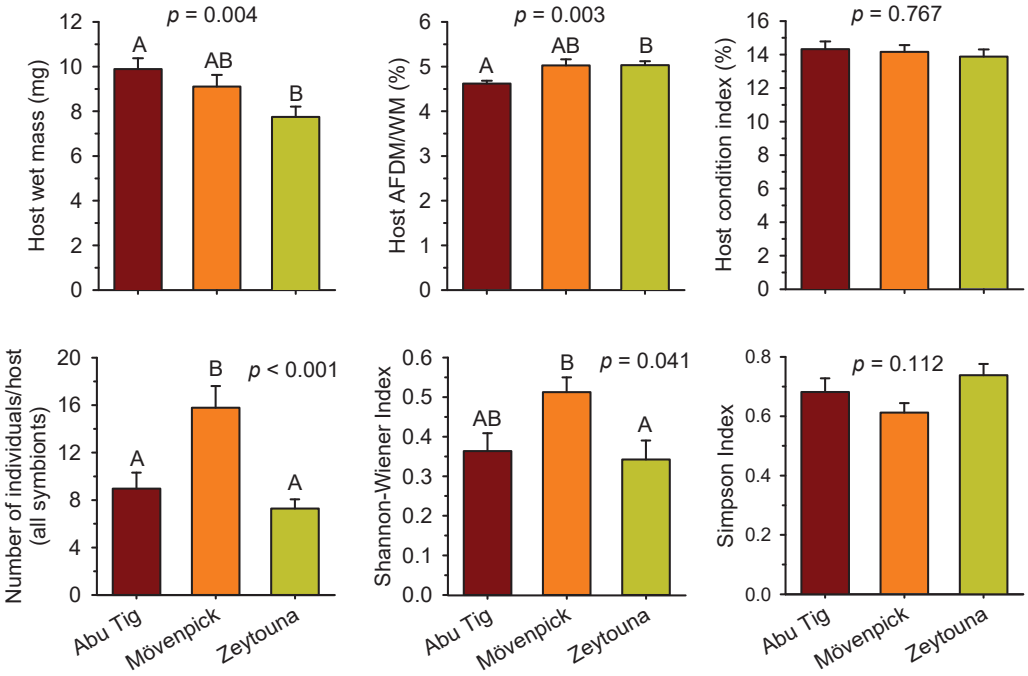

Figure 3. Wet mass, ash-free dry mass per wet mass (AFDM/WM), and condition of the ascidian *Phallusia nigra* collected at three reefs from El Gouna, Egypt (top row). Associated fauna (total ascidian symbionts) and two indices of species diversity of symbionts (Shannon-Wiener and Simpson indices) are presented on the bottom row. Bars represent means ± 1 SE. P values are from one-way ANOVA or Kruskal-Wallis tests, followed by appropriate pairwise comparisons as needed (see Methods). Same letters above bars indicate statistically equivalent means. Fill colors of bars are maintained between some figures to facilitate comparisons.

Approximately twice as many symbionts per ascidian were found in Mövenpick reef as in either of the two other sites ($p < 0.001$, one-way ANOVA [log-transformed data]; Figure 3). This pattern was largely related to the significantly higher abundances of the amphipod *L. furina* and the copepod *B. projecta* at that site ($p = 0.023$ and $p < 0.001$, respectively, Kruskal-Wallis; Figure 4). Interestingly, different measurements of symbiont diversity yielded different results. There was a significant difference in species diversity ($p = 0.041$, Kruskal-Wallis; Figure 3), with ascidians from Mövenpick reef having a more diverse symbiont community than those from Zeytouna Beach, and Abu Tig hosts having intermediate and equivalent diversity to the other two populations. In contrast, applying the Simpson Index, a dominance index in essence, did not detect differences among sites ($p = 0.112$, Kruskal-Wallis; Figure 3). As highlighted previously, there were significant differences among sites in the densities of amphipods (*L. furina*) and *B. projecta*, but overall, these two species comprised over 92% of all symbionts found regardless of reef (Figure 4, right panel). The largest number of *L. furina* in a single host was 31 (Mövenpick reef) and for *B. projecta* it was 50, most of which were males (Abu Tig reef).

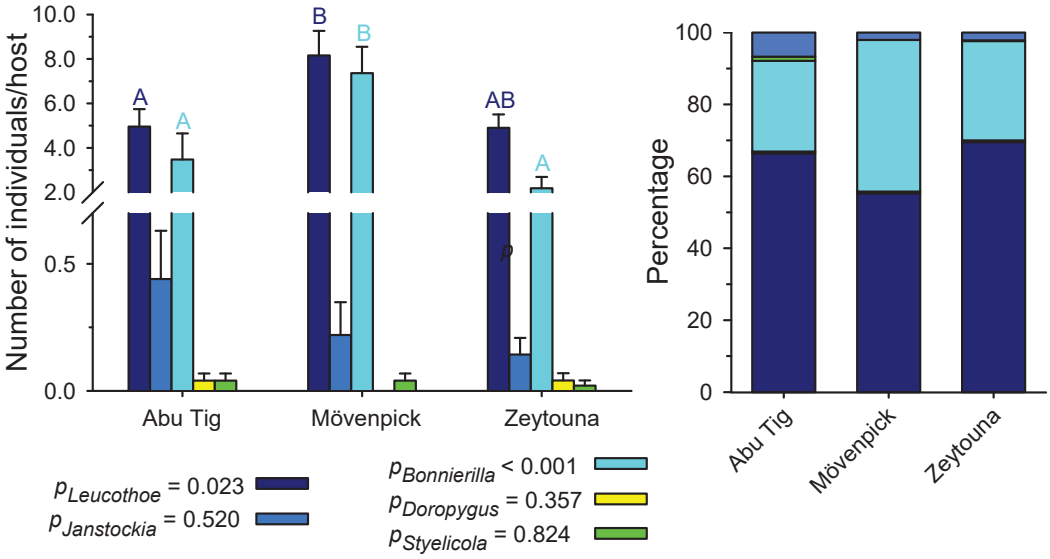

Figure 4. Numbers per host and relative abundances of *Phallusia nigra* symbionts collected at three reefs from El Gouna, Egypt. Left graph: Bars represent means ± 1 SE and *p* values are from Kruskal-Wallis tests on individual species. Same letters above bars indicate statistically equivalent means. Right graph: The same data are presented as percentages of total symbiont fauna for reference. These data are not analyzed. Fill colors of bars are as in the left figure.

To evaluate the potential effects of symbionts on their ascidian host, linear regressions were used (Figure 5, Table A1). No significant relations between amphipod, total copepods, or total symbionts were found against host WM, AFDM/WM, tunic AFDM/WM, or body AFDM/WM when data from all three reefs were pooled (Table A1). There was a weak but significant positive relation between total copepods or total symbionts, and host condition index; with a non-significant trend in the same direction for amphipods. When spatial variation was explored by analyzing data from the three reefs separately, few but stronger relations were observed. Data indicated that the total amount of symbionts was positively related with host WM ($p = 0.027$, $R^2 = 0.100$; Figure 5, Table A1) and that *P. nigra* AFDM/WM was also positively related to totals symbiont load (also $p = 0.027$, $R^2 = 0.100$; Figure 5, Table A1), but that these patterns only occurred in Zeytouna Beach. Similarly, *P. nigra* condition index was positively related to amphipod ($p = 0.020$, $R^2 = 0.110$; Table A1), total copepod ($p < 0.001$, $R^2 = 0.212$; Table A1), and total symbionts ($p < 0.001$, $R^2 = 0.363$; Table A1, Figure 5), only at Zeytouna Beach.

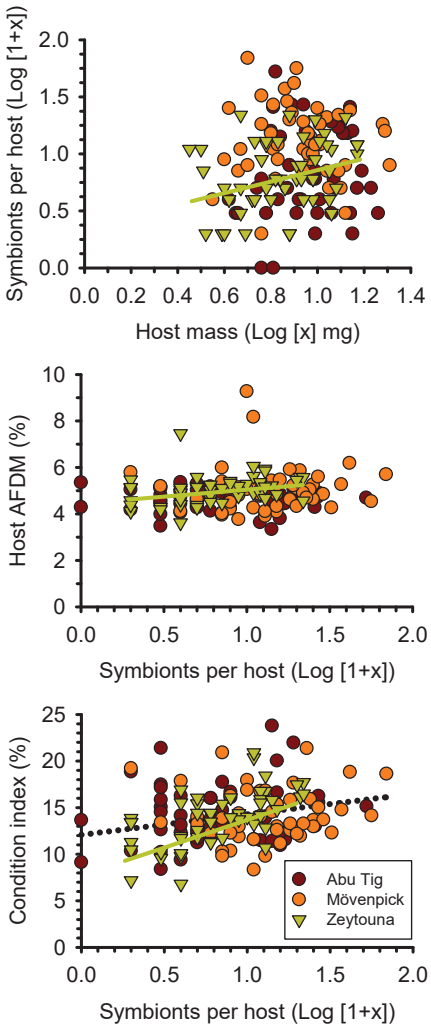

Figure 5. Selected regression analyses between host and total symbionts showing the variation of these patterns among reefs. Colored regression lines indicate the reef for which a significant relationship was found. The dotted line on the bottom graph shows the only case in which a general relationship between the two variables considered was found when all data for the three reefs were pooled. See Table A1 for results of all other comparisons performed.

4. Discussion

In this study, no strong negative or positive impacts of symbionts on their ascidian host were observed, consistent with a commensalistic interaction. Although a few relationships between host traits and symbiont densities could be detected, the predictability of those patterns was low (Figure 5, Table A1). Analyses also did not detect any evidence of tradeoffs in abundances, competition, or antagonism between different symbionts (Table 2). Inside the ascidian, the location of the symbionts is specific (Figure 2), which could result in decreased competition. For example *S. omphalus* attaches to the visceral mass of *P. nigra*, whereas *J. phallusiella* is found internally on the tunic, and *B. projecta* occurs in the pharyngeal basket [46]. However, the amphipod *L. furina*, and the copepods *B. projecta* and *D. humilis*, all share the pharyngeal basket of the host without apparent exclusion of one

another. In fact, among the very few significant correlations between symbionts, there was a positive (albeit weak) correlation between the abundances of the two most abundant symbionts, *L. furina* and *B. projecta* (pooled data and for Mövenpick reef), and also between *B. projecta* and *D. humilis* at Zeytouna Beach. These results suggest that these symbionts were not resource or space limited in the ascidians studied, and the environmental variables favoring one species would also favor the others. Space limitation may still operate for symbionts that specialize on organs or structures other than the relatively spacious host pharynx. Gage [75] hypothesized that an ascidicolid copepod was found overwhelmingly as single individuals inside their host because they associated with the ascidian food string, whereas a notodelphyid from the same host was found in densities as high as 17 per ascidian within the pharyngeal basket. Interestingly, the ascidicolid *S. omphalus* was always found as single females attached to the visceral mass of *P. nigra* during our study. The lack of negative correlation should not be interpreted as a complete rejection of antagonistic interactions, however. Although there is very little information on the diet of leucothoid amphipods, gut content analysis of a few species suggests those species feed on detritus and crustaceans [76]. If *L. furina* preys on symbiotic copepods living in the ascidian pharynx, a positive correlation can occur as long as the predator is not overexploiting its prey.

Host traits in general did not affect symbiont abundance or diversity. Despite prior studies showing positive correlations between ascidian size and symbiont numbers [77–79], that was not the case here. As seen in Figure 3, *P. nigra* from Abu Tig reef were significantly larger than those from Zeytouna Beach and similar in size to those at Mövenpick reef. However, the number of total symbionts was very similar at Abu Tig and Zeytouna, while Mövenpick reef ascidians contained almost twice as many associated animals. None of these patterns matched the observed anthropogenic influences on these reefs (see Methods). Symbiont diversity (Shannon-Wiener Index) was also significantly higher at Mövenpick than Zeytouna, but no dominance by any given symbiont was observed across reefs (Simpson Index). Thiel [58] found no relation between ascidian mass and numbers of a symbiotic amphipod, whereas Saito [80] found a negative non-linear relation between host mass and density of the copepod *Idomene purpurocincta* [=*Xouthous purpurocinctum* (Norman & Scott T., 1905)]. Both studies used dry mass as proxy for ascidian size, a less accurate approximation of ascidian structure, considering the high water content of the hosts (e.g., about 90% of WM in the *P. nigra* studied here).

Ascidian AFDM/WM showed the opposite pattern to size, with Abu Tig animals having a significantly lower organic content than those from Zeytouna Beach, but regression analyses yielded no indication that these patterns were related to amphipod, copepod, or total symbiont load. More importantly, we hypothesized that condition index of the ascidians could serve as indicator of the relation between symbionts and host: an inverse relation would indicate a negative effect of symbionts on host health (i.e., parasitism), while no relation would be consistent with commensalism, where the symbionts benefit at no expense from the host. Surprisingly, a positive overall relationship was observed between total copepods (considered often as parasites) and host condition, and between total symbionts and host condition when all three reefs were pooled (Figure 5, Table A1). These patterns appeared mostly influenced by the data from Zeytouna Beach, where a much stronger significant positive relationship between densities of amphipods, copepods and total symbionts, and host condition was detected (Figure 5, Table A1). Despite these results, to classify the relationship as a pairwise or diffuse mutualism is not supported. Firstly, only two of the 149 hosts samples were totally free of symbionts, precluding a thorough assessment of host health in the absence of any associated fauna. Second, the comparisons among reefs emphasized the role of spatial variance in understanding patterns. Our data would have suggested different interactions had we sampled only Zeytouna Beach (where a positive correlation was consistent across all symbiont groups and host condition), in comparison to the other two sites. Finally, while useful, condition indices such as the ones calculated here cannot be used as proxies of host fitness without further refinement. In fact, different indices are not equally accurate parallels for animal health and fitness for the

same species, and the same index may not be equally applicable to different species, sexes, or ages [24,25,81–83]. An estimation of gonad mass or reproductive output of *P. nigra* in relation to our calculated body condition index (i.e., gonadosomatic index) would greatly improve the application of this metric on ecological work as it would provide a more appropriate description of fitness (e.g., [14,25]).

The wide range of symbiont loads inside the ascidians sampled here (0–68) also points to a low per capita impact of the symbionts on the host. It is recognized that density-dependent effects are important in changing the nature of symbiotic relations through a parasite–mutualist continuum. Animals providing a net service to a host will fundamentally operate as parasites if their density exceeds a certain threshold [6,8,84,85]. Here, while some symbionts were consistently rare (e.g., *D. humilis*, *S. omphalus*), others varied at least one order of magnitude without any of our analyses detecting negative impacts on the ascidian host.

Our results support the historical treatment of leucothoid amphipods as commensals [45,48,52,53]. For the much more diverse symbiotic copepods [54–56], the existence of both commensal and parasitic species has been recognized [55,86]; yet, the tendency to classify Ascidicolidae and Notodelphyidae as parasitic without further assessment is widespread in the literature [86–90]. In some instances, conclusions about the nature of the interaction were reached after examination of mouth parts, formation of galls or cysts, and position of the symbiont in the host (e.g., [87,91–93]). Those are not unreasonable approximations; the formation of such structures or the intake of host fluids could result in reductions in host performance and fitness. However, feeding on host materials and induction of abnormal tissue growth occurs also with mutualists, such as senita moths, rhizobia, and gall-forming fig wasps [94–98]. A broader analysis of costs and benefits can avoid overgeneralizations about species for which little information, inability for manipulation, or historical treatment of certain related groups, have obscured our understanding of ecological interactions. Other recent studies on invertebrates [13] and vertebrates [12] have highlighted the need to reassess marine symbioses for groups that have been classified as symbionts and parasites.

5. Conclusions

The use of condition indices could help elucidate the nature of symbiotic interactions for instances in which symbiont loads cannot be manipulated in the host to quantify performance. Nevertheless, the application of these indices to ecological questions requires further refinement to include more directly related measurements of fitness, such as fecundity or gonad development and mass. A promising additional tool is the measurement of key stable isotopes in host and symbiont to establish the trophic status of the interacting animals [99]. For the Red Sea species studied here, the effects of five different symbionts on the host *P. nigra* appeared minimal, even for copepods with adaptations suggesting that their nutrition comes directly from host fluids or tissues (e.g., *J. phallusiella* and *S. omphalus* [46]) and despite the simultaneous presence of more than one symbiont in a single ascidian. Similarly, symbiont density was not shown to affect hosts within the variance sampled here. Data also suggested that local conditions could influence the trajectory of interactions, as evidenced by some significant patterns observed in single reefs alone. To avoid misclassification of host–symbiont interaction, geographically relevant sampling should be considered.

Author Contributions: Conceptualization, E.C.-R.; methodology, E.C.-R.; formal analysis, E.C.-R. and T.L.; investigation, E.C.-R., M.-E.-D.S. and S.E.-S.; resources, E.C.-R.; data curation, E.C.-R.; writing—original draft preparation, E.C.-R.; writing—review and editing, E.C.-R., M.-E.-D.S., S.E.-S. and T.L.; visualization, E.C.-R. and T.L.; project administration, E.C.-R.; funding acquisition, E.C.-R. All authors have read and agreed to the published version of the manuscript.

Funding: This research was funded by an American University in Cairo Research Development Grant to the lead author and by funds to M.-E.-D. Sherif from the Department of Biology of the American University in Cairo in support of a senior undergraduate thesis.

Institutional Review Board Statement: Not applicable.

Data Availability Statement: The data presented in this study are openly available in figshare at https://doi.org/10.6084/m9.figshare.17677787.

Acknowledgments: We thank the private administrations of Abu Tig Marina, Mövenpick Hotel, and Zeytouna Beach for access to our field sites. We gratefully acknowledge the staff of the J. D. Gerhart Field Station for logistical support during collections and sample processing.

Conflicts of Interest: The authors declare no conflict of interest. The funders had no role in the design of the study; in the collection, analyses, or interpretation of data; in the writing of the manuscript, or in the decision to publish the results.

Appendix A

Table A1. *p* values from linear regression analyses between symbiont abundances and various measurements of their ascidian hosts (*Phallusia nigra*). Note that host mass was treated as an independent variable against total amphipods (*Leucothoe furina*), total copepods (all four species found together) and log (1 + x) of all symbionts together. However, for ease to accommodate results in this table, host wet mass is placed on the top row. For all other analyses, amphipods, total copepods, and log (1 + x) of all symbionts were treated as the independent variable. Percent ash-free dry mass per wet mass (AFDM/WM) of the ascidian tunic and body were added to obtain total AFDM/WM. Analyses were conducted for all studied reefs together and individually. Numbers in bold indicate significant relations between variables. For those cases, R^2 is provided in parentheses. Only positive regressions were detected. Note that *p* and R^2 values were coincidentally similar in two separate analyses.

All Field Sites		**Host Wet Mass (log x)**	**Host Total AFDM/WM**	**Host Tunic AFDM/WM**	**Host Body AFDM/WM**	**Host Condition Index**
	Amphipods	0.644	0.444	0.960	0.829	0.054
	Copepods	0.944	0.219	0.666	0.871	**0.016 (0.039)**
	All symbionts (log 1 + x)	0.088	0.137	0.976	0.928	**0.001 (0.068)**
Individual sites						
Abu Tig	Amphipods	0.596	0.639	0.471	0.904	0.635
	Copepods	0.777	0.914	0.838	0.555	0.351
	All symbionts (log 1 + x)	0.359	0.602	0.588	0.128	0.173
Mövenpick	Amphipods	0.407	0.854	0.796	0.748	0.282
	Copepods	0.442	0.493	0.317	0.620	0.221
	All symbionts (log 1 + x)	0.756	0.692	0.519	0.799	0.617
Zeytouna Beach	Amphipods	0.113	0.260	0.976	0.989	**0.020 (0.110)**
	Copepods	0.410	0.100	0.606	0.427	**<0.001 (0.212)**
	All symbionts (log 1 + x)	**0.027 (0.100)**	**0.027 (0.100)**	0.653	0.780	**<0.001 (0.363)**

References

1. Castro, P. Animal symbioses in coral reef communities: A review. *Symbiosis* **1988**, *5*, 161–184.
2. Leung, T.L.F.; Poulin, R. Parasitism, commensalism, and mutualism: Exploring the many shades of symbioses. *Vie Milieu* **2008**, *58*, 107–115.
3. Glynn, P.W.; Enochs, I.C. Invertebrates and their roles in coral reef ecosystems. In *Coral Reefs: An Ecosystem in Transition*; Dubinsky, Z., Stambler, N., Eds.; Springer: Dordrecht, The Netherlands, 2011; pp. 273–325; ISBN 978-94-007-0113-7.
4. Hirsch, A.M. Plant-microbe symbioses: A continuum from commensalism to parasitism. *Symbiosis* **2004**, *37*, 345–363.
5. Cheney, K.L.; Côté, I.M. Mutualism or parasitism? The variable outcome of cleaning symbioses. *Biol. Lett.* **2005**, *1*, 162–165. [CrossRef]
6. Brown, B.L.; Creed, R.P.; Skelton, J.; Rollins, M.A.; Farrell, K.J. The fine line between mutualism and parasitism: Complex effects in a cleaning symbiosis demonstrated by multiple field experiments. *Oecologia* **2012**, *170*, 199–207. [CrossRef]
7. Hoeksema, J.D.; Bruna, E.M. Pursuing the big questions about interspecific mutualism: A review of theoretical approaches. *Oecologia* **2000**, *125*, 321–330. [CrossRef]

8. Silknetter, S.; Kanno, Y.; Kanapeckas Métris, K.L.; Cushman, E.; Darden, T.L.; Peoples, B.K. Mutualism or parasitism: Partner abundance affects host fitness in a fish reproductive interaction. *Freshw. Biol.* **2019**, *64*, 175–182. [CrossRef]
9. Saffo, M.B.; McCoy, A.M.; Rieken, C.; Slamovits, C.H. *Nephromyces*, a beneficial apicomplexan symbiont in marine animals. *Proc. Natl. Acad. Sci. USA* **2010**, *107*, 16190–16195. [CrossRef]
10. Cumbo, V.R.; Baird, A.H.; Moore, R.B.; Negri, A.P.; Neilan, B.A.; Salih, A.; van Oppen, M.J.H.; Wang, Y.; Marquis, C.P. *Chromera velia* is endosymbiotic in larvae of the reef corals *Acropora digitifera* and *A. tenuis*. *Protist* **2013**, *164*, 237–244. [CrossRef]
11. Kwong, W.K.; del Campo, J.; Mathur, V.; Vermeij, M.J.A.; Keeling, P.J. A widespread coral-infecting apicomplexan with chlorophyll biosynthesis genes. *Nature* **2019**, *568*, 103–107. [CrossRef]
12. Halliday-Isaac, A.K.; Robinson, J.B.; Cruz-Rivera, E.; Campbell, A.G.; Sikkel, P.C. Environmental correlates of prevalence of an intraerythrocytic apicomplexan infecting Caribbean damselfish. *Parasitologia* **2021**, *1*, 69–82. [CrossRef]
13. Carlton, J.T.; Blakeslee, A.M.H.; Fowler, A.E. Accidental associates are not symbionts: The absence of a non-parasitic endosymbiotic community inside the common periwinkle *Littorina littorea* (Mollusca: Gastropoda). *Mar. Biol.* **2020**, *167*, 97. [CrossRef]
14. Hirose, E.; Oka, A.T.; Akahori, M. Sexual reproduction of the photosymbiotic ascidian *Diplosoma virens* in the Ryukyu Archipelago, Japan: Vertical transmission, seasonal change, and possible impact of parasitic copepods. *Mar. Biol.* **2005**, *146*, 677–682. [CrossRef]
15. Parmentier, E.; Michel, L. Boundary lines in symbiosis forms. *Symbiosis* **2013**, *60*, 1–5. [CrossRef]
16. Dvoretsky, A.G.; Dvoretsky, V.G. Interspecific competition of symbiotic and fouling species of red king crab in the Barents Sea. *Doklady Biol. Sci.* **2011**, *440*, 300–302. [CrossRef]
17. Devlaming, V.; Grossman, G.; Chapman, F. On the use of the gonosomatic index. *Comp. Biochem. Physiol. A* **1982**, *73*, 31–39. [CrossRef]
18. Lucas, A.; Beninger, P.G. The use of physiological condition indices in marine bivalve aquaculture. *Aquaculture* **1985**, *44*, 187–200. [CrossRef]
19. Crosby, M.P.; Gale, L.D. A review and evaluation of bivalve condition index methodologies with a suggested standard method. *J. Shellfish Res.* **1990**, *9*, 233–237.
20. West, G. Methods of assessing ovarian development in fishes: A review. *Mar. Freshw. Res.* **1990**, *41*, 199–222. [CrossRef]
21. Fernandez, C.; Boudouresque, C.-F. Phenotypic plasticity of *Paracentrotus lividus* (Echinodermata: Echinoidea) in a lagoonal environment. *Mar. Ecol. Prog. Ser.* **1997**, *152*, 145–154. [CrossRef]
22. Fernandez, C.; Boudouresque, C.-F. Nutrition of the sea urchin *Paracentrotus lividus* (Echinodermata: Echinoidea) fed different artificial food. *Mar. Ecol. Prog. Ser.* **2000**, *204*, 131–141. [CrossRef]
23. Lowerre-Barbieri, S.K.; Brown-Peterson, N.J.; Murua, H.; Tomkiewicz, J.; Wyanski, D.M.; Saborido-Rey, F. Emerging issues and methodological advances in fisheries reproductive biology. *Mar. Coast. Fish.* **2011**, *3*, 32–51. [CrossRef]
24. Labocha, M.K.; Hayes, J.P. Morphometric indices of body condition in birds: A review. *J. Ornithol.* **2012**, *153*, 1–22. [CrossRef]
25. Ouréns, R.; Freire, J.; Fernández, L. Definition of a new unbiased gonad index for aquatic invertebrates and fish: Its application to the sea urchin *Paracentrotus lividus*. *Aquat. Biol.* **2012**, *17*, 145–152. [CrossRef]
26. Unglaub, B.; Steinfartz, S.; Kühne, D.; Haas, A.; Schmidt, B.R. The relationships between habitat suitability, population size and body condition in a pond-breeding amphibian. *Basic Appl. Res.* **2018**, *27*, 20–29. [CrossRef]
27. Dunphy, B.J.; Wells, R.M.G. Endobiont infestation, shell strength and condition index in wild populations of New Zealand abalone, *Haliotis iris*. *Mar. Freshwater Res.* **2001**, *52*, 781–786. [CrossRef]
28. O'Connell-Milne, S.A.; Poulin, R.; Savage, C.; Rayment, W. Reduced growth, body condition and foot length of the bivalve *Austrovenus stutchburyi* in response to parasite infection. *J. Exp. Mar. Biol. Ecol.* **2016**, *474*, 23–28. [CrossRef]
29. Bazterrica, M.C.; Bruschetti, C.M.; Alvarez, M.F.; Iribarne, O.; Botto, F. Effects of macroalgae on the recruitment, growth, and body condition of an invasive reef forming polychaete in a south-western Atlantic coastal lagoon. *J. Sea Res.* **2014**, *88*, 121–129. [CrossRef]
30. Shenkar, N. Ascidian (Chordata, Ascidiacea) diversity in the Red Sea. *Mar. Biodiv.* **2012**, *42*, 459–469. [CrossRef]
31. Vandepas, L.E.; Oliveira, L.M.; Lee, S.S.C.; Hirose, E.; Rocha, R.M.; Swalla, B.J. Biogeography of *Phallusia nigra*: Is it really black and white? *Biol. Bull.* **2015**, *228*, 52–64. [CrossRef]
32. Rocha, R.M.D.; Lotufo, T.M.D.C.; de Almeida Rodrigues, S. The biology of *Phallusia nigra* Savigny, 1816 (Tunicata: Ascidiacea) in Southern Brazil: Spatial distribution and reproductive cycle. *Bull. Mar. Sci.* **1999**, *64*, 77–88.
33. Kondilatos, G.; Corsini-Foka, M.; Pancucci-Papadopoulou, M.-A. Occurrence of the first non-indigenous ascidian *Phallusia nigra* Savigny, 1816 (Tunicata: Ascidiacea) in Greek waters. *Aquat. Inv.* **2010**, *5*, 181–184. [CrossRef]
34. Naser, H.A. Variability of marine macrofouling assemblages in a marina and a mariculture centre in Bahrain, Arabian Gulf. *Reg. Stud. Mar. Sci.* **2017**, *16*, 162–170. [CrossRef]
35. Goodbody, I. The biology of *Ascidia nigra* (Savigny). I. Survival and mortality in an adult population. *Biol. Bull.* **1962**, *122*, 40–51. [CrossRef]
36. Goodbody, I. The biology of *Ascidia nigra* (Savigny). III. The annual pattern of colonization. *Biol. Bull.* **1965**, *129*, 128–133. [CrossRef]
37. Goodbody, I.; Gibson, J. The biology of *Ascidia nigra* (Savigny) V. Survival in populations settled at different times of the year. *Biol. Bull.* **1974**, *146*, 217–237. [CrossRef]
38. Al-Sofyani, A.M.A.; Satheesh, S. Recruitment patterns of the solitary ascidian *Phallusia nigra* Savigny, 1816 on artificial substrates submerged in the central Red Sea, Saudi Arabia. *Oceanol. Hydrobiol. Stud.* **2019**, *48*, 262–269. [CrossRef]

39. Granot, I.; Shenkar, N.; Belmaker, J. Habitat niche breadth predicts invasiveness in solitary ascidians. *Ecol. Evol.* **2017**, *7*, 7838–7847. [CrossRef]
40. Ghazilou, A.; Koochaknejad, E.; Ershadifar, H.; Negarestan, H.; Kor, K.; Baskaleh, G. Infestation biology of *Phallusia nigra* (Tunicata, Phlebobranchia) on hard corals in a subtropical bay. *Mar. Ecol. Prog. Ser.* **2019**, *626*, 135–143. [CrossRef]
41. Hirose, E.; Yamashiro, H.; Mori, Y. Properties of tunic acid in the ascidian *Phallusia nigra* (Ascidiidae, Phlebobranchia). *Zool. Sci.* **2001**, *18*, 309–314. [CrossRef]
42. Odate, S.; Pawlik, J.R. The Role of vanadium in the chemical defense of the solitary tunicate, *Phallusia nigra*. *J. Chem. Ecol.* **2007**, *33*, 643–654. [CrossRef]
43. Mayzel, B.; Haber, M.; Ilan, M. Chemical defense against fouling in the solitary ascidian *Phallusia nigra*. *Biol. Bull.* **2014**, *227*, 232–241. [CrossRef]
44. Stock, J.H. Report on the Notodelphyidae (Copepoda, Cyclopoida) of the Israel South Red Sea Expedition. *Bull. Sea Fish. Res. Stat. Israel* **1967**, *27*, 1–126.
45. White, K.N. A Taxonomic review of the Leucothoidae (Crustacea: Amphipoda). *Zootaxa* **2011**, *3078*, 1–113. [CrossRef]
46. Kim, I.-H.; Cruz-Rivera, E.; Sherif, M.-E.-D.; El-Sahhar, S. Cyclopoid copepods (Ascidicolidae, Notodelphyidae) associated with *Phallusia nigra* Savigny, 1816 (Ascidiacea) in the Red Sea: A new ascidicolid and first descriptions of the males from two notodelphyids. *J. Crust. Biol.* **2016**, *36*, 553–566. [CrossRef]
47. Martin, D.; Nygren, A.; Cruz-Rivera, E. *Proceraea exoryxae* sp. nov. (Annelida, Syllidae, Autolytinae), the first known polychaete miner tunneling into the tunic of an ascidian. *PeerJ* **2017**, *5*, e3374. [CrossRef]
48. White, K.N.; Krapp-Schickel, T. Red Sea Leucothoidae (Crustacea: Amphipoda) including new and re-described species. *Eur. J. Taxon.* **2017**, *324*, 1–40. [CrossRef]
49. White, K.N. Caribbean Leucothoidae (Crustacea: Amphipoda) of Panama. *Gulf Caribb. Res.* **2011**, *23*, 23–35. [CrossRef]
50. Senna, A.R.; Andrade, L.F.; Ramos, B.S.; Skinner, L.F. A new ascidian-dwelling species of *Leucothoe* Leach, 1814 (Amphipoda: Leucothoidae) from Ilha Grande Bay, Rio de Janeiro State, Brazil. *J. Nat. Hist.* **2021**, *55*, 1441–1460. [CrossRef]
51. Hernández, J.E.; Bolaños, J.A.; Palazón, J.L.; Hernández, G.; Lira, C.; Baeza, J.A. The enigmatic life history of the symbiotic crab *Tunicotheres moseri* (Crustacea, Brachyura, Pinnotheridae): Implications for its mating system and population structure. *Biol. Bull.* **2012**, *223*, 278–290. [CrossRef]
52. Thomas, J.D.; Klebba, K.N. New species and host associations of commensal leucothoid amphipods from coral reefs in Florida and Belize (Crustacea:Amphipoda). *Zootaxa* **2007**, *1494*, 1–44. [CrossRef]
53. White, K.; Reimer, J. Commensal Leucothoidae (Crustacea, Amphipoda) of the Ryukyu Archipelago, Japan. Part I: Ascidian-dwellers. *ZooKeys* **2012**, *163*, 13–55. [CrossRef]
54. Ho, J.-S. Origin and evolution of the parasitic cyclopoid copepods. *Int. J. Parasitol.* **1994**, *24*, 1293–1300. [CrossRef]
55. Kim, I.-H.; Boxshall, G.A. Untold diversity: The astonishing species richness of the Notodelphyidae (Copepoda: Cyclopoida), a family of symbiotic copepods associated with ascidians (Tunicata). *Megataxa* **2020**, *4*, 1–660. [CrossRef]
56. Kim, I.-H.; Boxshall, G.A. Copepods (Cyclopoida) associated with ascidian hosts: Ascidicolidae, Buproridae, Botryllophilidae, and Enteropsidae, with descriptions of 84 new species. *Zootaxa* **2021**, *4978*, 1–286. [CrossRef]
57. Ortiz, M. Claves ilustradas para la clasificación de los anfípodos (Crustacea, Peracarida) de Cuba: Morfología y taxonomía. *Rev. Investig. Mar.* **2021**, *41*, 1–108.
58. Thiel, M. Host-use and population demographics of the ascidian-dwelling amphipod *Leucothoe spinicarpa*: Indication for extended parental care and advanced social behaviour. *J. Nat. Hist.* **1999**, *33*, 193–206. [CrossRef]
59. Boxshall, G.A.; Marchenkov, A. A new genus of notodelphyid copepod (Crustacea, Copepoda, Cyclopoida) from a compound ascidian host collected in the Suez Canal. *Zoosystema* **2005**, *27*, 483–497.
60. Schellenberg, A. Neuo Notodelphyiden des Berliner und Hamburger Museums mit einer Übersicht der ascidien bowohnenden Gattungen und Arten. *Mitt. Zool. Mus.* **1922**, *10*, 219–274.
61. Gurney, R. Report on the Crustacea:—Copepoda (littoral and semi-parasitic). *Trans. Zool. Soc.* **1927**, *22*, 451–577. [CrossRef]
62. El Sherbiny Ahmed, H.; Sherif Ahmed, H.; Hassan Ali, N. Model for environmental risk assessment of tourism project construction on the Egyptian Red Sea Coast. *J. Environ. Eng.* **2006**, *132*, 1272–1281. [CrossRef]
63. Vanderstraete, T.; Goossens, R.; Ghabour, T.K. The use of multi-temporal Landsat Images for the change detection of the coastal zone near Hurghada, Egypt. *Int. J. Remote Sens.* **2006**, *27*, 3645–3655. [CrossRef]
64. Marshall, N.A.; Marshall, P.A.; Abdulla, A.; Rouphael, T.; Ali, A. preparing for climate change: Recognising its early impacts through the perceptions of dive tourists and dive operators in the Egyptian Red Sea. *Curr. Issues Tour.* **2011**, *14*, 507–518. [CrossRef]
65. Nassar, K.; El-Adawy, A.; Zakaria, M.; Diab, R.; Masria, A. Quantitative appraisal of naturalistic/anthropic shoreline shifts for Hurghada: Egypt. *Mar. Georesour. Geotechnol.* **2021**. [CrossRef]
66. Moufaddal, W.M. Use of Satellite imagery as environmental impact assessment tool: A case study from the NW Egyptian Red Sea coastal zone. *Environ. Monit. Assess.* **2005**, *107*, 427–452. [CrossRef]
67. Ballarin, L.; Burighel, P. Tunicata and Cephalochordata. In *Biological Science Fundamentals and Systematics*; Encyclopedia of Biological, Physiological and Health Sciences; Minelli, A., Contrafatto, G., Eds.; EOLSS Publishers, UNESCO: Oxford, UK, 2009; Volume IV, pp. 43–67; ISBN 978-84826-189-1.
68. Cruz-Rivera, E.; Hay, M.E. Macroalgal traits and the feeding and fitness of an herbivorous amphipod: The roles of selectivity, mixing, and compensation. *Mar. Ecol. Prog. Ser.* **2001**, *218*, 249–266. [CrossRef]

69. Prado, P.; Heck, K.L. Seagrass selection by omnivorous and herbivorous consumers: Determining factors. *Mar. Ecol. Prog. Ser.* **2011**, *429*, 45–55. [CrossRef]
70. Cruz-Rivera, E.; Friedlander, M. Effects of algal phenotype on mesograzer feeding. *Mar. Ecol. Prog. Ser.* **2013**, *490*, 69–78. [CrossRef]
71. Okumuş, İ.; Stirling, H.P. Seasonal variations in the meat weight, condition index and biochemical composition of mussels (*Mytilus edulis*, L.) in suspended culture in two Scottish Sea lochs. *Aquaculture* **1998**, *159*, 249–261. [CrossRef]
72. Adjei-Boateng, D.; Wilson, J.G. Body condition and gametogenic cycle of *Galatea paradoxa* (Mollusca: Bivalvia) in the Volta River Estuary, Ghana. *Estuar. Coast. Shelf Sci.* **2013**, *132*, 94–98. [CrossRef]
73. Rainier, J.S.; Mann, R.L. A comparison of methods for calculating condition index in eastern oyster, *Crassostrea virginica* (Gmelin, 1791). *J. Shellfish Res.* **1992**, *11*, 55–58.
74. Zeng, Y.; Yang, H. Review of molluscan bivalve condition index calculations and application in northern quahogs *Mercenaria mercenaria*. *Aquac. Res.* **2021**, *52*, 23–36. [CrossRef]
75. Gage, J. Seasonal Cycles of *Notodelphys* and *Ascidicola*, copepod associates with *Ascidiella* (Ascidiacea). *J. Zool.* **1966**, *150*, 223–233. [CrossRef]
76. Guerra-García, J.M.; Tierno de Figueroa, J.M.; Navarro-Barranco, C.; Ros, M.; Sánchez-Moyano, J.E.; Moreira, J. Dietary analysis of the marine Amphipoda (Crustacea: Peracarida) from the Iberian Peninsula. *J. Sea Res.* **2014**, *85*, 508–517. [CrossRef]
77. da Silva Ramos, E.K.; Batista Rosa, A.H.; Cobo, V.J. Influence of the endo-symbiont *Leucothoe wuriti* (Thomas & Klebba, 2007) (Crustacea, Leucothoidae) on the biomass of *Phallusia nigra* (Savigny, 1816) (Tunicata, Ascididae), in the northeastern coast of the São Paulo State, Brazil. *Rev. Biociên.* **2015**, *21*, 38–43.
78. Egan, E.A. The seasonal occurrence of the copepod *Pachypygus australis* Gotto (Notodelphyidae) in its host *Pyura pachydermatina* (Herdman) Pyuridae: Ascidiacea. *J. Exp. Mar. Biol. Ecol.* **1984**, *76*, 247–262. [CrossRef]
79. Svavarsson, J. Life Cycle and population dynamics of the symbiotic copepod *Lichomolgus canui* Sars associated with the ascidian *Halocynthia pyriformis* (Rathke). *J. Exp. Mar. Biol. Ecol.* **1990**, *142*, 1–12. [CrossRef]
80. Saito, S. Density and adult ratio of the symbiotic harpacticoid copepod *Idomene purpurocincta* in the compound ascidian host *Aplidium yamazii*. *Plankton Benthos Res.* **2009**, *4*, 160–166. [CrossRef]
81. Jakob, E.M.; Marshall, S.D.; Uetz, G.W. Estimating fitness: A comparison of body condition indices. *Oikos* **1996**, *77*, 61–67. [CrossRef]
82. Peig, J.; Green, A.J. The paradigm of body condition: A critical reappraisal of current methods based on mass and length. *Funct. Ecol.* **2010**, *24*, 1323–1332. [CrossRef]
83. Labocha, M.K.; Schutz, H.; Hayes, J.P. Which body condition index is best? *Oikos* **2014**, *123*, 111–119. [CrossRef]
84. Addicott, J.F. A multispecies aphid–ant association: Density dependence and species-specific effects. *Can. J. Zool.* **1979**, *57*, 558–569. [CrossRef]
85. Drew, G.; King, K. More or less? The effect of symbiont density in protective mutualisms. *Am. Nat.* **2022**. [CrossRef]
86. Illg, P.L. North American copepods of the family Notodelphyidae. *Proc. US Natl. Mus.* **1958**, *107*, 463–649. [CrossRef]
87. Dudley, P.L. A light and electron microscopic study of tissue interactions between a parasitic copepod, *Scolecodes huntsmani* (Henderson), and its host ascidian, *Styela gibbsii* (Stimpson). *J. Morphol.* **1968**, *124*, 263–281. [CrossRef] [PubMed]
88. Ho, J.; Conradi, M.; López-González, P.J. A new family of cyclopoid copepods (Fratiidae) symbiotic in the ascidian (*Clavelina dellavallei*) from Cádiz, Spain. *J. Zool.* **1998**, *246*, 39–48.
89. Ho, J.; Kim, I.-H. Two species of copepoda parasitic in the algal-bearing ascidian, *Didemnum molle* (Herdman), in Okinawa, Japan. *Proc. Biol. Soc. Wash.* **2009**, *122*, 414–425. [CrossRef]
90. Marchenkov, A.; Boxshall, G.A. A new notodelphyid copepod, *Paranotodelphys illgi* n. sp. (Copepoda: Cyclopoida), parasitic in the ascidian *Corynascidia herdmani* Ritter in the North Pacific. *Syst. Parasitol.* **2003**, *54*, 43–52. [CrossRef]
91. Stock, J.H. Parasite or commensal? *Notodelphys weberi, a new South African ascidicole copepod. Amsterdam Nat.* **1950**, *1*, 36–42.
92. Illg, P.L. Occurrence in Sagami Bay, Japan, of *Scolecodes*, a remarkable copepod parasite of ascidians. *Publ. Seto Mar. Biol. Lab.* **1970**, *18*, 69–74. [CrossRef]
93. Thomas, J.D.; Taylor, G.W. Mouthpart morphology and feeding strategies of the commensal amphipod, *Anamixis hanseni* Stebbing. *Bull. Mar. Sci.* **1981**, *31*, 462–467.
94. Fleming, T.H.; Holland, J.N. The evolution of obligate pollination mutualisms: Senita cactus and senita moth. *Oecologia* **1998**, *114*, 368–375. [CrossRef] [PubMed]
95. Oldroyd, G.E.D.; Downie, J.A. Coordinating nodule morphogenesis with rhizobial infection in legumes. *Annu. Rev. Plant Biol.* **2008**, *59*, 519–546. [CrossRef] [PubMed]
96. Mortier, V.; Holsters, M.; Goormachtig, S. Never too many? How legumes control nodule numbers. *Plant Cell Environ.* **2012**, *35*, 245–258. [CrossRef] [PubMed]
97. Harris, M.O.; Pitzschke, A. Plants make galls to accommodate foreigners: Some are friends, most are foes. *New Phytol.* **2020**, *225*, 1852–1872. [CrossRef] [PubMed]
98. Zhang, Z.; Yan, C.; Zhang, H. Mutualism between antagonists: Its ecological and evolutionary implications. *Integr. Zool.* **2021**, *16*, 84–96. [CrossRef]
99. Alfaya, J.E.F.; Galván, D.E.; Machordom, A.; Penchaszadeh, P.E.; Bigatti, G. *Malacobdella arrokeana*: Parasite or commensal of the giant clam *Panopea abbreviata*? *Zool. Sci.* **2015**, *32*, 523–530. [CrossRef]

diversity

MDPI

Article

The Impact of Different Biotopes and Management Practices on the Burden of Parasites in Artificial Nests of *Osmia* spp. (Megachilidae) Bees

Ivana Tlak Gajger [1,*], Ivana Laklija [1], Mirko Jurković [1], Anja Košćević [1], Showket Ahmad Dar [2] and Marija Ševar [3,†]

[1] Department for Biology and Pathology of Fish and Bees, Faculty of Veterinary Medicine, University of Zagreb, 10000 Zagreb, Croatia; ilaklija@gmail.com (I.L.); mirkojurkovic90@gmail.com (M.J.); anja.katarinavet25@gmail.com (A.K.)
[2] Division of Agricultural Entomology, KVK-Kargil II, Sher-e-Kashmir University of Agricultural Sciences and Technology of Kashmir, Srinagar 191111, India; showketdar43@gmail.com
[3] Ministry of Agriculture, 10000 Zagreb, Croatia
* Correspondence: ivana.tlak@vef.unizg.hr; Tel.: +385-91-2390-041
† Deceased.

Abstract: The decline in pollinator insect abundance and diversity is increasing on a global scale. Major threats are the byproducts of numerous negative environmental pressures acting individually or in combination. They vary throughout different geographical areas, affecting the solitary bees differently. One of the most important negative pressures are the many parasites, predators and pests representing a threat to the successful reproduction of solitary bees in artificial nests. Especially vulnerable are the managed *Osmia* spp. bee populations reared for commercialization and trade. The primary goals of our monitoring study were: (i) to examine the presence and the prevalence of brood parasites in the various types of bees' nesting material and in semi-field rearing conditions using the nest section analyses; (ii) to determine the presence of *Nosema* spp. in samples of feces and homogenized bee abdomens using a multiplex PCR method; (iii) the evaluation of the survival success level and emergence mass of healthy bees at each of the four studied bee rearing locations separately, depending on different environments and on the implementation of different managing practices. We determined the presence and prevalence of nest destructor parasites and accompanying fauna. Their presence was positively correlated with bee rearing failures. The results of this study may be used as a baseline for further solitary bee nest parasites monitoring schemes.

Keywords: *Osmia cornuta*; *Osmia rufa*; biotope; semi-field conditions; artificial nests; section analysis parasites; pathogens

Citation: Tlak Gajger, I.; Laklija, I.; Jurković, M.; Košćević, A.; Dar, S.A.; Ševar, M. The Impact of Different Biotopes and Management Practices on the Burden of Parasites in Artificial Nests of *Osmia* spp. (Megachilidae) Bees. *Diversity* **2022**, *14*, 226. https://doi.org/10.3390/d14030226

Academic Editors: Luc Legal and William G. Meikle

Received: 1 January 2022
Accepted: 18 March 2022
Published: 19 March 2022

1. Introduction

In Europe, the most ubiquitous representatives of solitary bees are the mason bee species *Osmia bicornis* L. (syn. *Osmia rufa* L.) and *Osmia cornuta* L. These bee species live in similar environments but differ in phenology and time of emergence in the spring. These species are being increasingly used for pollination services in agricultural and natural environments [1,2]. *Osmia bicornis* is polylactic and collects pollen from a very broad spectrum of plants, while *O. cornuta* prefers Rosaceae, especially fruit trees. Both species are especially important in fruit tree pollination in orchards due to their specific foraging and nesting behavior [3]. They emerge early in spring and so they are important in pear plantations which bloom early [4]. Additionally, these bees forage readily among different trees and rows within the orchard, which is particularly important for self-incompatible fruit cultivars that require cross fertilization [2–4]. Because they are also common in non-agricultural environments, these bees are important for the preservation of natural

landscapes. Therefore, these bees have been introduced in urban areas as an environmental accompaniment [2,5].

Due to their importance for biodiversity and environmental health worldwide, losses in diversity and abundance of bees, including *Osmia* spp., are of great concern. The identity and status of wild bees in Europe are still unknown and incomplete [6]. However, losses of wild bees and diversity in northwestern Europe have been observed and Red Lists for bees under threat have been published [7]. These losses of populations are not limited to bees—alarming ongoing declines in the abundance and diversity of beneficial insects in general have been noted [8]. The main causes of the declines are the presence of various negative factors such as habitat unavailability, a lack of natural nest materials, new agricultural and agrochemical practices, climate changes, urbanization, the presence of non-native species and the spread of parasites and pathogens [3,9–12]. Those factors can act individually, in combinations or synergistically, varying in different geographical areas, affecting solitary bees differently [13]. For example, in urban environments, solitary bees have been found to change their behavior, including flight activity, and can have impaired development, a smaller body size, reduced immunity and longevity and lower biodiversity in general [14–19].

Many parasites, predators and pests found in the nests of *O. bicornis* and *O. cornuta* in areas of southeast Europe interfere with successful reproduction [20]. *Osmia* spp. are managed cavity-nesting bees. They nest in artificial nests in semi-field conditions and can be sold in the diapause stage of development, are transported and later hatched and developed into sexually mature adults for crop pollination [4]. The presence of nest parasites, predators or pests limits the number of solitary bees that can emerge from cocoons and can interfere with individual development [3]. Additionally, the limited access to pollen provisions within nests may affect the rate of reproductive success and even intensify the parasitism consequences. Bees reared in semi-field conditions tend to be kept in very high densities which are favorable conditions for the spread of parasites and pathogens. High densities of artificial nests promote increases in the density of predators which can also cause significant damage [3]. Accompanying fauna collected from *Osmia* spp. nests described by Krunić et al. (2005) included: cleptoparasites, parasitoids, predators, cleptobionts, nest destructors and accidental nest residents [20].

As part of strategies to improve the status of local insect pollinators, the *Osmia* spp. solitary bees are managed in semi-natural habitats or rearing conditions by beekeepers. Many different management practices aimed to reduce the effects of main drivers of decline, to contribute to biodiversity conservation and to improve yield. There are many protective short- and long-term measures that can be used to optimize the rearing system. For example, opening the artificial bees' nests in autumn months enables extraction of cocoons, and permits the mechanical removal of parasites, predators and pests. Nests can also be protected against natural enemies such as ants, mice, squirrels or birds through the use of sticky barriers or wire nets set in front of the aggregations of nest tube entries [3].

The primary goal of this study was to examine the presence and prevalence of brood parasites, predators and pests in various types of bees' nesting material and semi-field rearing conditions in Croatia.

2. Materials and Methods

2.1. Artificial Solitary Bee's Nests Sampling

Artificial nests were randomly chosen and taken in October 2019 on four semi-controlled rearing solitary bee stations (Location 1—L1, Location 2—L2, Location 3—L3, Location 4—L4) across the territory of Croatia (Figure 1). These locations were situated in the different biotopes of the continental part of the country. These selected locations were influenced by various factors such as environmental conditions, urbanization gradient and breeding management practices. Location 1 was settled in an urban environment close to the city center with a small percentage of greenery, mostly composed of balcony ornamental flowers and mini gardens, in an area approximately 200 m around the sam-

pling site (micro location). Location 2 represented the suburban environment in grassland surrounded by fields used for intensive agriculture and close to the city's built-up infrastructure. Its micro-location was under rapeseed and corn plantations earlier in the season. Location 3 was in a suburban area on the border with an industrial zone and intensive refinery activity, surrounded by meadows. Location 4 was in a pure rural environment surrounded with forest and hilly meadows. Therefore, the micro location was rich in different pollen sources. Sampled occupied artificial nests originated from different beekeepers with different management practices according to their pollination needs.

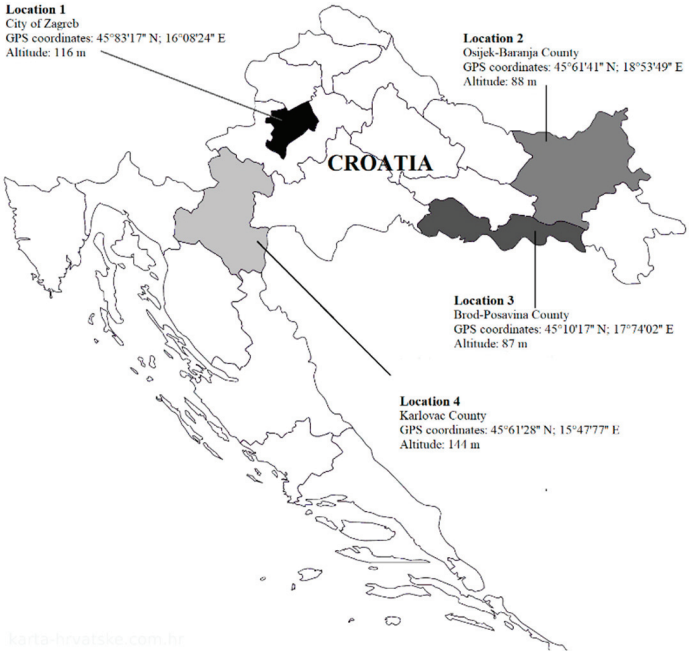

Figure 1. Sampling sites (Location 1, Location 2, Location 3 and Location 4) where few types of artificial nests of *Osmia* spp. bees were collected, from different environments in the continental part of Croatia.

At L1, beekeepers used different materials for artificial bee's nests. The length of the cane tubes used was between 12 and 16 cm and between 8 and 13 mm in inner diameter. They provide regular preventive disinfection during the winter months. The cane tube nests were opened and bees in cocoons proceeded with wintering in cardboard boxes at 2 °C and, during the darkness, to undergo diapause. At L2, only the long cane tubes were used (between 48 and 50 cm in length, and between 8 and 10 mm in width) bound in bigger bundles. At L3, the length of the used cane tubes was between 16 and 22 cm, with 8 to 11 mm in inner diameter combined with punched tree trunks of different sizes. At L4, beekeepers use cane tubes (between 10 and 14 cm long and between 9 and 12 mm in inner diameter) collected in thinner bundles (Figure 2). At all locations, one-year-old cane tubes were sampled and regularly used, except at L3 (combined with two- and three-year-old cane tubes and drilled tree trunks).

A total of 643 occupied dry cane tubes of different lengths and inner diameters (L1 = 221; L2 = 66; L3 = 286; L4 = 70) of marsh common reed (*Phragmites australis*), 192 plastic lamella (L1 = 192) and 80 individual bee cocoons (L1 = 80) were sampled. All collected nests and individual cocoons were placed into clean labelled cardboard boxes, transported

to the Laboratory for Honeybee Diseases APISlab at the Faculty of Veterinary Medicine University of Zagreb and stored in the refrigerator at 4 °C until the section analyses.

Figure 2. At semi-controlled rearing solitary bee stations (Location 1, Location 2, Location 3 and Location 4) different management practices were used.

2.2. Artificial Nests Section Analyses

The section of each nest was done by opening the reed tubes with horizontal cuts with a sharp scalpel to avoid disruption of the nest chambers. This has been done by the manual opening of the commercially available plastic lamella boxes for solitary bee rearing, and/or sections of individual cocoons using ophthalmological sterile scissors and tweezers. The visual inspection of the collected masoned nesting tubes and the lamellas with well-developed healthy cocoons (unchanged cocoon appearance), deceased larvae, leftovers of pollen provisions and soil chamber separators was done. The cocoons were classified into the groups of visually healthy, empty, destroyed or partially damaged cocoons as a consequence of infestations by different parasites and pests. Then, all the cocoons were pulled out from the nest brood chambers with sterile section tools; each was opened, and the content was taken out. For each vital solitary bee that emerged, the morphological identification (*O. bicornis* or *O. cornuta*) was done, as well as the weighting of the body mass (g) using digital scales (Sanitas, Hans Dinslage GmbH, Uttenweiler, Germany). Based on the sexual dimorphism, the gender of adult bees was determined.

The presence, prevalence and morphological identification of parasites, parasitoids, predators and the other accompanying fauna species stuck on the mason bee cocoons was done according to the previously published methods [20].

Additionally, abdomens of adult offspring bee specimens extracted from the healthy cocoons and feces samples were separately collected into the sterile 2 mL Eppendorf tubes. Those subsequent samples were stored at −20 °C until the further diagnosis was done.

2.3. Estimation of the Osmia spp. Bee's Survival Level

To estimate the level of survival and health status at each of the studied solitary bee rearing locations, during the nest tubes section the following parameters were evaluated:

I. Failures included:
   1. The number of nest brood chambers containing the undeveloped bee's offspring, e.g., mummified and dry larvae and pupae specimens;
   2. The number of nest brood chambers containing the individual dead adult bees outside of their cocoons;
   3. The number of nest brood chambers containing parasites, predators or pests;
   4. The number of nest brood chambers containing unused pollen pellets.

II. The number of live and healthy adult bee specimens (non-symptomatic bees, bees free of parasites and predation, bees without visible characteristic clinical symptoms of diseases) which are fully developed in cocoons.

The survival level of solitary bees (SL) for each sampling location was determined using the following formula:

$$SL = II./II. + (1. + 2. + 3. + 4.) \times 100\% \quad (1)$$

2.4. Laboratory Microscopic and Molecular Diagnostic of Nosema spp.

The microscopic examination of the presence of microsporidia *Nosema* spp. spores and genetic analysis confirmation were carried out on the abdomens of 30 adult bees and 30 samples of feces collected from the brood nest chambers at each location. Firstly, separated abdomens were thoroughly crushed and homogenized in a plastic container with 1 mL of water per bee. Feces samples were dissolved in the same amount of water. The magnifications of 400× under a bright field microscope—model Olympus Bx41 (Olympus Europa SE & Co., Hamburg, Germany)—were used to check the presence of *Nosema* spp. spores in freshly prepared smears of bees' gut content dispersed in water, according to the Office International des Epizooties guidelines [21]. Each diagnostic procedure was replicated three times. The microscopic equipment was carefully washed after each sample to avoid contamination with previous samples.

The extraction of total DNA from the smashed bees' abdomens was done using the DNAeasy Blood and Tissue Kit (Qiagen, Germany) according to the manufacturer's instructions. Further standard Polymerase Chain Reaction (PCR) molecular analysis was performed as was described elsewhere [5,21], through the literature within.

2.5. Statistical Analyses

The statistical analyses were performed using the statistical software package GraphPad Prism software version 7.00 for Windows (GraphPad Software, La Jolla, CA, USA). In order to assess and verify the differences between groups, the one-way analysis of variance (ANOVA) with Tukey's Post Hoc test was used. The results are presented as the mean values and standard deviations. The significance level of 0.05 was set to define the statistical differences (0.95 confidence interval).

3. Results

In this study, 4672 cocoons (6680 in total including the empty brood chambers) from artificial nests of *Osmia* spp. were examined and classified. Nests were located at four different bee rearing stations. Various nests per rearing station were analyzed, and various management practices were implemented at each studied location. The total number of healthy cocoons was 1379 (29.51%). Section analyses of artificial nests showed that

the studied localities differed in the number of determined healthy bees (L1 = 49.97%; L2 = 28.05%; L3 = 13.80%; L4 = 34.00%), number of brood parasites (L1 = 47.63%; L2 = 80%; L3 = 45.52%; L4 = 88.15%), mummified larvae (L1 = 24.70%; L2 = 10.98%; L3 = 2.73%; L4 = 2.66%) or dead adult bees (L1 = 10.77%; L2 = 5.57%; L3 = 2.48%; L4 = 0.87%), as well as chambers containing unused pollen pallets (L1 = 5.13%; L2 = 16.98%; L3 = 0.55%; L4 = 1.75%) (Table 1). Additionally, it is important to note that at L1 a different nest material was used (a, b, c).

Table 1. Comparison of the number of empty brood chambers with those which contain healthy *Osmia* spp. adult bees, and with rearing brood failures, in locations with different environment.

Number of Brood Chambers	Bee Rearing Station Location			
	L1 (a + b + c)	**L2**	**L3**	**L4**
Empty	0 + 403 + 592 Σ995	328	563	122
Brood failures	22 + 643 + 1166 Σ1831	218	1100	229
Healthy bee	58 + 453 + 404 Σ915	85	176	118

Note: a—individual cocoons; b—brood chambers in plastic lamella; c—brood chambers in reed tubes.

The weight of extracted healthy cocoons was significantly variable between the studied locations (F = 92.45, $p < 0.05$). In detail, the mean values of cocoon weight were as follows: L1 = 0.08 ± 0.02 g; L2 = 0.13 ± 0.04 g; L3 = 0.12 ± 0.05 g; and L4 = 0.12 ± 0.02 g. Results are presented in Figure 3.

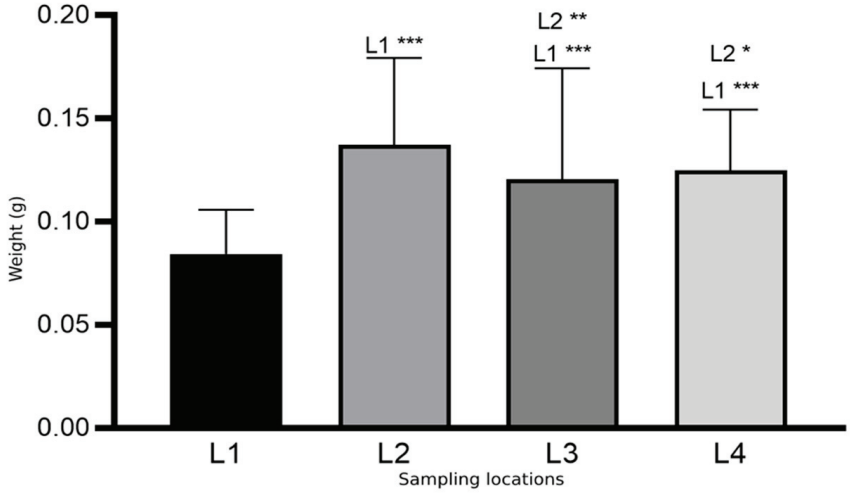

Figure 3. Weight means values of extracted cocoons from artificial nests situated at different locations. Asterisks indicates statistically significant differences: L1 vs. L2, L3, L4; L2 vs. L3, L4; * $p < 0.05$, ** $p < 0.001$, *** $p < 0.0001$; mean ± SD.

Adult specimens of *O. bicornis* differ in weight at emergence (Figure 4), particularly those significantly lightweight originating from L4, in comparison with those from L1, L2 and L3 (F = 97.45; $p < 0.0001$). The mean weight values of cocoons extracted from live bees increased as follows: L4 = 0.053 ± 0.007 g, L1 = 0.075 ± 0.006 g, L2, L3 = 0.75 ± 0.010 g.

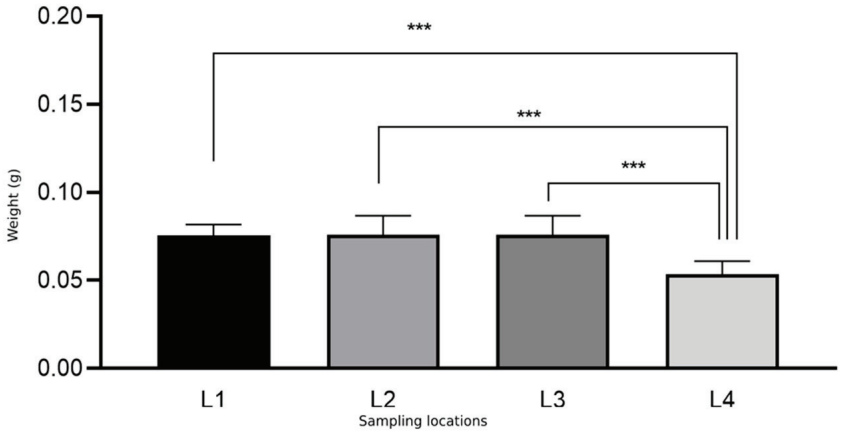

Figure 4. Weight means values of the emerged adult *Osmia bicornis* at different locations. Asterisks indicates statistically significant differences: L1, L2, L3 vs. L4, *** $p < 0.0001$; mean ± SD.

The weight means values of the emerged adult *O. cornuta* were highest at L2 (0.128 ± 0.028 g) and decreased as follows: >L4 (0.112 ± 0.028 g), >L1 (0.110 ± 0.029 g) and >L3 (0.070 ± 0.028) (Figure 5). Significant differences were observed between bees' weight between L2 and L1, L2, L4; between L3 and L1, L2, L4; and between L4 and L3 ($F = 168.7$; $p < 0.0001$).

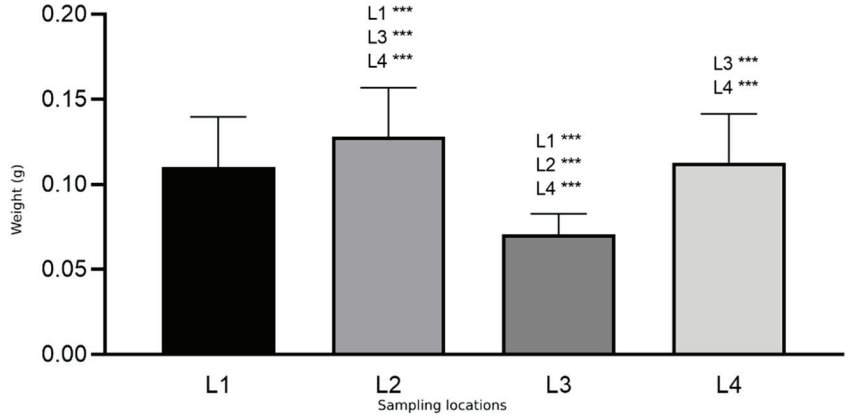

Figure 5. Weight means values of the emerged adult *Osmia cornuta* at different locations. Asterisks indicates statistically significant differences: L2 vs. L1, L3, L4; L3 vs. L1, L2, L4; L4 vs. L3; *** $p < 0.0001$; mean ± SD.

The overall bee emergence weight statistic based on the number of healthy bees and their species differentiation is shown in Table 2.

Table 2. Bee emergence weight means values based on the number of healthy bees and their species differentiation.

Species	Location	Sample Size (n)	Mean (g)	S.D.
Osmia bicornis	L1 (a + b + c)	613 (45 + 341 + 227)	0.075	0.006
	L2	38	0.076	0.010
	L3	122	0.076	0.010
	L4	66	0.053	0.007
Osmia cornuta	L1 (a + b + c)	302 (13 + 112 + 177)	0.110	0.029
	L2	47	0.128	0.028
	L3	53	0.075	0.012
	L4	52	0.112	0.028

Emergence success of solitary bees *Osmia* spp. at different rearing locations increased in following order: L1a > L1b > L1c > L4 > L2 > L3. Results are presented in Table 3.

Table 3. Summarized data of survival level and health status of solitary bees for different sampling location and management practices, based on number of healthy bees in comparison with determined individual rearing failures.

Location	Brood Chambers Contain					SL (%)
	Mummified Larvae and Pupae	Dead Adult Bees	Parasites, Predators or Pests	Unused Pollen Pellets	Live and Healthy Adult Bees	
L1a	2	7	13	-	58	72.5
L1b	256	152	216	19	453	41.33
L1c	286	108	657	115	404	34.64
	Σ613	Σ267	Σ886	Σ134	Σ915	
L2	30	16	128	44	85	28.05
L3	34	31	1028	7	176	13.80
L4	9	3	211	6	118	34.00

During the visual inspection of 80 cocoons at L1, 9.00% of the cocoons containing cleptoparasite *Cacoxenus indagator* and 8.00% containing the mite *Chaetodactylus osmiae* were found. In the nests of plastic lamella at L1, we determined that 6.00% of brood chambers were invaded by *C. indagator*, 7.00% by *C. osmiae* mites, 4.00% by parasitoid *Monodontomerus obscurus*, 0.27% containing predator larva *Trichodes apiarius*, 2.00% invaded by *Trogoderma glabrum* and 0.36% by *Ptinus fur* nest destroyers. Additionally, we determined characteristic clinical signs for chalkbrood in 0.55% of examined brood chambers. In reed tubes at the same rearing station, as in natural nest materials, we found higher parasitization rates. In detail, parasitization included: 12% of brood chambers invaded by *C. indagator*, 10.00% by *C. osmiae* mites, 12% by *T. glabrum*, 0.36% by *P. fur*, 4.00% containing *M. obscurus* and 3.00% with adult Eumenidae wasps.

In nests sampled at L2 during section analyses, we determined *C. osmiae* mites in 22.00% of examined brood chambers, 9.00% contained *T. glabrum* and 5.00% were invaded by Eumenidae wasp larvae. Additionally, in 6.00% of brood chambers there were mummies characteristic for chalkbrood disease.

In cane tubes from L3, 5% of *C. indagator*, 20% of *C. osmiae* mites, 20.00% of *T. glabrum*, 30.00% of Eumenidae wasp, and *T. apiarius* and Chalkbrood disease, each at 3.00%, were found.

After the section of cane nests originated from L4, it was determined that 12.00% of brood chambers were invaded by *C. indagator*, 20.00% by *C. osmiae* mites and 9.00% by parasitoid *M. obscurus*. Then, 20.00% of the chambers contained *T. glabrum*, 3.00% contained *T. apiaries*, 30.00% contained Eumenidae wasp larvae and 3.00% contained mummies characteristic of chalkbrood.

A detailed presentation of the determined occurrence and prevalence of brood parasites and clinically visible chalkbrood is shown in Figure 6. The most common parasites are shown in Figure 7.

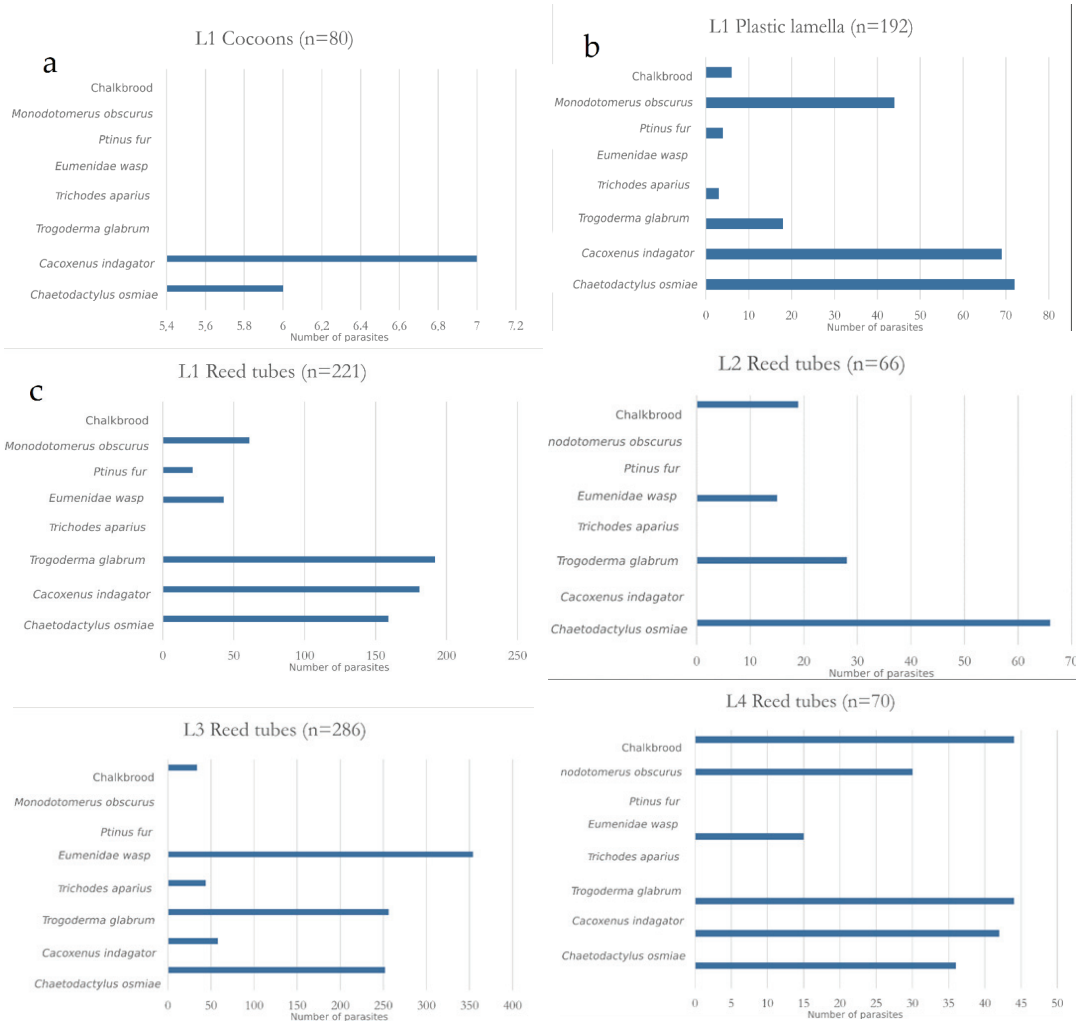

Figure 6. Occurrence and prevalence of brood parasites and clinically visible chalkbrood in various types of bees' nesting material and rearing conditions at four locations (L1—different nesting material: extracted cocoons—(**a**), plastic lamella—(**b**), reed tubes—(**c**), L2, L3, L4).

(**a**) (**b**)

Figure 7. *Cont*.

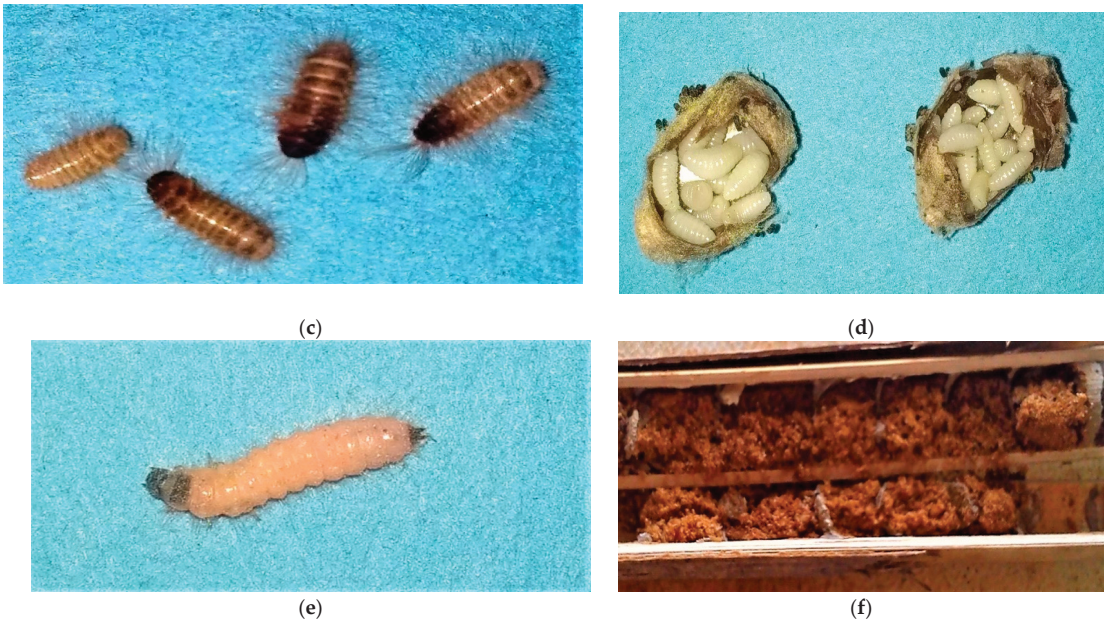

Figure 7. Common parasites of *Osmia* spp. bees' nests: (**a**)—*Cacoxenus indagator* young larvae; (**b**)—*C. indagator* adults; (**c**)—*Monodontomerus obscurus* overwintering prepupa inside cocoons; (**d**)—*Trichodes apiarius* larvae; (**e**)—*Trogoderma glabrum*; (**f**)—destroyed cocoons invaded by *Chaetodactylus osmiae* mites.

The results of the microscopic examination on the *Nosema* spp. spores' presence in homogenized abdomens and feces of natural watery smears were negative. Additionally, the results of multiplex PCR show that all analyzed samples were negative for the genetic material of both *Nosema apis* and *Nosema ceranae* when amplified with their specific primer pairs.

4. Discussion

In this monitoring-designed study, we firstly examined the occurrence and the prevalence of parasites in *Osmia* spp. bees artificial nests, settled at different locations in the continental part of Croatia. We found significant differences in the bees SL for different sampling locations, as well as between nesting materials used in implementing managing practices. Insect pollinators can be secondary carriers of the parasites in their nest surroundings [22,23]. However, it was recently reported that solitary *Osmia* spp. bees do not transmit or introduce the pathogen microorganisms in their nests from the environment [5]. Findings such as unused pollen provisions or brood failures in the early bees' developmental stages could be caused by other environmental or anthropogenic factors, such as pollution or urbanization. Additionally, the part of urban gardens and horticultural nurseries as solitary bees' food sources have just recently received attention and the consequent impacts are still unknown [24]. The highest percentage of unused pollen and dead younger brood was found at the urban environment in the reed tube nests (L1c). This can possibly be explained by the fact that the larval bacterial microbiome is linked with the available pollen [25], and an unusual environmental bacterial community might be harmful to the bee larvae [26]. Due to the limited sources of pure pollen from balconies, mini garden flowers and ornamental plants in the urban site micro location and the high possibility of its contamination with various xenobiotics or protein diet content of the changed microbiome, adult bees are not able for efficient detoxification. Additionally, they avoid laying the eggs on collected provisions and sealed young brood die in a short period. Generally, diversity

and overlapping of the bacterial communities between pollen and bee larvae is significantly lower in disintegrated than in the healthy solitary bee larvae [27]. In the protection of park plants and ornamental flowers, systemic insecticides are used at higher levels and various formulations than in the production of food crops [28,29]. Additionally, pollution mechanisms of their nectar and pollen are poorly understood.

Previously published results showed that in urban areas there is a lower level of parasite invasion in artificial bees nests than in the suburban and rural sites [5]. In our study, we included the results linked with parasitization rates in different nesting materials of the same rearing location and management practice. As was anticipated, in cocoons mechanically cleaned and extracted from reed nests before wintering, the highest bees SL was calculated, and we found only two parasites, *C. indagator* and mites *C. osmiae*. *C. indagator* females lay their eggs on the pollen provisions and larvae actively feed until the next pupal stage [1]. Here, we found it in a few noticeable smaller deformed neighboring cocoons without other content. Similarly, *C. osmiae* was found in partially damaged small cocoons with tiny walls inside which were dead but developed bees surrounded with hypopi. Such a finding was also previously described [30,31]. Despite prewinter disinfection being applied per recommendation [32], for 8% of the cocoons it was not successful. Comparison with other artificial nests is interesting due to a higher percentage of healthy bees in plastic lamella (41.33%) than in the natural reed tubes (34.64%). In both kinds of nests, we mostly found the same six parasites (*M. obscurus*, *P. fur*, Eumenidae wasp (just L1c), *T. apiarius* (just L1 b), *T. glabrum*, *C. indagator* and mites *C. osmiae*). Furthermore, in the plastic lamella in which moisture was higher, the characteristic signs of chalkbrood caused by fungi were also present. According to the results, we determined that in the urban environment (L1 a, b, c) there was a lower occurrence and prevalence of nest parasites, which agrees with previously published results for experimentally settled initial bee populations [5].

At L2 and L3, the manifestation of the nest parasites was higher than at the L1 and L4. This observation was especially visible at L3 where 80.56% of brood chambers contained parasites. Although the nests of solitary bees are not the reservoir of infectious pathogenic microorganisms [5], they can be the source of different parasites and nest destructors. At L3, management practice involved the combination of a few different nest materials. In detail, except two- and three-year-old cane tubes, there are drilled tree trunk nests. In this study, we sampled only one-year-old cane tubes, but the presence of older multiple-used nests could be a reason for the easier spread of the parasites. Earlier studies showed that the mason bee artificial nests should be used only once, because repeated use of tubes (or other kinds of nest material) increases the level of parasite infestations [33]. The same authors determined that in comparison with one-year-old tubes, in the two-year-old cane tubes there are more than ten times less healthy cocoons and three times more injured or destroyed cocoons, with a wider diversity of parasites [33]. Additionally, it was previously reported that continuous breeding in the same place for more than ten years means significantly higher numbers and diversity of brood parasites in nests [34,35]. Our results showed the lowest determined bees SL was at L3, which was 13.80% in total, while in a similar environment of L2, it was 28.05%. The bees SL was determined as almost equal at the L1c (34.64%) and L4 (34.00%) sites.

In the samples of *O. bicornis* adults caught near honeybee apiaries, Ravoet et al. (2014) confirmed the presence of *N. ceranae* genetic material [36]. Our finding, that adult bees collected from nests situated on different biotopes, as well as samples of their feces, were not invaded by microsporidia *Nosema* spp., is in agreement with other studies [5,37].

It is very interesting that a high percentage of brood chambers with unused pollen provisions were found during the section analyses of reed tube nests samples from L2 (17% of examined nest brood chambers; empty chambers were excluded from the calculation). It was a significantly higher percentage in comparison with the situation at L3 (0.55%). As around this bee rearing station there are fields for intensive agricultural production, there is also the possibility for chemical contamination of different nest materials, pollen and nectar, as well as mud, water and leaf nest material. Additionally, residues of agrochemicals or fer-

tilizers used in plant cultivar production, natural vegetation and soil can be detected [38,39]. Again, as at L1, these results indicate the possibility that bee females avoid laying eggs on contaminated or changed bacterial community composition of pollen provisions. Recently, the moderate impact of horticultural management practices including the imidacloprid application, which strongly reduced solitary bee reproduction success, was described [40–42]. Additionally, the water availability in artificial nest environments is strongly linked with insect pollinator's food quality and consequently to all bees' developmental stages, fitness and survival [43].

At L4, we found a small incidence of nest chambers with unused pollen provisions and early bee developmental stage failures in comparison with L1c, L2 and L3. Parasites' occurrence and their diversity were similar to the other rearing station locations.

The overall emergence success of *O. bicornis* and *O. cornuta* at different rearing locations cannot be determined because this study is not an experimental study with meaningful control of the independent variables. The number and diversity of parasites which act as nest destructors increased in the following order: urban, rural and suburban environments. Additionally, those parameters were positively correlated with the presence of solitary bee rearing failures. Those results are in accordance with the reports of Los et al. (2019) and Fliszkiewicz et al. (2012), who noticed lower parasite infestations and diversity in rural and urban sites than in suburban areas in experimental initial bee populations [5,44]. The mortality of *Osmia lignaria* offspring caused by brood parasites is also higher at natural and rural sites [45].

The differences in cocoon mass and emergence mass of healthy adult bees were determined between the observed locations. Interestingly, cocoon weight increased as follows: L1, L3, L4 and L2. Additionally, the weights of adult emerged bees were different depending on the rearing location and bee species (Figures 3–5; Table 2). However, due to morphological differences and the differences in metabolic rates between sexes, as well as the water content, body weight can differ between males and females [46]. The body weight of *O. bicornis* was significantly lower at L4, and all other rearing sites' mean values of bees' weight were similar. At L2, adults of *O. cornuta* were significantly weightier in comparison with the emerged bees originating from other nests at other locations. That may relate to the management practice of using longer reed tubes as artificial nests. Adults from L3 were significantly smaller, which may be linked with the high parasitization rate but also environmental factors, such as the lack of quality natural food. Here, it must be noted that we opened the nests during November and December, and until then the material was kept at fridge temperature. Schenk et al. (2018) reported that environmental temperature influences the emergence term and body weight [47]. The same authors concluded that the timing of emergence also depends on the individual's body condition, due to the variability in natural emergence terms among specimens which survive the winter period at the same or similar environmental temperatures [47]. As we did not measure weather conditions, it is hard to make any conclusions about the body weight variability among the bees from the different experimental rearing stations.

5. Conclusions

The number and diversity of solitary bees are declining in many landscapes. Therefore, pollination by these insects is vulnerable to ecosystem services. The results of this study include the presence and prevalence of brood parasites, predators and pests in various types of *Osmia* spp. bees' nesting material and the semi-field rearing conditions in Croatia for the first time. Managed rearing practices of *Osmia* spp. bees can be useful for agricultural and horticultural sustainable development in different biotopes. Therefore, this study may be used as a baseline for further solitary bee nest parasite monitoring schemes.

Author Contributions: Conceptualization, I.T.G. and M.Š.; methodology, I.T.G.; investigation, all authors; writing—original draft preparation, I.T.G.; writing—review and editing, all authors; visualization, I.T.G. All authors have read and agreed to the published version of the manuscript.

Funding: This research received no external funding.

Institutional Review Board Statement: Not applicable.

Informed Consent Statement: Not applicable.

Data Availability Statement: The data presented in this study are available in this paper.

Acknowledgments: The authors would like to thank G. Husinec for assistance in the laboratory and J. Vlainić for statistic technical support. Additionally, many thanks to I. Sabolek for critically reviewing this manuscript.

Conflicts of Interest: The authors declare no conflict of interest.

References

1. Krunić, M.; Stanisavljević, L.J. Augmentation of managed populations of *Osmia cornuta* and *O. rufa* (Hymenoptera: Megachilidae) in Southeastern Europe. *Eur. J. Entomol.* **2006**, *103*, 695–697. [CrossRef]
2. MacIvor, J.S.; Packer, L. The bees among us: Modelling Occupancy of Solitary Bees. *PLoS ONE* **2016**, *11*, e0164764. [CrossRef]
3. Sedivy, C.; Dorn, S. Towards a sustainable management of bees of the subgenus *Osmia* (Megachilidae; Osmia) as fruit tree pollinators. *Apidologie* **2014**, *45*, 88–105. [CrossRef]
4. Bosch, J.; Kemp, W.P. Developing and establishing bee species as crop pollinators: The example of *Osmia* spp. (Hymenoptera: Megachilidae) and fruit trees. *Bull. Entomol. Res.* **2002**, *92*, 3–16. [PubMed]
5. Łoś, A.; Skórka, P.; Strachecka, A.; Winiarczyk, S.; Adaszek, L.; Winiarczyk, M.; Wolski, D. The associations among the breeding performance of *Osmia bicornis* L. (Hymenoptera: Megachilidae), burden of pathogens and nest parasites along urbanisation gradient. *Sci. Total Environ.* **2020**, *710*, 135520. [CrossRef] [PubMed]
6. Carvalheiro, L.G.; Kunin, W.E.; Keil, P.; Aguirre-Gutiérrez, J.; Ellis, W.N.; Fox, R.; Groom, Q.; Hennekens, S.; Van Landuyt, W.; Maes, D.; et al. Species richness declines and biotic homogenisation have slowed down for NW-European pollinators and plants. *Ecol. Lett.* **2013**, *16*, 1416–1417. [CrossRef]
7. Nieto, A.; Roberts, S.P.M.; Kemp, J.; Rasmont, P.; Kuhlmann, M.; García Criado, M.; Biesmeijer, J.C.; Bogusch, P.; Dathe, H.H.; De la Rúa, P.; et al. *European Red List of Bees*; Publication Office of the European Union: Luxembourg, 2014.
8. Wagner, D.L. Insects declines in the Anthropocene. *Ann. Rev. Entomol.* **2020**, *65*, 457–480. [CrossRef] [PubMed]
9. Tlak Gajger, I.; Sakač, M.; Gregorc, A. Impact of Thiamethoxam on Honey Bee Qeeen (*Apis mellifera*) Reproductive Morphology and Physiology. *Bull. Environ. Contam. Toxicol.* **2017**, *99*, 297–302. [CrossRef]
10. Laurino, D.; Lioy, S.; Carisio, L.; Manino, A.; Porporato, M. *Vespa velutina*: An Alien Driver of Honey Bee Colony Losses. *Diversity* **2020**, *12*, 5. [CrossRef]
11. Strobl, V.; Bruckner, S.; Radford, S.; Wolf, S.; Albrecht, M.; Villamar-Bouza, L.; Maitip, J.; Kolari, E.; Chantawannakul, P.; Glauser, G.; et al. No impact of neonicotinoids on male solitary bees *Osmia cornuta* under semi-field conditions. *Physiol. Entomol.* **2021**, *46*, 105–109. [CrossRef]
12. Tlak Gajger, I.; Šimenc, l.; Toplak, I. The First Detection and Genetic Characterization of Four Different Honeybee Viruses in Wild Bumblebees from Croatia. *Pathogens* **2021**, *10*, 808. [CrossRef] [PubMed]
13. González-Varo, J.P.; Biesmeijer, J.C.; Bommarco, R.; Potts, S.G.; Schweiger, O.; Smith, H.G.; Steffan-Dewenter, I.; Szentgyörgyi, H.; Woyciechowski, M.; Vilà, M. Combined effects of global change pressures on animal-mediated pollination. *Trends Ecol. Evol.* **2013**, *28*, 524–530. [CrossRef] [PubMed]
14. McKinney, M.L. Urbanization, Biodiversity, and Conservation: The impacts of urbanization on native species are poorly studied but educating a highly urbanized human population about these impacts can greatly improve species conservation in all ecosystems. *BioScience* **2002**, *52*, 883–890. [CrossRef]
15. Giraudeau, M.; Mousel, M.; Earl, S.; McGraw, K. Parasites in the City: Degree of Urbanization Predicts Poxvirus and Coccidian Infections in House Finches (*Haemorhous mexicanus*). *PLoS ONE* **2014**, *9*, e86747. [CrossRef] [PubMed]
16. Giejdasz, K.; Fliszkiewicz, M. Effect of temperature treatment during development of *Osmia rufa* L., on mortality, emergence and longevity of adults. *J. Apic. Sci.* **2016**, *60*, 221–232. [CrossRef]
17. Kierat, J.; Szentgyörgyi, H.; Czarnoleski, M.; Woyciechowski, M. The thermal environment of the nest affects body and cell size in the solitary red mason bee (*Osmia bicornis* L.). *J. Therm. Biol.* **2017**, *68*, 39–44. [CrossRef] [PubMed]
18. Isaksson, C. Urbanization, oxidative stress and inflammation: A question of evolving, acclimatizing or coping with urban environmental stress. *Funct. Ecol.* **2015**, *29*, 913–923. [CrossRef]
19. Kierat, J.; Filipiak, M.; Szentgyörgyi, H.; Woyciechowski, M. Predation Cues in Solitary bee Nests. *J. Insect Behav.* **2017**, *30*, 385–393. [CrossRef] [PubMed]
20. Krunić, M.; Stanisavljević, L.J.; Pinzauti, M.; Felicioli, A. The accompanying fauna of *Osmia cornuta* and *Osmia rufa* and effective measures of protection. *Bull. Insectol.* **2005**, *58*, 141–152.
21. OIE—Office International des Epizooties. Chapter 2.2.4., Nosemosis of Honey Bees. In *Manual of Diagnostic Tests and Vaccines for Terrestrial Animals*; OIE: Pairs, France, 2013. Available online: http://www.oie.int/international-standard-setting/terrestrial-manual/access-online (accessed on 26 June 2021).

22. Maccagnani, B.; Giacomello, F.; Fanti, M.; Gobbin, D.; Maini, S.; Angeli, G. *Apis mellifera* and *Osmia cornuta* as carriers for the secondary spread of *Bacillus subtilis* on apple flowers. *BioControl* **2009**, *54*, 123. [CrossRef]
23. Graystock, P.; Goulson, D.; Hughes, W.O.H. Parasites in bloom: Flowers aid dispersal and transmission of pollinator parasites within and between bee species. *Proc. R. Soc. B* **2015**, *282*, 20151371. [CrossRef] [PubMed]
24. Egerer, M.; Cecala, J.; Cohen, H. Wild bee conservation within urban gardens and nurseries: Effects of local and landscape management. *Sustainability* **2020**, *12*, 293. [CrossRef]
25. Voulgari-Kokota, A.; Grimmer, G.; Steffan-Dewenter, I.; Keller, A. Bacterial community structure and succession in nests of two megachilid bee genera. *FEMS Microbiol. Ecol.* **2019**, *95*, fiy218. [CrossRef] [PubMed]
26. Anderson, K.E.; Ricigliano, V.A. Honey bee gut dysbiosis: A novel context of disease ecology. *Curr. Opin. Insect Sci.* **2017**, *22*, 125–132. [CrossRef] [PubMed]
27. Voulgari-Kokota, A.; Steffan-Dewenter, I.; Keller, A. Susceptibility of Red Mason Bee Larvae to Bacterial Threats Due to Microbiome Exchange with Imported Pollen Provisions. *Insects* **2020**, *11*, 373. [CrossRef] [PubMed]
28. Gierer, F.; Vaughan, S.; Slater, M.; Thompson, H.M.; Elmore, J.S.; Girling, R.D. A review of the factors that influence pesticide residues in pollen and nectar: Future research requirements for optimizing the estimation of pollinator exposure. *Environ. Pollut.* **2019**, *249*, 236–247. [CrossRef] [PubMed]
29. Cowles, R.S.; Eitzer, B.D. Residues of neonicotinoid insecticides in pollen and nectar from model plants. *J. Environ. Hortic.* **2017**, *35*, 24–34. [CrossRef]
30. Seidelman, K. Zur parazitenkontrolle in stammzuchten der roten mauerbiene *Osmia rufa* L. *Wissen-Schaften Z. Univ. Halle* **1990**, *39*, 25–34.
31. Stanisavljević, L.J. The Impact of Accompaining Fauna on the Populations of Newly Domesticated Solitary Bees *Osmia cornuta* (Latr.) and *O. rufa* (L.) (Megachilidae, Hymenoptera). Master's Thesis, Faculty of Biology, University of Belgrade, Belgrade, Serbia, 1996.
32. Krunić, M.; Stanisavljević, L.J.; Brajković, M.; Tomanović, Ž.; Radović, I. Ecological studies of *Osmia cornuta* (Latr.) (Megachilidae, Hymenoptera) populations in Yugoslavia with special attention to their diapause. *Acta Hortic.* **2001**, *561*, 297–301. [CrossRef]
33. Madras-Majewska, B.; Zajdel, B.; Boczkowska, B. The influence of nests usage on mason bee (*Osmia rufa* L.) survival. *Ann. Warsaw Agricult. Univ.-SGGW Anim. Sci.* **2011**, *49*, 115–119.
34. Zajdel, B.; Kucharska, K.; Kucharski, D.; Fliszkiewicz, M.; Gąbka, J. Accompanying fauna of red mason bees in annual and perennial nesting sites. *Med. Weter* **2014**, *70*, 745–749.
35. Zajdel, B.; Borański, M.; Kucharska, K.; Teper, D. Reproduction and Accompanying Fauna of Red Mason Bee *Osmia rufa* L. (syn. *Osmia bicornis* L.) in Areas with Different Levels of Urbanization. *J. Apic. Sci.* **2021**, *65*, 123–137. [CrossRef]
36. Ravoet, J.; De Smet, L.; Meeus, I.; Smagghe, G.; Wenseleers, T.; De Graaf, D.C. Widespread occurrence of honey bee pathogens in solitary bees. *J. Invertebr. Pathol.* **2014**, *122*, 55–58. [CrossRef] [PubMed]
37. Hedtke, S.M.; Blitzer, E.J.; Montgomery, G.A.; Danforth, B.N. Introduction of Non-Native Pollinators Can Lead to Trans-Continental Movement of Bee-Associated Fungi. *PLoS ONE* **2015**, *10*, e0130560. [CrossRef] [PubMed]
38. Kopit, A.M.; Pitts-Singer, T.L. Routes of Pesticide Exposure in Solitary, Cavity-Nesting Bees. *Environ. Entomol.* **2018**, *47*, 499–510. [CrossRef]
39. Cecala, J.M.; Wilson Rankin, E.E. Pollinators and plant nurseries: How irrigation and pesticide treatment of native ornamental plants impact solitary bees. *Proc. R. Soc. B* **2021**, *288*, 20211287. [CrossRef] [PubMed]
40. Stuligross, C.; Williams, N.M. Pesticide and resource stressors additively impair wild bee reproduction. *Proc. R. Soc. B* **2020**, *287*, 20201390. [CrossRef] [PubMed]
41. Klaus, F.; Tscharntke, T.; Bischoff, G.; Grass, I. Floral resource diversification promotes solitary bee reproduction and may offset insecticide effects—Evidence from a semi-field experiment. *Ecol. Lett.* **2021**, *24*, 668–675. [CrossRef] [PubMed]
42. Mokkapati, J.S.; Bednarska, A.J.; Laskowski, R. The development of the solitary bee Osmia bicornis is affected by some insecticide agrochemicals at environmentally relevant concentrations. *Sci. Total Environ.* **2021**, *775*, 145588. [CrossRef] [PubMed]
43. Wilson Rankin, E.E.; Barney, S.K.; Lozano, G.E. Reduced water negatively impacts social bee survival and productivity via shifts in floral nutrition. *J. Insect Sci.* **2020**, *20*, 15. [CrossRef]
44. Fliszkiewicz, M.; Kuśnierczak, A.; Szymaś, B. The accompanying fauna of solitary bee *Osmia bicornis* (L.) syn. *Osmia rufa* (L.) nests settled in different biotopes. *J. Apic. Sci.* **2012**, *56*, 51–58. [CrossRef]
45. Palladini, J.D.; Maron, J.L. Reproduction and survival of a solitary bee along native and exotic floral resource gradients. *Oecologia* **2014**, *176*, 789–798. [CrossRef] [PubMed]
46. Bosch, J.; Vicens, N. Body size as an estimator of production costs in a solitary bee. *Ecol. Entomol.* **2002**, *27*, 129–137. [CrossRef]
47. Schenk, M.; Mitesser, O.; Hovestadt, T.; Holzschuh, A. Overwintering temperature and body condition shift emergence dates of spring-emerging solitary bees. *PeerJ* **2018**, *16*, e4721. [CrossRef] [PubMed]

diversity

MDPI

Article

Citizen Scientists Record Significant Range Extensions for Tropical Sea Slug Species in Subtropical Eastern Australia

Stephen D. A. Smith [1,2,*] and Matt J. Nimbs [2]

[1] Aquamarine Australia, Mullaway, NSW 2456, Australia
[2] National Marine Science Centre, Southern Cross University, Coffs Harbour, NSW 2450, Australia; matthew.nimbs@scu.edu.au
* Correspondence: steve.smith@scu.edu.au

Abstract: The Sea Slug Census program in Australia engages with citizen scientists to record the diversity and distribution of sea slugs across multiple locations. The program has consistently recorded shifts in distribution patterns but a recent, nine-day census in subtropical eastern Australia recorded unprecedented range extensions of tropical species. Seven species (six chromodorids and one polycerid) were found further south of their previously known distribution with *Hypselodoris bertschi* being recorded for the first time in Australia. These observations suggested the recent transport of larvae via the East Australian Current with recruitment to coastal sites possibly promoted by a protracted period of strong onshore winds associated with the 2021/22 La Niña in the western Pacific. With the increasing frequency of poleward range extensions of marine taxa, citizen science programs such as the Sea Slug Census provide the opportunity to substantially increase monitoring efforts. Linking with iNaturalist strengthens the value of the observations through online peer review to confirm species identities as well as the incorporation of substantiated (Research Grade) records into international biodiversity databases such as GBIF.

Keywords: Heterobranchia; iNaturalist; Mollusca; Solitary Islands Marine Park; volunteer

Citation: Smith, S.D.A.; Nimbs, M.J. Citizen Scientists Record Significant Range Extensions for Tropical Sea Slug Species in Subtropical Eastern Australia. *Diversity* **2022**, *14*, 244. https://doi.org/10.3390/d14040244

Academic Editor: Michael Wink

Received: 10 March 2022
Accepted: 25 March 2022
Published: 27 March 2022

1. Introduction

Changes in the distribution patterns of species are occurring at unprecedented rates across the globe as anthropogenic effects, especially climate change, modify natural habitats and environmental conditions [1–3]. With these accelerating rates of change, arguably, there has never been a more important time to recruit members of the broader community to help quantify change. The importance of observations by community members as citizen scientists has long been recognized for terrestrial habitats but, possibly due to the comparative difficulty of observations and limited access for many would-be participants, marine-based citizen science programs lag behind their terrestrial counterparts. However, a range of recent programs has been implemented to encourage marine observations. The Sea Slug Census (SSC) is one such program. Commencing in Nelson Bay, New South Wales (NSW), Australia, in December 2013, participants (scuba divers, snorkelers, rock-pool ramblers) simply photograph each species of sea slug they encounter over nominated spatial and temporal scales (equivalent to a focused "bioblitz") and submit them to the event organisers [4]. Species records are added to the program database and a report illustrating all species found is distributed to all participants and made more widely available through various web and social media sites (primarily the Sea Slug Census site on Facebook (Meta)). The popularity of the program, especially amongst scuba divers, has led to its expansion to 11 locations within Australia as well as sites in Indonesia and Vanuatu.

Motivations for participating stem not only from the fact that many species in the focal taxonomic group (Heterobranchia) are highly photogenic (e.g., the colourful nudibranchs) but also because participants are keen to monitor the health of their local marine habitats [4].

As most marine heterobranch species have relatively short lifespans and often highly specific food and habitat requirements [5,6], they have been hypothesised to be sensitive to environmental change, detectable through changes in species presence and distribution (e.g., [7–9]). This is supported through several of the earlier observations in the SSC program with citizen scientists providing a number of observations of range extensions across NSW [10–14].

There are a number of important considerations when establishing a citizen science program (reviewed by [15]). Providing a program that is appealing to potential participants is a key consideration and, for marine volunteers, additional motivations primarily relate to increasing their own knowledge whilst adding to the accumulation of scientific knowledge [16]. However, at the other end of the data collection process, in order for the observations to have value outside the specific and often geographically restricted project, it is essential that identifications are accurate and available to a wider audience. Until recently (2021), observations from the SSC program were identified by the program organisers with input from external experts where necessary and data were shared amongst the program participants. In order to make the program more globally relevant, from October 2021 (during the Great Southern Bioblitz of iNaturalist), participants were asked to register and submit photographic observations through iNaturalist (Available online: https://www.inaturalist.org/, Accessed on 1 March 2022). This platform is rapidly becoming one of the most important for collating observations of global biodiversity and provides not only a crowd-sourced review process for gaining consensus for identifications (termed Research Grade) but also open access to all observations that are also incorporated into the main global biodiversity databases (such as GBIF and, in Australia, Atlas of Living Australia) (e.g., [17]). This paper reports on specific observations submitted through iNaturalist as part of the January 2022 Coffs Coast Sea Slug Census within the Solitary Islands Marine Park (SIMP).

The SIMP lies on the subtropical east coast of Australia (Figure 1) and covers estuarine, shore and subtidal habitats. Marine communities comprise a mix of algal-dominated habitats close to shore [18] with increasing representation of more tropically affiliated species offshore [19,20]. The outer islands (North and South Solitary islands; Figure 1) are regularly influenced by the southward-flowing East Australian Current (EAC) and thus experience water temperatures that are 1–1.5 °C higher than nearshore locations [21]. The influence of the EAC is cited as a key reason for the dominance of hard corals around the mid-shelf and offshore islands with coral cover approaching that of more tropical locations at several sites [22]. Range extensions have been reported for a number of taxa over the past decade but, although there has been a progressive loss of macroalgal cover at a few mid-shelf sites [23], coral-dominated communities at the outer islands show no evidence of broadscale tropicalisation [24]. A thriving diving industry and a dedicated group of underwater volunteers [25] ensure that most main island sites are regularly visited with the consequent likelihood that novel or unusual species will be observed and reported. It is against this backdrop that we evaluated the list of taxa recorded during the recent Coffs Coast Sea Slug Census with a specific focus on species recorded for the first time and south of their previously documented range.

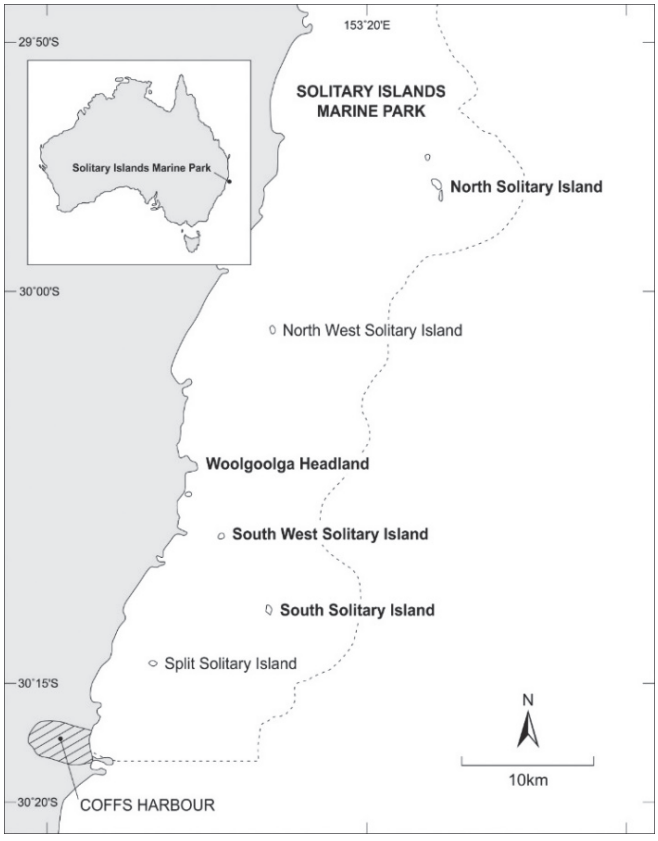

Figure 1. The Solitary Islands Marine Park (boundary shown as a dotted line), subtropical eastern Australia. The geographical scope of the Coffs Coast Sea Slug Census included the entire marine park. Locations of observations for the seven species covered in this paper appear in bold font.

2. Materials and Methods

For the recent Coffs Coast Sea Slug Census, participants searched for and photographed sea slugs (Mollusca; Heterobranchia) from marine habitats over a 9-day period from 22–30 January 2022 with additional observations on 15 February 2022. There were no restrictions on the time of day for observations although only one search was conducted at night, on a coastal headland. The spatial scope of the study was the entire Solitary Islands Marine Park (Figure 1). Participants conducted searches of tidepools, snorkeled in shallow habitats and/or explored subtidal habitats via scuba and took pictures of sea slugs in situ. Species captured in images were collated through iNaturalist and identifications were crowd-sourced to reach consensus (Research Grade). These were also checked, along with distribution records, against a range of resources including reference books [26–29], websites covering sea slugs (e.g., Sea Slug Forum) and databases (GBIF) including those compiled from recent records in the SSC program [11,30,31].

A determination of an extension to a species range was made by reference to the databases of the authors as well as publications detailing sea slug distributions in NSW [10–14,30,31]. The taxonomic structure of this paper follows the World Register of Marine Species [32].

3. Results

SYSTEMATICS
Class: Gastropoda
Subclass: Heterobranchia
Order: Nudibranchia Cuvier, 1817
Family: Chromodorididae Bergh, 1891
Genus: *Chromodoris* Alder & Hancock, 1855
Chromodoris quagga Bonomo & Gosliner, 2020
(Figure 1)

Chromodoris quagga is similar to *Chromodoris burni* in colour and pattern; however, the presence of brown body pigment and the absence of white spots on the gills and rhinophores in *C. quagga* are diagnostic. Additionally, *C. quagga* is three times larger at ~35 mm compared with *C. burni* at 9–11 mm [33].

As a recently described species (in 2020), there is the potential for historic observations to remain unrecognised, potentially recorded as *Chromodoris* sp. in the literature and in online data repositories. Nevertheless, there have been several recent observations outside the Philippines (type location) and also in Indonesia, Papua New Guinea and New Caledonia [34].

In Australia, *C. quagga* has only been observed at South Solitary Island, NSW. It was first recorded by Steve Smith on 24 January 2019. Since then, two more animals have been recorded [34] (Figure 2). These observations from a single location made over a four-year period represent a poleward range extension of ~900 km from the nearest observation in New Caledonia (orthodromic distance between the observation latitudes 22°16′–30°6′) and the most southern global record of this species (Table 1).

Figure 2. *Chromodoris quagga*, South Solitary Island, NSW, 29 January 2022. Photo: B. Touzell.

Table 1. Distribution records of *Chromodoris quagga* in Oceania.

Location	Date	Latitude	Longitude	Reference
Milne Bay, Papua New Guinea	2015	10°27′53.81″ S	150°42′6.36″ E	[34]
Mont Dore, New Caledonia	2022	22°16′20.86″ S	166°33′45.46″ E	[34]
South Solitary Island, NSW	2019, 2021, 2022	30°6′34.17″ S	153°12′43.42″ E	This paper

Genus: *Hypselodoris* Stimpson, 1855
Hypselodoris bertschi Gosliner & R. F. Johnson, 1999
(Figure 3)

Figure 3. *Hypselodoris bertschi*, Woolgoolga Headland, NSW, 22 January 2022. The only observation of this species in Australia. Photo: S. D. A. Smith.

Hypselodoris bertschi is characterised by a translucent white body with rows of indistinct purple-blue elliptical spots alternating with opaque narrow white lines on the dorsum and a light blue foot margin. The rhinophores exhibit a median orange band and the gills have an orange rachis [35,36].

The recent (1999) description of *H. bertschi* helped to resolve the historic taxonomic instability associated with this species [37] by bringing into synonymy several confusing names dating back as far as 1860 [38]. However, the new species, *H. bertschi*, as currently accepted, and its synonymous taxa were considered to be restricted to the Hawaiian Islands, USA.

Since then, *H. bertschi* has been observed in Japan in 2001 and 2009 [39], French Polynesia in 2006 [40] and South Africa in 2007 and 2010 [40]. With only three records from the southern hemisphere across two locations, any observations may be regarded as noteworthy. An observation of a 15 mm individual in a coastal tidepool (depth 0.5 m) by Steve Smith at Woolgoolga Headland, NSW, on 22 January 2022 (Figure 3)—approximately 5900 km southwest of the nearest observation at Moorea, French Polynesia—represents not only the fourth record of this species in the southern hemisphere but also the first for Australian waters (Table 2).

Table 2. South Pacific distribution records of *Hypselodoris bertschi*.

Location	Date	Latitude	Longitude	Reference
Moorea, French Polynesia	2007, 2010	17°28′55.25″ S	149°49′37.26″ W	[40]
Woolgoolga, NSW	2022	30°06′34.17″ S	153°12′43.42″ E	This paper

Hypselodoris imperialis (Pease, 1860)
(Figure 4)

Figure 4. *Hypselodoris imperialis*, South Solitary Island, NSW, 24 January 2022. Photo: N. Fripp.

Hypselodoris imperialis is a large white nudibranch with an undulating dark blue mantle that occasionally broadens onto the dorsum into wide patches that contain yellow spots. Yellow spots are also scattered across the body. The gills are white and lined with blue [29,41].

This species, considered by several authors to be restricted to Hawaii and the Marshall Islands, USA and French Polynesia [29,41], has been frequently confused with *Hypselodoris* sp. 11 (Gosliner et al. [29]); however, the latter exhibits white gills lined with red [29].

Prior to January 2022, *H. imperialis* was observed only three times outside its Central Pacific range [42]: Papua New Guinea in 1998; Vanuatu in 2006; and Currimundi Reef, Sunshine Coast, QLD in 2019 (Table 3).

Table 3. Selected Oceania distribution records of *Hypselodoris imperialis*.

Location	Date	Latitude	Longitude	Reference
Louisiade Archipelago, PNG	1998	10°57′10.57″ S	152°33′18.39″ E	[42]
Espiritu Santo, Vanuatu	2006	15°39′9.93″ S	167°0′40.46″ E	[42]
Currimundi Reef, QLD	2019	26°45′59.22″ S	153°8′50.42″ E	[43]
North Solitary Island, NSW	2022	29°55′44.55″ S	153°23′24.75″ E	This paper
South Solitary Island, NSW	2022	30°06′34.17″ S	153°12′43.42″ E	This paper

Two observations of *Hypselodoris imperialis* were made in January 2022 at the Solitary Islands, NSW. The first was at South Solitary Island on 24 January 2022 of an 80 mm specimen photographed at a depth of 15 m by Nathan Fripp (Figure 4). The second, at North Solitary Island, NSW, was of a 60 mm specimen on 30 January 2022 photographed by Craig Lewis and Brett Touzell (Table 3).

These observations represent a 380 km southward range extension from the previous southernmost observation at Currimundi, QLD.

Hypselodoris sagamiensis (Baba, 1849)

(Figure 5)

Figure 5. *Hypselodoris sagamiensis*, South Solitary Island, NSW, 25 January 2022. Photo: C. Lewis.

Hypselodoris sagamiensis has a translucent white body with opaque white patches on the mantle, occasionally raised into low pustules. Black spots may be distributed on the dorsum. The mantle exhibits a blue-purple margin that may be broken into lines or spots. There may also be a submarginal orange or yellow line, which may also be broken into spots. The rhinophore tips and gill edges are red or orange [44].

First described by Baba in 1949 (as *Glossodoris sagamiensis*) using type specimens collected by the Japanese Emperor at Sagami Bay, this species was considered to be restricted to Japanese waters until as recently as 2001 [44]. In 2006, Cobb and Willan [26] reported a putative first Australian observation of *H. sagamiensis* at Mooloolaba, QLD. However, 16 years earlier, in May 1990, *H. sagamiensis* had been photographed at Coffs Harbour, NSW, by Carol Buchanan but this image was only published in 2008 by Coleman [28] (p. 173) and therein mistakenly identified as *Hypselodoris* cf. *bertschi*. This observation was subsequently amended to *H. sagamiensis* in Coleman 2015 [27] (p. 149).

An observation of a 25 mm animal by Craig Lewis at a depth of 13 m at South Solitary Island on 25 January 2022 was the first observation of this species at its southern range limit for 32 years (Table 4).

Table 4. Australian distribution records of *Hypselodoris sagamiensis*.

Location	Date	Latitude	Longitude	Reference
Darwin Harbour, NT	2011	12°24′53.54″ S	130°49′04.68″ E	[45]
Mooloolaba, QLD	2005	26°40′49.68″ S	153°07′49.65″ E	[26,45]
Cook Island, NSW	2017	28°11′48.16″ S	153°34′38.07″ E	[45]
South Solitary Island, NSW	1990, 2022	30°06′34.17″ S	153°12′43.42″ E	This paper, [27]

Genus: *Goniobranchus* Pease, 1866
Goniobranchus kuniei (Pruvot-Fol, 1930)
(Figure 6)

Figure 6. *Goniobranchus kuniei*, South West Solitary Island, NSW, 23 January 2022. Photo: N. Fripp.

One of a group of similarly coloured mantle-flapping chromodorids, *Goniobranchus kuniei* was described from a specimen collected from the Isle of Pines, New Caledonia, from which it is named (*kuni* is the indigenous name for Île des Pins) [46]. This species is most similar in appearance to *Goniobranchus geminus* Rudman, 1987, which differs in the colour of the dorsal spots and marginal bands on the mantle. *Goniobranchus kuniei* has a broad Indo-West Pacific distribution from the Red Sea and Madagascar in the west to Tuamotu, French Polynesia, in the east and Okinawa, Japan, in the North.

In Australia, *G. kuniei* is known to occur on both the east and west coasts of Australia. In Western Australia it has been found as far south as Shark Bay [47,48]. In the east, it has been observed along much of the Queensland coast and offshore at Lord Howe Island, NSW [31,47]. However, the southernmost continental records are from the Sunshine Coast, QLD [43].

On 23 January 2022, a single 50 mm long specimen was observed at a depth of 12 m at South West Solitary Island, NSW, by Nathan Fripp (Figure 6). This observation represented a 400 km shift in the continental range from the Sunshine Coast, QLD, south into coastal NSW (Table 5).

Table 5. Selected East Australian distribution records of *Goniobranchus kuniei*.

Location	Date	Latitude	Longitude	Reference
Osprey Reef, GBR, QLD	2010	13°55′08.05″ S	146°38′00.38″ E	[47]
Lizard Island, GBR, QLD	2006	14°40′04.37″ S	145°28′16.87″ E	[47]
Heron Island, GBR, QLD	1980	23°26′50.49″ S	151°54′27.33″ E	[48]
Lady Musgrave Island, GBR, QLD	2021	23°54′24.39″ S	152°23′30.74″ E	[47]
Lady Eliot Island, GBR, QLD	2019	24°06′43.77″ S	152°42′46.40″ E	[47]
Sunshine Coast, QLD	Multiple	26°39′12.17″ S	153°06′33.80″ E	[43]
South West Solitary Island, NSW	2022	30°09′38.43″ S	153°13′37.75″ E	This paper
Lord Howe Island, NSW	2007	31°32′25.19″ S	159°03′40.01″ E	[31]

Goniobranchus rufomaculatus (Pease, 1871)
(Figure 7)

Figure 7. *Goniobranchus rufomaculatus*, South Solitary Island, NSW, 26 January 2022. Photo: S. D. A. Smith.

Goniobranchus rufomaculatus has a white mantle with scattered yellow spots and three translucent patches of varying sizes between the gills and rhinophores. The gills are white and the mantle margin is edged with purple lines or spots [49]. It is very similar in appearance to *Goniobranchus aureopurpureus* Collingwood, 1881, but *G. aureopurpureus* lacks the translucent patches on the dorsum and the gills are a translucent purple or puce [50].

Pease described *Goniobranchus rufomaculatus* (as *Chromodoris rufomaculata*) using a specimen found under rocks in the intertidal zone at Huanine-iti in French Polynesia in 1871 [51]. It has an Indo-West Pacific distribution and has been recorded on both the east and west coasts of Australia. In Western Australia, it has been recorded at Dirk Hartog Island (26.15° S) and, in the east, at several location as far south as Lord Howe Island, NSW [31].

A specimen measuring 50 mm was observed at a depth of 8 m at South Solitary Island, NSW, on 24 January 2019 by Steve Smith. A specimen of the same size was also found and photographed by Steve Smith during the recent Coffs Coast Seas Slug Census at the same location (Figure 7). Similar to the observation of *G. kuniei* reported above, these observations represent a 400 km southward shift in the continental range from the Sunshine Coast, QLD (Table 6).

Table 6. Selected distribution records of *Goniobranchus rufomaculatus* from Oceania.

Location	Date	Latitude	Longitude	Reference
Turtle Island, Espiritu Santo, Vanuatu	2006	15°22′10.21″ S	167°12′41.41″ E	[52]
Nouméa, New Caledonia	2009	22°17′18.33″ S	166°28′23.45″ E	[52]
Yule Detached Reef, GBR, QLD	1982	11°57′59.47″ S	143°59′01.14″ E	[52]
Heron Island, GBR, QLD	1981	23°26′50.49″ S	151°54′27.33″ E	[52]
Mooloolaba, QLD	2005	26°40′49.68″ S	153°07′49.65″ E	[27]
South Solitary Island, NSW	2019, 2022	30°06′34.17″ S	153°12′43.42″ E	This paper
Lord Howe Island, NSW	1994	31°32′25.19″ S	159°03′40.01″ E	[52]

Family: Polyceridae Alder & Hancock, 1845
Genus: Nembrotha Bergh, 1877
Nembrotha yonowae Goethel & Debelius, 1992
(Figure 8)

Figure 8. *Nembrotha yonowae*, South Solitary Island, NSW, 15 February 2022. Photo: N. Fripp.

Nembrotha yonowae is a large polycerid with a dark brown or black body with orange pustules scattered across the mantle [53]. Described using specimens from the Maldives, it has an Indo-West Pacific distribution with records spanning east to Papua New Guinea and north to the Philippines [53].

In Australian waters, *N. yonowae* has been found in northern Western Australia at the remote Ashmore Reef in the Arafura Sea and on the east coast at Heron Island, GBR, QLD, as well as at Julian Rocks in northern NSW (Table 7).

Table 7. Selected distribution records of *Nembrotha yonowae* from Oceania.

Location	Date	Latitude	Longitude	Reference
Milne Bay, Papua New Guinea	2017	10°27′53.81″ S	150°42′06.36″ E	[54]
Ashmore Reef, Arafura Sea	1994	12°14′19.15″ S	123°07′41.94″ E	[54]
Heron Island, GBR, QLD	2001	23°26′50.49″ S	151°54′27.33″ E	[54]
Julian Rocks, NSW	2007	28°36′40.44″ S	153°37′53.75″ E	[27,28]
South Solitary Island, NSW	2022	30°06′34.17″ S	153°12′43.42″ E	This paper

An observation of a 100 mm specimen by Nathan Fripp at a depth of 16 m at South Solitary Island on 15 February 2022 represented a 180 km southern range shift from its previous southernmost observation at Julian Rocks, NSW (Figure 8).

4. Discussion

The discovery of range extensions for seven species of tropical sea slug over a short survey period (9 days) during the Coffs Coast Sea Slug Census, and an additional dive 2 weeks later, is unprecedented within the SSC program. Although poleward range extensions have been sporadically recorded over the eight years of the program to date [13], the observations reported here were significant for a number of reasons. Firstly, *Hypselodoris bertschi* was recorded for the first time in Australia and at a nearshore, tidepool location (most previous records of range extensions have been at the offshore islands [13]). Secondly, the majority of new records were for species of Chromodorididae, a family with a predominantly tropical distribution comprising highly visible species that are unlikely to be overlooked by observers. Thus, most of these observations were highly likely to represent very recent additions to the local species pool. Two exceptions from the seven species reported here were *Chromodoris quagga*, which has now been recorded in three consecutive years at a

single location, and *Goniobranchus rufomaculatus,* which has been recorded in three out the past four years and at two locations. Despite the repeated observations of these two species, there was no evidence of increased abundance and establishment of populations; all these records consequently fitted into the first stage of range extension, arrival (*sensu* [1]). As such, it is highly likely that the presence of these species was dependent on the transport of larvae from more northerly locations via the East Australian Current (EAC) [13,55]. To our knowledge, and from the records from the SSC program as well as historical datasets from various citizen scientists, we are unaware of any native tropically affiliated heterobranch species that have recently established populations in the Solitary Islands Marine Park (we note, however, the establishment of populations of the introduced and invasive aeolid nudibranch, *Spurilla braziliana*, throughout south-east Australia [56]).

The ability of a novel species to successfully recruit depends on a range of factors that include physico-chemical conditions, the presence of a suitable habitat (e.g., [57]) and food as well as biotic interactions with the local community (e.g., [2]). There is little doubt that the individuals observed here were not only surviving but also feeding sufficiently to reach sizes that were at, or greater than, the published size within their usual geographic range [29,58]. Indeed, the specimen of *Hypselodoris imperialis* recorded from South Solitary Island measured ~80 mm (extended crawl length), which was substantially greater than the published size (50 mm [58]). This suggests that suitable food resources were available for these taxa within the SIMP. Unfortunately, as so little is known about the feeding habits for many species of heterobranch sea slugs [5], we could not speculate on whether the survival and growth of these species were facilitated by the presence of a specific food source at the receiving sites, or the ability of the species to feed on a range of food sources. Clearly, species with catholic feeding requirements are more likely to be successful in recruiting to novel locations; information on feeding will, therefore, be useful for predicting the likely progression of range extensions from arrival to the establishment of populations.

The presence of *Hypselodoris bertschi* in a coastal tidepool, the first confirmed sighting in Australia, was perhaps the most interesting observation reported here. With a few exceptions [13], most previous novel records have come from observations at the offshore Solitary Islands, which are regularly influenced by the EAC, the likely source of tropical recruits to the region [55,59,60]. Incursions of the EAC across the continental shelf regularly occur but with considerable variations in terms of strength and duration [21]. These episodes are predicted to become more frequent with the progression of climate change [61,62]. Although speculative, the transport of larvae of *H. bertschi* to the coast, as well as the presence of the six other species at the islands, may have been facilitated by the strong onshore winds associated with the 2021/22 La Niña in the western Pacific (commencing in November 2021) [63]. The protracted period of onshore winds led to the stranding of a large number of plastic debris items that had clearly been at sea for a considerable period based on the extensive marine growth and patterns of degradation. These included items whose source could be traced to New Caledonia (based on embossing [64]). These ancillary observations confirmed the transport of surface waters to coastal waters in the months leading up to our observation period.

Although this study reports on a just a few observations of novel species in a geographically restricted area, it potentially has important implications for ongoing investigations of climate-driven range extensions and the role of citizen scientists. Subtropical regions have been suggested as being amongst the first to experience changes related to range-shifting species, potentially acting as refuges for taxa driven poleward by warming seas [65]. Although recent research has suggested that there has been little change in the biotic composition of key structural species such as corals over the past 25 years at the Solitary Islands [24], the observations reported here and previously [13] clearly show that novel species arrive regularly. However, monitoring species of all taxa that occur within the region is impractical. Our results suggest that heterobranch sea slugs, and especially nudibranchs from the family Chromodorididae, have the potential as a focus group, not only because observations of species in this taxon dominate our records of range extensions

but also due to their popularity with recreational divers and naturalists, which can boost the search effort immensely [4]. One caveat is that a few species may be difficult to identify based solely on the external features captured in photographs [29] and mimicry is now known to occur in several species of chromodorid [66], necessitating circumspection in these cases. Programs such as the SSC can significantly contribute to documenting shifts in species distribution patterns, especially when linked with important databases. The recent association of the SSC program with iNaturalist has created a more powerful tool to monitor changing distributions and facilitated expert input to ensure that observations by participating citizen scientists effectively and accurately help update global species distribution patterns.

Author Contributions: Conceptualization, methodology, data curation, writing draft preparation, review and editing, S.D.A.S. and M.J.N. All authors have read and agreed to the published version of the manuscript.

Funding: This research received no external funding.

Institutional Review Board Statement: Not applicable.

Informed Consent Statement: Not applicable.

Data Availability Statement: Publicly available datasets were analysed in this study. These data can be found here: Available online. https://www.gbif.org/ (10 March 2022).

Acknowledgments: We thank all of the enthusiastic participants in the Sea Slug Census program for their passion and commitment to help document the diversity and distribution of sea slugs across the geographical range of the program. In particular, we would like to thank participants in the 2022 Coffs Coast Sea Slug Census with special mention to Nathan Fripp, Craig Lewis and Brett Touzell whose observations and photographs are featured in this paper. Determining the identity of species benefited from advice provided through the peer-review process on iNaturalist (especially from Hsini Lin, Erwin Koehler, Adrian Gale, Nick Lambert and Ben Travaglini), and advice from Marta Pola. The program was supported by members of the Solitary Islands Underwater Research Group and local businesses (Jetty Dive, Divequest Mullaway) who provided logistic support or small prizes as incentives for participants. Kathryn James prepared Figure 1. We are grateful to the three anonymous reviewers who helped improve the manuscript.

Conflicts of Interest: The authors declare no conflict of interest.

References

1. Bates, A.E.; Pecl, G.T.; Frusher, S.; Hobday, A.J.; Wernberg, T.; Smale, D.A.; Sunday, J.M.; Hill, N.A.; Dulvy, N.K.; Colwell, R.K. Defining and observing stages of climate-mediated range shifts in marine systems. *Glob. Environ. Chang.* **2014**, *26*, 27–38. [CrossRef]
2. Poloczanska, E.S.; Burrows, M.T.; Brown, C.J.; García Molinos, J.; Halpern, B.S.; Hoegh-Guldberg, O.; Kappel, C.V.; Moore, P.J.; Richardson, A.J.; Schoeman, D.S. Responses of marine organisms to climate change across oceans. *Front. Mar. Sci.* **2016**, *3*, 62. [CrossRef]
3. Gervais, C.R.; Champion, C.; Pecl, G.T. Species on the move around the Australian coastline: A continental-scale review of climate-driven species redistribution in marine systems. *Glob. Chang. Biol.* **2021**, *27*, 3200–3217. [CrossRef]
4. Smith, S.D.A.; Davis, T.R. Slugging it out for science: Volunteers provide valuable data on the diversity and distribution of heterobranch sea slugs. *Molluscan Res.* **2019**, *39*, 214–223. [CrossRef]
5. Rudman, W.B.; Willan, R.C. *Opisthobranchia. The Southern Synthesis*; Fauna of Australia; CSIRO: Melbourne, Australia, 1998.
6. Smith, S.D.A.; Nimbs, M.J. Quantifying temporal variation in heterobranch (Mollusca: Gastropoda) sea slug assemblages: Tests of alternate models. *Molluscan Res.* **2017**, *37*, 140–147. [CrossRef]
7. Goddard, J.H.R.; Gosliner, T.M.; Pearse, J.S. Impacts associated with the recent range shift of the aeolid nudibranch *Phidiana hiltoni* (Mollusca, Opisthobranchia) in California. *Mar. Biol.* **2011**, *158*, 1095–1109. [CrossRef] [PubMed]
8. Goddard, J.H.R.; Treneman, N.; Pence, W.E.; Mason, D.E.; Dobry, P.M.; Green, B.; Hoover, C. Nudibranch range shifts associated with the 2014 warm anomaly in the Northeast Pacific. *Bull. South. Calif. Acad. Sci.* **2016**, *115*, 15–40. [CrossRef]
9. Schultz, S.T.; Goddard, J.H.R.; Gosliner, T.M.; Mason, D.E.; Pence, W.E.; McDonald, G.R.; Pearse, V.B.; Pearse, J.S. Climate-index response profiling indicates larval transport is driving population fluctuations in nudibranch gastropods from the northeast Pacific Ocean. *Limnol. Oceanogr.* **2011**, *56*, 749–763. [CrossRef]
10. Nimbs, M.J.; Smith, S.D.A. Welcome strangers: Southern range extensions for seven heterobranch sea slugs (Mollusca: Gastropoda) on the subtropical east Australian coast, a climate change hot spot. *Reg. Stud. Mar. Sci.* **2016**, *8*, 27–32. [CrossRef]

11. Nimbs, M.J.; Larkin, M.; Davis, T.R.; Harasti, D.; Willan, R.C.; Smith, S.D.A. Southern range extensions for twelve heterobranch sea slugs (Gastropoda: Heterobranchia) on the eastern coast of Australia. *Mar. Biodivers. Rec.* **2016**, *9*, 289. [CrossRef]
12. Nimbs, M.J.; Smith, S.D.A. Revision of the southern distribution limit for the tropical marine herbivore *Syphonota geographica* (A. Adams & Reeve, 1850) (Heterobranchia: Aplysiidae) in a global climate change hot-spot. *Aust. Zool.* **2017**, *38*, 582–589. [CrossRef]
13. Nimbs, M.J.; Smith, S.D.A. Beyond Capricornia: Tropical Sea Slugs (Gastropoda, Heterobranchia) Extend Their Distributions into the Tasman Sea. *Diversity* **2018**, *10*, 99. [CrossRef]
14. Nimbs, M.J.; Willan, R.C.; Smith, S.D.A. Range extensions for heterobranch sea slugs (formerly opisthobranch) belonging to the families Diaphanidae, Plakobranchidae and Facelinidae on the eastern coast of Australia. *Mar. Biodivers. Rec.* **2015**, *8*, e76. [CrossRef]
15. Silvertown, J. A new dawn for citizen science. *Trends Ecol. Evol.* **2009**, *24*, 467–471. [CrossRef] [PubMed]
16. Martin, V.Y.; Christidis, L.; Lloyd, D.J.; Pecl, G. Understanding drivers, barriers and information sources for public participation in marine citizen science. *J. Sci. Commun.* **2016**, *15*, A02. [CrossRef]
17. Seltzer, C. Making Biodiversity Data Social, Shareable, and Scalable: Reflections on iNaturalist & citizen science. *Biodivers. Inf. Sci. Stand.* **2019**, *3*, e46670.
18. Smith, S.D.A.; Simpson, R.D. Nearshore corals of the Coffs Harbour region, mid north coast, New South Wales. *Wetl. Aust.* **1991**, *11*, 1–9. [CrossRef]
19. Malcolm, H.A.; Jordan, A.; Smith, S.D.A. Biogeographical and cross-shelf patterns of reef fish assemblages in a transition zone. *Mar. Biodivers.* **2010**, *40*, 181–193. [CrossRef]
20. Harrison, M.A.; Smith, S.D.A. Cross-shelf variation in the structure of molluscan assemblages on shallow, rocky reefs in subtropical, eastern Australia. *Mar. Biodivers.* **2012**, *42*, 203–216. [CrossRef]
21. Malcolm, H.A.; Davies, P.L.; Jordan, A.; Smith, S.D.A. Variation in sea temperature and the East Australian Current in the Solitary Islands region between 2001–2008. *Deep Sea Res. Part II Top. Stud. Oceanogr.* **2011**, *58*, 616–627. [CrossRef]
22. Harriott, V.J.; Smith, S.D.A.; Harrison, P.L. Patterns of coral community structure of subtropical reefs in the Solitary-Islands Marine Reserve, Eastern Australia. *Mar. Ecol. Prog. Ser.* **1994**, *109*, 67–76. [CrossRef]
23. Vergés, A.; Steinberg, P.D.; Hay, M.E.; Poore, A.G.B.; Campbell, A.H.; Ballesteros, E.; Heck, K.L.; Booth, D.J.; Coleman, M.A.; Feary, D.A. The tropicalization of temperate marine ecosystems: Climate-mediated changes in herbivory and community phase shifts. In *Proceedings of the Royal Society B: Biological Sciences*; The Royal Society: London, UK, 2014; Volume 281, p. 20140846.
24. Mizerek, T.L.; Madin, J.S.; Benzoni, F.; Huang, D.; Luiz, O.J.; Mera, H.; Schmidt-Roach, S.; Smith, S.D.A.; Sommer, B.; Baird, A.H. No evidence for tropicalization of coral assemblages in a subtropical climate change hot spot. *Coral Reefs* **2021**, *40*, 1451–1461. [CrossRef]
25. Hammerton, Z.; Dimmock, K.; Hahn, C.; Dalton, S.J.; Smith, S.D.A. Scuba diving and marine conservation: Collaboration at two Australian subtropical destinations. *Tour. Mar. Environ.* **2012**, *8*, 77–90. [CrossRef]
26. Cobb, G.; Willan, R.C. *Undersea Jewels: A Colour Guide to Nudibranchs*; ABRS: Canberra, Australia, 2006.
27. Coleman, N. *Nudibranchs Encyclopedia-Catalogue of Asia/Indo Pacific Sea Slugs*, 2nd ed.; Neville Coleman's Underwater Geographic: Springwood, Australia, 2015; ISBN 9780947325411.
28. Coleman, N. *Nudibranchs Encyclopedia*; Neville Coleman's Underwater Geographic: Springwood, Australia, 2008; ISBN 9780947325411.
29. Gosliner, T.M.; Valdés, Á.; Behrens, D.W. *Nudibranch and Sea Slug Identification: Indo-Pacific*, 2nd ed.; New World Publications: Jacksonville, FL, USA, 2018; ISBN 978-1-878348-67-8.
30. Nimbs, M.J.; Smith, S.D.A. An illustrated inventory of the sea slugs of New South Wales, Australia (Gastropoda: Heterobranchia). *Proc. R. Soc. Vic.* **2017**, *128*, 44–113. [CrossRef]
31. Nimbs, M.J.; Hutton, I.; Davis, T.R.; Larkin, M.F.; Smith, S.D.A. The heterobranch sea slugs of Lord Howe Island, NSW, Australia (Mollusca: Gastropoda). *Proc. R. Soc. Vic.* **2020**, *132*, 12–41. [CrossRef]
32. Horton, T.; Kroh, A.; Ahyong, S.; Bailly, N.; Boyko, C.B.; Brandão, S.N.; Gofas, S.; Hooper, J.N.A.; Hernandez, F.; Holovachov, O.; et al. *World Register of Marine Species (WoRMS) 2020*; World Register of Marine Species: Ostend, Belgium, 2020.
33. Bonomo, L.J.; Gosliner, T.M. Adding stars to the *Chromodoris* (Nudibranchia, Chromodorididae) galaxy with the description of four new species. *Zootaxa* **2020**, *4819*, zootaxa-4819. [CrossRef] [PubMed]
34. GBIF. *Chromodoris quagga* Bonomo & Gosliner, 2020. Available online: https://www.gbif.org/species/10730273 (accessed on 16 February 2022).
35. Gosliner, T.M.; Johnson, R.F. Phylogeny of *Hypselodoris* (Nudibranchia: Chromodorididae) with a review of the monophyletic clade of Indo-Pacific species, including descriptions of twelve new species. *Zool. J. Linn. Soc.* **1997**, *125*, 1–114. [CrossRef]
36. Sea Slug Forum: *Hypselodoris bertschi*. Available online: http://www.seaslugforum.net/showall/hypsbert (accessed on 16 February 2022).
37. Bertsch, H.; Gosliner, T.M. Chromodorid nudibranchs from the Hawaiian Islands. *Veliger* **1989**, *32*, 247–265.
38. Pease, W.H. Descriptions of new species of Mollusca from the Sandwich Islands. *Proc. Zool. Soc. Lond.* **1860**, *28*, 18–36.
39. Sea Slug Forum: Imamoto, J., *Hypselodoris bertschi*? from Japan. Available online: http://www.seaslugforum.net/find/5490 (accessed on 16 February 2022).
40. GBIF. *Hypselodoris bertschi* Gosliner & R.F. Johnson, 1999. Available online: https://www.gbif.org/species/4596896 (accessed on 16 February 2022).

41. Sea Slug Forum: *Risbecia imperialis* (Pease, 1860). Available online: http://www.seaslugforum.net/showall/risbimpe (accessed on 16 February 2022).
42. GBIF. *Hypselodoris imperialis* (Pease, 1860). Available online: https://www.gbif.org/species/6788184 (accessed on 16 February 2022).
43. Mullins, D.; Schubert, J.; Farr, T. Nudibranch Domain. Available online: https://nudibranchdomain.org/ (accessed on 16 February 2022).
44. Sea Slug Forum: *Hypselodoris sagamiensis* (Baba, 1949). Available online: http://www.seaslugforum.net/showall/hypssaga (accessed on 16 February 2022).
45. GBIF. *Hypselodoris sagamiensis* (Baba, 1949). Available online: https://www.gbif.org/species/6126803 (accessed on 16 February 2022).
46. Pruvot-Fol, A. Diagnose provisoirse (imcompètes) des espèces nouvelles et liste provisoire des mollusques nudibranches recueillis par Mme. A. Pruvot-Fol en nouvelle Cadédonie (Ile de Pins.). *Bull. Muséum Natl. d'Histoire Nat.* **1930**, *2*, 229–233.
47. GBIF. *Goniobranchus kuniei* (Pruvot-Fol, 1930). Available online: https://www.gbif.org/species/6519733 (accessed on 16 February 2022).
48. Sea Slug Forum: *Chromodoris kuniei* Pruvot-Fol, 1930. Available online: http://www.seaslugforum.net/find/chrokuni (accessed on 16 February 2022).
49. Sea Slug Forum: *Chromodoris rufomaculatus*. Available online: http://www.seaslugforum.net/find/chrorufo (accessed on 16 February 2022).
50. Rudman, W.B. The Chromodorididae (Opisthobranchia: Mollusca) of the Indo-West Pacific: *Chromodoris epicuria*, *C. aureopurpurea*, *C. annulata*, *C. coi* and *Risbecia tryoni* colour groups. *Zool. J. Linn. Soc.* **1986**, *90*, 305–407. [CrossRef]
51. Pease, W.H. Descriptions of nudibranchiate Mollusca inhabiting Polynesia. *Am. J. Conchol.* **1871**, *6*, 299–305.
52. GBIF. *Goniobranchus rufomaculatus* (Pease, 1871). Available online: https://www.gbif.org/species/6519729 (accessed on 16 February 2022).
53. Pola, M.; Cervera, J.L.; Gosliner, T.M. Revision of the Indo-Pacific genus *Nembrotha* (Nudibranchia: Doridida: Polyceridae), with a description of two new species. *Sci. Mar.* **2008**, *72*, 145–183. [CrossRef]
54. GBIF. *Nembrotha yonowae* Goethel & Debelius, 1992. Available online: https://www.gbif.org/species/165495130 (accessed on 16 February 2022).
55. Smith, S.D.A. Growth and population dynamics of the giant clam *Tridacna maxima* (Röding) at its southern limit of distribution in coastal, subtropical eastern Australia. *Molluscan Res.* **2011**, *31*, 37.
56. Bridle, T. *Spurilla braziliana*-a new sea slug in South Australia. *South Aust. Nat.* **2017**, *91*, 29–33.
57. Scott, A.; Harasti, D.; Davis, T.; Smith, S.D.A. Southernmost records of the host sea anemone, *Stichodactyla haddoni*, and associated commensal shrimps in a climate change hotspot. *Mar. Biodivers.* **2015**, *45*, 145–146. [CrossRef]
58. Epstein, H.E.; Hallas, J.M.; Johnson, R.F.; Lopez, A.; Gosliner, T.M. Reading between the lines: Revealing cryptic species diversity and colour patterns in *Hypselodoris* nudibranchs (Mollusca: Heterobranchia: Chromodorididae). *Zool. J. Linn. Soc.* **2018**, *186*, 116–189. [CrossRef]
59. Booth, D.J.; Figueira, W.F.; Gregson, M.A.; Brown, L.; Beretta, G. Occurrence of tropical fishes in temperate southeastern Australia: Role of the East Australian Current. *Estuar. Coast. Shelf Sci.* **2007**, *72*, 102–114. [CrossRef]
60. Figueira, W.F.; Booth, D.J. Increasing ocean temperatures allow tropical fishes to survive overwinter in temperate waters. *Glob. Chang. Biol.* **2010**, *16*, 506–516. [CrossRef]
61. Suthers, I.M.; Young, J.W.; Baird, M.E.; Roughan, M.; Everett, J.D.; Brassington, G.B.; Byrne, M.; Condie, S.A.; Hartog, J.R.; Hassler, C.S. The strengthening East Australian Current, its eddies and biological effects—an introduction and overview. *Deep Sea Res. Part II Top. Stud. Oceanogr.* **2011**, *58*, 538–546. [CrossRef]
62. Oliver, E.C.J.; Holbrook, N.J. Extending our understanding of South Pacific gyre "spin-up": Modeling the East Australian Current in a future climate. *J. Geophys. Res. Ocean.* **2014**, *119*, 2788–2805. [CrossRef]
63. Bureau of Metereology. Climate Driver Update. Available online: www.bom.gov.au/climate/enso/ (accessed on 16 March 2022).
64. Smith, S.D.A.; Banister, K.; Fraser, N.; Edgar, R.J. Tracing the source of marine debris on the beaches of northern New South Wales, Australia: The bottles on beaches program. *Mar. Pollut. Bull.* **2018**, *126*, 304–307. [CrossRef] [PubMed]
65. Beger, M.; Sommer, B.; Harrison, P.L.; Smith, S.D.A.; Pandolfi, J.M. Conserving potential coral reef refuges at high latitudes. *Divers. Distrib.* **2014**, *20*, 245–257. [CrossRef]
66. Layton, K.K.S.; Gosliner, T.M.; Wilson, N.G. Flexible colour patterns obscure identification and mimicry in Indo-Pacific *Chromodoris* nudibranchs (Gastropoda: Chromodorididae). *Mol. Phylogenet. Evol.* **2018**, *124*, 27–36. [CrossRef] [PubMed]

diversity

MDPI

Article

Understanding Extra-Pair Mating Behaviour: A Case Study of Socially Monogamous European Pied Flycatcher (*Ficedula hypoleuca*) in Western Siberia

Vladimir G. Grinkov [1,2,*], Andreas Bauer [3], Helmut Sternberg [4] and Michael Wink [3]

[1] Department of Biological Evolution, Faculty of Biology, Lomonosov Moscow State University, 119234 Moscow, Russia
[2] Biodiversity Monitoring Laboratory of the Biology Institute, Tomsk State University, 634050 Tomsk, Russia
[3] Institute of Pharmacy and Molecular Biotechnology, Heidelberg University, INF 364, 69120 Heidelberg, Germany; andy.bauer@freenet.de (A.B.); wink@uni-heidelberg.de (M.W.)
[4] OAG f. Populationsforschung Braunschweig, 38104 Braunschweig, Germany; helmut.sternberg@t-online.de
* Correspondence: grinkov@mail.bio.msu.ru; Tel.: +7-495-939-35-01

Abstract: Extra-pair copulation (EPC) occurred in most socially monogamous bird species. The mechanisms leading to the frequent occurrence of extra-pair offspring (EPO, EPY) in socially monogamous couples, as well as the 'function' of EPC, are the subjects of strong debates and raise many unanswered questions. We studied the relationship between extra-pair paternity (EPP) and the different characteristics of males and females in the European pied flycatcher in Western Siberia (Russia). The analysis was based on the genotyping of 232 males, 250 females, 1485 nestlings (250 nests). The European pied flycatchers were predominantly socially and genetically monogamous, but about 20% of birds could be involved in EPP. Loss of paternity tended to be more frequent in one-year-old males. EPCs could be multiple: one individual may have up to three extra-pair partners. The EPP rate was independent of the breeding time. The extra-pair mates of an individual were mainly its near neighbours. The EPC status of an individual was unrelated to most of its morpho-physiological traits. The occurrence of EPP was almost twice as high in females nesting in good quality territories. The fitness of within-pair offspring, EPO, paternal half-sibs of EPO and maternal half-sibs of EPO did not differ statistically significantly. Assuming very low heritability of extra-pair mating, we argued that EPCs could be incidental side effects (by-product) of selection. We believe that the evolution and maintenance of extra-pair mating are the episelective processes in the case of the European pied flycatcher.

Keywords: European pied flycatcher; *Ficedula hypoleuca*; extra-pair mating behaviour; extra-pair copulations; extra-pair paternity; Western Siberia; episelective evolution

Citation: Grinkov, V.G.; Bauer, A.; Sternberg, H.; Wink, M. Understanding Extra-Pair Mating Behaviour: A Case Study of Socially Monogamous European Pied Flycatcher (*Ficedula hypoleuca*) in Western Siberia. *Diversity* **2022**, *14*, 283. https://doi.org/10.3390/d14040283

Academic Editors: Fabián Casas and W. Douglas Robinson

Received: 28 October 2021
Accepted: 5 April 2022
Published: 10 April 2022

1. Introduction

Monogamy is the most common system of social relationships in birds, which has been recorded for more than 90 percent of species [1]. Social monogamy is a pairing system in which one male and one female stay together and cooperate in breeding for at least one breeding cycle [2]. Long-term social bonds (offspring rearing, for example) between mates maintained for several years are generally called long-term mutual monogamy or true monogamy [1,3]. Sexual or genetic monogamy implies sexual exclusivity along with the social living arrangements between a male and a female, and it is quite rare among birds [4,5]. In the social relationships of birds, serial monogamy [6], facultative polygamy and extra-pair copulations (EPCs) have been frequently reported.

Social monogamy occurs as serial monogamy in many bird species. Serial monogamy implies that pair bonds are formed sequentially for only one reproductive attempt or breeding season [6]. The genetic consequences of serial monogamy for individuals living

for several years differs only little from polygamy: one male fertilizes the eggs of several females [7]. Additionally, species with serial monogamy can exhibit facultative polygamy. In its most general meaning, the facultative polygamy of serially monogamous species can be viewed as the realization of serial monogamy within the same reproductive season [7,8].

EPCs as another type of 'mate infidelity' has been observed in many bird species [5,9]. The term refers to copulations that occur outside the social bonds. Individuals involved in EPCs do not show any social interactions (except the copulations), making such contacts and their consequences in natural populations difficult to identify without special methods, e.g., DNA profiling. The widespread use of DNA profiling [10] in studies of the mating systems of natural bird populations has revealed that EPP occurs in more than 75% of surveyed socially monogamous bird species [4,5,9,11–13]. Thus, it is obvious that monogamous social living arrangements are very often associated with genetic polygamy.

Attempts to explain the broad spread of EPP in socially monogamous bird species are still ongoing [5,9]. An EPC can be costly for both males and females [14–17]. However, females as well as males, despite these risks, still engage in extra-pair copulations [11,18–23].

The most common explanation of the evolutionary origin and maintenance of promiscuity in socially monogamous bird species is based on the assumption that birds have a propensity for EPC because there should be benefits from the promiscuous mating behaviour that outweigh all its negative consequences. Several hypotheses have been put forward on this issue [5,9,11,12,14,24]. The advantage of extra-pair mating is thought to be obvious for males who may sire additional offspring without the cost of care, and thus increase the number of their descendants in the population (increase fecundity). Indeed, where the costs of infidelity are low and EPC avoidance in females is weak, EPC may result from direct selection among males generating a self-interest male tactic [25]. This view appears to be well supported by accumulated data [26].

Female birds cannot take advantage of increased fecundity (the number of eggs in a clutch) from EPC, however, in socially monogamous relationships, females may mate multiply because of indirect genetic (e.g., 'good' and 'compatible genes' hypothesis) ([11,19,27–31], but see [26,32]) and direct benefits. Direct benefits include, for example, a better chance of fertilization of eggs [33], nuptial gifts from several mates [34,35], but see [36], or getting extra help from extra-pair mates in caring for offspring at the nest [18,37,38]. By mating with extra-pair males, females may construct a social network, which also could provide benefits to them (vigilance, alarm calls, calling networks, predator mobbing, and so on) [24,39].

Other hypotheses, also based on adaptive selective mechanisms, consider the possibility of EPC evolution among females in socially monogamous systems as a side correlative effect of selection on some fitness-related traits with the pleiotropic gene effects on the female 'inclination' towards EPC. A female 'propensity' for EPC may evolve and persist because it is positively genetically correlated with a male or female reproductive fitness component, and, consequently, experiences positive cross-sex or within-sex indirect selection [40]. These refer to 'intersexual' and 'intrasexual antagonistic pleiotropy' mechanisms, respectively [14,41,42], but see [43].

In view of the difficulties in attempts to explain inter- and intraspecific EPP variation based on differences in contemporary ecological factors and benefits from the promiscuous mating behaviour, the alternative explanations of EPP were proposed. They are based on fundamental differences in reproductive biology among avian lineages rather than differences in contemporary ecology. They consider the cost of being involved with EPC rather than differences in the opportunities for engaging in such behaviours. Indeed, in species with high annual mortality rates, females that participate in EPCs will be less likely to suffer any subsequent payback from their social partner [11,44,45]. It was shown that for EPP, over 50% of the interspecific variation is due to differences among taxonomic families and orders. High EPP rates are associated with high rates of adult mortality and reduced paternal care [45,46].

The above list of hypotheses (most likely the list is not all-inclusive) alone tells eloquently that the mechanisms of evolutionary persistence of EPP remain unclear. This may

be because all proposed hypotheses have limited general applicability, and can differ even within a species or population or between years. Consequently, obtaining new data that can reveal the causes both facilitating and refuting various hypotheses about EPP persistence among monogamous species may help to understand the high degree of variation in social relationships.

The European pied flycatcher (*Ficedula hypoleuca*) is a small (~12 g) insectivorous long-distance migratory bird species that breeds in Europe and winters in Africa. In nature, the European pied flycatchers nest in tree cavities but readily accept nest-boxes, which has made it a model species for studying population ecology and evolutionary biology. Birds breed once a year. The female incubates an average of six to seven eggs. Male and female together feed 5–6 nestlings in Western Siberia [47]. European pied flycatchers are relatively short-lived birds. The average lifespan of an individual is about two years from hatching [48,49]. The maximum life span in most populations does not exceed 8 years. However, the European pied flycatcher has a large pool of non-breeding individuals [50–53]. Males and females may first begin breeding at one to five years of age [50,53].

The European pied flycatcher is predominantly socially monogamous during a breeding cycle with an annual change of partners (serial monogamy) and with facultative polygyny. The proportion of socially monogamous pairs is rarely less than 80–90% [49]. However, like in most passerine birds with serial monogamy, some individuals are involved in EPCs that result in EPPs (for the variety of social relationships that may exist within the species, see [8]). The proportion of broods containing nestlings sired by extra-pair males varied from 6.5% to 40% [8,54–65].

In most studies of EPP in the European pied flycatcher, attempts were made to find phenotypic traits of males that could serve as criteria for 'extra-pair mate choice' [55,58,59,66,67]. It has been shown that different traits can be correlated with the involvement of males in EPP such as male-specific plumage ornaments [58,67,68], body size, age [59,61,67], polygyny status [56], and timing of breeding [60,61,65]. The relationship between phenotypic traits of females and their involvement in EPC has been studied much less frequently [64,69,70]. Moreover, despite the relatively large number of studies carried out on the European pied flycatcher, the actual effects of EPC on individual fitness are still ambiguous [8,57,65,71]. Consequently, our understanding of the factors affecting variation in the EPP rate between populations or individuals of the European pied flycatcher, as well as mechanisms persisting EPP, is rather limited.

This investigation was carried out as part of an ongoing long-term population study initiated in 2001 [8,53,69,72]. To determine parenthood and EPP status, we collected 1967 blood samples from 250 bird families in 2005 and genotyped them by microsatellite analysis [8]. We compared the traits of within-pair and extra-pair mates in both males and females. We attempted to find the phenotypic traits associated with the involvement of birds in EPCs. The recruitment rate of fledglings of the European pied flycatcher in the Western Siberian population is one of the highest among all populations of this species [53]. Therefore, we could directly estimate whether there are differences in the survival and the total fitness of the fledgling from different EPP backgrounds. Using these data, we tried to identify the most likely mechanisms of EPC evolution (ultimate explanation) in a given bird species and to identify the most likely environmental factors (proximate explanation) determining the involvement of individuals in EPCs.

2. Materials and Methods

2.1. Study System

This study was part of an ongoing long-term study of the European pied flycatcher population in Western Siberia in the Tomsk region. This region is now considered to be the eastern boundary of the species distribution range. We used nest-boxes (n = 381 in 2005) to attract these birds for breeding. The nest-box area of the study site was established in 2001. It is located 13 km southwards of Tomsk (56°21′ N 84°56′ E) in a mixed forest which consists of aspen (*Populus tremula*), birches (*Betula* spec.), spruce (*Picea abies*), Siberian fir

(*Abies sibirica*) and pine (*Pinus sylvestris*). The study site consists of four subplots—two 5 ha and two 10 ha areas equipped with nest-boxes (Figure 1). To build the map of the study area, we first GPS-referenced the coordinates of the corner nest-boxes of each subplot, and then, using the triangulation method, we determined the position of other nest boxes in the map. The map was created in Inkscape. The coordinates were recorded in pixels, which were back converted to meters for the calculations.

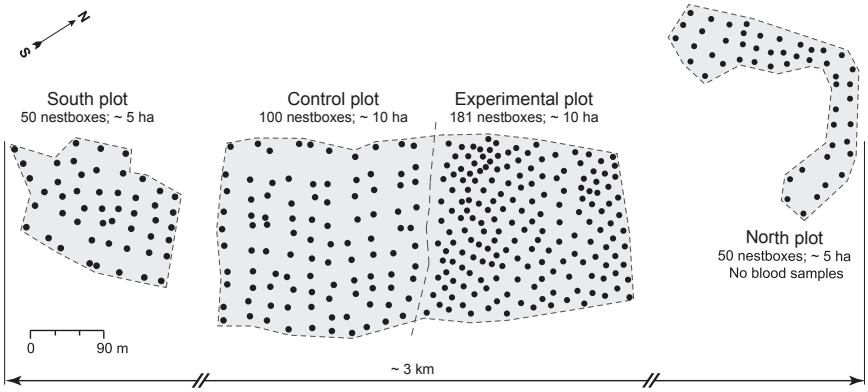

Figure 1. A simplified map of the study area. The map shows all the plots, their areas, and the number of nest-boxes at each site.

The distance between the most remote nest-boxes in the whole study site was approximately 3 km (Figure 1). On average, the interval between nest-boxes is about 30 m on the South, Control and North plots and about 20 m on the Experimental plot. The nest-box density was ~10 nest-boxes/ha for South, Control and North plots and 18.1 nest-boxes/ha for the Experimental plot (Figure 1). In 2005, the actual breeding density of European pied flycatchers was 8.2–9.1 pairs/ha (South, Control and North plots) and 11.5 pairs/ha (Experimental plot).

The European pied flycatcher is the only mass breeder at our sites. Other bird species (great tit, coal tit, Eurasian nuthatch, common redstart) occasionally nest in the nest boxes (1–3 pairs) and not every year.

During the breeding season, we checked each nest-box once every five days to record the laying date of the first egg, clutch size, brood size and the number of successfully fledged nestlings. To trap birds, we used small traps mounted inside the nest-box. We trapped females during the incubation period with active (spring-loaded) flap traps, which, when triggered by birds, close the entrance to the nest box from the inside. We trapped parents feeding nestlings with passive (springless) traps, which only allow birds to enter the nest box, but block their exit. We captured almost all females two times during the breeding season. For the first time, each female was captured on day 7 to 9 of clutch incubation, and for the second time, each female was captured when feeding 9–11-day-old nestlings. Males were captured only when feeding 9–11-day-old nestlings. When a bird was caught, we attached an aluminium ring to the bird's leg to enable individual identification. We did not use colour rings made of plastic for the birds' banding. No nest failed after the capture of adults. We measured weight, wing and tail length, tarsus length, fat index, post-breeding moult stage, and primary score index each time a European pied flycatcher was captured. For each caught male, we also recorded forehead spot size and the colour type of breeding plumage on Drost's colour scale [73]. The scale describes the degree of melanization of the upper-body feathers in the male breeding plumage and overall plumage brightness. Males of type 1 are the most conspicuous because of the deep black colouration of the body top and purely white colouration of the body bottom. Males of type 7 are most cryptically coloured because of the brown body top and dirty brownish-white body bottom.

The colouration of breeding plumage of males of type 7 is practically identical to that of females.

Immigrant flycatchers (all adults without rings) to the study population were trapped and ringed as described above and released; they can be identified individually throughout a lifetime. Flycatchers, born in the study area, were ringed and monitored from birth through all breeding attempts until they disappeared (when they most likely died).

Additional information about the monitoring scheme of the population, the bird treatment, as well as a description of the research area can be found in our earlier publications [8,74].

2.2. Paternity Analysis

To determine paternity, blood samples were taken from each bird. Both males and females were blood-sampled when feeding 9–11-day-old nestlings. Nestlings were blood-sampled on day 10–12 after hatching. We collected blood samples from all caught birds breeding in the three subplots in 2005 (South, Control and Experimental plots). This year, all nests in which females started incubation were successful, i.e., they survived until the time of blood sampling and the nestlings fledged. Therefore, blood samples were taken from all females. In 13 nests, we did not manage to detect/catch males. Some males could not be caught using our trapping methods, because they became extremely cautious (they stopped feeding their nestlings if they saw a trap inside the nest box). Some males were absent near the nests (males may have been predated, and it could be bigamous males who do not assist one of their females to feed nestlings). Therefore, we sampled 232 males, 250 females, 1485 nestlings (250 nests; 1967 blood samples). DNA fingerprinting was carried out using eight microsatellite loci, which were amplified by two multiplex-PCRs and analysed by capillary electrophoresis. For the analysis, we used FHU1/PTC2, FHU2/PTC3 [75]; FHU3, FHU5 [76]; FHY336, FHY403, FHY427, FHY452 [77] microsatellite loci. The degree of genetic relationships was determined by CERVUS 3.0 [78]. All work related to DNA genotyping of individuals and paternity analysis was completed at the Institute of Pharmacy and Molecular Biotechnology of Heidelberg University in Germany. Further details of genotyping by microsatellite analyses were described in the publication of Grinkov et al. [8].

For the present study, we assumed that the number of offspring sired by an extra-pair male is a good phenotypic measure of the extra-pair mating behaviour. Direct registration of copulation behaviour of all birds breeding in the study area was impossible in our case. In general, a linear dependence between the observed rate of EPCs and EPP was not demonstrated across an analysed species [79,80]. However, it seems that in the case of the European pied flycatcher there is a covariance between the observed rate of the EPP and the true rate of EPCs [74]. Nonetheless, we are unable to assume that females and males without EPY have not had EPCs at all. However, the assumption that EPP correlates positively with the degree of EPC behaviour across females and males within the population of the European pied flycatcher looks reliable and parsimonious [26,74].

2.3. Overlapping in Fertility Periods

The physiological readiness of females and the sexual activity and maturity of males primarily determine the chances that the EPC could lead to an EPY. We calculated fertility periods of females in this population to estimate the proportion of individuals in which it overlaps. Females of the European pied flycatcher can store sperm for 7–9 days [81]. Copulations can occur 9 days before the first egg is laid [66,82,83], but it seems that the earliest mating that can lead to fertilization was two days before the first egg is laid [81,83]. The extent and degree of sperm storage by females of the European pied flycatcher has not been determined in detail [81]. Males of the European pied flycatcher are physiologically ready for mating and fertilization from the arrival to the breeding area and until the hatching of the nestlings [84]. Therefore, we define a fertility period as following: the fertility period starts 6 days before the laying of the first egg and finishes when the last egg has been laid (a similar estimate was used, for example, in [56,85]). Obviously, among

males, the period in which they can inseminate eggs is longer, and they can visit females in different stages of egg-laying.

2.4. Nest Site Quality

To estimate the quality of the breeding territory, we used the number of recruits in the local population, which were produced in each nest-box from 2001 to 2009 (four years earlier and later than the year of parenthood determination). All territories were divided into four groups. In the 'best' nest site group, the number of recruited fledglings varied from 6 to 13 individuals, in the 'good' nest site group—from 3 to 5 individuals, in the 'bad' nest site group—from 1 to 2 individuals, and finally, in the 'worst' areas, no recruits were obtained for 9 years.

The boundaries were stated so that there were at least 30 nests in the categories (in fact, the number of nests in the smallest group is 31). This number of nests gives a number close to the recommended [4] number of offspring for EPP estimation. The European pied flycatchers have an average of 6 nestlings per brood, yielding about 180 nestlings in 30 broods (200 recommended in the publication; the smallest group in our analysis contains 195 nestlings).

2.5. Classification of Individuals

We used the following classification of individuals for the statistical processing of data. We divided all males into three groups:

$M_{EPY\ 0}$—Males that did not gain EPP, and did not lose paternity in their own nest, *EPY*-neutral, mostly monogamous in our opinion (but see [8]).
M_{EPY+}—Males that gained EPP, but could have also lost paternity in their own nest, *EPY*-positive males.
M_{EPY-}—Males that lost paternity in their own nest, but did not gain EPP elsewhere, *EPY*-negative males.

We again want to point out here that females of some EPY-positive males were involved in EPC, i.e., among EPY-positive males, there were also lost-paternity males [8]. We did not distinguish this group of males separately because of the small sample size. They were all part of the EPY-positive group of males.

We also divided females into three groups:

$F_{EPY\ 0}$—Females not obtained EPP and mated with *EPY*-neutral males, EPY-neutral, mostly monogamous females.
F_{EPY+}—Females obtained EPP, *EPY*-positive females.
F_{EPY-}—Females breeding with *EPY*-positive males.

We divided the nestlings according to their genetic background into four groups:

WPO—Within-pair offspring, the genetic descendants of the *EPY*-neutral males and *EPY*-neutral females.
Mat HSib of EPO—maternal (within-pair) half-siblings of extra-pair offspring.
EPO—Extra-pair offspring.
Pat HSib of EPO—Paternal (within-pair) half-siblings of extra-pair offspring.

Mat HSib of EPO and *EPO* are the genetic offspring of EPY-positive females, they are in this female's broods (nests). *Mat HSib of EPO* nestlings were sired by within-pair males of the EPY-positive females (M_{EPY-}). *EPO* nestlings were sired by extra-pair males (M_{EPY+}). Thus, *Mat HSib of EPO* and *EPO* nestlings were reared by EPY-positive females and their within-pair males (M_{EPY-}). *Mat HSib of EPO* and *EPO* nestlings are thus maternal half-siblings: they have a common mother but different genetic and social fathers. *Pat HSib of EPO* nestlings are genetic descendants of EPY-positive males, and these males have reared them together with their within-pair females (F_{EPY-}). *EPO* and *Pat HSib of EPO* nestlings are therefore paternal half-siblings. For reference, we list all types of social and genetic relationships between offspring and parents in Table S1 in the Supplementary Materials.

Sometimes we had to group individuals by other criteria for statistical calculations. Such instances are indicated and described in the legends of figures and tables or the text.

2.6. Fitness Estimates

We traced the survival and the reproduction of the nestlings of the 2005 cohort until 2012, until the last individual of the cohort was recorded. These data allowed us to calculate both the survival rate and the overall fitness of the nestlings in connection with their genetic origin and social parents. No experimental manipulations that could affect the fitness of birds were performed during this time.

Here, we define recruitment rate not as per capita recruitment probability, but instead as the number or proportion of individuals, i.e., what number or proportion of individuals of the 2005 cohort survived and returned to the population. We calculated apparent recruits, corrected recruits and local survival probability for different groups of nestlings (see above). Apparent recruits are the simple sum of returned individuals to the study area from nestlings ringed in 2005 during all subsequent years (e.g., if one individual returned in three different years, it was only counted as one). We calculated the corrected recruits using our earlier approach, which is based on the assumption of a 50% average annual individual mortality rate [50,51,53]. The corrected recruits make the adjustment for the fact that some recruits may have been missed (not bred) and, therefore, some may have died and may not have been captured in the following years. A more precise measure of the local survival probability, taking into account all possible inter-annual variation in mortality, we calculated based on the Cormack–Jolly–Seber (CJS) models [86–89] in the MARK program [90], using RMark [91] as R interface for the MARK.

The calculation of corrected recruits is much easier than the local survival probability with MARK. The two estimates are comparable (see results). The assumptions for the computing of corrected recruits are simple. The mean survival of individuals of different groups does not differ after the first year of life (50% as written above). The encounter probability is 0 before the first breeding for all individuals. In general, for most individuals, these assumptions are met, although not always.

We used lifetime reproductive success (LRS) and the individual intrinsic rate of increase (λ) calculated for a specimen (per capita) as an estimate of total fitness of fledglings [92]. The individual intrinsic rates of increase were calculated as the dominant eigenvalue of an age-structured population projection matrix constructed from life-history data, collected for an individual [93]. Both estimates were calculated from the number of fledglings and the number of recruits produced by an individual during a lifetime. These data were used to compare all groups of nestlings.

2.7. Statistical Analysis

We estimated the statistical significance of differences between the proportions (for example, proportions of apparent recruits and corrected recruits in all types of nestlings) using χ^2-test (prop.test() function in R). Inferences on whether there were statistically significant differences in local survival probability between nestlings groups were drawn based on Akaike's Information Criterion corrected for the effective sample size, AIC_c, and the normalized Akaike weights, ω_i, calculated for all CJS models (involving or not involving the variation in local survival probability between different nestlings groups and in different breeding years of pied flycatchers). We used the open-source R software environment for statistical computing and graphics (version 3.5.0) [94] under an integrated development environment for R-RStudio (RStudio Desktop version 1.1.447) [95] to analyse data.

In particular, to test statistical significance differences in the central tendency between the two groups, we used the Mann–Whitney U test. To estimate linear or monotonic relationships between variables, we used Spearman's correlation. Both between groups tests of the central tendency and correlations were used to describe associations between various variables pointed in previous parts of the Materials and Methods section. The use of either test in each case was determined by the type of the variable (numerical, nominal,

ordinal, etc.) under treatment. We used the false discovery rate method ("fdr") to correct *p*-values. We used spatstat package [96] in R to calculate distances.

3. Results

Paternity analysis revealed that 21.2% (53) of studied broods had EPY [8]. Therefore, 53 females definitely took part in EPCs. The number of extra-pair mates in EPY-positive females could be 1 (84.9%, N = 45), 2 (13.2%, N = 7) and 3 (1.9%, N = 1). Thus, the number of sexual partners in EPY-positive females varied from 2 to 4 including within-pair social males. Paternity analysis assigned 40 males as extra-pair sires. EPY-positive males successfully sire EPY in 1 extra-pair female in 85.0% cases (N = 34), in 2 extra-pair females in 12.5% cases (N = 5) and in 3 extra-pair females in 2.5% cases (N = 1). The number of sexual partners in EPY-positive males also varied from 2 to 4 including within-pair social females. We found that 8 females of EPY-positive males in turn also copulated with extra-pair males [8], i.e., there were 8 males that participated in EPCs whose social mates reciprocally cuckolded them.

We were able to reveal fathers for 65% (N = 67) of all EPY (N = 103) among the sampled males. The remaining 35% (N = 36) of EPYs for which genetic fathers were not identified are most likely the offspring of males that we were unable to detect or capture and the offspring of unmated non-breeding males [65].

3.1. Breeding Density and Breeding Time

Our study area consisted of several plots, differing in the number and density of nest-boxes. The density of nest-boxes ranged between 10 and 18.1 boxes per ha (Figure 1). In 2005, the actual breeding density of the European pied flycatcher was 8.8 pairs/ha, 9.1 pairs/ha and 11.5 pairs/ha on South, Control and Experimental plots, respectively. The corresponding EPP occurrence was 13.6%, 25.3% and 20.9%. We were not able to detect statistically significant differences in the level of EPP between plots (χ^2 = 2.42, df = 2, p = 0.298). The breeding density was on average very high, and the relatively small differences between subplots did not affect EPP rates (but see [8]).

In the Siberian European pied flycatcher population, breeding was rather synchronous (Figure 2). When the first egg was laid in the first nest-box, already 27 sexually receptive females (>10% of all females) were present in the population. When 50% of the clutches contained at least the first egg, about 70% of the females were in a fertile period. Even when the last female in the population started to lay eggs, about a dozen fertile females were still available (Figure 2). Thus, males of the Siberian population had the opportunity at any given time to find a sufficiently large number of females for EPC. Moreover, because the fertile period of males lasts from the time of arrival until the eggs hatch [84], the latest nesting males had the potential to mate with all females in the population. The extended fertility period of both males and females is most likely the reason why we were not able to detect signs of an uneven distribution of EPP within the nesting period. The proportion of nests with EPY was not correlated with the breeding time (Figure 3a).

The number of nests with EPY in each particular nesting period was directly proportional to the corresponding total number of nests (Figure 3b). Thus, the proportion of males and females, copulating with extra-pair mates, was more or less stable throughout the breeding season.

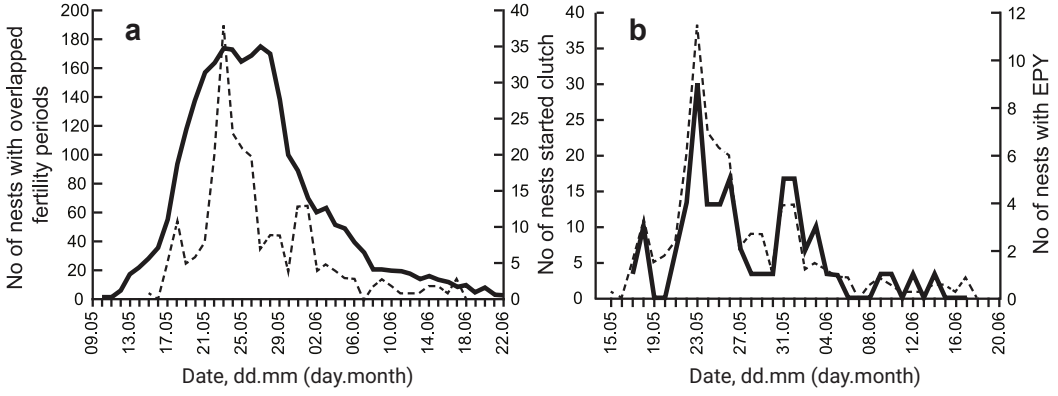

Figure 2. Clutch start dates, overlapping fertility periods (**a**) and number of nests with EPY (**b**). The dashed line on parts (**a**,**b**) is the number of nests that a clutch is started on the relevant date; the solid line on (**a**) is the number of nests whose female fertility periods overlap on the relevant date; the solid line on (**b**) is the number of nests with EPY on the respective date.

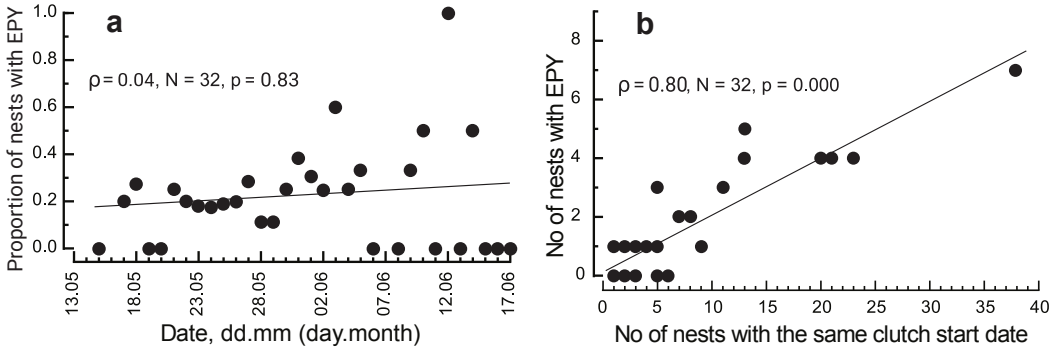

Figure 3. The link between the proportion of nests with EPY and the clutch start date (**a**) and between the number of nests with EPY and the total number of nests that a clutch has started on the respective date (**b**). The value of Spearman's correlation (ρ), sample size (N) and significance level (p) are given. Linear regression (solid line) is shown.

3.2. Distance between Extra-Pair Mates

Males and females copulated mainly with their near neighbours as extra-pair mates: the nests of extra-pair partners were spaced between 17.4 to 495.3 m apart (Figure 4). The distance between all nests (the set of distances from a nest-box to all others) varied from 12.1 to 1891.4 m at the plots where blood samples were taken. The mean distance between all nests was 594.14 m (SD = 578.1, N = 31,125), the median was 297.9 m (Figure 4). The average distance between the nests of extra-pair mates was 149.1 m (SD = 115.3, N = 46). In more than 90% of cases, nests of extra-pair mates were located between ~270–300 m from each other. No EPC could be detected between males and females nesting on different study plots, nor between partners nesting at the same site but which were more than 500 m apart (Figure 4). The distributions in distances of all nests and distances of nests of extra-pair mates differed significantly (Mann–Whitney U test W = 1,123,036, $p = 2.449 \times 10^{-11}$). A pronounced decrease in the likelihood of EPC between individuals, depending on the distance between their nests, had also been demonstrated in Spanish populations of the European pied flycatchers [61].

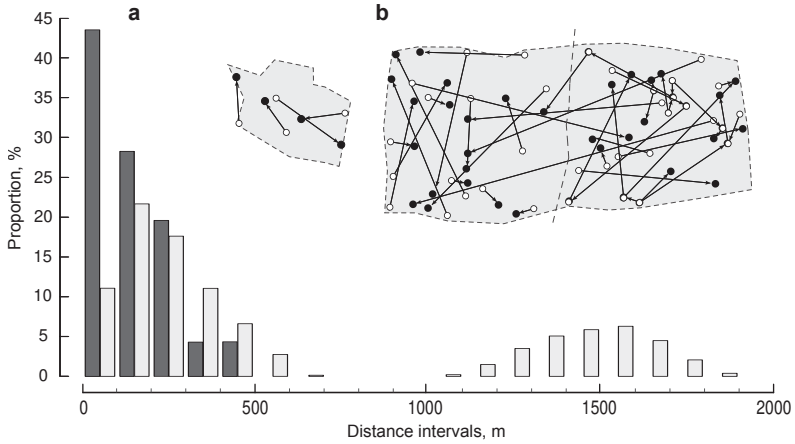

Figure 4. Occurrences of distances between nests of extra-pair mates (**a**) and the location of nests of extra-pair mates (**b**). In (**a**), the black bars indicate the distribution of distances between the nests of extra-pair mates, and the light bars depict the distribution of all possible distances between all nests. (**b**) Nests of extra-pair males (open circles) and extra-pair females (filled circles). The arrows mark the distance from the nest of the extra-pair male to the respective nest of the extra-pair female. Space between the plots is reduced. For the actual location of the areas, see Figure 1.

We found that the distance between nests of extra-pair mates was not associated with the probability of paternity loss in EPY-positive males (recall that 20% of them were EPY-negative males) (Mann–Whitney U test W = 154, $p = 0.40$), meaning that all EPY-positive males could lose paternity regardless of how far from their nest they found extra-pair females for EPC.

The distance between the nests of the extra-pair mates is positively correlated with the clutch start date of within-pair females of EPY-positive males (Figure 5a).

This is probably due to a smaller number of sexually receptive females at the end of the breeding period. A large distance between nesting sites of extra-pair mates would be the consequence.

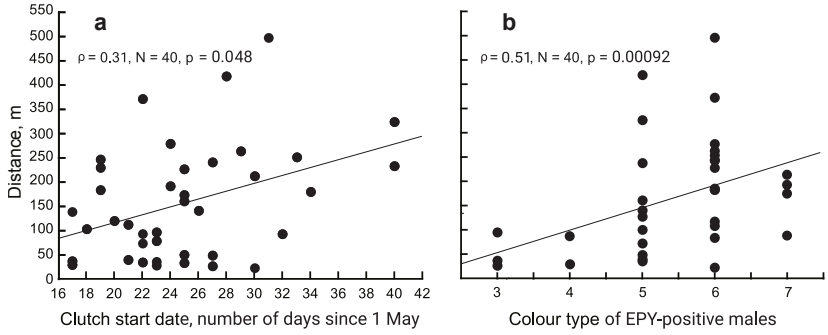

Figure 5. The distance between the nests of extra-pair mates depending on breeding timing of males (estimated as the clutch start date of within-pair female) (**a**) and the Drost's colour type of the male breeding plumage (**b**). The order of the categories of this scale denotes the degree of melanization of the upper-body feathers in the male breeding plumage and overall plumage brightness. Males of type 1 are the most conspicuous because of the deep black colouration of the body top and purely white colouration of the body bottom. Males of type 7 are most cryptically coloured because of the brown body top and dirty brownish-white body bottom. The colouration of breeding plumage of males of type 7 is practically identical to that of females. The value of Spearman's correlation coefficient (ρ), sample size (N) and significance level (p) are given. Linear regression (solid line) is shown.

3.3. Age of Birds

Among females with EPY (F_{EPY+}), the proportion of individuals older than one year was higher (58%, 31 out of 53 females) than among females without EPY ($F_{EPY\,0}$ and F_{EPY-}) (49%, 97 out of 197). These differences are not statistically significant (χ^2 = 1.1, df = 1, p = 0.3). EPY-positive males were older than EPY-negative males in overall terms (Figure 6).

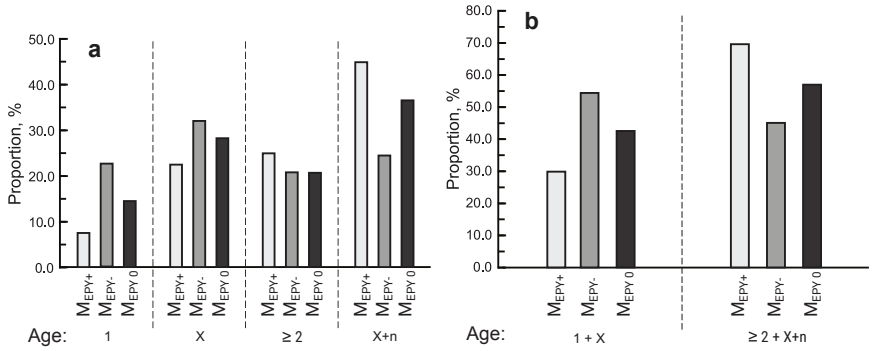

Figure 6. The age distribution (%) in males that mated with extra-pair females (M_{EPY+}), those who lost their paternity (M_{EPY-}) and monogamous males ($M_{EPY\,0}$). Bars painted in different shades of grey denote groups of males for which the proportions of age classes were calculated. Age groups are labelled as yearlings (1), males aged 2 years and older (≥2), males of uncertain age first caught in the study area (X), and males recaptured in the study area (X + n, where n = 1, 2, 3, etc.) One-year-old and older individuals (age 1 and ≥2) were born in the research area and were ringed as nestlings in previous reproductive seasons. Males of unknown age (X and X + n) were ringed as adult birds. (**a**) The age ratio of all four age groups. (**b**) The age ratio in the pooled samples.

Among males, whose age was accurately determined according to the ringing data (age 1, 2, 3, etc.), the proportion of one-year-old males (yearlings) was about two times higher than the proportion of older birds aged 2 years and older in the EPY-negative fathers in comparison with EPY-positive ones (52.6% (10 out of 19) and 23.1% (3 out of 13), respectively). Additionally, among males of unknown origin (age X, X + 1, X + 2, etc.), the proportion of newly caught birds (age class X) was higher than the fraction of recaptured individuals (age class X + n) in the EPY-negative fathers in comparison with EPY-positive males (57.7% (15 out of 26) and 33.3% (9 out of 27), respectively) (Figure 6). In a pooled sample, in which the yearlings were combined with the newly caught males and the older specimens with re-caught ones, respectively, the proportion of younger males (yearlings plus X) was higher among the EPY-negative males in comparison to EPY-positive males (55.6% (25 out of 45) and 30% (12 out of 40), respectively) (Figure 6). Only this difference is statistically significant (χ^2 = 4.63, df = 1, p = 0.031). The EPY-neutral males have a proportion of young individuals that are intermediate between EPY-negative and EPY-positive males. Pairwise comparison of the proportion of yearlings among males of different EPP status using correction for multiple testing revealed no statistically significant differences (please see Table S6 in the Supplementary Materials).

3.4. Morphological Characters

In our work, we evaluated the association of wing, tail, tarsus and beak length, beak height, body mass, fat and cloacal protuberance index (males), post-breeding moult stage, primary score index, Drost's colour type (males), and forehead spot size (males) with EPP status. We could find no differences in most morphological traits between EPY-positive males versus EPY-negative fathers (Table S6 in the Supplementary Materials). EPY-positive males tended to have a longer beak. Similarly, we were not able to identify morphological differences between EPY-neutral males and the two other groups of males that differed

in their EPP status (Table S6 in the Supplementary Materials). The distances between the nest-boxes of extra-pair mates were positively correlated to the colouration of the breeding plumage of EPY-positive males (Figure 5b): males with a blacker breeding plumage were more likely to copulate with extra-pair females in the nearer vicinity to their nests than were males with browner breeding plumage. Two explanations are possible: black top body males are more attractive than brown males ([97,98]; but see [99,100]). Alternatively, this may be due to the greater aggressiveness of resident males towards blacker males [101,102], which in turn may restrict their movement across the territory, unlike browner males. The remaining morphological traits of EPY-positive males (wing, tail, tarsus and beak length, beak height, body mass, fat and cloacal protuberance index, and forehead spot size) were not related to the distance between the nests of the extra-pair mates (Table S6 in the Supplementary Materials).

The females with EPYs (F_{EPY+}) tended to have shorter wing length and tail length in comparison with EPY-neutral females ($F_{EPY\ 0}$), although these differences are not statistically significant (Table S6 in the Supplementary Materials). Body mass, fat index, tarsus length, post-breeding moult stage, and primary score index were not differ statistically significant among EPY-neutral, EPY-positive, and EPY-negative females (Table S6 in the Supplementary Materials).

3.5. Territory (Nest Site) Quality

We calculated the proportion of EPY-positive mothers in 'best', 'good', 'bad' and 'worse' nest sites (Figure 7).

Females who were sampled in nest-boxes with higher recruitment rates showed an about twice higher EPP rate (Figure 7a). Comparison of the proportions of EPY-positive females among nests of different quality did not reveal the statistically significant differences ($\chi^2 = 3.34$, df = 3, $p = 0.34$).

The proportion of the EPY-positive males did not differ statistically significantly across different quality groups of their nesting sites (Figure 7b) (Table S6 in the Supplementary Materials). The overall variability in the number of recruits per nesting site is very high, and the linear dependence between the number of recruits and EPP estimates is weakly positive and not statistically significant (Spearman's correlation ρ: $\rho = 0.07$, $\rho = 0.07$, $\rho = 0.04$ for the presence/absence of the EPO in a brood, the EPO number in females and the EPO number in males, respectively; Table S6 in the Supplementary Materials).

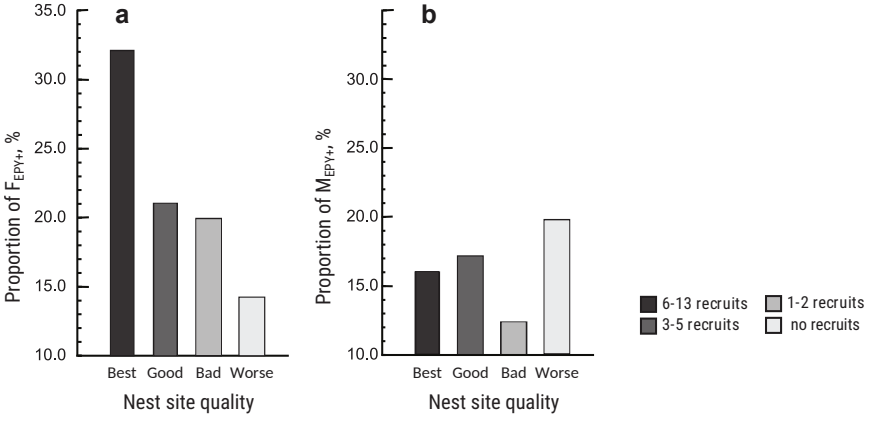

Figure 7. The proportion of females (**a**) and males (**b**) with EPY (F_{EPY+} and M_{EPY+}, respectively) among individuals nesting in territories of different quality. Territory quality was determined by the number of recruits born in the nest-box.

3.6. Fecundity of Adults, Fledglings Fitness

In our work, we cannot directly calculate and describe the variation in the total fitness of adults depending on their involvement in EPC. This requires long-term studies with annual genetic control of all descendants from all individuals. Using our material, we can estimate the effect of EPC on one of the components of fitness, namely, current fecundity. EPC can certainly increase the number of genetic offspring of male participants by simultaneously reducing the number of genetic offspring among EPY-negative males. The mean number of offspring of EPY-positive males, EPY-negative males and EPY-neutral was 7.0 (N = 40, SD = 1.89), 4.2 (N = 45, SD = 1.64) and 6.0 (N = 165, SD = 1.39), respectively. Pairwise comparisons using the Mann–Whitney U test showed statistically significant differences in all combinations with a significance level of $p = 0.00167$ (highest corrected *p*-value, Table S6 in the Supplementary Materials).

The mean number of descendants in EPY-positive, EPY-negative, and EPY-neutral females was roughly the same (6.1, N = 53, SD = 1.1; 5.7, N = 32, SD = 1.2; 6.0, N = 165, SD = 1.4, respectively; there are no statistically significant difference, Table S6 in the Supplementary Materials). The ratios of the number of fledglings to the number of eggs in EPY-positive, EPY-negative, and EPY-neutral females were 0.93 (N = 53, SD = 0.10), 0.88 (N = 32, SD = 0.12), and 0.91 (N = 165, SD = 0.15), respectively. This index incorporates two main causes of eggs' failure in females, i.e., fertilisation failure and embryo death. Here, we used it as the rough estimation of average female fertility. The clutch-to-brood ratio of EPY-negative females tended to be lower than that of EPY-positive and EPY-neutral females (the differences were not statistically significant, Table S6 in the Supplementary Materials). The mean clutch-to-brood ratio (average fertility) of EPY-neutral and EPY-positive females was nearly identical, as argued earlier [32].

The number of recruits and the recruitment rate of the fledglings related to the differences in genetic and social parents in the Western Siberian population of the European Pied Flycatcher are shown in Table 1. We compared the apparent and corrected recruitment rates of different types of offspring in all possible pairwise combinations (Table 1). We found that the differences in apparent recruitment rates of offspring were not statistically significant (Table S6 in the Supplementary Materials). The corrected recruitment of maternal (within-pair) half-siblings of EPO is significantly different from WPO, EPO and paternal (within-pair) half-siblings of EPO (χ^2 test; $p = 0.0009$, $p = 0.02$ and $p = 0.0009$, respectively; corrected *p*-values; Table S6 in the Supplementary Materials). A comparison of the models with the different type of variation of the local survival probability in the MARK program (Table S2 in the Supplementary Materials) revealed that the most parsimonious model best fitted the data was one in which the differences in the local survival probability between the types of offspring were not simulated (i.e., the local survival probability of all bird types was assumed to be the same). Thus, the survival of offspring of EPY-positive females from within-pair males (EPY-negative males) is at least as good (if not the best) as the survival of their half-sibs from extra-pair males (EPY-positive males) and offspring of EPY-positive males from their within-pair females (EPY-negative females).

The total fitness of the fledglings related to the differences in genetic and social parents in the Western Siberian population of the European pied flycatcher is presented in Table 2. A comparison of the mean intrinsic rate of increase and LRS values calculated from the number of fledglings and recruits between the different fledglings types in all possible pair combinations (Table 2) did not reveal statistically significant differences according to corrected *p*-values (Table S6 in the Supplementary Materials). However, in general, the fitness of EPY-positive females and EPY-negative males offspring was nearly twice that of all other offspring groups, although these differences were not statistically significant.

Table 1. The number of recruits and the recruitment rate of the fledglings related to the differences in genetic and social parents in the Western Siberian population of the European pied flycatcher.

Social and Genetic Mother	Sire	Social Father	Type	N	Recruited and Started Breeding in					Apparent Recruits		Corrected Recruits		φ [CI]
					2006	2007	2008	2009	2010	N	%	N	% [CI]	
$F_{EPY\ 0}$	$M_{EPY\ 0}$	$M_{EPY\ 0}$	*WPO*	981	30	28	–	1	1	60	6.1%	110	11.2% [9.2–13.2]	10.3% [7.4–14.1]
F_{EPY+}	M_{EPY-}	M_{EPY-}	*Mat HSib of EPO*	189	12	4	1	2	–	19	10.1%	40	21.2% [15.4–27.0]	14.6% [9.9–21.1]
F_{EPY+}	M_{EPY+}	M_{EPY-}	*EPO*	103	7	1	–	–	–	8	7.8%	9	8.7% [3.3–14.1]	10.6% [5.6–18.3]
F_{EPY-}	M_{EPY+}	M_{EPY+}	*Pat HSib of EPO*	212	5	4	1	–	–	10	4.7%	17	8.0% [4.3–11.7]	9.8% [6.1–15.2]

φ is the local survival probability from birth to the next breeding season as calculated in the MARK program, CI in square brackets denotes the lower and upper limits of the 95% confidence interval. $F_{EPY\ 0}$—EPY-neutral females, F_{EPY+}—EPY-positive females, F_{EPY-}—EPY-negative females, $M_{EPY\ 0}$— EPY-neutral males, M_{EPY+}—EPY-positive males, M_{EPY-}—EPY-negative males, *WPO*—within-pair offspring, *Mat HSib of EPO*—maternal (within-pair) half-siblings of extra-pair offspring, *EPO*—extra-pair offspring, *Pat HSib of EPO*—paternal (within-pair) half-siblings of extra-pair offspring (for details, see Classification of individuals section in Methods).

Table 2. The total fitness of the fledglings related to the differences in genetic and social parents in the Western Siberian population of the European pied flycatcher.

Social and Genetic Mother	Sire	Social Father	Type	N	$\overline{\lambda}_{Nfl}$ [CI]	$\overline{\lambda}_{Nrec}$ [CI]	$\overline{LRS}_{Nfl}$ [CI]	$\overline{LRS}_{Nrec}$ [CI]
$F_{EPY\ 0}$	$M_{EPY\ 0}$	$M_{EPY\ 0}$	*WPO*	981	0.15 [0–2.42]	0.02 [0–0.50]	0.28 [0–3.50]	0.02 [0–0.50]
F_{EPY+}	M_{EPY-}	M_{EPY-}	*Mat HSib of EPO*	189	0.27 [0–3.55]	0.04 [0–0.71]	0.53 [0–6.30]	0.04 [0–0.50]
F_{EPY+}	M_{EPY+}	M_{EPY-}	*EPO*	103	0.24 [0–3.47]	0.01 [0–0.00]	0.31 [0–3.95]	0.01 [0–0.00]
F_{EPY-}	M_{EPY+}	M_{EPY+}	*Pat HSib of EPO*	212	0.12 [0–2.14]	0.02 [0–0.36]	0.27 [0–3.36]	0.02 [0–0.36]

The per capita mean intrinsic rate of increase calculated using the number of fledglings and the number of recruits is written as $\overline{\lambda}_{Nfl}$ and $\overline{\lambda}_{Nrec}$, respectively. The per capita mean number of the lifetime fledglings and recruits produced by an individual is written as $\overline{LRS}_{Nfl}$ and $\overline{LRS}_{Nrec}$, respectively. CI in the square brackets denotes the location of 0.025 and 0.975 quantiles. $F_{EPY\ 0}$—EPY-neutral females, F_{EPY+}—EPY-positive females, F_{EPY-}—EPY-negative females, $M_{EPY\ 0}$—EPY-neutral males, M_{EPY+}—EPY-positive males, M_{EPY-}—EPY-negative males, *WPO*—within-pair offspring, *Mat HSib of EPO*—maternal (within-pair) half-siblings of extra-pair offspring, *EPO*—extra-pair offspring, *Pat HSib of EPO*—paternal (within-pair) half-siblings of extra-pair offspring (for details, see Classification of individuals section in Methods).

It is worth noting here, that our data on the fledglings fitness of different origin confirm that observations of a higher offspring fitness among broods containing EPY compared with those with only WPY do not provide conclusive evidence for indirect benefits of EPC behaviour among females because both a high offspring fitness and a high rate of EPY could be the result of a maternal and/or environmental effects [32].

4. Discussion

We carried out an observational analytical study of the EPP phenomenon in a Western Siberian population of the European pied flycatcher, attempting to find and quantify a relationship or association between registered variables (mainly individual phenotypical traits) and the involvement of a bird in extra-pair copulations. The revealed pattern of association between variables was rather complex.

In general, most of the associations between variables studied are weak. The statistical significance of most of the associations, with few exceptions, crosses only the uppermost threshold of significance level (0.05). The very revealing of statistically significant associations is very much dependent on the statistical analysis methods. This suggests that the data are poorly structured by the EPP status of individuals. Pure stochasticity seems to play a very important role in determining the involvement of individuals in EPC. Likely, many of the association of traits of individuals with their EPP status in the case of the European pied flycatcher researches are determined by the data structure per se, e.g., being data-specific.

We found that up to one-fifth of all birds can be involved in the EPP, which is just within the inter-population variability of the EPP rate described in this species so far (6 to 40%, see Introduction). Some of the relationships detected can be interpreted as a "function" of the EPCs, connecting this behaviour of an individual to its fitness and, hence, can be considered as support for selective scenarios persisting EPP (see Introduction). EPP tended

to be age-dependent, current fecundity was larger in EPY-positive males, offspring-to-eggs ratio in EPY-positive females (vs. EPY-negative ones) tended to be higher, distance to a nest of extra-pair females in EPY-positive males with bright and conspicuous breeding plumage was shorter. Many other relationships are more difficult to link to the presence of selective mechanisms. EPC was multiple, EPP rate was independent of breeding time, extra-pair mates were mainly near neighbours, association between most morpho-physiological traits and the EPC status of an individual was almost absent, the occurrence of EPP tended to be higher in good-quality territories, the average fertility of EPY-neutral and EPY-positive females were equal, and, finally, fitness between types of fledglings were roughly similar.

It is a challenging task to provide a coherent and logical explanation for our results based on all those hypotheses that assume the involvement of natural selection (in any of its forms) in the persistence of EPP in natural populations (most of such hypotheses were described in the Introduction). The difficulty is that many of the results we have obtained are contradictory and can be interpreted in different ways. Our results can be considered in favour or against a particular hypothesis about the function or evolution of EPC. To interpret the results within an adaptationist framework, we need knowledge about the genetic basis of EPC. However, the proportion of phenotypic variation in the number of EPOs and, apparently, in the involvement of individuals in EPC, due to genetic factors is very low among the European pied flycatcher [74]. This effectively means that selection can neither maintain EPP, nor change the mean EPP level among European pied flycatcher populations [74].

Therefore, when combined with earlier findings [8,74], the results of this study allow us to conclude that the extra-pair mating behaviour of the European pied flycatcher is an unpredictable side effect of selection on other phenotypic traits of an individual. Direct selection for fecundity, fertility and parental care performance is enough to produce EPCs as a by-product [8]. Here, our opinion is in general consistent with the repeated view that EPCs could be incidental side effects of behaviours (i.e., offensive male adaptations to gain sexual access to any females, resistance adaptations among females and defensive adaptations among males) that have evolved and are maintained primarily by direct benefits [32,103–105]. We believe that EPC evolved in the same way as all other non-monogamous forms of socially genetic relationships [8]. A very clear example of an incidental side effect of behaviour evolution is interspecific feeding [8,106,107], which no doubt does not arise evolutionarily by means of natural selection. The way in which a trait arises as an unpredictable by-product of selection for other properties of the phenotype, rather than as a correlative effect of it, is called episelective evolution [108,109]. Currently, within the field of ecological evolutionary developmental biology (Eco-Evo-Devo), this mechanism is considered as one of the main ways of evolution of novelties [110–112].

It appears that the extra-pair mating behaviour of the European pied flycatcher is, at present, a highly variable phenotypic trait or a plastic character. The involvement of birds in extra-pair mating seems to be almost entirely determined by phenotypic conditions of the individual, their hormonal status, behaviour and environmental factors [8,74]. The participation of each bird in EPCs seems to be a little predictable and depends entirely on the ecological environment in which the bird finds itself at a given point in its life cycle. Phenotypic trait values with low ontogenetic and environmental reproducibility (repeatability) and with a minuscule genetic component in overall phenotypic variability could be arbitrarily associated with fitness: weakly or strongly, negatively or positively. The effects of such traits on fitness may thus be population-specific. In this regard, comparative studies of inter-population variability in EPPs of the same species may be very important for understanding the population-specific ecological and behavioural mechanisms behind the involvement of birds in EPCs.

EPCs can only occur when there is physical contact between individuals. Consequently, all factors that may influence the probability of contact between males and females have the potential to alter the occurrence of EPO in broods of social pairs. Population density, operational sex ratios and environmental heterogeneity seem to be the most important

among them [3,113,114]. Low nesting density should correlate with a low EPP rate merely because the probability of meeting an extra-pair mate decreases sharply as the distance between them increases (European pied flycatchers engage in the extra-pair copulations virtually without going beyond their home range). In this study, the variation in breeding density at forest plots was insufficient to affect the EPP incidence on these sites. However, the larger differences in the overall structural characteristics of the environment between the urban and forest research areas strongly influence the occurrence of EPP in the European pied flycatcher in Western Siberia [8].

The general relationship of nesting density to the occurrence of EPP in populations may, however, be more complex. Among European pied flycatchers, it is known that males who have not formed pairs can participate in EPCs along with breeding territorial males [65]. We could not reveal genetic fathers for 35% (N = 36) of the EPYs. Certainly, non-breeding non-territorial males could be the genetic fathers of some of these nestlings. Consequently, in the case of very low nesting densities, it is the non-breeding males that may sire a substantial proportion of EPY, and it is likely that the occurrence of EPP in such case will be determined by the number of non-breeders, their fertilisation performance and territorial linkages. While the movements of nesting birds are highly spatially restricted as they are tethered to the nest site, non-breeding males have no such restrictions and are likely capable of exploring much larger areas.

Further, knowledge of the sex role in EPC initiation is crucial to the understanding which ecological interactions and behavioural patterns affect EPP [23,115]. Mating attempts can be initiated by a male [12,28,36] or female [18,19,33]. The male-initiated mating does not necessarily always have to be allowed or solicited by the female to result in successful copulations, i.e., in fertilization: EPP can be a consequence of sexual coercion [116] and forced extra-pair copulations [22]. Moreover, because resisting the male-initiated mating attempts can be costly to females [116], female 'cooperation' with a male could reduce the net costs of the encounter resulting in inconvenience polyandry [12,117]. European pied flycatcher EPC could occur, as argued here, as an unexpected side effect of the reproductive performance [8]. The male at the peak of the reproductive state in the corresponding hormonal status will copulate anyway with a within-pair or an extra-pair mate, and he could achieve his aim through sexual coercion and forced extra-pair copulations [8,23,64,116]. On the other hand, since the fertilization of an egg is the most important physiological need for a female in a reproductive state, the female could 'search' for extra-pair mates if her social partner is somehow absent 'soliciting' the EPC [83,118,119]. Thus, the presence of EPO in bird nests does not automatically imply the existence of a 'propensity' for EPCs of any gender.

Apparently, EPCs among birds are most commonly male-initiated, which proves that a female-initiated pursuit of extra-pair copulation is rare [12]. In the case of the European pied flycatcher, EPCs are mostly initiated by males as suggested by previous observations [118,120]. Through territorial intrusion tests and the measurement of excreted corticosterone metabolites, it has been demonstrated that the likelihood of paternity loss is associated with reduced aggressiveness and increased stress among males of the European pied flycatcher. It has been inferred that paternity is lost mostly among males who cannot effectively guard their within-pair females and territory against the male intruders sexually harassing females [59]. On the other hand, a negative correlation between the proportion of EPY in the brood and the age and wing length of the female lead to the conclusion that first-year and shorter-wing females are less likely to evade sexual abuse attempts by extra-pair males [64]. Our findings are generally consistent with those of the study. Among Spanish European pied flycatchers, gaps were temporarily created in the wings of females, resulting in a reduction of their wing area. Consequently, experimentally flight-impaired females had a higher proportion of EPYs, they were more likely to have EPYs and the number of extra-pair mates was also higher [70]. Thus, EPCs among European pied flycatchers are mostly the result of sexual abuse and are mainly driven by the extra-pair male pursuit of

females, capable of overruling female avoidance and mate defence from within the pair males [64,70].

Likely, this mechanism is also responsible for the fact that the incidence of EPP tends to be higher among females nesting in the best territories. We do not know the characteristics of the microhabitats that bring local nesting birds to the production of more recruits. However, if this is due to a fragmented distribution of insects, then rich food patches simply attract birds. This has resulted in such sites being visited more frequently by more specimens and, as a by-product, resident females of these microhabitats may be more often sexually abused by extra-pair males.

5. Conclusions

There are two ways of looking at biological phenomenon: ultimate (evolutionary explanations) and proximate (ecological and functional explanations). Ideally, a thorough explanation of biological phenomena must include both, although neither of them is mutually exclusive. Ecological events can always be considered profitably within an evolutionary framework and vice versa. However, these explanations are still different and, for example, not all ecological causes of a phenomenon can be mechanisms of its evolution without explicit assessment of the key parameters characterising that phenomenon. The key parameters that need to be documented to understand the evolution of extra-pair copulation behaviour are the magnitude of genetic correlations, the intensity of selection on mating biases, additive genetic variation in mating biases, preferred male traits and net fitness, as well as repeatable differences in these across ecological contexts [105]. Without an explicit assessment of these key parameters, all evidence that a given ecological process is an evolutionary factor for extra-pair mating behaviour would be incomplete. In our work, we used heritability as the main criterion discriminating hypotheses about the evolution and maintenance of EPCs [74]. We argue that the evolution and maintenance of extra-pair mating seem to be the episelective process [109,110]. Extra-pair mating behaviour among the European pied flycatcher is a plastic trait and can be determined by a whole set of proximate causes, and it appears that these causes may be different in particular populations of the species.

There also appears to be a hierarchy among the proximate factors that determine the extent to which birds are involved in extra-pair mating. Structural environmental characteristics that influence the probability of physical contact between individuals is one such top-level factor [8]. Sexual abuse seems to be a low-level behavioural proximate cause of the involvement of specimens in extra-pair copulations of the European pied flycatcher [70].

However, many details remain ambiguous or unstudied. For instance, the role of unmated non-breeding males in shaping EPP levels in populations is poorly investigated. Theoretically, in some circumstances, these individuals may contribute significantly to the proportion of broods containing EPY. The relationship between male–male interactions and the likelihood of EPCs is also not known in any detail. We have sometimes observed unsuccessful mating attempts of females with a within-pair male in nature, where the extra-pair male simply physically pushed aside the within-pair male and mated with the extra-pair female. The female did not change her inviting mating posture. In this situation, there was no sexual abuse from the extra-pair male to the extra-pair female. It simply was the case that the within-pair male failed to protect his interests at the critical moment when his social female needed to fertilize her eggs. Studies of these relationships between individuals and others like them are purely ecological and ethological in nature, but they do not lose their significance in the understanding of the extra-pair mating behaviour. This ecological research and observations as well as individual-based behavioural studies which combine a detailed description of behaviour with the genetic control of paternity will, therefore, be particularly beneficial in the future.

Supplementary Materials: The following supporting information can be downloaded at: https://www.mdpi.com/article/10.3390/d14040283/s1, Table S1: The list of all types of social and genetic relationships between offspring and parents, Table S2: The set of models investigated in the MARK program, Table S3: EPP, breeding and phenotypic trait data, Table S4: Encounter histories of offspring in connection with their origin, Table S5: Fitness of offspring, Table S6: The list of *p*-values generated during the analysis.

Author Contributions: Conceptualization, H.S. and M.W.; data curation, V.G.G. and A.B.; formal analysis, V.G.G. and A.B.; funding acquisition, M.W., H.S. and V.G.G.; investigation, V.G.G., H.S. and A.B.; methodology, M.W., H.S. and V.G.G.; project administration, V.G.G., H.S. and M.W.; resources, M.W. and V.G.G.; software, V.G.G.; supervision, M.W., H.S. and V.G.G.; validation, V.G.G. and A.B.; visualization, V.G.G.; writing—original draft preparation, V.G.G.; writing—review and editing, V.G.G., H.S. and M.W. All authors have read and agreed to the published version of the manuscript.

Funding: This work was supported by the Russian Fund of Basic Research RFBR (projects 05-04-49173-a, 06-04-49082-a, 09-04-00162-a, 13-04-01309-a, 18-04-00536-a). The research was carried out as part of the Scientific Project of the State Order of the Government of Russian Federation to Lomonosov Moscow State University No 121031600198-2.

Institutional Review Board Statement: Our work conforms to the legal requirements and guidelines in the Russian Federation as well as to international ethical standards. All our treatments and samplings have been intravital and have not required prolonged treatment and handling of birds. The species from our study is not included in the 'Threatened' category of the IUCN Red List of Threatened Species. The Bioethics Commission of Lomonosov Moscow State University provided full approval for this research (Protocol No 89-o of 22 March 2018).

Data Availability Statement: The data presented in this study are available in Supplementary Materials.

Acknowledgments: Authors are grateful to Moskvitin S.S. and Moskvitina N.S. for their help in lunching field research in the Tomsk region and for their constant facilitation in carrying it out, to Bulakhova N.A., Korobicyn I.G., Tjutenkov O.J., Kurbatskij D.V. for assistance in the field. We are grateful to Kathrin Henne for improving the English language of the manuscript.

Conflicts of Interest: The funders had no role in the design of the study; in the collection, analyses, or interpretation of data; in the writing of the manuscript, or in the decision to publish the results.

References

1. Lack, D. *Ecological Adaptations for Breeding in Birds*, 1st ed.; Methuen and Co. Ltd.: London, UK, 1968.
2. Erritzoe, J.; Kampp, K.; Winker, K.; Frith, C.B. *The Ornithologist's Dictionary: Or Ornithological and Related Technical Terms for Layman and Expert*; Lynx: Barcelona, Spain, 2007.
3. Wittenberger, J.F. The Evolution of Mating Systems in Birds and Mammals. In *Social Behavior and Communication*; Marler, P., Vandenbergh, J.G., Eds.; Springer: Boston, MA, USA, 1979; pp. 271–349. [CrossRef]
4. Griffith, S.C.; Owens, I.P.F.; Thuman, K.A. Extra pair paternity in birds: A review of interspecific variation and adaptive function. *Mol. Ecol.* **2002**, *11*, 2195–2212. [CrossRef] [PubMed]
5. Brouwer, L.; Griffith, S.C. Extra-pair paternity in birds. *Mol. Ecol.* **2019**, *28*, 4864–4882. [CrossRef] [PubMed]
6. Carey, M.; Nolan, V. Polygyny in Indigo Buntings: A Hypothesis Tested. *Science* **1975**, *190*, 1296–1297. [CrossRef]
7. Ford, N.L. Variation in Mate Fidelity in Monogamous Birds. In *Current Ornithology*; Johnston, R.F., Ed.; Plenum Press: New York, NY, USA, 1983; pp. 329–356. [CrossRef]
8. Grinkov, V.G.; Bauer, A.; Gashkov, S.I.; Sternberg, H.; Wink, M. Diversity of social-genetic relationships in the socially monogamous pied flycatcher (Ficedula hypoleuca) breeding in Western Siberia. *PeerJ* **2018**, *6*, e6059. [CrossRef] [PubMed]
9. Lifjeld, J.T.; Gohli, J.; Albrecht, T.; Garcia-del Rey, E.; Johannessen, L.E.; Kleven, O.; Marki, P.Z.; Omotoriogun, T.C.; Rowe, M.; Johnsen, A. Evolution of female promiscuity in Passerides songbirds. *BMC Evol. Biol.* **2019**, *19*, 169. [CrossRef]
10. Jeffreys, A.J. Highly variable minisatellites and DNA fingerprints. *Biochem. Soc. Trans.* **1987**, *15*, 309–317. [CrossRef]
11. Wink, M.; Dyrcz, A. Mating systems in birds: A review of molecular studies. *Acta Ornithol.* **1999**, *34*, 91–109.
12. Westneat, D.F.; Stewart, I.R. Extra-pair paternity in birds: Causes, correlates, and conflict. *Annu. Rev. Ecol. Evol. Syst.* **2003**, *34*, 365–396. [CrossRef]
13. Neudorf, D.L.H. Extrapair paternity in birds: Understanding variation among species. *Auk* **2004**, *121*, 302–307. [CrossRef]
14. Forstmeier, W.; Nakagawa, S.; Griffith, S.C.; Kempenaers, B. Female extra-pair mating: Adaptation or genetic constraint? *Trends Ecol. Evol.* **2014**, *29*, 456–464. [CrossRef]

15. McLeod, D.V.; Day, T. Sexually transmitted infection and the evolution of serial monogamy. *Proceed. Biol. Sci.* **2014**, *281*, 20141726. [CrossRef] [PubMed]
16. Lombardo, M.P. On the evolution of sexually transmitted diseases in birds. *J. Avian Biol.* **1998**, *29*, 314. [CrossRef]
17. Sheldon, B.C. Sexually transmitted disease in birds: Occurrence and evolutionary significance. *Philos. Trans. R. Soc. Lond. Ser. B Biol. Sci.* **1993**, *339*, 491–497. [CrossRef]
18. Davies, N.B. *Dunnock Behaviour and Social Evolution*; Oxford Series in Ecology and Evolution; Oxford University Press: Oxford, UK, 1992; Volume 3.
19. Kempenaers, B.; Verheyen, G.R.; van den Broeck, M.; Burke, T.; van Broeckhoven, C.; Dhondt, A. Extra-pair paternity results from female preference for high-quality males in the blue tit. *Nature* **1992**, *357*, 494–496. [CrossRef]
20. Sheldon, B.C. Sperm competition in the chaffinch: The role of the female. *Anim. Behav.* **1994**, *47*, 163–173. [CrossRef]
21. Westneat, D.F.; Gray, E.M. Breeding synchrony and extrapair fertilizations in two populations of red-winged blackbirds. *Behav. Ecol.* **1998**, *9*, 456–464. [CrossRef]
22. Brekke, P.; Cassey, P.; Ariani, C.; Ewen, J.G. Evolution of extreme-mating behaviour: Patterns of extrapair paternity in a species with forced extrapair copulation. *Behav. Ecol. Sociobiol.* **2013**, *67*, 963–972. [CrossRef]
23. Girndt, A.; Chng, C.W.T.; Burke, T.; Schroeder, J. Male age is associated with extra-pair paternity, but not with extra-pair mating behaviour. *Sci. Rep.* **2018**, *8*, 8378. [CrossRef]
24. Eliassen, S.; Jørgensen, C. Extra-pair mating and evolution of cooperative neighbourhoods. *PLoS ONE* **2014**, *9*, e99878. [CrossRef]
25. Albrecht, T.; Kreisinger, J.; Piálek, J. The strength of direct selection against female promiscuity is associated with rates of extrapair fertilizations in socially monogamous songbirds. *Am. Nat.* **2006**, *167*, 739–744. [CrossRef]
26. Arnqvist, G.; Kirkpatrick, M. The evolution of infidelity in socially monogamous passerines revisited: A reply to Griffith. *Am. Nat.* **2007**, *169*, 282–283. [CrossRef]
27. Weatherhead, P.J.; Robertson, R.J. Offspring quality and the polygyny threshold: "The sexy son hypothesis". *Am. Nat.* **1979**, *113*, 201–208. [CrossRef]
28. Yezerinac, S.M.; Weatherhead, P.J. Reproductive synchrony and extra-pair mating strategy in a socially monogamous bird, Dendroica petechia. *Anim. Behav.* **1997**, *54*, 1393–1403. [CrossRef] [PubMed]
29. Jennions, M.D.; Petrie, M. Why do females mate multiply? A review of the genetic benefits. *Biol. Rev.* **2000**, *75*, 21–64. [CrossRef] [PubMed]
30. Arct, A.; Drobniak, S.M.; Cichoń, M. Genetic similarity between mates predicts extrapair paternity—A meta-analysis of bird studies. *Behav. Ecol.* **2015**, *26*, 959–968. [CrossRef]
31. Cramer, E.R.A.; Greig, E.I.; Kaiser, S.A. Strong sexual selection despite spatial constraints on extrapair paternity. *Behav. Ecol.* **2020**, *31*, 618–626. [CrossRef]
32. Arnqvist, G.; Kirkpatrick, M. The evolution of infidelity in socially monogamous passerines: The strength of direct and indirect selection on extrapair copulation behavior in females. *Am. Nat.* **2005**, *165*, 26–37. [CrossRef]
33. Sheldon, B.C. Male phenotype, fertility, and the pursuit of extra-pair copulations by female birds. *Proc. R. Soc. Lond. Ser. B Biol. Sci.* **1994**, *257*, 25–30. [CrossRef]
34. Arnqvist, G.; Nilsson, T. The evolution of polyandry: Multiple mating and female fitness in insects. *Anim. Behav.* **2000**, *60*, 145–164. [CrossRef]
35. Tryjanowski, P.; Hromada, M. Do males of the great grey shrike, Lanius excubitor, trade food for extrapair copulations? *Anim. Behav.* **2005**, *69*, 529–533. [CrossRef]
36. Ledwoń, M.; Neubauer, G. True deception during extra-pair courtship feeding: Cheating whiskered tern *Chlidonias hybrida* females perform better. *J. Avian Biol.* **2018**, *49*, e01503. [CrossRef]
37. Stacey, P.B. Female promiscuity and male reproductive success in social birds and mammals. *Am. Nat.* **1982**, *120*, 51–64. [CrossRef]
38. Davies, N.B.; Harley, I.R.; Hatchwell, B.J.; Langmore, N.E. Female control of copulations to maximize male help: A comparison of polygynandrous alpine accentors, Prunella collaris, and dunnocks, P. modularis. *Anim. Behav.* **1996**, *51*, 27–47. [CrossRef]
39. Krams, I.A.; Mennerat, A.; Krama, T.; Krams, R.; Jõers, P.; Elferts, D.; Luoto, S.; Rantala, M.J.; Eliassen, S. Extra-pair paternity explains cooperation in a bird species. *Proc. Natl. Acad. Sci. USA* **2022**, *119*, e2112004119. [CrossRef] [PubMed]
40. Halliday, T.; Arnold, S.J. Multiple mating by females: A perspective from quantitative genetics. *Anim. Behav.* **1987**, *35*, 939–941. [CrossRef]
41. Forstmeier, W.; Martin, K.; Bolund, E.; Schielzeth, H.; Kempenaers, B. Female extrapair mating behavior can evolve via indirect selection on males. *Proc. Natl. Acad. Sci. USA* **2011**, *108*, 10608–10613. [CrossRef]
42. Hsu, Y.H.; Schroeder, J.; Winney, I.; Burke, T.; Nakagawa, S. Are extra-pair males different from cuckolded males? A case study and a meta-analytic examination. *Mol. Ecol.* **2015**, *24*, 1558–1571. [CrossRef]
43. Reid, J.M.; Wolak, M.E. Is there indirect selection on female extra-pair reproduction through cross-sex genetic correlations with male reproductive fitness? *Evol. Lett.* **2018**, *2*, 159–168. [CrossRef]
44. Mauck, R.A.; Marschall, E.A.; Parker, P.G. Adult survival and imperfect assessment of parentage: Effects on male parenting decisions. *Am. Nat.* **1999**, *154*, 99–109. [CrossRef]
45. Arnold, K.E.; Owens, I.P.F. Extra-pair paternity and egg dumping in birds: Life history, parental care and the risk of retaliation. *Proceed. Biol. Sci.* **2002**, *269*, 1263–1269. [CrossRef]

46. Valcu, C.M.; Valcu, M.; Kempenaers, B. The macroecology of extra-pair paternity in birds. *Mol. Ecol.* **2021**, *30*, 4884–4898. [CrossRef] [PubMed]
47. Kuranov, B.D. Nesting biology of the pied flycacther (Ficedula hypoleuca, Passeriformes, Muscicapidae) in the southeastern part of its distribution area. *Zool. Zhurnal* **2018**, *97*, 321–336. [CrossRef]
48. Lundberg, A.; Alatalo, R.V. *The Pied Flycatcher*; T 'I&' AD Poyser Ltd.: London, UK, 1992.
49. Artemev, A.V. *Populyatsionnaya Ekologiya Muholovki-Pestrushki v Severnoy Zone Areala*; Nauka: Moscow, Russia, 2008.
50. Sternberg, H. Pied flycatcher. In *Lifetime Reproduction in Birds*; Newton, I., Ed.; Academic Press Ltd.: London, UK, 1989; pp. 55–74.
51. Sternberg, H.; Grinkov, V.G.; Ivankina, E.V.; Ilyina, T.A.; Kerimov, A.B.; Schwarz, A. Evaluation of the size and composition of nonbreeding surplus in a pied flycatcher Ficedula hypoleuca population: Removal experiments in Germany and Russia. *Ardea* **2002**, *90*, 461–470.
52. Both, C.; Burger, C.; Ouwehand, J.; Samplonius, J.M.; Ubels, R.; Bijlsma, R.G. Delayed age at first breeding and experimental removals show large non-breeding surplus in Pied Flycatchers. *Ardea* **2017**, *105*, 43–60. [CrossRef]
53. Grinkov, V.G.; Sternberg, H. Delayed start of first-time breeding and non-breeders surplus in the Western Siberian population of the European Pied Flycatcher. *bioRxiv* **2018**, 387829. [CrossRef]
54. Lifjeld, J.T.; Slagsvold, T.; Lampe, H.M. Low frequency of extra-pair paternity in pied flycatchers revealed by DNA fingerprinting. *Behav. Ecol. Sociobiol.* **1991**, *29*, 95–101. [CrossRef]
55. Rätti, O.; Hovi, M.; Lundberg, A.; Tegelström, H.; Alatalo, R.V. Extra-pair paternity and male characteristics in the pied flycatcher. *Behav. Ecol. Sociobiol.* **1995**, *37*, 419–425. [CrossRef]
56. Lubjuhn, T.; Winkel, W.; Epplen, J.T.; Brün, J. Reproductive success of monogamous and polygynous pied flycatchers (Ficedula hypoleuca). *Behav. Ecol. Sociobiol.* **2000**, *48*, 12–17. [CrossRef]
57. Slagsvold, T.; Johnsen, A.; Lampe, H.M.; Lifjeld, J.T. Do female pied flycatchers seek extrapair copulations with familiar males? A test of the incomplete knowledge hypothesis. *Behav. Ecol.* **2001**, *12*, 412–418. [CrossRef]
58. Lehtonen, P.K.; Primmer, C.R.; Laaksonen, T. Different traits affect gain of extrapair paternity and loss of paternity in the pied flycatcher, Ficedula hypoleuca. *Anim. Behav.* **2009**, *77*, 1103–1110. [CrossRef]
59. Moreno, J.; Martínez, J.G.; Morales, J.; Lobato, E.; Merino, S.; Tomás, G.; Vásquez, R.A.; Möstl, E.; Osorno, J.L. Paternity loss in relation to male age, territorial behaviour and stress in the pied flycatcher. *Ethology* **2010**, *116*, 76–84. [CrossRef]
60. Canal, D.; Jovani, R.; Potti, J. Multiple mating opportunities boost protandry in a pied flycatcher population. *Behav. Ecol. Sociobiol.* **2012**, *66*, 67–76. [CrossRef]
61. Canal, D.; Jovani, R.; Potti, J. Male decisions or female accessibility? Spatiotemporal patterns of extra pair paternity in a songbird. *Behav. Ecol.* **2012**, *23*, 1146–1153. [CrossRef]
62. González-Braojos, S.; Ruiz de Castañeda, R.; Cantarero, A.; Sánchez-Tójar, A.; Martínez, J.G.; Moreno, J. Extra-pair matings, context-dependence and offspring quality: A brood manipulation experiment in pied flycatchers. *Behaviour* **2013**, *150*, 359–380. [CrossRef]
63. de la Hera, I.; Reed, T.E.; Pulido, F.; Visser, M.E. Feather mass and winter moult extent are heritable but not associated with fitness-related traits in a long-distance migratory bird. *Evol. Ecol.* **2013**, *27*, 1199–1216. [CrossRef]
64. Moreno, J.; Martínez, J.G.; González-Braojos, S.; Cantarero, A.; Ruizde-Castañeda, R.; Precioso, M.; López-Arrabé, J. Extra-pair paternity declines with female age and wing length in the pied flycatcher. *Ethology* **2015**, *121*, 501–512. [CrossRef]
65. Tomotani, B.M.; Caglar, E.; de La Hera, I.; Mateman, A.C.; Visser, M.E. Early arrival is not associated with more extra-pair fertilizations in a long-distance migratory bird. *J. Avian Biol.* **2017**, *48*, 854–861. [CrossRef]
66. Lifjeld, J.T.; Slagsvold, T.; Dale, S.; Ellegren, H. A sexually selected paradox in the pied flycatcher: Attractive males are cuckolded. *Auk* **1997**, *114*, 112–115. [CrossRef]
67. Canal, D.; Dávila, J.; Potti, J. Male phenotype predicts extra-pair paternity in pied flycatchers. *Behaviour* **2011**, *148*, 691–712. [CrossRef]
68. Møller, A.P.; Brohede, J.; Cuervo, J.J.; de Lope, F.; Primmer, C. Extrapair paternity in relation to sexual ornamentation, arrival date, and condition in a migratory bird. *Behav. Ecol.* **2003**, *14*, 707–712. [CrossRef]
69. Grinkov, V.G.; Bauer, A.; Sternberg, H.; Wink, M. Genetic background of social interactions in a Siberian population of Pied Flycatcher. *Ornithol. Sci.* **2014**, *13*, 1–2.
70. Plaza, M.; Cantarero, A.; Gil, D.; Moreno, J. Experimentally flight-impaired females show higher levels of extra-pair paternity in the pied flycatcher Ficedula hypoleuca. *Biol. Lett.* **2019**, *15*, 20190360. [CrossRef]
71. Moreno, J.; Velando, A.; González-Braojos, S.; Ruiz-de Castañeda, R.; Cantarero, A. Females paired with more attractive males show reduced oxidative damage: Possible direct benefits of mate choice in pied flycatchers. *Ethology* **2013**, *119*, 727–737. [CrossRef]
72. Bushuev, A.V.; Husby, A.; Sternberg, H.; Grinkov, V.G. Quantitative genetics of basal metabolic rate and body mass in free-living pied flycatchers. *J. Zool.* **2012**, *288*, 245–251. [CrossRef]
73. Drost, R. Ueber das Brutkleid männlicher Trauerfliegenfänger, Muscicapa hypoleuca. *Vogelzug* **1936**, *6*, 179–186.
74. Grinkov, V.G.; Bauer, A.; Sternberg, H.; Wink, M. Heritability of the extra-pair mating behaviour of the pied flycatcher in Western Siberia. *PeerJ* **2020**, *8*, e9571. [CrossRef] [PubMed]
75. Ellegren, H. Polymerase-chain-reaction (PCR) analysis of microsatellites: A new approach to studies of genetic relationships in birds. *Auk* **1992**, *109*, 886–895. [CrossRef]

76. Primmer, C.R.; Moller, A.P.; Ellegren, H. New microsatellites from the pied flycatcher Ficedula hypoleuca and the swallow Hirundo rustica genomes. *Hereditas* **1996**, *124*, 281–283. [CrossRef]
77. Leder, E.H.; Karaiskou, N.; Primmer, C.R. Seventy new microsatellites for the pied flycatcher, Ficedula hypoleuca and amplification in other passerine birds. *Mol. Ecol. Resour.* **2008**, *8*, 874–880. [CrossRef]
78. Kalinowski, S.T.; Taper, M.L.; Marshall, T.C. Revising how the computer program CERVUS accommodates genotyping error increases success in paternity assignment. *Mol. Ecol.* **2007**, *16*, 1099–1106. [CrossRef]
79. Dunn, P.O.; Lifjeld, J.T. Can extra-pair copulations be used to predict extra-pair paternity in birds? *Anim. Behav.* **1994**, *47*, 983–985. [CrossRef]
80. Griffith, S. The evolution of infidelity in socially monogamous passerines: Neglected components of direct and indirect selection. *Am. Nat.* **2007**, *169*, 274–281. [CrossRef] [PubMed]
81. Birkhead, T.R.; Briskie, J.V.; Slagsvold, T. Breeding-cycle patterns of sperm storage in the pied flycatcher (Ficedula hypoleuca). *Auk* **1997**, *114*, 792–796. [CrossRef]
82. von Haartman, L. Territory in the pied flycatcher Muscicapa hypolueca. *Ibis* **1956**, *98*, 460–475. [CrossRef]
83. Lifjeld, T.J.; Slagsvold, T.; Ellegren, H. Experimental mate switching in pied flycatchers: Male copulatory access and fertilization success. *Anim. Behav.* **1997**, *53*, 1225–1232. [CrossRef]
84. Silverin, B. Reproductive organs and breeding behaviour of the male pied flycatcher Ficedula hypoleuca (Pallas). *Ornis Scand.* **1975**, *6*, 15. [CrossRef]
85. Chek, A.A.; Lifjeld, J.T.; Robertson, R.J. Lack of Mate-guarding in a Territorial Passerine Bird with a Low Intensity of Sperm Competition, the Pied Flycatcher; (Ficedula hypoleuca). *Ethology* **1996**, *102*, 134–145. [CrossRef]
86. Cormack, R.M. Estimates of survival from the sighting of marked animals. *Biometrika* **1964**, *51*, 429–438. [CrossRef]
87. Jolly, G.M. Explicit estimates from capture-recapture data with both death and immigration-stochastic model. *Biometrika* **1965**, *52*, 225–248. [CrossRef]
88. Seber, G.A.F. A note on the multiple-recapture census. *Biometrika* **1965**, *52*, 249–260. [CrossRef]
89. Lebreton, J.D.; Burnham, K.P.; Clobert, J.; Anderson, D.R. Modeling survival and testing biological hypotheses using marked animals: A unified approach with case studies. *Ecol. Monogr.* **1992**, *62*, 67–118. [CrossRef]
90. White, G.C.; Burnham, K.P. Program MARK: Survival estimation from populations of marked animals. *Bird Study* **1999**, *46*, S120–S139. [CrossRef]
91. Laake, J.L. *RMark: An R Interface for Analysis of Capture-Recapture Data with MARK*; AFSC Processed Rep. 2013-01; Alaska Fisheries Science Center, NOAA, National Marine Fisheries Service: Seattle, WA, USA, 2013.
92. Brommer, J.E.; Merilä, J.; Kokko, H. Reproductive timing and individual fitness. *Ecol. Lett.* **2002**, *5*, 802–810. [CrossRef]
93. McGraw, J.B.; Caswell, H. Estimation of individual fitness from life-history data. *Am. Nat.* **1996**, *147*, 47–64. [CrossRef]
94. R Core Team. *R: A Language and Environment for Statistical Computing*; R Foundation for Statistical Computing: Vienna, Austria, 2020.
95. RStudio Team. *RStudio: Integrated Development Environment for R*; RStudio, PBC: Boston, MA, USA, 2021.
96. Baddeley, A.; Turner, R. Spatstat: An R Package for analyzing spatial point patterns. *J. Stat. Softw.* **2005**, *12*, 1–42. [CrossRef]
97. Sætre, G.P.; Dale, S.; Slagsvold, T. Female pied flycatchers prefer brightly coloured males. *Anim. Behav.* **1994**, *48*, 1407–1416. [CrossRef]
98. Saetre, G.P.; Moum, T.; Bures, S.; Kral, M.; Adamjan, M.; Moreno, J. A sexually selected character displacement in flycatchers reinforces premating isolation. *Nature* **1997**, *387*, 589–592. [CrossRef]
99. Alatalo, R.V.; Lundberg, A.; Glynn, C. Female pied flycatchers choose territory quality and not male characteristics. *Nature* **1986**, *323*, 152–153. [CrossRef]
100. Grinkov, V.G.; Palko, I.V.; Sternberg, H. Character displacement within the breeding area questions reinforcement in Ficedula flycatchers. *bioRxiv* **2019**, 515916. [CrossRef]
101. Huhta, E.; Alatalo, R.V. Plumage colour and male-male interactions in the pied flycatcher. *Anim. Behav.* **1993**, *45*, 511–518. [CrossRef]
102. Dale, S.; Slagsvold, T. Plumage coloration and conspicuousness in birds: Experiments with the pied flycatcher. *Auk* **1996**, *113*, 849–857. [CrossRef]
103. Cameron, E.; Day, T.; Rowe, L. Sexual conflict and indirect benefits. *J. Evol. Biol.* **2003**, *16*, 1055–1060. [CrossRef] [PubMed]
104. Chapman, T.; Arnqvist, G.; Bangham, J.; Rowe, L. Sexual conflict. *Trends Ecol. Evol.* **2003**, *18*, 41–47. [CrossRef]
105. Kokko, H.; Brooks, R.; Jennions, M.D.; Morley, J. The evolution of mate choice and mating biases. *Proc. R. Soc. Lond. Ser. B Biol. Sci.* **2003**, *270*, 653–664. [CrossRef]
106. Shy, M.M. Interspecific feeding among birds: A review. *J. Field Ornithol.* **1982**, *53*, 370–393.
107. Zubkova, O.A. Records of nest valence and visits of nest by stranger in the Pied Flycatcher. *Ornithologia* **2013**, *38*, 122–124. (In Russian)
108. Severtsov, A.S.; Kreslavsky, A.G.; Cherdantsev, V.G. Three mechanisms of evolution. In *Contemporary Problems of Evolutionary Theory*; Tatarinov, L.P., Ed.; Nauka: Moscow, Russia, 1993; pp. 17–42.
109. Cherdantsev, V.G.; Kreslavsky, A.G.; Severtsov, A.S. Episelective evolution. *Evoutionary Theory* **1996**, *11*, 69–87.
110. Moczek, A.P. On the origins of novelty in development and evolution. *BioEssays* **2008**, *30*, 432–447. [CrossRef]

111. Moczek, A.P. The nature of nurture and the future of evodevo: Toward a theory of developmental evolution. *Integr. Comp. Biol.* **2012**, *52*, 108–119. [CrossRef]
112. Gilbert, S.F.; Bosch, T.C.G.; Ledón-Rettig, C. Eco-Evo-Devo: Developmental symbiosis and developmental plasticity as evolutionary agents. *Nat. Rev. Genet.* **2015**, *16*, 611–622. [CrossRef]
113. Emlen, S.; Oring, L. Ecology, sexual selection, and the evolution of mating systems. *Science* **1977**, *197*, 215–223. [CrossRef] [PubMed]
114. Westneat, D.F.; Sherman, P.W.; Morton, M.L. The ecology and evolution of extra-pair copulations in birds. In *Current Ornithology*; Power, D.M., Ed.; Current Ornithology, Plenum Press: New York, NY, USA, 1990; pp. 331–369.
115. Ledwoń, M.; Szczys, P. Extra-pair paternity in a species with frequent extra-pair courtship feedings, few extra-pair copulations, and male-biased parental care. *J. Ornithol.* **2021**, *163*, 437–444. [CrossRef]
116. McKinney, F.; Evarts, S. Sexual coercion in waterfowl and other birds. *Ornithol. Monogr.* **1998**, *49*, 163–195. [CrossRef]
117. Wagner, R.H.; Schug, M.D.; Morton, E.S. Condition-dependent control of paternity by female purple martins: Implications for coloniality. *Behav. Ecol. Sociobiol.* **1996**, *38*, 379–389. [CrossRef]
118. Björklund, M.; Westman, B. Extra-pair copulations in the pied flycatcher (Ficedula hypoleuca). *Behav. Ecol. Sociobiol.* **1983**, *13*, 271–275. [CrossRef]
119. Slagsvold, T.; Drevon, T. When and from whom do female pied flycatchers (Ficedula hypoleuca) solicit copulations. *Behaviour* **2005**, *142*, 1059–1076. [CrossRef]
120. Lundberg, A.; Gottlander, K.; Alatalo, R.V. Extra-pair copulations and mate guarding in the polyterritorial pied flycatcher, Ficedula hypoleuca. *Behaviour* **1987**, *101*, 139–154. [CrossRef]

diversity

MDPI

Review

Evolutionary Ecology of Fixed Alternative Male Mating Strategies in the Ruff (*Calidris pugnax*)

Michel Baguette [1,2], Baptiste Bataille [3] and Virginie M. Stevens [2,*]

[1] Institut Systématique, Evolution, Biodiversité (ISYEB), UMR 7205 Muséum National d'Histoire Naturelle, CNRS, Sorbonne Université, EPHE, Université des Antilles, 75241 Paris, France; michel.baguette@mnhn.fr
[2] Centre National de la Recherche Scientifique, SETE Station d'Ecologie Théorique et Expérimentale, CNRS UAR 2029, 09200 Moulis, France
[3] Jozef De Windestraat 17, B-1700 Dilbeek, Belgium; baptiste@baptiste-bataille.com
* Correspondence: virginie.stevens@sete.cnrs.fr

Abstract: A few empirical examples document fixed alternative male mating strategies in animals. Here we focus on the polymorphism of male mating strategies in the ruff (*Calidris pugnax*, Aves Charadriiformes). In ruffs, three fixed alternative male mating strategies coexist and are signaled by extreme plumage polymorphism. We first present relevant data on the biology of the species. Then we review the available knowledge of the behavioral ecology of ruffs during the breeding season, and we detail the characteristics of each of the three known fixed male mating strategies. We next turn to the results of exceptional quality accumulated on both the structural and functional genomics of the ruff over the past few years. We show how much these genomic data can shed new, mechanistic light on the evolution and maintenance of the three fixed alternative male mating strategies. We then look if there is sufficient indication to support frequency-dependent selection as a key mechanism in maintaining these three strategies. Specifically, we search for evidence of equal fitness among individuals using each of the three strategies. Finally, we propose three lines of research avenues that will help to understand the eco-evolutionary dynamics of phenotypic differences within natural populations of this iconic model species.

Keywords: phenotypic polymorphism; structural genomics; chromosomal inversion; supergene; functional genomics; hormonal plasticity; frequency-dependent selection; cryptic female choice of sperm; sexual selection; eco-evolutionary dynamics

Citation: Baguette, M.; Bataille, B.; Stevens, V.M. Evolutionary Ecology of Fixed Alternative Male Mating Strategies in the Ruff (*Calidris pugnax*). *Diversity* **2022**, *14*, 307. https://doi.org/10.3390/d14040307

Academic Editor: Michael Wink

Received: 21 March 2022
Accepted: 17 April 2022
Published: 18 April 2022

1. Introduction

The most common occurrence of alternative male mating strategies (AMMS) in animals involves the coexistence of two extreme behaviors: (1) males that defend either a territory or a group of females and gain access to mates through their aggressive behavior, and (2) males that perform various forms of sneaking behavior by parasitizing the attractiveness of others [1]. In many animal species, AMMS are signaled by phenotypic polymorphism [2–5]. Earlier works focused on the mechanisms and evolutionary stability of alternative phenotype coexistence in populations while speculating on the environmental vs. genetic origin of this polymorphism. Most reported variation in reproductive behavior within populations is nongenetic, and even when genetically determined, most strategies turn out to be conditional and reversible [1,6]. In conditional strategies, the behavior an individual adopts is determined by some aspect of their state (e.g., age, size, conditional). However, in a few cases, genetically determined strategies are fixed all over an individual's lifetime [7]. Conditional strategies correspond thus to behavioral plasticity: individuals adopt well-defined behavioral tactics but can change them according to their state (e.g., age, size, condition). In genetically determined fixed strategies, behavioral tactics that the individual can adopt remain constant throughout their life, regardless of their condition. Theory suggests that conditional male mating strategies are most frequent at intermediate

levels of variance in male mating success, whereas fixed strategies evolve mainly when male mating success is highly skewed, but also when the costs and limits of being conditional are very high or the benefits of being conditional are very low [8]. Importantly, if there are either fitness costs or limits to behavioral plasticity, conditional strategies are never able to entirely replace fixed strategies, and equilibrium populations may frequently consist of a mixture of conditional and fixed strategies [8].

According to the evolutionary game theory, the maintenance of fixed AMMS based on genetic polymorphism should depend on a negative frequency-dependent selection that provides each strategy with equal fitness [2]. However, only a few empirical examples document genetic-based, fixed alternative strategies, and the evidence of frequency-dependent selection and/or equal fitness between strategies remain elusive [2,5]. A noticeable exception is the side-blotched lizard *Uta stansburiana*, in which three differently colored male phenotypes each have a distinct mating strategy. In this species, color phenotypes and thus mating strategies are genetically determined and have high heritability [3]. Each of them has a fitness advantage over one of the other two and is inferior to the last. There is frequency-dependent selection on these phenotypes, which translates into cycles of morph frequency in populations over time [3]. Sinervo and Lively [3] suggest that "frequency-dependent selection maintains substantial genetic variation in alternative male strategies, while at the same time prohibiting a stable equilibrium in morph frequency".

This well-documented study remains dramatically isolated, however. In particular, the scarcity of empirical demonstration that fixed AMMS are maintained by frequency-dependent selection raises questions about their origin, maintenance, and evolution. Austad, in 1984 [6], mentioned that in the ruff (*Calidris pugnax* (Linné 1758)), a Palearctic breeding shorebird that is a classic case of male mating strategy polymorphism, a genetic mechanism could interfere with frequency-dependent selection to maintain the different strategies documented in this species [6]. In the light of current knowledge, the simple genetic scenario of two alleles at a single locus proposed by Austad [6] does not correspond to the autosomal inversion and recombination that are at work to generate and retain the ruff male polymorphism [8,9]. However, it is a premonitory vision of the importance of the joint role of ecological (frequency-dependent selection) and evolutionary (complex genomic mechanisms) drivers of fixed AMMS that deserves to be highlighted.

Here we focus on the evolutionary ecology of the polymorphism of mating strategies in the ruff. We first present relevant data on the biology of the species. Then we review the available knowledge of the behavioral ecology of ruffs during the breeding season, and we detail the characteristics of each of the three known fixed male mating strategies. We next turn to the exceptional quality results accumulated on structural and functional genomics of the ruff over the past few years. We show how much these genomic data can shed new, mechanistic light on the origin and evolution of phenotypic polymorphism associated with the three alternative male mating strategies. We then examine whether currently available data do support frequency-dependent selection as a key mechanism in maintaining alternative male mating strategies. Specifically, we search for evidence of equal fitness among individuals using each of the three strategies. Finally, we propose three lines of research avenues that will help to understand the eco-evolutionary dynamics of phenotypic differences within natural populations in this iconic model species.

2. Biology of Ruffs

2.1. Systematics and Taxonomy

The ruff *Calidris pugnax* (Aves, Charadriiformes) is a shorebird belonging to the Scolopaci clade (suborder), the Scolopacini tribe, the Scolopacidae family, and the Calidridinae subfamily (e.g.,[10–13]. Ruff was initially described as belonging to the polytypic genus *Tringa* Linné 1758. The species was then placed into different monotypic genera (*Philomachus* Merrem 1804, *Pavoncella* Leach 1816, *Machetes* Cuvier 1817). This monotypic treatment is probably due to the many particularities of this species, which distinguish ruffs from other Charadriiformes. However, recent phylogenetic studies based on nuclear and

mitochondrial genes [14,15] revealed that the species was closely related to birds belonging to the genus *Calidris* MERREM 1804. Accordingly, *Calidris pugnax* is now acknowledged as the valid scientific name of the species [16–18].

2.2. Adult Description

The most conspicuous feature of ruffs is the polymorphism of male nuptial plumages. These plumages are progressively acquired by a prenuptial molt during the spring migration and lost during a post-breeding molt until mid-autumn [19]. Individual males can be assigned unambiguously to three different categories of nuptial plumages (Figure 1). The "darkish" males may wear a blackish-reddish-bluish ruff of elongated neck feathers, two tufts on top of their head, and a collection of small facial wattles between the bill and eyes [20]. The "whitish" males may wear the same ornamentation, but their color is here predominantly white [20]. Within these categories, the coloration patterns of individuals are highly variable, making reliable identification possible even with human eyes [19–22]. As male ruffs perform silent displays, which is unusual in birds, their voice cannot be used to signal individual identity. Lank and Dale [23] propose that the adaptive significance of this variation in ruff plumage is to signal the identity of each individual. The third category of males does not develop male nuptial plumage. Those males that are similar to females in nuptial plumages were first called "naked-nape males" by Hogan-Warburg [20,22] and then "faeder" by Jukema and Piersma [24]. Males maintain a single nuptial plumage phenotype throughout their adult lifetime [20,21,25]. Female nuptial plumage is only slightly different from their winter plumage, which is also similar to the prenuptial plumage of males [21]. Variation among female nuptial plumage exists in females but is usually too vague to allow individual identification of females [21].

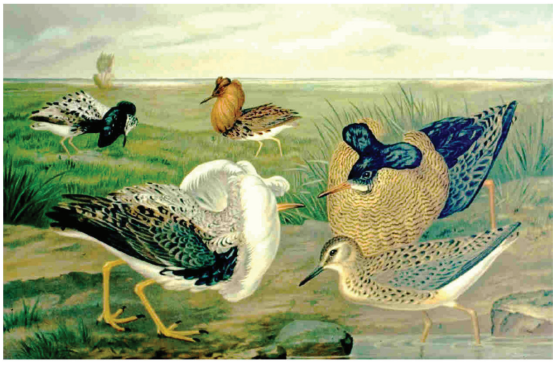

Figure 1. Illustration of ruff plumages: variable darkish males, a whitish male, and a female. The dark male in the background adopts the squat posture (see text). The posture adopted by the whitish male in the forefront is an artistic vision, as a satellite would probably never be seen facing off in this agonistic posture. Painting by Johann Friedrich Naumann (1780–1857), public domain.

Another characteristic of ruffs is sexual dimorphism in size and weight: males are larger and heavier (10% to 70% [26]) than females, which is unusual in shorebirds and especially in Calidridinae [27]. This sexual dimorphism is related to a polygynous mating system [27], which is indeed observed in ruffs (e.g., [21,28–30]). There are also size and weight differences among the three male plumage phenotypes: darkish males are usually heavier with longer wings, tarsus, and overall body size than whitish males [31] even there is extensive overlap, whereas wing length and weight of naked-nape males are distinctly smaller and fall in-between those of females and darkish and whitish males [24].

2.3. Distribution and Habitats

The ruff breeds in lowlands of high and low Arctic and subarctic, in boreal and temperate zones in Europe and Siberia almost to the Pacific, towards the oceanic fringe of west Palearctic, and overlaps steppe zone in the continental interior (Figure 2) [26,32–34]. The main wintering area is in Africa, where most Fennoscandian breeders overwinter in the Sahel zone, and most Siberian breeders overwinter in east and southern Africa [32]. Some western breeders spend the winter in western, south-western, and central Europa, whereas some Siberian breeders overwinter in the Middle East, India, and easternmost Asia (Figure 2) [26,32–34]. Stable isotope measurements in different tissues have proven to be excellent tools for tracing ruff migration routes by identifying stopovers from overwintering sites to nesting sites [35]. Sexes are not distributed evenly on the wintering grounds. Males tend to overwinter northerly, whereas females go further south [26,32,36]; the proportion of females wintering in Africa exceeds the female proportion in breeding populations, whereas almost all birds overwintering in western Europe are males [32]. This sex bias is explained by sexual selection for the earlier return of males to breeding grounds [36], which is a general pattern in birds in which male fitness depends on the number of matings (e.g., [37]). Migration departure of both sexes also differs in time; males leave their wintering areas earlier than females in March and their breeding areas in July several weeks before females. Juveniles fly northwards simultaneously or even later than females [36]. The ruff total world population is estimated at over two million individuals, with one million overwintering in western Africa and one million in the east and south Africa, and in Asia [26].

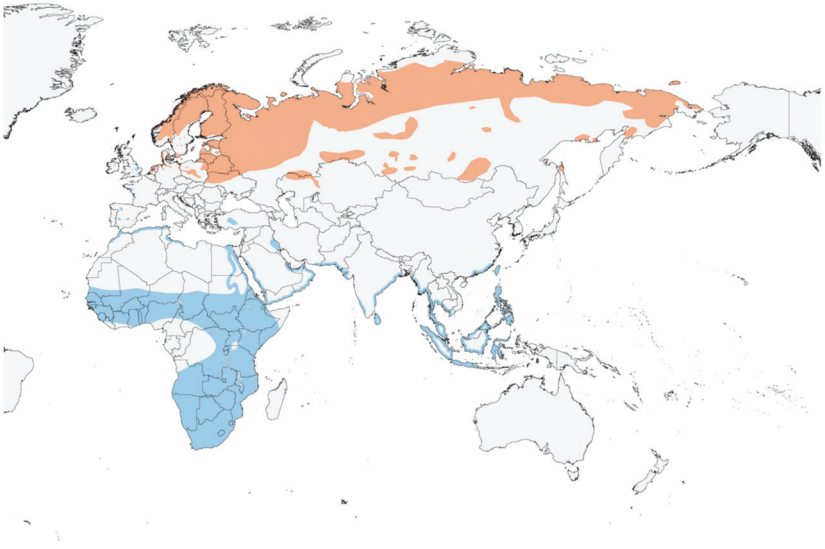

Figure 2. Distribution map of ruff (*Calidris pugnax*) breeding (orange) and wintering (blue) areas [14], © BirdLife International.

The breeding habitats of the ruff are coastal or inland wetlands with adjacent feeding, courtship, and nesting areas; usually in coastal tundra to forest-tundra near small lakes, in marshes and deltas with shallow-water margins in boreal zones; in damp to swampy meadows in Western and Central Europa (e.g., [26,34]). Outside breeding season, the proximity between feeding, resting, and roosting areas is relaxed. The ruff prefers wetlands but feeds on grass, wheat, or rice fields, not always close to water. Birds use night-time roosts on shallow water along lake edges (e.g., [26,34]).

2.4. Food and Foraging

The diet consists chiefly of invertebrates during the breeding season, mainly larval and adult insects (aquatic and terrestrial), but the ruff also feeds on mollusks and earthworms. Outside of the breeding season, birds feed on a wider range of animals, including amphipod crustaceans, spiders, frogs, and small fish, and on vegetal material, mainly seeds but also vegetative parts of plants (e.g., [26,34]). Individuals forage for food by walking on the ground or by wading in shallow water; their bill probes mud or soft soil or picks up material from soil or water surface and from vegetation. When foraging in water, birds sometimes immerse their heads [26].

2.5. Demography

The yearly survival is 0.52 ± 0.04 with a type II survivorship (constant over time), and no sex difference was reported [26,38]. The oldest ringed bird was 10 years 11 months old [26]. The age at first reproduction is 2 years, but probably older for males [26]. There is one brood per year. The mean clutch size is 3.72 eggs ± 0.31 (n = 18) [39]. The hatching success is 0.92 (n = 62) [37]. The fledging success is not yet documented. The sex ratio in juvenile and adult populations is ♂:♀0.34 [40].

3. Behavioral Ecology of Breeding Ruffs

3.1. Male Strategies on Leks

Lekking behavior is the most striking feature of the ruff. Males aggregate in mating arenas ("leks") and display close together [41]. Females visit the lek and are free to mate with any male on the lek. After mating, the female leaves the lek, whereas the male stays and continues to display towards other females. The female incubates the eggs and attends to the young all by herself. Males provide no resources, except the sperm necessary to fertilize the egg, and no parental care [41]. Lekking is most prevalent in birds across the Animal kingdom, even if there is a strong taxonomic bias towards a few bird families [41]. Apart from the ruff, there are only a handful of Scolopacidae species that use this mating system (the Great Snipe (*Gallinago media*) [42], the Buff-breasted Sandpiper (*Calidris subruficollis*) [43], and the Pectoral Sandpiper (*Calidris melanotos*) [44]). However, ruff's lekking behavior is even more particular because the three plumage phenotypes of males described above (darkish, whitish, and naked-nape males) correspond each to different courtship behaviors on the lek [20,21,23,29,30]. We will therefore use from now on the term "phenotype" to designate both the plumage and the courtship behaviors subsuming the three fixed AMMS used by males.

The *independent strategy* is used by darkish males. Some independent males set up small display territories (approximatively 30–60 cm in diameter) within the main arena. Those males are called *resident independents* [19,20]. The main arena (about 10 m in diameter) is located close (300–400 m) to suitable breeding sites [45] and may be used for several dozens of years [20,22]. Within the breeding habitat, ruffs form multiple smallish leks rather than aggregating into larger ones. Thus one finds clusters of leks [20,46]. Display territories are grassy areas that are trampled up to become bare ground at the end of the breeding season [20]. Each display territory has its own independent residence [20]. A peculiarity of displaying territories of residents is that they are not contiguous: there is a space in between, which is not specifically claimed by any of the resident males [20]. The size of this space is variable (100–150 cm) and seems directly dependent on the size of the lek [20,45]. Resident males defend their display territories vigorously against territorially independent neighbors or any independent males moving in between territories. Residents return to their display territory after an absence from the lek; they arrive before dawn, even when completely dark, and stay until dusk, or even spend the night there ([20], overall spending most of their time (*ca.* 90% of daylight) during the 6–8 weeks of the lekking season in their display territories [19]. Residents may leave the lek to forage nearby around midday, though any conspecific interaction on the lek entails immediate back flight [20]. The number of attending residents can vary greatly in space (across arenas) and time (over

the season) but average between three and eight [20]. Many residents males remain faithful to the same lek for up to five breeding seasons [19].

Some, but not all, independent males succeed in establishing a display territory in the arena. Those males that fail to own a display territory are called *marginal independents* because they are located at the margin of the arena, out of the area occupied by the display territories [20]. They spend less time on the lek and are less regular there than their resident counterparts. Marginals are frequently attacked by residents during their visit to the lek but usually lose their fights with territory owners [47]. These floater individuals are usually young, inexperienced, and low-ranking males that may become territorial in subsequent years [19,20,47]. Others are territory prospectors that may establish new territories, usually at the border of the lek. These new residents try to move towards the center of the arena if vacancies occur, which gives rise to fights with prospective neighbors [19]. More rarely, territory prospectors may oust resident males during the course of the breeding season [19,20]. Ousted resident males behave then as marginals and visit the lek even more rarely than other marginal males [20]. Whereas resident males rarely, if ever, visit another arena, they behave there as marginal males [20]. Marginal males are less faithful to the lek from one year to the next [48].

The *satellite strategy* is used by whitish males. Satellites are slightly smaller on average than independents and usually do not engage in aggressive behaviors or set up display territories. Rather, a satellite male will tend to form a coalition with a resident to perform a joint, ritualized display when females visit the lek (see below). Satellite males usually prefer high-ranking residents, and high-ranking residents can be visited by up to four satellites [19]. However, satellites behave opportunistically: they follow females visiting the arena, and in doing so, they can move among territories [20]. Satellites spend less time on the lek than residents [19,20]. Resident males have variable reactions towards satellites: they can attack and try to expel them, or on the contrary, they may allow the resident to come into their display territories and to stay there in their company [20]. The adoption of a given satellite by a resident male seems a progressive process: if the resident male is not tolerant, the satellite will "freeze" in a distinct posture (the "squat" posture) and accept pecks by the resident to possibly acquire a position on the display territory. If the resident male is tolerant, the satellite will adopt distinct postures ("oblique" and "upright" postures) [19]. Different satellites may have different preferences for display territories on the lek [19] and for resident males (one or two by satellite individual [21]), which suggests the establishment of a privileged relationship with the resident owner of the display territory, and, therefore reciprocal recognition made possible by the unique plumage of each individual [23].

Similar to what happens with independents, there are *central* and *peripheral satellite* males. Central satellites visit the display territories and the area in between them more often and for a longer period than marginal satellites. Central satellites are also more easily accepted by residents than peripheral ones. Peripheral satellites spend less time on the lek than central ones [20,48] and seem less faithful to the lek from one year to the next [48].

The *sneaker strategy*, i.e., the parasitism by some males of the attractiveness of others, is used by naked-nape males. Sneaker males have no ornamentation and do not perform display behavior [8,24,34]. They wander stealthily through the lek, where their female-like phenotype inhibits aggressive interactions with other males. Sneaker males rapidly sneak copulations when females solicit matings from ornamented displaying males [8,34]. However, precise and detailed quantitative data on the behaviors of sneaker males are still missing (see [48]).

The frequency of these three male phenotypes is rather constant over time and across space [19,20,22], even if there may be some discrepancies between frequency estimates on leks and within populations due to differences in patterns of lek attendance between resident independents, marginals independents, and satellites [45]. The respective proportions of the three phenotypes within populations are ca. 83%–85% of independents, 14%–16% of satellites, and 1% of sneaker males (e.g., [23,25,34,49]). The relative constancy of these

phenotypes does not support cyclic changes in phenotype proportions within populations as predicted by the rock-paper-scissor model for maintaining alternative male-mating strategies (e.g., [3,50].

3.2. Male-Female Interactions on Leks

Females return from migration and arrive later than males on breeding grounds [20]. They form mixed flocks with marginal and satellite males that forage on meadows and visit lekking areas. While males progressively install on leks, females begin their solitary life in the surroundings [20]. Males on leks have to incite flying flocks or single females to land. Usually, most ornamented males on leks, whatever their phenotype, perform a *reception ceremony* [19,20], in which they flap both wings and display their white underside, which results in flash-like signals showing the location of the lek unambiguously. Females visiting leks land in between territories. Resident males on their territory display up-down movements oriented towards females and then "freeze" in a "*squat*" posture, Figure 1). A chain reaction in the lek may occur from the movements of a resident male that drive all other males to resume their displays, including postures or attacks or residents that are directed towards their neighbors or towards satellites [19,20]. Females observe male displays, walking on the leks and either fly away or solicit copulation by crouching while installed on a display territory [20]. The installation of a female on a display territory is favored when the resident interrupts his squat posture. Van Rhijn [19] showed that this interruption and the subsequent series of short movements are higher when the resident male is accompanied by one or more satellites.

The advantage for a resident of having a satellite is thus the rise of his activity level that incites a female visit on his territory. In that sense, satellite males can be considered "kingmakers" [34]. However, Van Rhijn [19] suggests that the presence of satellites is no longer advantageous to the resident male after the arrival of a female on his territory. Satellites perturb the stimulation of females to crouch, and even when the female crouches, resident males are almost unable to copulate when a satellite is present [19]. Residents use two tactics to avoid having both satellites and females on their territory. Firstly, resident males who frequently copulate are strongly intolerant to the presence of satellites and prevent their presence on their display territory. Secondly, resident males become intolerant to the presence of satellites when a female visits their territory. During the interruption of the squat posture, these males harass their satellites by turning around them, pecking at their wattles, and even actually attacking them. Some satellites manage to resist such harassment and hinder resident copulation, even to the extent of mounting themselves on the crouching female [19,20]. The behavioral interactions between residents and satellites on leks include thus cooperative and competitive elements [50]. Hugie and Lank [50] emphasize that residents do not merely tolerate satellites but sometimes appear to actively recruit them onto their courts. Furthermore, most intolerant behavior appears to be an attempt to control rather than evict satellites. Such behavior suggests that resident males benefit from having a satellite on their court, even though they are reproductive competitors that must be controlled [50]. Another tactic used by satellites is to follow females walking on the lek. The visit of a female to a display territory often results in the resident male owner being attacked by a neighbor. On this occasion, a central satellite present in the immediate vicinity may take advantage of the presence of a receptive female attracted to the resident and mate with her, taking advantage of the resident owner settling accounts with his neighbor [43]. The sneaker mating tactic seems to follow the same scenario [8,19,20,24,34].

The comparison of independent-satellite copulation success on leks shows that males copulating with a female are mostly resident independents (61%–80% in [21], 83–92 in [23], 76% in [51], 82%–95% in the extensive study of Vervoort and Kempenaers [48]). The latter study reveals that among satellites, only central males manage to copulate on leks. Vervoort and Kempenaers mention that the rarity of sneakers has so far precluded a quantitative assessment of the mating success of this phenotype [48], but these authors make an excellent start doing this and report that sneaker males perform 7% of the copulations they observed

on their lek clusters. Another limitation of the comparison of phenotype mating success is the lack of data on possible copulation out of the leks. Satellite and marginal independent males frequently move with females between leks and foraging sites and often display to foraging females. Such highly mixed groups of birds are hard to follow, but observations at suitable foraging sites show that copulations do occur outside leks [22,52].

Widemo [22] mentions that satellites are remarkably quick to mount a female soliciting an independent male. Satellites complete copulation in less than a second, which means that in many cases, females are probably not able to terminate the copulation before its completion. Van Rhijn [19] reports that the mating duration of satellite males is shorter than that of residents, and Küpper et al. [8] makes the same observation for sneakers. However, at this stage, there does not seem to be a formal comparative study of the copulation duration between the three male phenotypes. Nonetheless, the faster copulation of both satellite and sneakers can be related to the larger testes of males belonging to these two categories. Jukema and Piersma [24] mention that sneakers had testes 2.5 times the size of "normal" males in April. Küpper et al. [8] showed that testes of satellites could be even larger than those of sneakers. Loveland et al. [53] examined the difference in testes' weight among phenotypes. Their conclusion from very direct data, albeit from captive birds, is that gonadal masses are similar among phenotypes, which represents a greater relative investment by sneakers and possibly as suggested in [8] by satellites as well. This conclusion differs from that of [8], which was measured with ultrasound and involved controlling for seasonal timing via regression analysis. So there is some difference here. Captivity could play a role, but the data from [53] are much more real. Taken altogether, these results suggest that these differences in testes' weight relative to body size might explain the persistence of the satellite and the sneaker phenotypes via successful sperm competition despite their lower mating success as measured on leks [22,48]. Ruffs have the longest sperm of any shorebird yet measured, which supports an evolutionary history of sperm competition [54,55]. Accordingly, it should be noticed that more than 50% of female ruffs are polyandrous, which is the highest rate of polyandry known in a lekking bird [56]. This observation leads Lank et al. to suggest that female ruffs actively genetically diversify their offspring [56]. A pedigree study actually demonstrates that in direct sperm competition, the male siring the majority of offspring is most often the least genetically similar to the female [57]. Thuman and Griffith [57] speculate that their results provide support for the preferential female cryptic choice of sperm from the least genetically similar male. As we will see, recent genetic and genomic investigations shed new light on what can be the proximate mechanism of this offspring's genetic diversification and the ultimate mechanism of the maintenance of stable genetic polymorphism for alternative reproductive strategies [8,9].

4. Genetics and Genomics of Male Alternative Strategies in Ruffs

Male plumages are thus reliable signals of the fixed behavioral strategies they will use on leks to gain successful copulations. Investigating if there is a genetic determinism in the transmission of these morphological and behavioral phenotypes would help to gain insights into the evolution and maintenance of the alternative mating strategies. Surprisingly, pedigree data of male phenotypes support an autosomal model of genetic inheritance, which contrasts with the sex-linked inheritance reported in other taxa using sex-limited alternative mating strategies [25,57]. As predicted by this autosomal model of genetic inheritance, testosterone-implanted females of known lineages show subsequent male mating behaviors that parallel those of their brothers and half-brothers [58]. Pedigree analyses reveal that the three male phenotypes are controlled by a single Mendelian locus with three alleles. Two alleles, *Faeder* (corresponding to the sneaker strategy of naked-nape males) and *Satellite* (corresponding to the independent strategy of whitish males), are dominant to *Independent* (corresponding to the independent strategy of blackish males), but the precise genetic architecture of phenotype determination remained unclear until the use of genomic methods [8,9,25,57,58].

4.1. Structural Genomics

Single loci controlling the polymorphism of complex phenotypes (known as supergenes) are indeed a target of choice for genomic studies [59]. Two independent studies published in 2016 in *Nature Genetics* managed to unravel the location and the structure of the ruff supergene that directs the three male phenotypes [8,9]. It consists of a block of ca. 90–125 genes located on a single chromosome (*ca.* 20% of chromosome 11) inherited together, mostly without recombination [8,9,34,59]. The structure of the block differs between the three alleles. The *Faeder* allele derives from the *Independent* allele by an inversion of the supergene [8,9] that probably happened ca. 3.8 million years ago [9] (Figure 3). The *Satellite* allele results from an exceptional recombination event between the *Independent* and the *Faeder* alleles that occurred later, ca. 500,000 years ago [9] (Figure 3). Satellite males have indeed intermediate phenotypic characteristics between the independent males, such as a ruff, and the sneaker males, such as a nonagonistic behavior. Satellite males also have their own characteristics, like the whitish color of the ruff [34,59]. Importantly, these two studies report that the inversion disrupts the gene coding for a protein playing an essential role in the formation of centromeres (the *CENPN* gene encoding centromere protein N) [8,9]. Homozygosity for the inversion is lethal ([8]), which means that there is no carrier of two *Satellite/Satellite* alleles, of two *Faeder/Faeder* alleles, but also of the *Faeder/Satellite* alleles. The results of Loveland et al. [53] suggest that the two inversion alleles, incomplete *CENPN* transcripts or proteins would make cell divisions impossible.

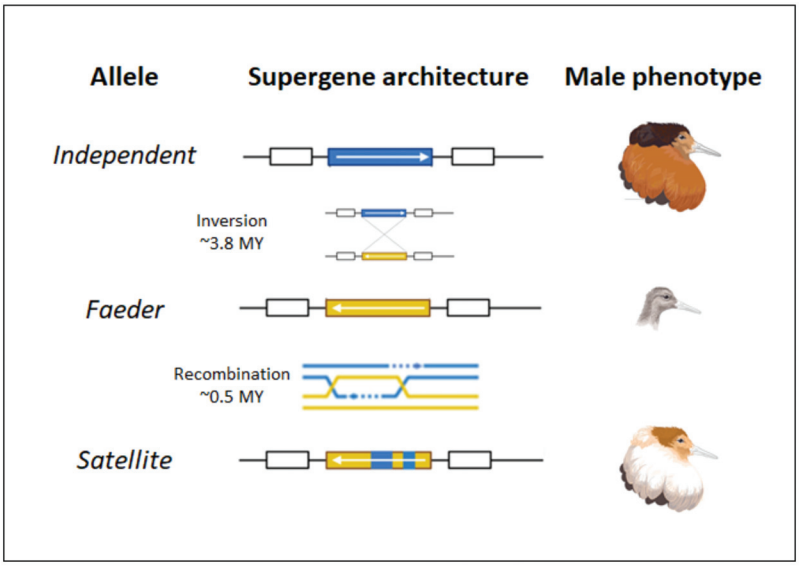

Figure 3. Schematic overview of the evolution of the ruff supergene that regulates the male phenotypes. The inversion of the ruff supergene that occurred ca. 3.8 million years ago on chromosome 11 gave rise to the sneaker phenotype. An exceptional viable recombination event between the *Independent* and *Faeder* allele (*ca.* 500.000 years ago) produced the *Satellite* allele that gives rise to the satellite phenotype. Modified from [53]. Male ruff head profiles from [60], with permission.

4.2. Functional Genomics

The two studies that document the inversion and the recombination of the ruff supergene provide a list of candidate genes located in this genomic region that could explain differences in male phenotypes [8,9]. These candidate genes can be assigned to three broad functional categories: (1) genes with roles in the metabolism of sex hormones, (2) genes controlling for either color polymorphism or feather morphogenesis in birds, and (3) genes

associated with sperm motility and gonadal expression [8,9]. Altogether, the functions allocated to the genes linked to the supergene and their molecular variation resulting from the inversion and recombination events are coherent with the variation of the ruff male phenotypes [8,9]. The analyses of nucleotide sequence divergence of candidate genes provided new insights into the evolution of the three phenotypes. Many gene sequences involved in steroid metabolism located on the inversion are more divergent between independents and the two other phenotypes. However, in the recombined areas of the inversion, gene sequences are more divergent between the sneaker and the two other phenotypes. A gene involved in sperm motility (*GAS8*) was more divergent between independent and the two other phenotypes than between satellite and sneaker males [8]. A candidate gene for variation in pigmentation, *MC1R* (encoding melanocortin 1 receptor), is located within the inverted region. The three male phenotypes have distinct alleles of the single *MC1R* exon [9]. These authors suggest that the *MC1R* allele on *Satellite* supergenes, possibly together with altered metabolism of sex hormones, underlies the white color of ornamental feathers in satellite males [9].

Recent studies go further than gene function assignment by showing changes in the expression of genes located in the inversion [53]. The key point is to investigate if gene expression is altered on genes located on the supergene and on other chromosomes [53]. As previously mentioned, one of the inversion breakpoints is located within the *CENPN* gene. In independent males carrying no inversion, the expression of exons belonging to the *CENPN* transcripts is broadly similar upstream and downstream of the inversion breakpoint, whereas, in both sneaker and satellite males, a *CENPN* exon that is downstream from the inversion breakpoint has at least twofold lower expression than that of an exon upstream from the inversion breakpoint [53]. Loveland et al. [53] detail allelic imbalance in recently recombined areas, as well as a correlation of expression between the inversion gene *SDR42E1* and aromatase that is shared by independents and satellites but completely lost in sneakers. Besides, Loveland et al. [53] show that divergence in gene sequence does not predict gene expression patterns.

The identification of the very molecular processes responsible for male morphological and behavioral differences is a complex task, as exemplified by a recent experimental study [61]. The role of steroid hormones, especially testosterone, in eliciting morphological and behavioral changes among the three phenotypes has been suggested by three lines of evidence: (1) castration of males prevents the molt of the nuptial plumage in independent, and satellite males [62], (2) sub-cutaneous implementation of physiological levels of testosterone to females induces the reversible acquisition of independent- and satellite-like plumage, body mass and behavior [50]; and (3) independent males have a higher physiological concentration of testosterone than satellite or sneaker males ([9,53]). Several genes located on the supergene (namely *HSD17B2*, *SDR42E1*, *CY5B5*) are involved in sex steroid synthesis and metabolism, which suggests a direct effect of supergene alleles on hormone production and regulation [53,61]. In particular, *HSD17B2* encodes the enzyme that converts testosterone back to its precursor, androstenedione. *HSD17B2* is thus a candidate gene to explain the hormonal difference among phenotypes [53]. Sneaker and satellite males have higher concentrations of the circulating precursor androstenedione than independent males [8]. The experimental elevation of circulating androstenedione results in increased aggression in independent males but fails to induce aggressive behavior in satellite males, even if courtship behavior of satellites males intensifies [63]. *HSD17B2* contains several deletions in the *Faeder and Satellite* alleles of the supergene and in their immediate surrounding [8,9]. The experimental stimulation of the pituitary gland that should induce sex steroid synthesis in male gonads fails to provide a durable increase in testosterone concentraion in both sneaker and satellite males [61]. A simple explanation could be higher levels of *HSD17B2* enzymes in these males. However, gonadal *HSD17B2* levels are similar between independent and inversion phenotypes [61,63]. This result suggests thus the existence of impairment in androstenedione to testosterone conversion in males carrying the *Faeder and Satellite* alleles [61]. Based on several similar differences in hormonal produc-

tion and regulation among phenotypes, these authors and others speculate that genomic rearrangements like inversion generate hormonal plasticity by modifying the expression of genes involved in hormone synthesis and receptivity [61,64,65]. Loveland et al. [61] went further by proposing that "over time, sequence evolution combined with selection on certain inversion haplotypes may further canalize hormonal profiles into a restricted range that becomes associated with specific behaviors and morphological traits" [61].

5. Evolution and Maintenance of Male Alternative Strategies in Ruffs

The evolution of fixed alternative male mating strategies in ruffs relies thus on genomic rearrangements that give rise to the sneaker and the satellite phenotypes. The timing of these rearrangements (3.8 MY for the inversion and 0.5 MY for the recombination, [9]) shows that there is a strong asynchrony in their appearance within ruff populations. There are also strong differences in population frequency of males using each of the strategies, at least on leks (independent: 83%–85%, satellite: 14%–16% of satellites and sneaker: 1%, e.g., [23,25,34,49]), which remain stable across space and over time. Game theory and population genetics predict that the spread and the long-term maintenance of these strategies from the event of genomic rearrangement are in agreement with the prediction of an equal fitness of the three phenotypes provided by frequency-dependent selection [2,4–7]. However, a detailed understanding of how frequency-dependent selection works should be based on a thorough analysis of the fitness costs-benefits associated with each phenotype. We summarize here the available information for such an analysis. We will see to what extent there is sufficient explanation for the coexistence of the three alternative fixed male strategies. We then propose research avenues that are needed to refine the diagnosis of frequency-dependent selection.

Our starting point is the lethality of homozygous individuals for inversion, i.e., the *Satellite/Satellite*, *Faeder/Faeder*, and *Faeder/Satellite* genotypes. Such lethality should purge these rare alleles in the long term, a situation that is not observed in the ruff. Some authors, therefore, conclude that carriers of the inversion in one or both sexes must have higher fitness than those individuals that are homozygous for the ancestral *Independent* allele [8,9]. For Lamichhaney et al. [9], those individuals that are heterozygous for the *Satellite* allele should have about 5% higher fitness to maintain an allele frequency of about 5% in compensating for the lethality of the homozygote [9]. Küpper et al. [8] propose that the costs related to the lethality of inversion homozygous carriers and to the alleged low survival of heterozygous individuals at the supergene they observed in experimental crossings might be balanced by a higher reproductive success of sneaker and satellite males [8].

In his review of alternative reproductive strategies, Gross [2] briefly mentions the ruff as a study system for fixed strategies and indicates that "there are presently no fitness measurements that include both mating success and life history differences, nor are there data to test for frequency-dependent selection" [2]. It must be said that more than 25 years later, many important data are still missing. However, some elements might help us to understand how this frequency-dependent selection is likely to occur.

Firstly, the copulation success of ruff males on leks is very unevenly distributed both among phenotypes and among males, which corresponds to the theoretical prediction of Plainstow et al. [7] that conditional male mating strategies are most frequent at intermediate levels of variance in male mating success, whereas fixed strategies evolve mainly when male mating success is highly skewed. As previously mentioned, resident independent males obtain the vast majority of copulations. Besides, there is a high level of mating skew among males of similar phenotype, with some males mating with many females and most mating with none [22,48,66,67]. Should we conclude that this success is responsible for the greater frequency of the independent phenotype in ruff populations? The answer could be negative for practical reasons. Copulation success is monitored on leks for practical facilities, but copulations can occur outside leks on foraging sites. These observations remain still anecdotal, however. Lank and Smith [52], in a rare study following individual

behavior on and off leks, mention that over 90% of the social displays they observed occurred away from leks. However, females very rarely mate with males off leks (D. Lank, pers. communication). So it should be useful to compare the frequencies of the copulations by phenotypes outside leks. It is possible that these might be biased towards satellites or sneakers more than those observed at leks because these birds spend more time with females. However, so do the many marginal independents, which also come and go from leks with females. Besides, more detailed monitoring of sneaker males' reproductive success on leks is also needed.

Secondly and much more important, it remains to be proved that the copulation success of males translates into effective paternity. Indeed, the above-mentioned pedigree analysis of Thuman and Griffith [56] provides evidence of disassortative mating in ruffs. The output of direct sperm competition depends mostly on the genetic dissimilarity between the male and the female, and the least similar male usually sires a larger proportion of the offspring [56]. Female cryptic choice by sperm competition, therefore, could play a role in maintaining the polymorphism of fixed alternative male mating strategies in the ruff. Disassortative mating by post-copulatory sperm competition [56] is supported by indirect evidence. Ruff males have large testes, which is unusual in lekking bird species [68], and both sneaker and satellite males have testes that are even 2,5 larger than those of independents [8]. Intraspecific variation in testis size in birds is positively related to variation in the number of sperm per ejaculate [68], and the chances of fertilization for a given male are proportional to the relative number of sperm simultaneously inseminated in a sperm competition situation [68]. A higher number of sperm per ejaculate may thus be viewed here as a considerable advantage for those phenotypes that copulate infrequently and, unlike independent males, cannot keep other males from mating with a female [68]. It should be remembered here that among the coding sequences located on the ruff supergene, there is a gene involved in sperm motility that is more divergent between independent males and the two other phenotypes than between satellite and sneaker males [8], which might result in a difference in sperm motility between phenotypes. As mentioned earlier, female ruffs hold the record of registered polyandry in lekking bird species, with more than 50% of polyandrous females [55]. Females visit leks about one week before laying their first egg and do not visit leks during incubation 55]. So there are many mating possibilities and time before egg-laying for cryptic mate choice by sperm competition. Finally, individual recognition plays an important role in relationships between independent and satellite males on leks. A model predicts that traits selected to signal individual identity are neither associated with fitness differences nor condition-dependent [69]. Accordingly, female ruffs should not have a visual indicator of the quality of the males with whom they wish to mate, except for the position and the display of residents on the lek. We suggest that cryptic female choice by sperm competition may have evolved because the plumage of the male is not an honest signal of its quality.

In the light of all these elements, we anticipate that every component of the life history of the three ruff phenotypes that can affect disassortative mating by post-copulatory sperm competition is likely to be involved in frequency-dependent selection. Besides, as the supergene is located on an autosomal chromosome, females carry the same alleles as males. As previously mentioned, testosterone implants on females generate the appearance of both independent and satellite male plumages and behaviors [58]. However, little is known about the allelic frequencies of the ruff supergene in females. How females carrying the inversion do differ from females carrying two ancestral alleles in reproductive success is a key question. Size differences similar to that of males also occur among female genotypes [57,70]. This difference in size corresponds to a lower reproductive success of the females carrying the *Faeder* allele: in a captive population with known individual pedigrees, females carrying the *Faeder* allele show a lower laying rate, smaller egg size, and lower offspring survival than females with two ancestral alleles [70]. From these data, the lower reproductive success of females carrying the *Faeder* allele calls further into question the maintenance of these phenotypes in ruff populations. Confirmation by field studies

is essential, however, because captivity is likely to mask compensation mechanisms for these differences in reproductive success, such as, for example, better foraging strategies for females carrying the *Faeder* allele or even an earlier return to wintering areas giving them an advantage in the choice of partners and nesting sites.

How differences in reproductive success or survival among phenotypes might explain the supergene allelic frequencies stability in space and time is investigated using a set of analytical models by Giraldo-Deck et al. [70]. Assuming no differences in survival, no assortative mating, and by using the difference of reproductive success among female phenotypes in a captive population and data on the lethality of inversion homozygous individuals, their model estimated that independent, satellite and sneaker males should fertilize 76%, 22% and 2% of the eggs, respectively [70] to maintain the stability of allelic frequencies. Given the differences in male phenotype frequencies in ruff populations, the *per capita* male fertilization success should therefore be 0.94, 1.20, and 2.94 for independent, satellite, and sneaker males, respectively [70]. Assuming no difference in reproductive success, sneaker males and females should survive 3.1 and 8.2 times longer than their independent counterparts to allow the allelic inversion frequencies to be stable in time [70]. This modeling exercise is a first step in the right direction to test for the existence of a frequency-dependent selection at work to maintain the coexistence of three fixed alternative male mating strategies in male ruffs. However, there are some caveats to the modeling procedure. Firstly, individual fitness depends on both survival and reproductive success, and it should be more informative to combine these two traits into a single model to adequately predict under which conditions allelic frequencies remain stable over time. Secondly, according to Thuman and Griffith [56], rather than assuming no assortative mating, the models should also consider the possibility of disassortative matings between mates on the basis of their genetic similarity. Thirdly, the availability of field data on survival and reproductive success for each of the male and female genotypes should increase the reliability of model predictions. The collection of such data may seem like wishful thinking now, but technological advances in remote data logging should meet this challenge in the near future.

6. Conclusions

Our review of alternative male mating strategies in the ruff shows the immense interest in combining ecological, genetic, and genomic data. Behavioral studies in the field started in the 1960s demonstrate the existence of different, well-defined male mating strategies. Genetic analyses in the 1980s using data issued from careful breeding confirm that they are fixed and show how they are transmitted from one generation to the next. Genomic studies initiated in 2016 provide insights into the molecular mechanisms involved in their origin, maintenance, and evolution. The integration of data produced by these different approaches makes now the ruff an iconic model species for understanding the eco-evolutionary dynamics of phenotypic differences within natural populations. We suggest that unraveling the eco-evolutionary dynamics of fixed AMMS in the ruff should combine three different but converging approaches.

Firstly, the study of the molecular mechanisms that determine each of the strategies should be developed. Investigating how molecular, cellular, and physiological mechanisms could result in cryptic female sexual selection is key not only to understand what is happening in the ruff but also to generalize across species. Another important point is to investigate signals of past or current selection on the loci involved in phenotypic differences among individuals carrying different alleles of the ruff supergene and to what extent it might confirm the hypothesis of Loveland et al. [53] of hormonal profiles canalization into a restricted range that becomes associated with specific behaviors and morphological traits. This is a fascinating point that would solve a question akin to the chicken or the egg causality dilemma. Here the autosomal rearrangement is clearly the starting event of the appearance within populations of mating strategies that differ from that used by independent males homozygous for the ancestral allele. However, remember that there

seems to be cooperation between independent males and satellites on the leks. How such a degree of sophistication in the relationship between these two phenotypes could evolve and be achieved without selection after the chromosomal rearrangement is an open question that the search for selection signals at specific loci could help answer.

Secondly, it would be necessary to understand the variation in the cost-benefits of the life histories among the three phenotypes while providing them with an equal fitness. As previously mentioned, careful studies of individuals in the field are essential to provide accurate estimates of the reproductive survival and success of males and females of each of the phenotypes. These studies should also cover all periods of the life history of individuals, including what happens during migration and wintering. We currently have only fragmentary elements, which often indicate differences between male phenotypes or between sexes.

Thirdly, another interesting research avenue would be to study if and how conditional strategies could be involved in the stabilization of the frequencies of each of the three fixed strategies. We have mentioned that the independent and satellite strategies are fixed, but also that the individuals using each of these strategies have access (independent residents and satellites residents) or not (marginal independents and peripheral satellites) to reproduction. Behavioral monitoring indicates possible shifts among these categories, i.e., independent or satellite residents become marginals or peripherals and vice-versa, both within and between breeding seasons. This means that conditional strategies in space use on leks, and hence in social interaction and access to reproduction, are nested within fixed strategies [66]. Besides, mating off lek exists and is understudied. It might appear that lekking itself would be a conditional strategy [52], but long-term studies of individuals are required to validate this hypothesis. We believe that the ruff is a model of choice to assess the interactive role of fixed and conditional strategies in maintaining the phenotypic variation in AMMS, offering here again the possibility of generalization across species.

Author Contributions: All authors contributed equally to the manuscript. All authors have read and agreed to the published version of the manuscript.

Funding: MB and VMS are members of the LabEx (Laboratory of Excellence) TULIP. This research was thus funded by grant TULIP 10-LABX-0041 from the ANR (Agence National de la Recherche, French National Research Agency).

Institutional Review Board Statement: Not applicable.

Informed Consent Statement: Not applicable.

Data Availability Statement: Not applicable.

Acknowledgments: We acknowledge support from the CHANGE-EVOL team of the Theoretical and Experimental Ecology Station of the CNRS in Moulis (CNRS UAR 2029), and especially from Delphine Legrand and Hervé Philippe. We warmly thank David B. Lank and two anonymous reviewers for their constructive comments and suggestions on the first drafts of the manuscript.

Conflicts of Interest: The authors declare no conflict of interest. The funders had no role in the design of the study; in the collection, analyses, or interpretation of data; in the writing of the manuscript, or in the decision to publish the results.

References

1. Waltz, E.C. Alternative mating tactics and the law of diminishing returns: The satellite threshold model. *Behav. Ecol. Sociobiol.* **1982**, *10*, 75–83. [CrossRef]
2. Gross, M.R. Alternative reproductive strategies and tactics: Diversity within sexes. *Trends Ecol. Evol.* **1996**, *11*, 92–98. [CrossRef]
3. Sinervo, B.; Lively, C.M. The rock-paper-scissors game and the evolution of alternative male strategies. *Nature* **1996**, *380*, 240–243. [CrossRef]
4. Shuster, S.M. Alternative mating strategies. In *Evolutionary Behavioral Ecology*; Fox, C., Westneats, D.F., Eds.; Cambridge University Press: Cambridge, UK, 2010; pp. 434–450.
5. Taborsky, M.; Brockmann, H.J. Alternative reproductive tactics and life history phenotypes. In *Animal Behaviour: Evolution and Mechanisms*; Kappeler, P., Ed.; Springer: Berlin/Heidelberg, Germany, 2010; pp. 537–586.

6. Austad, S.N. Classification of alternative reproductive behaviors and methods for field-testing ESS models. *Am. Zool.* **1984**, *24*, 309–319. [CrossRef]
7. Plaistow, S.J.; Johnstone, R.J.A.; Colegrave, N.; Spencer, M. Evolution of alternative mating tactics: Conditional versus mixed strategies. *Behav. Ecol.* **2004**, *15*, 534–542. [CrossRef]
8. Küpper, C.; Stocks, M.; Risse, J.E.; dos Remedios, N.; Farrell, L.L.; McRae, S.B.; Morgan, T.C.; Karlionova, N.; Pinchuk, P.; Verkuil, Y.I.; et al. A supergene determines highly divergent male reproductive morphs in the ruff. *Nat. Genet.* **2016**, *48*, 79. [CrossRef]
9. Lamichhaney, S.; Fan, G.; Widemo, F.; Gunnarsson, U.; Thalmann, D.S.; Hoeppner, M.P.; Kerje, S.; Gustafson, U.; Shi, C.; Zhang, H.; et al. Structural genomic changes underlie alternative reproductive strategies in the ruff (*Philomachus pugnax*). *Nat. Genet.* **2016**, *48*, 84. [CrossRef]
10. Piersma, T.; van Gils, J.; Wiersma, P. Family Scolopacidae (sandpipers, snipes and phalaropes). In *Handbook of the Birds of the World, Vol. 3. Hoatzin to Auks*; del Hoyo, J., Elliott, A., Sargatal, J., Eds.; Lynx Edicions: Barcelona, Spain, 1996; pp. 444–533.
11. Colwell, M.A. *Shorebirds Ecology, Conservation and Management*; University of California Press: Berkeley, CA, USA; Los Angeles, CA, USA, 2010; 328p.
12. Jehl, J.R., Jr. It's Calidridine. *Wader Study Group Bull.* **2010**, *117*, 195.
13. Van Gils, J.P.; Wiersma, G.M. Kirwan. Ruff (*Calidris pugnax*), version 1.0. In *Birds of the World*; del Hoyo, J., Elliott, A., Sargatal, J., Christie, D.A., de Juana, A., Eds.; Cornell Lab of Ornithology: Ithaca, NY, USA, 2020.
14. Gibson, R.; Baker, A. Multiple gene sequences resolve phylogenetic relationships in the shorebird suborder Scolopaci (Aves: Charadriiformes). *Mol. Phyl. Evol.* **2012**, *64*, 66–72. [CrossRef]
15. Chen, T.-Y.; Zhang, F.; Wang, G.-H.; Zhang, M.-Y.; Liang, T.; Lu, C.-H. Complete mitochondrial genome of the Ruff, *Calidris pugnax* (Aves, Scolopacidae). *Mitochondrial DNA Part B* **2020**, *5*, 1246–1247. [CrossRef]
16. Banks, R.C. Classification and nomenclature of the sandpipers (Aves: Arenariinae). *Zootaxa* **2012**, *3513*, 86–88. [CrossRef]
17. Chesser, R.T.; Banks, R.C.; Barker, F.K.; Cicero, C.; Dunn, J.L.; Kratter, A.W.; Lovette, I.J.; Rasmussen, P.C.; Remsen, J.V., Jr.; Rising, J.D.; et al. Fifty-Fourth Supplement to the American Ornithologists' Union Check-list of North American Birds. *The Auk* **2013**, *130*, 558–571. [CrossRef]
18. Crochet, P.-A.; Barthel, P.H.; Bauer, H.-G.; van den Berg, A.B.; Bezzel, E.; Collinson, J.M.; Dubois, P.J.; Fromholtz, J.; Helbig, A.J.; Jiguet, F.; et al. AERC TAC's Taxonomic Recommendations: 2015 Report. 2015. Available online: http://www.aerc.eu/tac.html (accessed on 21 January 2022).
19. Van Rhijn, J.G. *The Ruff*; T. & A.D. Poyser: London, UK, 1991; 209p.
20. Hogan-Warburg, A.J. Social behavior of the Ruff (*Philomachus pugnax* (L.). *Ardea* **1966**, *54*, 109–229. [CrossRef]
21. Andersen, F. Contributions to the breeding biology of the Ruff (*Philomachus pugnax* (L.)): II. *Dan. Ornithol Tidssk* **1948**, *42*, 125–148.
22. Widemo, F. Alternative reproductive strategies in the ruff, *Philomachus pugnax*: A mixed ESS? *Anim. Behav.* **1998**, *56*, 329–336. [CrossRef]
23. Lank, D.B.; Dale, J. Visual signals for individual identification. The silent "song" of ruffs. *Auk* **2001**, *118*, 759–765.
24. Jukema, J.; Piersma, T. Permanent female mimics in a lekking shorebird. *Biol. Lett.* **2006**, *2*, 161–164. [CrossRef]
25. Lank, D.B.; Smith, C.M.; Hanotte, O.; Burke, T.; Cooke, F. Genetic polymorphism for alternative mating behaviour in lekking male ruff *Philomachus pugnax*. *Nature* **1995**, *378*, 59–62. [CrossRef]
26. Cramp, S.; Simmons, K.E.L. *The Birds of the Western Palearctic*; Volume III. Waders to Gulls; Oxford University Press: Oxford, UK; New York, NY, USA, 1983; 913p.
27. Jehl, J.R.; Murray, B.G. The evolution of normal and reverse sexual size dimorphism in shorebirds and other birds. In *Current Ornithology*; Johnston, R.F., Ed.; Plenum Press: New York, NY, USA, 1986; pp. 1–86.
28. Tinbergen, N. Ruff. *Brit. Birds* **1959**, *52*, 302–306.
29. Van Rhijn, J.G. Behavioural dimorphism in male ruffs, *Philomachus pugnax* (L.). *Behaviour* **1973**, *47*, 153–227. [CrossRef]
30. Van Rhijn, J.G. A scenario for the evolution of social organization in ruffs *Philomachus pugnax* and other Charadriiform species. *Ardea* **1985**, *73*, 25–37.
31. Höglund, J.; Lundberg, A. Plumage color correlates with body size in the ruff (*Philomachus pugnax*). *Auk* **1989**, *106*, 336–338.
32. Zwarts, L.; Bijlsma, R.; van der Kamp, J.; Wymenga, E. *Living on the Edge. Wetlands and Birds in a Changing Sahel*; KNNV Publishing: Zeist, The Netherlands, 2009; 564p.
33. Verkuil, Y.I. The Ephemeral Shorebird. Population History of Ruffs. Ph.D. Thesis, University of Groningen, Groningen, The Netherlands, 2010; 192p.
34. Shorebird, R. *Encyclopedia of Evolutionary Psychological Science*; Shackelford, T.K., Weekes-Shackelford, V.A., Eds.; Springer International Publishing: Cham, Switzerland, 2016; pp. 1–4.
35. Schmaltz, L.E.; Loonstra, A.H.J.; Wymenga, E.; Hobson, K.A.; Piersma, T. Quantifying the non-breeding provenance of staging Ruffs, Philomachus pugnax, using stable isotope analysis of different tissues. *J. Ornithol.* **2018**, *159*, 191–203. [CrossRef]
36. Gill, J.A.; Clark, J.; Clark, N.; Sutherland, W.J. Sex differences in the migration, moult and wintering areas of British-ringed Ruff. *Ringing Migr.* **1995**, *16*, 159–167. [CrossRef]
37. Kokko, H.; Gunnarsson, T.G.; Morrell, L.J.; Gill, J.A. Why do female migratory birds arrive later than males? *J. Anim. Ecol.* **2006**, *75*, 1293–1303. [CrossRef] [PubMed]

38. Schmaltz, L.E.; Juillet, C.; Tinbergen, J.M.; Verkuil, Y.I.; Hooijmeijer, J.C.E.W.; Piersma, T. Apparent annual survival of staging ruffs during a period of population decline: Insights from sex and site-use related differences. *Popul. Ecol.* **2015**, *57*, 613–624. [CrossRef]
39. Andersen, F. Contributions to the breeding biology of the Ruff (*Philomachus pugnax*). *Dan. Ornithol Tidssk* **1944**, *38*, 26–30.
40. Jaatinen, K.; Lehikoinen, A.; Lank, D.B. Female-biased sex ratios and the proportion of cryptic male morphs of migrant juvenile ruffs (*Philomachus pugnax*) in Finland. *Ornis Fenn.* **2010**, *87*, 125–134.
41. Höglund, J.; Alatalo, R.V. *Leks*; Princeton University Press: Princeton, NJ, USA, 1995; 248p.
42. Höglund, J.; Lundberg, A. Sexual selection in a monomorphic lek-breeding bird: Correlates of male mating success in the great snipe *Gallinago media*. *Behav. Ecol. Sociobiol.* **1987**, *21*, 211–216. [CrossRef]
43. Lanctot, R.B.; Scribner, K.T.; Kempenaers, B.; Weatherhead, P.J. Lekking without a paradox in the Buff-Breasted Sandpiper. *Am. Nat.* **1997**, *149*, 1051–1070. [CrossRef]
44. Kempenaers, B.; Valcu, M. Breeding site sampling across the Arctic by individual males of a polygynous shorebird. *Nature* **2017**, *541*, 528–531. [CrossRef] [PubMed]
45. Höglund, J.; Widemo, F.; Sutherland, W.J.; Nordenfors, H. Ruffs, *Philomachus pugnax*, and distribution models: Can leks be regarded as patches? *Oikos* **1998**, *82*, 370–376. [CrossRef]
46. Höglund, J.; Montgomerie, R.; Widemo, F. Costs and consequences of variation in the size of ruff leks. *Behav. Ecol. Sociobiol.* **1993**, *32*, 31–39. [CrossRef]
47. Widemo, F. Competition for females on leks when male competitive abilities differ: Empirical test of a model. *Behav. Ecol.* **1998**, *9*, 427–430. [CrossRef]
48. Vervoort, R.; Kempenaers, B. Variation in lek attendance and copulation success of independent and satellite male ruffs *Calidris pugnax*. *Ardea* **2019**, *107*, 303–320. [CrossRef]
49. Verkuil, Y.I.; Jukema, J.; Gill, J.A.; Karlionova, N.; Melter, J.; Hooijmeijer, J.C.E.W.; Piesma, T. Non-breeding fæder ruffs *Philomachus pugnax* associate according to sex, not morphology. *Bird Study* **2008**, *55*, 241–246. [CrossRef]
50. Hugie, D.M.; Lank, D.B. The resident's dilemma: A female choice model for the evolution of alternative mating strategies in lekking male ruffs (*Philomachus pugnax*). *Behav. Ecol.* **1997**, *8*, 218–225. [CrossRef]
51. Mustonen, J. Influence of Intraspecific Relationships on the Allocation of Temporal Resources in the Lekking Ruff, Calidris pugnax. Master's Thesis, University of Oulu, Oulu, Finland, 2020; 52p.
52. Lank, D.B.; Smith, C.M. Conditional lekking in ruff (*Philomachus pugnax*). *Behav. Ecol. Sociobiol.* **1987**, *20*, 137–145. [CrossRef]
53. Loveland, J.L.; Lank, D.B.; Küpper, C. Gene expression modification by an autosomal inversion associated with three male mating morphs. *Front. Genet.* **2021**, *12*, 641620. [CrossRef]
54. Johnson, D.D.P.; Briskie, J.V. Sperm competition and sperm length in shorebirds. *Condor* **1999**, *101*, 848–854.
55. Lank, D.B.; Smith, C.M.; Hanotte, O.; Ohtonen, A.; Bailey, S.; Burke, T. High frequency of polyandry in a lek mating system. *Behav. Ecol.* **2002**, *13*, 209–215. [CrossRef]
56. Thuman, K.A.; Griffith, S.C. Genetic similarity and the nonrandom distribution of paternity in a genetically highly polyandrous shorebird. *Anim. Behav.* **2005**, *69*, 765–770. [CrossRef]
57. Lank, D.B.; Farrell, L.L.; Burke, T.; Piersma, T.; McRae, S.B. A dominant allele controls development into female mimic male and diminutive female ruffs. *Biol. Lett.* **2013**, *9*, 20130653. [CrossRef] [PubMed]
58. Lank, D.B.; Coupe, M.; Wynne-Edwards, K. Testosterone-induced male traits in female ruffs (*Philomachus pugnax*): Autosomal inheritance and gender differentiation. *Proc. R. Soc. Lond. Ser. B* **1999**, *266*, 2323–2330. [CrossRef]
59. Jiggins, C.D. A flamboyant behavioral polymorphism is controlled by a lethal supergene. *Nat. Gen.* **2016**, *48*, 7–8. [CrossRef] [PubMed]
60. Taylor, S.; Campagna, L. Avian supergenes. *Science* **2016**, *351*, 446–447. [CrossRef]
61. Loveland, J.L.; Giraldo-Deck, L.M.; Lank, D.B.; Goymann, W.; Gahr, M.; Küpper, C. Functional differences in the hypothalamic-pituitary-gonadal axis are associated with alternative reproductive tactics based on an inversion polymorphism. *Horm. Behav.* **2021**, *127*, 104877. [CrossRef]
62. Van Oordt, G.J.; Junge, G.C.A. Die hormonal Wirkung der Gonaden auf Sommer- und Prachtkleid III. Der Einfluss der Kastration auf männliche Kampfläufer (*Philomachus pugnax*). *Wilhelm Roux Arch. Entwicklungsmech. Org.* **1936**, *134*, 112–121. [CrossRef]
63. Morgan, T. Hormonal Regulation of Alternative Reproductive Strategies. Master's Thesis, University of Alaska, Fairbanks, AK, USA, 2010; 76p.
64. Horton, B.M.; Michael, C.M.; Prichard, M.R.; Maney, D.L. Vasoactive intestinal peptide as a mediator of the effects of a supergene on social behaviour. *Proc. R. Soc. B* **2020**, *287*, 20200196. [CrossRef]
65. Merritt, J.R.; Grogan, K.E.; Zinzow-Kramer, W.M.; Sun, D.; Ortlund, E.A.; Yi, S.V.; Maney, D.L. A supergene-linked estrogen receptor drives alternative phenotypes in a polymorphic songbird. *Proc. Natl. Acad. Sci. USA* **2020**, *117*, 2011347117. [CrossRef]
66. Hill, W.L. Correlates of male mating success in the ruff *Philomachus pugnax*, a lekking shorebird. *Behav. Ecol. Sociobiol.* **1991**, *29*, 367–372. [CrossRef]
67. Widemo, F.; Owens, I.P.F. Lek size, male mating skew and the evolution of lekking. *Nature* **1995**, *373*, 148–151. [CrossRef]
68. Möller, A.P. Sperm competition, sperm depletion, paternal care, and relative testis size in birds. *Am. Nat.* **1991**, *137*, 882–906. [CrossRef]

69. Dale, J.; Lank, D.B.; Reeve, H.K. Signaling individual identity versus quality: A model and case studies with ruffs, queleas, and house finches. *Am. Nat.* **2001**, *158*, 75–86. [CrossRef] [PubMed]
70. Giraldo-Deck, L.M.; Loveland, J.L.; Goymann, W.; Tschirren, B.; Burke, T.; Kempenaers, B.; Lank, D.B.; Küpper, C. Intralocus conflicts associated with a supergene. *Nat. Commun.* **2022**, *13*, 1384. [CrossRef] [PubMed]

diversity

MDPI

Article

Identifying Complex DNA Contamination in Pig-Footed Bandicoots Helps to Clarify an Anomalous Ecological Transition

Matthew J. Phillips *, Manuela Cascini and Mélina Celik

School of Biology and Environmental Science, Queensland University of Technology, 2 George Street, Brisbane, QLD 4000, Australia; manuelacascini@gmail.com (M.C.); melina.celik@gmail.com (M.C.)
* Correspondence: m9.phillips@qut.edu.au

Abstract: Our understanding of the biology of the extinct pig-footed bandicoots (*Chaeropus*) has been substantially revised over the past two decades by both molecular and morphological research. Resolving the systematic and temporal contexts of *Chaeropus* evolution has relied heavily on sequencing DNA from century-old specimens. We have used sliding window BLASTs and phylogeny reconstruction, as well as cumulative likelihood and apomorphy distributions, to identify contamination in sequences from both species of pig-footed bandicoot. The sources of non-target DNA that were identified range from other bandicoot species to a bird—emphasizing the importance of sequence authentication for historical museum specimens, as has become standard for ancient DNA studies. Upon excluding the putatively contaminated fragments, *Chaeropus* was resolved as the sister to all other bandicoots (Peramelidae), to the exclusion of bilbies (*Macrotis*). The estimated divergence time between the two *Chaeropus* species also decreases in better agreement with the fossil record. This study provides evolutionary context for testing hypotheses on the ecological transition of pig-footed bandicoots from semi-fossorial omnivores towards cursorial grazers, which in turn may represent the only breach of deeply conserved ecospace partitioning between modern Australo-Papuan marsupial orders.

Keywords: Peramelemorphia; marsupials; phylogeny; ecospace; DNA authentication

Citation: Phillips, M.J.; Cascini, M.; Celik, M. Identifying Complex DNA Contamination in Pig-Footed Bandicoots Helps to Clarify an Anomalous Ecological Transition. *Diversity* **2022**, *14*, 352. https://doi.org/10.3390/d14050352

Academic Editor: Michael Wink

Received: 8 March 2022
Accepted: 27 April 2022
Published: 29 April 2022

1. Introduction

Bandicoots and bilbies (Peramelemorphia) are unusual among living marsupials in possessing a rudimentary chorio-allantoic placenta with umbilicus [1], and a robust patella [2] (also *Notoryctes* and Caenolestidae [3,4]). The two extant peramelemorphian families include the lone surviving bilby (*Macrotis*: Thylacomyidae) and ~22 species of bandicoots (Peramelidae). To varying extents, all are semi-fossorial omnivores, digging and foraging terrestrially for invertebrates, bulbs, fungi and fruit. Pig-footed bandicoots (*Chaeropus*) appear to have evolved into novel ecospace for peramelemorphians. They are proposed to have been cursorial grazers [5,6], characterized by gracile, two-toed forelimbs and higher-crowned teeth. Their relationships and temporal divergence from other peramelemorphians have been contentious. Morphological assessments [7–10] have been tentative and may be compromised by Oligo-Miocene fossil taxa being drawn (apparently artefactually) towards the plesiomorphic or secondarily "primitive" [11] and primarily New Guinean Peroryctinae (among which we include *Peroryctes*, *Echymipera*, *Rhynchomeles* and *Microperoryctes*). Nevertheless, these studies tended to toggle between placing *Chaeropus* as sister to Thylacomyidae (*Macrotis*) or close to Perameliinae (*Isoodon* and *Perameles*), within Peramelidae.

Analyses of DNA sequences have further inflated the uncertainty surrounding *Chaeropus* affinities (see Figure 1). The study by Westerman et al. [12] was the first molecular phylogenetic study to include *Chaeropus*. They employed mitochondrial 12S rRNA sequences and placed *Chaeropus* as the sister to all other extant bandicoots and bilbies.

Meredith et al. [13] published a partial, nuclear *RAG1* sequence from *Chaeropus*, which they favoured grouping with Peramelidae to the exclusion of *Macrotis*. Additional, partial 16S rRNA and *Cytb* mtDNA sequences were published in association with Westerman et al. [14], although only the 16S sequence was included for analysis alongside the available 12S and *RAG1* sequences. That study strengthened support for *Chaeropus* falling outside all other peramelemorphians. May-Collado et al. [15] utilized all sequences available at the time to construct their marsupial supermatrix tree, in which *Chaeropus* was sister to the peroryctine bandicoots. Subsequently, Travouillon and Phillips [16] combined the mtDNA sequences with morphological data (including for fossil taxa) and placed *Chaeropus* as sister to *Macrotis* or outside all extant peramelemorphians (as did Kear et al. [17] and Beck et al. [18]). Travouillon and Phillips [16] cautioned the use of the *Chaeropus RAG1* sequence, because its phylogenetic signal is largely confined to ambiguous sites and, unusually, the inferred substitutions along this lineage are dominated by transversions over transitions. *Cytb* provided the most remarkable result, with Upham et al. [19] nesting the *Chaeropus yirratji* sequence within a different marsupial order (Dasyuromorphia), among the dunnarts (*Sminthopsis*).

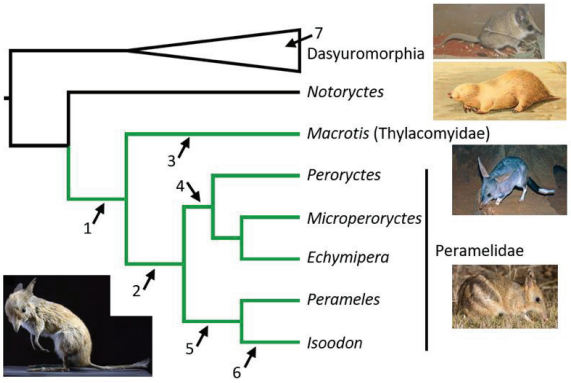

Figure 1. Peramelemorphia phylogeny (in green) for all extant genera, with dasyuomorphian and *Notoryctes* outgroups. The potentially extinct *Rhynchomeles* may fall within *Echymipera* [16]. Placements of *Chaeropus* in molecular and combined molecular-morphological studies; 1. Westerman et al. [12,14], Kear et al. [17], Travouillon and Phillips [16], Beck et al. [18], 2. Meredith et al. [13], Travouillon et al. [20], 3. Travouillon and Phillips [16], 4. May-Collado et al. [15], 5,6. Travouillon et al. [6], 7. Upham et al. [19]. Note that alternative analyses in some studies favoured differing placements. Images: Left; *Chaeropus yirratji* (Muséum national d'histoire naturelle, Paris), Right, from the top; *Sminthopsis crassicaudata* (A Couch), *Notoryctes typhlops* (R Lydekker), *Macrotis lagotis* (B Dupont), *Perameles gunnii* (JJ Harrison).

Travouillon et al. [6] provided the most comprehensive phylogenetic examination yet, for the affinities of *Chaeropus*. They obtained new mtDNA (12S/16S rRNA and *Cytb*) sequences and scored craniodental morphological characters across extant and fossil bandicoots. Both datasets placed *Chaeropus* in a clade with *Perameles* and *Isoodon*; the DNA favoured a closer relationship with *Isoodon* and the morphology tended to favour a closer relationship with *Perameles*. Travouillon et al.'s [6] study is also important for lending molecular and morphological support for splitting *Chaeropus* into two species, *C. ecaudatus* with a semi-arid distribution and *C. yirratji* with a more arid distribution. Several morphological characters supported this taxonomic distinction, including maxillary fenestrae in *C. ecaudatus*, and larger metaconules in *C. yirratji*, lending additional blades for processing plant material. Travouillon et al.'s [6] molecular divergence estimate for these two recently extinct species of 8.6 (95% CI: 3.2–13.4) Mya is surprisingly old in view of the 2.92–2.47 Mya age of the more plesiomorphic stem fossil taxon, *C. baynesi* from the Fisherman's Cliff Local Fauna [21,22].

It is important to examine the authenticity of published *Chaeropus* DNA sequences in light of substantial, apparent phylogenetic incongruence between genes and the potential temporal discrepancy between the divergences of stem and crown taxa. Enormous strides have been made in the authentication of DNA sequences in the fields of ancient DNA and forensics, with protocols ranging from replicating sequences in different labs (e.g., [23]) to profiling patterns of DNA fragment length and damage [24]. These methods tend to be upstream in the experimental and analytical process. Once sequences are published, however, authentication typically requires phylogenetic methods, such as analysis of evolutionary rates [25], similarity measures [26] and topological agreement [27].

To authenticate published *Chaeropus* sequences, we employed phylogenetic authentication methods within a sliding window framework (e.g., [28,29]). This approach allowed smaller non-target DNA fragments to be identified within longer sequences. Phylogenetic analyses of the remaining set of more confidently attributed sequences were undertaken to clarify the affinities and temporal divergence of *Chaeropus*, which in turn lend a novel context for understanding their ecological transition from semi-fossorial omnivores towards cursorial grazers.

2. Materials and Methods

2.1. Sequence Authentication of GenBank DNA Accessions

Nine mtDNA sequences attributed to *Chaeropus* have been published to date. These include Sanger sequenced 12S rRNA (AF131247), 16S rRNA (JF706364) and *Cytb* (JF718363) from *Chaeropus yirratji*, published by Westerman et al. [12,14], and Illumina sequenced 12S rRNA (MK359293, MK359294), 16S rRNA (MK359295, MK359296) and *Cytb* (MK359297, MK359298) from *Chaeropus ecaudatus*, published by Travouillon et al. [6]. The two *C. ecaudatus* sequences for each of these genes are identical. Hence, 12S rRNA, 16S rRNA and *Cytb* are effectively available for two taxonomic units, which are the two species. These published *Chaeropus* mtDNA sequences were initially BLASTed against other mammal sequences in GenBank, using The NCBI's discontinuous megablast [30]. These BLASTs were undertaken for windows of 150 bp that were slid in steps of 75 bp until the end of each sequence. We tried several window widths and 150 bp was an acceptable compromise, as it was long enough to be informative on potential contamination, whilst not being too long to isolate the position of contaminated fragments. Sequences that did not closely match any mammals were subsequently BLASTed without taxonomic constraint.

Sliding window analysis was extended to maximum parsimony (MP) phylogeny reconstruction, with *Chaeropus* allowed to float on a backbone constraint tree of 190 other marsupials, allowing fine-grained assessment of contamination. MP Bootstrap trees were obtained in PAUP 4.0b10 [31] from 250 heuristic search pseudoreplicates for windows of 300 bp that were slid in steps of 100 bp until the end of each sequence. These longer windows were necessary to improve phylogenetic resolution. Subsequent parsimony apomorphy reconstructions in PAUP employed the MP tree for the concatenated mtDNA with the backbone constraint and monophyly enforced for *C. ecaudatus* and *C. yirratji*. In these apomorphy reconstructions, *Chaeropus* was sister to Peramelidae, which is in agreement with the maximum likelihood and Bayesian inference trees (see below).

Alternative phylogenetic placements for *Chaeropus* that were identified in the MP bootstrap sliding window analyses were subsequently compared for cumulative site likelihood along each of the three genes. Site likelihoods were inferred in IQ-TREE [32] for each of the alternative placements, using the partition schemes, substitution modelling, and the Mt_{192} constraint tree that are outlined below.

2.2. Phylogenetic Inference

Two primary data sets were employed to infer the phylogenetic relationships of *Chaeropus*. The first of these, the 3149 bp Mt_{192} dataset, included only the three mtDNA genes that are available for *Chaeropus* (12S and 16S rRNA, *Cytb*). In addition to the two *Chaeropus* species, these data include 190 other taxa that cover all modern marsupial families

and all Australo-Papuan marsupial genera except for two monotypic ringtail possum genera (*Hemibelideus* and *Petropseudes*), for which mtDNA sequences were unavailable.

To enhance the potential for identifying contamination with the short (300 bp) sliding windows, we constructed a constraint tree for the 190 non-*Chaeropus* taxa. The first step was inferring an unconstrained ML tree in IQ-TREE for the Mt_{192} data matrix, without *Chaeropus*. This 12/16S-*Cytb* tree (Figure S1) provides close agreement with the most comprehensively gene-sampled and well-resolved genome-scale marsupial tree [33] and also with more densely taxon-sampled nuclear-mitogenomic supermatrix trees (e.g., [16,34–36]). Minor differences from expected relationships were corrected in a second ML analysis with topological constraints conforming to Duchêne et al. [33] and enforcing monophyly for each of Peroryctinae, *Perameles*, *Pseudantechinus*, and *Sarcophilus-Dasyurus*. This produced the final Mt_{192} constraint tree on which *Chaeropus* placement could float for the sliding window and cumulative site likelihood analyses of the mtDNA (see Figure S2). For the present work, it is important that this constraint tree conforms to the mitochondrial tree, not the marsupial species tree. As such, the swamp wallaby (*Wallabia bicolor*), which has an introgressed mitogenome [37,38], was constrained to be sister to the other large kangaroos and wallabies (*Macropus*, *Osphranter*, *Notamacropus*).

The second dataset ($MtNuc_{26}$) is modified from Travouillon and Phillips [16] by adding the *C. ecaudatus* sequences alongside *C. yirratji*, 16 extant peramelemorphian species, and nine outgroup marsupials. The three mtDNA genes are included and supplemented with five nuclear genes (*BRCA1*, *IRBP*, *RAG1*, *ApoB* and *vWF*) that have been broadly sampled across extant bandicoots. The additional gene sampling for the 9314 bp $MtNuc_{26}$ is intended to clarify relationships and divergences among extant bandicoots and in turn, to improve inference of the relationships and timescale of *Chaeropus* evolution.

The two data matrices (Mt_{192} and $MtNuc_{26}$) were manually aligned in Se-Al 2.0a [39]. Model partitions followed Travouillon and Phillips [16] for $MtNuc_{26}$. The mtDNA was partitioned into rRNA stems, rRNA loops and the three *Cytb* protein-codon positions, while the five nuclear gene sequences were concatenated and partitioned into their three protein-coding positions. Given the emphasis on cumulative site likelihoods across genes with the Mt_{192} data, for those analyses, the rRNA data were instead sequentially partitioned as 12S and 16S rRNA. Substitution models for each partition (Table S1) were assigned in accordance with ModelFinder results obtained with IQ-TREE v1.6.10 [32]. Maximum likelihood analyses were performed in IQ-TREE. Corrected AIC (AICc) favoured estimating the branch lengths independently across partitions (-sp option) for $MtNuc_{26}$ and with branch length multipliers (i.e., proportional across partitions, -spp option) for Mt_{192}.

Bayesian phylogenetic inference of $MtNuc_{26}$ was carried out with MrBayes 3.2.7 [40]. Two independent runs each included three Markov Chain Monte Carlo (MCMC) chains for five million generations. The same partitions and substitution models (or the next most general available in MrBayes) were used as described above for ML. Models were unlinked across all partitions for the substitution matrix, (empirical) state frequencies, proportions of invariant sites and the shape parameter of the rates-across-sites gamma distribution. Branch lengths were unlinked between the nuclear and mtDNA data, but they were proportionally scaled across partitions within each of these genomes. Trees were sampled every 5000 generations, with the first 25% discarded as burn-in. Clade frequencies across the two independent runs reached convergence (clade frequency standard deviations < 0.01) and estimated sample sizes for likelihood, prior and substitution parameter estimates were all above 200 (Tracer v1.7.1 [41]).

Mitochondrial protein 3rd codon sites are particularly susceptible to a combination of phylogenetic signal erosion and nucleotide compositional heterogeneity, which can mislead phylogenetic inference, including for marsupials [42,43]. Hence, we ran the primary maximum likelihood and Bayesian inference phylogenetic analyses ($MtNuc_{26}$) with all sites standard (NT) coded and alternatively, with *Cytb* 3rd codon positions RY-coded (A,G $\rightarrow$ R; C,T $\rightarrow$ Y). Having identified potentially contaminated regions in several of the *Chaeropus* sequences, our primary phylogenetic analyses excluded those regions.

2.3. Molecular Dating

Divergence times were estimated in BEAST v.1.8.1 [44] using the uncorrelated relaxed clock model with lognormally distributed branch rates [45]. The $MtNuc_{26}$ data matrix was partitioned as described for the MrBayes phylogenetic analyses and was run alternatively with standard NT-coding and with RY-coding for the *Cytb* 3rd codon positions. Eight fossil-based prior age distributions were modified from Travouillon and Phillips [16] to provide node calibration (see Table S2).

Each BEAST analysis was run for 40,000,000 MCMC generations, with the chain sampled every 5000th generation, following a burn-in of 4,000,000 generations. This resulted in estimated sample size values >100 (estimated in Tracer v1.71) for $-\ln L$, tree and substitution parameters, and importantly, for all node heights. However, ESS values for the prior and consequently for the posterior were low (between 20–50). Therefore, we ran two additional, independent 15,000,000 generation runs for verification. These gave posterior node heights that were essentially identical to the primary analyses.

3. Results

3.1. Authentication of GenBank DNA Sequences

The Mt_{192} data matrix includes 12S/16S rRNA and *Cytb* accessions for 192 marsupials, including both *Chaeropus ecaudatus* and *C. yirratji*. ML analyses of these data fail to recover *Chaeropus* as monophyletic. *C. ecaudatus* is sister to Peramelidae and *C. yirratji* is sister to all bandicoots and bilbies (Figure S1). To identify potential contamination, a sliding window approach with BLASTs and MP bootstrap was employed to examine phylogenetic signal variation along individual sequence accessions.

As a starting point for authentication, three systematic expectations for pig-footed bandicoots can be confidently derived from morphology (see [6]): *Chaeropus* is (1) unambiguously peramelemorphian, (2) a distinct genus, separate from other lineages, and (3) monophyletic. Thus, in principle, authentic *Chaeropus* sequences should BLAST and phylogenetically group with peramelemorphians, but not with far closer affinity to any particular peramelemorphian species or genus to the exclusion of others (except for congeneric *Chaeropus* accessions). To gauge how these expectations might fare with real data, which involves biases from sources such as base compositional heterogeneity and stochastic artefacts with short windows, we first applied our sliding window BLAST and MP bootstrap approach to the bilby (*Macrotis lagotis*, AJ639871). *Macrotis* is valuable for guiding prior expectations for *Chaeropus* sequences, because both are taxonomically isolated lineages that are most often thought to have diverged along the stem lineage leading to peramelid bandicoots.

Using *Macrotis* as a control shows that authentic peramelemorphian sequences diverging from the peramelid stem lineage will not necessarily BLAST or phylogenetically place closest to other bandicoots. Among the *Macrotis* rRNA and *Cytb* BLAST windows, respectively, 23% and 64% of top hits were outside of Peramelemorphia (Table S3). Similarly, 25% and 67%, respectively, of rRNA and *Cytb* sliding window MP bootstraps favoured *Macrotis* placements outside of Peramelemorphia (Table S4). We found better success in circumscribing expectations for authentic sequences by using two metrics. The first metric we refer to as the "identity ratio", which is the specificity of the top BLAST hit. Where the top BLAST hit (percentage identity) with any taxon is I_A and the next highest BLAST hit to a peramelemorphian is I_B:

$$\text{Identity ratio} = (1 - I_A)/(1 - I_B) \quad (1)$$

Since congeneric taxa will often be highly similar and thus may mask the specificity of potential contamination, if I_A is a peramelemorphian, then I_B will be taken as the highest hit for another peramelemorphian genus.

The second metric we refer to as "anomalous MP bootstrap support", which is the highest bootstrap support for any placement of the focal taxon that is incongruent with

prior expectations. For *Chaeropus*, this will be whichever is higher, the bootstrap support for its exclusion from other peramelemorphians and *Notoryctes* or the bootstrap support for being a shallow-level sister group with or within another genus (peramelemorphian or not). We do not assume that *Chaeropus* is not sister to another bandicoot genus, but it is unlikely to be so close to (or within) another genus that a 300 bp window would provide high (e.g., ≥95% bootstrap support).

Plotting the identity ratio versus anomalous MP bootstrap support for each sliding window (Figure 2) shows a close match between the distributions for *Macrotis* and *C. ecaudatus*. The area bounded by 95% of these *Macrotis* and *C. ecaudatus* sliding window data points sets an expectation for authentic *Chaeropus* sequences. It may even be somewhat conservative, since the *C. ecaudatus* cluster tends to fall within the lower half (17–58%) of anomalous MP bootstrap support values. It is also notable that the MP bootstrap results for the two outlier *Macrotis* BLAST windows still do not reject peramelemorphian affinities at $p = 0.05$, given the anomalous MP bootstrap support is 94% (both of the 150 bp BLAST windows are covered by the same 300 bp MP window in the centre of 16S rRNA). Moreover, that anomalous support is not primarily linked to a particular taxon (the highest genus-level affinity is *Petaurus*, at 7%). Instead, the anomaly relates to these two overlapping BLAST windows being an apomorphic sequence in peramelids, leaving the *Macrotis* sequence plesiomorphically similar to numerous non-peramelemorphians. These considerations lessen concern for the *Macrotis* windows being non-target DNA.

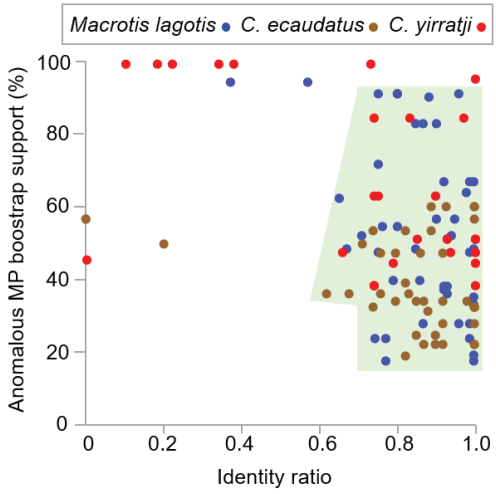

Figure 2. Scatterplot of the identity ratio from 150 bp BLAST windows versus highest anomalous MP bootstrap support among 300 bp MP windows that fully include that BLAST window, for *Macrotis lagotis* (blue), *C. ecaudatus* (brown) and *C. yirratji* (red). All BLAST windows are included from 12S/16S rRNA and *Cytb*. In the MP bootstrap analyses, the *Cytb* 3rd codon positions were RY coded. The shaded area covers 95% of *Macrotis* and 95% of *C. ecaudatus* windows. Identity ratio is a metric for the specificity of the identity to the top hit (I_A) relative to the identity for the next most similar peramelemorphian genus (I_B). Identity ratio = $(1 - I_A)/(1 - I_B)$. Anomalous MP bootstrap support is whichever is the higher discrepancy with prior expectations, the support for the focal taxon either being excluded from other peramelemorphians and *Notoryctes* or being a shallow-level sister group with or within another genus. Scores on these metrics for each window are provided in Tables S3 and S4.

Thus, by considering *Macrotis* as a control, we are able to preliminarily define *Chaeropus* sliding window sequences as either likely authentic, likely non-target DNA or potentially non-target DNA. Likely non-target DNA includes windows corresponding to data points

in Figure 2 that fall outside the shaded 95% distribution for BLAST identity ratio versus highest anomalous MP support and have an identity ratio < 0.30 (lowest for *Macrotis* is 0.37) or anomalous MP bootstrap $\geq$ 95%. Potential non-target DNA includes windows for which two or more of the following conditions are met (see Table S3): (1) the other *Chaeropus* species is not the top hit, (2) the identity ratio is below 0.7, (3) the top hit is outside of Peramelemorphia, (4) both windows immediately before and after are likely or potential non-target DNA or (5) a highly unusual sequence is included that does not closely match any accession.

3.1.1. Chaeropus Ecaudatus Sequence Authenticity

The *Chaeropus ecaudatus* 12S rRNA sequences (MK359293, MK359294) sequences match our BLAST and MP bootstrap authenticity expectations for all windows (Tables S3 and S4) and fall within the shaded 95% distribution for BLAST identity ratio versus highest anomalous MP support (Figure 2). Top hits for each of the (150 bp) BLAST windows were bandicoots, closely followed by other bandicoots, such that all identity ratios were high (0.74–1.00). The corresponding 300 bp window MP bootstraps all favoured *Chaeropus* grouping with or within Peramelemorphia, without strong affinity to any particular genus or species.

All of the 300 bp sliding window MP bootstrap analyses for *C. ecaudatus* 16S rRNA (MK359295, MK359296) favour peramelemorphian affinities, without strong support for placements with any particular taxon (Table S4). However, the finer-scaled BLAST (Table S3) and log likelihood (ln*L*, Figure 3D) accumulation results identify two sections that deserve further consideration. There is rapid fluctuation in ln*L* advantage across the first 100 bp for placements within Peramelidae (Figure 3D). Moreover, much of this segment is difficult to align, it shows no closer similarity to marsupials than to placentals (especially otariids) and it is not clear how the first two 16S stem-loop structures from this 5′ end would form. The alignment and authenticity of the MK359295/MK359296 16S sequences are more assured from base position 99, until a stretch of 49 ambiguous "N" nucleotides that is closely followed by a 392 bp fragment (pos 710–1101) that is almost identical to *Isoodon macrourus* (391/392–only a single transition apart). Next most similar is *Isoodon obesulus* (382/392). Such extensive convergence upon *Isoodon* and *I. macrourus,* in particular, is implausible, especially as the variation derives largely from the less functionally constrained 16S rRNA "loop" sites. These windows in the middle of 16S rRNA are the *C. ecaudatus* outliers in Figure 2, with identity ratios of 0.00 and 0.20. Comparison with the Westerman et al. [14] 16S *C. yirratji* sequence supports the authenticity of MK359295/MK359296 from position 1104 onwards.

Examining the authenticity of the *Cytb* sequences is complex, because their rapid evolution facilitates biases (such as nucleotide compositional biases) that can mask true (inherited) phylogenetic similarity. This may help to explain why most *C. ecaudatus Cytb* (MK359297, MK359298) windows BLAST outside of Peramelemorphia (Table S3), similar to *Macrotis*. This hypothesis is consistent with the average anomalous BP bootstrap support across the *Cytb* windows being reduced from 55% to 35% by RY coding the *Cytb* 3rd codon positions. All of the *C. ecaudatus Cytb* windows fall within the shaded 95% distribution for BLAST identity ratio versus highest anomalous MP support (Figure 2) and we find no basis for rejecting their authenticity.

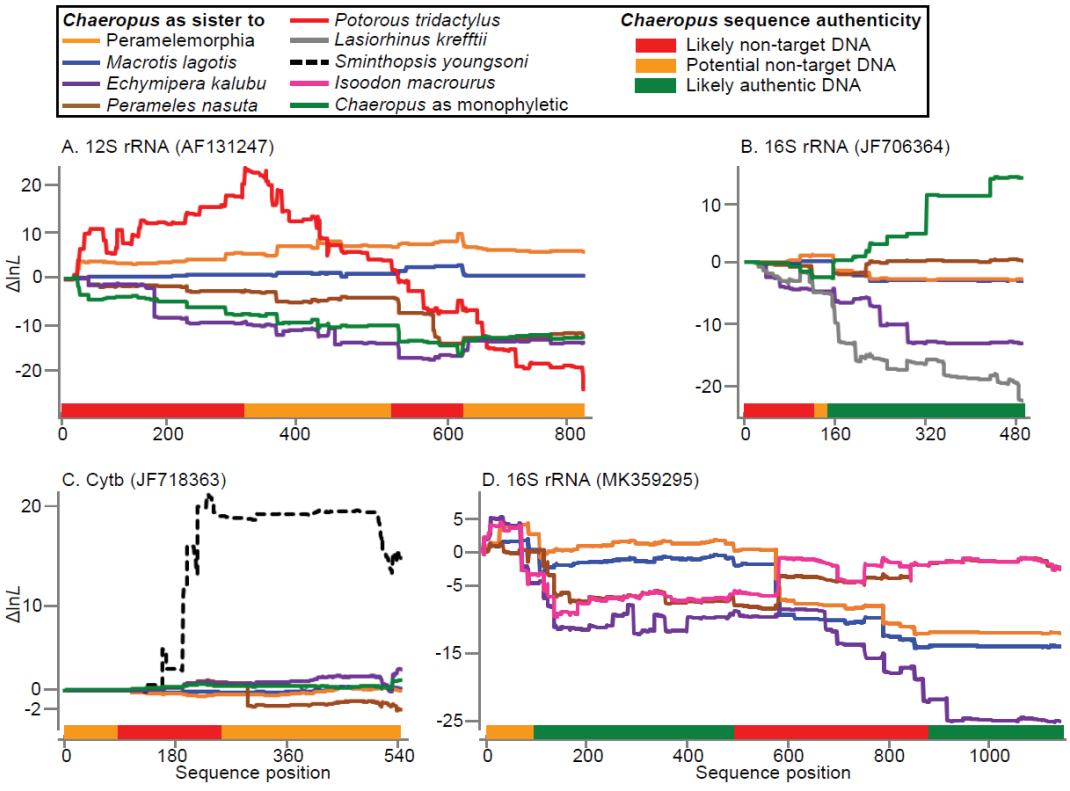

Figure 3. Cumulative ln*L* differences along gene sequences, for alternative sister group relationships for the published *Chaeropus yirratji* sequences, (**A**) 12S rRNA (AF131247), (**B**) 16S rRNA (JF706364), (**C**) *Cytb* (JF718363) and the published *Chaeropus ecaudatus* sequence, (**D**) 16S rRNA (MK359295 and MK359296 are identical). In each case, the null (zero Δln*L*) is for the focal *Chaeropus* sequence as sister to Peramelidae. Inferences of the authenticity of these sequences are indicated above the x-axes, as likely non-target DNA (red), potential non-target DNA (orange) or likely authentic DNA (green), based primarily on sliding window BLAST and MP bootstrap with densely sampled marsupial alignments (see Tables S3 and S4).

3.1.2. *Chaeropus yirratji* Sequence Authenticity

Chaeropus yirratji 12S rRNA (AF131247) appears to be a chimera of several marsupial sequences, including a potoroo (*Potorous tridactylus*), a bilby (*Macrotis lagotis*) and other bandicoots (potentially including *Chaeropus*), and an unidentified fragment. BLAST and MP bootstrap (Tables S3 and S4) show the *Potorous* contamination covers the first third of the sequence and one of the middle windows matches 100% to a bilby sequence. Each of those windows are outliers in Figure 2, either with an identity ratio of 0.0 or anomalous MP bootstrap support of 100%. Cumulative likelihood variation traces ln*L* support along the gene sequences for alternative *Chaeropus* placements on the 192-taxon tree (relative to ln*L* for the *Chaeropus* placement as sister to Peramelidae that was favoured on the full concatenated dataset). The clearest anomaly for 12S rRNA is support for *Potorous* affinities over the first third of the sequence (Figure 3A, red line). Authentic *C. yirratji* sequence is not rejected for the last third of the 12S rRNA accession, but that segment is substantially more similar to other bandicoots than to *C. ecaudatus*. This in itself does not identify which of these *Chaeropus* sequences is artefactual. However, there is otherwise no hint of non-target DNA in the *C. ecaudatus* 12S rRNA sequences (MK359293/359294). In contrast, those final

two sliding window BLASTs for *C. yirratji* 12S (AF131247) include a 31 bp segment that does not closely match any GenBank sequence. Therefore, we suggest that the cautious approach of excluding all of AF131247 is currently expedient.

16S rRNA (JF706364) is the only published sequence for *C. yirratji* with all windows falling within the shaded 95% distribution for BLAST identity ratio versus highest anomalous MP support (Figure 2). It also exhibits the expected close similarity and sister grouping with *C. ecaudatus*, at least for the last two thirds of the sequence (Figure 3B, green line, also Table S3). JF706364 matches 98.8% to *C. ecaudatus* (MK359295/359296) from base 174 onwards, and the next most similar sequences are other bandicoots with several percent lower identity (e.g., *Isoodon obesulus*, 94.9%). This congeneric similarity (and monophyly) shows what could also have been expected from the 12S rRNA and *Cytb* sequences had the accessions from both *Chaeropus* species been authentic.

The first third of the *C. yirratji* 16S rRNA (JF706364) sequence is anomalous. The first 150 bp sliding window BLAST most closely matches the wombat, *Lasiorhinus krefftii* from another order (Diprotodontia) at 98.0% identity. This alone is not necessarily cause for concern, because there is only a small uptick in cumulative ln*L* for this wombat affinity (Figure 3B, grey line) and BLAST matches to bandicoots are not far behind (e.g., *Perameles nasuta* at 97.3%). However, two results raise concern. These are (1) the similarity to wombats is specific to *Lasiorhinus krefftii* (98.0%) but not its close relative *Vombatus ursinus* (92.7% identity) and (2) the first third of 16S is dominated by autapomorphies along the lineage leading to the JF706364 sequence (Figure S3). Alternative explanations could include miscalled bases on an unclear electrophoretogram or that this fragment of sequence has rapidly diverged in *Vombatus* and is contaminated by another bandicoot in the other *Chaeropus* (*ecaudatus*) sequence.

We can only be confident in the JF706364 *C. yirratji* sequence from position 174 onwards and recommend excluding at least the first 130 bp as potentially non-target DNA until confirmed authentic. The intervening sequence (130–174 bp) is identical to *C. ecaudatus*. Therefore, clarifying the authenticity of those 16S sites in the *C. ecaudatus* sequence (see above) could lend veracity for *C. yirratji*. Unfortunately, this segment of 16S does not stem-pair with sites in the remainder of the 16S sequence, precluding another avenue for verification.

The *C. yirratji Cytb* sequence (JF718363) does not appear to be authentic. Most windows fall outside the shaded 95% distribution for BLAST identity ratio versus highest anomalous MP support (Figure 2). Moreover, no similarity (Table S3) or likelihood support for grouping with *C. ecaudatus* emerges along this partial *Cytb* sequence (Figure 3C, green line). All MP bootstrap windows favour placements outside Peramelemorphia (Table S4). The first two of those have 100% and 95% bootstrap support for JF718363 grouping with two dunnarts (*Sminthopsis youngsoni* and *S. ooldea*) within Dasyuromorphia. This coincides with a strong ln*L* signal (Figure 3C, dashed line). Relevant BLAST windows (76–225 bp and 151–300 bp) provide <80% identity to the other bandicoots, but have 96–98% identity to the crested bellbird (*Oreoica gutturalis*) and the above-noted dunnarts. The last two JF718363 BLAST windows provide curious results. They BLAST closest to another dasyurid genus, *Pseudantechinus* (though only ~90%). For the MP bootstrap window that covers those BLASTs, JF718363 falls outside of all other peramelemorphians and marsupial moles, and ML support plateaus then falls for the dasyurid (*Sminthopsis*) in Figure 3C. Taken together, these results for the last two JF718363 BLAST windows might be explained by a chimera of dasyurid and bandicoot sequences.

3.2. Phylogenetic Affinities of Chaeropus

To reconstruct the phylogenetic placement of *Chaeropus*, we excluded gene sequence fragments that could not be authenticated and that we considered to be contaminated DNA (Figure 3, *x*-axis: red) or suspected of being non-target DNA (Figure 3, *x*-axis: orange). This leaves *C. ecaudatus* represented for *Cytb*, 12S and the majority of 16S rRNA, whereas *C. yirratji* is represented only by a partial 16S rRNA sequence. Phylogenetic analyses

of the resulting 26-taxon MtNuc$_{26}$ data provide strong support for *Chaeropus* as sister to Peramelidae, to the exclusion of *Macrotis* (Figure 4A). Results are similar regardless of whether the rapidly evolving *Cytb* 3rd codon positions were RY-coded, with 1.00 BPP and 87–98% ML bootstrap support for both Peramelidae and the *Chaeropus*-Peramelidae grouping. Alternative placements for *Chaeropus* (including those in Figure 1) are strongly rejected by ML hypothesis testing (Table S5), except being sister to all extant peramelemorphians (p = 0.199). The primarily New Guinean bandicoots (*Peroryctes*, *Echymipera*, *Microperoryctes*) and the primarily Australian bandicoots (*Perameles*, *Isoodon*) were both strongly supported as monophyletic.

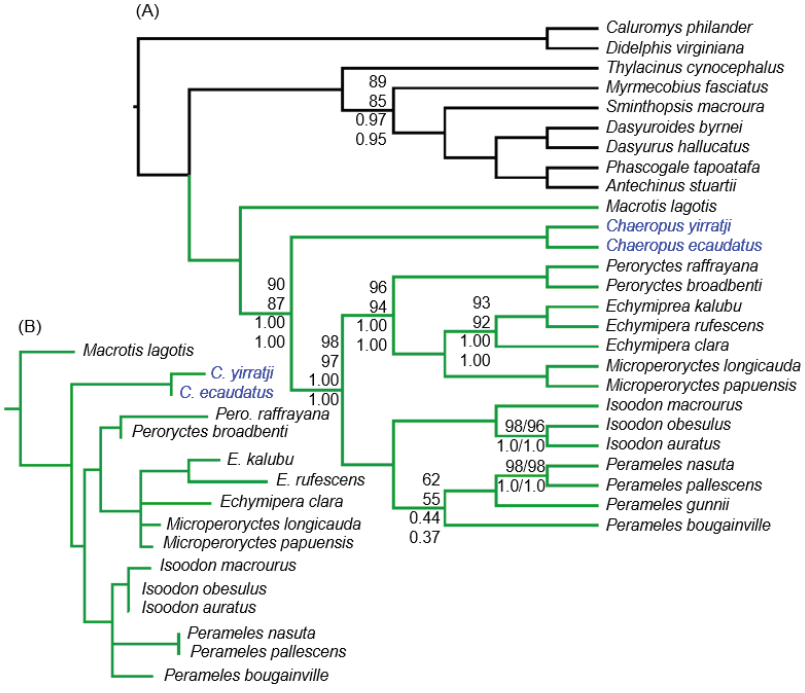

Figure 4. (**A**) MtNuc$_{26}$ maximum likelihood phylogeny focusing on Peramelemorphia (bandicoots and bilby, green branches) and without phylogenetic constraints. Clade support values at nodes, from top to bottom are ML-BP (NT data), ML-BP (RY-coded *Cytb* 3rd positions), BI-BPP (NT data), BI-BPP (RY-coded *Cytb* 3rd positions). Support values are not shown for clades when 100% for each measure. BP is ultrafast bootstrap in IQ-TRRE (-bb 10,000). BPP is Bayesian posterior probability in MrBayes. (**B**) IQ-TREE ML phylogram for the 361 bp segment of 16S rRNA that was deemed to be authentic (non-contaminated) for both *Chaeropus* species. The topology was constrained in agreement with the MtNuc$_{26}$ tree to ensure the appropriate phylogenetic context for inferring branch lengths with the truncated sequences.

Although the MtNuc$_{26}$ phylogenies help to clarify the genus-level placement of *Chaeropus*, the exclusion of putative non-target DNA and sites of uncertain homology in the alignment left the two pig-footed bandicoot species sharing only a 361 bp segment of 16S rRNA. To avoid branch length estimation biases associated with missing and non-overlapping sequences, we also inferred branch lengths on this short segment of the alignment. This resulted in the phylogeny shown in Figure 4B when constraining the topology to the MtNuc$_{26}$ tree (Figure 4A). *C. ecaudatus* has essentially zero branch-length for this 361 bp segment (Figure 4B).

3.3. Timescale of Chaeropus Evolution

The BEAST timetrees for the $MtNuc_{26}$ data with *Cytb* 3rd codon positions RY-coded (Figure 5) or treated as standard nucleotides (see Figure S4) have near-identical divergence times right across the marsupial tree. We will focus here on the RY-coded timetree. The median (and 95% HPD) estimate for *Chaeropus* diverging from their peramelid sister group is 16.8 (10.9–23.6) Mya. Peramelemorphia diverged from Dasyuromorphia at 55.9 (48.3–66.5) Mya, with the crown divergence of Peramelemorphia (bandicoots versus bilbies) at 22.6 (17.6–29.1) Mya. The two *Chaeropus* species were estimated to have diverged at 2.4 (0.3–6.1) Mya. That median estimate is roughly in the middle of the range of estimated divergences for bandicoot species pairs (Figure 5), and is most similar to the divergence of *Echymipera rufescens* versus *E. kalubu* at 2.38 (1.5–3.7) Mya. However, the divergence estimate between *C. yirratji* and *C. ecaudatus* is less precise, with the upper bound more than 20-fold older than the lower bound.

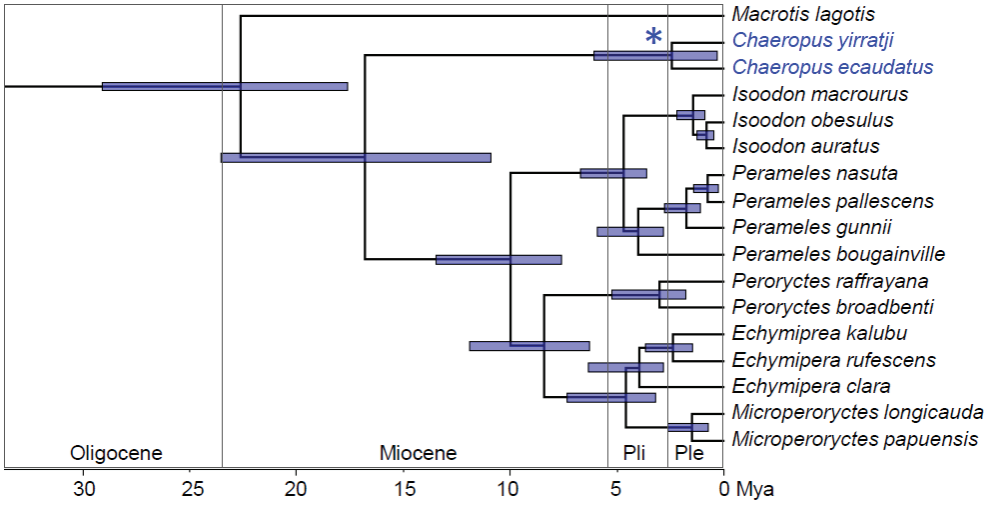

Figure 5. Molecular dated evolutionary timescale for peramelemorphian evolution, inferred in BEAST on the $MtNuc_{26}$ data matrix with *Cytb* 3rd codon positions RY coded. Blue bars show 95% highest posterior density for node ages. The asterisk indicates the approximate age of *Chaeropus baynesi* from the Fisherman's Cliff Local Fauna. Outgroup taxa and divergence times are provided in the Supplementary Information. Abbreviations: Pli; Pliocene, Ple; Pleistocene.

4. Discussion

4.1. MtDNA Authentication

Molecular systematics and evolutionary biology depend upon DNA sequences being authentic. Distinguishing target and non-target DNA with high probability is achievable by replicating sequences in different labs [23]. This is effectively achieved for *Chaeropus* only for a fragment of 16S rRNA (Figure 3B, green line), albeit with different species replicated. The absence of such replication for the other published *Chaeropus* sequences places the burden of evidence on phylogenetic methods. Here, we emphasize a cautious approach for accepting sequence authenticity, because contamination often does not manifest as 100% similarity to non-target taxa. This may be because GenBank does not cover the full diversity of potential non-target sequences or because contamination may be incorporated as a heterogenous mix of target and non-target DNA.

We employed a multi-pronged approach to identify non-target DNA fragments among published *Chaeropus* sequences. Initial sliding window BLASTs [46] provided fine precision, but this trades off against accuracy, due to being a similarity (phenetic) metric and using

narrow (150 bp) windows. BLAST similarity comparisons can be confounded by compositional bias and autapomorphy. We complemented the BLASTs with wider window (300 bp) MP bootstrap analyses on the densely sampled (Mt_{192}) backbone tree and by examining apomorphy distributions. Cumulative site likelihood (Figure 3) provided clear visualization of stark contamination examples, but ln*L* volatility associated with different substitution categories may obscure shorter or less evolutionarily distant non-target sequences.

Substitution rate variation between genes is an obstacle to circumscribing objective rules for identifying non-target DNA. For example, apparently authentic *Chaeropus* sequences among the slower evolving ribosomal RNA genes fit the expectation of sliding window MP affinities with Peramelemorphia, but faster evolving *Cytb* sequences often do not (Table S4). One solution was to run the sliding window MP bootstrap analyses for *Cytb* with the 3rd codon positions RY coded (Table S4), which removes the rapidly saturating transition signal, and has been shown to enhance deeper-level phylogenetic inference, including for marsupials [47]. The primary key to controlling for variation in substitution patterns within and between genes was to calibrate our BLAST and MP bootstrap expectations for *Chaeropus* by reference to a similarly evolutionarily distinct peramelephorphian, the bilby (*Macrotis lagotis*), which has well-accepted modern sequences, (Tables S3 and S4).

RY coding *Cytb* 3rd codon positions and using *Macrotis* as a control provided a basis for deriving metrics that capture null expectations for *Chaeropus* sliding window BLAST and MP bootstrap results. Plotting BLAST identity ratio and highest anomalous MP bootstrap support metrics for each sliding window provided an expected distribution in which 95% of *Macrotis* and *C. ecaudatus* sliding windows clustered (Figure 2). With the exception of two outlier *Macrotis* windows that were explained by symplesiomorphy, other, more extreme sliding window outliers among *C. ecaudatus* and *C. yirratji* are best explained as non-target DNA.

Several of the published *C. yirratji* sequences include non-target DNA. 12S rRNA (AF131247) includes *Potorous* and *Macrotis* sequence (Figure 3A, Tables S3 and S4). Conversely, 16S rRNA (JF706364) was the first largely authentic DNA sequence published for *Chaeropus* (Westerman et al. [14]). This was a substantial achievement at that time. The specimen is relatively young (1901 CE); however, several leading ancient DNA labs failed to retrieve authentic DNA sequences from similarly preserved *Chaeropus* specimens, and Meredith et al. [13] noted the difficulty of amplifying *Chaeropus* DNA. The *C. ecaudatus* sequences are inferred to be mostly authentic, except for 16S rRNA (MK359295, MK359296), which includes a 392 bp *Isoodon macrourus* fragment (Table S3). This is surprising because these replicate sequences are identical (albeit from the same laboratory). However, this putative contamination may have originated in silico, since Travouillon et al. [6] used *I. macrourus* as the bioinformatic reference sequence.

The *C. yirratji Cytb* (JF718363) sequence provides a complex example of contamination. The sequence BLASTs with the marsupial order Dasyuromorphia, closest to two dunnarts (*Sminthopsis*). Closer inspection revealed that the sequence is a chimera of marsupial DNA and a fragment of avian DNA that also contaminates the two dunnart sequences. That avian fragment in JF718363 and in both dunnarts matches (129/130 bp) to several crested bellbird (*Oreoica gutturalis*) sequences. This avian contamination explains both *Chaeropus* nesting within *Sminthopsis*, based on *Cytb* in Upham et al. [19], and the anomalous *Sminthopsis Cytb* phylogeny noted by Krajewski et al. [48]. Recognizing non-authentic DNA on GenBank remains a vexed issue. However, we recently proposed a mechanism for updating taxonomic attributions [49] that gives original contributors the first option for revision, and may also assist with flagging or correcting non-authentic sequences.

4.2. Peramelemorphian Systematics

Non-target DNA incorporated in published *Chaeropus* sequences has further blurred the affinities of pig-footed bandicoots and inflated estimates of the temporal divergence between *C. ecaudatus* and *C. yirratji*. Phylogenetic analysis of the combined mitochondrial and nuclear dataset ($MtNuc_{26}$) after excluding the likely and suspected non-target DNA

fragments brings *C. ecaudatus* and *C. yirratji* into closely divergent monophyly. In turn, *Chaeropus* is supported as sister to Peramelidae (Figure 4A). The alternative affinities of *Chaeropus* found in previous studies (Figure 1) will have been substantially influenced by the inclusion of non-target DNA fragments. All of the *Chaeropus* DNA used here is mitochondrial. Good agreement between mtDNA and nuclear DNA for similar magnitudes of statistical and branch length support in other marsupial studies lends confidence to the present result being robust to incomplete lineage sorting (see [33,34,42,50]). However, deep mitochondrial introgression needs to be ruled out. Although rare, the swamp wallaby (*Wallabia bicolor*) provides a cautionary example, with its mtDNA captured from a now extinct, deeper diverging kangaroo [37,38]. Hence, nuclear data will be required to confirm the placement of *Chaeropus* as sister to Peramelidae.

The sister relationship of *Chaeropus* to extant peramelids, and inferred temporal divergence between these two clades of 16.8 (10.9–23.6) Mya (Figure 5) are equivocal for assigning pig-footed bandicoots to their own family. Several other marsupial family crown ages may be older, such as Dasyuridae, Acrobatidae and Burramyidae (see [33,34]). However, *Chaeropus* morphology alludes to functional and ecological distinctiveness that sets them apart from both extant peramelemorphian families, Peramelidae and Thylacomyidae, and in our view justifies Groves [51] placing *Chaeropus* in its own family, Chaeropodidae.

Deeper in the tree, the estimate for the crown Peramelemorphia (bandicoots versus bilby) divergence of 22.6 (17.6–29.1) Mya accords with the earliest relatively well-supported crown fossil taxon being the ~14 Mya thylacomyid, *Liyamayi dayi* [52]. Unfortunately, the absence of tight calibration limits molecular dating precision. The 95% credible interval for the peramelemorphian crown divergence is also consistent with the more tentative assignment of the 24.9 Mya *Bulbadon warburtonae* to Thylacomyidae [20]. However, Travouillon et al.'s [20] matrix-based phylogenetic analysis placed *B. warburtonae* in a polytomy that leaves its crown affinity unresolved. Further investigation into the affinities of *B. warburtonae* and other Late Oligocene peramelemorphians, ideally with more complete material, will be important for clarifying basal bandicoot (and bilby) relationships and for more precisely calibrating molecular or total evidence dating.

4.3. Chaeropus Evolution

Only one fossil chaeropodid has been published. The 2.92–2.47 Mya *Chaeropus baynesi* from the Fisherman's Cliff Local Fauna is known from several molars that showcase the transition towards increased herbivory, but not yet grazing [21]. Although dental microwear analysis has not yet been undertaken, Travouillon [21] concluded from gross molar morphology that grazing specialization in *Chaeropus* was more recent, and was probably a response to Pleistocene drying. Travouillon et al.'s [6] subsequent molecular dates appear out of step with this scenario, instead implying far earlier grazing, with the more specialized *C. ecaudatus* and *C. yirratji* diverging at 8.6 (95% CI: 3.2–13.4) Mya. This temporal anomaly is resolved in the present study by excluding the non-target DNA, whereby the divergence between the modern species falls to 2.4 (0.3–6.1) Mya (Figure 5). Our date may even be overestimated if branch length asymmetry on the tree inferred from the 361 bp fragment that is shared by both *Chaeropus* species hints at the *C. yirratji* Sanger sequence retaining some errors compared to the zero-branch length *C. ecaudatus* (Figure 4B). However, such speculation is premature, since the same tree shows similar branch length asymmetry among other bandicoot species pairs. Nevertheless, our more recent divergence timing for *Chaeropus* is consistent with grassland expansion [53] and increased grazing adaptation among kangaroos [32,54] from 6 Mya or younger. The shallow divergence between *C. ecaudatus* and *C. yirratji* (Figure 5) does lessen the molecular case for their species-level distinctiveness, but is not inconsistent with Travouillon et al.'s [6] taxonomy. Indeed, with so little DNA contributing to *C. yirratji*, it is prudent to prioritise the morphological arguments for recognising both *C. ecaudatus* and *C. yirratji*.

All crown bandicoots and bilbies had ancestors that were semi-fossorial omnivores [34,55] and it is from this ancestry that *Chaeropus* evolved an array of appendicular, dental and

digestive system traits indicative of cursorial and grazing behaviours (see [6]). The extent to which *Chaeropus* retained an insectivorous component to its diet is clouded by conflicting evidence. Examination of several faecal pellets found only grass [5,56]. Conversely, some Aboriginal observations attributed ant and termite feeding to *Chaeropus* [57], while theoretical considerations place their ~200–500 g mass below size thresholds for exclusive grazing [58,59]. The pointed snout is also suggestive of insectivory, even soil/sand probing as in other bandicoots. A relevant question here, is whether this reflects the habits of pig-footed bandicoots or evolutionary inertia— is this a ghost of their recent ecological past?

Plio-Pleistocene evolution of predominantly grazing bandicoots would be remarkable as a possible incursion across foraging ecospaces that map to marsupial orders (Figure 6A) and may have been phylogentically conserved for 50 million years. *Chaeropus* may have evolved into ecospace occupied by the order Diprotodontia, particularly macropodoids (kangaroos and bettongs). Indeed, *Chaeropus* might be the only example among recent marsupial fauna, of an incursion across an evolutionarily stable niche discontinuity (ESND, see [60]). An earlier broad-scale foraging ecospace overlap between orders involved dasyuromorphians and thylacoleonids (marsupial lions) [61].

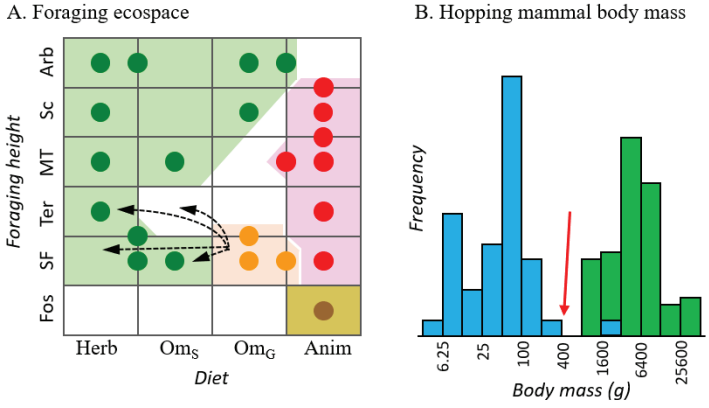

Figure 6. (**A**) Foraging ecospace distribution among extant Australian marsupials, with genera denoted as circles for the four orders, Diprotodontia (green), Peramelemorphia (orange), Notoryctemorphia (brown) and Dasyuromorphia (red). Diet axis: Herb (herbivorous), Om$_S$ (plant-specialized omnivorous), OmG (generalized omnivorous), Anim (Animalivory). See Table S6 for definitions and scoring. Foraging height axis: Fos (fossorial), SF (semi-fossorial), Ter (terrestrial), MT (mostly terrestrial), Sc (scansorial) and Arb (arboreal). Dashed arrows indicate four alternative foraging ecospace transitions along the lineage leading to *Chaeropus*. (**B**) Frequency distribution average adult body mass (g) among all extant hopping mammals, which include rodents (blue) and macropodoids (green). The red arrow indicates estimated body mass for *Chaeropus*.

Three of the four possible foraging ecospace placements for *Chaeropus* in Figure 6A (into green patches) would represent an incursion across the ESND between bandicoots and diprotodontians, albeit into new (grassland) ecospace. Two aspects of the biology of *Chaeropus* and potential competition with macropods may be relevant: (1) In the ancestors of pig-footed bandicoots, small size near the energetic feasibility limit for a grazer may shift the balance of selection pressure in favour of gracile, ungulate-like legs for energetically efficient cursorial locomotion over selection for mechanical advantage in digging. The smallest predominantly grass-feeding macropods (see [62]), such as the rufus hare-wallaby (*Lagorchestes hirsutus*) are larger, averaging ~1.3 kg. (2) The mass of the quadrupedal *Chaeropus* falls in the trough of the binomial body mass distribution for mammalian hoppers (Figure 6B). Hopping appears to be most advantageous for predator avoidance at small body sizes [63] and imparts energetic advantages principally at larger sizes [64]. Moreover, macropod locomotion tends to be inefficient at low speeds [65]. Thus, an ecological

opportunity for a small grazer feeding more or less constantly across the landscape rather than between more distant patches might be more accessible for a bandicoot evolving specialized quadrupedal locomotion than for further shrinking a macropod.

Chaeropus evolution may have instead not violated the conservation of ESNDs between marsupial orders—if invertebrates remained an important component of their diet, even seasonally, and if they foraged terrestrially as their limb morphology may imply [6], then *Chaeropus* evolved into an ecospace that is largely unoccupied by other modern marsupials (Figure 6A, open patch). The paucity of marsupials and dominance of rodents now occupying Australia's mammalian terrestrial omnivore foraging ecospace alludes to the potential importance of looking beyond the intrinsic biology of pig-footed bandicoots to understand their evolution. In particular, the temporal coincidence of the *Chaeropus* ecological shift revealed by the transitional *C. baynesi* and the Pliocene diversification of murid rodents begs the question of how the newly arrived placental omnivores shifted the balance of competition among marsupials for ecospace occupation. This broader view will be critically informed by further fossil evidence. However, genomics may offer valuable insights for testing the alternative ecological transition pathways for *Chaeropus*, by identifying functional mutations, such as in chitinase genes, which have marked dietary transitions from omnivory to more exclusive herbivory among placental mammals [66].

Supplementary Materials: The following supporting information can be downloaded at: https://www.mdpi.com/article/10.3390/d14050352/s1, Figures S1–S4: Supplementary figures.pdf; Tables S1–S7: Supplementary tables.pdf.

Author Contributions: Conceptualization, M.J.P.; methodology, M.J.P.; formal analysis, M.J.P. and M.C. (Manuela Cascini); investigation, M.J.P., M.C. (Manuela Cascini) and M.C. (Mélina Celik); data curation, M.J.P., M.C. (Manuela Cascini) and M.C. (Mélina Celik); writing—original draft preparation, M.J.P.; writing—review and editing, M.J.P., M.C. (Manuela Cascini) and M.C. (Mélina Celik); visualization, M.J.P. and M.C. (Mélina Celik); supervision, M.J.P.; funding acquisition, M.J.P. All authors have read and agreed to the published version of the manuscript.

Funding: This research was funded by The Australian Research Council, grant number "DP190103636".

Institutional Review Board Statement: Not applicable.

Informed Consent Statement: Not applicable.

Data Availability Statement: Body mass and foraging ecospace data are provided in the Supplementary information. Original DNA sequences are available at GenBank and alignments are available upon request.

Acknowledgments: We thank Kenny Travouillon, Robin Beck and three anonymous reviewers for valuable comments on the manuscript.

Conflicts of Interest: The authors declare no conflict of interest. The funders had no role in the design of the study; in the collection, analyses, or interpretation of data; in the writing of the manuscript, or in the decision to publish the results.

References

1. Hughes, R.L. Morphological studies on implantation in marsupials. *Reproduction* **1974**, *39*, 173–186. [CrossRef] [PubMed]
2. Szalay, F.S. *Evolutionary History of the Marsupials and an Analysis of Osteological Characters*; Cambridge University Press: Cambridge, UK, 1994.
3. Denyer, A.L.; Regnault, S.; Hutchinson, J.R. Evolution of the patella and patelloid in marsupial mammals. *PeerJ* **2020**, *8*, e9760. [CrossRef] [PubMed]
4. Szalay, F.S.; Sargis, E.J. Model-based analysis of postcranial osteology of marsupials from the Palaeocene of Itaboraí (Brazil) and the phylogenetics and biogeography of Metatheria. *Geodiversitas* **2001**, *23*, 139–302.
5. Wright, W.; Sanson, G.D.; McArthur, C. The diet of the extinct bandicoot *Chaeropus ecaudatus*. In *Vertebrate Palaeontology of Australasia*; Vickers-Rich, P., Monaghan, J.M., Baird, R.F., Rich, T.H., Eds.; Pioneer Design Studio: Melbourne, Australia, 1991; pp. 229–245.

6. Travouillon, K.J.; Simões, B.F.; Miguez, R.P.; Brace, S.; Brewer, P.; Stemmer, D.; Price, G.J.; Cramb, J.; Louys, J. Hidden in plain sight: Reassessment of the pig-footed bandicoot, *Chaeropus ecaudatus* (Peramelemorphia, Chaeropodidae), with a description of a new species from Central Australia, and use of the fossil record to trace its past distribution. *Zootaxa* **2019**, *4566*, 1. [CrossRef] [PubMed]
7. Groves, C.P.; Flannery, T. Revision of the families and genera of bandicoots. In *Bandicoots and Bilbies*; Seebeck, J.H., Wallis, R.L., Brown, P.R., Kemper, C.M., Eds.; Surrey Beatty: Sydney, Australia, 1990; pp. 1–11. ISBN 978-0-94932-433-7.
8. Muirhead, J.; Dawson, L.; Archer, M. *Perameles bowensis*, a new species of *Perameles* (Peramelemorphia, Marsupialia) from the Pliocene faunas of Bow and Wellington Caves, New South Wales. *Proc. Linn. Soc. N. S. W.* **1997**, *117*, 163–173.
9. Gurovich, Y.; Travouillon, K.J.; Beck, R.M.D.; Muirhead, J.; Archer, M. Biogeographical implications of a new mouse-sized fossil bandicoot (Marsupialia: Peramelemorphia) occupying a dasyurid-like ecological niche across Australia. *J. Syst. Palaeontol.* **2014**, *12*, 265–290. [CrossRef]
10. Travouillon, K.J.; Archer, M.; Hand, S.J.; Muirhead, J. Sexually dimorphic bandicoots (Marsupialia: Peramelemorphia) from the Oligo-Miocene of Australia, first cranial ontogeny for fossil bandicoots and new species descriptions. *J. Mamm. Evol.* **2015**, *22*, 141–167. [CrossRef]
11. Travouillon, K.J.; Gurovich, Y.; Beck, R.M.D.; Muirhead, J. An exceptionally well-preserved short-snouted bandicoot (Marsupialia; Peramelemorphia) from Riversleigh's Oligo-Miocene deposits, northwestern Queensland, Australia. *J. Vert. Paleont.* **2010**, *30*, 1528–1546. [CrossRef]
12. Westerman, M.; Springer, M.S.; Dixon, J.; Krajewski, C. Molecular relationships of the extinct pig-footed bandicoot *Chaeropus ecaudatus* (Marsupialia: Perameloidea) using 12S rRNA sequences. *J. Mamm. Evol.* **1999**, *6*, 271–288. [CrossRef]
13. Meredith, R.W.; Westerman, M.; Springer, M.S. A timescale and phylogeny for "bandicoots" (Peramelemorphia: Marsupialia) based on sequences for five nuclear genes. *Mol. Phylogenet. Evol.* **2008**, *47*, 1–20. [CrossRef]
14. Westerman, M.; Kear, B.P.; Aplin, K.; Meredith, R.W.; Emerling, C.; Springer, M.S. Phylogenetic relationships of living and recently extinct bandicoots based on nuclear and mitochondrial DNA sequences. *Mol. Phylogenet. Evol.* **2012**, *62*, 97–108. [CrossRef] [PubMed]
15. May-Collado, L.J.; Kilpatrick, C.W.; Agnarsson, I. Mammals from 'down under': A multi-gene species-level phylogeny of marsupial mammals (Mammalia, Metatheria). *PeerJ* **2015**, *3*, e805. [CrossRef] [PubMed]
16. Travouillon, K.J.; Phillips, M.J. Total evidence analysis of the phylogenetic relationships of bandicoots and bilbies (Marsupialia: Peramelemorphia): Reassessment of two species and description of a new species. *Zootaxa* **2018**, *4378*, 224. [CrossRef] [PubMed]
17. Kear, B.P.; Aplin, K.P.; Westerman, M. Bandicoot fossils and DNA elucidate lineage antiquity amongst xeric-adapted Australasian marsupials. *Sci. Rep.* **2016**, *6*, 37537. [CrossRef]
18. Beck, R.M.D.; Voss, R.; Jansa, S. Craniodental morphology and phylogeny of marsupials. *Bull. Am. Mus. Nat. Hist.* 2021; *accepted*. [CrossRef]
19. Upham, N.S.; Esselstyn, J.A.; Jetz, W. Inferring the mammal tree: Species-level sets of phylogenies for questions in ecology, evolution, and conservation. *PLOS Biol.* **2019**, *17*, e3000494. [CrossRef]
20. Travouillon, K.J.; Beck, R.M.D.; Case, J.A. Upper Oligocene–Lower-Middle Miocene peramelemorphians from the Etadunna, Namba and Wipajiri Formations of South Australia. *Alcheringa Australas. J. Palaeontol.* **2021**, *45*, 109–125. [CrossRef]
21. Travouillon, K.J. Oldest fossil Remains of the enigmatic pig-footed bandicoot show rapid herbivorous evolution. *R. Soc. Open Sci.* **2016**, *3*, 160089. [CrossRef]
22. Whitelaw, M.J. Magnetic polarity stratigraphy of the Fisherman's Cliff and Bone Gulch vertebrate fossil faunas from the Murray Basin, New South Wales, Australia. *Earth Planet. Sci. Lett.* **1991**, *104*, 417–423. [CrossRef]
23. Poinar, H.N.; Cooper, A. Ancient DNA: Do it right or not at all. *Science* **2000**, *289*, 1139.
24. Key, F.M.; Posth, C.; Krause, J.; Herbig, A.; Bos, K.I. Mining metagenomic data sets for ancient DNA: Recommended protocols for authentication. *Trends Genet.* **2017**, *33*, 508–520. [CrossRef]
25. Hebsgaard, M.B.; Phillips, M.J.; Willerslev, E. Geologically Ancient DNA: Fact or artefact? *Trends Microbiol.* **2005**, *13*, 212–220. [CrossRef] [PubMed]
26. Buckley, L.B.; Jetz, W. Linking global turnover of species and environments. *Proc. Natl. Acad. Sci. USA* **2008**, *105*, 17836–17841. [CrossRef] [PubMed]
27. Hedges, S.B.; Schweitzer, M.H. Detecting dinosaur DNA. *Science* **1995**, *268*, 1191–1194. [CrossRef] [PubMed]
28. Hassanin, A.; Bonillo, C.; Nguyen, B.X.; Cruaud, C. Comparisons between mitochondrial genomes of domestic goat (*Capra hircus*) reveal the presence of numts and multiple sequencing errors. *Mitochondrial DNA* **2010**, *21*, 68–76. [CrossRef] [PubMed]
29. Westbury, M.; Baleka, S.; Barlow, A.; Hartmann, S.; Paijmans, J.L.A.; Kramarz, A.; Forasiepi, A.M.; Bond, M.; Gelfo, J.N.; Reguero, M.A.; et al. A mitogenomic timetree for Darwin's enigmatic South American mammal *Macrauchenia patachonica*. *Nat. Commun.* **2017**, *8*, 15951. [CrossRef] [PubMed]
30. Ma, B.; Tromp, J.; Li, M. PatternHunter: Faster and more sensitive homology search. *Bioinformatics* **2002**, *18*, 440–445. [CrossRef] [PubMed]
31. Swofford, D.L. *PAUP*: Phylogenetic Analysis Using Parsimony (and Other Methods)*; Version 4.0b10; Sinauer Associates: Sunderland, MA, USA, 2002.
32. Nguyen, L.-T.; Schmidt, H.A.; von Haeseler, A.; Minh, B.Q. IQ-TREE: A fast and effective stochastic algorithm for estimating maximum-likelihood phylogenies. *Mol. Biol. Evol.* **2015**, *32*, 268–274. [CrossRef] [PubMed]

33. Duchêne, D.A.; Bragg, J.G.; Duchêne, S.; Neaves, L.E.; Potter, S.; Moritz, C.; Johnson, R.N.; Ho, S.Y.W.; Eldridge, M.D.B. Analysis of phylogenomic tree space resolves relationships among marsupial families. *Syst. Biol.* **2018**, *67*, 400–412. [CrossRef]
34. Mitchell, K.J.; Pratt, R.C.; Watson, L.N.; Gibb, G.C.; Llamas, B.; Kasper, M.; Edson, J.; Hopwood, B.; Male, D.; Armstrong, K.N.; et al. Molecular phylogeny, biogeography, and habitat preference evolution of marsupials. *Mol. Biol. Evol.* **2014**, *31*, 2322–2330. [CrossRef]
35. Westerman, M.; Krajewski, C.; Kear, B.P.; Meehan, L.; Meredith, R.W.; Emerling, C.A.; Springer, M.S. Phylogenetic relationships of dasyuromorphian marsupials revisited. *Zool. J. Linn. Soc.* **2016**, *176*, 686–701. [CrossRef]
36. Celik, M.; Cascini, M.; Haouchar, D.; Van Der Burg, C.; Dodt, W.; Evans, A.R.; Prentis, P.; Bunce, M.; Fruciano, C.; Phillips, M.J. A molecular and morphometric assessment of the systematics of the *Macropus* complex clarifies the tempo and mode of kangaroo evolution. *Zool. J. Linn. Soc.* **2019**, *186*, 793–812. [CrossRef]
37. Dodt, W.G.; McComish, B.J.; Nilsson, M.A.; Gibb, G.C.; Penny, D.; Phillips, M.J. The complete mitochondrial genome of the eastern grey kangaroo (*Macropus giganteus*). *Mitochondrial DNA* **2016**, *27*, 1366–1367. [CrossRef] [PubMed]
38. Nilsson, M.A.; Zheng, Y.; Kumar, V.; Phillips, M.J.; Janke, A. Speciation generates mosaic genomes in kangaroos. *Genome Biol. Evol.* **2018**, *10*, 33–44. [CrossRef] [PubMed]
39. Rambaut, A. Sequence Alignment Editor. 1996. Available online: http://tree.bio.ed.ac.uk/software/seal (accessed on 23 March 2014).
40. Ronquist, F.; Teslenko, M.; van der Mark, P.; Ayres, D.L.; Darling, A.; Höhna, S.; Larget, B.; Liu, L.; Suchard, M.A.; Huelsenbeck, J.P. MrBayes 3.2: Efficient Bayesian phylogenetic inference and model choice across a large model space. *Syst. Biol.* **2012**, *61*, 539–542. [CrossRef]
41. Rambaut, A.; Drummond, A.J.; Xie, D.; Baele, G.; Suchard, M.A. Posterior summarization in Bayesian phylogenetics using tracer 1.7. *Syst. Biol.* **2018**, *67*, 901–904. [CrossRef]
42. Phillips, M.J.; Pratt, R.C. Family-level relationships among the Australasian marsupial "herbivores" (Diprotodontia: Koala, wombats, kangaroos and possums). *Mol. Phylogenet. Evol.* **2008**, *46*, 594–605. [CrossRef]
43. Cascini, M.; Mitchell, K.J.; Cooper, A.; Phillips, M.J. Reconstructing the evolution of giant extinct kangaroos: Comparing the utility of DNA, morphology, and total evidence. *Syst. Biol.* **2019**, *68*, 520–537. [CrossRef]
44. Drummond, A.J.; Rambaut, A. BEAST: Bayesian evolutionary analysis by sampling trees. *BMC Evol. Biol.* **2007**, *7*, 214. [CrossRef]
45. Drummond, A.J.; Ho, S.Y.W.; Phillips, M.J.; Rambaut, A. Relaxed phylogenetics and dating with confidence. *PLoS Biol.* **2006**, *4*, e88. [CrossRef]
46. Grant, J.R.; Katz, L.A. Building a phylogenomic pipeline for the eukaryotic tree of life—Addressing deep phylogenies with genome-scale data. *PLoS Curr.* **2014**, *6*. [CrossRef]
47. Phillips, M.J.; McLenachan, P.A.; Down, C.; Gibb, G.C.; Penny, D. Combined mitochondrial and nuclear DNA sequences resolve the interrelations of the major Australasian marsupial radiations. *Syst. Biol.* **2006**, *55*, 122–137. [CrossRef] [PubMed]
48. Krajewski, C.; Anderson, F.E.; Woolley, P.A.; Westerman, M. Molecular evidence for a deep clade of dunnarts (Marsupialia: Dasyuridae: *Sminthopsis*). *J. Mamm. Evol.* **2012**, *19*, 265–276. [CrossRef]
49. Phillips, M.J.; Westerman, M.; Cascini, M. The value of updating GenBank accessions for supermatrix phylogeny: The case of the New Guinean carnivore genus *Myoictis*. *Mol. Phylogenet. Evol.* **2022**, *160*, 107328. [CrossRef] [PubMed]
50. Meredith, R.W.; Westerman, M.; Springer, M.S. A phylogeny of Diprotodontia (Marsupialia) based on sequences for five nuclear genes. *Mol. Phylogenet. Evol.* **2009**, *51*, 554–571. [CrossRef] [PubMed]
51. Groves, C. Order Peramelemorphia. In *Mammal Species of the World: A Taxonomic and Geographic Reference*, 3rd ed.; Wilson, D.E., Reader, D.M., Eds.; Johns Hopkins University Press: Baltimore, MA, USA, 2005; pp. 38–42.
52. Travouillon, K.J.; Hand, S.J.; Archer, M.; Black, K.H. Earliest modern bandicoot and bilby (Marsupialia, Peramelidae and Thylacomyidae) from the Miocene of the Riversleigh World Heritage Area, Northwestern Queensland, Australia. *J. Vertebr. Paleontol.* **2014**, *34*, 375–382. [CrossRef]
53. Martin, H. Cenozoic climatic change and the development of the arid vegetation in Australia. *J. Arid. Environ.* **2006**, *66*, 533–563. [CrossRef]
54. Couzens, A.M.C.; Prideaux, G.J. Rapid Pliocene adaptive radiation of modern kangaroos. *Science* **2018**, *362*, 72–75. [CrossRef]
55. Warburton, N.M.; Travouillon, K.J. The biology and palaeontology of the Peramelemorphia: A review of current knowledge and future research directions. *Aust. J. Zool.* **2016**, *64*, 151. [CrossRef]
56. Dixon, J. Notes on the diet of three mammals presumed to be extinct: The Pig-footed bandicoot, the lesser bilby and the desert rat kangaroo. *Vic. Nat.* **1988**, *105*, 208–211.
57. Burbidge, A.A.; Johnson, K.A.; Fuller, P.J.; Southgate, R.I. Aboriginal knowledge of the mammals of the central deserts of Australia. *Austr. Wildlife Res.* **1988**, *15*, 9–39. [CrossRef]
58. Lee, A.K.; Cockburn, A. *Evolutionary Ecology of Marsupials (Monographs on Marsupial Biology)*; Cambridge University Press: Cambridge, UK, 1985.
59. Cork, S.J. Digestive constraints on dietary scope in small and moderately-small mammals: How much do we really understand? In *The Digestive System in Mammals: Food, Form and Function*; Chivers, D.J., Langer, P., Eds.; Cambridge University Press: Cambridge, UK, 1994; pp. 337–369.
60. Poole, A.M.; Phillips, M.J.; Penny, D. Prokaryote and eukaryote evolvability. *Biosystems* **2003**, *69*, 163–185. [CrossRef]
61. Gillespie, A.K.; Archer, M.; Hand, S.J. A tiny new marsupial lion (Marsupialia, Thylacoleonidae) from the early Miocene of Australia. *Palaeontol. Electron.* **2016**, *19*, 1–26. [CrossRef]

62. Arman, S.D.; Prideaux, G.J. Dietary classification of extant kangaroos and their relatives (Marsupialia: Macropodoidea): Diets of extant macropodoids. *Austral Ecol.* **2015**, *40*, 909–922. [CrossRef]
63. Moore, T.Y.; Cooper, K.L.; Biewener, A.A.; Vasudevan, R. Unpredictability of escape trajectory explains predator evasion ability and microhabitat preference of desert rodents. *Nat. Commun.* **2017**, *8*, 440. [CrossRef] [PubMed]
64. McGowan, C.P.; Collins, C.E. Why do mammals hop? Understanding the ecology, biomechanics and evolution of bipedal hopping. *J. Exp. Biol.* **2018**, *221*, jeb161661. [CrossRef]
65. Webster, K.; Dawson, T. Is the energetics of mammalian hopping locomotion advantageous in arid environments? *Aust. Mammal.* **2004**, *26*, 153. [CrossRef]
66. Emerling, C.A.; Delsuc, F.; Nachman, M.W. Chitinase genes (*CHIAs*) provide genomic footprints of a post-Cretaceous dietary radiation in placental mammals. *Sci. Adv.* **2018**, *4*, eaar6478. [CrossRef]

diversity

MDPI

Review

A Review of Coastal Anthropogenic Impacts on Mytilid Mussel Beds: Effects on Mussels and Their Associated Assemblages

Leandro Sampaio [1,2], Juan Moreira [3], Marcos Rubal [1,2,*], Laura Guerrero-Meseguer [4] and Puri Veiga [1,2]

[1] Interdisciplinary Centre of Marine, Environmental Research (CIIMAR) of the University of Porto, Novo Edifício do Terminal de Cruzeiros do Porto de Leixões, Avenida General Norton de Matos, 4450-208 Matosinhos, Portugal; leandro.sampaio@fc.up.pt (L.S.); puri.sanchez@fc.up.pt (P.V.)
[2] Department of Biology, Faculty of Sciences, University of Porto, Rua do Campo Alegre s/n, 4169-007 Porto, Portugal
[3] Departamento de Biología (Zoología), Centro de Investigación en Biodiversidad y Cambio Global (CIBC-UAM), Facultad de Ciencias, Universidad Autónoma de Madrid, 28049 Madrid, Spain; juan.moreira@uam.es
[4] Mediterranean Institute for Advanced Studies, IMEDEA (CSIC-UIB), Miquel Marqués, 21, 07190 Esporles, Spain; laura.meseguer@fc.up.pt
* Correspondence: marcos.garcia@fc.up.pt

Abstract: Mussel beds are an important habitat in many coastal systems, harboring a high diversity of biota. They are threatened by anthropogenic impacts that affect mussels and their associated assemblages. Pollution, harvesting, trampling, dredging and trawling are major threats faced by these communities. Most of the studies on the effects of such impacts on the mussel beds overlook the associated fauna. Since mussels are very resilient, especially to pollution, the associated fauna can provide a better footprint of the impacts' effects. In this review, we looked into the main remarks regarding the effects of anthropogenic impacts in mussel bed communities. Organic pollution was the best studied impact and the Atlantic region was the best studied zone. Low values of abundance, biomass, diversity, evenness and species richness were reported for all categories of impacts, with some studies describing declines in at least three of these descriptors. Among the associated fauna, some tolerant species benefited from the impacts, particularly organic enrichment, and became more abundant, but sensitive species suffered considerable declines in density, mainly in dredging and trawling impacts. Therefore, fauna associated with mussel beds is a suitable indicator of anthropogenic disturbances.

Keywords: Mytilidae; ecosystem engineer; coastal systems; macrobenthos; associated fauna; pollution; harvesting; trampling; dredging; trawling

Citation: Sampaio, L.; Moreira, J.; Rubal, M.; Guerrero-Meseguer, L.; Veiga, P. A Review of Coastal Anthropogenic Impacts on Mytilid Mussel Beds: Effects on Mussels and Their Associated Assemblages. *Diversity* **2022**, *14*, 409. https://doi.org/10.3390/d14050409

Academic Editor: Michael Wink

Received: 16 April 2022
Accepted: 19 May 2022
Published: 22 May 2022

1. Introduction

Anthropogenic disturbances are among the greatest threats for many coastal systems around the world [1–3]. The lack of environmental protecting laws or their effective enforcement prolong this threat [4,5]. Macroinvertebrate communities either have to adapt to the changes, move or perish [6–8].

Mussels of the family Mytilidae are often key species in marine environments and traditionally cluster to form beds on the surface of several substrates. Therefore, mussels provide additional habitat for many other species. Barnacles, algae and other sessile species find an extra substrate on top of the shells of mussels [9]. The byssus that holds bivalves in place creates a very complex habitat forming huge tight clumps [10,11]. This intricate structure easily traps sediment from the water column. The fecal pellets excreted by mussels and other ecosystem engineer bivalves (e.g., oysters, [12]) mix with this sediment creating organic enriched particles that attract many deposit feeders [10,11,13].

The mussel communities supply shelter and food to a rich assemblage of diverse species, making these habitats a good biodiversity hotspot [9,14]. Since mussels are efficient

suspension-feeders, they are very important in cleaning the water column of suspended solids and contaminated particles [10]. Mussels have a high resilience to contamination and often bioaccumulate the pollutants extracted from the water column. This bioaccumulation makes them unsafe for consumption but promote the restoration of polluted environments [11,15]. In heavy contaminated sites mussels can die. However, while mussels remain alive, their associated assemblages might change due to pollution [1,2]. By studying the mussel beds' communities, we can look into the health status of the aquatic systems. Since the loss of the mussel beds carries the loss of their associated assemblages [4,6,14,16], it is important to protect them. Protection can be achieved either by creating marine reserves, banning their harvesting or establishing restrictions to safeguard the ecological quality of the aquatic systems [5,17,18].

In order to understand the importance of mussel beds for ecosystem health, we reviewed scientific papers about the biodiversity of fauna associated with mussel beds under different anthropogenic impacts. These papers deal with how the assemblages cope with the impacts and whether the extension or regression of the mussel clumps and their complex structure influences the recovery of impacted ecosystems.

2. Literature Selection

The study of the assemblages associated with mussel beds has been increasingly discussed in the last years, and the existing literature on the subject is still emerging. The literature survey conducted in the present review and the information gathered provide an important insight into the relevance of mussels as ecological engineers that sustain and protect many species and contribute to a better ecological quality of ecosystems. We started with an examination of the literature using SCOPUS and the string search in the title, abstract and keywords: Mussels AND ('Pollution' OR 'Contamination' OR 'Enrichment' OR 'Pollutant*' OR 'Harvesting' OR 'Trampling' OR 'Anthropog*' OR 'Human' OR 'Farm*' OR 'Fisher*') AND ('Assemblages' OR 'Biota' OR 'Communit*' OR '*diversit*').

A large volume of scientific papers was found that met the selected criteria, but we focused our selection on marine environments and considered only the papers that studied the communities associated with mussels in a scenario of anthropogenic impact. By doing so, we further narrowed our results to 68 scientific papers. Then, after a full paper review, we excluded those studies with very limited taxa information, those that used transplanted mussels, those associated with offline platforms or those where mussels did not form relevant clumps, being too scattered and/or scarce, or even those where anthropogenic impacts only referred to adjacent areas and did not affect mussel communities.

The final body of literature was reduced to 31 scientific papers, that were reviewed in the following impact categories: large-scale physical impacts (dredging, trawling), pollution impacts (organic compounds, heavy metals) and small to medium-scale physical impacts (harvesting, trampling). The impact of alien species was not the target of this study, but some papers highlight that the effects of alien species added to those of the considered target impacts. A summary of the studied impacts, target mussel species, main effects and data analysis conducted can be found in Table 1, for each reviewed scientific paper. The location, type of impact and target species is exhibited in Figure 1. Species names were revised using WoRMS [19].

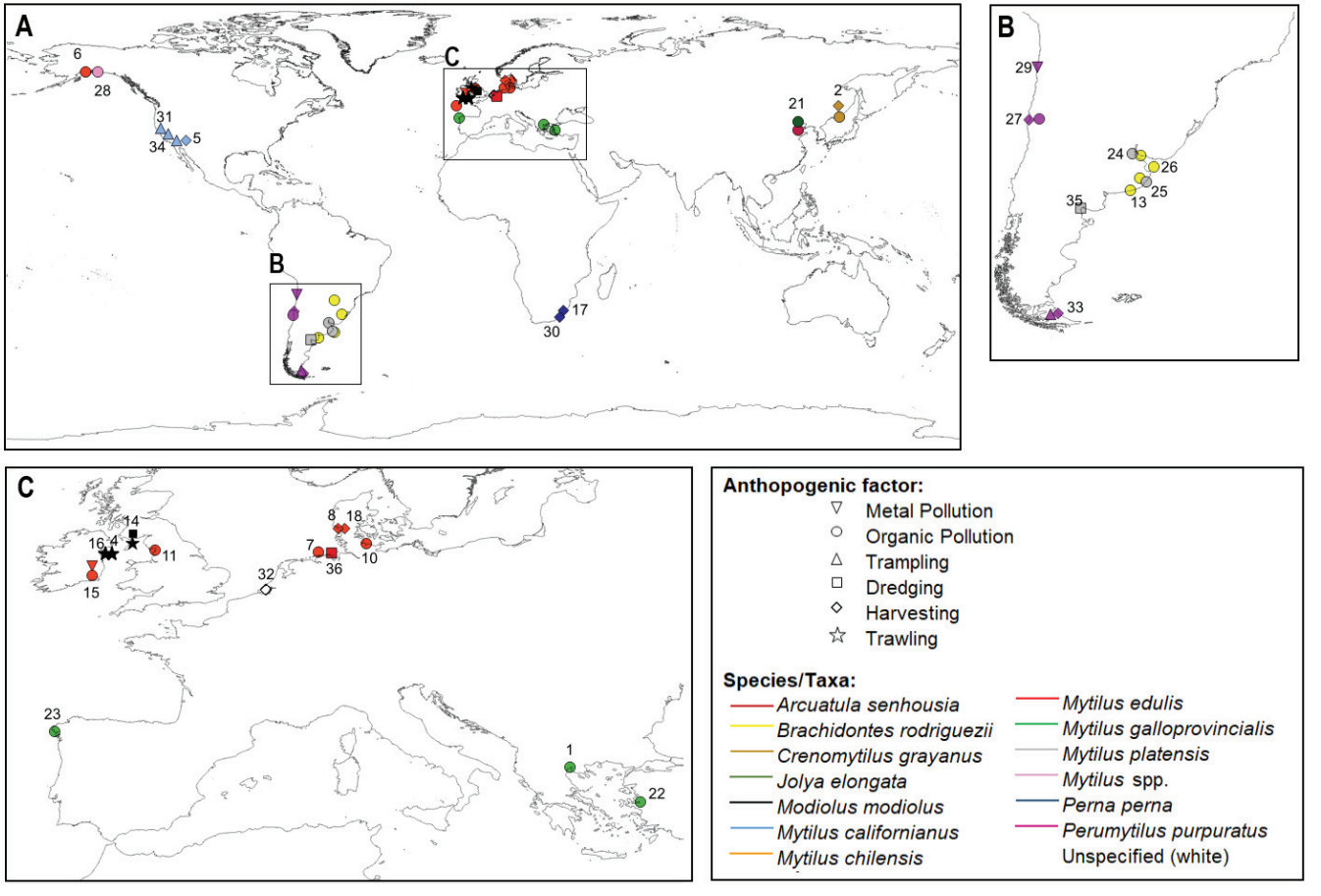

Figure 1. (**A**)—Study distribution around the world with indication of each anthropogenic descriptor and taxa investigated; (**B**)—Detail of studies conducted in South America; (**C**)—Detail of studies held in Europe. Numbers identify the reference studies included in the review.

3. Geographic Area and Taxa

The reviewed scientific papers investigated several anthropogenic impacts (dredging, harvesting, pollution, trampling and trawling) that affected different mussel bed communities around the world (Figure 1, Table 1). More than half of the studies (18, Figure 1, Table 1) were done in the Atlantic region, two thirds at the north (12, Figure 1, Table 1) and one third at the south (6, Figure 1, Table 1). This region was also the best studied concerning the different impacts under review. Organic pollution was the most examined impact here (9, Figure 1, Table 1), while trampling was the least studied (1, Figure 1, Table 1), but all dredging and trawling impacts were investigated in this region (5, Figure 1, Table 1). The Pacific region gathered nine studies, the vast majority at the east (7, Figure 1, Table 1), but a few were done at the west (2, Figure 1, Table 1). At the west, organic pollution and harvesting were the only impacts researched, while at the east, additionally to those, metal pollution and trampling were analyzed (Figure 1, Table 1). Furthermore, this region had more studies concerning trampling effects on mussel beds than anywhere else in the world (3, Figure 1, Table 1). The remaining studies were done in the Indian region (2, Figure 1, Table 1) concerning harvesting impacts, and in the Mediterranean (2, Figure 1, Table 1), investigating organic pollution effects. Until recently there were no mussels in Antarctica, but with the discovery of a first settlement of mussels in this continent one might expect new follow-up studies in the near future in this pristine region [20].

The total number of mussel species considered in the reviewed studies was twelve (sometimes two species were present in a single study), distributed among eight genera: *Arcuatula senhousia* (Benson, 1842), *Brachidontes rodriguezii* (d'Orbigny, 1842), *Crenomytilus grayanus* (Dunker, 1853), *Jolya elongata* (Swainson, 1821), *Modiolus modiolus* (Linnaeus, 1758), *Mytilus californianus* Conrad, 1837, *Mytilus chilensis* Hupé, 1854, *Mytilus edulis* Linnaeus, 1758, *Mytilus galloprovincialis* Lamarck, 1819, *Mytilus platensis* d'Orbigny, 1842, *Perna perna* (Linnaeus, 1758) and *Perumytilus purpuratus* (Lamarck, 1819) (Figure 1, Table 1). Additionally, two studies did not specify the target species, but it could possibly be *M. edulis* mixed with a similar related species (Figure 1, Table 1). Indeed, nearly two thirds of the studies investigated the *Mytilus* species (20, Figure 1, Table 1), while four studies involved a single species of *Brachidontes* (*B. rodriguezii*; Figure 1, Table 1), and three analyzed one *Perumytilus* species (*P. purpuratus*; Figure 1, Table 1) and a *Modiolus* species (*M. modiolus*; Figure 1, Table 1). Moreover, the genus *Mytilus* had by far the highest number of studied taxa, corresponding to five species (*M. californianus*, *M. chilensis*, *M. edulis*, *M. galloprovincialis*, *M. platensis*; Figure 1, Table 1). The other target species, each belonging to a different genus, were researched in four studies (Figure 1, Table 1), among which the genus *Perna* was investigated in two different studies (*P. perna*; Figure 1, Table 1), while two other species (*A. senhousia*, *J. elongata*; Figure 1, Table 1) were investigated in the same study.

The mussels *A. senhousia*, *C. grayanus* and *J. elongata* (Figure 1, Table 1) were only investigated in the west Pacific in areas prone to some degree of organic pollution, although *C. grayanus* (Figure 1, Table 1) was also examined for the impact of harvesting in this region. *M. galloprovincialis* (Figure 1, Table 1) was also employed to observe the effect of organic pollution in mussel beds, both in the northeast Atlantic and in the Mediterranean. *P. perna* (Figure 1, Table 1) was only analyzed in the Indian region in studies that dealt with the effects of harvesting in rocky shores, while *M. modiolus* (Figure 1, Table 1) was only encountered in trawled or dredged areas around the UK. In the southwest Atlantic, *B. rodriguezii* (Figure 1, Table 1) was solely considered in organic pollution studies, alone or in the presence of *M. platensis* (Figure 1, Table 1), while the latter was also examined in a dredging study (Figure 1, Table 1). The other species found in this region, further south, were *M. chilensis* and *P. purpuratus* (Figure 1, Table 1), and were used to investigate harvesting and trampling impacts. Moreover, *P. purpuratus* was also encountered in the east Pacific Chilean coast and employed to study harvesting effects, as well as organic and metal pollution impacts. On the northeast Pacific region, *M. californianus* and *M. edulis* were used in anthropogenic impact studies on mussel bed communities (Figure 1, Table 1). While *M. edulis* was restricted to Alaska, in the Pacific (Figure 1, Table 1), and used to examine

the organic pollution impacts there, *M. californianus* was utilized to address the effects of harvesting and trampling further south, in California (Figure 1, Table 1). Moreover, *M. edulis* (Figure 1, Table 1) was the most studied mussel species in the northeast Atlantic and of all the mussel species anywhere else. With the exception of trampling studies, this species was employed as the model to study the effects of every anthropogenic impact dealt with in this review.

4. Anthropogenic Perturbations

4.1. Pollution Impacts

The aquatic environment has been polluted by organic compounds, heavy metals and other pollutants due to anthropogenic activities [1,7,21]. In most cases these compounds bioaccumulate in the food chains, being harmful for some organisms and sometimes leading to indirect effects outside the contaminated areas [1,11].

4.1.1. Organic Compounds

The presence of mussel beds in an area usually mitigates the pollutant effects on the associated community. When their biomass decreases the associated communities are more severely affected [11,22]. We analyzed 16 papers that studied the effects of organic pollution on the mussel beds and their associated fauna.

The studies done in the North Atlantic include the coasts of Ireland, Spain, UK and the North and Baltic Seas. On a shallow soft sediment inshore region in the South of Kiel Bay, Anger [10] found that biomass and the abundance of the macrofauna community increased at short and intermediate distances from a sewage outfall. This enhancement was less pronounced at mussel beds than on adjacent sand bottoms or eelgrass communities. However, the overall diversity and mean species richness was higher in mussel communities. Nevertheless, there was a clear negative effect of pollution on both species' richness and evenness in the mussel beds of the study area [10].

In another pollution study, Crowe and colleagues [11] found a good relationship between hydrocarbon concentration in *M. edulis*, scope for growth (SFG) and the associated assemblages diversity. Fauna associated with mussels had a reduced diversity at sites with low SFG compared with the control sites that had high SFG. Low SFG was due to high hydrocarbon concentrations but also to the high levels of sewage input in one site. According to the authors, the relationship between SFG and diversity was not confounded by environmental factors, but other pollutants could also be at play [11]. Furthermore, experiments with both copper and biocide chlorpyrifos in Ireland, also among *M. edulis* assemblages, revealed consistent plumes of contamination within patches of mussels, but which were not detected in the water outside the patches [15]. Ecotoxicological assays revealed that mussel assemblages exposed to chlorpyrifos had an 81% decrease in amphipod numbers and a 40–70% decrease in annelids when copper was also present. The synergistic effects of the pollutant input, addiction of non-indigenous species and range-related community alterations can produce long-term ecological changes in intertidal mussel bed communities [7]. At Helgoland, North Sea, an invasive alga outcompeted a native alga within the mussel bed in the mid intertidal zone when the study site was revisited 18 years later [7]. Although species richness remained very similar in both surveys, there was a turnover of nearly 60 species, with 27 new records and 32 displacements between surveys. Crustacea had more new records and less species losses compared to annelids and mollusks that lost more species. These community structure changes were the result of combined pollution, alien species and distribution shifts [7].

García-Regueira and colleagues [23] studied oil spilling effects on the diversity and abundance of annelids inhabiting intertidal rocky shores non-impacted and impacted by the Prestige oil spill. The temporal evolution of the annelid assemblage on mussel and algal beds showed positive and negative impacts depending on the tidal level. At the lowest tidal level, the impacted site presented the greatest diversity compared to the control while at higher elevations the control had a higher number of species [23]. However, statistical

analyses did not show any clear temporal trend, maybe because other anthropogenic disturbances might overlap with those of the Prestige oil spill [23].

In the South Atlantic, all the studies were done in Argentina in areas with a sewage outfall, using *B. rodriguezii* [13,24–26], although *M. platensis* was also present in two studies [24,25]. The area adjacent to the sewage outfalls was dominated by the opportunistic annelids *Boccardia polybranchia* (Haswell, 1885) and/or *Capitella capitata* (Fabricius, 1780) [13,24–26] that were rarer at other locations [24]. Sometimes their abundance could increase significantly near the outfall in response to temporary increases in sewage discharges [13,26]. Close to the outfall, the mussel abundance was low but at intermediate distances the mussel beds were conspicuous [13], sediments retained by mussels reached their maximum values, and the abundance of other annelids was also high [13] or crustaceans dominated [25]. In this same area, a follow-up research encompassing a 10-year period showed that the impacted sites exhibited significant differences compared to the reference site, and a pattern of increasing disturbance was evident [26].

In the Mediterranean, the studies were focused in the eastern Mediterranean using *M. galloprovincialis*. In a polluted port with high levels of commercial shipment, dense subtidal mussel beds developed at the lower midlittoral. This mussel dominance led to the replacement of an algal-dominated community and its associated fauna [1]. Despite the existence of biogenic mussel structures, the associated fauna diversity decreased due to organic enrichment, and most species were tolerant to pollution and took advantage of the existing enriched conditions [1]. In an area in the Aegean Sea subjected to various pollution discharges since the 1960s, annelids had the highest species richness and abundance within the mussel beds' faunal assemblage [22]. Moreover, there were several invasive species, including the annelid *Hydroides elegans* (Haswell, 1883), that, together with mollusks, had the highest biomass [22]. The less impacted station outside the harbor had the highest species richness and diversity, whereas the abundance and biomass were generally higher inside the harbor [22].

In the Pacific region, in a polluted area of the Vostok Bay where sewage discharges are frequent, Galysheva [2] studied the composition and structure of *C. grayanus* communities impacted since the 1970s. Due to pollution, the diversity and evenness of the mussel communities became lower, and pollution-tolerant species invaded and dominated the assemblages [2]. Further south, in an area impacted for over 20 years through over-fishing and pollution, important changes occurred between two periods of study [21]. The authors found changes in community structure from the 1980s to the 1990s and across geographical regions. The mussel *A. senhousia* disappeared from the surveyed area in the 1990s, while it was abundant in the 1980s at Laizhou Bay, but another mussel, *J. elongata*, replaced *A. senhousia* in the surveyed area. While at Laizhou Bay diversity increased, in the other areas some species dominated and significantly decreased evenness. Annelids and bivalves accounted for over 50% of abundance while crustaceans contributed for a species richness increase between periods [21]. In Chile, Valdivia and Thiel [27] evaluated the effects of direct nutrient addition on the species diversity of the epibenthic assemblage associated with the mussel *P. purpuratus*. However, nutrient addition only had minor effects on diversity compared to another treatment that included mussel removal. The authors concluded that physical and biological stress acting on exposed hard-bottom communities surpasses the possible effects of nutrient addition [27].

Oil spilling can have a low to moderate impact in the intertidal communities of exposed shores [23], but the treatment methods employed to clean a shore can sometimes have a more severe impact [6,28]. For instance, studies at Prince William Sound reported severe impacts to intertidal epibenthos of treatments widely used to remove stranded oil. Moreover, the type and number of significant changes observed varied considerably by elevation and type of treatment, perhaps reflecting the position of the zone relative to washing activities and rigor of washing [6,28]. At upper and mid-levels, where mussels were most abundant, the most significant variations corresponded to abundance declines. Dispersant and beach cleaner treatments had less significant changes in abundance, perhaps

due to a less vigorous washing, whereas the hot water treatment was associated with the highest number of negative alterations. In rocky beaches that received no treatment or where the treatment was less severe, the majority of the dominant species, including mussels and associated fauna, survived the oiling [6]. However, the severe effects of hot water treatment remained noticeable three years later. Thus, there were few statistically significant differences between the biota of unoiled rocky shores and those treated with hot water, but a full recovery was still far from being achieved [6,28].

4.1.2. Heavy Metals

The amount of contamination that can be absorbed by an ecosystem before the detection of structural or functional changes can be estimated through manipulative experiments. This information is relevant, in turn, to regulate the use of heavy metals. In situ experimental studies can help manage the dose administrated and the frequency of pollutants to which fauna is exposed [15]. We analyzed one paper reporting an experimental study of the effects of metal pollution on the mussel communities.

In the Pacific, Acevedo and colleagues [29] evaluated the effects of copper on *P. purpuratus* communities using three treatments (continuous, intermittent and no copper administration) on three mussel areas for a short period of time. Here, the effects of copper were less severe than in the Atlantic study. The continuous administration of copper decreased species richness and diversity compared to the other treatments, but only significant effects were found for diversity when analyzing *a priori* orthogonal contrasts between the continuous and intermittent treatments [29]. No significant effects were detected on mussel density, length and number of strata, or faunal species richness, evenness and diversity. Nevertheless, non-metric multidimensional scaling showed a significant effect of the copper treatments compared to the control, suggesting that the associated fauna responds differentially to copper frequency administration [29].

4.2. Small- to Medium-Scale Physical Impacts

Organisms on rocky shores are subjected to physical perturbations when many people visit intertidal zones for recreation, collection of food, fish bait or ornamentation [2,30]. Visitor activities can result in the loss or damage of individuals and cause alterations of the community structure [2,5,31]. We analyzed 11 papers that studied the effects of harvesting and trampling on the mussel beds and their associated assemblages. We found three studies for the North-East Atlantic (North Sea), one study for the South-West Atlantic (Argentina), five studies in the Pacific (SE Russia, USA and Chile) and two studies for the Indian Ocean (South Africa), while other areas remain unstudied.

4.2.1. Harvesting

All the studies aimed at investigating the effects of harvesting impacts in the Atlantic were done in the North Sea using *M. edulis* [8,18,32], except for a study conducted in the Argentinian coast that investigated *M. chilensis* and *P. purpuratus* [33]. No other studies were conducted in the east coast of Brazil, Canada and USA, or in more exposed rocky habitats of the northeast Atlantic coasts. In the North Atlantic, a study in 1980 found major changes in the community of subtidal fauna at the Wadden Sea compared to historical studies of the mid-1920s. These changes were attributed to anthropogenic disturbances and human interference [8]. However, the shell fishery promoted the spread of *M. edulis* across the entire region. Barnacles and many annelids took advantage of the mussel expansion and increased their abundances compared to 1920s, but mollusks and crustaceans decreased in species richness, diversity and evenness. Overall, the total number of species remained approximately the same, but mollusks suffered losses and annelids diversified; nonetheless, the abundance increased with the dominance of a few species (*M. edulis*, *Balanus crenatus* Bruguière, 1789, *Cerastoderma edule* (Linnaeus, 1758), *Scoloplos armiger* (Müller, 1776)) [8]. Twenty years later, Saier [18] studied the epifauna in the same region and found a higher diversity, abundance and species richness in the subtidal zone compared to the intertidal

zone. Abundances significantly declined with increasing depth, mainly due to significantly higher densities (97%) of juvenile periwinkles and crabs in intertidal mussel beds [18]. On the other hand, in subtidal mussel beds, species' abundances were more evenly distributed. Therefore, the author suggested an extension of the protective measures against mussel harvesting towards the subtidal zone to keep the high epifaunal diversity and maintain the integrity of the mussel bed communities [18]. High diversity is a common feature among healthy mussel bed communities. For instance, in the Netherlands, unexplored mussel beds had the highest densities and biomass, indicating an unstressed community [32]. When evaluated under the abundance/biomass comparison method, an area with an exploited mussel bed showed moderate stress, and the benthic community had not been able to reach an equilibrium [32].

In the South Atlantic, defaunation was used to simulate a physical disturbance comparable to an extreme harvesting [33]. At the start of the experiment, bivalves appeared in at least two layers with *M. chilensis* over *P. purpuratus*. Beneath the bivalves, there was a variable layer of sediment in which there were mainly annelids, crustaceans and other mollusks. This layer gradually disappeared for reasons still to be investigated but coincided with a massive recruitment of *M. chilensis*. *P. purpuratus* dominated the assemblage in June 2001. However, due to a recruitment event of *M. chilensis* in December 2001, their numbers were higher than those of *P. purpuratus* in the disturbed plots [33]. By February 2002, the proportion of *M. chilensis* in both the disturbed and control plots was over 60% and much higher than at the beginning (about over 20%). Changes in the relative abundance of both mussel species due to disturbance conditioned the presence of the associated fauna. In fact, the diversity, richness and evenness of the associated fauna was significantly lower in the disturbed plots. Moreover, the frequency of some opportunistic annelids and isopods increased, while that of some amphipods and bivalves decreased.

In the Indian region, *P. perna* was the only mussel investigated in the Transkei coast of South Africa. There was a reduction in biomass of the exploited mussels and their associated fauna in both studies considered [17,30]. In some cases, although there were changes in the community structure (e.g., decline in the abundance of certain filter-feeders), they were balanced with an increase in the abundance of some associated seaweeds. Species richness and diversity values were not consistent with the presence or absence of exploitation, but biomass was significantly altered in the exploited sites [30]. The presence of marine reserves safeguarded mussels from harvesting, mollusks increased their densities within reserves, and annelids were more abundant in the exploited sites.

In the Pacific region, three harvesting studies were conducted, each using a different mussel species. At Vostok Bay, in the East Pacific, the biomass of *C. grayanus* declined due to poaching (unselective harvesting, [2]). Since the 1970s, the total biomass of the assemblages and the size–age composition of the population had changed because of poaching effects. At an exposed rocky shore of northern-central Chile, the removal of *P. purpuratus* also had significant and negative effects on the associated assemblages, particularly on species richness, and the abundance of suspension-feeders and sessile organisms. Furthermore, the abundance of top consumers declined significantly with mussel removal in the presence of nutrient addition, but there was no effect on the evenness of the associated fauna [27]. Further north, in California, high human visitation resulted in a significantly lower abundance of *M. californianus* than in less frequented sites. Moreover, the percentage cover, biomass and size measures of mussels were reduced within harvested sites. Nevertheless, the diversity of the fauna associated with the mussel beds was not significantly affected by the level of intertidal use, and neither were the evenness or species richness [5].

4.2.2. Trampling

Studies about the trampling effects on the fauna associated with mussel beds were conducted mainly in the Pacific region with *M. californianus*, except for one study conducted in the Atlantic coast of Argentina, that involved *M. chilensis* and *P. purpuratus*. However, many other areas still lack studies on this subject. In Tierra del Fuego, mussel crushing was

done to simulate a physical disturbance comparable to extreme trampling [33]; the diversity of the associated fauna declined in the disturbed plots. Furthermore, sediment trapped among the two mussel species (to less than 5 mm) almost disappeared for unknown reasons, and was not restored until the end of the study period. Species richness and evenness were also significantly lower in the disturbed plots. In general, opportunistic annelids and some isopods endured the disturbance well, while sensitive amphipods and bivalves were more affected. Due to the slow recovery of *P. purpuratus*, the initial structure of multilayers with sand, *P. purpuratus* and *M. chilensis* found at the start of the trial was never completely recovered by the end of the four-year experiment [33].

The remaining studies investigated the human trampling in the Californian coast [5,31,34]. In Santa Cruz, the abundance and diversity among the associated fauna in mussel beds was higher in less trampled sites. However, there was no significant decline of these descriptors in areas subjected to trampling, except at a higher ground [31,34]. At the most trampled site, some small bivalves were less abundant and some algae were absent, compared to less trampled sites. 17 years later, Van de Werfhorst and Pearse [34] employed a different sampling design in their follow-up study. They created a contour map and stratified sampling according to tidal height and found a large variability above the 2 m tidal level. This time, mussel beds and the associated species' richness declined with increased human trampling; they concluded that these differences could be attributed to the sampling strategy and argued that sampling scale and design are important for evaluating and monitoring trampling impacts [34]. In a broader study encompassing ca. 1000 km of the Californian coast, the effect of human visits and trampling impact was evaluated and compared between regulated reserves and unprotected areas [5]. In areas with higher levels of human visits, the mussel cover was significantly lower than in low-use sites, but the diversity of associated species was not affected by the level of use.

4.3. Large-Scale Physical Impacts

Dredging and trawling (where fishing gear is towed near or along the seabed) can physically damage benthic habitats and biota [14,16,35]. These practices can also stir up sediment from the bottom, creating sediment plumes that can impact sensitive species [5,14]. Recovery times for disrupted habitats are usually long and depend on their species sensitivity, the area affected and the intensity of the impact [4,35]. We analyzed five papers that studied the effects of dredging and/or trawling on the mussel communities and adjacent habitats.

4.3.1. Dredging

Among the large-scale physical impacts, dredging seems to be less severe than trawling for the mussel communities [14]. Mussel epifauna is the most affected by dredging, with reductions in abundance of up to 60% following the pass of a dredge [14]. Along the Wadden Sea, the presence of *M. edulis* allowed for a reduction of the impact of dredging, contributing to a higher abundance and diversity than in other mussel-free fishing grounds [36]. Heterogeneous sediments that were inhabited by *M. modiolus* also provided high epifaunal diversity and density. Crustaceans were dominant among the dredged epibenthos, and mussels could provide them with refuge [36].

In the South Atlantic, Morsan [35] (Table 1) observed that dredging causes high disturbance to the whole benthic ecosystem. Multivariate analysis showed that macrofaunal assemblages were altered on each fishing ground between 1987 and 1997, according to fishing intensity and time-lapse, since the last fishing action. However, no significant alterations occurred on the fishing grounds that were not dredged during the 10-year period. In general, the mean density of almost all species declined in dredged fishing grounds. However, in 1997, the abundance of other non-commercial species increased, probably because of the reduction of the commercial target species, that dominated the dredged fishing grounds ten years earlier [35].

Table 1. Reviewed anthropogenic disturbances that impacted mussel beds and associated assemblages. spp. = species; N = abundance; S = species richness; H = Shannon–Wiener's diversity index; J = Pielou's evenness index; ANOSIM = analysis of similarities; ANOVA = analysis of variance; BIOENV = best subset of environmental variables; MANOVA = multivariate analysis of variance; nMDS = non-metric multidimensional scaling; PERMANOVA = permutational analysis of variance; PERMDISP = homogeneity of dispersions; SIMPER = similarity percentage analysis. (+) = Positive impact; (−) = negative impact; null = not mentioned.

Article	Mussel Species	Habitat	Disturbance	Sampling Period	Metazoan Taxa	Mussel Response	Impact on Fauna	Indices and Statistics	Other Measures	Location
[1]	*Mytilus galloprovincialis*	Intertidal, Subtidal: Rock, Sand	Organic pollution (hydrocarbons and sewage)	2004	88 spp. [only mussel beds]: Arthropoda (20.5%); Echinodermata (1.1%), Mollusca (18.2%), Annelida (36.4%), Other (23.8%)	(+)	Moderate impact	N, S, H, J, ANOVA, ANOSIM, nMDS	-	Thermaikos Gulf, Northern Aegean Sea, Greece
[2]	*Crenomytilus grayanus*	Subtidal: Rock, Sand	Organic pollution (sewage), Harvesting	2000–2004	138 spp.: Arthropoda (11.6%), Echinodermata (11.6%), Mollusca (23.2%), Annelida (32.6%), Other (21.0%)	(−)	High impact	N, S, H, J	Biomass, trophic guilds	Vostok Bay, Sea of Japan, Russia
[4]	*Modiolus modiolus*	Subtidal: Mud, Rock, Shells	Trawling	2010	273 spp.: Annelida (34.1%), Arthropoda (17.9%), Echinodermata (6.2%), Mollusca (17.2%), Other (24.6%)	(−)	High impact	N, S, H, J, Margalef, PERMANOVA, PERMDISP, SIMPER	-	Strangford Lough, Ireland
[5]	*Mytilus californianus*	Intertidal: Rock	Harvesting, Trampling	not specified	22 spp. [highest species richness in a site]: not specified	(−)	Low impact	N, S, H, J, *t*-test	Biomass, cover, size, thickness	CA, USA
[6]	*Mytilus edulis*	Intertidal: Rock	Organic pollution (hydrocarbons)	1989	18 spp. [highest species richness in a site]: not specified	(−)	High impact	N, S	Cover	Prince William Sound, AK, USA
[7]	*Mytilus edulis*	Intertidal: Rock	Unspecified pollutants Alien species	2002	154 spp.: Annelida (18.2%), Arthropoda (27.9%), Echinodermata (1.9%), Mollusca (18.2%), Other (33.8%)	-	Moderate impact	S, Conspicuousness, Cluster Analysis, nMDS	-	Helgoland, German Bight, North Sea
[8]	*Mytilus edulis*	Subtidal: Gravel, Mud, Rock, Sand, Shell	Human interference: Harvesting (*Ostrea edulis*),	1980	89 spp.: not specified	(+)	High impact	N, S, Cluster Analysis, Linear Regression	-	Island of Sylt, German Bight, North Sea
[10]	*Mytilus edulis*	Subtidal: Mud, Sand	Organic pollution (sewage)	1971, 1972	38 spp. [only mussel beds]: Annelida (44.7%), Arthropoda (28.9%); Mollusca (21.1%), Echinodermata (2.6%), Other (2.6%)	(-)	Moderate impact	N, S, H, J, Simpson	Biomass	Kiel Bay, Baltic Sea
[11]	*Mytilus edulis*	Intertidal: Rock, Sand, Shells	Organic pollution (hydrocarbons)	1999	57 spp.: Annelida (22.8%), Arthropoda (35.1%), Mollusca (31.6%), Other (10.5%)	(−)	Moderate impact	S, H, BIOENV, MANOVA, nMDS, SIMPER	-	West Coast of UK

Table 1. *Cont.*

Article	Mussel Species	Habitat	Disturbance	Sampling Period	Metazoan Taxa	Mussel Response	Impact on Fauna	Indices and Statistics	Other Measures	Location
[13]	*Brachidontes rodriguezii*	Intertidal: Rock, Sand	Organic pollution (sewage)	1997–2000	12 spp.: only Polychaeta	(−)	Moderate impact	ANOSIM, SIMPER	-	Mar del Plata, Argentina
[14]	*Modiolus modiolus*	Subtidal: Rock	Dredging, Trawling	2007–2009, 2012	29 spp.: not specified	(−)	High impact	N, S, H, J, Margalef, ANOVA, nMDS, PERMANOVA, PERMDISP, SIMPER	-	Isle of Man and Wales, UK
[15]	*Mytilus edulis*	Subtidal: Artificial structures	Metal and Organic pollution (experimental)	2010	not specified	(−)	High impact	ANOVA	-	Malahide Marina, Ireland
[16]	*Modiolus modiolus*	Subtidal: Mud, Rock, Shells	Trawling	not specified	not specified	(−)	High impact	Cluster Analysis, DECORANA	-	Strangford Lough, Ireland
[17]	*Perna perna*	Intertidal: Rock	Harvesting	2008	not specified	(−)	Moderate impact	N, S, PERMANOVA	Cover	Transkei, South Africa
[18]	*Mytilus edulis*	Intertidal, Subtidal: Rock	Harvesting (subtidal)	1997, 1998	19 spp. [Intertidal], 22 spp. [Subtidal]: not specified	(−)	Moderate impact	N, S, H, J, Sørensen's index, Renkon's index, ANOVA, Kruskal-Wallis Test, Mann-Whitney U-Test	-	Island of Sylt, German Bight, North Sea
[21]	*Arcuatula senhousia*, *Jolya elongata*	Subtidal: Mud, Sand	Organic pollution (unspecified),	1985–1987, 1997–1999	460 spp.: not specified	(−)	Moderate impact	N, S, H, J, ANOSIM, nMDS	-	Bohai Sea, China
[22]	*Mytilus galloprovincialis*	Intertidal: Artificial structures	Organic pollution (unspecified)	2004	155 spp.: Annelida (43.2%); Arthropoda (18.1%) Echinodermata (0.6%), Mollusca (9.7%), Other (28.4%)	(+)	Moderate impact	N, S, H, J, Margalef, ANOVA, ANOSIM, BIOENV, nMDS, SIMPER	Biomass	Izmir Bay, Eastern Mediterranean, Turkey
[23]	*Mytilus galloprovincialis*	Intertidal: Rock	Organic pollution (hydrocarbons)	2004, 2005	104 spp.: only Annelida	-	Moderate impact	N, S, H, nMDS	-	Caldebarcos and O Segaño, Galicia, Spain
[24]	*Brachidontes rodriguezii*, *Mytilus platensis*	Intertidal: Rock, Sand	Organic pollution (sewage)	1999, 2000	24 spp.: Annelida (33.3%), Arthropoda (29.2%), Mollusca (20,8%), Other (16.7%)	(+)	Moderate impact	S, H, Margalef, ANOVA, ANOSIM, nMDS	Biomass	Quequén and Necoche, Argentina
[25]	*Brachidontes rodriguezii*, *Mytilus platensis*	Intertidal: Rock, Sand	Organic pollution (sewage)	1997	43 spp.: not specified	(−)	Moderate impact	N, S, H, J, Jack-Knife test	-	Mar del Plata, Argentina

Table 1. *Cont.*

Article	Mussel Species	Habitat	Disturbance	Sampling Period	Metazoan Taxa	Mussel Response	Impact on Fauna	Indices and Statistics	Other Measures	Location
[27]	*Perumytilus purpuratus*	Intertidal: Rock	Harvesting, Organic enrichment (experimental)	2004	45 spp.: Annelida (17.8%), Arthropoda (31.1%), Mollusca (35.6%), Echinodermata (4.4%) Other (11.1%)	-	Moderate impact	N, S, ANOVA, ANOSIM, SIMPER	Trophic guilds	Bahía Totoralillo, Northern-Central Chile
[28]	*Mytilus* sp.	Intertidal: Rock, Heterogenous sediment	Organic pollution (hydrocarbons),	1990, 1991	42 spp. [highest species richness in a site]: not specified	(−)	High impact	N, S, H, ANOVA	Cover	Prince William Sound, AK, USA
[29]	*Perumytilus purpuratus*	Intertidal: Rock	Metal pollution (experimental)	2007	46 spp.: Annelida (30.4%), Arthropoda (19.6%), Echinodermata (8.7%), Mollusca (23.9), Other (17.4%)	null	Moderate impact	S, H, J	-	Bahia San Jorge, Northern Chile
[30]	*Perna perna*	Intertidal: Rock	Harvesting	not specified	not specified	(−)	Low impact	N. S, H, nMDS	Biomass, trophic guilds	Transkei, South Africa
[31]	*Mytilus californianus*	Intertidal: Rock	Trampling	1977, 1978	67 spp.: not specified	null	Low impact	N, S, H, Dominance curves, Kruskall-Wallis Test, Mann-Whitney U-Test	-	Santa Cruz, CA, USA
[32]	unspecified	Intertidal: Mud, Sand	Harvesting	1981–1984, 1987	44 spp. [unpolluted site]: Annelida (50.0%), Arthropoda (20.4%), Echinodermata (3.7%), Mollusca (25.9%)	(−)	Moderate impact	ABC K-Dominance curves	-	Netherlands and Belgium
[33]	*Perumytilus purpuratus*, *Mytilus chilensis*	Intertidal: Mud, Rock, Sand	Harvesting, Trampling (experimental)	2001	not specified	(−)	Moderate impact	ANOVA, Mann-Whitney U-Test	Biomass, cover, size	Rio Grande, Tierra del Fuego, Argentina
[34]	*Mytilus californianus*	Intertidal: Rock	Trampling	1995	20 spp. [highest species richness in a site]: not specified	(−)	Low impact	S, H, ANOVA, ANCOVA, *t*-test	Cover	Santa Cruz, CA, USA
[35]	*Mytilus platensis*	Subtidal: Gravel, Mud, Sand, Shells	Dredging	1986–1997	46 spp. [highest species richness in a site]: not specified	(−)	Moderate impact	S, ANOSIM, MDS	-	Golfo de San Matías, Argentina
[36]	*Mytilus edulis*	Subtidal: Gravel, Sand, Shells	Dredging	1988, 1992	42 spp.: Arthropoda (23.8%), Echinodermata (4.8%), Mollusca (21.4%), Annelida (4.8%), Other (45.2%)	(+)	High impact	Mann-Whitney U-Test	-	Schleswig-Holstein, Wadden Sea, North Sea

The recovery of dredging-impacted areas takes a long time [14]. Comparisons with historical surveys in the Wadden Sea suggested that a decline of nearly 50% of all epifaunal species within the last hundred years could be attributed to fishery impacts [36]. Moreover, the community structure may not return to pre-harvest conditions, but lead instead to new assemblages [14,35].

4.3.2. Trawling

An obvious effect of trawling was the destruction of the mussel clumps, the flattening of the mussel structure and the removing of epifauna [4,16]. In some cases, the substrate was not totally removed, and a few live mussels remained among a noticeable amount of shell debris [16]. Magorrian and Service [16] visually documented the effects of trawling, but their 'Visual Fast Count' approach did not provide as much taxonomic information as traditional methods, mostly due to the difficulty in identifying organisms on video. However, this research could have a potential role in the management of epifaunal communities in future broader assessment studies.

Declines in the abundance of mussels and epifaunal organisms following the passage of a trawl could reach up to 90% of the total fauna abundance [4,14]. Declines in diversity were also observed, mainly for anthozoans, ascidians, bivalves, echinoderms, hydrozoans, sponges or tunicates. A repeated exploitation led to a major reduction in mussel distribution in Northern Ireland since the 1970s, until a fishing ban enforcement was implemented in 2003 [4]. The loss of the structure formed by *M. modiolus* and its role in pelagic-benthic coupling probably accounts for the diversity and abundance declines of most higher taxa [14,16]. Distinct species also respond to the impact in different ways; for instance, the abundance of tunicates or some infaunal annelids increases while vagile taxa or mussel epifauna decline because of the reduction or disappearance of the host [4]. This is reflected in significant decreases of overall values of species richness, diversity and evenness in trawled areas [4,14].

Trawling impacted areas have a very slow recovery, compared to dredging [14]. Therefore, some authors suggest a direct intervention, including habitat restoration, to speed up the process, since the designation of Marine Protected Areas and the introduction of fishing bans alone could not be enough to reverse the negative effects caused by trawling [4].

5. Synthesis and Final Remarks

Mussel beds are very important habitats, forming complex structures and creating niches that harbor a great number of species [9,14]. The biota depends on the mussels' shelter, their water purification abilities or the sediment and fecal pellets trapped amid the byssus, that contribute to the presence of many deposit-feeders and predators [10,11,13]. When the ecosystem is impacted, the assemblages rely on the mussels for protection and/or mitigation. The mussels are capable of bioaccumulating a huge amount of organic and inorganic pollutants, removing them from the water column or making them less available to other species [11,15,27]. Therefore, the removal and killing of mussels by harvesting, trampling, dredging, trawling or pollution threatens the ecological quality of the mussel communities. This is especially prominent when the systems are afflicted by other disturbances and synergistic effects lead to a poor ecological status, reducing biodiversity [2,23,27,33].

Low values of abundance, biomass, diversity, evenness or species richness were reported for all categories of impacts, with some studies describing declines in at least three of these descriptors [2,4,5,8,33]. However, some species, like annelids, opportunistically profited from the perturbations, particularly from organic enrichment, and increased their abundance and biomass [10,22,25]. Regarding the mussel species, some were able to recover faster than others in the same disturbed system [33]. In moderate impacted areas, species tolerant to pollution were thriving, benefiting from the enriched sediments [1,2,13,22,24–26]. Moreover, the presence of heterogenous habitats colonized by mussels also helped to

mitigate severe impacts like dredging, since mussels, as ecosystem-engineers, increased biodiversity [36].

Most of the studies here reviewed concern the effects of organic pollution, mainly in the Atlantic–Mediterranean region, and only two discussed the effects of metals in this region. Moreover, organic pollution effects have been less studied in the Pacific region and remain to be studied in the Indian Ocean. In comparison, harvesting or trampling have been less studied but encompass different regions of the world, including the Indian Ocean. However, dredging or trawling have only been studied in the Atlantic region even though trawling, for instance, is a widespread practice in other known mussel regions [37]. The assessment of both impacts in other regions is needed due to their severe effects, particularly trawling. In general, this applies to many areas with mussel beds, regardless of the type of impact, in order to get a better comprehension of their effects on the mussel communities and overall biodiversity.

It is important to protect mussel beds by promoting marine reserves conservation, managing harvesting or establishing limitations to allow for a good restoration [5,17,18]. A direct intervention in the restoration of mussel beds can have a huge impact in habitat degradation reversion and be useful to improve resources and ecosystem function [38]. This should be an approach to follow in the future.

Author Contributions: Conceptualization, P.V., L.G.-M., L.S., J.M. and M.R.; methodology, L.G.-M., L.S., M.R. and P.V.; resources, M.R., and P.V.; writing—original draft preparation, L.S.; writing—review and editing, J.M., L.G.-M., M.R. and P.V.; project administration, P.V.; funding acquisition, P.V. All authors have read and agreed to the published version of the manuscript.

Funding: This research was developed under the Project No. 30181 (PTDC/CTA-AMB/30181/2017), co-financed by COMPETE 2020, Portugal 2020 and the European Union, through the ERDF, and by the FCT (Foundation for Science and Technology) through national funds within the scope of UIDB/04423/2020 and UIDP/04423/2020.

Data Availability Statement: Not applicable.

Acknowledgments: We would like to thank the two reviewers for their constructive comments, which helped to improve the manuscript. Puri Veiga was hired through the Regulamento do Emprego Científico e Tecnológico—RJEC, from the Portuguese Foundation for Science and Technology (FCT) (CEECIND/03893/2018). Laura Guerrero-Meseguer was funded by the "Recovery, Transformation and Resilience Plan of the Ministry of Universities of Spain", "NextGenerationEU" and the University of the Balearic Islands.

Conflicts of Interest: The authors declare no conflict of interest.

References

1. Antoniadou, C.; Sarantidis, S.; Chintiroglou, C. Small-scale spatial variability of zoobenthic communities in a commercial Mediterranean port. *J. Mar. Biol. Assoc. U. K.* **2011**, *91*, 77–89. [CrossRef]
2. Galysheva, Y.A. Current state and long-term changes of the *Crenomytilus grayanus* community in Vostok Bay, Sea of Japan. *Russ. J. Ecol.* **2008**, *39*, 272–278. [CrossRef]
3. Veiga, P.; Ramos-Oliveira, C.; Sampaio, L.; Rubal, M. The role of urbanisation in affecting *Mytilus galloprovincialis*. *PLoS ONE* **2020**, *15*, e0232797. [CrossRef]
4. Fariñas-Franco, J.M.; Allcock, A.L.; Roberts, D. Protection alone may not promote natural recovery of biogenic habitats of high biodiversity damaged by mobile fishing gears. *Mar. Environ. Res.* **2018**, *135*, 18–28. [CrossRef]
5. Smith, J.R.; Fong, P.; Ambrose, R.F. The Impacts of Human Visitation on Mussel Bed Communities Along the California Coast: Are Regulatory Marine Reserves Effective in Protecting These Communities? *Environ. Manag.* **2008**, *41*, 599–612. [CrossRef] [PubMed]
6. Lees, D.C.; Houghton, J.P.; Driskell, W.B. Effects of shoreline treatment methods on intertidal biota in Prince William Sound. In Proceedings of the International Oil Spill Conference, Tampa, FL, USA, 29 March–1 April 1993; American Petroleum Institute: Washington, DC, USA, 1993; Volume 1993, pp. 345–354.
7. Reichert, K.; Buchholz, F. Changes in the macrozoobenthos of the intertidal zone at Helgoland (German Bight, North Sea): A survey of 1984 repeated in 2002. *Helgol. Mar. Res.* **2006**, *60*, 213–223. [CrossRef]
8. Riesen, W.; Reise, K. Macrobenthos of the subtidal Wadden Sea: Revisited after 55 years. *Helgoländer Meeresunters.* **1982**, *35*, 409–423. [CrossRef]

9. Gestoso, I.; Arenas, F.; Rubal, M.; Veiga, P.; Peña, M.; Olabarria, C. Shifts from native to non-indigenous mussels: Enhanced habitat complexity and its effects on faunal assemblages. *Mar. Environ. Res.* **2013**, *90*, 85–95. [CrossRef]
10. Anger, K. On the influence of sewage pollution on inshore benthic communities in the South of Kiel Bay. *Helgoländer Wiss. Meeresunters.* **1975**, *27*, 408–438. [CrossRef]
11. Crowe, T.P.; Smith, E.L.; Donkin, P.; Barnaby, D.L.; Rowland, S.J. Measurements of sublethal effects on individual organisms indicate community-level impacts of pollution. *J. Appl. Ecol.* **2004**, *41*, 114–123. [CrossRef]
12. Quintino, V.; Azevedo, A.; Magalhães, L.; Sampaio, L.; Freitas, R.; Rodrigues, A.M.; Elliott, M. Indices, multispecies and synthesis descriptors in benthic assessments: Intertidal organic enrichment from oyster farming. *Estuar. Coast. Shelf Sci.* **2012**, *110*, 190–201. [CrossRef]
13. Elías, R.; Rivero, M.S.; Palacios, J.R.; Vallarino, E.A. Sewage-induced disturbance on polychaetes inhabiting intertidal mussel beds of *Brachidontes rodriguezii* off Mar del Plata (SW Atlantic, Argentina). *Sci. Mar.* **2006**, *70*, 187–196. [CrossRef]
14. Cook, R.; Fariñas-Franco, J.M.; Gell, F.R.; Holt, R.H.F.; Holt, T.; Lindenbaum, C.; Porter, J.S.; Seed, R.; Skates, L.R.; Stringell, T.B.; et al. The Substantial First Impact of Bottom Fishing on Rare Biodiversity Hotspots: A Dilemma for Evidence-Based Conservation. *PLoS ONE* **2013**, *8*, e69904. [CrossRef] [PubMed]
15. Browne, M.A.; Brooks, P.R.; Clough, R.; Fisher, A.S.; Pinto, M.M.; Crowe, T.P. Simulating regimes of chemical disturbance and testing impacts in the ecosystem using a novel programmable dosing system. *Methods Ecol. Evol.* **2015**, *7*, 609–618. [CrossRef]
16. Magorrian, B.H.; Service, M. Analysis of underwater visual data to identify the impact of physical disturbance on horse mussel (*Modiolus modiolus*) beds. *Mar. Pollut. Bull.* **1998**, *36*, 354–359. [CrossRef]
17. Cole, V.J.; McQuaid, C.D.; Nakin, M.D.V. Marine protected areas export larvae of infauna, but not of bioengineering mussels to adjacent areas. *Biol. Conserv.* **2011**, *144*, 2088–2096. [CrossRef]
18. Saier, B. Subtidal and intertidal mussel beds (*Mytilus edulis* L.) in the Wadden Sea: Diversity differences of associated epifauna. *Helgol. Mar. Res.* **2002**, *56*, 44–50. [CrossRef]
19. World Register of Marine Species. At VLIZ. Available online: http://www.marinespecies.org (accessed on 12 January 2021).
20. Cárdenas, L.; Leclerc, J.-C.; Bruning, P.; Garrido, I.; Détrée, C.; Figueroa, A.; Astorga, M.; Navarro, J.M.; Johnson, L.E.; Carlton, J.T.; et al. First mussel settlement observed in Antarctica reveals the potential for future invasions. *Sci. Rep.* **2020**, *10*, 5552. [CrossRef]
21. Zhou, H.; Zhang, Z.N.; Liu, X.S.; Tu, L.H.; Yu, Z.S. Changes in the shelf macrobenthic community over large temporal and spatial scales in the Bohai Sea, China. *J. Mar. Syst.* **2007**, *67*, 312–321. [CrossRef]
22. Çinar, M.E.; Katagan, T.; Koçak, F.; Öztürk, B.; Ergen, Z.; Kocatas, A.; Önen, M.; Kirkim, F.; Bakir, K.; Kurt, G.; et al. Faunal assemblages of the mussel *Mytilus galloprovincialis* in and around Alsancak Harbour (Izmir Bay, eastern Mediterranean) with special emphasis on alien species. *J. Mar. Syst.* **2008**, *71*, 1–17. [CrossRef]
23. García-Regueira, X.; Tato, R.; Moreira, J.; Urgorri, V. Temporal evolution of polychaete assemblages on intertidal hard substrata at two localities of the Galician coast after the 'Prestige' oil spill. *Thalassas* **2010**, *26*, 33–45.
24. Adami, M.L.; Tablado, A.; Gappa, J.L. Spatial and temporal variability in intertidal assemblages dominated by the mussel *Brachidontes rodriguezii* (d'Orbigny, 1846). *Hydrobiologia* **2004**, *520*, 49–59. [CrossRef]
25. Vallarino, E.A.; Rivero, M.S.; Gravina, M.C.; Elías, R. The community-level response to sewage impact in intertidal mytilid beds of the Southwestern Atlantic, and the use of the Shannon index to assess pollution. *Rev. Biol. Mar. Oceanog.* **2002**, *37*, 25–33. [CrossRef]
26. Sánchez, M.A.; Jaubet, M.L.; Garaffo, G.V.; Elías, R. Spatial and long-term analyses of reference and sewage-impacted sites in the SW Atlantic (38° S, 57° W) for the assessment of sensitive and tolerant polychaetes. *Mar. Pollut. Bull.* **2013**, *74*, 325–333. [CrossRef]
27. Valdivia, N.; Thiel, M. Effects of point-source nutrient addition and mussel removal on epibiotic assemblages in *Perumytilus purpuratus* beds. *J. Sea Res.* **2006**, *56*, 271–283. [CrossRef]
28. Houghton, J.P.; Fukuyama, A.K.; Lees, D.C.; Driskell, W.B.; Shigenaka, G.; Mearns, A.J. Impacts on Intertidal Epibiota: Exxon Valdez Spill and Subsequent Cleanup. In Proceedings of the International Oil Spill Conference, Tampa, FL, USA, 29 March–1 April 1993; American Petroleum Institute: Washington, DC, USA, 1993; Volume 1993, pp. 293–300.
29. Acevedo, J.; Orellana, I.F.; Guiñez, R. Evaluación experimental de la toxicidad de cobre in situ sobre la fauna asociada a *Perumytilus purpuratus* (Bivalvia: Mytilidae), un ingeniero ecosistémico. *Rev. Biol. Mar. Oceanog.* **2010**, *45*, 497–505. [CrossRef]
30. Lasiak, T.A.; Field, J.G. Community-level attributes of exploited and non-exploited rocky infratidal macrofaunal assemblages in Transkei. *J. Exp. Mar. Biol. Ecol.* **1995**, *185*, 33–53. [CrossRef]
31. Beauchamp, K.A.; Gowing, M.M. A quantitative assessment of human trampling effects on a rocky intertidal community. *Mar. Environ. Res.* **1982**, *7*, 279–293. [CrossRef]
32. Meire, P.M.; Dereu, J. Use of the Abundance/Biomass Comparison Method for Detecting Environmental Stress: Some Considerations Based on Intertidal Macrozoobenthos and Bird Communities. *J. Appl. Ecol.* **1990**, *27*, 210–223. [CrossRef]
33. Calcagno, J.A.; Curelovich, J.N.; Fernandez, V.M.; Thatje, S.; Lovrich, G.A. Effects of physical disturbance on a sub-Antarctic middle intertidal bivalve assemblage. *Mar. Biol. Res.* **2012**, *8*, 937–953. [CrossRef]
34. Van de Werfhorst, L.C.; Pearse, J.S. Trampling in the rocky intertidal of central California: A follow-up study. *Bull. Mar. Sci.* **2007**, *81*, 245–254.
35. Morsan, E.M. Impact on biodiversity of scallop dredging in San Matías Gulf, northern Patagonia (Argentina). *Hydrobiologia* **2009**, *619*, 167–180. [CrossRef]

36. Buhs, F.; Riese, K. Epibenthic fauna dredged from tidal channels in the Wadden Sea of Schleswig-Holstein: Spatial patterns and a long-term decline. *Helgolander Meeresun.* **1997**, *51*, 343–359. [CrossRef]
37. Amoroso, R.O.; Pitcher, C.R.; Rijnsdorp, A.D.; McConnaughey, R.A.; Parma, A.M.; Suuronen, P.; Eigaard, O.R.; Bastardie, F.; Hintzen, N.T.; Althaus, F.; et al. Bottom trawl fishing footprints on the world's continental shelves. *Proc. Natl. Acad. Sci. USA* **2018**, *115*, E10275–E10282. [CrossRef] [PubMed]
38. Kristensen, L.D.; Stenberg, C.; Støttrup, J.G.; Poulsen, L.K.; Christensen, H.T.; Dolmer, P.; Røjbek, M.; Thorsen, S.W.; Holmer, M.; Deurs, M.V.; et al. Establishment of blue mussel beds to enhance fish habitats. *Appl. Ecol. Environ. Res.* **2015**, *13*, 783–798.

MDPI
St. Alban-Anlage 66
4052 Basel
Switzerland
www.mdpi.com

Diversity Editorial Office
E-mail: diversity@mdpi.com
www.mdpi.com/journal/diversity

Academic Open
Access Publishing

mdpi.com

ISBN 978-3-0365-9958-8